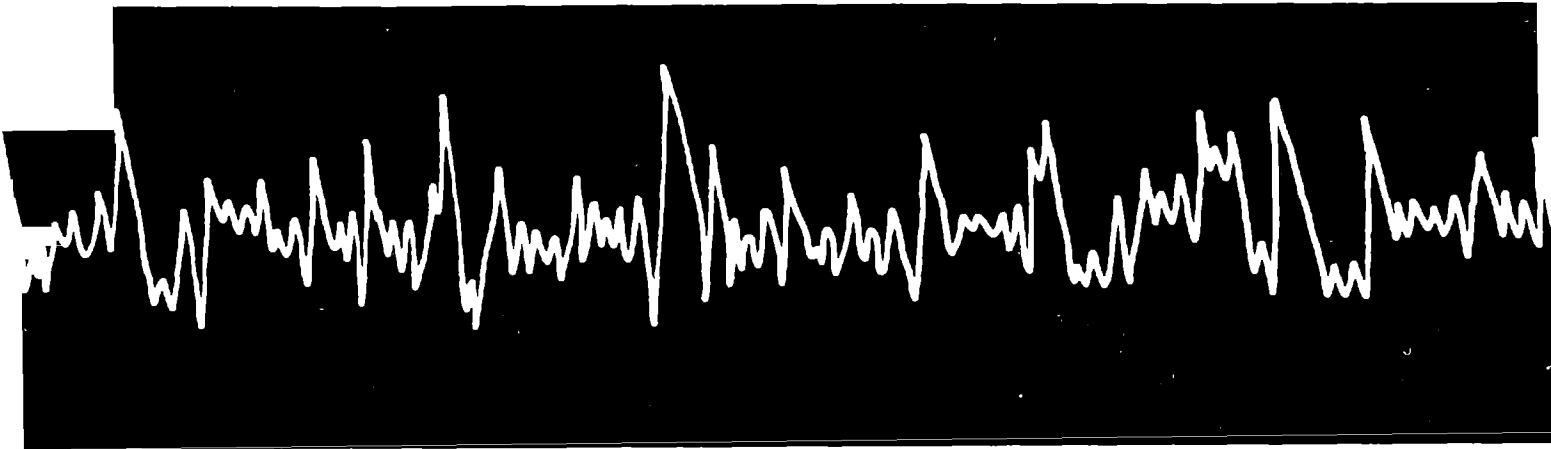


PB300-308



**PROCEEDINGS OF
THE SECOND INTERNATIONAL CONFERENCE ON
MICROZONATION
FOR SAFER CONSTRUCTION—RESEARCH AND APPLICATION**



VOLUME

I

Any opinions, findings, conclusions or recommendations expressed in this publication are those of the author(s) and do not necessarily reflect the views of the National Science Foundation.

Sponsored by:
National Science Foundation
UNESCO
American Society of Civil Engineers
Earthquake Engineering Research Institute
Seismological Society of America
Universities Council for Earthquake Engineering Research

REPRODUCED BY
U.S. DEPARTMENT OF COMMERCE
NATIONAL TECHNICAL
INFORMATION SERVICE
SPRINGFIELD, VA 22161

SAN FRANCISCO, CALIFORNIA, U.S.A.

NOVEMBER 26-DECEMBER 1, 1978

PROGRAM COMMITTEE

Conference Chairman

Mehmet A. Sherif
University of Washington
Seattle, Washington

Steering Committee

S.T. Algermissen
U.S. Geological Survey
Denver, Colorado

Bruce A. Bolt
University of California
Berkeley, California

Michael P. Gaus
National Science Foundation
Washington, D.C.

Henry J. Lagorio
University of Hawaii
Honolulu, Hawaii

George Mader
William Spangle and Associates
Portola Valley, California

Norton S. Remmer
Code Inspection Department
Worcester, Massachusetts

H. Bolton Seed
University of California
Berkeley, California

Karl V. Steinbrugge
Insurance Services Office
Earthquake Department
San Francisco, California

Robert E. Wallace
U.S. Geological Survey
Menlo Park, California

Robert V. Whitman
Massachusetts Institute of Technology
Cambridge, Massachusetts

Clarence R. Allen
California Institute of Technology
Pasadena, California

Lloyd S. Cluff
Woodward-Clyde Consultants
San Francisco, California

George W. Housner
California Institute of Technology
Pasadena, California

S. Chi Liu
National Science Foundation
Washington, D.C.

Marion E. Marts
University of Washington
Seattle, Washington

Christ Sanidas
Chief Building Official
Memphis, Tennessee

Haresh C. Shah
Stanford University
Palo Alto, California

Ralph H. Turner
University of California
Los Angeles, California

Gilbert F. White
University of Colorado
Boulder, Colorado

John H. Wiggins
J.H. Wiggins Company
Redondo Beach, California

Conference Secretary

Isao Ishibashi
University of Washington
Seattle, Washington

CONFERENCE SESSIONS AND CHAIRMEN

I. *STATE-OF-THE-ART*

Richard H. Jahns, Stanford University, Palo Alto, California
Michael P. Gaus, National Science Foundation, Washington, D.C.

II. *MICROZONATION*

Robert M. Hamilton, U.S. Geological Survey, Washington, D.C.
Haresh C. Shah, Stanford University, Palo Alto, California

III. *GEOLOGY, SEISMOLOGY, GEOPHYSICS AND SITE EFFECTS*

Lloyd S. Cluff, Woodward-Clyde Consultants, San Francisco, California
Clarence R. Allen, California Institute of Technology, Pasadena, California

IV. *SOIL DYNAMICS, SOIL-STRUCTURE INTERACTION AND GROUND EFFECTS*

H. Bolton Seed, University of California at Berkeley
Kenji Ishihara, University of Tokyo

V. *ENGINEERING MECHANICS AND STRUCTURAL DESIGN*

Ray W. Clough, University of California at Berkeley

VI. *OFFSHORE MICROZONATION*

I.M. Idriss, Woodward-Clyde Consultants, San Francisco, California

VII. *URBAN PLANNING, SOCIO-ECONOMICS AND GOVERNMENT RESPONSIBILITY*

Ralph H. Turner, University of California at Los Angeles

VIII. *PANEL DISCUSSION*

John A. Blume, URS/J.A. Blume Associates, San Francisco, California

INTRODUCTORY STATEMENT

The Second International Conference on Microzonation for Safer Construction—Research and Application has succeeded in bringing together representatives from diverse fields of interest, such as geology, seismology, engineering, sociology, economics, planning, architecture, insurance, and government, to summarize the state of knowledge in the zoning of areas for earthquake effects and to identify future research needs in seismic microzonation. This broadly based participation reflects the general notion that real and enduring solutions to the social and economic problems resulting from earthquakes can best be achieved through genuine interdisciplinary cooperative effort among scientists who are involved in the discovery and expansion of knowledge, engineers who are engaged in the application of scientific principles to improve the performance of manmade structures during earthquakes, and public officials who are responsible for implementing and enforcing land-use planning and building code requirements.

These three volumes of Conference Proceedings include between their covers an impressive number of high-quality technical papers by authors from different countries. On behalf of the Organizing Committee, I take this opportunity to express our most sincere thanks and appreciation to these authors for devoting much time and effort to the preparation of these papers.

Mehmet A. Sherif
Conference Chairman

San Francisco U.S.A.
November 1978

TABLE OF CONTENTS

VOLUME I

STATE-OF-THE-ART SESSION		Page
C. Kisslinger	Seismicity and Global Tectonics as a Framework for Microzonation	3
P. C. Jennings D. V. Helmberger	Strong-Motion Seismology	27
N. C. Donovan	Soil & Geologic Effects on Site Response	55
M. A. Sherif I. Ishibashi	Soil Dynamics Considerations for Microzonation	81
A. S. Veletsos	Soil-Structure Interaction for Buildings during Earthquakes	111
L. S. Cluff	Geologic Considerations for Seismic Microzonation	135
V. J. Murphy	Geophysical Engineering Investigative Techniques for Site Characterization	153
J. R. Hutton D. S. Mileti	Social Aspects of Earthquakes	179
H. J. Lagorio E. E. Botsai	Urban Design and Earthquakes	193
K. V. Steinbrugge	Earthquake Insurance and Microzonation	203
N. S. Remmer	Government Responsibility in Microzonation	215

MICROZONATION SESSION

Progress on Seismic Zonation in the San Francisco Bay Region

E. E. Brabb R. D. Borchardt	1. Introduction and Summary	229
D. G. Herd	2. Neotectonic Framework of Central Coastal Cali- fornia and Its Implications to Microzonation of the San Francisco Bay Region	231
R. D. Borchardt J. F. Gibbs T. E. Fumal	3. Progress on Ground Motion Predictions for the San Francisco Bay Region, California	241
R. J. Archuleta W. B. Joyner D. M. Boore	4. A Methodology for Predicting Ground Motion at Specific Sites	255

T. L. Youd J. C. Tinsley D. M. Perkins E. J. King R. F. Preston	5. Liquefaction Potential Map of San Fernando Valley, California	267
D. K. Keefer G. F. Wieczorek E. L. Harp D. H. Tuel	6. Preliminary Assessment of Seismically Induced Landslide Susceptibility	279
S. T. Algermissen K. V. Steinbrugge	7. Earthquake Losses to Buildings in the San Francisco Bay Area	291
W. J. Kockelman E. E. Brabb	8. Examples of Seismic Zonation in the San Francisco Bay Region	303
J. B. Perkins	9. The Use of Earthquake and Related Information in Regional Planning--What We've Done and Where We're Going	315
W. G. Milne D. H. Weichert	The Sensitivity of Seismic Risk Maps to the Choice of Earthquake Parameters in the Georgia Strait Region of British Columbia	323
J. A. Fischer J. G. McWhorter	The Microzonation of New York State: Progress Report No. 2	329
J. Kuroiwa E. Deza H. Jaén J. Kogan	Microzonation Methods and Techniques Used in Peru	341
E. L. Harp R. C. Wilson G. F. Wieczorek D. K. Keefer	Landslides from the February 4, 1976 Guatemala Earthquake: Implications for Seismic Hazard Reduction in the Guatemala City Area	353
S. T. Mau C. S. Kao	A Risk Model for Seismic Zoning of Taiwan	367
H. K. Acharya	Ground Motion Attenuation in the Philippines	379
K. Moazami-Goudarzi H. Parhikhteh	A Quantitative Seismotectonic Study of the Iranian Plateau	391
N. Mândrescu	The Vrancea Earthquake of March 4, 1977 and the Seismic Microzonation of Bucharest	399
J. Petrovski	Need for Experimental Evidence in Development of Seismic Microzoning Methods	413
S. Hattori	A New Proposal of the Seismic Risk Map Based on the Maximum Earthquake Motions, the Ground Characteristics and the Temporal Variations of the Seismicity	421
E. Shima	Seismic Microzoning Map of Tokyo	433

S. Yoshikawa Y. T. Iwasaki M. Tai	Microzoning of Osaka Region	445
D. R. Packer L. S. Cluff D. P. Schwartz F. H. Swan, III I. M. Idriss	Auburn Dam - A Case History of Earthquake Evaluation for a Critical Facility	457
E. J. Bell D. T. Trexler J. W. Bell	Computer-Simulated Composite Earthquake Hazard Model for Reno, Nevada	471
A. S. Patwardhan D. D. Tillson R. L. Nowack	Zonation for Critical Facilities Based on Two-Level Earthquakes	485
W. W. Hays S. T. Algermissen R. D. Miller K. W. King	Preliminary Ground Response Maps for the Salt Lake City, Utah, Area	497
C. E. Glass	Application of Regionalized Variables to Micro- zonation	509
J. L. Alonso L. Urbina	A New Microzonation Technique for Design Purposes	523
A. S. Patwardhan L. S. Cluff	The Concept of Residual Risk in Earthquake Risk Assessments	535
S. Murakami K. Midorikawa	Land Use Technique for Microzonation	547
J. G. Anderson M. D. Trifunac	Application of Seismic Risk Procedures to Problems in Microzonation	559
B. A. Schell	Seismotectonic Microzoning for Earthquake Risk Reduction	571
A Report on the Miyagiken-oki, Japan, Earthquake of June 12, 1978		
	Abstract	587
H. Kobayashi K. Seo S. Midorikawa	I. Strong Ground Motions and Seismic Microzoning	588
Y. Yoshimi I. Tohno K. Tokimatsu	II. Geotechnical Aspects of Damage	600
T. Katayama	III. Damage to Lifeline Utility Systems (A) . . .	606
H. Shibata	IV. Damage to Lifeline Utility Systems (B) . . .	612

Index of Authors

VOLUME II

GEOLOGY, SEISMOLOGY, GEOPHYSICS AND SITE EFFECTS SESSION

B. A. Bolt	Fallacies in Current Ground Motion Prediction . . .	617
E. W. Hart	Zoning for the Hazard of Surface Fault Rupture in California	635
M. R. Ploessel	High-Resolution Geophysical Surveys, A Technique for Microzonation of the Continental Shelf	647
L. Esteva E. Bazán	Seismicity and Seismic Risk Related to Subduction Zones	657
W. D. Page W. U. Savage J. N. Alt L. S. Cluff D. Tocher	Seismic Hazards along the Makran Coast of Iran and Pakistan: The Importance of Regional Tectonics and Geologic Assessment	669
S. Kh. Negmatullaev G. S. Seleznyov D. W. Simpson C. Rojahn	Engineering and Seismological Observations at Dams	681
R. A. Wiggins G. A. Frazier J. Sweet R. Apsel	Modeling Strong Motions from Major Earthquakes . .	693
F. T. Wu	Prediction of Strong Ground Motion Using Small Earthquakes	701
T. Iwasaki T. Katayama K. Kawashima M. Saeki	Statistical Analysis of Strong-Motion Acceleration Records Obtained in Japan	705
A. F. Shakal M. N. Toksöz	Analysis of Source and Medium Effects on Strong Motion Observations	717
F. J. Sánchez-Sesma	Ground Motion Amplification due to Canyons of Arbitrary Shape	729
E. Mardiross	A Method for Assessment of Seismic Design Motions	739
A. M. Rogers W. W. Hays	Preliminary Evaluation of Site Transfer Functions Developed from Earthquakes and Nuclear Explosions	753
K. Kudo	The Contribution of Love Waves to Strong Ground Motions	765
I. S. Oweis	The Relevancy of One Dimensional Shear Models in Predicting Surface Acceleration	777

N. Goto Y. Ohta H. Kagami	Deep Shear Wave Velocity Measurement for Evaluation of 1-10 Sec Seismic Input Motions	793
K. Sadigh M. S. Power R. R. Youngs	Peak Horizontal and Vertical Accelerations, Velocities, and Displacements on Deep Soil Sites during Moderately Strong Earthquakes	801
F. J. Sabina I. Herrera R. England	Theory of Connectivity: Applications to Scattering of Seismic Waves. I. SH Wave Motion	813
S. Midorikawa H. Kobayashi	On Estimation of Strong Earthquake Motions with Regard to Fault Rupture	825

SOIL DYNAMICS, SOIL-STRUCTURE INTERACTION AND GROUND EFFECTS SESSION

W. D. L. Finn Y. P. Vaid S. K. Bhatia	Constant Volume Cyclic Simple Shear Testing	839
Y. Yoshimi K. Tokimatsu	Two-Dimensional Pore Pressure Changes in Sand Deposits during Earthquakes	853
A. S. Arya P. Nandakumaran V. K. Puri S. Mukerjee	Verification of Liquefaction Potential by Field Blast Tests	865
H. Dezfulian S. R. Prager	Use of Penetration Data for Evaluation of Liquefaction Potential	873
T. Iwasaki F. Tatsuoka K. Tokida S. Yasuda	A Practical Method for Assessing Soil Liquefaction Potential Based on Case Studies at Various Sites in Japan	885
K. Ishihara K. Ogawa	Liquefaction Susceptibility Map of Downtown Tokyo	897
J. Isenberg D. K. Vaughan	Three-Dimensional Nonlinear Analysis of Soil-Structure Interaction in a Nuclear Power Plant Containment Structure	911
E. Alarcón J. Dominguez A. Martín F. Paris	Boundary Methods in Soil-Structure Interaction	921
Y. Sugimura	Seismic Shear Strain Induced in Soil Deposits	933
R. D. Singh W. S. Gardner R. Dobry	Post Cyclic Loading Behavior of Soft Clays	945

S. Nemat-Nasser A. Shokoh	A New Approach for the Analysis of Liquefaction of Sand in Cyclic Shearing	957
K. Tanimoto M. Nishi T. Noda	A Study of Shear Deformation Process of Sandy Soils by the Observation of Acoustic Emission Response	971
W. P. Grant I. Arango D. N. Clayton	Geotechnical Data at Selected Strong Motion Accelerograph Sites	983
Y. Shioi T. Furuya M. Okahara	Recent Earthquake Resistant Design Methods for Different Types of Foundations in Japan	1001
W. F. Marcuson, III R. F. Ballard, Jr. S. S. Cooper	Comparison of Penetration Resistance Values to In Situ Shear Wave Velocities	1013
C. M. Duke G. C. Liang	Site Effects from Fourier Transforms	1025
A. M. Abdel-Ghaffar R. F. Scott	Dynamic Characteristics of an Earth Dam from Two Recorded Earthquake Motions	1037
B. Tucker J. King K. Aki J. Brune I. Nersesov W. Prothero G. Shpilker G. Self	A Preliminary Report on a Study of the Seismic Response of Three Sediment-Filled Valleys in the Garm Region of the USSR	1051
K. W. Campbell	Empirical Synthesis of Seismic Velocity Profiles from Geotechnical Data	1063
S. D. Werner H. S. Ts'ao	Effect of Local Site Conditions on Spectral Amplification Factors	1077
I. Lam C. F. Tsai G. R. Martin	Determination of Site Dependent Spectra Using Non-linear Analysis	1089
M. L. Traubenik J. E. Valera W. H. Roth	Effects of Soil Inertia Forces on Design of Buried Pipelines Crossing Faults	1105
C. B. Crouse B. E. Turner	Analysis of Ground Motion Spectra	1117

Index of Authors

VOLUME III

ENGINEERING MECHANICS AND STRUCTURAL DESIGN SESSION

G. C. Hart C. Rojahn	Selection of Buildings for Strong-Motion Instrumentation Using Zonation Information and Decision Theory	1135
V. V. Bertero S. A. Mahin	Need for a Comprehensive Approach in Establishing Design Earthquakes	1145
A. R. Chandrasekaran D. K. Paul	Velocity Response Spectra for Sites on Rock or Soil	1157
P. C. Chen J. H. Chen	Generation of Floor Response Spectra Directly from Free-Field Design Spectra	1169
T. Hisada Y. Ohsaki M. Watabe T. Ohta	Design Spectra for Stiff Structures on Rock	1187
A. H. Hadjian	On the Correlation of the Components of Strong Ground Motion	1199
T. Iwasaki K. Kawashima	Seismic Analysis of a Highway Bridge Utilizing Strong-Motion Acceleration Records	1211
G. C. Delfosse J. C. Miranda	Buildings on Isolators for Earthquake Protection	1223
W. J. Hall J. R. Morgan N. M. Newmark	Traveling Seismic Waves and Structural Response . .	1235
R. V. Whitman	Effective Peak Acceleration	1247
B. Mohraz M. L. Eskijian	A Study of Earthquake Response Spectra for Offshore Platforms	1257
J. Petrovski	Influence of Soil-Structure Interaction Effects on Dynamic Response of Large Panel Prefabricated Buildings	1269

OFFSHORE MICROZONATION SESSION

I. M. Idriss L. S. Cluff A. S. Patwardhan	Microzonation of Offshore Areas - An Overview . . .	1281
A. S. Patwardhan	Factors Influencing Seismic Exposure Evaluation for Offshore Areas	1291
R. G. Bea M. R. Akky	Seismic Exposure and Reliability Considerations in Offshore Platform Design	1307

J. A. Fischer C. T. Spiker	Preliminary Microzonation of the Baltimore Canyon Lease Area	1329
L. A. Selzer R. T. Eguchi T. K. Hasselman	Seismic Risk Evaluation of Southern California Coastal Region	1341
J. R. Benjamin F. A. Webster C. Kircher	The Uncertainty in Seismic Loading and Response Criteria	1369
D. Nair J. B. Weidler R. A. Hayes	Inelastic Seismic Design Considerations for Offshore Platforms	1383
H. Kappler G. I. Schuëller	The Influence of Microzonation on the Reliability- Based Design of Offshore Structures	1399
B. J. Watt R. C. Byrd	Aseismic Design Considerations for Concrete Gravity Platforms	1409
Y. Moriwaki E. H. Doyle	Site Effects on Microzonation in Offshore Areas . .	1433
H. J. Swanger D. M. Boore	Importance of Surface Waves in Strong Ground Motion in the Period Range of 1 to 10 Seconds	1447
J. Kallaby W. W. Mitchell	Guidelines for Design of Offshore Structures for Earthquake Environment	1459

URBAN PLANNING, SOCIO-ECONOMICS AND GOVERNMENT RESPONSIBILITY SESSION

R. A. Olson	The Policy and Administrative Implications of Seismic Microzonation: Toward Logic or Confusion	1475
M. Abolafia A. L. Kafka	Toward a Measure of Socio-Seismicity	1489
E. Kuribayashi T. Tazaki	An Evaluation Study on the Distribution of Property Losses Caused by Earthquakes	1499
H. C. Cochrane	Potential for Inflated Building Costs after Disaster	1511
R. Themptander	Earthquake and Insurance	1525
D. R. Nichols R. A. Matthews	The U.S. Geological Survey's Role in Geologic- Related Hazards Warning	1531

Index of Authors

STATE OF THE ART SESSION

INTENTIONALLY BLANK

SEISMICITY AND GLOBAL TECTONICS AS A FRAMEWORK FOR MICROZONATION

by

Carl Kisslinger^I

ABSTRACT

Improved seismographs, widely deployed, combined with good computational facilities and better methods for treating complex velocity structure, have led to more nearly complete detection and more accurate location of earthquakes. Seismic zones, especially at active oceanic plate margins are clearly defined. Seismicity along plate boundaries within continents is more diffuse and the boundaries are not clearly delineated. Tectogenesis in plate interiors is a major, unresolved problem. Regional seismograph networks are contributing important detailed information concerning concentrations of activity, including delineation of linear trends where faults are not readily mappable.

Accurate hypocenter locations have led to the development of the seismic gap concept. The identification of gaps with high potential for a large earthquake is an important contribution to hazards assessment. The determination of the stress levels along seismic belts, especially within gaps, can help in the evaluation of the seismogenic potential of a particular place. New techniques based on interpretation of the spectral properties of the seismic signals offer a feasible approach to stress determination. Changes in temporal and spatial patterns of seismic activity may be useful as precursors of impending large earthquakes.

INTRODUCTION

The past decade has been remarkably productive in the increase of knowledge of what an earthquake is, where earthquakes occur, why they occur where they do, and, perhaps equally important, the definition of unresolved problems of global seismicity and tectonics that will require our best research efforts for their solution. However, the gap between improved knowledge of the general, world-wide distribution of earthquakes in time and space and the estimation of the seismic hazard during some specified time interval at a particular site remains great. This conference is devoted to the latter subject. I shall try in this paper to evaluate some contributions which progress in global scale research provide to an improved framework within which microzonation can be accomplished.

I assume a general familiarity with the broad pattern of global seismicity: the existence of well-defined belts of high seismic activity, the existence of diffuse and poorly defined zones of intracontinental

I Professor of Geological Sciences and Director, Cooperative Institute for Research in Environmental Sciences, University of Colorado, Boulder, Colorado.

earthquakes, and the nature of long-time average earthquake recurrence as a function of magnitude. I also assume basic familiarity with the tenets of plate tectonics theory, on which current attempts to explain seismicity are based.

IMPROVED ACCURACY OF HYPOCENTER LOCATIONS

Knowledge of where earthquakes occur is fundamental to the problem of estimating seismic hazards. Significant improvement in definition of the details of the geographic distribution of earthquakes has been achieved during the past two decades as a result of the wide deployment of better instruments, the availability of facilities for processing large amounts of high quality data and research leading to practical techniques for handling the effects of complicated earth structure on travel-times.

Much of the improvement in world-wide coverage resulted from the installation of the World-Wide Network of Standardized Seismographs (WWNSS) by the United States in the early 1960's, and comparable standardized networks within a few large countries, especially Canada and the Soviet Union. There has been little support for major improvements in WWNSS until very recently. A program of upgrading selected stations of WWNSS, by changing some sites, borehole installation of some seismometers and the addition of digital recording, is now being carried out with funding from the Defense Advanced Research Projects Agency.

The most significant improvements in both detection capability and location accuracy has come from the installation of relatively dense regional networks in a few selected places of special interest for seismological research. The support for these networks has come mostly from the Earthquake Hazards Reduction Program of the U.S. Geological Survey. Portions of the following important seismic areas in the United States are now covered by such networks: Alaska and the Aleutian Islands, the State of Washington, central and southern California, Utah, the New Madrid seismic zone, New York State, and the Charleston, S.C. area. A network in the Caribbean is monitoring parts of that seismic region under the U.S.G.S. program.

The claimed improvement in location accuracy refers principally to relative locations of events with reference to other nearby events. Various methods for correcting for the effects of complex structure in the source region have been developed. Nevertheless, systematic biases in locations of sets of events may still be present in the solution, so that the absolute locations, referred to a geographical reference, may still be in error by substantial amounts.

Detection thresholds and location accuracy depend strongly on the position of the event relative to the distribution of seismograph stations. At present, even in the worst case, it is likely that any event bigger than m_b 5 will be detected at enough stations to permit a location to be calculated and the event will appear in some catalogue, even if not in the comprehensive summaries of the National Earthquake Information Service and the International Seismological Center. The threshold is much lower for routine monitoring

of events in places like Europe, Japan and North America, which are covered much more adequately than, say, the Indian Ocean. Regional networks, which are often installed for specific research purposes for a limited time, push the limit for nearby earthquakes down to very small events, the cut-off depending on local noise conditions. Typical uncertainties in good teleseismic locations are given as 10 km or less in geographical position and somewhat greater in depth. Systematic bias may cause errors in even these good locations of 25 km or more. Events within good regional networks can be located with uncertainties less than 2 km if good velocity information is available.

Large numbers of reliably located events define the active seismic zones of the world in considerable detail. In many places, especially at active margins of oceanic plates, narrow bands of epicenters can be associated with major geological or topographic features, marking the zones of divergent, convergent or transcurrent plate motions. Convergent plate boundaries within continents are often not well defined by either the distribution of epicenters, which may be diffuse, or geologically. Tectonic relations that appear to be simple under the oceans, or that can be unravelled as a combination of simple elements, may be almost undecipherable within continents.

Tectogenesis, including earthquakes, within plate interiors is not understood and remains one of the challenges to students of large scale tectonic processes. Earthquake activity at passive continental margins, such as the east coast of North America, and in continental interiors, such as the seismic zones of the midcontinent of the United States, has not been explained in terms of a unifying theory. Those who attempt rational, quantitative hazard assessment know the difficulties that arise from our inability to associate intraplate earthquakes with distinct structural systems or individual structures. It appears likely that intraplate earthquakes are manifestations of a variety of processes, and even the definition of "intraplate earthquake" is fuzzy. The earthquakes in the interior of China, for example, seem to be related to continental-scale tectonics in a different way than those near New Madrid, Missouri.

Regional networks contribute important information about the details of the hypocentral distributions within broader seismic zones. The resulting detailed patterns are useful both for associating the earthquakes with regional geological structures and processes and for detecting changes in patterns of occurrence that may be premonitory of future large events. The data are especially valuable where the faults are not easily mapped. An excellent example is the result for the New Madrid region obtained by Stauder et al. (1976). Although some features of the distribution began to emerge from observations with a small network in the 1960's, it was not until the 16 station network was available that fine detail, Figure 1, showing linear active zones presumably corresponding to faults, could be seen. Results for the central Aleutian Islands (Engdahl, 1977; Engdahl and Scholz, 1977), Figure 2, further illustrate the importance of carefully controlled locations in clarifying the details of regional tectonics. A double seismic zone within the descending lithospheric slab is interpreted by Engdahl and Scholz as due to stresses caused by the unbending of the plate at depth.

The redetermination of the locations of old earthquakes can be important for hazard assessment. Old instrumental data can be reworked using better velocity information, but the fundamental limitations of sparse data of questionable quality (especially timing) cannot be easily overcome. An example is the work of Gawthrop (1978) on the M7.3 Lompoc, California earthquake of November 4, 1927. His conclusions, based on a recalculation of the epicenter from P-wave arrivals at 80 stations and all of the macroseismic and geological data he could find, is that the earthquake occurred much closer to the coastline than Byerly's original solution and is probably associated with an active fault just off-shore. Events for which only macroseismic, descriptive information in historical documents is available are even more problematic, though workers in countries such as China and Japan have extracted a great deal of information from such records and have produced seismicity maps on this basis. A systematic program of relocation of old U.S. earthquakes, incorporating research on the techniques to derive the maximum amount of reliable information from whatever data are available, is to be encouraged.

SEISMIC GAPS

As our ability to locate earthquakes with better accuracy has increased, the details of the distribution of events have become more meaningful. Only when we are confident that the epicenters on our maps are close to the correct positions, can we proceed to assign significance to observations of currently active and long-inactive segments of seismic belts. Thus, the notion of a seismic gap has emerged as a useful indicator of the possible site on a plate boundary of a great earthquake within the relatively near future. We so far restrict the application of the gap concept to plate boundaries because we think we are justified in expecting continuity of relative motion of adjacent material along these features. When a portion of an otherwise continuous belt of earthquakes has been quiet for a long time, we are led to ask if strain is accumulating at that place, preparatory to a great earthquake, or whether the relative motion of the adjoining plates is either locally accommodated by aseismic movements or interfered with by some other process.

The significance of the seismic gap as a means of predicting the location and magnitude of future large events was first recognized and successfully applied by Fedotov, for the Kuril Islands - Kamchatka seismic zone (Fedotov, 1965; Fedotov, et al., 1970). Mogi contributed important ideas concerning the migration of large earthquakes along seismic belts (e.g., Mogi, 1968). Kelleher and Sykes, in a series of papers (Kelleher, 1970; Kelleher et al., 1973; Sykes, 1971) suggested criteria for identifying a gap and roughly estimating its seismogenic potential and proceeded to map plate-boundary segments that they thought met these criteria. An excellent review of the history of the gap concept and a systematic description of some current gaps is provided by McCann, et al. (1978).

The validity of the gap concept depends on the observation that sections of plate boundaries break as units at the time of great earthquakes and the sources of adjacent earthquakes abut each other without much overlap. The

evidence for this behavior is primarily the distribution of the aftershocks of the big earthquakes. The data for Alaska and the Aleutian Islands, Figure 3, (Engdahl, personal communication) illustrates the point. Because we depend on the aftershock locations to define the source dimensions of the strong earthquakes, the accuracy of these locations becomes important in determining whether or not a gap exists. Especially for older earthquakes, for which magnitude 4-5 aftershocks may be mislocated by 50 km or more, caution in deciding whether a gap exists is required.

Because the identification of a gap depends on recognition of a prolonged interval without a large earthquake, we are faced with the question of the expected variability of activity within an active region. Departures from average rates of occurrence, either intervals with few events or with many, are expected in a randomly distributed time series. Only if the data base is sufficiently long to permit the determination of the statistics of the series with reasonable confidence can decisions be made as to whether intervals with few or large numbers of events are significant departures from expected behavior (cf, e.g., Garza and Lomnitz, 1978). For much of the world, the length of the period of observation is very short for description of a geological process. Where historical records covering a number of centuries are available, clustering of activity is seen, e.g., Figure 4 for north China (Qiu Qun, 1976). For this intracontinental setting, observations covering only 100 years or so could give a very misleading impression of the long-time average rate of big earthquakes.

Gaps are defined in terms of large events, with source dimensions that fill the gap. The relation of smaller earthquakes that may occur frequently even within a gap to the occasional big one is not understood. For example, within the portion of the Aleutian arc covered by our regional network, there is a place that was the site of a M7.1 event in 1971, with a few moderate sized aftershocks (La Forge, 1977). This place has not been the location of any event large enough to be located from teleseismic data (greater than body-wave magnitude 4) since that time. Nevertheless, the distribution of smaller events, located with the data from the regional network, shows no break at this place. Is this a gap within which strain is accumulating for another large event? The whole region lies within the long segment broken by the great 1957, M8.2 earthquake (Figure 3) and it seems early to expect another very strong event. But the data suggest that there are shorter gaps related to fairly strong earthquakes within the large gaps.

Plate tectonics provides a rationale for estimating the recurrence time for great earthquakes on plate boundaries. Rikitake (1974, 1975, 1976) has estimated recurrence times for selected subduction zones on the assumption that great earthquakes occur when some critical strain value is exceeded, that they relieve all of the accumulated strain and that strain accumulates at a constant rate determined by the velocity of the relative motion of the plates at the boundary. Of course, we do not know that plate motions are continuous with a constant velocity, even though the velocities appear to be quite constant when averaged over millions of years. Uncertainties in the critical strain value and the rate of strain accumulation appear in the

result of Rikitake's analysis as uncertainties in the recurrence time. These, in turn, can be restated as the probability at any time since the last great earthquake that another one as large will occur. One then has to make a judgment as to how large this probability must be before a significant enhancement of the local seismic hazard is announced. As an example, Rikitake (1975) concludes that the probability of recurrence in the region of the 1923 Kanto earthquake will not reach 0.8 until about 2020 A.D. For the most active subduction zones around the Pacific, Rikitake (1976) derives a range of recurrence intervals from 27 ± 9 years for the Aleutian-Alaska zone to 170 ± 69 years for the Nankai-Tokai region, off southern Honshu.

Estimates of recurrence times based on relative plate motions assume that all or most of the relative motion eventually appears as slip during great earthquakes. Some appreciable part of this motion may take place as aseismic creep in parts of the seismic zone. The evaluation of the earthquake generating potential of a gap in which no great earthquake has occurred in history depends critically on whether normal plate boundary motions are interfered with (Kelleher and McCann, 1977) or creep is in progress. Although creep is measured along major faults within continents, no good way of estimating creep in ocean-covered subduction zones has been worked out. The exception to this is the estimation of slow post-seismic displacements on an active fault from time-dependent level changes on adjacent land areas, but this is a separate problem. If creep can occur over very long times along limited portions of a subduction zone, the mechanical properties of the materials in this segment must be different from those in the adjacent, seismic sectors. We are then led to ask if the mechanical properties themselves are time-dependent, so that a creeping segment may "lock" eventually, or a seismogenic part go into a creeping mode for a long time.

One direct approach to the evaluation of the earthquake potential or state of readiness of a gap is available in principle through measurements of local stress as a function of time. If stress is increasing, so is strain, and a place at which the stress is high must be considered as a possible earthquake site. Direct measurements of stress in the crust are few and none have been made at the depths at which most hypocenters occur. We do have indirect methods of estimating stress, from the properties of the waves generated by the earthquakes. Conventional focal mechanism solutions yield the orientation of the principal stress axes, subject to assumptions about the relation between the orientation of the present stress field and pre-existing fault surfaces on which the earthquakes occur. Determination of the magnitudes of the stress components is more difficult, but we can get some estimates from the spectra of the earthquake signals. A typical spectrum is shown schematically in Figure 5 (Brune, 1970). It is characterized by a low-frequency level, a corner frequency, and a high-frequency fall-off of f^{-2} for f^{-3} . The corner frequency is inversely proportional to the length of the slip zone and is roughly the frequency at which the wavelength is the same as the fault dimensions. The low-frequency level is proportional to the seismic moment and, thus, depends on the area over which slip occurs and the average amount of slip that takes place. By application of theoretical models of the source, these geometrical para-

meters can be interpreted in terms of the change in shear stress that occurs across the fault during the earthquake. The change in shear stress is not necessarily equal to the total shear stress acting before the event, though it is probably close to it for very large earthquakes. An earthquake with a large magnitude can be generated by a low average stress drop across a large area of slip or a high stress drop on a smaller area. Observations of the spectral characteristics of moderate background earthquakes within a seismic zone can give an idea of the size of the shear stress in the zone.

One practical approach to applying this principle is to compare the surface-wave and body-wave magnitudes of an earthquake. The surface-wave magnitude is measured by wave amplitudes at frequencies near 0.05 Hz; body-wave magnitude at around 1 Hz. For many earthquakes (fault lengths between roughly 5 to 50 km) the corner frequency falls between these two values. As illustrated in Figure 5, if two earthquakes have the same surface wave magnitude (same signal amplitude at 0.05 Hz), but the radius of the slip area for one is half that for the other, the stress drop, from the source theory of Brune (1970) for the geometrically smaller event is about 8 times that of the other and the body wave magnitude about 0.6 greater. This illustrates in a simplified way that the difference between M_s and m_b is a function of the stress drop during the earthquake and can be used to determine the stress drop once a fault geometry, depth and theoretical source model have been adopted.

C. Archambeau (1978) has used his relaxation source theory to calculate theoretical curves of M_s vs. m_b for a variety of kinds of faulting, over a range of crustal depths. An example of one set of his theoretical curves is shown in Figure 6. He has used such curves to derive stress drops for a large number of earthquakes and presents the results as contour maps of stress. A closed contour of high stress marks a place with a high potential for a strong earthquake. One such place is offshore of the Alaskan peninsula, at about 160°W longitude, a location previously and independently identified as a gap by Kelleher *et al.* (1973). Another high stress area is close to the source of a M7.5 earthquake off the coast of northeast Honshu on June 12, 1978, Figure 7. This map is for events 33-40 km deep. The earthquake was at about 40 km. The epicenter map, Figure 8, was compiled by the Japan Meteorological Agency for the period 599-1975. The June 12 earthquake occurred close to the mapped positions of events in 1936 and 1937, on the southern edge of an area that has not experienced a large earthquake for over 60 years. A similar impression is gained from the map of seismic energy release for 1926-1974, Figure 9, also prepared by JMA. The numbers plotted are the \log_{10} of the energy released at each point, calculated from a standard empirical equation relating magnitude and energy. 23 corresponds to M7.5, 22 to M6.8, 20 to M5.5, etc. The aftershock regions of the larger earthquakes are outlined. The JMA and NEIS locations for the June 12 earthquake disagree somewhat, but it occurred either at the mapped position of the 1933 M7.3 event or an event in 1937 of about the same size. Of course, the locations of these old earthquakes are even less certain than those of recent events.

Thus, the June 12 event occurred in a place that was a gap, with no strong earthquake for at least 40 years, and a region of high shear stress.

A considerable gap still exists to the north of this place and it will be interesting to see if a sequence of M7.5 events, similar to the 1938 sequence to the south, or a single larger event occurs in this gap.

SEISMICITY PATTERNS AS EARTHQUAKE PRECURSORS

Seismicity information is the foundation of conventional analysis of expected locations and frequencies of occurrence of future earthquakes, in some long-term average sense. Recent research shows, in addition, that characteristic patterns of occurrence of small and moderate earthquakes may be valid indicators of the approach of a large event. Of course, the preceding discussion of gaps focussed on the idea that the prolonged absence of a large event at a place known to be active in the past is an indication that strain energy to be released in the next big earthquake is accumulating. However, the determination that a large event is imminent, with an estimate of the time of occurrence, is a problem in earthquake prediction. Although a review of prediction is outside of the scope of this paper, some comments on the ways in which seismicity patterns seem to foreshadow large earthquakes in some cases are in order. Typical of the research on pre-shock seismicity is that reported by Sekiya (1977), Ishida and Kanamori (1977), Wyss, *et al.* (1978), Caputo, *et al.* (1978), and our group working on Aleutian Islands' earthquakes (Price, *et al.*, 1978).

All of these studies have revealed the occurrence of a surge, or swarm of activity in the neighborhood (distances allowed by different investigators are highly variable) of the epicenter of the future major event, at a relatively long time, several months to years, beforehand. Foreshocks in the conventional sense, i.e., events near the main event preceding it by a few minutes to a few weeks, may also occur, but these precursory swarms are a distinct phenomenon. In all cases the pre-shock surge is limited in time duration and spatial extent. Some investigators have noted an alignment or migration of preshocks. A period of very low activity follows the swarm in some cases, but not all.

The problem of precursory swarms is made up of several parts: the identification of a group of earthquakes as a swarm, the decision that the swarm is precursor to a larger event, and the determination of the time of occurrence of the main shock. The first part of the problem is the only one for which useful approaches have been developed so far. A swarm can be defined on the basis of a number of events in excess of some measure of the normal rate of occurrence, during some limited interval of time, confined within a small area. Keilis-Borok and Wyss have set up formal rules for defining a group of earthquakes to be a swarm.

Figure 10 shows pre-shock data associated with a M6.5 event near Adak Island, November 4, 1977. The number of events during each month since the local network was placed in operation that occurred within 5 km and 10 km of the main shock is plotted, along with the running mean values for these same distances. Only once did the number of events within 5 km exceed the 24 month mean by more than two standard deviations, during mid-November 1976 to mid-January 1977. A period of quiescence occurred from November 1975 to May 1976. We consider this to be a precursory swarm associated with

the November 4 event. In this case the activity remained at a fairly high level after the swarm.

The same information is shown in another format in Figure 11, a time-distance plot out to 10 km from the main shock epicenter. We see in this figure that the activity began to build up some 5 to 6 km away from the epicenter and then migrated toward it to form the November-to-January swarm.

We have not yet identified any properties of these swarm earthquakes that distinguish them from all of the other small events in this seismic zone. In general, no one has suggested a technique for identifying a swarm as a precursor. Various characteristics of the individual events, such as orientation of the focal mechanisms and spectral properties are being examined in the search for some unique, discriminatory features. Without a reliable means of separating precursory swarms from other swarms, false alarms will occur.

Although retrospective studies suggest a regular relation between the length of time between the swarm and the main shock and the magnitude of the main shock (Sekiya, 1977), we have no approach to projecting the time to the main shocks, or equivalently the expected magnitude, at the time the swarm occurs. This is a critical question for prediction. It seems that some kinds of independent information, for example, the size of the region in which large strains have accumulated, will be required for a solution.

Foreshocks in the usual sense, i.e., events clustered close to the main shock hypocenter and occurring shortly before, are an important aid to short-term prediction where they occur. Jones and Molnar (1976) found by analysis of the NOAA hypocenter file that 44 percent of large shallow earthquakes, magnitude 7 or greater, between 1950 and 1973 had foreshocks strong enough to be recorded teleseismically. They defined a foreshock as an event within 100 km and 40 days of the main event. We are again faced with identifying foreshocks as such as they occur. In some cases (e.g., Engdahl and Kisslinger, 1977), the foreshocks have distinct focal mechanisms.

SUMMARY AND CONCLUSIONS

Modern observational facilities enable us to acquire very detailed information about the distribution of earthquakes, as well as some of their important physical properties. The delineation of active structures can be done more accurately than in the past with the use of local networks, a capability that is especially important in places where faults are not readily recognized or easily accessible to direct observation. With epicentral distributions known well, we can investigate and assign significance to particular patterns and features, especially seismic gaps. The gap concept is useful in identifying possible sites for large earthquakes in the near future, but each gap must be evaluated in terms of basic tectonics to determine whether it is seismogenic. The distribution of stress in the crust is a key factor in the assessment of the likelihood of occurrence of earthquakes, not only in gaps, but in any seismic zone. We presently have poor knowledge of this parameter. Finally, temporal and spatial patterns of background seismicity seem to be useful as precursors of future large earthquakes.

ACKNOWLEDGMENT

The research in the central Aleutian Islands is supported by the U.S. Geological Survey under Contract 14-08-0001-16716. M. Wyss critically reviewed the manuscript and offered several valuable suggestions.

BIBLIOGRAPHY

- Archambeau, C.B., 1978, Estimation of Non-Hydrostatic Stress in the Earth by Seismic Methods: Lithospheric Stress Levels along Pacific and Nazca Plate Subduction Zones, in Proceedings of Conference V: Defining Seismic Gaps and Soon-to-Break Gaps, ed. J.F. Evernden, U.S. Geological Survey open file report, in press.
- Brune, J., 1970, Tectonic Stress and the Spectra of Seismic Shear Waves from Earthquakes, J. Geophys. Res., 75:4997-5010.
- Caputo, M., V. Keilis-Borok, P. Gasperini, L. Marcelli and I. Rotwain, 1978, Earthquake Swarms as Forerunners of Strong Earthquakes in Italy (abstract), EOS, Trans. Amer. Geophys. Union, 59:330.
- Engdahl, E.R., 1977, Seismicity of Plate Subduction in the Central Aleutians, in Island Arc, Deep Sea Trenches and Back-Arc Basins, ed. M. Talwani and W.C. Pitman III, Washington, D.C., Amer. Geophys. Union, 259-271.
- Engdahl, E.R. and C. Kisslinger, 1977, Seismological Precursors to a Magnitude 5 Earthquake in the Central Aleutian Islands, J. Physics Earth, 25, Suppl., S243-S250.
- Engdahl, E.R. and C. Scholz, 1977, A Double Benioff Zone beneath the Central Aleutian: An Unbending of the Lithosphere, Geophys. Res. Lett., 4: 473-476.
- Fedotov, S.A., 1965, On Regularities in Distribution of Strong Earthquakes of Kamchatka, Kurile Islands and Northeastern Japan, Tr. Inst. Phys. Zemli Akad. Nauk S.S.S.R., 36 (203):66-93.
- Fedotov, S.A., N.A. Dolbilkina, V.N. Morozov, V.I. Myachkin, V.B. Preobrazhensky and G.A. Sobolev, 1970, Investigation on Earthquake Prediction in Kamchatka, Tectonophysics, 9:249-258.
- Garza, T. and C. Lomnitz, 1978, The Oaxaca Gap: A Case History, in Proceedings of Conference V: Defining Seismic Gaps and Soon-to-Break Gaps, ed. J. F. Evernden, U.S. Geological Survey open file report, in press.
- Gawthrop, W., 1978, The 1927 Lompoc, California, Earthquake, Bull. Seism. Soc. Amer., in press.
- Ishida, M. and H. Kanamori, 1977, The Spatio-Temporal Variation of Seismicity before the 1971 San Fernando Earthquake, California, Geophys. Res. Lett., 4:345.
- Jones, L. and P. Molnar, 1976, Frequency of foreshocks, Nature, 262:677-679.
- Kelleher, J., 1970, Space-Time Seismicity of the Alaska-Aleutian Seismic Zone, J. Geophys. Res., 75:5745-5756.

- Kelleher, J. and W. McCann, 1977, Bathymetric Highs and Development of Convergent Plate Boundaries, in Island Arcs, Deep Sea Trenches and Back-Arc Basins, ed. M. Talwani and W. C. Pitman III, Washington D.C., Amer. Geophys. Union., pp. 115-122.
- Kelleher, J., L. Sykes and J. Oliver, 1973, Possible Criteria for Predicting Earthquake Motions and Their Application to Major Plate Boundaries of the Pacific and the Caribbean, J. Geophys. Res., 78:2547-2585.
- LaForge, R., 1977, Tectonic Implications of Seismicity in the Adak Canyon Region, Central Aleutians, unpublished M.S. thesis, University of Colorado.
- McCann, W., S. Nishenko, L. R. Sykes and J. Krause, 1978, Seismic Gaps and Plate Tectonics, in Proceedings of Conference V: Defining Seismic Gaps and Soon-to-Break Gaps, ed. J. F. Evernden, U.S. Geological Survey open file report, in press.
- Mogi, K., 1968, Sequential Occurrence of Recent Great Earthquakes, J. Phys. Earth, 16:30-36.
- Price, S. J., C. Kisslinger and E. R. Engdahl, 1978, Microearthquake Activity Precursory to the Magnitude 6.5 Adak Earthquake of November 4, 1977 (abstract), EOS, Trans. Amer. Geophys. Union, 59:330.
- Qiu Qun, 1976, On the Background and Seismic Activity of the M = 7.8 Tangshan Earthquake, Hopei Province of July 28, 1976, Acta Geophysica Sinica, 19.
- Rikitake, T., 1974, Probability of Earthquake Occurrence as Estimated from Crustal Strain, Tectonophysics, 23:299-312.
- Rikitake, T., 1975, Statistics of Ultimate Strain of the Earth's Crust and Probability of Earthquake Occurrence, Tectonophysics, 26:1-21.
- Rikitake, T., 1976, Recurrence of Great Earthquakes and Subduction Zones, Tectonophysics, 35:335-362.
- Sekiya, H., 1977, Anomalous Seismic Activity and Earthquake Prediction, J. Phys. Earth, 25:S85-S93.
- Stauder, W., M. Kramer, G. Fischer, S. Schaefer and S. T. Morrisey, 1976, Seismic Characteristics of Southeast Missouri as Indicated by a Regional Telemetered Microearthquake Array, Bull. Seism. Soc. Amer., 66:1953-1964.
- Sykes, L., 1971, Aftershock Zones of Great Earthquakes, Seismicity Gaps and Earthquake Prediction for Alaska and the Aleutians, J. Geophys. Res., 76:8021-8041.
- Wyss, M., R. E. Habermann and A. C. Johnston, 1978, Long Term Precursory Seismicity Fluctuations, in Proceedings of Conference V: Defining Seismic Gaps and Soon-to-Break Gaps, ed. J. F. Evernden, U.S. Geological Survey open file report, in press.

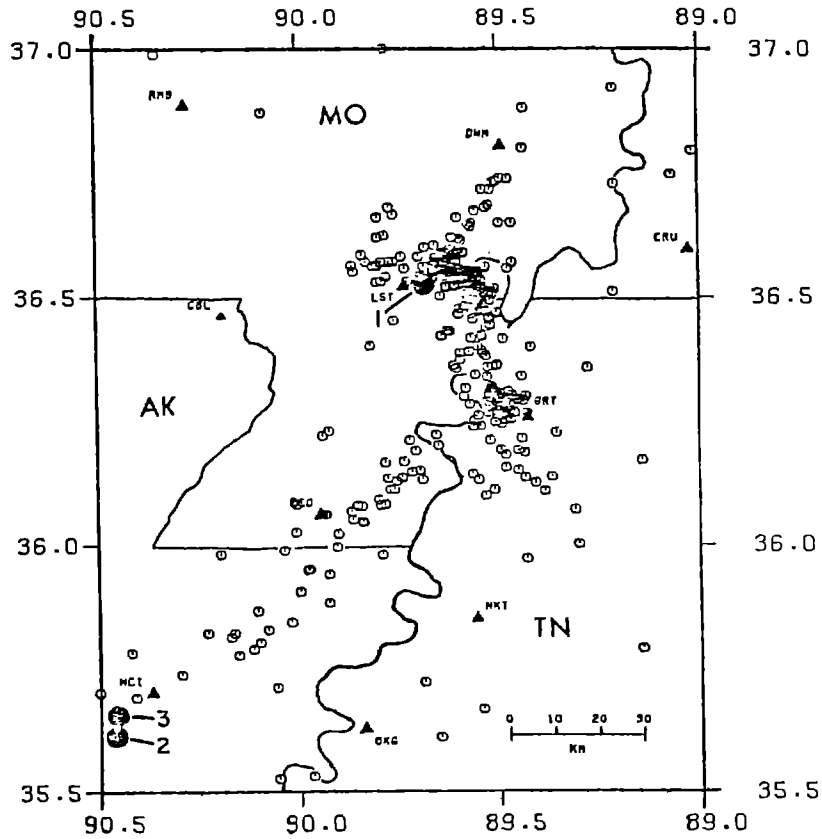


Figure 1. Epicenters of all earthquakes located in the St. Louis University network in region around New Madrid, Mo., during 1 July 1974-31 March 1976 (from Stauder, *et al.*, 1976).

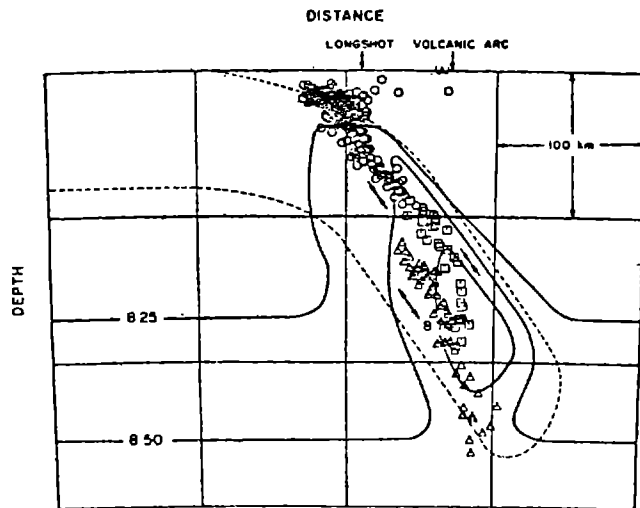


Figure 2. Vertical section perpendicular to central Aleutian arc, showing the double-layered Benioff zone. The arrows indicate down-dip compression or tensions (from Engdahl and Scholz, 1977).

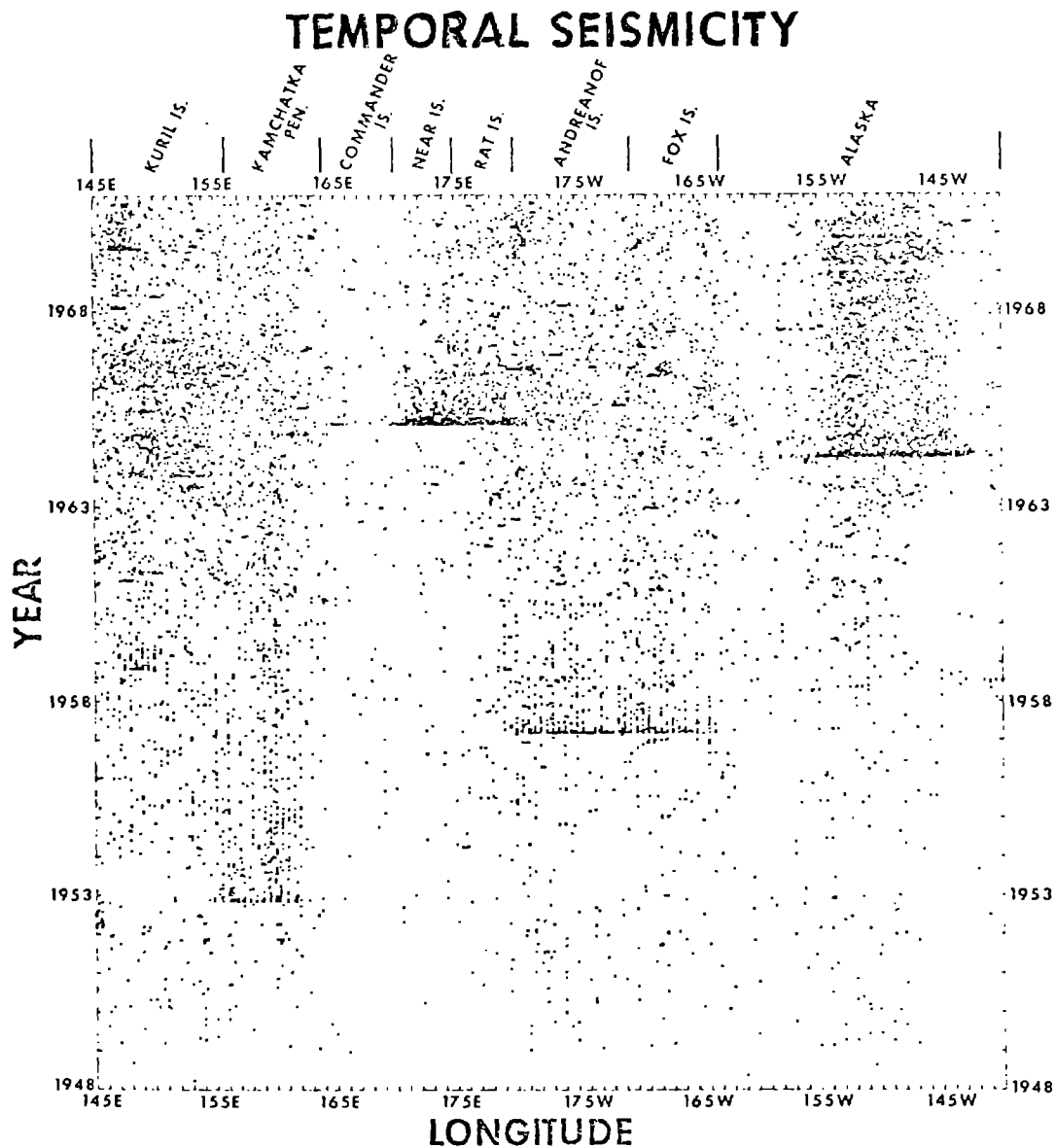


Figure 3. Time-space diagram of Alaska-Aleutian seismicity, 1948-1971. Each point is one earthquake. Elongated rows are aftershock sequences of the great earthquakes. (From Engdahl, 1971, private communication.)

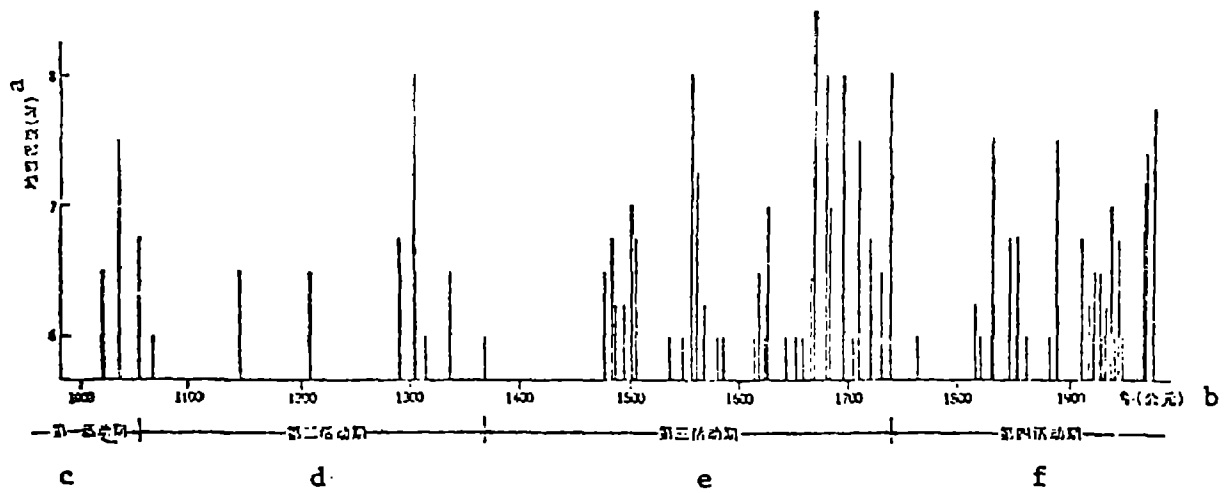


Figure 4. Plot of magnitude vs time for earthquakes in Northern China.

- Legends: a -- Earthquake magnitude (M)
 b -- Time (year A.D.)
 c -- First active period
 d -- Second active period
 e -- Third active period
 f -- Fourth active period

(From Qiu Qun, 1976, translation by W.H.K. Lee, 1977.)

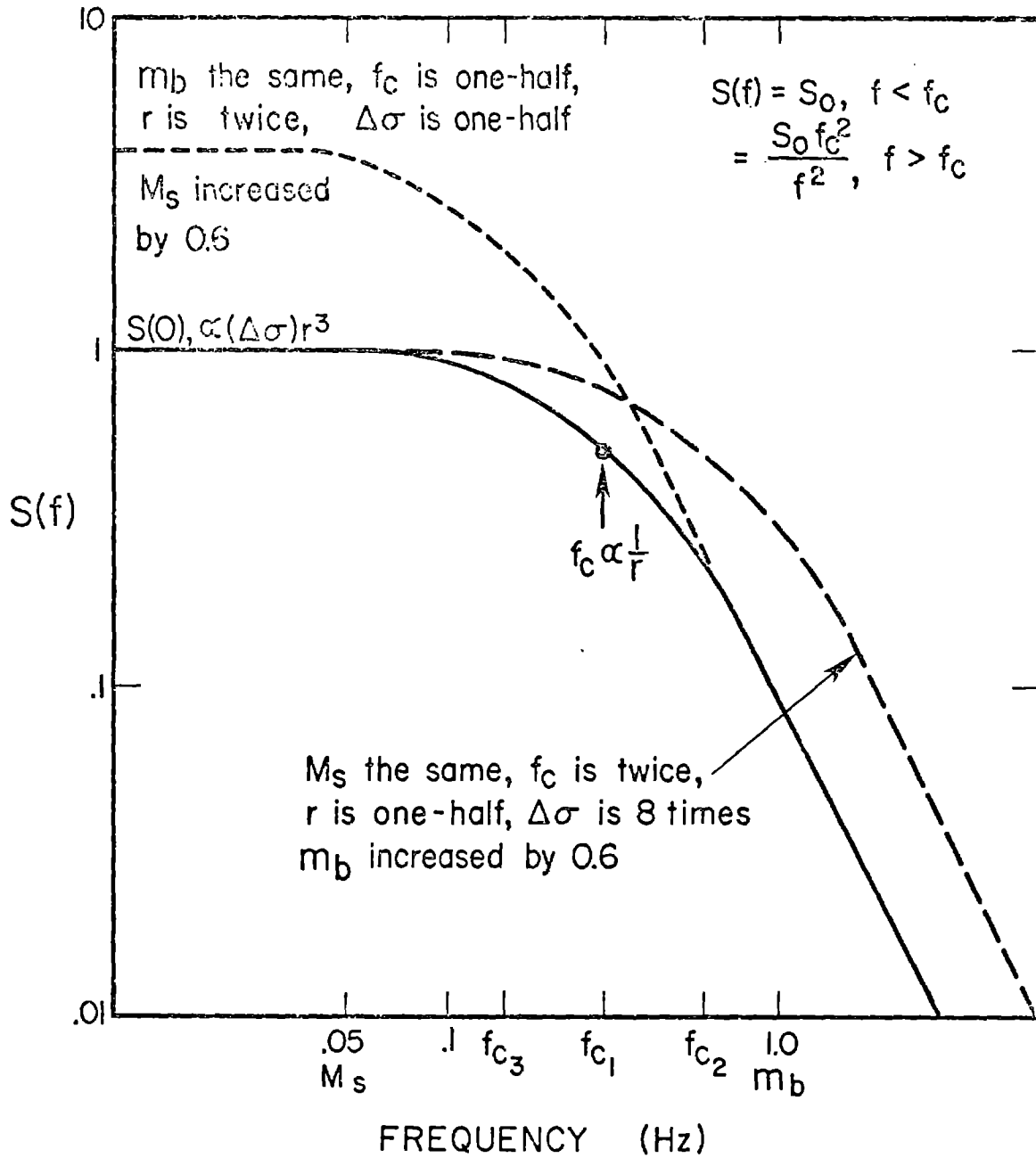


Figure 5. Schematic seismic spectrum, illustrating relations between source dimensions, stress drop and magnitudes.

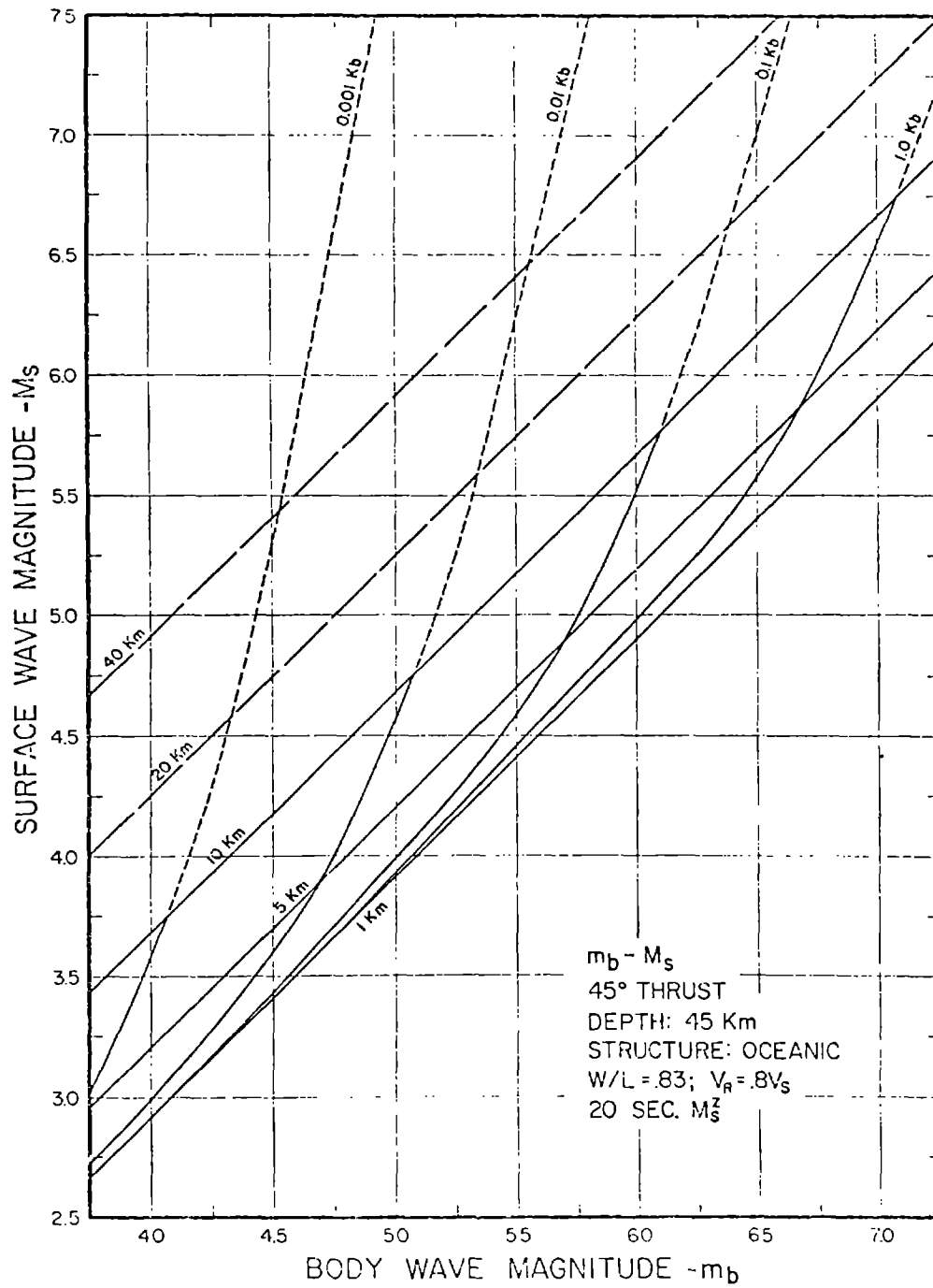


Figure 6. Typical theoretical M_s vs. m_b curves, with fault length and stress drop as parameters (Archaubeau, 1978).

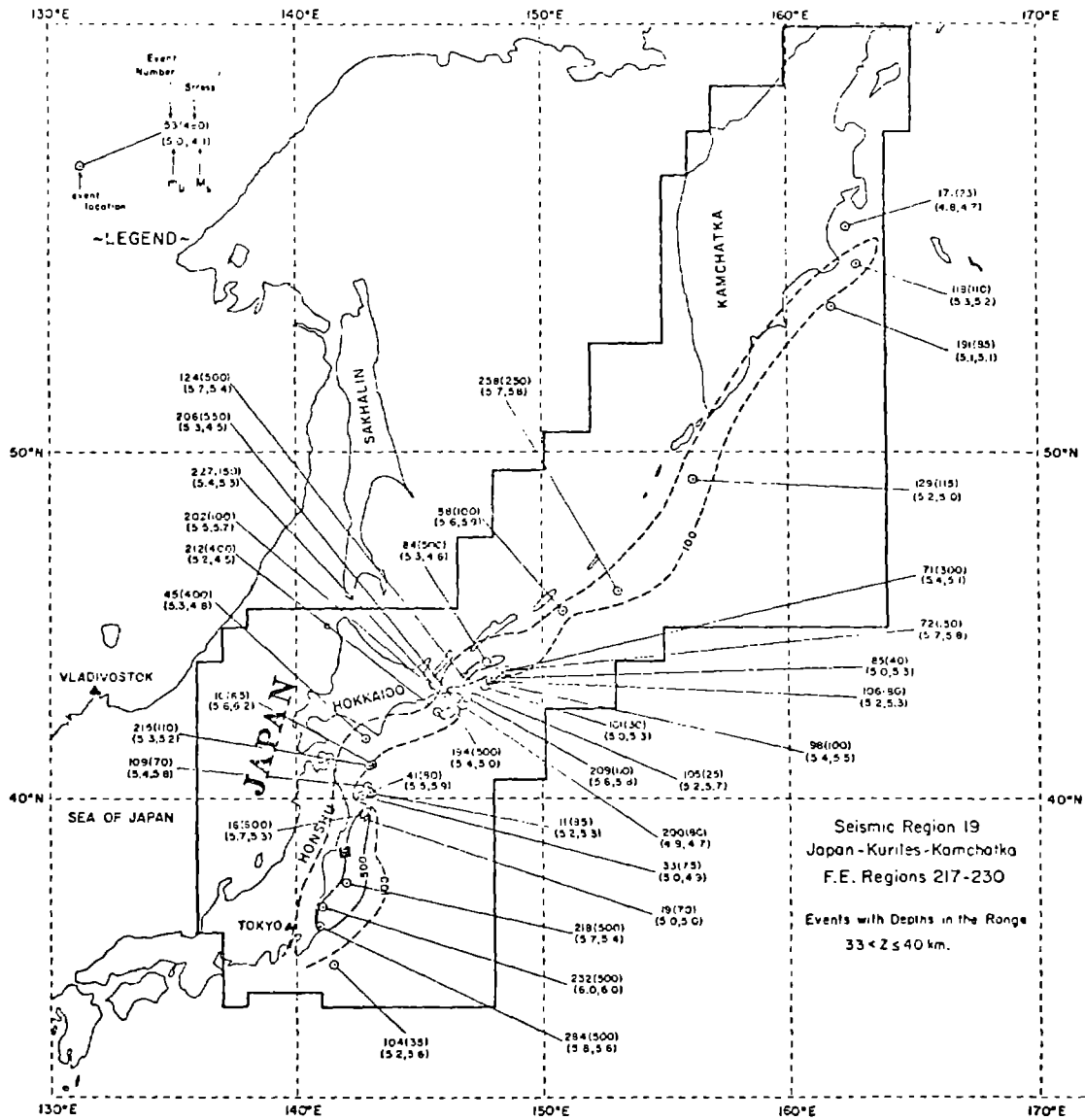


Figure 7. Stress map for Japan-Kurile Islands-Kamchatka seismic zone, based on $M_s - m_b$ data. The black square near 38°N , 142°E is the location of the June 12, 1978 earthquake.

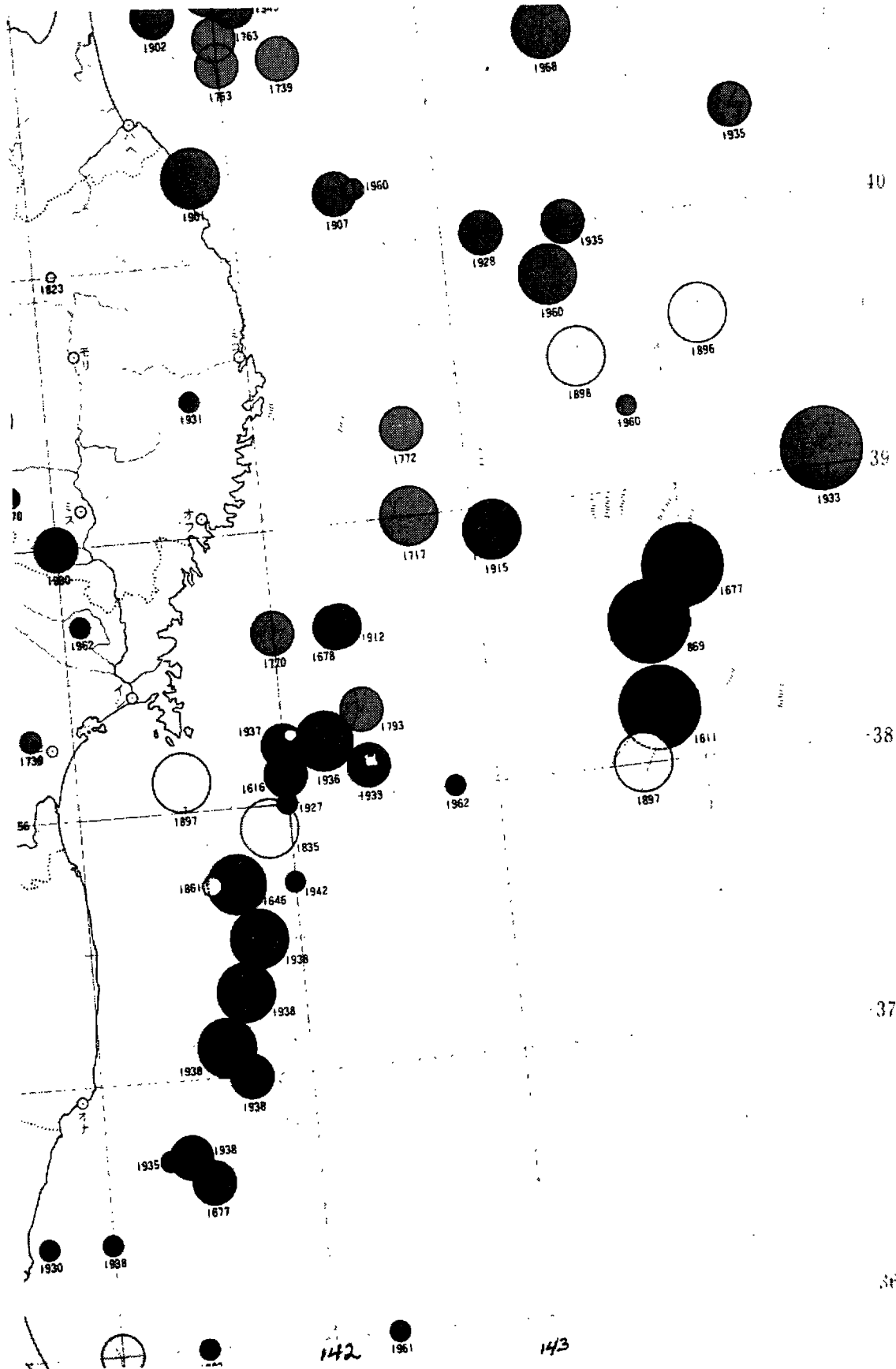


Figure 8. Large earthquakes in vicinity of northeastern Honshu, 599-1975. White dot near 38°N, 142°E is the NEIS epicenter of the June 12, 1978 earthquake. The white square is the location computed by the Japan Meteorological Agency. Prepared by Japan Meteorological Agency.

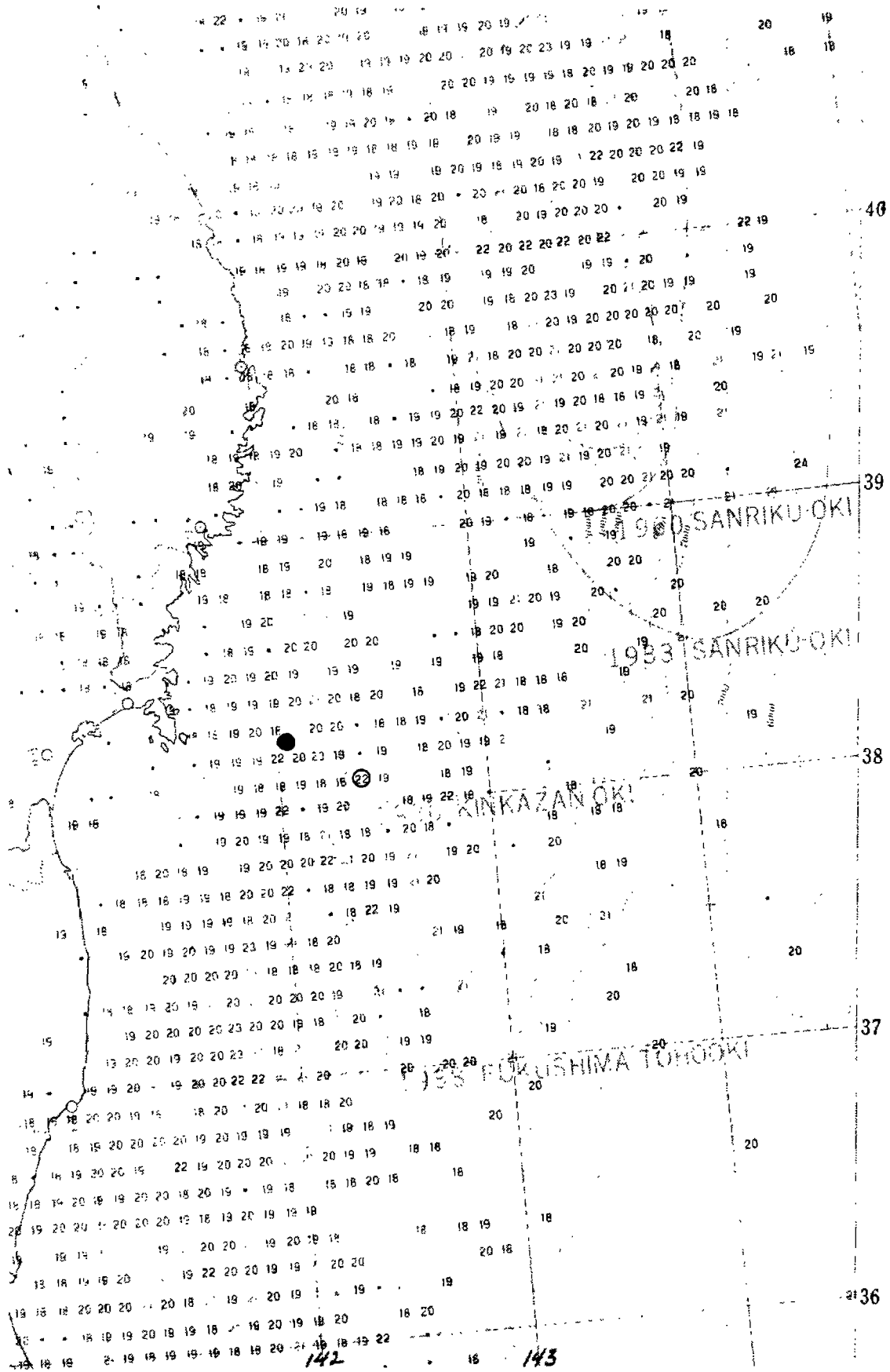


Figure 9. Cumulative seismic energy release in vicinity of northeastern Honshu, 1926-1974. Black dot near 38°N , 142°E is the NEIS location of the June 12, 1978 earthquake. The open circle is the location computed by the Japan Meteorological Agency, the same as the epicenter of a M7.3 event in 1933. Prepared by Japan Meteorological Agency.

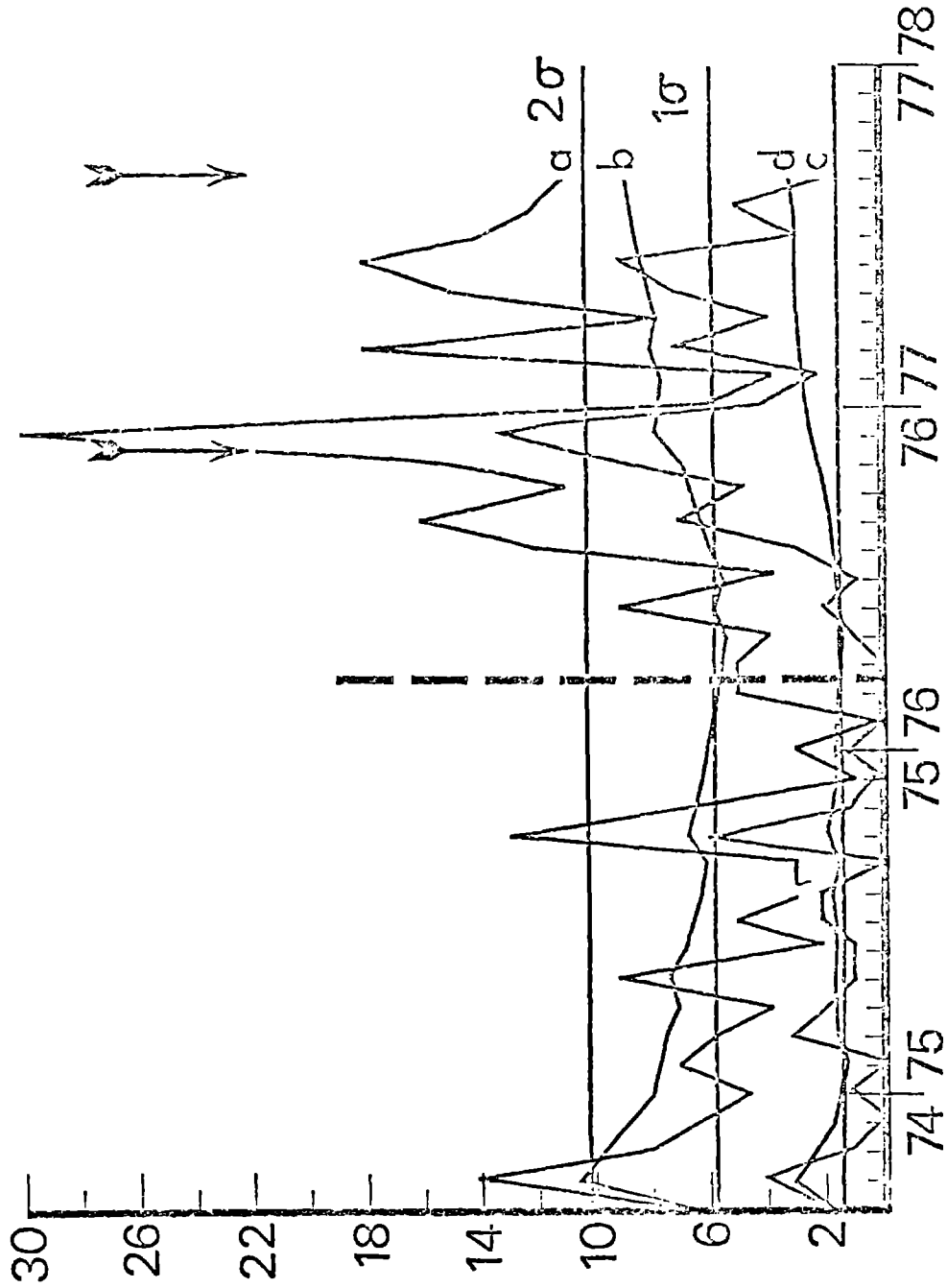


Figure 10. Seismic activity as a function of time in the vicinity of a M6.5 earthquake near Adak Island, November 4, 1977. The number of earthquakes per month within 10 km (curve a) and 5 km (curve c) of the main event are plotted, as well as the running mean number per month, curves b and c. The one- and two-standard deviation levels for the 5 km mean after 24 months are also shown.

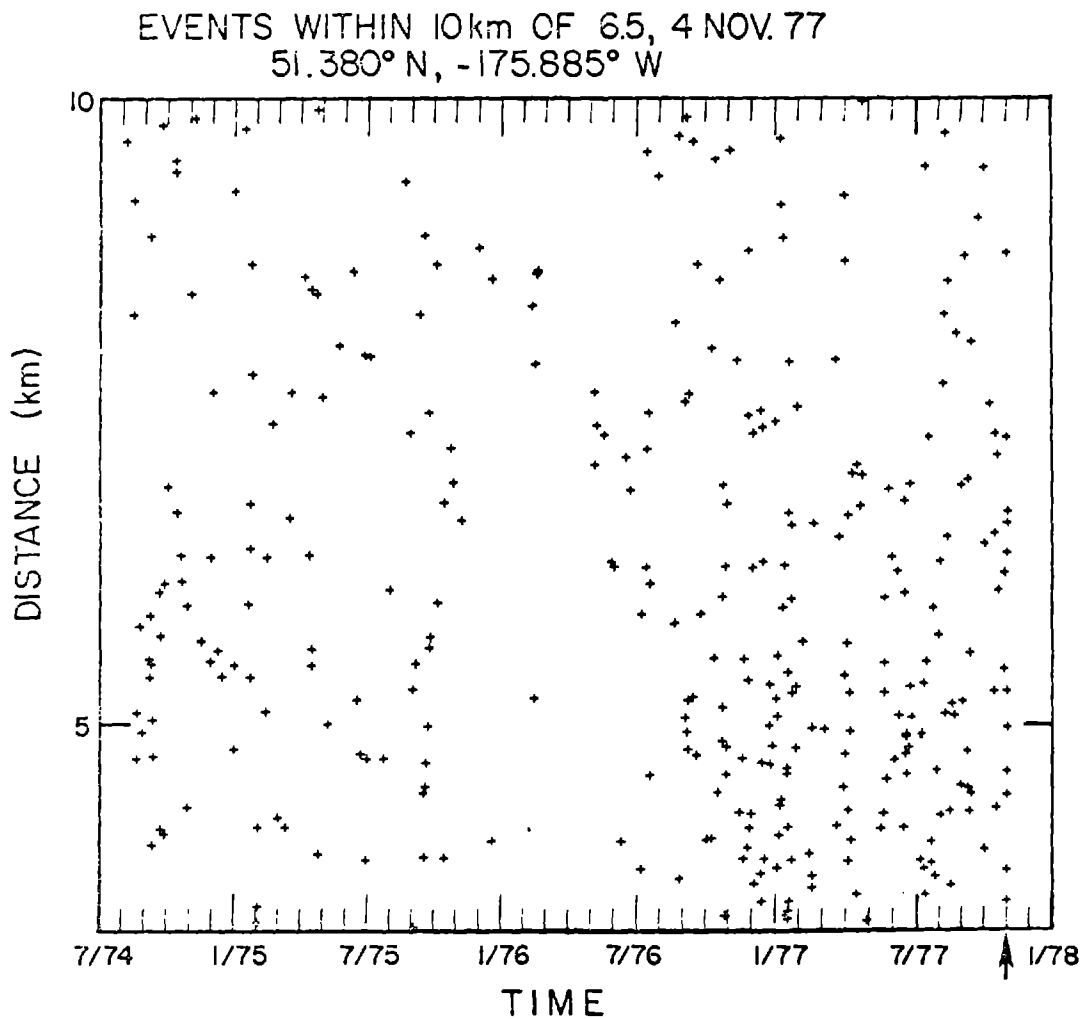


Figure 11. Time-distance plot to 10 km for November 4, 1977 Adak earthquake. The distance coordinate is plotted on a squared-scale to preserve the areal density of the events. The absence of events in March-April 1976 is due to network outage.

INTENTIONALLY BLANK

STRONG-MOTION SEISMOLOGY

By

P. C. Jennings^I and D. V. Helmberger^{II}

ABSTRACT

The paper presents a summary of the status of strong-motion instrumental networks and records in the United States followed by a discussion of some recent results in strong-motion seismology that are believed to be of interest to the conference. The results selected for presentation are the seismological modeling of seismic sources using strong-motion records, with application to the Borrego Mountain earthquake of 1968, the Brawley earthquake of 1976, and the San Fernando earthquake of 1971; the relation between the spectral descriptions of strong motion used in engineering and seismology; and the use of strong-motion instruments to determine Local Magnitude, M_L .

^IProfessor of Civil Engineering and Applied Mechanics, California Institute of Technology.

^{II}Associate Professor of Geophysics, California Institute of Technology.

INTRODUCTION

In preparing this paper it was necessary to select a few topics for emphasis rather than attempt to cover the entire field. The subject has grown over the years until it would take a sizeable volume to present accurately the state-of-the-art, even with a narrow definition of strong-motion seismology that includes only the measurement and interpretation of strong ground-motion during earthquakes, and excludes the measured response of structures. Consequently, we have selected a few topics with which we are familiar and which we believe to be appropriate to the interests of this conference. The reader is referred to the literature for subjects not addressed here, such as details of the instrumentation (7, 18) and techniques for the processing of strong-motion data (20, 32), as well as details of some of the observed and calculated effects of local conditions upon the ground motion which are the subject of other papers in these volumes.

INSTRUMENTS AND NETWORKS

Strong-Motion Instruments

The basic strong-motion instrument is the accelerograph which, in its most common form, generates a film record of three mutually perpendicular components of acceleration: vertical and two horizontal. Samples of accelerograms are shown in Figures 1 and 2. The instruments also record an internally generated time signal and reference traces. The sensitivity is commonly $\pm 1g$, and the instrument is self-triggering. The basic transducer typically has a natural frequency near 25 hz and damping is of the order of 60 percent of critical. These are nominal properties of common instruments such as shown in Figure 3, and the reader is referred to the literature (e.g., 7) for properties of specific accelerographs. Although the basic instrument is the three-component accelerograph, there are a number of important variations that are becoming increasingly important in strong-motion seismology. One such instrument is the central recording accelerograph, which allows up to 12 channels of data to be recorded on a single, 7-inch film strip. This instrument is particularly useful for installation in structures and in arrays, where the small size of the transducers, which are separate from the recording mechanism, is an advantage. Another important development is the digital-recording accelerograph which has obvious advantages for data processing. Some instruments of this type have been installed in the field, but not enough experience has been accumulated so far to place them in a category of reliability comparable to the film-recording systems. Another modification, of particular interest to seismology, is the addition of a timing signal. The internal timing mechanism in the instrument is supplemented by a WWVB receiver and associated electronics which results in a digitally encoded time signal on the edge of the accelerogram.

The power for the accelerometers is usually provided by batteries, which are kept at peak charge by means of slow-acting chargers connected to standard electrical outlets. Under favorable circumstances, the

accelerograph will require maintenance at intervals of 6 months or longer. Under less favorable conditions more frequent maintenance is required. About 90 to 95 percent of the accelerographs in a network can be expected to function properly with proper service. Discharged batteries and problems with the film transport system are the most common causes of difficulty.

Another important strong-motion recorder is the seismoscope (19), illustrated in Figure 4. This instrument is basically a spherical pendulum which scratches its displacement record on a smoked watch glass, as seen in Figure 5. The natural period is commonly 0.75 second and the damping is nominally 10 percent of critical. The instrument and its properties are such that the maximum displacement can be converted to a point on the displacement response spectrum of the ground motion. Although it provides less information than the accelerograph, the seismoscope has proven to be extremely reliable and in the Guatemalan earthquake of 1976, for example, provided the only significant strong-motion record. In addition to direct reading of the instrument, there have been instances when it has been possible to estimate the history of ground acceleration from the seismoscope response, using a higher mode response of the transducer as a timing signal (30).

Other strong-motion instruments include such special purpose devices as peak-recording accelerographs for nuclear powerplants, Carder "displacement" meters, elevator shut-off mechanisms, and shut-off mechanisms (jiggle valves) for gas lines.

Status of Instrumental Networks

The principal agency involved in the deployment and maintenance of strong-motion instruments, and in the processing of the records obtained, is the Seismic Engineering Branch of the U. S. Geological Survey. This agency installs and maintains its own instruments and performs similar services for instruments owned by other organizations. The operating funds for the Seismic Engineering Branch are provided by the National Science Foundation under a 5-year agreement, scheduled to be renewed. Other sizeable networks are operated by the California State Division of Mines and Geology, and by the City of Los Angeles. There are additional, smaller networks operated by university research groups, utilities and other organizations. Foreign accelerograph networks exist in several countries including Japan, Mexico, Yugoslavia, Iran, Italy, New Zealand, Peoples Republic of China, and Soviet Russia among others.

At the present time (26), the Seismic Engineering Branch is maintaining the following instruments under its basic program:

- 184 USGS accelerographs
- 59 accelerographs owned by other agencies
 - 1 14-channel digital system
 - 3 analog systems
- 20 accelerographs in foreign countries (chiefly South and Central America), and
- 1 12-channel analog system, in a foreign country.

An even larger number of accelerometers are owned by other agencies, (e.g., Corps of Engineers, U. S. Bureau of Reclamation) but are maintained by the Seismic Engineering Branch on a contract basis. This instrumentation includes:

- 301 accelerographs
 - 7 installations, with a total of 72 channels of digitally-recorded data
 - 4 installations, with a total of 38 channels of analog-recorded data.

These figures give a total of 580 installations, with approximately 1864 channels of data. The instruments are distributed throughout the United States, with concentrations in more seismic regions.

The Seismic Engineering Branch also owns and services approximately 150 seismoscopes and maintains 25 peak recording accelerographs owned by other agencies. A few Carder displacement meters are also owned and serviced by the Branch.

The program of the California Division of Mines and Geology was established in 1972 and is operated by the Office of Strong-Motion Studies. The status of their installations, as of June 30, 1978, is summarized below (33):

<u>Installation Type</u>	<u>Number</u>	<u>Data Channels</u>
Surface free-field	247	741
Down-hole free-field	2	18
Buildings	35	374
Dams	16	176
Bridges	3	58
TOTALS	303	1,367

The free-field phase of the California program is approximately 50 percent completed now, and emphasis in this phase has been shifted from general distribution throughout the state toward the installation of special-purpose free-field instrumentation, including linear and down-hole arrays.

The major emphasis of the installation effort has recently been shifted to instrumentation of structures, including bridges, buildings, dams and port facilities. The instrumentation of structures is about 10 percent complete.

The plans for the near future include instrumenting approximately 20 structures and 10 free-field sites per year, and the development of a capability for record processing and dissemination.

The City of Los Angeles maintains a network of strong-motion instruments that have been installed in tall buildings in accordance with the City Building Code. At the end of August last year there were 158 buildings instrumented in this program, with a total of 486 three-channel

accelerographs (29). The City of Los Angeles is maintaining 143 of these buildings, while the others were maintained by other groups, including 10 serviced by the Seismic Engineering Branch.

The remaining networks of strong-motion instruments are smaller and are generally devoted to special purposes of individual groups, such as the measurement of the response of dams, the measurement of soil-structure interaction, or as complementary instrumentation for seismological research. An exception to this is the recently-funded array being installed by the University of Southern California. When completed this will comprise a grid of about 90 accelerographs in the Los Angeles Basin.

The need for increased coverage by strong-motion instrumentation is recognized by all seismically active countries, and there are plans underway for an international project to install detailed arrays at selected locations in the world (22).

STRONG-MOTION DATA

Status of Strong-Motion Records

The Seismic Engineering Branch has the primary responsibility for processing, storing and disseminating strong-motion records. They do this not only for the instruments they maintain, but also for the California Division of Mines and Geology, the City of Los Angeles and for nearly all of the smaller, special purpose networks. They also try to obtain copies of important records obtained in foreign countries.

As of June 1978, the Seismic Engineering Branch had in its archives approximately 2800 records recorded from 750 separate events (4). With a few exceptions, each record contains three components of ground acceleration. Of these 2800 records about 800 are from upper stories of buildings, crests of dams, etc., leaving about 2000 records of basement or free-field motion. Approximately 100 of the 2800 records are from foreign stations. As might be expected, most of these records are of small motions and of the 2000 ground-level accelerograms only 250 are classified as being significant on the basis of having a peak acceleration of 10 percent g or more, or of being of special interest. On the same basis, some 200 of the 800 records of structural response are classified as significant.

This gives a total of about 450 significant records, with about half coming from the San Fernando earthquake. Of these 450 records, 420 have been digitized and processed and are on computer tape at the Seismic Engineering Branch in Menlo Park, the National Information Service for Earthquake Engineering (NISEE) at Berkeley and at the Environmental Data Service (EDS-NOAA) at Boulder. Copies of accelerograms can be obtained from these agencies. There is also a large file of accelerograms at the California Institute of Technology, where many of the records were digitized and processed.

In addition, there is a significant data base obtained from strong-motion recordings of aftershocks of the Oroville earthquake (9). In a period of 3 months, 313 records from 86 events were obtained from 15 stations. Of these 120 records from 14 events have been digitized. The aftershocks include records with amplitudes up to 70 percent g, although most are much smaller.

The Seismic Engineering Branch also analyzes significant seismoscope records and archives the originals. Over 140 useable seismoscope records were obtained from the San Fernando earthquake, and a detailed report of the results has been prepared (3).

Additions to the strong-motion data, and developments in the networks are published in the program reports of the Seismic Engineering Branch (e.g., 28).

Assessment of Strong-Motion Data from the Engineering Viewpoint

The strong-motion data is fundamental to earthquake engineering. Along with the experience obtained from structural performance during earthquakes, it is the determining factor in setting the seismic design provisions of building codes and the earthquake design criteria for major engineering projects. The records of ground motion and response are also primary factors in assessing the seismic hazard of cities, in improving design practices through understanding of structural response, and in virtually all phases of earthquake engineering research.

The strong-motion data collected since the first accelerogram was obtained in the Long Beach earthquake of 1933 have greatly increased our understanding of the potential effects of strong shaking, frequency content and duration of strong ground motion. We also have some appreciation of how these quantities are related to measures of the size of the earthquake and to the geometrical relations between source and site. There are experimental data indicating the way that strong ground motion can be affected by soil-structure interaction, by very soft soil deposits, by topography and by the presence of surface waves. We are also in a position to make meaningful estimates of some of the inherent variations that exist in strong ground shaking.

Although the general picture is encouraging, there are some very important questions for which the data are insufficient. In addition, almost none of the points described above are understood in sufficient detail, even given that complete understanding should not be expected or required for applications in earthquake engineering practice. There are two very important gaps in the data from the engineering viewpoint. First, there is a paucity of records in the near field (e.g., $\Delta < 20$ km) of major, potentially damaging earthquakes. This lack of information introduces great difficulties, and occasionally controversy, into setting the earthquake-resistant design criteria for major projects. The second major gap is the lack of strong motion records from a great (e.g., $M_S > 8$) earthquake. These earthquakes have, of course, the largest potential for disaster and knowledge of the amplitude, duration and areal extent of strong shaking is required to deal with the hazard posed

by these extreme events. It should be pointed out also that there are parallel gaps in our knowledge of the response of structures to ground motions in these two categories.

There are major deficiencies in the data needed to clarify our understanding of the effects of source mechanisms, travel paths and local conditions upon strong ground motion. This is perhaps most apparent when relations between measures of the strength of ground motion (e.g., peak acceleration, peak velocity, spectral intensity) and measures of distance (e.g., epicentral distance, hypocentral distance, distance to the center of the aftershock zone) and earthquake size (e.g., local magnitude, M_L , surface-wave magnitude, M_S) are investigated. Figures 6 and 7 are plots of peak acceleration and velocity, respectively, for different magnitude classes. The figures illustrate the variability in the data and suggest the difficulty in establishing simple relations among these variables. The unsatisfactory state of present affairs is indicated by the fact that in a recent report (21), 26 different studies were identified in which relations between peak acceleration, magnitude and distance have been advanced. Clearly there is not yet a consensus on this subject. An additional feature requiring experimental clarification and verification is the effects of different source mechanisms on the strong motion. For example, theoretical studies indicate, and some data support, the concept that thrust-type earthquakes produce significantly stronger near field shaking than strike-slip events.

Similarly, there is no clear professional consensus on the details of how local site conditions can affect strong ground motion. Although there is general agreement on the qualitative nature of such effects, there is a divergence of judgements on the degree of the effects as seen in the data, the role of surface waves, and the degree to which engineering solutions can be reliably obtained from analyses of simplified models of the phenomenon. More strong-motion data clearly is required to further the understanding of the potential effect of local conditions on the ground motions, and several of the strong-motion arrays now being installed are designed to yield some of this data.

Additional strong-motion data are also needed to clarify the role of soil-structure interaction in modifying the earthquake motion transmitted to the structure. The interaction problems include the effects of the compliance of the foundation, the effects of embedment, and the effects of foundations with large areas in suppressing motions of high frequency. Some instrumental arrays now installed will provide records bearing on these problems, but improvement is needed. For example, the effects of large foundations on high frequency motion appear to be quantitatively similar to effects soft soils are thought to have on these motions. In the very common case of a record obtained in the base of a sizeable building founded on fairly soft alluvium, it may not be possible to separate the two effects without additional instrumentation.

Finally, it should be stated that the strong-motion data base is insufficient to determine the variability in strong ground motion under specified circumstances. The problem arises, for example, when the level

of the mean plus one standard deviation is sought for the expected response spectra at a site of a nuclear power plant. Different investigations of the existing data and different approaches to the assessment of the variability can lead to significantly different results, with large economic implications for the project.

MODELING EARTHQUAKES WITH DISLOCATION THEORY

One of the most interesting uses of strong-motion data has been in seismology, where the records are used to help deduce properties of the source mechanism. Some applications of this type are reviewed in this section.

The basic problem we address is the inference of the spatial and temporal distribution of faulting at depth based on a set of observed motions at the surface, where the motions can be severely distorted by the intervening earth structure. In other words, we wish to explain observed motions in terms of the source excitation after separating out those complexities associated with propagation through a heterogeneous earth. To achieve this goal we characterize earthquakes in a way that is closely related to the driving tectonic stresses by assuming a distributed shear dislocation as the fault description, an approach amenable to analysis. Then, we characterize the properties of the earth that affect the propagation in a way that can be predicted by geophysical means. The simplest model one can devise that still contains some features of reality is that of a layered earth where the layering can be assumed to be locally flat and parallel to the surface. In what follows, we will apply recently developed synthetic modeling techniques to the interpretation of the faulting characteristics for two relatively simple events, the Borrego Mountain earthquake of 1968, and the Brawley event of 1976, and a complex event, the San Fernando earthquake of 1971.

Earthquakes as Seismic Sources

The seismic radiation field produced by earthquakes can be represented by several means. Following the stress relaxation approach, one assumes the initial stress and frictional conditions and performs the proper dynamics using analytical or numerical techniques to obtain the displacements. Another particularly useful approach is due to Haskell (10), called the shear-dislocation model. Schematic diagrams of this type of model are displayed in Figure 8, where one does not attempt to understand the detailed mechanics involved in the actual fault zone but simply states that slip occurs on a specified surface, referred to as a dislocation. This information is all that is necessary to propagate the field to a more distant point assuming elastic conditions. In many situations the faulting reaches the earth surface yielding the average slip (D_0) and the fault dimension (r). The ratio (D_0/r) multiplied by the rigidity (μ) leads to an estimate of stress-drop or the amount of stress released by the faulting process, (5), although the actual slip along the fault is probably highly variable. Another more precise measure of some of these fault parameters can be obtained by synthesizing the observations obtained on a worldwide basis, for example see Figure 9. The coherency

between neighboring stations such as the three east coast stations (WES, OGD, SCP) is remarkable and is a common feature of most earthquakes. Note that the faulting had a strike-slip orientation along a line 69° west of north, similar to the strike slip of Figure 8a, with the northeastern side moving south relative to the southwestern side. This dislocation results in a positive first motion or compression in the eastern and western quadrants and negative first motion or dilatation in the northern and southern quadrants. (Engineers: Compare with Mohr's circle for pure shear.) Seismologists have used such polarization plots for many years to determine the orientation of faulting to aid in the interpretation of tectonic processes and in the understanding of surface breakage. Following the waveform analysis (6) for this event indicates that the faulting started at a depth of about 9 km and developed into an average dislocation of 2.5 meters on a faulting surface of about 150 km^2 . Modeling these long period waveforms tells us about the strength, orientation, depth, and overall duration, but does not tell us about the details of rupture, that is, its direction and velocity. These quantities can only be determined by strong motion seismology or by modeling the local field. However, to accomplish this we must model or account for propagational distortions caused by local crustal structure.

Point Dislocations in Layered Models

The basic technique used in constructing synthetic strong motion displacement records is to assume that an arbitrary distribution of dislocations representing a fault can be modeled by a summation of a large number of point shear dislocations distributed properly in space and time. The actual number of points required is related directly to the wavelength of interest. Next, one computes the Green's function which represents the response of the local structural model, usually assumed to be a layered halfspace, to a point shear dislocation with a delta function slip. An example calculation using the generalized ray method (14), is displayed in Figure 10. In general, the delta function response is somewhat difficult to handle numerically and we use the temporal integral of the Green's function, called the step response. As seen in Figure 10, the difference in response between the halfspace and the layer over the halfspace is especially noticeable for the shallow source. The classical type of Love wave dispersion becomes well developed when the layer contains the source and is well understood in terms of the interference of rays. Comparing the responses with the source situated just above and below the layer boundary, see $d = 3.5$ and $d = 4.5$, one finds similar long period behavior as expected from physical considerations.

To produce a theoretical displacement for a given slip history, $s(t)$, requires a convolution integration of $s(t)$ with the derivative of the step response. Some example calculations for a layer over a halfspace are given in Figure 11 where the difference in radiation pattern becomes especially apparent. This is because of the quadrupole nature of the earthquake source and because any site will, in general, receive phases departing from several sectors of the focal sphere. In the dip-slip case, the vertical radiation pattern is such that rays leaving the source horizontally are weak compared to those leaving vertically and thus the

multi reflected pulses are relatively strong. The reverse is true for the strike-slip case. Finally, since the development of the surface wave-train involves a critical reflection effect, it is not surprising that its development depends on Δ as well as source depth. With this brief introduction of how to handle point source excitations, it becomes possible to model the ground motion resulting from realistic faulting motions, at least the longer periods, by superposition of these simple point source elements.

Modeling Strong Motions

We next show some example observations that can be largely explained by applying the above technique. The three data sets chosen for illustration are from the Borrego Mountain earthquake, Brawley earthquake, and the San Fernando earthquake.

Unfortunately, not many local recordings are available for the Borrego event because of its remote location. El Centro was the nearest site ($\Delta = 60$ km) where the event was recorded by Carder displacement meters and by a standard accelerograph. An example of the strongest component of motion is displayed in Figure 12 which shows the acceleration and processed velocity and displacement. Since the earthquake was essentially a strike-slip event, see Figure 8a, and the station is only 8° from the strike of the fault, we expected predominantly SH motion with small motions on the vertical and radial components, all of these features are well documented (12). The observed SH displacement is displayed on the top of Figure 13 with a highly idealized synthetic model on the bottom. Several models have been constructed to fit the first 40 sec of motion. A 2.9 km thick layer with shear velocity of 1.5 km/sec overlaying a halfspace with shear velocity of 3.3 km/sec gives a good overall fit to the Love wave portion of the record for a variety of distributed sources at depths ranging from 4 to 10 km. The source distribution in this example is particularly simple, that is, two point sources with slip histories chosen to be compatible with the teleseismic information. The interpretation is that massive faulting occurred at a depth of 9 km producing the powerful direct arrival followed by rupturing in the upward direction, thus producing the proper amount of Love waves. The detailed or fine scale properties of the faulting are still not resolved due to lack of near-field data. Some synthetic displacements displaying various plausible assumptions about the rupture parameters are given in Figure 14. In this exercise we assumed a rectangular fault with different epicentral locations, Δ_E , and allowed the elements to turn on in sequence, simulating a rupture velocity. The seismic moment was adjusted to obtain record strengths comparable to the data. Note that the horizontal rupture direction and slip history are particularly important with respect to the short period or high frequency information. Thus, the strong acceleration and velocity spike at the beginning of the record in Figure 12 could be caused either by a point source or by substantial faulting motion directed towards the station.

In the above efforts we adjusted the crustal model to fit the observations in a rather idealistic fashion, since the crustal structure is known to be complicated in this region. In our second example, the Brawley earthquake, we chose an event where the crustal structure is well

represented by a layered model as determined by geophysical means (2), and secondly, the event is small enough to be treated as a point source. Since this event occurred in the well instrumented Imperial Valley region we know its orientation and location accurately with the duration or slip history being the only unknown parameter (13). A plot of the observed tangential component obtained at the Imperial Valley College station is displayed in Figure 15 along with synthetics for various assumptions about duration. It appears that the 1.5 sec triangular slip history yields excellent results and furthermore, we would have predicted about this duration for a $M = 5$ event based on previous studies (15). However, we still were not able to determine the detailed rupture properties, but only an overall duration.

For our last example, we will consider the San Fernando earthquake, which is well enough recorded to actually determine the rupture parameters independently. The data set obtained from this event is huge (20) and has been discussed at length (8) showing the applicability of seismological techniques to the interpretation of strong motion records. He demonstrates the existence of surface waves and displays numerous examples of the coherency of signals from neighboring stations. The near-in stations show particularly large accelerations and have been discussed at length (27, 8, 31). The latter author obtained relatively good fits for the three components of motion obtained from the Pacoima Dam site. In fact, it is the data from this station that allows relatively tight bounds to be put on the rupture process.

We approached this data set following the same strategy used in the Borrego Mountain study, namely we will initially constrain the fault description to fit the teleseismic waveform data. Unfortunately, the waveforms produced by San Fernando, while being as coherent from station to station as those displayed in Figure 9, are quite complicated with rupturing occurring on two fault planes, starting at depth and propagating towards the surface (25). A rectangular model similar to the one proposed is displayed in Figure 16. We assumed a halfspace in modeling the nearest stations and computed the Green's functions on a .5 km spacing. After a diligent search (11), the slip distribution given by the contours explains many of the observed properties including the static offsets. Although it is necessary to present numerous observations and possible slip distributions to support this proposed model, the comparison between the synthetic displacements and data for PAC and LKH are the most indicative; that is, to produce the required change in amplitude between PAC and LKH requires very strong focusing to the south. This requires a relatively narrow fault at depth, probably less than 6 km wide, with about 2 meters of displacement. The rupture velocity is 2.8 km/sec for the bottom segment and 1.8 km/sec for the top section. Note that this model indicates rather small offsets beneath PAC and massive faulting towards the south, probably within a km of the surface. Because of the high apparent accelerations in the region just to north of the surface break and because of the large stress drop implied (approaching the breaking strength of rocks), this portion of the faulting surface is of special seismological interest.

It is seen from these examples that relatively simple models of the

source mechanism and of the travel path can be used to describe the observed low-frequency ground motion. Thus, the frequencies of ground motion that show most clearly in the displacement traces are believed to be determined by source mechanics and by geological layering. The frequency ranges that dominate the velocity and acceleration records, however, are not as yet modeled by this approach. To replicate motions at these frequencies would require more detailed models of the source mechanism and more detailed knowledge of the intervening geological structure. From a practical viewpoint this knowledge will probably not be available for typical sites, and the statistical models developed in earthquake engineering may be useful.

SPECTRAL DESCRIPTIONS OF STRONG GROUND MOTION

The concept of modeling strong-motion acceleration by a random process was first advanced by Housner (16). A significant body of work has been performed on the subject since that time and there are now available a variety of statistical models of strong ground motion. Some of these models are quite sophisticated and include consideration of such effects as temporal variations in amplitude and frequency content. The results of this work also include the construction of artificial accelerograms for use in design calculations, and computer programs for generating artificial accelerograms for Monte-Carlo studies of structural response. These stochastic approaches have been able to model many of the observed characteristics of strong ground shaking in the sense that sample accelerograms and derived velocities, displacements, response spectra, etc. show many features exhibited by actual ground motion. In addition to being directly useful, the statistical modeling of ground motion has furnished additional insight into the degree of complexity of strong ground motion, particularly at shorter periods. The approach is, however, essentially mathematical and while modeling what is observed, does not clarify the basic mechanics of the generation or propagation of strong ground motion.

It is interesting for the purpose of this paper, to try to relate the statistical concepts underlying the simpler models of strong ground motion to the spectral characterization of source mechanisms, as recently developed in seismology. Figure 17 shows schematically the average undamped response spectra of strong ground shaking found from examination of strong, potentially damaging accelerograms (17). The records considered are obtained from major earthquakes and have durations of strong-motion of about 20 seconds. If such accelerograms are modeled by comparably long segments of a statistically stationary random process, the following statement can be made: The average of the undamped velocity spectra is proportional to the average of the Fourier Spectra of the model accelerograms, and to the square root of the power spectral density of the underlying random process from which the accelerograms are generated. The curve in Figure 17 can therefore be interpreted as the observed, average Fourier spectra of accelerograms of major earthquakes. It is seen that the spectrum starts at low amplitude at small frequencies, rises fairly rapidly to a roughly level central portion and then falls away. There is insufficient data to determine the details of the shape, but it is consistent with the data to take the initial size as proportional

to ω^2 , the central portion as level and the decay for high frequencies as proportional to ω^{-1} . It should be pointed out that the spectral shape in the figure is for major earthquakes; if smaller earthquakes are considered, the spectral shape would change. In this case, the ascending part of the curve would be shifted to the right, decreasing the width of the central portion.

The spectral curve for acceleration can be transformed to one for displacement by using the relation that in the frequency domain, the spectrum of acceleration is ω^2 times that of displacement. The resulting displacement spectra is shown also in Figure 17. It is seen to begin horizontally, then decay as ω^{-2} . For still higher frequencies the decay is as ω^{-3} . This interpretation of strong-motion spectra is consistent with spectra of the source mechanism of major earthquakes, as interpreted by seismologists (1). For example, the amplitude of the horizontal part of the displacement spectrum is proportional to the seismic moment. Another important parameter is the corner frequency, the transition between the horizontal and ω^{-2} segments of the displacement spectrum. The decay rates ω^{-2} and ω^{-3} are also consistent with seismological interpretations of earthquake generation and propagation.

Figure 17 and the accompanying discussion are intended to show that seismological and engineering description of strong ground motion, although different in approach and detail, are consistent in their descriptions of the energy content of strong ground motion. This consistency, once appreciated, should aid the application of the results of source mechanism studies into engineering practice and some of the statistical models of strong ground motion developed by engineers may be used to augment seismological source mechanism models at high frequencies.

DETERMINATION OF LOCAL MAGNITUDE FROM STRONG-MOTION INSTRUMENTS

A recent development in strong-motion seismology is the use of strong-motion instruments to determine local magnitude, M_L , which is determined by the peak response of a Wood-Anderson torsion seismograph. The instrument is, in essence, a one-degree-of-freedom oscillator with a gain of 2800, a period of 0.8 sec and 80 percent critical damping. The magnitude of an earthquake has come to play a dominant role in earthquake engineering, and of the several magnitude scales in use, the local magnitude is the most directly related to most engineering applications because it is determined within a frequency band, and at distance most pertinent to the response of structures. The surface wave magnitude, M_S , is usually determined by waves of near 20 sec period recorded at distances of hundreds or thousands of kilometers, and is a better indicator of the extent of faulting and the duration of shaking. It is not, however, a good measure of the strength of the ground motion at much shorter periods.

The response characteristics of the strong-motion accelerometers and the Wood-Anderson seismograph are such that it is possible to use the recorded acceleration as an input to the equation of motion

of the seismograph. This process generates a synthetic seismogram which can then be read in the usual manner. This calculation has been performed for many of the more important accelerograms and the results are available in a recent paper (24). There are two major results of this study. The first is that the local magnitude, M_L , can be determined from very large earthquakes for which no standard measurement is possible. An example is the Kern County earthquake of 1952 which was found to have a local magnitude of $M_L = 7.2$, the largest reported so far. (The commonly used value of $M = 7.7$ was determined on the basis of body and surface waves recorded at large distances.) A second result of this research is that a large number of accelerograms are available from many recent earthquakes, particularly in southern California, and these can be used to determine reliable values of M_L by averaging.

It is clearly advantageous in the construction of attenuation relations and in other engineering applications to use a consistent magnitude scale, which this study allows. Another potential application occurs in the design of major projects in which the design earthquake is often specified by geologists and seismologists in terms of a shock of a given magnitude, occurring on a specified location on a fault. Under these conditions, if accelerograms can be selected which are representative of the design earthquake in terms of duration and frequency content, they can be scaled to give the predetermined magnitude. This can be done because the local magnitude indicated by an accelerogram depends only on the acceleration history and the ascribed distance. Thus, in some cases, it appears possible to avoid statistical relations between magnitude and strength of ground motion, and also to verify the appropriateness of design acceleration histories determined by other means. Additionally, it is possible to investigate the inherent variation in response spectra of ground motions giving the same magnitude at the same distance, and studies along these lines are in progress.

In a related study (23) not yet completed, the method has been extended to determine M_L from seismoscope records. The technique uses a basic result from the theory of random vibrations to extrapolate from the response of the seismoscope to that of the Wood-Anderson seismograph by making corrections for the different gains, periods and dampings of the two instruments. The accuracy of the extrapolation has been verified by application to data from the San Fernando and Parkfield earthquakes wherein both accelerograph and seismoscope records are available from the same sites. The accelerograph data from these sites was used to synthesize the Wood-Anderson response which was then compared to that estimated from the seismoscope records. The average magnitude determined by the approaches are very nearly equal, as are the dispersions about the averages. The approach is being applied to important earthquakes in which seismoscope data, or similar information, comprise the only strong-motion data available. In particular, the Guatemalan earthquake of 1976 and the 1906 San Francisco earthquake are being examined. Preliminary determinations of M_L for these earthquakes give values significantly less than the magnitude determined on the basis of surface waves. This is consistent with the saturation of the local magnitude with increasing surface-wave magnitude noted (24).

SUMMARY

We have tried in this brief presentation to highlight some of the recent developments in strong-motion seismology. Also, the status of the strong-motion networks in this country and the data so far obtained were reviewed. In closing, we would like to make the point that the recent increase in the quantity of strong-motion data, particularly that from the San Fernando earthquake, has permitted advances in strong-motion seismology to the point where some of the features of ground motion of interest to engineers can be modeled by seismological techniques previously applied only to more distantly obtained seismograms. The mechanics used in these approaches are, however, familiar to many engineers who deal in stress analysis and wave propagation and we believe that earthquake professionals can look forward to a coming together of the engineering and seismological viewpoints on the generation, propagation and interpretation of strong ground motion.

Contribution Number 3138, Division of Geological and Planetary Sciences, California Institute of Technology, Pasadena, California 91125.

REFERENCES

1. Aki, K. (1972). Scaling law of earthquake source time function, Geophys. J. R. astr. Soc., 31, 3-25.
2. Biehler, S. (1964). Geophysical study of the Salton Trough of Southern California, Ph.D. Thesis, California Institute of Technology, Pasadena.
3. Borrill, B. J. (1971). Seismoscope results -- San Fernando earthquake of 9 February 1971, Chapter 3 of Strong-Motion Instrumental Data on the San Fernando Earthquake of February 9, 1971, D. E. Hudson (Ed.), Earthquake Engineering Research Laboratory, California Institute of Technology, and Seismological Field Survey, National Oceanic and Atmospheric Administration, U. S. Department of Commerce, Pasadena, California.
4. Brady, A. G. (1978). Personal communication.
5. Brune, J. N. (1970). Tectonic stress and the spectra of seismic waves from earthquakes, J. Geophys. Res., 75, 4997-5009.
6. Burdick, L. J. and G. R. Mellman (1976). Inversion of the body waves from the Borrego Mountain earthquake to the source mechanism, Bull. Seism. Soc. Am., 66, 1485-1499.
7. Halverson, H. (1974). A technical review of recent strong motion accelerographs, Proceedings of the Fifth Work Conference on Earthquake Engineering, I, 1046-1055, Edigraph, Rome.
8. Hanks, T. C. (1974). The faulting mechanism of the San Fernando earthquake, J. Geophys. Res., 79, 1215-1229.
9. Hanks, T. C. and L. C. Seekins (1978). Strong motion accelerograms of the Oroville aftershocks and peak acceleration data, Bull. Seism. Soc. Am., 68, no. 3, 677-689.
10. Haskell, N. A. (1964). Total energy and energy spectral density of elastic wave radiation from propagating faults, Bull. Seism. Soc. Am., 54, 1811-1831.
11. Heaton, T. H. (1978). Generalized ray models of strong ground motion, Ph.D. Thesis, California Institute of Technology, Pasadena.
12. Heaton, T. H. and D. V. HelMBERGER (1977). A study of the strong motion of the Borrego Mountain, California earthquake, Bull. Seism. Soc. Am., 67, 315-330.
13. Heaton, T. H. and D. V. HelMBERGER (1978). Predictability of strong ground motion in the Imperial Valley, Bull. Seism. Soc. Am., 68, 31-48.

14. HelMBERGER, D. V. and S. D. MALONE (1975). Modeling local earthquakes as shear dislocations in a layered half-space, J. Geophys. Res., 80, 4881-4888.
15. HelMBERGER, D. V. and L. R. JOHNSON (1977). Source parameters of moderate size earthquakes and the importance of receiver crustal structure in interpreting observations of local earthquakes, Bull. Seism. Soc. Am., 64, 301-313.
16. HOUSNER, G. W. (1947). Characteristics of strong-motion earthquakes, Bull. Seism. Soc. Am., 37, no. 1, 19-31.
17. HOUSNER, G. W. and P. C. JENNINGS (1965). Generation of artificial earthquakes, J. Eng. Mech. Div., ASCE, 90, no. EM1, 113-150.
18. HUDSON, D. E. (1970). Ground motion measurements, Chapter 6 of Earthquake Engineering, R. L. WIEGEL (Ed.), Prentice-Hall, Englewood Cliffs, New Jersey.
19. HUDSON, D. E. and W. K. CLOUD (1961). A simplified instrument for recording strong motion earthquakes, Bull. Seism. Soc. Am., 51, 159-174.
20. HUDSON, D. E., M. D. TRIFUNAC and A. G. BRADY (1969 to 1976). Analyses of strong-motion accelerograms, I-IV, Parts A-Y, Index Vol. (EERL Report 76-02), Earthquake Engineering Research Laboratory, California Institute of Technology, Pasadena.
21. IDRISSE, I. M. (1978). State of the art -- ground motions, presented at the ASCE Earthquake Engineering and Soil Dynamics Conference and Exhibit, Pasadena, California, June 19-21.
22. IWAN, W. D. (Ed.) (1978). Proceedings of the International Workshop on Strong Motion Earthquake Instrument Arrays, Honolulu, May 2-5. Earthquake Engineering Laboratory, California Institute of Technology.
23. JENNINGS, P. C. and H. KANAMORI (1978b). The determination of local magnitude, M_L , from seismoscope records (abstract), Earthquake Notes, 49, no. 1, 9.
24. KANAMORI, H. and P. C. JENNINGS (1978a). Determination of local magnitude, M_L , from strong-motion accelerograms, Bull. Seism. Soc. Am., 68, no. 2, 471-485.
25. LANGSTON, C. A. (1978). The February 9, 1971 San Fernando earthquake, Bull. Seism. Soc. Am., 68, 1-30.
26. MALEY, R. P. (1978). Personal communication.
27. MIKUMO, T. (1973). Faulting process of the San Fernando earthquake of February 9, 1971 inferred from static and dynamic near-field displacements, Bull. Seism. Soc. Am., 63, 249-269.

28. Porcella, R. L. (Ed.) (1978). Seismic engineering program report, September - December 1977, Geological Survey Circular 762-C.
29. Robb, J. O. (1978). Personal communication.
30. Scott, R. F. (1973). The calculation of horizontal accelerations from seismoscope records, Bull. Seism. Soc. Am., 63, no. 5, 1637-1661.
31. Trifunac, M. D. (1974). A three-dimensional dislocation model for the San Fernando, California earthquake of February 9, 1971. Bull. Seism. Soc. Am., 64, 149-172.
32. Trifunac, M. D., F. E. Udvardia and A. G. Brady (1973). Analysis of errors in digitized strong-motion accelerograms, Bull. Seism. Soc. Am., 63, no. 1, 157-187.
33. Wooten, T. M. (1978). Personal communication.

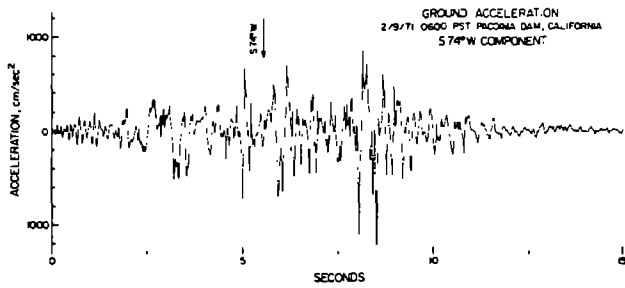


Figure 1. S74°W component of acceleration recorded at Pacoima Dam during the San Fernando earthquake of February 9, 1971.

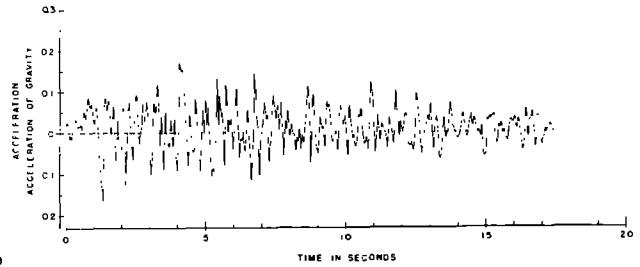


Figure 2. S69°E component of acceleration recorded at Taft during the Kern County earthquake of July 21, 1952.

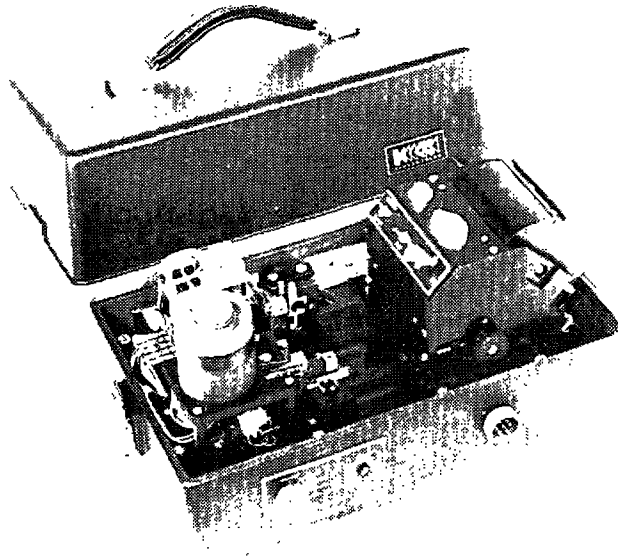


Figure 3. SMA-1 film-recording strong-motion accelerograph.

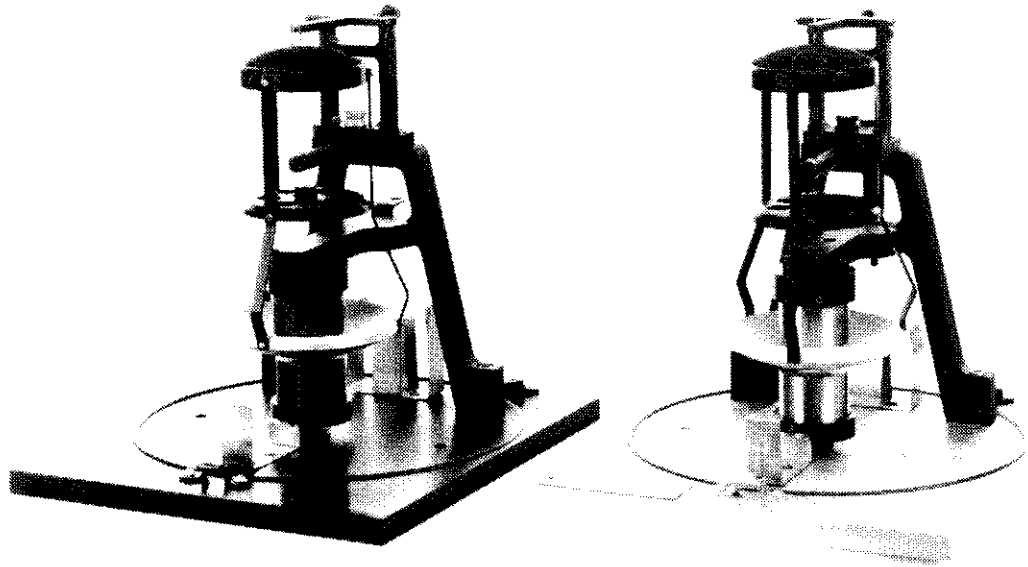


Figure 4. Strong-motion seismoscopes. Record is scribed on smoked glass dish at top of instrument.

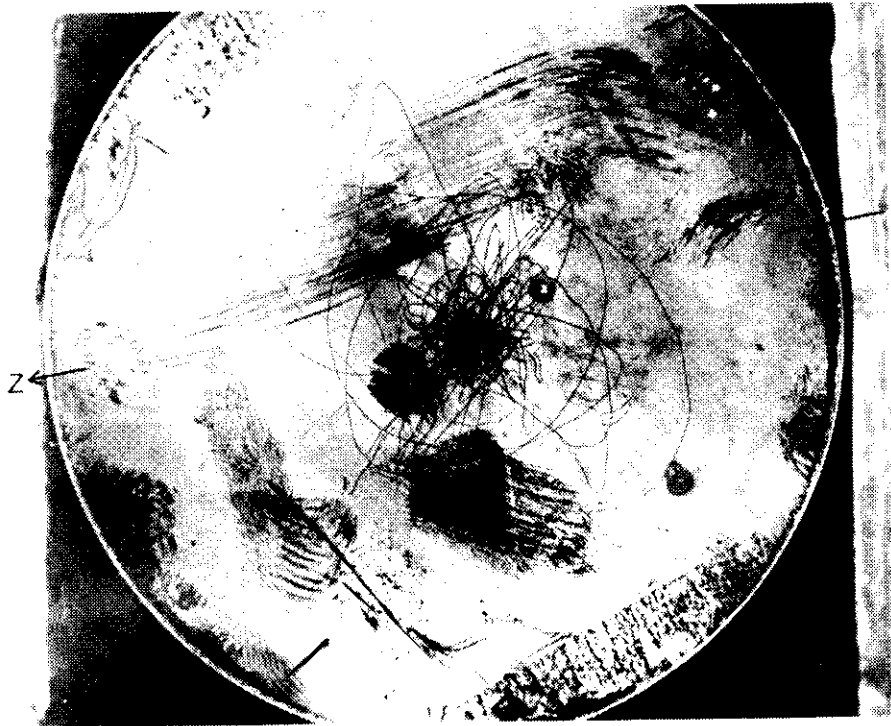


Figure 5. Seismoscope record obtained at the University Administration building during the Guatemalan earthquake of February 4, 1976. North is to the left.

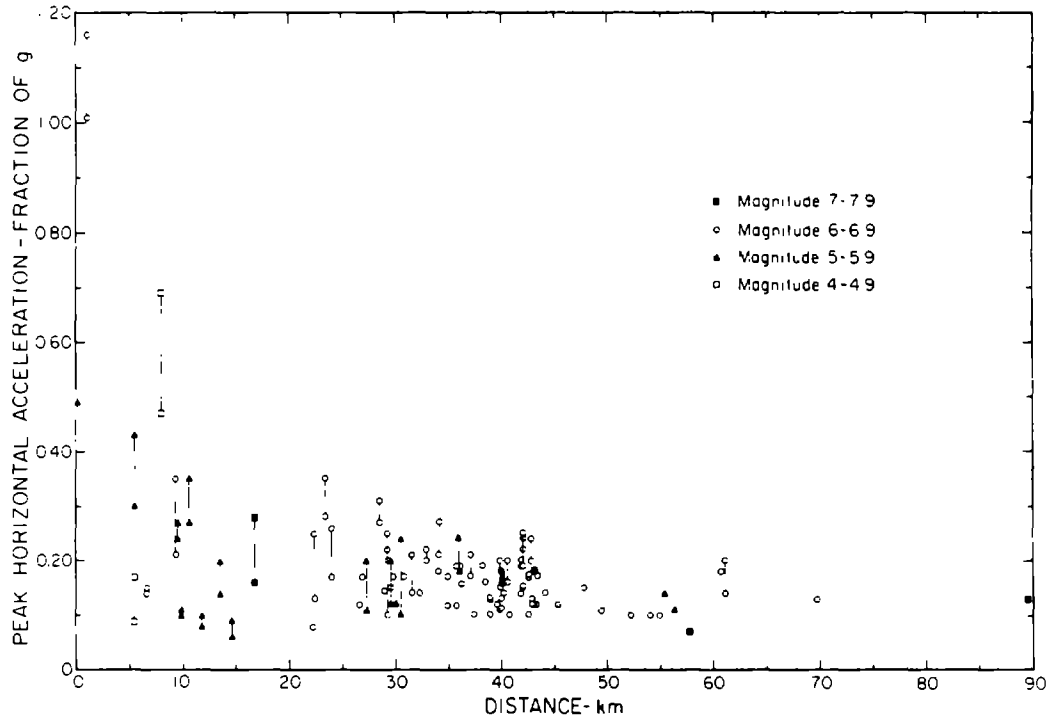


Figure 6. Peak acceleration vs. distance for four magnitude classes. Lines join the two horizontal components of larger and closer motions.

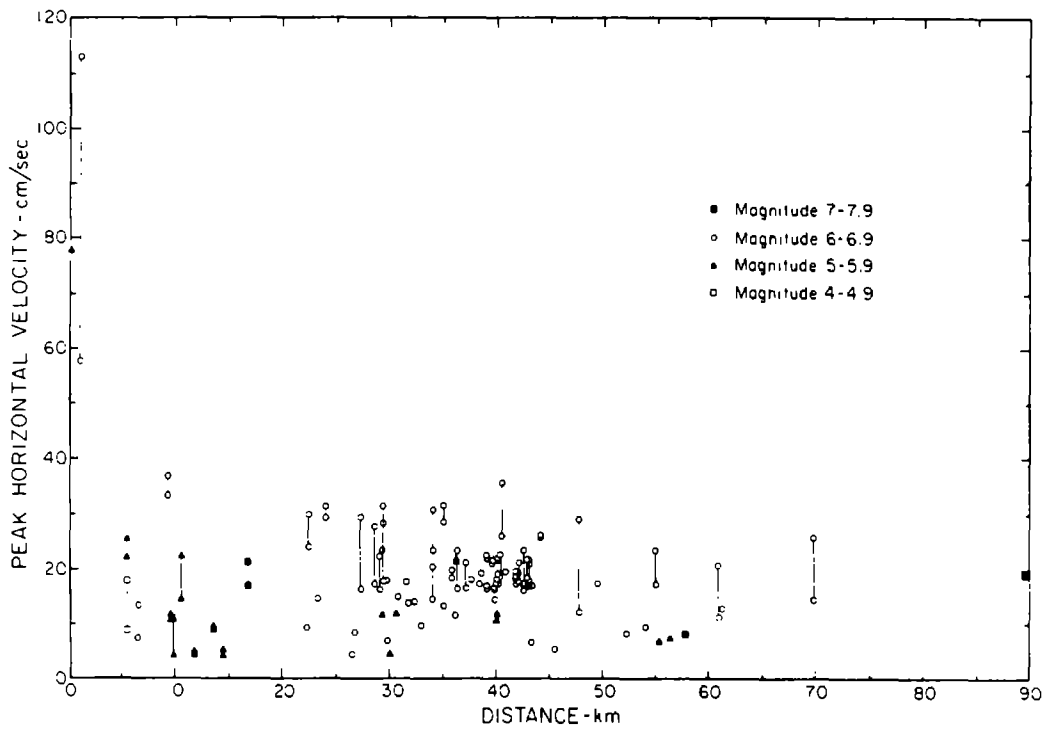


Figure 7. Peak velocity vs. distance for four magnitude classes. Lines join the two horizontal components of larger and closer motions.

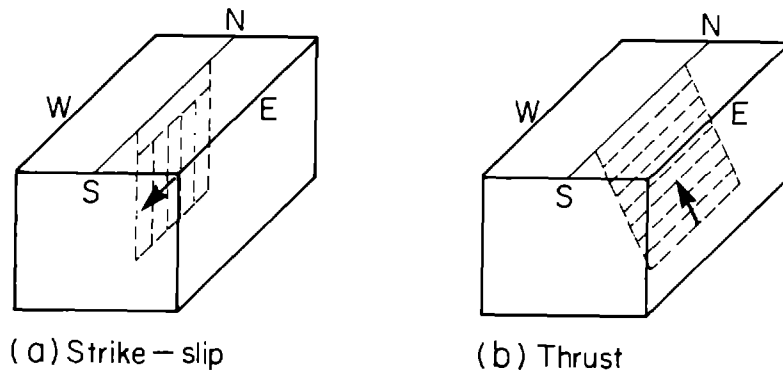


Figure 8. Apparent movement in vertical section for dislocation models of a strike-slip (a) and a thrust (b) type faulting.

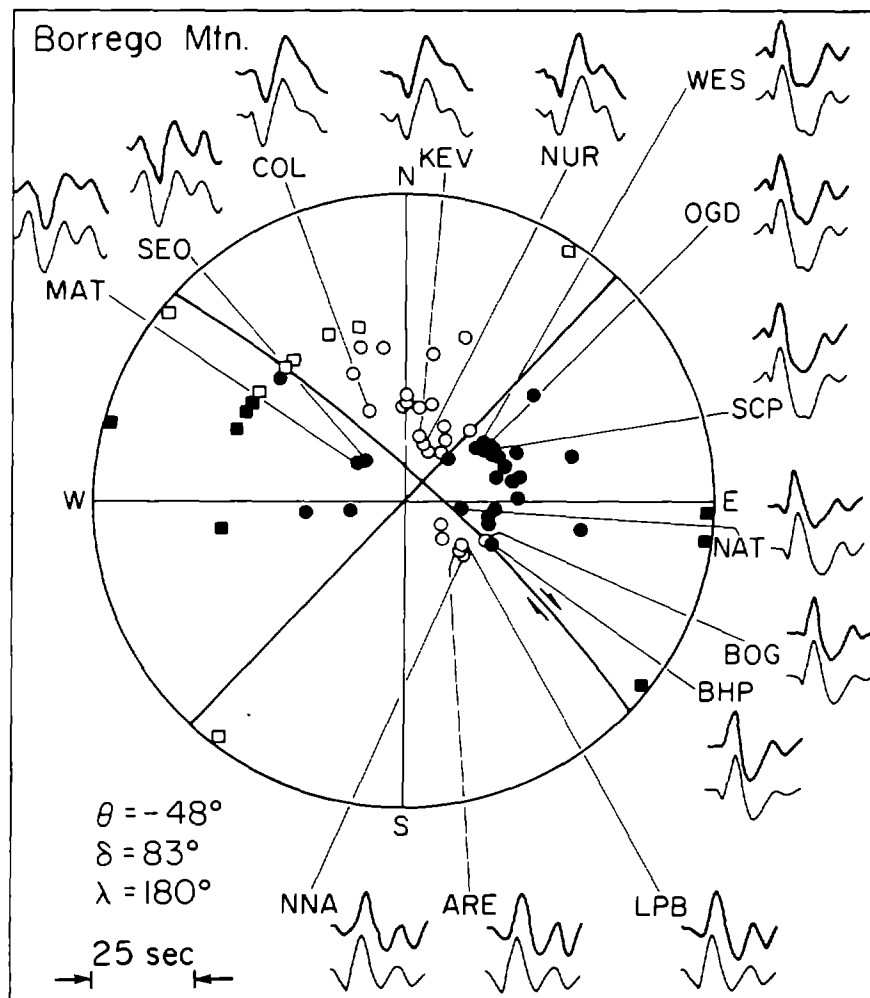


Figure 9. Observed (top) and synthetic (bottom) long period P wave forms at 14 WSS stations, MAT (Japan), SEO (Korea), COL (Alaska), KEY (Finland), NUR (Finland), WES (Mass.), OGD (New Jersey), SCP (Penn.), NAT (Brazil), BOG (Colombia), BHP (canal Zone), LPB (Bolivia), ARE (Peru), NNA (peru). The P-first motion plot is represented by the equal area stereographic projection of the lower half of the focal sphere. Black dots indicate compression (upward breaking P) and open circles indicate dilatation (downward breaking P). The heavy solid lines denote the nodal planes used in determining the fault orientation, θ (strike), δ (dip), λ (slip direction). Modified (6).

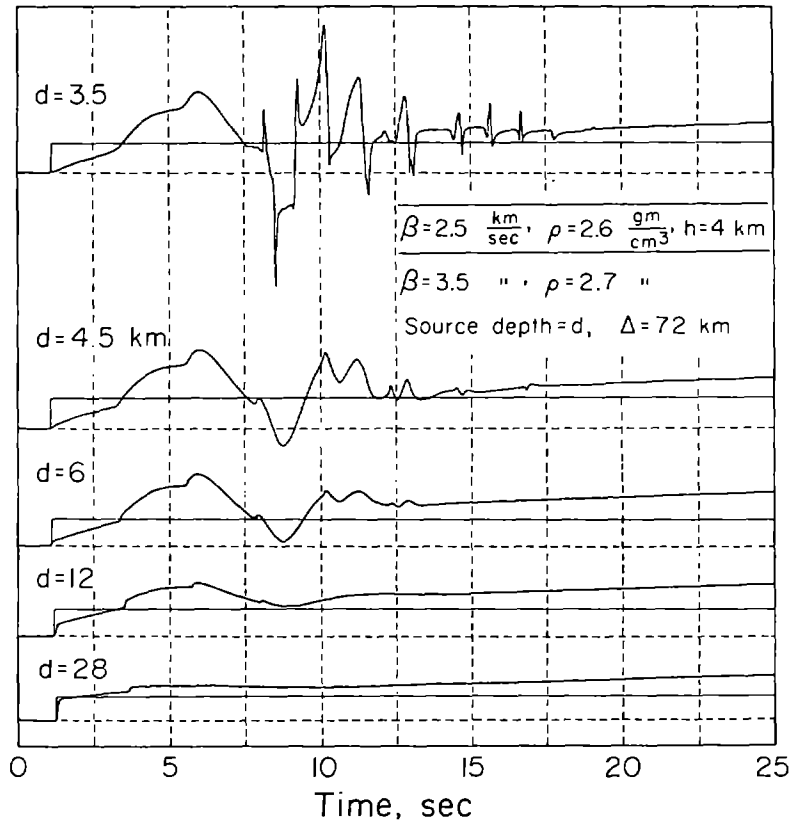


Figure 10. Step function responses at the surface assuming a point strike-slip dislocation situated at various depths. The amplitudes are scaled relative to the top trace with the step response for a homogeneous halfspace (bottom properties) displayed for comparison. After (14).

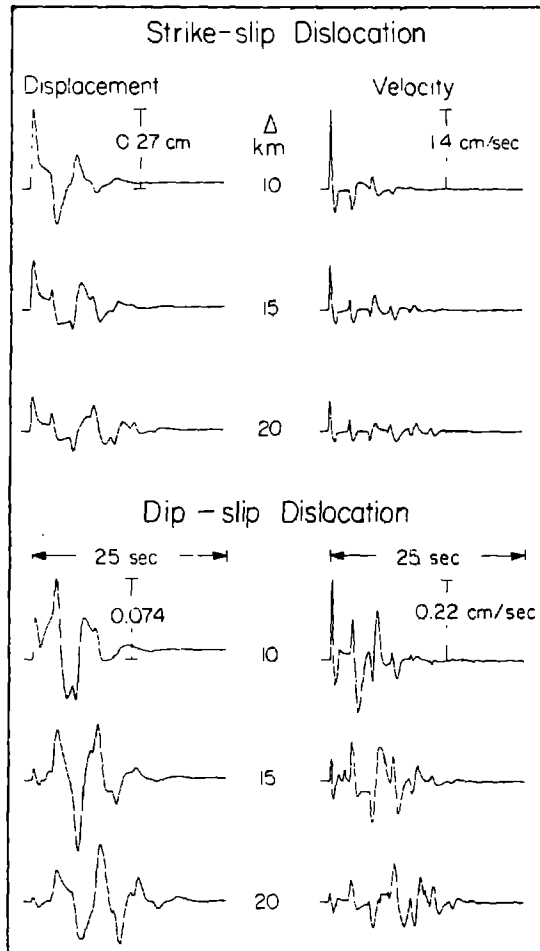


Figure 11. SH displacements and velocity components for a strike-slip and dip-slip dislocation in a layer over a half-space model. The elastic parameters are $\beta = 3.3$ km/sec, $\rho = 2.7$ gm/cm³ for the halfspace and $\beta = 1.5$ km/sec, $\rho = 1.9$ gm/cm³ for the layer. The source is buried at a depth of six km with a 2 km surface layer. The far-field source time function is assumed to be a trapezoid of unit height described by three time parameters, $\delta t_1 = .1$, $\delta t_2 = .2$, and $\delta t_3 = .5$. The time integral of this pulse is proportional to $M_0 = 1.66 \times 10^{23}$ dyne-cm, which fixes the magnitude of faulting displacements. Signal amplitudes are plotted relative to the top trace for each type of fault.

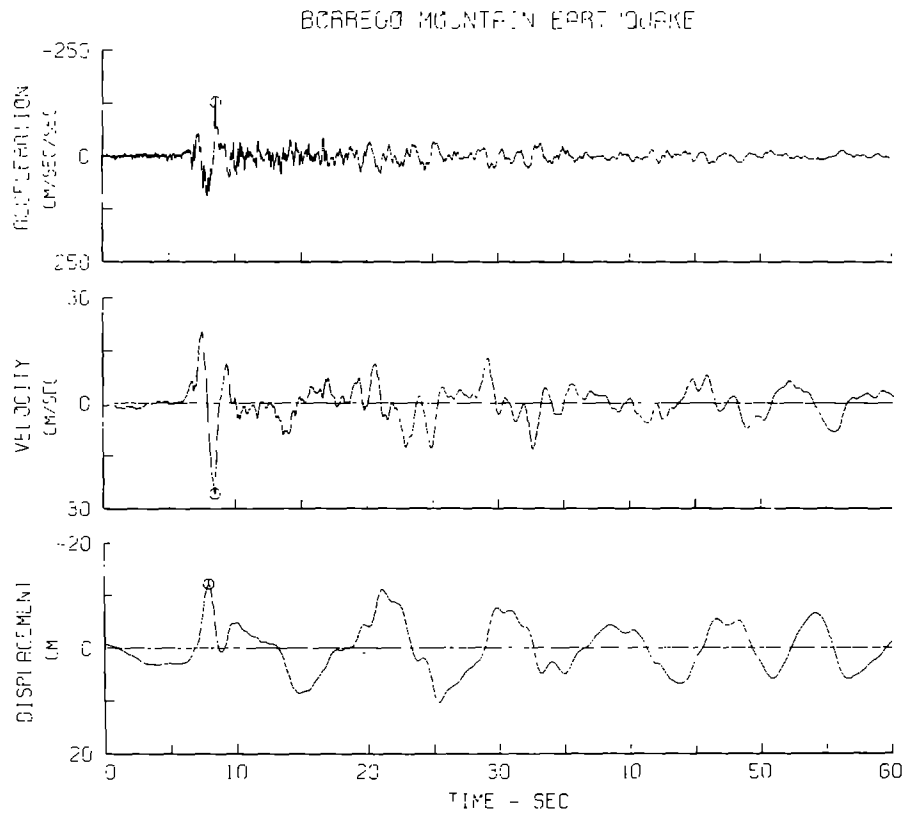


Figure 12. Acceleration, velocity and displacement motions for the north-south component recorded at El Centro of the April 8 Borrego Mountain earthquake 1968 (U. S. Coast and Geodetic Survey *et al.*, 1968).

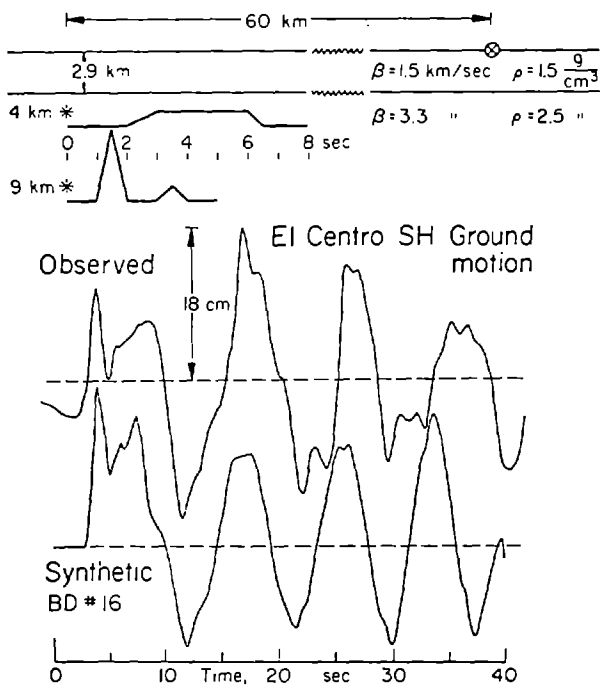


Figure 13. Comparison of the observed strong ground motion (transverse component) of the Borrego Mountain earthquake (April 9, 1968; $M_L = 6.4$) at El Centro, California, with ground motion computed on the basis of the simple source model schematically illustrated in the upper left embedded in the crustal structure parameterized in the upper right.

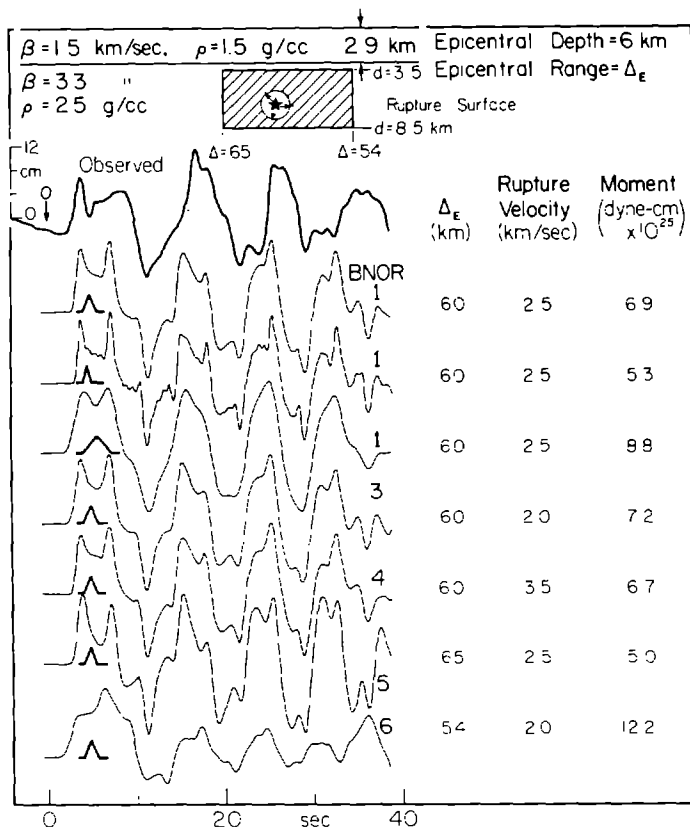


Figure 14. Comparison of observed with synthetic SH ground motion for models consisting of a rectangular fault with uniform offset which initiates at a point and propagates radially to the edge of the rectangle. In models BNOR5 and BNQR6 the rupture propagates unilaterally toward and away from El Centro, respectively. Rupture propagation is bilateral in the other models shown. The far-field time function for each point on the fault is displayed directly beneath the beginning of each synthetic. After (12).

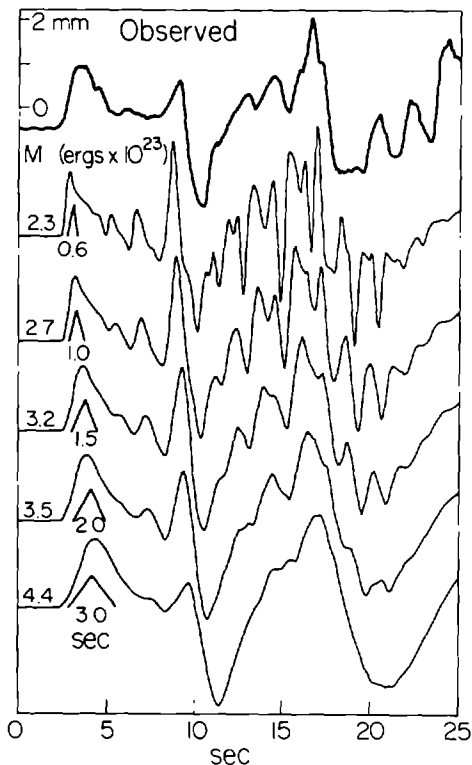


Figure 15. Comparison of IVC tangential ground motion with synthetics which have different duration triangular far-field time functions. The far-field time functions are displayed directly under the first pulse in the corresponding synthetic. A strike-slip point source with a depth of 6.9 km and a range of 33 km was used in all of these synthetics. The crustal parameters are P-velocity $\alpha_1 = 2.0$ km/sec, $\alpha_2 = 2.6$, $\alpha_3 = 4.2$, $\alpha_4 = 6.4$; and S-velocity $\beta_1 = .88$ km/sec, $\beta_2 = 1.5$, $\beta_3 = 2.4$, $\beta_4 = 3.7$; and density $\rho_1 = 1.8$ g/cc, $\rho_2 = 2.35$, $\rho_3 = 2.6$, $\rho_4 = 2.8$; layer thickness $Th_1 = .95$, $Th_2 = 1.15$, $Th_3 = 3.8$. After (13).

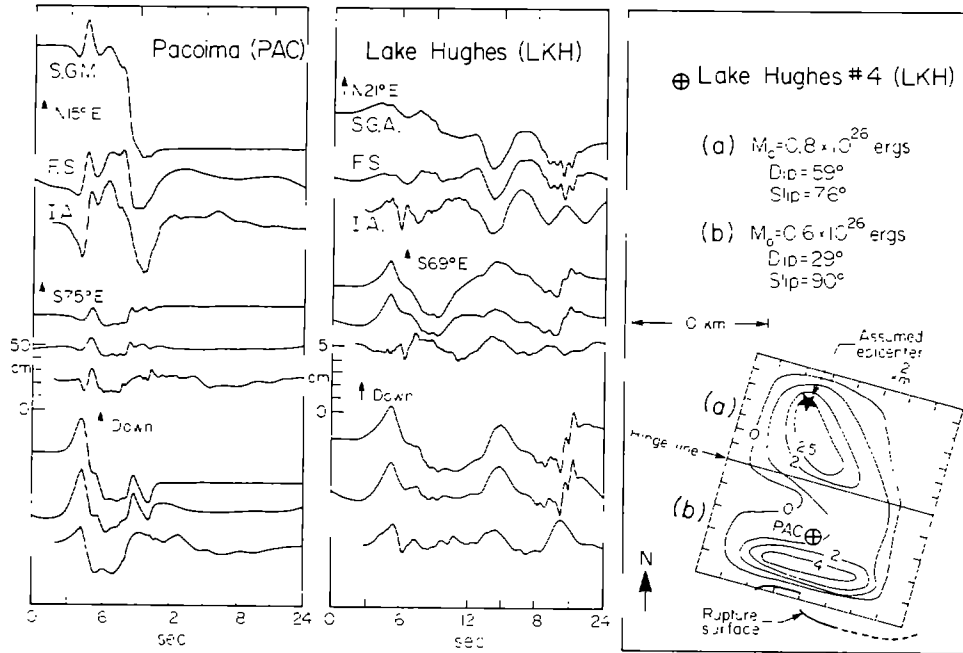


Figure 16. Relative geometry showing the locations of PAC (Pacoima Dam) and LKH (Lake Hughes) relative to the San Fernando fault and a comparison of displacements (top) synthetic with instrument (middle) and observed (bottom). Note the factor of 10 difference in amplitude scales between PAC and LKH which indicates the strong dependence on rupture direction (modified after [11]).

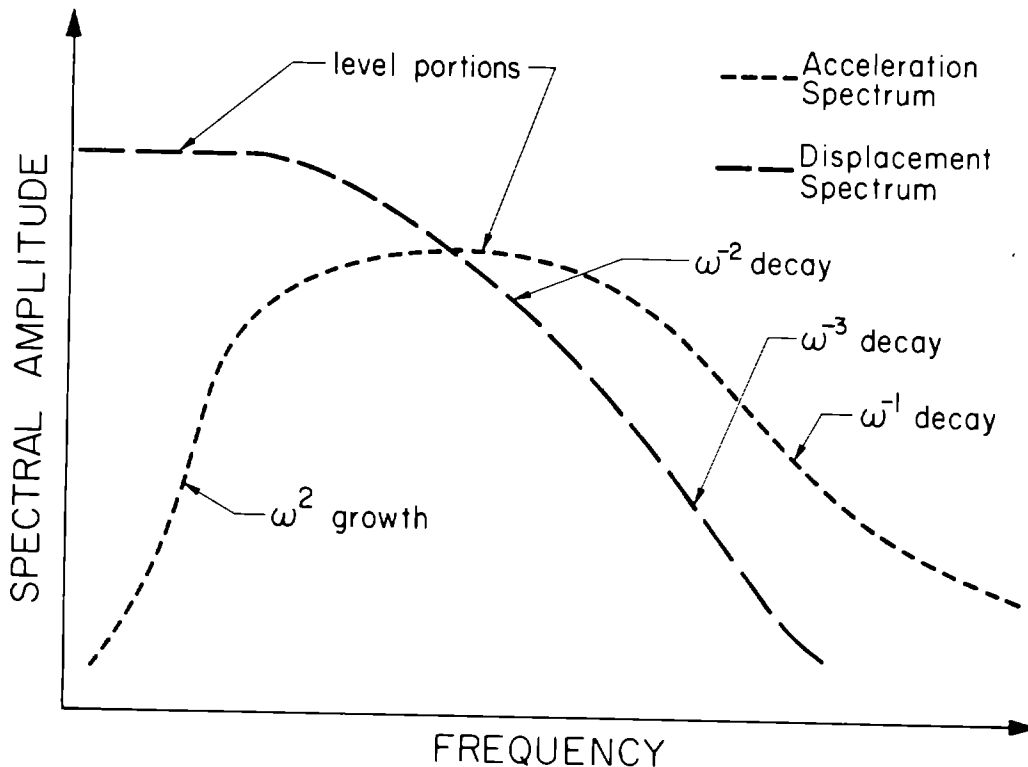


Figure 17. Spectra of acceleration and displacement of strong ground motion.

INTENTIONALLY BLANK

SOIL & GEOLOGIC EFFECTS ON SITE RESPONSE

by
Neville C. Donovan*

ABSTRACT

During the past decade the profession has gone from a feeling of optimism to a growing degree of caution over the use of one-dimensional site response analyses as a means of quantitatively developing site specific design parameters. The success of demonstrating site effects by analytic means was a significant advance, but also led to neglect of other equally significant parameters. The ability to model a special case and the weaknesses of the model are demonstrated in this paper by a comparison of computer and recorded motions.

Much attention has been given in the literature to the extremes of strong motion recording. A more rational approach is described in this paper where the mean value of data sets are used in conjunction with the distribution of data values about that mean. Procedures for developing site specific design criteria are described based on mean values with the use of a known measure of conservatism.

INTRODUCTION

A short historical review is useful for placing some perspective on the state-of-the-art. For the purpose of this paper considering the effects of soils and local geology on site response in the United States, it is sufficient to start from 1968. The pioneering efforts of Kanai (21) in Japan and the work by Herrera and Rosenblueth (17, 18) demonstrating the ability to analyse the effects of distant earthquakes in Mexico City must not be overlooked. At a 1968 symposium organized by the Earthquake Engineering Research Institute in San Francisco a paper by Seed and Idriss (33) showed that local soil effects in San Francisco could be effectively modelled by an equivalent lumped mass system. A companion paper by Donovan and Matthiesen (8) showed that wave propagation theory using vertically ascending shear waves could also be used to explain the local effects in San Francisco.

ANALYTICAL PROCEDURES

Computational difficulties in the early use of the wave propagation theory led to development and more extensive use of the lumped mass system even though it was much more difficult to model soils systems and especially hysteretic damping in this way. Whitman and his coworkers (7) showed that the two methods could give similar results. After the wave propagation method using the Fast Fourier Transform was incorporated by Schnabel, Lysmer, and Seed into the program SHAKE (31), wave propagation became the dominant method used throughout the profession for the computation of ground profile effects on earthquakes.

*Principal Engineer - Partner, Dames & Moore, San Francisco, CA.

The method is restricted to analysis of a linearly elastic model with nonlinear effects represented only by a reduction of the shear modulus to a value proportional to some assumed average strain.

Because analyses are usually performed by using a complete program which takes as input a rock or deep soil acceleration record together with the soil properties and then computes an acceleration or stress record at the surface or some intermediate level, the power and sophistication of the component parts are often not recognized. The method consists first of transforming the record, such as an acceleration time history, from the time domain to the frequency domain by the use of Fast Fourier Transform techniques. This is combined with the transfer function of the soil profile using complex arithmetic and then the product is inverted, again using Fast Fourier techniques, to obtain the output in the time domain. It is little recognized that, except for relatively minor changes due to the iterative differences in computing an equivalent linear modulus, the transfer function or soil effect which can be represented by an amplification spectrum will be the same for similar strength time records. In estimating effects of different profiles, the use of an amplification spectrum which does not include the effects due to source mechanism and other travel path properties can show site effects much more efficiently than analyses based on time history outputs from the profile model.

The Fourier Transform of the motion is a complex variable which can be represented in real quantities by a phase and an amplitude. Phase has often been neglected in favor of the absolute value of the amplitude spectra which is usually referred to simply as the Fourier spectra. Phase is important especially in near field studies where a large displacement pulse may be present. Such a displacement pulse may be retained following considerable tapering of the amplitude spectra provided the phase spectra is not changed.

Let us examine the situation resulting from different approaches to analysis of a well known site where motions have been recorded, the Southern Pacific Building at the foot of Market Street in San Francisco. This site has alternating sand and clay layers over rock at a depth of 220 feet. Figure 1 shows the amplification spectra for this site using a linear model with the modulus and damping for each layer compatible with an average strain equal to 65 percent of the maximum value. Figure 2 shows the input and output response spectra for a sample application of a wave propagation analysis. In this case the input motion used was one component of the 1952 Taft record used without any scaling of amplitude.

The computed profile effects shown in these first figures are based on the use of a linear model. Weaknesses of a linear model are readily apparent. The motion at the fundamental period of the profile, in this case 1.25 seconds, is very strongly amplified with a rapid fall off away from this frequency. If we examine the actual response spectra computed from the motion recorded during the 1957 San Francisco earthquake shown on Fig. 3, we see a maximum response at the fundamental period of the profile. However there is a much wider response containing other frequencies so that the attenuation away from the fundamental period is much less rapid than that computed using linear

vertical wave propagation analyses. It was perhaps the ability to model the peaks of response spectra that led to great optimism over one-dimensional analyses. The Taft record which was also used in the Fig. 3 example was scaled down in amplitude so that the resultant response was different from that shown in Fig. 2. The Taft record has much energy in the range of periods between 0.4 and 1 second so the computed response exceeds the recorded motion response in this area, but fails to transmit the short period motion evident in the recorded motions. This difference between measured and computed response is pronounced even in the case of the 1957 earthquake, a small amplitude event for which a linear approximation would be expected to work well.

There have been many recent developments in the application of non-linear approaches to the computation of site response. Such analyses must be performed in the time domain. Computational procedures may be based on, but are not restricted to the method of characteristics (Streeter et al, 36) and finite difference techniques (Taylor and Larkin, 37).

The preceding discussion, while raising the weaknesses of the linear analysis of vertical wave propagation, has not questioned the basic assumption of vertical propagation. This too should be questioned. The arrival of motion at a site is not a simple process involving only vertical wave propagation. If this assumption was correct then there would be little difference between the response spectra of individual components in the horizontal directions at the same site. These often differ from each other by amounts equal to the effects we seek to demonstrate. The ratio of spectral amplitudes for the two horizontal components shown on Fig. 3 are plotted on Fig. 4. The spectral amplitude ratio when the N45W component response is divided by the N45E component has values between 0.6 and 2.3. This variation between individual components at the same site during the same event should be considered in the discussion of uncertainties later in the paper.

Another example illustrating difficulties with the simple assumption can be taken from records made at the Southern Pacific Building during the 1969 Santa Rosa earthquakes. These records which were obtained from a distant event with low levels of motion would be expected to give excellent agreement with a linear response analysis. The recorded motion lasting 24 seconds was digitized and response spectra were computed. Two sets of spectra are shown on Fig. 5. The spectra shown in Figure 5(a) were computed from the actual records. It is readily apparent that the fundamental period of the Southern Pacific site was not excited by the actual record while the site response study suggests there should have been a significant response at that period. Spectra shown in Fig. 5(b) were obtained from a site response study of 20 second duration. It was only when the duration was severely repressed in the analytical study that response spectra similar to those recorded were obtained.

An examination of the response time history of one component of the 1968 recorded motion at two different periods is shown on Figure 6. The dispersion of the wave motion can be readily seen in the different responses and is especially apparent after 3 seconds where the 0.29

second motion reaches its peak value while the large period amplitude is still very small. If the earthquake motion reached the site as surface waves, the longer period motion would be expected to be within the first arrivals. This is obviously not so and leads to the conclusion that the short period motion is produced by body waves taking a deep travel path and reaching the site first while the longer period motion is probably produced by surface waves which reach the site at a slightly later time.

The suggestion is offered, therefore, that any means of site modelling that represents site response as being based on a simple response to a single type of motion, either as vertically propagating shear waves, or other motions such as Rayleigh waves, should be considered only as a guide to estimating the site effects on ground motion and not for the development of acceleration time histories for design.

GROUND MOTION PARAMETERS

It is perhaps in response to these difficulties in the analytical methods that much more attention has recently been given to the empirical evaluation of design spectra by using average response spectra. There were insufficient records to perform such studies until recently. Average spectra were first prepared on the basis of exclusion of site and distance effects, [Newmark (26), Blume et al (3)]. Subsequent work by Seed et al (34) and Mohraz (25) has included site effects. The methods adopted by different investigators are not the same but comparison of the end results are similar. This is not surprising as the separate studies all use the same strong motion records as the primary data base.

The starting point for developing both non site-specific and site matched design spectra is the choice of an acceleration value to which the spectra is scaled. The choice of peak acceleration as the basic design parameter is a poor one. This has been discussed at length within the profession and will not be continued here. Where acceleration is used as a scaling parameter against which other ground motion terms can be related it is a useful quantity. A term defining an acceptable scaling parameter is believed to be "Effective Peak Acceleration" (EPA) developed by the Applied Technology Council (1). The definition of EPA which is summarized in Donovan et al (12) can be defined in the following way. "For a specified actual ground motion of normal duration, EPA and EPV (effective peak velocity) can be determined as illustrated in Figure 7. The 5 percent damped spectrum for the actual motion is drawn and fitted by straight lines between two sets of periods (see figure). The ordinates of the smoothed spectrum are then divided by 2.5 to obtain the EPA and EPV. The EPA and EPV thus obtained are related to peak ground acceleration and peak ground velocity but are not necessarily the same as or even proportional to peak acceleration and velocity."

The introduction of an EPV term as a second scaling parameter was required because a single parameter related to acceleration cannot even approximately describe response spectra which result from large distant

earthquakes. The effective peak acceleration will be similar in magnitude to the average instrumental maximum value but should not be expected to be equal to any individual value.

If effective peak acceleration defined on the basis of a probabilistic assessment is taken as the starting point, it is then possible to construct design response spectra using velocity and displacement motion directly. Before doing so, it is important that the level of uncertainty that is present in the development of each of the necessary parameters including peak acceleration be considered.

Peak Acceleration Uncertainty

The extent and effect of the level of uncertainty are best illustrated by considering some examples. Figure 8 shows data points obtained from strong motion instrumentation during a magnitude 5.5 earthquake which occurred near Ferndale, California, on June 7, 1975. These are compared with estimates of peak acceleration using different relationships. Some of the values on Figure 8 lie more than 2 standard deviations beyond the mean values upon which the curves are based. In the near field, recent work by Hanks and Johnson [16] suggests, that for magnitudes above 4.5, peak acceleration may have no relationship to either the earthquake size or the true severity of ground shaking on structures.

Attempts have been made to correlate Modified Mercalli Intensity (MMI) values to acceleration. These can lead to several inconsistencies which are best illustrated by considering data from a single event. Figure 9 shows the isoseismal map for the February 9, 1971 San Fernando earthquake as prepared by the United States Coast and Geodetic Survey which is now the Seismic Engineering Branch within the United States Geologic Survey. The most common procedure in estimating attenuation of MMI with distance is to compute the radius of the equivalent circle having the same area as the isoseismal line and use this value as a single data point. Bollinger (4) has shown that this can produce a conservative bias to the interpretation. This bias is demonstrated on Figure 10 where the individual reporting stations from which Intensities were derived are shown as solid circles. The values of the equivalent radii are shown as triangles. The biasing effect of the equivalent radii method is immediately evident. If least squares procedures are used to produce a best fit curves such as a straight line or a parabola it can then be seen that the extent of this bias is approximately one unit of Intensity and is nearly constant. The constant bias shows that the procedure by which isoseismals are drawn is consistent. Because most acceleration to Intensity relationships show an approximate doubling as MMI increases by one unit the bias effect is a very significant parameter. It may be claimed that as most of the data values are based on small Intensity values with consequently small acceleration levels the interpretations are not valid. While the claim may be valid it should not be honored because all MMI attenuation relationships, especially those from eastern U.S. earthquakes are based on small Intensity values.

If the intensity to distance curves on Figure 10 are used and converted to acceleration and distance using an MMI to acceleration relationship, the results illustrated on Figure 11 are obtained. The actual MMI to acceleration relationship used is unimportant as all show the same general trend. The mean attenuation relationship for peak acceleration obtained using the recorded strong motion instrument data is also shown on Fig. 11. The discrepancy in the shapes of the two types of curves on Fig. 11 confirms the known poor correlation between acceleration and Intensity. MMI values are based wherever possible on observed damage. As design criteria should be based on these observations and used to prevent future damage the results shown on Fig. 11 can be interpreted as an alternate means of justifying design acceleration or EPA values that are less than peak acceleration values in the near field region of large earthquakes and larger than peak instrumental values in areas where distant earthquakes are more important (12).

Values of the uncertainty associated with the computation of acceleration for derived attenuation relationships are shown in Table 1. As the relationships are expressed in exponential terms and the variability is known to be lognormally distributed, the factor listed is more significant than the standard deviation. This factor is the quantity by which the mean value must be multiplied to find the value one standard deviation higher than the mean value.

TABLE 1

Estimates of Uncertainty

	Author		Standard Deviation	
			Lognormal	Factor
a) acceleration				
	Esteva	1970	1.02	2.8
	Esteva & Villaverde	1973	0.64	1.9
	Donovan*	1973	0.48	1.6
	Donovan	1973	0.71	2.0
	Donovan & Bornstein**	1975	0.3 >0.5	1.3 >1.6
	Seed et al***	1976	0.34 >0.51	1.4 >1.7
	McGuire	1974	0.51	1.7
b) velocity				
	Esteva	1970	0.84	2.3
	Esteva & Villaverde	1975	0.74	2.1
	McGuire	1974	0.63	1.9
c) displacement				
	McGuire	1974	0.76	2.1

* San Fernando data only

** Site specific relationship

*** Seed et al data are sorted by site characteristics and consider only one magnitude level

The values show that when a complete data set is considered without the classification of site conditions, the standard deviation factor may be as large as 2. There is little data published regarding the standard deviation for site specific acceleration data but Donovan and Bornstein have estimated that for accelerations on rock and stiff soil sites the standard deviation factor may be reduced to approximately 1.5. What this implies is that even when the site conditions and the location of the probable source are known there is only a 70 percent chance of measuring a value within plus or minus 50 percent of the computed quantity.

The attenuation equations referenced above are only a selection of those available. A comprehensive list of those presently available was compiled by Idriss (19). Together with the compilation Idriss presented somewhat detailed comparisons of the results obtained by using the equations in a deterministic way. Direct use of any attenuation equation should not be undertaken without consideration of the uncertainty associated with that relationship when uncertainties as large as those shown in Table 1 exist. An example of correct usage of an equation is demonstrated in a seismic risk analysis where the mean attenuation relationship is used throughout the analysis but is always taken in combination with the probability distribution of the data about that mean.

Velocity and Displacement Uncertainty

Velocity and displacement have been examined in two different ways. The more common method in use at the present time is a comparison of the peak velocity and displacement with the peak acceleration. Some efforts have been made by Esteva (13) and McGuire (22) to develop direct attenuation equations for peak velocities and displacements. Velocity and displacement data exhibit much more scatter than acceleration and are greatly affected by site conditions but in a different way. Whereas high rock accelerations may be attenuated by a soil profile and small accelerations may be amplified, velocity and displacement values tend to be amplified at most motion levels. The standard deviation factors for some velocity and displacement equations are also included in Table 1.

The direct comparison of peak velocity and peak acceleration was first undertaken by Newmark and Hall (27) and has been repeated by others. Site conditions have not been considered by Newmark and Hall but Mohraz (25) has extended work initially performed with Hall and Newmark to include these effects. Some of the basic relationships are given in Table 2. While Table 2 shows the similarity of results by different investigators, Mohraz is the only one to show the standard deviation multiplier. These values in Table 2 show that the uncertainties in the quantity ratios from specific events is approximately equal to the uncertainty between the individual quantities themselves. The attenuation relationships proposed by Esteva and McGuire are magnitude dependent and will give different v/a ratios for different magnitude and distance values. The values in Table 2 do not include magnitude and distance so a comparison of the range of values predicted by use of the mean attenuation equations of Esteva and McGuire can provide additional insight. If the range of magnitudes is varied between 4.5 and 7.0 and epicentral distances are varied between 1 and 65 kilometers (0.6 to 40

miles), then the variation of the v/a ratio for Esteva (1973) is between 81 and 119 cm/sec/g (32 to 47 inches/sec/g) with a mean value of 102 cm/sec/g (40 inches/sec/g). Similar values for McGuire vary between 60 and 133 cm/sec/g (23 to 52 inches/sec/g) with a mean value of 89 cm/sec/g (35 inches/sec/g). The variation in the ratios computed directly from the equations are in accord with seismological observation that the velocity to acceleration ratio should increase with both increasing magnitude and increasing distance from the source. Some of the difficulties in working with statistics using limited data sets are shown in Seed et al (35) where the conclusions reached are not in agreement with observation and imply that velocity attenuates more rapidly than acceleration for deep cohesionless soil sites.

TABLE 2

Profile Type	Ground Motion Parameter Ratios				Standard Deviation	
	v/a	v/a	v/a	v/a	Factor	
	Newmark-Hall	Seed et al	Mohraz		Mohraz	
	cm/sec/g	cm/sec/g	cm/sec/g	cm/sec/g	L	S
Rock	61(24)**	66(26)	61(24)	69(27)	1.58	1.63
Stiff Soil	--	144(45)	--	--	--	--
Deep Sand	--	--	76(30)	91(36)	1.53	1.61
Alluvium	122(48)	142(55)	122(48)	145(57)	1.44	1.49

* Mohraz considered horizontal data in two sets. L comprises the set containing the largest horizontal component from each site and the S set contains the lower value.

** Numbers in parentheses are in units of inches/sec/g.

Response Spectra

The procedure for construction of a design response spectra should be reviewed briefly. The most common procedure follows the method developed by Newmark and Hall where the basic ground motion parameters based on particle acceleration, velocity and displacement are used as the starting points. The velocity and displacement values are usually obtained by scaling from the statistical v/a ratios and the dimensionless term ad/v^2 . These ground parameters, the starting point for spectral construction, are shown on Figure 12 for a site on a deep soil profile with an effective peak acceleration of 0.1g. Using the v/a ratio of Newmark and Hall the equivalent particle velocity would be 4.8 inches per sec. With an ad/v^2 ratio of 5 the equivalent particle displacement would then be 3 inches. From these ground parameter values, spectral amplification values are used to draw the design spectra for the appropriate damping levels. Two spectra are shown for a damping level of 5 percent on Figure 12. The lower spectra is based on mean amplification values and the upper curve represents the 84 percentile or one standard deviation beyond the mean.

The uncertainty in the spectral amplification must also be considered. Estimates of the uncertainty appear to vary slightly across the spectrum at different periods but are not great enough to warrant special attention. In Table 3 the average ratio between the mean response spectra coefficients and the mean plus one standard deviation coefficients are shown for three different damping levels. As these spectra are computed from selected data sets and are not based on the total data, the standard deviation should be expected to be slightly reduced.

TABLE 3

Spectral Uncertainty

Damping Level	Averaged Across Spectra		
	Blume-Newmark	Mohraz	Seed et al
.02	1.42	1.41	--
.05	1.32	1.36	1.4
.10	1.30	1.31	--

It can be seen that no matter how ground motion input for design is defined a large amount of uncertainty exists. This uncertainty must be recognized. It is imperative that the uncertainty be included as a part of the design study for the whole project rather than by separately compounding the uncertainty of each individual part. Unbridled conservatism could quickly lead to ridiculous criteria. If a conservative acceleration is chosen and spectra are then constructed using conservative ground motion ratios and spectral amplification factors, it is an easy step to end up with criteria that are up to 4 or 5 times the most probable or mean value. This conservative factor only relates to the ground motion portion of the design criteria. When each step is considered in this way the use of maximum conservatism is unconscionable.

To some extent the problem in making a reasonable design choice has been compounded by the separation of parts of the problem between disciplines. The seismologist and geophysicist may recognize the uncertainty of the representative peak parameters, but consider they have failed if an event should occur with peak parameters larger than their recommendations. The earthquake engineer in turn may not know the amount of conservatism in these parameters and include the uncertainty in the spectral parameters on the basis that the prior numbers are mean values.

RECOMMENDED USAGE OF PARAMETERS

Although the difficulties in the compounding of uncertainties should be avoided it is important that the uncertainty be considered in the selection of design values. This inclusion of uncertainty should be only to the extent that the total degree of conservatism is not much

greater than that existing in the selection of individual parts. For example, the choice of mean acceleration and ground motion ratios with 84 percentile spectral amplification ratios is one useful concept.

It was the stated intent of Hall, Mohraz and Newmark (15) in recommending the use of mean plus one standard deviation (or 84 percentile) response spectral amplification values that mean values would be used for the basic ground parameters including acceleration. Unfortunately this intent is often ignored. Page (30) has made the spurious assertion that the measures of peak acceleration is primarily a function of the number of instruments deployed. It is reasonable to expect that a rare but ever larger maximum will be recorded as the data set increases in size. At the same time as the maximum of the maximum values increases, the mean value will become more firmly established. Statistical evaluations and studies must be based on mean values even if they are from a set of maximum values.

The difficulties in the choice of parameters for design have been pointed out in the previous sections of this paper with almost complete abandon. It becomes necessary, therefore, to describe in a step by step fashion how some of these difficulties can be avoided in a logical manner. The first step in current design procedures is the selection of an acceleration value to be used as a scaling parameter for development of the design spectra. This acceleration value may be developed from a seismic risk analysis (6, 24, 11) or obtained by other means such as assuming a known source and using an attenuation relationship. What attenuation relationship should be used? While the writer has a preference to those he has developed, (9, 11) this is a reaction based on familiarity. Others can also be recommended for use in developing design acceleration values if they are based on a large data base (22). The need for a wide range of data rather than selected data is to ensure that the mean peak acceleration will closely approximate the design acceleration or EPA value. The attenuation relationship by Schnabel and Seed (32) and those by Page et al (29) do not satisfy these criteria. Many factors are known to affect acceleration levels but few are yet sufficiently understood. There is sometimes a strong directional effect for example, (2) and at present little is known about the difference in ground motion on strike slip faults in contrast to the ubiquitous data from San Fernando. The writer usually uses several attenuation relationships and attempts whenever possible to logically reconcile the differences between them before making a choice of the design acceleration level.

Where the site under study is different from those upon which the attenuation data was obtained, selection of a value for a stiff soil or rock site is recommended as a first step. This value can then be converted to a design acceleration for the appropriate soil profile by use of Fig. 13 which was developed by Seed et al (35).

Once the acceleration has been chosen a v/a ratio appropriate for the site conditions and the magnitude and distance of the event should be selected. At the present time this is preferable to direct use of any velocity attenuation relationship. For moderate distances (20 to 40 km) the values of v/a listed in Table 2 would be appropriate. For other distances some adjustment should be made recognizing that the ratio

increases with increasing distance and with increasing magnitude (23).

There has been apparent disagreement in the literature because Newmark and Hall (27) have apparently not considered the effects of different soil profiles. This difference however, is more apparent than real and can be shown as follows. The effect of a soft soil site is to reduce the acceleration level and increase the v/a ratio. For example using Fig. 13, a rock acceleration of 0.2g would be reduced to 0.16g for a deep soil or alluvium site. At the same time the v/a ratio would be increased beyond the 122 cm/sec recommended by Newmark and Hall (which is not a mean value) to 142 cm/sec. The actual ground motion velocity values to which the spectral amplification values are applied would be 24.4 cm/sec and 22.7 cm/sec respectively and show that except for the short period portion of the response spectra there is very little real difference in the two seemingly disparate approaches.

Displacement can be computed using a value of ad/v^2 of 5 or 6 and the previously developed acceleration and velocity values. Nuttli (28) has noted that displacements on soft sites are approximately 4 times those on rock. This is in agreement with the factor of 2 noted in the v/a ratio for the same conditions.

With the ground motion parameters established and constructed as shown on Fig. 12 the spectral amplification values for acceleration, velocity, and displacement can be obtained from tables prepared by Hall et al (14) or Mohraz (25) for the desired damping levels. Although there are differences in the amplification values for the different soil profile types these values are comparatively small so that the major effects or spectral shape are directly controlled by the ground motion parameters.

Where the design event magnitude is close to 6.5 an alternate procedure would be to use the average spectra of Seed et al (34) directly. The average spectra recommended by Seed et al, and Mohraz for different soil types normalized to 0.1g are shown on Fig. 14(a) and 14(b). Also shown on Fig 14(c) is the recommendation of Hall et al. The difference in spectral amplitude in the Hall spectra comes about because the v/a ratio is not based on a mean quantity.

The spectra shown in Fig. 14 are mean spectra based on mean ground motion parameters. If the design acceleration to which the spectra will be proportioned has been chosen using a mean value these should not be recommended as design spectra. No conservatism has been included. Instead the recommended procedure would be to take the 84 percentile values from the spectral amplitude tables of either Hall et al, or Mohraz and prepare design spectra in this fashion. Fig. 15 shows the recommended design spectra with a damping of 5 percent for the design acceleration of 0.2 g on rock and the comparable value of 0.16 g on a deep soil profile using the suggested procedures of Mohraz and Seed et al which are site specific and the method of Hall et al which is not.

Where it is intended that design be based on use of an acceleration time history the choice of the ground motion record should be undertaken with great care. While it is not a difficult problem to develop a time history that can match a specified average response

spectrum as demonstrated by Tsai (38) it is neither unique nor truly representative of the average when used in a multi degree of freedom analysis (10). It is beyond the scope of this paper to discuss this problem in detail, but it is believed that methods that seek to closely model the actual propagation of fault rupture such as suggested by Guzman and Jennings (14, 20) offer the most promise at this time. Strong motion seismology is also achieving success in modelling the displacement records in strong motion (5). As the acceleration values are largely controlled by irregularities in geology and fault rupture the theoretical modelling of acceleration records other than in a probabilistic sense is not yet possible.

CONCLUSIONS AND RECOMMENDATIONS

There has been considerable progress made in the study of the effects of soil and geology on site response. This progress became very rapid during the early part of this decade. At that time the flush of success in explaining some of the observed effects during earthquakes by using simple site models led to overuse and some misuse of the models. The large amount of data obtained from the San Fernando earthquake showed that simple models were not adequate to explain observed phenomenon. At the same time the large amount of data has enabled direct empirical evidence of site effects to be compiled. These empirical procedures carefully applied with the use of mean values and a reasonable degree of conservatism offer a much more attractive means of evaluating site effects on ground motion than is possible with any presently available one or two dimensional linear or non linear site model. Analytical procedures still have a wide role. Analytical techniques involving soil and structure models are required for soil and structure interaction studies. The loss of strength of cohesive soils during cyclic loading and the generation of pore pressures in sands and silts need the understanding that comes from detailed studies to provide the ability to make a rational extrapolation of field observation from past earthquakes to problems of present design.

REFERENCES

1. Applied Technology Council, 1977, Final Review of Draft of Recommended Comprehensive Seismic Design Provisions for Buildings, Palo Alto, California, January 7.
2. Arnold P., and Vanmarcke, E.H., 1977, "Ground Motion Spectra, The Influence of Local Soil Conditions and Site Azimuth," Sixth World Conference on Earthquake Engineering, New Delhi, India, Vol. 2, pp. 113-118, January.
3. Blume, John A. & Associates, 1973, "Recommendations for Shape of Earthquake Response Spectra" Report prepared for the directorate of licensing United States Atomic Energy Commission,
4. Bollinger, G. A., 1977, "Reinterpretation of Intensity Data for the 1886 Charleston, South Carolina Earthquake", United States Geological Survey Professional Paper 1028.

5. Bouchon, Michel, 1978, "Synthesis of Strong Motion for Arbitrary Three-Dimensional Seismic Sources" Paper presented at 73rd Annual Meeting, Seismological Society of America, Sparks, Nevada, April 6-8.
6. Cornell, C. Allin and Vanmarcke, Erik H., 1969, "The Major Influences of Seismic Risk", Proceedings of the Fourth World Conference on Earthquake Engineering, Santiago, Chile, Volume I, 1969, pp. 69-83.
7. Dobry, R., Whitman R. V., and Roesset, J. M., 1971, "Soil Properties and the One-Dimensional Theory of Earthquake Amplification", Department of Civil Engineering, Massachusetts Institute of Technology, Research Report R71-18.
8. Donovan, N. C., and Matthiesen, R. B., 1968, "Effects of Site Conditions on Ground Motion during Earthquakes", State-of-the-Art Symposium, Earthquake Engineering Research Institute, San Francisco, California, February
9. Donovan, N. C., 1973, A Statistical Evaluation of Strong Motion Data, Including the February 9, 1971 San Fernando Earthquake, Proceedings of the Fifth World Conference on Earthquake Engineering, Rome, Italy, June, pp. 1252-1261.
10. Donovan, N. C., Valera, J. E., and Beresford, P. J., 1975, "Statistical Uncertainty of Design Based on Smoothed Response Spectra", Proceedings of the U.S. National Conference on Earthquake Engineering, Ann Arbor, Michigan, pp. 53-59
11. Donovan, N. C. and Bornstein, A. E., 1978, "Uncertainties in Seismic Risk Procedures," Journal of the Geotechnical Engineering Division, ASCE, Vol 104, No GT7, Proceedings Paper 13896, July pp. 869-887.
12. Donovan, N. C., Bolt, B.A., and Whitman, R. V., 1978 "Development of Expectancy Maps and Risk Analysis," Journal of the Structural Engineering Division, ASCE, Vol 104, No. 58, August.
13. Esteva, Luis and Villaverde, R., 1973, "Seismic Risk, Design Spectra and Structural Reliability", Proceedings 5th World Conference on Earthquake Engineering, Rome, Italy, pp. 2586-2596.
(note: not in published preprints)
14. Guzman, R., and Jennings, P.C., 1976, "Design Spectra for Nuclear Power Plants", Journal of the Power Division, ASCE, No P02, November.

15. Hall, W. J., Mohraz, B., and Newmark, N. M., 1976, "Statistical Studies of Vertical and Horizontal Earthquake Spectra", prepared for the United States Nuclear Regulatory Commission, NUREG-003, January.
16. Hanks, T.C., and Johnson, D.A., 1976, "Geophysical Assessment of Peak Accelerations", Bulletin of the Seismological Society of America, Vol. 66, No. 4, August, pp. 1155-1158.
17. Herrera, I and Rosenblueth, E., 1965, "Response Spectra on Stratified Soil" Proceedings of 3rd World Conference on Earthquake Engineering, Auckland & Wellington, New Zealand, pp. I44-I60.
18. Herrera, I, Rosenblueth, E., and Rascon, O. A., 1965, "Earthquake Spectrum Prediction for the Valley of Mexico" Proceedings of 3rd World Conference on Earthquake Engineering, Auckland & Wellington, New Zealand, pp. I61-I74.
19. Idriss, I.M., 1978, "Ground Motion - State-of-the-Art" to be published in Volume 3 of Proceedings of ASCE Specially Conference Earthquake Engineering and Soil Dynamics, Pasadena, California, June 19-21.
20. Jennings, P. C. & Guzman R., 1975, "Seismic Design Criteria for Nuclear Powerplants", Proceedings of the United States National Conference on Earthquake Engineering, Ann Arbor, Michigan, June, pp. 474.
21. Kanai, Kiyoshi, "Relations between the Nature of Surface Layer and Amplitudes of Earthquake Motions: Parts I to IV", Bulletin of the Earthquake Research Institute, Tokyo University.
 Part I: Volume 30, 1952, pp. 31-37
 Part II: Volume 31, 1953, pp. 219-226.
 Part III: Volume 31, 1953, pp. 276-279.
 Part IV: Volume 34, 1956, pp. 167-183.
22. McGuire, Robin K., 1974, "Seismic Structural Response Risk Analysis, Incorporating Peak Response Regressions on Earthquake Magnitude and Distance", School of Engineering, Massachusetts Institute of Technology, Cambridge, Mass. 02139, R74-51 Structures Publication 99.
23. McGuire, Robin K., 1978, "Seismic Ground Motion Parameter Relations" Journal of the Geotechnical Engineering Division, ASCE Vol 104, No. GT4, Proc. Paper 13661, April, pp. 481-490
24. Merz, H. A., and Cornell, C. A., 1973, "Seismic Risk Analysis Based on a Quadratic Frequency Law", Bulletin of the Seismological Society of America, Volume 63, No. 6, December, pp. 1999-2006.
25. Mohraz, B., 1976, "A Study of Earthquake Response Spectra for Different Geological Conditions", Bulletin of the Seismological Society of America, Vol. 66, No. 3, June, pp. 915-935.

26. Newmark, Nathan M., 1973, "A Study of Vertical and Horizontal Earthquake Spectra" Report prepared for the Directorate of Licensing, United States Atomic Energy Commission Report WASH-1255, April.
27. Newmark, N. M., and Hall., W. J., 1969, "Seismic Design Criteria for Nuclear Reactor Facilities", Proceedings of the Fourth World Conference on Earthquake Engineering, Santiago, Chile, Volume II, pp. B4 37-50.
28. Nuttli, O. W., 1973, "State-of-the-Art for Assessing Earthquake Hazards in the United States" Miscellaneous Paper 5-73-1, U.S. Army Engineer Waterways Experiment Station, Vicksburg, Mississippi, January.
29. Page, Robert A., Boore, David M., Joyner, William B., and Coulter, Henry W., 1972, "Ground Motion Values for Use in the Seismic Design of the Trans-Alaska Pipeline System", U.S. Geological Survey, No. 672.
30. Page, Robert A., 1977, "Correlation of Peak Acceleration with Earthquake Magnitude, Epicentral Distance and Site Conditions", presentation to Advisory Committee on Reactor Safeguards, Seismic Activity Subcommittee Meeting, February 8 in Bethesda, Maryland.
31. Schnabel, P.B., Lysmer, J., Seed, H., Bolton, 1972, "SHAKE -a computer program for earthquake response analysis of horizontally layered sites" Earthquake Engineering Research Center Report No. EERC 72-12, Univeristy of California, Berkeley, December.
32. Schnabel, Per B., and Seed, H., Bolton, 1973, "Accelerations in Rock for Earthquakes in the Western United States", Bulletin of the Seismological Society of America, Vol. 63, No. 2, April, pp. 501-516.
33. Seed, H., Bolton, & Idriss I.M., 1968, "Influence of Soil Conditions on Ground Motions during Earthquakes" State-of-the-Art Symposium, Earthquake Engineering Research Institute, San Francisco, California, February.
34. Seed, H., Bolton, Ugas, C., and Lysmer, J., 1976, "Site Dependent Spectra for Earthquake-Resistant Design", Bulletin of the Seismological Society of America, Vol. 66, No. 1, February, pp. 221-244.
35. Seed, H.B., Murarka, R., Lysmer, J., and Idriss, I.M., 1976, "Relationships between maximum acceleration, maximum velocity, distance from source and local site conditions for moderately strong earthquakes", Bulletin of the Seismological Society of America, Vol. 66, No. 4, pp. 1323-1342.

36. Streeter, J. L., Wylie, E. B., and Richart, F. E., Jr., 1974, "Soil Motion Computations by Characteristic Methods", Journal of the Geotechnical Engineering Division, ASCE, Vol 100, No. GT3, March, pp. 247-263.
37. Taylor, Peter W., and Larkin, Thomas J., 1978, "Seismic Site Response of Nonlinear Soil Media", Journal of the Geotechnical ASCE, Vol, 104, No. GT3, Proc. Paper 13597, March. pp. 369-583.
38. Tsai, Nien-Chien, 1972, "Spectrum-Compatible Motions for Design Purposes", Journal of the Engineering Mechanics Division, ASCE, Vol. 98, No. EM2, Proc. Paper 8807, April, pp 345-356.

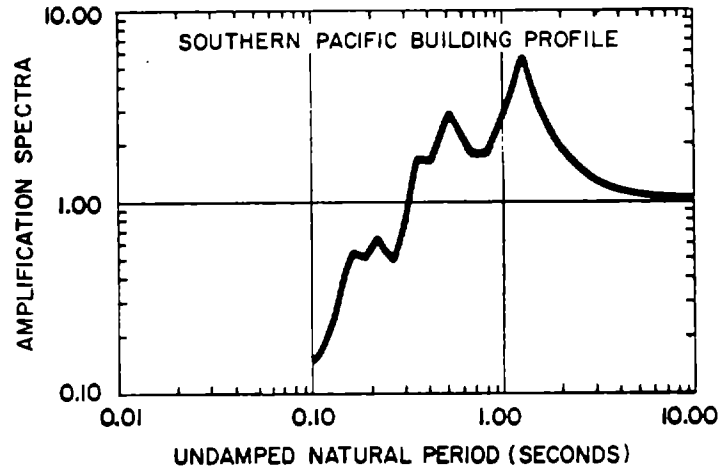


Fig. 1. Computed amplification spectra for the Southern Pacific Building site, San Francisco.

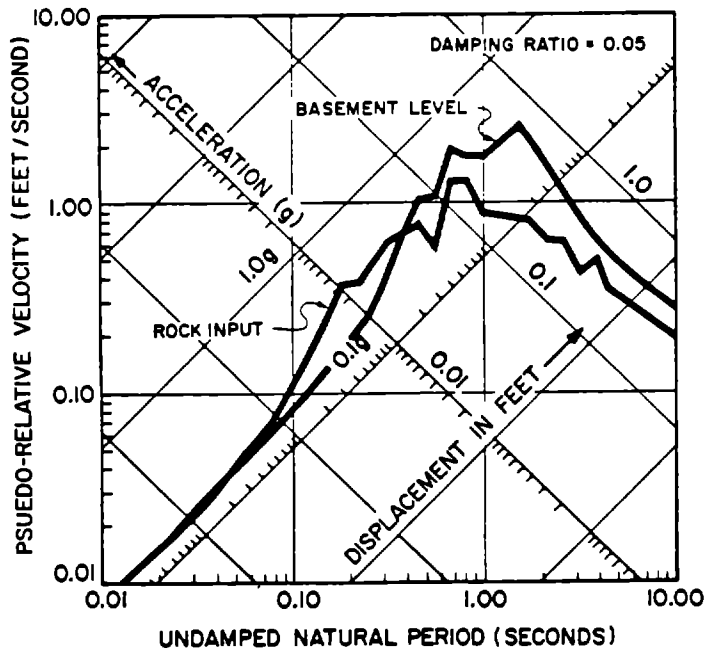


Fig. 2. Response spectra of input motion used at rock level and the computed basement level motion for the Southern Pacific Building site. The input motion was the N21E component of the Taft record for the July 21, 1952, Kern County earthquake. Linear analysis using program SHAKE.

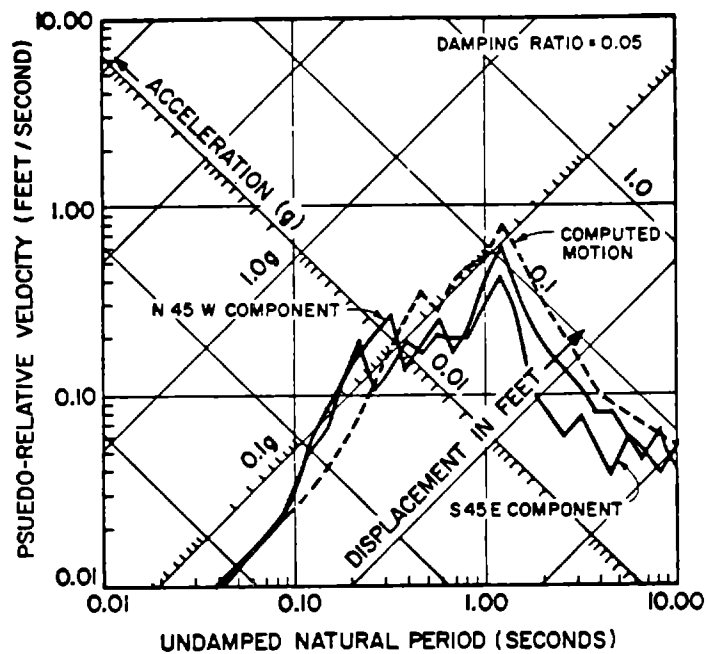


Fig. 3. Comparison of computed basement level motion response spectrum with the response spectra of motions recorded during the March 22, 1957 earthquake.

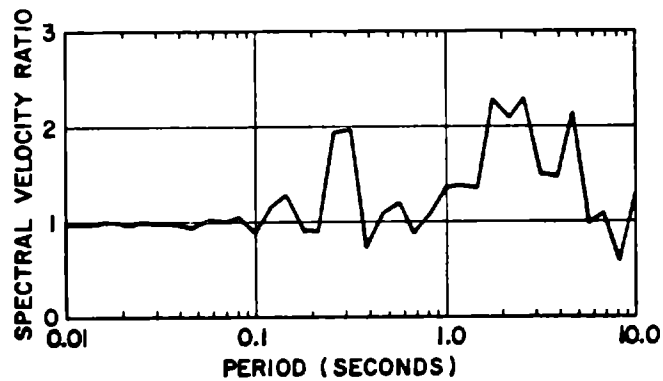


Fig. 4. Ratio of spectral amplitudes for the two recorded components of March 27, 1957 recorded in Southern Pacific Building basement: Ratio of N45W spectrum divided by N45E spectrum. Both spectra have a damping ratio of 0.05.

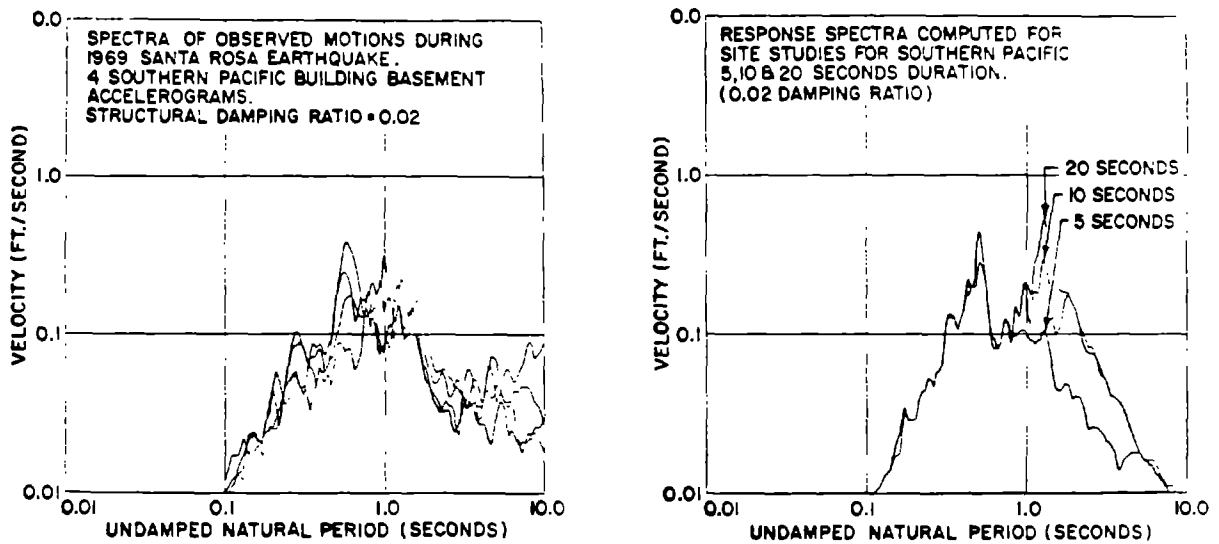


Fig. 5. Response spectra recorded at basement level in Southern Pacific Building during the 1969 Santa Rosa Earthquakes compared with response obtained by one dimensional site study.

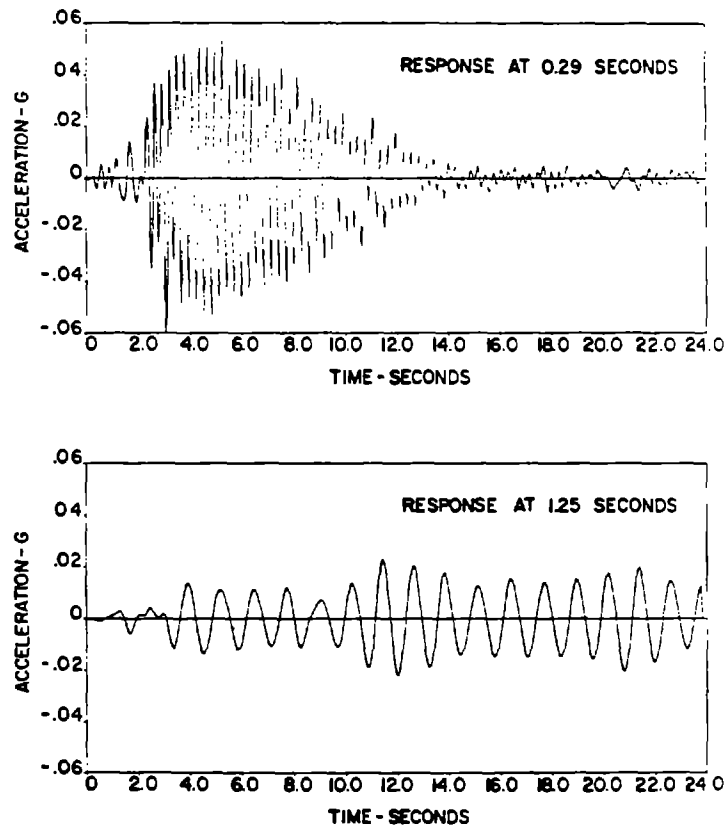


Fig. 6. Response time histories for one component of 1969 Santa Rosa record. The occurrence of the peak values at different times shows the dispersion of the wave motion between the source and the recording site.

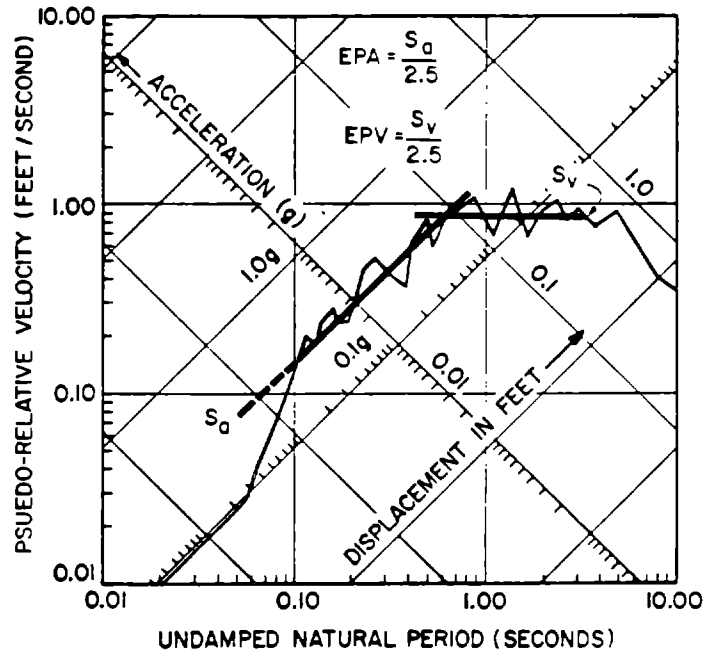


Fig. 7. Illustration of how Effective Peak Acceleration (EPA) and Effective Peak Velocity (EPV) are defined from a response spectrum with 5 percent damping.

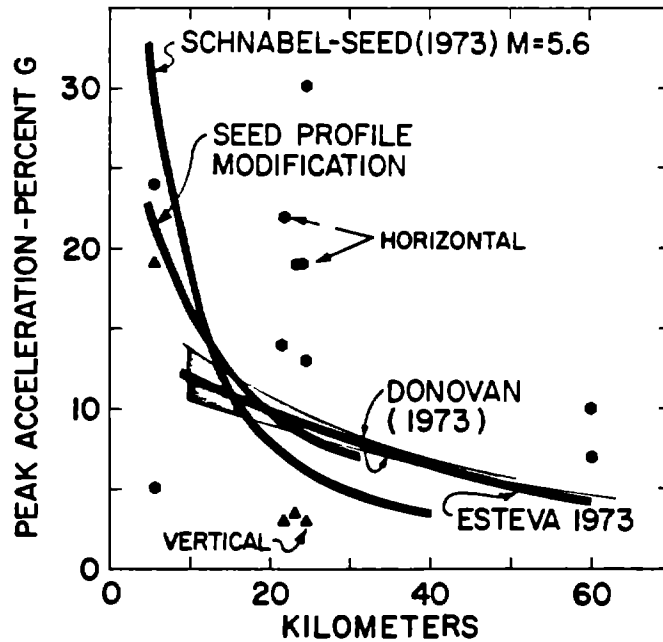


Fig. 8. Peak accelerations recorded during a magnitude 5.5 event near Ferndale California on June 7, 1975. The inability of available attenuation relationships to predict these peak motions is readily apparent.

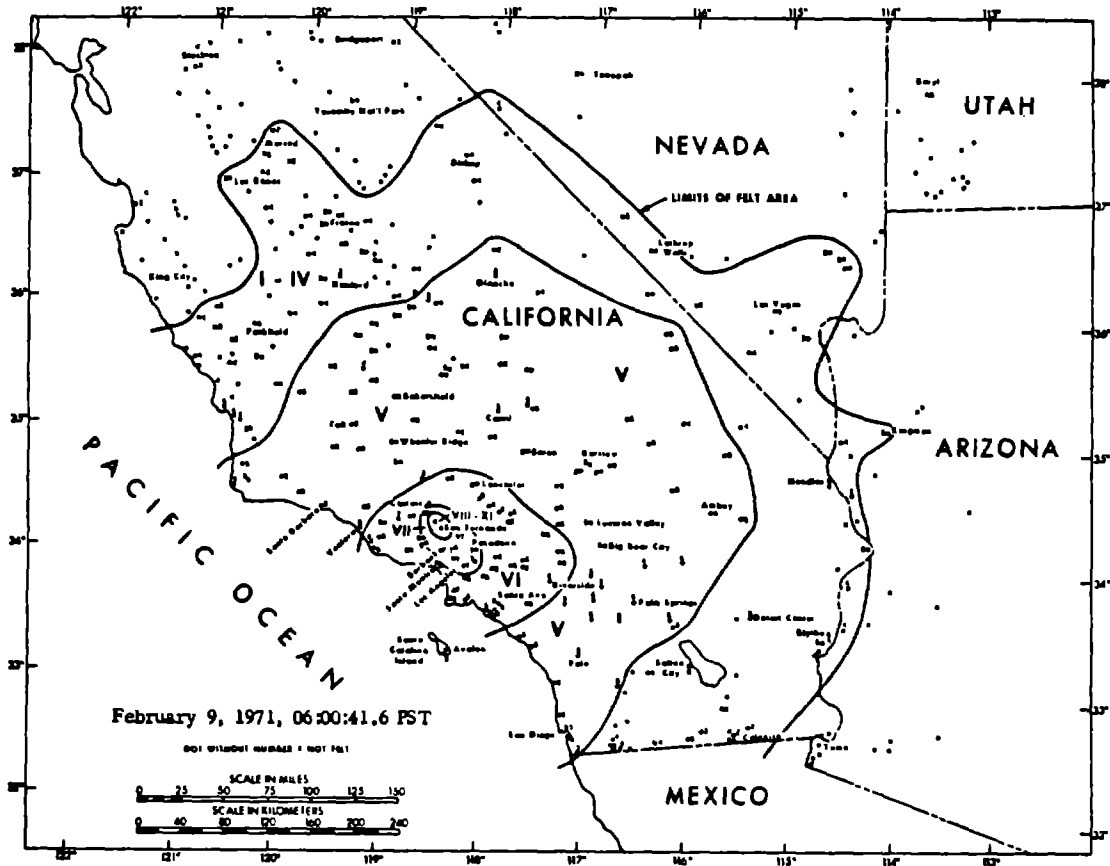


Fig. 9. Isoseismal map of the Feb. 9, 1971 San Fernando event.
Map prepared by the United States Coast and Geodetic Survey.

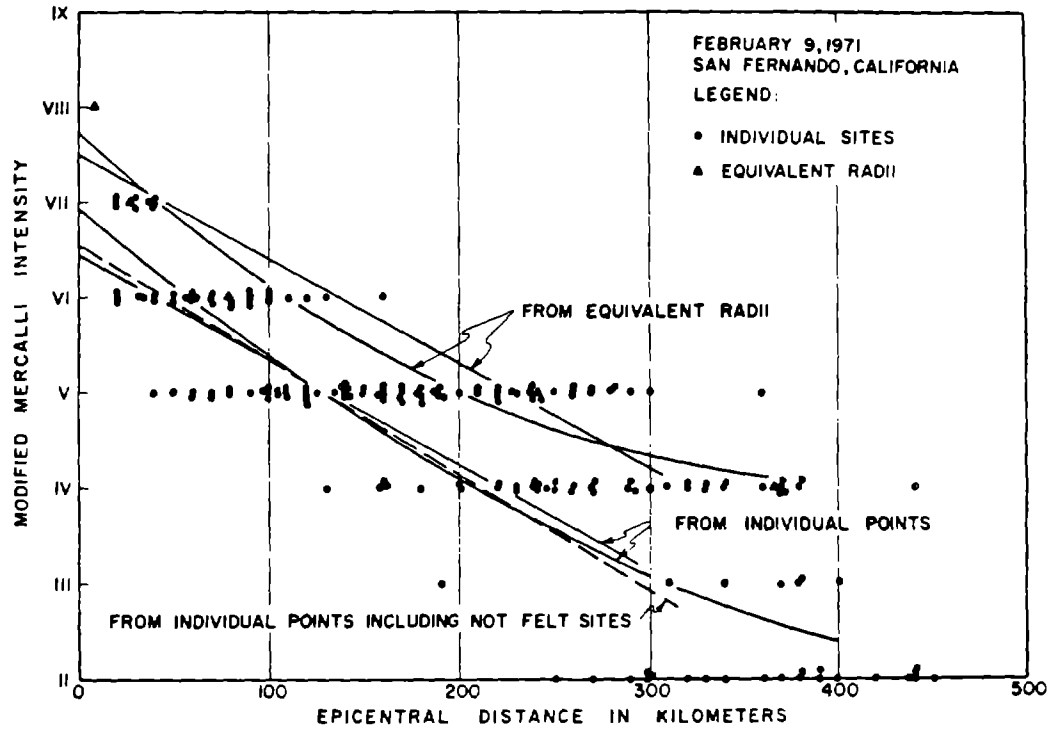


Fig. 10. Comparison of attenuation of Modified Mercalli Intensity with distance using equivalent radii computed from isoseismals and by using individual data points.

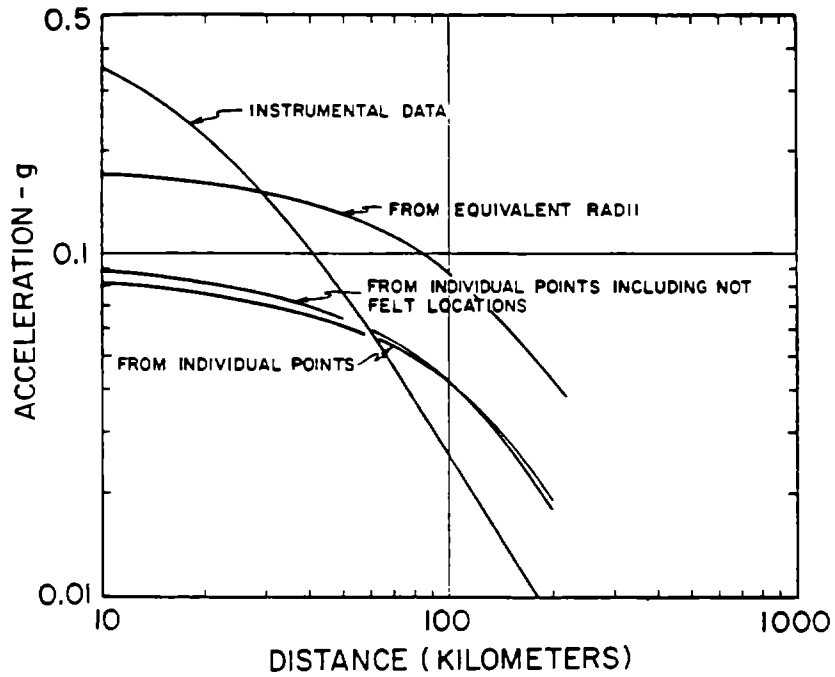


Fig. 11. Acceleration attenuation computed from MMI attenuation are compared with observed acceleration attenuation. All curves are based on mean relationships and suggest that instrumental peak acceleration may be a poor measure of the strength or damage potential of an earthquake in the near field.

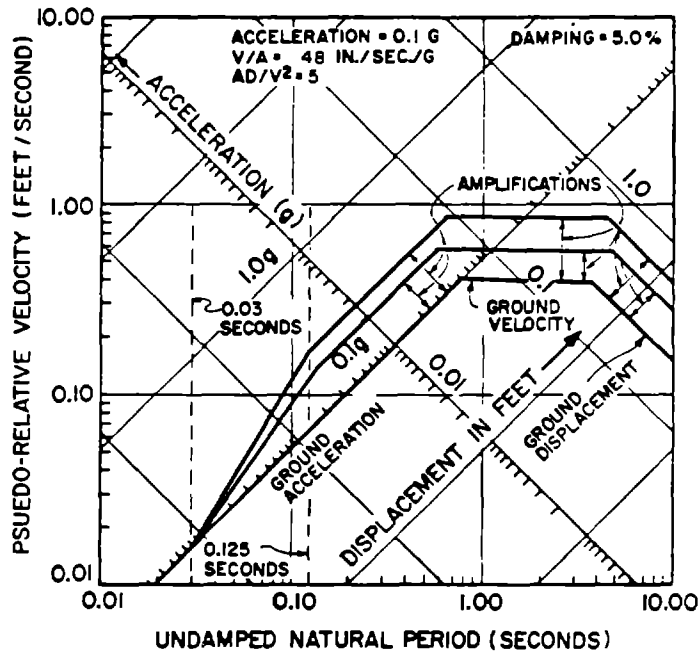


Fig. 12. Method used to construct response spectra on tripartite graph paper using ground motion parameters and spectral amplification values. Response spectra shown represent the mean and 84 percentile relationships.

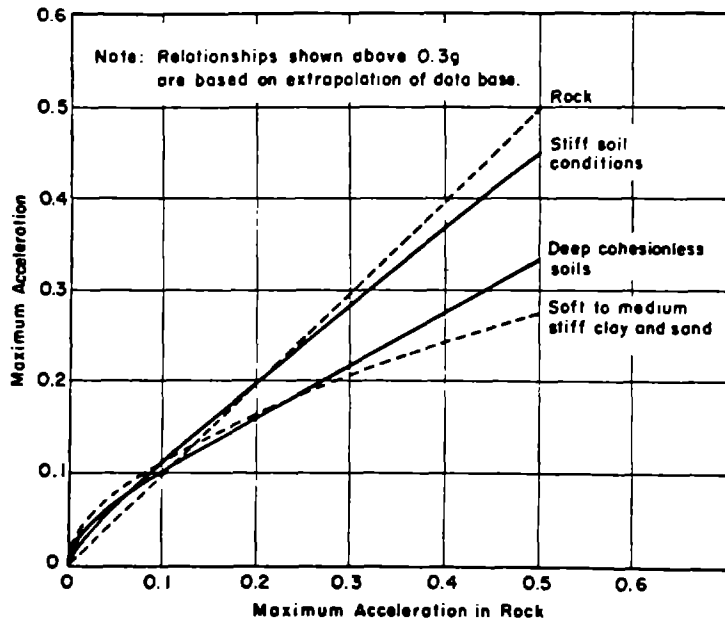
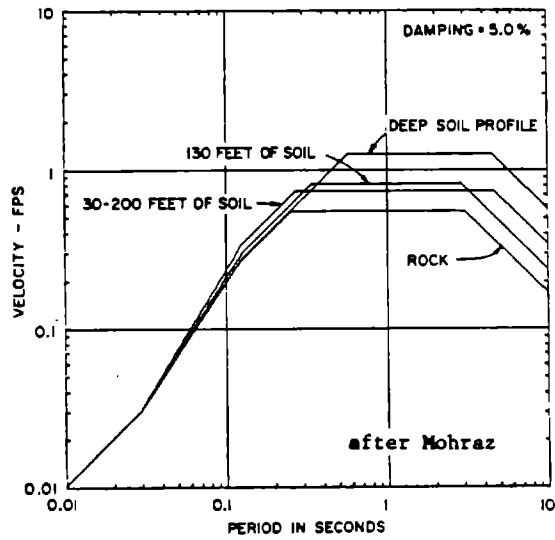
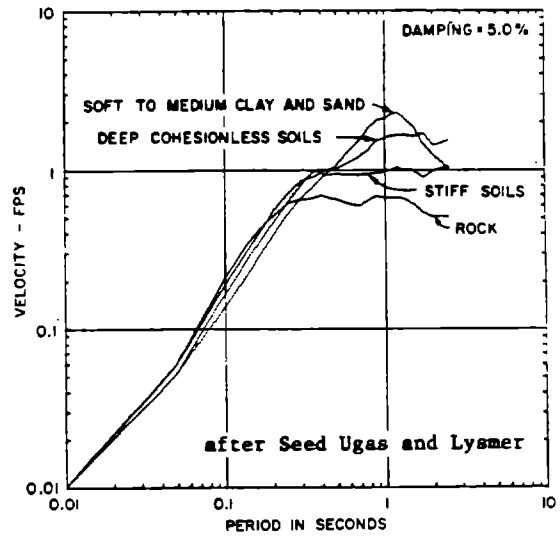


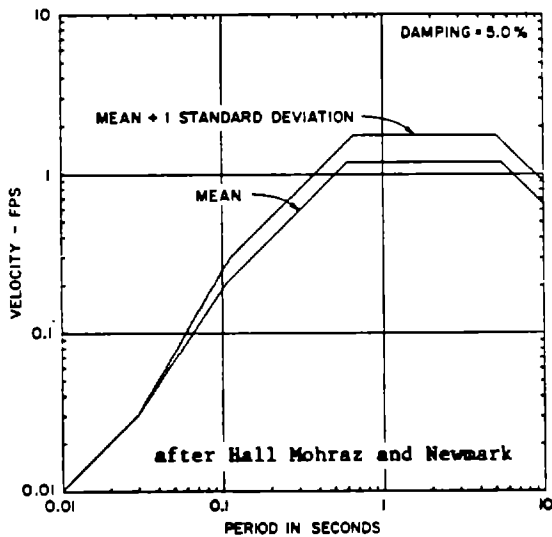
Fig. 13. Typical relationship between acceleration on rock and other local site conditions [after Seed et al (34)].



14 (a)



14 (b)



14 (c)

Fig. 14. Recommended average response spectra for different site conditions. All spectra have been normalized to a ground acceleration of 0.2g.

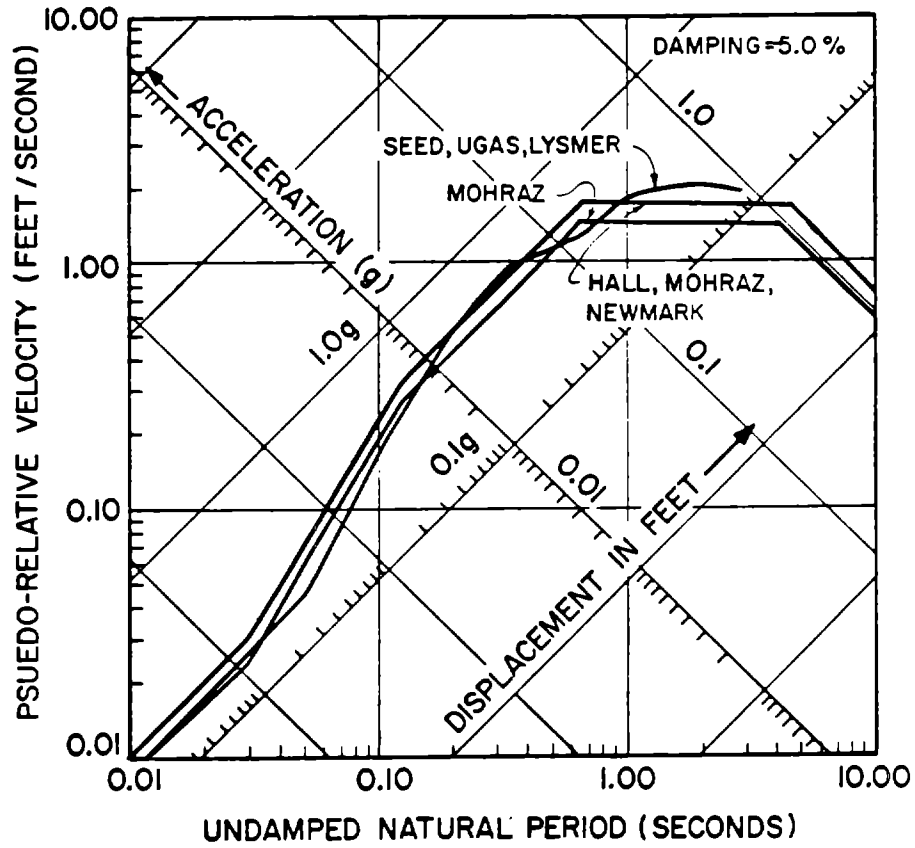


Fig. 15. Recommended design response spectra for a deep soil profile with a surface acceleration of 0.16g based on criteria recommended in this paper and spectra from Newmark, Mohraz and Seed.

SOIL DYNAMICS CONSIDERATIONS FOR MICROZONATION

by

M. A. Sherif^I and I. Ishibashi^{II}

ABSTRACT

Microzonation for earthquake effects involves the determination of relevant site characteristics and their incorporation into land-use planning and the design of earthquake-resistant structures to reduce damage to human life and property in the event of seismicity. The engineering behavior of soils plays an important role in the microzonation of regions for earthquake effects. In considering soil effects that enter into seismic microzonation, engineering interest focuses on assessing (1) soil liquefaction potential, (2) soil densification characteristics, (3) loss of soil strength due to dynamic loading and (4) shear moduli and damping properties of soils. The first three soil factors provide information on the strength and stability of the soil deposits in the area, while the fourth (shear moduli and damping) is used in analytical estimation of ground response, from which the magnitudes of accelerations, and hence the forces to which the structures in the area will be subjected during earthquakes, are determined.

I. SOIL LIQUEFACTION

Liquefaction is recognized as a phenomenon whereby certain sands and sandy soils totally lose their supportive capacity and behave almost like liquids under dynamic or earthquake-type loading. Liquefaction in sands is brought about to a great extent as a consequence of pore-pressure buildup and to a lesser extent due to favorable reorientation of soil particles in such a way that the soil-water system enters a stage at which it exhibits least resistance to applied forces. In engineering practice the soil is considered to have liquefied when the pore-pressure rise reaches the value of the total overburden stresses on the soil. When this happens, the strength of the soil reduces to zero, as indicated in Eq. 1.

$$\tau = (\sigma_T - u)\tan\phi \quad (1)$$

where τ = shear strength; σ_T = total overburden pressure; u = pore pressure; and ϕ = angle of internal friction.

I.1. Preliminary Evaluation of Site Liquefaction Potential

In order to make a preliminary assessment of the liquefaction potential of soil deposits over a large area in a seismically active region, it is suggested that the following preliminary liquefaction-potential evaluation procedure, outlined in Fig. 1, be followed. First, field investigations are conducted to determine whether any liquefiable soils exist within 50 feet below the ground surface (sand, silty sand and clayey sand

-
- I Professor of Civil Engineering and Adjunct Professor of Quaternary Research, University of Washington, Seattle, Washington
 II Research Assistant Professor of Civil Engineering, University of Washington, Seattle, Washington.

are liquefiable; clay, silt, loam, organic soil, gravel and others are less susceptible to liquefaction). The second step is to see whether the above-determined liquefiable soils lie below or above the water table. Liquefaction is considered less of a problem if the liquefiable soils lie above the water table. There is evidence to suggest that if a non-liquefiable soil layer extends to a depth of 10 feet or more immediately below the ground surface, structures founded on it do not suffer appreciable damage, even if liquefiable soils exist below the non-liquefiable surface soil layer (Ishihara, 1973). Next, if the grain-size distribution curves are available, screening is performed to determine whether the gradation of the liquefiable soil falls within the liquefaction-susceptible range, as shown in Fig. 2. The last step in preliminary liquefaction evaluation involves checking the standard penetration blow count N at the site. Several critical curves regarding N_{CR} have been proposed. Fig. 3 shows envelopes of those curves, which could be used for liquefaction evaluation. By using the above process of evaluation and coupling it with the geological map and seismological data on the area, the sites could be zoned on a preliminary basis into liquefiable, questionable, and non-liquefiable categories.

I.2. Detailed Evaluation of Site Liquefaction Potential

When engineers require more accurate information regarding soil liquefaction potential under an important structure, detailed liquefaction evaluation could be carried out by (1) using an analytical prediction involving the time history of pore-pressure buildup in saturated sands, or (2) comparing the induced shear stresses (calculated through response analysis) with the shear stresses causing soil liquefaction during laboratory testing under uniform cyclic shear loading. Each of the above procedures is discussed in the following paragraphs.

Prediction of Time History of Pore-Pressure Buildup

Several analytical methods of predicting the time history of pore-pressure generation leading to assessment of liquefaction potential of saturated sands have been proposed, by Martin et al. (1975), Seed et al. (1975), Ishihara et al. (1976), Liou et al. (1976), Ishibashi et al. (1977), and Ghaboussi and Dikmen (1978). Most recently, Sherif et al. (1978) proposed a detailed analytical procedure for predicting the time history of pore-pressure buildup in dense, medium dense and loose saturated sands as expressed by Eq. 2. It is significant to note that Eq. 2 is a general equation which applies to all kinds of loadings, including the random earthquake type.

$$(\Delta U_N^*)_p = (1 - U_{N-1}^*) \cdot \frac{C_1(N_{eq})_p}{(N_{eq})_p^{C_2} - C_3} \cdot \left(\frac{\tau_{Np}}{\sigma'_{N-1}} \right)^\alpha \quad (2-a)$$

$$(N_{eq})_p = \sum_{i=1}^N \left(\frac{\tau_{ip}}{\tau_{Np}} \right)^\alpha \quad (2-b)$$

$$(\Delta U_N^*)_n = (1 - U_{N-1}^*) \cdot \frac{C_1(N_{eq})_n}{(C_{eq})_n^{C_2} - C_3} \cdot \left(\frac{\tau_{Nn}}{\sigma'_{N-1}} \right)^\alpha \quad (2-c)$$

$$(N_{eq})_n = \sum_{i=1}^N \left(\frac{\tau_{in}}{\tau_{Nn}} \right)^\alpha \quad (2-d)$$

$$U_N^* = U_{N-1}^* + \frac{1}{2} \left[(\Delta U_N^*)_p + (\Delta U_N^*)_n \right] \quad (2-e)$$

where $(\Delta U_N^*)_p$ or $(\Delta U_N^*)_n$ are normalized pore-pressure increments per cycle (pore-pressure rise divided by the initial confining pressure) in positive or negative shear stress regions under cyclic shear stresses τ_{Np} or τ_{Nn} during the Nth cycle; and U_{N-1}^* and U_N^* are normalized pore pressures at the end of the (N-1)th and Nth cycles. The terms $(N_{eq})_p$ and $(N_{eq})_n$ are equivalent numbers of cycles in positive and negative regions. The term σ_{N-1}^* is the effective confining pressure at the end of the (N-1)th cycle; and α , C_1 , C_2 and C_3 are material constants which are functions of void ratio or density, as shown in Fig. 4.

To apply Eqs. 2-a through 2-e in practice, an illustrative problem is shown in Fig. 5, in which the top graph shows the time history of an earthquake-induced shear stress at a given depth in a soil mass with a void ratio $e = 0.70$. Corresponding to $e = 0.70$ in Fig. 4, the material constants C_1 , C_2 , C_3 and α are determined to be 6.13, 1.77, 0.46 and 2.40 respectively. If the stress time history and material constants are known, the values of the pore pressures at the end of each cyclic stress can be calculated by following the procedure outlined in Fig. 6. Fig. 5(b) shows a plot of the normalized pore-pressure rise as a function of time under the above stress history. It is seen from this figure that at the end of the third cycle the value of the normalized pore pressure U_N^* is 0.465.

Fig. 7 shows a comparison between the actual pore-pressure buildup in saturated Ottawa sand under random loading in the laboratory and that predicted by Eq. 2.

If at any time during the time history of an earthquake the value of U_N^* in Eq. 2-e approaches unity, the soil will liquefy under that given earthquake loading. For example, under the earthquake stress history shown in Fig. 7, the soil in that area will not totally liquefy, since the maximum value of U_N^* during the time history of the earthquake is 0.55.

Liquefaction Assessment by Stress-Comparison Method

This method involves comparing the stresses causing liquefaction during laboratory testing with the expected earthquake-induced shear stresses (calculated by response analysis). The detailed analysis could be carried out according to the procedure outlined in Fig. 8.

Step I

This step involves field investigation; soil sampling and determination of soil depth and stratification; and laboratory testing for the determination of shear modulus G , damping ratio λ , soil density γ and other relevant soil properties for use in site-response calculations in Step III.

Step II

This step is normally carried out in conjunction with Step I, and it involves the study of seismic history and the location of active fault lines with respect to the site, for the purpose of establishing a design bedrock acceleration history.

Step III

This step involves conducting laboratory liquefaction tests to determine the magnitudes of the shear stresses that cause liquefaction of the soil in the laboratory as a function of the number of uniform shear stress cycles.

Based on the liquefaction test results obtained, a liquefaction-potential curve is established as a function of soil type and relative density. One such series of curves is shown in Fig. 9. Engineers should be cautioned as to the unreliability of the present relative-density determination procedures, as cited by Finn (1972). In view of the fact that liquefaction potential is highly sensitive to variations in relative density, it is apparent that a serious need exists for the development of a viable standard test procedure for relative-density determination that would yield more consistent results than those now being used.

In presenting liquefaction-potential curves, such as those in Fig. 9, Ishibashi and Sherif (1974) recommend the use of $\Delta\tau_{\max}/\sigma_{\text{oct}}$ on the vertical axis because when the data are presented as such, the resulting liquefaction-potential curves become independent of the coefficient of earth pressures at rest, as shown in Fig. 10.

The uniqueness of the $\Delta\tau_{\max}/\sigma_{\text{oct}}$ parameter for determining liquefaction potential of sand under isotropically and anisotropically consolidated conditions can be used to establish a correlation between the simple or torsional shear test data and the triaxial test data, as shown below.

$$\left(\frac{\tau_{\text{vh}}}{\sigma_{\text{vo}}} \right) \text{ in simple shear} = \frac{1 + 2K_0}{3} \cdot \left(\frac{\sigma_{\text{dp}}}{2\sigma_{\text{vo}}} \right) \text{ in triaxial} \quad (3-a)$$

$$C_r = \frac{1 + 2K_0}{3} \quad \text{or} \quad \tau_{\text{vh}} = C_r \cdot \frac{\sigma_{\text{dp}}}{2} \quad (3-b)$$

where τ_{vh} = cyclic shear stress on horizontal plane in simple shear or torsional shear; σ_{vo} = initial effective vertical confining stress in triaxial, simple and torsional shear tests; σ_{dp} = dynamic deviatoric stress in triaxial testing; K_0 = coefficient of lateral earth pressure at rest; and C_r = correlation factor.

In Fig. 11 the reporters have plotted the correlation factor in Eq. 3-b against the coefficient of earth pressure at rest K_0 and obtained the solid line. Fig. 11 also includes the correlation factors suggested by other researchers. It is evident from this figure that the correlation factor $C_r = (1 + 2K_0)/3$ provides reasonable representation of the cumulative research data to date; therefore, it is proposed that the above correlation

factor be utilized for all practical purposes to translate simple-shear data to triaxial and vice versa.

Step IV

Complete site-response analysis could be performed by the lumped-mass technique (Seed and Idriss, 1969), the wave-propagation method (Schnabel et al., 1972), or the finite-element method (Idriss et al., 1973). Finn et al. (1976) performed effective stress-response analysis utilizing the lumped-mass method and introducing the pore-pressure generation equation developed by Martin et al. (1975). Using any of these response analyses, the time history of shear stress can be calculated at any depth of soil deposit. In all of these analyses, the equivalent dynamic shear modulus G_{eq} and soil damping ratio λ had to be used in the calculations.

To translate the earthquake stresses determined by any of the above methods into laboratory experiments, Seed and Idriss (1971) have proposed that an equivalent uniform shear stress equaling $0.65 \times \tau_{max}$ be applied on the soil during laboratory liquefaction study, where τ_{max} is the maximum shear stress induced in the soil during an earthquake. The above investigators also proposed the following relationship between the magnitudes of earthquakes and the corresponding numbers of significant cycles:

Earthquake Magnitude	7.0	7.5	8.0
Number of Significant Stress Cycles	10.0	20.0	30.0

Based on analyses of many earthquakes, Lee and Chan (1972) suggested the use of $0.75 \times \tau_{max}$ and the following corresponding numbers of significant stress cycles:

Earthquake Magnitude	5.0	5.5	6.0	6.5	7.0	7.5	8.0
Number of Significant Stress Cycles	5.0	6.0	7.5	9.5	12.0	15.5	20.0

A comparison between these two sets of data (Fig. 12) implies that liquefaction will occur under slightly smaller earthquakes than suggested by Seed and Idriss.

Even though the Lee and Chan proposal represents an advancement over the procedure previously suggested by Seed and Idriss, further research in this area is in order, especially in view of the fact that the pore pressures generated in the soil deposit are very much influenced whether the peak stresses are introduced into the ground at the beginning or at later stages of an earthquake. Ishibashi et al. (1977) have shown that the pore pressures generated in the soil deposit are higher if the peak stresses are introduced near the beginning of an earthquake.

Step V

This step involves a comparison between the induced equivalent uniform earthquake shear stresses throughout the soil profile, as determined in Step IV, and the uniform shear stresses causing liquefaction during laboratory tests, established in Step III.

By comparing shear stresses causing liquefaction in the laboratory with the induced shear stresses in the soil deposit, a determination is made regarding the liquefiability of a soil deposit in a particular site.

II. SOIL DENSIFICATION

During seismic vibration, cohesionless soils densify and produce settlement of the ground surface. Excessive settlement can cause severe damage to structures of all kinds.

II.1. Settlement of Dry Sands

There is conflicting research information on the densification of dry sands. Seed and Silver (1972) have assumed that the effects of vertical vibration on densification are almost negligible until it exceeds 1.0g and that the overburden pressure does not significantly affect soil settlement. Later, in 1975, Pyke et al. conducted shaking-table experiments and found that (1) the settlement caused by combined horizontal motions is almost the same as the sum of the settlements caused by each component acting separately; and (2) while vertical acceleration of less than 1.0g induces no appreciable settlement by itself, it causes marked increase in settlement (about 50%) when superimposed on horizontal acceleration. This finding suggests that actual field settlement could be three times as great as would be predicted by the earlier Seed and Silver method.

Finn and Byrne (1976) studied the effects of relative density, surcharge loads, and maximum base acceleration on densification of dry sands under earthquake-type random loading by using the equation of volumetric strain increment for liquefaction study that was originally developed by Martin et al. (1975). Their results showed that even very dense, dry sands ($D_r = 80\%$) settle under cyclic loading and that the structures on top of the sand increase the total ground settlement, thus implying that free field settlement of sands provides a lower bound to the settlement to be expected under a structure during an earthquake.

In view of the practical importance of the subject matter, and because of the conflicting points of view at the present time, there is a definite need for research in this area.

II.2. Settlement of Saturated Sands

When saturated sands are subjected to cyclic shear loading in drained conditions, they undergo densification. Youd (1972) showed from simple-shear tests that the effect of initial moisture content on the final void ratio reached is negligible during drained tests, and that the effects of vertical stress and frequency on densification are almost insignificant. In contrast, Krizek and Fernandez (1971) showed that the initial moisture content significantly influences the maximum vibratory density attained.

Lee and Albaisa (1974) investigated settlement due to pore-pressure dissipation following partial and complete liquefaction. In these studies, pore pressures were generated in saturated undrained cyclic triaxial tests. The tests were stopped after a certain number of cycles and the pore pressures were allowed to dissipate. The investigators found that the amount of volume change was dependent only on the magnitude of excess pore pressure, irrespective of the type of cyclic loading. They also concluded that the effects of confining pressure and relative density on volume

change are small and that the effect of grain size is quite important. The above investigators also found that the cyclic volumetric strains the soil undergoes after it has been dynamically excited can be determined by static tests, provided that the magnitude of the maximum pore pressure generated during dynamic loading is known. The static tests involve applying on the soil samples back-pressure equal in magnitude to those that may have been induced by dynamic loading, and measuring the volume changes in the sample after the drainage lines are opened.

Settlement of a model building on saturated sands during vibration was investigated by Yoshimi and Tokimatsu (1977) on a shaking table. Yoshimi et al. concluded that (1) the amount of settlement under a heavy structure is more dependent on soil density than under a light structure; and (2) artificial lateral confinement (by sheet piles, for example) of the soil immediately beneath the building reduces building settlement due to liquefaction.

Based on the above information, it appears that certain procedures and methodologies are now available to assist engineers to a limited extent in assessing densification characteristics of soil for microzonation purposes. Further research in soil-structure interaction effects, the effect of multi-directional shaking, and the influences of initial moisture content on final settlement could provide highly useful information for practical design and land-use planning purposes.

III. LOSS OF SOIL STRENGTH

Certain soils lose strength when subjected to repeated dynamic loading. In some cases, the loss of strength is partial, and in others it is total, such as during liquefaction of saturated sands. The quantitative measure of partial loss of strength is expressed by the cyclic strength ratio, which is defined as the ratio of the undrained static shear strength (after dynamic excitation) to the undrained static strength of the soil (prior to dynamic loading).

Lee and Focht (1976) collected previously published data and presented it as the cyclic stress ratio (applied cyclic stress S_p to undrained static shear strength S_u) versus the number of cycles to failure n_{cf} , as shown in Fig. 13. This figure includes data from cyclic simple shear and cyclic triaxial tests for both consolidated undrained (CU) and unconsolidated undrained (UU) tests obtained at frequencies ranging from 0.1 to 2Hz. It is apparent from Fig. 13 that the number of cycles necessary to fail these soils under a given S_p/S_u ratio is a function of soil type and that in all cases it is possible to fail these soils under relatively low dynamic stresses if a sufficiently large number of cycles is applied. The fact that each of the curves in Fig. 13 appears to flatten out and assume nearly a constant ratio at higher n_{cf} implies that for each soil there exists a threshold dynamic stress level that does not cause failure, regardless of the number of times the loads are applied on the sample.

In most practical cases the applied stress ratio S_p/S_u is not large enough to cause total loss of strength within a short time span; and yet the soil does undergo partial strength reduction as a consequence of dynamic excitation. When this happens, natural and man-made clayey slopes fail, with resulting adverse social and economic consequences. For this reason, it is important that the amount of strength loss cohesive soils exhibit as a result of dynamic loading be known.

Based on the static and cyclic strain-controlled triaxial compression test results on San Francisco Bay mud and Anchorage silty clay, Thiers and Seed (1969) concluded that the application on any soil of a peak cyclic strain of less than one-half of the static failure strain would result in retention of 80% of the soil's original static shear strength, as shown in Fig. 14. In the above study, the researchers applied cyclic strains for 200 cycles at 1Hz for each of the soils tested.

Castro and Christian (1976) interpreted Thiers and Seed's curve to mean that 90% of the original shear strength would be recovered, so long as the applied cyclic strain was less than one-half the static failure strain. In fact, Castro et al. concluded from their study that the cyclic strength is equal or very close to the static undrained strength for saturated soils subjected to stress-controlled triaxial tests.

Lee and Focht (1976), based on limited studies on North Sea soils, concluded that essentially no, or minimal, reduction in strength would occur if the applied dynamic strains were less than 50% of the static failure strain. Two of the data points obtained by Lee and Focht are shown in Fig. 14.

Koutsoftas (1978) studied the strength loss of two marine clays, one normally consolidated and the other overconsolidated, in a stress-controlled triaxial device. He concluded that as the imposed strain ratio increases, the reduction in undrained shear strength also increases; and yet, even at large strain ratios, the reduction in undrained shear strength is relatively small (between 10% and 20%), as shown in Fig. 14, and not as large as previously reported by Thiers and Seed.

The results obtained by Sherif et al. (1976B and 1977B) from tests conducted on Northwest Pacific pelagic marine clays which came from an area where the depth of water was about 22,000 feet, showed that these soils lose strength even if the applied dynamic strain is as low as 10% of the static failure strains (see Fig. 14). Furthermore, Sherif et al. have found that the amount of strength loss was very much dependent on the number of strain cycles applied, as well as on the magnitudes of effective confining pressures, as shown in Fig. 15.

It should be apparent from the above discussion that there is a considerable amount of diversity in laboratory test data on the subject of loss of soil strength due to dynamic loading. In view of the importance of the subject for the design of safe structures in terrestrial and marine environments, further research in this area is extremely desirable.

IV. DYNAMIC SHEAR MODULI AND DAMPING

The analytical procedures, such as the lumped-mass, wave-propagation and finite-element methods, used in the determination of ground response during earthquakes, require a knowledge of dynamic shear moduli and damping. In this section the current knowledge on these two important soil parameters is discussed.

When soil is subjected to high earthquake strain levels, it behaves in a non-linear fashion. Fig. 16 shows a non-linear shear stress-strain relationship for a soil under dynamic loading. To take this non-linear behavior into consideration in practice, the soil behavior can be represented by an equivalent linear model, where the slope of the line AO in

Fig. 16 represents the equivalent shear modulus G_{eq} , and the equivalent damping ratio λ_{eq} is defined as:

$$\lambda_{eq} = \frac{A_L}{4\pi A_T} \quad (4)$$

where A_L equals the shaded area within the closed loop, and A_T is the area of triangle OAB in Fig. 16.

For brevity, G_{eq} and λ_{eq} will be referred to hereafter as shear modulus G and damping ratio λ . Currently, several procedures exist for the determination of shear moduli and damping.

Fig. 17 shows the approximate strain ranges associated with each method of determination. Since field procedures are described elsewhere in the proceedings of this conference (Murphy, 1978), the reporters will focus their attention on laboratory determination of G and λ . In general, G and λ for sands and clays are determined by resonant-column tests for low strain levels and by simple shear or torsional simple shear devices for higher strains, such as those experienced during strong earthquakes.

IV.1. Dynamic Properties of Sands

Dynamic Shear Moduli for Sands

It is generally agreed by researchers that the dynamic shear moduli of sands are most affected by (1) the shear strain amplitude; (2) confining pressure; and (3) soil density or void ratio. Based on other researchers' test data, Seed and Idriss (1970) proposed an average shear modulus curve as a function of the above three variables.

Hardin and Drnevich (1972A and B) proposed the following equations for clean, dry sands:

$$G = \frac{G_{max}}{1 + \frac{G_{max}}{\tau_{max}} \left[1 - 0.5 \cdot e^{-0.16 \frac{G_{max}}{\tau_{max}} \gamma} \right]} \quad (5)$$

where

$$G_{max} = 1230 \frac{(2.973 - e)^2}{1 + e} \cdot \bar{\sigma}_0^{0.5} \quad (6)$$

$$\tau_{max} = \left\{ \left[\frac{1 + K_0}{2} \cdot \bar{\sigma}_v \sin \bar{\phi} + \bar{C} \cos \bar{\phi} \right]^2 - \left[\frac{1 - K_0}{2} \bar{\sigma}_v \right]^2 \right\}^{1/2} \quad (7)$$

where K_0 = coefficient of earth pressure at rest; $\bar{\phi}$, \bar{C} = effective angle of internal friction and true cohesion; e = void ratio; $\bar{\sigma}_0$ and $\bar{\sigma}_v$ = effective confining pressure and effective vertical pressure; G_{max} = shear modulus at strain levels nearly approaching zero strain; and τ_{max} = strength obtained from static shear tests.

Sherif and Ishibashi (1976) have found that the rate of decrease in shear modulus becomes much larger with increasing shear strains when the imposed shear strains exceed 0.03%. Accordingly, they proposed the following equations for shear modulus G in psi.

$$G = 2.8\bar{\phi}(\bar{\sigma}_0)(11.67\gamma + 0.5) \cdot 40(0.205)^{(\gamma/0.03)} \quad 0 \leq \gamma \leq 0.03\% \quad (8)$$

$$G = 2.8\bar{\phi}(\bar{\sigma}_0)^{0.85} \cdot \gamma^{-0.6} \quad 0.03 \leq \gamma \leq 1.0\% \quad (9)$$

where $\bar{\sigma}_0$ = effective confining pressure in psi; $\bar{\phi}$ = angle of internal friction in degrees; and γ = cyclic shear strain amplitude in percentage.

To simplify the determination of G , the above authors presented Eqs. 8 and 9 in nomograph form, as shown in Fig. 18. Most recently, Iwasaki et al. (1978) proposed the relationship shown in Eq. 10.

$$\frac{G}{G_{\gamma=10^{-6}}} = K(\gamma) \cdot p^{m(\gamma)} \quad (10)$$

where $G_{\gamma=10^{-6}}$ is the shear modulus at $\gamma = 10^{-6}$, p is the mean principal stress, and $K(\gamma)$ and $m(\gamma)$ are functions of strain and are presented by Iwasaki et al. by experimental curves. Iwasaki et al. also plotted other researchers' data in the form of $G/G_{\gamma=10^{-6}}$ versus shear strain γ , as shown in Fig. 19. It is seen from this figure that, except for the Shibata and Soelarno (1975) data, the differences among the rest are small.

To determine the value of G from Fig. 19 at a specific strain level, the shear modulus at $\gamma = 10^{-6}$ (which nearly equals G_{\max}) should first be known. The G_{\max} values are given by Hardin in Eq. 6, by Sherif and Ishibashi in Eq. 11, and by Iwasaki et al. in Eq. 12.

$$G_{\max} = 112 \bar{\phi} \sqrt{\bar{\sigma}_c} \quad (\text{Sherif and Ishibashi}) \quad (11)*$$

$$G_{\max} = 4385 \frac{(2.17 - e)^2}{1 + e} (\bar{\sigma}_c)^{0.40} \quad (\text{Iwasaki et al.}) \quad (12)$$

where G_{\max} and $\bar{\sigma}_c$ are in psi and $\bar{\phi}$ is in degrees.

In Fig. 20, the reporters have plotted the G_{\max} values calculated by Eqs. 6, 11 and 12 for four types of sands (Ottawa, Del Monte, Golden Gardens and Seward Park sands) in loose and dense states under effective confining pressures of 10 and 40 psi. The material properties e and $\bar{\phi}$ of these four sands were known from previous studies by Sherif and Ishibashi (1976).

It is seen from Fig. 20 that G_{\max} varies randomly and is dependent on soil type and density. Therefore, additional research in this area is suggested.

* This equation is obtained from Eq. 8 at $\gamma = 0$.

Damping Ratio for Sands

Damping is a measure of energy dissipation in a system and is quantitatively defined by Eq. 4 and Fig. 16. The factors that have the greatest influence on damping ratio of sands are (1) cyclic strain amplitudes, (2) confining pressures, (3) soil type (gradation and angularity), and (4) number of stress cycles. The effect of soil density or void ratio is so small as to be almost negligible (Silver and Seed, 1971; Sherif et al., 1977A).

Seed and Idriss (1970) reviewed the available data on damping ratios of sands and presented an average curve with about ± 4 to 6% variations in λ , as a function of shear strain amplitude.

Hardin and Drnevich (1972A and B) proposed the following equations, based on torsional shear and resonant-column test results on a dry uniform quartz sand.

$$\left. \begin{aligned} \lambda &= \frac{\lambda_{\max} \gamma/\gamma_r}{1 + \gamma/\gamma_r} \\ \lambda_{\max} &= 33 - 1.5 \log N_c \\ \gamma_r &= \frac{\tau_{\max}}{G_{\max}} \end{aligned} \right\} \quad (13)$$

where N_c is the number of stress cycles and τ_{\max} and G_{\max} are as defined earlier, in Eqs. 6 and 7.

Sherif et al. (1977A) investigated the effects of soil type (gradation and angularity) on damping ratio for four different types of sands and proposed the following equation for damping λ (%) as a function of effective confining pressure $\bar{\sigma}_c$ (psi), shear strain amplitude γ (%) and soil gradation and sphericity factor F:

$$\lambda = \frac{50 - 0.6\bar{\sigma}_c}{38} (73.3F - 53.3)\gamma^{0.3} \quad (14)$$

The above researchers defined the new soil gradation and sphericity factor F as:

$$F = \frac{1}{\psi^2 C_g} \quad (15)$$

where $\psi = S'/S$ represents soil sphericity, and $C_g = D_{30}^2/(D_{10} \times D_{60})$ is the coefficient of gradation. The terms S' and S refer, respectively, to the surface area of a sphere of the same volume as the soil particle and the actual surface area of the soil. Fig. 21 shows a plot of all the experimental data points for the four sands tested by Sherif et al. during the above investigation at dense and loose states, together with the curve, based on Eqs. 14 and 15. It is apparent from this figure that a good correlation exists between the experimental data and the relationship expressed by Eqs. 14 and 15. The above investigators have also proposed a nomograph, based on Eqs. 14 and 15, for easy determination of damping

ratios, as shown in Fig. 22. Fig. 23 shows a comparison among experimental data obtained by Sherif et al. and others. This figure suggests that soil gradation and angularity strongly affect the damping values for sands.

IV.2. Dynamic Soil Properties of Cohesive Soils

Dynamic Shear Moduli for Clays

Because cohesive soils are more complex than sands, there is little information covering these soils in general. Important factors affecting dynamic shear moduli of clays are (1) shear strain amplitudes; (2) confining pressures; (3) void ratio; (4) degree of saturation; (5) number of stress cycles; and (6) time effects. Factors 2, 3 and 4 may be combined into one parameter, that being the strength of clay.

Seed and Idriss (1970) gathered available data and presented an average shear modulus curve for clays. They presented the curve as G/S_u versus shear strain, where S_u is the undrained shear strength of the clay. Kovacs et al. (1971) presented a curve similar to the one proposed by Seed and Idriss for a soft clay tested in a simple-shear device and shaking table, and obtained lower values than Seed and Idriss.

Hardin and Drnevich (1972A and B) claim that their Eqs. 5, 6 and 7 apply for normally consolidated clays as well as sands. Anderson and Richart (1976) presented G values for five different cohesive soils tested in a high-amplitude resonant-column device and found data that could have been predicted by Hardin and Drnevich's empirical equation, if τ_{max} were taken equal to S_u .

Damping Ratio for Clays

Test data for damping ratios for saturated cohesive soils are limited. An average curve compiled by Seed and Idriss (1970) shows more scatter than the one for sands.

Hardin and Drnevich (1972A and B) believe that their Eq. 13 also applies for clays, provided that λ_{max} is defined in the following form:

$$\lambda_{max} = 31 - (3 + 0.03f)\bar{\sigma}_o^{0.5} + 1.5f^{0.5} - 1.5 (\log N) \quad (16)$$

where f is frequency in cycles per second, $\bar{\sigma}_o$ is effective mean principal stress in kg/cm^2 and N is the number of stress cycles.

It is apparent from the foregoing that no general relationship for the determination of shear moduli and damping for clays has yet been found, principally because the effects of several complex factors, including shear strength, plasticity index, water content, overconsolidation ratio and secondary consolidation, are not fully understood. There is a definite need for future research in this important area.

IV.3. Dynamic Properties of Other Types of Soils

There are very limited data available on dynamic shear moduli and damping ratios of gravelly soils, peat, deep-ocean sediments, frozen soils and others. Seed and Idriss (1970) reported some data for gravelly soil and peats. Sherif et al. (1976A and B, 1977B) conducted dynamic tests on very soft ocean-bottom clays and presented the data shown in Fig. 24.

REFERENCES

- Anderson, D.G. and Richart, F.E., Jr.(1976) "Effects of Straining on Shear Modulus of Clays," J. Geotechnical Engineering Div., ASCE, Vol. 102, No. GT9, pp. 975-987.
- Castro, G.(1975) "Liquefaction and Cyclic Mobility of Saturated Sands," J. Geotechnical Engineering Div., ASCE, Vol. 101, No. GT6, pp. 551-569.
- Castro, G. and Christian, J.T.(1976) "Shear Strength of Soils and Cyclic Loading," J. Geotechnical Engineering Div., ASCE, Vol. 102, No. GT9, pp. 887-894.
- Cho, Y., Rizzo, P.C. and Humphries, W.K.(1976) "Saturated Sand and Cyclic Dynamic Tests," Liquefaction Problems in Geotechnical Engineering, ASCE National Convention, Philadelphia, October 2.
- DeAlba, P., Seed, H.B. and Chan, C.K.(1976) "Sand Liquefaction in Large-Scale Simple Shear Tests," J. Geotechnical Engineering Div., ASCE, Vol. 102, No. GT9, pp. 909-927.
- Finn, W.D.L., Pickering, D.J. and Bransby, P.L.(1971) "Sand Liquefaction in Triaxial and Simple Shear Tests," J. Soil Mechanics and Foundations Div., ASCE, Vol. 97, No. SM4, pp. 639-659.
- Finn, W.D.L.(1972) "Liquefaction of Sands," Proc. International Conf. on Microzonation, Seattle, Vol. 1, pp. 87-111.
- Finn, W.D.L., Byrne, P.M. and Martin, G.R.(1976) "Seismic Response and Liquefaction of Sands," J. Geotechnical Engineering Div., ASCE, Vol. 102, No. GT8, pp. 841-856.
- Finn, W.D.L. and Byrne, P.M.(1976) "Estimating Settlement in Dry Sands during Earthquakes," Canadian Geotechnical Journal, Vol. 13, No. 4., Nov.
- Ghaboussi, J. and Dikmen, S.U.(1978) "Liquefaction Analysis of Horizontal Layered Sands," J. Geotechnical Engineering Div., ASCE, Vol. 104, No. GT3, pp. 341-356.
- Hardin, B.O. and Drnevich, V.P.(1972A) "Shear Modulus and Damping in Soils: Measurement and Parameter Effects," J. Soil Mechanics and Foundations Div., ASCE, Vol. 98, No. SM6, pp. 603-624.
- Hardin, B.O. and Drnevich, V.P.(1972B) "Shear Modulus and Damping in Soils: Design Equations and Curves," J. Soil Mechanics and Foundations Div., ASCE, Vol. 98, No. SM7, pp. 667-692.
- Idriss, I.M., Lysmer, J., Hwang, R. and Seed, H.B.(1973) "QUAD-4, A Computer Program for Evaluating the Seismic Response of Soil Structures by Variable Damping Finite Element Procedures," Report No. EERC 73-16, University of California, Berkeley, July.
- Ishibashi, I. and Sherif, M.A.(1974) "Soil Liquefaction by Torsional Simple Shear Device," J. Geotechnical Engineering Div., ASCE, Vol. 100, No. GT8, pp. 871-888.

- Ishibashi, I., Sherif, M.A. and Tsuchiya, C.(1977) "Pore-Pressure Rise Mechanism and Soil Liquefaction," Soils and Foundations (Japan) Vol. 17, No. 2, June, pp. 17-27.
- Ishihara, K. and Li, S.E.(1972) "Liquefaction of Saturated Sand in Triaxial Torsion Shear Test," Soils and Foundations (Japan), Vol. 12, No. 2, pp. 19-39.
- Ishihara, K.(1973) "Review on the Liquefaction in Sandy Ground," Tsuchi-to-kiso, Vol. 21, No. 6, pp. 21-22 (Japanese).
- Ishihara, K., Lysmer, J., Yasuda, S. and Hirao, H.(1976) "Prediction of Liquefaction in Sand Deposits during Earthquakes," Soils and Foundations (Japan), Vol. 16, No. 1, pp. 1-16.
- Iwasaki, T., Tatsuoka, F. and Takagi, Y.(1978) "Shear Moduli of Sands under Cyclic Torsional Shear Loading," Soils and Foundations (Japan) Vol. 18, No. 1.
- Japan Society of Civil Engineers (1973) Earthquake Resistant Design for Civil Engineering Structures, Earth Structures and Foundations in Japan, p. 58.
- Koutsoftas, D.C.(1978) "Effect of Cyclic Loads on Undrained Strength of Two Marine Clays," J. Geotechnical Engineering Div., ASCE, Vol. 104, No. GT5, pp. 609-620.
- Kovacs, S.D., Seed, H.B. and Chan, C.C.(1971) "Dynamic Moduli and Damping Ratios for a Soft Clay," J. Soil Mechanics and Foundations Div., ASCE, Vol. 97, No. SM1, pp. 59-75.
- Krizek, R.J. and Fernandez, J.I.(1971) "Vibratory Densification of Damp Clayey Sands," J. Soil Mechanics and Foundations Div., ASCE, Vol. 97, No. SM8.
- Lee, K.L. and Albaisa, A.(1974) "Earthquake Induced Settlements in Saturated Sands," J. Geotechnical Engineering Div., ASCE, Vol. 100, No. GT4, pp. 387-406.
- Lee, K.L. and Chan, C.K.(1972) "Number of Equivalent Significant Cycles in Strong Motion Earthquakes," Proc. International Conf. on Microzonation, Seattle, Vol. 2, pp. 609-627.
- Lee, K.L. and Focht, J.A.(1976) "Strength of Clay Subjected to Cyclic Loading," Marine Geotechnology, Vol. 1, No. 3, pp. 165-185.
- Liou, C.P., Streeter, V.L. and Richart, F.E., Jr. (1976) "A Numerical Model for Liquefaction," Liquefaction Problems in Geotechnical Engineering, ASCE National Convention, pp. 313-341.
- Martin, G.R., Finn, W.D.L. and Seed, H.B.(1975) "Fundamentals of Liquefaction under Cyclic Loading," J. Geotechnical Engineering Div., ASCE, Vol. 101, No. GT5, pp. 423-438.
- Murphy, V.J. (1978) "Geophysical Engineering Investigative Techniques for Site Characterization," Proc. Second International Conf. on Microzonation, San Francisco.

- Nishiyama, H., Yahagi, K., Nakagawa, S. and Wada, K.(1977) "Practical Method of Predicting Sand Liquefaction," Proc. Ninth International Conf. on Soil Mechanics and Foundation Engineering, Tokyo, Vol. 2, pp. 305-308.
- Pyke, R.H., Seed, H.B. and Chan, C.K.(1975) "Settlement of Sands under Multidirectional Shaking," J. Geotechnical Engineering Div., ASCE, Vol. 101, No. GT4, pp. 379-398.
- Schnabel, P.B., Lysmer, J. and Seed, H.B.(1972) "SHAKE: A Computer Program for Earthquake Response Analysis of Horizontal Layered Sites," Report No. EERC 72-12, Univ. of California.
- Seed, H.B. and Silver, M.L.(1972) "Settlement of Dry Sands during Earthquakes," J. Soil Mechanics and Foundations Div., ASCE, Vol. 98, No. SM4.
- Seed, H.B. and Idriss, I.M.(1969) "Influence of Soil Conditions on Ground Motion during Earthquakes," J. Soil Mechanics and Foundations Div., ASCE, Vol. 95, No. SM1, pp. 99-137.
- Seed, H.B. and Idriss, I.M.(1970) "Soil Moduli and Damping Factors for Dynamic Response Analyses," Report No. EERC 70-10, Univ. of California.
- Seed, H.B. and Idriss, I.M.(1971) "Simplified Procedure for Evaluating Soil Liquefaction Potential," J. Soil Mechanics and Foundations Div., ASCE, Vol. 97, No. SM9, pp. 1249-1273.
- Seed, H.B., Martin, P.P. and Lysmer, J.(1975) "The Generation and Dissipation of Pore Water Pressures during Soil Liquefaction," Report No. EERC 75-26, Univ. of California.
- Seed, H.B. and Peacock, W.H.(1971) "Test Procedures for Measuring Soil Liquefaction Characteristics," J. Soil Mechanics and Foundations Div., ASCE, Vol. 97, No. SM8, pp. 1099-1119.
- Shannon & Wilson, Inc., and Agbabian-Jacobsen Assoc(1972) Soil Behavior under Earthquake Loading Conditions, State of the Art, Evaluation of Soil Characteristics for Seismic Response Analyses, January.
- Sherif, M.A. and Ishibashi, I.(1976) "Dynamic Shear Moduli for Dry Sands," J. Geotechnical Engineering Div., ASCE, Vol. 102, No. GT11, pp. 1171-1184.
- Sherif, M.A., Khalid, R. and Ishibashi, I.(1976A) "Dynamic Soil Properties of Deep-Pacific Ocean Clays," Soil Engineering Research Report No. 16, Univ. of Washington.
- Sherif, M.A., Ling, S.C. and Ishibashi, I.(1976B) "Strength Degradation and Dynamic Properties of Pelagic Submarine Clays," Soil Engineering Research Report No. 14, Univ. of Washington.
- Sherif, M.A., Ishibashi, I. and Gaddah, A.H.(1977A) "Damping Ratio for Dry Sands," J. Geotechnical Engineering Div., ASCE, Vol. 103, No. GT7, pp. 743-756.
- Sherif, M.A., Ishibashi, I. and Ling, S.C.(1977B) "Dynamic Properties of Marine Sediments," Proc. Ninth International Conf. on Soil Mechanics and Foundation Engineering, Tokyo.

Sherif, M.A., Ishibashi, I. and Tsuchiya, C.(1978) "Pore-Pressure Prediction during Earthquake Loadings," Soils and Foundations (Japan) (accepted for publication).

Shibata, T. and Soelarno, D.S.(1975) "Stress-Strain Characteristics of Sands under Cyclic Loading," Proc. Japanese Soc. Civil Engrs., No. 239, July, pp. 57-65 (Japanese).

Silver, M.L. and Seed, H.B.(1971) "Deformation Characteristics of Sands under Cyclic Loading," J. Soil Mechanics and Foundations Div., ASCE, Vol. 97, No. SM8, pp. 1081-1098.

Thiers, G.R. and Seed, H.B.(1969) "Strength and Stress-Strain Characteristics of Clays Subjected to Seismic Loading Conditions," ASTM, STP 450, pp. 3-56.

Yoshimi, Y. and Tokimatsu, K.(1977) "Settlement of Buildings on Saturated Sand during Earthquakes," Soils and Foundations (Japan), Vol. 17, No. 1, pp. 23-28.

Youd, T.L.(1972) "Compaction of Sands by Repeated Shear Straining," J. Soil Mechanics and Foundations Div., ASCE, Vol. 98, No. SM7.

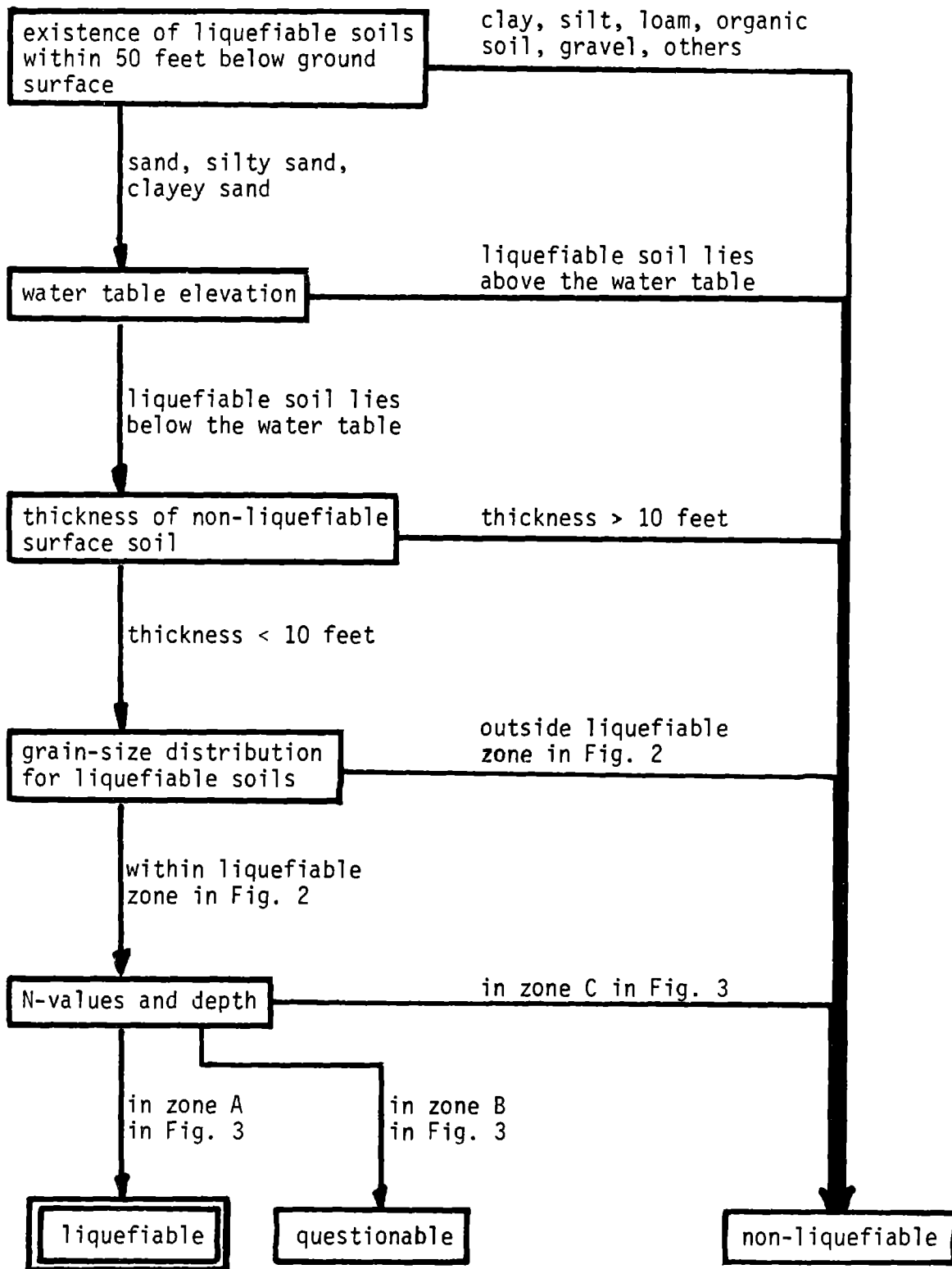


Fig. 1 Preliminary Evaluation of Soil-Liquefaction Potential

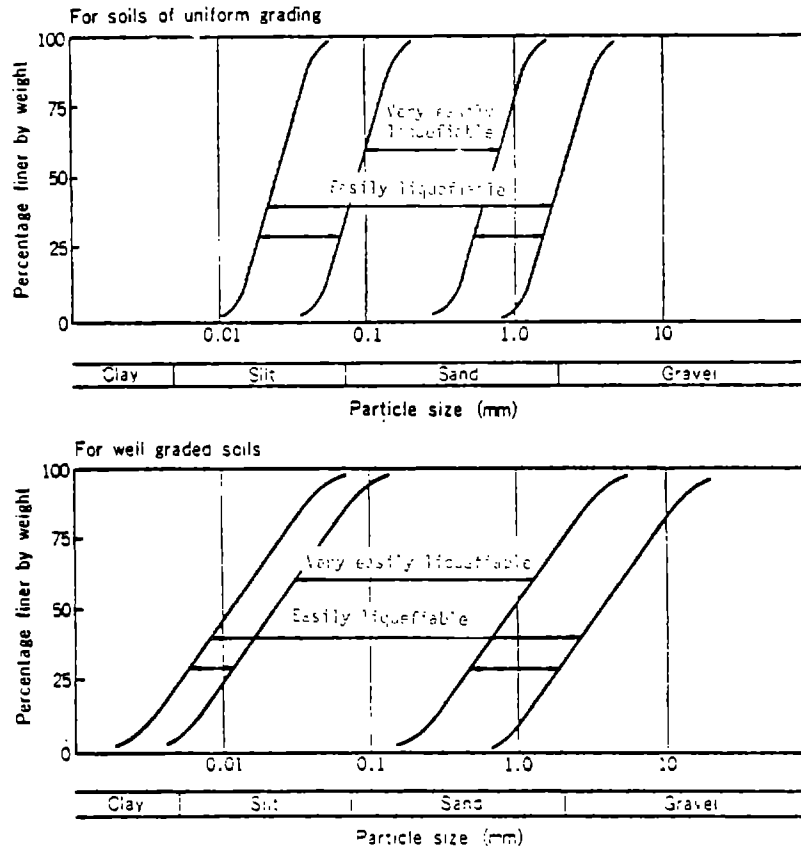


Fig. 2. Ranges of Particle Size Distribution Curves of Sands Which Have Possibility of Liquefaction (Japan Society of Civil Engineers, 1973)

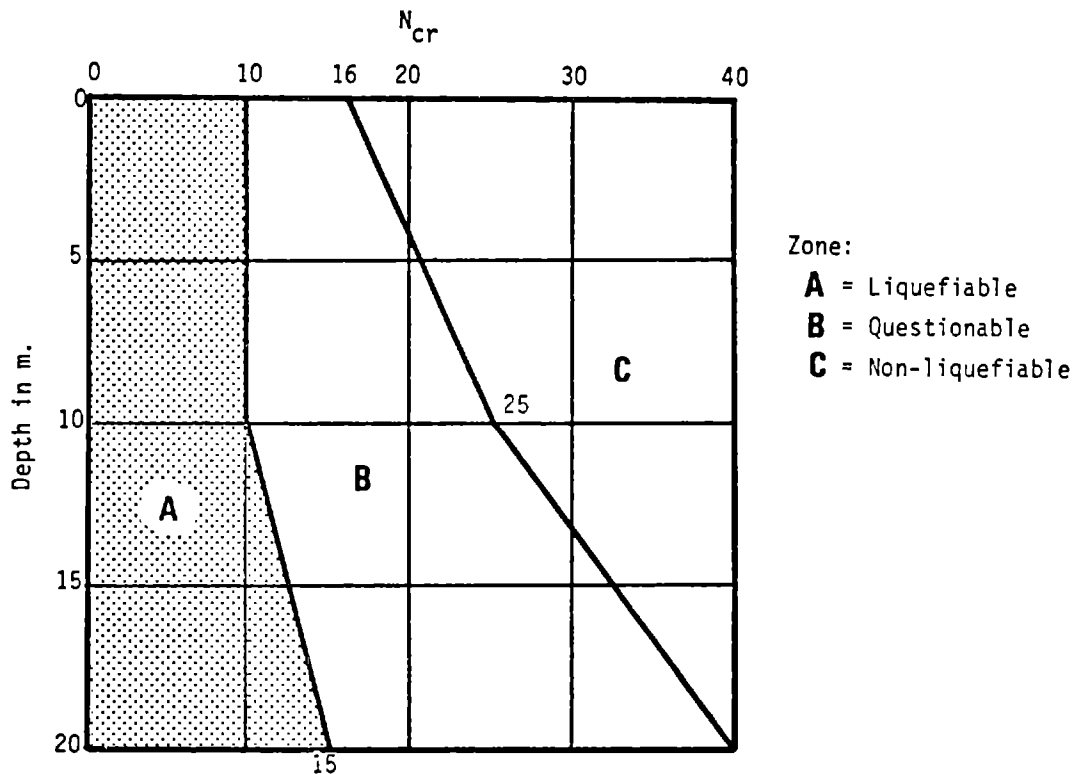


Fig. 3. Critical N-values vs. Depth (Nishiyama et al., 1977)

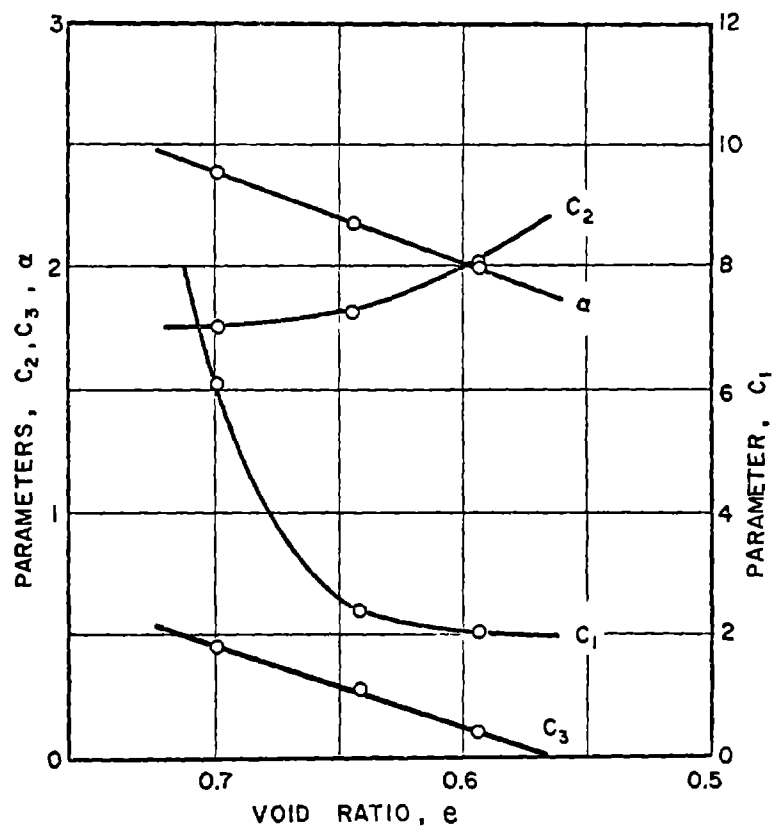


Fig. 4. Variation of Parameters C_1 , C_2 , C_3 and α with Void Ratio for Ottawa Sand (Sherif et al., 1978)

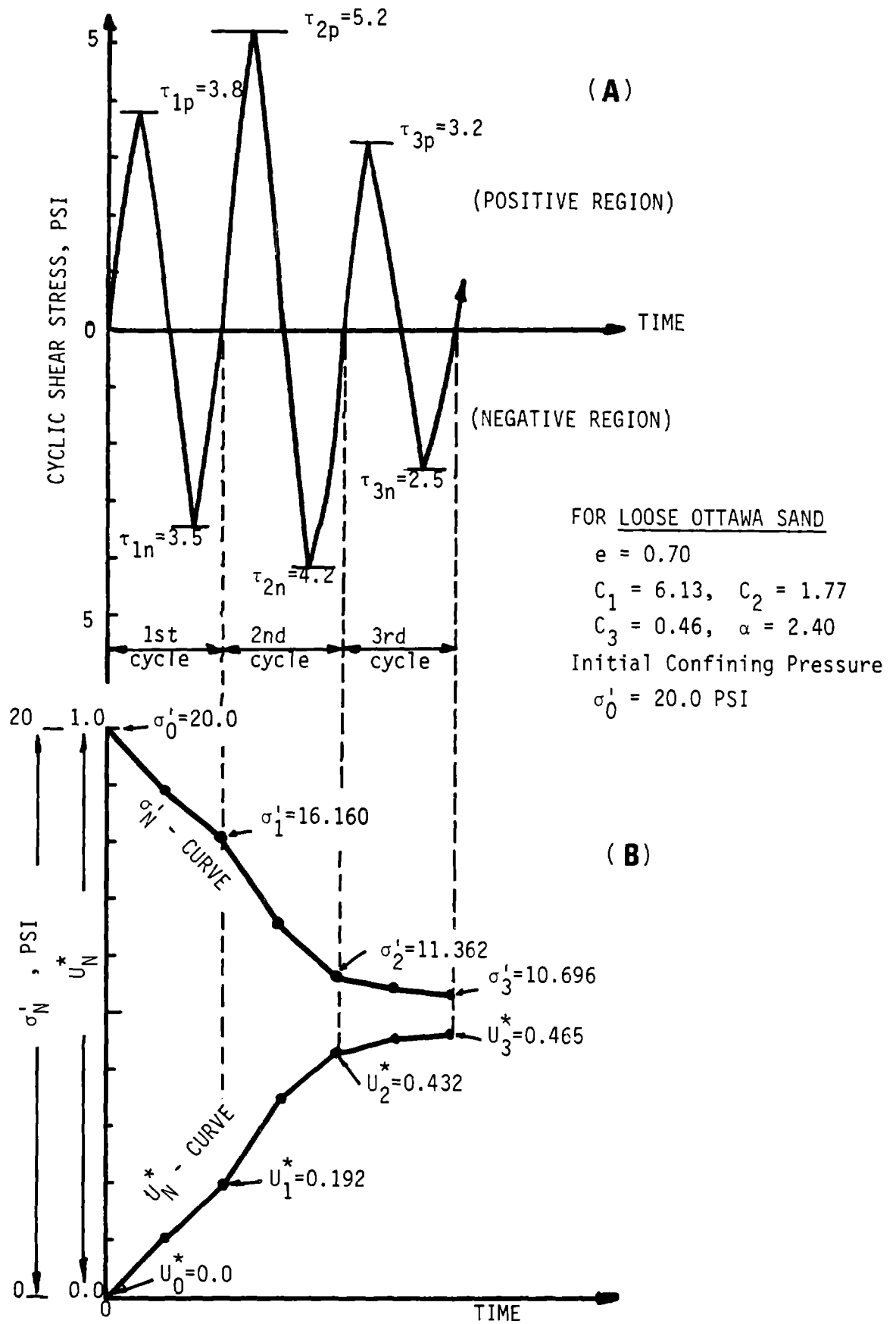


Fig. 5. Illustrations of Stress History and Pore Pressure Buildup

CYCLE NUMBER, N	SHEAR STRESS τ_N , PSI	$(N_{eq})^{\alpha} = \sum \left(\frac{\tau_i}{\tau_N} \right)^{\alpha}$	$\frac{\Delta U_{Np}^* \text{ or } \Delta U_{Nn}^*}{(1-U_{N-1})^{\alpha} \frac{N_{eq} C_2 - C_3}{N_{eq} C_1} \left(\frac{\tau_N}{\sigma_{N-1}} \right)^{\alpha}}$	$\Delta U_N^* = \frac{1}{2} (\Delta U_{Np}^* + \Delta U_{Nn}^*)$	$U_N^* = U_{N-1}^* + \Delta U_N^*$	$\sigma'_N = \sigma'_0 (1 - U_N^*)$ PSI
1	Positive	$\left(\frac{3.8}{3.8} \right)^{2.4} = 1.0$	$(-0) \frac{1 \times 6.13}{1.77} \left(\frac{3.8}{20} \right)^{2.4} = 2.11$	$\frac{1}{2} (0.211 + 0.173) = 0.192$	$0 + 0.192 = 0.192$	$20(1 - 0.192) = 16.16$
	Negative	$\left(\frac{3.5}{3.5} \right)^{2.4} = 1.0$	$(-0) \frac{1 \times 6.13}{1.77} \left(\frac{3.5}{20} \right)^{2.4} = 1.73$	0.192	0.192	16.16
2	Positive	$\left(\frac{3.8}{5.2} \right)^{2.4} + \left(\frac{5.2}{5.2} \right)^{2.4} = 1.47$	$(-0.192) \frac{1.47 \times 6.13}{1.77} \left(\frac{5.2}{16.16} \right)^{2.4} = 3.16$	$\frac{1}{2} (0.316 + 0.164) = 0.240$	$0.192 + 0.240 = 0.432$	$20(1 - 0.432) = 11.362$
	Negative	$\left(\frac{3.5}{4.2} \right)^{2.4} + \left(\frac{4.2}{4.2} \right)^{2.4} = 1.65$	$(-0.192) \frac{1.65 \times 6.13}{1.77} \left(\frac{4.2}{16.16} \right)^{2.4} = 1.64$	0.240	0.432	11.362
3	Positive	$\left(\frac{3.8}{3.2} \right)^{2.4} + \left(\frac{5.2}{3.2} \right)^{2.4} + \left(\frac{3.2}{3.2} \right)^{2.4} = 5.72$	$(-0.240) \frac{5.72 \times 6.13}{1.77} \left(\frac{3.2}{11.362} \right)^{2.4} = 0.44$	$\frac{1}{2} (0.44 + 0.022) = 0.233$	$0.432 + 0.233 = 0.665$	$20(1 - 0.665) = 10.696$
	Negative	$\left(\frac{3.5}{2.5} \right)^{2.4} + \left(\frac{4.2}{2.5} \right)^{2.4} + \left(\frac{2.5}{2.5} \right)^{2.4} = 6.72$	$(-0.240) \frac{6.72 \times 6.13}{1.77} \left(\frac{2.5}{11.362} \right)^{2.4} = 0.22$	0.233	0.665	10.696

For Loose Ottawa Sand: $C_1 = 6.13$, $C_2 = 1.77$, $C_3 = 0.46$, $\alpha = 2.40$; $\sigma'_0 = 20$ psi (Void Ratio = 0.70)

Fig. 6. Illustrative Calculations of Pore Pressure Buildup Corresponding to Stress History Shown in Fig. 5(A)

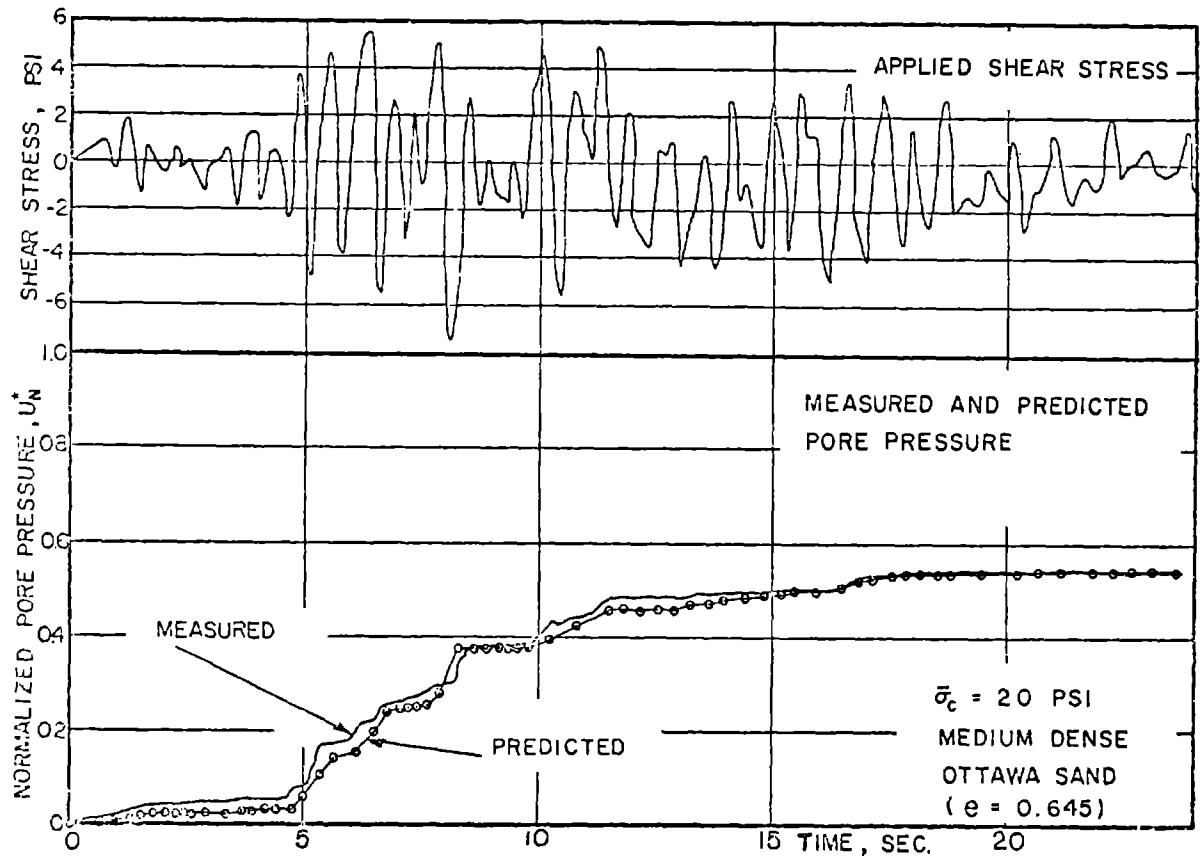


Fig. 7 Comparison between Predicted and Measured Pore-Pressure Rise under Earthquake-type Loading (Sherif et al., 1978)

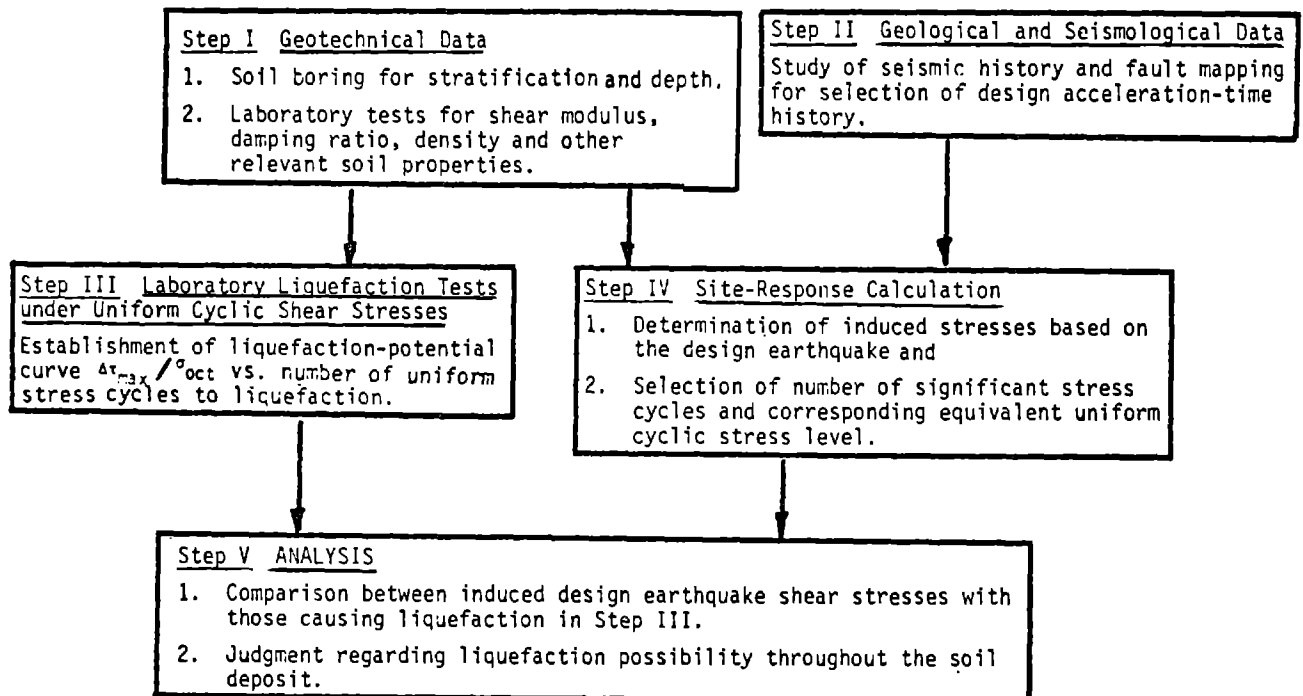


Fig. 8 Liquefaction-Potential Evaluation by Stress-Comparison Method

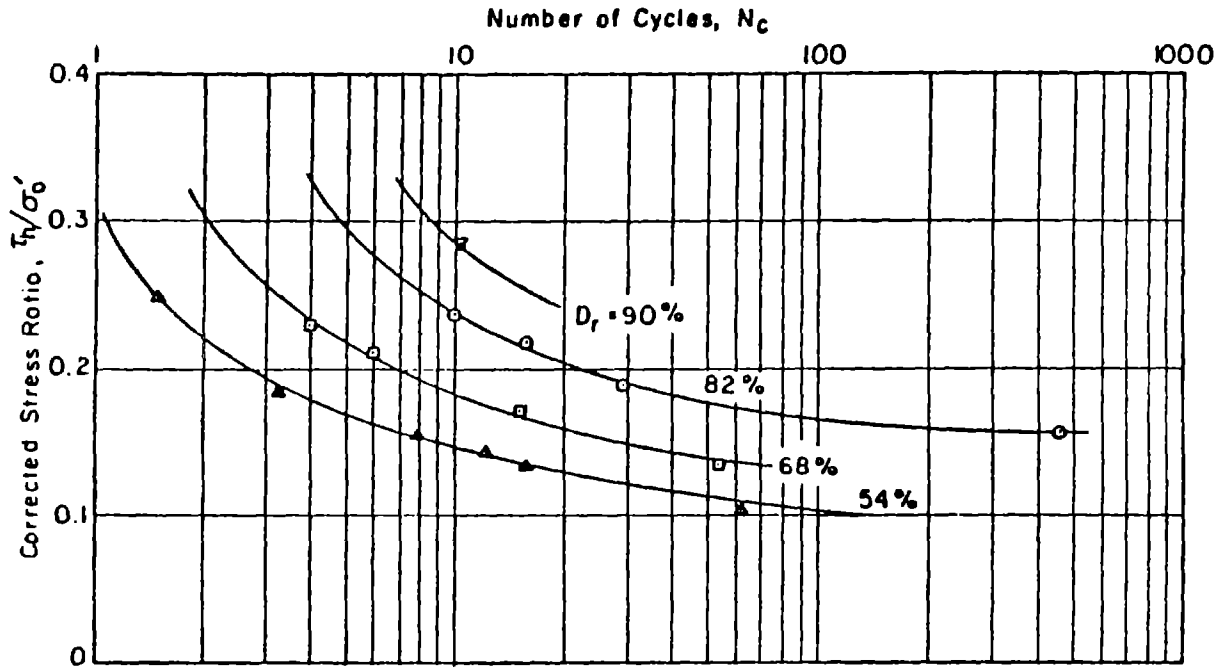


Fig. 9 Corrected τ_h/σ'_0 vs. N_c for Initial Liquefaction (DeAlba et al., 1975)

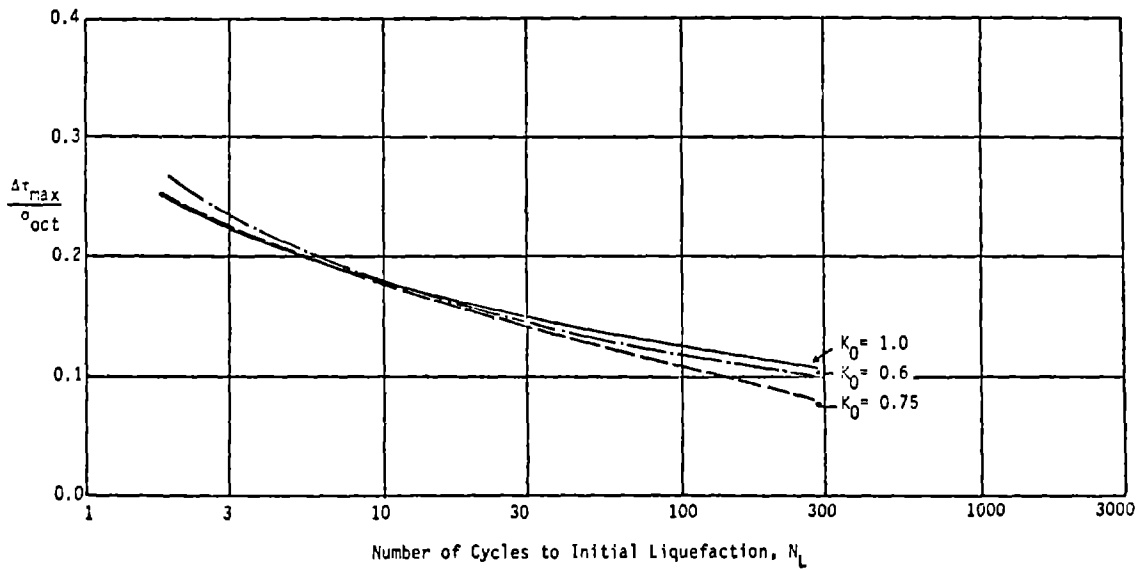


Fig. 10 Relationship between $\Delta\tau_{max}/\sigma_{oct}$ and Number of Cycles to Liquefaction for Various K_0 Values (Ishibashi and Sherif, 1974)

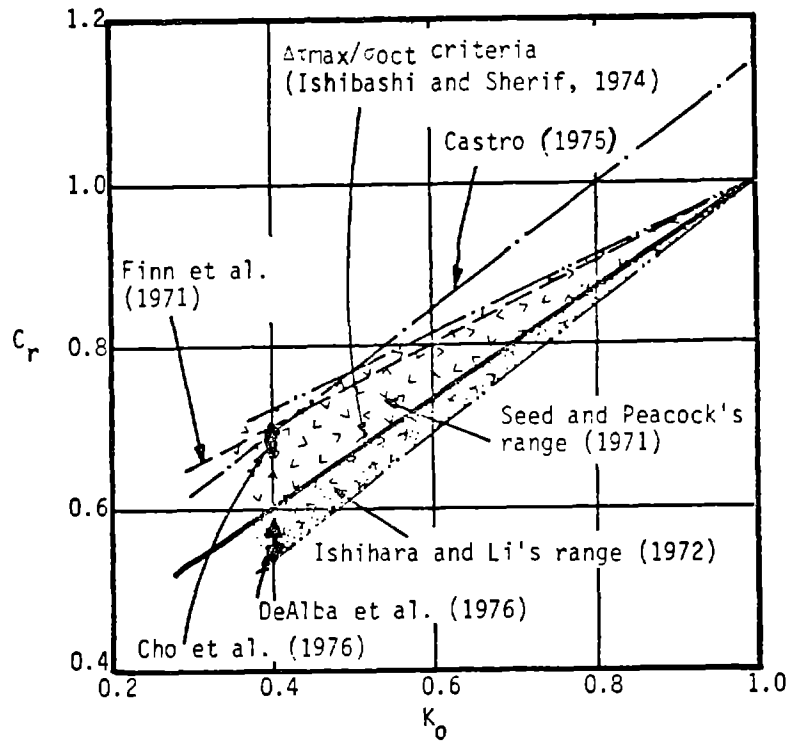


Fig. 11 Correlation Factor C_r against Coefficient of Lateral Earth Pressure K_0

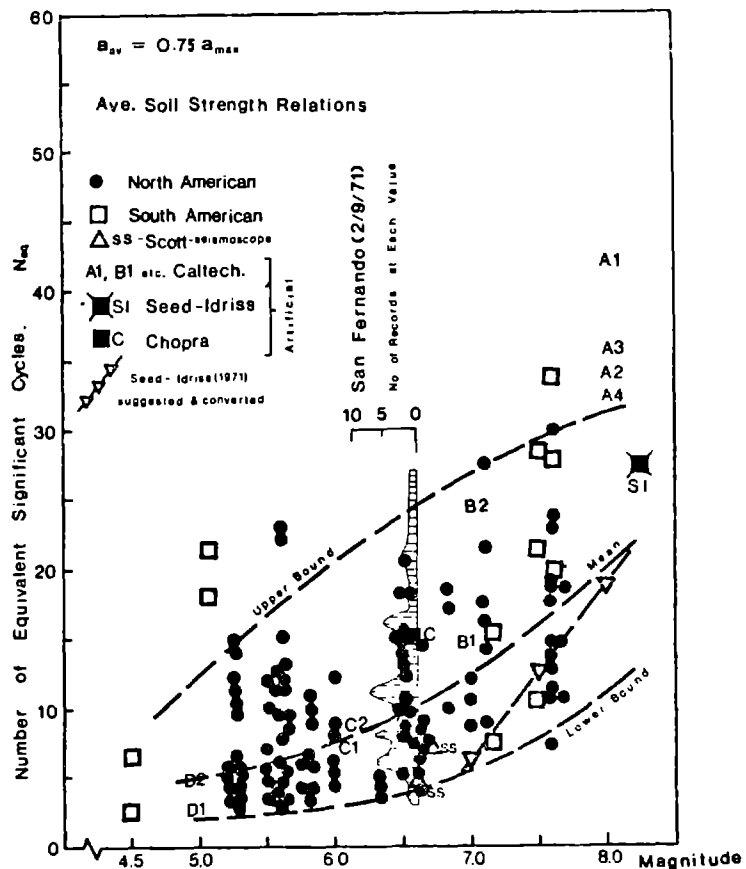


Fig. 12. Calculated Number of Equivalent Cycles from Strong Motion Accelerograms (Lee and Chan, 1972)

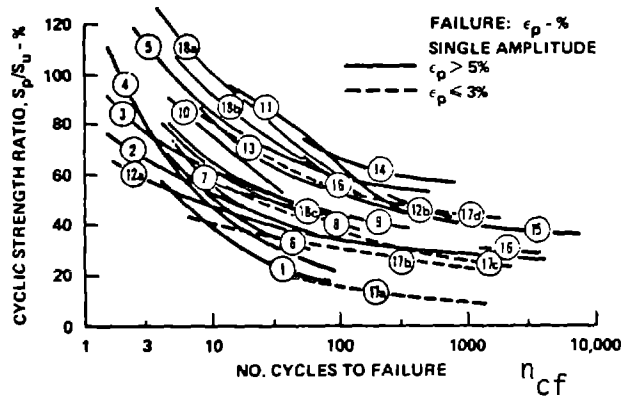


Fig. 13 Compilation of Cyclic Stress Ratio Data for Saturated Clays (Lee and Focht, 1976)

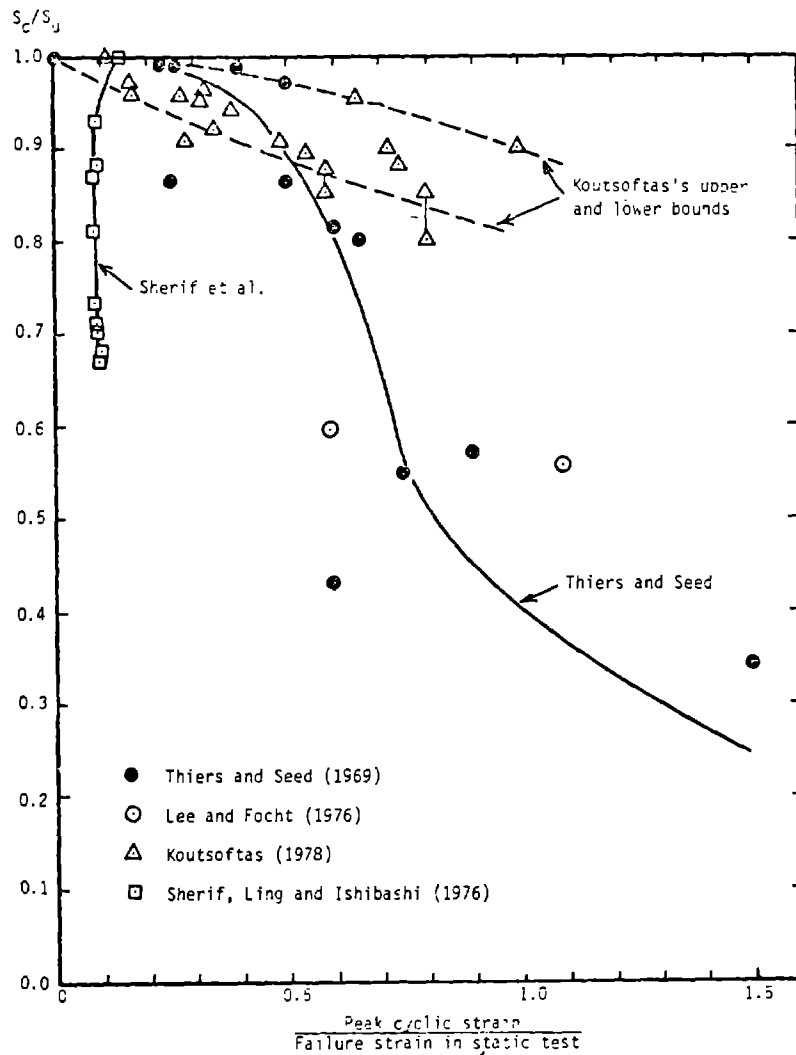


Fig. 14 Cyclic Strength Ratio versus Cyclic Strain Ratio

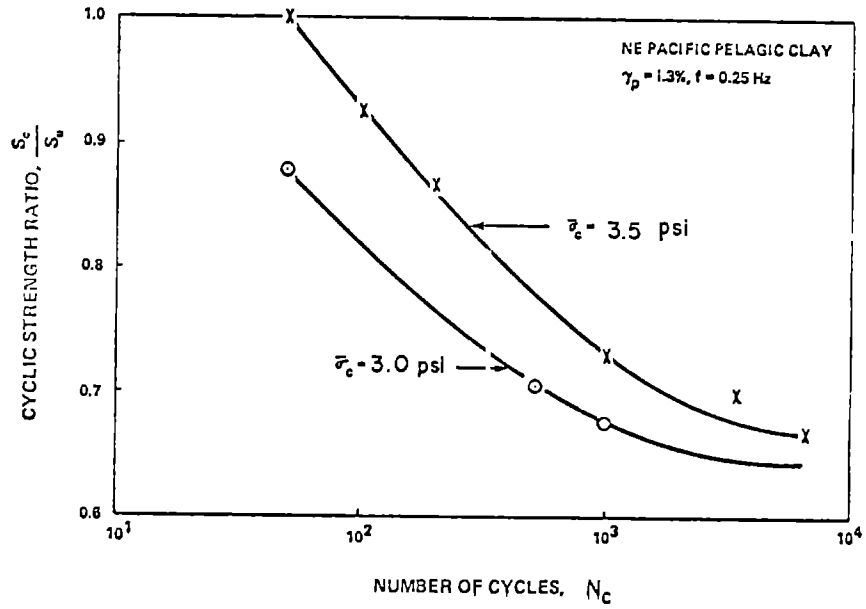


Fig. 15 Effect of N_c on a NE Pacific Clay (Sherif et al., 1977B)

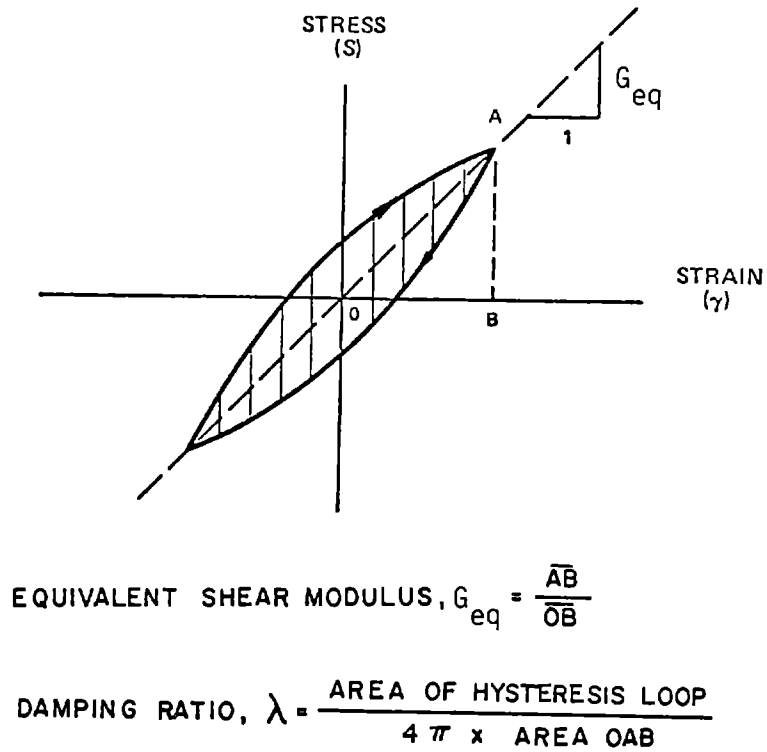
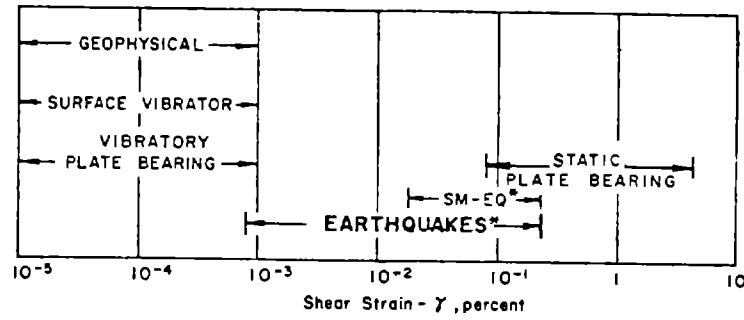
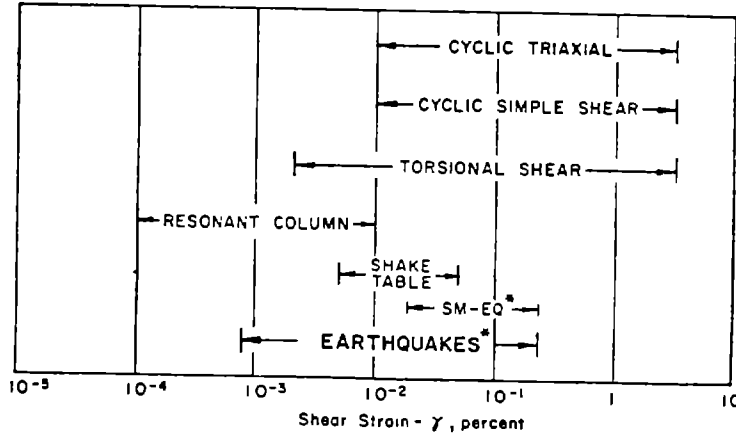


Fig. 16 Definition of Equivalent Shear Moduli and Damping Ratio



a. FIELD TESTS



* Note: Range of shear strain denoted as "Earthquakes" represents an extreme range for most earthquakes. "SM-EQ" denotes strains induced by strong motion earthquakes.

b. LABORATORY TESTS

Fig. 17. Field and Laboratory Tests Showing Approximate Strain Ranges of Test Procedures (Shannon & Wilson, Inc., and Agbabian-Jacobsen Assoc., 1972)

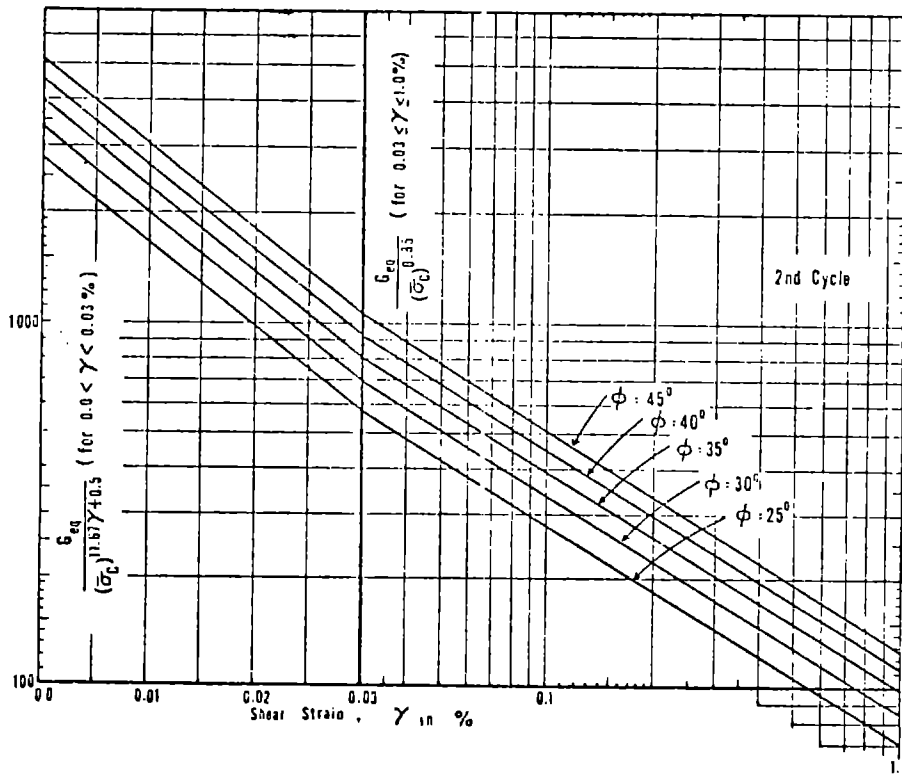


Fig. 18. Nomograph for G_{eq} Determination for Dry Sands (Sherif and Ishibashi, 1976)

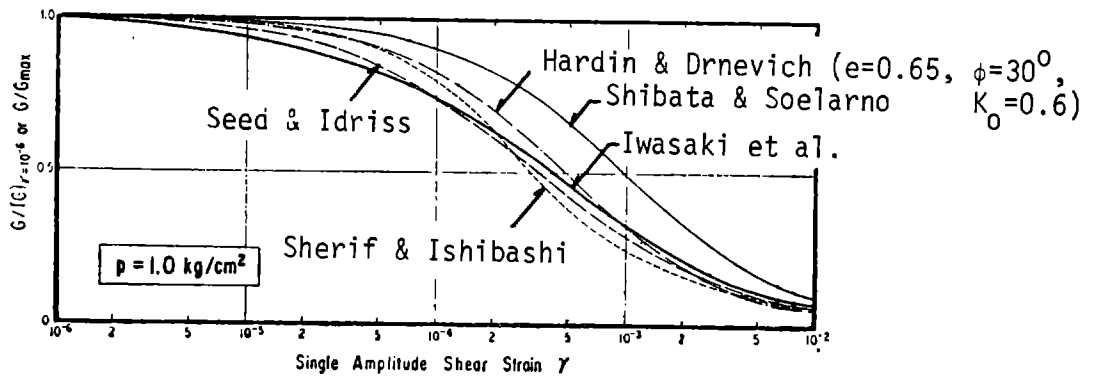


Figure 19 Comparison among G/G_{max} versus γ Relationships (Iwasaki et al., 1978)

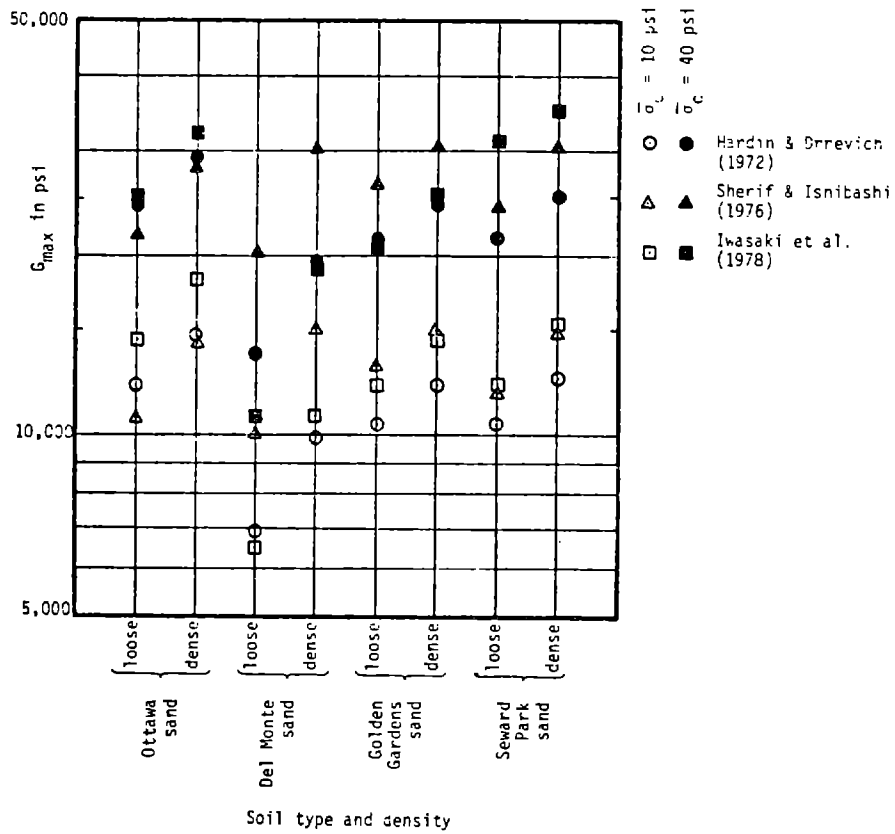


Fig. 20. G_{max} Values as a Function of Soil Type and Density

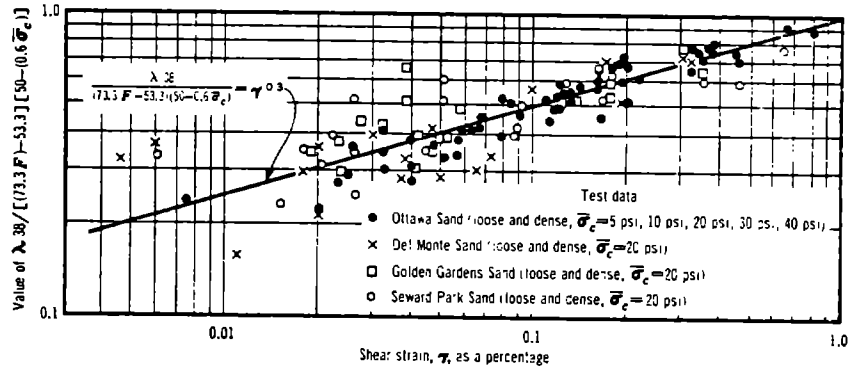


Fig. 21 $\text{Log} \lambda_{38} / \{50 - (0.6 \bar{\sigma}_c)\} \{ (73.3 F) - 53.3 \}$ versus $\text{Log} \gamma$ for Four Types of Sand (1 psi = 6.89 kN/m²) (Sherif et al., 1977)

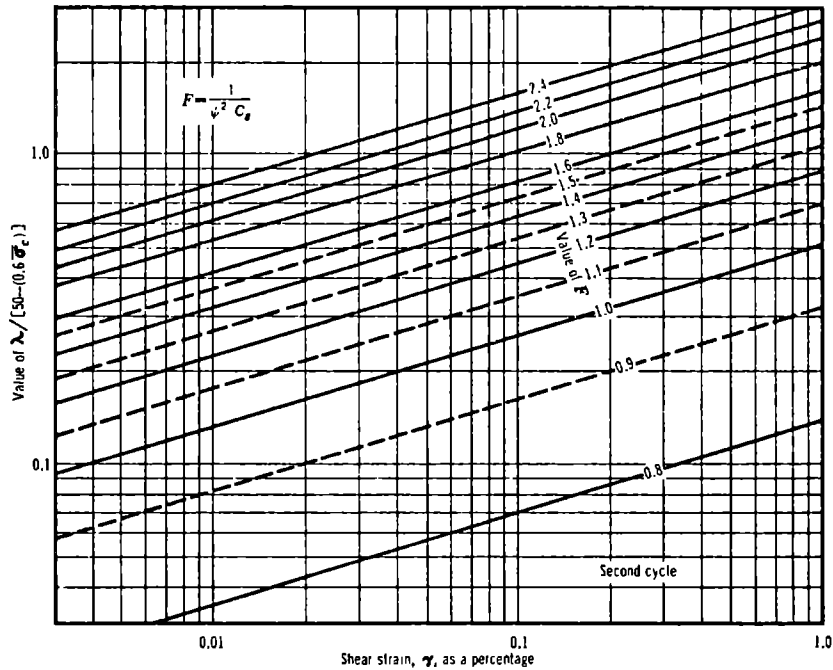


Fig. 22. Nomogram for λ Determination for Dry Sands (Sherif et al., 1977)

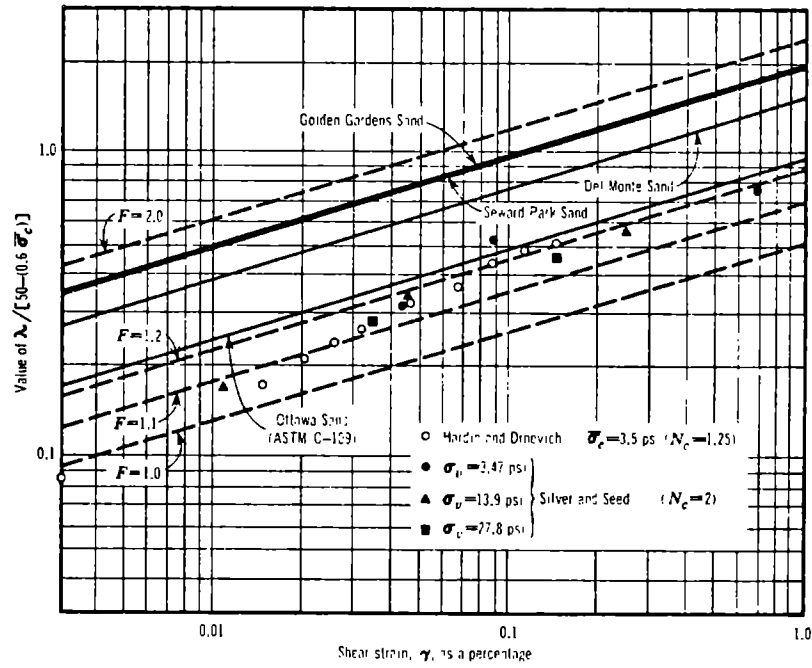


Fig. 23 Comparison of Reporters' Results with Other Researchers' Experimental Data (1 psi = 6.89 kN/m²) (Sherif et al., 1977)

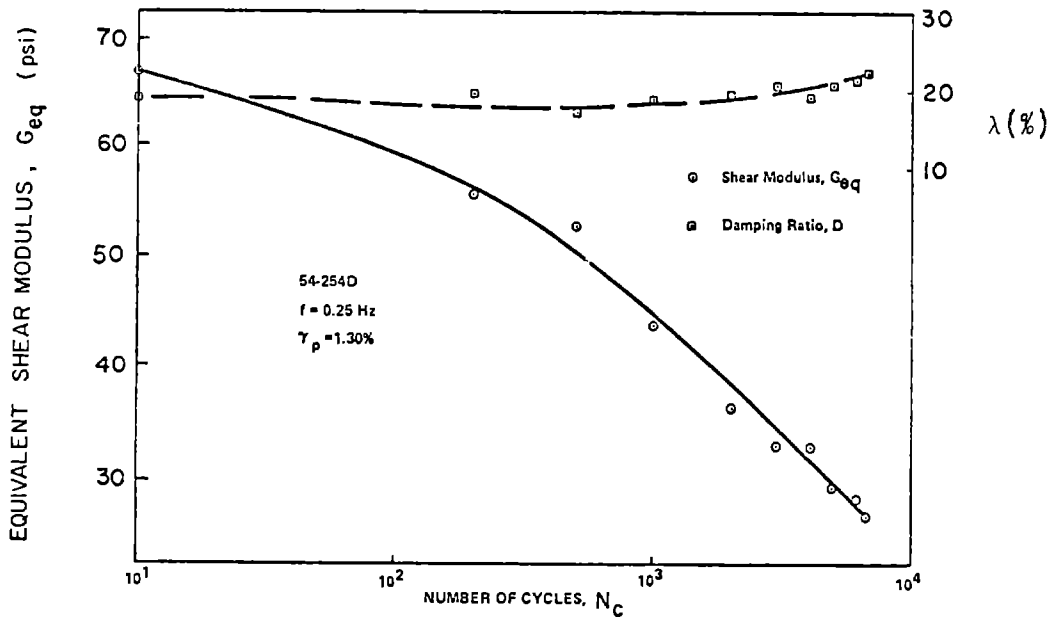


Fig. 24 . Shear Modulus and Damping Ratio versus Number of Cycles (Sherif et al., 1977B)

SOIL-STRUCTURE INTERACTION FOR BUILDINGS DURING EARTHQUAKES

by

A. S. Veletsos^I

ABSTRACT

After a brief review of the principal effects of soil-structure interaction on the response of structures subjected to ground motions, a simple practical procedure is presented for evaluating these effects. The procedure utilizes standard response spectra for fixed-base systems. A brief account also is given of how the concepts underlying this approach have been used recently in the formulation of recommended seismic design provisions.

INTRODUCTION

The dynamic behavior of a structure during an earthquake depends on the characteristics of the motion transmitted through the ground to the base of the structure.

For structures supported on rock or extremely stiff soil, the base or foundation motion is essentially the same as the free-field ground motion, a term that refers to the motion which would take place at the foundation level of the site under consideration if no structure were present. The deformation of the supporting medium due to the motion of the structure itself is negligible in this case in comparison with that due to the earthquake-induced stress waves, and the structure can correctly be analyzed by considering the foundation motion to be the same as the free-field ground motion.

For structures supported on soft soil, on the other hand, the foundation motion may be influenced significantly by the motion of the superimposed structure, and the response can correctly be evaluated only by taking proper account of the feedback or interaction effects between the vibrating structure and the underlying soils. The foundation motion in this case may include an important rocking component in addition to a lateral or translational component. The contribution of the rocking component may be particularly significant for tall structures.

Two factors are responsible for the difference in the responses of a rigidly supported structure and an elastically supported identical structure. First, the elastically supported structure has more degrees of freedom than the rigidly supported structure and hence different dynamic characteristics. Second, a substantial part of the vibrational energy of the elastically supported structure may be dissipated into the supporting medium by radiation of waves and by hysteretic action in the soil itself. There is, of course, no counterpart of this effect of energy dissipation in a rigidly supported structure.

^I Brown & Root Professor of Engineering, Department of Civil Engineering, Rice University, Houston, Texas

The objectives of this paper are: (1) to identify the principal effects of soil-structure interaction on the response of building structures to earthquakes; (2) to review a simple practical procedure for evaluating these effects; (3) to present the more important elements of recently recommend code provisions for incorporating these effects in design; and (4) to discuss the origin and rationale of these provisions.

The soil-structure interaction effects provided for herein represent the difference in the responses of a structure computed by (1) assuming the motion of its foundation to be the same as the free-field ground motion, and (2) considering the modified or actual foundation motion, including the effects of energy dissipation in the supporting medium. This difference depends on the characteristics of the free-field ground motion, as well as on the properties of the structure and the supporting soils.

The characteristics of the free-field motion for a given site depend on a variety of factors, including the magnitude of the anticipated earthquake; the distance of the site from the earthquake source; the source mechanism of the earthquake; the characteristics of the travel path, such as the size, orientation and physical properties of the surface and subsurface strata through which the waves must travel to reach the site; and the local geology and soil conditions of the site. It is important to note that these factors are provided for in the specification of the design free-field ground motion and need not be reconsidered explicitly in the evaluation of the interaction effects.

Fundamental to the information presented in this paper is the assumption that the structure and the underlying soil are bonded and remain so throughout the period of ground shaking. It is further assumed that there is no soil instability or large foundation settlement. The design of the foundation in a manner to ensure satisfactory soil performance, e.g., avoid soil settlement and instability associated with the compaction and liquefaction of loose granular soils, is beyond the scope of this paper. Finally, no account is taken of the interaction effects among neighboring structures.

POSSIBLE APPROACHES TO PROBLEM

Two different approaches may be used to assess the effects of soil-structure interaction (1,2). The first and more natural one involves modifying the stipulated free-field design ground motion and evaluating the response of the structure to the modified motion of the foundation. The second approach involves modifying the dynamic properties of the structure and evaluating the response of the modified structure to the prescribed free-field ground motion. When properly implemented, both approaches lead to equivalent results. However, the second approach, which involves the use of the free-field ground motion, or of the associated response spectra for fixed-base systems, is more convenient for design purposes, and will be used exclusively in this presentation.

It will be shown that the interaction effects in the second approach may be expressed by an increase in the fundamental natural period of vibration of the structure, and by a change (usually increase) in its effective damping. The increase in period results from the flexibility of the foundation soil, whereas the change in damping results mainly from the effects of energy dissipation in the soil due to radiation and material damping.

These concepts are clarified in the following sections by comparing the responses of rigidly supported and elastically supported simple systems to a harmonic excitation of the base.

PRINCIPAL EFFECTS OF INTERACTION

Consider the linear structure of weight W , lateral stiffness k , and coefficient of viscous damping c , shown in Fig. 1, and assume that it is supported by a foundation of weight W_0 at the surface of a homogeneous, elastic halfspace. The foundation mat is considered to be a rigid circular plate of negligible thickness which is bonded to the supporting medium, and the columns of the structure are presumed to be weightless and axially inextensible. Both the foundation weight and the weight of the structure are assumed to be uniformly distributed over circular areas of radius r . The base excitation is specified by the free-field motion of the ground surface, and it is taken as a horizontally directed, simple harmonic motion with a period T_0 and an acceleration amplitude a_m .

This system, which has three degrees of freedom when flexibly supported and a single degree of freedom when fixed at the base, may be viewed either as the direct model of a one-story building frame, or more generally, as a model of a multistory, multimode structure that responds as a single-degree-of-freedom system in its fixed base condition. In the latter case, h must be interpreted as the distance from the base to the centroid of the inertia forces associated with the fundamental mode of vibration of the fixed-base structure; and W , k and c must be interpreted, respectively, as the generalized or effective weight, stiffness, and damping coefficient for that mode. The evaluation of these quantities is considered in subsequent sections.

The configuration of the system at any time is specified by the lateral displacement and rotation of the foundation, $x(t)$ and $\theta(t)$, and by the deformation of the structure, $u(t)$. The foundation displacement $x(t)$ is, of course, generally different from the free-field ground displacement, $d(t)$. For a fixed-base structure, $x(t) = d(t)$ and $\theta(t) = 0$.

The solid lines in Figs. 2 and 3 represent response spectra for the steady-state amplitude of the total shear in the columns of the system considered in Fig. 1. Two values of h/r and several values of ϕ_0 are considered. The latter parameter, which is a dimensionless measure of the relative flexibilities of the soil and the structure, is defined by the equation

$$\phi_0 = \frac{h}{v_s T} \quad (1)$$

in which h is the height of the structure, as previously indicated; v_s is the velocity of shear wave propagation in the halfspace; and T is the natural period of the structure in its fixed-base condition. A value of $\phi_0 = 0$ corresponds to a rigidly supported structure.

The results in Figs. 2 and 3 are displayed in a dimensionless form. The abscissa represents the ratio of the period of the excitation, T_0 , to the fixed-base natural period of the system, T ; and the ordinate represents the ratio of the amplitude of the actual base shear, V , to the amplitude of

the base shear induced in an infinitely stiff, rigidly supported structure. The latter quantity is given by the product ma_m , in which $m=W/g$; g is the acceleration of gravity; and a_m is the acceleration amplitude of the free-field ground motion. The inclined scales on the left represent the deformation amplitude of the superstructure, u , normalized with respect to the displacement amplitude of the free-field ground motion,

$$d_m = \frac{a_m T_o^2}{4\pi^2} \quad (2)$$

The damping of the structure in its fixed-base condition, β , is considered to be 2 percent of the critical value, and the additional parameters needed to characterize completely these solutions are identified in Ref. 3, from which these figures have been reproduced.

Comparison of the results presented in these figures reveals that the effects of soil-structure interaction are most strikingly reflected in a shift to the right of the peak of the response spectrum, and in a change in the magnitude of the peak. These changes, which are particularly prominent for the taller structures and the more flexible soils (larger values of ϕ_o), can conveniently be expressed by an increase in the natural period of the system over its fixed-base value and by a change in its damping factor.

Also shown in these figures in dotted lines are response spectra for single-degree-of-freedom (SDF) oscillators, the natural periods and dampings of which have been adjusted so that the absolute maximum (resonant) value of the base shear and the associated period are, in each case, identical to the corresponding quantities of the actual interacting system. The base motion for the replacement oscillators in these solutions is considered to be the same as the free-field ground motion.

With the properties of the replacement oscillators determined in this manner, it can be seen that the response spectra for the actual and the replacement systems are in excellent agreement over wide ranges of the exciting period on both sides of a resonant peak.

In the context of Fourier analysis, a transient ground motion may be viewed as a combination of harmonic motions of different periods and amplitudes. Inasmuch as the components of the excitation with periods close to the resonant period are likely to be the dominant contributors to the response, the maximum responses of the actual system and of the replacement oscillator can be expected to be in satisfactory agreement for earthquake motions as well. This expectation has been confirmed by the results of comprehensive numerical studies that have been carried out (1,2,3,4).

It follows that, to the degree of approximation involved in the comparison of the results summarized in Figs. 2 and 3, the effects of soil-structure interaction on the maximum response of the structure may be expressed by

- an increase in the fundamental natural period of vibration of the structure; and
- a change in its effective damping.

In the remainder of this paper, the fundamental natural period of the

interacting system will be denoted by \tilde{T} , and the associated damping factor will be denoted by $\tilde{\beta}$. These quantities, which will also be referred to as the effective period and effective damping of the system, may be determined as follows.

EFFECTIVE PERIOD AND DAMPING OF SYSTEM

The effective natural period \tilde{T} is given approximately by the equation

$$\tilde{T} = T \sqrt{1 + \frac{k}{K_x} \left[1 + \frac{K_x h^2}{K_\theta} \right]} \quad (3)$$

in which T is the natural period of the fixed-base structure; K_x is the horizontal translational stiffness of the foundation, defined as the horizontal force at the level of the foundation necessary to produce a unit deflection at that level; K_θ is the rocking stiffness of the foundation, defined as the moment necessary to produce a unit rotation of the foundation; and k and h are as previously defined.

The stiffnesses K_x and K_θ depend on the geometry of the foundation-soil contact area, the properties of the soil beneath the foundation, and the characteristics of the foundation motion. For the circular foundation considered in Fig. 1, the translational stiffness is given approximately by

$$K_x = \frac{8}{2 - \nu} G r \quad (4)$$

and the rocking stiffness is given by

$$K_\theta = \frac{8}{3(1 - \nu)} G r^3 \quad (5)$$

where r is the radius of the foundation; G is the shear modulus of the soil; and ν is its Poisson's ratio. The shear modulus, G , is related to the shear wave velocity, v_s , by the equation

$$G = \frac{v_s^2 \gamma}{g} \quad (6)$$

Although strictly valid for statically loaded foundations, Eqs. 4 and 5 may be used with good accuracy for dynamically excited foundations as well. The approximation involved in the application of these equations to harmonically excited systems is discussed in Ref. 2.

The damping factor of the elastically supported structure, $\tilde{\beta}$, may be expressed in the form

$$\tilde{\beta} = \beta_o + \frac{\beta}{(\tilde{T}/T)^3} \quad (7)$$

where β represents the damping factor of the structure in its fixed-base

condition, and β_0 represents the contribution of the foundation damping. Note that β and β_0 are not directly additive but must be combined in accordance with Eq. 7.

Since \tilde{T} is greater than T , it follows from Eq. 7 that soil-structure interaction reduces the effectiveness of the structural damping, and that the resulting reduction may be quite important when \tilde{T}/T is large. In fact, unless this reduction is offset by the increase due to the effect of foundation damping, the overall damping of the interacting system will be less than that of the fixed-base system.

The foundation damping factor, β_0 , incorporates the effects of energy dissipation in the soil due to the following factors: (1) radiation of waves away from the foundation, known as radiation or geometric damping; and (2) hysteretic or dissipative action in the soil itself, also known as soil material damping.

For the system considered in Fig. 1, the three more important parameters that affect the value of β_0 are:

- the ratio of natural periods of the elastically supported and fixed-base structures, \tilde{T}/T ;
- the ratio h/r of the height of the structure to the radius of the foundation; and
- the damping capacity of the soil itself, defined by the factor

$$\tan \delta = \frac{1}{2\pi} \frac{\Delta W_s}{W_s} \quad (8)$$

The quantity ΔW_s in Eq. 8 represents the area of the hysteresis loop in the stress-strain diagram for a soil specimen undergoing harmonic shearing deformation, and W_s represents the strain energy stored in a linearly elastic material that is subjected to the same maximum stress and strain (i.e., the area of the triangle in the stress-strain diagram between the origin and the point of the maximum induced stress and strain). This ratio is a function of the magnitude of the imposed peak strain, increasing with increasing intensity of excitation or level of straining, and may be considered to be independent of the frequency of motion.

The variation of β_0 with \tilde{T}/T and h/r is shown in Fig. 4 for two values of $\tan \delta$. The dashed lines, which refer to systems supported on a purely elastic medium, represent the effect of radiation damping only, whereas the solid lines, which refer to a viscoelastic medium with $\tan \delta = 0.10$, represent the combined effect of radiation damping and material damping. It can be seen that the foundation damping may be a significant contributor to the overall damping of the system, and that the component contributed by material soil damping may be particularly significant for the taller structures, for which the contribution of radiation damping is generally quite small.

The data in Fig. 4 are for systems of the type considered in Fig. 1 with $W_0 = 0$ and $W = 0.15 \pi r^2 h \gamma$. The latter value represents a weight equal to 15 percent of the weight of the structure when filled with soil. Similar results have been obtained for other weight ratios as well (1,2,3,4).

ANALYSIS PROCEDURE

With the information presented in the preceding sections, the analysis of the system shown in Fig. 1 may be implemented as follows:

1. Evaluate the fixed-base natural period of the structure, T .
2. By application of Eq. 3, evaluate the fundamental natural period of the interacting system, \tilde{T} .
3. Estimate the structural damping factor, β , and the soil damping parameter, $\tan \delta$, and by application of Eq. 7 and the data presented in Fig. 4 and Ref. 2, determine the effective damping factor, $\tilde{\beta}$, for the structure-foundation-soil system. The considerations involved in the choice of the values of β and $\tan \delta$ are discussed in subsequent sections.
4. From the basic response spectrum for fixed-base systems, evaluate the lateral force coefficient, \tilde{C} , corresponding to the natural period \tilde{T} and the damping factor $\tilde{\beta}$. It may be recalled that this coefficient is equal to the ratio of the spectral pseudo-acceleration and the gravitational acceleration.
5. With the value of \tilde{C} established, the maximum value of the base shear for the interacting system, \tilde{V} , may be determined from the equation

$$\tilde{V} = \tilde{C} W \quad (9)$$

6. The maximum deformation of the structure, u_m , may then be determined from

$$u_m = \frac{\tilde{V}}{k} \quad (10)$$

and the maximum horizontal displacement of the mass of the structure relative to its base, Δ_m , may be determined from

$$\Delta_m = \frac{\tilde{V}}{k} + \frac{\tilde{V} h^2}{K_\theta} = u_m \left(1 + \frac{k h^2}{K_\theta} \right) \quad (11)$$

The second term on the right side of Eq. 11 represents the contribution of the rotation of the base.

ATC DESIGN PROVISIONS

The concepts outlined in the preceding sections have provided the basis of the design provisions for soil-structure interaction formulated recently by the Applied Technology Council (ATC). The results of a much broader project that included the development of a comprehensive set of new design recommendations for earthquake-resistant building design, these provisions represent the first known attempt explicitly to incorporate the effects of soil-structure interaction in design codes. Funded by the National Science Foundation and the National Bureau of Standards, this project involved the efforts of 85 participants. A brief account of this effort is presented in Ref. 5, and the complete set of recommendations is

available in Ref. 6.

In the following sections, the more important of the ATC provisions for soil-structure interaction are presented, and their origin and rationale are discussed. Special attention is given to the provisions governing the total lateral seismic design force.

Two different methods have been recommended for the analysis of structures with or without regard for interaction. The first involves the use of equivalent static lateral forces, and is in the spirit of the current design provisions of the Seismology Committee of the Structural Engineers Association of California (7). The second approach is a simplified version of the modal superposition method. Only the equivalent static lateral force method of analysis is considered in this paper.

Provisions for Rigidly Supported Structures

For buildings analyzed without regard for soil-structure interaction, the earthquake-induced total static lateral force or base shear, V , is expressed in the form

$$V = C_s W \quad (12)$$

where W is the total weight of the building, including the dead weight and the effective portion of the design live load; and C_s is a dimensionless coefficient that depends on the following parameters:

- The effective ground acceleration, A , which is an index of the severity of the anticipated seismic activity in a given region. Its value is taken in the range between 0.05 g and 0.40 g, and it is specified in terms of contour maps making due provision for the category and importance of the structure involved.
- The soil factor, S , which accounts for the type of local soil conditions. Three soil categories are considered, including rock or firm sites, deep alluvium sites, and soft soil sites.
- The response modification factor, R , which is a function of the structural type and materials involved. This factor accounts for the different ductility capabilities of different structural types, materials and framing systems, and provides for the better performance observed in actual earthquakes of some types of structures and materials compared with others.
- The fundamental natural period of vibration of the building, T . This quantity may be determined either from empirical equations included in the recommended provisions or by application of fundamental principles of structural dynamics. The variation of C_s with T is shown in Fig. 5.

The damping of the structure does not appear explicitly in these provisions, but a value of 5 percent of critical damping has been used in the development of the basic design spectra.

It should be noted from Fig. 5 that C_s is considered to be a non-increasing function of T . Furthermore, since C_s decreases with increasing damping, an increase in the overall damping of the structure above the value of $\beta = 0.05$ implied in the basic response spectrum will further reduce the

design base shear, V .

In the provisions for interacting systems presented in subsequent sections, the minimum damping for flexibly supported structures is considered to be the same as that for rigidly supported structures (i.e., 5 percent of the critical value). The rationale for this decision is explained later. As a consequence of this decision and the form of the response spectrum presented in Fig. 5, consideration of soil-structure interaction will *decrease* the design values of the base shear, lateral forces and overturning moments from the levels applicable to a rigid-base condition. Therefore, these forces can be evaluated conservatively without the adjustments recommended in the following sections.

Because of the influence of foundation rocking, however, the horizontal displacements relative to the base of the elastically supported structure may be *larger* than those of the corresponding fixed-base structure, and this may increase both the required spacing between buildings and the secondary design forces associated with the P-delta effects. Such increases are generally small and have a minor influence on the final design.

Provisions for Flexibly Supported Structures

For structures analyzed with due regard for soil-structure interaction, the total static lateral design force or base shear, \tilde{V} , is expressed in the form

$$\tilde{V} = V - \Delta V \quad (13)$$

in which V is the base shear for the rigidly supported structure, determined in accordance with Eq. 12; and ΔV is the reduction due to soil-structure interaction. The reduction, ΔV , is defined by the equation

$$\Delta V = \left[C_s - \tilde{C}_s \left(\frac{0.05}{\tilde{\beta}} \right)^{0.4} \right] \bar{W} \quad (14)$$

where

C_s = the seismic design coefficient determined from the basic response spectrum (Fig. 5) using the fundamental natural period of the fixed-base structure, \bar{T} ;

\tilde{C}_s = the value of C_s corresponding to the fundamental natural period of the flexibly supported structure, \tilde{T} ;

$\tilde{\beta}$ = the fraction of critical damping for the structure-foundation-soil system; and

\bar{W} = the effective weight of the building, which is taken as 70 percent of the total weight, W , subject to the following exception. When W is effectively concentrated at a single level, \bar{W} is taken equal to W .

The evaluation of the quantities \tilde{T} and $\tilde{\beta}$ is considered in the next two sections, and the derivation of Eq. 14 is given in the Appendix.

Fundamental to the development of Eq. 14 is the assumption that soil-structure interaction affects only the response component contributed by

the fundamental mode of vibration. This has been demonstrated to be a good approximation for typical building structures (1,2).

In Eq. 14 the difference between C_s and \tilde{C}_s provides for the effect of the increased period of the elastically supported structure compared to that of the rigidly supported structure; the factor raised to the 0.4 power accounts for the change in the effective damping of the elastically supported structure from the value of $\beta = 0.05$ used in the development of the basic design spectrum; and the use of the effective instead of the total weight provides for the fact that soil-structure affects almost exclusively the response component contributed by the fundamental mode of vibration.

Strictly speaking, the relationship between \bar{W} and W depends on the detailed characteristics of the structure. The constant value of $\bar{W} = 0.7W$ is used in the interest of simplicity and because it is a good approximation for typical buildings. For example, for buildings with a constant weight per floor level and a fundamental mode of vibration that increases linearly with height, the exact value of $\bar{W} = 0.75W$.

The maximum permissible reduction in base shear due to the effects of soil-structure interaction is set at 30 percent of the value calculated for a rigid-base condition. It is expected, however, that this limit will control only infrequently, and that the calculated reduction will usually be less.

Effective Building Period. The effective period, \tilde{T} , is determined from Eq. 3, with k interpreted as the effective stiffness of the structure when vibrating in its fixed-base fundamental mode, and h interpreted as the height from the base to the centroid of the inertia forces associated with motion in that particular mode. The latter quantities will be identified by the symbols \bar{k} and \bar{h} , respectively.

The effective stiffness, \bar{k} , is defined by the equation

$$\bar{k} = 4\pi^2 \frac{\bar{W}}{g T^2} \quad (15)$$

and the effective height, \bar{h} , is taken as 70 percent of the total height, except when the weight of the structure is effectively concentrated at a single level, in which case it is taken as the height to that level. Strictly speaking, the relationship between \bar{h} and h depends on the characteristics of the structure and the supporting soil. The constant value of $\bar{h} = 0.7h$ is used in the interest of simplicity and consistency with the approximation used in the definition of W . For structures with the same total weight per floor level and a fundamental mode of vibration that increases linearly with height, the exact value of $\bar{h} = (2/3)h$.

For mat foundations of arbitrary shape, the stiffnesses K_x and K_θ in Eq. 3 may be computed from Eqs. 4 and 5 subject to the following modifications. The radius r in Eq. 4 must be interpreted as

$$r_a = \sqrt{\frac{A_o}{\pi}} \quad (16)$$

and in Eq. 5, it must be interpreted as

$$r_m = \sqrt[4]{\frac{4 I_o}{\pi}} \quad (17)$$

The quantity r_a represents the radius of a disk which has the area of the actual foundation, A_o ; and r_m represents the radius of a disk the static moment of which about a horizontal centroidal axis, I_o , is equal to that of the actual foundation in the direction in which the response is being evaluated.

Equations 4 and 5 in combination with Eqs. 16 and 17 are strictly valid only for mat foundations supported at or near the ground surface. They can also be used for embedded foundations when there is no positive contact between the soil and the walls of the structure, or when any existing contact cannot reasonably be expected to remain effective during the stipulated design ground motion. The effect of foundation embedment may be accounted for by use of a corrective factor specified in the recommended provisions (6). Also included in the recommendations are guidelines for evaluating the stiffnesses of footing foundations and pile foundations. It should be noted, however, that there is only a small amount of information available concerning the interaction effects for structures supported on such foundations (8, 9,10). The recommended provisions in these cases represent the Committee's best interpretation of, and judgement relative to, the current state of knowledge.

Soil Properties. The soil properties of interest are the shear modulus, G , the associated shear wave velocity, v_s , the unit weight, γ , and Poisson's ratio, ν .

These quantities are likely to vary from point to point of a construction site, and it is necessary to use average values for the region of the soil significantly affected by the forces acting on the foundation. The depth of significant influence is a function of the dimensions of the foundation base and of the direction of the motion involved. It may be considered to extend to about $4 r_a$ below the foundation base for horizontal and vertical motions, and to about $1.5 r_m$ for rocking motion. For mat foundations, the depth of significant influence is related to the total plan dimensions of the mat, whereas for buildings supported on widely spaced spread footings, it is related to the dimensions of the individual footings. For closely spaced footings, the depth of significant influence may be determined by superposition of the 'pressure bulbs' induced by the forces acting on the individual footings.

Since the stress-strain relations for soils are nonlinear, the values of G and v_s are functions of the severity of ground shaking and should be determined so as to correspond to the dominant strain levels associated with the design ground motion. The recommended values of G and v_s are listed below as a function of the effective ground acceleration, A :

Value of A , in g's	≤ 0.10	0.15	0.20	≥ 0.30
Value of G/G_o	0.81	0.64	0.49	0.42
Value of v_s/v_{s0}	0.9	0.8	0.7	0.65

The normalizing quantity v_{s0} in this tabulation represents the average shear wave velocity for the soils beneath the foundation at small amplitude strains (of the order of 10^{-3} percent or less); and $G_0 = \gamma v_{s0}^2$ represents the associated shear modulus.

The values of v_{s0} and G_0 depend on a number of factors, of which the more important are the void ratio of and the average confining pressure for the soil. The confining pressure at a given depth depends, in turn, on the weight of the overlying soil and the weight of the superimposed structure and foundation. These values may be determined approximately from empirical relations summarized in Ref. 6, or more accurately by means of field or laboratory tests. Field evaluations may be carried out by standard refraction methods or the cross-hole method, whereas laboratory tests may be carried out with resonant column devices (11).

It should be emphasized that the tabulated values of G/G_0 and v_s/v_{s0} represent first-order approximations. More precise evaluations would require field tests or laboratory tests on undisturbed samples from the site, and studies of wave propagation for the site to determine the magnitudes of the soil strains associated with the stipulated design ground motion. However, such precision is seldom warranted in building design.

Effective Damping. The effective damping of the structure-foundation-soil system is determined from Eq. 7, with the structural damping factor taken as $\beta = 0.05$ and the minimum value of $\tilde{\beta}$ taken as $\tilde{\beta} = \beta = 0.05$.

The foundation damping factor, β_0 , is determined from Fig. 6. The dashed lines in this figure, which are recommended for values of A equal to or less than $0.10g$, correspond to a soil material damping value of $\tan \delta \approx 0.5$; and the solid lines, which are recommended for values of A equal to or greater than $0.20g$, correspond to a value of $\tan \delta \approx 0.15$. These curves are based on the results of extensive parametric studies (1,2,3,4) and represent average values. For the ranges of parameters that are of interest in the design of ordinary building structures, however, the dispersion of the results is small.

For mat foundations of arbitrary shape, the radius r in Fig. 6 should be interpreted as a characteristic length that is related to the length, L_0 , of the foundation in the direction in which the structure is being analyzed. For short, squatty structures for which $\bar{h}/L_0 \leq 0.5$, the overall damping of the structure-foundation system is dominated by the translational motion of the foundation, and r is interpreted as r_a (see Eq. 16.) On the other hand, for structures with $\bar{h}/L_0 \geq 1$, the interaction effects are dominated by the rocking motion of the foundation, and r is interpreted as r_m (see Eq. 17). For intermediate values of \bar{h}/L_0 , the value of r is determined by interpolation.

The curves in Fig. 6 may also be used for embedded mat foundations and for foundations involving spread footings or piles. In the latter two cases, the quantities A_0 and I_0 in the expressions for r should be interpreted as the area and moment inertia, respectively, of the *load carrying* foundation.

In the evaluation of the overall damping of the structure-foundation system, no distinction has been made between surface-supported foundations and embedded foundations. Since the effect of embedment is to increase the

damping capacity of the foundation (12,13), and since such an increase is associated with a reduction in the magnitude of the forces induced in the structure, the application of the recommended provisions to embedded structures will err on the conservative side.

Equation 7, in combination with the information presented in Fig. 6, may lead to damping factors for the structure-soil system, $\tilde{\beta}$, which are smaller than the structural damping factor, β . However, since the representative value of $\beta = 0.05$ used in the development of the design provisions for rigidly supported structures is presumably based on the results of tests on actual buildings, it reflects the damping of the entire structure-soil system, not merely of the component contributed by the superstructure. Therefore, the value of $\tilde{\beta}$ determined from Eq. 7 should not be taken less than β , and a low bound of $\tilde{\beta} = \beta = 0.05$ has been imposed. The use of values of $\tilde{\beta} > \beta$ is justified by the fact that the experimental values correspond to extremely small-amplitude motions and do not reflect the effects of the higher soil damping capacities associated with the large soil strains that correspond to the design ground motions. The effects of the higher soil damping capacities are appropriately reflected in the values of β_0 presented in Fig. 6.

For buildings supported on point bearing piles, and in all other cases where the foundation soil consists of a soft stratum of reasonably uniform properties underlain by a much stiffer, rock-like deposit with an abrupt increase in stiffness, the radiation damping effects may be substantially less than those for nearly uniform soil deposits, and it is necessary to reduce the foundation damping factors determined from Fig. 6. For such cases, special relations have been proposed in Ref. 6 for the computation of both the foundation damping factor, β_0 , and the foundation stiffnesses, K_x and K_θ .

Distribution of Seismic Forces and Other Effects

The vertical distributions of the equivalent lateral forces for flexibly and rigidly supported structures are generally different. However, the differences are inconsequential for practical purposes, and it is recommended that the same distribution be used in both cases, changing only the magnitude of the forces to correspond to the appropriate base shear. A greater degree of refinement in this step would be incompatible with the approximations involved in the provisions for rigidly supported structures. The relevant distribution is identified in Chapter 4 of Ref. 6.

With the vertical distribution of the lateral forces established, the overturning moments and the torsional effects about a vertical axis are computed as for rigidly supported structures. Finally, the lateral floor displacements relative to the base are computed from a generalized version of Eq. 11. For additional details, reference should be made to Ref. 6.

CONCLUDING REMARKS

It is hoped that the information presented in this paper has provided improved insight into the major effects of soil-structure interaction on the behavior of buildings during earthquakes and into the more important factors that affect the interaction phenomenon.

The ATC provisions for incorporating these effects in design provide

sufficient flexibility and accuracy for practical applications. Only for unusual structures of major importance, and only when the recommended provisions indicate that the interaction effects are indeed of definite consequence in design, would the use of more elaborate procedures be justified.

Following are some of the refinements that are possible, listed in order of more or less increasing complexity:

1. Improve the estimates of the static stiffnesses of the foundation, K_x and K_θ , and of the foundation damping factor, β_0 , by considering in a more nearly precise manner the foundation type involved, the effects of foundation embedment, variations of soil properties with depth, and hysteretic action in the soil. The relevant solutions may be obtained by analytical or semi-analytical formulations, or by application of finite difference or finite element techniques (9,10,14,15).
2. Improve the estimates of the average properties of the foundation soils for the stipulated design ground motion. This would require both laboratory tests on undisturbed samples from the site and studies of wave propagation for the site. The laboratory tests are needed to establish the actual variations with shearing strain amplitude of the shear modulus and damping capacity of the soil, whereas the wave propagation studies are needed to establish realistic values for the predominant soil strains induced by the design ground motion.
3. Incorporate the effects of interaction for the higher modes of vibration of the structure, either approximately by application of the procedures recommended in Refs. 16, 17 and 18, or by more precise analyses of the structure-soil system. The latter analyses may be implemented either in the frequency domain by use of Fourier transform techniques (1,2,19), or directly in the time domain (1) by application of the impulse response functions presented in Ref. 20. However, the frequency domain analysis is limited to systems that respond within the elastic range, whereas the approach involving the use of the impulse response functions is limited at present to soil deposits that can adequately be represented as a uniform elastic half-space. The effects of yielding in the structure and/or supporting medium can be considered only approximately in this approach, by representing the supporting medium by a series of springs and dashpots whose properties are independent of the frequency of the motion, and by integrating numerically the governing equations of motion (21).
4. Analyze the structure-soil system by the finite element method (22, 23,24), taking due account of the nonlinear effects in both the structure and the supporting medium.

It should be emphasized that, while they may be appropriate in special cases for design verification, the more elaborate methods referred to above involve their own approximations, and do not eliminate the uncertainties that are inherent in the modeling of the structure-foundation-soil system, and in the specification of the design ground motion and the properties of the structure and soil.

At a time when the trend in analysis seems to be toward the use of ever more complex structural models and sophisticated methods, it is worth emphasizing that increased complexity and sophistication in analysis does not necessarily ensure improved design. Because of the numerous factors that

influence the dynamic response of structural systems and because of the sensitivity of the response to variations in many of these factors, it is generally quite difficult, if not impossible, intelligently to interpret the results of a limited number of highly complex analyses. Because of limitations of funds and time, such solutions are often limited to a small set of conditions, and design decisions are reached without adequate assessment of the effects upon the final design of the numerous uncertainties embodied in the analyses. The problem is aggravated by the fact that the computer programs used to implement these analyses are often used with inadequate appreciation of the assumptions and approximations embodied in the idealization of the problem and the method of analysis itself. The end product under such conditions may be no better than, and may in fact be inferior to, what could be achieved at far lower cost by simpler approaches with which the effects of variations in the more important factors can be evaluated readily.

The design provisions for soil-structure interaction summarized in this paper are believed to be as simple, rational and potentially useful as they can be made at the present stage of knowledge. Furthermore, they are capable of refinement in light of new information without the need for revising the basic approach. There is, to be sure, need for additional basic research in this area. The sections of the provisions that stand to benefit most from further research are those relating to buildings supported on piles or spread footings.

ACKNOWLEDGEMENT

This paper is based on Chapter 6 and the associated Commentary of Ref. 6, which were prepared by a committee on the Applied Technology Council composed of Drs. M. S. Agbabian, J. Bielak, P. C. Jennings, F. E. Richart, Jr., and J. M. Roesset, with the author serving as Chairman. Mr. R. L. Sharpe was Project Director of the program for ATC, and Dr. N. M. Newmark was Chairman of Task Group II, of which the committee referred to was a part. In addition to acknowledging the contributions of my associates in this effort, I wish to thank Drs. M. Novak and J. H. Rainer of Canada for several helpful comments.

REFERENCES

1. Nair, V. V. D., "Dynamics of Certain Structure-Foundation Systems," Ph.D. Dissertation submitted to Rice University, Houston, Texas, 1974.
2. Veletsos, A. S., "Dynamics of Structure-Foundation Systems," Structural and Geotechnical Mechanics, A Volume Honoring N. M. Newmark (W. J. Hall, Editor), Prentice-Hall, Inc., Englewood Cliffs, N. J., 1977, pp. 333-361.
3. Veletsos, A. S., and Meek, J. W., "Dynamic Behavior of Building-Foundation Systems," Earthquake Engineering and Structural Dynamics, Vol. 3, No. 2, 1974, pp. 121-138.
4. Veletsos, A. S., and Nair, V. V. D., "Seismic Interaction of Structures on Hysteretic Foundations," Journal of the Structural Division, Proc. ASCE, Vol. 101, No. ST1, January, 1975, pp. 109-129.
5. Newmark, N. M., et al, "Seismic Design and Analysis Provisions for the United States," Proceedings of the Sixth World Conference on Earthquake Engineering, New Delhi, India, 1977.

6. "Tentative Provisions for the Development of Seismic Regulations for Buildings," will be available in 1978 as ATC-3-06 Report from Applied Technology Council, Palo Alto, California, and as NBS Special Publication 510 from Superintendent of Documents, Washington, D. C.
7. "Recommended Lateral Force Requirements and Commentary," Seismology Committee of the Structural Engineers Association of California, 171 Second Street, San Francisco, California 94105.
8. Nair, K., Gray, H., and Donovan, N. C., "Analysis of Pile Group Behavior," ASTM Special Technical Publication No. 44, 1969.
9. Novak, M., "Dynamic Stiffness and Damping of Piles," Canadian Geotechnical Journal, Vol. 11, 1974, pp. 574-598.
10. Blaney, G. W., Kausel, E., and Roesset, J. M., "Dynamic Stiffnesses of Piles," Proceedings, Second International Conference on Numerical Methods in Geomechanics, Blacksburg, Virginia, Vol. 2, pp. 1001-1012.
11. Richart, F. E., Jr., Hall, J. R., and Woods, R. D., "Vibrations of Soils and Foundations," Prentice-Hall, Inc., Englewood Cliffs, N. J., 1970.
12. Novak, M., "Effects of Soil on Structural Response to Wind and Earthquake," Earthquake Engineering and Structural Dynamics, Vol. 3, 1974, pp. 79-96.
13. Bielak, J., "Dynamic Behavior of Structures with Embedded Foundations," Earthquake Engineering and Structural Dynamics, Vol. 3, 1975, pp. 259-274.
14. Luco, J. E., "Impedance Functions for a Rigid Foundation on a Layered Medium," Nuclear Engineering and Design, No. 31, 1974, pp. 204-217.
15. Veletsos, A. S. and Verbic, B., "Vibration of Viscoelastic Foundations," Earthquake Engineering and Structural Dynamics, Vol. 2, No. 1, 1973, pp. 87-102.
16. Roesset, J. M., Whitman, R. V., and Dobry, R., "Modal Analysis for Structures with Foundation Interaction," Journal of the Structural Division, Proc. ASCE, Vol. 99, No. ST3, 1973, pp. 399-416.
17. Tsai, N. C., "Modal Damping for Soil-Structure Interaction," Journal of the Engineering Mechanics Division, Proc. ASCE, Vol. 100, No. EM2, 1974, pp. 323-341.
18. Bielak, J., "Modal Analysis for Building-Soil Interaction," Journal of the Engineering Mechanics Division, Proc. ASCE, Vol. 102, No. EM5, 1976, pp. 771-786.
19. Jennings, P. C. and Bielak, J., "Dynamics of Building-Soil Interaction," Bulletin of Seismological Society of America, Vol. 63, No. 1, February, 1973, pp. 9-48.
20. Veletsos, A. S., and Verbic, B., "Basic Response Functions for Elastic Foundations," Journal of Engineering Mechanics Division, Proc. ASCE, Vol. 100, No. EM2, 1974, pp. 189-202.

21. Parmelee, R. A., Perelman, D. S., and Lee, S. L., "Seismic Response of Multistory Structures on Flexible Foundations," Bulletin of the Seismological Society of America, Vol. 29, 1969, pp. 1061-1070.
22. Seed, H. B., Lysmer, J., and Hwang, R., "Soil-Structure Interaction Analysis for Seismic Response," Journal of the Geotechnical Engineering Division, Proc. ASCE, Vol. 101, No. GT5, 1974, pp. 439-457.
23. Seed, H. B., Whitman, R. V., and Lysmer, J., "Soil-Structure Interaction Effects in the Design of Nuclear Power Plants," Structural and Geotechnical Mechanics, A Volume Honoring N. M. Newmark (W. J. Hall, Editor), Prentice-Hall, Inc., Englewood Cliffs, N. J., 1977, pp. 220-241.
24. Vaish, A. K., and Chopra, A. K., "Earthquake Finite Element Analysis of Structure-Foundation Systems," Journal of the Engineering Mechanics Division, Proc. ASCE, Vol. 100, No. EM6, 1974, pp. 1011-1016.
25. Arias, A. and Husid, R., "Influence of Damping on Earthquake Response of Structures," Revista del IDIEM, Vol. 1, No. 3, December 1962 (in Spanish).
26. Newmark, N. M., Blume, J. A., and Kapur, K. K., "Seismic Design Spectra for Nuclear Power Plants," Journal of the Power Division, Proc. ASCE, Vol. 99, No. P02, November 1973, pp. 873-889.

For additional references, see Ref. 2 and Commentary for Chapter 6 of Ref. 6.

APPENDIX

DERIVATION OF EQUATION 14

Upon adding and subtracting the term $C_s(T, \beta) \bar{W}$, Eq. 12 may be written in the form:

$$V = C_s(T, \beta) \bar{W} + C_s(T, \beta) [W - \bar{W}] \quad (A-1)$$

where \bar{W} represents the generalized or effective weight of the structure when vibrating in its fundamental natural mode, and the terms in parentheses are used to emphasize the fact that C_s depends upon both T and β . The first term on the right side of this equation approximates the contribution of the fundamental mode of vibration, whereas the second term approximates the contributions of the higher natural modes.

Inasmuch as soil-structure interaction may be considered to affect only the contribution of the fundamental mode, and inasmuch as this effect can be expressed by changes in the fundamental natural period and the associated damping of the system, the base shear for the interacting system, \tilde{V} , may be stated in a form analogous to Eq. A-1 as follows:

$$V = C_s(\tilde{T}, \tilde{\beta}) \bar{W} + C_s(T, \beta) [W - \bar{W}] \quad (A-2)$$

The value of C_s in the first term on the right should be determined for the natural period and damping of the elastically supported system, \tilde{T} and $\tilde{\beta}$; and the value of C_s in the second term should be determined for the corresponding quantities of the rigidly supported system, T and β .

Next, rewrite Eq. A-2 in the same form as Eq. 13. On making use of Eq. 12 and rearranging terms, one obtains the following expression for the reduction in the base shear,

$$\Delta V = \left[C_s(T, \beta) - C_s(\tilde{T}, \tilde{\beta}) \right] \bar{W} \quad (A-3)$$

Within the ranges of natural period and damping that are of interest in studies of building response, the values of C_s corresponding to two different damping values but the same natural period, say \tilde{T} , are related approximately as follows:

$$C_s(\tilde{T}, \tilde{\beta}) = C_s(\tilde{T}, \beta) \left(\frac{\beta}{\tilde{\beta}} \right)^{0.4} \quad (A-4)$$

This expression, which appears to have been first proposed in Ref. 25, is in good agreement with the results of recent studies of earthquake response spectra for systems having different damping values (26).

Substitution of Eq. A-4 in Eq. A-3 leads to

$$\Delta V = \left[C_s(T, \beta) - C_s(\tilde{T}, \beta) \left(\frac{\beta}{\tilde{\beta}} \right)^{0.4} \right] \bar{W} \quad (A-5)$$

where *both* values of C_s are now for the damping factor of the rigidly supported system, and may be evaluated from the standard response spectrum. If the values corresponding to the periods T and \tilde{T} are denoted more simply as C_s and \tilde{C}_s , respectively, and if the damping factor β is taken as 0.05, Eq. A-5 reduces to Eq. 14.

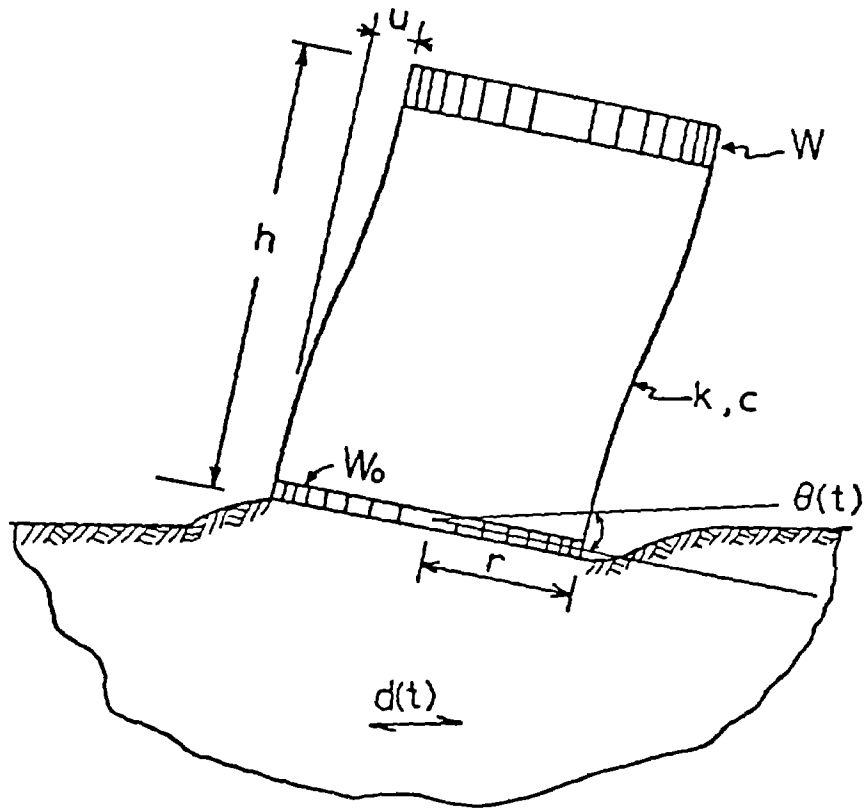


Fig. 1 Simple System Investigated

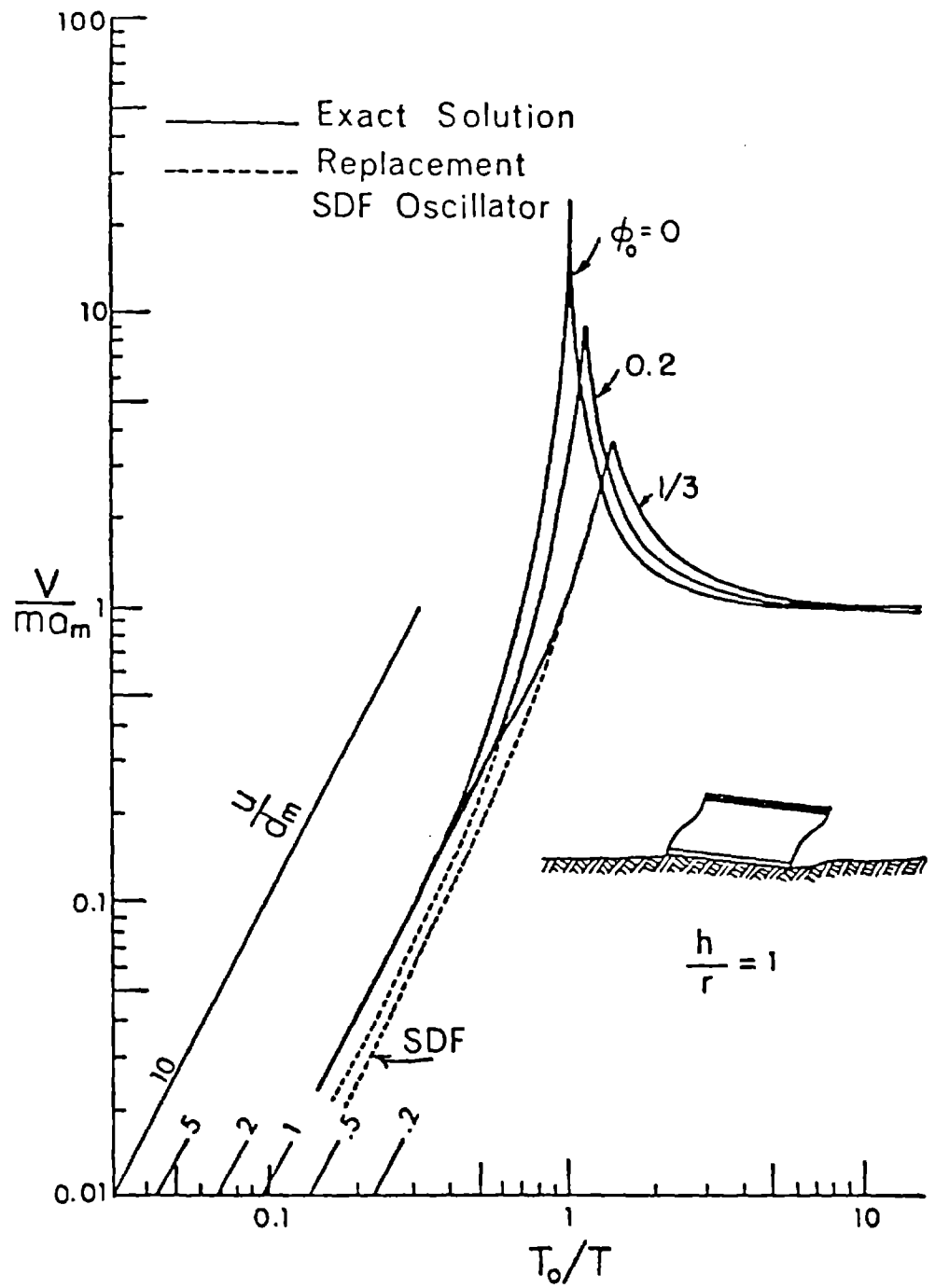


Fig. 2 Response Spectra for Systems with $h/r = 1$

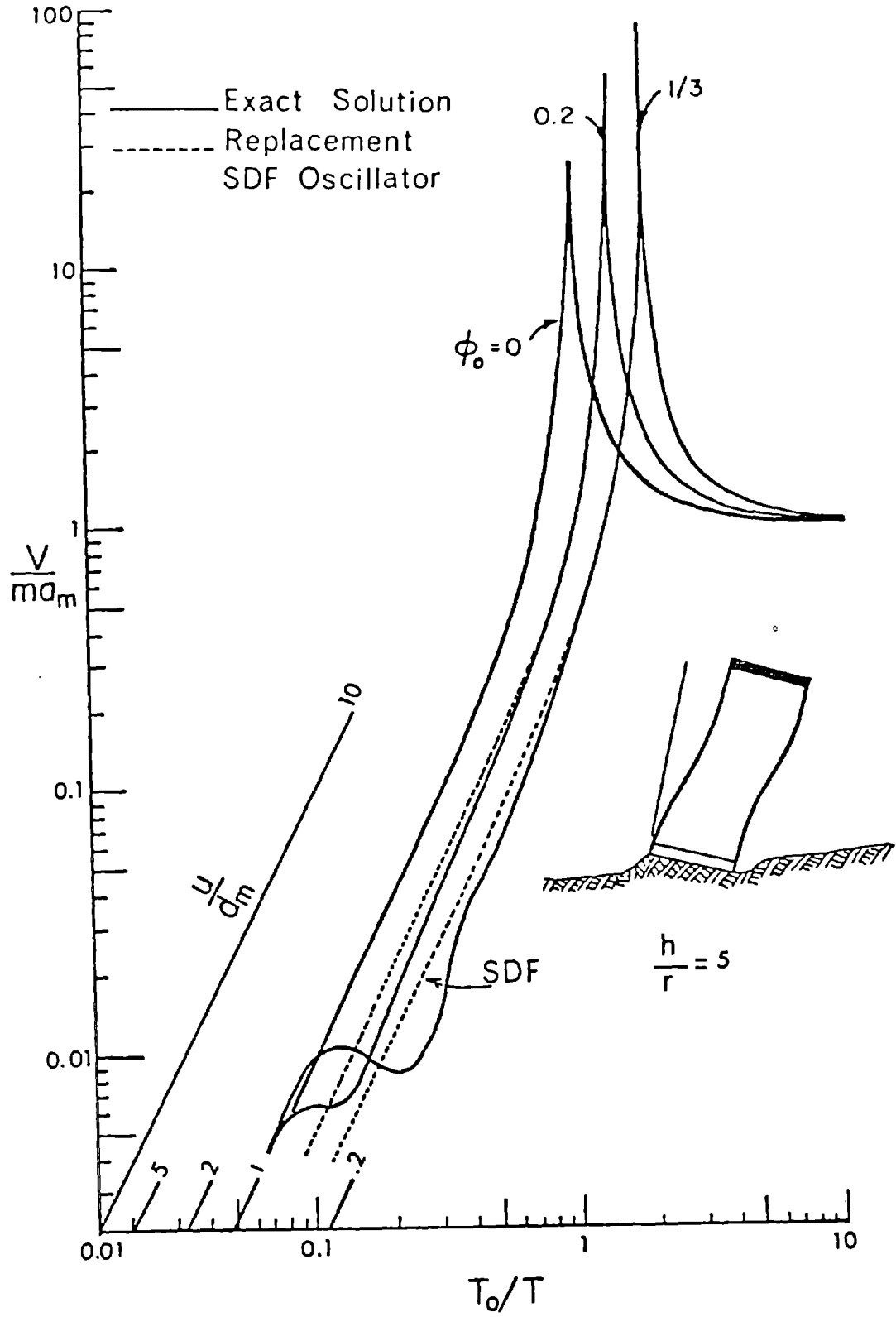


Fig. 3 Response Spectra for Systems with $h/r = 5$

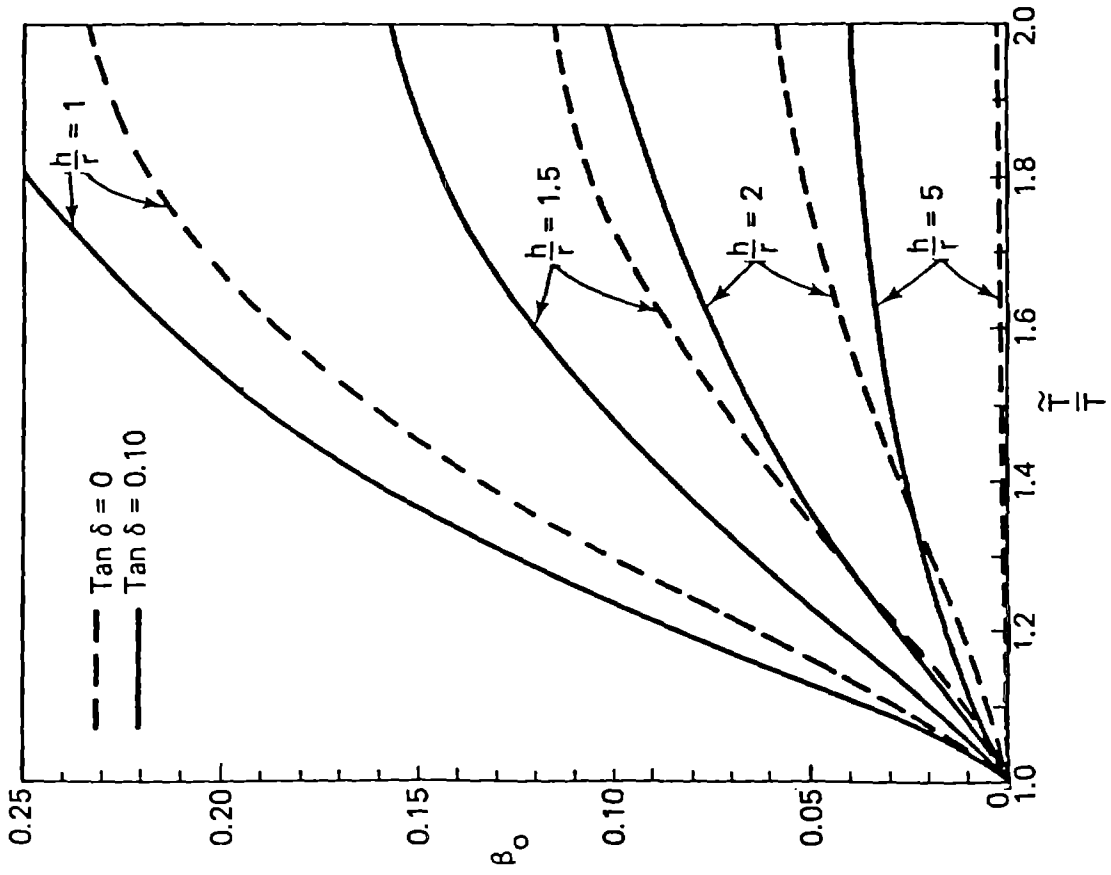


Fig. 4 Foundation Damping Factor, β_0

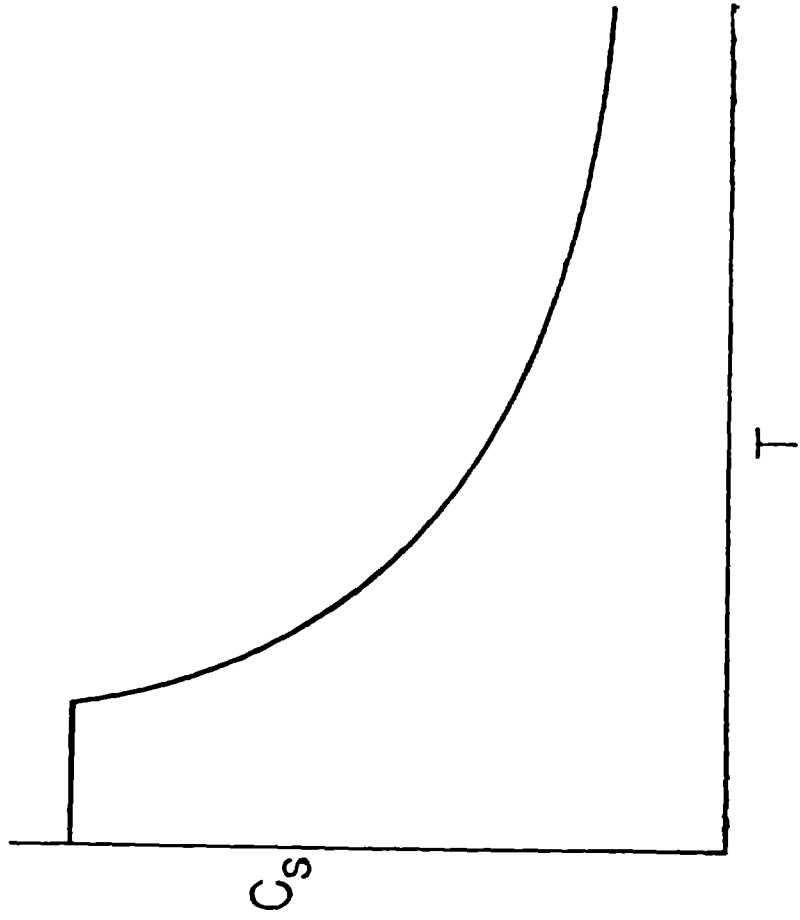


Fig. 5 Standard Response Spectrum

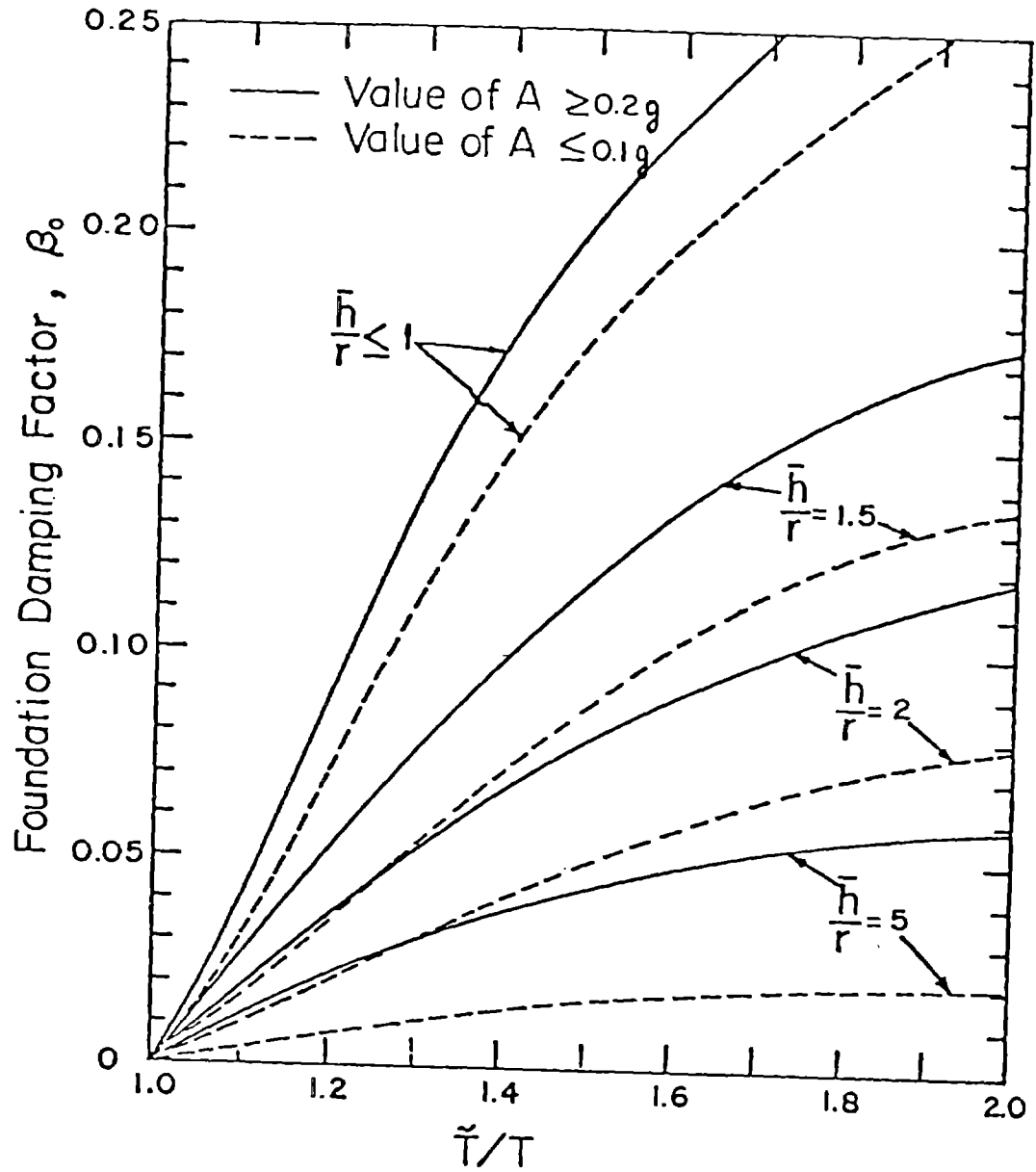


Fig. 6 Design Value of Foundation Damping Factor, β_0

INTENTIONALLY BLANK

GEOLOGIC CONSIDERATIONS FOR SEISMIC MICROZONATION

By

LLOYD S. CLUFF⁽¹⁾

INTRODUCTION

Seismic microzonation is herein defined as the subdivision of a region into areas or zones that have relatively similar exposure to various earthquake-associated effects (such as surface fault rupture, ground shaking, ground failure, and water inundation). The aim of microzonation is to estimate the location, recurrence interval, and relative severity of future seismic events in an area so the potential hazards can be assessed and the effects can be mitigated or avoided.

Seismic microzonation studies are most definitive and useful when conducted as integrated multidisciplinary efforts combining data and judgments from geology, seismology, geophysics, engineering, and planning (1). The objective of this paper is to discuss the contributions of geologic data and judgments to interdisciplinary microzonation studies, to recognize some of the problems that have developed in attempting to assess and classify seismic hazards, and to suggest alternatives for consideration to advance the science of microzonation to come to more realistic assessments of seismic hazards.

GEOLOGIC ASPECTS OF MICROZONATION

The geologic discipline has recently made several major contributions to seismic microzonation studies. Geologic studies contribute data for the identification and delineation of earthquake sources, assessment of earthquake size, estimation of earthquake recurrence intervals, and evaluations of the potential for surface fault rupture, the ground shaking hazard, and the ground failure hazard. Following is a discussion of the state of the geologic practice in these areas.

Identification and Delineation of Earthquake Sources

Geologic and seismologic researchers are generally agreed that earthquakes are caused by displacements along faults within the shallow part of the earth's crust. These faults have appropriately been referred to as "causative faults". Even where earthquakes are associated with volcanic activity, those earthquakes represent fault displacements associated with volcanic processes. The sources and locations of future earthquakes, therefore, will be along faults, and will be most likely to occur along faults having a history of repeated fault displacements in the relatively recent geologic past (several million years).

(1) Vice President and Chief Geologist
Woodward-Clyde Consultants
Three Embarcadero Center, Suite 700
San Francisco, California 94111

Displacement along causative faults may or may not reach the ground surface during a particular earthquake depending upon size, depth, and extent of the rupture surface. Large, shallow-focus earthquakes are nearly always associated with surface fault rupture along the causative fault zone. Magnitude 5-1/2 to 6 appears to be the threshold value of earthquakes associated with surface fault rupture, although surface faulting has been associated with earthquakes as small as magnitude 3.6 (2). Repeated surface fault rupture along fault zones produces recognizable geomorphic features that are more or less distinct, depending upon the relationship between the frequency of surface faulting and other geologic processes such as erosion and deposition. Zones of characteristic geomorphic features are especially common along faults associated with major plate boundaries, where repeated surface faulting occurs. These diagnostic features have been described in detail by Cluff and Brogan (3) and Slemmons (4) and recognition of them has proved to be the most fundamental tool in identifying and delineating potential earthquake sources.

Within large plates, such as the North American plate, some relatively infrequent but damaging intraplate earthquakes have not yet been satisfactorily identified with causative faults. The geologic evidence of these faults is sometimes extremely subtle, and past investigations have generally not been designed to detect such subtle features. Recently, however, detailed studies in the New Madrid region have begun to reveal evidence for the causative faults associated with the 1811 and 1812 earthquakes in that region (5, 6). Thus, given appropriately designed detailed studies, it is being shown that geologic investigations can provide much more reliable data on locations of future major earthquakes.

Assessment of Earthquake Size

The size of future large earthquakes can be estimated by analysis of the geometry, amount, and extent of fault displacement. Techniques for this analysis have been most recently summarized by Slemmons (4). Such geologic studies have been applied to microzonation efforts in several locations along or near major plate boundary causative fault zones, such as in the San Francisco Bay Area (7), and in New Zealand (8).

In intraplate regions, more work is needed to develop causative fault data to the point where it can be reliably utilized as effectively as along faults associated with plate boundaries. In the central United States, joint efforts by the U.S. Geological Survey and other cooperating groups are producing encouraging results (5).

Because of the difficulty of recognizing and delineating active faults in the eastern United States, it is the practice to use the "tectonic province" approach in estimating the size of potential earthquakes, rather than to assign earthquakes to specific faults. Using the tectonic province approach, the size of the largest earthquake that has occurred anywhere within an area, or "tectonic province," is conservatively increased in magnitude and then assumed to be capable of occurring anywhere in the entire province (9). This approach results in controversies over the bases for delineating the boundaries of the tectonic provinces, and these boundaries often have been defined on the

basis of ancient geologic structures that may not have any relevance to present earthquake-producing mechanisms. The tectonic province approach has undoubtedly resulted in costly overconservatism in the earthquake design of many engineering structures, as well as the risk that some facilities may be located directly across active faults, faults that remain to be identified at a later time, either as the result of the application of more definitive geologic and geophysical techniques, or as the result of a surprise earthquake. In the future, the procedures and techniques presently utilized in the western United States⁽¹⁾ should be applied to studies in the eastern United States⁽¹⁾; that is, procedures that are based on identifying individual geologic structures responsible for causing earthquakes. Considering the low degree of activity in most parts of the eastern United States, there is a need for significantly greater geologic and geophysical efforts than have been required in the western United States. These new efforts in the east may also require the development of new and innovative techniques in order to detect small fault displacements and to date the most recent geologic history of fault behavior.

Estimation of Earthquake Recurrence Intervals

The estimation of earthquake recurrence intervals frequently has primarily relied on the temporal pattern of past earthquakes, as evidenced by the historical earthquake record; however, one of the most widespread and significant problems confronted during seismic microzonation studies is the relatively short earthquake record. Even where this record is one thousand or more years (such as in China, Japan, and Italy), the irregular pattern of earthquake occurrence indicates that this interval is too short to record long-term periodicity that may be operating (10, 11). However, through the understanding and application of the Quaternary geologic record, the available earthquake record can be significantly lengthened (to one million or more years).

An increasing number of studies during the past decade have utilized the Quaternary geologic record to detect Quaternary fault displacements and to estimate recurrence intervals at particular locations along causative faults. Allen (10, 12) has summarized the results of such studies in California, Turkey, Japan, the Philippines, and China, and has succinctly described the value of the Quaternary geologic record in overcoming "many of the statistical inadequacies of the relatively short instrumental and historical records." York and others (13) utilized LANDSAT-1 imagery of China in an analysis of Quaternary faulting and earthquakes. In New Zealand, Quaternary faulting and seismicity have been studied for several decades (14, 15) and have formed the basis for more recent microzonation efforts (8). Ambraseys (16, 17) has utilized archeological data in the Middle East together with Quaternary geology in documenting the irregular time distribution of earthquakes in that area.

Studies of Quaternary geology are particularly helpful in areas having very short earthquake histories, such as California. In a recent California study by Sieh (18), one segment of the San Andreas fault has

(1) For the purpose of this paper, the boundary between the western and eastern U.S. is the eastern front of the Rocky Mountains (Denver).

geologic evidence of eight prehistoric earthquakes similar to an 1857 event (magnitude 8+). These have occurred since 575 \pm 45 years A.D., and have an average recurrence interval of 160 years.

To estimate the frequency of fault displacements, it is necessary to know the age of the faulted rock, the age of the younger deposits and soils that cover the faulted rock, and the age of the material along the fault plane or filling the fault zone (often gouge or mineral deposits). Therefore, there is an increasing demand for accurate absolute dates of geologic deposits. The absolute dating of geologic materials can be difficult because of a lack of suitable geologic materials or because the age of the available materials is not within the age range of the available techniques. Moreover, erroneous or misleading age dates can be derived due to sample contamination or alteration, or because secondary geologic processes have affected the datable component of the sample. Geologic dating problems require an interpretation of a wide variety of information from many disciplines, and an understanding of the geologic processes involved to select the technique or combination of techniques that will be most effective in assessing the age of the materials. Packer and others (19) have prepared an overview of age dating techniques available to the geologist in solving geologic dating problems. Quaternary geology and dating of geologic materials are key research areas for the future to increase the ability to accurately estimate earthquake recurrence intervals.

Evaluation of the Potential for Surface Fault Rupture

Geologic information is critical to the identification and evaluation of the potential for surface fault rupture. Ground deformation associated with surface fault rupture is often complex, involving both discrete displacements across narrow fault traces and warping across a wide zone. The zone of deformation will vary from a meter or two to a hundred meters or more in width, depending upon the following variable factors: (1) type and style of faulting, (2) attitude of the fault plane, (3) amount of displacement, (4) direction of displacement, and (5) surficial geology (1, 20).

Numerous studies have been made of surface fault rupture patterns produced during historical earthquakes. Bonilla and Buchannan (21) have summarized such data and originated nomenclature for various parts of the observed patterns that are applicable to most cases of surface faulting. Oborn (22) provides a thorough summary of previous evaluations of surface fault rupture as applied to engineering geologic situations. Wesson and others (7) applied these data, together with data on fault creep, to a regional microzonation study in the five-county San Francisco Bay Area. Rogers and Williams (23) applied similar data to microzonation of one county in the San Francisco Bay Area. At the site-specific level, Cluff and others (1) considered the complexities of surface fault rupture deformation, and identified ten separate zones of significantly distinct deformation types. Taylor and Cluff (20) have recently assessed the importance of surface fault rupture and associated tectonic deformation to the problems of lifeline earthquake engineering.

The Managua, Nicaragua earthquake of 1972 provided an excellent example of the effects of surface fault rupture through a major urban area

along several separate faults (24, 25). Detailed geologic studies of the deformation associated with fault displacement and the geologic conditions in the vicinity of Managua were made and translated into microzonation products (26, 27). One interesting observation during this investigation was the Banco Central de Nicaragua, a large, modern structure situated astride one of the faults that experienced a few centimeters of surface fault rupture. The bank survived without significant damage due to fault displacement (28). The massive structure, designed to house the National Treasury, was sufficiently strong to resist the surface faulting that occurred, and caused the fault displacement to deflect around the building. This illustrates that if structures must be sited within active fault zones, it is possible to design them to resist or deflect ground deformation to the extent that they retain their usefulness provided detailed information is known regarding the exact fault locations, the type and style of displacement, the amount and direction of displacement, fault geometry, and surficial geologic conditions.

Evaluation of the Ground Shaking Hazard

The geologic data important to the evaluation of the shaking hazard are the understanding of the regional geologic conditions, and especially an understanding of the location and distribution of bedrock, and the location, distribution, relative thickness, and geometry of surficial materials. These data, when combined with geophysical data such as shear wave velocity profiles at specific locations, can be used to enhance the interpretation of site-specific ground motion data (strong motion records). Examples of microzonation studies utilizing this approach are Borchardt (29) and McCrory (30) for the San Francisco and Monterey areas of California, and Grant-Taylor (8) for the Wellington, New Zealand area. Both studies also utilize the observed modified Mercalli intensity distribution from previous major earthquakes to calibrate observed geologic and other conditions, and to produce microzone maps showing areas of anticipated future maximum intensity.

Evaluations of the ground shaking hazard are currently hampered by the paucity of strong motion records of damaging earthquakes, the lack of understanding of the seismicity of large areas, and the need to better understand the phenomena and processes responsible for damaging ground motion (31). Future studies and research, including the development of dynamic rupture models and the collection of instrumental data on damaging ground motions close to causative faults and correlating these motions with actual damage to buildings will do much to increase the understanding of the ground shaking hazard for microzonation.

Evaluation of Ground Failure Hazard

Secondary ground failures that can occur in surface deposits during strong ground shaking include seismically induced landslides, liquefaction, and subsidence. Geologic investigations can provide data on the location and extent of cohesionless soils, lithology and physical properties of surface deposits, depth to groundwater, and locations of historical landslides. These data can be used to assess future landslide susceptibility, liquefaction potential, and potential for compaction and settlement for microzonation of the ground failure hazard. When

identified at a particular site, these hazards can be mitigated by correcting the condition by removal of the incompetent deposits, or by special design of the foundation of the structure. Examples of maps of existing landslides and maps depicting landslide potential that were produced specifically for seismic hazard evaluation and microzonation studies in the San Francisco Bay Area are Brabb and Pampeyan (32), Brabb and others, (33), Nilsen and Brabb (34), and Rogers and Williams (23). Regarding liquefaction, lithologic data and hydrologic setting have been utilized by Youd and others (35), Youd (36), and Borchardt (29) in describing ground failures associated with earthquakes and in constructing maps of areas of liquefaction potential. In New Zealand, similar considerations have been made in a microzonation study of Wellington (8).

Sometimes, the current lack of understanding of the mechanics of ground failure processes such as liquefaction precludes mitigating the hazard. In these cases, through adequate geologic studies, these earthquake-related problems can be identified and addressed by complete avoidance rather than mitigation. Lee and others (31) summarized the basic studies of soils subject to liquefaction and collapse and the development of new empirical techniques that will be needed before the loss of strength of various soils under earthquake effects can be assessed more definitively.

CURRENT PROBLEMS IN ASSESSING AND CLASSIFYING SEISMIC HAZARDS

Microzonation Studies That Are Not Interdisciplinary

In an interdisciplinary microzonation study, various geoscience and engineering disciplines consider different aspects of the seismic hazard. To optimize the results of an integrated study, all disciplines should be represented in, or be aware of, all the aspects of the study. Disciplines most active early in the study should maintain sufficient presence throughout the study to 1) explain their assumptions, judgments, and levels of confidence and conservatism; 2) prevent inadvertent misuse of interpretations and results; and 3) observe the full implications and effects of their judgments. Disciplines most active later in the study should maintain sufficient presence throughout the study to: 1) foresee the implications of early judgments and data; 2) communicate these implications to the disciplines involved; and 3) maximize the efficiency of their own studies through more complete understanding of previous results. During this process, mutual understanding can be enhanced and overall problems can be addressed.

Numerous studies have been conducted to depict zones of relative seismic hazard that have utilized only one or two of the geoscience or seismologic disciplines. Because of the limited data base, these studies are less credible in describing the type and distribution of various seismic effects that may constitute hazards, and may result in misleading conclusions concerning potential hazards, which may in turn lead to inappropriate or inconsistent assumptions of risk. The following examples will serve to illustrate this.

In the case of the Romanian earthquake of March 4, 1977, a detailed microzonation study had previously been prepared for the Bucharest area based primarily on geophysical modeling techniques. Apparently, no

consideration was made of a previous major earthquake (1941) that produced damage in the Bucharest area, or regional geologic or seismologic data. After study of the damage pattern produced by the 1977 earthquake, it was apparent that the detailed microzones previously delineated bore little resemblance to the 1977 intensity distribution. However, a reconstruction of the 1941 intensity distribution was remarkably similar to that of 1977. Based on the available data, the 1941 and 1977 earthquakes were very similar in location, size, and apparent source characteristics. Thus, in this case, the pre-1977 Bucharest microzonation study proved inadequate to describe relative seismic hazards due to lack of an integrated approach that considered regional geologic, seismologic, geophysical, and historical data.

Other examples of non-integrated studies are those utilizing the historical earthquake record as the primary data source. These are often called "seismic risk" studies, a term which implies much more analysis than the studies usually contain. Most of these studies involve sophisticated statistical treatment of data from historical earthquake catalogs. By not considering regional and local geologic conditions, such studies overlook data that may contradict or invalidate the apparent results of the primarily statistical analysis. Often, the type of geologic data needed does not exist in available published form, and must be obtained by original field studies. An illustration of this point is the Makran Coast in southeastern Iran and southwestern Pakistan. A study based primarily on the historical seismic record led to the conclusion that the Makran Coast area in southeastern Iran represents the least seismic hazard of any area in Iran due to the paucity of recorded historical earthquakes (37). Data from a recent geologic study of the Quaternary geology along the Makran Coast (38) lead to precisely the opposite conclusion. The Quaternary geologic data extend the relatively short historical record along the Makran Coast and clearly indicate that major earthquakes have occurred there many times during the recent geologic past and the potential for the largest earthquakes in Iran exists in that region.

Deterministic Classification of Fault Activity

Geologists experienced in assessing fault activity in seismic regions throughout the world have usually recognized there is a significant difference in the degree of activity between faults. This difference is dependent upon the relationship of a fault to a particular tectonic stress environment. However, because of the lack of uniform knowledge about the location and extent of potential earthquake sources, combined with the need of various regulatory agencies in the United States to assess the safety of critical facilities, faults have been classified as either "active" or "inactive", often depending on the judged degree of hazard based upon the recency of fault displacement. One of the first fault activity classification systems was developed by the New Zealand Geological Survey (39). This system is based on evidence for late Quaternary faulting and formed the basis for the first fault activity classification for nuclear power plants in the United States (40). Present siting criteria for nuclear power reactors developed by the U.S. Nuclear Regulatory Commission (9) and criteria for fault classification for the safety of dams developed by the U.S. Bureau of Reclamation and the U.S. Army Corps of Engineers have used the terms "active" and "inactive"

and "capable" and "noncapable"; these terms have taken on somewhat rigid legal definitions. All these definitions are based on certain time intervals since the most recent displacement to define fault activity or capability. Each agency's criteria for fault activity is summarized as follows:

U.S. Nuclear Regulatory Commission: evidence for multiple fault displacements in 500,000 years, single fault displacement in 35,000 years;

U.S. Bureau of Reclamation: evidence for fault displacement in 100,000 years;

U.S. Army Corps of Engineers: evidence of fault displacement in 35,000 years;

State of California: evidence of fault displacement in 11,000 years.

This deterministic "active fault concept" for assessing fault activity resulted mostly from a fundamental lack of confidence regarding the understanding of earthquake mechanics and the behavior of faults, and the inability to confidently identify and delineate the sources of potential earthquake activity uniformly across the United States. The problem in using the active fault concept is that rigid definitions do not allow the degree of fault activity to be appropriately taken into consideration and, under these presently developed criteria, once a fault is classified as active according to any of these definitions, it appears to be equally as hazardous as any other active fault. This is clearly not a correct assessment of the potential for slip on a fault as it exists in nature.

A problem that will become increasingly important with time is the discovery of new active or capable faults in regions where none were previously thought to exist. As an example, past general procedures for selecting the sites for dams and other critical facilities have not always adequately evaluated fault activity and earthquake hazards. Too often, the site evaluation focused on the historical earthquake record and gave little attention to geologic evidence for fault activity and associated earthquake hazards. Thus in the absence of pertinent information, conclusions regarding earthquake hazards often relied on published geologic literature that was not prepared for the purpose of earthquake hazard assessment. The discovery of active faults in regions where none were previously thought to exist is becoming commonplace as greater emphasis is placed on comprehensive regional tectonic evaluation of fault activity. A specific case is the proposed Auburn Dam, which was located in a region not previously known to have active faults. It was not until the Oroville earthquake of August 1, 1975 that geologists and seismologists found conclusive evidence for geologically young faulting in the western Sierran foothills of California. If active faults exist there, why did we not know about them prior to the occurrence of a destructive earthquake? The answer to this question is the same as in many other similar cases; adequate geologic and seismologic studies had not been aimed at looking for fault activity. Now that circumstances have developed to focus scientific attention on a region previously thought to be relatively aseismic, and appropriate techniques especially developed to

evaluate fault activity have been systematically applied to the region, several active faults have been found in the western Sierran foothills of California.

The implication of newly discovered active faults is beginning to be realized with the release of a map by the U.S. Geological Survey entitled "Preliminary Map of Young Faults in the United States as a Guide to Possible Fault Activity" (41). Most of the hundreds of faults shown on this map are generally known to experienced geologists, however they are a real surprise to most engineers and public officials involved in the regulatory process regarding earthquake safety of critical facilities. While some of the faults shown on the map will be classified as inactive or noncapable utilizing the present deterministic criteria for fault activity, many of the faults shown on the map will undoubtedly be classified as active or capable. This preliminary map is only the beginning from the standpoint of the implications for existing and future critical facilities. Research on the evaluation of fault activity will continue to discover active faults were none were thought to exist and some of the newly discovered active faults will be near or beneath existing or planned critical facilities such as nuclear reactors, dams, and LNG plants.

Probabilistic Calculations of Earthquake Recurrence Intervals

One of the most important questions that needs to be answered is, what is the frequency of occurrence of damaging earthquakes? Several statistical models that are supposed to represent the process of earthquake occurrence have been proposed to answer this question. The most common is the Poisson model, which assumes spatial and temporal independence of all earthquakes; that is, the occurrence of one earthquake does not affect the likelihood of a similar earthquake at the same location in the next unit of time. Other models such as those proposed by Estevea (42) and Shlien and Toksoz (43) consider the clustering of earthquakes in time. A few other probabilistic models have been used to represent earthquake sequences as strain energy release mechanisms such as in Knopoff and Kagan (44). They used a stochastic branching process that considers a stationary rate of occurrence of main shocks and a distribution function for the space, time and location of foreshocks and aftershocks. These models are all useful in the general broad context of estimating earthquake recurrence sequences over large tectonic regions; however, they are not adequate to characterize specific occurrences of earthquakes. While the Poisson process does provide estimates for a region of the probability of occurrence of earthquakes of a specific magnitude or of the formation of a seismic gap, the estimates are independent of the size of and time elapsed since the most recent earthquake, and they are insensitive to location. Therefore, precise calculations of earthquake recurrence based on these methods must be viewed with extreme caution, especially when they are based on an often inadequate historical earthquake record.

DEGREE OF FAULT ACTIVITY -- A CONCEPT WHOSE TIME HAS COME

A recent comparison of fault activity rates between faults associated with different tectonic environments (Table 1) shows that there can be a

FAULT	SLIP RATE (CM/YEAR)	CALCULATED CUMULATIVE SLIP (M)				MAXIMUM SLIP/EVENT (METERS)	RECURRENCE INTERVAL (YEARS)
		10K yrs	35K yrs	100K yrs	500K yrs		
Fairweather, Ak.	5.8	580	2030	5800	29000	10	170
San Andreas, Ca.	3.7	370	1295	3700	18500	10	270
Hayward, Ca.	.6	60	210	600	3000	2	300
Coyote Creek, Ca.	.3	30	105	300	1500	1.5	500
Lower Rhine Graben, Germany	.023	2.3	8.5	23	115	.5	2000
Upper Rhine Graben, Germany	.005	.5	1.75	5	25	.3	6000
Cleveland Hill, Ca.	.0006	.06	.21	.60	3	.2	33000

Table 1 -- COMPARISON OF DEGREE OF FAULT ACTIVITY

difference of several orders of magnitude in the degree of activity of different faults. As an example, a given fault in a highly active tectonic environment may have a slip rate of 6 centimeters per year and may have the potential for as much as 10 meters of displacement in a single event. The recurrence interval for the 10-meter-slip event may be approximately 150 years. The cumulative slip, representing multiple slip events, that results from 100,000 years of strain accumulation along that fault will be 6000 meters. Conversely, a fault in a tectonic environment of moderately low degree of activity may have a slip rate of 0.0006 centimeters a year and may have the potential for only 20 centimeters of slip in a single event. The recurrence interval for the 20-centimeter-slip event may be approximately 33,000 years. The cumulative slip resulting from 100,000 years of strain accumulation across the fault in this environment will be only 60 centimeters. This is a significant contrast to 6000 meters in a highly active tectonic environment. Both faults may be of engineering significance; however, it is unrealistic to call both faults active as though they were of comparable hazard.

Another way of illustrating the relative degree of fault activity is shown on Figure 1. On this figure, faults having a slip rate from 1 to 10 centimeters per year, such as the Fairweather fault in Alaska and the San Andreas fault in California, have a very high rate of activity. Faults having lower rates of slip, smaller displacements, and longer recurrence intervals have relative degrees of fault activity that are significantly lower.

The slip rate line shown as A in Figure 1 illustrates a fault having a very high degree of activity. Two different forms of behavior are indicated on this fault; one showing long recurrence intervals interrupted

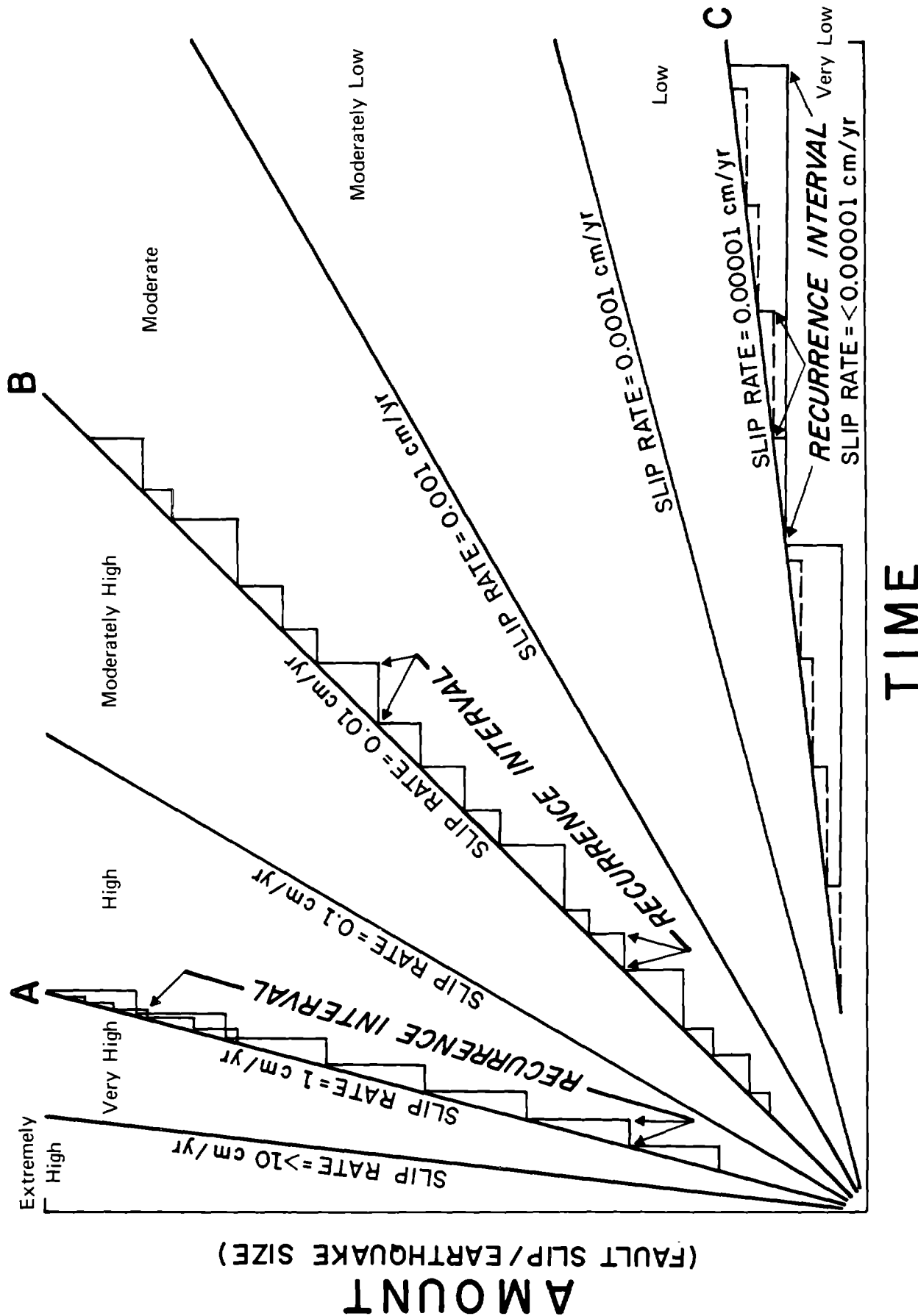


Figure 1 - RELATIVE DEGREE OF FAULT ACTIVITY

by large fault displacements releasing large earthquakes (lower part of line A), and one (upper part of line A), representing shorter recurrence intervals interrupted by episodes of smaller amounts of fault slip releasing more frequent, smaller earthquakes. Recent studies of fault behavior indicate that some faults may be consistently uniform in the size of earthquakes released, as well as uniform in the length of the recurrence interval between major earthquakes (11). On the other hand, some very long faults, especially plate boundary faults, which may have the same slip rate along their entire length, show distinct behavioral differences in both size of earthquakes and recurrence intervals along certain segments (45, 46).

Slip rate line B on Figure 1 represents a fault having a moderate degree of activity. The recurrence intervals shown are a mixture of long intervals followed by large displacements and shorter intervals followed by smaller displacements.

The slip rate line shown as C in Figure 1 represents faults having a low degree of activity. Two possible interpretations of recurrence and size of earthquakes is shown. In this tectonic environment, the longer recurrence intervals may be several tens of thousands of years and the shorter recurrence intervals may be several thousand years, with a corresponding decrease in amount of strain accumulation and displacement.

All the faults represented by the relative degrees of activity in Figure 1 may meet the deterministic criteria to be classified as active or capable faults, even though the faults range from having an extremely high to a very low degree of activity.

The deterministic criteria created to define active or capable faults are being regarded by society and some professionals in regulatory agencies as legal descriptions that categorize a fault as safe or unsafe. Therefore, these criteria have a tendency to become the basis for value judgments on safety. We must work towards the phasing out of terms such as "active" and "capable", descriptions that tend to categorize a fault as safe or unsafe. Instead, we must aim toward assessing the degree of activity of individual faults on a quantitative basis, answering the following questions: (1) What is the probability of fault slip during the life of a facility? (2) What is the probability of exceeding a given amount of slip in a single event? (3) What is the probability of a certain size earthquake occurring during the life of the facility? (4) What is the magnitude of the earthquake that has a high probability of occurring during a certain time interval? and (5) What is the probability of the estimated maximum earthquake occurring along a given fault?

Using the deterministic active fault concept in the earthquake safety regulatory process has undoubtedly resulted in critical facilities being constructed using excessive conservatism to compensate for our ignorance in being able to confidently answer these questions. Also, some unsafe structures have probably been built at hazardous sites because of this same ignorance. Improved basic scientific knowledge that will allow us to confidently answer these questions will obviously result in increased confidence in the safety of critical facilities, and the additional knowledge will permit such facilities to be located and built more economically, avoiding the waste that is presently inherent in our conservatism.

Probabilistic values, even though based on considerable professional judgment, are what are needed to allow realistic assessment of hazards so that rational value judgments can be made regarding the levels of acceptable risk.

REALISTIC PROBABILISTIC MODEL FOR EARTHQUAKE RECURRENCE

The evaluation of the Quaternary geologic evidence for seismicity, combined with the historical record of seismicity, shows that significant earthquakes exhibit nonrandom patterns in terms of location, size, and frequency of occurrence. The occurrence of significant earthquakes can be represented by a relatively continuous, gradual process of strain accumulation, interrupted periodically by episodes of sudden energy release caused by fault slip. Several factors influence the size of earthquakes in a given area; the area available to accumulate strain, the rate of strain accumulation, the shearing resistance along faults, and the amount of sudden fault displacement. This physical model suggests a dependence on at least two conditions; the size of and the time elapsed since the most recent significant earthquake. Since both conditions will vary from fault to fault, the probability of occurrence of a significant earthquake or continuation of a seismic gap can be expected to vary from location to location, even within the same tectonic region.

Patwardhan and others (47) have utilized a semi-Markov process, which can model the spatial and temporal tendencies of great, main-sequence earthquakes. A semi-Markovian representation of earthquake sequences is consistent with a generalized understanding of earthquake generation consisting of gradual, uniform strain accumulation and periodic release of a significant amount of strain energy by fault displacement. Since the build up of strain energy sufficient to generate another significant earthquake along a given fault would take some time, the occurrence of a significant earthquake along the same segment of the fault is less likely within some time following an earthquake of similar size than along the segment of the fault that has not experienced a similar earthquake for a long time. As the time elapsed without the occurrence of another significant earthquake increases, so does the probability of its occurrence. It is reasonable to assume that both the size and the waiting time to the next significant earthquake is influenced by the amount of strain energy released along that segment of the fault in the previous significant earthquake and the length of time over which strain has been accumulating along that segment of the fault. For example, assuming a constant strain rate along a major fault, the strain build up required to generate a large magnitude earthquake will take longer than the strain build up to generate a moderate magnitude earthquake. These considerations are well modeled by a semi-Markovian representation of earthquake sequences. In addition, a semi-Markov process has the basic Markovian property of a one-step memory (the probability that the next significant earthquake is of a given magnitude depends on the magnitude of the previous significant earthquake). The development and application of the semi-Markov model for estimating the probabilities of great earthquakes is discussed in detail by Patwardhan and others (47).

The purpose of discussing the semi-Markov process is to bring it to the attention of geologists and seismologists who have been critical of inaccurate and unrealistic, albeit sophisticated, statistical treatments

of earthquake recurrence that have not taken into consideration the fact that the earthquake process is one of gradual strain accumulation interrupted periodically by sudden fault slip. The semi-Markov model appears to be closer to representing the true earthquake process, rather than being based on an over simplified assumption that earthquakes are spatially and temporally independent, and that the occurrence of one earthquake does not affect the likelihood of similar earthquakes along the segment of a fault during the next unit of time. The primary result obtained from the semi-Markov model is the probabilities of occurrences of different magnitude earthquakes in a given zone during a specified period of interest. The probabilities are location and time-specific; that is, they are dependent on the initial condition of the zone and are applicable for the duration of real time. For example, if a period of interest of the next 100 years is specified, the probabilities are applied to the next 100 years, rather than to all 100-year intervals. The probabilities derived from this method provide contributions to a seismic risk model that are more consistent with the earthquake mechanism of strain accumulation and cyclic energy released by faulting.

The continuing research in refinement of the semi-Markov model, together with the potential of incorporating geologic data (data on the degree of fault activity), will allow a more realistic assessment of earthquake hazards that will result in a more realistic quantification of seismic risk. However it is important to understand that the confidence in the final answers are directly related to our ability to understand the fundamental aspects of earthquake mechanisms and fault behavior.

CONCLUSION

We must face earthquake safety issues knowing that there are uncertainties, and attempt to quantify the uncertainties probabilistically so that value judgments about the level of acceptable risk are based on the best and most reliable data at the time of the decision. There has always been uncertainty in the geologic and geophysical sciences and the time has come to accurately communicate this uncertainty and estimate the degree of fault activity so that decision makers have a realistic basis for earthquake hazard mitigation and risk management. We must give the most accurate answer now, while periodically revising our estimates as more reliable data become available. An adequately completed probabilistic approach allows scientific assessments to be made with a clear indication of the degree of confidence in the data.

Considering the results of basic earthquake research that are beginning to be realized, and anticipated future research programs, we are truly on the threshold of an exciting phase of earthquake hazard assessment and risk quantification that, when appropriately applied, will allow realistic assessment of the degree of hazard so that confident value judgments can be made regarding acceptable earthquake risk.

REFERENCES

- (1) Cluff, L.S., Hansen, W.R., Taylor, C.L., Weaver, K.D., Brogan, G.E., McClure, F.E., Idriss, I.M., and Blayney, J.A., 1972, Site evaluation in seismically active regions--an interdisciplinary team approach, in Proceedings of International Conference on Microzonation for Safer Construction Research and Application, Seattle, Washington, v. 2, p. 957-987.
- (2) Brune, J.N. and Allen, C.R., 1967, A low-stress-drop, low-magnitude earthquake with surface faulting: the Imperial, California, earthquake of March 4, 1966: Seismological Society of America Bulletin, v. 57, no. 3, pp. 501-514.
- (3) Cluff, L.S. and Brogan, G.E., 1974, Investigation and evaluation of fault activity in the U.S.A: proceedings for the Second International Congress of the International Association of Engineering Geology, Sao Paulo, Brazil.
- (4) Slemmons, D.B., 1977, Faults and earthquake magnitude, Report 6 of State of the Art for Assessing Earthquake Hazards in the United States: U.S. Corps of Engineers Miscellaneous Paper S-73-1, 129 p.
- (5) Buschbach, T.C., 1977, New Madrid seismotectonic study--activities during fiscal year 1977: Illinois State Geological Survey, Report prepared for the Division of Reactor Safety Research, Office of Nuclear Regulatory Research, U.S. Nuclear Regulatory Commission, 61 p.
- (6) McKeown, F.A., 1978, Mississippi Valley seismotectonics, in Summaries of Technical Reports, volume 5, Prepared by participants in National Earthquake Hazards Reduction Program, January 1978, p. 84-85.
- (7) Wesson, R.L., Helley, E.J., Lajoie, K.R., and Wentworth, C.M., 1975, Faults and earthquakes, in Studies for Seismic Zonation of the San Francisco Bay Region: U.S. Geological Survey Professional Paper 941-A, p. A5-A30.
- (8) Grant-Taylor, T.L., Adams, R.D., Hatherton, T., Milne, J.D.G., Northey, R.D., and Stephenson, W.R., 1974, Microzoning for earthquake effects in Wellington, New Zealand: New Zealand Department of Scientific and Industrial Research, Bulletin 213, 62 p.
- (9) Code of Federal Regulations, 1973, Reactor site criteria: Title 10, Part 100, Appendix A, U.S. Atomic Energy Commission, Washington, D.C.
- (10) Allen, C.R., 1975, Geologic criteria for evaluating seismicity: Geological Society of America, v. 86, p. 1041-1057.
- (11) Wallace, R.E., 1978, How often will earthquakes occur on the San Andreas fault?: U.S. Geological Survey Earthquake Information Bulletin, v. 10, no. 3, p. 76-81.

- (12) Allen, C.R., 1978, Quaternary geology--an essential clue to evaluating seismicity: U.S. Geological Survey Earthquake Information Bulletin, v. 10, no. 1, p. 4-11.
- (13) York, R.K., Cardwell, R., Ni, J., 1976, Seismicity and Quaternary faulting in China: Bulletin of the Seismological Society of America, v. 66, no. 6, p. 1983-2002.
- (14) Wellman, H.W., 1955, New Zealand Quaternary tectonics: Geologischen Rundschau, v. 43, no. 1, p. 248-257.
- (15) Lensen, G.L., 1965, Active faults and major earthquakes in New Zealand: New Zealand Journal of Geology and Geophysics, v. 8, no. 6.
- (16) Ambraseys, N.N., 1962, A note on the chronology of Willis's list of earthquakes in Palestine and Syria: Seismological Society of America Bulletin, v. 52, no. 1, pp. 77-80.
- (17) Ambraseys, N.N., 1971, Value of historical records of earthquakes: Nature, v. 232, p. 375-379.
- (18) Sieh, K.E., 1977, Prehistoric large earthquakes produced by slip on the San Andreas fault at Pallet Creek, California: Journal of Geophysical Research, v. 82, no. B8, p. 3907-3939.
- (19) Packer, D.R., Biggar, N.E., and Hee, K.S., 1976, Age dating of geologic materials, a survey of techniques: Woodward-Clyde Consultants, San Francisco, California.
- (20) Taylor, C.L., and Cluff, L.S., 1977, Fault displacement and ground deformation associated with surface faulting: Proceedings of Current State of Knowledge of Lifeline Earthquake Engineering, ASCE, Los Angeles, California, p. 338-353.
- (21) Bonilla, M.G., and Buchanan, J.M., 1970, Interim report on worldwide historic surface faulting: U.S. Geological Survey Open File Report, December 1970.
- (22) Oborn, L.R., 1974, Seismic phenomena and engineering geology, in proceedings of the Second International Congress of the International Association of Engineering Geology, Sao Paulo, Brazil, v. 1, p. II-GR.1 through GR.41.
- (23) Rogers, T.H., and Williams, J.W., 1974, Potential seismic hazards in Santa Clara County, California: California Division of Mines and Geology Special Report 107.
- (24) Cluff, L.S. and Carver, G.A., 1973, Geological observations, in Managua, Nicaragua Earthquake of December 23, 1972: Earthquake Engineering Research Institute Reconnaissance Report, Oakland, California.
- (25) Brown, R.D. Jr., Ward, P.L., and Plafker, G., 1973, Geologic and seismologic aspects of the Managua, Nicaragua earthquakes of December 23, 1972: U.S. Geologic Survey Professional Paper 838.

- (26) Cluff, L.S., Weaver, K.D., and Niccum, M.R., 1977, Zoning for surface fault rupture, Managua, Nicaragua, in proceedings, Sixth World Conference on Earthquake Engineering, New Delhi, India, v. 1, p. 817-822.
- (27) Woodward-Clyde Consultants, 1975, Investigation of active faulting in Managua, Nicaragua and vicinity, Report prepared for Vice Ministerio de Planificacion Urbana, November 1975.
- (28) Niccum, M.R., Cluff, L.S., Chamorro, F., Wyllie, L., 1976, Banco Central de Nicaragua--A case history of a high-rise building that survived surface fault rupture: Annual Symposium on Engineering Geology and Soils Engineering, Boise State University, Boise, Idaho.
- (29) Borchardt, R.D. (editor), 1975, Studies for seismic zonation of the San Francisco Bay Region: U.S. Geological Survey Professional Paper 941-A, 102 p.
- (30) McCrory, P.A., Greene, H.G., and Lajoie, K.R., 1977, Map showing earthquake intensity, zonation and distribution of Quaternary deposits, San Mateo, Santa Cruz, and Monterey Counties, California: U.S. Geological Survey Miscellaneous Field Studies Map MF-903, scale 1:250,000.
- (31) Lee, K.L., Marcuson, W.F., III, Stokoe, K.H., II, and Yokel, F.Y., 1978, Research needs and priorities for geotechnical earthquake engineering applications: prepared for the National Science Foundation, NSF Grant No. AEN77-09861.
- (32) Brabb, E.E. and Pampeyan, E.H., 1972, Preliminary maps of landslides in San Mateo County, California: U.S. Geological Survey Miscellaneous Field Studies Maps MF-344, scale 1:62,500.
- (33) Brabb, E.E., Pampeyan, E.H., and Bonilla, M.G., 1972, Landslide susceptibility in San Mateo County, California: U.S. Geological Survey Miscellaneous Field Studies Maps MF-360, scale 1:62,500.
- (34) Nilsen, T.H., and Brabb, E.E., 1975, Landslide, in Studies for Seismic Zonation of the San Francisco Bay Region: U.S. Geological Survey Professional Paper 941-A, p. A75-A87.
- (35) Youd, T.L., Nicols, D.R., Helley, E.J., and Lajoie, K.R., 1973, Liquefaction potential, in Studies for Seismic Zonation of the San Francisco Bay Region: U.S. Geological Survey Professional Paper 941-A, p. A68-A74.
- (36) Youd, T.L., 1978, Historic ground fractures in northern California triggered by earthquakes: U.S. Geological Survey Professional Paper 993, 177 p.
- (37) Neghabat, F., and Liu, S.C., 1977, Earthquake regionalization of Iran, in proceedings, Sixth World Conference on Earthquake Engineering, New Delhi, India, v. 1, p. 859-865.
- (38) Page, W.D., Alt, J.N., Cluff, L.S., and Plafker, G., Evidence for the recurrence of large magnitude earthquakes along the Makran coast

- of Iran and Pakistan: Tectonophysics, Special Issue, 1977 International Symposium on Recent Crustal Movements (in press).
- (39) New Zealand Geological Survey, 1966, Late Quaternary faulting: Department of Scientific and Industrial Research, New Zealand.
- (40) U.S. Atomic Energy Commission, 1971, Nuclear power plant seismic and geologic siting criteria: Federal Register, v. 36, NO228, P. 22, 602.
- (41) Howard, K.A., Aaron, J.M., Brabb, E.E., Brock, M.R., Gower, H.D., Hunt, S.J., Milton, D.J., Muehlberger, W.R., Nakata, J.K., Plafker, G., Prowell, D.C., Wallace, R.E., and Witkind, I.J., 1978, A preliminary map of young faults in the United States as a guide to possible fault activity: U.S. Geological Survey, Map MF-916.
- (42) Esteva, L., 1976, in Seismic risk and engineering decisions; developments in geotechnical engineering 15: Elsevier Scientific Publishing Company, New York.
- (43) Knopoff, L. and Kagan, Y., 1977, Analysis of the theory of extremes as applied to earthquake problems: Journal of Geophysical Research, v. 82, no. 36, December.
- (44) Shlien, S. and Toksoz, M., 1970, A clustering model for earthquake occurrences: Seismological Society of America Bulletin, v. 60, no. 6, p. 1765-1787.
- (45) Wallace, R.E., 1978, Behavior of different segments of the San Andreas fault: Earthquake Information Bulletin, v. 10, no. 4.
- (46) Wallace, R.E., 1970, Earthquake recurrence intervals on the San Andreas fault: Geological Society of America Bulletin, v. 81, p. 2875-2890.
- (47) Patwardhan, A.S., Kulkarní, R.B., and Tocher, D., A semi-Markov model for characterizing recurrence of great earthquakes: proceedings of the EHRP Conference on Methodology for Defining Seismic Gaps and Soon-to-Break Gaps, Boston, Massachusetts, May, 1978, U.S. Geological Survey Open File Report (in press).

GEOPHYSICAL ENGINEERING INVESTIGATIVE TECHNIQUES
FOR SITE CHARACTERIZATION

by

Vincent J. Murphy^I

ABSTRACT

Geophysical surveys that are of a regional nature and those for site-specific studies, usually including in-situ measurements of seismic wave velocity values, are the most generally accepted applications of geophysical engineering techniques for microzonation/site characterization.

The need to know where earthquakes are apt to occur, as well as the effects of those earthquakes on different geologic materials/foundation conditions, has both increased the use as well as the acceptance of geophysical surveys. On the one hand, delineation of tectonic elements is desirable; on the other hand, the values of moduli at various depths below ground surface is a design requirement.

A myriad of geophysical techniques is readily available from a number of consultants and contractors. There appears to be a universal acceptance of gravity and magnetic surveys for the regional considerations, and seismic refraction and cross-hole velocity measurements for the in-situ parameters; occasionally, seismic reflection surveys are useful for delineating specific structures (such as offshore faulting) and tracing such features.

Of all the geophysical techniques that are in any way related to specific site parameters, the in-situ measurement of shear wave, "S", velocity values is the most widely used. The method of measurement, that is, the type of energy source and the specific array of boreholes (either closely spaced or spread at relatively great distances) varies with the organization conducting the measurement:

INTRODUCTION

The ever increasing use of geophysical techniques for zoning applications, in general, and for soil dynamics considerations, in particular, is evident upon a brief perusal of the proceedings of recent conferences, such as the Fifth and Sixth World Conferences on Earthquake Engineering (Rome and New Delhi - 1973 and 1977) and specialty conferences, such as ASCE (Pasadena - 1978), etc. In the Fifth WCEE, Perrinetti (1) referred to numerous geophysical studies performed other

^IVice President, Senior Consultant: Weston Geophysical Corporation, Westboro, Massachusetts, 01581.

than for microzonation which (could) should be included with geologic information in the course of compiling a "geoseismic map". In the Sixth WCEE, Medvedev (2) called for map compilations including "...velocities of propagation of longitudinal and shear waves, and the structure of soils are determined with the methods of seismic prospecting". Whitman et al (3) noted that the soil profile factor, "G", varies from 1 to 1.5 for conditions varying from rock to soft clays and soils (conditions that are readily assessed with geophysical techniques).

Background

The most widespread use of geophysical techniques for projects that would quite properly fall within the context of "Microzonation" is in Japan and the United States; in Italy, Turkey, and other countries bordering the Mediterranean Sea, there are lesser amounts of documented geophysical/zoning experiences. In numerous worldwide areas, geophysics is used for engineering-type projects - not specifically for zoning. At the First Microzonation Conference, this writer (4) considered techniques and applications that dated over a period of nearly 20 years; for this Second Conference, the reader will find that an effort is made to consider relevant materials and developments that have become available in the interim period.

Extensive new data banks are available; careful searching through various public agencies and private company files will disclose useful information in the form of profiles, contour maps, and specific parameter values.

It is interesting to note that both Japanese and United States investigators pioneered the type of measurements that are considered as site specific, namely, in-situ velocity/moduli for individual building sites; however, investigators in the United States also pioneered the broader type of investigations, such as long geophysical profile lines and gravity/magnetic contour maps of extensive areas.

In this state-of-the-art presentation, the attempt is made to crossover from a classical type of geophysics to engineering/site characterization work and from engineering back to geophysics.

Objectives of Findings

The topical questions that are asked of geophysics usually concern soil/rock conditions (deep or shallow, hard or soft) and tectonics (structures, trends, and delineations of active/capable zones).

Knowledge of soil and rock conditions is achieved by seismic wave velocity measurements and profiling of the various velocity layers; knowledge of the tectonics of an area is provided by gravity and magnetic surveys. Closely related to those specific tasks and techniques is the ultimate question of what intensity would result from a certain earthquake.

Typical data correlations that are indicative of the value of geophysical techniques for site characterization are as follows: mafic masses, detected by magnetic and/or gravity surveys, are reported to be spatially related (in a number of instances) with isolated areas of seismicity; it appears, with regard to liquefaction, that materials with seismic shear wave velocity values exceeding 200 to 250 m/sec (700 to 800 ft/sec) probably would not be a problem, and intensity values of VIII(MM) or greater have apparently not been observed for structures built on materials with a "P"-wave velocity of over 4,000 m/sec (13,000 ft/sec) and/or an "S"-wave velocity exceeding 2,000 m/sec (6,600 ft/sec).

Structural geologic features that have near-vertical attitudes and are buried at depths greater than trenching limits are oftentimes detectable only with geophysical techniques.

LITERATURE

The methods and theoretical background concerning the various techniques covered in this paper are adequately considered in recent texts and reference works. Since the time of the First Microzonation Conference (1972), a significant number of new texts and reference works has become available.

Texts and Journals

Some of the more popular and widely used texts are a new edition of the well-known one by Dobrin (5) and a most comprehensive paperback by Telford et al (6); an earlier edition of Dobrin is also available in Spanish. A text that originally appeared in German and contains extensive consideration of "digital seismics" is by Dohr (7). A volume concerned specifically with gravity and magnetics and an elementary monograph on the same subject matter are by Nettleton (8a, 8b). United States Geological Survey monographs of greater suitability than their titles would imply are by Zohdy et al (9a) and by Keys and MacCory (9b). A recent text from England that covers a number of techniques, but specifically addresses offshore applications, is by McQuillin and Ardu (10). New volumes that are specialized for seismic surveys are by Coffeen (11) and Payton (12); these volumes also contain numerous data samples demonstrating faulting, folding, and other relevant structural features from notable areas.

A technique that has widespread application for zonation and soil dynamics, but is rarely considered in geophysical text books, is the in-situ measurement of shear wave velocity values (covered as a separate topic later in this paper).

Several professional geophysical journals contain papers on both techniques and applications: "Geophysics" of the Society of Exploration Geophysicists, "Geophysical Prospecting" of the European Association of Exploration Geophysicists, the "Journal of the American Association of Petroleum Geologists", and the "Bollettino di Geofisica" from the Geophysical Observatory-Trieste. These journals contain numerous data/survey case histories and examples such that the reader will find information that is useful not only for the techniques themselves but also for real geologic conditions in many diverse parts of the world.

It should be recognized that most geophysical exploration takes place in oil provinces or potential province areas; as a result, much of these data apply to relatively deep sedimentary sections rather than to shallow crystalline rock areas.

If an area considered for zoning is fortunate enough to be within an oil province, it is most probable that extensive seismic reflection profiling has taken place and at least some published data are available in the journals. Such data may be in the form of actual recordings, seismic profile sections, or structural contour maps. It is recognized that some structural features, such as slump and growth faulting, may be due to nontectonic factors; judgment, therefore, is necessary in the use of these data.

Although a significant amount of data by explorationists is classed under a proprietary cover, it is often available for limited usage at a fraction of the acquisition cost; commercial data banks are helpful for locating such data.

In virtually all conferences on earthquake engineering, from the International and World Conferences through the United States National Conference and local ASCE Section Conferences, shear modulus and small strain/in-situ measurement of shear wave velocity values are subjects of frequent discussion.

REGIONAL GEOPHYSICAL STUDIES

In order to fully utilize geophysical data for microzonation of areas of varying size, available data banks are, and should be, augmented by on-site field measurements. After the preparation of epicenter maps for the historical record, aeromagnetic survey contour maps and gravity station data are then assembled; some processing, such as filtering for delineation and separation of localized (residual) anomalies from those of more regional extent will result in data that can be correlated with the epicenter map. This use of available data banks is an economical and significant first step. The need for additional data (closer flight lines and/or greater density of stations) also must be assessed.

The detection and delineation of the mafic masses considered by Kane (13a), Hildenbrand et al (13b), and McKeown (14) are readily attainable by geophysics (refer also to Figure 5).

Reflection surveys for petroleum and refraction surveys for routine foundation investigation are types of data that should also be sought after in initial data searches. The northern Venezuelan and the Californian coasts are areas where existing data are useful for zonation. Much of the data was not originally acquired there for that purpose; also, it may have been obtained some tens of years ago, but the indications of faulting occurrences are as valuable today for zonation as they were originally for oil and foundation evaluation.

Gravity and Magnetic Surveys

The spatial correlation of earthquake epicenters with various geophysical anomalies, such as magnetic and gravity "highs" and trends of gravity contours with steep gradients, is a recent development for sections of the United States where earthquakes have been known to occur for considerable time based on historical records. Typical areas are northeast and northwest United States (Figures 1, 2, 3, and 4) and central and southeast United States (Figure 5). Gravity station data must all be referenced to a common base and field checked by repeating selected station readings; where the aeromagnetic survey coverage is rather sparse, such as widely-spaced flight line (10 kilometer) and/or no tie lines, and where adjacent surveys are flown at different flight elevations or at different ground clearances, entirely new data may be necessary. The preferred spacing of gravity stations appears to be in the order of a kilometer, and the preferred interval between adjacent aeromagnetic survey flight lines is in the order of a kilometer with tie-line spacings that do not exceed 10 kilometers. For the aeromagnetic survey, a constant ground clearance of 300 to 500 meters is usually desirable; areas of steep and irregular topography will require some adjustment in ground clearance or possible draping.

The use of gravity and magnetics is usually involved with broader geologic structures that are of interest for zoning in order to relate anticipated earthquake occurrences with specific geologic structures; the extent of the structures is usually a few to as many as tens of kilometers.

Recent studies in two divergent areas of the United States, the northeast and northwest, have taken advantage of the latest state-of-the-art techniques and methods to provide geophysical data significant for zoning in general, and nuclear power plant siting in particular. Contour maps, resulting from processed gravity and aeromagnetic surveys, became especially useful to identify areas where earthquakes would not be anticipated as well as localized geologic structures that correlate with historical activity (Reference Nos. 15a and 15b, and Figures 1, 2, 3, and 4). The significance for zoning is obvious.

The interpretation of gravity and aeromagnetic survey contour maps is largely of a qualitative nature. Trends, magnitudes, linears, and patterns are some of the characteristics with which a geophysical interpreter is usually concerned. Very recently, however, Simmons et al (16a) and Simmons (16b) has evaluated gravity anomalies located in parts of the northeast and northwest United States in a quantitative manner; the mathematical modeling for those areas demonstrated significant stress fields at or near locations where earthquake activity is known to occur.

Seismic Reflection Surveys

Seismic reflection profiling, on land and underwater, includes applications that vary from truly regional considerations (such as detection and delineation of deeply buried structures and the extent of offshore faulting) to very site-specific considerations, such as the

possibility of faulting at proposed nuclear or other power plant locations. Since the cost usually varies directly with the depth of penetration required (deep profiling requires more expensive systems and more sophisticated data processing), most of the seismic reflection work related in any way to zoning is usually shallow underwater profiling with equipment that is portable and suitable for small boat operations. A particular note in this regard for the offshore profiling is that accurate locationing is essential and requires a highly reliable radio navigation system.

Advances in instrumentation by digital recording, wide band amplifiers, etc., allow more exacting evaluation of recorded data than has previously been available. The ability to play-out and replay certain segments of the recorded data has a distinct advantage over analog recording, which may have an unfavorable noise level and/or amplification and/or adverse frequency pass-band selection.

Data samples from the United States east and west coasts illustrate the detail of layering and structure that is readily attainable with the reflection technique (Figures 6 and 7).

SITE-SPECIFIC SURVEYS AND MEASUREMENTS

Depth to rock and the configuration of the rock surface, as well as velocity values for both rock and overburden layers, are frequent objectives for seismic refraction surveys and in-situ type measurements (Reference Nos. 17, 18, 19, 20, 21, 22, 23, 24, 31, 32, and Figures 11 and 12). These data often constitute input for analyses by other professionals concerned with amplification, liquefaction, etc.; the 1967 Caracas earthquake is a particular instance of such an involvement of different disciplines (Reference Nos. 27, 28, 29, 30, and Figure 15). The continuity of layering and the presence or absence of faulting are often the objective of seismic reflection profiling. Moduli determinations require in-situ measurements of both "P" and "S" velocity values.

Seismic Reflection Surveys

Extensive seismic reflection survey coverage off the California coast, as exemplified in the sections of Figure 7, and land coverage in areas such as the Atlantic coastal plain shown in Figure 8, readily demonstrate the absence or presence of geologic structural features. In the first example, evenly bedded sediments are disturbed by faulting; in the second example, a notably smooth, gently-dipping crystalline rock surface extends for significant distances.

Seismic Refraction Surveys

Seismic refraction profiling which has been used extensively for some tens of years as a foundation exploration tool for various engineering projects has recently been used successfully for near-surface fault detection. Where faults are truly "active" (or to use a nuclear siting term - "capable"), the fault zone often acts as a barrier to groundwater movement, resulting in different depths to the water table on either side of the fault zone. This technique has widespread application

for areas, such as parts of California - the Calaveras fault (Figure 9) and faults subsidiary to the San Andreas in southern California; applications for microzonation are numerous--the siting of all lifelines and structures. Existing dams and other earth embankments are being explored with refraction (Ballard and McLean (24), Figures 13 and 14), as well as with borehole techniques.

In-situ Velocity Measurements

For a period of approximately 10 years, there has been an ever increasing use of these cross-hole type measurements (Figure 10) to determine in-situ values of seismic shear-wave velocity (Reference Nos. 25, 26, 33, 34, 39, 40, 41). From the recent ASCE Conference (Pasadena), the paper by Woods (42) includes a rather exhaustive treatment of this matter and includes numerous references and data samples (Figure 16). Although much of the original and referenced material in that paper is drawn from studies where the source of energy was mechanical (that is, some sort of a weight drop or other mechanical impact device), the actual velocity value for any layer ought to be the same regardless of the energy source, if the strain level along the path of transmission is of approximately the same magnitude.

In addition to obtaining specific data for the design of a specific structure, cross-hole velocity values can also be used to assess the uniformity of soil dynamics properties over extensive areas. Typical arrays of holes and suites of data are displayed in Figures 10, 14, and 16. The spacing of holes and the measurement intervals are selected by reference to the probable geologic sequence that is penetrated; thin soft or hard layers require special attention.

Energy sources and spacings of holes are a controversial item in the practice of in-situ velocity measurements; explosives, mechanical or electromechanical, air guns, and most recently, "sparkers", probably comprise the full spectrum of available sources. Adaptations of these sources to borehole orientations and size is a further subjective element. Consistency of measured values for the same section of material at a specific site is most desirable for all velocity measurements no matter how the measurements are made; variations up to plus or minus 10 percent are probably acceptable. Repeated measurements by the same organization with the same equipment and field procedures usually result in a data value scatter of less than 5 percent. When 50 or 100 percent differences between sets of measured data for the same layer become evident (from the same or different investigators), either the nature of the material has undergone a significant change in the period between measurements, or one set of data is clearly in error.

The increased use and emphasis on in-situ determination of velocity values have also brought about a greater awareness of the limitations of these geophysical measurements (Reference Nos. 35, 36, 37, 38, and 43).

Gravity and Magnetic Surveys

Localized, structural geologic features can often be delineated with closely-spaced ground survey traverses made with gravity meters and/or magnetometers. The portability and ease of use of these instruments result in significant amounts of data at any area within a short time framework. It should be noted, however, that gravity surveys take place in virtually any environment, whereas magnetic surveys are often affected by cultural features (buildings, fences, pipelines, etc.).

Borehole Logging

Borehole logging is one of the few geophysical techniques where advances in the equipment state-of-the-art and applications have been notably lacking with regard to zonation-type applications. Relatively rapid techniques for stratigraphic continuity studies are gamma logging and sonic logging, but only a few professionals are actively using them. This technique is probably the fastest and most inexpensive of all the geophysical techniques and enables the site explorationist to rapidly drill a number of holes without coring or sampling and merely compare the gamma log signature from one hole to the other. For this type of measurement, it is imperative that accurate locationing, both vertically and horizontally, is provided for dependable correlations.

RECOMMENDED PROGRAMS

Based on the current practice of national agencies and private organizations, a sequence of geophysical evaluations allows zoning from a regional scale down to and including site-specific objectives.

Aeromagnetic and gravity contour maps, processed and interpreted to disclose linears and other anomalous features and trends, should be correlated with historical seismicity maps. For many parts of the world, it will become readily apparent that the locales of certain types of anomalies will require different zoning criteria than others, such as along the trend of gravity contours where steep gradients exist, and at near-circular magnetic anomalies with both steep gradients and high magnitudes. If such anomalous features correlate with geologic structures that are old and seismically inactive, then it may be possible to revise the zoning requirement.

For localized considerations, such as for cities and similarly small regions, programs should include seismic profiling and the in-situ measurement of seismic wave velocity values. High resolution reflection and refraction profiling will readily distinguish those areas where rock or other firm foundation materials are shallow from areas where deep, extensive deposits of loose materials exist. A further benefit of such profiling is the detection and delineation of near-surface faulting that is probably active/capable, and bedrock features, such as ridges and depressions, that may have significance for both geologic and engineering considerations.

With regard to the most widely used geophysical technique suitable for both zoning and design requirements, the in-situ measurement of "P"-wave and "S"-wave velocity values is useful and often required for determination of moduli and the layering sequence where those values apply.

REFERENCES

- (1) Perrinetti, U., 1973, "Proposals for a More Thorough Evaluation of Seismic Risk in Italy", Fifth World Conference on Earthquake Engineering, Rome, pp. 1715-1728.
- (2) Medvedev, S. V., 1977, "Complex Method of Microzoning", Sixth World Conference on Earthquake Engineering, New Delhi, pp. 2-504.
- (3) Whitman, Robert V., 1977, "Seismic Design Regionalization Maps for the United States", Sixth World Conference on Earthquake Engineering, New Delhi, Vol. 2, pp. 387-392.
- (4) Murphy, V. J., 1972, "Geophysical Engineering Investigation Techniques for Microzonation", First International Conference on Microzonation, Seattle, pp. 135-159.
- (5) Dobrin, M. B., 1976, Introduction to Geophysical Prospecting, 3rd Edition, McGraw-Hill Book Company, 630 p.
- (6) Telford, W. M., L. P. Geldart, R. E. Sheriff, and D. A. Keys, 1976, Applied Geophysics, Cambridge University Press, Cambridge, Massachusetts, 860 p.
- (7) Dohr, Gerhard, 1974, Applied Geophysics, "Introduction to Geophysical Prospecting", John Wiley & Sons, New York, Vol. 1, 272 p.
- (8a) Nettleton, L. L., 1976, Gravity and Magnetics in Oil Prospecting, McGraw-Hill, Inc., New York, 464 p.
- (8b) Nettleton, L. L., 1971, "Elementary Gravity and Magnetics for Geologists and Seismologists", Monograph Series, The Society of Exploration Geophysicists, Tulsa, Oklahoma, No. 1, 121 p.
- (9a) Zohdy, A. A. R., G. P. Eaton, and D. R. Mabey, 1974, "Application of Surface Geophysics to Ground-Water Investigations", Techniques of Water-Resources Investigations of the United States Geological Survey, United States Government Printing Office, Washington, Book 2, Chapter D1, 116 p.
- (9b) Keys, W. Scott and L. M. MacCory, 1972, "Application of Borehole Geophysics to Water-Resources Investigations", Techniques of Water-Resources Investigations of the United States Geological Survey, United States Government Printing Office, Washington, Book 2, Chapter E1, 126 p.
- (10) McQuillin, R. and D. A. Arduis, 1977, Exploring the Geology of Shelf Seas, Graham & Trotman Limited, London, 234 p.
- (11) Coffeen, J. A., 1978, Seismic Exploration Fundamentals, The Petroleum Publishing Company, Tulsa, Oklahoma, 277 p.

- (12) Payton, Charles E., 1977, Seismic Stratigraphy - applications to hydrocarbon exploration, The American Association of Petroleum Geologists, Tulsa, Oklahoma, Memoir 26, 516 p.
- (13a) Kane, M. F., 1977, "Correlation of Major Eastern Earthquake Centers with Mafic/Ultramafic Basement Masses", Studies Related to the Charleston, South Carolina, Earthquake of 1886 - A Preliminary Report, Geological Survey Professional Paper 1028-0 J, pp. 199-204.
- (13b) Hildenbrand et al, 1977, "Magnetic and Gravity Anomalies in the Northern Mississippi Embayment and Their Spatial Relation to Seismicity", U.S.G.S., Map Folio MF-914.
- (14) McKeown, F. A., 1978, "Hypothesis: Many Earthquakes in the Central and Southeastern United States are Causally Related to Mafic Intrusive Bodies", Journal Research United States Geological Survey, Vol. 6, No. 1, pp. 41-50.
- (15a) Boston Edison Company, 1976, Pilgrim Unit II, Preliminary Safety Analysis Report.
- (15b) Washington Public Power Supply System, 1977, WNP 1 and 4, Amendment 23, Preliminary Safety Analysis Report.
- (16a) Simmons, G. et al, 1976, "The Ossipee Mountains, New Hampshire: Earthquakes and a Stress Model", Field Velocity Measurements and Rock Mechanics Studies, Boston Edison Company, Docket No. 50-471, BE-SG 7606.
- (16b) Simmons, G., 1978, "Stress, Gravity Anomalies, and the Location of Earthquakes in Washington State - Two-Dimensional Models", Washington Public Power Supply System, WNP 1 and 4, Amendment 23, Preliminary Safety Analysis Report.
- (17) Shima, Etsuzo, 1977, "On the Base Rock of Tokyo Metropolis", Sixth WCEE, Rome, Vol. 2, pp. 161-166.
- (18) Tanaka, T., S. Yoshizawa, T. Morishita, K. Osada, and Y. Osawa, 1973, "Observation and Analysis of Underground Earthquake Motions", Fifth WCEE, Rome, pp. 658-667.
- (19) Fujiwara, Toshiro, 1977, "Seismic Motions of Very Soft Ground", Sixth WCEE, New Delhi, Vol. 2, pp. 69-74.
- (20) Asada, A., F. Kawakami, and M. Kamiyama, 1973, "On the Characteristics of Seismic Motion in Soft Soil Layers" Fifth WCEE, Rome, pp. 319-323.
- (21) Campbell, K. W. and C. M. Duke, June 1976, "Correlations Among Seismic Velocity, Depth and Geology in the Los Angeles Area", School of Engineering and Applied Science, University of California, 43 p.

- (22) Lajoie, K. R. and E. J. Helley, 1975, "Differentiation of Sedimentary Deposits for Purposes of Seismic Zonation", Geological Survey Professional Paper 941-A, United States Government Printing Office, Washington, pp. A39-51.
- (23) Wilson, R., R. Warrick, and M. Bennett, 1975, "Seismic Velocities of San Francisco Bayshore Sediments", In-Situ Measurements of Soil Properties, American Society of Civil Engineers, Vol. II, pp. 1007-1023.
- (24) Ballard, Robert F., Jr. and Francis McLean, 1975, "Seismic Field Methods for In Situ Moduli", In Situ Measurement of Soil Properties, American Society of Civil Engineers, Vol. I, pp. 121-150.
- (25) Durgunoglu, H., S. Texcan, S. Erden, and Y. Acar, 1978, "A Comparison of Insitu and Laboratory Measured Dynamic Soil Properties", Bogazici University, Istanbul, 8 p.
- (26) Muzzi, F. and A. Pugliese, 1977, "Analysis of the Dynamic Response of a Soil Deposit in Locality 'Ca'dant' (Cornino-Forgaria)", Specialist Meeting on the 1976 Friuli Earthquake and the Antiseismic Design of Nuclear Installations, Rome, Paper III.4.
- (27) Linehan, D. and V. J. Murphy, 1973, "Caracas Earthquake of July 1967, Geophysical Field Measurements", Fifth WCEE, Rome, pp. 767-770.
- (28) Seed, H. B. and J. L. Alonso, 1973, "Soil-Structure Interaction Effects in the Caracas Earthquake of 1967", Fifth WCEE, Rome, pp. 2108-2111.
- (29) Espinosa, A. F. and S. T. Algermissen, 1973, "Ground Amplification Studies in the Caracas Valley and the Northern Coastal Area of Venezuela", Fifth WCEE, Rome, pp. 741-744.
- (30) Alonso, J. L. and J. Larotta, 1977, "Seismic Risk and Seismic Zoning of the Caracas Valley", Sixth WCEE, New Delhi, Vol. 2, pp. 419-423.
- (31) Arnold, P. and Erik Vanmarcke, 1977, "Ground Motion Spectral Content: The Influence of Local Soil Conditions and Site Azimuth", Sixth WCEE, New Delhi, Vol. 2, pp. 113-118.
- (32) Hadjian, A. and J. Luco, 1977, "On the Importance of Layering on the Impedance Functions", Sixth WCEE, New Delhi, Vol. 4, pp. 205-210.
- (33) Duke, C. M. et al, 1976, "Shear Velocities and Near-surface Geologies at Accelerograph Sites that Recorded the San Fernando Earthquake", School of Engineering and Applied Science, University of California, 63 p.

- (34) Hattori, S., 1973, "Determination of Under Ground Structure at Tsukuba Experimental Site", Bulletin of the International Institute of Seismology and Earthquake Engineering, Vol. II, pp. 73-89.
- (35) Stokoe, K. H. and F. E. Richart, Jr., 1973, "Shear Moduli of Soils, In-situ and from Laboratory Tests", Fifth WCEE, Rome, pp. 356-359.
- (36) Richart, F., Jr., D. Anderson, and K. Stokoe, II, 1977, "Predicting In Situ Strain-Dependent Shear Moduli of Soil", Sixth WCEE, New Delhi, Vol. 6, pp. 159-164.
- (37) Iwasaki, T. and F. Tatsuoka, 1977, "Dynamic Soil Properties with Emphasis on Comparison of Laboratory Tests and Field Measurements", Sixth WCEE, New Delhi, Vol. 6, pp. 153-158.
- (38) Troncoso, J. H., F. R. Brown, and R. P. Miller, 1977, "In Situ Impulse Measurements of Shear Modulus of Soils as a Function of Strain", Sixth WCEE, New Delhi, Vol. 6, pp. 165-170.
- (39) Billi, E. et al, 1977, "Misura della velocità di propagazione delle onde longitudinali e trasversali nel sito del Brasimone", CNEL, Rome, 21 pp.
- (40) Goto, N., H. Kagami, K. Shiono, and Y. Ohta, 1977, "An Easy-Capable and High-Precise Shear Wave Measurement by Means of the Standard Penetration Test", Sixth WCEE, New Delhi, Vol. 6, pp. 171-176.
- (41) Imai, Tsuneo, 1977, "P- and S-Wave Velocities in Subsurface Layers of Ground in Japan", Sixth WCEE, New Delhi, Vol. 6, p. 234.
- (42) Woods, Richard W., 1978, "Measurement of Dynamic Soil Properties", Earthquake Engineering and Soil Dynamics, American Society of Civil Engineers, Vol. 1, pp. 91-178.
- (43) Stokoe, II, K. H. and R. J. Hoar, 1978, "Variables Affecting In Situ Seismic Measurements", Earthquake Engineering and Soil Dynamics, Vol. II, pp. 919-939.

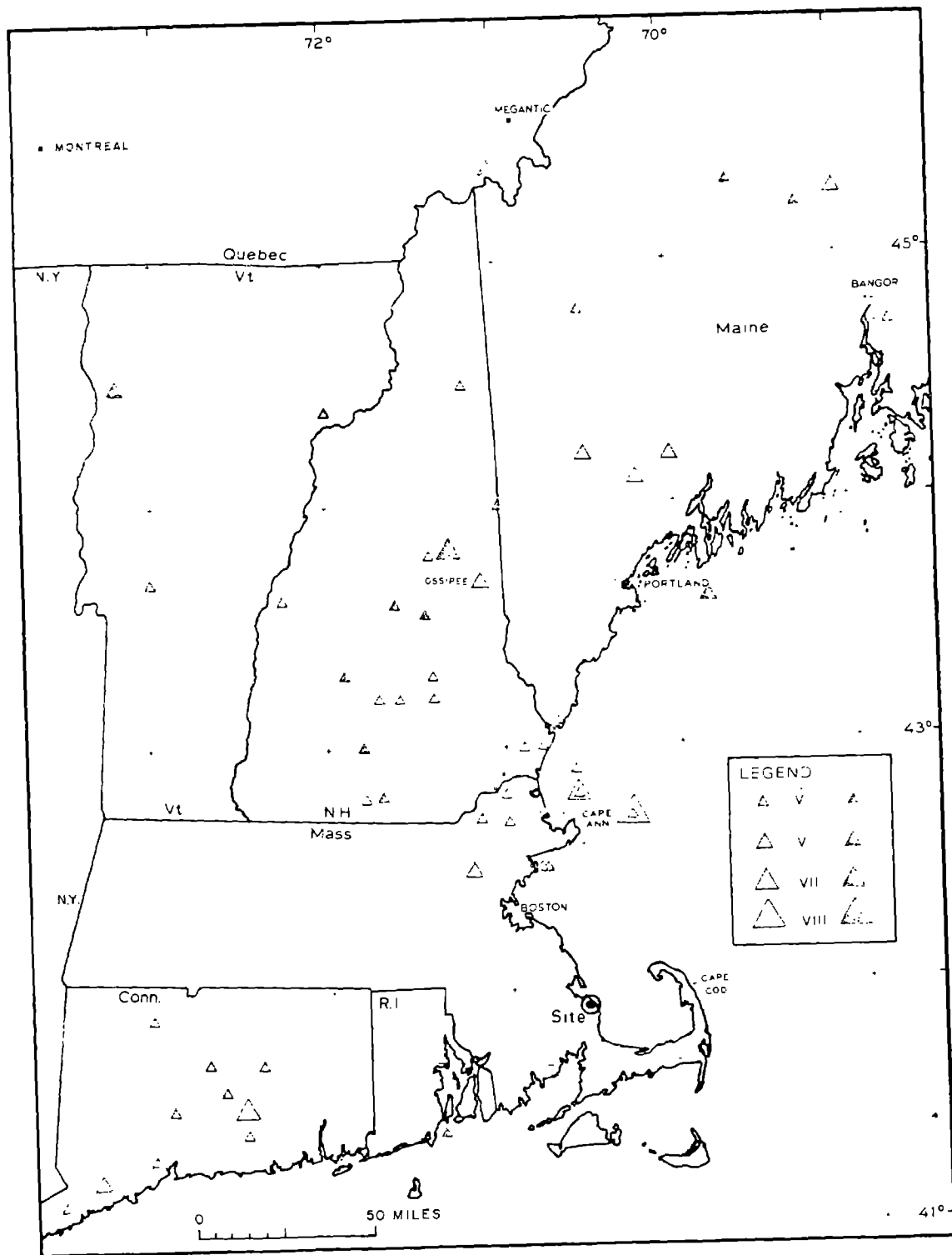
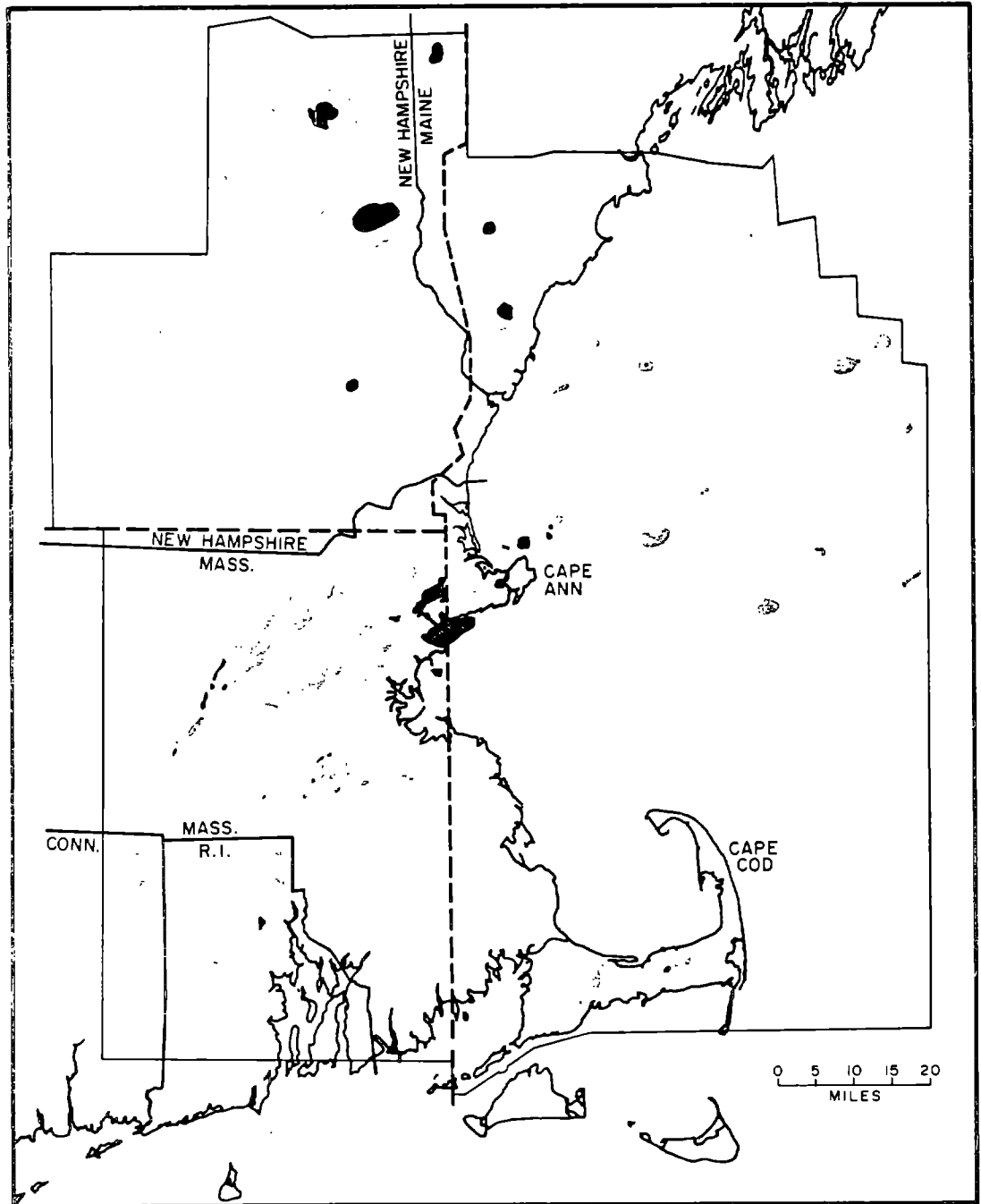


Figure 1. Locations of the New England earthquakes.

Size of the symbol indicates intensity of the earthquake. An open symbol indicates that the location was based on historical data. A solid symbol indicates that the location was determined instrumentally.

FIGURE 1
(adapted from 15a)



LEGEND:



Figure 3. Magnetic field.

The strength of the earth's magnetic field was measured in an airplane that flew 22,000 miles within the area. Additional data in the southwest area were available from maps of the U.S. Geological Survey. The pattern indicates the strength of the magnetic field: the darker the pattern, the stronger the field. The magnetically strong regions, termed magnetic anomalies, correspond to the plutons. One pluton, previously unknown, was discovered near Cape Ann during the project.

FIGURE 2
(adapted from

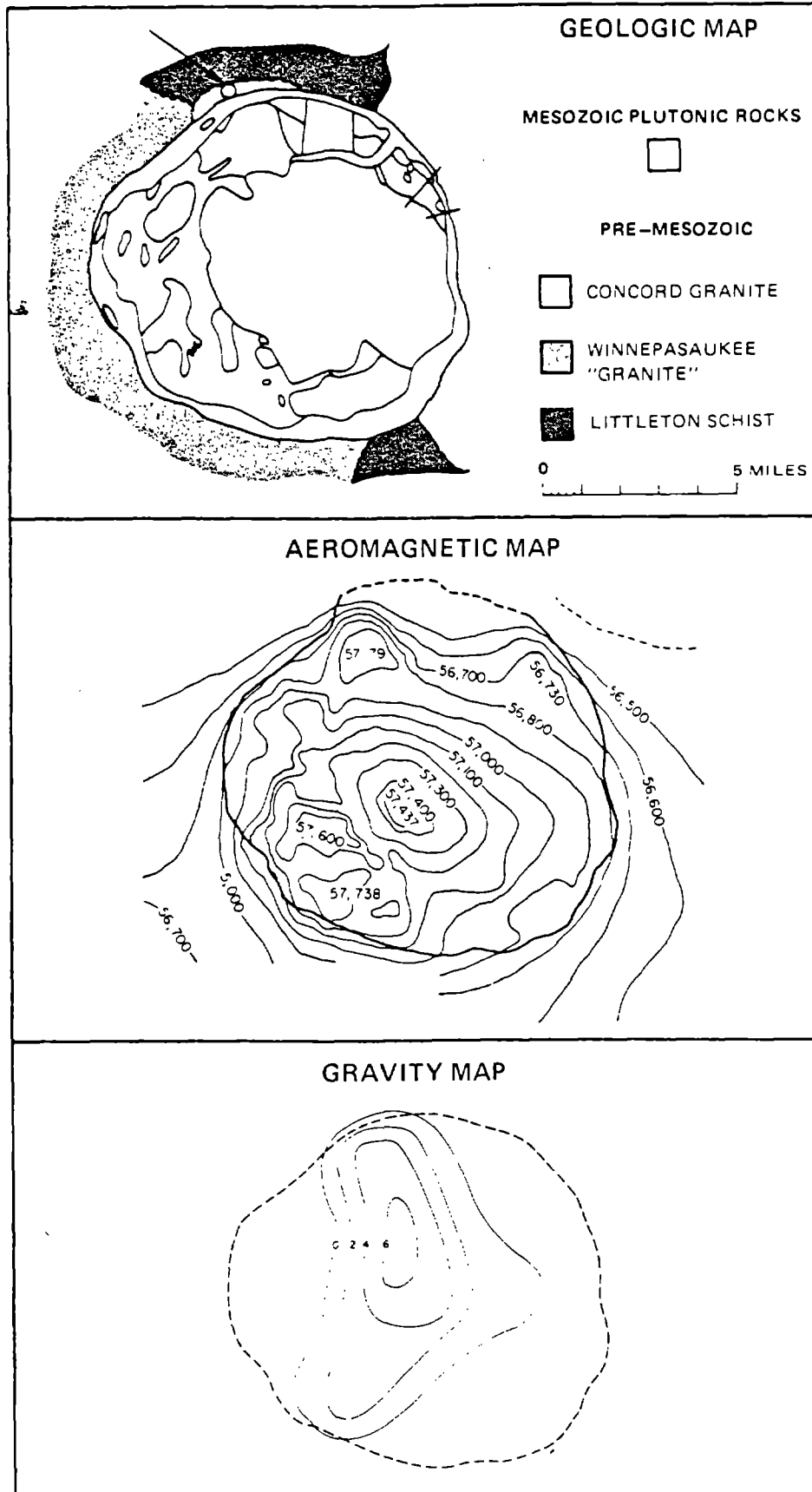
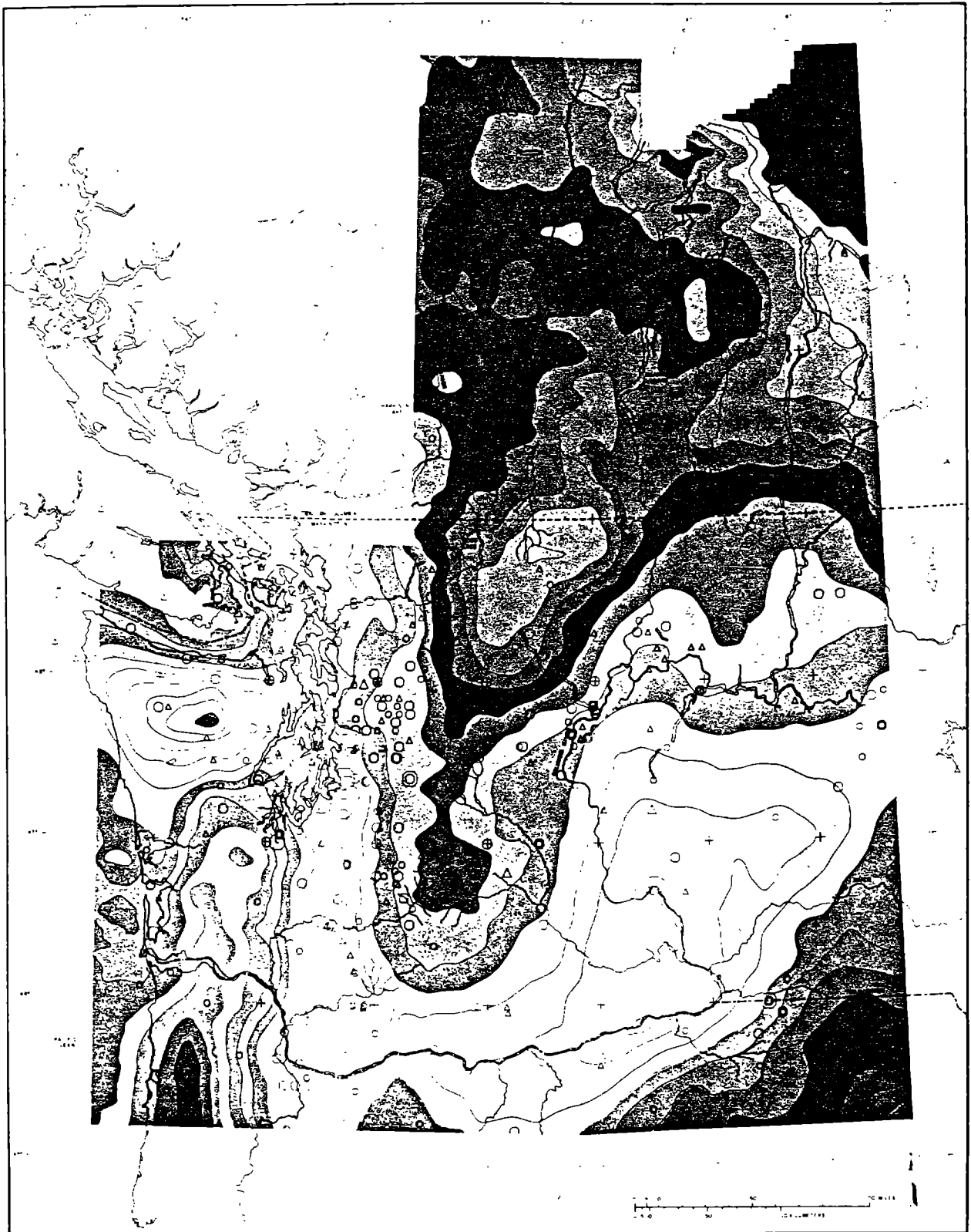


FIGURE 3
(adapted from 15a)



INTENSITY	MAGNITUDE
IX	7
VIII	6
VII	5
VI	4
V	3

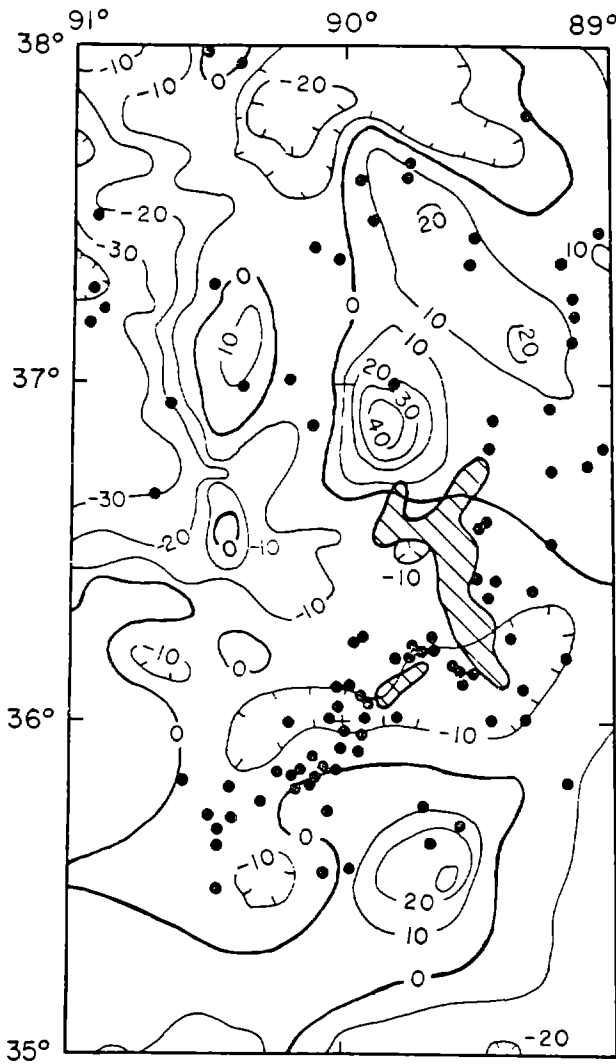
NOTE
EARTHQUAKES PLOTTED BY
INTENSITY WHEN ASSIGNED

VALUES IN MGALS
107 1/2
107 1/4
107 1/2
107 3/4
108
108 1/4
108 1/2
108 3/4
109
109 1/4
109 1/2
109 3/4
110
110 1/4
110 1/2
110 3/4
111
111 1/4
111 1/2
111 3/4
112
112 1/4
112 1/2
112 3/4
113
113 1/4
113 1/2
113 3/4
114
114 1/4
114 1/2
114 3/4
115
115 1/4
115 1/2
115 3/4
116
116 1/4
116 1/2
116 3/4
117
117 1/4
117 1/2
117 3/4
118
118 1/4
118 1/2
118 3/4
119
119 1/4
119 1/2
119 3/4
120

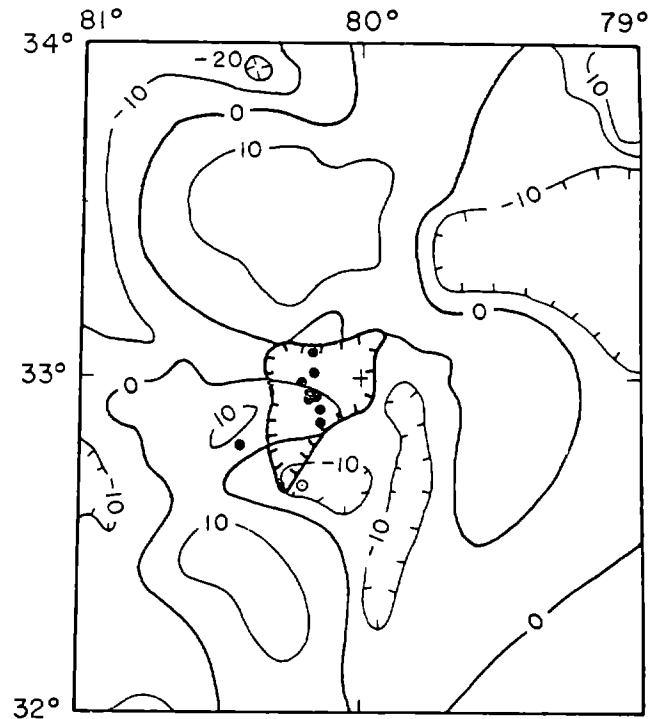
REGIONAL BOUGUER ANOMALY MAP
WITH EPICENTERS
OF WASHINGTON AND ADJACENT AREAS
prepared by
WESTON GEOPHYSICAL
1977
WASHINGTON PUBLIC POWER SUPPLY SYSTEM

FIGURE 4
(from 15b)

STUDIES RELATED TO CHARLESTON, SOUTH CAROLINA, EARTHQUAKE OF 1886



A, New Madrid, Mo., area



B, Charleston, S. C., area

EXPLANATION



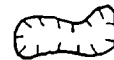
Bouguer gravity contour in milligals relative to sea level. Hachures indicate areas of relatively lower gravity.



Location of a well-determined recent seismic event



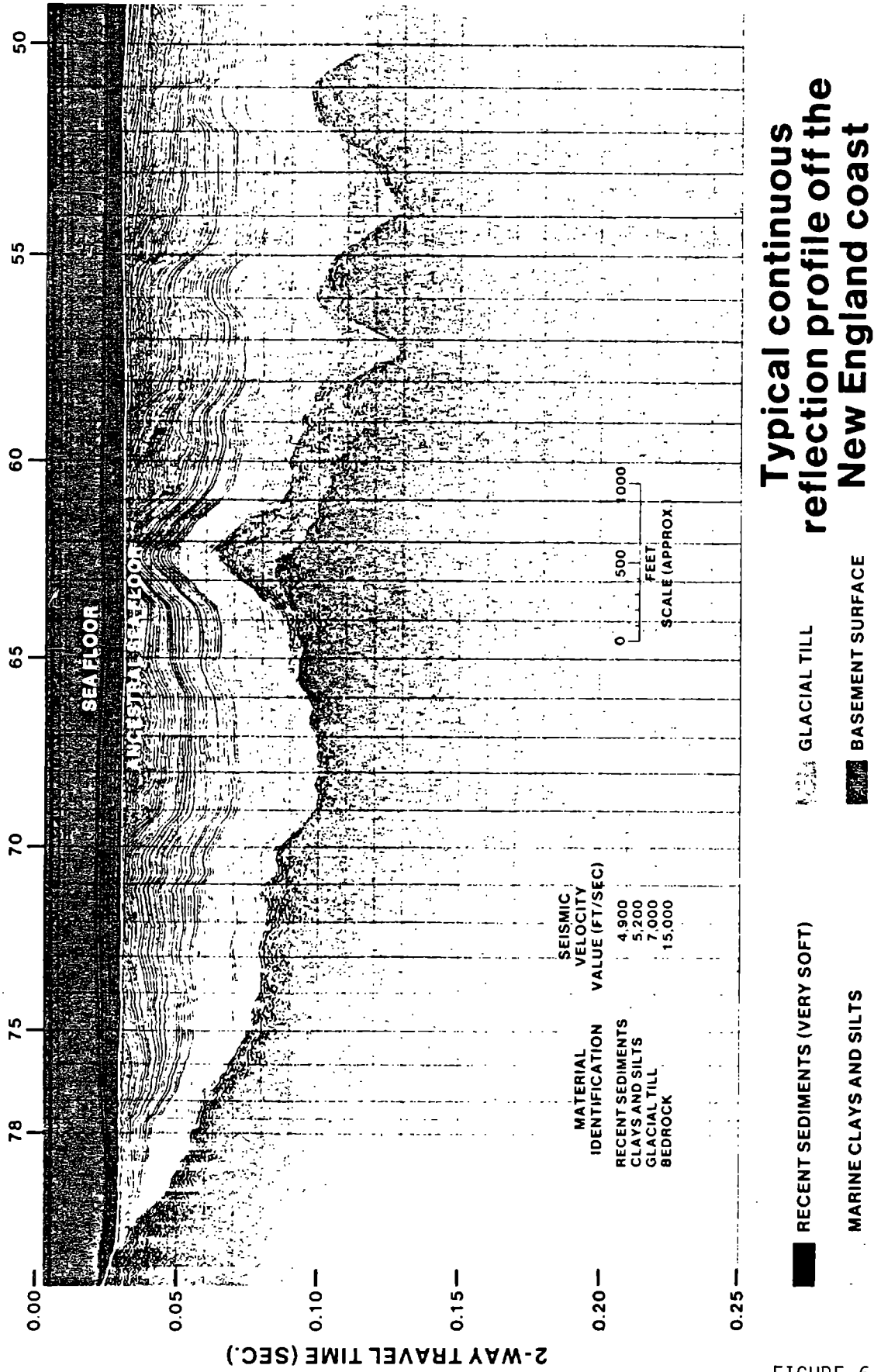
Area where seismic events are too closely grouped to be shown separately



Isoseismal zone of the 1886 Charleston, S. C. earthquake

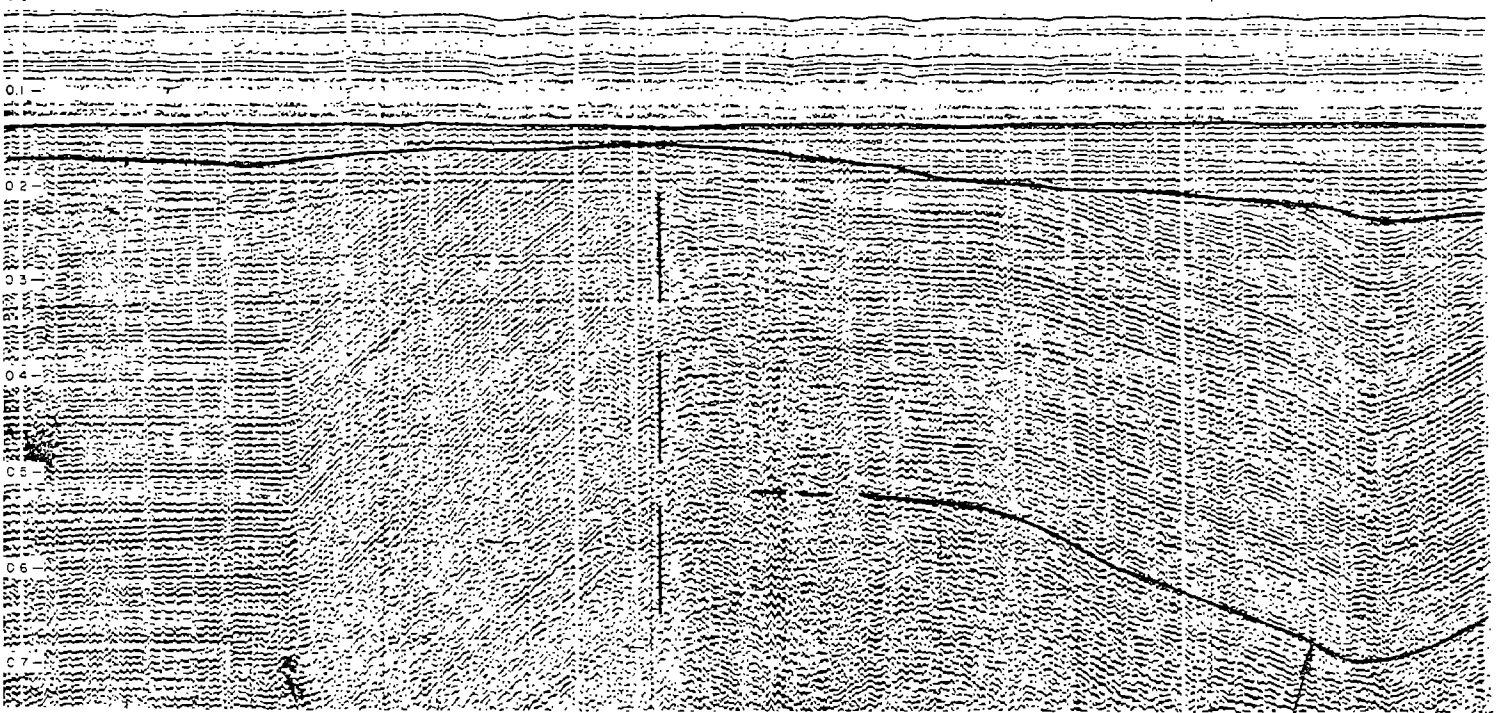
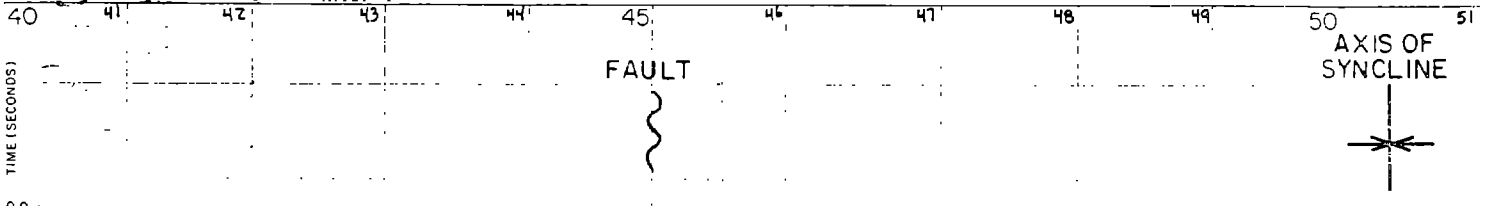
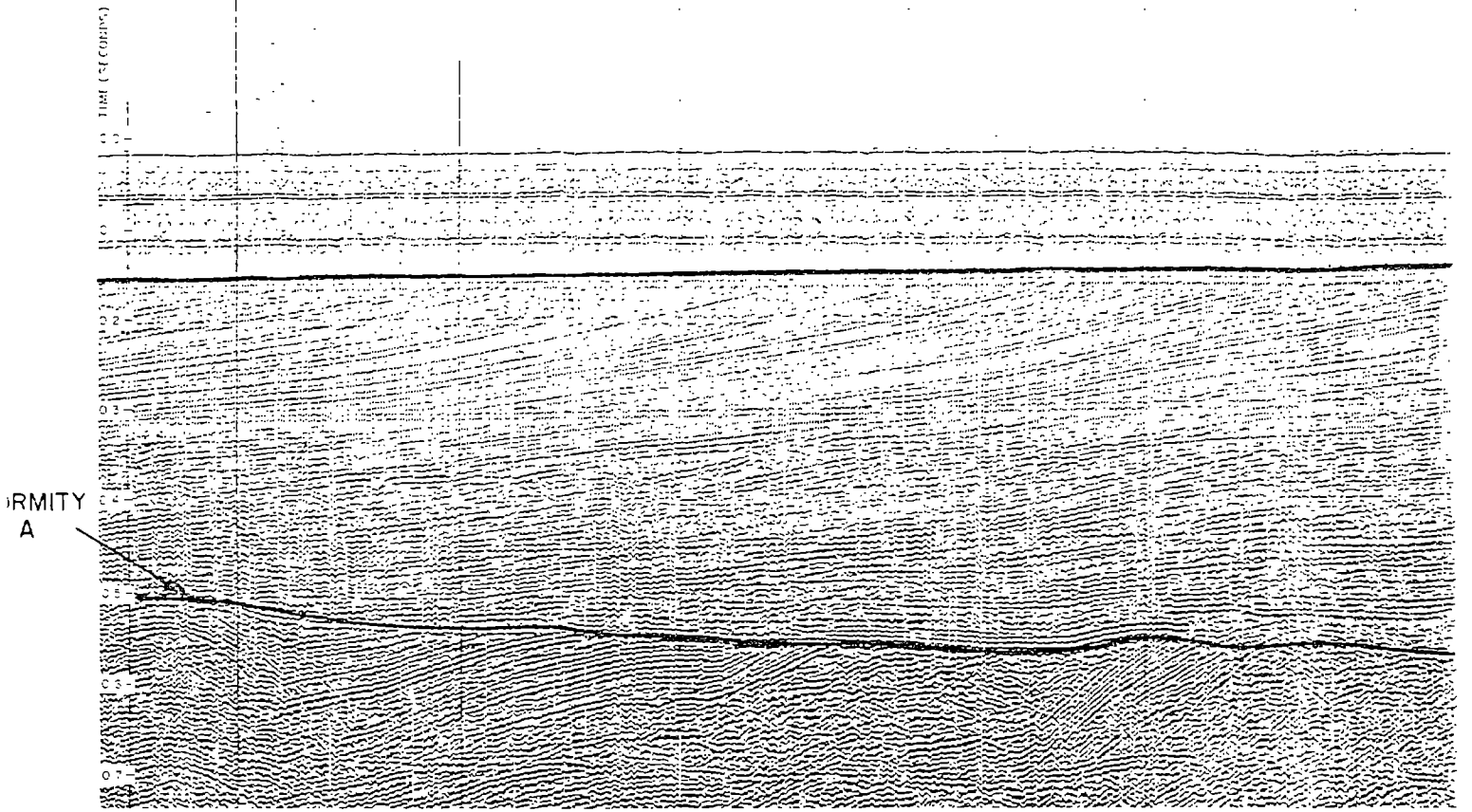


FIGURE 2.—Sketch maps showing gravity and contemporary epicenter data for the New Madrid, Mo., and Charleston, S. C., earthquake areas. Sources of gravity data are given in figure 1. Epicenter data in the New Madrid, Mo., area are from Stauder and others (1976). Epicenter data in the Charleston, S. C., area are from Tarr (this volume). Isoseismal boundary is from Dutton (1889).



Typical continuous reflection profile off the New England coast
by
Weston Geophysical

FIGURE 6



NOTE : FAULT PLANE LOCATIONS AND ATTITUDES ARE SHOWN FOR POSITIONAL REFERENCE ONLY.

HORIZON A'

FIGURE 7
SEISMIC REFLECTION SURVEY
OFFSHORE CALIFORNIA

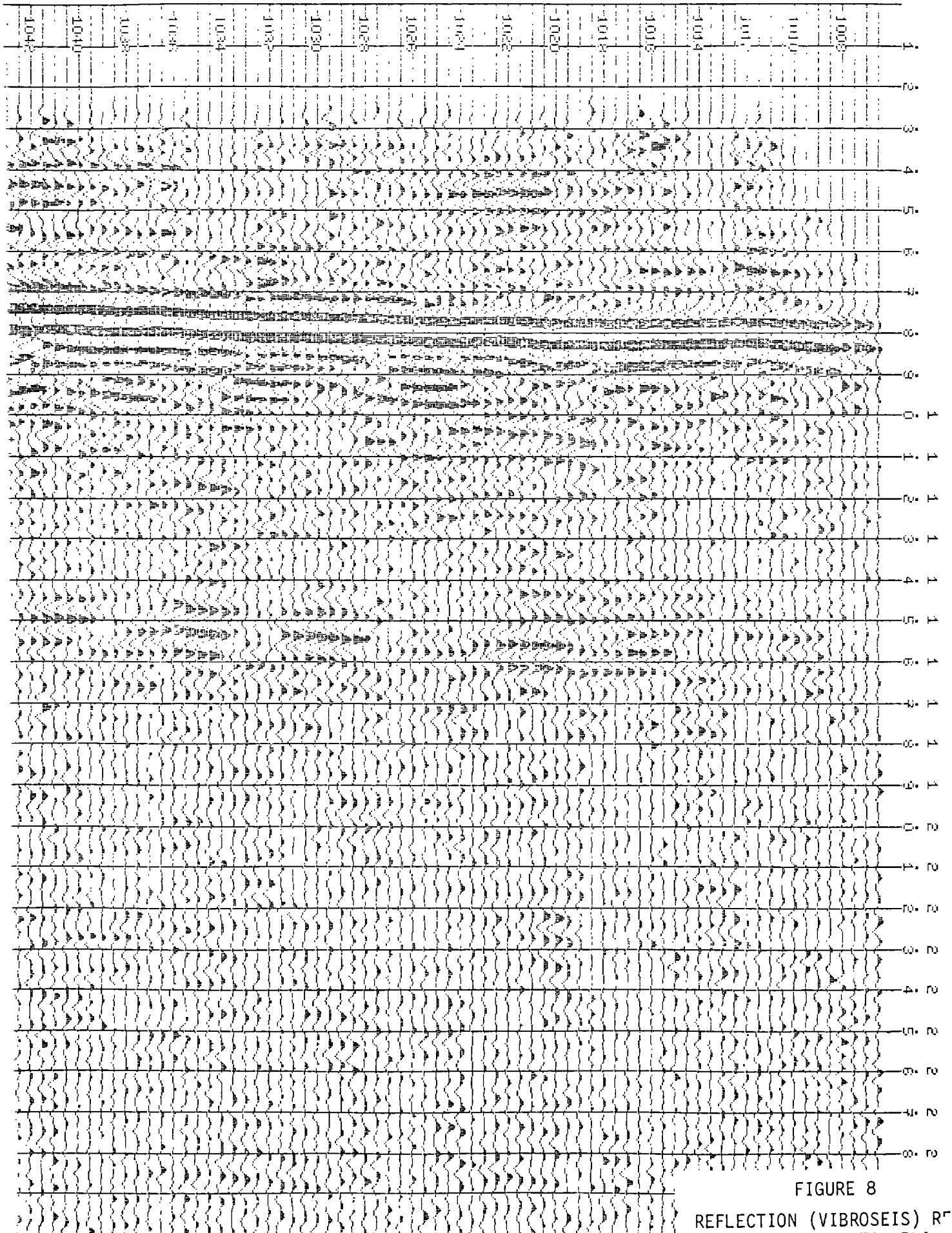


FIGURE 8

REFLECTION (VIBROSEIS) RT
ATLANTIC COASTAL PL

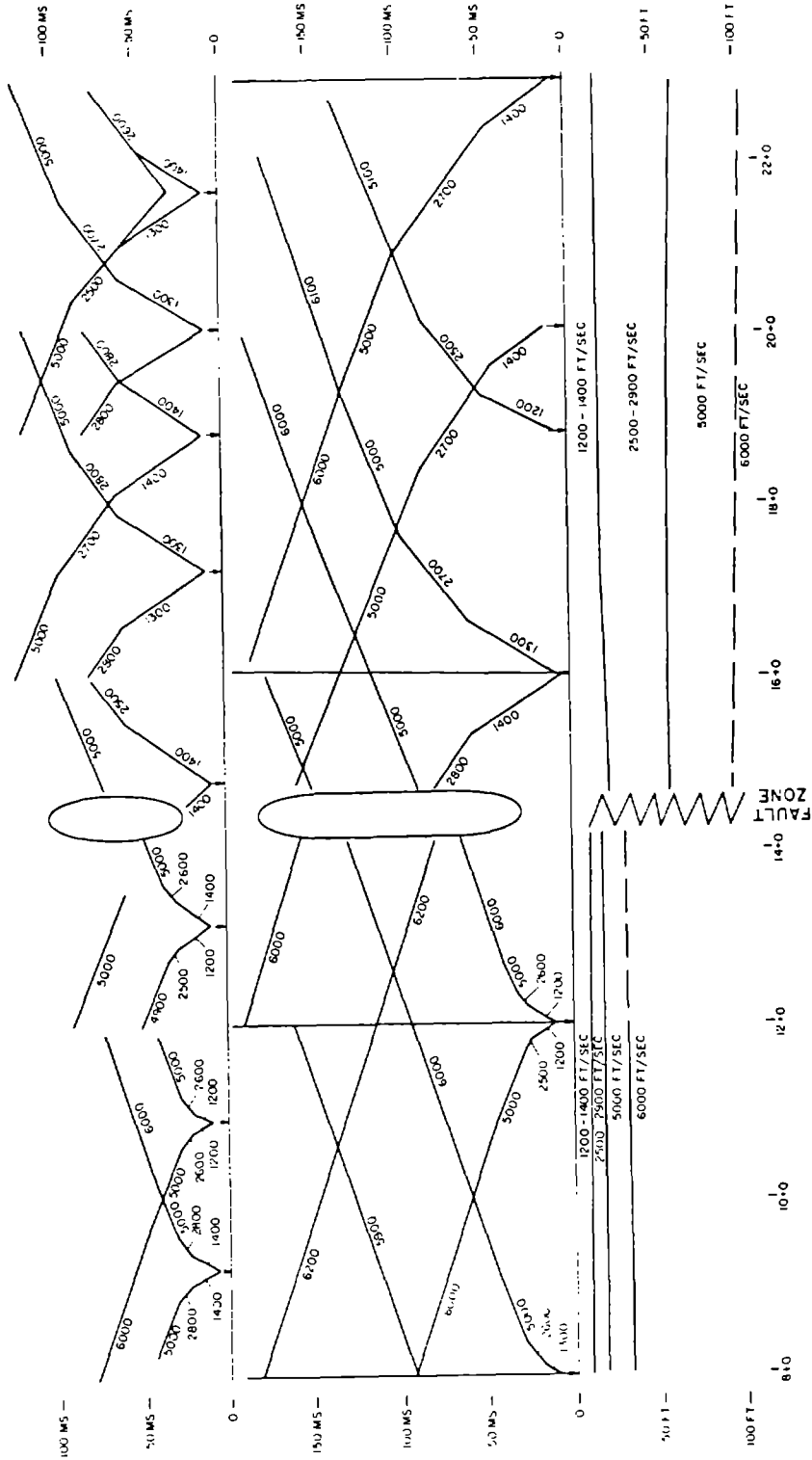


FIGURE 9
REFRACTION PROFILE
CALAVERAS FAULT, CALIFORNIA

174

CROSSHOLE

$$V_2 > V_3$$

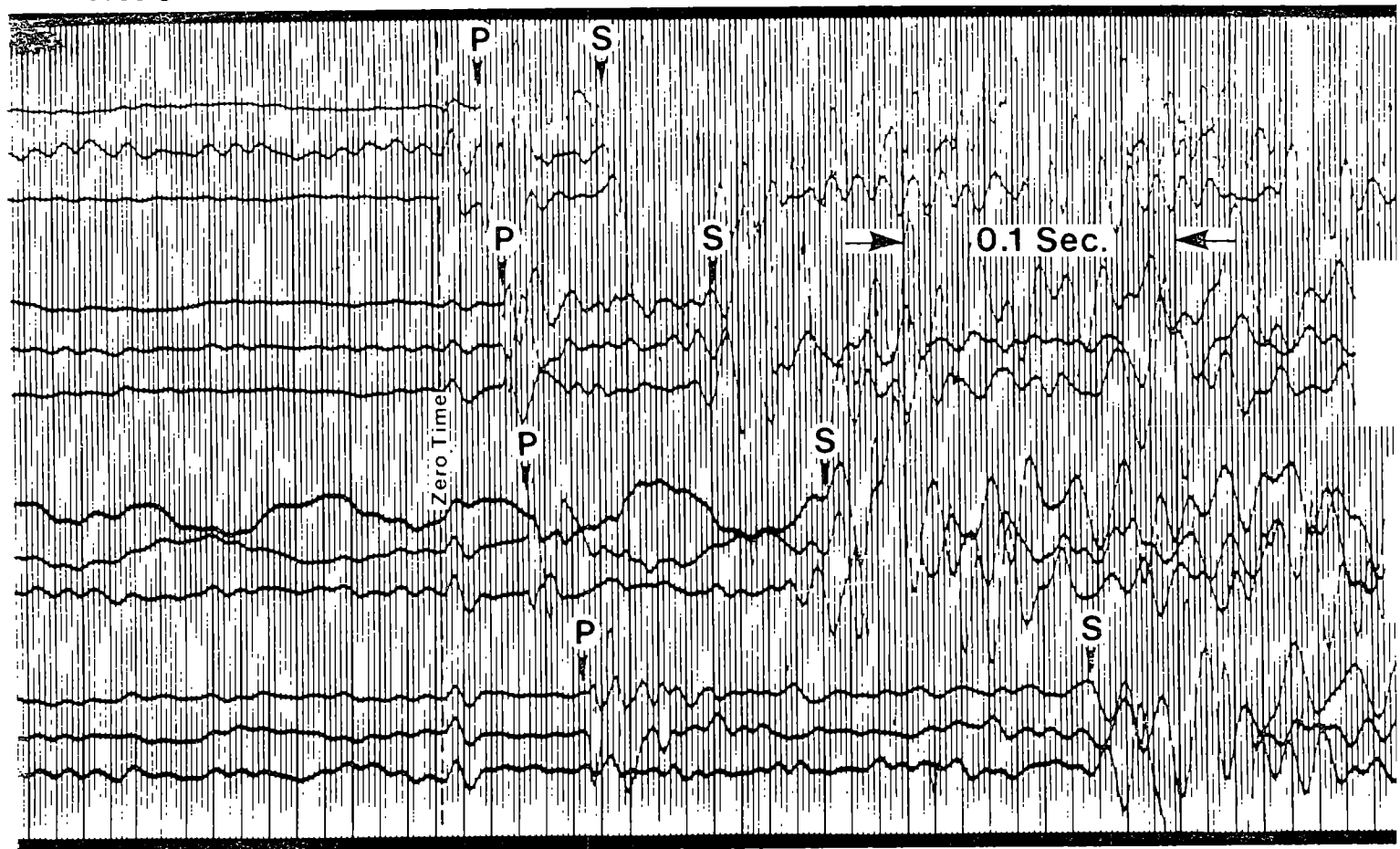
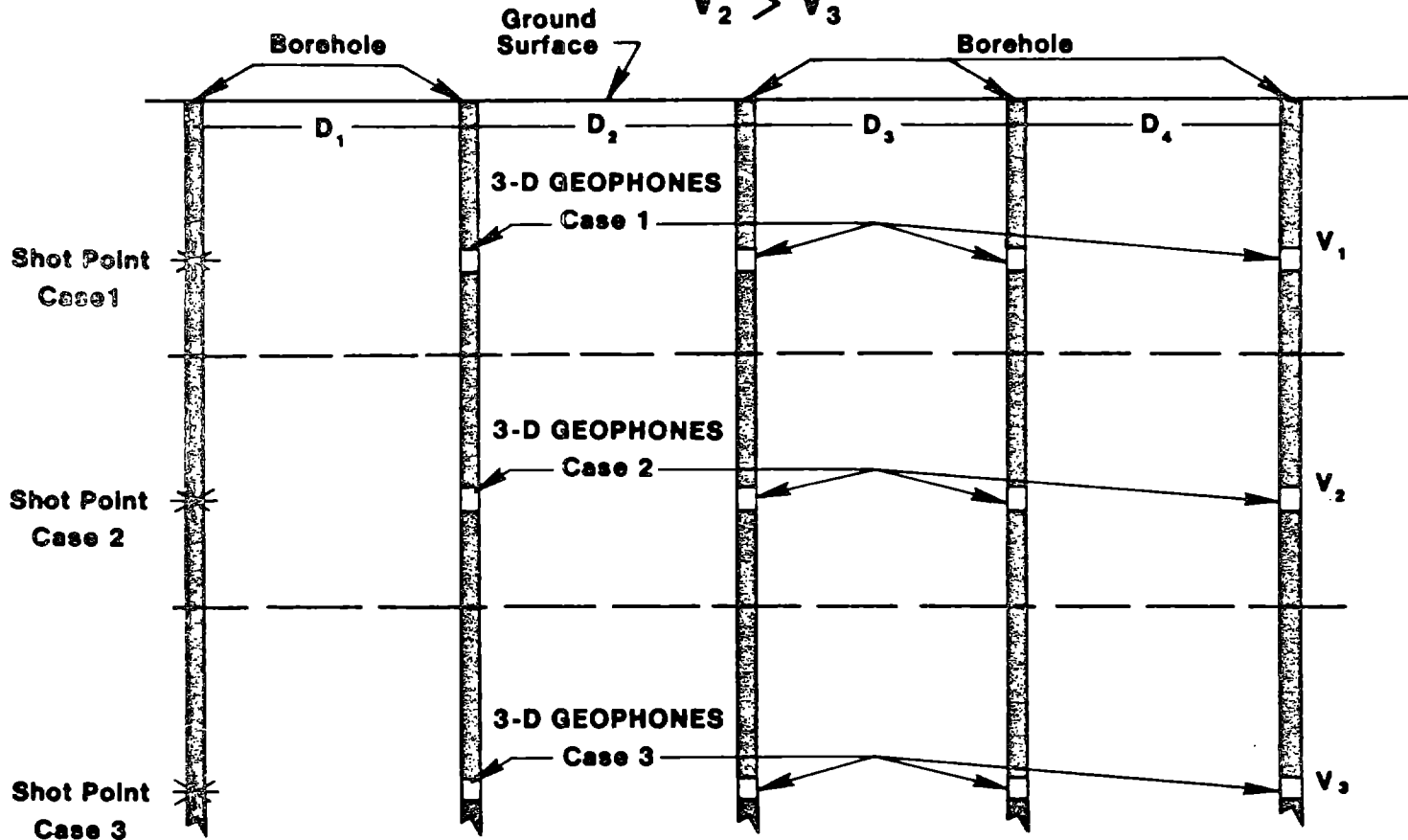
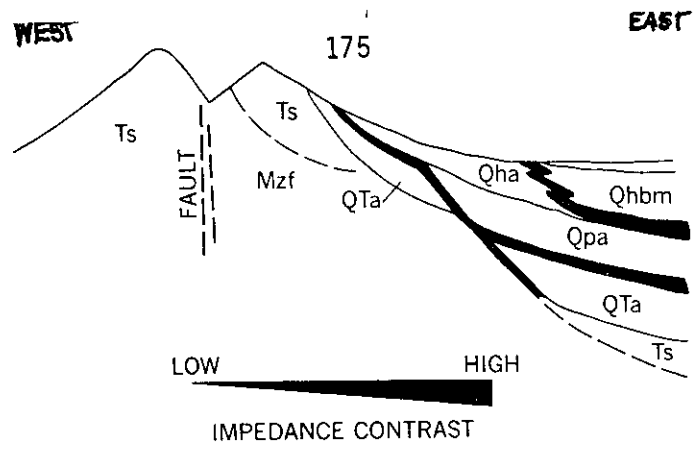


FIGURE 10
CROSS-HOLE ARRAY
AND "P"/"S" RECORDING



Unit	Thickness (m)	Relative bulk density, ρ (g/cm ³)	Penetration resistance ¹ (blows/ft)	P-wave velocity, V_p (m/sec)	S-wave velocity, V_s (m/sec)	Impedance, $V_s \rho$
Qhbm	0-36	1.3-1.7	0	<i>1400</i> ⁴	<i>90-130</i> ²	117-153
Qha	0-15	1.9	20-80	300-600 ³	200-300	380-570
Qpa	10-45	2.1	100	1500-2100	200-400 ⁵	420-630
QTa	0-250?	2.0	100-refusal	2500	1200	2400
Ts	0-300	2.4	Refusal	1500-3300	500-1400	1200-3360
Mzf	2.7	Refusal	2800-4000	1400-2000	3780-5400

¹ Test used 140-lb hammer dropped 30 in.
² From Warrick (1974)
³ Above water table. Below water table $V_p = 1500-1700$
⁴ Figures in italics are estimated values
⁵ Warrick (oral commun., 1974)

FIGURE 31.—Schematic cross section of southern San Francisco Bay region and description of certain physical properties of the generalized geologic units. Qhbm, bay mud; Qha, Holocene alluvium; Qpa, late Pleistocene alluvium; QTa, early Pleistocene and Pliocene alluvium; Ts, Tertiary sandstone; Mzf, Franciscan Formation.

FIGURE 11
(from 22)

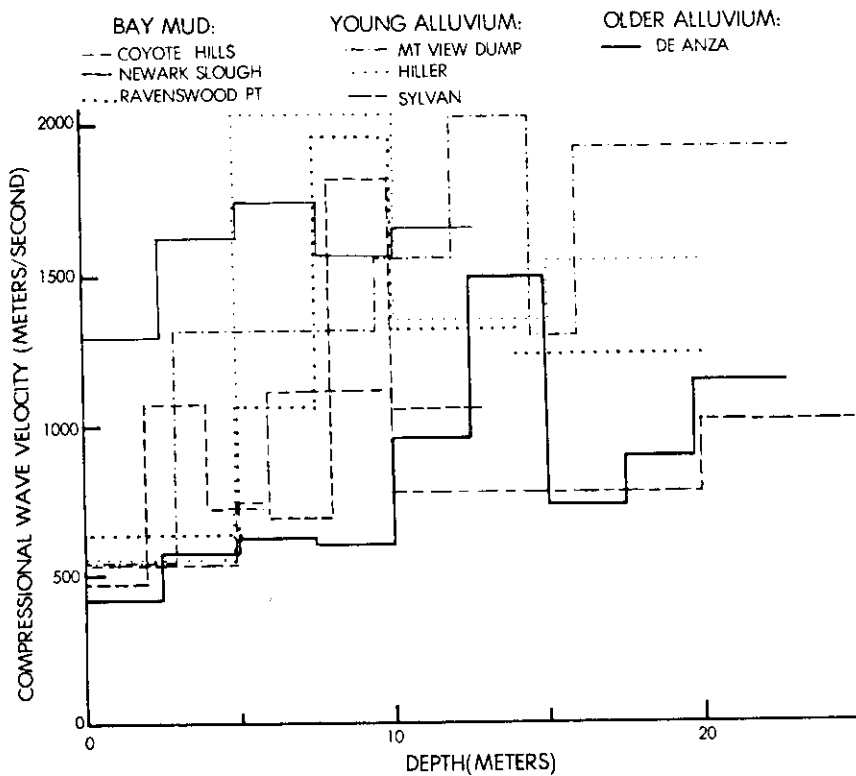


FIGURE 12
(from 23)

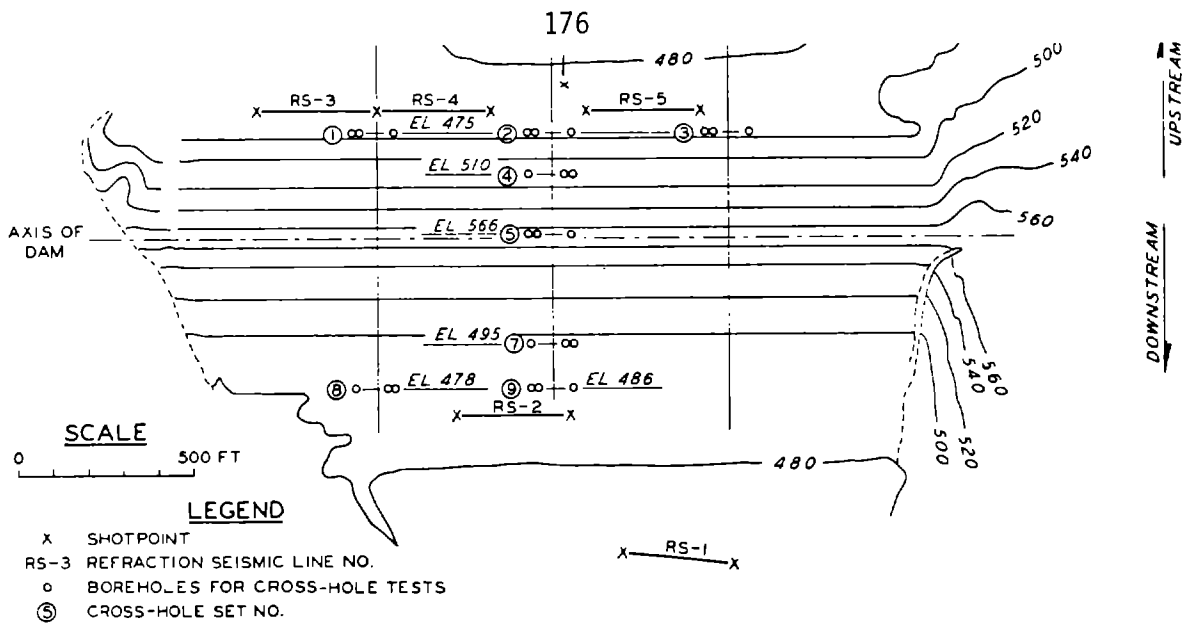
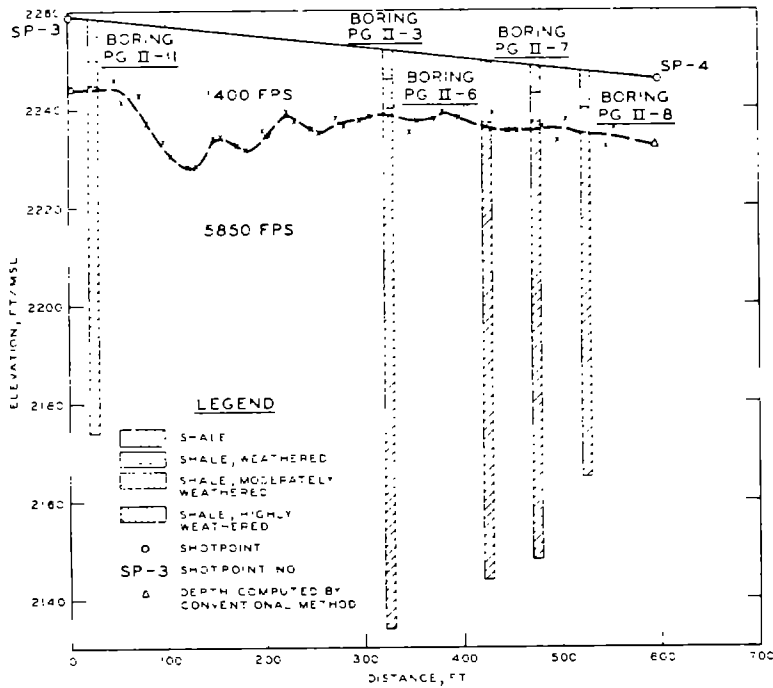
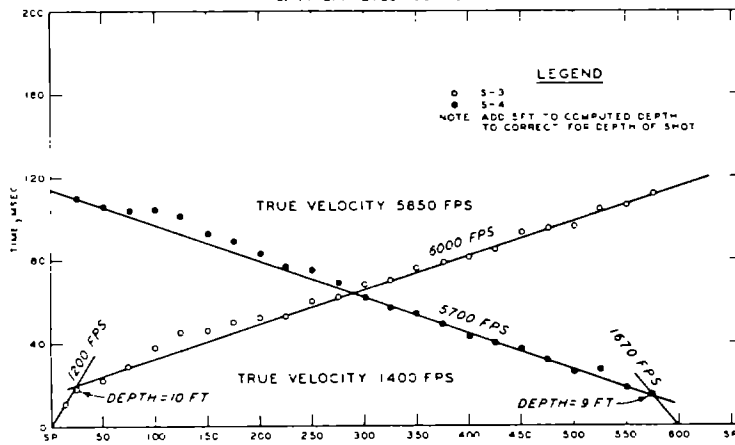


FIG. 2.--SEISMIC INVESTIGATION PLAN FOR AN EARTH DAM

FIGURE 13
(from 24)



a. INTERPRETED ROCK SURFACE



b. APPARENT TIME-DISTANCE PLOT

FIG. 4.--TIME-DELAY INTERPRETATION OF REFRACTION SEISMIC SURVEY

FIGURE 14
(from 24)

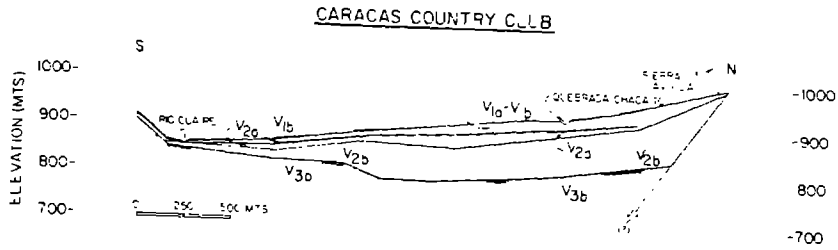


Figure 2a

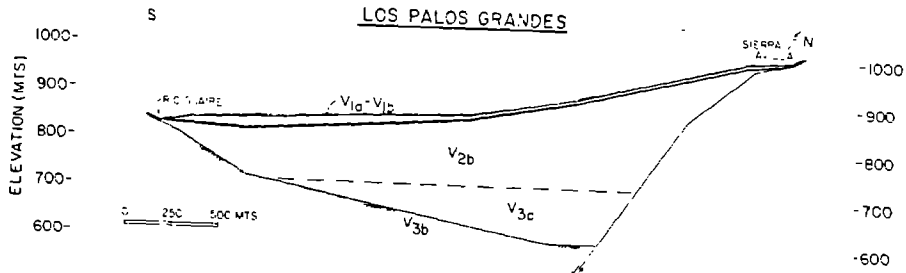


Figure 2b

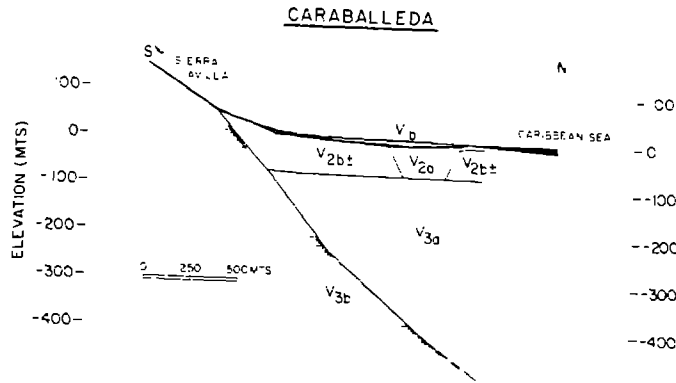
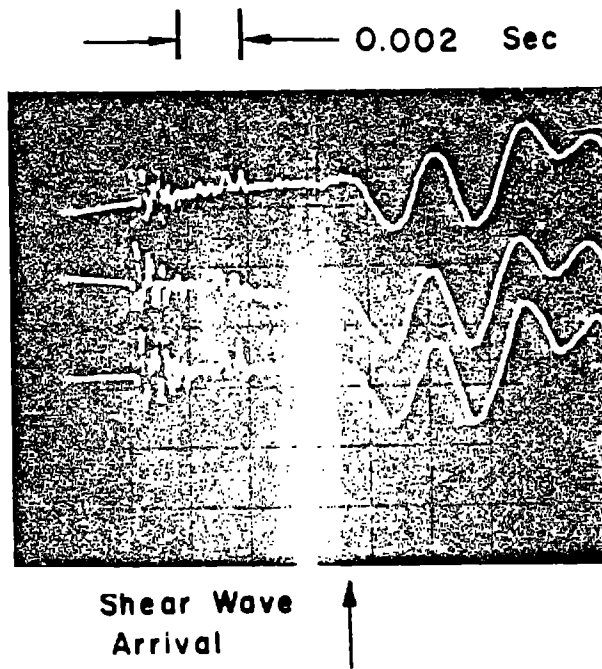


Figure 2c

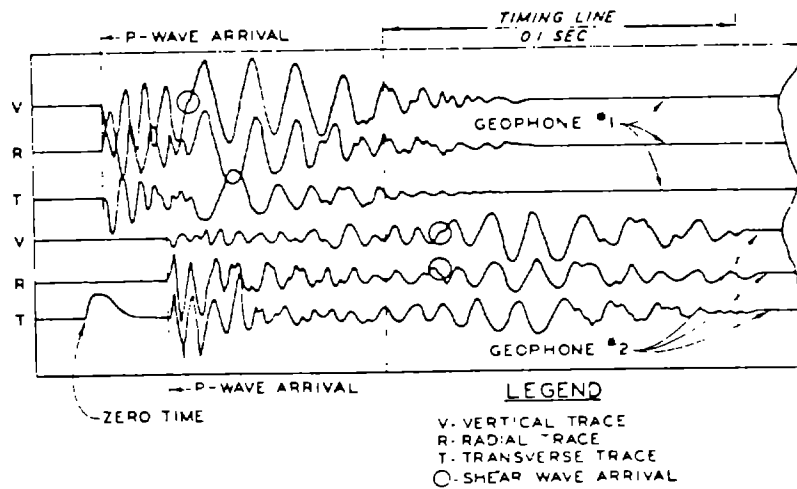
CARACAS - SEISMIC VELOCITY VALUES

<u>SYMBOL</u>	<u>VELOCITY ("P" WAVE) (MTS / SEC)</u>	<u>IDENTIFICATION</u>
V _{1c}	400 - to 500±	SOILS, PROBABLY LOOSE
V _{1b}	900±	SOILS
V _{2a}	1500±	SOILS, SATURATED
V _{2b}	1700 - to 1850±	SOILS, COMPACTED VALLEY FILL, ALSO LAYERS OF SOFT AND/OR WEATHERED ROCK
V _{3a}	2400±	SEDIMENTARY ROCK AND/ OR CEMENTED SOILS
V _{3b}	4000±	ROCK, GNEISS OR MASSIVE SCHIST

Figure 2



a) OSCILLOSCOPE TRACES FOR CROSS-HOLE TEST
MECHANICAL SOURCE



b) OSCILLOGRAPH RECORDS FOR CROSS-HOLE TEST
BLASTING CAP SOURCE
(from Ballard and McLean, 1975)

Fig. 44 Identification of Shear Wave Arrivals.

SOCIAL ASPECTS OF EARTHQUAKES

by

Janice R. Hutton¹ and Dennis S. Mileti^{II}

ABSTRACT

Recent natural hazards policy studies illustrate discouraging trends in earthquake losses and in the use of adjustments to mitigate earthquake hazards. The potential for catastrophic losses from large earthquakes is increasing. Adjustment use trends indicate that some current practices do help reduce losses from moderate earthquakes but may ultimately increase losses from large earthquakes. Furthermore, research indicates only a comprehensive approach, one that encourages the use of a locally appropriate mix of adjustments, can curb the increasing rise in catastrophe potential from large earthquakes.

Potentially, microzonation has a substantial contribution to make to efforts to mitigate the effects of large earthquakes and associated hazards. Microzoning studies may also provide a stimulus to initiate comprehensive programs of earthquake hazard management. In order to provide the basis for effective hazard reduction programs, microzonation studies must be performed by experienced multidisciplinary technical teams working in direct conjunction with a variety of public and private officials.

INTRODUCTION

Prior to the 1960's, poverty in America was socially understood as a fact of life; a reflection of individual choice, a product of God's will. But in 1961 Michael Harrington discovered that poverty in America was not a fact at all, it was instead a problem (8). The distinction between facts and problems is that problems have solutions; while social facts have no solutions. Harrington's study focused on the distribution of poverty. The patterns of distribution allowed him to discern the interactive causes of poverty which implied a more systematic approach to solving poverty in America. Lyndon Johnson instituted a set of solutions to the institutional causes of poverty implied in Harrington's work. Called to "Economic Opportunity Act of 1964", the Federal government launched a full scale attack on the causes of poverty in America. Poverty became a social problem rather than a fact. Legislative and organizational solutions abounded, and some of these solutions have enabled purposeful interventions to break the cycle of poverty.

Prior to the 1970's earthquakes and their destructive potential were socially defined as facts of life; a reflection of individual choice; or a product of God's will. Spurred by funding emphasis of the National Science Foundation in the early 70's, studies identified more systematically the physical and social distributions of earthquake effects and

-
- I Janice R. Hutton, Senior Staff Scientist, Woodward-Clyde Consultants, San Francisco, California.
II Dennis S. Mileti, Associate Professor, Colorado State University, Ft. Collins, Colorado.

losses (1), (2), (3), (6), (12), (13), (14), (15). The patterns of distribution enabled scientists to better describe the interactive causes of earthquake losses which imply a more systematic approach to reducing the growing hazards from earthquakes.

Coupled with the impact of the 1971 San Fernando Earthquake, study findings gave rise to the definition of earthquakes as a National social problem. With passage of the "Earthquake Hazards Reduction Act of 1977", the Federal government has instituted a set of solutions to the interactive causes of earthquake losses. The 1970's could mark the beginning of comprehensive solutions aimed at altering the cycle of increasing potential for catastrophic losses. Microzonation has a large potential contribution in solving earthquake problems.

Microzoning studies could provide an important first step toward instituting comprehensive damage-reduction programs for seismic events and associated hazards. The studies should be undertaken with a view to their serving as a basis for a variety of planning efforts related to hazard abatement.

DEFINITIONS OF CAUSE AS BLINDERS

The nature and content of proposals for solving problems is highly related to the shared and accepted definitions of the causes of problems. Hence, when Harrington discovered systematic biases in the opportunity structure for getting jobs, affirmative action programs were offered as a solution to break down the biases. This program and others began to compete with the more commonly held view that poverty in America, since the time of the Great Depression of the 1930's, was caused by laziness, an inherited lack of intelligence, individual choice and God's will. This later view of causes of poverty defined it as an individual's problem. No social system cause or social problem was defined and therefore no social solution was offered.

Causes of Earthquakes

Similarly, an overwhelming majority of people asked about the causes of disasters in their own localities, said they view them as either unaccountable or as an act of nature or of God (2). Recent work by Burton, et. al. discerned three perspectives on the cause of disasters. Casual factors are either nature, technology or society. People and their decisions and habits are rarely viewed as causes of disaster.

From the natural science point of view disasters are natural events which are solved by an emphasis on scientific research on natural causes. From this definition of cause the choices of solution emphasize increasing and using knowledge from the natural sciences to mitigate hazards.

The implication of the Burton, et. al. line of argument is that those who view the cause of hazard as technological or as social are biased in suggesting solutions which are almost wholly technological or social, respectively. Social, economic and political variables are, in fact, just beginning to surface as possible causes of hazards. "They need to be examined in harmony with physical and technical factors" (14). None of these three casual explanations alone (nor any two of them) will provide

adequate solutions to the earthquake problem, just as Mother Nature casual explanations have not led to reliable solutions.

Trends in Earthquake Losses

Recent U.S. research in natural hazards and policy has presented decision makers with better documentation regarding the causes of earthquake damages, and the extent and distribution of expected losses from earthquakes.

More than 70 million people in the U.S. live in the two highest (of four) seismic risk zones. Most of the nation is subject to some risk from seismic disturbance. Major earthquakes have occurred in the interior of the country and on the eastern seaboard, thus undermining the popular conception that earthquakes are limited to the Pacific Coast.(1) Despite a considerable seismic history, the United States has been extraordinarily lucky; only 1,200 deaths have resulted from earthquakes in this country (13). But, earthquake damage has been on the increase. Dollar loss per capita shows an upward trend in recent years (1). Danger from earthquakes is increasing in the U.S. because in recent decades the population has concentrated in urban centers subject to risk from major earthquakes and associated hazards. It is estimated that by the year 1200, 15% of the nation's people will be subject to major earthquakes in California alone (13).

Increasing concentration of people and property at risk leads to increasingly high estimates of loss potential from large earthquakes in urban areas. Estimates of losses from a repeat of the 1906 San Francisco quake are staggeringly high. The death toll could reach 40,000 with economic loss estimates ranging from 13 to 20 billion dollars (5), (13). A major earthquake in Los Angeles is estimated to cost 25 billion dollars with as many as 12,000 deaths and thousands more injured (13). These discouraging trends in the U.S. losses are roughly reflected throughout the seismically active world.

Causes of Earthquake Losses

When we come to agree that earthquake problems stem from a combination of natural, technological and social causes then we will begin to assess earthquake risk by using information about all three causes. Specific causes and interactions among them that contribute to earthquake losses are difficult to identify and measure. To illustrate the complexity, Ayre, et. al. summarized some of the relationships in a 1975 study (1). Drawing on their work, there are at least five sets of factors or effects which combine to identify the level of hazardousness of a place. The earthquake hazard is an interactive function of:

- (1) Physical Effects
- (2) Static Human-use Effects
- (3) Systemic Human-use Effects
- (4) Associated Hazards Effects
- (5) Adjustment Levels Effects

Physical effects, which define the character of the earthquake event are hard to estimate because interactions among them are complex and difficult to predict. Earthquake damage may result from three separate physical sources: (1) strong ground motion (shaking); (2) surface fault ruptures; and (3) ground failure (landsliding, settlement, liquifaction). In turn, these effects are influenced by other earthquake parameters: (1) magnitude of the earthquake; (2) epicentral location; (3) hypocentral depth; (4) extent and magnitude of surface faulting; and (5) intensity and duration of ground motion (4). All of these physical characteristics of the natural event are causes of damage and should be considered when estimating the earthquake risk at a particular location.

To further complicate the attempt to evaluate local risk are a host of human use characteristics which combine with the physical effects to determine risk. Included in the evaluation will be static estimates of the amount and distribution of exposure of people and various classes of structures, according to age, use, type, height and density of occupation.

A particularly important consideration in estimating earthquake risk is that earthquakes sometimes result in compound disasters. Fires are the most common secondary hazard, although the dangers from flooding (from tsunamis or dam failures) are particularly important at some locations. Locally, landslides and avalanches must also be considered in risk estimates.

Future efforts to estimate and quantify the earthquake risk of an area should consider the indirect, systemic effects. Indications and geographic location of especially vulnerable structures, systems or economic sectors whose demise would have implications beyond their direct damage are considerations to be estimated. For instance, an especially large employer or the concentration of an industry wide distribution center upon whom many jobs are dependent are examples of indicators. Losses like these appear to be a very significant cost associated with a large earthquake disaster. An interesting study by Cochrane of losses from a repetition of an earthquake in San Francisco of the same magnitude of that in 1906 indicates that indirect and systemic effects are, at a minimum, equivalent to direct property damages (5), (6).

Estimates of levels of mitigating measures in use in the area are also determinants of damage potential. Local capacity to respond to an earthquake emergency can greatly affect the influence of secondary hazards on damage levels.

Our capacity to measure potential effects of earthquakes has increased in recent years although further refinement of measures is desirable. Which and how many of these measures are included in an assessment of risk is a matter of choice. We believe that this choice should be a matter of wide scientific and policy debate so that some indicators of each type of cause of earthquake damage is included in an overall assessment of local area earthquake risk.

The ways in which earthquakes are measured is very much a matter of cultural convention, scientific knowledge, data availability and functional need. For the present multitude of purposes, the ideal measure of

earthquake bigness includes various dimensions of the hazard rather than merely some indexical measure of physical effects (2). In order to serve as a basis for comprehensive planning for the reduction of earthquake hazard potential, risk assessments should encompass measures of each category of earthquake effects and describe their geographic distributions. The resulting, more comprehensive description and evaluation of hazard potential may yield more comprehensive solutions to hazard problems.

LIMITATIONS OF AVAILABLE SOLUTIONS

Any effort to design programs for comprehensive earthquake hazards reduction is very difficult. Not only are the physical and social interactions complex, but our knowledge about the relationships is quite incomplete. Nevertheless, reliable knowledge is increasing and some trends in the effectiveness of preventive actions are emerging for interpretation.

Briefly stated, hazard adjustments is a phrase which refers to intentional actions which are taken by decision makers to cope with the risk and uncertainties of earthquakes. III Adjustments are purposefully chosen solutions to a perceived hazard problem. The particular choices imply assumptions as to hazard cause. A conventional classification of adjustments includes three categories of actions: (1) modify the event (earthquake control); (2) modify vulnerability (earthquake-resistant design of structures); and (3) redistribute losses (emergency relief aid).

Adjustments which comprise the modification of vulnerability to earthquakes include:

- (1) earthquake-resistant construction;
- (2) land use management;
- (3) prediction and warning systems;
- (4) community preparedness for emergency response; and
- (5) pre-event planning for post event reconstruction. IV

An attempt to estimate and assess current levels of earthquake adjustment use and effectiveness was conducted by the Institute of Behavioral Science, University of Colorado in 1975 (1), (14). The study concluded that the U.S. is currently over-relying or encouraging the use of some adjustments at the expense of stimulating the use of others; thus inhibiting a mixed approach in stemming vulnerability from earthquakes.

In an all hazard summary evaluation of adjustment use and effectiveness the research concluded that a "... substantial portion of the

III For a more thorough review of hazard adjustments and the complexities of evaluating their interactions and use see White, Gilbert F. and J. Eugene Haas, Assessment of Research on Natural Hazards. Cambridge, Mass.: The MIT Press, 1975, pp 57-66 and 323-324.

IV The discussion of adjustments and their use is adapted from Ayre, Mileti and Trainer, Earthquake and Tsunami Hazards in the United States: A Research Assessment. Boulder, Colorado: Institute of Behavioral Science, University of Colorado, 1975.

adjustments being used appear to contribute to enlargement of catastrophe potential as a result of increasing reliance upon technological measures" (14). So far, our approaches to coping with earthquake hazards do not reflect an awareness of the tendency to over-rely on technological adjustments.

Optimum structural resistance to earthquakes involves responsible action by the owner, financing agency, architect, engineer, builder, foreman of construction, manufacturer of components, insurer, and appropriate government officials. There are many special problems with the use of building codes and regulations for protection against earthquake, fire and other hazards. The codes themselves, even if in effect and thoroughly enforced, are often inadequate. Codes establish no more than minimum requirements for public safety -- they are not designed to prevent damage although they aim to reduce damage to a tolerable minimum. With the occurrence of a large earthquake, many "built to code" structures may be total economic losses. Furthermore, old hazardous buildings -- not subject to codes -- pose a very serious problem in some cities because many of them have evolved into densely occupied housing for low-income people.

On the other hand, effective implementation of earthquake-resistant design and construction undoubtedly reduces damages from moderate earthquakes, and should be encouraged. But codes should not become the sole collective adjustment. It is just not clear that persons who should know, know that present codes and uneven enforcement may contribute to a false sense of security leading to decisions to locate in areas prone to large earthquakes. Dense occupation of expensive structures in areas of high hazard continues and contributes to the staggering growth in potential catastrophic losses.

Land Use Management

Although there are a few examples of the use of land use management for reducing seismic hazards, little has been done in the United States to encourage the application of this adjustment. The most encouraging example exists in the City of Long Beach, California, where a long term program for phasing out the use of old and hazardous buildings is in effect.

The State of California has made two attempts to encourage recognition of seismic safety considerations in local planning efforts. The Alquist-Priolo Special Studies Zones Act aimed to guard against building inhabitable structures (except single family dwellings) across active faults. And, the California Council on Intergovernmental Relations adopted guidelines to be enforced under previous planning legislation which require California cities to take seismic hazards into account in their planning programs. The experience with both efforts is uneven. Both attempts have been hindered by ambiguity and interpretation of what is expected (13). Many studies conducted to comply with the seismic element have provided only highly generalized information and several studies are reported to be of low technical quality. Even if these two provisions were being enforced to the letter and intent of the legislation, problems with their use

remain. Foremost, there is a common misconception that damage from fault shippage is a major source of loss from earthquakes. When evaluating total damages from a given earthquake, damage resulting from surface fault displacements will generally be minor when compared with damages from other earthquake effects, such as local ground conditions. (4)

An implication of sole reliance on land use schemes based on incomplete or technically poor information is similar to the implication previously drawn about the sole use of building codes as a strategy to achieve earthquake loss reduction. In consciously meeting the laws, development decision makers may be lulled into believing they have adhered to all practical guidelines for safe location. Decisions to locate in areas of high hazard are likely encouraged by guidelines which are either incomplete in their concept or coverage of hazard effects or inadequately implemented and enforced. Further study of the effectiveness of these laws are needed to explore the hypothesis that these two laws are exacerbating the trend of growing catastrophe potential.

Prediction and warning systems

Specific forecasts of damaging earthquakes may be available in less than a decade but a reliable system for prediction and warning may not be available in the foreseeable future. Some mechanisms are already in place to assist responsible officials who must cope with the many uncertainties involved in advantageously using the new technology (11). Scientifically successful prediction and warning of an event cannot be expected to lead, of itself, to desirable social response. In the event of inaccurate predictions or false warning, which in the nature of the problem will inevitably occur, the social response may be highly undesirable and may lead to greater economic and social disruption than would have occurred without warning. Encouraging the use of this adjustment at the expense of applying other, more reliable, forms of protection would be a major error in policy direction for the United States.

Emergency Response

Community preparedness for emergency response is a hazard adjustment of special importance for earthquakes in order to minimize the potential for a compound disaster. Associated hazards of fire and flooding are particularly in need of immediate attention after an earthquake. While some level of preparedness planning for emergency exists in most communities, present levels of preparedness fail to provide for all eventualities of an earthquake disaster. In most areas subject to large earthquakes there is a lack of detailed information on which to base viable contingency planning. Information about special physical problems such as gas and water lines rupture and vulnerability of communications and health services needs to be detailed. Planning should take better account of the implications inherent in the failure of vital life lines and inaccessible services due to earthquake damage. The NOAA/FDAA studies of Los Angeles and San Francisco which identified patterns and extent of earthquake

losses in relation to emergency response are exemplary models, and they are being followed in Salt Lake/Ogden and Seattle/Tacoma. Other communities subject to large and compound earthquake disasters should be provided with similar analytic information.

Furthermore, there is evidence that these studies provide impetus, by their conduct and publication, for hazard reduction actions taken by private sector decision makers. Identification of hazard producing dams which are particularly vulnerable to earthquake damage is a study component. Acting independently, and at considerable expense, the East Bay Municipal Utility District immediately undertook corrective action for those dams under their jurisdiction which were identified in the study. Other dam operators have not been so responsive to the new information, but this is a good example that some hazard reduction measures will be undertaken once hazardous facilities and high risk areas are identified.

Pre-event preparation for reconstruction

Pre-event planning for post event reconstruction as an idea is relatively new. In practice, it is non-existent. From a study of disaster reconstruction issues Kates concluded that the reconstruction process is ordered, knowable and predictable.

"The central issues and decisions (involved in the reconstruction process) are value choices that give varying emphasis to the easy return to normalcy, to the reduction of future vulnerability, or to opportunities for improved efficiency, equity, or amenity. Over ambitious postconstruction planning to reduce future vulnerability or improve efficiency or amenity appears to be counter-productive. And the major opportunities to improve the reconstruction process lie in three areas: the early recognition of certain overlooked problems, people, functions and areas; the reduction of uncertainty about the future for those who live and work in the city; and the preparation for reconstruction before the disaster comes" (9).

Kates is quick to point out that, he is not calling for elaborate and formal studies, plans and designs put forth by professionals. Experience shows that elaborate and inflexible community plans are, most often abandoned for a host of reasons. Pre-event planning for post disaster reconstruction is a call for recognizing explicitly factors that are now implicit. There is already a plan for reconstruction -- it is the on-going plan of the pre-disaster city. Predisaster inventories and catalogs of current processes and resources plus provision for moratoriums and organizational aids should be instituted prior to disaster to help limit the extraordinary influence of entrepreneurial interests which often prevail during reconstruction.

Sole solutions are inadequate

The idea of comprehensive management of earthquake prone areas in the United States is not new. The idea developed from research investigations that postulate and demonstrate the inadequacies of exclusive reliance on a limited range of adjustments designed to curb the effects of moderate earthquakes in areas prone to earthquakes of relatively frequent moderate events (1), (2), (6), (7), (14).

The occurrence of a large earthquake will emphasize conclusions which already are apparent: that earthquake prediction and warning proficiency will not alone prevent catastrophe; that slowness to plan with land use will build up the catastrophe potential; that reliance upon a few technological improvements such as earthquake resistance in buildings will not avert broader disaster; that sustained local awareness and responsibility are essential to prevent incompatible encroachment of vulnerable zones; that provision must be made to deal in an integrated fashion with earthquakes of moderate size as well as with large events (4).

Factors affecting the mix of adjustments

Burton, et. al. identified four overriding factors which affect the selection of adjustments and adjustment combinations for reducing hazard problems. The factors are: some characteristics of extreme events; experience with extreme events and adjustment success; intensity of resource use of the area at risk; and the level of material wealth attained by the decision making entity (2). The direction of the relationships of these factors to human response to hazards does not bode well for the success of comprehensive earthquake hazard reduction programs in the areas of highest damage potential in the U.S.

Earthquakes are characterized as very intensive on an intensive-pervasive scale of hazard characteristics. Drought, for instance is highly pervasive. According to Burton, et. al., an intensive event is readily forgotten and if there is a long time between events, permanent shifts in adjustment patterns is unlikely.

Shifts in adjustment use have almost always come in the immediate aftermath of a disaster. If the event size and frequency of occurrence to which adjustment levels are desired are also very rare events, then the opportunity to shift adjustment trends is also rare. Earthquakes of large magnitude, which are the source of great catastrophes, are extremely rare events.

Areas in which intensive use of capital and labor is in effect, such as urban centers, are more likely to employ hazard reduction measures than areas not so intensively used. However, areas of intensive resource use are slower to change use or location as the means of adjustment.

Wealthy societies seem to tolerate recurrent disasters for a longer period prior to actively reducing the hazards. Whereas, poorer societies have less tolerance for the impact of even small disasters. When these societies do act the poorer tend to reduce hazards through migration while wealthier nations reduce hazards through other means.

Given these constraining factors, prosperous, urban centers -- the areas of greatest earthquake hazard potential -- are unlikely to choose by themselves to reduce hazards through shifts in land uses or changes in location. More detailed specification of risk may alter these patterns.

MICROZONATION AND ADJUSTMENT CHOICE

Microzonation could provide information to stimulate the beneficial use of hazard reduction adjustments. The information provided in a given study will depend on the use to which the study is to be put. Narrowly defined utility will yield narrowly scoped studies. The Proceedings of the International Conference on Microzonation for Safer Construction Research and Application defined microzonation in fairly narrow terms.

Microzonation was referred to as zoning for potential earthquake effects in detail on a local geographic level. This rather broad definition of what information could be included was conceived as useful only to structural architects.

Microzonation was conceived as a guide to architects to avoid over or under design of earthquake resistant structures in hazardous region. The users of this information are the architect and building inspector who set and meet design criteria for new structures. The utility of this conceptualization is limited to encouraging one adjustment; that of earthquake-resistant design and, if implemented, earthquake-resistant construction. This use of microzonation assumes that the building of such structures in hazardous areas is desirable. In six short years, an expanded conception of the utility of microzone studies is already conventional.

One invited paper uses a substantially broader concept of microzonation utility:

"The aim of microzonation is to estimate the location, recurrence interval, and relative severity of future seismic events in a local area so the potential hazards can be assessed and the effects can be mitigated or avoided" (3).

Armed with this concept of microzonation, comprehensive programs for earthquake hazard reduction in local areas could proceed to be designed and implemented. Accurate and interdisciplinary delineation of differential risk areas within a local jurisdiction can be used to stimulate the use of an appropriate mix of adjustments. Such studies have the potential to:

1. enhance design and application of practicable land use subdivisions and zoning programs;
2. enhance regional application of appropriate building design and practice;
3. enhance public awareness of risks from geologic hazards;
4. enhance emergency response planning;
5. enhance planning for compatible reconstruction after an event; and

6. enhance socially appropriate responses to earthquake warnings.

With the advent of the Earthquake Hazards Reduction Act of 1977, and the thoughtful development of a plan for implementing the law's provisions (see 15), comprehensive earthquake hazards management is in prospect. The plan emphasizes the need for balance in the use of hazard adjustments at the local level of planning and provides possible assistance to state and local governments for achieving a reduction of earthquake hazards. In order to design comprehensive programs, comprehensive risk information should be forthcoming.

Microzone studies have a tremendous potential contribution to make to planning efforts made by public and private managers to reduce earthquake hazards. In order to make the contribution, many obstacles must be overcome. Some of the more obvious next steps are:

1. A thoughtful specification of the elements comprising ideal microzonation is needed. For microzonation to be most useful to local decision makers the information needs to go beyond delineating soil and foundation data. Maps may include judgments about especially vulnerable segments of population, secondary hazard potential (fire), and especially hazardous facilities, including structures. More detailed information may better illustrate mitigation decision priorities to local decision makers. More detailed information may better illustrate needs for coordinating earthquake mitigation programs with other hazard mitigation programs such as those of the California Coastal Zone Commissions, the National Flood Insurance Program, and the National Environmental Protection Agency. New programs may be instituted at the Federal level for hazardous land acquisition or subsidized earthquake insurance. Ongoing microzonation efforts will allow communities a basis for informed participation.

2. Formal criteria are needed to determine the priority areas for microzoning earthquake effects. Earlier candidates for microzonation may be those places where growth has yet to occur rather than areas where population density is high. Preventing incompatible development is cheaper than correcting existing facilities.

3. The Alquist-Priolo Studies Zones Act of 1972 (as amended) provides the foundation from which a building block program of microzonation needs to be developed. Ultimately, local decision makers need more detailed information than currently provided, with which to make more comprehensive land use decisions for earthquake and other hazard mitigation efforts. If the new provision of information to local areas (under Alquist-Priolo) is not soon accompanied by more detailed information, the current law could act as a deterrent to more comprehensive decision making. From the National Flood Insurance Program experience we have learned that too little information and regulation may be worse in the long run than no information or regulation at all (10).

CONCLUSION

Programs and information bases which stimulate use of a locally appropriate mix of adjustments to reduce earthquake risks are urgent needs in hazard mitigation planning. We have reviewed the experience with current solutions to emphasize two points. First, some of the efforts we have made and are about to make have the potential to make the hazard greater. Second, risk assessments which include estimates from each category of hazard effects will provide a better basis for comprehensive hazard reduction programs. An implication of these points is that we must sustain our new efforts to work together in providing integrated evaluations of hazard causes and in designing integrated solutions for hazard reduction. Further, we must broaden our vision of participation to include elected officials, private sector managers and representatives of interested publics. For even if we ultimately achieve our idealized goal of providing perfect risk information it is not us who will be burdened with effective implementation of hazard reduction; it is they who must ultimately perform.

BIBLIOGRAPHY

-
1. Ayre, Robert S. with Dennis S. Mileti and Patricia B. Trainer
1975 Earthquake and Tsunami Hazards in the United States: A Research Assessment. Boulder, Colorado: Institute of Behavioral Science, University of Colorado.
 2. Burton, Ian, Robert W. Kates and Gilbert F. White
1978 The Environment as Hazard. New York: Oxford University Press.
 3. Cluff, Lloyd S.
1978 "Geologic Considerations for Seismic Microzonation," Draft mimeographed paper to be presented at the Second International Conference on Microzonation. San Francisco: Woodward-Clyde Consultants.
 4. Cluff, L.S., W.R. Hansen, C.L. Taylor, K.D. Weaver, G.E. Brogan, I.M. Idriss, F.E. McClure and J.A. Blayney
1972 "Site Evaluation in Seismically Active Regions-- An Interdisciplinary Team Approach." In Proceedings of the International Conference on Microzonation for Safer Construction Research and Application. Prepared for the National Science Foundation. Springfield, Virginia: NTIS, U.S. Department of Commerce, pp. 957 - 987.
 5. Cochrane, Harold C.
1974 "Predicting the Economic Impact of Earthquakes." In Social Science Perspectives on the Coming San Francisco Earthquake: Economic Impact, Prediction and Reconstruction. Natural Hazards Research Working Paper #25. Boulder, Colorado: Institute of Behavioral Science, University of Colorado.
 6. 1975 Natural Hazards: Their Distributional Impacts. Boulder, Colorado: Institute of Behavioral Science, University of Colorado.
 7. Friedman, Don G.
1975 Computer Simulation in Natural Hazard Assessment. Boulder, Colorado: Institute of Behavioral Science, University of Colorado.
 8. Harrington, Michael
1961 Poverty in America

9. Kates, Robert W.
1977 "Major Insights: A Summary and Recommendations,"
in Reconstruction Following Disaster, J. Eugene
Haas, Robert W. Kates and Martyn J. Bowden, Eds.
Cambridge, Mass.: MIT Press, pp. 261 - 293.
10. Mileti, Dennis S. and Janice R. Hutton
1978 Analysis of Adoption and Implementation of Community
Land Use Controls for Floodplains Management. An
interim draft report to the National Science Foun-
dation. San Francisco: Woodward-Clyde Consultants.
11. Mileti, Dennis S., Janice R. Hutton and John H. Sorensen
1978 Earthquake Prediction and Public Action. A report
to the National Science Foundation, (forthcoming).
12. Nichols, Thomas C., Jr.
1974 "Global Summary of Human Response to Natural Hazards:
Earthquakes," in Natural Hazards Local, National,
Global, Gilbert F. White, Ed. New York: Oxford
University Press, pp. 274 - 284.
13. U.S. Senate
1977 "Hearings on the Earthquake Hazards Reduction Act."
Printed for Committee on Commerce, Science and
Transportation. Washington, D.C.: U.S. Government
Printing Office.
14. White, Gilbert F. and J. Eugene Haas
1975 Assessment of Research on Natural Hazards.
Cambridge, Mass.: MIT Press.
15. Working Group on Earthquake Hazards Reduction
1978 Earthquake Hazards Reduction: Issues for an
Implementation Plan. Washington, D.C.: Office
of Science and Technology, Executive Office of
the President.

URBAN DESIGN AND EARTHQUAKES

by

H. J. Lagorio^I, and E. Botsai^{II}

ABSTRACT

Despite many technological advances in earthquake engineering and prediction, major U.S. cities remain vulnerable to major seismic events. Since the 1906 San Francisco earthquake, it is fortunate that a major U.S. metropolitan center has not been hit directly by a severe earthquake or even a moderate one.

In the U.S., an early beneficiary of the industrial revolution, large-scale urbanization began in the latter half of the 19th Century. Risk to populations exposed to earthquake is most critical for those living in highly congested urban centers in contrast to those in the suburbs. Because of rapid urbanization and the continued development in existing, well-established urban concentrations, recurrence of a major earthquake would result in much greater damage and life loss than ever before.

Urban Design as an emerging field of Architecture is identified with the rapid urbanization of the last three decades. Assessment of the physical growth of cities indicates that potential urban design principles in hazards mitigation are overlooked or that some consequences of urban design decisions are not foreseen due to the complexity of required interdependent activities, services, and functions.

INTRODUCTION

In the United States, as well as in other highly developed countries which were early beneficiaries of the industrial revolution, large scale urbanization began in the latter half of the 19th Century. Since then there has been a steady migration from rural areas to urban centers -- from the countryside to towns and cities. In the past few decades the number of urban places is still increasing with most of the population growth taking place in existing, well-established urban concentrations. It has been predicted that by the year 1990, more than half the world's people will be living in cities with a population of 100,000 or more.

I Professor of Architecture, Department of Architecture, University of Hawaii, Manoa Campus, Honolulu, Hawaii.

II President of the American Institute of Architects, Washington, D.C., and Chairman, Department of Architecture, University of Hawaii, Manoa Campus, Honolulu, Hawaii.

It is clear that the risks of natural environmental hazards are most critical for that population living in highly congested urban concentrations in contrast to those in the suburbs. Regarding this high risk exposure, the San Fernando earthquake in 1971 is noteworthy because of what might have happened had it occurred at the center instead of the edge of the Los Angeles metropolitan area, or if the Van Norman dam had collapsed completely without prior evacuation of the 70,000 downstream population.

Records of testimony given by expert witnesses during U.S. Senate hearings on "Governmental Response to the California Earthquake Disaster of 1971" clearly indicate that the increasing growth of population density in our cities is creating problems whereby a very localized earthquake in an urban setting can cause a major catastrophe such as was not possible some years ago. The pressures of population growth in the urbanization of our country are causing expansion into areas which are more difficult to develop safely than those of past decades.

VULNERABILITY OF URBAN CENTERS

The urban environment is a complex and closely knit fabric composed of many interdependent activities, services, functions, life systems and facilities. Due to this interdependency, the failure of any single component can severely affect the functioning of others. The recent "brown out" experienced in New York City with the failure of one public utility company's capacity to supply power is but one example of how one element of any interdependent life system can become compounded into a full crisis and result in total "collapse" of the function and integrity of a metropolitan center.

While much research has focused on the separate, individual elements of the urban environment, such as independent studies on: a) Life Lines, b) Building Design, c) Land Use, d) Contingency Planning, e) Public Policy, and f) Post-earthquake Recovery Programs, little or no work to date has been done in approaching the problem from a balanced urban design focus to mitigate the earthquake vulnerability of large metropolitan areas. The United States has been most fortunate that since the San Francisco earthquake in 1906, no major metropolitan center has been centrally impacted by a severe earthquake. Many authorities on the subject believe that such a seismic event is long overdue and that several of our major cities represent "catastrophies awaiting to occur". It is evident that almost all of our large urban centers located in areas of high seismicity are not prepared for such an event.

Table I is a selected and brief listing of some of the major American metropolitan centers located in zones subject to moderate or severe earthquake activity, being located in Seismic Zones 2, 3, or 4 as designated by the Uniform Building Code (UBC), 1976 Edition. Not listed in the table are other major cities like Chicago, Cleveland, or Detroit which, although not located in critical seismic zones, will none-the-less be affected by "long period" damage patterns resulting from the occurrence of major seismic events in other highly active seismic areas miles distant. Also not listed are those major coastal cities located in lesser earthquake prone areas but still vulnerable to tsunami damage caused by earthquakes originating thousands of miles away.

TABLE I

SEISMIC ZONE LOCATION OF SELECTED U.S. METROPOLITAN STATISTICAL AREAS

<u>Name of Area:</u>	<u>Seismic Zone 1976 - UBC</u>	<u>Potential Total Population at Risk</u>
Anchorage, Alaska	4	166,000
Los Angeles, California	4	8,960,000
San Francisco, California	4	4,450,000
Boston, Massachusetts	3	3,795,000
Charleston, S. Carolina	3	296,000
Salt Lake City, Utah	3	561,000
Seattle-Tacoma, Washington	3	1,788,000
San Diego, California	3	1,355,000
Atlanta, Georgia	2	1,780,000
Cincinnati, Ohio	2	1,162,000
St. Louis, Missouri	2	1,747,000

SOURCE: (a) 1977 Commercial Atlas & Marketing Guide
Rand McNally & Company

(b) UBC, 1976 Edition

As can be seen from Table 1, the population at risk in the metropolitan areas indicated is very high when dealing with major urban developments. Recent earthquake studies completed by NOAA and USGS reveal that the potential recurrence of a severe earthquake in a selected high density urban area would result in a major disaster with staggering casualties and high death ratios. Table 2 lists the damage and life safety implications of these studies in the urban centers selected for analysis. It is significant to note in Table 2 that a recurrence of the 1906 San Francisco earthquake today would result in over 10,000 deaths and 40,000 hospitalized injuries (not counting the possibility of dam failure in the study areas). The dollar loss in terms of repair costs to single family wood frame dwellings alone would approach \$1,240,000,000. In contrast, documented statistics of the actual San Francisco earthquake in 1906 indicate that there were only 700 deaths and a total dollar loss at that time of \$524,000,000 caused by the original event and fire.

CHARACTERISTICS OF URBAN DESIGN

The evolution of urban design as an emerging field and a recently recognized professional discipline within architecture has been identified with the rapid urban development which took place during the early 1940's through the late 1950's. In the mid-1960's, an assessment and evaluation of the physical results of this growth indicated that many fundamental design approaches were overlooked or that the critical consequences of some design decisions were not foreseen due, in part, to the fact that the urban environment is a complex and tightly knit fabric composed of many interdependent activities, services, and facilities. As indicated previously, due to its complexity, the failure of any of its components can severely affect the functioning of others. Consequently, urban designers are becoming sensitive to the fact that their decisions must be developed from a balanced and holistic program to include the design professions, social and economic concerns, and public policy when dealing with the intricate relationships found in metropolitan areas.

As a profession, urban design focuses on the three-dimensional physical planning and design of the urban environment. Although overlap exists in many areas, it is a field distinct from other disciplines normally associated with city and regional planning issues and the public policy aspects of cities as applied through local, regional and Federal government intervention. The fundamental objective of urban design is to synthesize and develop three-dimensional solutions to:

1. The physical, spatial arrangement of all urban activities including their nature, location, type, scale, density, and circulation patterns.
2. The physical three-dimensional form of urban activities through the interaction of design determinants with climate, topography, natural hazards, and other environmental relationships.

TABLE 2

E.Q. VULNERABILITY OF SELECTED U.S. URBAN AREAS

<u>Metropolitan Area</u>	<u>Injuries*</u>	<u>Deaths*</u>	<u>Homeless*</u>
San Francisco, California	40,000	10,000	58,000
Los Angeles, California	75,200	18,800	140,000
Salt Lake City, Utah	9,200	2,300	29,600
Seattle/Tacoma, Washington	28,000	7,000	45,000

* NOTE: Excluding dam failure

SOURCE: USGS & NOAA Reports: 1972, 1973, 1975, 1976.

- a) A Study of Earthquake Losses in the San Francisco Bay Area.
- b) A Study of Earthquake Losses in the Los Angeles, California Area.
- c) A Study of Earthquake Losses in the Puget Sound, Washington Area.
- d) A Study of Earthquake Losses in the Salt Lake City, Utah Area.

3. The physical organization of urban linkages relating to community and social requirements exemplified by buildings, transportation systems, communication networks, redevelopment, energy utilization, land-use, and local government programs.
4. The quality of urban living which recognizes and measures the positive attributes of physical development in terms of public health and life safety.

The urban designer must not only be skilled in the design process and three-dimensional physical planning, but must also have extensive knowledge of the city's broad planning goals and implementation processes as they relate to the dynamic nature of urban growth and decay. The social, cultural needs of people as well as the physical, economic foundations of the community must be understood and considered as part of the design professional's responsibility in maintaining the quality of life in our cities.

URBAN DESIGN AND SEISMIC SAFETY

Government, private enterprise and local communities have responded or adapted in a variety of ways to the problems induced by earthquakes. Their level of preparedness and ability to address hazard reduction programs vary to considerable degrees. Some communities ignore the potential risk of earthquakes; others might be unable to apply known information to effective policy and program implementation; others might have changed city management and building practices to mitigate earthquake hazards.

Physical urban design characteristics of cities should be assessed and reviewed considering the potential danger of earthquakes. Local ordinances, internal city structure, city lifelines, activity location, infrastructure design, land utilization, urban form, building codes and typologies, construction materials and practices, real estate financing and insurance can be orchestrated to increase a community's resilience to such disastrous natural events. Urban design and planning policies for emergency and preparedness programs can minimize catastrophies; post-earthquake planning programs for reclamation, resiting, redeveloping and resettling can accelerate the recovery phase of a community and point it in the proper direction.

Significant interactions exist between urban design concerns and the vulnerability of cities to earthquakes and post-earthquake recovery. Two examples on record, among others, may be cited as follows:

Example 1:

The dependence of a major city on the continued functioning of its transportation system, freeways and highways, as a component of life line considerations came into sharp focus as a result of the 1971 San Fernando earthquake. A total of 58 State highway bridges were damaged and, of these, 7 either collapsed or were demolished according to a

report prepared by the State Division of Highways. Large sections of Interstate 5, the San Diego Golden State Freeway, were closed to traffic which had to be rerouted through local streets. Accordingly, important sections of the north-south transportation systems of the Los Angeles metropolitan area were severely crippled and removed from significant participation in post-earthquake recovery. If the situation had become further complicated by the collapse of the Van Norman dam, critical failure of the entire urban system to respond to the disaster was prognosticated.

Example 2:

Conflagration due to fire following earthquake is one of the most dreaded hazards facing our urban centers. In the 1972 Managua, Nicaragua, earthquake large areas damaged by the earthquake were later completely razed by the fire which followed. The fact that the fire remained unchecked and resulted in conflagration was due, in major part, to the fact that failures occurred in: (a) the water supply system when two major 24-inch lines were severed by ground breaks and pumping stations blocked by landslides; and (b) the inability of the Fire Department to respond to the emergency when two major fire stations, including the headquarters building, suffered major damage and most of the fire fighting equipment was trapped under the rubble. These two isolated events had drastic consequences for the entire urban fabric of Managua. Fires broke out in four or five places within a very short period after the earthquake, and within two days fires were burning in all parts of the city.

These two examples, and many others not cited indicate that the combination of two or more isolated but closely inter-related events, is the crux of the problem. Accordingly, it is an urban design problem and not solely an earthquake engineering or earthquake prediction one. It is not enough to attempt to mitigate the problem by strengthening isolated buildings or unilaterally legislating public policy, but rather it is appropriate that by working in a multidisciplinary manner, a range of urban design skills can be the integrating factor in reducing risks assumed by our metropolitan centers. Urban design requires a holistic, balanced approach to the problem through joint cooperative efforts by the design professions and local government in order to develop and implement a coordinated effort in earthquake hazards reduction programs. At the moment, many urban areas are subject to recurrent earthquake related hazards; others, in the future, will suffer even greater the brunt of these natural disasters because more people and facilities are being concentrated in vulnerable areas.

Patterns of urban location, expansion, form, structure and management must be considered against the natural phenomena related to earthquake events and classified to include ground shaking, ground displacement along fault traces, structurally poor ground, landslides, soil-structure interaction and water inundation by earthquake-generated waves or dam failures.

APPLICABILITY OF MICROZONATION TO URBAN DESIGN

Microzonation techniques represent a potentially important tool for the design professional seeking physical solutions to the earthquake hazards vulnerability of cities from an urban design focus. Microzonation maps can serve as one of the initial "check points", among others, in the general, overall configuration or redevelopment of metropolitan areas and the corresponding location of life line systems. Such maps of cities have the potential of providing essential preliminary information which the urban designer should consult prior to presenting alternative three-dimensional solutions for consideration by governing bodies in coordination with codes and ordinances. It is essential therefore that these maps be prepared from a common base by utilizing similar techniques and the same technical language in order to allow uniform interpretation on a nation-wide basis. Only in this way would it be possible to analyze alternatives as to their effectiveness, cost-benefits, political feasibility and management efficiencies.

A hypothesis which must be explored is that urban design concerns in earthquake hazards reduction programs can lead to the different location, design, configuration, planning and management of cities than currently practiced. On a long term basis, urban design practices coordinated with microzonation techniques could provide the basis for targeting redevelopment areas in metropolitan centers which are vulnerable to potentially damaging earthquakes.

Most city planning provisions and building ordinances throughout the nation normally do not take into account the possibility of surface faulting due to earthquake. In recent times, responsible design professionals and practitioners have been known to sometimes persuade clients to consider alternative sites only to have the faulty site developed by others who may have been uninformed of the hazard. Currently only the State of California has a fault-zone hazards ordinance in effect which mandates cities to take fault-line hazards into account before site development begins. In other major cities outside of California, it is entirely conceivable that major structures will continue to be constructed in fault zones. Even in California some major facilities, such as general hospitals and portions of the San Francisco Bay Area Rapid Transit System (BART), prior to enactment of the Alquist-Priolo Fault-Zoning Hazards Act of 1974, were located across known fault zones without having taken special precautions. In all probability the pressures of urban growth, economic expediency and increased population needs were responsible for such design decisions at the time. Certainly there is less chance by far that such questionable design procedures are found in sparsely settled rural areas where urban design is not a critical issue at the moment in terms of earthquake vulnerability. Accordingly, due to public risk involved, an emphasis might be placed on urban design and its potential role in earthquake hazards reduction by using microzonation techniques as a starting point.

SUMMARY AND CONCLUSION

In terms of earthquake disaster mitigation, urban design represents a new, emerging field which has been underutilized as a profession. Its role and usefulness in earthquake hazards reduction programs should be reviewed

and assessed as a potential tool in devising an integrated design approach to the problem. As a discipline, it involves a multidisciplinary, team approach to problem solving relative to the physical three-dimensional design of major urban centers. Proper utilization of urban design principles could have significant potential for application to seismic safety concerns and goals.

Microzonation techniques should enable urban designers, representing a specific sector of the design professions, to improve the manner in which they give consideration to earthquake hazards reduction measures. This activity should help both governmental and private sector agencies plan for and implement physical design principles in urban development and redevelopment efforts. An integrated, multidisciplinary urban design approach should also allow public officials an additional method of responding to earthquake hazards. Such an approach would also be of long-term use to design professionals as they design new communities and redevelop existing city centers.

In the planning of new communities and the redevelopment of existing metropolitan areas, design professionals and public officials should consider the integration of the urban design process into their planning and design activities when addressing alternatives directed to the mitigation of earthquake hazards. Because of the increased risk faced by urban areas due to population growth, design professionals must embark on a firm course of earthquake hazards reduction which makes the most effective use of every tax dollar received. Efficiencies and savings can be maximized by coordinating efforts in a balanced, multidisciplinary approach to the seismic safety of cities. Without adequate safety, very little can be said about the quality of life in those metropolitan areas which are located in zones of high seismicity.

ACKNOWLEDGEMENTS

Special acknowledgement is given to David O. Meeker, Jr., FAIA, Executive Vice-President of the American Institute of Architects in Washington, D.C., and to Gordon D. C. Tyau, AIA, Professor of Architecture of the Department of Architecture at the University of Hawaii Manoa Campus in Honolulu, who reviewed the manuscript from their own personal areas of expertise. Their comments and advice were appreciated and incorporated into the text where appropriate.

Wherein much data were available to the co-authors from many official sources and reference documents, any recommendations made or conclusions drawn in this paper are based on personal judgement and remain the responsibility of the co-authors.

SELECTED BIBLIOGRAPHY

- Algermissen, S. T., Karl V. Steinbrugge, et al; NOAA and USGS Reports:
- a) "A Study of Earthquake Losses in the San Francisco Bay Area", 1972.
 - b) "A Study of Earthquake Losses in the Los Angeles, California Area", 1973.
 - c) "A Study of Earthquake Losses in the Puget Sound, Washington Area", 1975.
 - d) "A Study of Earthquake Losses in the Salt Lake City, Utah Area", 1976.
- Botsai, E., Henry J. Lagorio, A. Goldberg, et al; "Architects and Earthquakes", AIA Research Corporation and NSF/RA-770156, 1977.
- Joint Committee on Seismic Safety, "Meeting the Earthquake Challenge", California State Seismic Safety Commission, Sacramento, California, January 1976.
- Lagorio, Henry J., "Urban Design and Seismic Safety", Invited Paper, AIA Research Corporation, Summer Seismic Safety Institute for Architecture Faculty, Stanford University, 1978.
- Minerbi, L., "Earthquake Impact on Human Settlements of the Pacific Basin", Unpublished Report, Department of Architecture and Pacific Urban Studies and Planning Program, University of Hawaii, Honolulu, 1978.
- Office of Emergency Preparedness, Executive Office of the President, "Disaster Preparedness", Washington, D.C., January 1972.
- Steinbrugge, Karl V., "Earthquake Hazard in the San Francisco Bay Area, A Continuing Problem in Public Policy", Institute of Governmental Studies, University of California, Berkeley, 1968.
- Steinbrugge, Karl V., Chairman, et al; "Earthquake Hazards Reduction: Issues for Implementation Plan" Office of Science and Technology Policy, Executive Office of the President, Washington, D. C., 1978.

EARTHQUAKE INSURANCE AND MICROZONATION

by

Karl V. Steinbrugge^I

ABSTRACT

Microzonation applications to earthquake insurance are cost limited by the size of insurance premiums. High value buildings with high premiums allow a detailed examination of site specific geotechnical information. On the other end of the economic scale, low value buildings (such as wood frame dwellings) have low rates and resulting premiums are low. It follows, then, that generalized microzonation maps have best utility for low valued buildings. Experience indicates that effective usage of generalized microzonation maps comes from maps relating soil characteristics to monetary loss patterns by class of construction material. Applying microzonation maps showing active faulting to dwellings is difficult for economic reasons while landsliding has difficult technical-economic problems.

A review of public response to earthquake insurance in geologically hazardous areas indicates that insurance penalties do not deter the house-buying or insurance-buying public.

INTRODUCTION

The possible increased use of microzonation techniques by public and private financial institutions has been of increasing interest to engineers and scientists. The most obvious point of this interest would seem to be in its application to earthquake insurance. One purpose of this paper is to examine some of the economic limitations under which user institutions operate so that researchers may better understand the application of their studies.

Additionally, some public officials have suggested using earthquake insurance as a vehicle for public policy, namely, as a method for providing the financial resources necessary for post-earthquake recovery in lieu of Federal disaster assistance in a form of grants and low cost loans. It is also frequently held by those interested in land use and earthquake hazard abatement that differentials in earthquake insurance rates based on the quality of construction (including earthquake resistive design) should encourage improvements in new construction. Microzonation is often mentioned as being one important step to strengthen incentives for improvements in locations (or land use). A second intent of this paper is to examine the validity of this public policy approach.

I Manager, Earthquake Department, Pacific Region, Insurance Services Office, San Francisco, California

Microzonation has different meanings among members of the research community and those who apply the results of their research. In this paper, the definition of microzonation is restricted to mean local maps which delineate varying degrees of each of three earthquake geologic hazards with respect to construction: (1) active fault traces, (2) potential land-slide areas, and (3) structurally poor ground areas such as marshes. Resulting damage patterns are normally determined by others, doing so on an individual building analysis basis or on a building materials class basis. Seismicity (frequency of occurrence) is considered on a different map or set of maps. The two kinds of maps (geologic hazards and seismicity) complement each other and must be used together.

Recently an examination of the overall scope of insurance and other financial problems was conducted by a committee under the Office of Science and Technology Policy, Executive Office of the President (Steinbrugge, chairman, 1978), henceforth cited as the "OSTP Issues" report. Among other findings, this study concluded that except for earthquake insurance, little is known of the possible impacts on public and private financial institutions if an earthquake were to destroy property worth 25 to 100 billion dollars. Considering the order of magnitude of potential monetary losses should earthquake insurance be mandated, it is quite appropriate to examine the roles of microzonation in controlling these losses.

ENGINEERING/SCIENCE COMPONENTS OF EARTHQUAKE INSURANCE

An understanding of the engineering and science components of earthquake insurance rating is necessary in order to perceive the role of microzonation. It must be remembered that building owners pay for the costs of engineering and science via earthquake insurance premiums, and these premiums must include costs such as those for inspection, engineering analysis, plus taxes and other costs of doing business.

Two fundamental components determine the basic rate for an individual building (or "risk" in insurance terminology). First, the building's probable monetary loss must be determined for a maximum probable earthquake using a given recurrence interval (often 300 years). Second, the seismicity of the area must be reflected in the insurance rate. The resulting basic rate may be modified by many factors, including geologic factors, hazardous roof appendages, exposure hazards from adjoining structures, unrepaired previous earthquake damage, and the like.

The first rating component (probable damage) may be based on a building classification system determined by either (1) materials of construction or by (2) the extent and adequacy of its damage control features. More often than not, economics dictate that the first of these two methods be applied to older non-earthquake resistive buildings of any value as well as modern low-value buildings. Moderate and high-value earthquake resistive buildings may warrant significant engineering attention, consistent with the economic caveat that these engineering expenses must be reasonable with respect to the premiums or justified by rate reductions based on this engineering attention. One major building classification and rating system is the "Commercial Earthquake Insurance Manual" issued

by the Insurance Services Office. Table 1 is a simplification of this manual and is applicable in San Francisco and Los Angeles to buildings insured to their full value. It will be noted that the lowest rates apply to wood frame construction which is normally associated with lowest value structures (specifically, dwellings, which will receive emphasis in a following section).

MICROZONATION APPLICATION IN INSURANCE

General Considerations:

Earthquake premiums from a high valued building (such as a high-rise) normally warrant an engineering review of construction drawings and geotechnical reports which, for modern buildings, should consider the factors included on microzonation maps. On the other end of the building value scale, geotechnical reports rarely exist on individual single-family wood frame dwellings, although they do exist for many modern housing subdivisions in California. However, their availability through the homeowner and insurance agent is usually another question. Nevertheless, microzonation maps of cities and other jurisdictions are important for the evaluation of low value structures. As a result, in the balance of this paper, emphasis is given to wood frame dwelling earthquake insurance.

From an equity standpoint, it is imperative that insurance rating methods be fair and be uniformly applied. This means that criteria for the preparation of microzonation maps must be such that all independent investigators will develop essentially the same results from the same source data. This is hardly true for the more complicated types of microzonation maps developed by some investigators. One should also bear in mind that the insurance user of these maps normally does not have a professional background; alternatively, others must be able to adapt these maps for use by non-professionals on some consistent and economical basis.

Structurally Poor Ground:

Insurance oriented microzonation maps of metropolitan areas in California and a few areas elsewhere have existed for many years. This kind of map, which is associated with intensified damage for a variety of reasons, exists where property values are high and substantial amounts of earthquake insurance are written. One basis for these maps is discussed by Steinbrugge (1969) and in the companion papers. The further application of various kinds of insurance microzonation maps showing structurally poor ground awaits the development and general acceptance of consistent mapping criteria.

Additionally, it may be some time before certain special microzonation problems have generally accepted solutions. Significant special problem areas have been identified in Santa Rosa, California from damage patterns observed after the 1906 and 1969 earthquakes, in Caracas after the 1967 earthquake, and in San Fernando after the 1971 earthquake. While some explanations have been published, there appear to be no generally accepted mapping criteria to identify and map similar areas elsewhere.

TABLE 1

SIMPLIFIED EARTHQUAKE BUILDING CLASSIFICATIONS AND RATES
 SAN FRANCISCO AND LOS ANGELES
 (After Insurance Services Office)

Building Class	Summary Description	Story Height Limit	Major Special Conditions	Building Rate Cents/\$100	Deductible (in %)	Evaluation Required by Professional Engineer
11 (1)	Wood frame -- habitational	2	-	12.9	** 5	
11 (2)	Wood frame -- small	3	Non-dwellings up to 3,000 sq. ft.	21.4	** 5	
12	Wood frame -- other	-	-	21.4	** 5	
21	All-metal -- small	1	Up to 20,000 sq. ft. area	12.9	5	
22	All-metal -- large	-	-	21.4	5	
31	Steel frame -- superior	-	Superior earthquake resistive	21.4	5	Yes
32	Steel frame -- ordinary	-	Monolithic concrete floors	30.0	5	Yes
33	Steel frame -- intermediate	-	Intermediate earthquake resistive	25.7	5	Yes
34	Steel frame -- other	-	Wood, metal, precast concrete floors	42.8	5	
41	Reinf. concrete -- superior	-	Superior earthquake resistive	25.7	5	Yes
42	Reinf. concrete -- ordinary	-	Monolithic concrete floors	42.8	5	
43	Reinf. concrete -- intermediate	-	Intermediate earthquake resistive	34.2	5	Yes
44	Reinf. concrete -- precast	-	Structural precast concrete	42.8	10	
45	Reinf. concrete -- other	-	Wood, metal floors; mixed concrete & steel frame	42.8	10	
52	Mixed constr. -- superior	1	Superior earthquake resistive	34.2	5	Yes
53	Mixed constr.	1	Ordinary earthquake resistive	42.8	10	*Yes
54	Mixed constr. -- intermediate	-	Intermediate earthquake resistive	51.3	10	*Yes
55	Mixed constr.	-	***Ordinary non-earthquake resistive	90.0	10	
56	Mixed constr.	-	Hollow masonry, adobe	135.0	10	
61 thru 65	Special earthquake resistive	-	Special design for damage control	12.9 to 30.0	5	Yes

*Unless exempted (in certain specified jurisdictions).

**Masonry veneered structures may take variable penalty.

***Excluding hollow tile, hollow masonry, adobe, and cavity walls when used as part of a structural system.

Geologically Active Faults:

In California, microzonation maps show certain active faults within well-defined "special studies zones." These maps, required by California's Alquist-Priolo Act, are prepared by the California Division of Mines and Geology and are available to the public.

Despite the substantial amounts of public attention given to faults, the amount of potential destruction to buildings from surface faulting is comparatively small. As shown in Table 2, Algermissen (1972) determined the number of wood frame dwellings in the metropolitan San Francisco area subjected to possible damage from vibration and from surface faulting in the event of a recurrence of the 1906 earthquake on the San Andreas fault and also from a magnitude 7.0 earthquake on the Hayward fault.

TABLE 2

DWELLINGS SUBJECTED TO VIBRATION AND TO FAULTING
SAN FRANCISCO BAY AREA

	<u>*Dwellings at Risk</u>	<u>**Dwellings on or Near Fault Trace</u>
San Andreas Fault:		
Recurrence of 1906	1,203,121	237
Hayward Fault:		
M = 7.0	1,203,121	1,138

*Limited to a study area consisting of the 10 San Francisco Bay Area Counties.

**Dwellings within 50 meters of the fault. Hayward fault figure proportionally adjusted from 300 meter zone to 50 meter zone.

Table 2 shows that the probability of a dwelling being in the 50 meter fault zone was about 1:1000 along the Hayward fault and about 1:5000 along the San Andreas fault. However, based on experience from previous strike-slip fault movements, the damage probabilities would appear to be even more remote than the ratios suggest.

As a result, most insurance companies do not find it economically feasible to locate dwellings to be insured with respect to active faults, and fault proximity is not a component of the rate making process. Therefore, the excellent Alquist-Priolo maps have negligible insurance impact on low value structures. The opposite, of course, is true for large value risks such as major hospitals or high value electronic plants where underwriting practices can determine and use the facts.

Landsliding (Earthquake Induced):

Landslide microzonation maps have been difficult to interpret and apply on an equitable and consistent basis by non-professional personnel. Consider, for example, a map showing existing landslides in an area before development begins. Is one to assume that all new construction will include provisions which will correct existing landslide conditions according to best practice as required by law (building code)? If not, then how can an insurance rate be made without evaluating a soil report, and how can this be economically done? Does an old landslide now represent a stable condition, or is it a most likely candidate for further movement? Or will the next movement take place at a location between two recent landslides? What about hillside construction which is 10, 20, or 30 years old?

It would seem that substantial amounts of study are needed, including clarification of criteria, before landslide hazard maps will have their rightful place in microzonation use by financial institutions.

EARTHQUAKE INSURANCE IN CALIFORNIA

Earthquake insurance has been marketed by American insurance companies since at least 1916. However, it has never been widely purchased, being an estimated 7% of dwellings carrying fire insurance in metropolitan San Francisco and Los Angeles. In spite of the availability of the coverage, aggregate premiums in California in 1977 were only \$19,759,536 for all coverages identifiable as earthquake on all classifications of property including habitational.

For example, insurance rates for single-family, wood frame homes in coastal California (San Francisco, Los Angeles, San Diego, etc.) average \$2.00 per \$1,000 insurance, with a 5 percent deductible. However, probably less than 5 percent of California homeowners currently have earthquake coverage. Promotional campaigns by companies after the 1971 San Fernando earthquake had not noticeable effect. Residents in other earthquake-prone areas of the United States have shown even less interest. The 5 percent deductible is often blamed as a deterrent to the purchase of dwelling earthquake insurance; however, many who do so are not familiar with catastrophe insurance and the relation between deductibles and rates. On the other hand, Kunreuther, et al (1978) concluded: "It seems likely that, unless the hazard appears probable, it will not be viewed as a problem and the individual will not consider protective measures such as insurance" (p. 243).

On the other hand, the size of the potential dwelling losses are very large. For example, Rinehart, et al (1976) showed potential losses to wood frame dwellings from "a maximum credible earthquake" to be:

1. San Andreas fault - San Francisco Bay Area: \$2.2 billion.
2. Newport-Inglewood fault - Los Angeles Basin: \$4.0 billion.

At 1978 prices, these would amount to 4.1 and 7.5 billion dollars, respectively.

ECONOMIC CONSIDERATIONS

Homeowner Viewpoint:

Apart from psychological reasons (Kunreuther, 1978), economic considerations should influence an individual's decision on purchasing earthquake insurance. A uniform 25% rate penalty for structurally poor ground is applied to all non-dwelling properties in mapped areas; let us examine its comparative economic impact if it is also applied to dwellings.

Table 3 may give an insight into this viewpoint. Loan data in this table are based on information furnished by major mortgage organizations and these data apply to single-family wood frame dwellings in the San Francisco Bay Area. A 25% rate penalty for structurally poor ground has been separately listed and brings the total earthquake premium to \$12.50 monthly. Fire insurance premiums and property taxes have not been included. While the mortgage in the example is \$60,000, the sale price of the land and improvements would be \$75,000 (with a 20% down payment). Experience has shown that a home buyer or developer is not greatly swayed by a \$10 monthly increase in payments. (The change of 0.25% in the mortgage interest rate from 1976 to 1977 was of a greater dollar amount than the earthquake insurance premium. Housing sales were not significantly affected by this change in interest rates.) Undoubtedly, a \$2.50 further increase based on adverse microzonation information would have even lesser effect.

TABLE 3

COMPARISON OF
MORTGAGE AND EARTHQUAKE INSURANCE PAYMENTS
SAN FRANCISCO BAY AREA

	Year		
	1976	1977	1978
<u>Mortgage:</u>			
30 year, \$60,000 mortgage, 20% down payment*			
Mortgage interest rate	8 3/4%	9%	10%
Monthly payment (interest plus principal)	\$472.03	\$482.78	\$526.55
<u>Earthquake Insurance:</u>			
Monthly "Homeowners Policy" earthquake premium**	\$ 10.00	\$ 10.00	\$ 10.00
Increased monthly earthquake premium for structurally poor ground	\$ 2.50	\$ 2.50	\$ 2.50

*Land at 30% of land plus improvement (Bay Area average in 1978)

**Based on amount of mortgage at its inception. 5% deductible applies. Rate is \$2.00 per \$1,000.

One recent private study conducted by the author on the geographic distribution of almost one billion dollars in earthquake dwelling insurance showed:

<u>Area</u>	<u>Homeowner Earthquake Policies to Total Homeowner Policies</u>
San Francisco Bay Area	7:100
Waterfront housing in San Mateo County	21 to 32:100

It appears that homeowners may be aware of their geologic hazards on the San Mateo waterfront and be willing to pay for added insurance in their highly publicized hazard area. But they are not discouraged from living there. Quadrupling this geologic hazard penalty to \$10 per month probably would not discourage a sailing enthusiast from wanting to anchor his boat at his backyard.

What if "in the interest of improved construction and land-use practices," the rate penalties were increased solely on the basis of public policy? There currently is a general public feeling that "insurance rates are too high," although the Federal Insurance Administrator's Office once declared that dwelling earthquake insurance rates were fair and equitable. Whether the public's view is correct or not, it is hardly likely that state insurance regulators would press for a major rate increase in order to improve land-use and construction practices.

One may conclude from the foregoing that economic incentives through present rate penalties are not an effective means to influence most homeowners or builders.

Our findings can be contrasted with the situation in the National Flood Insurance Program where there is a much greater rate variation reflecting risk. For instance, the rate for a one-to-four family no-basement residential structure in any zone is one cent when the first floor is five feet above the base flood elevation. The rate for the same structure if it were located in flood zone A15 to A17 with its first floor eight feet below the elevation of the base flood would be \$2.67. The resulting premium range for the example in Table 3 would be \$6.00 to \$1,602.00. It should be added that the flood insurance program is under Federal Government operation.

This is not the case for dwelling earthquake insurance, and improved construction and land use must rely principally on local regulations. Such local regulation, however, presents the opportunity for effective utilization of microzonation techniques and maps.

Insurance Company Viewpoint:

An insurance company must pragmatically examine the cost of a microzonation program in the processing of dwelling policies which include earthquake coverage against the available additional premiums generated by the program. If a microzonation program were introduced into a company's procedure, it would be necessary to apply it nationwide to all dwelling property on which earthquake is written to avoid the charge of unfair discrimination.

Experience data do not exist on premium income vs. costs for microzonation, but a hypothetical case will give indicative answers. It is reasonable to estimate that perhaps 1 in 50 dwellings in California are in areas for which a 25% rate surcharge could be made for insurance microzoned structurally poor ground. Further, assume a statewide average value for insured dwellings at \$50,000. The annual premium increase for the 25% rate penalty on a \$2.00/\$1,000.00 homeowners/dwelling policy would be \$25.00. Since every policy would have to be reviewed to see if the rate penalty should be applied, then the \$25.00 premium must be spread over 50 policies, or \$0.50 for each policy.

In company operations, premiums for homeowner policies are allocated on percentages such as the following:

Losses and adjustment expense	65.2%
Production and outside costs	18.5%
Internal expense and inspection costs	10.1%
Federal and state taxes	2.9%
Profit and contingency reserves	<u>3.3%</u>
	100.0%

After "Bests Aggregates and Averages, Property-Casualty, 1977," stock companies, p. 113.

On this basis, 10.1% of the surcharge premium of \$25.00, or \$2.53, would be available to pay the cost of the microzonation program for 50 policies, or 5 cents per policy. This 5 cents can be multiplied by the number of years that the policy may be renewed without re-examination -- possibly ten years. Business judgment has indicated that the final result is not economically feasible.

One may conclude that present rate penalties are not economically feasible under today's marketing conditions. The situation in the event of mandated dwelling insurance, of course, would require a more thorough economic examination.

SUMMARY AND CONCLUSION

Microzonation applications to earthquake insurance are cost limited by the size of insurance premiums. High value buildings with high premiums allow a detailed examination of site specific geotechnical information of buildings constructed in the last several decades.

On the other end of the economic scale, low valued buildings (such as wood frame dwellings) have low rates (Table 3) and resulting premiums are quite low. Further, geotechnical information is rarely economically available for site specific insurance evaluations. It follows, then, that generalized microzonation maps have theoretically best utility for low valued buildings. Experience indicates that most effective usage comes from maps relating soil characteristics to monetary loss patterns by class of construction material. Applying microzonation maps of active faulting to dwellings is difficult for economic reasons while landsliding has difficult technical-economic problems. There are clear needs to improve microzonation techniques to suit insurance and other financial problems.

Improved construction and land-use practices using earthquake insurance for this means have been suggested by public officials to suit various public policy viewpoints. A brief examination of homeowner cost shows that relevant insurance rate differentials have little potential for economic "clout" on individual homeowners. This would also apply to the development of housing tracts, because the developer passes insurance costs to the buyer who, in many cases, is not aware of them.

Microzonation maps are useful to the various branches of the financial sector, but the potential of these maps has not yet been achieved for various reasons. With respect to earthquake insurance, its use has been limited by the state-of-the-art of microzonation. In this regard, the best potential lies in the development of better criteria for relating ground vibration characteristics to building class, particularly for low value structures.

Mandation of dwelling insurance requires legislation as well as changes in public policies and public attitudes. In the event of mandation, microzonation maps will perform a useful economic role due to the large inventory of dwellings, but would not likely improve hazard mitigation practices nor educate the public adequately. Microzonation maps in hazard mitigation will probably have much greater impact as a part of the building construction regulatory process, that is, in building codes, land-use zoning, and urban redevelopment policies.

ACKNOWLEDGMENTS

Information and advice were kindly furnished by many persons. Mr. Robert L. Odman (State Farm Fire and Casualty), Mr. Charles R. Ford (Fireman's Fund Insurance Companies), and Mr. David R. Simmons (Insurance Information Institute) provided specific insurance data and background therefor. Professor of Architecture Henry J. Lagorio and Dr. S. T. Algermissen (U.S.G.S.) critically examined the manuscript from the viewpoint of their disciplines. Finally, and certainly not least, Dr. Theodore Levin of the Federal Insurance Administrator's Office provided flood insurance information. We are grateful to all of these persons.

While the assistance and resources of insurance organizations and governmental agencies were available to the author, all opinions and conclusions are the sole responsibility of the author.

SELECTED BIBLIOGRAPHY

- Algermissen, S. T., W. A. Rinehart, and J. C. Stepp. "A Technique for Seismic Zoning: Economic Considerations", Vol. II, pp. 943/956 in Proceedings of the International Conference on Microzonation, Seattle, 1972.
- Insurance Services Office. "Commercial Earthquake Insurance Manual". New York, New York, 1976.
- Kunreuther, Howard, et al. "Disaster Insurance Protection: Public Policy Lessons". New York: John Wiley & Sons, 1978.
- Rinehart, W., S. T. Algermissen, and Mary Gibbons. "Estimation of Earthquake Losses to Single Family Dwellings". USGS Open File Report 76-156 (1976).
- Steinbrugge, Karl V. "Seismic Risk to Buildings and Structures on Filled Land in San Francisco Bay", pp. 103/115, in Geologic and Engineering Aspects of San Francisco Bay Fill, California Division of Mines and Geology, Special Report 97, 1969.
- Steinbrugge, Karl V., Chairman. "Earthquake Hazards Reduction: Issues for an Implementation Plan", Office of Science and Technology Policy, Executive Office of the President, Washington, D. C. 1978.

214

INTENTIONALLY BLANK.

GOVERNMENT RESPONSIBILITY IN MICROZONATION

by

Norton S. Remmer, P.E.^I

ABSTRACT

On June 22, 1978, the President of the United States presented to the Congress a report entitled "A National Earthquake Hazards Reduction Program." The program identifies the guidelines, priorities and responsibilities for the Federal, State and local governments, and private responsibilities. The significance of the program at this time is that it provides the context and the basis for determining government responsibility at all levels. It also reviews technical capabilities and projects future capabilities which will provide essential elements in any government plan of action. The importance of regional, local and site seismic hazard characteristics is emphasized in relation to government land use control programs and specific site evaluation responsibilities.

The programs of California and Massachusetts for earthquake hazard reduction provide interesting examples of the present status of state and local government, at opposite ends of the earthquake hazard spectrum, and their relation to the Federally promulgated program. Finally, the potential of linking land use control and prediction capability for existing buildings presents the possibility for state and local governments, especially, to fulfill their responsibility for existing buildings in a realistic way.

INTRODUCTION

The subject of the "State of Art" relative to government responsibility in microzonation is addressed in this paper in a relatively narrow scope. The scope is restricted as far as possible to what can be described as documented aspects of acts or policies which involve microzonation or concepts of microzonation and involve government at various levels. The paper is not an attempt to analyze or imply the obligations of government responsibility or how one assesses that responsibility. There are several good reasons for this approach at this time. And the phrase "This time" is intended to imply a significant period in defining the state of the art in government responsibility based on the recent delivery of the report entitled "The National Earthquake Hazards Reduction Program" delivered by the President to the Congress of the United States. The importance of this program will be reviewed in the next section of this paper.

With the availability of this program report, this paper and this conference is a good time to review the status of all levels of government programs which involve aspects of microzonation and to consider the Federal role, the State and local role, and the implications for the future.

I Commissioner, Department of Code Inspection, Worcester, Massachusetts
Formerly Technical Director, Massachusetts State Building Code Commission

In some cases, such as California, the implications of risk and hazard due to earthquakes are relatively obvious and the necessity for creating programs to deal with the risk and hazard have become a recognized and significant part of the government's responsibility. Programs have been developed and are being developed, laws passed and systems of controls created, to deal effectively with what is generally agreed is a significant hazard and a high risk in many areas of that state.

In other cases, such as Massachusetts, the hazard exists but is somewhat marginal and the risk is of significance but does not demand the same government concerns as the hazard and risk in California.

And of course, in many other places in the United States where both the hazard and risk exist at a level which appears to require some government responsibility, there is virtually no program evident. While no program may be evident, this does not necessarily imply that there has not been a definitive decision made by government to ignore any or all hazards and risks.

It may be simply that based on either state or local concerns isolated from any Federal influence, the decision has been made that the cost or necessity of such a program is not justified.

It appears reasonable to say that all government decisions relative to hazard and risk due to earthquakes rely on the existence or absence of information on microzonation and the assessment of the importance of acting on that information or acquiring the necessary detailed information. Government responsibility can incorporate very stringent requirements in very small specific locales, such as neighborhoods, streets, building sites, etc., where there is a significant hazard. This is common in California and the number of options and the character of government responsibility reflects a concern for microzoning areas down to the smallest practical scale of use and control.

In Massachusetts after considerable deliberation of the characteristics of relatively small zones, such as the Boston Back Bay and different regions of the state, the characteristics of microzoning were based on a single risk zone for the state with design force equation modifications based on soil conditions for local area or site considerations.

Many of the options available for identifying responsibility, evaluating risk and benefit to the community and establishing land use control programs, before and after earthquakes, and developing and using modern seismic building codes to reflect the earthquake hazard have been reported elsewhere in great detail. The potentials for reducing hazard and the means have been explored as a preliminary to the current report to Congress in the "Newmark" report, using extensive experience and documentation, and most recently in the report entitled "Earthquake Hazards Reduction: Issues for an Implementation Plan." In addition, the future potentials for earthquake prediction and the correlations with microzoning capabilities have been explored in detail in the publication "Earthquake Predictions and Public Policy" by the National Academy of Sciences.

The intent of this paper is not to review these concepts but to consider where government responsibility lies in respect to the mandates created by the report to the Congress. To do this the rest of the paper will deal with the following:

1. Review the report and its significance relative to government responsibility at all levels concerning microzonation.
2. Review briefly the state of the art of government responsibility in two extreme and informative cases:
 - a.) California
 - b.) Massachusetts
 with respect to the mandates and implications of the report to Congress.
3. Consider the significance of the Federal program with respect to existing buildings, earthquake predictions, and future research.

THE NATIONAL EARTHQUAKE HAZARD REDUCTION PROGRAM

On June 22, 1978, the President transmitted to the Congress of the United States a plan for a National Earthquake Hazards Reduction Program. The program presented by the President is intended to provide the means for implementing the Earthquake Hazards Reduction Act of 1977 (Public Law 95-124). In the message to the Congress, the President stated that the National Earthquake Hazards Reduction Program "deals with, predicting and preparing for earthquakes: ways in which government, industry, and the public can apply knowledge of seismic risk when making land-use decisions; and achieving earthquake-resistant design and construction."

Within the context of the program presented by the President is clearly defined the Federal government's policy for the means of implementing earthquake hazard reductions. Further than this, the details of the program spell out the federal government's perceptions of its own responsibilities in such a program, and the correlated responsibilities of other levels of governments and the private sector.

Unquestionably, within the text of the program document, the statements of government responsibility relative to microzonation at the federal level constitutes a clear statement of the "State of the Art", and the elements which pertain to other levels of government imply some of the directions of government responsibility which will guide local governments in their decisions relative to earthquake hazard reduction.

It is important to review the program to extract the implications for microzonation. There are several reasons why the document is important for understanding the current "State of the Art" for government responsibility. One obvious reason is that it tells with some precision what the Federal government expects to do and what it expects other levels of government to do, or, alternatively, to consider, whether they do something or not.

Another reason is that the program says what federal government responsibility is not, and therefore shifts certain burdens of responsibility to lower levels of government.

Another reason is that overall, the program now establishes a uniform context for government responsibility at all levels and for those things which, by implication, have been reviewed by experts and have been determined to be considerations to demand attention, or at least a proper degree of address, and a reasoned disregard.

And finally, the program establishes a measuring stick by which existing earthquake hazard reduction programs at federal, state and local levels can be reviewed and evaluated and perhaps modified.

1. General Aspects

- Partnership: The federal government places the principal responsibility and the essential burden of action on state and local governments for all aspects of the program.
- Implementation: There is an implied responsibility at the federal level to ensure that local governments recognize a responsibility to use existing and developing knowledge about regional and local variations of seismic risk in making their land use decisions.

2. Guiding Principals

- The Federal government's responsibility is to provide a strong exemplary position with regard to its own facilities and to develop guidelines and standards for Federally-assisted or licensed critical facilities. Improvements in local land use and building codes to accomplish earthquake hazard reduction is to be accomplished by persuasion and encouragement.
- "The priorities of hazards reduction are to be based on relative risk; that is, the probability of significant loss of life and property, considering the population exposed, the nature and magnitude of the hazards posed by manmade structures to the population, and the likelihood and character of significant earthquakes. Regional differences in the nature and magnitude of the risk and of perception of the risk require a flexible approach."
- "Earthquake hazards reduction must not only take into account the direct natural hazards from faulting and vibration, but also the indirect natural hazards from tsunamis, seiches, landslides, floods, soil consolidation, soil failure and slumping....."
- "To be acceptable in regions characterized by lower, but significant, seismic risk, earthquake hazards mitigation activities should lead to the reduction of risks from hazards other than earthquakes and be coordinated with efforts to protect people and property from other potential hazards and disasters."

Some of the priorities for immediate action which are of interest are as follows:

- "The determination of the interest of States for the development of State and local strategies and capabilities for earthquake hazards reduction."
- "The development of seismic resistant design and construction standards for application in Federal construction and encouragement for the adoption of improved seismic provisions in state and local building codes."

- "The estimation of the hazard posed to life by possible damage to existing Federal facilities of this type will rest with the Director of the U.S. Geological Survey." "The Director will be assisted in this task by the National Earthquake Evaluation Council, a Council to be composed of scientists from inside and outside government." "The responsibility for warning the people about the imminent danger from a natural hazard and to advise or direct them on how to respond is principally a function of State and local government."

The Federal government has also assumed the responsibility for assessing the "frequency and characteristics of earthquakes in the United States." The maps envisioned, however, "are not intended for local zoning or the evaluation of specific sites but for showing the broad variation of seismic risk throughout the Nation."

The program calls for the continuing work of the Geological Survey in "identifying and evaluating earthquake hazards, such as active faults and ground conditions that affect the distribution of damage." The program includes the evaluation and regional delineation of earthquake hazards, particularly in regions of highest risk." However, it is emphasized that the work encompassed by this task is probably not adequately detailed to be used in making decisions about local conditions and land use. The responsibility is clearly directed to the discretion of local or state authorities, although there is implied that discretion for some facilities may be tempered by Federal or State influences.

The Federal government identifies clearly its responsibility for earthquake hazard reduction in developing and managing its own land and construction projects and the need to provide an example for other levels of government and the private sector.

In addressing facilities such as dams, hydraulic structures, nuclear reactors, liquid natural gas plants and storage facilities for explosive and hazardous materials and lifelines the Federal mandate for responsibility is not clearly outlined although it implies increased participation by State governments. There is, however, one example given of legislation which encourages "early identification of geological conditions at prospective power plant sites and the banking of sites for future use." It is clear, although understated, that there is a compelling responsibility at all levels of government to link the geologic and seismologic characteristics of the immediate site with planned or existing "critical" use in evaluating either suitability or existing threat. For the normal facilities associated with public services and responsibilities such as hospitals, fire and police stations, communications and administration centers the program implies that the means of establishing state or local government responsibility, based presumably on the local hazard, is through the control of any funds provided for such facilities by the Federal government.

In the final section of the program a definitive listing of responsibilities is provided for the Federal government, State and local governments. The Federal role has already been identified to a great extent previously. It is to set an example in the use of its own lands and buildings and in new construction; to provide the latest information available to local governments on regional hazard assessment and seismic codes; to work with

professional groups and model code groups in order to create vehicles for adoption locally of national standards; and to provide assistance as appropriate and as required in the development of state and local strategies and implementation plans.

The program provides a undefinable sense of moral obligation for the State and local governments to do something that will meet certain standards, the determination of which most appropriately lies with the local government or State. "State and local governments bear responsibilities for preparedness, response, warning, regulating construction, and regulating the use of land. The National Earthquake Hazards Reduction Program must, to be successful, include development of state and local strategies for defining and meeting their responsibilities in earthquake hazards mitigation."

"The most severely threatened states need to analyze their own problems and find their own solutions. This process should include the modification of decision making processes to include considerations of earthquake hazards where appropriate."

One of the possible solutions for mitigating earthquake hazards is proposed as "the acquisition of lands or facilities in seismic hazard zones, identification and mapping of local hazard zones for land use planning, and retrofitting, razing or relocation of structures."

The program goes on to say, "the opportunity exists for state and local governments to mandate, through legislation, including the adoption of building codes and zoning ordinances, earthquake hazards reduction actions on private property." "In the rapidly urbanizing areas of the country susceptible to earthquakes, regulation of land use through building codes or local zoning is the most effective way to avoid some earthquake hazards."

The conclusions which can be drawn are as follows: state and local government has two basic responsibilities:

- a.) To establish programs of earthquake hazard mitigation which mesh with the programs, policies and impetus of the Federal government and
- b.) With the help, encouragement and persuasion of the Federal government to define their own perceptions of risk and based on their evaluation of the hazard to establish programs of mitigation.

Implicit in the programs at all levels is the fundamental need to assess risk at ageographic level which is inversely proportional to the apparent hazard and to relate solutions to site and regional geological and seismological characteristics. Land Use control emerges as a significant fundamental tool.

In the next section two ongoing programs of earthquake hazard mitigation are reviewed in relation to the Federal program - the programs in the States of California and Massachusetts. These two states represent two limits of the spectrum of considerations for State and local government responsibility and the character of microzonation implicit in responsibility at the two extremes of seismic hazard.

CALIFORNIA

The history of developments in California relative to earthquake hazard mitigation generally represent the most comprehensive and current programs of government responsibility at any given period of time in the United States. Both the need for such programs and the reasons for the implementation are subjects which don't require detailed explanation here. It is interesting, however, to note briefly the features of earthquake hazard mitigation developments in California in chronological sequence:

- 1906 San Francisco - After the earthquake - rebuilt under a code providing 30 pounds per square foot loading for both wind and earthquake resistance.
- 1927 Uniform Building Code
Included provision for lateral earthquake forces proportional to masses.
- 1928 California State Chamber of Commerce
Recognized need for building code "dedicated to the safeguarding of buildings against earthquake disaster."
Initiated studies by leading structural engineers of the State which formed the basis for the codes which followed.
- March 1933 Long Beach earthquake destroyed many public school buildings.
- 1933 State Legislation adopted "Field Act" controlling design and construction of public school buildings.
- 1933 Riley Act adopted requiring all buildings except dwellings and farm buildings to be designed to resist a specified lateral force.
- 1933 Los Angeles building ordinance required a lateral force equal to 8% of the dead load plus half the live load.
- 1935 Uniform Building Code adopted provisions similar to Los Angeles.
- 1943 Los Angeles incorporated a coefficient recognizing the influence of flexibility in the design of structures.
- 1947 San Francisco adopted a table of varying coefficients applied to vertical design loads for buildings of different heights with variations for soil conditions.
- 1971 San Fernando Earthquake
- 1971 Seismic Safety Element - As a part of legislation requiring all cities and counties to adopt a general plan as included in the following:
"A seismic safety element consisting of an identification and appraisal of seismic hazards such as susceptibility to surface ruptures from faulting, to ground shaking, to ground failures, or to effects of seismically induced waves such as tsunamies and seiches."

1971 Public School Siting Bill

1973 Hospital Safety - Required that hospitals remain "completely functional" during and after an earthquake.

Since 1971 California has passed additional legislation including bills for the control of construction near active faults, and a strong motion instrumentation program.

The gradual increase of control over more specific items and sites is apparent in this historical perspective. Looking at areas like San Francisco in detail would show an even greater attention to the recent increased development of specific land use controls and the linkage of site characteristics to specific development policies. In fact within the state there are many instances of examples of effective land use controls and these have been reported extensively in the literature.

There appears to be little doubt that California is actively addressing its earthquake hazard problem and in most efforts fulfilling the objectives of the Federal program.

It is of interest, however, to note the period of time required to put into places so many of the objectives, even recognizing what appears to be a hazard time scale closely equivalent to the time scale of government action.

MASSACHUSETTS

Perhaps the time to begin with Massachusetts is in 1969 when the U.S. Geological Survey permitted the publication of a revised seismic risk map of the United States prepared by S.T. Algermissen. The Algermissen map placed Boston and the Northshore immediately north of Boston in zone 3, and most of the rest of the state in zone 2. Based on this event there evolved the apparent possibility that buildings in Boston might be required to meet the same design requirements as Los Angeles and San Francisco. Until that time it is safe to say that Massachusetts had no seismic requirements.

In July, 1970 the City of Boston issued a new building code which adopted zone 2 and referenced the 1967 edition of the Uniform Building Code, Volume 1, Section 2314, "Earthquake Regulations" which basically required only the capability to withstand lateral forces while remaining vague about required ductility. This represented the first introduction of seismic requirements in the Boston Code.

In 1972 legislation was passed in Massachusetts establishing a State Building Code Commission and the provision for promulgation on January 1, 1975 of a uniform mandatory state code. In 1973 a Seismic Committee was formed to advise the State Building Code Commission. On January 1, 1975 the Seismic provisions were published with the new state code, incorporating a zone approximately equal to the Uniform Building Code zone 1.5 and incorporating a site soil factor and requirements for evaluation of liquefaction potential under various specified site conditions. At the present time the code is being revised and the question of dividing the state into more than one zone has been considered.

At this point it is worthwhile analyzing the development of certain aspects of the seismic provisions in more detail in order to consider some of the aspects of government responsibility contained in the Federal program as reflected in the decisions in Massachusetts.

As the fundamental basis of the decision - making process the two criteria of reasonable life-safety and economics were established. Life-safety reflected the characteristics of hazard and risk especially of the Boston area, and economics was the economics of developing construction, not the economics of disaster and disaster recovery. The balance sought was a realistic level of public safety recognizing a return period of 10,000 years for the design basis earthquake, and the desire not to create an unwarranted cost burden for construction. A single zone was chosen for the state in the interest of maintaining simplicity.

Subsequent review of the zonation of the state in early 1978 established that there is "ample reason to argue for a reduction in seismic requirements" for the western part of the state.

It was decided, however, to leave the state as one seismic zone for two fundamental reasons:

1. Uniformity of enforcement
2. The error inherent in setting an east-west boundary for two zones in the state is so great that it is not meaningful.

It appears that the efforts to date in Massachusetts meets both the intent and the spirit of the Federal program. There is, of course the question of whether the actions taken, and they appear now to be relatively limited in scope, adequately fulfills the concept of responsibility established for state and local government given the state's own perception of its hazard and risk.

It is clear that California has need of assuming more responsibility and has a far more comprehensive program of land-use control which reflects many more of the objectives of the Federal program. Massachusetts is perceived by those making decisions as being at the other end of the seismic spectrum, despite the publication of the survey map in 1969 which raised the question of assessment of hazard. With some relatively minor modifications to the structural provisions in the next issue of the building code Massachusetts appears to be satisfied that it has assumed virtually all the responsibility required for its efforts, including land use control.

EXISTING BUILDINGS, PREDICTIONS AND THE FUTURE

Existing buildings pose the greatest threat. As outlined in the Federal program, the cost of upgrading existing buildings to an acceptable level for seismic safety, especially in California, is beyond the scope of practical reality. Ignoring the threat of existing buildings, as has been done until now, is a risk assumed by the Federal, State and local governments.

Responsibility for action on the part of government must represent the "state of the art" in terms of practical reality.

The Federal program looks forward to the potential of earthquake prediction as a major mitigating factor for existing buildings. It appears that, depending on the risk perceived by the government responsible, there are several potential approaches for existing buildings. The Federal program speaks of the development of a strategy and methodology, in conjunction with several Federal agencies and the California Seismic Safety Commission, to identify Federal buildings which present "unacceptable" risks. The possible strategies shown for mitigating hazards impose overwhelming financial burdens which it may not be possible for any state, including California, to reasonably assume.

However, it appears that it may be reasonable to assume that state and local governments should, at some level of hazard, possibly equal to that perceived in Boston, and certainly as perceived in California, assess critical facilities and high occupancy buildings based on their particular site characteristics and their effective design capacity.

In some cases the acquisition of the knowledge of these two parameters implies a responsibility to make a decision on the risk. In other cases, such as Boston, the question of what is responsible action, especially in view of the lack of guidelines in the Federal program is still open to question. If Boston takes action and, say, Memphis does not, is Boston being excessively responsible or is Memphis ignoring their responsibilities?

Perhaps the most realistic responsible approach for existing buildings in many seismic areas depends on the coupling of four factors; the use of the building, the site characteristics, the design capacity of the building and the threat implied at the specific site based on the prediction. While prediction may be a long time from becoming a practical tool, state and local governments who project return periods of the order of thousands of years for earthquakes which represent significant hazards may be acting most responsibly, within the full context of all their scope of responsibilities, by waiting until prediction becomes a functional tool.

BIBLIOGRAPHY

1. "The National Earthquake Hazards Reduction Program", Executive Office of the President, Office of Science and Technology Policy, Washington, D.C. 20500, June 22, 1978.
2. Message to the Congress of the United States, President Carter, June 22, 1978.
3. Fact Sheet on the National Earthquake Hazards Reduction Program, Executive Office of the President, Office of Science of Technology Policy, June 22, 1978.
4. Steinbrugge, Karl V. et al., "Earthquake Hazards Reduction: Issues for an Implementation Plan", Working Group on Earthquake Hazards Reduction, Office of Science and Technology Policy, Executive Office of the President, 1978.
5. Proceedings of the International Conference on Microzonation for Safer Construction, Research and Application, Seattle, Washington, U.S.A., 1972 (Sponsored in part by the University of Washington, and the National Science Foundation). Volumes I and II.
6. "Earthquake Prediction and Public Policy", National Academy of Sciences, Washington, D.C., 1975.
7. Reed, Richard E., Editor, "Living with Seismic Risk, Strategies for Urban Conservation", The American Association for the Advancement of Science, Washington, D.C. 20036, 1977.
8. Olson, Robert A., and Wallace, Mildred, Editors, "Geologic Hazards and Public Problems", Conference Proceedings, Office of Emergency Preparedness, Region Seven, Federal Regional Center, Santa Rosa, California, 95403.
9. Newmark, Nathan et al., "Earthquake Prediction and Hazard Mitigation Options for USGS and NSF Programs", National Science Foundation, September, 1976.
10. Krimgold, Frederick, "Seismic Design Decisions for the Commonwealth of Massachusetts State Building Code", MIT Department of Civil Engineering, June 1977.
11. Remmer, Norton S., "Government Responsibility", AIA Research Corporation, Summer Seismic Institute, University of Illinois, June, 1978.
12. Massachusetts State Seismic Advisory Committee, Minutes of Public Meetings, 1978. Massachusetts State Building Code Commission, Boston, Massachusetts.

226

INTENTIONALLY BLANK

Preceding page blank

227

MICROZONATION SESSION

INTENTIONALLY BLANK

PROGRESS ON SEISMIC ZONATION IN THE SAN FRANCISCO BAY REGION

INTRODUCTION AND SUMMARY

by

Earl E. Brabb^I and Roger D. Borchardt^{II}

Studies by 16 researchers in various earth-science and engineering disciplines were summarized at the First International Conference on Microzonation in 1972. These reports, published in expanded form as U.S. Geological Survey Professional Paper 941-A, established that seismic zonation of the San Francisco Bay region was feasible and showed the necessity for a multidisciplinary approach to the problem. The reports emphasized methodologies for constructing seismic zonation maps from earth-science data that were currently available on a regional scale. The maps showed maximum earthquake intensity, active faults, geologic units, qualitative ground response, liquefaction susceptibility, landslide susceptibility, and areas of potential tsunami inundation. These maps served to delineate areas with potential earthquake problems, identify the problem, and indicate its possible severity.

These basic tools and a number of other products developed as part of a cooperative project between the U.S. Geological Survey and the Department of Housing and Urban Development have been utilized by most of the 91 cities and all of the counties in the San Francisco Bay region. They have also been used in the preparation of seismic safety, public safety, conservation, and open-space elements of general plans together with ordinance administration policy and environmental impact statements. They are the basic building blocks for derivative maps prepared by the Association of Bay Area Governments for regional planning, such as the appropriate location for toxic waste disposal, industrial development, population concentration, and transportation. This wide application of the products has resulted in a significantly increased demand for new and improved earth-science data that can be used for development of policies for earthquake hazard reduction.

Since the initial study, a number of new data have been collected and a number of new approaches have been developed concerning communication of these data to the planning communities. The following set of papers discusses some of these new results in detail. Some of the highlights are as follows:

Discovery of three new potentially active fault systems;

Mapping of all faults with Quaternary displacement in northern San Francisco Bay region at scales of 1:125,000 and 1:24,000;

-
- I Research Geologist, U.S. Geological Survey, 345 Middlefield Road, Menlo Park, California, 94025
- II Supervisory Geophysicist, U.S. Geological Survey, 345 Middlefield Road, Menlo Park, California, 94025

Seismic and geologic logging of 59 drill holes in southern San Francisco Bay region to develop a data base for improved regional ground motion predictions;

Development of new Methods utilizing synthetic seismograms to improve quantitative ground motion predictions;

Mapping liquefaction susceptibility of Santa Cruz County at a scale of 1:62,500 using new techniques;

Development of new techniques for mapping regional slope stability during earthquakes; and

Development of improved methods for estimating earthquake-induced damage to buildings on a regional scale.

The need for new and improved data in all metropolitan areas of high seismic risk is becoming increasingly apparent. The recent Earthquake Hazards Reduction Act of 1977 (P.L. 95-124) calls for the identification, evaluation and characterization of seismic hazards in all areas of high or moderate risk and the development of means to coordinate information about seismic risk with land-use policy decisions. Some of the methods and policies developed in the San Francisco Bay region will be directly applicable to other areas of the United States; however, where earthquake problems and basic data sets are different, additional methods and policies will be needed.

NEOTECTONIC FRAMEWORK OF CENTRAL COASTAL CALIFORNIA
AND ITS IMPLICATIONS TO MICROZONATION
OF THE SAN FRANCISCO BAY REGION

by

Darrell G. Herd^I

ABSTRACT

Microzonation of the San Francisco Bay region must consider future earthquakes on several major northwest-trending faults. Principal among these, the San Andreas fault zone extends through the central Coast Ranges to San Francisco, and then north along the Pacific coastline. Paralleling it offshore to the west is the San Gregorio-Hosgri fault system, which joins with the San Andreas near San Francisco. At Hollister, the Hayward-Lake Mountain fault system branches eastward from the San Andreas, extending north beyond Eureka. The Calaveras-Sunol, Concord, and Green Valley faults form a line that splays from the Hayward-Lake Mountain fault system near San Jose. East of San Francisco, the San Joaquin fault zone bounds the east flank of the Coast Ranges.

Large earthquakes ($M > 7$) are credible on several fault zones in the San Francisco Bay area and have a basic recurrence of tens to hundreds of years on a few.

INTRODUCTION

Microzonation of the San Francisco Bay region for seismic shaking must consider future earthquakes that likely will occur along several predominantly northwest-trending faults. The San Francisco Bay region lies astride the San Andreas fault zone at its intersection with two other major fault systems. These faults, which constitute the neotectonic framework of central coastal California, have been repeatedly active throughout the Quaternary Period (last 1.8 m.y.).

Most historic California earthquakes have originated along such recently active faults (1, 2). An assessment of the length, character, and rate of displacement along them, with reference to historic worldwide seismicity, can be used to estimate the magnitude and frequency of large earthquakes expectable in the San Francisco Bay area.

NEOTECTONIC FRAMEWORK

Recently active faults. The San Francisco Bay region (fig. 1) is cut by several major northwest-trending right-slip faults. These faults, which have been active in both historic (Table 1) and geologically recent time, sliver coastal California into narrow crustal blocks. Principal among these faults, the San Andreas fault zone extends from southern California through the central Coast Ranges of San Francisco. From there north, the San Andreas skirts the Pacific coastline to near Cape Mendocino (see fig. 3), where the fault zone intersects the Mendocino fracture zone. The San Andreas is paralleled offshore to the west by the San Gregorio-Hosgri fault system (3), which begins west of Point Conception and joins the San

^IGeologist, U.S. Geological Survey, Menlo Park, California

Andreas just west of San Francisco. Approximately 120 km southeast of San Francisco a second system of faults, the Hayward-Lake Mountain (4), branches eastward from the San Andreas fault zone at Hollister. This line of large en echelon, recently active right-slip fault zones parallels the San Andreas northward, passing east of Cape Mendocino. The fault system extends beyond Eureka onto the continental shelf southwest of Crescent City. A much shorter line of three faults, the Calaveras-Sunol, Concord, and Green Valley, splays from the Hayward-Lake Mountain fault system near San Jose. To the south, the Sargent fault zone joins the Calaveras-Paicines fault zone and the San Andreas (5).

Southwest of San Jose, an imbricate system of thrust faults (collectively referred to here as the Berrocal fault zone) abuts the northeast side of the San Andreas fault zone (5). East of San Francisco, the San Joaquin fault zone bounds the east flank of the Coast Ranges. The zone is predominantly normal in character (east side down), with local reverse faults.

Faulting and plate tectonics. The northward movement of the Pacific plate relative to North America (fig. 3) is manifested in coastal California as slip along the San Andreas fault zone and the subsidiary faults. The relative rate of movement across the plate boundary is not uniform and is difficult to measure because the area is slivered by intersecting and branching fault systems. One of the crustal slivers, the Humboldt plate (4), moves independently of the Pacific and North American plates. This small plate, bounded on the east by the Hayward-Lake Mountain fault system and on the west by the San Andreas, converges northwestward with the Gorda plate. Near San Jose, the Humboldt plate locally overrides and is crushed by the Pacific plate (along the Berrocal thrust faults). The crustal extension at the east side of the Coast Ranges (evidenced by normal faulting along the San Joaquin fault zone) may be due to the northwestward movement of the Humboldt plate away from the North American plate.

Fault slip. Movement on the recently active faults in the San Francisco Bay region occurs catastrophically in seismic slip events (as much as 5 m of right-lateral displacement was measured (2) across the San Andreas fault after the 1906 earthquake) as well as gradually by fault creep.

An average of 3.7 cm/yr of long-term slip (determined from the right-lateral offset of a 3,000-year-old stream channel (6) in the Carrizo Plain) occurs along the San Andreas fault zone south of Hollister (fig. 1, inset).

Table 1.--Historic surface fault displacements associated with earthquakes in the San Francisco Bay region (2)

Date	Fault	Rupture length	Magnitude
Late June, 1838	San Andreas	Unknown	
July 3, 1861	Calaveras-Sunol	Unknown	
October 22, 1868	Hayward	>30 km	7+1/2 (estimated)
April 24, 1890	San Andreas	>10 km?	
April 18, 1906	San Andreas	~430 km	8.3

Surface faulting has previously been reported (2) for the June 10, 1836 earthquake on the Hayward fault zone. However, re-examination of the original newspaper accounts (referenced in 7) does not support such an interpretation. The described earth fissures were probably due to ground shaking and slope failure rather than faulting.

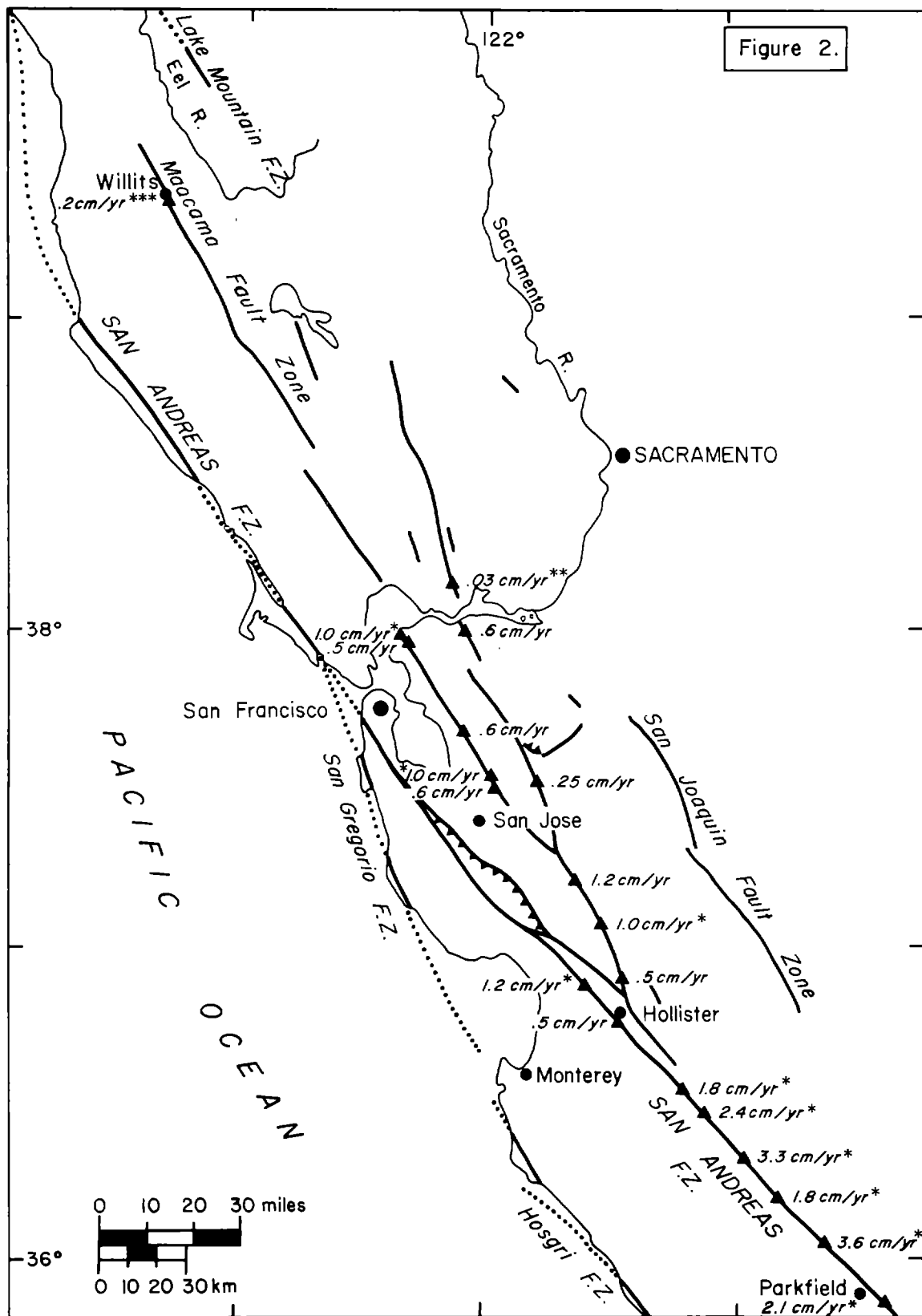


Figure 2.--Documented creep on faults in central coastal California. Data marked by * are from R. O. Burford (8), ** from Frizzell and Brown (9), *** from Harsh and others (10). Other data from Wesson and others (2).

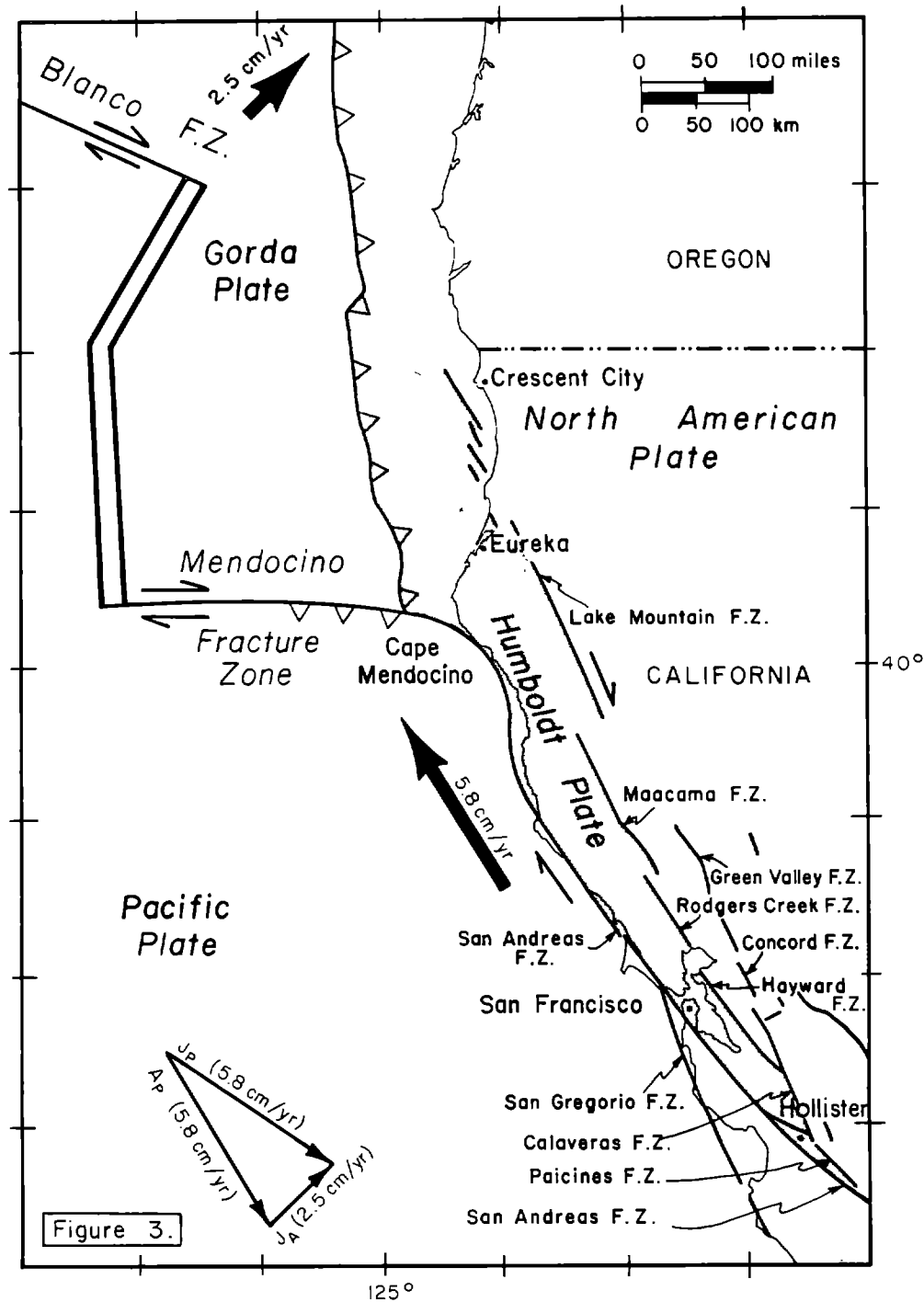


Figure 3.--Map showing plate tectonics of coastal northern California and Oregon (4). Recently active faults of coastal California are represented. Large black arrows show movement of Pacific and Gorda plates relative to the North American plate deduced from vector diagram in bottom center. Motion of the North American plate with respect to the Pacific plate (A_p) is assumed to be 5.8 cm/yr parallel to the San Andreas fault zone. Motion of the Gorda plate with respect to the Pacific plate (J_p) is assumed to be 5.8 cm/yr parallel to the Blanco fracture zone. The resultant motion of the Gorda plate with respect to the North American plate (J_a) is a compression in a north-northeast direction of 2.5 cm/yr.

Part of the displacement (currently as much as 3.6 cm/yr) occurs locally as creep (fig. 2). North of Hollister, near San Francisco (fig. 1), only 2 cm/yr of long-term slip has been documented along the San Andreas fault zone, 0.6-2.2 cm/yr in displaced Pliocene (1.8-5.0 m.y.) rocks (11), and 1-3 cm/yr in offset deposits 1-3 m.y. old (12).

Most of the 1.7 cm/yr of slip that is not carried northward along the San Andreas beyond Hollister is apparently transferred to the Calaveras-Paicines fault zone, which branches from the San Andreas just south of Hollister (fig. 1). Although the actual long-term rate of slip along the Calaveras-Paicines fault zone is not known (a minimum of 0.14-0.71 cm/yr slip has been determined (13) from offset 3.5-m.y.-old volcanic rocks north of Hollister, fig. 1), the long-term rate is maybe at least 1.2 cm/yr and more probably about 1.5 cm/yr. Southeast of San Jose (fig. 2), 1.0-1.2 cm/yr of creep has been documented on the Paicines-Calaveras fault zone. The rate of creep along the Calaveras-Paicines fault zone, like the San Andreas south of Hollister, is presumably equal to or less than the long-term slip rate (the difference being made up in catastrophic seismic slip events).

Slip along the Calaveras-Paicines fault zone is apportioned at San Jose between the Hayward-Lake Mountain fault system and the Calaveras-Sunol--Concord--Green Valley fault system (fig. 1). Although no geologic rates of offset have been locally determined along either fault system, the measurement of 0.6 cm/yr of creep on both the Hayward and Concord fault zones at about the same latitude suggests that the 1.5 cm/yr (?) of slip along the Calaveras-Paicines is equally divided between the two. A marked diminution in long-term slip rate northward along the respective fault systems is suggested by only 0.2 cm/yr of creep along the Maacama fault zone at Willits (fig. 2), and 0.03 cm/yr of creep on the Green Valley fault zone.

About 1 cm/yr (0.63-1.3 cm/yr) of movement for the last 200,000 years has been measured (14) across the San Gregorio fault zone at Año Nuevo (fig. 1). This amount of slip is added to the San Andreas fault zone west of San Francisco, apparently increasing the long-term slip rate along the San Andreas north of Bolinas to about 3.0 cm/yr.

"BASIC" EARTHQUAKE RECURRENCE

Curves of Wallace's (15) "basic" earthquake recurrence can be determined for earthquakes of different magnitude at given points on faults in the San Francisco Bay area if (a) the rate of displacement on the fault is known; (b) the slip rate is constant; (c) all the long-term offset or slip on the fault was the cumulative effect of sudden slips accompanying earthquakes, interspersed with periods of elastic strain build-up; and (d) all earthquakes are assumed to be of the same size. These curves (fig. 4) can be generated for the Hayward, Calaveras-Sunol, Calaveras-Paicines, and San Gregorio fault zones, and parts of the San Andreas (for which average geologic slip rates can be approximated) by the formula

$$R_M = \frac{D}{S}$$

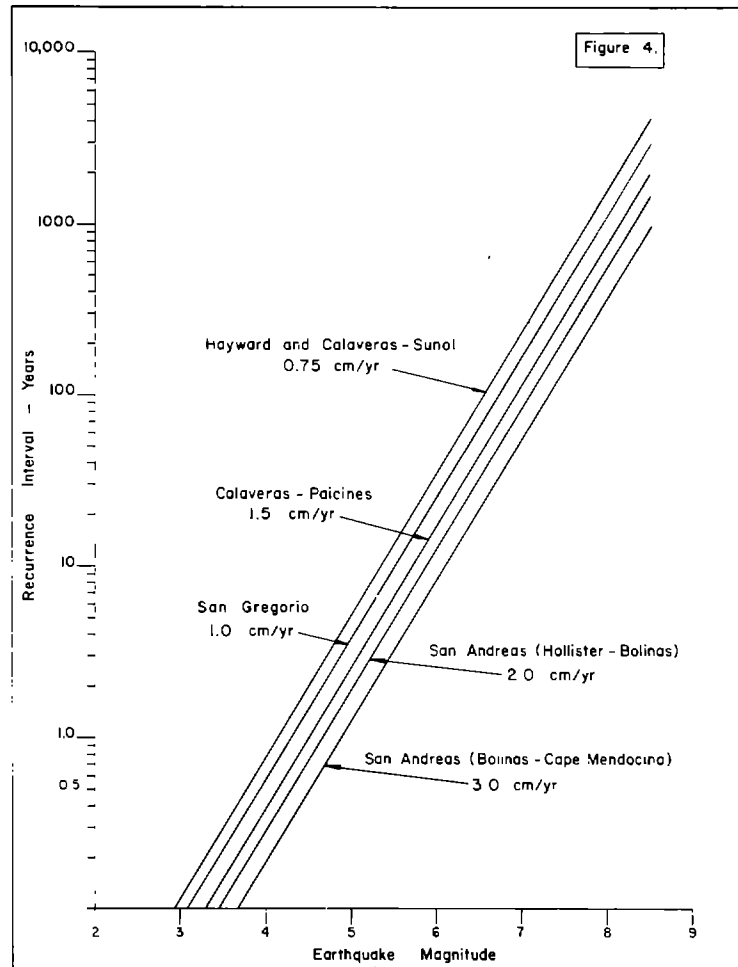


Figure 4.--Basic recurrence intervals (15) at a given point on fault zones in the San Francisco Bay region, assuming average displacement rates indicated. The earthquake magnitudes have been calculated from the empirical relation of Slemmons (17) $M = 6.717 + 1.214 \log_{10} (D)$, where M is magnitude and D is displacement in meters ($n = 30$, $r^2 = 0.408$, $s = 0.639$).

where R_M = recurrence interval, at a point on the fault of an earthquake of magnitude M ,

D = most probable surface displacement associated with an earthquake of magnitude M , determined from a linear regression of earthquake magnitude on surface displacement from data on historical magnitude and surface rupture, and

S = long-term strain rate.

The curves suggest that large earthquakes ($M > 7$) have a "basic" recurrence of tens to hundreds of years on the faults. However, the curves are only a first approximation of estimated earthquake recurrence since the energy released during earthquakes of other magnitudes is not deducted. Moreover, the effect of fault creep, which may be considered a noncatastrophic mode of fault slip and thus an inhibiting factor in the accumulation of elastic strain and the generation of earthquakes, is not considered.

"MOST PROBABLE" EARTHQUAKE MAGNITUDES

Estimates of the "most probable" earthquake magnitudes that can be expected along faults in the San Francisco Bay area if one-half the total fault length ruptured (Table 2) can be used to calculate ground response for microzonation. These estimates, which have commonly been called "maximum credible" or "maximum expectable" earthquake magnitudes (16), are made from linear regressions of earthquake magnitude on length of surface rupture using historical earthquake magnitudes and lengths of surface ruptures (17, 18, 19).

The earthquake magnitudes estimated in Table 2 imply that $M > 6$ earthquakes are credible on most principal fault zones in the San Francisco Bay area. The values differ from those previously determined for faults in the Bay area (2) because they are based on newly mapped fault lengths, and because they are not calculated from regressions of fault length on earthquake magnitude (18).

Table 2.--Most probable magnitudes of earthquakes that would be expected, provided that rupture of one-half the total length of faults or fault segments in the San Francisco Bay region occurred.

Fault zone	Character of motion	Length (L) km	Most probable magnitude 1/2 L
San Andreas			
Hollister - Cape Mendocino	Right-slip	430	7.8
Hollister - Bolinas	do	160	7.2
Bolinas - Cape Mendocino	do	270	7.5
Paicines-Calaveras	do	100	6.9
Hayward	do	90	6.9
Rodgers Creek	do	50	6.5
Maacama	do	140	7.1
Calaveras-Sunol	do	70	6.7
Concord	do	20	6.0
Green Valley	do	90	6.9
San Gregorio	do	140	7.1
San Joaquin	Predominantly normal	120	7.3
Sargent	Right-slip	60	6.6
Berrocal	Thrust	60	7.4

The magnitudes are calculated using the empirical relations of Slemmons (17): $M = 0.597 + 1.351 \log_{10} (L)$ for strike-slip faults ($n = 31$, $r^2 = 0.601$, $s = 0.694$); $M = 1.845 + 1.151 \log_{10} (L)$ for normal faults ($n = 18$, $r^2 = 0.331$, $s = 0.521$); and $M = 4.145 + 0.717 \log_{10} (L)$ for reverse faults ($n = 9$, $r^2 = 0.869$, $s = 0.167$), where M is magnitude and L is fault length in meters.

REFERENCES CITED

1. Allen, C. R., St. Amand, P., Richter, C. F., and Nordquist, J. M., 1965, Relationship between seismicity and geologic structure in the southern California region: Bulletin of the Seismological Society of America, v. 55, no. 4, p. 753-797.
2. Wesson, R. L., Helley, E. J., Lajoie, K. R., and Wentworth, C. M., 1975, Faults and future earthquakes, in Borcherdt, R. D., ed., Studies for seismic zonation of the San Francisco Bay region: U.S. Geological Survey Professional Paper 941-A, p. A5-A30.
3. Graham, S. A., and Dickinson, W. R., 1978, Evidence for 115 kilometers of right slip on the San Gregorio-Hosgri fault trend: Science, v. 199, no. 4325, p. 179-181.
4. Herd, D. G., 1978, An intracontinental plate boundary east of Cape Mendocino, California: Geology, in press.
5. McLaughlin, R. J., 1974, the Sargent-Berrocal fault zone and its relation to the San Andreas fault system in the southern San Francisco Bay region and Santa Clara Valley, California: Journal of Research of the U.S. Geological Survey, v. 2, no. 5, p. 593-598.
6. Hall, N. T., and Sieh, K. E., 1977, Late Holocene rate of slip on the San Andreas fault in the northern Carrizo Plain, San Luis Obispo County, California (abst.): Geological Society of America Abstracts with Programs, v. 9, no. 4, p. 428-429.
7. Louderback, G. D., 1947, Central California earthquakes of the 1830's: Seismological Society of America Bulletin, v. 37, p. 33-74.
8. Savage, J. C., and Burford, R. O., 1973, Geodetic determination of relative plate motion in central California: Journal of Geophysical Research, v. 78, no. 5, p. 832-845.
9. Frizzell, V. A., Jr., and Brown, R. D., Jr., 1976, Map showing recently active breaks along the Green Valley fault, Napa and Solano Counties, California: U.S. Geological Survey Miscellaneous Field Studies Map MF-743, scale 1:24,000.
10. Harsh, P. W., Pampeyan, E. H., and Coakley, J. M., 1978, Slip on the Willits fault, California (abst.): Seismological Society of America Earthquake Notes, v. 49, no. 1, p. 22.
11. Addicott, W. A., 1969, Late Pliocene mollusks from San Francisco Peninsula, California, and their paleogeographic significance: Proceedings of the California Academy of Sciences, Fourth Series, v. 37, no. 3, p. 57-93.
12. Cummings, J. C., 1968, The Santa Clara Formation and possible post-Pliocene slip on the San Andreas fault in central California, in Dickinson, W. R., and Grantz, Arthur, eds., Proceedings of conference on geologic problems of San Andreas fault system: Stanford University Publications in the Geological Sciences, v. 11, p. 191-207.

13. Nakata, J. K., 1977, Distribution and petrology of the Anderson-Coyote Reservoir volcanic rocks: San Jose State University, California, Master of Science Thesis, 105 p.
14. Weber, G. E., and Lajoie, K. R., 1977, Late Pleistocene and Holocene tectonics of the San Gregorio fault zone between Moss Beach and Point Año Nuevo, San Mateo County, California (abst.): Geological Society of America Abstracts with Programs, v. 9, no. 4, p. 524.
15. Wallace, R. E., 1970, Earthquake recurrence intervals on the San Andreas fault: Geological Society of America Bulletin, v. 81, p. 2875-2890.
16. Wesson, R. L., Page, R. A., Boore, D. M., and Yerkes, R. F., 1974, Expectable earthquakes in the Van Norman Reservoirs area: U.S. Geological Survey Circular 691-B, 9 p.
17. Slemmons, D. B., 1977, State-of-the-art for assessing earthquake hazards in the United States: U.S. Army Engineer Waterways Experiment Station Miscellaneous Paper S-73-1, Report 6, var. pag.
18. Mark, R. K., 1977, Application of linear statistical models of earthquake magnitude versus fault length in estimating maximum expectable earthquakes: Geology, v. 5, p. 464-466.
19. Mark, R. K., and Bonilla, M. G., 1977, Regression analysis of earthquake magnitude and surface fault length using the 1970 data of Bonilla and Buchanan: U.S. Geological Survey Open-file Report 77-614, 8 p.

PROGRESS ON GROUND MOTION PREDICTIONS
FOR THE SAN FRANCISCO BAY REGION, CALIFORNIA

by

Roger D. Borcherdt^I, James F. Gibbs^I, and Thomas E. Fumal^{II}

ABSTRACT

The amount of damage in the San Francisco Bay region from the 1906 earthquake depended strongly on the geologic character of the ground. This dependence indicates the need for seismic zonation maps of the region to outline areas where special earthquake resistant design is necessary to reduce losses from future earthquakes.

Current research is directed at defining methodologies for improved quantitative estimates of ground response on a regional scale. This research includes determination of seismic and geologic logs in 59 drill holes to a depth of 30 meters.

Relations derived between site amplifications (Amp), 1906 earthquake intensity increments (δI), and shear-wave velocity are, respectively,

$$\text{Amp} = -11.4 \log (S\text{-vel, m/s}) + 33.6$$

and

$$\delta I = -0.0027 (S\text{-vel, m/s}) + 2.25$$

Geotechnical parameters such as texture, standard penetration, and depth, for sediments, and fracture spacing and hardness, for rocks, show strong correlations with seismic velocities and provide a useful means of defining 13 units with distinct seismic characteristics. Utilizing the preceding empirical relations, quantitative estimates of ground response at 59 sites, recently developed numerical models, and the classification of seismically distinct units on the basis of geotechnical parameters, improved quantitative estimates of variations in ground shaking can be provided on a regional scale for seismic zonation of the San Francisco Bay region. In addition, the seismic velocity relations permit extrapolation of these data to other regions.

Introduction

The most widespread earthquake damage is generally due to ground shaking and is strongly dependent on the geologic character of the ground. After the 1906 earthquake, Lawson (12) reported evidence for increased damage due to geologic conditions in 18 California communities. This strong dependence of damage on the geological character of the ground defined a strong need for predictions of regional ground motion that can

I

Geophysicists

II

Geologist; U.S. Geological Survey, Menlo Park, CA

be used for economical earthquake-resistant design. This paper describes a new data base for developing a methodology to prepare predictions of regional ground motion that account for variations in geologic conditions.

The problem of predicting regional ground motion is quite distinct from that of predicting for specific sites. For specific sites (for example, siting of a nuclear power plant or a high-rise structure), detailed geologic and seismic data are available. As a result, recently developed numerical modeling procedures can be used to predict reasonably detailed time histories of ground motion. However, such detailed seismic and geologic information is not available on a regional basis, and predictions must necessarily be more generalized.

Previous Work on Regional Problem

At the time of the First International Conference on Microzonation, Borcherdt, et al., (5) reported on data available for regional ground motion predictions in the San Francisco Bay region. These data included observed 1906 earthquake intensities, recordings of the 1957 earthquake, comparative measurements at 99 sites of ground shaking generated by nuclear explosions, and high-strain laboratory measurements of dynamic soil properties.

Comparative measurements of ground shaking generated by the nuclear explosions and the 1957 earthquake showed that a significant and consistent difference in the response to shaking exists between different geologic units in the San Francisco Bay region (Borcherdt, 1). Comparison of the measured amplifications with the high quality 1906 intensity data showed that an increase in amplification corresponds to an increase in intensity. This correlation suggested that sites at equal distance from the fault with large observed amplifications may also be sites of relatively high intensity in future earthquakes. These data together with available geologic information were used to predict the maximum intensity that sites in the San Francisco Bay region might sustain from large earthquakes on either the San Andreas fault or the Hayward fault (Borcherdt, Gibbs, and Lajoie, 4). (See Fig. 1 for map).

The intensity map delineates general areas susceptible to problems from earthquakes in the San Francisco Bay region, and, when properly interpreted, it provides a preliminary form of seismic zonation. The map has been used in the required Seismic Safety Elements of several bay region communities and for development of general land-use policies designed to reduce earthquake losses. The map does not provide quantitative estimates of ground shaking nor does it predict the nature and areal extent of such problems as surface faulting or liquefaction. It does delineate many potentially hazardous areas and provides a qualitative estimate of the overall hazard from shaking on a regional scale. In addition to their use for the maximum predicted intensity maps, the data available in the San Francisco Bay region were considered adequate to prepare a map showing that the expected effects of amplified ground shaking would be least on bedrock, intermediate on alluvium, and greatest on bay mud (Borcherdt et al., 2). However, the data were not considered adequate to prepare more quantitative maps depicting such parameters as peak acceleration, velocity and displacement. Such predictions require not only detailed models of the earthquake source and the seismic wave transmission path, but also detailed knowledge of the geometry and configuration of near-surface geologic deposits.

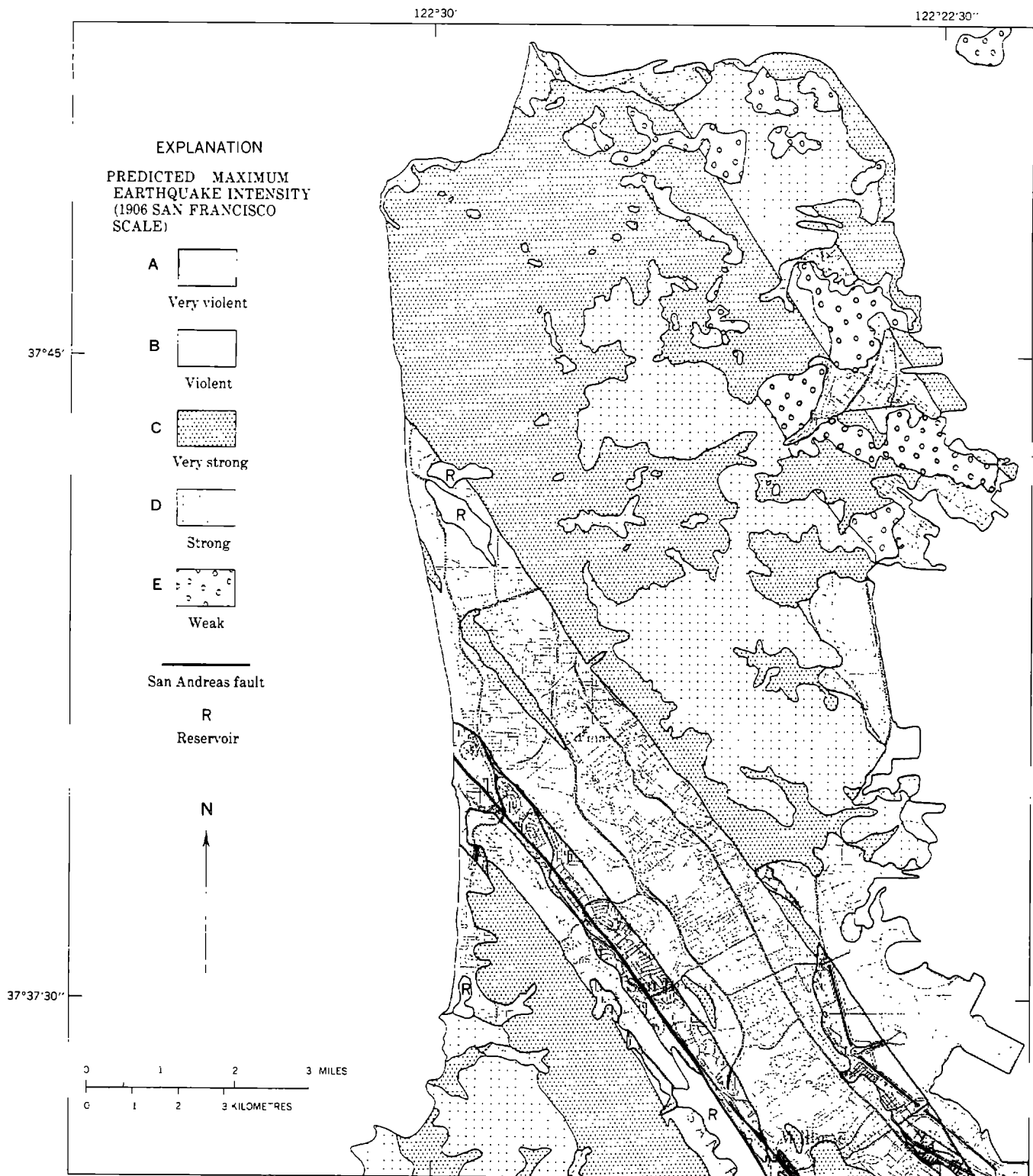


Figure 1.—Maximum earthquake intensities predicted for San Francisco (map is excerpt from Borchardt, Gibbs, and Lajoie, 4). Each value is maximum of those predicted assuming a large earthquake on San Andreas or Hayward fault. Intensity values are predicted from empirical relations based on only good intensity data for the 1906 earthquake together with a generalized geologic map compiled by K. R. Lajoie (written comm., 1974). Letters A-E indicate grades of San Francisco intensity scale.

New Data Base for Regional Problem

To develop an improved data base for more quantitative predictions of ground motion on a regional scale, a program was undertaken by the U.S. Geological Survey to determine detailed seismic and geologic logs for a large number of sites in all major geologic units in the San Francisco Bay region. To date, seismic velocity logs of P- and S- waves, together with geologic logs, have been determined for 59 sites in drill holes to a depth of 30 meters (Fig. 2) (Gibbs *et al.*, 7, 8, 9, 10). Seismic velocities (Fig. 3) were measured at 2.5-meter intervals using an in-hole technique developed by Kobayashi (11) and Warrick (13). (See Gibbs *et al.*, 7, for detailed description of technique). Interpretive geologic logs were compiled for each hole using field data, including descriptions of three to six samples taken at lithologic contacts and at points where changes in physical properties were indicated (see Fumal, 6, for details). Drill hole sites were selected on the basis of available high-quality 1906 intensity data, measured ground response from nuclear explosions, and detailed geologic mapping.

Seismic Velocity vs. Intensity Increments

To compare seismic velocities with the 1906 intensity data, the effect of distance on the observed 1906 intensities was removed by computing increments in observed intensity with respect to a mean attenuation curve for intensities observed on the Franciscan Formation (Borcherdt and Gibbs, 3). Those intensity increments, based on the better 1906 data and collected at sites for which no ground failure was observed, are plotted as a function of average shear wave velocity to the bottom of the hole determined at the corresponding site (Fig. 4). The plot shows considerable scatter in the data, but a decrease in seismic shear wave velocity clearly corresponding to a decrease in observed intensity increment. The relations without regard to geologic setting suggests that sites equidistant from the fault with average shear wave velocities of about 250 m/s could expect to experience an intensity of approximately 2 units higher than sites with velocities near 1000 m/s. In addition, the relations helps to establish that seismic velocity may be a significant parameter for evaluating seismic hazards.

Seismic Velocity vs. Measured Ground Response

To compare seismic velocities with ground response determined from nuclear explosions, the average of the horizontal spectral amplification curves (Borcherdt and Gibbs, 3) were plotted as a function of average shear wave velocity to the bottom of the hole (Fig. 5). The data show a strong correlation between shear wave velocity and measured amplification. In particular, at sites with average shear velocities of 250 m/s, low-strain ground motions over the frequency band 0.5 to 2.5 Hz are likely to be about seven times greater than those at sites with velocities near 900 m/s.

The data from drill holes more than 100 m from the site of the measured amplification show considerably more scatter, and this scatter suggests that amplification effects are very localized and that care is required in extrapolating site-specific measurements to a regional scale.

The data suggest that the seismic shear wave velocity of the upper 30

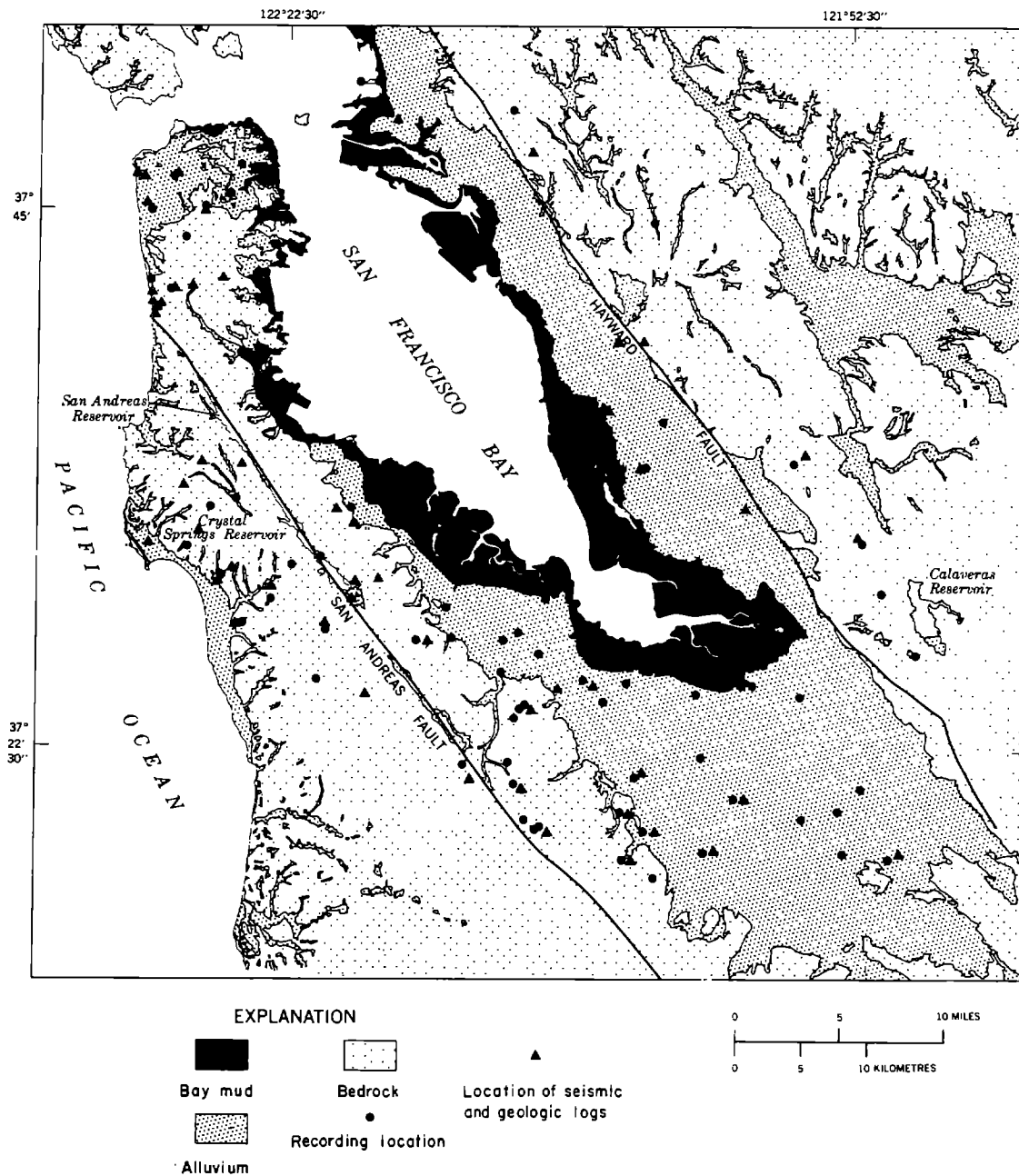


Figure 2.-Distribution of generalized geologic units, locations where seismic and geologic logs have been compiled in drill holes to 30 m depth, and locations where ground response has been measured from a nuclear source.

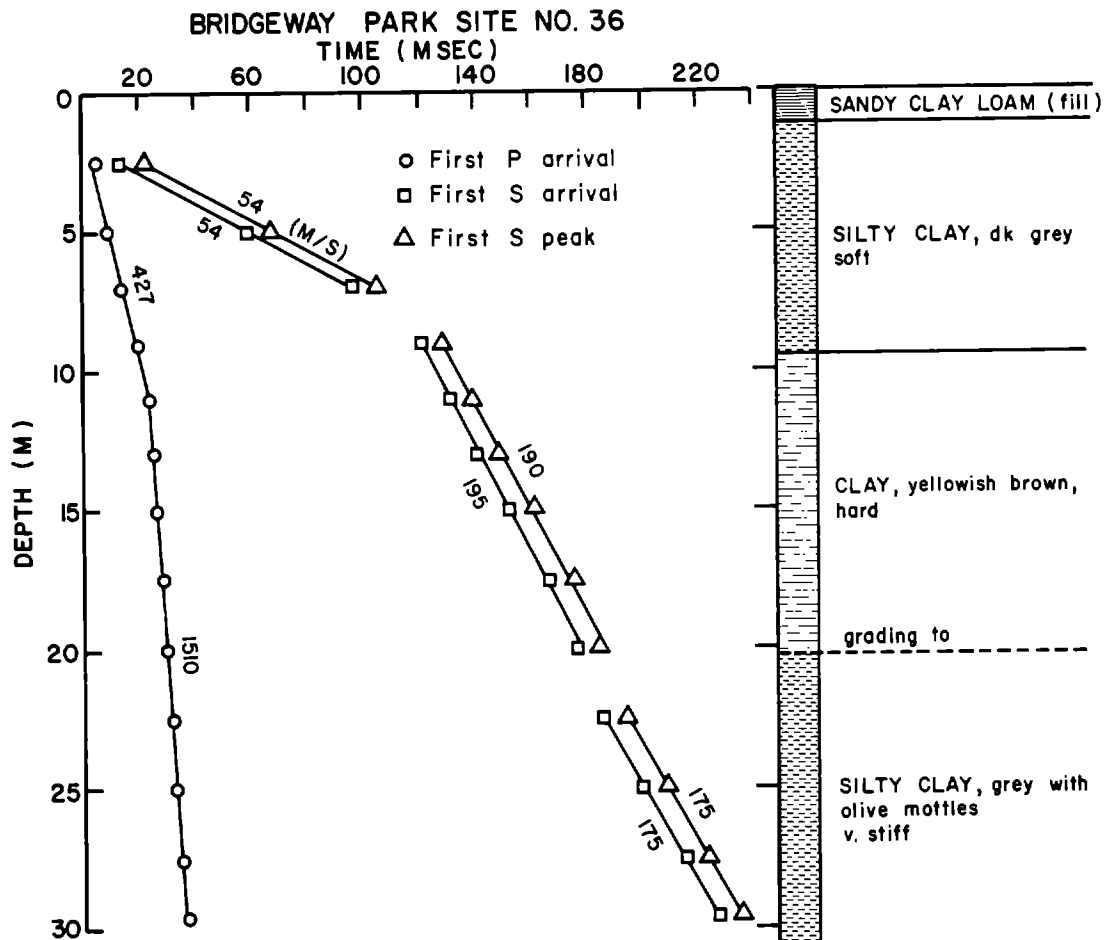


Figure 3.-Example of traveltime curves for P and S waves and simplified geologic log. Two picks are shown for the S-wave group--first S arrival and first S peak.

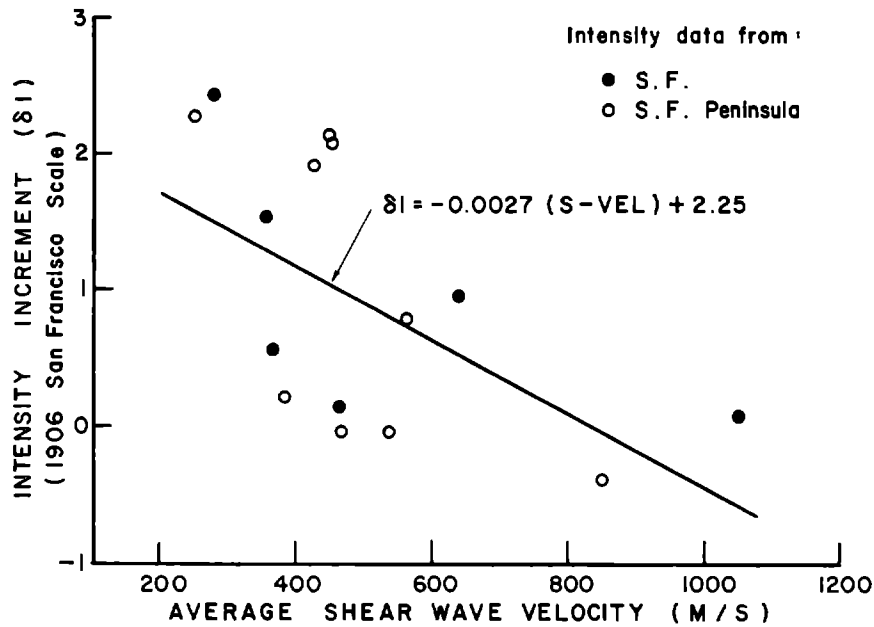


Figure 4.-Intensity increment (δI) determined from data of 1906 San Francisco Earthquake vs. shear wave velocity averaged from surface to approximately 30 m depth. Dots are observed data using San Francisco intensity scale and circles are data using Rossi-Forel scale. Intensity increments are expressed in terms of the San Francisco intensity scale converting the letters A-E to 4-0, respectively. Observed data expressed in Rossi-Forel scale were converted to San Francisco scale using X \rightarrow A, IX \rightarrow B, VIII-IX \rightarrow C, VII-VIII \rightarrow D, and VI-VII \rightarrow E.

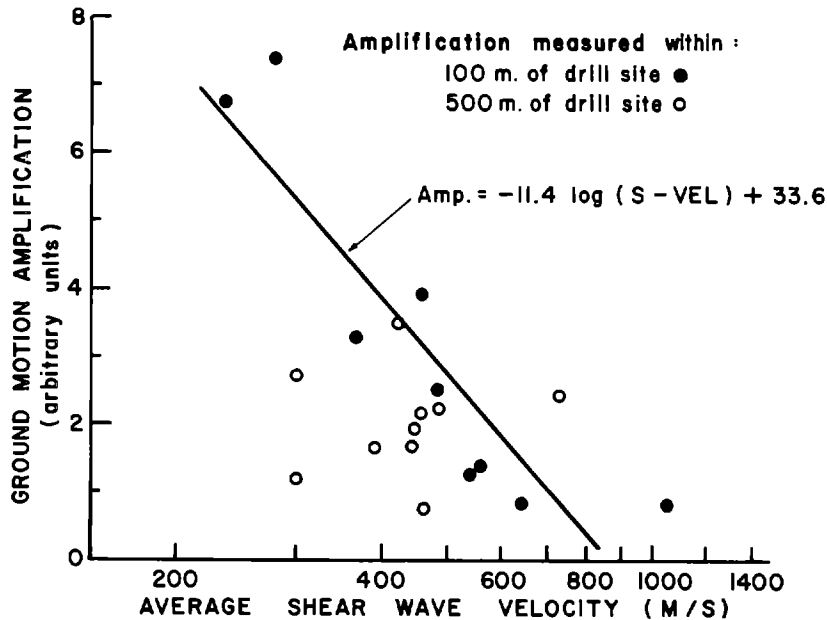


Figure 5.-Amplification (Amp.) as determined from recordings of ground motion generated by nuclear explosions vs. shear wave velocity averaged from surface to approximately 30 m depth. Dots represent ground motion amplification measured within 100 m; and circles, within 500 m of drill site.

meters of a surficial deposit plays a significant role in changing the anticipated characteristics of seismic waves in certain frequency bands.

Geologic and Physical Properties of Seismically Distinct Units

Preparation of regional ground response maps requires utilization of data available on a regional scale. In most urban areas this data base is limited to standard geologic mapping. Most such maps, however, are compiled for purposes of inferring geologic history and are not immediately applicable to preparing special-purpose interpretive maps. Mapped units commonly contain materials with a wide range of physical properties and seismic characteristics.

In order to adapt the geologic data base for purposes of regional seismic zonation, a detailed study was undertaken to investigate correlations between geologic and physical descriptions of the various units and seismic velocities (Fumal, 6). The study identified a suite of physical properties of geologic materials that can be used to identify seismically distinct units and can be readily determined in the field and thus incorporated in geologic mapping schemes.

Seismic wave velocities were measured in each of the geologic map units in the San Francisco Bay region. The range of seismic velocities for a given unit is dependent on the variety of materials included in the unit, which is largely a function of the age of the deposit. Each of the Holocene map units shows a distinct and relatively narrow range of shear wave velocity. Older sedimentary deposits and bedrock materials show relatively wide and overlapping velocity ranges. For these materials, age has been an important factor in defining geologic units. Differences in age, however, frequently do not correlate with significant variation in the physical properties that affect seismic velocities.

For the unconsolidated to semiconsolidated sedimentary units, texture or relative grain size distribution was found to have the most significant effect on seismic shear wave velocity. On the basis of texture alone, the unconsolidated sedimentary deposits in the San Francisco Bay region can be divided into four categories: (1) clay and silty clay, (2) sandy clay and silt loam, (3) sand, (4) and gravel. Utilizing standard penetration resistance measurements (SPR), the clay and silty clay unit and the sand unit each can be subdivided into two additional units. Each unit identified according to physical properties is clearly identifiable seismically (lower abscissa Fig. 6, Table 1) with the exception of the sand unit, which was classified separately because it is easily distinguishable in the field and because its compaction varies over a broad range. Each of the units identified according to texture and SPR is also easily recognized in the field and should be readily differentiated in areas that have existing geologic maps.

For the bedrock materials in the San Francisco Bay region, fracture spacing was found to have the most significant effect on seismic shear wave velocity for various rock types. Hardness has the second largest effect and lithology can be used to distinguish between hard sedimentary and igneous rocks like the sedimentary units, each bedrock unit identified according to physical properties is seismically distinct (lower abscissa, Fig. 7; Table 1). The seismically distinct bedrock units can not be so easily mapped as the unconsolidated sediments because fracture spacing

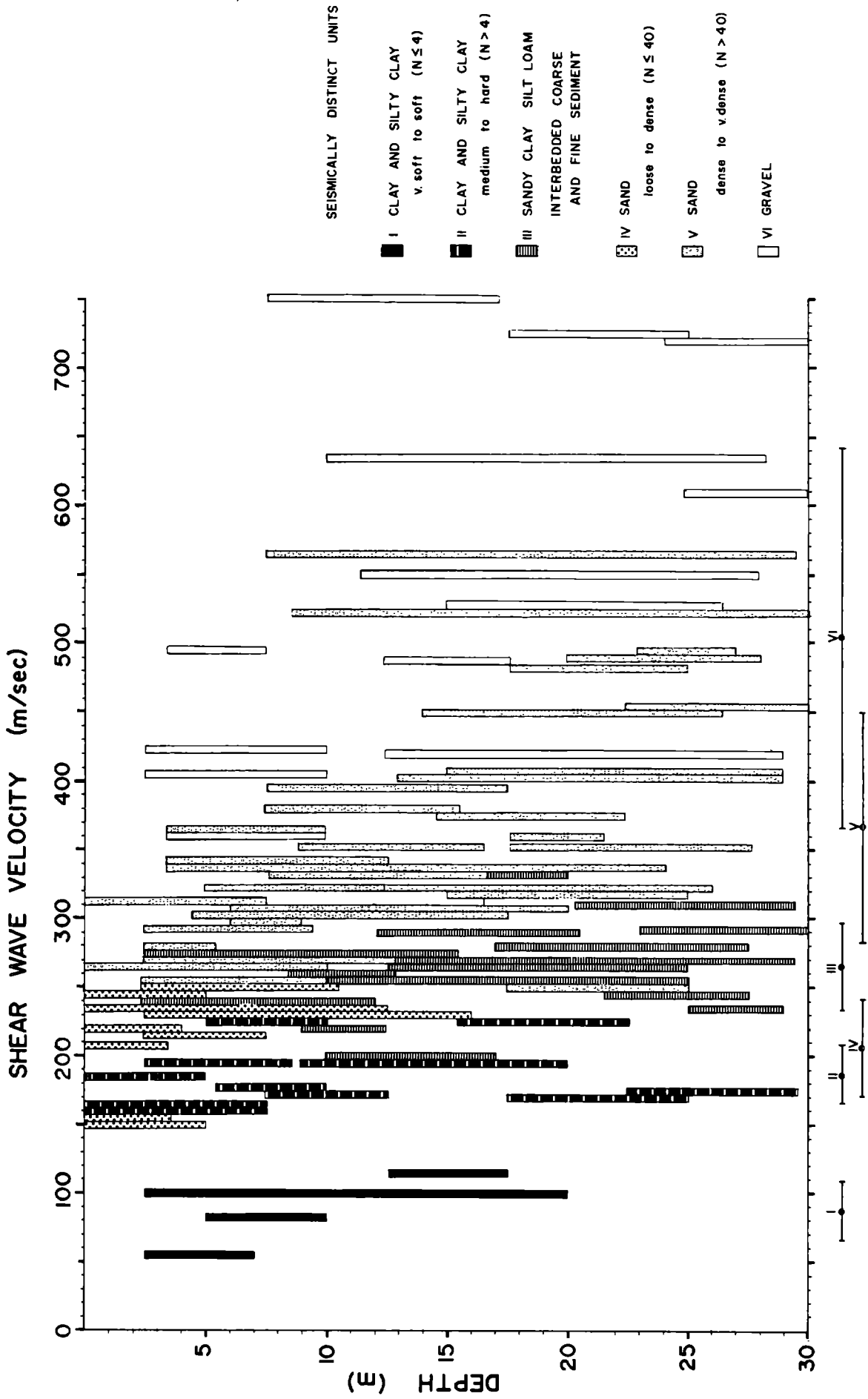


Figure 6.-Shear wave velocity for various depth intervals determined in drill holes for unconsolidated to semiconsolidated sedimentary deposits. Seismically distinct units are classified according to the physical properties of texture or relative grain size and standard penetration resistance. Means and standard deviations for each unit are shown along lower abscissa by dots and error bars, respectively.

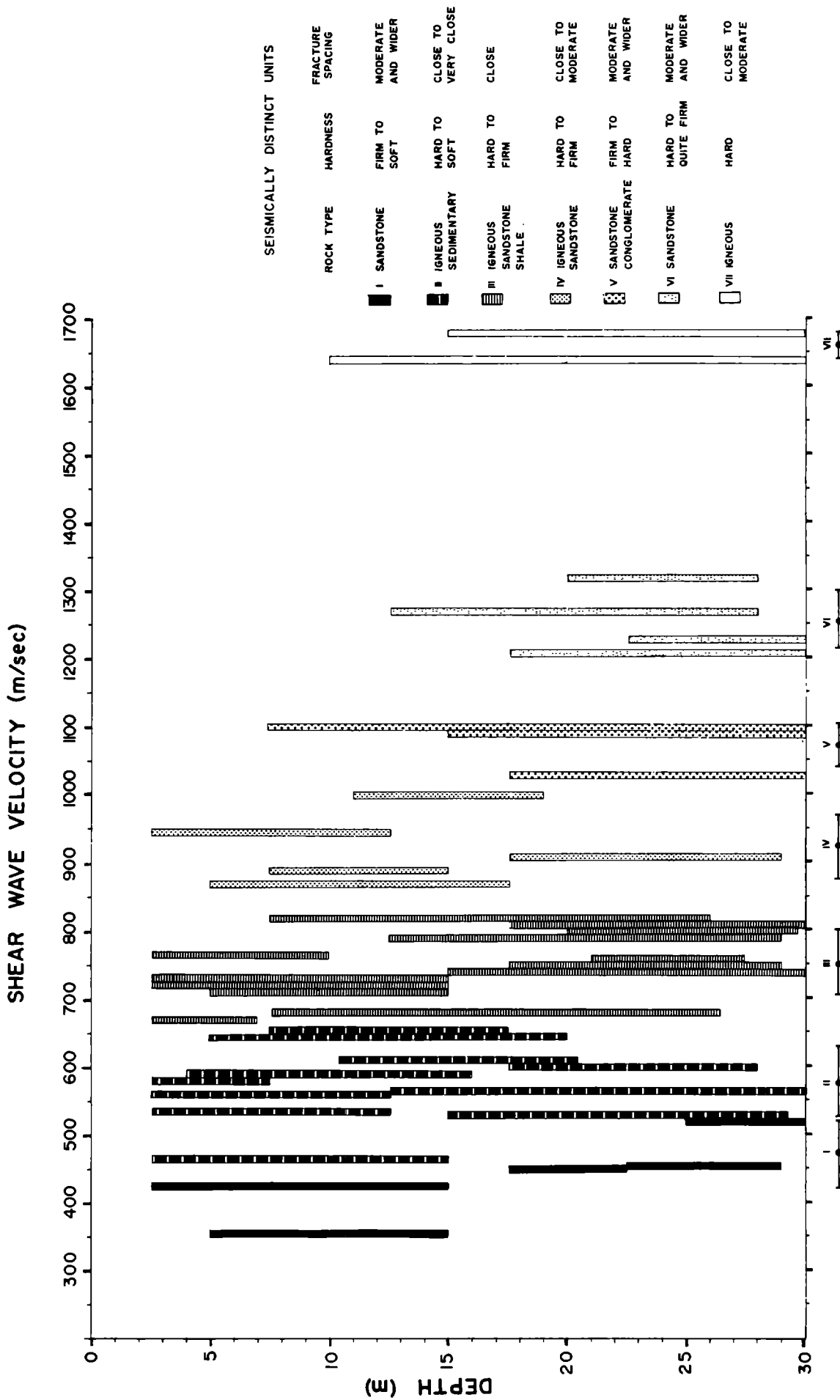


Figure 7.-Shear wave velocity for various depth intervals determined in drill holes for bedrock materials. Seismically distinct units are classified according to the physical properties of fracture spacing, hardness, and lithology. Means and standard deviations for each unit are shown along lower abscissa by dots and error bars, respectively.

TABLE I

SHEAR WAVE VELOCITIES IN GEOLOGIC MATERIALS

Distinct Seismic Units	Shear Wave			Intensity Increment (Pred.)	Distinct Seismic Units	Physical Properties			Shear Wave			Intensity Increment (Pred.)	
	Physical Properties	Vel. (m/s) Mean	Std. Dev.			Amp. (Pred.)	Rock Type	Hardness	Fracture Spacing	Vel. (m/s) Mean	Std. Dev.		
<u>Sedimentary Deposits</u>													
I	Clay-Silty Clay very soft-soft (N ≤ 4)	88	22	11.43	2.01	I	Sandstone	Firm to Soft	Moderate and wider	470	48	3.14	0.98
II	Clay-Silty Clay medium-hard (N ≥ 4)	186	22	7.73	1.75	II	Igneous Sedimentary	Hard to Soft	Close to very close	577	51	2.12	.69
III	Sandy Clay-Silt Loam Interbedded Coarse and Fine Sediment	265	32	5.97	1.53	III	Igneous Sandstone Shale	Hard to Firm	Close	751	46	.82	.22
IV	Sand loose to dense (N ≤ 40)	206	36	7.22	1.69	IV	Igneous Sandstone	Hard to Firm	Close to Moderate	923	48	-.20	-.24
V	Sand dense to very dense (N ≥ 40)	366	84	4.38	1.26	V	Sandstone Conglomerate	Firm to Hard	Moderate and wider	1073	31	-.95	-.65
VI	Gravel	504	138	2.79	.89	VI	Sandstone	Hard to quite firm	Moderate and wider	1257	42	---	---
VII						VII	Igneous	Hard	Close to	1660	20	---	---

and hardness vary widely within many map units. For purposes of mapping regional ground response, however, subdivision of the bedrock materials is not so important, and fewer subdivisions may be adequate for many areas.

Methodology for Regional Maps

Regional maps depicting expected variations in ground response must be based on data available on a regional scale. Geologic and physical property data can be readily tied to more quantitative estimates of ground response such as amplifications and intensity increments utilizing seismic velocity data.

Intensity increments and amplifications are predicted for 11 of the 13 units in the San Francisco Bay region using relations in figures 4 and 5 (Table 1). Both the intensity increments and amplifications predicted are easily distinguishable for the various units and show that a considerable geographic variation can be expected in ground response to earthquake generated shaking. These predictions, together with appropriate bedrock attenuation curves from a potential earthquake source, provide a technique for developing a preliminary but improved regional ground motion map for the San Francisco Bay region. To prepare ground response maps for other areas where similar intensity and amplification data are not available, measurement of seismic velocities in a relatively few seismically distinct units would permit extrapolation of the San Francisco data. A program is currently under way to compare data in the San Francisco and Los Angeles regions.

REFERENCES

1. Borcherdt, R.D. (1970), Effects of local geology on ground motion near San Francisco Bay, *Bull. Seis. Soc. Am.*, v. 60, pp. 29-61.
2. Borcherdt, R.D. (Editor) (1975), Studies for seismic zonation of the San Francisco Bay region, U.S. Geological Survey Professional Paper 941-A.
3. Borcherdt, R.D. and Gibbs, J.F. (1976), Effects of local geological conditions in the San Francisco Bay region on ground motions and the intensities of the 1906 earthquake, *Bull. Seis. Soc. Am.*, v. 66, pp. 467-500.
4. Borcherdt, R.D., Gibbs, J.F. and Lajoie, K.R. (1975), Prediction of maximum earthquake intensity in the San Francisco Bay region, California, for large earthquakes on the San Andreas and Hayward faults, U.S. Geological Survey, MF 709.
5. Borcherdt, R.D., Joyner, W.B., Nichols, D.R., Chen, A.T.F., Warrick, R. E., and Gibbs, J. (1972), Ground motion predictions, abs., Proceedings of the international conference on microzonation, p. 862, Seattle, WA.
6. Fumal, T.E. (1978), Correlations between seismic wave velocities and physical properties of near-surface geologic materials in the southern San Francisco Bay region, U.S. Geological Survey, Open-file report (in progress).
7. Gibbs, J.F., Fumal, T.E. and Borcherdt, R.D. (1975), In-situ measurements of seismic velocities at twelve locations in the San Francisco Bay region, U.S. Geological Survey, Open-file report 75-564.
8. Gibbs, J.F., Fumal, T.E. and Borcherdt, R.D. (1976), In-situ measurements of seismic velocities in the San Francisco Bay region...Part II, U.S. Geological Survey, Open-file report 76-731.
9. Gibbs, J.F., Fumal, T.E., and Borcherdt, R.D. (1978), In-situ measurements of seismic velocities at 59 locations in the San Francisco Bay region, abs., 73rd Annual Meeting, Seis. Soc. of Am., Sparks, Nv.
10. Gibbs, J.F., Fumal, T.E., Borcherdt, R.D. and Roth, E.F. (1977), in-situ measurements of seismic velocities in the San Francisco Bay region...Part III, U.S. Geological Survey, Open-file report 77-850.
11. Kobayaski, N. (1959), A method of determining the underground structure by means of SH waves, *Zisin*, ser. 2, v. 12, pp. 19-24.
12. Lawson, A.C. (Chairman) (1908), The California earthquake of April 18, 1906, report of the state earthquake commission, Carnegie Inst. Washington, p. 160-253.
13. Warrick, R.E. (1974), Seismic investigation of a San Francisco Bay mud site, *Bull. Seism. Soc. Am.*, v. 64, pp. 375-385.

254

INTENTIONALLY BLANK

A METHODOLOGY FOR PREDICTING GROUND MOTION AT SPECIFIC SITES

Ralph J. Archuleta^I, William B. Joyner^{II} and David M. Boore^{III}

ABSTRACT

An important development in current research on earthquake ground motion is the synthesis of ground motion records based on the physics of a propagating fracture. Different techniques are used for generating synthetic records depending upon the frequency range of interest. For frequencies below about 1-2 Hertz we used a finite element method to simulate a propagating fracture; for higher frequencies we used a stochastic dislocation model. With the finite element method we have been able to simulate a dynamic earthquake in a fully three-dimensional geometry. We compute the ground motion from two hypothetical earthquakes that differ only in their shear stress distribution with depth. On the free surface we have contoured the maximum particle velocity. From such contours one could approximate the areas most likely to suffer damage during an earthquake. We have also used the fault slip generated by a propagating stress relaxation as input for the stochastic model. Acceleration is computed using a statistical source model in which the amplitude of the dislocation-time function varies randomly along the fault while the shape of the function and the rupture velocity are constant.

INTRODUCTION

One of the fundamental assumptions for any microzonation plan is that one can realistically estimate the ground motion resulting from an earthquake. We are developing methods for computing complete time histories of earthquake ground motion from physical models of the source and propagation path. We expect that the time histories will be useful, not only in the detailed dynamic analysis of structures, but also in estimating ground motion parameters, e.g., peak particle velocity and peak particle acceleration, for microzonation purposes.

A major difficulty in making estimates of the ground motion in the near field is that the frequencies of interest range from d.c. to tens of hertz. In order to span this wide range of frequencies we have modeled the earthquake source by using a three-dimensional, finite element model of a propagating stress relaxation (1) in combination with a stochastic propagating dislocation (2). The finite element provides estimates of the dislocation time history (2). In addition the finite element method

-
- I. Research Associate, U.S. Geological Survey, 345 Middlefield Rd., Park, CA. 94025
 - II. Geophysicist, U.S. Geological Survey, 345 Middlefield Rd., Menlo Park, CA, 94025.
 - III. Professor of Geophysics, Stanford University, Stanford, CA. 94305.

provides estimates of particle displacement and particle velocity while the stochastic dislocation gives some estimate of the particle acceleration. The finite element method has been used successfully to model real ground motion data from the 1966 Parkfield earthquake (3). In this paper we illustrate the method by applying it to two hypothetical earthquakes: the first has a shear prestress distribution that is uniform over the width of the fault; the second has a prestress distribution that varies with depth, Figure 1. A comparison illustrates the influence of one of the important aspects of the earthquake source model.

METHODS

To simulate an earthquake in a prestressed medium we use the method of Archuleta and Frazier (1) that allows the fracture to nucleate at a hypocenter and spread with a prescribed rupture velocity over a given finite-sized fault area embedded within a halfspace. As the fracture spreads, it relaxes the stress enclosed by its rupture front. This model was based on the generally accepted elastic rebound hypothesis (4) as the mechanism for shallow, tectonic earthquakes. This method is fully three-dimensional and the rupture surface may or may not intersect the traction-free surface of the halfspace. Driven by the stress relaxation the medium adjusts to the new stress state. The particle displacement and particle velocity can be computed everywhere including the rupture surface and the free surface.

To demonstrate that their numerical method correctly simulated the physics of a propagating stress relaxation, Archuleta and Frazier (1) compared their numerically computed dislocations for a circular fault in a full space with the dislocations analytically determined by Kostrov (5) for a continuously expanding circular stress relaxation. Until the arrival of edge effects due to the finiteness of the fault in the numerical method, the numerical and analytical dislocations showed exceptional agreement including the square root behavior of the dislocation at the arrival of the rupture front.

As an example of using such an earthquake model, together with the response of a layered medium, Archuleta and Day (3) have computed synthetic seismograms to compare with those recorded during the 1966 Parkfield earthquake at Stations 2, 5, 8 and 12 which were about .8, 3.4, 9.1, and 14 km off the fault, respectively. A comparison of displacement time histories for Station 5 in the Cholame-Shandon array is shown in Figure 2. One can see that the match between components is close. The phases could probably be made to match better by adjusting the rupture velocity. The other stations showed similar agreements between synthetic and recorded displacements.

The frequency resolution of waves propagated using the finite element method depends critically on the number of nodal points per wavelength (6). Thus the finite element (and finite difference) methods

cannot economically resolve the high frequencies found in acceleration records. It can also be argued that on a scale of several hundred meters which corresponds to wavelengths associated with a 10 Hertz wave that we neither know the spatial variation of stress on the fault nor the inhomogeneities of the medium. Thus we have chosen to estimate the high frequencies from a propagating stochastic dislocation along a line at a fixed depth. A representative dislocation function is selected from the dislocations computed using the finite element stress relaxation. The dislocation is propagated with the same velocity from the same hypocenter. However, the amplitude of the dislocation is allowed to vary randomly about a mean value calculated from the stress relaxation model. The width of the fault is taken into account by assigning the dislocation function a weighting factor related to the width used in the stress relaxation problem.

EARTHQUAKE MODEL

We will model a strike-slip earthquake that occurs on a vertical fault that is 32 km in length and 8 km in width. The plane of the fault intersects the traction free surface of a homogeneous, isotropic, linearly elastic halfspace. The halfspace is characterized by a compressional wave speed (α) 6.0 km/sec, shear wave speed (β) 3.5 km/sec and density of 2.7×10^3 kg/m³. To designate the spatial positions we use a Cartesian coordinate system X_1, X_2, X_3 with the origin at the midpoint of the strike of the fault at the traction free surface, Figure 1. Components of motion referred to as parallel, vertical and transverse are the components in the X_1, X_2, X_3 directions, respectively. The fracture nucleates at (0., 5., 0.) and spreads radially over the fault surface with a rupture velocity of $.9\beta$, Figure 1. As the fracture spreads it relaxes the σ_{31} component of stress.

We consider two different shear prestress distributions on the fault as a function of depth ($\sigma_{31}(X_2)$); however both shear stress distributions have the same average value. We also assume that the sliding friction stress does not vary with depth. The shear prestress does not vary along the strike of the fault. The parameter σ_E is the magnitude of the difference between the tractions on the fault before the fracture nucleates and the tractions on the fault during sliding. Because the sliding friction stress is uniform, σ_E varies with depth exactly as does the prestress. The amplitude of the particle motion scales directly with σ_E (7).

RESULTS

To illustrate the particle motion on the fault we show in Figure 3 time histories of particle velocity for points starting at the hypocenter and progressively moving toward the end of the fault on a line of constant depth. An important feature for microzonation is that the amplitude of the particle velocity increases in the direction of rupture propagation.

As pointed out by Archuleta and Frazier (1) this focusing of energy is a combination of both the directivity associated with a moving source (8) and the buildup of stresses on the fault ahead of a subsonic rupture. This focusing can be an important consideration in microzonation because the largest amplitude ground shaking depends not only on the stress but also the rupture velocity and its direction of propagation. It should be mentioned that if the rupture nucleates at depth and propagates towards the free surface, the particle velocity will increase in amplitude as it approaches the free surface. The free surface has the additional effect of nearly doubling the amplitude of the particle velocity should the rupture front break through the surface (1).

To see how the earth's surface might respond to an earthquake we have plotted contours of maximum horizontal particle velocity in Figure 4 for the cases of uniform stress with depth and variable stress with depth. Maximum horizontal particle velocity is calculated by first taking the absolute value of the vector sum of the parallel and transverse components of particle velocity for each node on the free surface for every time step of the computation. The maximum value attained during the entire process is then contoured using a linear interpolation between adjacent nodes. Depending on what information is considered important other variables such as peak displacement or maxima of individual components of particle velocity could be contoured.

In order to provide numerical estimates of the peak horizontal particle velocity we have assumed an average value for σ_E of 55 bars for both stress distributions. σ_E can underestimate the static stress drop by about 20 to 25 percent (1) due to the inertial effects of a dynamic rupture (9). With σ_E of 55 bars, $\mu = 3.3 \times 10^5$ bars, $\alpha = 6$ km/sec and $\beta = 3.5$ km/sec the contours are drawn at 0.9 m/sec, 0.8 m/sec, etc. One can see that in the case of variable stress with depth the areas near the ends of the fault have the highest values; whereas if the stress were uniform over the entire fault, the distribution of horizontal particle velocity is nearly uniform along the entire strike of the fault with a gradual flaring of the contours near the ends. It should be pointed out that the maximum values of horizontal particle velocity anywhere on the free surface were 1.0 m/sec and 1.9 m/sec for the variable stress and uniform stress, respectively. Thus the contour of 0.9 m/sec for a uniform prestress not only encloses a larger area but also encloses larger values of peak horizontal particle velocity. Although the uniform stress produces larger values near the fault and over a larger area, the differences in the contours between the uniform and variable stress cases decreases with distance from the fault. At a distance of approximately one fault depth the contours are almost indistinguishable. Although the finite element propagating stress-relaxation can be used to compute variables such as particle velocity and particle displacement, it is too expensive an approach for computing particle acceleration where the frequencies of interest are around 10 Hertz.

To calculate particle accelerations we have characterized the source as a propagating dislocation along a line at constant depth with the amplitude of the dislocation varying randomly from point to point. The form of the dislocation is derived from the dislocation computed in the stress relaxation problem. Since the method of Joyner and Boore (2) is strictly applicable only for the farfield, the dislocation rate rather than the dislocation is necessary to compute the accelerograms. We have taken the particle velocity function shown in Figure 3 at position (12., 5., 0.) as a representative for the entire faulting process. Using the Green's function for a full space and taking into account the free surface interaction by applying complex plane wave reflection coefficients we have computed accelerograms for the point(14.,0.,10.). A representative of the ensemble of accelerograms based on the stochastic method is shown in Figure 5. The acceleration records have been operated on by both the instrument response of an accelerograph with a natural frequency of 20 Hertz and damping 0.6 critical and by an attenuation operator (10) using a quality factor of 150 for shear values. The peak values of acceleration are 0.52g, 0.22g, and 0.19g, for the parallel, transverse and vertical directions, respectively where $g = 9.8 \text{ m/sec}^2$.

The methods of computing ground motion presented in this paper are approximations to our understanding of the earthquake source and the propagation paths. Further refinement of these methods plus the development of new techniques should lead to even better estimates of ground motion near a propagating fracture.

REFERENCES

- (1) Archuleta, R. J. and G. A. Frazier (1978). Three-dimensional numerical simulation of dynamic faulting in a halfspace, Bull. Seis. Soc. Am., 68, No. 3, p. 541-572.
- (2) Joyner, W. B. and D. M. Boore (1978). A statistical source model for synthetic strong motion seismograms, Earthquake Notes, 49, No. 1, p. 3.
- (3) Archuleta, R. J. and S. M. Day (1977). Near-field particle motion resulting from a propagating stress relaxation over a fault embedded within a layered medium, EOS, 58, p. 445.
- (4) Reid, H. F., (1910). Mechanics of the Earthquake, in California Earthquake, of April 18, 1906, II: Carnegie Inst., of Washington D. C. (updated in 1969).
- (5) Kostrov, B. V. (1964). Self-similar problems of propagation of shear cracks, J. App. Math. Mech. 38, p. 1077-1087.
- (6) Day, S. M. (1977). Finite element analysis of seismic scattering problems, Ph.D. Dissertation, University of California, San Diego.
- (7) Madariaga, R. (1976). Dynamics of an expanding circular fault, Bull. Seism. Soc. Am. 66, p. 639-666.

REFERENCES (continued)

- (8) Ben-Menahem, A. (1962). Radiation of seismic body waves from a finite source in the Earth, J. Geophys. Res. 67, p. 345-350.
- (9) Savage, J. C. and M. D. Wood (1971). The relation between apparent stress and stress drop, Bull. Seism. Soc. Am. 61, p. 1381-1388.
- (10) O'Neill, M. E. and D. P. Hill (1978). Frequency-dependent anelasticity and its effect on synthetic seismograms, Earthquake Notes 49, No. 1, p. 54.

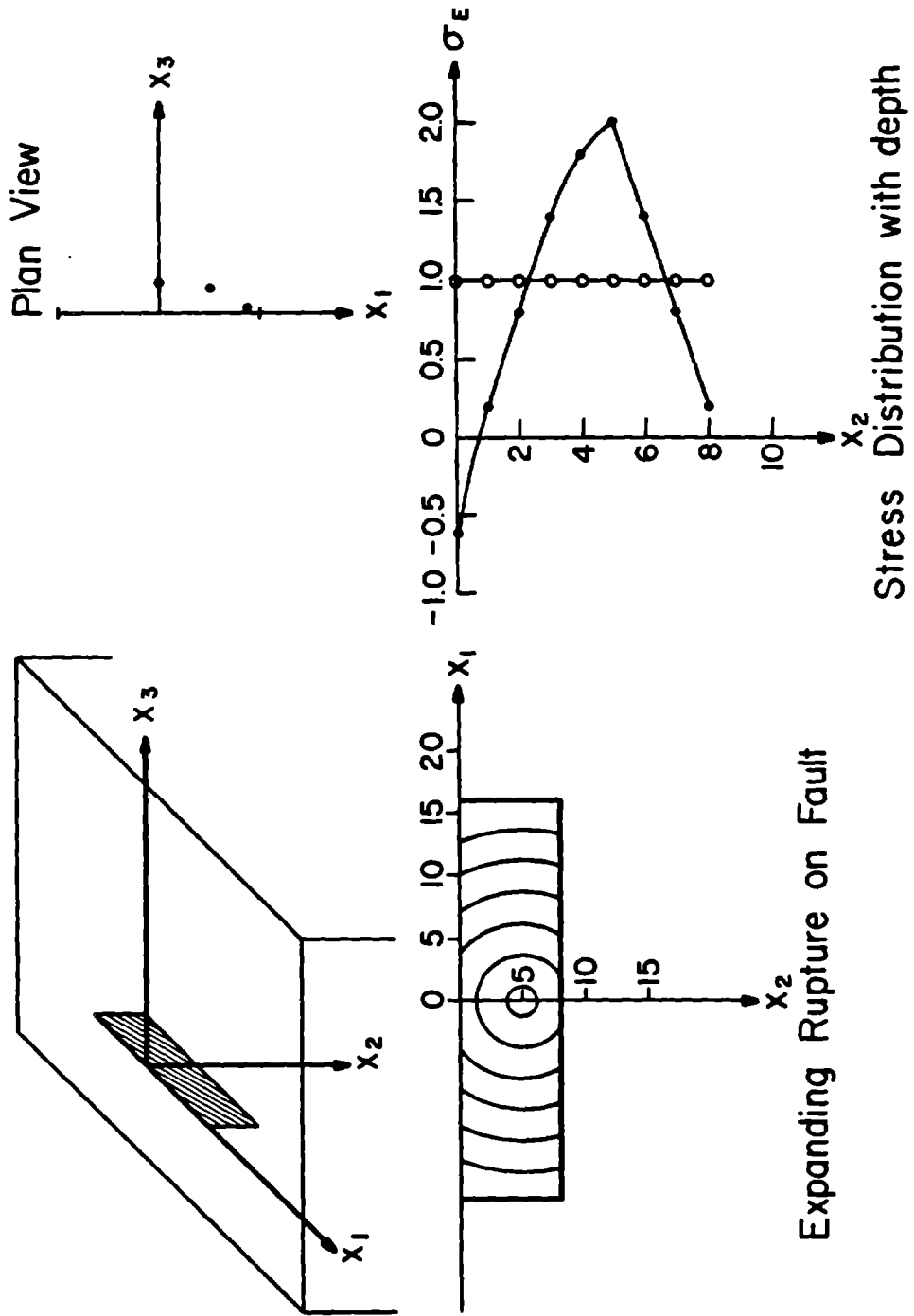


Figure 1. Schematic of fault, rupture surface and stress distribution.

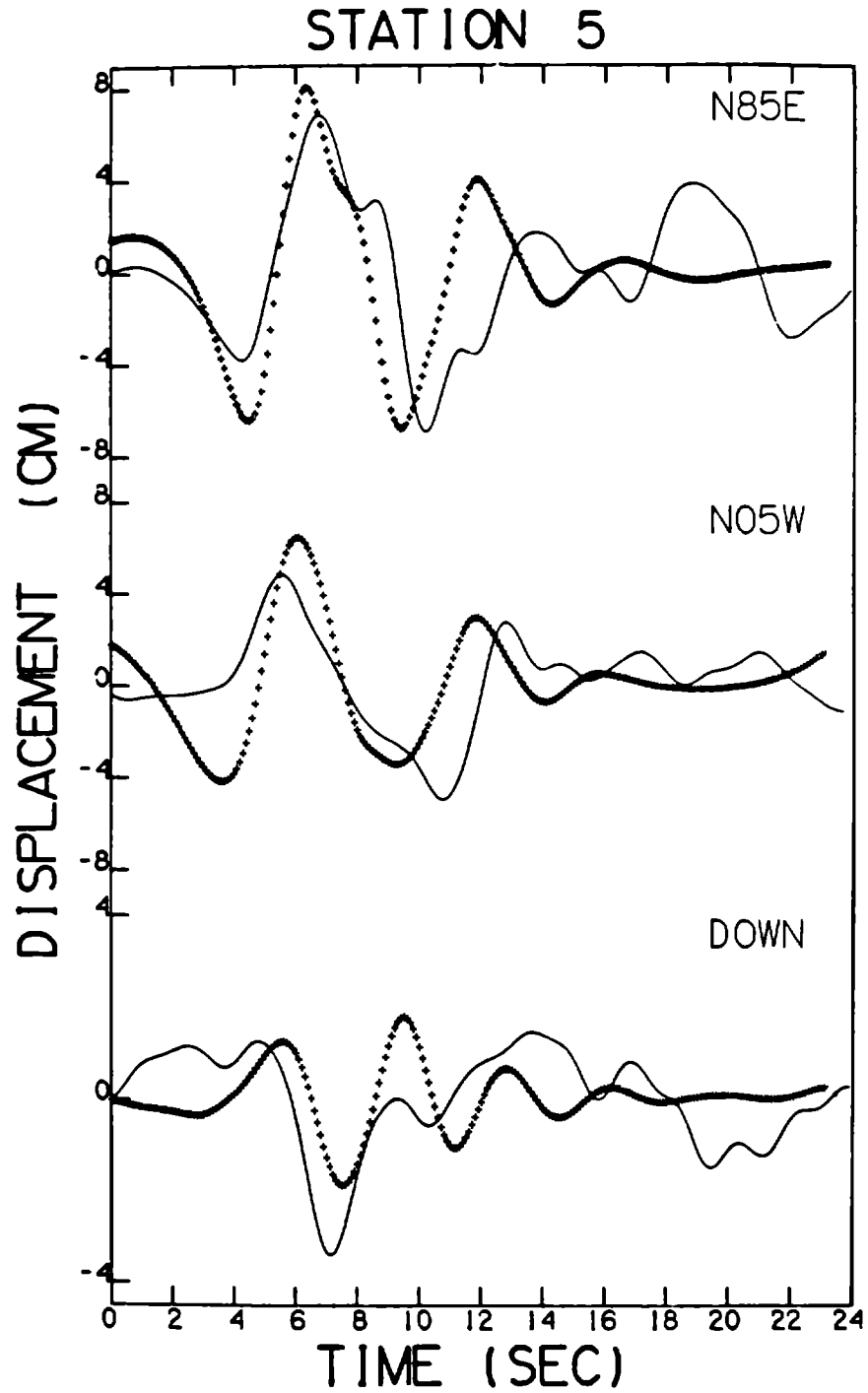


Figure 2. Comparison of synthetic (+) and recorded (-) ground motion of the 1966 Parkfield earthquake.

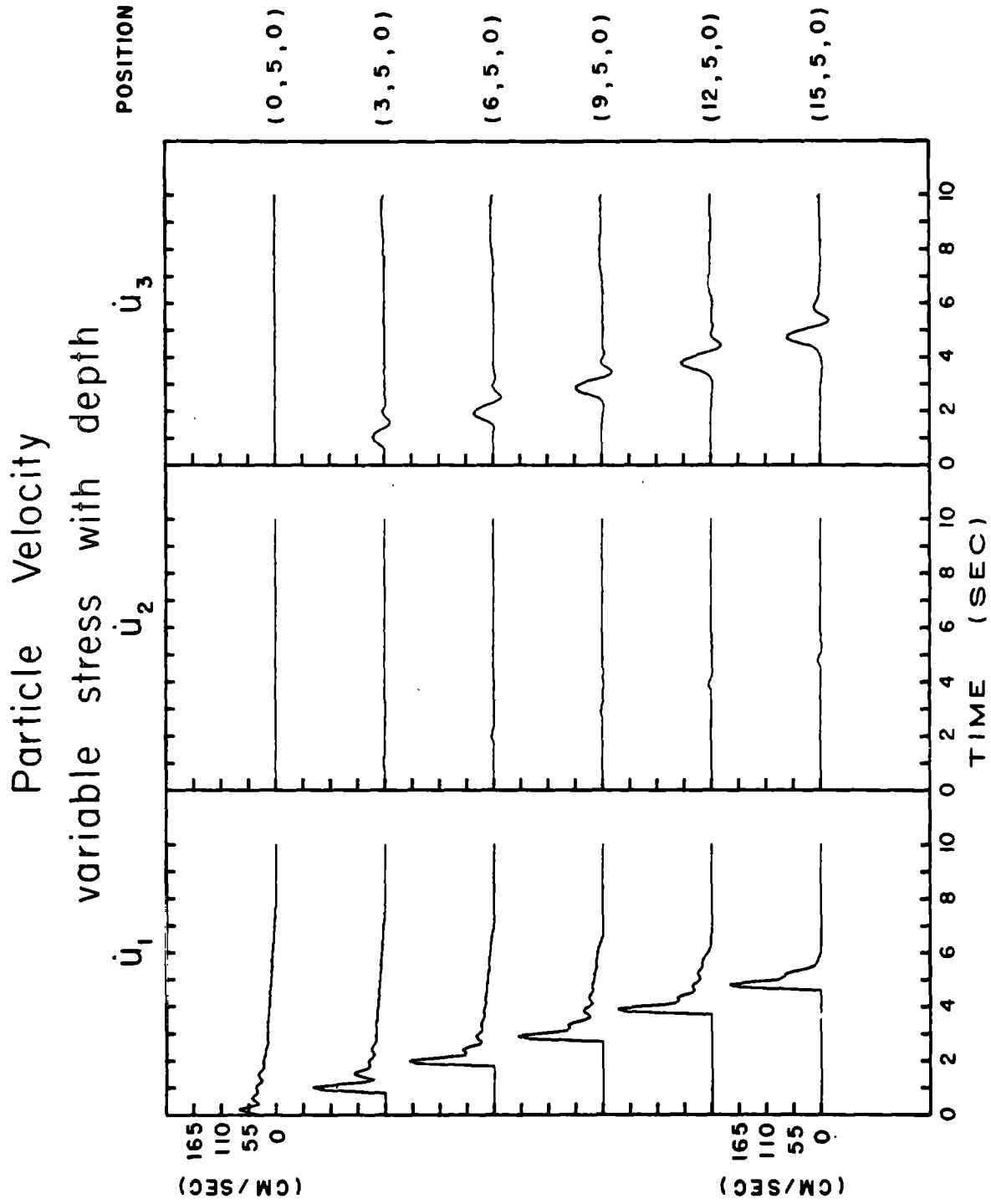
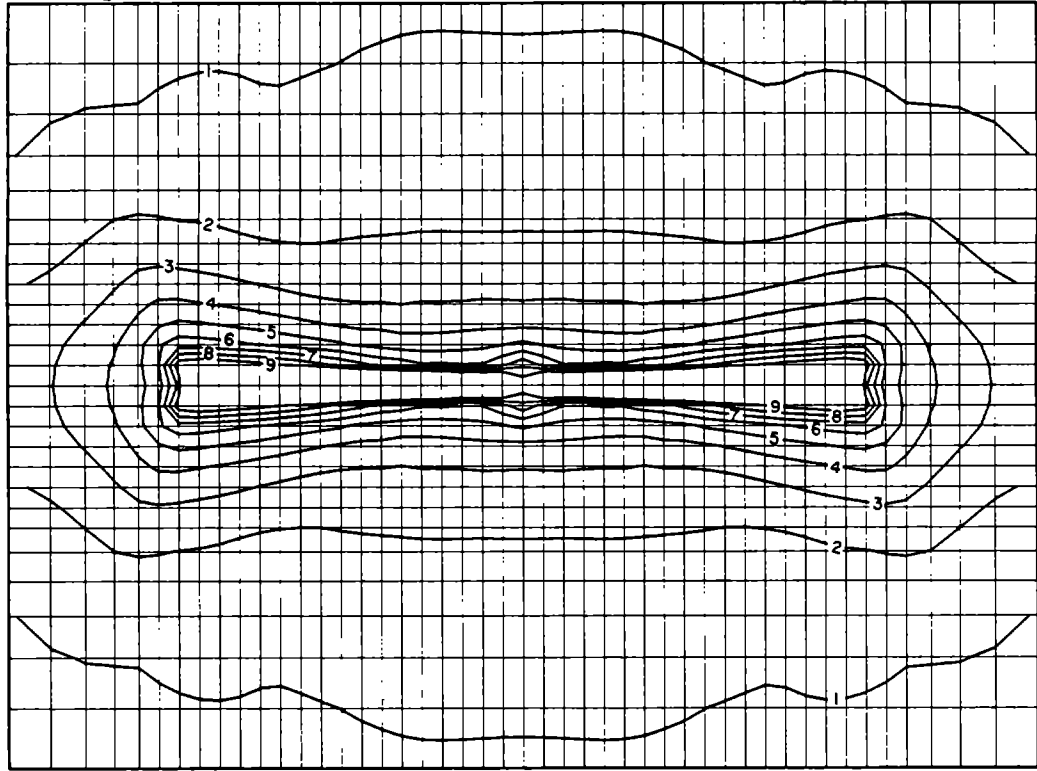


Figure 3. Particle velocity time histories on the fault surface.

Contours of Maximum Horizontal Particle Velocity
 Uniform effective stress (σ_e) Fault 32 X 8 Hypocenter (0, 5, 0)
 $\alpha = 6.0$ Km/sec $\beta = 3.5$ Km/sec $\rho = 2.7$ Kg/m³ $v = 0.9 \beta$
 For $\sigma_e = 55$ bars, contours are drawn for 0.9 m/sec, 0.8 m/sec....



Contours of Maximum Horizontal Particle Velocity
 Variable effective stress (σ_e) Fault 32 X 8 Hypocenter (0, 5, 0)
 $\alpha = 6.0$ Km/sec $\beta = 3.5$ Km/sec $\rho = 2.7$ Kg/m³ $v = 0.9 \beta$
 For $\sigma_e = 55$ bars, contours are drawn for 0.9 m/sec, 0.8 m/sec....

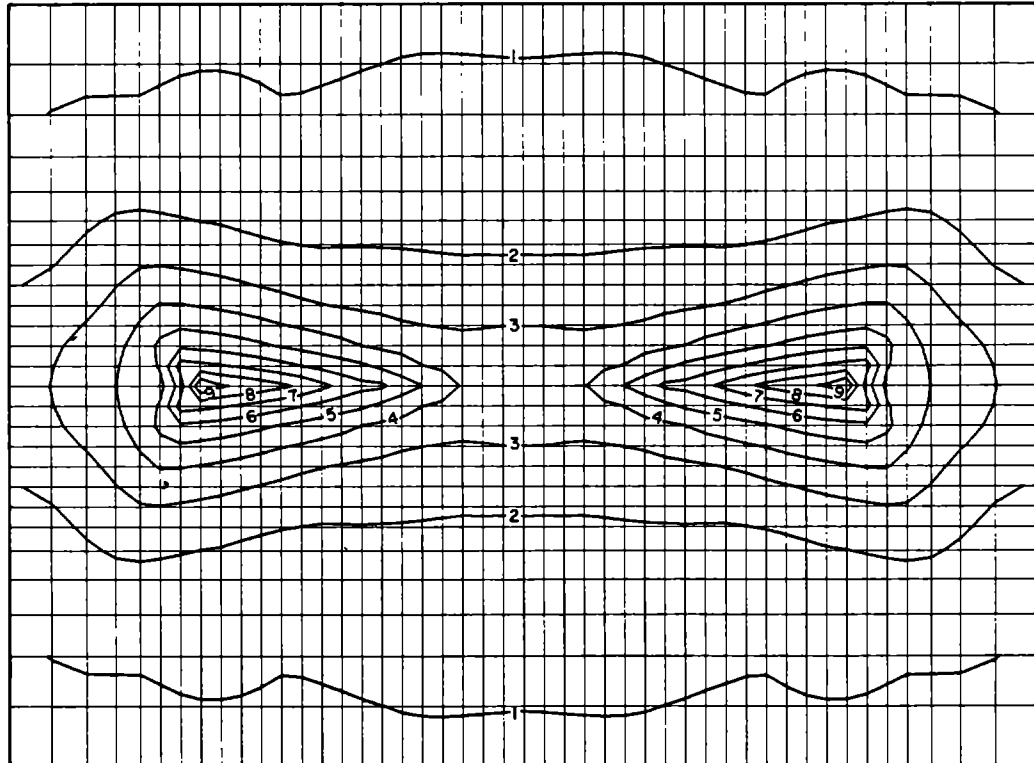


Figure 4. Contours of particle velocity on the free surface.

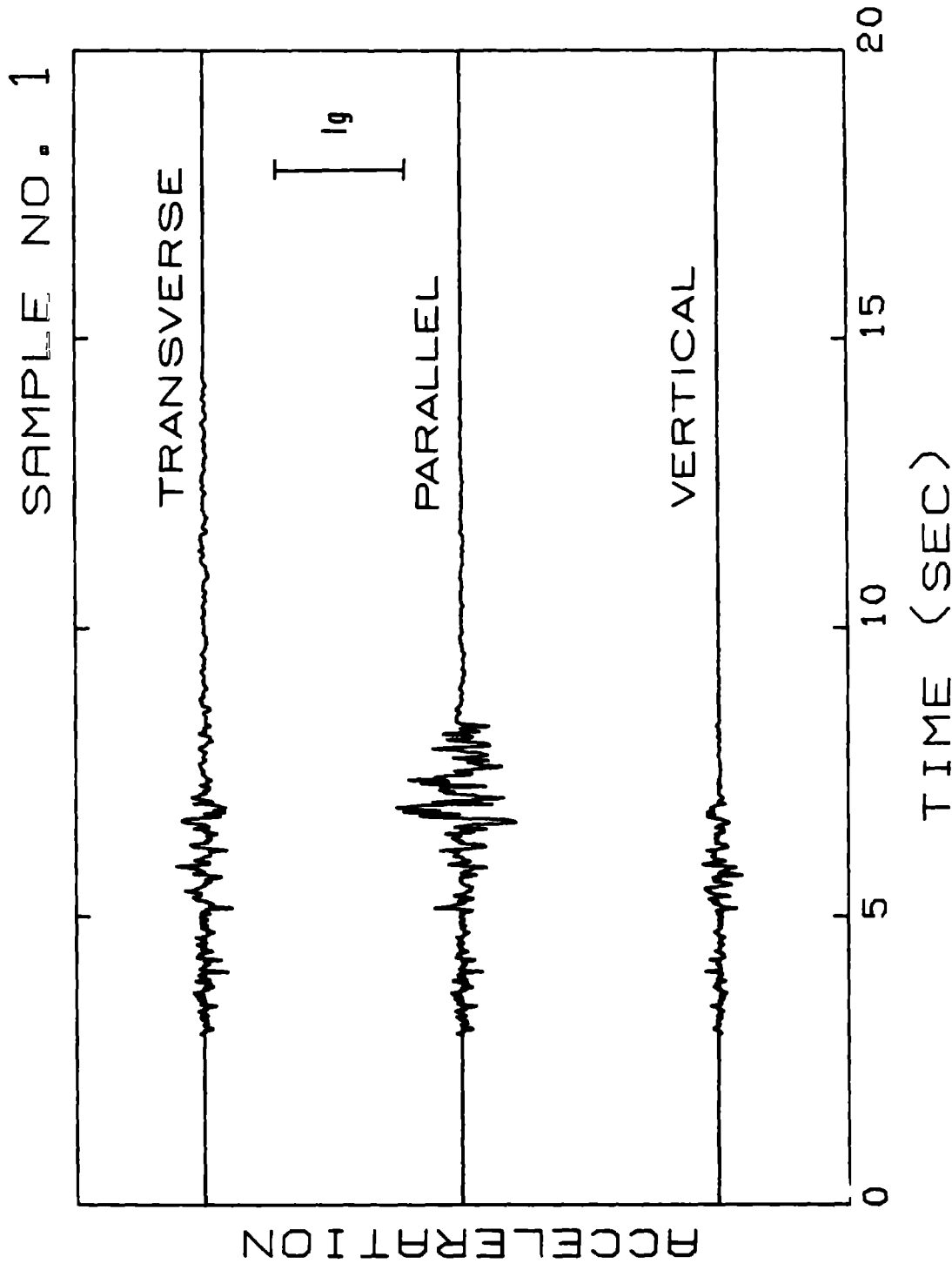


Figure 5. Components of acceleration computed for a particle on the free surface at (14.,0.,10.)

INTENTIONALLY BLANK

Liquefaction Potential Map of San Fernando Valley, California

by

T.L. Youd¹, J.C. Tinsley², D.M. Perkins³, E.J. King⁴
and R.F. Preston⁴

ABSTRACT

Ground failure caused by liquefaction is a primary hazard associated with earthquakes. A first step in avoiding or mitigating this hazard is to recognize where liquefaction is likely to occur. A liquefaction potential map has been compiled for the San Fernando Valley, California, showing areas where conditions may be favorable for the development of liquefaction. The map incorporates assessments of age and type of sedimentary deposits, ground water depth, and expected seismicity into the delineated zones. This map is useful to planners, building officials, engineers, and others responsible for minimizing seismic risk because it points out areas where potential hazards exist and where further investigation, regulation, zoning, or other measures might be required. The map is not sufficient for evaluation of the actual liquefaction potential at an individual site. Site-specific geotechnical investigations are required to make such an assessment.

INTRODUCTION

Ground failures generated by liquefaction have been a major cause of damage during past earthquakes and pose considerable potential for damage and injury during future temblors. For example, during the 1971 San Fernando, California, earthquake, liquefaction-induced ground failures inflicted irreparable damage to several buildings at the San Fernando Valley Juvenile Hall and caused major damage to the partly completed Jensen Water Filtration Plant. Such failures do not occur at random, but rather are limited to certain geologic and hydrologic settings and to certain types of materials. A threshold seismic shaking intensity is also required to generate ground failure. This paper presents an analysis of these factors and their geographical distribution in the San Fernando Valley and a map to show general areas where potential for liquefaction and associated ground failure may exist. Site-specific studies are required to evaluate the potential beneath any specific parcel of land.

The procedure used to develop the liquefaction potential map is a combination of the techniques proposed by Youd and Perkins (9) and Youd and others (8). The technique of Youd and others was used to make a liquefaction potential map for the southern San Francisco Bay area. The procedure used here requires the development of two constituent maps, a liquefaction susceptibility map and a liquefaction opportunity map. The susceptibility map delineates areas where liquefiable materials are most

¹Research Civil Engineer, U.S. Geological Survey, Menlo Park, Calif.

²Geologist, U.S. Geological Survey, Menlo Park, Calif.

³Geophysicist, U.S. Geological Survey, Golden, Colo.

⁴Physical Science Technician, U.S. Geological Survey, Menlo Park, Calif.

likely to occur. The opportunity map shows recurrence intervals for earthquake shaking strong enough to generate liquefaction in susceptible materials. These maps are then superimposed to form a liquefaction potential map.

LIQUEFACTION SUSCEPTIBILITY MAP

The liquefaction susceptibility map developed herein incorporates the following factors that affect liquefaction susceptibility: age and type of sedimentary deposits; standard penetration resistance of cohesionless sediments; and depth to perched or other ground water.

Sedimentary Deposits

Analyses of historical occurrences of liquefaction, in general, indicate that the more recently a sediment is deposited, the more likely it is to be susceptible to liquefaction, and that certain types of deposits, such as river channel and flood-plain deposits, are more susceptible to liquefaction than other deposits, such as alluvial fan deposits (9). Grain size distribution and packing also influence susceptibility. Sand and silty sand are the textural classes most likely to be adversely affected. In general, the more loosely the grains are packed, the more susceptible the sediment is to liquefaction. Standard penetration resistance is commonly used by engineers as an index of density of packing; the smaller the penetration resistance, the more likely the sediment will liquefy.

The San Fernando Valley lies in the Transverse Ranges structural province of southern California. The valley is an asymmetric basin filled chiefly with Miocene and younger (less than 20 million years old) sedimentary rocks. The relatively flat surface of the valley is underlain by unconsolidated sediments of middle to late Pleistocene or younger age that are as thick as 650 ft (200 m) (7). The exposed unconsolidated sediments are herein subdivided into three units -- most recent Holocene sediments (R), other Holocene sediments (H), and late Pleistocene deposits (P). The distribution of these units is shown on the map in Fig. 1. The margins of the basin comprise undifferentiated Pliocene to middle Pleistocene deposits (TQ) which include the Saugus and Pacoima Formations of Oakeshott (4), undifferentiated Tertiary sedimentary rocks (T), undifferentiated Mesozoic sedimentary rocks (K), and pre-Tertiary igneous and metamorphic rocks in the mountains mapped collectively as basement complex (BC).

Areas mapped as most recent Holocene sediments are chiefly those known to have been flooded historically, where the most recent deposition is known or presumed to have occurred. The primary data used to delineate the extent of flooding include field notes and unpublished maps prepared by the Los Angeles Flood Control District that show and describe areas inundated during floods in 1934, 1938, 1941, 1943, 1944, 1952, 1954, and 1956. Other data used include comparative photo-interpretive studies of 1928 and 1938, aerial photography at a scale of 1:24,000 or larger. The 1938 photographs were taken three to five months after the major floods of March, 1938. Features on the photographs used to delineate areas of recent deposition or flooding include changes in patterns of distributary channels or alluvial fans, areas where row crops, roads and other cultural features were washed out, areas adjacent to streams that were incised to depths less than 5 ft (1.5 m), and areas characterized topographically by bar and swale channel deposits. We have specifically excluded from the most recent Holocene unit areas that were locally inundated along streets where culverts

plugged and water simply backed up. In all cases, interpretations reflect our efforts to identify and delineate the youngest stages of a very youthful depositional system because these are most likely to contain sediments susceptible to liquefaction.

Areas mapped as other Holocene sediments are differentiated chiefly on the basis of lack of record of recent inundation, a topographic position slightly higher than the most recent Holocene unit and by undeveloped to very weakly developed cumulative pedogenic soil profiles (chiefly entisols, inceptisols, and vertisols) typical of Holocene deposits. Soil maps prepared by the U.S. Bureau of Soils (2), and the U.S. Department of Agriculture (6) were the primary data used to delineate this Holocene unit.

Areas mapped as late Pleistocene deposits were differentiated on the basis of morphology and pedological development. They generally are exposed as topographic benches and terraces near the margins of the valley and on the up-thrown side of thrust faults in the northern part of the valley. They are also characterized by surface soils with textural "B" horizons. Under present climatic conditions, to form such a soil profile requires a period of development that began in Pleistocene time.

By the criteria set out in Youd and Perkins (9), water-saturated, clay-free sediments in the most recent Holocene unit generally are expected to have high susceptibility to liquefaction; clay-free sediments in the other Holocene unit generally would be expected to have moderate susceptibility, and clay-free sediments in the late Pleistocene unit would be expected to have low susceptibility. The qualitative assessments of liquefaction susceptibilities were further verified by comparing them with liquefaction susceptibilities determined from standard penetration data. The evaluation of liquefaction susceptibility from standard penetration data followed the procedure previously used to compile a liquefaction potential map for the southern San Francisco Bay region. Plots were made of standard penetration resistance versus depth for the three youngest (R, H, and P) sedimentary units. Thicknesses of the two Holocene units have been inferred from descriptive logs of boreholes by identifying subsurface features such as, (a) an oxidized clay-rich layer which may indicate an ancient soil horizon that likely formed on the late Pleistocene unit before deposition of the Holocene unit, (b) an abrupt increase in penetration resistance not caused by intersecting a gravel layer, and (c) an estimated maximum thickness of the most recent Holocene unit of about 12 ft (3.6 m), based on rates of vertical accretion.

Using the criteria developed for the southern San Francisco Bay region (8), percentages of penetration data were grouped into high, moderate, and low liquefaction susceptibility categories for each sedimentary unit (Table 1). These categories are based on analyses developed in the simplified procedure for evaluating soil liquefaction potential formulated by Seed and Idriss (5) and analyses used by Youd and others (8) to map the San Francisco Bay area. The high susceptibility category represents saturated sediments that would be likely to liquefy in a nearby moderate ($M=6.5$) earthquake (energy source within 10 mi or 16 km) or a distant, very large ($M=8$) earthquake (energy source within about 60 mi or 100 km). The moderate susceptibility category indicates sediments that might liquefy during a nearby large ($M=8$) earthquake (energy source within 10 mi or 16 km). Low susceptibility indicates sediments that should not liquefy even when shaken by a nearby large earthquake. Assumptions made in deriving these categories are the same as those used in the San Francisco Bay region (8)

Table 1.--Evaluation of liquefaction susceptibility in clay-free granular layers from standard penetration data.

Sedimentary unit	Percentage of standard penetration data in susceptibility categories			Number of tests
	High	Moderate	Low	
Most recent Holocene	61	33	6	153
Other Holocene	39	49	12	618
Late Pleistocene	20	39	41	443

and include unit weight of 100 lb/ft³ (1.6 gm/cm³), a maximum surface acceleration of 0.2 *g* and 10 significant loading cycles for the nearby moderate (M=6.5) earthquake, and a 0.5 *g* maximum surface acceleration and 30 significant loading cycles for the nearby large (M=8) earthquake. The influence of depth to water table was taken into account in the calculation. These data (Table 1) show that saturated clay-free sediments in the youngest unit can be expected to have high susceptibility to liquefaction; similar sediments in the other Holocene unit can be expected to have moderate susceptibility; and saturated clay-free sediments in the late Pleistocene unit generally have moderate or low susceptibility to liquefaction.

Ground Water Depth

One of the primary factors controlling the distribution of liquefiable sediments in the San Fernando Valley is depth to ground water including perched ground water. Liquefaction susceptibility generally decreases with depth of the ground water table for two reasons: (a) The deeper the water table, the greater is the normal effective stress acting on saturated sediments at any given depth. Liquefaction susceptibility decreases with increased normal effective stress. (b) Age, cementation, and compactness of sediments generally increase with depth. Each of these factors also increases resistance to liquefaction. Thus, as depth to the water table increases, and as the saturated sediments become older, more cemented, more compact, and more stressed, the less likely they are to liquefy during an earthquake.

A map showing depth to ground water, including perched ground water, was prepared for part of the San Fernando Valley (Fig. 2). The lines on the map are not contour lines in the usual connotation used by hydrologists, i.e., an equipotential surface. Rather, they enclose areas where our data show that either perched or unconfined ground water has been recently found within the specified intervals of depth. This map was compiled from borehole data and well information supplied by the several agencies and firms acknowledged in this report. Because of sparsity of data in some areas and variations in amounts and elevations of ground water, construction of the map required considerable averaging, generalizing, interpolation, and extrapolation. Where depth lines are not tightly constrained, they are dashed; where they are speculative or positioned by factors other than borehole and well data, they are queried. The following problems are among those that arose in construction of the map. (a) Borings that intersect the water table are sparse in many areas. (b) Water levels in some deep wells may have been higher than the phreatic surface in the surrounding

soil because of artesian pressures at depth. (c) Some measurements, particularly along freeways and certain major storm drains, were recorded as much as 30 years ago, and water levels may have changed in the interim. Where several measurements have been made in one well over a period of years, the average of the measurements taken in the past seven years was used. (d) Seasonal fluctuations in water levels perturb the consistency of the data. (e) Irregular impermeable layers with poorly defined boundaries commonly retain perched water. (f) Errors may have been made in measuring water table levels in some boreholes. These difficulties were accounted for and corrected to the extent possible, but space does not allow enumeration here of these corrections.

With respect to depth to ground water, the following criteria were applied to liquefaction susceptibility: For ground water depths less than 10 ft (3.0 m), maximum possible susceptibility is very high. For water depths between 10 ft (3.0 m) and 30 ft (9.1 m), maximum possible susceptibility is high. For depths between 30 ft (9.1 m) and 50 ft (15.2 m) maximum susceptibility is low. For water depths greater than 50 ft (15.2 m) maximum possible susceptibility is very low. These criteria are based in part on criteria suggested by Youd and Perkins (9).

Map Compilation

The criteria developed in the preceding section and summarized in Table 2 were used to compile a liquefaction susceptibility map for the San Fernando Valley. These criteria were applied to the data compiled on Figs. 1 and 2 to derive the susceptibility map in Fig. 3. In order to show better the detail with which this type of map can be constructed for areas where sufficient data are available, a segment of the susceptibility map is shown at larger scale in Fig. 4. Note that the susceptibility maps presented here represent estimated average climatic conditions. Ground water levels and hence susceptibilities are likely to be higher during wet seasons and lower during extremely dry cycles.

Table 2.--Criteria used in compiling liquefaction susceptibility map

Sedimentary unit	Probable susceptibility of clay-free granular layers		
	Ground water depth, ft(m)		
	<30(9.1)	30(9.1)-50(15.2)	>50(15.2)
Most recent Holocene	High	Low	Very Low
Other Holocene	Moderate	Low	Very Low
Late Pleistocene	Low	Low	Very Low
Late Pliocene and early Pleistocene	Very Low	Very Low	Very Low
Tertiary	Very Low	Very Low	Very Low

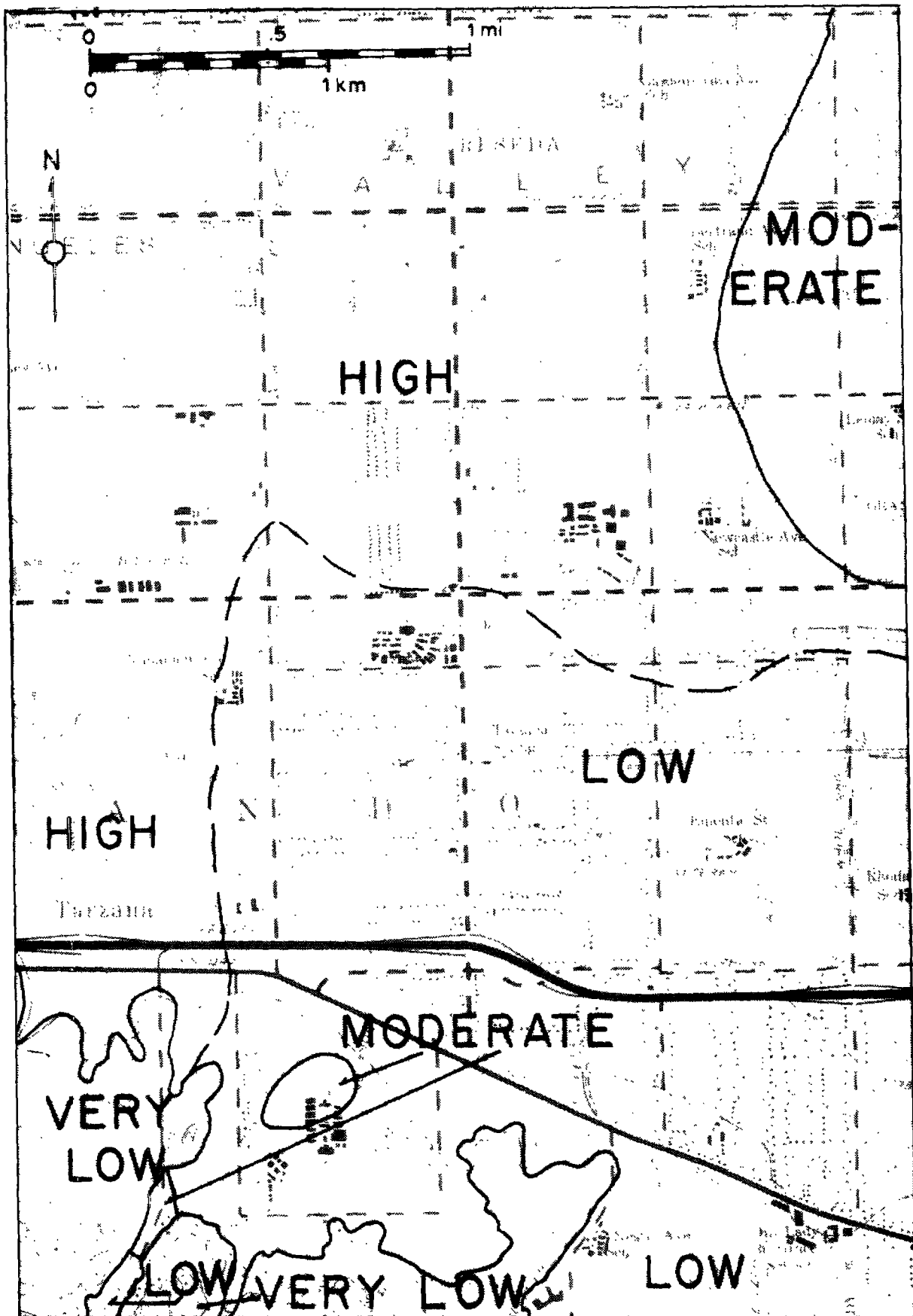


Fig. 4. Enlarged liquefaction susceptibility map for Tarzana area of the San Fernando Valley, California. Susceptibility categories same as Fig.

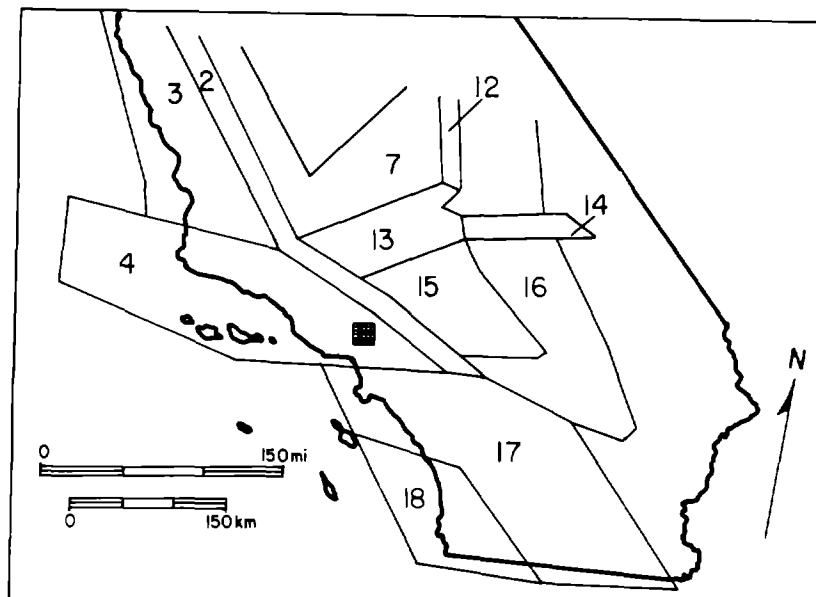


Fig. 5. Seismic source zones in the vicinity of the San Fernando Valley. Only zones 2,4,13, and 17 are significant to liquefaction opportunity in the San Fernando Valley. San Fernando Valley (hachured area) lies in the eastern corner of zone 4. San Andreas fault province corresponds to zone 4.

Table 3.--Normalized seismic parameters for source zones

Zone No.	Number of intensity V's/100 yrs/10 ⁴ km ² N	b-value for epi-central intensity ² b _I	Maximum intensity ¹ I _o	Maximum magnitude ¹ M _c
2	60.6	-.40 up to XI then flat	XII	8.5
3	12.5	-.45	XI	7.9
4	24.2	-.45	XI	7.9
13	129.65	-.45	XI	7.9
14	136.56	-.45	XI	7.9
15	----	-.53	VIII	6.1
16	20.8	-.50	X	7.3
17	70.4	-.45	XI	7.9
18	2.5	-.50	X	7.3

¹Modified Mercalli Intensity

²b-value for magnitude (b_M) = 0.6 b_I

Liquefaction Opportunity Map

A liquefaction opportunity map delineates recurrence intervals for earthquake shaking strong enough to produce liquefaction in susceptible materials. Information needed to compile an opportunity map includes an estimate of frequencies, magnitudes, and location of expectable future earthquakes and a relation between earthquake source characteristics and the distance from the source to the bound of a zone encompassing sites where liquefaction could be generated. The estimated earthquake sources and frequencies of occurrence in the San Fernando Valley region used in this study (Fig. 5, Table 3) are those previously defined by Algermissen and Perkins (1). The distance relation used is that given by Youd and

Perkins (9). The liquefaction opportunity map plotted on Fig. 6 was derived from these two sets of information. The map shows the return period (inverse annual probability) for liquefaction opportunity from the San Fernando Valley north to the San Andreas fault. The liquefaction opportunity varies only about 20 percent over this area and is effectively constant across the San Fernando Valley; the return period is about 46 years. Figure 7 shows the contribution of the various sources to the annual probability along a meridian section of the map in Figure 6. In general, earthquakes of magnitude less than 6 contribute an insignificant amount to the overall probability of liquefaction. Roughly half of the contribution comes from large-magnitude events occurring locally in the Transverse Ranges province (zone 17, fig. 5) and along the San Andreas fault (zone 2, fig. 5). This contribution is roughly constant across the San Fernando Valley. Large-magnitude events occurring near the Garlock fault to the north are balanced by large-magnitude events occurring south of the Transverse Ranges. As the effect of one region decreases across the San Fernando Valley, the effect of the other region increases.

Liquefaction Potential Map

Superposition of the maps in Figs. 3 and 4 with the map in Fig. 6 yields a liquefaction potential map. In this instance, the return period is constant at 46 years across the area in question, and hence no return period contours appear on the San Fernando Valley area. Thus, for a 46-year return period, the maps in Figs. 3 and 4 show the areas where strong ground shaking is likely to produce liquefaction in sediments with high susceptibility.

SUMMARY AND CONCLUSIONS

A liquefaction potential map has been compiled for the San Fernando Valley, California. The map incorporates assessments of age and type of sedimentary deposits, ground water depth, and expected seismicity into the delineated zones. This map is useful to planners, building officials, engineers, and others responsible for minimizing seismic risk by pointing out areas where potential hazards exist and where further investigation, regulation, zoning, or other measures might be required. The map is not sufficient for evaluation of the actual liquefaction potential at an individual site. Site specific geotechnical investigations are required to make such an assessment.

ACKNOWLEDGMENTS

Appreciation and acknowledgement are given to the following governmental agencies and private firms, who freely provided information for use in this study: U.S. Army Corps of Engineers, California Department of Transportation, California Department of Water Resources, Los Angeles County Flood Control District, Los Angeles County Engineer.

References Cited

- (1) Algermissen, S.T., and Perkins, D.M., 1976, A Probabilistic Estimate of Maximum Ground Acceleration in the Contiguous United States; U.S. Geological Survey Open-File Report 76-416.
- (2) Holmes, L.C., 1919, Soil Survey of the San Fernando Valley area, Calif., *in* Field Operations of the Bureau of Soils 1915; U.S. Department of Agriculture, Bur. Soils, 17th rept., pl. 63, scale 1:62,500.

- (3) Jennings, C.W. and Strand, R.G., 1969, Geologic Map of California, Los Angeles sheet (scale 1:250,000): Calif. Division of Mines and Geology.
- (4) Oakeshott, G.B., 1958, Geology and Mineral Deposits of San Fernando Quadrangle, Los Angeles County, Calif: Calif. Division of Mines Bulletin 172, 147 p., 3 pls.
- (5) Seed, H.B., and Idriss, I.M., 1971, Simplified Procedure for Evaluating Soil Liquefaction Potential: Journal of the Soil Mechanics and Foundations Division, Amer. Soc. of Civil Engineers, v. 97, no. SM9, p. 1249-1273.
- (6) U.S. Department of Agriculture, 1977, Soil Survey of Los Angeles County, Calif. west San Fernando Valley area: an interim, unedited report. 186 p. 5 pl.
- (7) Wentworth, C.M. and Yerkes, R.F., Geologic Setting and Activity of Faults in the San Fernando Area, Calif; *in* The San Fernando, Calif. Earthquake of February 9, 1971: U.S. Geological Survey Professional Paper 733, p. 6-16.
- (8) Youd, T.L., Nichols, D.R., Helley, E.J., and Lajoie, K.R., 1975, Liquefaction Potential, *in* Studies for Seismic Zonation of the San Francisco Bay Region: U.S. Geological Survey Professional Paper 941-A, p. A68-A74.
- (9) Youd, T.L., and Perkins, D.M., 1978, Mapping Liquefaction-Induced Ground Failure Potential: Journal of the Geotechnical Engineering Division, Amer. Soc. of Civil Engineers, v. 104, No. GT4, p. 433-446.

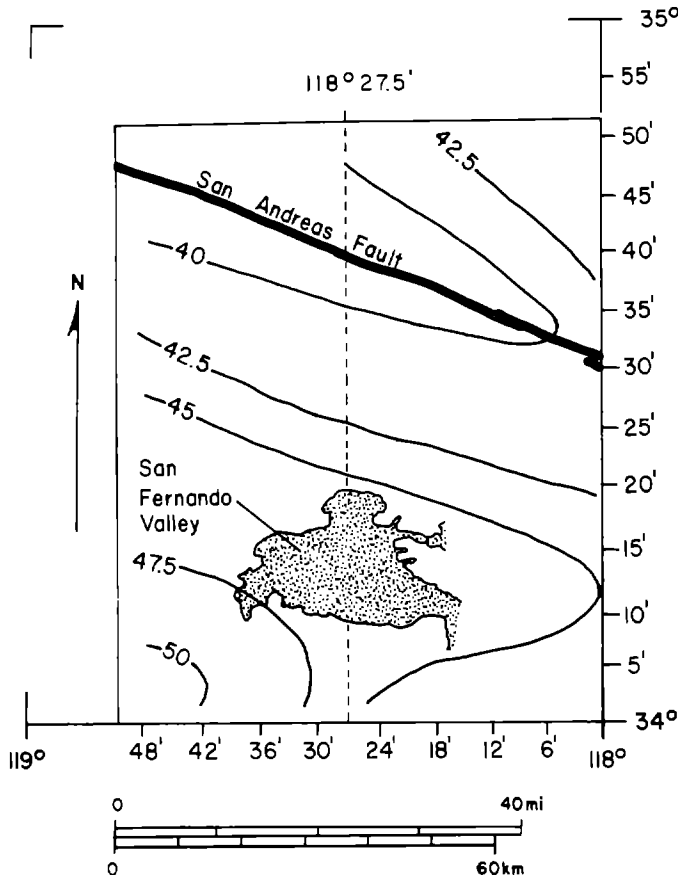


Fig. 6. Return period for liquefaction opportunity in the vicinity of the San Fernando Valley

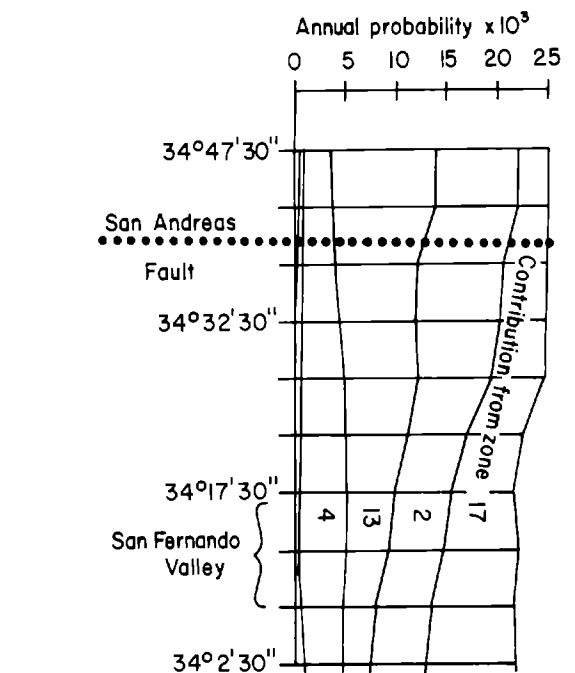


Fig. 7. Contributions to annual probability of liquefaction opportunity for sites along 188° 27.5' meridian. Major contributions to annual probability are due to large magnitude ($M > 6.4$) earthquakes located south of the Transverse Ranges (zone 17), along the San Andreas fault (zone 2), in the vicinity of the Garlock fault (zone 13), and in the vicinity of the Transverse Ranges

PRELIMINARY ASSESSMENT OF SEISMICALLY INDUCED LANDSLIDE SUSCEPTIBILITY

by

D. K. Keefer^I, G. F. Wieczorek^{II}, E. L. Harp^I and D. H. Tuel^{III}

ABSTRACT

Earthquake-induced landslides have taken a large toll in loss of life and property. We are currently engaged in studies aimed at determining which types of landslides are most common during earthquakes and at establishing criteria for mapping susceptibility of slopes to earthquake-induced landsliding. This preliminary summary of our findings deals primarily with the types and abundance of landslides that occurred during 15 historic earthquakes. Preliminary criteria have also been developed for mapping susceptibility to some kinds of landsliding, and these criteria are used herein to prepare an experimental susceptibility map of an area near San Francisco, Calif.

INTRODUCTION

On Sunday afternoon, May 31, 1970, an earthquake of magnitude 7.7 struck Peru. The shock caused a large mass of ice and rock to break away from Mount Huascaran, the highest mountain in the Peruvian Andes. The debris cascaded 600 m down the steep upper slopes of the mountain and landed on the surface of a glacier. It accelerated as it slid across the glacier and poured into the Llanganuco Valley. Below it lay the towns of Yungay and Ranrahirca. Mixed with glacial ice, surface water, and saturated soil, the mass became a huge debris flow and swept down the valley at velocities of 280 to 400 km per hour (28). Eleven kilometers from its source, a relatively small lobe of debris splashed over a ridge 200 to 250 m high and buried the town of Yungay. Almost simultaneously, the main debris lobe crashed into Ranrahirca, devastating it and the small villages around it. Within four minutes the landslide had killed more than 18,000 people (28).

Past Ranrahirca, the debris followed the Llanganuco Valley to its confluence with the Rio Santa. It then turned and flowed down the Santa Valley for more than 50 km, inundating many agricultural fields and causing extensive damage to dwellings, highways, communication networks, and a hydroelectric facility. The Peruvian earthquake was one of the most destructive shocks in recent history, and this single landslide caused approximately 40% of the deaths and a large but undetermined portion of the property damage attributed to that shock (28).

Geologic and historic evidence indicated that Yungay and Ranrahirca were in areas of severe landslide hazard. Eight years earlier, a debris flow not triggered by an earthquake had buried Ranrahirca, killing approximately 4,000 people. In fact, during the 30 years before the earthquake, eight destructive rock fall-avalanches and debris flows had occurred in the Santa Valley (28). None of these landslides were triggered by earthquakes indicating that the landslide hazard is acute there even under non-seismic conditions. According to geologic evidence, many large prehistoric

I Geologist, U. S. Geological Survey, Menlo Park, Calif.

II Research Civil Engineer, U. S. Geological Survey, Menlo Park, Calif.

III Clerk-Typist, U. S. Geological Survey, Menlo Park, Calif.

avalanches and flows also occurred in this area, and Yungay itself was probably built on a flow or avalanche deposit (28). If this evidence had been properly evaluated and acted on before the earthquake, the catastrophes at Yungay and Ranrahirca might have been averted by moving the communities to safer areas.

Many hundreds of thousands of landslides have been triggered by earthquakes, and they have caused enormous losses of life and property. Many landslides occurred in areas where the historic evidence of landslide hazard was not as clear as in the Mount Huascaran area. In fact, many occurred in areas with little or no record of slope instability under nonseismic conditions. We are, therefore, presently studying data from historic earthquakes to determine which types of landslides are most commonly triggered by earthquakes and which geologic environments are most susceptible to seismically triggered slope failure. Our goal is to apply this kind of information to the development of criteria for mapping earthquake-induced landslide susceptibility. Our results are preliminary. This paper presents data on landslides in 15 historic earthquakes and an experimental susceptibility map prepared as a demonstration of how criteria developed in this study can be used.

LANDSLIDE OCCURRENCE DURING HISTORIC EARTHQUAKES

Landslide data have been compiled (Table 1) from 15 historic earthquakes which range in size from the great M 8.6 Kansu, China event of 1920 to the moderate-size M 5.7 Fortuna-Rio Dell, Calif. shock of 1975. We have participated in field investigations following the 1977 San Juan, Argentina, the 1976 Guatemala (11) and the 1975 Fortuna-Rio Dell (18) earthquakes. For the other earthquakes, we have relied almost exclusively on published reports.

Landslide names used in Table 1 conform to those of Varnes (33), which is a revision of Varnes' earlier landslide classification system (32). One major difference in terminology between this report and that of Varnes (33) is in the use of the term "landslide." In this report, all types of slope failures, including falls, avalanches, and flows as well as true slides are considered types of landslides. In Varnes (33), "slope movement" is the general term used to denote all types of movement. In some of the categories in Table 1, two or more types of landslides are lumped together because the published data did not permit more subdivision.

Only landslides that were clearly outlined and that moved far enough to form clearly identifiable deposits were included in Table 1. Thus, sets of cracks or fissures that may have been incipient landslides were not considered. Where more than one type of material or more than one mode of movement were involved in the landslide, it was classified by the predominant material and mode of movement.

Abundances of landslides are grouped into three classes in Table 1. Data on landslide abundances were not always expressed quantitatively in published reports, so in many cases judgments were based on brief accounts of the geographic limits of the regions within which landsliding occurred and our estimates of the number of landslides per unit area in these regions. Geographic coverage of post-earthquake investigations was probably not complete for the 1920 Kansu, 1960 Chile, 1931 Hawke's Bay, or 1968 Inangahua earthquakes, so the information in Table 1 may underestimate the true extent of landsliding for those events. Relative abundance

TABLE 1: LANDSLIDES TRIGGERED BY EARTHQUAKES

LANDSLIDE TYPE ^I	EARTHQUAKE NAME, DATE, AND MAGNITUDE														
	Fortuna-Rio Dell, Calif. 1975 M 5.7	Managua, Nicaragua 1972 M 6.2	Borrego Mountain, Calif. 1968 M 6.4	San Fernando, Calif. 1971 M 6.4	Inangahua, New Zealand 1968 M 7.0	Hebgen Lake, Mont. 1959 M 7.1	San Juan, Argentina 1977 M 7.4	Guatemala 1976 M 7.5	New Madrid, Mo. 1811 MMI XII	Peru 1970 M 7.7	Hawke's Bay, New Zealand 1931 M 7.9	San Francisco, Calif. 1906 M 8.3	Chile 1960 M 8.4	Alaska 1964 M 8.4	Kansu, China 1920 M 8.6
A. LANDSLIDES IN ROCK															
ROCK FALL - AVALANCHES					S				S						
SLUMPS AND BLOCK SLIDES					S				S						
FALLS AND SHALLOW, DISINTEGRATING SLIDES															
B. LANDSLIDES IN UNCONSOLIDATED OR POORLY CONSOLIDATED DEPOSITS (ENGINEERING SOILS)															
FALLS, AVALANCHES, AND SHALLOW, DISINTEGRATING SLIDES	E	M	M	E	E	E	E	E	E	E	E	E	E	E	E
SLUMPS AND BLOCK SLIDES															
RE-ACTIVATION OF DORMANT LANDSLIDES															
LATERAL SPREADS ^{II}															
WET FLOWS ^{II}															
SUB-AQUEOUS LANDSLIDES ^{II}															
C. LANDSLIDES INVOLVING ARTIFICIAL CUTS OR FILLS															
CUT-SLOPE FAILURES															
LIQUEFACTION-INDUCED LANDSLIDES IN ARTIFICIAL FILLS															
LANDSLIDES IN ARTIFICIAL FILLS NOT CAUSED BY LIQUEFACTION															

^IClassifications after Varnes (33).

^{II}Liquefaction may be primary or contributing cause of failure.

^{III}Small landslides are those judged to contain less than 10,000 m³ of material.

^{IV}Large landslides are those judged to contain more than 10,000 m³ of material.

Explanation

E - Large number of landslides > 5,000 small III landslides, or > 100 large IV landslides, or Landslides common over >1000 km² area

M - Moderate number of landslides 500 to 5000 small III landslides, or 10 to 100 large IV landslides, or Landslides common over 100 to 1000 km² area

S - Small number of landslides < 500 small III landslides, or < 10 large IV landslides, or Landslides common over <100 km² area

No symbol - No landslides of this type reported

References:


Kansu, China: 5, 15
 Alaska: 19, 31
 Chile: 6, 26
 San Francisco: 36
 Hawke's Bay: 20
 Peru: 2, 8, 28
 New Madrid: 10
 Guatemala: 11, 12
 San Juan, Argentina: T. L. Youd, D. K. Keefer, and others, unpub. data
 Hebgen Lake: 1, 4, 9, 25, 29, 30
 Inangahua: 21, 22, 23, 27
 San Fernando: 14, 16, 17, 35
 Borrego Mountain: 3
 Managua: 7
 Fortuna-Rio Dell: 18

categories are defined in Table 1. Because of limitations in the data, numbers used to divide the categories should be regarded as first-order approximations. Classifications based on numbers of landslides rather than on area were applied wherever possible.

The number of landslides triggered by an earthquake correlates strongly with earthquake magnitude. The M 8.4 Alaska earthquake of 1964 probably triggered more landslides than any other seismic event in recent history. In Alaska, landslides were reported from an area of more than 210,000 km², which is equivalent in size to half the state of California (19, 31). At the other end of the scale in Table 1, the M 5.7 Fortuna-Rio Dell event of 1975 caused only one large rock fall and a few small debris slides. The Fortuna-Rio Dell earthquake should not be regarded as the lowest magnitude event to cause landsliding. Smaller shocks have triggered landslides, but we have not yet evaluated data from smaller earthquakes.

In Table 2, landslides in the various categories are ranked on the basis of their total abundance in the earthquakes listed in Table 1. The ranking was developed by assigning a numerical value to the abundance classification of each landslide category in each earthquake: E=3, M=2, S=1, No symbol=0. For each category, these numbers were totaled for all 15 earthquakes. The landslide categories were then ranked in order from highest total value through lowest.

TABLE 2: RELATIVE ABUNDANCE OF DIFFERENT TYPES OF LANDSLIDES.

Most Abundant	Falls and shallow, disintegrating slides in rock Avalanches, falls, and shallow disintegrating slides in soil Lateral spreads Cut-slope failures Slumps and block slides in soil Slumps and block slides in rock Wet flows Rock fall-avalanches Liquefaction-induced landslides in artificial fills ^I Re-activation of dormant landslides ^I Landslides in artificial fills not due to liquefaction
	
Least Abundant	Sub-aqueous landslides

The most abundant types of landslides were not necessarily the most damaging. The distribution of landslide damage in past earthquakes is partly due to the location of dwellings or other constructed works in certain landslide source areas or in the paths of certain landslides. However, landslides of several types do appear to have an inherently high potential for causing damage either because they tend to be large, because they tend to move long distances at high velocities, or both. On the basis of data from the 15 earthquakes listed in Table 1, the most hazardous landslides in natural materials are rock fall-avalanches, debris avalanches, wet flows, sub-aqueous landslides, and lateral spreads. Fortunately, some of these types of failures occur in relatively small numbers.

I Identical total numerical value

LANDSLIDE DESCRIPTIONS

Rock fall-avalanches: Rock fall-avalanches are large landslides that travel long distances at high velocities. The Mount Huascaran rock fall-avalanche contained 90 million m³ of material and flowed more than 60 km at velocities up to 400 km per hour. Nearly all of the rock fall-avalanches listed in Table 1 originated on steep mountain slopes that were hundreds of meters high. Most of these slopes were oversteepened by active fluvial or glacial erosion. The failures occurred in a wide variety of rock types. They were particularly common in closely jointed or deeply weathered rock, many broke loose where planes of weakness dipped out of slopes, and many occurred in unsaturated materials.

Slumps and block slides in rock: Deep-seated slumps and block slides are less common during earthquakes than rock falls and shallow, disintegrating rock slides. They commonly originate on steep slopes, but some continue to move on surprisingly gentle slopes. For example, two block slides triggered by the 1968 Inangahua earthquake moved on shear planes that dipped about 4° (21,22,23). Many slumps and block slides disintegrate into avalanches, but because of their relatively small size and short distance of travel, they generally are not as hazardous as rock fall-avalanches.

Rock falls and shallow, disintegrating rock slides: Landslides of these types are the most abundant slope failures listed in Table 1. It also appears that most shallow rock slides and falls originate on slopes of 35° or steeper (11,30). These landslides are particularly common in rocks that are poorly cemented, closely jointed, or highly weathered. Many slopes where these landslides occur have talus accumulations at their bases below where the earthquake-induced landslides originate (19,30,31).

Falls, avalanches, and shallow, disintegrating slides in soil: On December 16, 1920, a large earthquake shook Kansu Province in China, parts of which were underlain by thick deposits of loess. Loess is a windblown silt held together by a clayey or calcareous binder. Under nonseismic conditions, it is capable of standing in high, nearly vertical slopes. The earthquake apparently disrupted the binder holding the loess particles together. The result was probably the most spectacular and destructive series of earthquake-induced landslides in recent history. Whole villages and towns were buried by huge loess avalanches, and many valleys were filled with debris. These landslides were responsible for a large portion of the 200,000 deaths attributed to the shock (5).

The 1976 Guatemala earthquake also triggered thousands of soil avalanches and slides in a weakly cemented material that forms steep, high slopes under nonseismic conditions (11). There, the susceptible material is a soil derived from volcanic pumice (11). In many other earthquakes, soil avalanches, falls, and shallow, disintegrating slides have occurred in unsaturated, sandy or silty soils with little or no cohesion. The landslides take place most commonly on steep stream banks, ridge flanks, and artificial cuts (3,7,8,10,16,17,19,26,28,31,36).

Slumps and block slides in soil: Deep-seated soil slumps and block slides have also been triggered by many earthquakes listed in Table 1 (3, 16,17,19,20,21,26,28,31,36). They take place in soils derived from many different types of rocks, and they originate on moderate to steep slopes.

Many earthquake-induced slumps and block slides occur in regions where landslide deposits are already abundant (3,16,17,36).

Re-activation of dormant landslides in soil: A surprisingly low number of dormant landslides in soil were re-activated by the earthquakes listed in Table 1. In part, this low number reflects the lack of data on pre-earthquake landslides in many areas. However, the data are remarkably consistent and hold true even for areas such as Guatemala (11), San Fernando (16,17), and Fortuna-Rio Dell (18) where the pre-earthquake landslide distribution was known and where the landslide distribution was re-examined after the shock. It appears that earthquakes do not reactivate large numbers of dormant landslides in soil.

Lateral spreads: Lateral spreads are characterized by coherent blocks of material that move laterally on layers of liquefied sand or silt or of weakened, sensitive clay. The blocks commonly break up along internal fissures, and they may also rotate or subside. The large lateral spread at Turnagain Heights in Anchorage, Alaska was one of the more destructive landslides triggered by the 1964 earthquake (19,24,31). It started at the edge of a steep, flat-topped, coastal bluff, 20 m high, and progressively retrograded back from the face. It caused irreparable damage to 72 houses. The lateral movement took place primarily on a layer of sensitive clay, but liquefaction in sand and silt lenses almost certainly contributed to the failure (19,24,31). Similar, large lateral spreads from steep, high bluffs also took place during the 1811 New Madrid (10) and 1970 Chile earthquakes (26). Lateral spreads also occurred in areas of generally low relief such as river flood plains and deltas during several earthquakes (10,19,20,26,31,35,36).

Many seismically triggered lateral spreads, wet flows, and sub-aqueous landslides (see below) are caused by liquefaction. Techniques of assessing liquefaction susceptibility on a regional basis have been developed by others (37) and are briefly summarized here. Liquefaction commonly develops in saturated, cohesionless sediments such as sands and silts. The liquefaction susceptibility of a deposit is related to its age and depositional environment. River channel deposits, deltaic deposits, and uncompacted fills less than 500 years old have the highest liquefaction susceptibility. Other materials with a significant susceptibility to liquefaction include Holocene flood plain, fan delta, lacustrine, colluvial, dune, loess, and tephra deposits, and several materials deposited in coastal environments (37).

Wet flows: Wet flows are composed chiefly of saturated soils that lose much of their internal cohesion during earthquakes. Flows have been triggered by several earthquakes. Most originated in sandy or silty soils, and many formed where the slope was only a few degrees. Because they can travel long distances at high velocities, they are significant hazards in many areas. Methods of assessing the susceptibility of a soil to liquefaction-induced flow failure are discussed by Youd and Perkins (37).

Sub-aqueous landslides: Sub-aqueous landslides triggered by the 1959 Hebgen Lake (30), 1960 Chile (26), 1964 Alaska (19,31), and 1976 Guatemala (12) earthquakes were complex features involving a combination of slumping, lateral spreading and flow. The most common failure environments were the fronts of deltas or fan deltas, and most sub-aqueous slides were caused, at least partially, by liquefaction. In the Alaska earthquake, massive sub-aqueous slides severely damaged the towns of Valdez,

Whittier, Seward, and Homer (19,31). At least five sub-aqueous landslides in the Valdez area, but not in Valdez proper, had occurred during earthquakes in the preceding 70 years. Largely as a result of the 1964 slide the town was relocated on a non-liquefiable site (19,31). The relatively small number of reported sub-aqueous landslides during earthquakes (Table 2) probably reflects, in part, the difficulty of observing landslides of this type.

Cut-slope failures: Cuts increase landslide susceptibility by locally increasing slope steepness and by disturbing material adjacent to the cuts. Cut-slope failures are widespread during earthquakes (3,7,11,16,17,19,20,26,28,30,31,36).

Landslides in artificial fills: The most damaging failures in artificial fills have been caused by liquefaction (26,36,37), and these have occurred most frequently in uncompacted saturated sandy fills (37). In addition, much damage to artificial fills has been caused by liquefaction in subjacent materials (19,31). Other landslides not induced by liquefaction have occurred in artificial fills during earthquakes (3,7,16,17,20,26,28,36). Most failures of this type were small slumps or debris slides. The relatively small number of reported landslides in artificial fills is due, in part, to the fact that artificial fills are much less abundant than natural slopes.

SUMMARY OF LANDSLIDE TYPES AND FAILURE ENVIRONMENTS

Our study has identified several types of landslides that are triggered by earthquakes and some environments in which failures occur. Our preliminary findings are summarized in Table 3. As our study progresses, we anticipate that other environments with high susceptibilities to seismically induced landsliding will be identified and that categories listed in Table 3 will be refined and subdivided for better assessments.

PRELIMINARY MAP OF SEISMICALLY INDUCED LANDSLIDE SUSCEPTIBILITY OF THE LA HONDA AREA

Figure 1 is an experimental susceptibility map of an area near the town of La Honda, in the Santa Cruz Mountains, 40 km south of San Francisco, Calif. The map was prepared to demonstrate how the preliminary criteria summarized in Table 3 can be used to evaluate susceptibility to earthquake-induced landsliding. The preliminary La Honda map (Fig. 1) is subject to revision as our study of landsliding during historic earthquakes progresses. Furthermore, it is a regional map which shows only zones where unfavorable site conditions may exist. Local site conditions, not determined in this study, govern whether specific sites within these zones are actually susceptible to failure. Therefore, it is not intended for use in determining the susceptibility to failure of any given site. Any such site-specific assessment should be carried out by a professional engineering geologist.

Data on the La Honda area came from a detailed engineering geologic field investigation (34), a published map of unconsolidated Quaternary materials (13), and a computer-generated slope map. On the basis of this information and our review of landsliding during historic earthquakes, three types of zones with high susceptibilities to earthquake-induced landslides were identified (Fig. 1). These are areas with slopes greater than 35°, areas underlain by saturated sandy and silty Holocene alluvium,

and areas underlain by active and recently active landslides (34). Landslides judged to be dormant (34) are not included in the zones of high susceptibility.

TABLE 3: PRELIMINARY ASSESSMENT OF SEISMICALLY INDUCED
LANDSLIDE SUSCEPTIBILITY

LANDSLIDE TYPES	SOME ENVIRONMENTS IN WHICH LANDSLIDES ARE LIKELY TO OCCUR
Rock fall-avalanches	Very steep, very high slopes that are composed chiefly of deeply weathered, closely jointed, or highly sheared rock and that are being oversteepened by active erosion
Slumps and block slides in rock	Moderate to steep slopes in many different types of rock
Rock falls and shallow, disintegrating rock slides	<ol style="list-style-type: none"> 1. Rock slopes steeper than 35° 2. Rock slopes with talus accumulations at their bases 3. Slopes containing weathered, sheared, or closely jointed rock
Falls, avalanches, and shallow, disintegrating slides in soil	<ol style="list-style-type: none"> 1. Steep, high slopes containing certain kinds of weakly cemented materials such as some kinds of loess and some volcanic pumice soils 2. Steep ridge flanks and stream banks containing unsaturated sandy or silty soils with little or no cohesion
Slumps and block slides in soil	Moderate to steep slopes in soils derived from many different types of rocks, particularly in areas with abundant, preexisting landslide deposits
Re-activation of dormant landslides in soil	Only relatively small numbers of dormant landslides are re-activated by earthquakes
Lateral spreads	<ol style="list-style-type: none"> 1. Areas of generally low relief underlain by many different kinds of unconsolidated saturated Holocene sandy or silty materials 2. Steep, high bluffs containing layers of sensitive clay or liquefiable sand or silt as defined in 1. above 3. Uncompacted saturated sandy artificial fills
Wet flows	Steep to very gentle slopes underlain by some kinds of saturated sandy or silty soils

TABLE 3: (con't.)

TYPES (con't.)	ENVIRONMENT (con't.)
Sub-aqueous landslides	Fronts of deltas or fan deltas, particularly in areas underlain by saturated, liquefiable sand or silt
Cut-slope failures	Artificial cuts
Liquefaction- induced landslides in artificial fills	Uncompacted, saturated, sandy fills
Landslides in arti- ficial fills not caused by lique- faction	Many different types of fills

CONCLUSIONS

Predominant types of earthquake-induced landslides and some environments with high susceptibilities to failure have been identified from data about 15 historic earthquakes. Landslides that occurred in greatest numbers in the 15 earthquakes were: falls and shallow, disintegrating slides in rock; falls, avalanches, and shallow, disintegrating slides in soil; lateral spreads; cut-slope failures; slumps and block slides in soil; and slumps and block slides in rock. Many other kinds of earthquake-induced landslides occur relatively infrequently but have high inherent potentials for causing loss of life and property. Landslides that have caused extensive loss of life or property during historic earthquakes include rock fall-avalanches, soil avalanches, lateral spreads, wet flows, sub-aqueous landslides, and liquefaction-induced landslides in artificial fills. Some environments with high susceptibilities to seismically induced landsliding have been identified on a preliminary basis. As our studies progress, it is anticipated that these categories will be refined and that new environments with high susceptibilities will be identified.

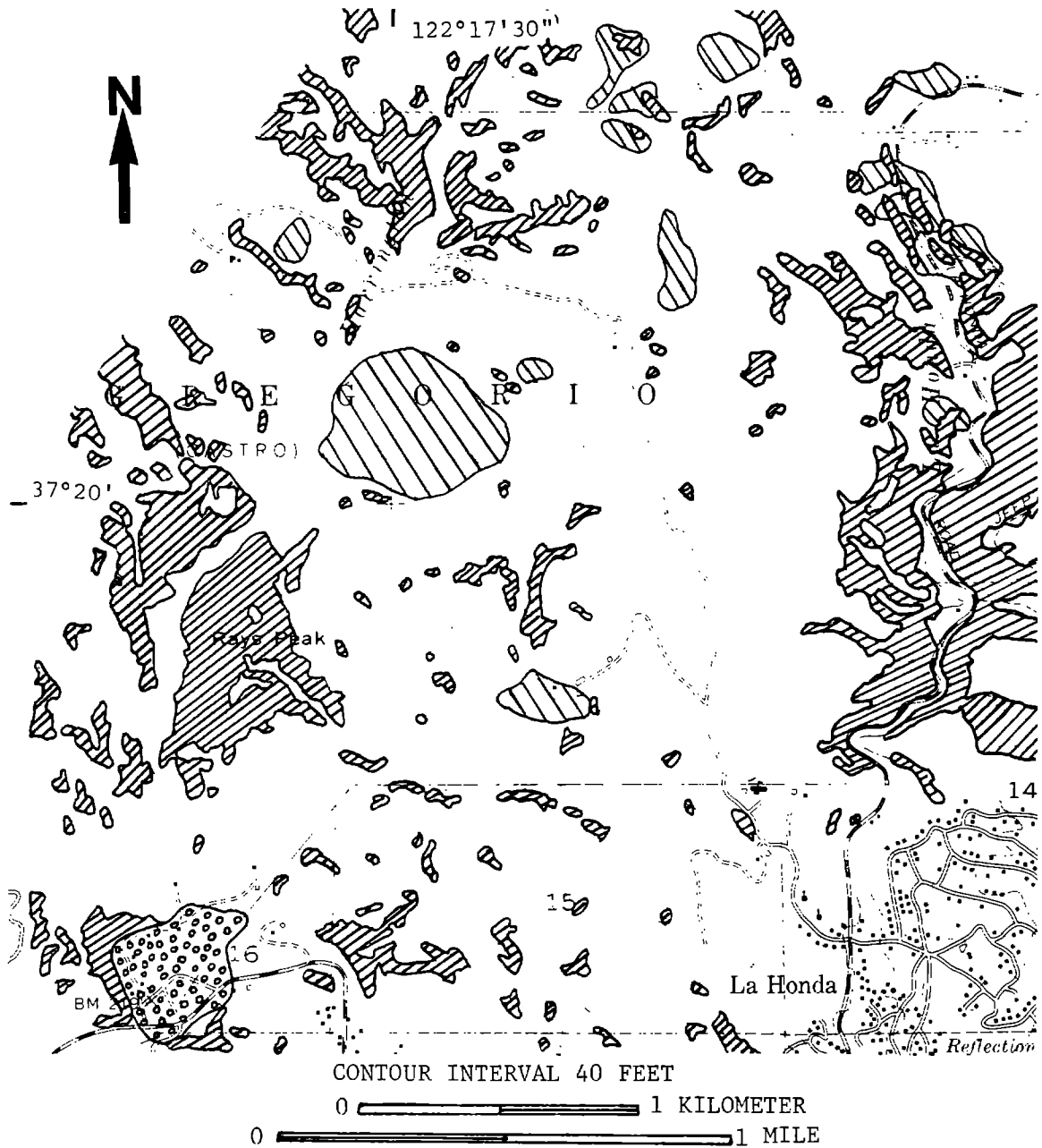
REFERENCES

- (1) Billings Geological Society, 1960, Earthquake papers: Billings, Montana, Eleventh Annual Field Conference Guidebook, p. 24-85.
- (2) Browning, J.M., 1973, Catastrophic rockslide, Mount Huascarán, North-central Peru, May 31, 1970: American Association of Petroleum Geologists Bulletin, v. 57, no. 7, p. 1335-1341.
- (3) Castle, R.O., and Youd, T.L., 1972, Engineering geology, *in* The Borrego Mountain earthquake of April 9, 1968: U.S. Geological Survey Professional Paper 787, p. 158-174.
- (4) Christiansen, R.L., and Blank, H.R., 1972, Volcanic stratigraphy of the Quaternary rhyolite plateau in Yellowstone National Park: U.S. Geological Survey Professional Paper 729-B, 18p.
- (5) Close, U. and McCormick, E., 1922, Where the mountains walked: National Geographic, v. 41, no. 5, p. 445-472.




- (6) Duke, C.M., and Leeds, D.J., 1963, Response of soils, foundations, and earth structures: Seismological Society of America Bulletin, v. 53, no. 2, p. 309-357.
- (7) Earthquake Engineering Research Institute Conference Proceedings, 1973, Managua, Nicaragua earthquake of December 23, 1972: v. 1, p. 8-264.
- (8) Earthquake Engineering Research Institute Earthquake Report Committee, 1970, Peru earthquake of May 31, 1970, preliminary report: Earthquake Engineering Research Institute, 55 p.
- (9) Fischer, W.A., 1960, Highlights of Yellowstone geology with an interpretation of the 1959 earthquakes and their effects in Yellowstone National Park: Yellowstone National Park, 62 p.
- (10) Fuller, M., 1912, The New Madrid earthquake; U.S. Geological Survey Bulletin 394, 118 p.
- (11) Harp, E.L., Wieczorek, G.F., and Wilson, R.C., 1978, Earthquake-induced landslides from the February 4, 1976, Guatemala earthquake and their implications for landslide hazard reduction: International Symposium on the February 4th, 1976 Guatemalan Earthquake and the Reconstruction Process, v. 1.
- (12) Hoose, S.N., Wilson, R.C., and Rosenfeld, J.H., 1978, Liquefaction-caused ground failure during the February 4, 1976, Guatemala earthquake: International Symposium on the February 4th, 1976 Guatemalan Earthquake and the Reconstruction Process, v. 2.
- (13) Lajoie, K.R., Helley, E.J., Nichols, D.R., and Burke, D.B., 1974, Geologic map of unconsolidated and moderately consolidated deposits of San Mateo County, California: U.S. Geological Survey Miscellaneous Field Studies Map MF-575, Basic Data Contribution 6.
- (14) Marachi, N.D., 1973, Dynamic soil problems at the Joseph Jensen Filtration Plant *in* Murphy, L.M., scientific coordinator, San Fernando, California earthquake of February 9, 1971: National Oceanic and Atmospheric Administration, v. 1, part B, p. 815-820.
- (15) Meyers, H., and von Hake, C.A., 1976, Earthquake data summary: Boulder, Colorado, National Oceanic and Atmospheric Administration, Environmental Data Service, Key to Geophysical Records Documentation No. 5, 54 p.
- (16) Morton, D.M., 1971, Seismically triggered landslides in the area above the San Fernando Valley, *in* The San Fernando, California earthquake of February 9, 1971: U.S. Geological Survey Professional Paper 733, p. 99-104
- (17) Morton, D.M., 1975, Seismically triggered landslides in the area above the San Fernando Valley, *in* The San Fernando, California earthquake of February 9, 1971: California Division of Mines and Geology Bulletin 196, p. 145-154
- (18) Nason, R., Harp, E.L., La Gresse, H., and Malley, R.P., 1975, Investigations of the 7 June 1975 earthquake at Humboldt County, California, U.S. Geological Survey Open-File Report 75-404, 37 p.
- (19) National Academy of Sciences, 1968-73, The great Alaska earthquake of 1964: Washington, D.C., National Academy of Sciences Printing and Publishing Office, v. 1, Geology, and v. 3, Hydrology.
- (20) New Zealand Department of Scientific and Industrial Research, 1933, The Hawke's Bay earthquake of 3rd February, 1931: New Zealand Journal of Science and Technology, v. 15, no. 1, p. 1-116.
- (21) New Zealand Department of Scientific and Industrial Research, 1968, Preliminary report on the Inangahua earthquake, New Zealand, May, 1968: Research Bulletin 193, 39 p.

- (22) New Zealand Society for Earthquake Engineering Bulletin, 1968, The 1968 Inangahua earthquake (conference seminar papers): v. 2, no. 1, 148 p.
- (23) New Zealand Society for Earthquake Engineering Bulletin, 1969, Special Inangahua reports: v. 2, no. 1, 148 p.
- (24) Seed, H.B., 1968, Landslides during earthquakes due to soil liquefaction: Journal Soil Mechanics and Foundations Div., American Society of Civil Engineers, v. 94, no. SM 5, p. 1055-1122.
- (25) Seismological Society of America Bulletin, 1962, The earthquake at Hebgen Lake, Montana on August 18, 1959 (GCT): v. 52, no. 2, p. 153-273.
- (26) Seismological Society of America Bulletin, 1963, Special issue on Chilean earthquakes of May 1960: v. 53, no. 6, p. 1123-1441.
- (27) Seismological Society of America Bulletin, 1970, The 1968 Inangahua earthquake: Report of the University of Canterbury Survey team: v. 60, no. 5, p. 1561-1606.
- (28) Seismological Society of America Bulletin, 1971, Special issue on Peru earthquake of May 31, 1970: v. 61, no. 3, p. 511-640.
- (29) U.S. Coast and Geodetic Survey, 1961, Abstracts of earthquake reports for the Pacific Coast and Western Mountain region, MSA-103, July, August, September, 1959: p. 51-189.
- (30) U.S. Geological Survey, 1963, The Hebgen Lake, Montana earthquake of August 17, 1959: U.S. Geological Survey Professional Paper 435, 242p.
- (31) U.S. Geological Survey, 1965-1970, The Alaska earthquake, March 27, 1964: U.S. Geological Survey Professional Papers 542-A, 542-B, 542-C, 542-D, 542-E, 542-G, 543-B, 543-E, 543-F, 544-A, 544-B, 544-D, 545-A, 545-C, 545-D.
- (32) Varnes, D.J., 1958, Landslide types and processes, *in* Eckels, E.B., ed., Landslides and engineering practice: Highway Research Board Special Report 29, National Academy of Science - National Research Council Publication 554, p. 20-47.
- (33) Varnes, D.J., in press, Slope movement types and processes: Chapter 2 *in* Schuster, R.L., and Kryzek, R.S., eds., Landslides--analysis and control: Transportation Research Board Special Report 176, National Academy of Sciences.
- (34) Wieczorek, G.F., 1978, Landslide susceptibility evaluation in the Santa Cruz Range, San Mateo County, California, Ph.D. thesis, University of California, Berkeley, 278 p.
- (35) Youd, T.L., 1971, Landsliding in the vicinity of the Van Norman Lakes *in* the San Fernando, California earthquake of February 9, 1971: U.S. Geological Survey Professional Paper 733, p. 105-109.
- (36) Youd, T.L., and Hoose, S.N., 1978, Historic ground failures in northern California triggered by earthquakes: U.S. Geological Survey Professional Paper 993, 177 p.
- (37) Youd, T.L., and Perkins, D.M., 1978, Mapping liquefaction-induced ground failure potential: Journal of the Geotechnical Engineering Div., American Society of Civil Engineers, v. 104, no. GT4, p. 433-446.

FIGURE 1: PRELIMINARY SEISMICALLY INDUCED LANDSLIDE SUSCEPTIBILITY MAP OF THE LA HONDA AREA



ZONES OF HIGH SUSCEPTIBILITY TO SEISMICALLY INDUCED LANDSLIDES

<u>SYMBOL</u>	<u>POSSIBLE LANDSLIDE TYPES</u>	<u>MAPPING CRITERIA</u>
	SOIL AVALANCHES; FALLS, SLUMPS, BLOCK SLIDES AND SHALLOW DISINTEGRATING SLIDES IN SOIL AND/OR ROCK	SLOPES STEEPER THAN 35°
	LATERAL SPREADS AND WET FLOWS	UNDERLAIN BY SATURATED SANDY AND SILTY HOLOCENE ALLUVIUM
	SLUMPS AND BLOCK SLIDES IN SOIL AND/OR ROCK	ACTIVE AND RECENTLY ACTIVE LANDSLIDES

EARTHQUAKE LOSSES TO BUILDINGS
IN THE
SAN FRANCISCO BAY AREA

by

S. T. Algermissen^I and K. V. Steinbrugge^{II}

ABSTRACT

Losses in the San Francisco Bay area are simulated for five broad classes of buildings which include the majority of building types found in the area. Losses are expressed in terms of the average percentage of the total actual cash value required to fully repair, in kind, any building in a particular building class. The inventory of dwellings was obtained from census data, and the inventory for buildings other than dwellings is derived from land-use classification in the San Francisco Bay area supplemented by minimal field work. Long-term annual losses for the various building classes range from 0.1 to 1.6 percent. For a large earthquake on the San Andreas fault, the range in percent loss is about 5.0 to 25 percent, depending on the building class. The 1970 value of dwellings in the nine-county Bay area was \$30.289 billion. Annual average losses to dwellings is estimated at \$271 per dwelling. The average loss per dwelling as a result of a large earthquake on the San Andreas fault would be about \$1,355; the total loss (1970), about \$1.5 billion.

INTRODUCTION

The primary economic losses to buildings as a result of earthquakes depend on three principal factors: (1) the spatial distribution of the various kinds of buildings exposed to ground shaking and geological hazards (landslides, liquefaction, surface faulting, etc.); (2) the spatial distribution of earthquake shaking and geological hazards associated with an earthquake; and (3) the susceptibility of each building class to loss. The purpose of this study is to present a methodology for the estimation of losses to buildings other than dwellings to complement earlier studies of single-family dwellings and to provide a general technique for the estimation of (a) total losses from single large earthquakes and (b) average losses resulting from earthquakes over a period of time. The nine-county San Francisco Bay area (fig. 1) is used to test the methodology for the calculation of losses resulting from earthquakes. The losses computed are expressed in terms of percent loss by class of construction. The percent loss is defined here to mean the average percentage of the total actual cash value required to fully repair, in kind, any building of a particular class represented by a particular degree of Modified Mercalli Intensity Scale. Only losses associated with ground shaking are estimated.

I Geophysicist, U.S. Geological Survey, Denver, Colorado.

II Manager, Earthquake Department, Insurance Services Office, San Francisco, California.

METHODOLOGY

Losses to buildings other than one- to four-family dwellings have been calculated as follows:

- (1) The spatial distribution of buildings throughout the nine-county area is approximated by class of construction for each U.S. Census Tract in the study area.
- (2) Relationships are developed between percent loss (as previously defined) and the various degrees of the Modified Mercalli (MM) Intensity Scale--the measure of ground shaking used in this study.
- (3) MM intensities for each census tract are determined for (a) individual earthquakes of interest and (b) ensembles of earthquakes.
- (4) The results from (1), (2), and (3) are used to calculate the loss to each class of construction that can be attributed to the occurrence of a particular earthquake or series of earthquakes.

For example, the percent loss to buildings in, say, class C, due to a particular earthquake, is

$$\sum_i [P(C)_i][L_C(I)_i] \quad (1)$$

where:

$P(C)_i$ = percent of the buildings of class C in the nine-county area that are located in census tract (i)

$L_C(I)_i$ = percent loss to buildings of class C when shaken at MM intensity I in census tract (i).

The summation is made over the census tracts of interest.

Methods for the estimation of earthquake losses to dwellings in California were developed in earlier studies (references 1, 2, 3, 4), and so no detailed description of the methods will be given here.

BUILDING CLASSIFICATION

An abridged description of the building classification used in this earthquake-loss simulation study is shown in table 1. These classifications are similar to those used by the majority of the property-casualty insurance companies in the United States and have the advantage of over 50 years experience, including testing after earthquakes.

Table 1.--Building classification used in this study

Notation used in loss tables 3 and 4	Brief description of subclasses of five broad building classes
1A	Wood-frame and frame-stucco dwellings.
1B	Wood-frame and frame-stucco buildings not qualifying under 1A (usually large-area nonhabitational units); (not considered in this study).
2A	One story, all metal; floor area less than 20,000 feet ² .
2B	All metal buildings not considered under 2A.
3LA	Steel frame, superior damage-control features; less than four stories.
3LB	Steel frame; ordinary damage-control features; less than four stories.
3LC	Steel frame; intermediate damage-control features (between 3LA and 3LB); less than four stories.
3LD	Floors and roofs not concrete; less than four stories.
3HA, 3HB, 3HC, 3HD	Descriptions are the same as for 3LA, 3LB, 3LC, and 3LD except that buildings have four or more stories.
4LA	Reinforced concrete; superior damage-control features; less than four stories.
4LB	Reinforced concrete; ordinary damage-control features; less than four stories.
4LC	Reinforced concrete; intermediate damage-control features (between 4LA and 4LB); less than four stories.
4LD	Precast reinforced concrete, lift slab, less than four stories.
4LE	Floors and roofs not concrete, less than four stories.
4HA, 4HB, 4HC, 4HD, 4HE	Descriptions are the same as for 4LA, 4LB, 4LC, 4LD, and 4LE except that buildings have four or more stories.
5A	Dwellings, not over two stories in height, constructed of (a) poured-in-place reinforced concrete, with roofs and second floors of wood frame or (b) adequately reinforced brick or hollow-concrete-block masonry, with roofs and floors of wood (not considered in this study).
5B	One-story buildings having superior earthquake damage-control features, including exterior walls of (a) poured-in-place reinforced concrete, and (or) (b) precast reinforced concrete, and (or) (c) reinforced brick masonry or reinforced-concrete brick masonry, and (or) (d) reinforced hollow-concrete-block masonry. Roofs and supported floors are of wood or metal-diaphragm assemblies. Interior bearing walls are of wood frame or any one, or a combination, of the aforementioned wall materials.
5C	One-story buildings having construction materials listed for Class 5B, but with ordinary earthquake damage-control features.
5D	Buildings having reinforced concrete load-bearing walls and floors and roofs of wood, but not qualifying for Class 4E; and buildings of any height having Class 5B materials of construction, including wall reinforcement; also included are buildings with roofs and supported floors of reinforced concrete (precast or otherwise) not qualifying for Class 4.
5E	Buildings having unreinforced solid-unit masonry of unreinforced brick, unreinforced concrete brick, unreinforced stone, or unreinforced concrete, where the loads are carried in whole or in part by the walls and partitions. Interior partitions may be wood frame or any of the aforementioned materials. Roofs and floors may be of any material. Not qualifying are buildings having nonreinforced load walls of hollow tile or other hollow-unit-masonry, adobe, or cavity construction.
5F	Buildings having load-carrying walls of hollow tile or other hollow-unit-masonry construction, adobe, and cavity-wall construction, and any building not covered by any other class (not considered in this study).

BUILDING INVENTORY

The inventory was developed in the following manner:

- (1) A direct correlation was assumed to exist between specific building classes and land-use designations. For example, large-area buildings that constitute subclass 2B, all-metal structures, are usually aircraft hangars, steel plants, major manufacturing facilities, or large warehouses, and, accordingly, are situated in land-use areas primarily zoned for industrial purposes. This assumption makes possible the determination of the geographic distribution of building classes throughout the study area. Modification of this assumption for any one building class or subclass was made on the basis of field sampling and personal knowledge.
- (2) All building classes and building values were assumed to be uniformly distributed within the designated mapped zones. An equal distribution of building value is reasonably consistent with policy assumed in zoning ordinances formulated by the respective county planning commissions and regional agencies. This assumption was modified when field sampling and personal knowledge of the authors indicated that it gave obviously incorrect results.
- (3) Nonconforming uses are not included in the geographic distribution of building classes. In addition, small isolated pockets of semicommercial developments in suburban areas are not considered. In comparison to the major commercial areas tabulated, the values of these semicommercial developments are relatively insignificant. Insofar as possible, their values are included in the nearest major commercial area and are accounted for by a factor related to population distribution based on the 1970 census. In any event, visual surveys indicate that, except for the all metal gasoline service stations located in these random pockets, the majority of these structures are wood-frame buildings.
- (4) Land-use data obtained from the "Atlas of Urban and Regional Change" (5) were plotted on the "Census Tract Outline Map" (6), and the land-use designations were converted to the appropriate building class. Data compatibility with the respective land-use maps provided by the various county planning commissions was confirmed by cross-checking data sources. Mapped results were partially verified through data collected from the detailed city and street maps available for urban centers located in the San Francisco Bay area.
- (5) Final mapping results were checked using visual field surveys of critical areas.
- (6) Special service areas found in the San Francisco Bay area, such as San Francisco Presidio, Port of San Francisco, Hamilton Air Force Base, Moffett Naval Air Field, U.S. Naval Magazines at Port Chicago and Concord, Oakland Army Base, Oakland Naval Supply Center, Nimitz Field Naval Air Station in Alameda, San Quentin Penitentiary, and Mare Island, among others, were not included in the mapping of building classes.

- (7) The area within each census tract having a particular land-use code (equated to building class) was measured. The area of each building class in each census tract was then summed to determine the total area of a particular building class in the nine counties considered in this study. The percentage of any building class in any census tract is then:

$$\frac{\text{Area of the particular building class in the census tract}}{\text{Total area of that building class in the nine-county area}} \times 100$$

A more complete discussion of the development of the building inventory, together with examples, may be found in (7).

GROUND SHAKING - LOSS RELATIONSHIPS

The estimation of losses resulting from earthquakes requires that relationships be known or developed between the intensity of ground shaking and the degree of damage to structures by class of construction (fig. 2). The measure of the intensity of ground shaking used in this study is the Modified Mercalli Intensity Scale (8). Limitations of the scale have been discussed in several papers (for example, 9, 10).

Development of the loss-intensity relationships used in this study entailed three steps: (1) examination of loss for a number of earthquakes; (2) analysis of existing building cost data; and (3) integration of (1) and (2), using engineering judgment based on actual earthquake experience, into loss-intensity relationships. Because of the large number of classes of construction and the many construction components included in nondwelling classes, the present attempt to develop loss-intensity relationships must be considered as preliminary.

The most useful published sources of loss data are found in the studies of the most recent earthquakes, although data extending back to the 1906 San Francisco shock still have substantial value. A review of several publications showed that the damage data in the publications are not usually compatible. Further, a more detailed review of all major sources shows that data are far from complete for all intensities for all building classes. It then follows that interpolation and judgment must be used with the published record of actual losses to produce loss values.

Analysis of existing building cost data has shown that the variations in the cost percentages among construction components for any particular building class permit only very approximate loss estimates when applying loss averages to any particular building.

The development of loss-intensity relationships, then, requires the integration of actual earthquake loss with current cost data. It also requires the interpretation of earthquake loss data and their relation to each class of construction in terms of the Modified Mercalli Intensity Scale. Actual earthquake losses must be analyzed with relation to iso-seismal maps that have been prepared for recent earthquakes. It is

important to note that this step effectively amounts to a more definitive description of losses at each intensity level than exist in the original MM Intensity Scale. In this sense, development and loss-intensity relationships for the various construction classes represents a further definition or refinement of the MM scale based on an analysis of loss experience and cost. At the present time we believe that MM intensity maps, together with the loss-intensity relationships developed using relevant experienced judgment, are the best bases for this kind of study. Indeed it is the only basis for which extensive data are available.

For damage-analysis purposes, the lower intensity limit of the Modified Mercalli Intensity Scale is the threshold of damage, which varies with the kind of building as well as with the kind of ground motion but is generally VI or VII. The threshold normally includes "imaginary" damage, which may decrease the actual lower limit by one intensity unit. By "imaginary" damage we mean damage that the owner/occupant believes occurred during the shock, but which was actually in existence before the earthquake. On the other hand, the upper intensity limit is determined by the intensity at which ground-vibration effects to buildings are overshadowed by geologic effects, such as landsliding, faulting, and failures of structurally poor ground. This upper limit is normally given as MM intensity IX in insurance practice. This limit of IX is somewhat arbitrary since vibrational effects on buildings will increase somewhat with increasing intensity, but becomes overshadowed by building damage resulting from geological effects.

Percent loss-MM intensity relationships are, in general, not linear. The general, qualitative characteristics of loss-intensity curves for various building classes have been discussed elsewhere (2, 7); the preliminary nature of this study precluded the determination of the detailed shape of the intensity-loss curves. As usable approximations, linear relationships were developed. In figure 2, percent losses from 0 to 10 have been estimated to the nearest 1 percent. Percent losses above 10 percent are estimated to the nearest 5 percent.

ESTIMATION OF GROUND SHAKING

MM intensities were assigned to all census tracts for all earthquakes of interest. Two techniques were used to assign intensities to census tracts. For earthquakes having maximum epicentral intensities from VI to VIII, average isoseismal maps were used. For earthquakes having maximum intensities greater than VIII, isoseismal maps were constructed using data from special studies (11, 12).

Average isoseismal maps (for earthquakes $VI < I_0 < VIII$) were constructed in the following manner:

- (1) The average area shaken at each intensity level was determined for each earthquake in the San Francisco Bay area for which an isoseismal map was available. The same general approach was used in an earlier study of single-family dwellings (3, 4), and all of the intensity data used in that study, together with additional new material, was used to construct average isoseismal maps.

- (2) Isoseismal patterns were considered to be elongated in the direction of faulting. This holds true in the San Francisco Bay area because earthquakes are shallow (< 15 km) and strike-slip faulting predominates, at least in the larger earthquakes that are of most interest to this study.
- (3) Using $M=1+2/3 I_o$, where I_o is the maximum MM intensity and M is magnitude, and $\log L=-0.39+0.34 M$, where L is fault rupture length (3) in kilometers, the shapes of average isoseismal maps were constructed using

$$A_I = 2W_I L + \pi W_I^2, \quad (\text{see fig. 3})$$

where A_I =area enclosed by the intensity I isoseismal plus higher intensities

and

W_I =width of zone bounded by the intensity I isoseismal plus higher intensities.

- (4) The orientation of the isoseismals (the strike of L in fig. 3) for any particular historical earthquake was taken to be the same as the strikes of faults in the San Francisco Bay area that are known to have been active near the earthquake epicenter during or since Quaternary time (13). Earthquakes that could not be associated with specific faults were assumed to have circular isoseismals. Table 2 gives the values of W (fig. 3) and L for elongated isoseismals and the radius R for circular isoseismals for all intensities associated with earthquakes of maximum intensities VI through VIII.

Table 2.--Parameters for construction of average isoseismals
for $VI \leq I_o \leq VIII$

Maximum intensity I_o and associated intensities I	Fault length L (km)	Width ¹ W (km)	Radius ² R (km)
VIII:	58	1.65	8.00
VII	--	5.90	15.55
VI	--	17.54	30.90
VII:	35	3.17	8.92
VI	--	9.98	17.84
VI	20	3.95	8.18

¹The width (W) and radius (R) are the maximum distances for each intensity.

²The radius (R) is for the circular isoseismals, which are assigned to earthquakes not associated with specific faults.

- (5) The isoseismals constructed for earthquakes having $VI \leq I_0 \leq VIII$ average the effects on surficial materials over broad areas. Consequently, the intensity of shaking at individual sites may differ considerably from on the average intensity map. The effect of site amplification was, to some extent, taken into account by dividing the surficial geology throughout the area into three units. Incremental intensities were assigned to these three units and added to or subtracted from the average intensities. The units and incremental intensities are bay mud (+1.0); alluvium (0); and bedrock (-1.0). These units are defined in more detail and discussed by Borchardt *et al.*, (12). The incremental intensities assigned here differ slightly from, but are in general agreement with, those suggested in (12).

LOSS CALCULATIONS

Losses were calculated for each class of construction using earthquakes that occurred during the following time intervals: 1800-1974 (175 years); 1800-1899 (100 years); 1900-1974 (75 years); and 1907-1974 (68 years). The losses are expressed as the average annual percent loss to buildings of each construction class in the nine-county San Francisco Bay area. The inventory, exclusive of wood-frame dwellings (Class 1A), is updated to 1973. Class 1A inventory is based on 1970 United States census data. The results are shown in table 3. Losses for two large earthquakes of interest in the Bay area--one, a maximum intensity X on the San Andreas fault, and the other, a maximum intensity IX on the Hayward fault--are shown in table 4.

DISCUSSION OF RESULTS

The four samples of historical seismicity data shown in table 3 indicate that, in general, the largest losses are associated with the 100-year period 1800-1899. This is a consequence of the three large earthquakes that occurred during the period: in 1838 on the San Andreas fault, and in 1836 and 1868 on the Hayward fault. In addition, the percent losses to buildings are considered constant (at the intensity IX level) for intensities above IX. Actual losses increase for intensities greater than IX, but the losses are increasingly caused by geologic effects that have not been considered in this report. The earthquakes of 1836, 1838, and 1868 are believed not to have been as large as the 1906 earthquake, but they would be about as effective in causing vibration damage. It is interesting to note also that, even though the earthquake history of the San Francisco Bay area is probably not complete for damaging shocks for the 1800-1899 period, the losses are generally the highest of any time interval considered. Best long-term average loss estimates are probably obtained from the losses simulated using either the 175-year seismicity sample (1800-1974), the 100-year sample (1800-1899), or the 75-year sample (1900-1974) even though the average losses computed using these three seismicity samples are all low, but for different reasons: The time spans that include 19th century data are incomplete, whereas the 1900-1975 sample contains only one large shock (1906). Data for the 68-year period, 1907-1974, are reasonably complete for damaging shocks, but yield useful average losses only if one believes that large damaging earthquakes will not occur in the Bay area during some period of interest in the future.

The losses shown in table 4, simulated for a maximum MM intensity X earthquake on the San Andreas fault and a maximum intensity IX earthquake on the Hayward fault, seem to indicate that the percent losses for the two earthquakes would be very similar from the point of view of vibration damage. Nearly equal losses result partly from the flat shape of the intensity-loss curves for intensities above IX and partly from the geometry of the Bay area and the high concentration of buildings in the east Bay area. Dollar loss estimates are available only for one- to four-family dwellings, the value of the dwellings being obtained from census data as previously reported (1, 2, 3, 4). There were approximately 1.1175 million one- to four-family dwellings in the nine-county study area having a replacement cost value of \$30.3 billion and an average value of \$27,100 in 1970. A conservative long-term annual average loss (based on table 3) might be 1 percent of the replacement cost value or about \$271. Average total losses to dwellings as a result of a large earthquake would be about 5 percent of value, or \$1.51 billion, or an average loss per dwelling of \$1,360.

Table 3.--Estimated average annual percent losses in the nine-county San Francisco Bay area, based on the historical seismicity during four time intervals

Building Subclass	175 years (1800-1974)	100 years (1800-1899)	75 years (1900-1974)	68 years (1907-1974)
I/ 1A	0.702	0.663	0.755	0.692
2A	0.131	0.153	0.102	0.043
2B	0.160	0.201	0.106	0.028
3LA	0.166	0.198	0.123	0.032
3LB	0.822	0.820	0.826	0.652
3LC	0.208	0.248	0.154	0.040
3LD	0.822	0.820	0.826	0.652
3HA	0.260	0.357	0.132	0.008
3HB	0.539	0.705	0.317	0.098
3HC	0.325	0.446	0.165	0.010
3HD	0.539	0.705	0.317	0.098
4LA	0.208	0.248	0.154	0.040
4LB	1.175	1.171	1.180	0.931
4LC	0.291	0.347	0.215	0.056
4LD	1.410	1.406	1.416	1.117
4LE	1.292	1.288	1.298	1.024
4HA	0.325	0.446	0.165	0.010
4HB	0.769	1.007	0.453	0.139
4HC	0.539	0.705	0.317	0.098
4HD	0.923	1.208	0.543	0.167
4HE	0.846	1.108	0.498	0.153
5B	0.208	0.248	0.154	0.040
5C	0.822	0.820	0.826	0.652
5D	1.057	1.054	1.062	0.838
5E	1.521	1.589	1.430	1.083

^IClass 1A inventory is based on 1970 census data.

Table 4.--Estimated percent losses for two large earthquakes in the nine-county San Francisco Bay area

Building Subclass	Percent losses for MM intensity X on the San Andreas fault	Percent losses for MM intensity IX on the Hayward fault
1A	5.04	4.03
2A	4.17	3.38
3LA	6.59	5.15
3LB	13.07	11.47
3LC	8.24	6.44
3LD	13.07	11.47
3HA	9.34	9.42
3HB	16.73	16.82
3HC	11.67	11.78
3HD	16.73	16.82
4LA	8.24	6.44
4LB	18.68	16.30
4LC	13.07	11.47
4LD	22.47	19.56
4LE	20.54	20.65
4HA	11.67	11.78
4HB	23.89	24.04
4HC	16.73	16.82
4HD	28.67	28.84
4HE	26.28	26.44
5B	8.24	6.44
5C	13.07	11.47
5D	16.81	14.74
5E	25.41	22.51

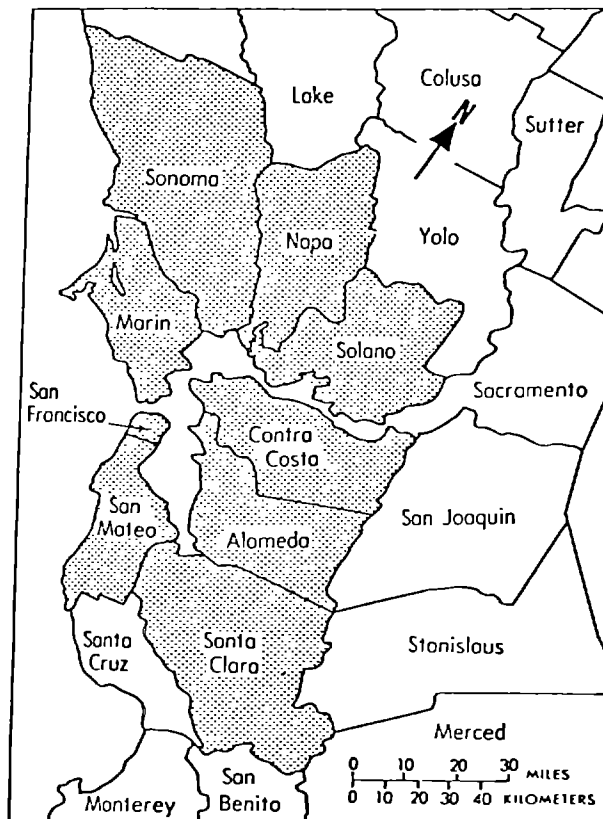


Figure 1.--Location map of northern California showing the nine-county area studies in this report.

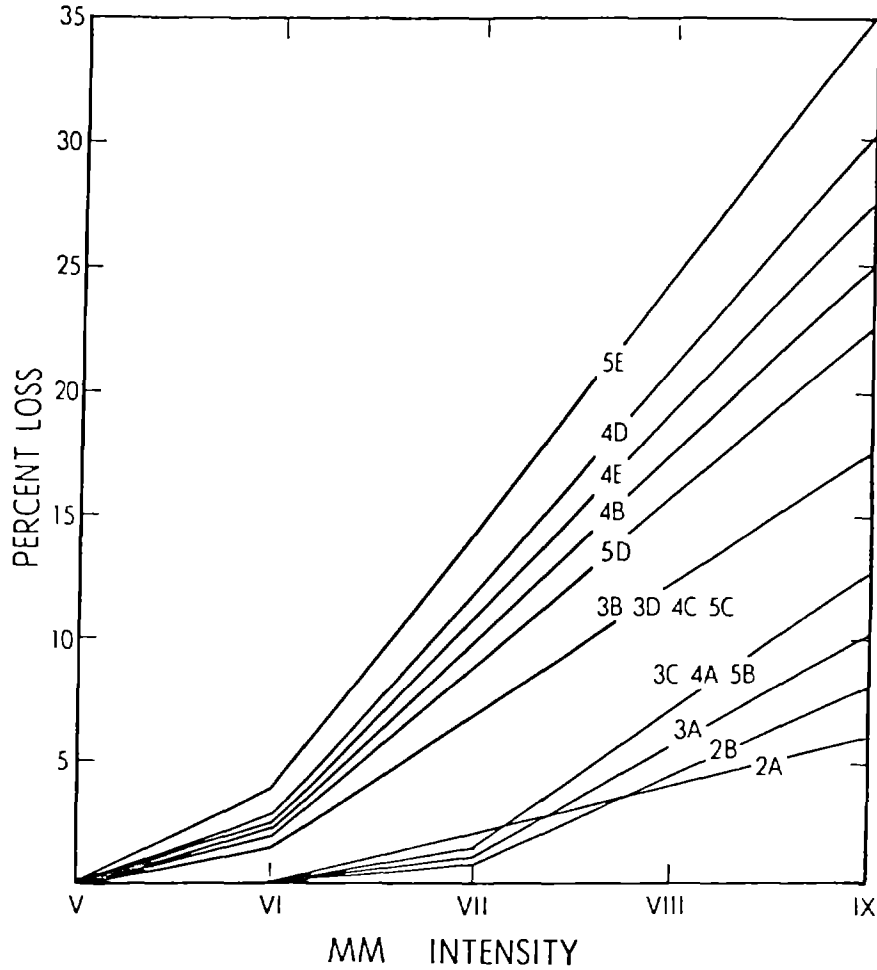


Figure 2.--Modified Mercalli intensity--loss relationship (by class of construction) used in this study. Descriptions of the various classes may be found in table 1. High-(H) and low-(L)rise subclasses of class 3 and class 4 have been combined.

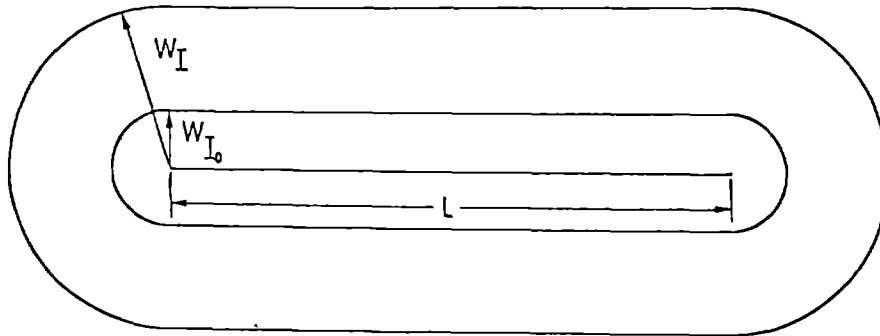


Figure 3.--Schematic showing the construction of average isoseismal maps (see text, p. 7, for discussion).

REFERENCES

1. U.S. Coast and Geodetic Survey, 1969, Summary and recommendations, in Studies in seismicity and earthquake damage statistics, 142 p.
2. Steinbrugge, K. V., McClure, F. E., and Snow, A. J., 1969, Appendix A, in Studies in seismicity and earthquake damage statistics: U.S. Coast and Geodetic Survey, 142 p.
3. Algermissen, S. T., Stepp, J. C., Rinehart, W. A., and Arnold, E. P., 1969, Appendix B, in Studies in seismicity and earthquake damage statistics: U.S. Coast and Geodetic Survey, 68 p.
4. Rinehart, W. A., Algermissen, S. T., and Gibbons, Mary, 1976, Estimation of earthquake losses in single-family dwellings: U.S. Geological Survey Open-File Report 76-156, 57 p., plus appendices.
5. U.S. Geological Survey, 1973, Atlas of Urban and Regional Changes, San Francisco Bay area: U.S. Geological Survey Open-File Report, 44 maps, 1:62,500.
6. Western Economic Research Company, 1973, Census Tract Outline Map of the Bay Area and Vicinity: Sherman Oaks, Calif., Scale 1:125,000.
7. Algermissen, S. T., Steinbrugge, K. V., and Lagorio, H. J., 1978, Estimation of earthquake losses to buildings (except single-family dwellings): U.S. Geological Survey Open-File Report 78-441, 146 p., plus appendices.
8. Wood, H. O., and Neumann, Frank, 1931, Modified Mercalli Scale of 1931: Seismological Society of America Bulletin, v. 21, p. 277-283.
9. Voight, D. S., and Byerly, P., 1949, The intensity of earthquakes as rated from questionnaires: Seismological Society of America Bulletin, v. 39, p. 21-26.
10. Richter, C. F., 1958, Elementary seismology: San Francisco, Calif., W. H. Freeman & Co., 768 p.
11. Algermissen, S. T. (principal investigator), Rinehart, W. A., Dewey, J. W., Steinbrugge, K. V. (principal consultant), Lagorio, H. J., Degenkolb, H. J., Cluff, L. S., McClure, F. E., Scott, Stanely, and Gordon, R. F., 1972, A study of earthquake losses in the San Francisco Bay area--A report prepared for the Office of Emergency Preparedness: U.S. Department of Commerce, National Oceanic and Atmospheric Administration, Environmental Research Laboratories, 220 p.
12. Borchardt, R. D., Joyner, W. B., Warrick, R. E., and Gibbs, J. F., 1975, Response of local geologic units to ground shaking, in Studies for seismic zonation of the San Francisco Bay area: U.S. Geological Survey Professional Paper 941-A, p. A52-A67.
13. Wesson, R. L., Helley, E. J., Lajoie, K. R., and Wentworth, C. M., 1975, Faults and future earthquakes: U.S. Geological Survey Professional Paper 941-A, p. A5-A30.

EXAMPLES OF SEISMIC ZONATION IN THE SAN FRANCISCO BAY REGION

by

W. J. Kockelman^I and E. E. Brabb^{II}

ABSTRACT

Six examples of seismic zonation at various scales by cities and counties in the San Francisco Bay region show that scientific information can be used effectively in avoiding earthquake hazards and mitigating damage. The zonation method involves postulating an earthquake, grouping geologic materials with similar physical properties, predicting the geologic effects of an earthquake, and combining the geologic effects on a map. The method has been used by the Cities of Mountain View, Novato, and San Francisco and the Counties of Marin, Santa Clara, and San Mateo to develop zones which were used as a basis for their general plans, seismic safety plans, development policies or ordinances.

INTRODUCTION

The proceedings of the International Conference on Microzonation for Safer Construction Research and Application, Seattle, 1972 included papers on the state of the art, various techniques, and a preliminary analysis of zonation methods. The papers lack uniform definition of "seismic zones," lack consensus on the scale and detail of seismic zone maps, and reveal the need for an unambiguous zonation method (10).

Three events have encouraged communities to attempt seismic zonation: passage of the Alquist-Priolo Act by the California Legislature requiring special studies in zones encompassing potentially and recently active faults (5), preparation and adoption of seismic safety plan elements by cities and counties as required by California statute (4), and further development of a seismic zonation method (2). The method has four steps: postulating an earthquake of a given size and location; grouping geologic materials with similar physical properties; predicting effects of the postulated earthquake for each geologic unit by type of hazard or failure, namely surface rupture, ground shaking, flooding, liquefaction potential, and landsliding; and combining geologic effects by zones on a map (1).

The following six examples of seismic zonation by cities and counties in the San Francisco Bay region illustrate applications of the method.

INVESTIGATION ZONES

Three "investigation zones" are derived and mapped at a scale of

-
- I Environmental Planner, U.S. Geological Survey, 345 Middlefield Road, Menlo Park, California, 94025
 - II Research Geologist, U.S. Geological Survey, 345 Middlefield Road, Menlo Park, California, 94025

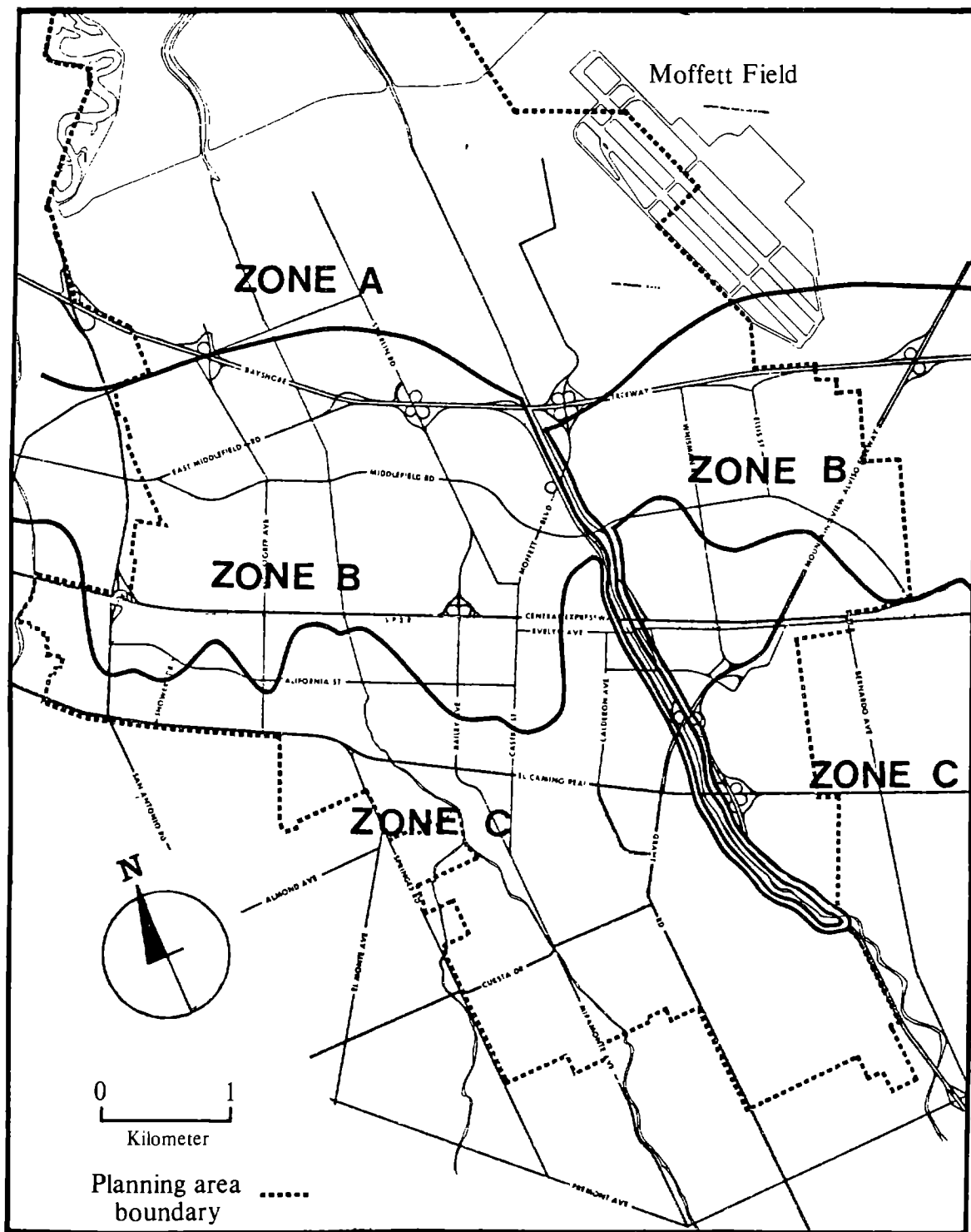


Figure 1.--City of Mountain View "investigation zones." The boundaries of the zones separate areas with different geologic properties. Zone A, for example, is underlain by water-saturated bay mud with a moderate to high liquefaction potential whereas zone B contains seasonally saturated alluvial fan deposits that may liquefy only when the water table is high (6, 20). Different development policies have been adopted for each of the zones (8).

1:48,000 (fig. 1) by the City of Mountain View Planning Department from its review of various earth-science information. Ground shaking and ground failure are considered the primary earthquake problems (8).

An earthquake on either the San Andreas or Hayward fault systems is assumed (7). Design earthquakes of magnitudes 8.0 and 6.5 may be implied from the Department's use of potential liquefaction data (6, 20).

Each "investigation zone" contains geologic units with similar physical properties. Zone A is underlain mostly by water-saturated bay mud. Zone B is underlain by weakly consolidated mud, silt and sand that are seasonally saturated. Zone C is underlain by somewhat coarser grained alluvium that is generally well drained and unsaturated (8, 9).

Geologic effects are predicted for each group of geologic units having similar properties. For example, "Moderate to substantial settlement and/or differential settlement may occur" in zone A, "Deep liquefaction and significant settlement ... is possible" in zone B, and "Neither significant settlement nor ground failure is likely to be experienced" in zone C (8).

With the aid of the zone map (fig. 1), areas of "relative seismic concern," such as those where loss of life, property damage and economic dislocation may occur, are delineated on the City's existing "General Plan Map." Land uses are subdivided into categories by importance, such as hospitals and fire stations that must provide emergency services after an earthquake; by occupancy, such as schools and other buildings that contain large numbers of people; and by type of construction, such as single-family dwellings. Development policies, such as "open space and low intensity uses shall be encouraged for sites most susceptible to earthquake damage," and "Uses should be limited to those when risk of loss of life, property damage, and social and economic dislocations are acceptable if liquefaction or settlement takes place," are specified for each land use group in each zone (8).

The zones, areas of "relative seismic concern," and land-use development policies have been incorporated into the City's Safety Element and adopted by the City Council as part of its general plan (8).

BUILDING DAMAGE LEVELS

Four levels of building damage aggregated on a block basis are estimated and mapped at a scale of 1:48,000 (fig. 2) for the San Francisco City Planning Department (3, 14).

A repetition of the 1906 earthquake (magnitude 8.3) originating on the San Andreas fault is assumed. Earthquakes with smaller magnitudes are also considered (3).

Soil and rock types are combined on the basis of similar engineering properties, and their susceptibility to earthquake failure is discussed (3). Their properties are reconsidered in estimating the types of potential ground motion such as peak ground acceleration, spectral response acceleration, and predominant periods for deep or soft soil deposits (14).

City Assessor's data on construction type, year built, number of

stories, floor area, and use of each building along with earthquake history were considered to obtain average damage factors for each block. The factors were then weighted to obtain the four levels of estimated building damage shown in figure 2 (14).

Hazards such as seiches, tsunamis, landslides, and dam failures are considered and mapped but are not generally used in developing the four levels of damage. These hazards are to be treated as "additional hazards;" for example, a building with a "slight" damage rating (fig. 2) that is apt to slide down a hill with a landslide should have its rating changed to "severe" (3).

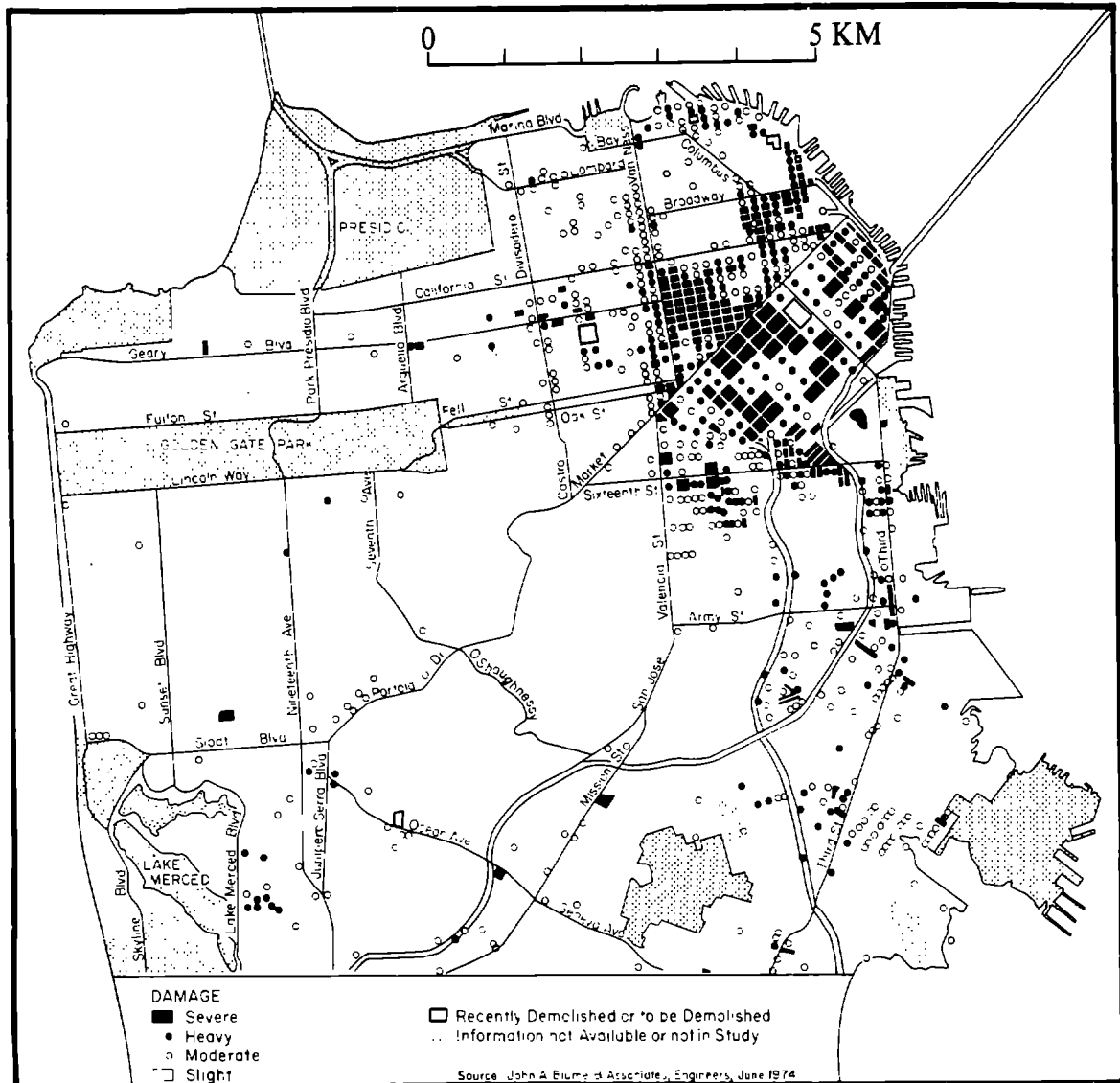


Figure 2.--Estimated building damage for a severe earthquake in the San Francisco area. Abatement of hazards associated with these buildings is recommended in San Francisco's Community Safety Plan (14).

Policies related to building damage levels such as "Initiate orderly abatement of hazards from existing buildings and structures" and "Abate existing hazards in all critical community facilities" are recommended (14).

The building damage levels, "additional hazards" and policies have been incorporated into the City's Community Safety Plan and adopted by the Board of Supervisors as part of the City's comprehensive plan (14).

EARTHQUAKE RISK ZONES

Five "earthquake risk" zones are developed and mapped at a scale of 1:12,000 (fig. 3) for the Novato area by the California Division of Mines and Geology in cooperation with the County of Marin and the City of Novato (13). Ground shaking, surface rupture, ground failure, and landslides are considered as having the highest potential for damage, whereas tsunamis are considered not to be significant potential hazards (12, 13). An earthquake of approximately magnitude 8 with an epicenter in the northern San Francisco Bay area is postulated (13).

Geologic materials are grouped into five zones on the basis of similar physical properties; for example, "firm, relatively unweathered bedrock" in zone A, "relatively shallow compacted alluvium and colluvium" in zone B, "deep upslope landslide deposits" in zone D, and "bay mud" in zone E. In addition, a symbol is placed over the trace of the potentially active Burdell Mountain fault (13).

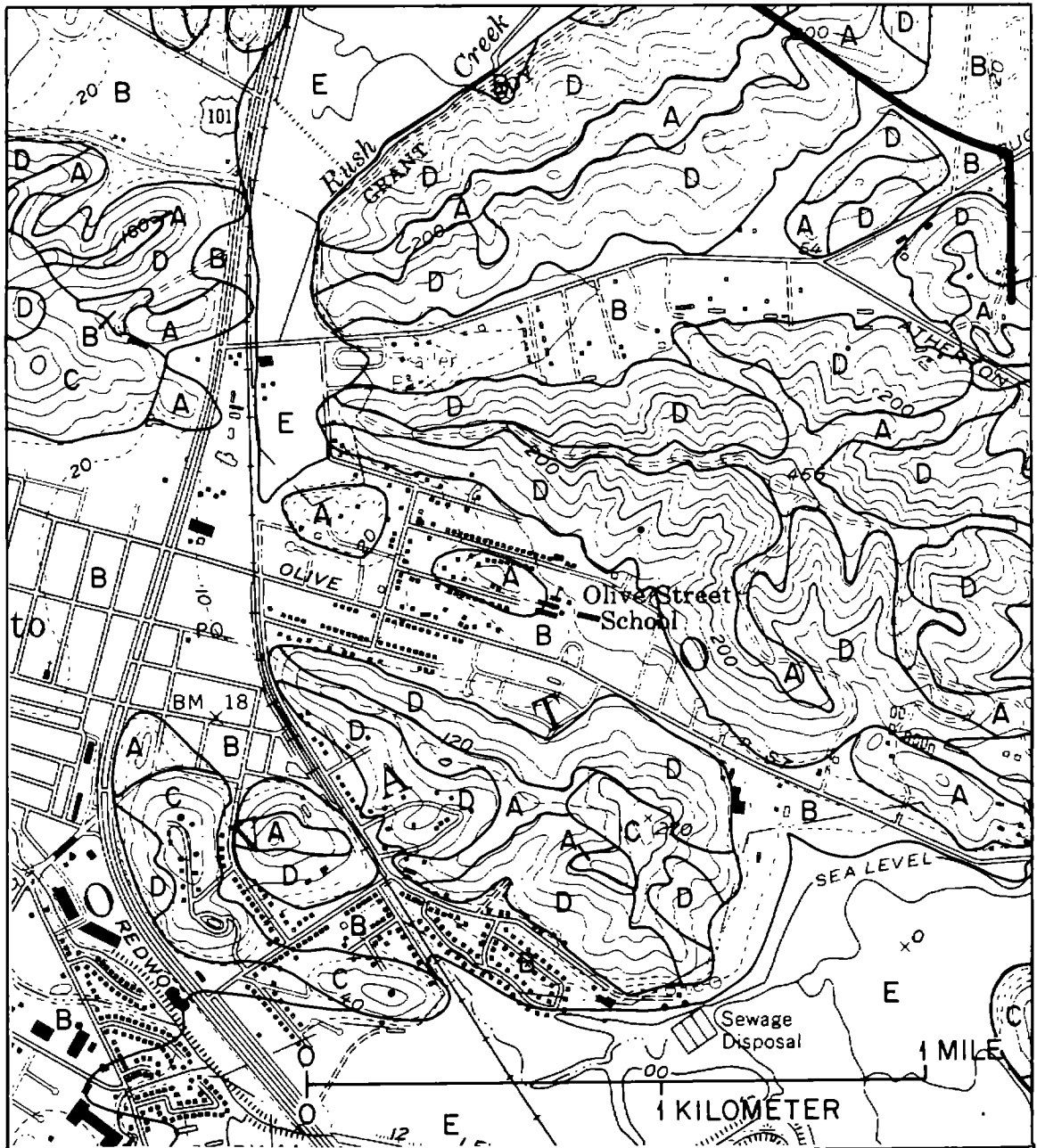
Some geologic effects of the postulated earthquake are predicted for each zone; for example, "subject to relatively high frequency vibrations" in zone A, "may be threatened by landsliding" in zone B, and "rapid differential settlement" in zone E. In addition, each zone is rated from probable low to probable high damage. The geologic materials, geologic effects, and damage ratings are combined and mapped by zone on figure 3 (13).

Recommendations related to the risk zones, such as "large public structures ... not be located on any demonstrated fault trace," "residential developments on fill may not be a fitting use" in zone E, and "Engineering geology reports, based on detailed geological mapping, [should] be required" in zone D, are made (13).

The "earthquake risk" zones and recommendations have been considered by the City of Novato and the County of Marin and used as a basis for their seismic safety plan elements.

SEISMIC SAFETY ZONES

Three "seismic safety zones" are developed and mapped at a scale of 1:62,500 (fig. 4) by the Santa Clara County Planning Department with assistance or contributions from the California Division of Mines and Geology, private consultants, and members of the U.S. Geological Survey (18). Dam failures, tectonic creep, dike failures, tsunamis, seiches, landslides, ground-shaking and surface ruptures were considered and the potentially hazardous ones were combined in zones on a "relative seismic stability" map (18). This map also includes nonseismic geologic hazards, such as landslides triggered by rainfall. The original map is printed in



- A** Areas of probable low damage. These areas are underlain by firm, relatively unweathered bedrock that crops out at the surface or is covered by only thin layers of soil or colluvium.
- B** Areas of probable low to moderate damage. These areas are underlain by relatively shallow, compacted alluvium and colluvium on flat or gently sloping surfaces.
- C** Areas of probable low to moderate damage. These areas are underlain by sheared bedrock.
- D** Areas of potentially high damage. These areas are underlain by landslide deposits and by thick deposits of colluvium or deeply weathered bedrock on steep slopes.
- E** Areas of probable high damage. These areas are underlain by bay mud ranging in thickness from a few feet to more than 100 feet.

— Fault

Figure 3.--Earthquake risk zones in the Novato area, Marin County, California (13).

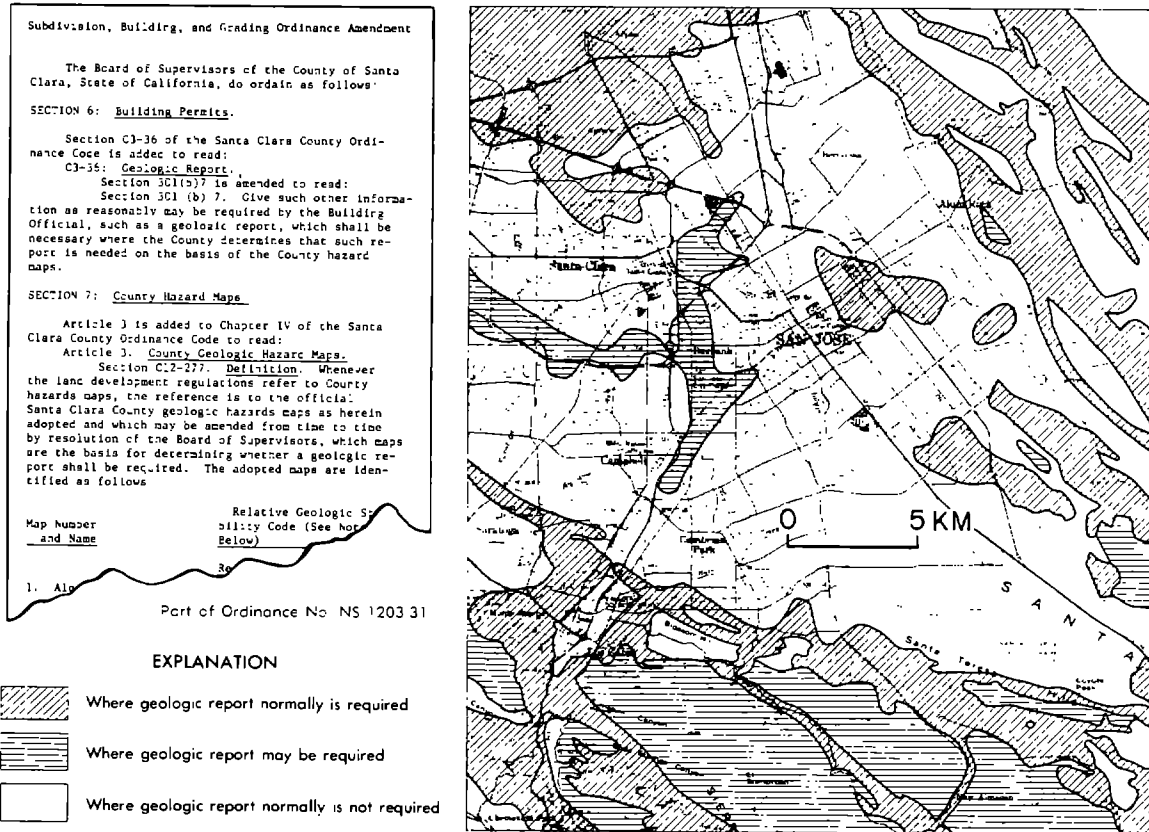


Figure 4.--Part of the official seismic stability map for Santa Clara County (18). Scale 1:250,000.

stoplight colors--red, yellow, and green--to make the information more easily understood by the general public.

A recurrence of the 1906 earthquake (magnitude 8.3) along the San Andreas fault zone in the San Francisco Bay area may be implied from the Department's discussion of the various seismic hazards (18).

Geologic units are grouped on the basis of similar physical properties, and the geologic effects are predicted for each group. For example, fine-grained water-saturated sand or silt within 6 meters of the ground surface would be considered to have a high potential for liquefaction and would normally require geologic investigation before any development is approved. The same materials within 6 to 15 meters of the surface are considered to have a moderate potential for liquefaction and might require a geologic investigation. In most cases, the county geologist decides whether and what level of geologic investigation is required.

Maps of other county plan elements, such as utility, transportation, community facilities, and urban development, are compared with the zone map to indicate their relation to the seismic safety zones (18). Recommendations to minimize the possible loss of life and property are made for each

county plan element. For example, "Emergency operations center structures should be evaluated for seismic vulnerability and should be designed and constructed to assure the continuity of vital services following a damaging earthquake," and "Proposed transportation routes, facilities and structures should be evaluated for potential vulnerability and built only if problems can be sufficiently mitigated" (18).

The three zones and recommendations are included in the County's Seismic Safety Plan which was unanimously adopted by the County Planning Commission and Board of Supervisors. In addition, the seismic safety zones have been adopted by the Board of Supervisors as the County's official geologic hazard maps. The County Ordinance Code has been amended so as to require site investigations and geologic reports based on the official geologic hazards map. Four sections of the code are affected: major subdivisions, minor land divisions, building sites, and grading. The amendment provides for site investigations and geologic reports so as to discourage development on, or adjacent to, known potentially hazardous areas. The reports are to be prepared by an engineering geologist registered in the State, be submitted to the County for approval, and specify the remedial measures that will make a safe development (17).

GEOTECHNICAL HAZARD SYNTHESIS

Thirteen geologic materials and seven geologic hazards are compiled, combined, and mapped at a scale of 1:24,000 (fig. 5) by the San Mateo County Planning Department and its consultant. Primary consideration is given to the extent and location of faults and to liquefaction potential; however, landslides, dam failure, and tsunamis are also considered and mapped. Seiches are considered but not mapped (11).

A magnitude 7.5-8.3 earthquake on the San Andreas fault is assumed for ground shaking. For fault displacement, a maximum expected magnitude 8.25 earthquake for the San Andreas fault and magnitude 7.0 for the Seal Cove-Gregorio fault are used (11).

Geologic materials are grouped on the basis of similar physical properties; for example, "younger estuarine mud and artificial fill" as no. 1, "beach and dune sand" as no. 4 "colluvium" as no. 5, and various "bedrock" hardnesses as nos. 6-13 (11).

Earthquake stability is predicted for each geologic material--"poor, fair, or good" depending upon geologic structure, slope angle and landslide and soil creep potential. Earthquake intensity is predicted for each geologic material unit--"strong, very strong, violent, very violent, and weak" depending upon the distance from the San Andreas fault (11).

The geotechnical hazard synthesis is part of the County's Seismic and Safety Elements of the General Plan. These elements include recommended policies and implementation programs regarding existing land use, future land use and development, zoning and division of land, and critical-use structures that are directly related to the geotechnical hazard synthesis maps; for example, "Determine the level of acceptable risk which can be borne, utilizing the ... Maps," and "Integrate geotechnical hazard data ... into zoning and subdivision ordinances" (16). The elements, including the geotechnical hazard synthesis maps and recommended policies and implementa-

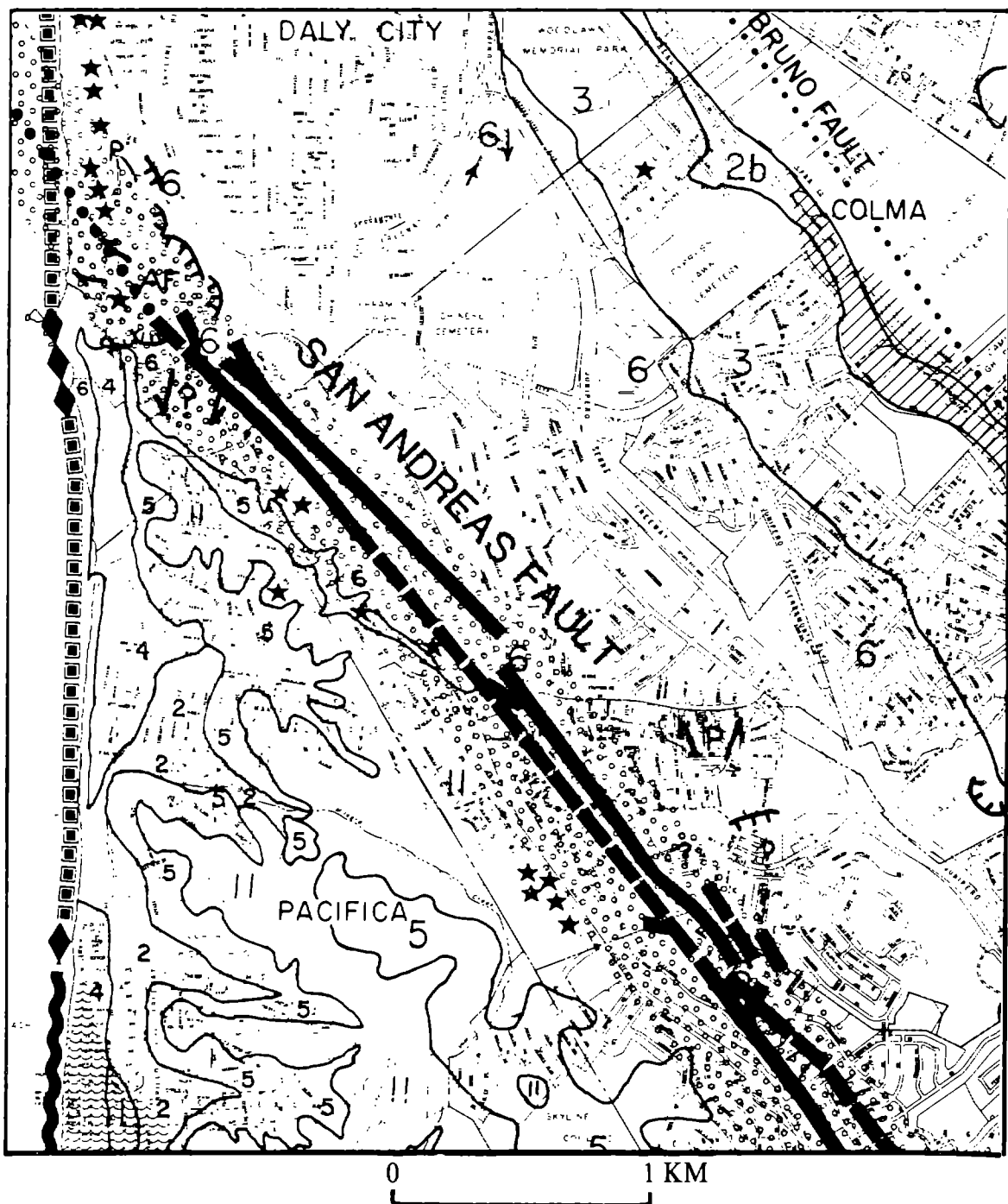


Figure 5.--Part of the geotechnical hazard synthesis map for San Mateo County (11), scale 1:24,000. The explanation for this map is complex, combining information on geologic processes, such as faulting, landsliding, coastal erosion, and liquefaction, with information on geologic materials, shown by numbers on the map. The material units are further subdivided by both seismic and engineering characteristics. For example, areas designated "2b" are underlain by alluvial fan deposits ranging in coarseness from silt to gravel, have poor to fair slope stability, moderate liquefaction potential, good to fair stability in terms of the intensity of ground shaking during a 7.5-8.3 M earthquake, and have good foundation properties.

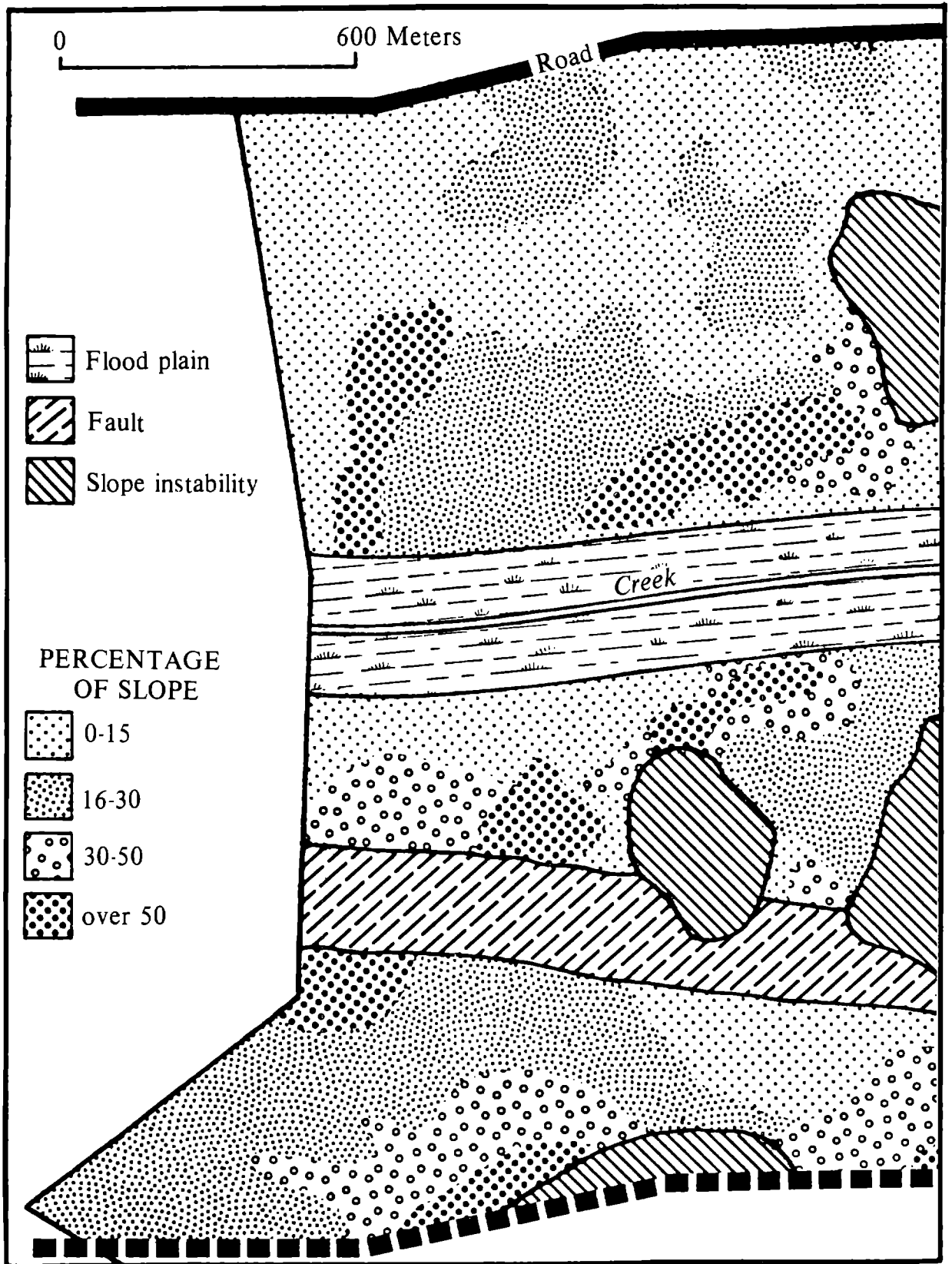


Figure 6.--Hypothetical property in San Mateo County with seismic and geologic constraints. Dwelling units in the fault zone and on landslides are limited to one per 16 hectares (40 acres). Similar low dwelling-unit densities are required along flood plains and on steep slopes (19).

tion programs, have been adopted by the County Board of Supervisors (16).

RESOURCE MANAGEMENT ZONING DISTRICT

Eleven land categories are derived and mapped at various scales by the San Mateo County Planning Department. Seven of the categories (fig. 6) were considered serious seismic or geologic constraints to development (19).

A 7.5-8.3 magnitude earthquake on the San Andreas fault is implied from the seismic hazard information used by the Department (19).

The seismic and geologic constraints are grouped on the basis of similar physical properties--faults, slopes, flood plains, and slope instability. Geologic effects are predicted for two categories; "potential surface deformation due to fault movement," and high, moderate, and low "susceptibility of slopes to failure landslides" (19).

The Department recommended that the permitted density of residential development proposed in each category be reduced to minimize risk exposure and to carry out the objectives and policies of the County's open-space and conservation plans (19).

The Board of Supervisors adopted an ordinance creating a resource management zoning district (15). In addition to the principal uses permitted in the district, the maximum number of dwelling units is limited by special density regulations. The regulations are applied to each application for a zoning permit through the use of a density matrix worksheet (15, 19). For example, 100 hectares (250 acres) of the hypothetical property shown on figure 6 would lie in the fault and slope instability zones where the number of dwellings would be only one per 16 hectares (40 acres).

CONCLUSION

The seismic zonation method can be applied by cities and counties to avoid earthquake hazards, to reduce loss of life, and to mitigate damage. The examples help clarify the definition, scale, and detail of "seismic zones" and provide a workable method for presenting earthquake effects in a form usable by scientists, engineers, land-use planners, decisionmakers, and other citizens.

REFERENCES CITED

- (1) Borcherdt, R. D., Brabb, E. E., Joyner, W. B., Helley, E. J., Lajoie, K. R., Page, R. A., Wesson, R. L., and Youd, T. L., 1975, Predicted geologic effect of a postulated earthquake in Borcherdt, R. D., ed., Studies for seismic zonation of the San Francisco Bay region: U.S. Geological Survey Professional Paper 941-A, p. 88-94.
- (2) Borcherdt, R. D., ed., 1975, Studies for seismic zonation of the San Francisco Bay region: U.S. Geological Survey Professional Paper 941-A, 102 p.
- (3) Blume, John A. and Associates, 1974, San Francisco seismic safety investigation: San Francisco, CA, 124 p.
- (4) California Legislature, Amendment to the local planning chapter,

- 1972: California Government Code, sec. 65302 (f), West's annot. Codes.
- (5) _____ Alquist Priolo special studies zones act, 1975: California Public Resources Code, secs. 2621 et seq., West's annot. Codes.
 - (6) City of Mountain View Planning Department, 1974, Safety element: Earth science data interpretive report, Background report I, Mountain View, CA, 31 p.
 - (7) _____ 1975, Relative concern zones, structural hazards, critical facilities and fire hazards: Background report II, Mountain View, CA, 47 p.
 - (8) _____ 1975, Safety element of the general plan: Resolution no. 10392, Amend. No. 16, adopted February 24, 1975, Mountain View, CA, 14 p.
 - (9) Helley, E. J., and Brabb, E. E., 1971, Geologic map of late Cenozoic deposits, Santa Clara County, California: U.S. Geological Survey Miscellaneous Field Studies Map MF-335.
 - (10) International Conference on Microzonation for Safer Construction Research and Application, Seattle, 1972: Proceedings, Seattle, WA, Vols. I and II, 987 p.
 - (11) Leighton & Associates and San Mateo County Planning Department, 1976, Geotechnical hazard synthesis map: Redwood City, CA, 7 sheets.
 - (12) Rice, Salem J., 1973, Geology and geologic hazards of the Novato area: California Division of Mines and Geology, 47 p.
 - (13) _____ 1975, Geology for planning - Novato area: California Division of Mines and Geology, 56 p., 6 pls.
 - (14) San Francisco Department of City Planning, 1974, Community safety plan - A proposal for citizen review: 68 p.
 - (15) San Mateo County Board of Supervisors, 1973, Ordinance No. 2229, adding a Resource Management District and regulations to the county zoning ordinance: Adopted December 20, 1973, 24 p.
 - (16) San Mateo County Planning Department, 1976, Seismic and safety elements of the general plan: Redwood City, CA, Vol. I, 57 p., Vol. II, 141 p.
 - (17) Santa Clara County Board of Supervisors, 1974, Ordinance No. NS 1203.31, amending the subdivision, building, and grading ordinances, and adding geologic hazard maps to the County Ordinance Code: Adopted November 6, 1974, 11 p.
 - (18) Santa Clara County Planning Department, 1975, Seismic safety plan, An element of the general plan: San Jose, CA, 119 p.
 - (19) Woolfe, Donald A., 1973, San Mateo County Planning Depart, Adoption of the resource conservation area density matrix and policy statement: Memorandum dated September 21, 1973, 32 p.
 - (20) Youd, T. L., Nichols, D. R., Helley, E. J., and LaJoie, K. R., 1975, Liquefaction potential in Borcherdt, R. D., ed., Studies for seismic zonation of the San Francisco Bay region: U.S. Geological Survey Professional Paper 941-A, p. 68-74.

THE USE OF EARTHQUAKE AND RELATED INFORMATION
IN REGIONAL PLANNING--WHAT WE'VE DONE AND WHERE WE'RE GOING

by

Jeanne B. Perkins^I

ABSTRACT

ABAG has used several techniques for combining earth science maps. These techniques include land capability analysis and various methods of calculating maximum earthquake intensity and cumulative economic risk due to earthquake damage. The resulting maps and data are more easily used in ABAG's planning programs, including:

- o providing data on characteristics of large vacant industrial sites and potential seaports
- o locating areas deserving further study for use as potential disposal sites for hazardous wastes
- o assessing the impacts of alternative future land use alternatives
- o reviewing regionally-significant development proposals on a continuing basis
- o providing information to city and county staff

ABAG's earthquake program plans to refine the existing earthquake maps by experimenting with the ways in which other relationships among geology, faults, topography, earthquake recurrence intervals and damage affect these maps. ABAG also expects to relate these maps more systematically to various land development patterns.

INTRODUCTION

ABAG is a regional comprehensive planning agency that is owned and operated by the local governments of the San Francisco Bay Area. It was established in 1961 to meet regional problems through the cooperative action of its member cities and counties.

The Bay Area is one of the most seismically active areas in the United States. The effects of earthquakes also usually cross city and county boundaries. Consequently, earthquake preparedness is a major regional concern.

SOME TECHNIQUES FOR COMBINING MAPS

Because it is difficult for planners and elected officials to deal directly with the reams of social, environmental, and economic information available concerning any given area or issue, ways of consolidating

^I Regional Planner, Association of Bay Area Governments, Berkeley, California

earth science data to slant that information to each application become valuable. Two techniques for combining earthquake and other earth science maps that ABAG staff have found useful are described below.

Maximum Earthquake Intensity and Cumulative Economic Risk

An earthquake intensity map groups together a variety of different causes of earthquake damage; although shaking is the dominant cause of damage, other factors such as liquefaction, landsliding, fault rupture, and changes in ground level can also contribute to intensity. Figure 1 is an example of a maximum earthquake intensity map for the San Francisco Bay Area based on the techniques developed by Borchardt, *et al.* (1). This map is not the only maximum intensity map that can be developed; altering the way that intensity is related to distance from a fault can produce a different map. This type of map can be used with information on existing buildings to forecast locations of maximum damage for use in planning emergency response measures and for designating areas of critical concern.

A cumulative economic risk map can relate the expected damage to particular types of buildings over time. Such maps rely on intensity information as well as information on the amount of damage that can be expected for each intensity and general type of building and information on how often a particular earthquake is likely to occur. Figures 2A - D are examples of risk maps. They indicate the total expected percent damage due to earthquakes resulting from any of the major active faults in part of the Bay Area for any given area for two types of small buildings: wood-frame (Figures 2A and C) and other types (Figures 2B and D). Risk maps may be used in evaluating the relative costs due to earthquakes for new buildings in various locations throughout the region and for designating areas where special precautions may be needed. However, the intensity-cost information is not a sufficient basis for engineering decisions at a specific site, for these require specific knowledge of the process causing damage. The graphic appearance of a risk map is very dependent on how often earthquakes are assumed to occur on each fault. Figures 2A and B use a different set of recurrence intervals than Figures 2C and D.

Land Capability Analysis

Any microzonation map, though a representation of the earthquake problem, cannot by itself represent the problems due to all geologic constraints, let alone all environmental, social or economic constraints. By relating each geologic problem to some common denominator, such as cost or lives lost, one can effectively compare the geologic concerns or can add these concerns together, using traditional or computerized map overlaying techniques. Figure 3 is an example of such a map, based on cost information for residential development in Santa Clara County.

SAMPLE USES

Solid Waste Planning

The earthquake intensity map and other geologic and hydrologic maps were used with map-related criteria to screen the Bay Area to find those general areas that warranted further study for use as disposal sites for hazardous waste.

After additional screening using other social and environmental criteria, ABAG staff discovered that only four of the nine Bay Area counties had areas worthy of additional study.

Special Facilities

The problem of overlaying maps may be avoided by simply providing a listing of the level of concern (high, moderate or low) for environmental safety issues in the form of a computer display. If land capability information is also available, a general indicator of overall concern for environmental safety also can be included. Separate displays have been prepared for approximately 450 vacant industrial sites and 173 proposed seaport sites in the Bay Area.

Assessment of Development Patterns

As part of assessing the environmental impacts of planning programs, it is important to know the relationship of geologic hazards to alternative land use or development patterns. Earthquake intensity and related information has been used in assessing the implications of policies that encourage more dense central city growth as opposed to less compact development in suburban and rural areas in the region. It has also been used in assessing development patterns intended to reduce commute distances for Santa Clara County.

Implementing Regional Policies

As the designated areawide clearinghouse, ABAG reviews local plans and projects that propose to use Federal and State funds. One of the review criteria used is the completeness of the description of geologic and seismic hazards affecting the site. Microzonation maps and information on other geologic hazards is used in the reviews.

In addition, ABAG assists cities and counties in obtaining earthquake information and incorporating that information into their programs as time permits.

FUTURE PLANS

Updating Information

Because earthquake microzonation is such a dynamic field, it is essential that all maps can be easily updated. All of the basic information, including geology and land use, the modeling techniques, and the

products, including maps and displays, are integrated in ABAG's computerized Bay Area Spatial Information System (BASIS). Thus, as better information on correlations between geologic materials and earthquake intensity or on recurrence intervals becomes available, the interpretive maps and the related information will be modified easily. The system also allows cities and counties to modify the maps for their own uses. Maps can be produced at non-standard scales, such as 1:60,000 for Santa Clara County. Requests can be fulfilled to group peat soils with Bay mud, rather than with alluvium, for generating a maximum intensity map for Contra Costa County.

Future Applications

Several interesting projects using earthquake and related information should be completed by December 1979. The displays for special facilities will be expanded to include existing and proposed airports and solid waste disposal sites. The work on assessment of development patterns should be dramatically improved when detailed information on current and projected land use is placed in BASIS. Such information also will be extremely valuable for planning emergency services. A more formal program will be instituted for ensuring that cities and counties more actively use the earthquake map information.

BIBLIOGRAPHY

1. Borchardt, R.D., Gibbs, J.F., and Lajoie, K.R., 1975, Maps Showing Maximum Earthquake Intensity Predicted for Large Earthquakes on the San Andreas and Hayward Faults, Southern San Francisco Bay Region, California, U.S. Geological Survey Miscellaneous Field Studies Map MF-709.

FIGURE 1

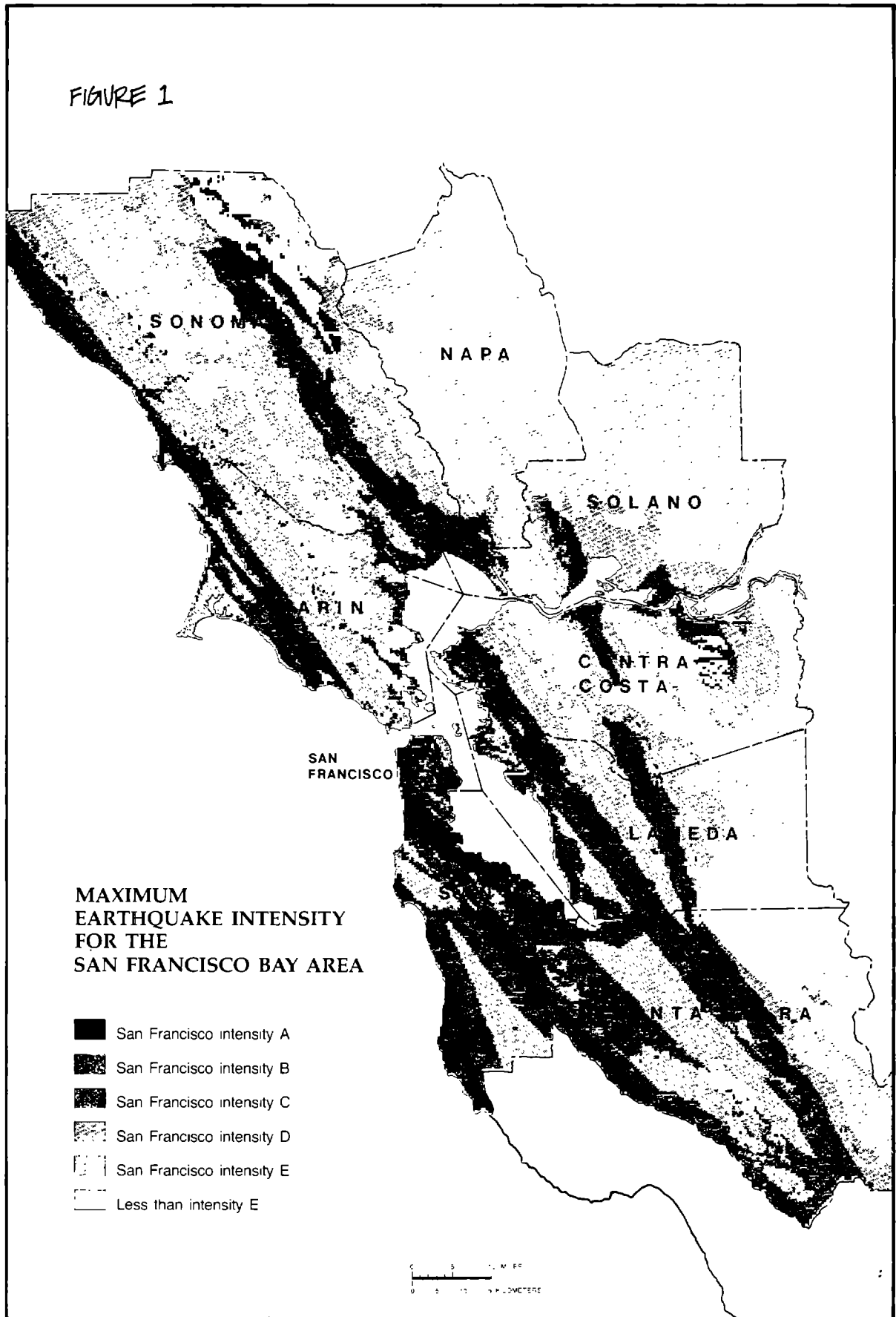
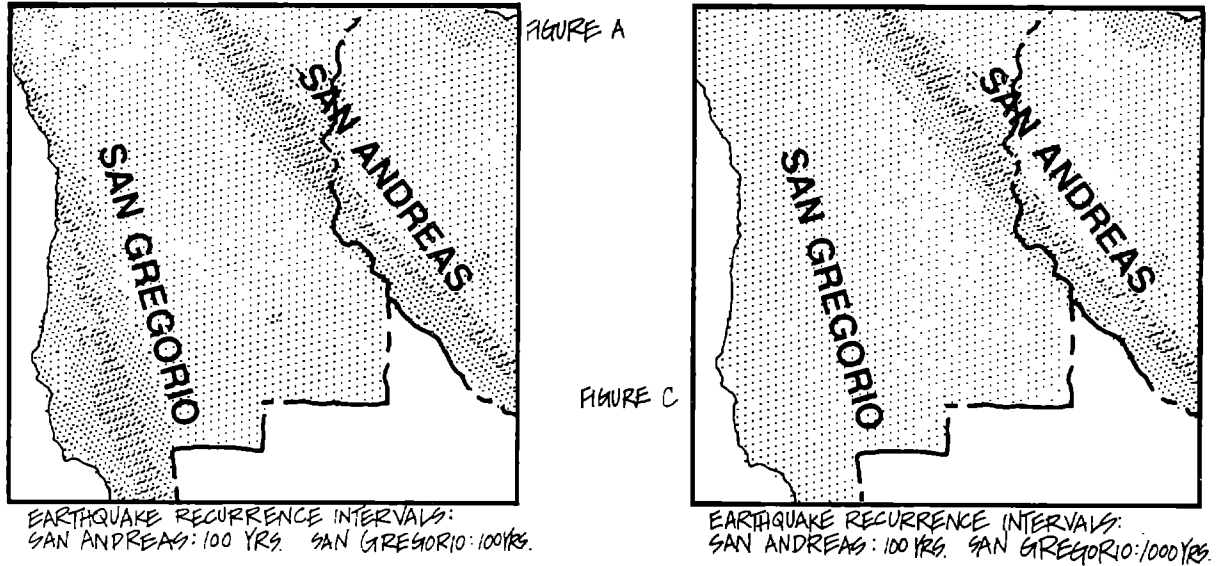


FIGURE 2:
**SAMPLE CUMULATIVE
 ECONOMIC RISK MAPS
 FOR EARTHQUAKE DAMAGE**

SMALL WOOD-FRAME BUILDINGS



OTHER SMALL BUILDINGS

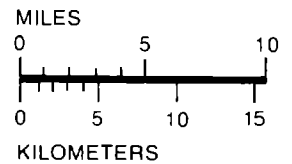
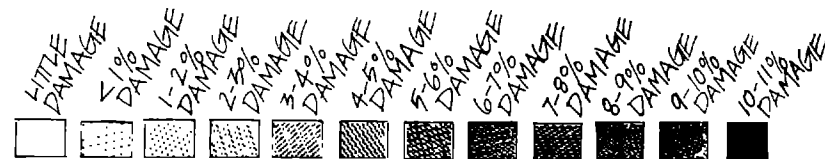
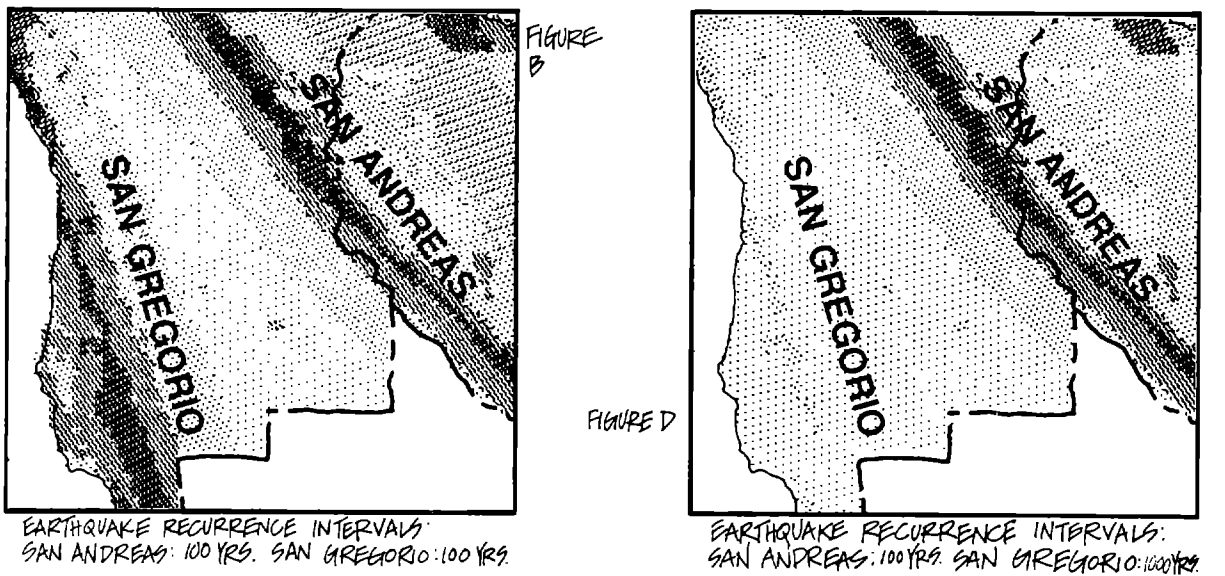
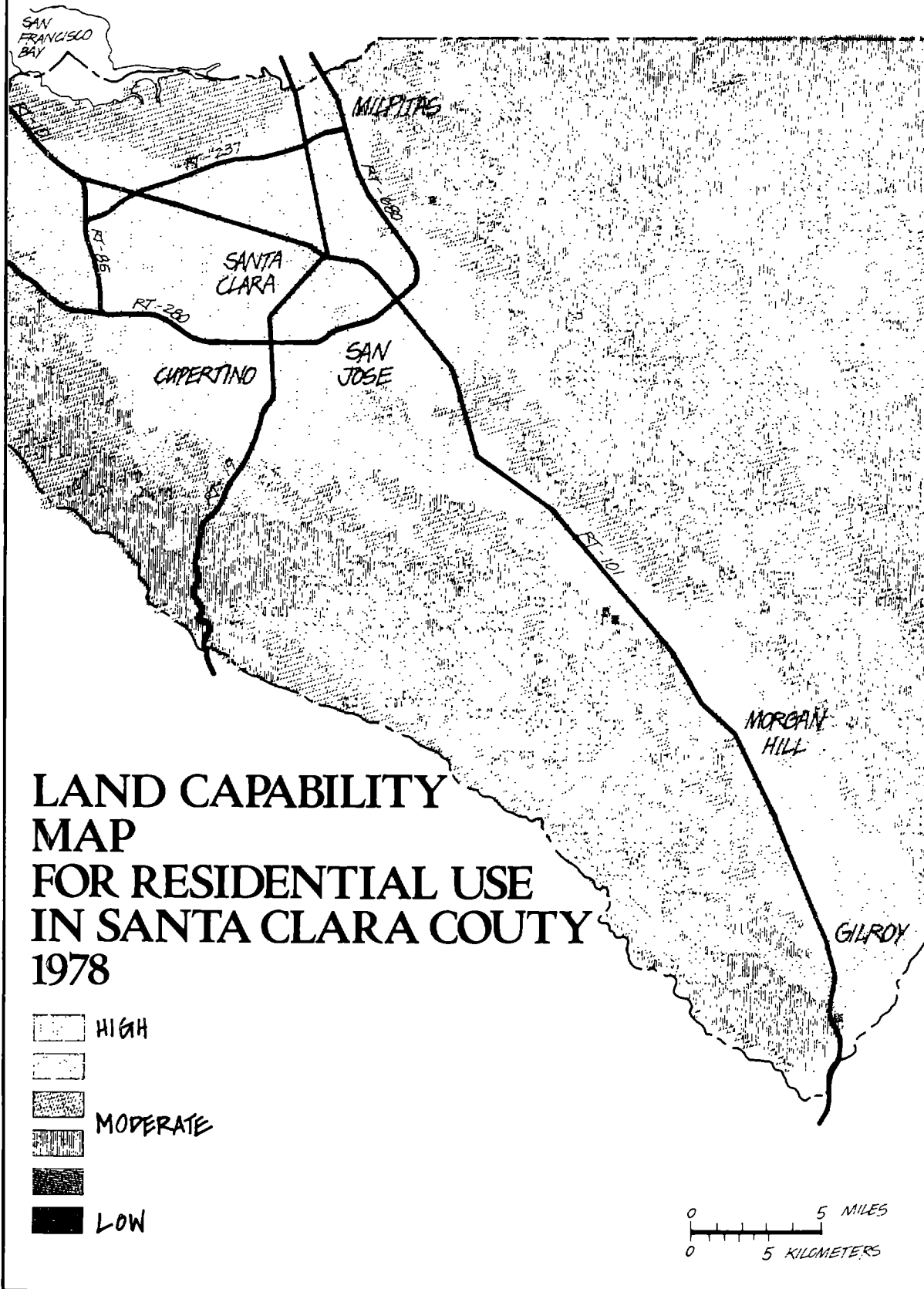


FIGURE 3



322

INTENTIONALLY BLANK

THE SENSITIVITY OF SEISMIC RISK MAPS TO THE CHOICE OF EARTHQUAKE
PARAMETERS IN THE GEORGIA STRAIT REGION OF BRITISH COLUMBIA

by

W.G. Milne and D.H. Weichert^I

ABSTRACT

A comparison is made between the calculated values of peak horizontal ground acceleration with an annual probability of exceedance of 0.01 for three sites in the Strait of Georgia. The acceleration amplitudes are calculated by extreme value, and average amplitude techniques using two different acceleration functions over two periods of time. The results show a scatter within the quoted error of data which are used in the National Building Code of Canada.

INTRODUCTION

The seismic zoning map, which is included in Supplement 1 of the National Building Code of Canada, was produced by methods outlined by Milne and Davenport (1969). The regional catalogue of Canadian earthquakes, from 1899 to date, forms the input to a Gumbel unlimited extreme value analysis of site specific accelerations. By this process, peak horizontal ground acceleration amplitudes with an annual probability of exceedance of 0.01 are calculated for specific sites or at a number of locations over an area to be zoned. The values of ground acceleration provide the basic input for drawing the contours of the seismic zoning map, and also provide an input to the dynamic analysis design method allowed by the code. Different methods were used for calculating the values of ground acceleration. This paper indicates the range of values which can be obtained, and points out the problems of unduly emphasizing a particular level of ground motion.

Since the original work, approximately 10 years ago, a number of modifications to the program have taken place. These have included a revised amplitude attenuation function, a revised alternate average amplitude method, and revision of some earthquake epicentres and magnitudes. This paper shows how these revisions have altered the acceleration levels at certain sites in the Strait of Georgia region. At these same sites, the stability of the risk model is examined as new data are added, or, as in the northern Strait, no new data have been observed.

ATTENUATION FUNCTION

The initial western acceleration attenuation function (Milne and Davenport, 1969) was derived from the strong motion seismic data that were available at that date. The formula used for this purpose was

I Pacific Geoscience Centre
Earth Physics Branch
9860 West Saanich Road
Sidney, B.C., Canada, V8L 4B2

$$ACC = \frac{0.69e^{1.64M}}{1.12^{1.1M} + \Delta^2} \quad (1)$$

where M is magnitude, Δ is epicentral distance, and ACC is a percentage of g. Data at close distances were not available at this date.

A revised formula (Milne 1977) takes a form which can more easily be adopted to a least squares fit. This form is

$$ACC = b_1 e^{b_2 M} \frac{b_3}{R} \quad (2)$$

$$\text{or } \log_e ACC = b_4 + b_2 M + b_3 \log_e R$$

where ACC is peak horizontal ground acceleration in units of g, M is magnitude (M_L where available, M_S where no M_L is available, m_b where M_L or M_S are missing, and M_N where it is the only magnitude available), R is hypocentral distance except for the Parkfield, 1966 earthquake where station to surface rupture by the causative fault is used. Where there is no published depth, a nominal value of 18 km is used. The analysis uses peak horizontal acceleration amplitudes from the maximum component of the data published by the California Institute of Technology, Volume II, parts A to Y. The 197 amplitudes are from accelerometers placed in free field locations, or in basements of buildings. All available data were used, which means that of the 197 readings, 103 are from the San Fernando earthquake on February 9, 1971. This data set is therefore biased by an earthquake of a particular type and in a particular region. The coefficients b_4 , b_2 , b_3 were fitted by a least squares subroutine using acceleration amplitude as the dependent variable. RMS errors for the coefficients are calculated.

$$\begin{aligned} \text{Values are } b_4 &= -3.23 \pm .38 \\ b_2 &= +0.99 \pm 0.01 \\ b_3 &= -1.39 \pm 0.08 \\ b_1 &= 0.04(25) \end{aligned}$$

CALCULATION OF ACCELERATION AMPLITUDES

In order to examine the stability of the model for computing seismic risk from historical seismic events, a number of computations have been made for three sites in the Strait of Georgia region. The first site is in the north, in the vicinity of the magnitude 7.3 earthquake in 1946. The second site is in the central portion of the Strait, near a major population centre at Vancouver, and near a locus of several minor earthquakes in 1975. The final site is at the south end of the Strait in a region of moderate earthquakes assumed to be shallow but also near epicentres of moderately deep (60-70 km) earthquakes in the Puget Sound. Table 1 lists the peak horizontal ground acceleration amplitudes with an annual probability of exceedance of 0.01 calculated by the following procedures:

a) - by the application of the original Milne/Davenport extreme value

analysis on earthquake epicentres from 1899 to 1963 using the attenuation curve in equation 1. Some of the epicentres have been recalculated; for instance, the epicentre of the 1946 earthquake has shifted to the west, but its magnitude remains unchanged. The lower threshold amplitude is set to the equivalent of intensity I, and focal depths are not involved.

- b) - by the application of method (a) using earthquakes from 1899 to 1977 inclusive. This is an extension of 14 years beyond the original data set during which some significant acceleration amplitude data were added, and during which some areas have been quiet.
- c) - by the application of the average amplitude method from the Milne Davenport paper to obtain the results using data from 1899 to 1963, with the attenuation curve of equation 1, with no allowance for varying focal depths, and with a lower threshold amplitude equivalent to intensity I.
- d) - by the application of the average amplitude method using data for the years from 1899 to 1977 inclusive.
- e) - by the application of the extreme value method using the attenuation curve of equation 2, data from 1899 to 1963, a threshold amplitude equivalent to intensity I, and focal depths which are published or are set to a nominal value of 18 km.
- f) - by the application of method (e) using data from 1899 to 1977.
- g) - by the application of the average amplitude method using the attenuation curve of equation 2, data from 1899 to 1963, a threshold amplitude equivalent to intensity I, and focal depths which are published or are a nominal 18 km.
- h) - by the application of method (g) using data from 1899 to 1977.

STABILITY OF THE MODEL

Comparison of the values of acceleration amplitude between methods a and b, c and d, e and f, and g and h shows that the extension of the data set from 65 to 79 years has increased the calculated risk at one site and decreased it at the other two. Clearly, the absence of contribution earthquakes has produced a lower risk level at site 1. A continuation of the earthquake experiences in the Puget Sound area has resulted in only a slight change at site 3, but an increase in activity near site 2 in late 1975 has raised the level here by an increase in the constant term in the least squares analysis without a corresponding change in slope. The maximum change is approximately 60%, at site 1.

The variation produced by the use of different attenuation curves is on the average lower than the variation produced by a difference in the period of observation. At site 3, the variation due to the change of attenuation curves is greatest, because of the presence of moderate nearby earthquakes.

The variation in amplitude levels between the extreme value method and the average amplitude method may also be seen in Table 1. This variation, on the average, is greatest, and at two of the sites the extreme value method is the lower of the two. This appears to indicate that in the central or northern Strait regions the low level, or background seismic activity is missing from the data set because it is in fact low or else it has been missed in the cataloging of events.

In summary, the variation in the .01 probability of exceedance of acceleration amplitudes is a function of the methods used, of the time period of the observations, and of the attenuation function in decreasing order of importance. The largest divergence is approximately a factor of two, generally quoted as the error of amplitude for the NBC.

BIBLIOGRAPHY

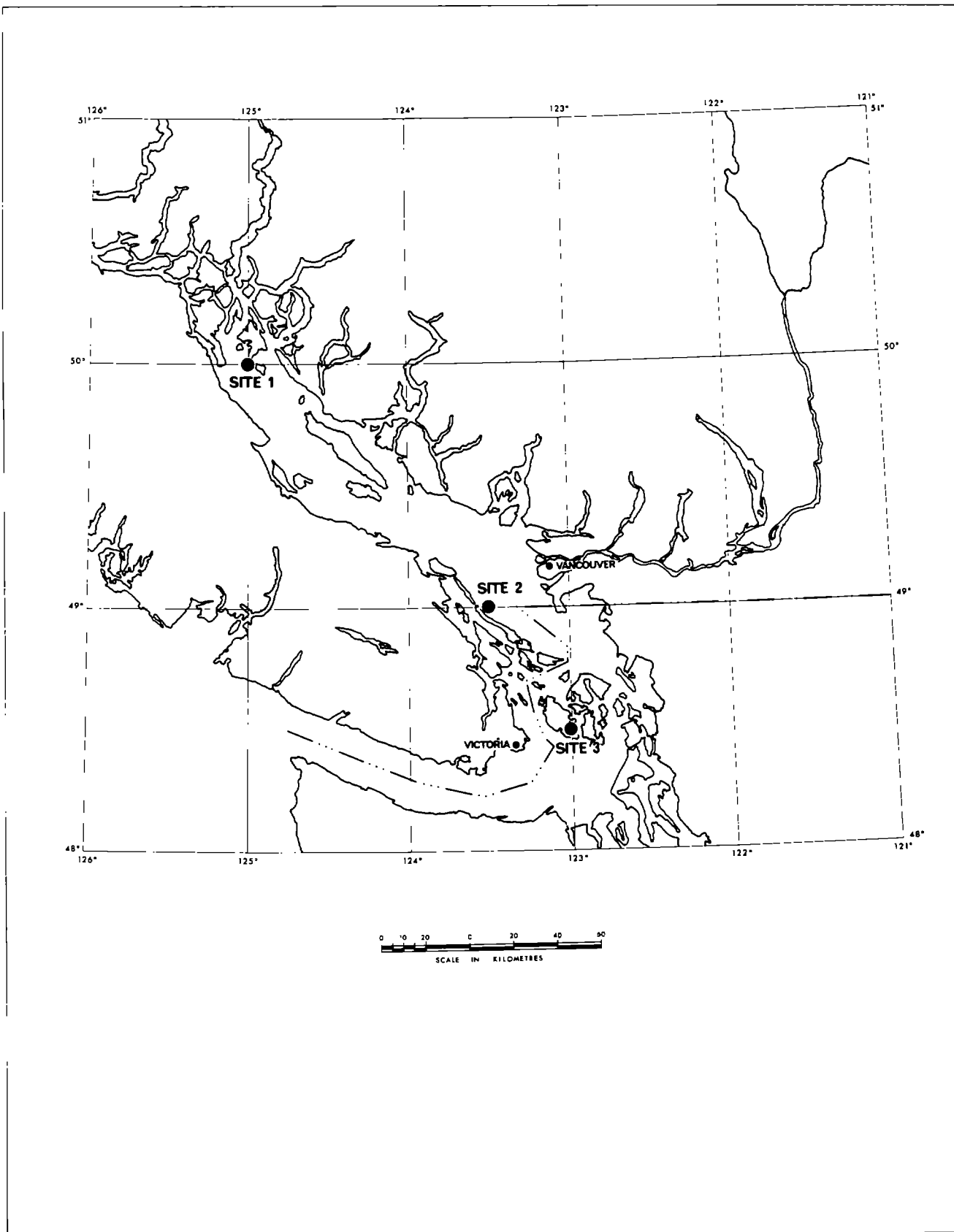
Milne, W.G., and Davenport, A.G. (1969). Distribution of earthquake risk in Canada, Bull. Seism. Soc. Am. 59, 729-754.

Milne, W.G. (1977). Proceedings of the 6th International Association of Earthquake Engineering.

Table 1

PEAK HORIZONTAL GROUND ACCELERATION AMPLITUDES (UNITS OF g)
(ANNUAL PROBABILITY OF EXCEEDANCE = 0.01)

Method	1969 attenuation function			1977 attenuation function		
	Extreme Value	Average Amplitude		Extreme Value	Average Amplitude	
	1896 to 1963 (a)	-1977 (b)	-1963 (c)	-1977 (d)	-1963 (e)	-1977 (f)
Site 1	.13	.08	.16	.12	.11	.09
Site 2	.12	.15	.14	.21	.12	.13
Site 3	.14	.13	.09	.08	.17	.16
					-1963 (g)	-1977 (h)
					.18	.14
					.15	.18
					.14	.12



THE MICROZONATION OF NEW YORK STATE: PROGRESS REPORT NO. 2

by

Joseph A. Fischer^I and James G. McWhorter^{II}

ABSTRACT

Some six years ago at the First International Conference on Microzonation, the authors described their interpretation of the spatial relationship of New York State earthquakes to the regional tectonics and the possible effects of New York seismicity upon man's construction. Since that time an abundance of information has been developed, much from nuclear plant studies and much from New York State Geological Survey research.

Of particular interest have been fault studies along the south shore of Lake Ontario and in southeastern New York/northeastern New Jersey. These studies have utilized geologic and geomorphic mapping, geophysical surveying and fluid inclusion study techniques. Geodetic measurements, earthquake fault plane analyses, and a number of insitu stress measurements have aided our attempts to develop an understanding of both the states' previous geologic history and its neo-tectonics.

Thus a number of the original authors' hopes for future (post-1972) research have been undertaken (although nowhere near completed).

This progress report reviews the recent studies, defines their effects upon the previous attempt at microzonation and defines the technical disciplines and geographical areas of needed research.

INTRODUCTION

In 1972, the authors presented the first paper on the Microzonation of New York State. At that time it was thought New York State would be a prime center of microzonation because of a number of reasons. These reasons included: a) relatively high seismicity in the St. Lawrence area along the northeastern part of the state; b) disagreements concerning the continuation of the high seismic activity to an area of the western portion of the state; c) high urbanization; and d) construction of major structures such as nuclear power plants. The state is of even greater interest when one considers the various assorted authors who have attempted to provide some form of seismic zoning for the state. The earliest was perhaps 1948 when F. P. Ulrich published zones of earthquake probability in the United States. The latest regionalization was in 1976 by Algermissen and Perkins and many of these are summarized by Kulhawy and Ninyo in 1977.

I Partner, Dames & Moore, Cranford, New Jersey.

II Senior Geologist, Dames & Moore, Cranford, New Jersey.

In addition to these various concepts of New York State seismology, recently another tempest in a teapot has brewed concerning the Indian Point nuclear reactors and the Ramapo Fault. Most of the Ramapo is in New Jersey, however, its northeast extension goes through the southeastern part of New York State.

Therefore, this paper will attempt to synthesize the various investigations in the State and present the results of not only the author's studies, but also the results of the work that has been undertaken by New York State Geological Survey, Lamont Doherty Geological Observatory, Cornell University, and others within the area. Although the authors have drawn upon the work of many in the State, they will accept the responsibility for the conclusions drawn herein.

TECTONIC HISTORY AND TECTONIC PROVINCES

An important aspect of siting critical structures, such as nuclear power plants, in the eastern United States is the identification of tectonic provinces within the region of influence about a proposed site. The authors have been involved recently with the development of such provinces (Dames & Moore, 1975). Studies of the inherent characteristics of the regional and subregional geology (the structure of petrographic assemblages and faunal zones), together with the plate tectonic theory, allow us to distinguish four major stages in the evolution of the Appalachian orogen and its individual components or tectonic provinces within New York and surrounding areas. These stages are:

1. Initial crustal divergence in Late Precambrian-Early Paleozoic time;
2. Crustal convergence in Ordovician to Carboniferous time;
3. Crustal translation in Carboniferous time; and
4. Renewed crustal divergence in Mesozoic time.

The tectonic framework of the provinces (Figure 2) which New York State is composed appears to have been found in Late Precambrian time. When crustal divergence created a northeasterly trending linear symmetric scheme of a medial depositional trough flanked by cratonic margins and cratons. Subsequent convergence created fold and thrust structures parallel to this symmetry. Still later, the cratonic margins, as the most fundamental and profound structures, served as a loci for translational and final divergent plate movements. The initial crustal divergence occurred in Late Precambrian time, following the completion of the Grenvillian orogenic cycle. This process caused the separation of North American and African plates and resulted in the formation of the proto-Atlantic Ocean (Williams and Stevens, 1974; Wilson, 1966; Rankin, 1975). In the initial rifting phase, an eastward thickening wedge of clastic sediments interbedded with volcanic rocks were deposited unconformably on a Grenvillian basement and water filled basins within the ancient continental margin (Hadley, 1970).

As rifting progressed, the proto-Atlantic Ocean opened and the previous system of isolated rift basins gave way to the long depositional trough underlain by oceanic crust. The trough was located primarily between the ancient margin of eastern North American and the ancient western margin of the Avalon Platform (Wilson, 1966; Williams & Stevens, 1974). This latter phase of the initial crustal divergence is marked by two rock assemblages representing the continental margin and oceanic trough:

1. A miogeosynclinal wedge developed either as a great carbonate bank over the stabilized ancient continental margin, or as a middle to late Cambrian basal clastic sequence lying transgressively on Grenvillian basement;
2. An ophiolitic sequence, remnants of which are known only from the northeastern portion of the orogen.

Otherwise, the oceanic crust was largely consumed by subduction during the subsequent convergence stage.

A transverse trough (transverse of the ancient continental margin) formed in the area from Ottawa to northern New Hampshire (Wilson, 1946; Cady, 1969; Rickett, 1973). This history of the closing of the proto-Atlantic is reflected in the convergence stage of the Appalachian Orogen. During this stage the tectonic provinces' began to develop their individuality and by its close all but one of the provinces is distinguished. This stage begins in Ordovician time with the onset of a tectonic orogeny. The close of the tectonic orogeny marked the destruction of the ancient continental margin and the development of the mature arc-trench-subduction zone system. The subsequent Acadian orogeny represents continent collision and shortening in limited metamorphism. A result of the final closure of the already contracted proto-Atlantic ocean in northern Appalachian.

During both the Taconic and Acadian orogenies the previously mentioned transverse trough from Ottawa to northern New Hampshire became a zone of greater tectonic mobility (Cady, 1969). Cady has named this northwest-trending trough a relatively more mobile zone, then New England salient. This unusual mobility is indicated by early Taconic crossfolds (Cady, 1969, Beland, 1967; St. Julien, 1967) and Late Taconic and Acadian rotation of longitudinal structural elements about a pivot on the south flank of the salient.

The translational stage followed the final closure of the proto-Atlantic in the north and was contemporary in use of the final process of convergency in the south. This stage of the orogens evolution is recognized on the northern Appalachians where it caused development of a series of Carboniferous to lower Permian sedimentary basins. Ballard and Uchupi (1975) noted that the translation may have resulted from an oblique collision of the North American and North African continents.

The post-middle Triassic development of the orogen, that is the final divergence initiated the opening of the North Atlantic Ocean. The last stage has originally been shown to be more complex than what is formally

believed. This structural development, which is the youngest regionally recognizable diastrophism in the northeastern United States (about 250-80 m.y.), is characterized by vertical movements (basining) and related continental marine sedimentation, transcurrent faulting along preexisting plains of crustal weakness, and extrusive and intrusive igneous activity.

The resultant tectonic province divisions are shown on Figure 1.

NEOTECTONICS

Seismicity

Historical seismicity of New York State is largely confined to two areas. One is the area around Attica, New York, where seismicity there has been related to the Clarendon-Linden Fault. Other important seismic activity is confined to the lower St. Lawrence Valley region from Messena, New York to Montreal and Quebec, Canada. Other minor seismicity lies in the Hudson Valley from the general Albany area to the New York City area. Earthquakes of New York State are shown on Figure 2.

Much work has been done in the area of monitoring seismic events in the state, as well as the rest of the northeast U.S., since 1972. Lamont-Doherty Geological Observatory has installed a rather extensive network of stations within and adjacent to New York State. The New York State network is part of the Northeast Seismic Network, with other contributing organizations being Weston Geophysical Observatory, Mass., Inst. of Technology, Univ. of Conn., State of Pennsylvania, and the Canadian Government. It is through the access of data recorded by these individual networks that has added to the insight of seismic processes and seismic risk in the state and elsewhere in the Northeast. Much still needs to be done in this area, however, as the authors recommended in 1972, before a definitive evaluation can be made.

As previously mentioned, somewhat of a controversy is brewing concerning the Ramapo Fault and its extension into southeastern New York being the loci for the occurrence of earthquakes. Contrary to Aggarwal's (1977) findings, in which he stated "earthquake locations in southeastern New York and New Jersey show remarkable correlation with mapped or inferred faults", it was found after a lengthy geologic and seismic investigation in which the authors were involved (Dames & Moore, 1975 and 1977) that the Ramapo Fault was not capable (according to Appendix A 10 CFR Part 100, U.S. NRC Criteria) and is no more seismically active than any other fault, mapped or unmapped, in the surrounding region. The investigation included the use of detailed geologic mapping, geomorphic studies, determination of in-situ stresses through the overcoring (strain-relief) method, age dating fault zone materials, construction of focal mechanism solutions for instrumentally recorded earthquakes, identification of vertical crustal movements through published and unpublished first-order leveling data and geophysics. Based on the non-unique focal mechanisms of several earthquakes near the Ramapo Fault zone, it was concluded by the ASLAB* that a direct relationship of these events with the Ramapo Fault was not established.

*Atomic Safety and Licensing Appeal Board, Decision, in the Matter of Con Ed and PASNY, October 12, 1977.

In western New York State, the dominant earthquake activity still remains associated with specific segments of the Clarendon-Linden Structure. Van Tyne (1975) has reinterpreted the structural geometry of the Clarendon-Linden based on additional subsurface data made available since 1970. Fletcher and Sykes (1977) showed very convincingly a correlation of earthquake activity and the Clarendon-Linden Fault near Dale. One important aspect has not changed, however, and that is the spatial association of earthquakes to the Fault near Attica. It remains to be seen whether additional monitoring in Western New York by Lamont will show earthquakes in association with other segments of the Clarendon-Linden Fault outside the Attica-Dale area.

Fox and Lastrico (1977) have recently reported the results of a study of bedrock accelerations and the 1929 Attica, N.Y. earthquake, where a correlation was obtained between computed ground motions at different locations in Attica and observed variations in damage reported at the different locations. The study about which Fox and Lastrico reported was designed to provide realistic bedrock accelerations from observed surface effects in the epicentral area to minimize the difficulties of developing rational design criteria from a remote, but significant, seismic event where little or no information exists concerning the direction, frequency content and accelerations caused by the earthquake. Additional studies like the one reported by Fox and Lastrico will continue to be helpful in making design decisions in New York State on a data base that is largely historic in nature.

State of Stress

Another important development in the last six years, along the lines of the second recommendation made by the authors in our 1972 paper, has been the wider identification, determination and use of in-situ stresses in analyzing seismotectonic conditions in the state. Most important has been the systematic study of the regional state of stress in an area encompassing the northern part of New York State (Dames & Moore, 1978). Besides the study of vertical crustal movements, four data groups have been identified: 1) focal mechanism solutions of earthquakes (see Figure 3); 2) in-situ stress determinations performed at depths using hydrofracturing techniques 3) in-situ determinations of near-surface lateral stress performed at different sites utilizing overcoring (strain-relief) techniques (see Figure 4); and 4) numerous geologic observations regarding stress conditions at specific localities. Throughout the northern portion of New York State, small structures of post-glacial age occur. These structures are frequently referred to as "pop-up" features, as either chevron style anticlines or as broad sinusoidal folds with no disruption at their crests. Typically these structures are asymmetric and opposing limbs dipping at different angles. The axial planes of these folds are generally oriented west-northwest to northwest. This preferred orientation is approximately parallel to the inferred axis of crustal tilting, which, in turn, is commonly believed to be related to glacial isostatic rebound. Additionally, the preferred orientation in the folds is approximately perpendicular to the greatest principal stress in the region, which provides additional evidence to support the observations of high horizontal stresses measured in-situ.

During the Pleistocene epoch, there were several advances of continental ice sheets over New York State. These advances were separated by warmer inter-glacial stages. Each advance contributed to isostatic downwarping of the earth's crust and during each interglacial stage the crust rebounded. The ice sheet reached its maximum extent approximately 18,000 years B.P. During this time the crustal depression introduced by the ice sheet may have been as much as 1300 to 1700 feet in the Lake Ontario area. Uplift on the order of 250 feet is estimated to have occurred in the Lake Ontario area in the last 12,000 years. Contemporary vertical crustal movements in the New York State area are based upon geodetic leveling of several first order survey lines and data from Lake Ontario Tidal Stations and Tidal Stations in the New York City area. These studies have revealed that the upper free surface of the lithosphere is undergoing vertical movements. The relative rate of the movements varies up to two millimeters per year. The general southward tilting of the land surface conforms to the inferred axis of post-glacial upwarping indicated by studies of ancient Lake Iroquois shorelines. Thus, it may be inferred that the pattern of vertical crustal movements indicate the continuation of glacial isostatic rebound to the present time.

The entire New York State area where stress conditions have been measured indicate that the stress field is considerably different than that which would be expected solely due to present gravitational loading. The state of stress in Upstate New York is manifested by the development of post-glacial deformation structures (pop-up structures) and by the occurrence of shallow seismic events of low magnitude. The regional stress field appears to be spatially continuous and homogeneous in character from one locality to the other. The most consistent observation regarding the stress field in the upstate area is that the intermediate principal stresses are either horizontal or subhorizontal. The least principal stress tends to be nearly vertical. The focal mechanism solutions in the state indicate that a range of stress conditions exist at the depth of the hypocenter.

The magnitude of the maximum horizontal normal stress is high and ranges from several hundred to several thousands of pounds per square inch. From the region reported in the literature it appears that the nature of strain energy stored in the rock masses is not known. The stress could be the result of applied boundary tractions, residual stresses locked into the rock material, or a combination of these systems. The only reported investigation in which attempts were made to assess whether the in-situ stresses were residual or applied boundary tractions is the work of Engelder and Sbar (1976) and more recently Engelder (in press). It is apparent that although a healthy body of data is beginning to form on this subject, much more intensive research must be conducted before an understanding can be reached as to: 1) the genesis of these high stresses; 2) whether these near-surface stresses have any relation to stresses (principal) at hypocentral depths; and 3) whether these high near-surface stresses have any relationship to the occurrence of shallow seismicity.

As the authors indicated in 1972, the process of evaluating the site within a complex geologic environment such as New York State will remain weighted towards the empirical side without the benefit of the results of research oriented investigations into 1) the nature and magnitude of in-situ

stresses; 2) the analysis of the response of various soil profiles to actual earthquake ground motion; and 3) development of strong ground motion parameters for recorded earthquakes. Much work has been accomplished towards these ends in the last six years in New York, but just as much or more remains to be accomplished in order to achieve a breakthrough in the area of earthquake hazards and the ability to make rational and cost-effective design decisions.

BIBLIOGRAPHY

Aggarwal, Y.P., 1977; Study of Earthquake Hazards in New York and Adjacent States - Phase IV Annual Technical Report for the New York State Energy Research and Development Authority.

Algermissen, S.T., and Perkins, D.M., 1976; A Probabilistic Estimate of Maximum Acceleration in Rock in the Contiguous United States; U.S. Geological Survey Open File Report 76-416.

Atomic Safety and Licensing Appeal Board (ASLAB), Decision, October 12, 1977, in the matter of Consolidated Edison Company of New York, Inc. and the Power Authority of the State of New York, ASLAB-436, (Show Cause).

Ballard, R.P. and Uchupi, E., 1975; Triassic Rift Structure in Gulf of Maine; American Association of Petroleum Geologists Bulletin, v. 59, 7, p. 1041-1072.

Beland, J., 1967; Contributions from Systematic Studies of Minor Structures in the Southern Quebec Appalachians; in Clark, T.H., (ed.), 1967, p. 48-56.

Cady, W.M., 1969; Regional Tectonic Synthesis of Northwestern New England and Adjacent Quebec; Geol. Soc. Amer. Memoir 120, 181 p.

Dames & Moore, 1975; Tectonic Provinces in the Northeastern United States and the Relationship of Historic Earthquakes to the Indian Point Site; for Consolidated Edison Company of New York, Inc.

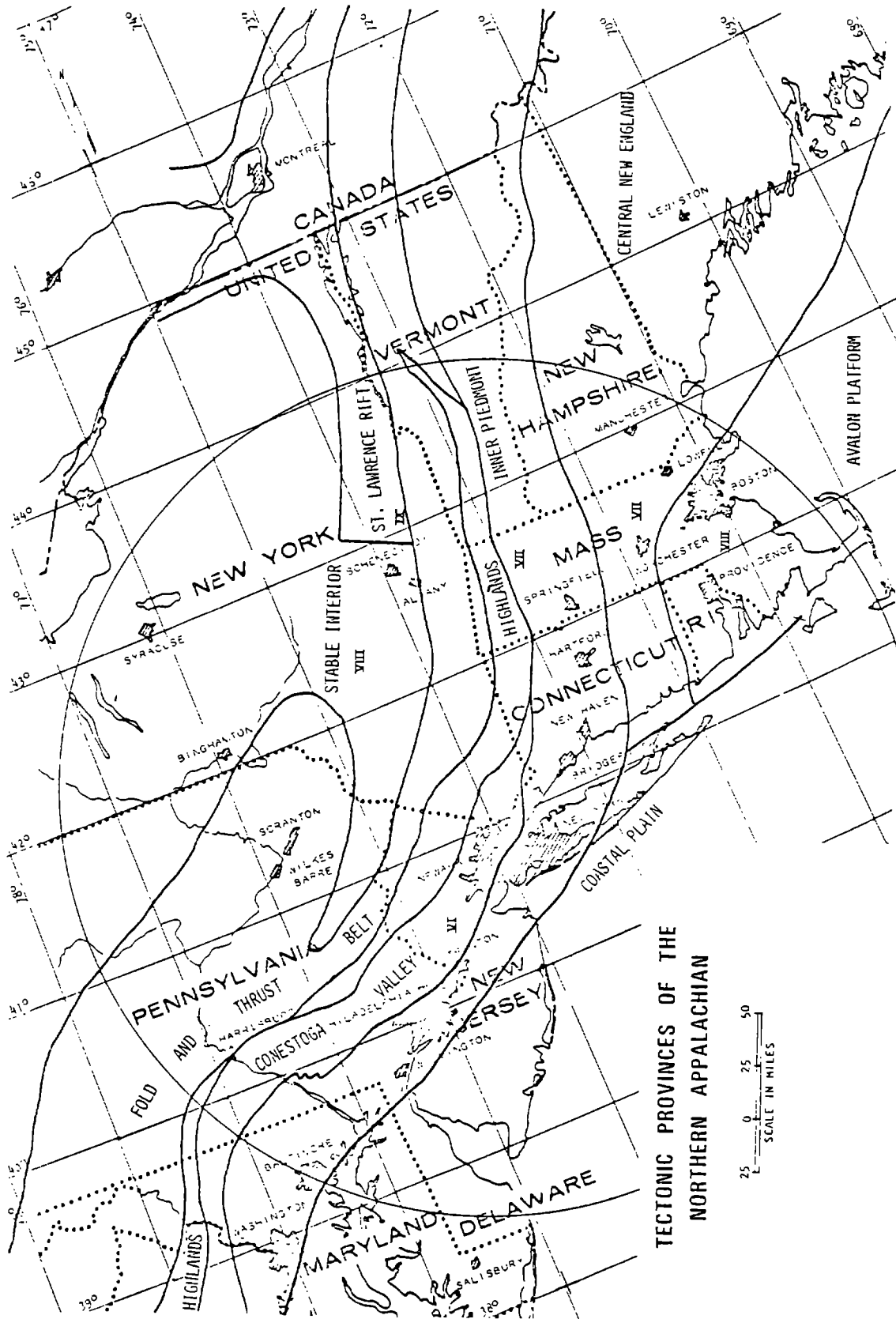
Dames & Moore, 1977; Geotechnical Investigation of the Ramapo Fault System in the Region of the Indian Point Generating Station; for Consolidated Edison Company of New York, Inc., Vols. I and II.

Dames & Moore, 1978; Geologic Investigation, Nine Mile Point Nuclear Station Unit 2; for Niagara Mohawk Power Corporation, Vols. I-III.

Engelder, T. and Sbar, M.L., 1976; Evidence for Uniform Strain Orientation in the Postdam Sandstone, Northern New York, from in situ Measurements; Journal of Geophysical Research, 81: pp. 3013-3017.

Engelder, T., 1978; The Nature of Deformation Within the Outer Limits of the Central Appalachian Foreland Fold and Thrust Belt in New York State, Tectonophysics (in press).

- Fletcher, J.B. and Sykes, L.R., 1977; Earthquakes Related to Hydraulic Mining and Natural Activity in Western New York State (submitted to Jour. Geophys. Research).
- Fox, F.L. and Lastrico, R., 1977; Bedrock Accelerations Determined from Surface Effects of the 1929 Attica, New York, Earthquake; Bull. Assoc. Eng. Geol., vol. XIV, No. 4, pp. 187-204.
- Hadley, J.B., 1970; The Ocoee Series and Its Possible Correlations; in Studies of Appalachian Geology, Fischer, J., Pettijohn, F., Weaver, K.; and Reed, J. (eds.), pp. 247-259, J. Wiley and Sons.
- Kulhawy, F. and Ninyo, A., 1977; Earthquakes and Earthquake Zoning in New York State; Bull. Amer. Assoc. Eng. Geol., Vol XIV, 2, pp. 69-87.
- Rankin, D.W., 1975; The Continental Margin of Eastern North America in the Southern Appalachians, Amer. Journ. Sci., v. 275-A, pp. 298-330.
- Rickard, L.V., 1973; Stratigraphy and Structure of the Subsurface Cambrian and Ordovician Carbonates of New York: Correlation of the Cambro-Ordovician Carbonates Within New York State, Extending into Adjacent States and Canada; N.Y. State Museum and Science Service, Map and Chart Ser., N18, 26 p.
- St. Julien, P., 1967; Tectonics of Part of the Appalachian Region of South-eastern Quebec (Southwest of the Chandiere River); in Clark, T.H. (ed.) 1968, p. 319-327.
- Ulrich, F. P., 1948; Zones of Earthquake Probability in the United States; in Building Standards Monthly, V.17, No. 3, pp. 11-12.
- Van Tyne, A.M., 1975; Clarendon-Linden Structure, Western New York; New York State Geological Survey Open File Report.
- Williams, H. and Stevens, R.K., 1974; The Ancient Continental Margin of Eastern North America; in Burk, C.A. and Drake, C.L. (eds.), The Geology of Continental Margins, pp. 781-796, Springer Verlag, pub.
- Wilson, A.E., 1946; Geology of the Ottawa-St. Lawrence Lowlands, Ontario, and Quebec, Geological Survey of Canada, Mem. 241.
- Wilson, J.T., 1966; Did the Atlantic Close and Then Reopen?; Nature, vol. 211, No. 5050, pp. 676-681.



TECTONIC PROVINCES OF THE
NORTHERN APPALACHIAN

FIGURE 1

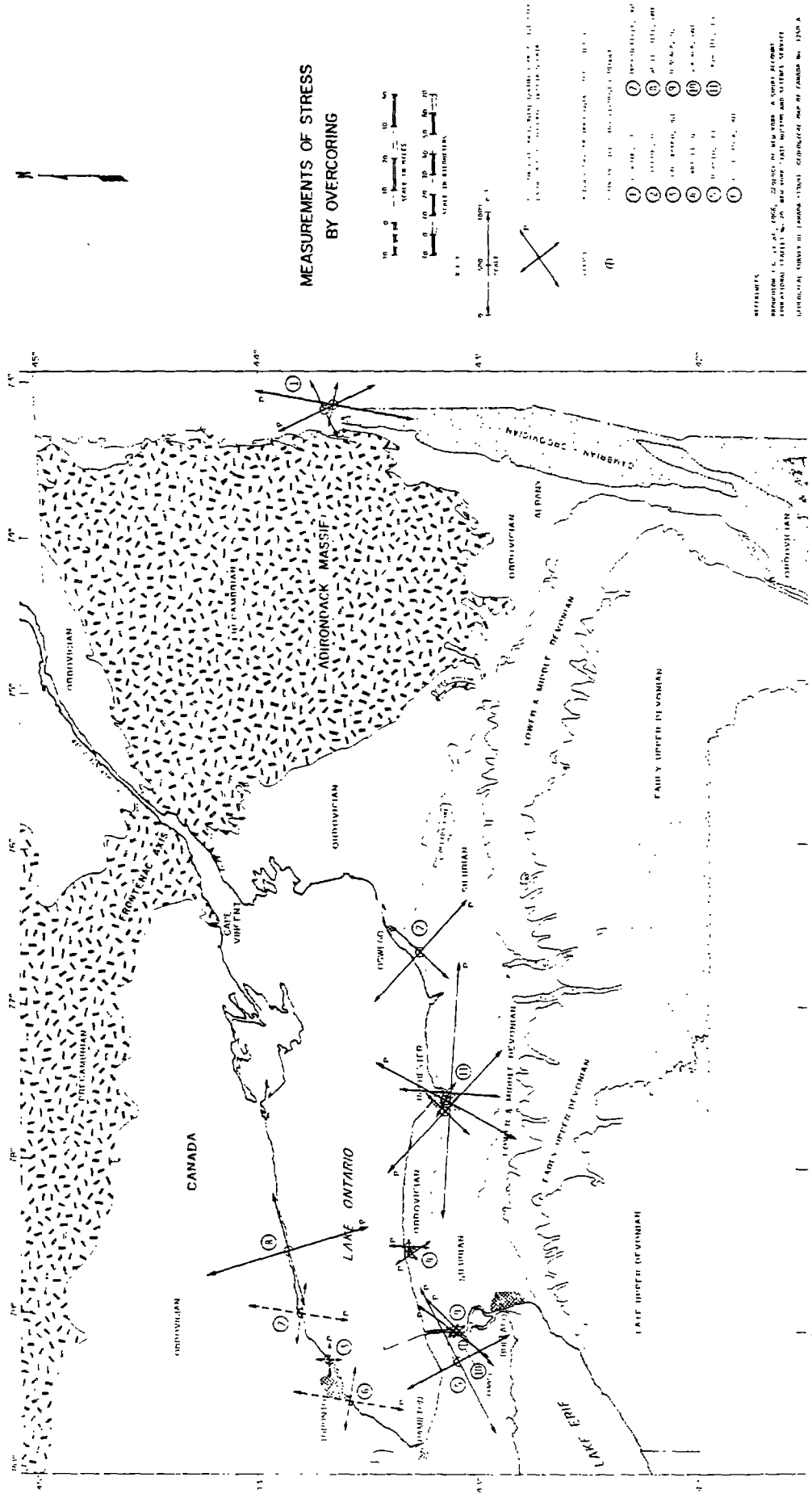


FIGURE 4

MICROZONATION METHODS AND TECHNIQUES USED IN PERU

By J.Kuroiwa^{I*}, E.Deza^{II*}, H.Jaén^{III}, and J.Kogan^{IV}

ABSTRACT

After Peru 1970 earthquake (official death toll: 67,000) an interdisciplinary group was set up to carry out the microzonation studies of the destroyed cities and towns, to reconstruct them. Up to the present, the same group whose main members are the authors of this paper, have made the microzonation studies of 8 cities and towns, and has carried out many site investigations, including new industries and harbor locations, and the Peru Nuclear Center.

The main disciplines included are: Seismology, Geology, Soil Mechanics, Soil Dynamics and Earthquake Engineering. The methods used in Soil Dynamics are based mainly, in those developed in the last 6 years at the University of California, Berkeley, and the University of Tokyo, but were modified and arranged to the local conditions.

The peculiarity of the peruvian territory, which consist of a very arid coastal region, the high Andes Range region, and the Amazon Jungle, make necessary to pay special attention to the External Geodynamics studies, in addition to the usual site and seismic investigations.

The paper includes the methods developed by the authors and the experience acquired by the working group in the investigations carried out in different locations in Peru in the last 8 years.

1.- INTRODUCTION. Past earthquake in Peru have clearly shown that the local geology and soil conditions have important influence in the damage distribution. Particularly in the Lima Metropolitan area, this century earthquake of 1904, 1932, 1940, 1966 and 1974 have caused the worst destruction at the same locations: La Molina, Callao and Chorrillos, all of them situated at the edge of the Rimac Valley, where Lima is seated. At those places the intensity have been 2 to 3 MM degrees higher than at the central part of the Valley. They are located few kms apart and the earthquakes parameters: magnitude, epicentral locations and focal deeps have been different every time. In addition, during Peru 1970 earthquake, with its epicenter located 300 kms away from Lima, the only places in this city where damages were reported are those above listed. In Huaraz during 1970 earthquake the intensity was 3 degrees MM different in points located only 2 kms apart (1).

On the other hand, in Table 1, are shown the most important geodynamical phenomena occurred between 1925 and 1978 in Peru II Region of Civil Defense, that cover an area of 236,300 km² roughly 1/5 of country area, are the most developed, and Lima are located there. Infrequency, earthquakes are fifth behind avalanches, land slides, flood and alluvions, being some of them triggered by earthquakes. However in number of victims and material losses, earthquakes are first followed by alluvions and avalanches (see Table 2)

I Profesor, National University of Engineering. Lima - Peru

II Seismologist, Geophysical Institute of Peru Lima

III Geologist, GEOTEC, Consulting Engineers. Lima

IV Research Engineer, Kuroiwa - Kogan and Associates, Consulting Engs. Lima.

* Member, Scientific Committee, Peru Civil Defense.

Note that flood damages are practically negligible there, but in Peru's Civil Defense Region, which corresponds to the low land Amazon Jungle, by far the flood damage are first and every year cause big losses there (see Fig. 1).

From the above remarks, two conclusions may be stated:

First; it is very important to perform microzonation studies before any important investment in construction made in Peru. The Peru Seismic code of 1977 according to this idea, makes compulsory to perform microzoning studies for the new cities expansion areas and at the location of new industries.

Secondly; If the main object of the microzoning studies is to protect the structures from any natural catastrophe, it is necessary to consider all the potential geodynamical danger in the area.

The methods being used, consider the following fields in the microzoning studies: Seismology, Geology, Soil Mechanics, Soil Dynamics, and Earthquake Engineering giving emphasis to the investigations which are most important according to topography of the area and the statistical information of past natural catastrophies.

The coordination among the different specialists are constant. When the analysis of the information in every field has been completed, the final evaluation, and the division of the studied area in subareas of similar characteristics are made by with the direct participation of the whole team. This method has been called seismogeological microzonation (2)

2.- INTERNAL GEODYNAMICS RISK. This discipline investigates the regional condition of seismotectonics and seismicity. It determines the degree of seismotectonic activity for establishing not only the seismic levels, that is the maximum possible earthquake, the "normal" one, and the "Design Earthquake", but also the areas of different earthquake occurrence.

It estimates the maximum possible intensities which may occur sometime on the areas and also the recurrence and probability of earthquake occurrence. Briefly the seismotectonic regionalization map must be prepared, as the example, that may be seen in figure 2, the seismotectonics regionalization map of the Lima area showing the maximum possible intensities.

The statistical seismic risk as a result of the evaluation of the possible intensities of the earthquake which have occurred during the last 400 years in Lima according to historical information is shown in figure 3.

The attenuation factors of the seismic energy is also found using isosismal maps of some earthquake. The resulting curve is shown in figure 4.

3.- GEOLOGICAL STUDIES. Geology is one of the basic disciplines in the microzonation studies. Hydrogeology, Geomorphology and Geological Engineering (known in some countries as Geotecnic), play an important role in the detection and identification of the different natural phenomena which threaten the security of a population or a civil engineering work as well as in the decision to choose the prevention methods for the risk attenuation and/or defense works construction.

In Peru, the geological methodology formerly used in microzonation was the classical one, that is survey of the stratigraphic, tectonic, geohistoric

and the study of the hydrogeological features. However, the morphology of the peruvian territory with strong topographic contrasts which delimit different fisiographic units with different lithological, structural and climatic characteristics, made necessary to introduce to the classical methodology, the study of the External geodynamic phenomena applying very particular rules and secuencia for the investigation of populated centers and civil works locations.

So, the study of the wide range of gradation or degradation processes is added to the investigation of the endomorphic phenomena which contribute permanently to the modeling of the earth surface. Thus, this approach may constitute a contribution to the classical studies being carried out in different parts of the world where the natural conditions are similar to those existing in Peru and the Andean countries.

The number of victims and the material losses per year caused by the External Geodynamic phenomena such as landslides, alluvions, avalanches, downfalls, soil slithering and solifluxion, floods, etc, are considerable in Peru as shown in Tables 1 and 2. For a period of 30 years (1943-1973) it was stimated that a volumen of two millions of m^3 of material was mobilized by these phenomena, which affected 4,000 hectares of soil and caused 50,000 victims.

As an example of these type of phenomena may be mentioned the Yungay alluvion, (locality situated 454 km NE from Lima), trigged by the Peru 1970 earthquake, when a city of 25,000 people was buried, mobilizing 244 millions m^3 of material along 14 kms.at a speed of 400 km/h. Another example is the Cochacay Landslide Alluvion, located in the Central Sierra, 398 km. SE from Lima, occurred in April 1974. The phenomenon displaced 1,600 millions m^3 of material repressing the important Mantaro river by means of a dike of 4 kms. long, 1 km wide and 170 meters high. The damming had a length of 30 kms. upstream, storing 670 millions cubic meters of water. The dead toll was 45 and the material losses about USA. \$ 7 million.

These examples emphasized the need of considering these phenomena in every seismogeological microzoning study, specially in the Andean countries and in those where the natural conditions are similar.

The External Geodynamics studies are oriented toward the location of the phenomena, the risk determinatión and the establishment of prevention measures, and/or defense construction methods, zoning the different sectors of the site being investigated and establishing their safety limits.

So, according to the above discussion, the following aspects should be considered:

- Analysis of the site morphological aspect.
- Study of the nature of the bed rock and foundation soil.
- Identification of the risky phenomena to people and constructions.
- Study of the phenomena origen, its evolution, and the factors contributing to its existance.
- Establishment of prevention methods to minimized or avoid the risk.
- Establishment of the safety limits.

The mentioned methodology have been applied in different localities of Peru.

4.- SOIL MECHANICS AND SOIL DYNAMICS. The soil Dynamics for amplification studies are made under stable conditions and basically considering: firstly a suitable soil exploration program, where the boring distribution and depth depend on the project needs, and previous site geological exploration.

The soil statics properties thus measured at the site and the samples taken to laboratories where the tests are made under different levels of solicitations, provide important information.

On the other hand, geophysical seismic exploration using modern measuring P and S wave velocities equipment, and by releasing small amount of energy by means of an explosion, or hitting a pressed wooden piece with a hammer the soil elasto-dynamics properties, internal and radiation damping and the soil dynamic stratification are found.

To obtain the idealized representative soil models, (usually one dimensional) (8), in addition to the soil mechanics data and the soil properties found dynamically, properly correlated, it is necessary to account for the site geology and topography. Due to economics and practical considerations, it is not possible to study a large number of positions, so the chosen positions have to be representative of an area and need to be located accordingly. In case of irregular soil stratification, bidimensional model is used (5)

In Peru only few accelerographs are installed, specially in populated areas. At the sites of new cities or civil works, where most of the microzonation and site investigations have been made, there are not earthquakes records, so artificial ones have been used. These earthquakes are generated according to seismological and geological informations: expected earthquake magnitude, possible epicentral distance, waves attenuation, duration etc. Basically two types of artificial are used: a nonstationary white noise, to determine the soil filtering properties in a wide range frequency band, and a second one also nonstationary, with its frequency contents defined by appropriate filters, such that its periods are close to the soil predominant periods to obtain the maximum soil amplification and having an upper bound. The soil response to a real intense earthquake is assured to be between these two limits by an appropriately weighted average.

The soil idealized models and the input earthquakes at the base are processed using computer programs (4). These programs consider the soil incursion into the inelastic range by the lineal equivalent method, using the criteria proposed by Seed (5), but with the deterioration curves adjusted to laboratories tests in the level of stresses and deformations caused by intense earthquakes. The response are computed in time and frequency domain in the chosen degrees of freedom, and the response spectra at the foundation level, are computed for use in the seismic design (see fig. 4, 5, 6, 7, 8).

5.- OTHERS INVESTIGATIONS. For certain types of projects such as port and harbor facilities it is necessary to perform investigations not previously included, for example the potential of noncohesive soil liquefaction, and the tsunami danger.

For the determination of sandy soils liquefaction, one of the most important soil instability during earthquakes three approaches are used (7):

1) Comparing the statistical information of sand deposits performance in past earthquakes in different part of the world (i.e., Niigata, Alaska, Chile 1960) in relation to representative soils properties such as the grains size and relative density of the deposit, etc. 2) In addition to the representative soil properties an equivalent stationary earthquake determined according to the local conditions (Soil Dynamic Response) and correlations abacus obtained in USA and Japan Laboratories by large scale dynamic texts. and 3) Solving the Terzaghi consolidation equation, using as data the soil hydraulic properties, its compressibility, and the earthquake influence which causes the increment in the pore water pressure (4). See fig (8).

Comparing the results of these three criterias it is possible to establish in a reasonable way the potential soil liquefaction occurrence and it is possible to give recommendations for design purpose.

For investigating the local tsunami in Perú, it is necessary to have batimetric information of few tens of kilometers from the coast, which may be get from the Peruvian Navy, but many times it is necessary perform detailed batimetric measurement for water depth less than 100 meters. Emphasis is given in the study to the tsunami energy concentration in areas of unfavorable batimetric and topographic configuration. The arrival times of local tsunamis are estimated by means of the sea waves refraction curves. If the line that passes through the 1966 and 1974 Peru earthquakes epicenters, both located offshore, is used as the major axis of the ellipse where the tsunami is assumed to be generated, the tsunami waves arrive to the Lima coast in about 1/2 hours, which agree with the arrival time of the 1746 tsunami which destroyed Callao, the near by sea port.

Detailed topographic information which is essential for the development of the engineering project is useful the determination of inundation possibility as well as to guess the direction of avalanches and other external geodynamics phenomena.

In some areas in Peru it is important to study the Glaciology and lagoon control.

6.- EARTHQUAKE ENGINEERING. The Peru Earthquake Code practically cover only regulations for building and the design spectra included there are "theoretical" based in foreign experience for hard, medium and soft soils.

In the microzoning studies applied for buildings, in addition to dividing the zone in subareas of similar soil properties, the seismic characteristic of each of them are defined by its respective design spectrum found for the site, which substitute the code ones. If there are some type of building not covered by the code, or correspond to projects of civil engineering structures such as quaywalls, piers, bridges, water supply systems etc, the seismic coefficient for such structures are given in the report, along with special recommendations which take into consideration the site characteristics as well as the properties of the structures.

For example in Fig. 9 are given the design spectra for different structures of the Peru Nuclear Center to be built in Huarangal, located about 28 kms NE of Lima, These spectra are accompanied by the classification of buildings, equipment and piping in class I, IA, II and III elements, accord

ing to the degree of importance from the view-point of plant safety. The permissible stresses are also given: The class I and IA elements shall be maintained within the elastic limits of the material under the action of level S2 earthquake. The class II elements shall be maintained below the elastic limits under S1 earthquakes, but may enter into inelastic range under S2 earthquakes. The deformations shall be as not to endanger their functioning. The class III elements shall be designed in accordance with the Peruvian Code for Seismic Design. Suggestion is also made how to distribute the different structures on the site to get the rational use of the land.

Past experience have shown that in Peru more than 80% of the earthquake damages have been caused by; stress concentration in certain elements as short columns due to wrong structural conception; torsion, impact, etc. The recommendation try to minimized such a kind of mistakes and put emphasis in a good design criteria learned from past earthquakes performance of structures in the country. Looking for an equilibrium between cost and safety it is try to give simple and clear guidelines to the designer.

CONCLUDING REMARKS

Starting in 1970 when a microzoning studies were made for the first time in the country for Chimbote city, by a Japanese Scientific Mission, headed by Dr. Ryohei Morimoto, by then Director of the Earthquake Research Institute of the University of Tokyo (11), the local group set up to assist that Mission has continue working up the present. The microzoning of 7 more cities and towns destroyed by the Peru 1970 earthquake were made in 1970-71. In 1974, the Peru Ministry of Housing and Construction asked the group to perform the microzoning studies of Cerro de Pasco. Part of that city needed to be moved because the mine open pit operations were going to invade the city old section. In 1974-75 Lima was zoned in areas of equal expected intensity to study the possible impact of a destructive earthquake in the Metropolitan area where near 30% country population are concentrated (12).

Site investigations for a nuclear centre, a fishing harbor, new industries and important buildings locations have been made at different locations of Peru. The method also have been applied to select new urban expansion areas at different locations of uncultivated land around Lima in order not to destroy the existing scarce green areas.

The fact that the group have prepared in the period 1970-1978, the restoration projects of more than 100 reinforced concrete buildings and near 3000 bricks houses damaged by the Peru 1970 and 1974 earthquake (14) correlating the damages with the site, soil and geologic conditions, have been very useful in developing the methods used in the microzoning studies.

These methods are mainly based in those developed in USA and Japan, but take into consideration as much as possible the local conditions not only on the types of the geodynamical phenomena that may endanger the structure, but also the limitations existing in the country; for example, as a general rule it has been chosen modern instrument, but easy to operate and maintain. The field and laboratory tests have been practical and simple. With these rules practically there have not been complications during the works.

- 11.- MORIMOTO R., KOIZUMI Y., MATSUDA T. and N. HAKUNO.- Seismic microzoning of Chimbote Area, Peru; Overseas Technical Cooperation Agency; Government of Japan 1971.
- 12.- KUROIWA J.- "Protección de Lima Metropolitana ante sismos Destructivos", Investigaciones efectuadas en el período 1973-1976, 136 pags., Universidad Nacional de Ingeniería. S/E C.N. Defensa Civil, Lima - Peru, 1977
- 13.- DEZA E., JAEN H., and J. KUROIWA.- Investigation of the Peruvian Earthquake of October 3, 1974, and Seismic Protection Studies of the Metropolitan Area. 6WCEE, New Delhi, Jan 1977.
- 14.- KUROIWA - KOGAN INGS. ASOCIADOS Memorias reparación y reforzamiento de estructuras dañadas por sismos, 1970-1978.

TABLE -1

MOST IMPORTANT GEODYNAMIC PHENOMENA OCCURRED IN THE PERU II CIVIL DEFENSE REGION BETWEEN 1,925 AND 1,978

DEPARTMENTS *	TYPES OF NATURAL DISASTERS					TOTAL
	HUAICOS	LAND SLIDES	FLOODS	AVALANCHES	EARTH-QUAKES	
LIMA	880	7	7	—	4	898
ANCASH	600	22	3	10	2	637
AYACUCHO	320	15	2	—	—	337
JUNIN	280	5	3	—	2	290
PASCO	280	8	3	—	—	291
HUANUCO	240	5	5	1	—	251
HUANCAVELICA	200	20	3	—	—	223
ICA	200	—	4	—	2	206
TOTAL	3,000	82	30	11	10	3,133

* POLITICALLY THE PERUVIAN TERRITORY IS DIVIDED IN 25 DEPARTMENTS

TABLE -2

EVALUATION OF DAMAGES CAUSED BY NATURAL DISASTERS IN THE PERU II CIVIL DEFENSE REGION (1,925 - 1,978)

DISASTER TYPES	FREQUENCY		DEAD TOLL		COST	
	NUMBER	%	NUMBER	%	AMOUNT* IN USA \$	%
HUAICOS	3,000	95.7	80	0.1	37'5	4.7
LAND SLIDES	82	2.8	850	1.1	8'0	1.0
FLOODS	30	1.0	30	0.1	0'5	0.1
AVALANCHES	11	0.4	34,015	44.0	250'0	31.4
EARTHQUAKES	10	0.3	42,249	54.7	500'0	62.8

* SPENT DIRECTLY BY THE PERUVIAN GOVERNMENT IN THE RESTORATION WORKS ONLY

ACKNOWLEDGEMENTS

The authors express their thanks to the authorities of the National University of Engineering and the Geophysical Institute of Peru of Lima. To the members of the 1970 Japanese Scientific Mission to Peru.

The authors also take this opportunity to thank the University of California at Berkeley, the University of Tokyo, the California Institute of Technology and the Massachusetts Institute of Technology, for providing them for a long time, with great generosity, with publications used in this study. Their gratitude to Prof. Shima of the University of Tokyo and to Dr. Suyama, President of Oyo Corporation, Tokyo

REFERENCES

- 1.- KUROIWA J., DEZA E., and H. JAEN.- Investigation of the Peruvian earthquake of May 31, 1970, Proc. 5WCEE, 447-456, Rome, June, 1973.
- 2.- DEZA E., Microzoning in a Broad Sense (seismogeological microzoning) 2nd International Congress of the International Association of Engineering Geology, 1974.
- 3.- JAEN H. and V. TAYPE - Ocurrencia de Fenómenos de Geodinamica Externa en el Perú. Bol.Soc. Geologica del Perú, 27-38, Tomo 52, 1976.
- 4.- KOGAN A.J..- Sistema Integrado de Programas para Análisis Dinámico de Suelos y Estructuras en Medianas Computadoras. Versión Extendida 1978. Kuroiwa-Kogan Ings. Asoc. Lima - Perú
- 5.- G. LYSMER, B. SEED Y OTROS.- Efficient Finite Element Analysis of Seismic Structure-Soil-Structure Interaction. University of California Berkeley - 1975.
- 6.- Y. OHSAKY.- Dynamic Characteristics and one Dimensional amplification teory of soil deposits. University of Tokyo 1975.
- 7.- H. BOLTON SEED AND I. ARANGO.- Evaluation of Soil licuefaction potencial during earthquakes, October 1975, University of California, Berkeley U.S.A.
- 8.- O.I.E.A.- Guia de Seguridad sobre análisis y ensayo sísmico de las Centrales nucleares. División de Seguridad Nuclear y Protección del medio ambiente, 1977
- 9.- GEC REACTOR EQUIPAMENT LTD-TAYLOR WOODROW CONSTRUCTION LIMITED and KUROIWA-KOGAN INGS. ASOC.- Estudio del emplazamiento propuesto para la construcción del Centro Nuclear de Investigación, Huarangal, Ejecutado para el Ministerio de Energía y Minas, Febrero de 1977.
- 10.- HOB INGS. ASESORES S.C.R. LTDA. y KUROIWA-KOGAN INGS. ASOC. Estudios Sismológicos, Geológicos y de Mecánica de Suelos para el Proyecto del Complejo Pesquero del Centro ubicado en Ventanilla-Callao. Efectuado para la Unidad Ejecutora del Ministerio de Pesquería. Lima Peru, Marzo 1978.

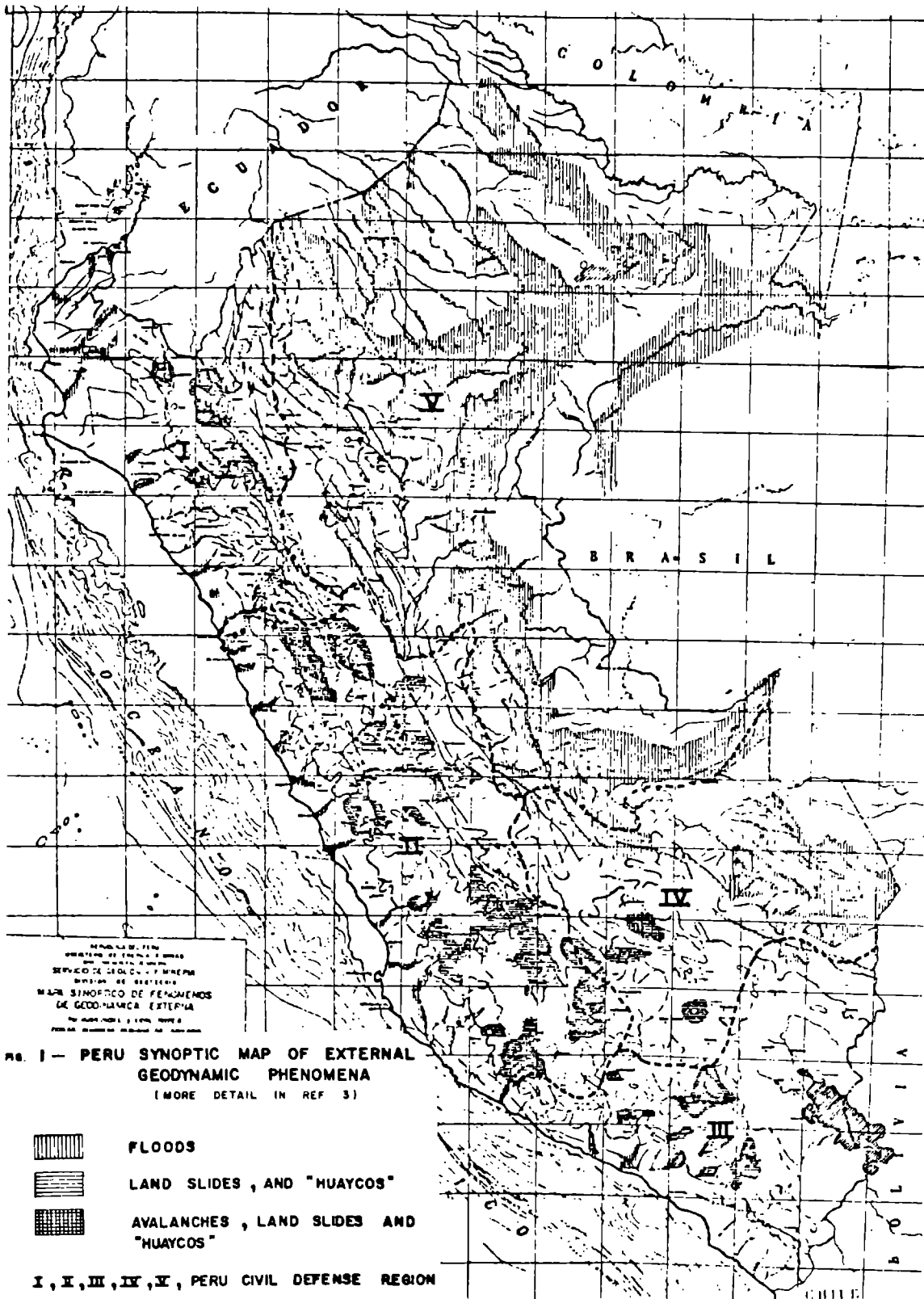
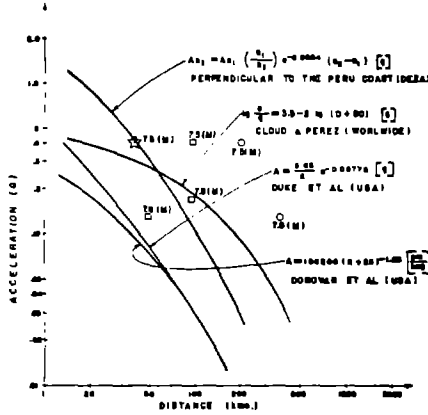
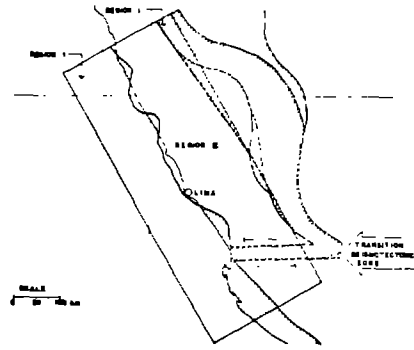


FIG 2 - ATTENUATION CURVES



□ DISTANCE FROM THE FAULT
 ○ DISTANCE FROM THE EPICENTER
 ☆ DISTANCE FROM THE FAULT PLANE (LIMA EARTHQUAKE 11-20-70)
 * MAXIMUM ACCELERATION RECORDED IN LIMA FOR M > 7.
 M = MAGNITUDE

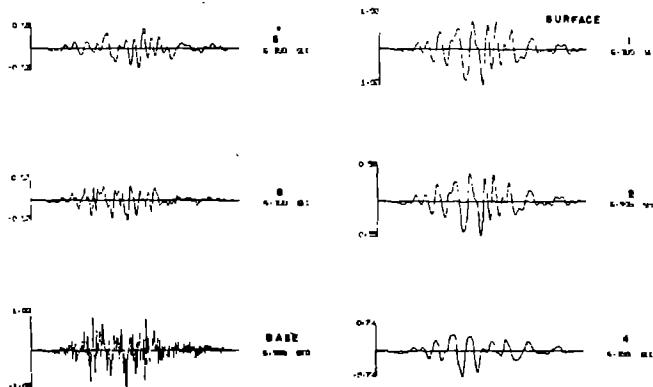
FIG 3 - SEISMOTECTONIC REGIONALIZATION MAP OF WESTERN CENTRAL PERU AND MAXIMUM POSSIBLE INTENSITIES



REGION I - INTENSITIES > IX MM
 □ SHALLOW AND INTERMEDIATE EARTHQUAKE AREA OF DESTRUCTIVE EARTHQUAKES
 ▨ SHALLOW EARTHQUAKES ASSOCIATED WITH STRIKE SLIP FAULTS, INVERSE FAULTS AND OVER THRUST FAULTS INTERMEDIATE EARTHQUAKE AREA OF DESTRUCTIVE EARTHQUAKES

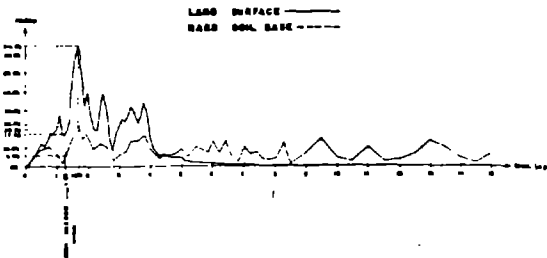
REGION II - INTENSITIES VIII - IX
 □ FEW EARTHQUAKES OCCUR IN THIS AREA AND ARE DEEPER THAN IN REGION I

FIG 4 - ARTIFICIAL EARTHQUAKE NO 1
 WATER RESONANCE THROUGH SHEARWAVE
 SOIL LAYER 1000-0, ... 10



1. AMPLIFICACION SISMICA COMPLEJO PESQUERO DEL CENTRO VENTANILLA

FIG 5 - FOURIER SPECTRUM
 ARTIFIC. EARTHQUAKE NO 1



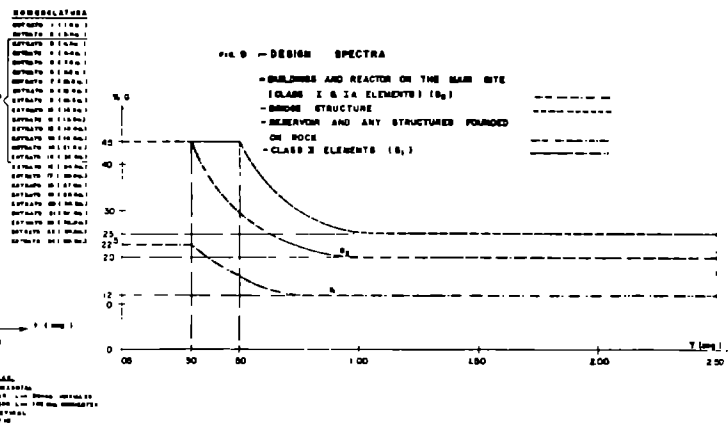
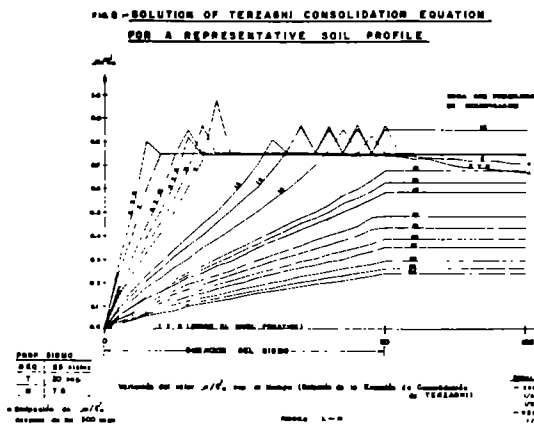
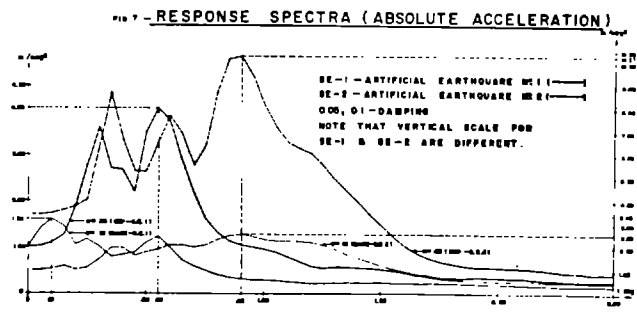
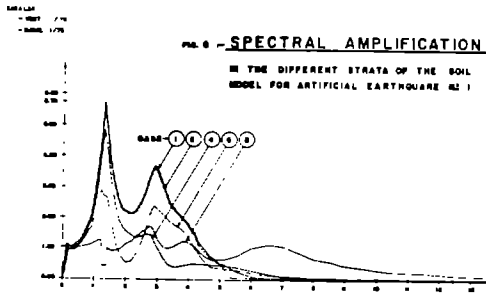


PHOTO 1.- Cordillera Blanca in An-cash (Photo SAN-PERU)

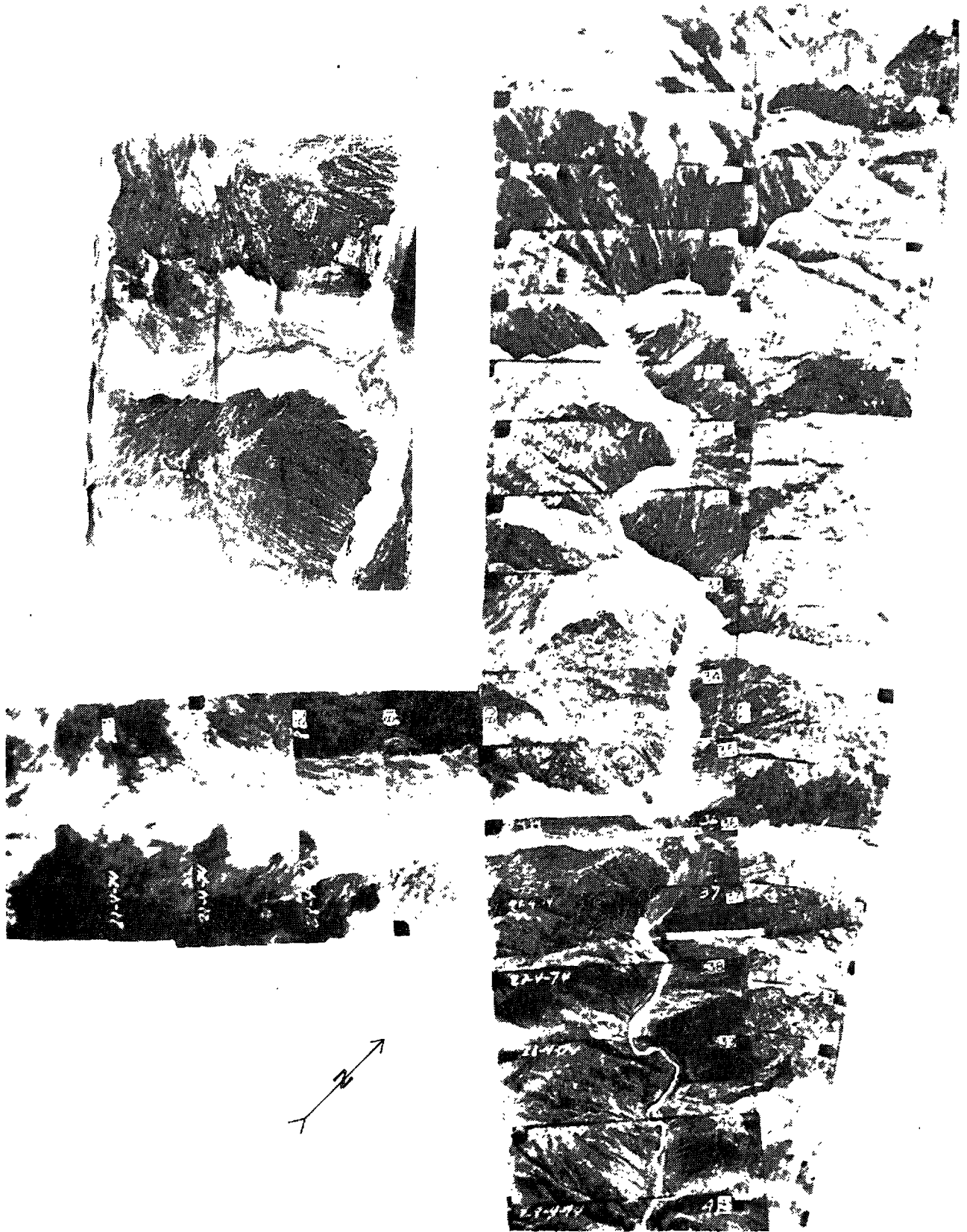


PHOTO 2 (SAN- PERU) Vertical view of the Cochacay Landslide
Alluvion of April 1974. Top left, side view.

LANDSLIDES FROM THE FEBRUARY 4, 1976 GUATAMALA EARTHQUAKE:
 IMPLICATIONS FOR SEISMIC HAZARD REDUCTION
 IN THE GUATEMALA CITY AREA

by

Edwin L. Harp^I, Raymond C. Wilson^I, Gerald F. Wieczorek^{II},
 and David K. Keefer^I

ABSTRACT

The February 4, 1976, earthquake (M=7.5) in Guatemala generated more than 10,000 landslides which were particularly destructive in the Guatemala City area. Rockfalls and shallow debris slides of less than 15,000 m³ in volume were the predominant landslide types.

Guatemala City occupies a relatively flat-lying intermontane plateau of Pleistocene pumice. The plateau is deeply incised by streams that have cut steep-walled canyons, and development throughout most of the city has extended to within a few meters of these canyon margins. Without exception, rockfalls and debris slides from the earthquake were located along the steep canyon slopes. Rockfalls occurred as spalling failures on canyon slopes generally steeper than 50°; most of these failures were near vertical slices of rock less than 6 m thick. Debris slides occurred on slopes of between 30° and 50°, mainly in sandy soils developed on the pumice, and were generally less than 1 m thick. Both rockfalls and debris slides were heavily concentrated along narrow ridges and spurs, which suggests that the existing topography markedly amplified the level of seismic ground motion.

From postearthquake U-2 photographs, 1:10,000 scale aerial photographs, and field investigations, individual landslides triggered during this earthquake were mapped at a scale of 1:12,500 for the Guatemala City area. The distribution of seismically induced rockfalls and debris slides suggests that slope gradient, topographic form, and lithologic features were primary factors controlling the occurrence of these failures. Utilizing these data, a map of the earthquake-induced landslide concentration for the Guatemala City area has been prepared showing areas of high landslide concentrations in which there is a high probability of landslide occurrence during future earthquakes.

INTRODUCTION

The M = 7.5 Guatemala earthquake of February 4, 1976, generated at least 10,000 landslides, which caused hundreds of fatalities as well as extensive property damage. This report depicts the landslide distribution in the Guatemala City area in terms of zones of relative concentration and correlates these with geologic and geophysical parameters in order to assess the probabilities of similar landslide distributions during future earthquakes.

Guatemala City, which suffered significant property damage and loss of life from landsliding during this earthquake, is built on a plateau along the continental divide (fig. 1). This plateau is deeply incised by a number

I Geologist, United States Geological Survey, Menlo Park, Calif.

II Research Civil Engineer, United States Geological Survey, Menlo Park, Calif.

of streams, forming a network of steep, narrow canyons (locally called "barrancos") that may be as deep as 100 m. The plateau is underlain by more than 100 m of Pleistocene pumice (6), a brittle material of very low tensile strength. However, the interlocking texture of the pumice provides sufficient shear strength under nonseismic conditions to support nearly vertical slopes as high as 100 m. Thus, slopes in the network of canyons that dissect Guatemala City exist in a state of metastable equilibrium.

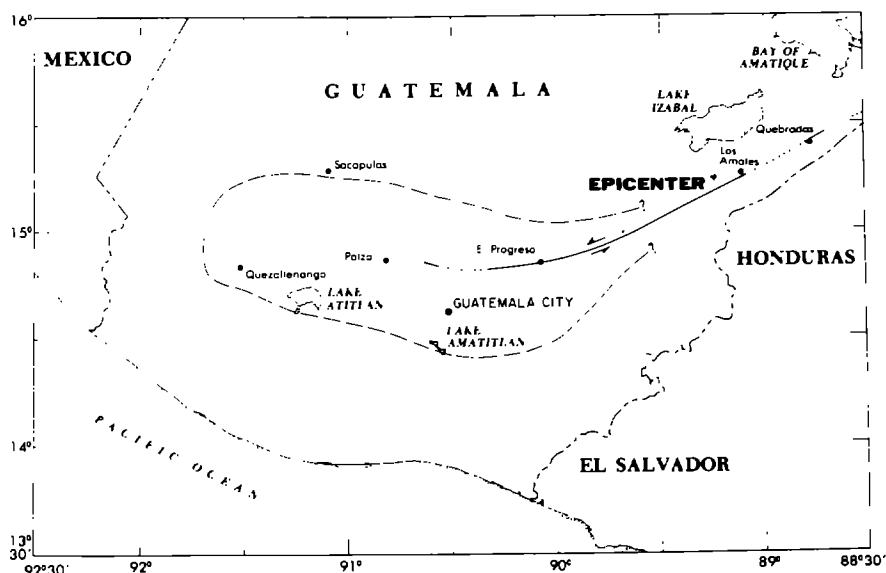


Figure 1.--Epicenter (7), fault rupture (8), and approximate limits of landslide-affected area (dashed line, (4)) from February 4, 1976, earthquake.

Not surprisingly, the barrancos of Guatemala City underwent extensive failure during the 1976 earthquake, with consequent damage to several dwellings and other structures located on the steep slopes or along edges of the canyons. It is not known precisely how much property damage or loss of life in the Guatemala City area was the direct result of landsliding, but a conservative estimate would be approximately 500 dwellings damaged and at least 200 deaths. Most damage to structures occurred to houses built on the plateau but located too close to the canyon rim (fig. 2). These houses were either undermined by failure of the adjacent slopes or deformed by fissures that appeared as incipient landslide scarps. Some neighborhoods situated on the slopes or bottoms of barrancos were also damaged by slope failures and falling debris.

The epicenter of the main event was in the Motagua fault zone near Los Amates (fig. 1), about 157 km northeast of Guatemala City (7). This earthquake triggered landslides over an area of approximately 16,000 km² extending from near Quebradas on the east to Quezaltenango on the west and from near Lake Amatitlan on the south to near Sacapulas on the north (fig. 1). This zone is only a few kilometers wide in the epicentral area, but expands to the southwest, reaching a width of about 80 km in the highlands. There were relatively few landslides near the epicenter and along the Motagua Valley northeast of Guatemala City; most landslides occurred on the steep slopes of the rugged Guatemalan highlands, with particularly heavy concentration along canyons of the major rivers in this region (figs. 1 and 3).

The predominant types of landslides occurring from this earthquake were rockfalls and debris slides of less than 15,000 m³. In some areas, however,

individual landslides coalesced so extensively that there was almost continuous failure, with as much as 80 percent of slopes denuded. There were also 11 large landslides with individual volumes of more than 100,000 m³ (4), several of which blocked stream drainages, posing an additional hazard from flooding. In all the cases observed, most landslide debris appeared relatively dry because the earthquake occurred at the height of the dry season when ground-water levels were low.



Figure 2.--Remains of house in northern Guatemala City built too close to canyon margin. Collapse occurred from rockfall failure beneath the house during an early aftershock.

Landslides also disrupted major highways and the national railroad system, greatly hindering rescue efforts. The Atlantic Highway, CA9, was blocked by landslides at numerous points between Guatemala City and El Progreso. The Pan American Highway, CA1, was blocked by landslides in the Mixco area west of Guatemala City, and also near Tecpan; Highway 10 was buried by a massive slide at Los Chocoyos. These highway blockages seriously hindered rescue and relief efforts in the severely damaged towns and villages of the Guatemala highlands. The railroad between Guatemala City and the Caribbean port, Puerto Barrios, was also blocked in over 30 places (Chang, Engineer, Ferrocarriles de Guatemala, personal comm.).

The distribution and types of seismically induced landslides were determined by an interpretation of aerial photographs coupled with aerial reconnaissance and ground-based fieldwork. The interpretation of aerial photographs and mapping of both postearthquake and obvious preearthquake landslides were based on U-2 photography taken on February 13, 1976, by the U.S. Air Force under contract to the Office of Foreign Disaster Assistance of A.I.D., U.S. Department of State. The U-2 photography was at altitudes of approximately 21 km (70,000 feet) with a resolution of about 1 m. These photographs afforded stereoscopic coverage of the entire area in which earthquake-induced landslides occurred. Landslides were mapped on a scale of 1:50,000 for the entire landslide-affected area, and of 1:12,500 for the Guatemala City area. The topographic base sheets were obtained from the Instituto Geografico Nacional de Guatemala. Fieldwork conducted to check

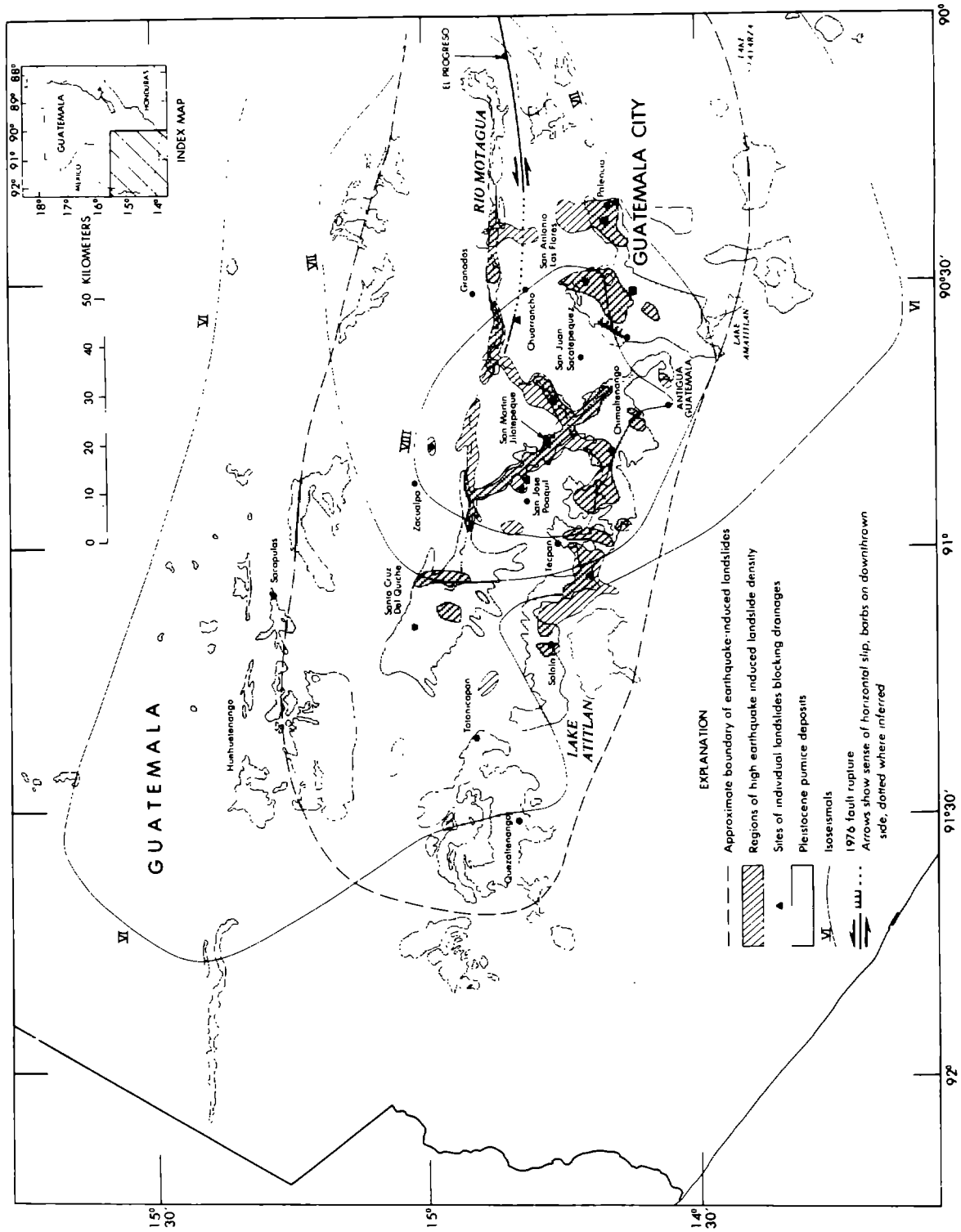


Figure 3.--Map of southwestern Guatemala showing areas of highest seismically induced landslide occurrence and distribution of Pleistocene pumice (1, 6). Also shown are isoseismals (2), fault rupture (8), and approximate limits of seismically induced landslides (4).

to check the accuracy from aerial photographs and to investigate landslide characteristics and mechanisms was undertaken over a period of 2 weeks in April and 2 weeks in June 1976.

PREDOMINANT LANDSLIDE TYPES: CHARACTERISTICS AND PROBABLE MECHANISMS

Rockfalls^I and debris slides^I were by far the most common types of landslides occurring from this earthquake. Although most slides were relatively small in volume (less than 15,000 m³), they had the highest overall impact on people and property because of their widespread occurrence and extremely high incidence in many areas. Rockfalls occurred as spalling failures on canyon slopes generally steeper than 50°. Over 90 percent of rockfalls and debris slides occurred within Pleistocene pumice deposits or the soils developed on them.

Debris slides were most extensive in areas where thin soils on slopes of between 30° and 50° (less than 1 m deep) overlie pumice bedrock (fig. 4). These soils are composed of medium to coarse sand-size fragments of weathered pumice and have a low clay content. Failure resulted from a decoupling at or near the soil-bedrock interface; subsequent movement took place by sliding along this discontinuity.

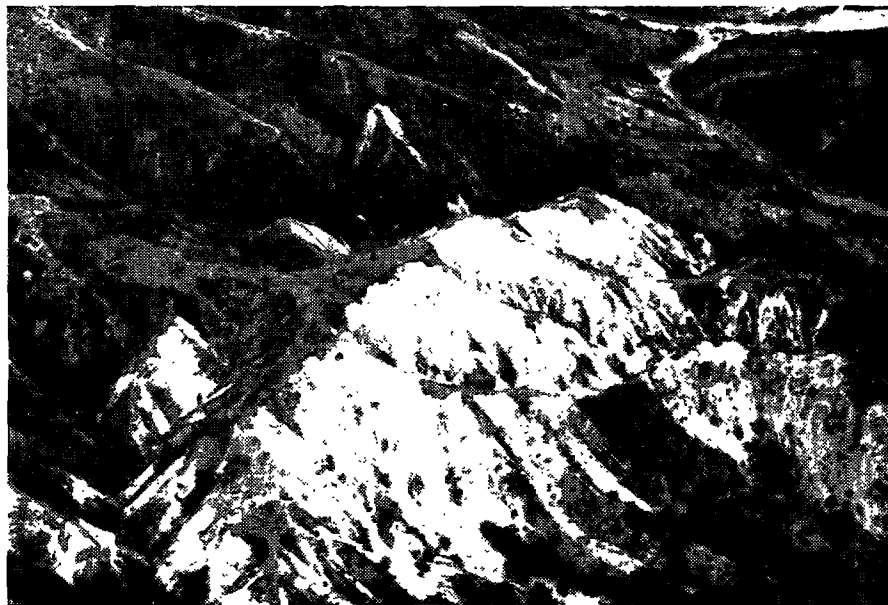


Figure 4.--View of pumice slopes near Motagua River, about 25 km north of Guatemala City, that have undergone extensive failure and coalescence of debris slides. Debris slides are shallow, typically less than 1 m thick.

A typical rockfall scarp was an irregular, more or less concave outward surface such as the one illustrated in figure 5. The mechanism of rockfall formation within the pumice appears to have been tensile fracture from interaction of seismic waves and the free faces of canyon walls. The average tensile strength of the pumice is probably less than 5 psi; this estimate is based on our observations that the pumice bedrock, though massive in outward appearance, could easily be broken apart and

I Landslides were classified according to the nomenclature of Varnes (9).

disaggregated by hand. The ability of pumice to stand as vertical cliffs and yet to undergo brittle fracture from seismic shaking seems to derive from the apparent cohesion caused by the mechanically interlocking fabric of highly angular pumice clasts.

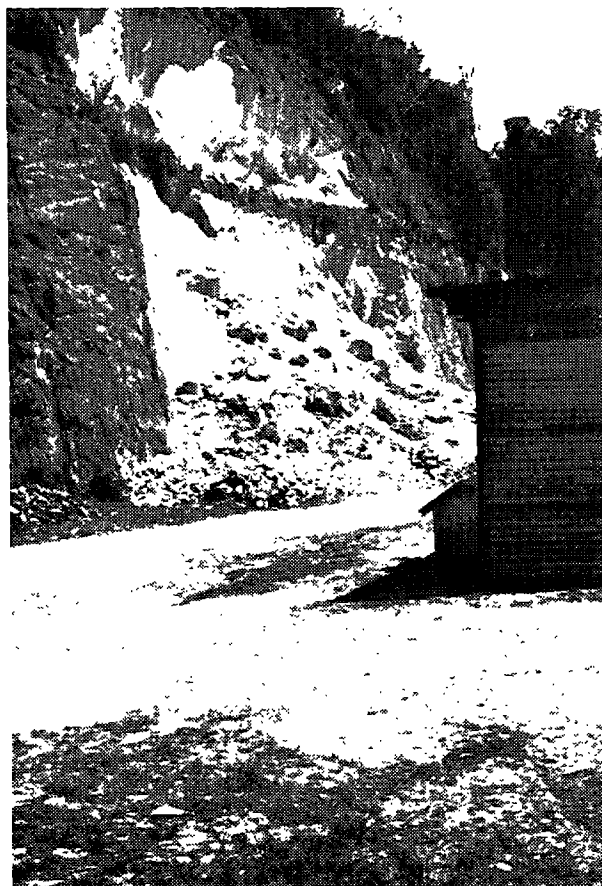


Figure 5.--Typical sesimically induced rockfall in pumice along canyon margin near Puente Belize in Guatemala City. Failure is no more than 1-2 m thick (normal to canyon face) and has overall concave outward shape. Rockfall scarp is unslickensided, indicating that failures such as this were caused by tensile spalling, possibly from seismic wave reflection at free faces.

Rockfalls most commonly happened when slices of pumice, in many cases bounded by nearly vertical cracks, broke away from the upper parts of canyon slopes, usually near the slope crest. These rockfalls were generally less than 6 m in thickness; some places, multiple 'scarps indicated incipient failures as far as 15 - 30 m from plateau margins. In such instances, one or more thin slices of the canyon wall fell, leaving additional blocks on the verge of failure, with extension fractures defining their boundaries in the flat plateau surface. Accelerated sloughing of slope material has been observed at sites of both rockfalls and debris slides during the two years following the earthquake.

LANDSLIDE CONCENTRATION IN THE GUATEMALA CITY AREA

The relative abundance or concentration of landslides is depicted for the Guatemala City area on the map in figure 6, which is a generalized from a landslide inventory map prepared from aerial photography and field reconnaissance. This landslide concentration map, which quantifies and categorizes the concentration of landslides along discrete areas, is a more useful graphic presentation for the purposes of planning and decision-making in Guatemala City than the earlier landslide inventory map.

Landslide concentrations were calculated in the following manner. The concentrations (percentage of slope failure) of discrete, 0.5-km-long segments of canyon were determined by measuring the width of landslide scarps along the segment under consideration, summing the measurements, and dividing by the total length of segment (0.5 km,) as diagrammed in figure 7. The widths of landslide scarps were used in the calculations rather than the areas, because the width (and thickness) of the scarps more accurately reflects the hazard to people and property situated close to the canyon rim. The width of landslide scarps is also an approximate measure of the width of the path swept out by landslide debris falling or sliding down to the canyon bottom, which also reflects the hazard posed to residents located in a few areas on canyon slopes below the plateau edge. In constructing the concentration map in figure 6, the concentration factor calculated for a segment of rim at the top of the slope was also used to characterize the area of the canyon slope and the runout area below a given rim segment.

The landslide concentration map was compiled according to the following procedure. Landslide concentrations were calculated for all canyon segments in the Guatemala City area where landslides occurred; these were then divided into four categories. Percentages ranging from 0 to 5% were termed low, 5 to 20% moderate, 20 to 50% high, and >50% severe; the zones corresponding to these categories are denoted on the map.

A high variation in landslide concentration is evident in figure 6. For example, in the central part of the map area along the Rio La Barranca, landslide concentration zones classified as severe and moderate are juxtaposed. Immediately to the north, severe concentrations lie adjacent to a stretch of low and moderate concentrations along the Rio El Naranjo; this stretch of canyon slopes was markedly unaffected by landslides, although it is practically surrounded by morphologically similar areas of high and severe concentrations. A high variability in landslide concentration also can be seen in the area north of the city and along many canyon slopes to the southwest. These examples indicate the extreme variability of landslide distribution in many places along canyon slopes.

FACTORS AFFECTING LANDSLIDE CONCENTRATION

An analysis of landslide concentration patterns suggests that the wide variation in landslide concentration within canyons in the Guatemala City area is caused by many geologic and seismic factors. In addition to the canyon topography, the following factors appear particularly significant: (1) lithologic features, both of bedrock and of overlying residual soil; (2) preexisting fractures, and (3) the severity of seismic shaking.

Although virtually the entire area affected by seismically induced landslides in Guatemala City is underlain by Pleistocene pumice, the

landslide concentration appears to have been dramatically influenced by lateral variations in rock types within these deposits and in the residual soils developed upon them. Exposures provided by vertical canyon walls in the Guatemala City area show that individual units within the pumice deposits vary greatly in thickness within horizontal distances of tens of meters. Although all pumice deposits are extremely weak in tension,

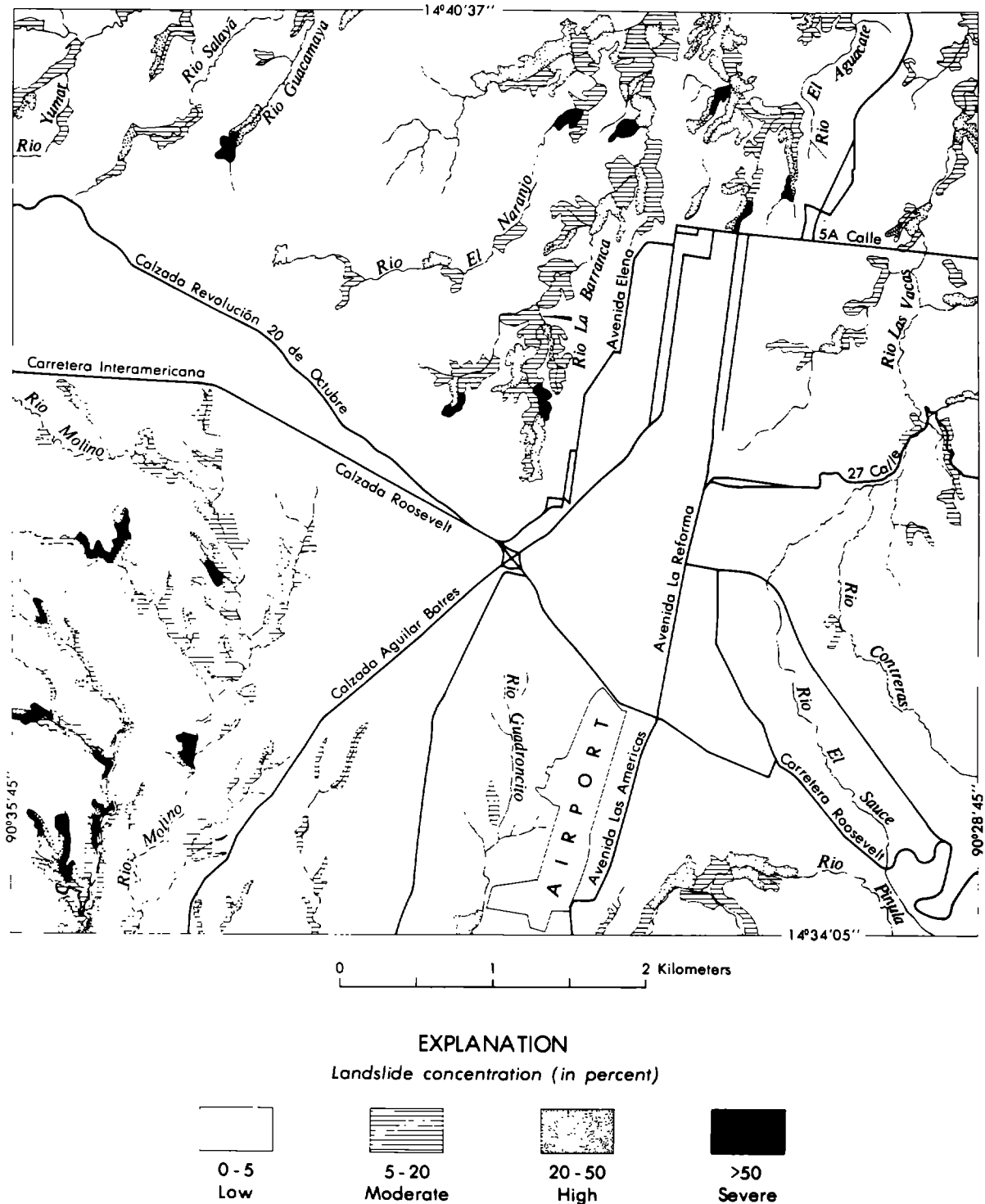


Fig. 6--Landslide concentration map for Guatemala City area (after Harp and others, (4)).

sorting and grain-shape characteristics of the various deposits impart specific differences to their strength properties. Tephros, for example, are the products of airborne ash falls; they are therefore less dense, better sorted, and have generally lower strength than ash-flow tuffs, which are generally poorly sorted, unworked pumice mixtures of coarse ash, pumice, and lithic fragments with little stratification, denser than the tephros. The tephros are only several meters in maximum thickness in the Guatemala City basin, whereas the ash-flow tuffs compose the bulk of basin fill (6), which may be as thick as 100 m. Because of lateral variability in the thickness of pumice units, the relative percentages of various pumice deposits within a vertical sequence may vary greatly over short distances. Such variations result in differences in overall rock strength from place to place and were probably responsible in large part for the variability in rockfall concentrations within the canyons.

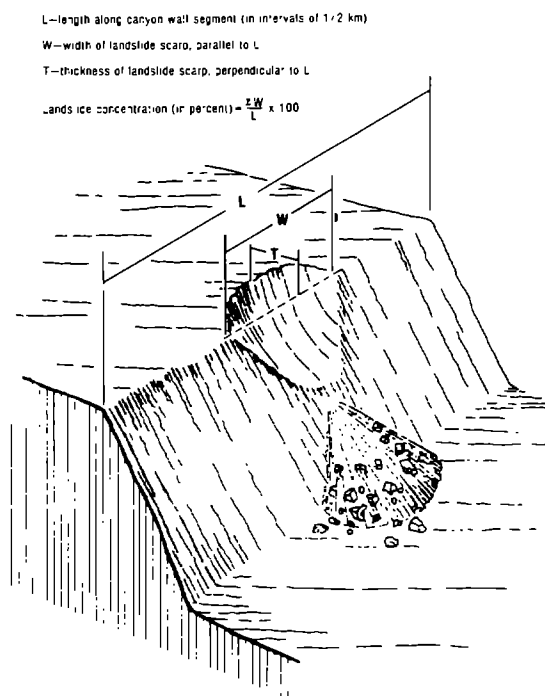


Figure 7.--Diagram of landslide dimensions and method of calculating landslide concentrations for map in figure 6 (after Harp and others (4)).

Perhaps the best example of these effects has a scope extending beyond the Guatemala City area. Variations in the lithology of the pumice and the overlying residual soils had a striking effect on the relative abundance of rockfalls versus debris slides. Within the Guatemala City area, debris slides were scarce in comparison to rockfalls, but along the Motagua River, 25 km north of Guatemala City, debris slides were far more abundant. In Guatemala City, the soils on the pumice are 1 to 2 m thick; these soils consist mainly of sand-size pumice particles, but contain enough clay to provide some cohesion, which inhibits the formation of debris slides. The Motagua soils are thinner (less than 30 cm) and contain little organic

material or clay. This northward decrease in soil thickness and clay content coincides with a rain shadow to the north of the continental divide which transects Guatemala City. In addition, slopes composed mainly of semi-rounded fluvial pumice gravels and lacustrine deposits along the Motagua River are not as steep as those composed primarily of ash flow tuffs and tephras in the Guatemala City area; the primary particles of the latter deposits are highly angular and interlock to provide sufficient strength to support nearly vertical slopes. As a result, the ash flow tuffs and tephras of the Guatemala City area and their soils failed as rockfalls, whereas the deposits along the Motagua River produced mainly debris slides. Although lithologic variations within the pumice deposits of the Guatemala City area are less dramatic, they exert a significant control upon the relative seismic stability of canyon slopes.

The spacing and orientation of preexisting fractures may also have influenced the concentration of seismically induced landslides in the Guatemala City area. In many places, weathered, planar surfaces formed parts of the scarps of rockfalls and were interpreted to be preexisting fractures that served as planes of weakness. Other weathered fracture surfaces were observed intersecting the scarp surfaces. In the Guatemala City area, a strong preferred orientation of N. 10 E. to N. 20 E. was observed in the fractures exposed in the rockfall scarps. This direction is approximately parallel to the Mixco fault zone, which bounds the western margin of the Guatemala City graben.

Because seismic shaking served as a trigger for these landslides, one would expect that the landslide concentrations correlated closely with the distribution of isoseismals from the 1976 earthquake. On a regional scale (fig. 3), this correlation seems to be true, because the highest landslide concentrations fall within the MMI (Modified Mercalli Intensity) VIII contour. At a local scale, however, (fig. 8), there is no close correlation between plotted isoseismals and landslide concentrations. At the 1:12,500 scale of the Guatemala City quadrangle, landslide concentrations are extremely inconsistent with the plotted intensity data. High landslide concentrations are found within areas of MMI VI, VII, and VII, (fig. 8), thus, there are no apparent differences in landslide concentrations that correspond to these zones. However, a noticeable concentration of landslides was related to slope geometry (described below), which suggests that the level of ground shaking (or seismic intensity) within the canyons varied over distances on the order of tens of meters.

Topographic variations appear to have influenced the concentration of landslides within the canyon network of Guatemala City. In many places, narrow ridges and promontories had very high concentrations of rockfalls, whereas nearby slopes without these topographic distinctions remained relatively unaffected (fig. 9). The concentration of failures on promontories suggests a topographic amplification of ground motion similar to that predicted theoretically by Wong and Jennings (10). Observations of this effect were confined largely to the canyon slopes where there were no buildings and hence were not incorporated into the intensity mapping.

The effect of topography on local ground shaking points out a very real difference between an intensity survey and a survey of ground failure. The difference is one of sampling and arises from the fact that the two surveys commonly sample different territories and different effects. The intensity survey is based largely on structural behavior. The ground failure survey reflects ground shaking, slope, rock type, jointing and

other factors that influence the site conditions of slopes. We believe that both ground failure and shaking intensity surveys are necessary to depict the true ground shaking.

Most observations suggest that lithologic and topographic factors were the most influential in affecting landslide distribution on a local scale. This evidence of the influence of physical site conditions is of great importance in answering the question of whether future earthquakes will produce similar landslide concentrations should seismic source conditions vary greatly.

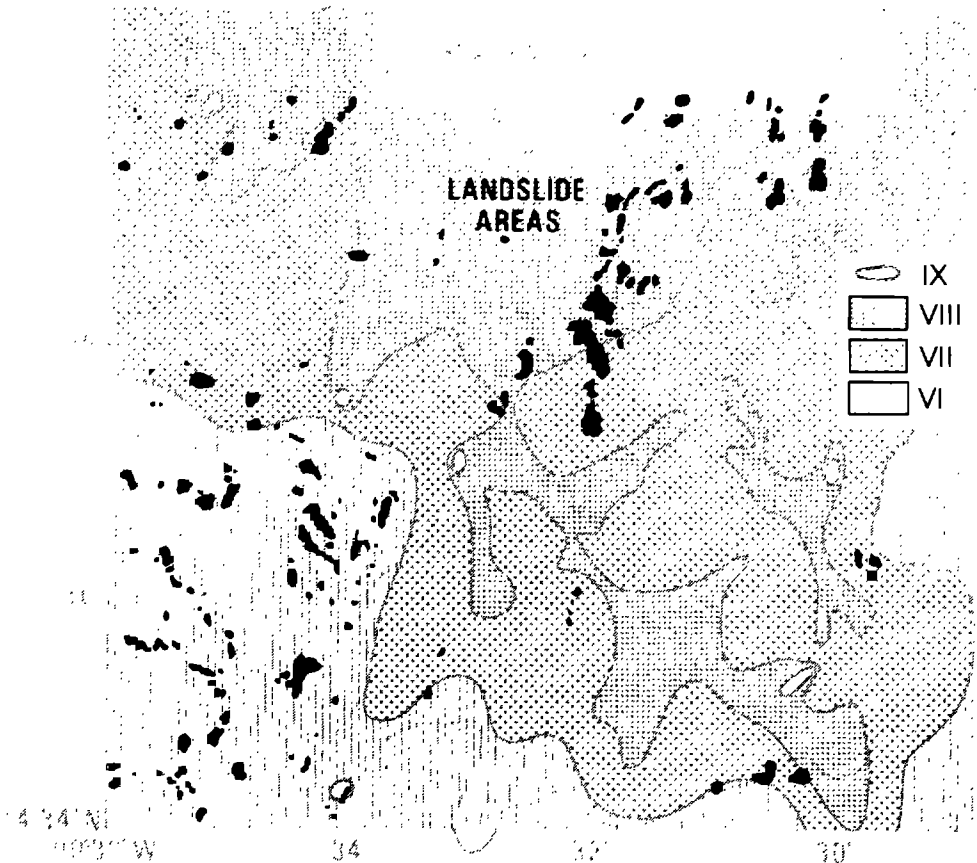


Figure 8.--Distribution of intensities and landslides from 1976 earthquake. Note scatter of landslides throughout area within zones of MMI VI through VIII (after Espinosa and others (3)).

IMPLICATIONS FOR REDUCTION OF SEISMIC-INDUCED LANDSLIDE HAZARDS IN GUATEMALA CITY

At present the canyon slopes in the Guatemala City area remain as susceptible to earthquake-induced landsliding as they were prior to the 1976 earthquake. It is likely that the areas of high and severe landslide concentrations from this earthquake will again be sites of extensive landslide activity in future earthquakes. It is possible that future earthquakes with stronger shaking, longer duration, and markedly different source characteristics may also cause failures on other slopes. Thus, it cannot be generally assumed that steep canyon slopes that did not fail in 1976 are safe simply because they did not fail in that event. Rather the areas of high and severe landslide concentrations in the 1976 earthquake are likely

to be sites of renewed failure in future events, and some slopes may fail that did not fail in 1976.

In view of this, it would seem prudent, in the future, for critical structures such as hospitals, communication systems, schools, and major lifelines to be placed outside of high landslide concentration areas within 10 m of the canyon margins and the slopes below. In zones of severe or high landslide concentration (fig. 6) in the 1976 earthquake, caution should be exercised in placing any inhabited structure.

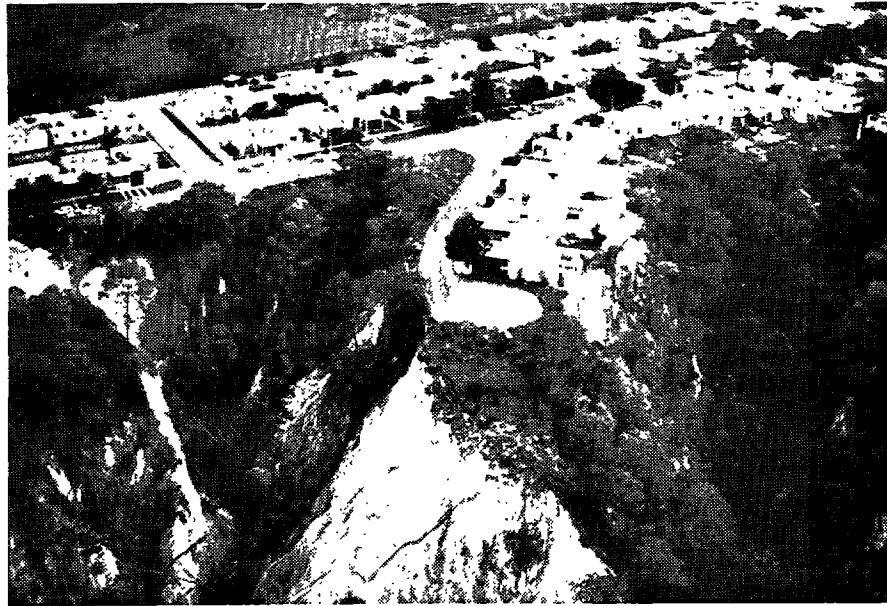


Figure 9.--Aerial photograph of a housing development in northeastern Guatemala City showing numerous rockfalls and extensive bedrock fracturing at end of a narrow ridge.

APPLICATION OF RESULTS TO OTHER AREAS OF SEISMIC HAZARD

The geologic and physiographic setting of Guatemala City is perhaps unique because of the comparatively uniform underlying lithology and the characteristics of the pumice. However, documentation of landslide occurrence in many other moderate to strong earthquakes suggests that the mechanisms and characteristics of rockfalls and debris slides are common in many earthquakes (5). Thus, with further study, these criteria may be generalized to other seismic regions with steep slopes and weakly cemented and heavily jointed rocks.

The data gathered on the Guatemala landslides were vital to the development of a complete picture of the landslide distribution and mechanisms. Similar postearthquake investigations in the future are needed to produce comprehensive case studies of earthquake-induced ground failure so that predictive criteria coming from earthquakes such as that in Guatemala can be refined and improved.

CONCLUSIONS

The total of more than 10,000 landslides triggered by the Guatemala earthquake makes it one of the more significant earthquakes in recent

history in terms of generating ground failures. Because of the widespread distribution of landslides, this earthquake has provided a great deal of information about and insight into processes involved in the generation of seismically induced landslides, particularly rockfalls and shallow debris slides. Our interpretation from aerial photographs, mapping, field reconnaissance, and statistical investigation of these landslides has led to the following conclusions:

1) The predominant landslide types generated in this earthquake were shallow rockfalls and debris slides. The rockfalls most commonly occurred on slopes steeper than 50° , were generally less than 6 m thick, and appeared to be tensile failures resulting from reflection of seismic waves at canyon walls. Debris slides occurred on gentler slopes between 30° - 50° within thin, noncohesive soil layers developed on Pleistocene pumice.

2) The regional distribution of landslides is similar to the overall pattern of seismic intensities.

3) The local landslide distribution within the Guatemala City area is inconsistent with the detailed intensity data. Landslide concentrations along canyon slopes cannot be correlated with the different MMI zones.

4) The lithologic, structural, and topographic characteristics of the steep canyon slopes are the most important factors in determining landslide locations in a given local area.

5) Similar landslide concentrations are likely to be produced during future earthquakes with the same general characteristics as the 1976 event. A future earthquake with greatly differing characteristics, for example, a larger magnitude or longer duration event, may produce landslide distributions involving additional canyon slopes.

The results of this study were used to make a landslide concentration map for the Guatemala City area. If, as concluded, the 1976 landslide concentration primarily reflects physical conditions of canyon slopes, then this map may be used to predict areas most susceptible to landslides in future strong earthquakes.

ACKNOWLEDGMENTS

The authors wish to acknowledge the assistance of Oscar Salazar and Sam Bonis of the Instituto Geografico Nacional de Guatemala in providing logistic support for our field investigations, and the offices of USAID/ROCAP for financial support and the arrangement of ground and air transportation.

REFERENCES CITED

- (1) Bonis, Samuel, Bohnenberger, O.H., and Dengo, Gabriel, 1970, Mapa Geologico de la Republica de Guatemala (1st ed.): Guatemala Instituto Geografico Nacional.
- (2) Espinosa, A.F., Husid, Raul, and Quesada, Antonio, 1976, Intensity distribution and source parameters from field observations, *in* Espinosa, Alvaro F., ed., The Guatemalan earthquake of February 4, 1976, a preliminary report: U.S. Geol. Survey Prof. Paper 1002, p. 52-66.

- (3) Espinosa, A.F., Asturias, Jose, and Quesada, A., 1978, Applying the Lessons learned in the 1976 Guatemalan Earthquake to Earthquake-Hazard-Zoning Problems in Guatemala: International Symposium on the February 4, 1976 Guatemalan Earthquake and the Reconstruction Process, Guatemala City, Proceedings.
- (4) Harp, E.F., Wieczorek, G.F., and Wilson, R.C., 1978, Earthquake-induced landslides from the February 4, 1976 Guatemala earthquake and their implications for landslide hazard reduction: International Symposium on the February 4, 1976 Guatemalan Earthquake and the Reconstruction Process, Guatemala City, Proceedings.
- (5) Keefer, D.K., Wieczorek, G.F., Harp, E.L., and Tuel, D.H., 1978, Preliminary assessment of seismically induced landslide susceptibility: 2nd International Conference of Microzonation, Proceedings, (in press).
- (6) Koch, A.J., and McLean, Hugh, 1975, Pleistocene tephra and ash flow deposits in the volcanic highlands of Guatemala: Geol. Soc. America Bull., v. 86, no. 4, p. 529-541.
- (7) Person, Waverly, Spence, William, and Dewey, J.W., 1976, Main event and principal aftershocks from teleseismic data, in the Guatemalan earthquake of February 4, 1976, a preliminary report: U.S. Geol. Survey Prof. Paper 1002, p. 17-23.
- (8) Plafker, George, Bonilla, M.G., and Bonis, S.B., 1976, Geologic effects, in The Guatemalan earthquake of February 4, 1976, a preliminary report: U.S. Geol. Survey Prof. Paper 1002, p. 38-51.
- (9) Varnes, D.J., 1978, Slope movement types and processes, chap. 2 of Schuster, R.L., and Krizek, R.J., eds., Landslides--analysis and control: National Academy of Sciences, Transportation Research Board Spec. Report 176 (in press).
- (10) Wong, H.L., and Jennings, P.C., 1975, Effects of canyon topography on strong ground motion: Seismol. Soc. America Bull., v. 65, no. 5, p. 1239-1257.

A RISK MODEL FOR SEISMIC ZONATION OF TAIWAN

by

S. T. Mau^I and C. S. Kao^{II}

ABSTRACT

A hybrid point-line source model is used for the seismic risk analysis of Taiwan. Any point with a past earthquake record of magnitude five or larger is recognized as a source. At each source, the rate of earthquake occurrence and the distribution of earthquake magnitude are established separately. A Poisson process is assumed first, and the rate of occurrence is estimated through a Bayesian procedure. The resulting occurrence model takes the form of a Polya process. For the magnitude distribution, the commonly used negative exponential distribution is initially assumed. Again the parameter of this distribution is estimated through a Bayesian procedure. An upper bound as well as a lower bound is imposed on the magnitude distribution. In calculating the ground acceleration at a site resulting from an earthquake at a source, the attenuation distance is measured from the site to a line centering at the source. The orientation of the line is made parallel to that of nearby faults. A map of contours of acceleration, that has a probability of 10% of being exceeded in 50 years, is constructed. A simplified zoning map is proposed accordingly.

INTRODUCTION

Although the size of Taiwan is small, a mere 36,000 sq. km, the frequency of earthquake in and around the island is high. The yearly average of the number of earthquakes with magnitude of four or larger is over 70 since 1936. A network of earthquake stations established in 1936, following a disastrous earthquake in 1935, keeps a complete record of earthquakes with magnitude 4.7 or greater(1). A record also exists for magnitude 6 or greater since 1900. The distribution of epicenters is shown in Figure 1. Since 1972 a modernized strong motion network has been established, but no major earthquake has been recorded yet.

The epicenters shown in Figure 1 scatter all over the area, and precise correlation with faults is rather difficult. Existing information on the location and nature of faults is so incomplete that a realistic line source model can not be set up. Under such circumstances, a point source model is convenient. By following an established approach of seismic risk analysis (2), a risk map of northern Taiwan was constructed with a modified occurrence model for each point source(3). The modification resulted in a non-stationary Polya process. The magnitude distribution for the whole region was established as usual(2), and no upper bound was imposed. Accordingly, the point sources differed only in the number of earthquakes attributed to them, not in the magnitudes. This is unrealistic. An effort was made to

I Professor of Civil Engineering, National Taiwan University, also Center for Earthquake Engineering Research, National Taiwan University, Taipei, Taiwan, Republic of China.

II Graduate Student of Civil Engineering, National Taiwan University, Taipei, Taiwan, Republic of China.

remedy this by redistributing the number of earthquakes according to their magnitudes(4). Again, no upper bounds were imposed, and the resulting values of accelerations were unreasonably high. Besides, the redistribution of the number of earthquakes tended to overemphasize the large earthquakes. In a subsequent study, the redistribution was abandoned, but an upper bound was imposed for each point source. The area of Taiwan was divided into two regions with different magnitude distributions, and a map of contours of accelerations was constructed(5).

All the above-mentioned efforts for the seismic risk analysis of Taiwan are based on a general approach which has been used for other areas of the world(6,7,8), despite the variations made in the detail modelling procedure. The present study still uses the same framework, but seeks to improve the magnitude distributions for each source and the attenuation relation between a site and a source. The result is a hybrid point-line source model that considers a source as a point in developing its characteristics, but considers a source as a line in determining the attenuation from the source. It becomes known to the authors during the course of the present study that a similar idea has been used before(9) with a discrete type of modelling. The present study also differs with previous efforts in that each point source is considered individually without establishing any regional characteristics. This necessitates the use of Bayesian approach in determining source parameters, because the number of earthquakes attributed to each source is usually small.

THE RISK MODEL AND NUMERICAL RESULTS

Within a source area bounded by the lines of 118°E, 123.0°E, 21.0°N, and 26.0°N, a grid-work of 0.1° in each direction is constructed. Every node of the grid-work with a minimum earthquake magnitude record of five is considered a source. The probability density function of magnitude, m , knowing a lower bound $m_0 (=5)$ and a parameter β can be expressed as

$$f(m|\beta, m_0) = \beta \exp(-\beta(m-m_0)) \quad (1)$$

Assuming a diffuse prior for the distribution of β , and knowing the n_0 earthquake magnitudes m_i , $i=1,2,\dots,n_0$, the posterior distribution of β can be found.

$$f(\beta|m_i, m_0) = \frac{(n_0 \bar{m} - n_0 m_0)^{n_0+1}}{n_0!} \beta^{n_0} \exp(-\beta n_0 (\bar{m} - m_0)) \quad (2)$$

where $\bar{m} = (\sum m_i) / n_0$. By combining Eqs. 1 and 2, the density and cumulative distribution functions of m can be obtained. If an upper bound m_u also exists in addition to the lower bound m_0 , then the resulting functions are

$$f(m|m_i, m_0, m_u) = k \frac{(n_0+1) (n_0 \bar{m} - n_0 m_0)^{n_0+1}}{(n_0 \bar{m} - n_0 m_0 + m - m_0)^{n_0+2}} \quad (3)$$

$$F(m|m_i, m_0, m_u) = k \left(1 - \frac{(n_0 \bar{m} - n_0 m_0)^{n_0+1}}{(n_0 \bar{m} - n_0 m_0 + m - m_0)^{n_0+1}} \right) ; m_0 \leq m \leq m_u \quad (4)$$

with

$$k = \left(1 - \frac{(n_0 \bar{m} - n_0 m_0)^{n_0+1}}{(n_0 \bar{m} - n_0 m_0 + m_u - m_0)^{n_0+1}} \right)^{-1} \quad (5)$$

Examples of this distribution are shown in Figure 2.

For every value of m , there is an assumed length of slipped fault, and an idealized relation between the magnitude and the length is used(10,11):

$$\begin{aligned} L &= 2.93 \times 10^{-2} \exp(m) & m < 6.7 \\ L &= 3.62 \times 10^{-5} \exp(2m) & m \geq 6.7 \end{aligned} \quad (6)$$

where the length is measured in km. The line is centered at the source with an orientation made consistent with that of nearby faults. A sketch of the orientations is shown in Figure 3. The ground acceleration, a , at a site is estimated with a modified distance R , calculated from $R = (E^2 + h^2 + 400)^{1/2}$, in which h is the depth of an assumed line and E is the distance measured from the site to the nearest point on the line, all expressed in km. The following law of attenuation is then used,

$$a = b_1 \exp(b_2 m) R^{-b_3} \quad (7)$$

The parameters are $b_1 = 372.5$, $b_2 = 0.876$, and $b_3 = 1.836$, estimated from isoseismal maps of past earthquakes in Taiwan(3,4). This equation gives higher acceleration values near an epicentral region than the attenuation in rocks of western United States(12).

For every value of acceleration at a site, a probability can then be calculated for the event that the acceleration will be exceeded due to an earthquake at a site. This probability is denoted as $p_e(a)$, or simply p_e . For the occurrence of earthquakes at a source, the Poisson process is assumed first. By adopting also a diffuse prior on the rate of occurrence, the posterior distribution of the rate of occurrence becomes a Gamma distribution. The resulting distribution on the number of occurrence, n , in t years, given n_0 occurrence in the past t_0 years, takes the form of a Polya distribution.

$$P(n, t) = \binom{n+n_0}{n} \left(\frac{t}{t_0+t} \right)^n \left(\frac{t_0}{t_0+t} \right)^{n_0+1} \quad (8)$$

This approach was first used for earthquake occurrence modelling in 1968 (13), although it is well known that this distribution can be obtained from a Poisson distribution by assuming a Gamma distribution on the rate of occurrence and by using a "stratification" concept(14).

By combining Eq. 8 and the probability p_e , the following probability of having an acceleration, a , being exceeded n times in a duration of t years is obtained(3):

$$P(n, t) = \binom{n+n_0}{n} \left(\frac{t p_e}{t_0 + t p_e} \right)^n \left(\frac{t_0}{t_0 + t p_e} \right)^{n_0+1} \quad (9)$$

The probability that an acceleration ,a, will not be exceeded in t years is then

$$P(0,t) = \left(\frac{t_0}{t_0+t_{pe}} \right)^{n_0+1} \quad (10)$$

If a total of j sources are relevant to the site, then by assuming no correlation among these sources, a simple expression is obtained:

$$P(0,t) = P_1(0,t)P_2(0,t)\cdots P_j(0,t) \quad (11)$$

For any site, the acceleration corresponding to a given $P(0,t)$ value can be found by interpolating $P(0,t)$ between probabilities corresponding to given levels of accelerations. By repeating the procedure for enough sites, a contour map can be constructed.

For the area of Taiwan, deterministic upper bounds of magnitudes and depth of sources are assumed. For a source, an upper bound on magnitude is made equal to the maximum magnitude ever occurred at the source plus an increment. This increment is roughly proportional to the inverse of the maximum magnitude. For maximum magnitude over 7, for example, an increment of 0.1 is used, and for magnitude below 5.5, an increment of 0.5 is used. The depth of a source is chosen from past focal depths, such that the chosen one corresponds to a past earthquake which produced the largest acceleration at the epicenter.

The record from 1900 to 1975 is used. For magnitude 6.5 or below, the number of earthquakes at each source is estimated by extending the record of 1936-1975 to 1900-1975 proportionally. This is justified by an examination of the completeness(15) of the record, which shows that the number of small earthquakes has been relatively stabilized during the period of 1936-1975. Since the risk analysis is meant for building designs, the exposure time is chosen to be 50 years, which is roughly the life span of buildings. A 10% probability is assigned to $P(0,50)$, and the resulting contours of acceleration are plotted in Figure 4. From Figure 4, and with the help of a geological map of Taiwan, a simplified zoning map is constructed and shown in Figure 5, which gives three seismic zones. The relative value of a zoning coefficient, conforming to the present format of a building code(16), are suggested to be 1:0.8:0.4 for the three zones.

CONCLUSION

A systematic way of seismic risk analysis is presented. The utilization of distributed point sources and Bayesian estimation of source parameters is particularly suitable for the situation where information on active faults is incomplete and risk assessment is required for a relatively small area, such as Taiwan. The use of line source attenuation simulates better a slipped fault of finite length. The assumptions of diffuse prior distributions in the Bayesian estimation process are convenient, but certainly can, and should, be changed to other forms of probability distributions, if data is available to justify so. In fact, one of the salient features of the present formulation is the capability of including subjective judgments in the form of a non-diffuse prior distribution. As new knowledge on active faults accumulates, the present formulation can be easily modified and results updated.

ACKNOWLEDGMENT

The work reported herein contains part of a research project supported by the National Science Council of the Republic of China, through Grant No. NSC-67E-0204-02(01). The critical review of the manuscript by Professor C. L. Yen of the Department of Civil Engineering, National Taiwan University is deeply appreciated.

BIBLIOGRAPHY

1. Hsu, M. T., "Seismicity of Taiwan and Some Related Problems," Bulletin of International Institute of Seismology and Earthquake Engineering, Vol. 8, 1971, pp. 115-234.
2. Cornell, C. A., "Engineering Seismic Risk Analysis," Bulletin of the Seismological Society of America, Vol. 58, No. 5, 1968, pp. 1583-1606.
3. Shih, T. Y., "The Application of Polya Process with Random Selection to Seismic Risk Analysis," in Chinese, Master Degree Thesis, Mau, S. T. advisor, Department of Civil Engineering, National Taiwan University, 1974.
4. Mau, S. T., Shih, T. Y. and Kuo, J. F., "Seismic Risk Analysis of Taiwan." Proceedings, Central American Conference on Earthquake Engineering, San Salvador, El Salvador, Vol. I, 1978, pp. 11-18.
5. Mau, S. T., "A Model of Engineering Seismic Risk Analysis and Its Applications," in Chinese, Journal of Civil and Hydraulic Engineering, Chinese Institute of Civil and Hydraulic Engineering, Vol. 5, No. 1, 1978, pp. 35-40.
6. Algermissen, S. T. and Perkins, D. M., "A Technique for Seismic Zoning: General Consideration and Parameters," Proceedings, International Conference on Microzonation for Safer Construction, Research and Application, Seattle, Washington, U. S. A., 1972, pp. 865-878.
7. Liu, S. C. and DeCapua, N. J., "Microzonation of Rocky Mountain States," Proceedings, U. S. National Conference on Earthquake Engineering, Ann Arbor, Michigan, U. S. A., 1975, pp. 128-135.
8. Kiremidjian, A. S. and Shah, H. C., "Seismic Hazard Mapping for Guatemala," Proceedings, Central American Conference on Earthquake Engineering, San Salvador, El Salvador, Vol. I, 1978, pp. 629-636.
9. Algermissen, S. T. and Perkins, D. M., "A Probabilistic Estimate of Maximum Acceleration in Rock in the Contiguous United States," U. S. Geological Survey, Open File Report, 76-416, 1976.
10. Bonilla, M. G., "Historic Surface Faulting in Continental United States and Adjacent Parts of Mexico," U. S. Geological Survey, 1967.
11. Housner, G. W., "Engineering Estimates of Ground Shaking and Maximum Earthquake Magnitude," Proceedings, Fourth World Conference on Earthquake Engineering, Santiago, Chile, 1969, pp. A1-A13.

12. Schnabel, P. B. and Seed, H. B., "Accelerations in Rock for Earthquakes in the Western United States," Bulletin of the Seismological Society of America, Vol. 63, 1973, pp. 501-511.
13. Benjamin, J. R., "Probabilistic Models for Seismic Force Design," Journal of the Structural Division, Proceedings of ASCE, Vol. 94, No. ST5, 1968, pp. 1175-1195.
14. Feller, N., An Introduction to Probability Theory and Its Applications, Vol. II, John Wiley and Sons, New York, 1966, pp. 56-57.
15. Stepp, J. C., "Analysis of Completeness of Earthquake Samples in the Puget Sound Area and Its Effects on Statistical Estimations of Earthquake Hazard," Proceedings, International Conference on Microzonation for Safer Construction, Research and Application, Seattle, Washington, U. S. A., 1972, pp. 897-910.
16. Chiu, C. P., Lin, T. W., Mau, S. T., Chen, C. C. and Yeh, C. S., "Recommended Earthquake Resistant Design Provisions for the Chinese Building Code, first draft," in Chinese, Journal of Civil and Hydraulic Engineering, Chinese Institute of Civil and Hydraulic Engineering, Vol. 5, No. 1, 1978, pp. 47-66.

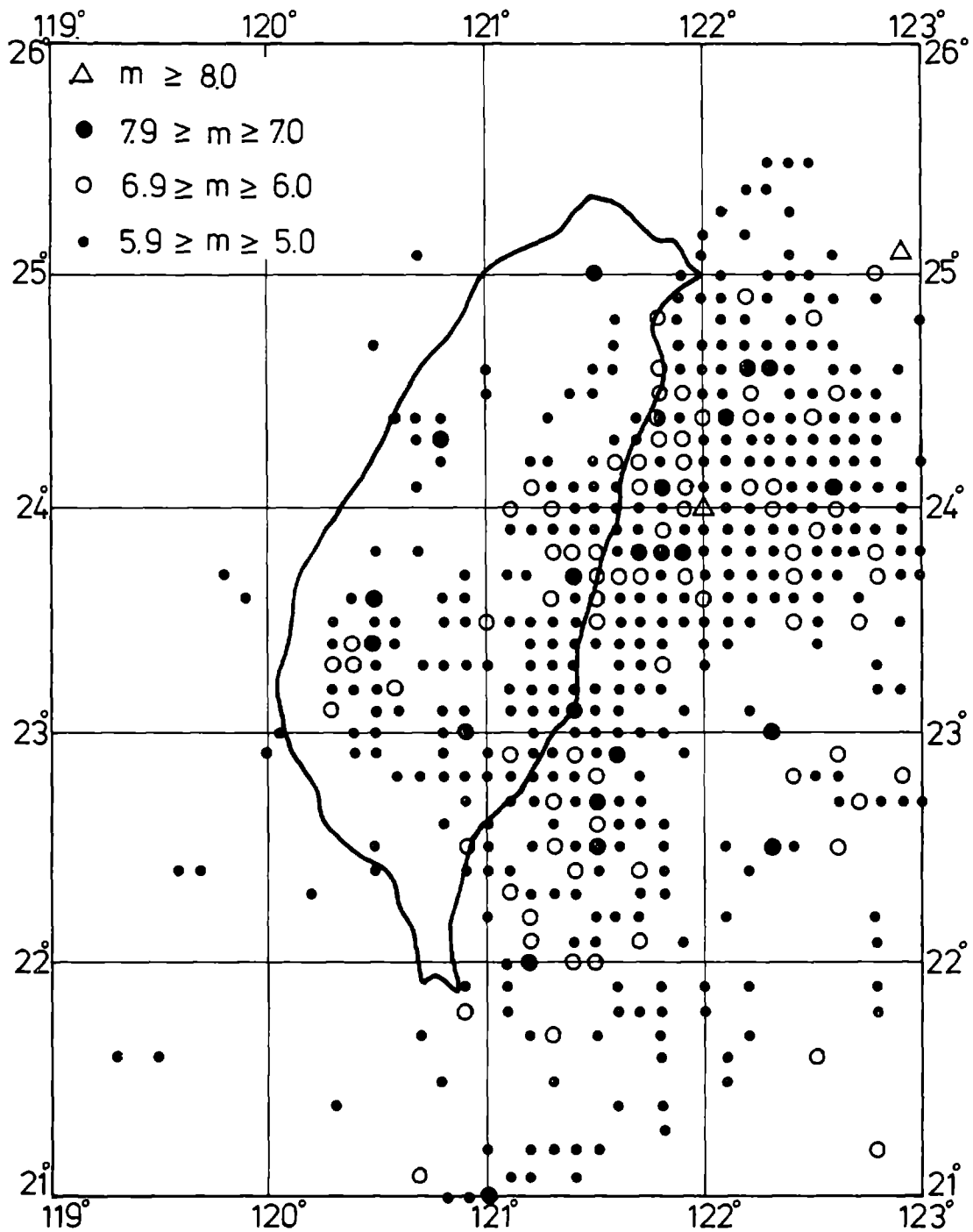


FIGURE 1. EPICENTRAL DISTRIBUTION SHOWING MAXIMUM MAGNITUDES

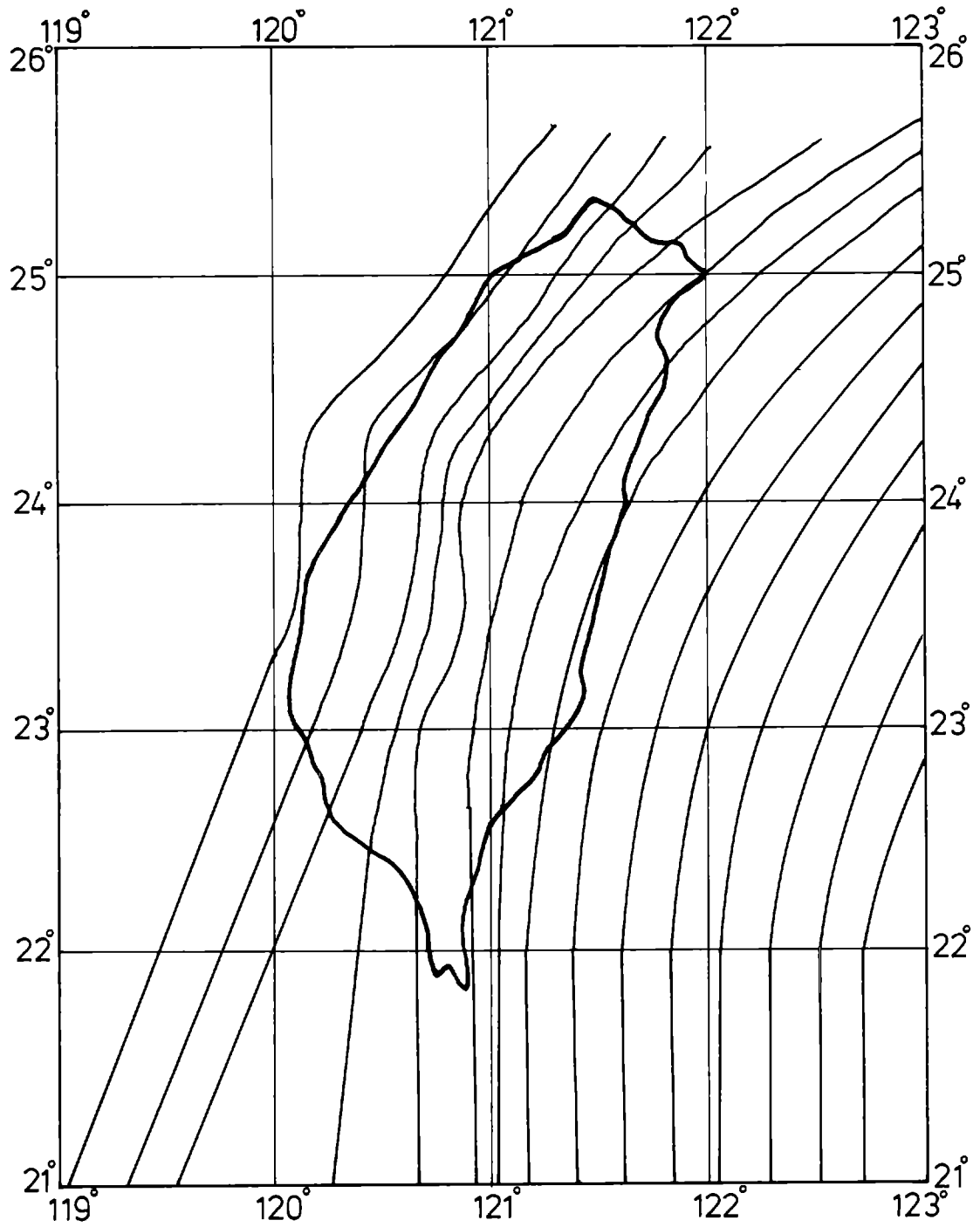


FIGURE 2. ORIENTATIONS FOR HYBRID POINT-LINE SOURCES

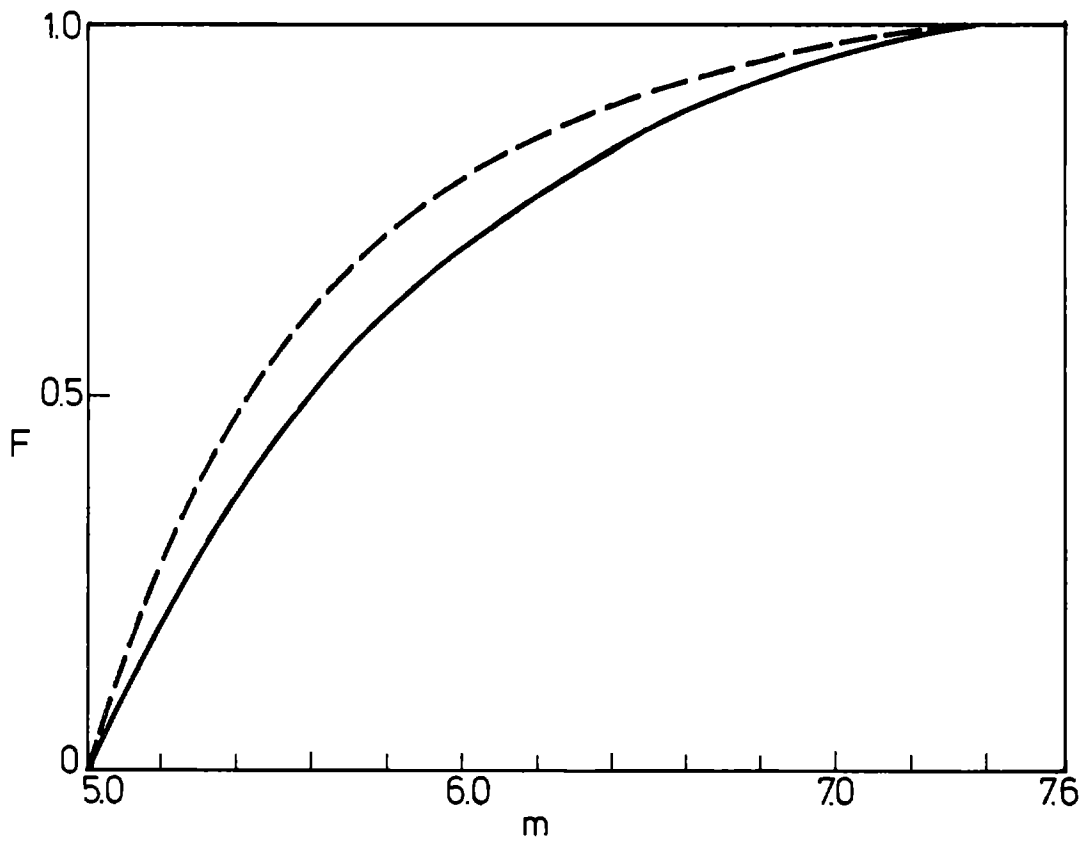
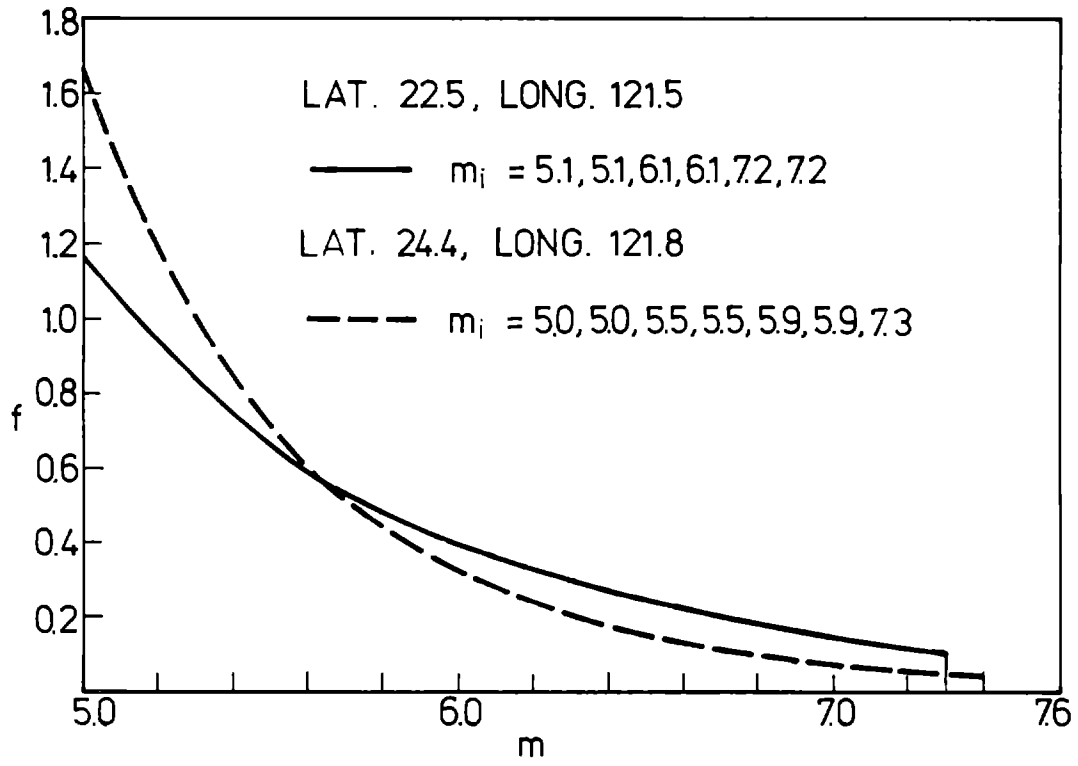


FIGURE 3. EXAMPLES OF PROBABILITY DISTRIBUTIONS OF MAGNITUDES

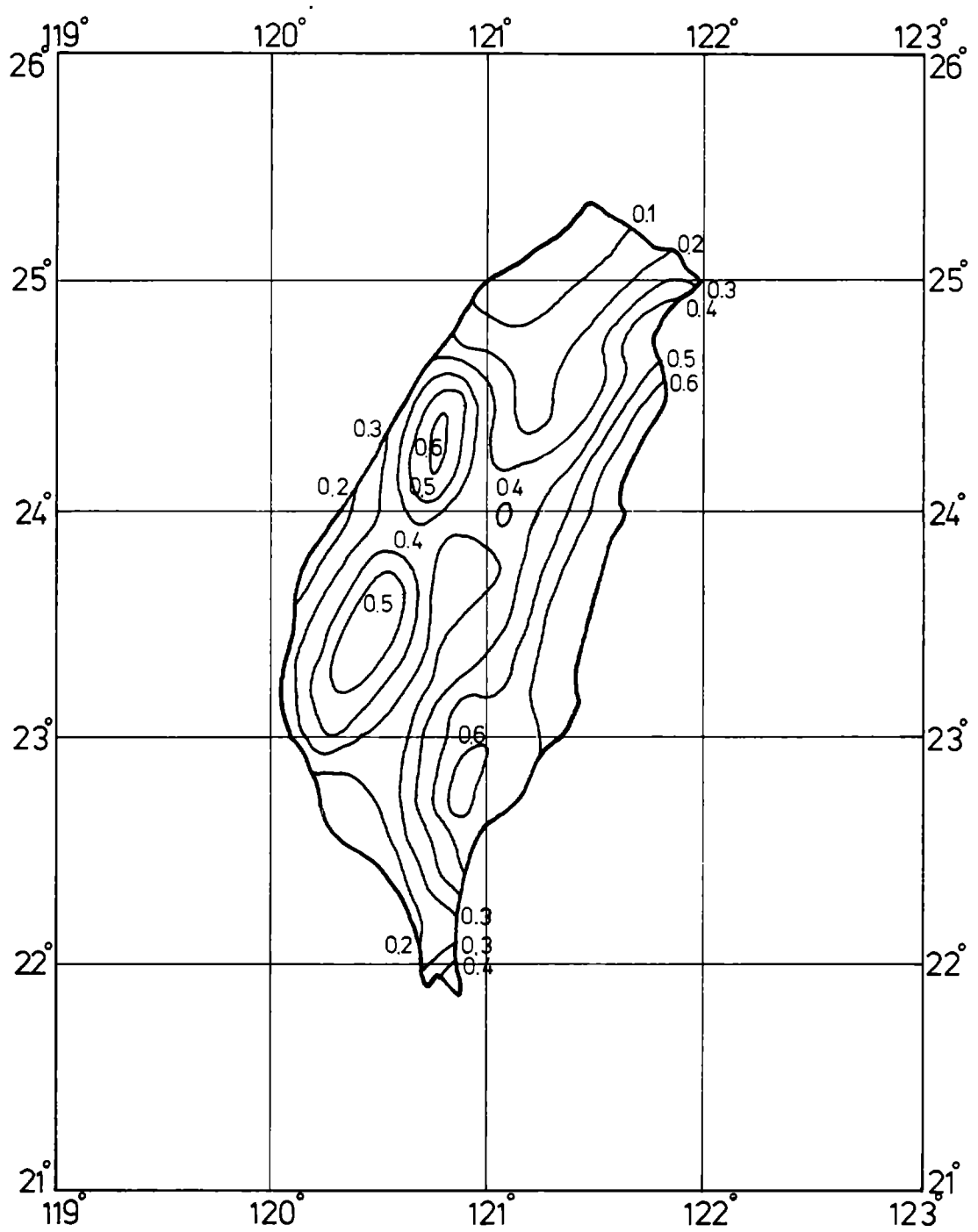


FIGURE 4. CONTOURS OF ACCELERATION WITH 10% PROBABILITY OF BEING EXCEEDED IN 50 YEARS

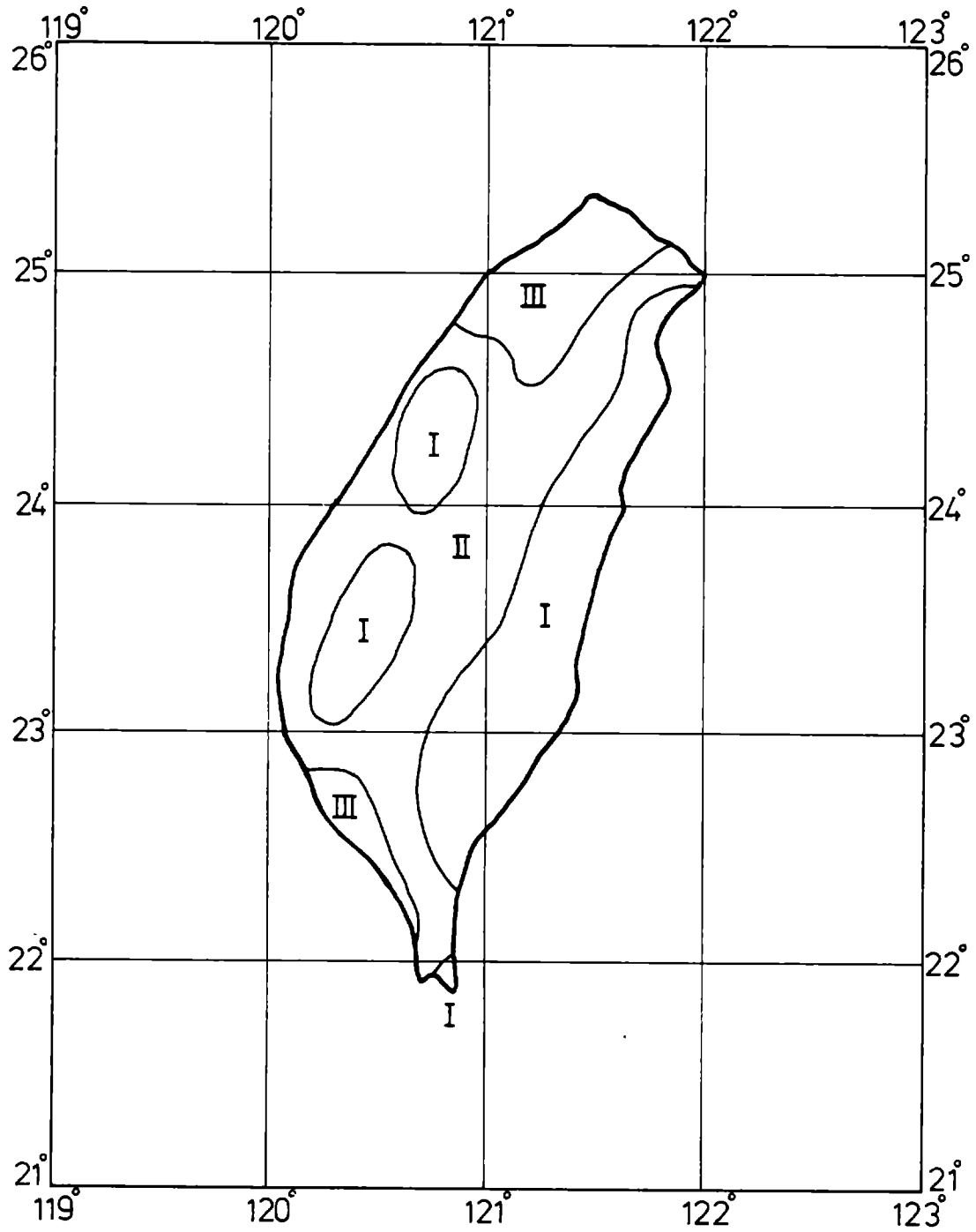


FIGURE 5. RECOMMENDED SEISMIC ZONING MAP OF TAIWAN

INTENTIONALLY BLANK

GROUND MOTION ATTENUATION IN THE PHILIPPINES

by

H. K. Acharya^I

ABSTRACT

Large earthquakes occur frequently in the Philippines and cause considerable damage to life and property. In order to assess the potential for damage, it is necessary to have some knowledge of the attenuation of ground motion. As strong motion data are practically nonexistent in the Philippines, the only available technique for assessing the attenuation of ground motion is the examination of isoseismals. All earthquakes (during the period 1949-1974) for which three or more intensity contours could be developed were used. A major difficulty arises, however, since most large earthquakes occur in the oceanic areas, and, therefore, the epicentral intensity is unknown. The intensity at a place is, therefore, expressed in terms of magnitude (M) and epicentral distance (Δ Km) by a relationship of the form:

$$\ln I = \ln (1.5M - 1.5) + 0.327 - 0.13 \ln \Delta - 0.00089 \Delta$$

where I is the intensity in the Philippine Rossi-Forel scale.

It is concluded that the ground motion attenuation in the Philippines is more severe than in the Cordilleran and the eastern section of United States but less severe than in the California coastal range section. A comparison of the isoseismal maps of the 1906 San Francisco earthquake, 1811-1812 New Madrid earthquake, and the 1976 Mindanao earthquake leads to the conclusion that attenuation in southern and central Philippines is much greater than in the eastern United States but slightly less than in California.

INTRODUCTION

The Philippine Islands are affected by large earthquakes from time to time, causing considerable destruction of life and property. In historic times 51 earthquakes, with maximum Intensity IX or X on the original Rossi-Forel scale, have been reported in the Philippines (1). Since 1897 an earthquake of magnitude 7.0 or greater has occurred in the Philippines almost every year. (Figure 1 shows the location of large earthquakes in the Philippines since 1897 based on NOAA tape listing and Damasco (2).) Manila has experienced Intensity VIII to X several times. The seismicity and tectonics of the Philippines have been recently investigated by Acharya and Aggarwal (3). However, in order to mitigate earthquake hazard in the Philippines, it is necessary to have not only an understanding of the seismicity of the area but also knowledge of the attenuation of ground motion.

^I Consultant, Stone & Webster Engineering Corporation,
Boston, Massachusetts 02110

METHOD OF INVESTIGATION

In the Philippines, the effects of earthquakes are known only through intensities, which since 1931 are specified on the Philippine Rossi-Forel scale. This adapted version is described in Table 1. At present, two strong motion instruments are operating in the Philippines. However, as there are practically no strong motion data, the attenuation of ground motion has to be investigated, principally using intensity data available for large earthquakes.

The Philippines Atmospheric Geophysical and Astronomical Services Administration (PAGASA) determines intensity at the weather stations it operates in the country. In addition, it conducts special investigations for large destructive earthquakes. For the period 1949-1959 Minoza et al (4) listed intensities at various locations and also presented isoseismal maps for large earthquakes. PAGASA reports, for subsequent years, list intensities at all affected places for significant earthquakes. For earthquakes in 1968, 1973, 1974, and 1976, it has published isoseismal maps in its special reports. These data form the base for determining the attenuation of ground motion with distance in the Philippines. Figure 2 shows the location of seismographic and weather bureau stations operated by PAGASA and the locations of earthquakes used for this investigation.

In the absence of strong motion data, ground motion attenuation in eastern and central United States has also been evaluated on the basis of isoseismal maps (5, 6, 7, and 8). However, in most cases in the eastern and central United States, the epicentral intensity can be estimated on the basis of felt reports. As can be seen in Figures 1 and 2, most large earthquakes in the Philippines occur on various faults and trenches in the oceanic areas, and the epicentral intensity is therefore unknown. Thus, ground motion attenuation cannot be estimated by examining intensity at various locations in terms of epicentral intensity. However, since the magnitude of these earthquakes is known, following Howell and Schultz (7) and Gutenberg and Richter (9), intensity is investigated as a function of magnitude and epicentral distance in a relationship of the form:

$$\ln I = \ln (1.5M - 1.5) + a - b \ln \Delta - c \Delta \quad (1)$$

where I is the intensity in Philippine Rossi-Forel scale, at an epicentral distance (Δ Km), M is the earthquake magnitude, and a , b , and c are constants. The coefficient b defines the rate of geometric spreading of the energy, coefficient c defines the rate of exponential absorption, and coefficient a is related to the conditions at the source (7).

INTENSITY DATA IN THE PHILIPPINES

Large earthquakes for which isoseismal maps are either available or could be developed are listed in Table 2. For the earthquakes in 1949,

1955, 1961, 1968, 1973, 1974, and 1976, isoseismal maps published by the Minoza et al (4) or PAGASA are directly used. For the remaining earthquakes, PAGASA reports were used to construct isoseismal maps. Only intensities greater than III were used in this endeavor, and at least three isoseismals were required for each earthquake. The areas occupied by isoseismals of Intensity III or greater were measured using a planimeter. The average isoseismal radius R is then given by $(A/\pi)^{1/2}$, where A is the area occupied by an isoseismal contour. In this way 47 different values of radii were determined for an equal number of values of intensity. These 47 equations in three unknowns a , b , and c were solved for the best values of three constants using the method of least squares. The following attenuation relationship was thereby obtained:

$$\ln I = \ln (1.5M - 1.5) + 0.327 - 0.13 \ln \Delta - 0.00089 \Delta \quad (2)$$

For the three provinces of United States, Howell and Schultz (7) obtained the following relationships:

San Andreas Province

$$\ln I = \ln (1.5M - 1.5) + 0.274 - 0.0953 \ln \Delta - 0.0022 \Delta \quad (3)$$

Cordilleran Province

$$\ln I = \ln (1.5M - 1.5) + 0.434 - 0.152 \ln \Delta - 0.00053 \Delta \quad (4)$$

Eastern Province

$$\ln I = \ln (1.5M - 1.5) + 0.517 - 0.155 \ln \Delta - 0.00064 \Delta \quad (5)$$

From these three relationships Howell and Schultz (7) concluded that it is the exponential absorption coefficient c which produces the great contrast in attenuation between east and west. They also observed that the effect of allowing focal depth is to increase the values of a and b and to decrease c .

It is clear from equations (2) - (5) that the exponential absorption factor c in the Philippines is less than its value for the San Andreas Province but greater than for Cordilleran and eastern United States. This factor for the Philippines and Eastern and Cordilleran Provinces will decrease further when the greater depth of focus for earthquakes in these regions is taken into consideration. It means that the attenuation of ground motion in Philippines is less severe than for San Andreas Province, but considerably greater than for Eastern Province. Differences in focal mechanism and intensity scales are reflected in the values of ' a ' and, therefore, values of coefficient ' a ' cannot be compared.

COMPARISON OF ISOSEISMAL MAPS OF LARGE EARTHQUAKES

A comparison of isoseismal maps of the largest earthquakes in the Philippines, California, and eastern United States confirms the ground

motion attenuation characteristics of Philippines deduced above. Nuttli (10) examined the isoseismal maps for (i) 1811-1812 New Madrid earthquake and (ii) 1906 San Francisco earthquake and concluded that the ground motion attenuation is lower in the eastern part of United States than in the western part. The isoseismal maps of these two earthquakes are compared in this study (Table 3) with a similar map prepared by PAGASA (11) for the Mindanao earthquake of August 16, 1976 ($M = 8.0$). This earthquake was felt up to 500 miles in the north in Luzon and up to 500 miles towards the southwest in Borneo (11). The isoseismal map for this earthquake is reproduced in Figure 3. The intensity data for all three earthquakes are available only for the regions east of the fault zones and, therefore, distances to various isoseismal countours were measured perpendicular to the fault zones. The 1906 earthquake was on the San Andreas Fault and its direction is well known. The New Madrid earthquake of 1811-1812 is postulated to be on the NE trending faults in the area (12). The distribution of aftershocks and fault plane solution indicate that the 1976 Mindanao earthquake was associated with the Celebes Sea Trench trending northwest (13, 14, and 15).

The isoseismals for the 1906 and 1811-1812 earthquakes are in the MM scale (16 and 17) whereas the isoseismals for the Mindanao earthquake are in the Philippine Rossi-Forel scale. A comparison of the description of two scales lead to the following equivalence:

<u>Philippine Rossi-Forel Scale</u>	<u>Modified Mercalli Scale</u>
II	II
III	III
IV	IV
V	IV-V
VI	V-VI
VII	VII
VIII	VIII
IX	IX-XII

Although conversion of intensity values from one scale to another involves some uncertainty, it appears from above that the two intensity scales are similar except near the upper limit.

It is interesting to note the Philippine Rossi-Forel scale defines Intensities VIII and IX primarily in terms of geological effects. Structural damage is included only in Intensities VI and VII, reflecting the construction practices in the Philippines.

The distances up to which various intensities were felt for all three earthquakes (normal to the strike of the fault) are listed in Table 3. Examination of this table indicates that intensity attenuation is most severe for the San Francisco earthquake and least severe for New Madrid shock, with Mindanao earthquake data in between. The comparison would be even more accentuated because, compared to the Mindanao earthquake, the San Francisco earthquake was of slightly higher magnitude while the New Madrid earthquake was of slightly lower magnitude.

The differences in attenuation characteristics of these areas can also be seen in a comparison of distances up to which the three earthquakes were felt. The 1906 earthquake was felt up to distance of about 270 miles, the 1976 earthquake was felt up to about 500 miles, and the 1811-1812 earthquake for about 1000 miles. Even considering the uncertainty in the drawing of the smallest intensity contours, it is clear that the ground motion attenuation in southern and central Philippines is less than in California and Nevada but much more than in eastern United States. This conclusion will be valid even if some uncertainties exist in the conversion of Philippine Rossi-Forel scale to MM scale.

CONCLUSION

On the basis of determination of exponential attenuation factor and comparison of isoseismal maps, it is concluded that ground motion attenuates in the Philippines much more rapidly than in eastern United States but less so than in California. The exponential attenuation factors in the Philippines and the Cordilleran Province in Western United States are 0.00089 and 0.00053, respectively. Thus, ground motion attenuation in the Philippines is greater than in the Cordilleran Province.

The attenuation relationships derived here, are based on the measurement of observed isoseismal areas, without any regard to the possible presence of regions of anomalous surficial geology which can significantly affect the observed intensity values. The method used here also does not consider the effect of elongation of isoseismals due to factors such as azimuthal variation in attenuation, finite fault length, and focal mechanism.

Ground motion attenuation characteristics developed above for the Philippines can be used for seismic risk analysis by determining intensity at a location, in terms of magnitude and epicentral distance. The intensity at a site can then be converted into ground acceleration using available relationships (18 and 19). This technique provides an easy method of using relevant ground motion attenuation for zonation and microzonation purposes in the Philippines and other countries with no strong motion data.

REFERENCES

1. Sevilla, F. Q.; Valenzuela, R. G.; and Bellosillo, S., Jr. Seismicity of the Philippines (1907-1964). International Institute of Seismology and Earthquake Engineering, Individual Studies, 2, p 34-63, 1965.
2. Damasco, Z., Seismicity of the Philippines (1897-1967). International Institute of Seismology and Earthquake Engineering, Individual Studies, 6, p 53-58 and appendix, 1970.
3. Acharya, H. K., and Aggarwal, Y. Seismicity and Tectonics of the Philippines. Submitted for publication, 1978.
4. Minoza, W. H.; Ocampo, A. T.; and Bellosillo, S., Jr. Significant Philippine Earthquakes (1949-1959). Philippine Weather Bureau Scientific Paper 101, 1960.
5. Brazee, R. J. Attenuation of Modified Mercalli Intensities with Distance for the United States East of 106°W. Earthquake Notes, 43, p 41-52, 1972.
6. Evernden, J. F. Seismic Intensities, 'Size' of Earthquakes and Related Parameters. Seismological Society of America Bulletin, 65, p 1287-1313, 1975.
7. Howell, B. F., and Schultz, T. R. Attenuation of Modified Mercalli Intensity with Distance from the Epicenter. Seismological Society of America Bulletin, 65, p 651-665, 1975.
8. Gupta, I. N., and Nuttli, O. W. Spatial Attenuation of Intensities for Central United States Earthquakes. Seismological Society of America Bulletin, 66, p 743-751, 1976.
9. Gutenberg, B., and Richter, C. F. Earthquake Magnitude, Intensity, Energy and Acceleration. Seismological Society of America Bulletin, 32, p 163-191, 1942 and 46, p 105-145, 1956.
10. Nuttli, O. W. Magnitude, Intensity and Ground Motion Relations for Earthquakes in the Central United States. Proc. Intern. Conf. Microzonation, Seattle, p 307-318, 1972.
11. Philippine Atmospheric Geophysical and Astronomical Services Administration (PAGASA), Preliminary report on the Moro Gulf Earthquake of August 17, 1976, Prepared by National Geophysical and Astronomical Services, Manila, 1976, p 13.
12. Nuttli, O. W. The Seismicity of the Central United States. Nuclear Geology (in press), 1978.

13. Wallace, R. E.; Pararascarayannis, G.; Valenzuela, R.; and Taggert, J. N. Earthquake and Tsunamis of August 17, 1976, Mindanao, Philippines (abstract). Geological Society of America (Abstract with Programs), 9, p 523, 1977.
14. Stewart, G. S., and Cohn, S. N. The August 16, 1976, Mindanao Philippine Earthquake ($M_s = 7.8$) - Evidence for a Subduction Zone South of Mindanao. (abstract), EOS, Trans. Am. Geophys. Union, 58, p 1194, 1977.
15. Acharya, H. K. The Mindanao Earthquake of August 16, 1976 - Preliminary Seismological Assessment. Seismological Society of America Bulletin, October 1978.
16. Bolt, B. A. Hazards from Earthquakes. in Geological Hazards, ed. B. A. Bolt, W. L. Horn, G. A. MacDonald, and R. F. Scott, Springer Verlag, New York, p 1-62, 1975.
17. Nuttli, O. W. The Mississippi Valley Earthquakes of 1811 and 1812: Intensities, Ground Motion and Magnitudes. Seismological Society of America Bulletin, 63, p 227-248, 1973.
18. Trifunac, M. D, and Brady, A. G. On the Correlation of Seismic Intensity Scales with Peaks of Recorded Strong Ground Motion. Seismological Society of America Bulletin, 65, p 139-163, 1975.
19. Murphy, J. R., and O'Brien, L. J. The Correlation of Peak Ground Acceleration Amplitude with Seismic Intensity and Other Physical Parameters. Seismological Society of America Bulletin, 67, p 877-917, 1977.

TABLE 1

ROSSI-FOREL SCALE OF EARTHQUAKE INTENSITIES (ADAPTED) (4)

- I. HARDLY PERCEPTIBLE SHOCK: Felt only by an experienced observer under favorable conditions.
- II. EXTREMELY FEEBLE SHOCK: Felt by small number of persons at rest.
- III. VERY FEEBLE SHOCK: Felt by several persons at rest. Duration and direction may be perceptible. Sometimes dizziness and nausea are experienced.
- IV. FEEBLE SHOCK: Felt generally indoors, outdoors by a few. Hanging objects swing slightly. Cracking of frames of houses.
- V. SHOCK OF MODERATE INTENSITY: Felt generally by everyone. Hanging objects swing freely. Overturn of tall vases and unstable objects. Light sleepers awaken.
- VI. FAIRLY STRONG SHOCK: General awakening of those asleep. Some frightened persons leave their houses. Stopping of pendulum clocks. Oscillation of hanging lamps. Slight damage in very old or poorly built structures, old walls, etc. Some landslides from hills and steep banks. Cracks in road surfaces.
- VII. STRONG SHOCK: Overturn of movable objects. General alarm, all run outdoors. Damage slight in well-built houses, considerable in old or poorly built structures, old walls, etc. Some landslides from hills and steep banks. Cracks in road surfaces.
- VIII. VERY STRONG SHOCK: People panicky. Trees shaken strongly. Changes in flow of spring and wells. Sand and mud ejected from fissures in soft ground. Small landslides. Slides in river banks.
- IX. EXTREMELY STRONG SHOCK: Panic general. Partial or total destruction of some buildings. Fissures in ground. Landslides and rock falls.

TABLE 2

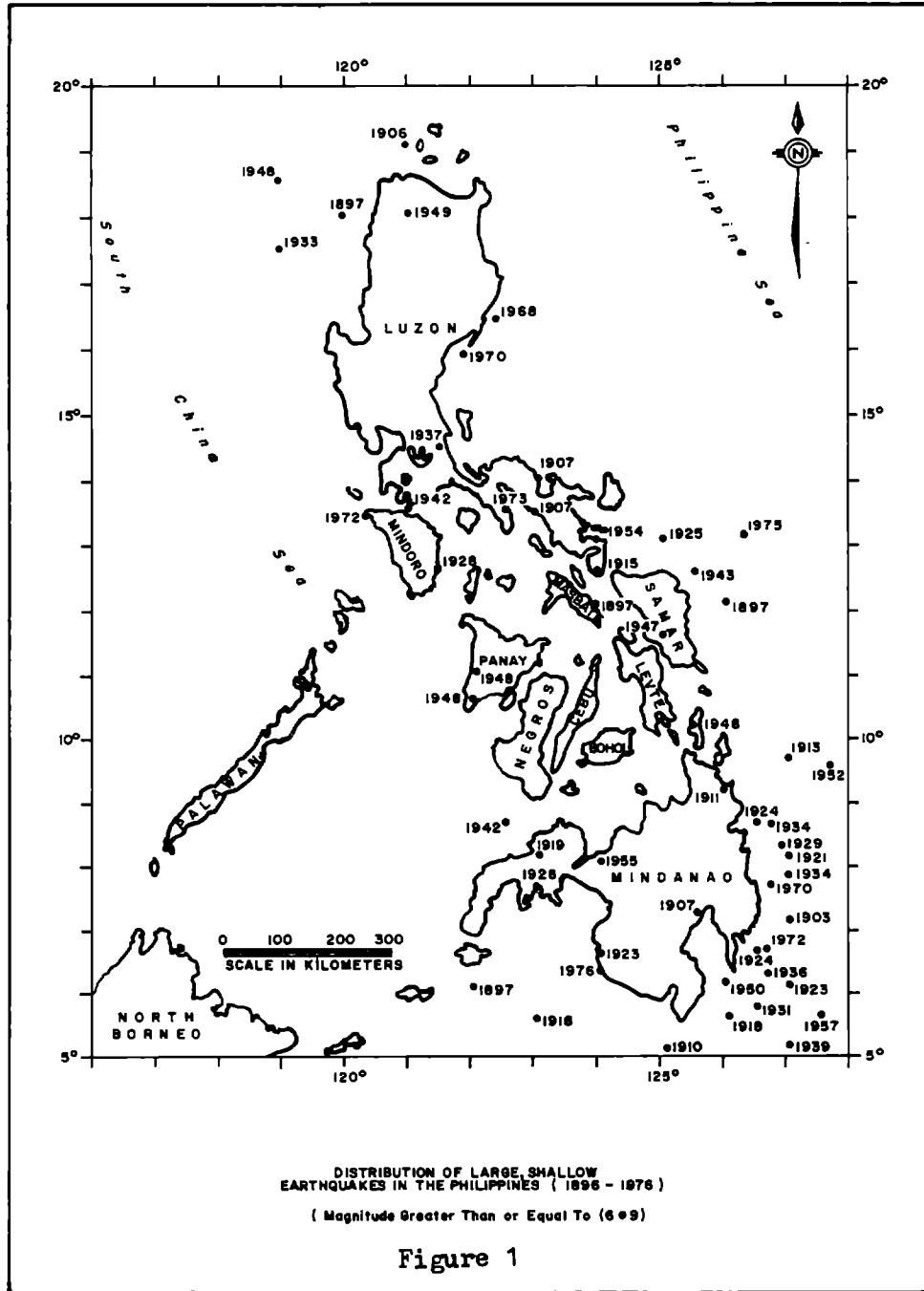
List of earthquakes for which isoseismal contours were examined. Coordinates of epicenters from NOAA and USGS listings.

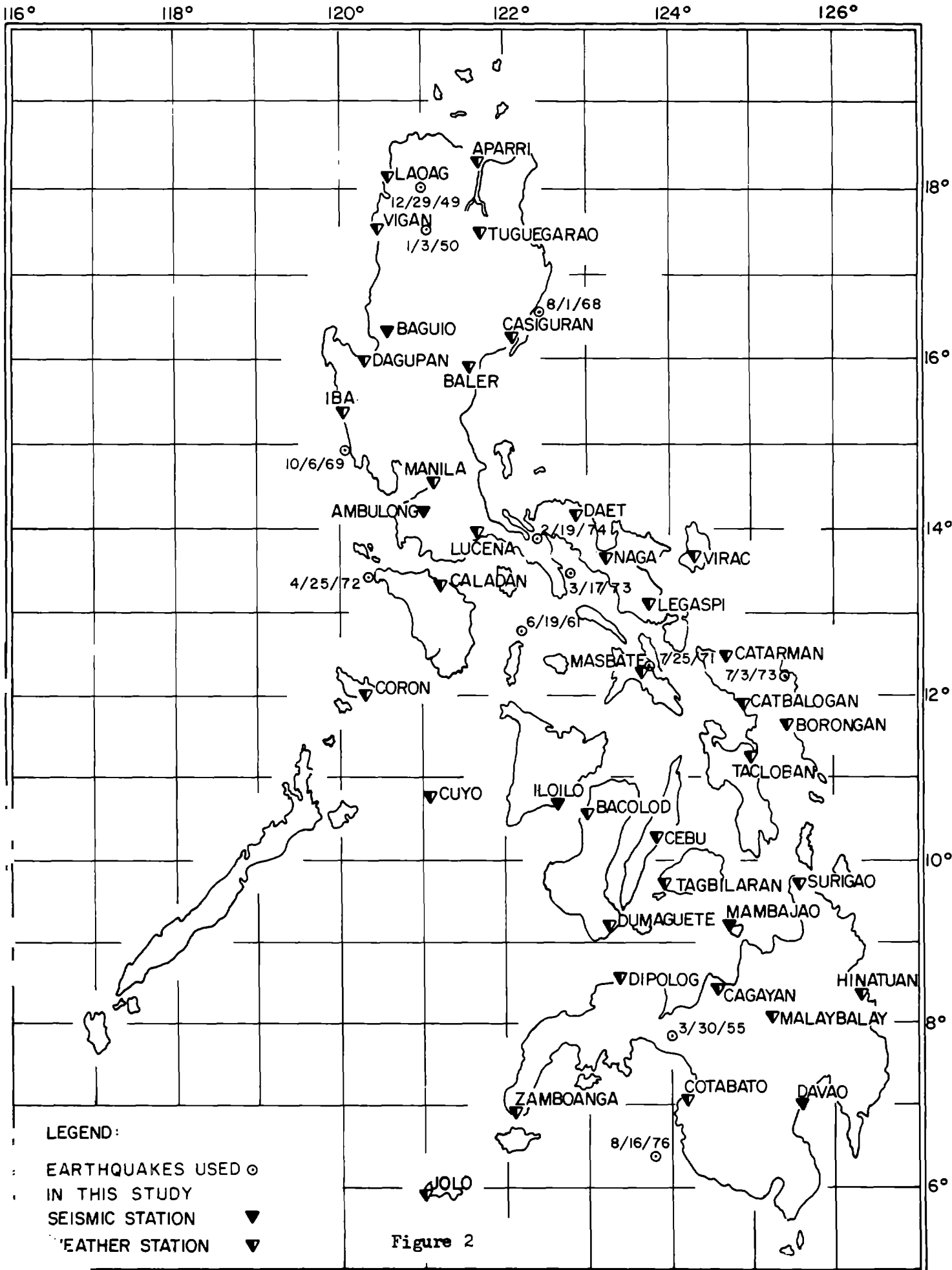
<u>Location</u>	<u>Date</u>	<u>Magnitude</u>	<u>Max. Intensity (P.R.F.)</u>	<u>Latitude (Deg)</u>	<u>Longitude (Deg)</u>	<u>Depth (Km)</u>
1. Isabella	12/29/49	7.4	8	18.0	121.0	
2. Tuguegarao	1/3/50	6.5	6	17.6	121.0	
3. Lanao	3/30/55	6.5	8	7.9	124.0	64
4. Romblon	6/19/61	5.8	6	12.7	122.1	48
5. Casiguran	8/1/68	7.3	8	16.522	122.2	37
6. Zambales	10/6/69	5.6	6	14.968	120.064	59
7. Masbate	7/25/71	5.6	5	12.363	123.685	33
8. Mindoro	4/25/72	7.3	6	13.37	120.309	50
9. Ragay Gulf	3/17/73	7.0	8	13.4	122.8	25
10. Samar	7/3/73	6.3	5	12.271	125.433	44
11. Calauag	2/19/74	7.4	8	13.9	122.1	17
12. Mindanao	8/16/76	8.0	7	6.261	124.032	25

TABLE 3

A comparison of distance normal to the fault up to which different intensities were felt for the three earthquakes.

<u>MM Int.</u>	<u>1906 San Francisco (Km)</u>	<u>1811-1812 New Madrid (Km)</u>	<u>1976 Mindanao (Km)</u>
IX	11	92	
VIII	21	185	
VII	38	400	90
VI	70	675	220
V	191	830	313
IV	284	985	470





LEGEND:

- EARTHQUAKES USED \odot
- IN THIS STUDY
- SEISMIC STATION \blacktriangledown
- WEATHER STATION \blacktriangledown

Figure 2

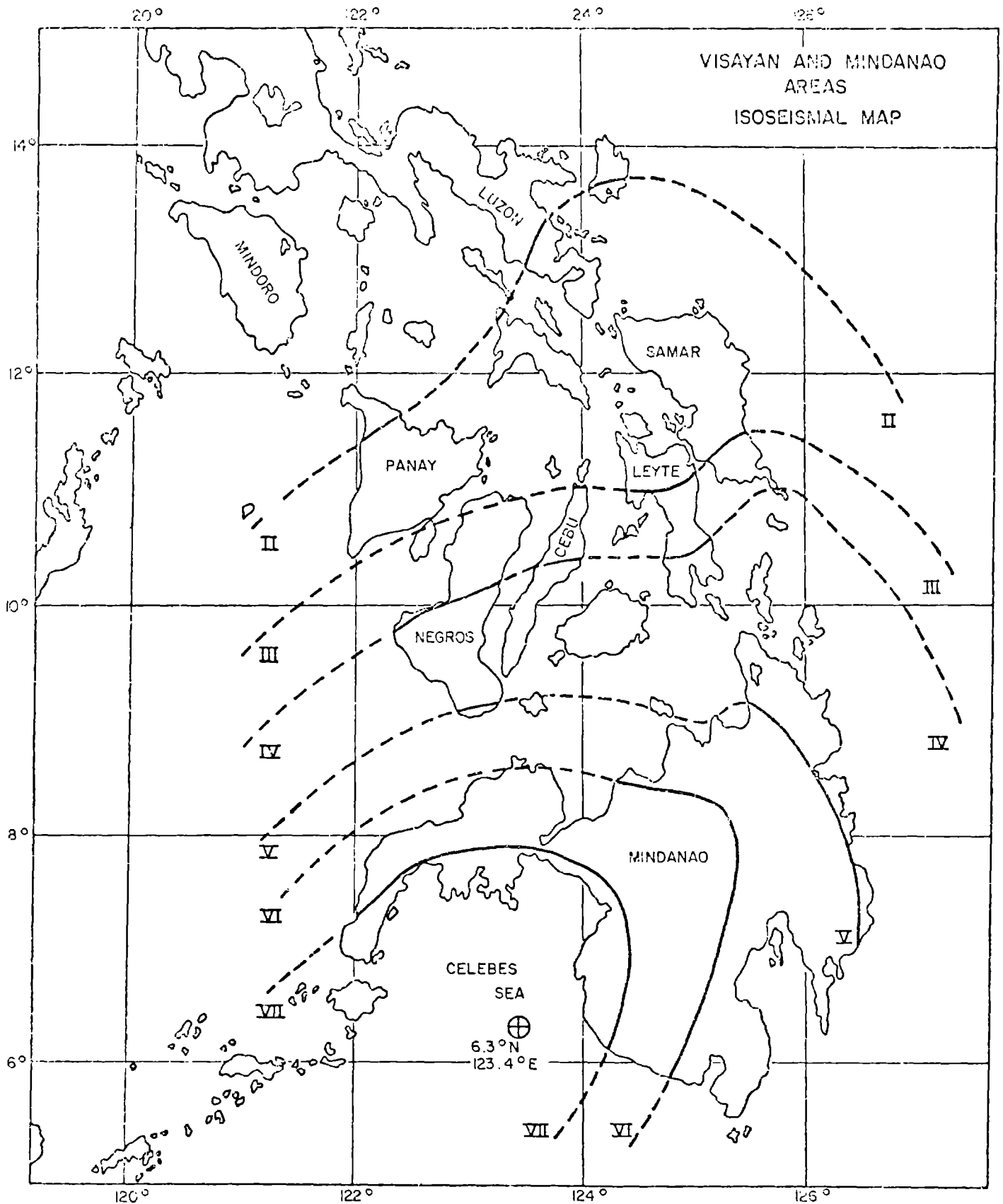


Figure 3 - Isoseismal Map for the August 16, 1976 Mindanao Earthquake. Prepared by PAGASA (1976)

A QUANTITATIVE SEISMOTECTONIC STUDY
OF THE IRANIAN PLATEAU

by

K. Moazami-Goudarzi^I, and H. Parhikhteh^{II}

ABSTRACT

The Iranian Plateau has been divided into 35 different quadrangles. Three normalized seismic activity coefficients, the A-value, the B-value and the ratio A/B have been computed twice for each quadrangle first by using the seismological data for the period 1900 to 1975 and second for the period 1965 to 1975.

It was found that the A-values were somehow in the same order of magnitude from Bam to Dezful regions, following the Zagros ranges, as well as from Shahpour to Eshghabad, along the Alborz ranges. But the frequency of occurrence of the $M \geq 7$ earthquakes was higher in the former ranges while in the latter one the most dangerous earthquakes of the plateau are more likely.

The A/B values were found to be the most significant factor for the earthquake engineering purposes due to its precise physical meaning. The seismotectonic aspects of the plateau have been discussed with respect to the quantitative values.

INTRODUCTION

In his book on seismology, K. Moazami-Goudarzi(1) divided Iran into 35 different quadrangles each covering 2 degrees of latitude and 2.5 to 3.5 degrees of longitude. This division was done in respect of the 1/250,000 map available for the Iranian plateau and of course had no relation with the seismotectonical aspects of the plateau.

The purpose of this paper is to ascribe some quantitative values of seismicity to each quadrangle and to see if by means of these values :

- 1) a quantitative factor could be given to each region to indicate its activity rate
- 2) it could be possible to compare quantitatively the activity of two different regions
- 3) different seismotectonical aspects of the plateau, could be demonstrated

I Associate Professor of Geophysics, Tehran University, Tehran, Iran

II Post graduate student of Physics, Tehran University; Tehran, Iran

4) different seismotectonical zones could be recognized.

METHOD

The earthquakes of each quadrangle were divided into 5 categories : $M \geq 7$, $M \geq 6$, $M \geq 5$, $M \geq 4$ and those without any given magnitude considered as $M \geq 3.5$.

The frequency distribution logarithm of the number of earthquakes versus magnitude for each region was studied by using the $\log N = A - BM$ formula. The value of A, B and A/B was found for each region, for two periods : 1900-1975 and 1965-1975. N in the above formula was considered as the number of earthquake occurrences per year and it was normalized to be for an area equal to the Shahpour region. The choice of the Shahpour region was of course arbitrary.

In table 1 we are giving the normalized values of A, B, and A/B for different regions in both periods.

It was found that the amount of data for the following regions were not sufficient to have a realistic result : these regions are Sarakhs, Torbatjam, Mandel, Zabol for both periods and Bakhardon, Zahedan, Boushehr, Oman Sea and Yazd for the second period only.

As it can be seen in table 1, some values for the same region vary from one period to another. It is rather hard to make a global decision and to prefer the results of one period to those of another. While the first set (1900-1975) has the advantages of covering a much longer period than the other, the second contains more accurate data especially for lower magnitudes. The reliability of each case should then be examined separately.

A-VALUE

The A-value could obviously be respected as the logarithm of the number per year of the shallow earthquakes ($\log N_0$) of positive magnitude. As it was pointed out by Housner (2), N_0 can indicate the "average seismicity" of a region. But this independently could not necessarily indicate the frequency of occurrence of the major earthquakes which is important for earthquake engineering. In other words, the A-value might be greater in one area and the frequency of occurrence of the major shocks higher in another area. Numerical examples could be found in the work of Parhikhteh (3). It seems to us that this characteristic of A-value, important for engineering seismology has not been well emphasized in the literature.

The normalized A-values for the period 1900 to 1975 and

TABLE 1

NAME OF REGIONS	Coordinates		1900 - 1975			1963 - 1975		
	N	E	A	B	A/B	A	B	A/B
SHAHPUR	38-40	42.5-46	2.1	0.55	3.3	2.5	0.60	4.2
TABRIZ	38-40	46 -49.5	2.1	0.55	3.8	3.3	0.80	4.1
CASPIAN SEA	38-40	49.5-56.5	1.3	0.50	2.6	2.8	0.80	3.5
BAKARDAN	38-40	56.5-60	1.6	0.50	3.2	-	-	-
ESHGH-ABAD	36-38	56.5-60	2.1	0.50	4.2	2.6	0.50	4.3
SHAHROUD	36-38	53 -56.5	2.9	0.67	4.3	2.8	0.56	5.0
RASET	36-38	49.5-53	2.1	0.52	4.0	2.6	0.59	4.1
ZANJAN	36-38	46 -49.5	1.0	0.38	2.6	1.8	0.43	4.2
MOUSEL	36-38	42.5-46	2.1	0.56	3.8	2.3	0.55	4.2
KARKOUK	34-36	42.5-46	1.3	0.41	3.2	2.1	0.53	4.0
HAMEDAN	34-36	46 -49.5	2.1	0.50	4.2	3.4	0.73	4.7
TEHRAN	34-36	49.5-53	2.0	0.50	4	3.6	0.88	4.1
SEM NAN	34-36	53 -56.5	1.3	0.40	3.3	1.3	0.36	3.6
TORBAT-HIDRIE	34-36	56.5-60	2.2	0.55	4	2.3	0.48	4.8
BIRJAND	32-34	56.5-60	1.7	0.48	3.5	2.1	0.44	4.8
ARDEKAN	32-34	53 -56.5	1.2	0.43	2.8	1.6	0.42	3.8
ESFAHAN	32-34	49.5-53	1.2	0.45	2.7	3.7	0.95	3.1
DEZFOUL	32-34	46 -49.5	2.8	0.65	4.3	2.7	0.50	5.4
AHV AZ	30-32	48 -51	2.6	0.60	4.3	2.7	0.47	5.7
ABADEH	30-32	51 -54	0.9	0.43	3.7	1.8	0.39	4.6
YAZD	30-32	54 -57	0.8	0.42	2.1	-	-	-
KERMAN	30-32	57 -60	0.8	0.32	2.5	1.2	0.34	3.5
ZAHEDAN	28-30	60 -63	0.6	0.37	1.6	-	-	-
BAM	28-30	57 -60	2.6	0.71	3.6	3.6	0.89	4.3
SAIED-ABAD	28-30	54 -57	2.0	0.47	4.2	2.4	0.51	4.7
SHIRAZ	28-30	51 -54	3.5	0.78	4.5	4.2	0.83	5.1
BOUSEHR	28-30	48 -51	2.2	0.64	3.4	-	-	-
PERSIAN-GULF	26-28	51 -54	1.3	0.34	3.8	1.9	0.39	4.9
MASGHAT & OMAN	26-28	54 -57	2.6	0.54	4.8	3.6	0.70	5.1
OMAN SEA	26-28	57 -60	1.6	0.46	3.5	1.4	0.36	3.9
SARAVAN	26-28	60 -62.5	1.0	0.35	2.9	1.4	0.35	4.0

1965 to 1975 are plotted in figure 1 and 2 respectively. The quadrangles are divided into 4 categories according to the rate of these values. For several regions two results are quite similar. The A-values have the same order of magnitude from Bam to Dezful, along the Zagros ranges, as well as from Shahpour to Esghabad, following the Alborz ranges. But the frequency of the occurrence of the earthquakes of positive magnitude is higher in the former ranges than along the latter one. Meanwhile, as it was pointed out before, this does not necessarily mean that the major shocks are more frequent in the south of Iran. For example during the period 1900 to 1975, 10 earthquakes of $M \geq 7$ have occurred in the Northern part of Iran, ($40 N \geq 9 \gg 36 N$) while during the same period in the Southern part of Iran ($30 N \geq 9 \gg 26 N$) only one earthquake of $M \geq 7$ occurred and even in a vast area limited by $34 N \geq 9 \gg 26 N$, this number rises only to 4. Altogether, against 12 earthquakes of $M \geq 7$ in the Alborz range, during this century, we observe 8 earthquakes of the same order in the rest of the plateau (including the Zagros ranges). For the earthquakes of $M \geq 6$, the situation is reversed and the frequency of the occurrence of these earthquakes are higher in the South. Comparing figure 1 to figure 2 it could be noted that (see also table 1) the normalized A-values are higher in the second period. For example the A-value of the Tehran quadrangle for the first period is 2.0 against 3.6 for the second period. It might be interesting to note that the same quadrangle has experienced 4 earthquakes of magnitude equal or greater than 6 during the first period against no earthquake of $M \geq 6$ during the second period. Generally speaking the average A-value of the plateau for the first period is 1.87 against 2.51 for the second period. This might arise from the definition of the A-value which, as we mentioned before, is influenced by the number of the earthquakes of low magnitude. In fact our knowledge about the frequency of low magnitude earthquakes occurred since 1965 has improved, as the numbers of the seismological stations have increased during this year from 2 to 6.

B-VALUES

If N_0 is the number per year of the shallow earthquakes of positive magnitude ($M \geq 0$), then we can write $\log N_0 = A$ and $B = \frac{1}{M} \log \frac{N_0}{N}$. If M^* is defined in such a way that the number per year of the earthquakes of $M \geq M^*$ is $N^* = \frac{1}{10} N_0$, then we get a simple definition of $b = \frac{1}{B}$ value, that is $b = M^*$. The b-value now can have a simple physical meaning; the b-value of a region is the minimum magnitude of the earthquake which is 10 times less frequent than the $M \geq 0$ events of that region. As far as the Iranian plateau is concerned this value varies from 1.2 to 3. These magnitudes seem to be too low to be interesting for earthquake engineering.

Furthermore the B-value, under the influence of the A-value, is not independently capable to give a precise quantitative

feature of the seismicity of the region and could be used to compare the seismicity of two different regions only if the A-values of those regions are nearly the same. It is true that the B-value does not depend on the period and the area of observation (see for example Kaila et al.⁽⁴⁾), but this does not necessarily mean that it could characterize the seismic activity of a region when the comparison of the seismicity of different regions, with different A-values, are concerned. This is exactly the case of Iran, where the different regions South of Zagros have A-values which are higher than those of the Alborz ranges. In fact the average of the A-values for Tabriz, Eshghabad, Shahroud, Rasht, Zangan, Tehran and Semnan situated along the Alborz ranges, is 1.9 while along Zagros ranges for Mousel, Hamedan, Dezful, Ahvaz, Bam, Said-abad and Shiraz it is 2.5.

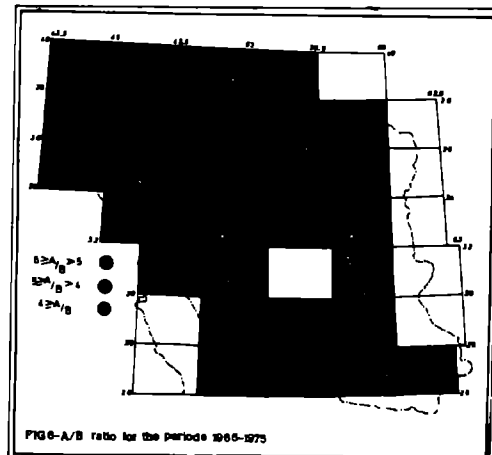
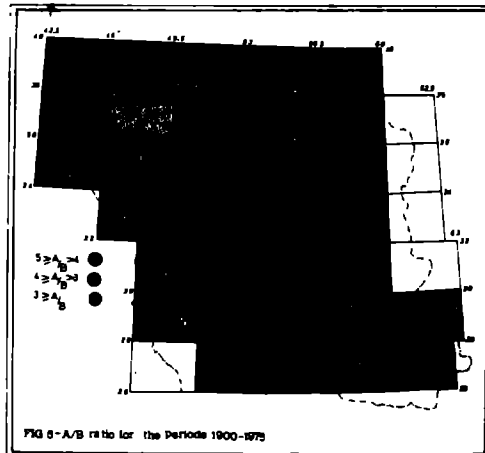
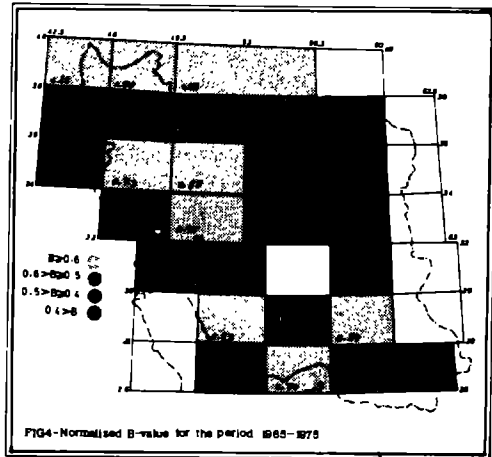
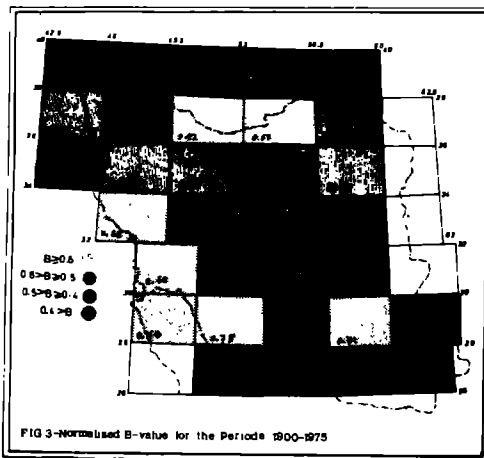
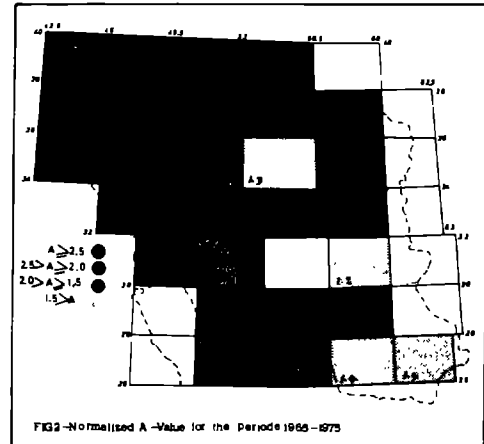
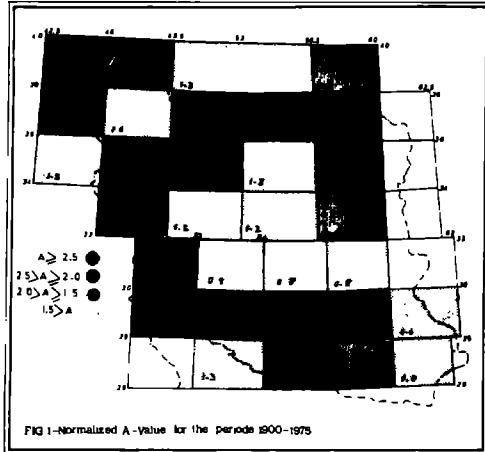
Figures 3 and 4 show the rate of B-values in Iran for the period 1900 to 1975 and 1965 to 1975 respectively. These values vary from 0.4 to 0.6, and as it could be expected, the B-value for the two different periods, and for the same quadrangle, are nearly the same and the 2 figures are much more comparable than the figures 1 and 2 were.

A/B VALUE

The ratio of A/B is obviously the minimum magnitude of the earthquake which occurs one single time per year in the region. For example, as the figure 5 indicates all over the Zagros and Alborz ranges, one could expect every year one earthquake of magnitude 4 to 4.8. This could be an important factor to compare the seismicity of two different regions and in our opinion the value of A/B is much more significative than the A or B values independently. If we divide the A/B values into 4 different ranges that is to say $\frac{A}{B} \geq 5$, $5 > \frac{A}{B} \geq 4$, $4 > \frac{A}{B} \geq 3$ and $\frac{A}{B} < 3$, then according to figure 5, 3 different zones could be distinguished in the Iranian plateau.

The most dangerous zone ($\frac{A}{B} \geq 4$) includes Zagros and Alborz ranges, the least dangerous zone is situated in the central Iran and Lut Blocks.

In figure 6, one may note that in the Zagros range and in the Shahroud region the value of A/B is even more than 5. But we believe that for the important earthquakes, the figure 5 which covers a much longer period is more relevant than the data of figure 6. This might simply indicate that during the period 1965-1975 the above regions have experienced more important earthquakes than the other high active area.



RETURN PERIOD

The A/B values, as we know, give the minimum earthquake magnitude of a given region for a return period of one year. This is not an adequate period for engineering problems. According to the age of a structure a return period of 10, 20 or 50 years might be required. If the adequate return period is τ then we can write: $M_{\tau} = \frac{A + \log \tau}{B}$ (I). In this equation M_{τ} is the minimum magnitude of the most important event which could be expected to occur only once during the period τ . For example for a return period of let us say ten years, M_{10} , for the Tehran quadrangle situated in the Alborz range is 6.1 and for the Shiraz quadrangle situated in the Zagros ranges it is 5.8. Reversally from this equation the return period τ of the most dangerous earthquake expected in the area could be estimated. The choice of this magnitude might be related to the maximum strength of the crustal rocks in a given region or any other physical or engineering argument. For example the return period of a magnitude, let's say, equal or greater than 7 for the two above mentioned quadrangles, according to the results of table 1 are about 30 and 90 years respectively.

It should be noted that for each region there is a magnitude beyond which the dependence of $\log N$ to the M is not linear and consequently the equation (I) does no more stand. This magnitude should be identified whenever the equation (I) is used.

CONCLUSION

Starting from the 1/250,000 geographical map of Iran, this quantitative study has traced the most important seismotectonical regions of the plateau and showed that A/B or $(A + \log \tau)/B$ ratio could be used to compare the seismotectonical activity of two different areas. When sufficient geological and tectonical data are not available the comparison of these values could be used to recognize whether any homogeneous and well bounded seismotectonical region exists. When the different seismotectonical regions are recognized, then the above quantitative values could be computed for each region in order to compare the rate of their activity quantitatively. As far as this study is concerned, three distinct zones of activity have been recognized in the Iranian plateau: the Zagros ranges with frequent earthquakes, the Alborz ranges, where the frequency of smaller events is lower than in the Zagros but where the most dangerous earthquakes of the plateau are more likely, and finally the Central Iran and the Lut Blocks where the minimum rate of the activity of the plateau has been observed.

BIBLIOGRAPHY

- (1) Moazami-Goudarzi, K., (1972), Seismology Pub. n° 1. Ministry of Sciences and Higher Education of Iran
- (2) Housner, G.W., (1970), Design Spectrum, Earthquake Engineering, Prentice Hall Inc. Englewood cliffs, N.J. (USA)
- (3) Parhikhteh, H., (1977), Study of A and B values in Iran M. Sc. Thesis, Tehran University
- (4) Kaila, K.L., et al., (1974), Seismotectonic maps of Southwest Asia region comprising Eastern Turkey, Caucasus, Persian plateau, Afghanistan and Hindukush. B.S.S.A. Vol. 64 n° 3, PP. 657-669.

THE VRANCEA EARTHQUAKE OF MARCH 4, 1977
AND THE SEISMIC MICROZONATION OF BUCHAREST

by N. Mândrescu^I

ABSTRACT

The 7.2 magnitude earthquake that occurred in the Vrancea region on March 4, 1977 was extremely damaging throughout the country and particularly in Bucharest, Craiova, Zimnicea, Vălenii de Munte, Ploiești and Cîmpina.

In Bucharest, the greatest damages occurred in the center of the city, where 32 older buildings of 8-12 storeys collapsed and many other buildings were seriously damaged. Many small dwellings and nearly all modern apartment buildings were not at all damaged.

In order to estimate the intensity of the seismic shock in Bucharest, some thousand masonry, reinforced concrete frames and large panel buildings, distributed on the whole town area, were examined. For this aim it was taken into account soil and subsoil characteristics, type of structure, height, age and state of the buildings a.s.o. Territorial repartition of damages for each class of buildings are plotted on the maps and have been used for new seismic microzonation map of Bucharest. The map has been compared with the similar map elaborated after November 10, 1940 earthquake and with the microzonation map performed in 1973 according to Medvedev method. It was pointed out a relationship between the spectral composition of the Vrancea intermediate earthquake of March 4, 1977 and selective damaging of the tall buildings in the Bucharest area.

INTRODUCTION

The Vrancea earthquake of March 4, 1977, ($M = 7.2$) caused great damages in Bucharest. During the seismic motion 32 apartment buildings of 8 to 12 storeys collapsed and around 150 buildings of over 4 storeys suffered severe damages; many of these buildings were subsequently demolished. The earthquake killed 1391 people and injured 7576.

Right after the earthquake investigations were started on the premises to appraise the distribution of the seismic intensity on the city area. As already known, one of the usual ways of appraising seismic intensity, when direct recording instruments are missing, is to appreciate the buildings behavior during the earthquake. However, an appreciation of the seismic intensity founded on the analysis of the suffered damage is particularly difficult as it depends not only on the amount of energy that reaches the investigated buildings but also on the state and character of the ground on which the structure stands

I Senior Geologist, Central Institute of Physics,
Centre for Earth Physics and Seismology, Bucharest, Romania.

and on the design, materials, workmanship and so forth, of the structure and its interaction with the ground. In spite of these drawbacks numerous attempts have been made to appraise in this way seismic intensity (10, 14, 17, 20, 22, 24, 31, 35).

The present paper gives the first results of a complex study regarding the seismic conditions of Bucharest city and of the neighbouring zones.

SEISMIC HISTORY OF THE VRANCEA REGION

The Romanian territory is affected by two kinds of earthquakes: subcrustal intermediate earthquakes and other earthquakes scattered in several fault zones all over the country (8, 30, 34). The intermediate earthquakes of Vrancea, limited to a very restricted area (2000-9000 sq. km.) at the Carpathian curvature, determines the seismicity of an area exceeding one third of the Romanian territory.

Among the particularly violent former earthquakes we have to mention those of 1471, 1620, 1738, 1802, 1829 and 1838 (36). These earthquakes have caused great damage in Bucharest and destroyed many dwellings and historical monuments.

The earthquake of November 10, 1940 (M=7.4), greatly damaged many towns in Romania. Panciu was almost totally destroyed and Focșani, Bîrlad, Galați, Rîmnicu Sărat, Ploiești and Cîmpina, were heavily damaged. Very many buildings were severely damaged in Bucharest (3) and the new 13-storey reinforced-concrete Carlton Hotel, sited in the central area of the city collapsed.

The earthquake of 1977 struck Bucharest very severely (2, 6). The earthquake parameters, provided by CSEM, Strasbourg are : 45.8° N - 26.78° E at a depth of 93 kilometres. The seismic motion was recorded in Bucharest at a focal distance of 185 kilometres, by a SMAC-B strong-motion accelerograph set up in the basement of the Building Research Institute, sited in the north-eastern part of the city (Fig. 1b). The peak acceleration values obtained on the NS, EW directions and vertically are 0.20g, 0.16g and 0.10g respectively. The duration of the strong shaking ($a \approx 0.05g$) was of 14.7 sec. The motion was recorded by a Wilmot seismoscope also set up in the Building Research Institute. This record shows (2) a double amplitude of 41 mm, which is consistent with the 44 mm amplitude response of the SMAC record at $T=0.75$ sec. and 10 p.c. damping.

GEOLOGICAL AND SOIL CHARACTERISTICS IN THE BUCHAREST AREA

Bucharest is sited in the central part of the Walachian platform (a great structural unit of the Romanian territory), at a distance of around 160 kilometres from the epicentral region of Vrancea (Fig. 1a).

The town relief is generally plane with a light bent towards the south-east. The rivers Dîmbovița and Colentina divide the town into a series of morfologic units: the plains

of Bucharest, Pipera-Pantelimon and Cotroceni-Văcărești and the meadows of the Dâmbovița and Colentina rivers (Fig.1b).

The geological formation and structural particularities of the Walachian (Moesian) platform are dealt with at large in various studies (12,13,27,29); we shall further attempt to present the geological conditions of the Bucharest zone.

1.Stratigraphy

The Walachian platform has a basement with two structural stages, a lower one with chloritic and sericitic schists of Precambrian age and an upper one made up of old Paleozoic folded marine formations going back to Middle Carboniferous age. The sedimentary cover of the Walachian platform is relatively thick (exceeding 6000 meters). The Mesozoic cover including also the Upper Permian, is almost continuous up to the Neogene; however, the Eocene, Oligocene and Lower Miocene deposits are lacking. The sedimentary deposits are made of argillites, conglomerates, graywacke, clay slates, limestone and dolomites.

The unconsolidated Quaternary deposits are greatly developed in the Bucharest zone (Fig.1c). The following lithological succession was established for the Middle and Upper Quaternary deposits through geologic drillings: sands and gravels; clayey marls and sands; fine sands and sandstone insertions; gravels and sands with lenticular clay intercalation sandy-clayey dusts (loesslike deposits) and sandy clays with lenticular silt intercalation (alluvial deposits from the meadows of the Dâmbovița and Colentina rivers).

2.Structure

The Walachian platform, consolidated during the last stages of the Baikalian orogenesis, beginning with the Paleozoic behaved as an unstable platform, sensitive to the orogenic movements of the neighbouring geosinclinal zones. These movements caused the formation of a system of longitudinal faults whose reactivity at various periods of time is reflected in the disorders of the sedimentary cover. The extension of the fractures, generally oriented east-west, gets considerably reduced in the upper stratigraphic layers and thus at the level of the Meotian we find only a major tectonic accident, the Tîrgu Fierbinți-Urziceni fault (sited some 40 kilometres north of Bucharest). In the Pliocene and in the Quaternary the region was continuously affected by negative movements on the vertical, this fact being emphasized by the continuous sedimentation of these deposits.

3.Soil characteristics

The foundation soil of Bucharest is formed by fluvial-lacustrine, loesslike and alluvial deposits. The fluvial-

lacustrine deposits are formed by fragments of quartz, mica-schists, gneiss and sandstone. The loesslike deposits, extending on over 10 p.c. of the city area, are formed by 13 p.c. sand, 47 p.c. dust and 40 p.c. clay. Greatest thickness of these deposits (10-16 meters) is to be found in the Cotroceni-Văcărești and the Pipera-Pantelimon plains and thinnest cover (3-5 meters) in the Bucharest plain. The alluvial deposits, encountered particularly on the meadow of the Dîmbovița river, show a high granulometric variety ranging from clay, silty clay of high plasticity to sandy dusts. The geotechnical conditions and the physico-mechanical features of the foundation soil are well known, due to the many geotechnical drillings performed on the city area (19,23,34).

4. Hydrogeology

According to the morphologic unit taken into consideration the hydrostatic level ranges from 0 to 5 meters (in the Dîmbovița and Colentina river meadows), to between 5 and 10 meters in the Bucharest plain and to over 10 meters in the Pipera-Pantelimon and Cotroceni-Văcărești plains.

EARTHQUAKE EFFECTS IN BUCHAREST

A well known fact is that earthquake cause direct damage to the buildings by the vibrations they transmit on the foundation and indirect damage as a result of the ground deformation under their action; sometimes the permanent deformation of the soil may debase the building even more severely than the seismic shock itself (4,5,17,18,20).

No permanent deformation that would have jeopardized the buildings during the March 4, 1977 earthquake, occurred in Bucharest. The settlements, pointed out in some zones, did not exceed 1.5-2.0 centimetres, while liquefaction of some sandy deposits in the Dîmbovița meadow occurred only in zones devoid of buildings. It may be considered that the Bucharest foundation soil behaved well during the earthquake (25,26).

1. Method of building behavior evaluation

The attempt to rate the distribution of the seismic intensity on the city area is based on a comparative study of how the buildings behaved during the earthquake, while bearing in mind their damage degree correlated to the seismic intensity according to the MSK scale. To this purpose 2429 buildings, belonging to the widest spread types of buildings in Bucharest were examined. These buildings were grouped in the following classes:

- A. Masonry buildings;
- B. Reinforced concrete frame structures;
- C. Large-panel precast concrete structures & cast-in-place reinforced concrete shear wall structures.

The first two classes were divided into two sub-classes, according to age: old and new buildings, built before and after 1940, respectively.

Evaluations were made in 106 spots, distributed on nearly all the city area (Fig. 1b). In each spot were examined around 20-25 buildings in succession, without preliminary selection. In most of these spots items, belonging to at least two of the three classes taken into focus, could be investigated.

The buildings response to the seismic shock was noted (33) with marks from 0 (zero) to 5 (five). Based on these marks mean values of damage degree were calculated for the buildings of the same class and so were mean values of damage degree considering all examined buildings in the respective spot.

2. Field observation and results

A. Masonry buildings. In this class were examined 1293 buildings. Highest damage was suffered by the old 3 to 5 story buildings; many of these collapsed during the earthquake while others, greatly damaged, were subsequently demolished. In contrast, the low and old 1 and 2 story buildings behaved well.

B. Reinforced concrete frame structures. A number of 739 high, 4 to 12 story buildings, were investigated. The buildings in this class suffered severe damage. Thirty-two of these buildings collapsed during the earthquake and over 150, 6 to 9 story buildings were considerably damaged; many of these were subsequently demolished. Most of the collapsed or severely damaged apartment buildings of this class were situated in the city central zone.

C. Large-panel precast concrete structures & cast-in-place reinforced concrete shear wall structures. A number of 397 buildings sited mainly in the new city districts was examined. These buildings behaved generally very well during the earthquake

The territorial distribution of the damage degree for the first two classes of buildings is given in figure 2.

The correlation between the damages degree and building height is given in figure 4; it emphasizes the reduced damage degree increase in the C class buildings, as compared to that in class A and B. This is due to the great difference between the fundamental period of class C buildings which, based on experimental investigations (9), ranged from $0.3N$ to $0.5N$ (N being the number of stories), and fundamental periods for soil deposits in Bucharest (7).

In order to transform damage degree into seismic intensity the transforming coefficients suggested by Shebalin (33) were adopted, however with certain changes. Considering all the examined buildings of each class, the following values were obtained: 7.5 degrees for A and C class buildings and 8 degrees for B class buildings. The apparently reduced 7.5 degrees value is justified by the very good behaviour of the 1 and 2 story brick buildings as well as of the large-panel precast concrete structures & cast-in-place reinforced concrete shear wall structures.

In figure 5 are delimited the areas of seismic intensity of the Bucharest territory. In the central zone of the city a

restricted area may be observed in which seismic intensity has a value exceeding 8 degrees (8^+), surrounded by seismic zones of 8, 7.5 and 7 degrees, respectively. Considering this map (Fig.5) the question arises: does this map show the real distribution of the earthquake energy in the city area?

COMMENTS AND CONCLUSIONS

Before attempting to formulate an answer about above mentioned question, we shall give some complementary data.

Based on the estimation of the November 10, 1940 earthquake effect a map was elaborated (31) with the distribution of the damages in the Bucharest area (Fig.6). Although the seismic microzones were not delimited, the author emphasizes the good behavior of the buildings in the central part of the city area (the area delimited in the figure by the dash line).

During the March 4, 1977 earthquake, 8 buildings of 6 to 9 stories collapsed and a lot of 3 to 5 story brick buildings suffered severe damage; part of these buildings were subsequently demolished. Those familiar with the local soil conditions can difficultly admit that the foundation soil has to such an extent changed its features in the period between the two earthquakes.

As already known, most of the buildings that collapsed had been built before 1940, without earthquake design provisions; these buildings had suffered greater and smaller damages during the November 10, 1940 earthquake and during the second world war. Moreover, some of the buildings had been submitted to important structural alterations, dictated by successive changes in their vocation, while the initial design was ignored.

As may be noted, there is a pronounced disagreement between the seismic microzonation map (Fig.7) elaborated in 1973 according to the Medvedev method (21) and the distribution of damages caused by the March 4, 1977 earthquake. Although quality and state of the existing buildings were obviously not taken into account, a fact that could to a certain extent explain the mentioned disagreement, the criterium resorted to of seismic rigidity of the foundation soil (first 10-15 m. of ground surface) did not prove satisfactory with respect to the city of Bucharest.

It is obvious that for the microzonation of cities situated at relatively great distances from the epicenter of a large earthquake the response of much thicker deposits than those used in the Medvedev method should be considered. In the case of Bucharest, the seismic motion involved very thick deposits, probably the whole unconsolidated Quaternary deposits, consist of gravel and sand, alternating with clays and clayey marls. The attempt to estimate the predominant ground period by making use of the known relations (15, 16, 28), led to values ranging from 0.9 to 1.6 sec., in satisfactory agreement with the peak values of the acceleration response spectrum (Fig.3).

The concentric distribution of the damages, usual in great cities struck by strong earthquake, obviously follows the city areal evolution (Fig.8). The old, central zone, involved at different stages in urbanization processes, was submitted to a great construction boom at the beginning of the century, particularly in the period between the two world wars, when the town population nearly trebled.

The following conclusions may be drawn from this study:

1. According to MSK scale, earthquake intensity reached its highest value of 8 degrees on the Bucharest territory.

2. The foundation soil behaved well during the earthquake; no permanent deformations, with damaging effect on the buildings occurred.

3. The high, elastic buildings were affected to a greater extent; this was due to the closeness of the values of their fundamental periods to the values of the underlying soil deposit ;

4. The large-panel precast concrete structures & cast-in-place reinforced concrete shear wall structures behaved very well.

5. Although the damages were very high in Bucharest, no fires were registered and economic activity was resumed shortly after the earthquake.

6. Although seismic intensity could be appreciated by help of the performed analysis, we consider that the elaborated map shows rather the distribution of the damages than the earthquake energy on the city territory.

ACKNOWLEDGEMENTS

In the activity developed to investigate the effects of the March 4, 1977 earthquake, considerable help was provided by the Soviet research team led by late Prof. S.V. Medvedev. We herewith thank Dr. Shebalin and Dr. V. Shtejnberg for their help and for the particularly precious advice they gave us.

BIBLIOGRAPHY

1. Ambraseys W.W., " An Engineering Seismology Study of the Skopje Earthquake of 26 July, 1963", Report of the UNESCO Technical Assistance Mission, 1964, pp. 66-85.
2. Ambraseys W.W., " Long-period Effects in the Romanian Earthquake of March 1977", Nature, Vol. 268, July, 1977, pp. 324-325
3. Beleş A.A., " Cutremurul și construcțiile", Bul. Soc. Tehnice din România, Anul LV, N^o 10, 1941.
4. Berg Glen V., " Response of Buildings in Anchorage ", The Great Alaska Earthquake of 1964, Engineering, National Academy of Sciences, Washington D.C., 1973, pp. 242-282.
5. Berg Glen V., Husid R., "Structural Behavior in the 1970 Peru Earthquake", Fifth World Conference on Earthquake-Engineering, Rome, 1975.
6. Bolt Bruce A., " The Romanian Earthquake of March 4, 1977 " (Preliminary Notes), March 24, 1977
7. Carydis P., Private communication, August, 1977.
8. Constantinescu L., Cornea I., Lăzărescu V., " Seismotectonic Map of Romania", Proceedings of the Seminar on the Seismotectonic Map of the Balkan Region, Dubrovnik, 1973.
9. Diaconu D., Manolovici M., Mihai C., Iticovici M., Vasilescu D., " Seismic Response of a Great Panel Structure with ten Stories ", Fifth World Conference on Earthquake Engineering, Rome, 1975.
10. Espinosa A.F., and S.T. Algermissen " Soil Amplification Studies in Areas Damaged by the Caracas Earthquake of July 29, 1967", Proceedings of the International Conference on Microzonation for Safer Construction Research and Application Vol. 2, 1972, pp. 455-464.
11. Espinosa A.F., R. Husid, S.T. Algermissen and J De Las Casas, " The Lima Earthquake of October 3, 1974 : Intensity Distribution", Bull. Seism. Soc. Am. Vol. 67, N^o 5, 1977, pp. 1429-1439.
12. Grigoraș N., Pătruț I., Popescu M., " Contribuții la cunoașterea evoluției geologice a Platformei Moesice de pe teritoriul R.P.R. " Congr. V. Asoc. Geol. Carpato-Balcanică, București, 1963.
13. Herz N., H. Savu " Plate Tectonics History of Romania", Bull. Geol. Soc. Am. Vol. 85, 1974, pp. 1429-1440.
14. Husid R., A.F. Espinosa and J De Las Casas " The Lima Earthquake of October 3, 1974 : Damage Distribution", Bull. Seism. Soc. Am. Vol. 67., N^o 5, 1977, pp. 1441-1472.
15. Kanai K., T. Tanaka and S. Yoshizawa., "Comparative Studies of Earthquake Motions on the Ground and Underground"., (Multiple Reflection Problem), Bull. Earthq. Res. Inst., Vol. 37, 1959, pp. 53-87
16. Kanai K., "On the Spectrum of Strong Earthquake Motions", Bull. Earthq. Res. Inst., Vol. 40, 1960, pp. 71-90.
17. Kuroiwa J., E. Deza and H. Jaen., " Investigations on the Peruvian Earthquake of May 31, 1970", Fifth World Conference on Earthquake Engineering, Rome, 1975.
18. Lee K.L., Monge J., " Effect of Soil Conditions on Damage in the Peru Earthquake of October 17, 1966", Bull. Seism. Soc. Am. Vol. 58, N^o 3, 1968, pp. 937-962.
19. Liteanu E., " Geologia zonei orașului București", Studii Tehnico-Economice, Seria E, Hidrogeologia, N^o 1, 1951.

20. Lomnitz C., and Cabré Ramón S.J. "The Peru Earthquake of October 17, 1966", Bull. Seism. Soc. Am. Vol. 58, N^o 2, 1968.
21. Medvedev S.V., "Injenernaia seismologhia", Moskva, 1962.
22. Mândrescu N., "Microzonarea seismică a oraşului Bîrlad", Stud. Cerc. Geol. Geof. Geogr., Seria Geofizică, Vol. 4, N^o 1, 1966, pp. 237-244.
23. Mândrescu N., "Cercetări experimentale de microzonare seismică", Stud. Cerc. Geol. Geof. Geogr., Seria Geofizică Vol. 10, N^o 1, 1972, pp. 103-116.
24. Mândrescu N., "Microzonation of a Populated Area by Analysis of Seismic Damage and Instrumental Data", Rev. Roum. Géol. Géophys. et Géogr., Serie Géophysique, Vol. 17, N^o 1, 1973, pp. 93-102.
25. Mândrescu N., "Seismic Microzoning of Areas with Difficult Ground Conditions", Rev. Roum. Géol. Géophys. et Géogr., Serie Géophysique, Vol. 20, N^o 1, 1976, pp. 121-132.
26. Mândrescu N., "Behavior of Soils During the Vrancea Earthquake of March 4, 1977 (in press)
27. Mutihac V., L. Ionesi "Geologia României", Ed. Tehnică, Bucureşti, 1974.
28. Omote S., Komaki S., and Kobayashi N., "Earthquake Observations in Kawasaki and Turumi Areas and the Seismic Qualities of the Ground", Bull. Earthq. Res. Inst., Vol. XXXIV, 1956, pp. 358-360.
29. Paraschiv D., "Geologia zăcămintelor de hidrocarburi din România", Studii Tehnico-Economice, Seria A, Vol. 10, 1975.
30. Radu C., "Contribution à l'étude de la séismicité de la Roumanie et comparaison avec la séismicité du bassin Méditerranéen et en particulier avec la séismicité du Sud-Est de la France", Thèse Dr. Sci., Strasbourg (France), 1974.
31. Rădulescu Al. N., "Consideraţiuni geografice despre cutremurul din 10 XI 1940", C.R. Acad. Rom. Tom. V., N^o 3, 1941.
32. Seed H.B., Idriss I.M., Dezfulian H., "Relationships Between Soil Conditions and Building Damage in Caracas Earthquake of July 29, 1967", Report N^o 70-2, EERC.
33. Shebalin N., "Ob oţenke seismiceskoi intensivnosti", Seismiceskaia şkala i metodî izmerenia seismiceskoi intensivnosti, Nauka, 1975, pp. 87-109.
34. Şerbănescu Gh., Mândrescu N., Cornea I., "Report on Seismic Microzoning Investigations in Romania", Meeting of the Working Group on Microzoning, UNDP/UNESCO Project (Survey of Seismicity of the Balkan Region), Ankara, 1974.
35. Stojković M., and V. Mihailov "Some Results of the Investigations in the Seismic Microzoning of Banja Luka", Fifth World Conference on Earthquake Engineering, Rome, 1975.
36. Ştefănescu Gr., "Cutremurele de Pământ în România în timp de 1391 de ani, de la anul 455 pînă la 1874", Analele Academiei Române, Seria II, Tom. XXIV, 1901.

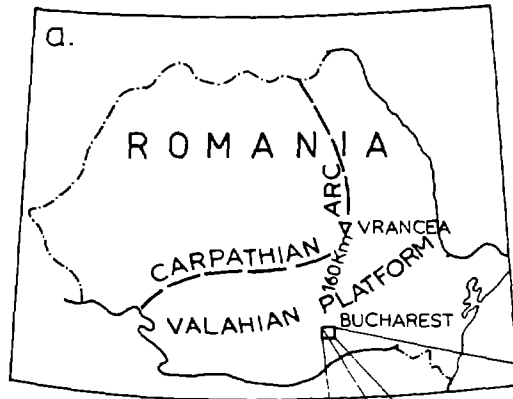
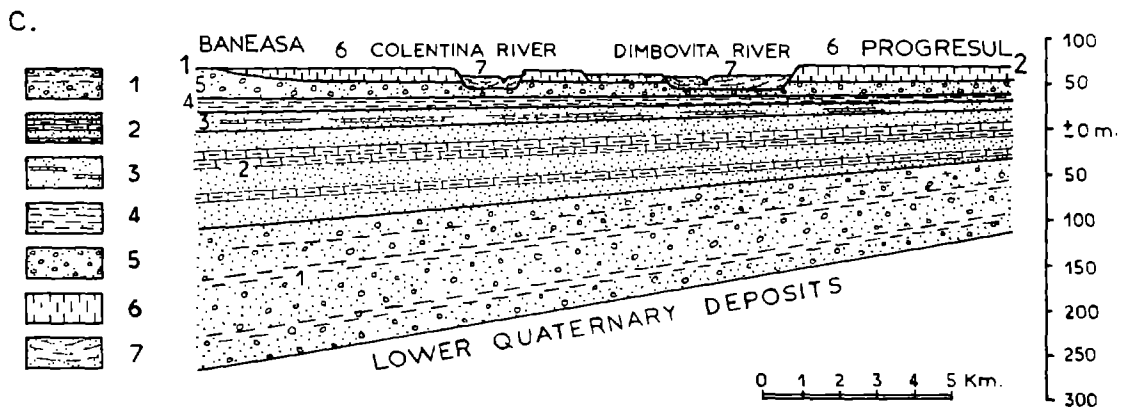
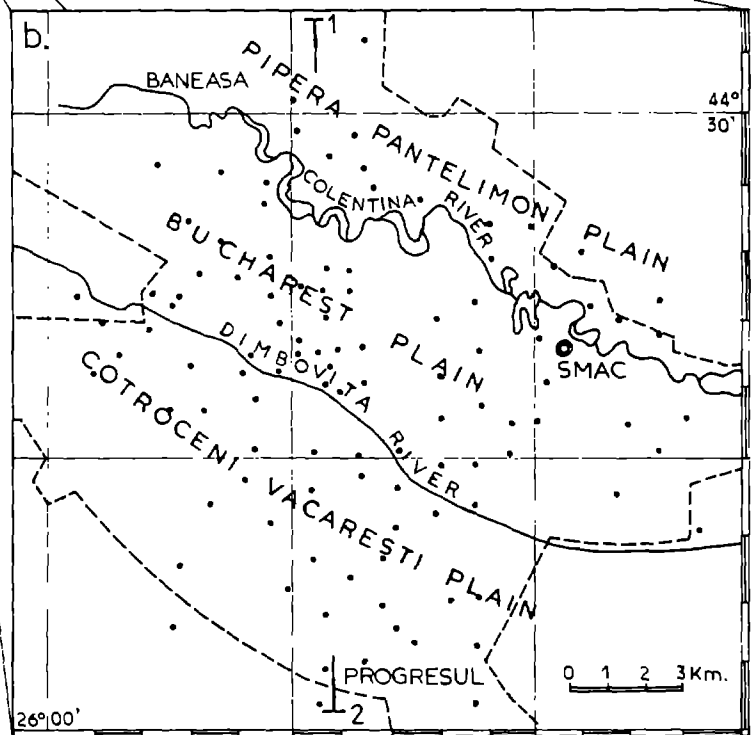


Fig. 1 VRANCEA MARCH 4, 1977 EARTHQUAKE

- a. LOCATION OF THE ANALYSED AREA
- b. SAMPLED SPOTS DISTRIBUTION IN BUCHAREST
- c. GEOLOGICAL CROSS SECTION

- ▽ VRANCEA EPICENTER
- SAMPLED SPOT
- BORDERLINE OF POPULATED AREA
- ↗ CROSS SECTION POSITION
- ACCELEROMETER SMAC



- 1. Sands & gravels ; 2. marl clay & sands ; 3. fine sands with intercalation of sandstone ; 4. clay with sands intercalation ; 5. gravels & sands with clay lens ; 6. loesslike deposits ; 7. alluvial deposits .

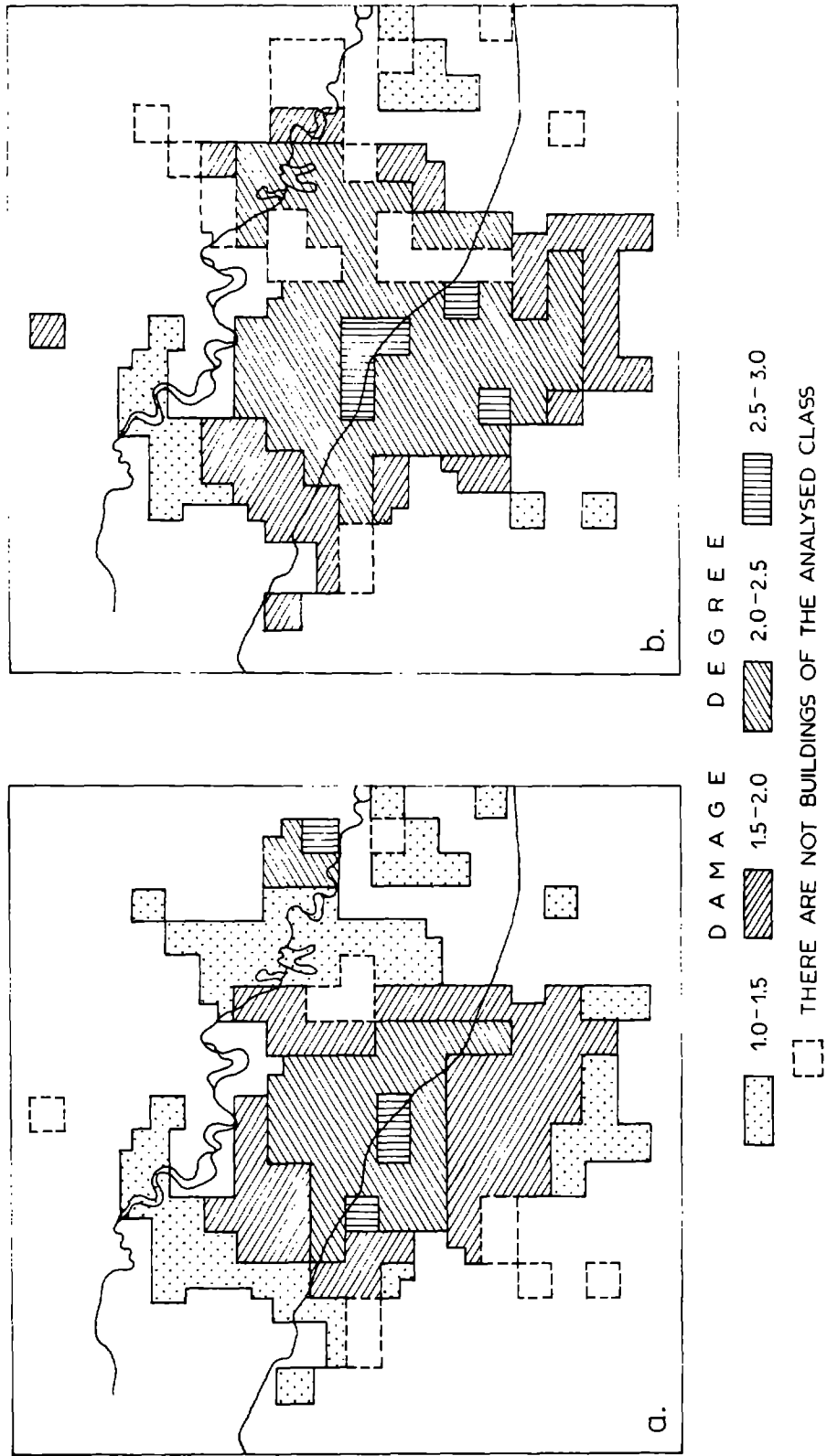


Fig. 2 VRANCEA MARCH 4, 1977 EARTHQUAKE. AREAL DISTRIBUTION OF THE DAMAGE DEGREE IN BUCHAREST FOR: a. MASONRY BUILDINGS; b. REINFORCED CONCRETE FRAME STRUCTURES

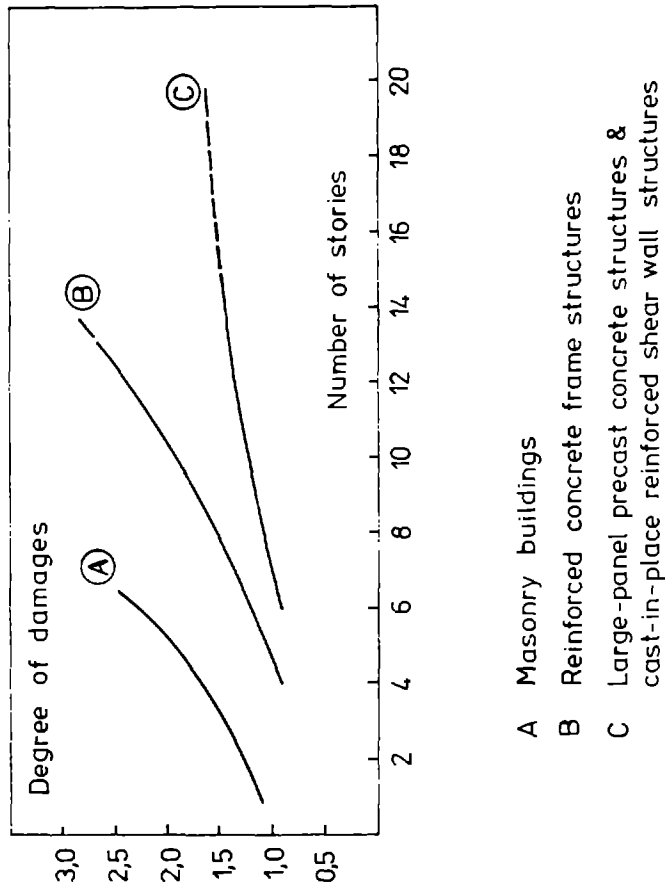


FIG. 4 RELATIONSHIP BETWEEN DAMAGE DEGREE AND NUMBER OF STORIES

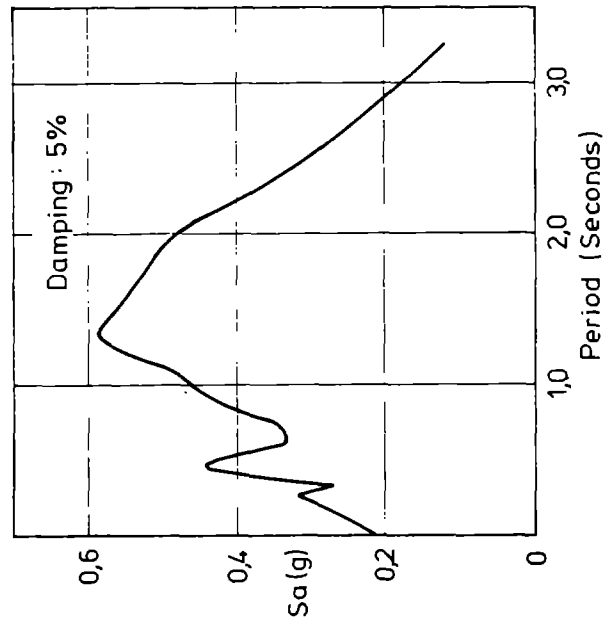
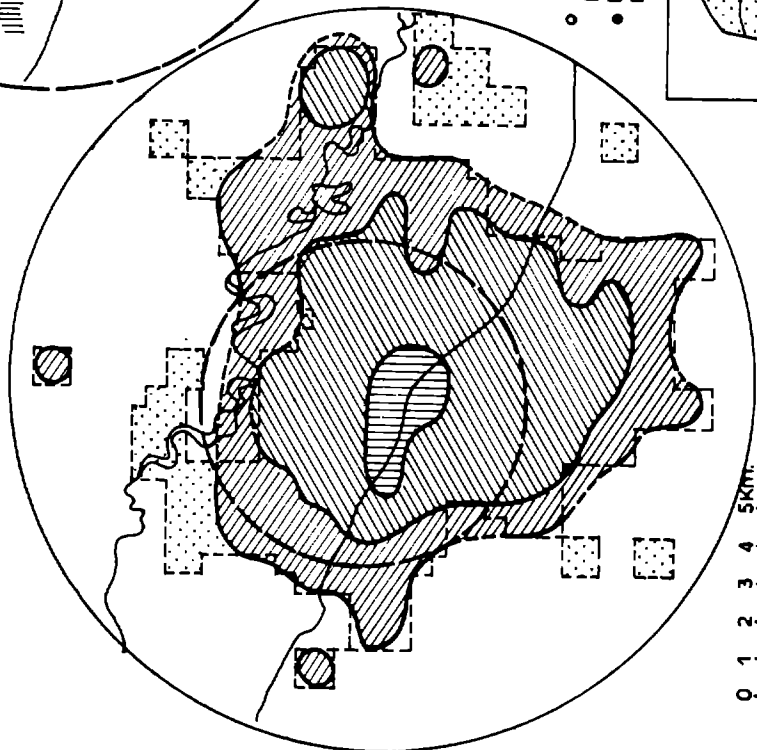


FIG. 3 ACCELERATION RESPONSE SPECTRUM OF THE MAIN PORTION OF THE NORTH-SOUTH COMPONENT OF MOTION IN THE BUCHAREST-VRANCEA EQ. 1977 (MADE AFTER P. G. CARYDIS)

Fig. 5 VRANCEA MARCH 4, 1977 EQ.
GENERALIZED COUNTOUR MAP OF
OBSERVED INTENSITY IN BUCHAREST



INTENSITY DISTRIBUTION
M S K DEGREE

	VIII*
	VII-VIII
	VII
	THE SAMPLED AREA

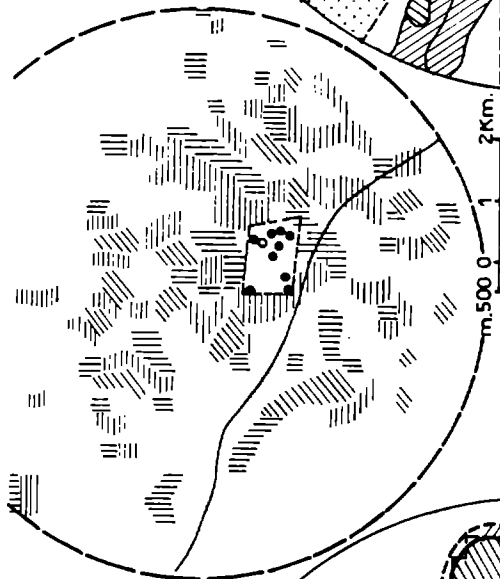


Fig. 6 VRANCEA NOVEMBER
10, 1940 EQ. DAMAGE DISTRIBUTION
(AFTER AL. N. RADULESCU)

HEAVY DAMAGE
 SCATTERED DAMAGE
 MINOR DAMAGE

○ THIRTEEN STORES BUILDING COLLAPSED
DURING THE NOVEMBER 10, 1940 EQ.
● BUILDINGS COLLAPSED DURING THE
MARCH 4, 1977 EQ.

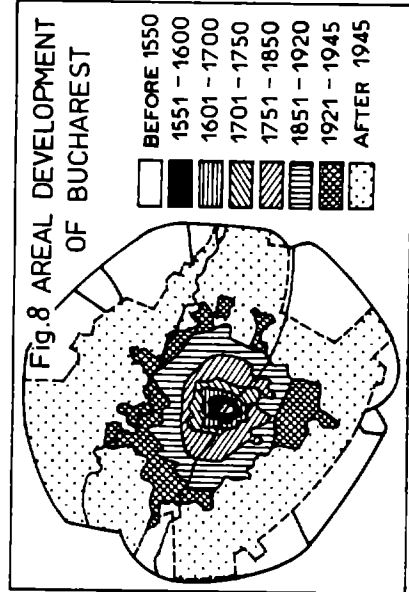
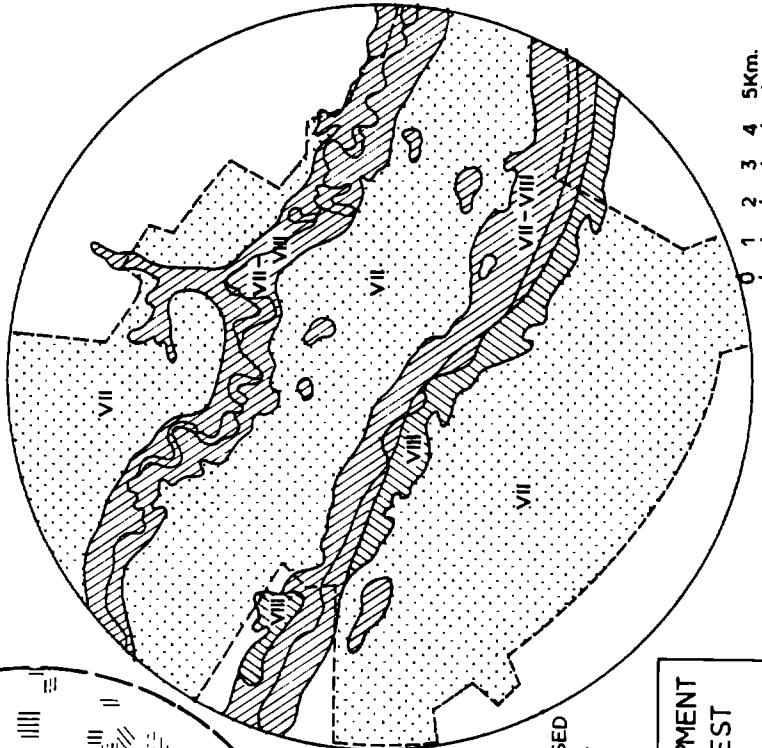


Fig. 8 AREAL DEVELOPMENT
OF BUCHAREST

□ BEFORE 1550
▨ 1551 - 1600
▩ 1601 - 1700
▧ 1701 - 1750
▦ 1751 - 1850
▤ 1851 - 1920
▣ 1921 - 1945
▢ AFTER 1945

Fig. 7 SEISMIC MICROZONING MAP (1973)
(ACCORDING TO MEDVEDEV'S PROCEDURE)



EXPECTED INTENSITY DISTRIBUTION
M S K DEGREE

	VIII
	VII-VIII
	VII

BORDERLINE OF POPULATED AREA

412

INTENTIONALLY BLANK

NEED FOR EXPERIMENTAL EVIDENCE IN DEVELOPMENT
OF SEISMIC MICROZONING METHODS

by

Jakim Petrovski^I

ABSTRACT

The existing empirically developed seismic microzoning methods and the new proposed methods and techniques for development of earthquake design parameters are presented and their critical aspects discussed.

The need of experimental data from the critical consideration of the existing methods and limited records in the past earthquakes for development of appropriate mathematical models and analysis techniques is analysed.

Three dimensional instrumentation dense array for recording ambient and forced-vibrations, small and strong earthquakes has been developed for the purpose of experimental examination of the validity of the existing methods and techniques, and development of possible new methods.

INTRODUCTION

A proper understanding of the nature of structural damage caused by large earthquakes has been essential in the evaluation and improvement of the criteria for the earthquake design of structures. However, most of the studies dealing with the distribution of the damage cost by earthquakes indicate that large differences in the extent of damage often occur over relatively short distances, that the areas of intensive damage are highly localized, and that the amount of damage may change abruptly over distances as short as 0.5 to 1 km. Some of these variations in structural damage have often been attributed to the local geology and soil conditions, specially when weak foundation materials have been involved. Even in the absence of such foundation problems, the overall intensity of ground shaking has been observed to be widely varying over short distances (7).

Damage to engineering structures caused by earthquakes is known to depend on the nature of the arriving seismic energy as well as on the characteristics of structures. For the purpose of engineering design, the characteristics of ground shaking that are of primary importance are the amplitude, the frequency content, and the duration of ground shaking. These characteristics are dependent on various elements such as the earthquake source mechanism, the orientation of the site with respect to the source (19), the surface topography, nonuniform surface configuration (18), and the material properties of the earth media through which the waves propagate. The complex nature of earthquake source mechanism and the irregularities and nongomogeneities of surface layers make it difficult to determine their actual influence on the local ground shaking. Because of the relatively small number of significant measurements of a strong earthquake motion in the epicentral regions, little is known about many factors that effect ground motions at the site. One of these factors, that has been most thoroughly studied, is related to the local site geology and subsoil effects on the earthquake ground motions.

I Director and Professor, Institute of Earthquake Engineering and Engineering Seismology, University of Skopje, Yugoslavia.

Conclusions derived from these studies of local soil conditions have influenced in an important way the methodology of seismic microzoning, that primarily considers the influence of local soil conditions on modification of the earthquake ground motions.

The existing empirical methods and new technique for seismic microzoning based on experience from damage of the structures in the past earthquakes and consideration of local site conditions determined from the studies of microtremors and small earthquakes are hardly reliable methods for evaluation of the seismic design parameters without having a specific evidence of the effect of local soil and geologic conditions for multiple recordings at the same stations from different location and different level of excitation sources. Verification is ultimately needed for the possibility of extrapolation of small earthquake records to predict local soil behaviour in the case of strong earthquake motions as well as to verify laboratory techniques for elaboration of dynamic soil properties under high strain levels.

In order to study local site effect on the modification of strong ground motions and dynamic response of structural systems a three-dimensional strong motion instrumentation array under development, able to record high and low level of excitation is discussed. The continuous recording of high level of excitations is in the range of 5×10^{-4} g to 1 g and the low level of excitations during field studies is in the amplitude range of 10^{-5} g to 2×10^{-2} g. With intensive recording of microtremors, force-vibrations, small and strong earthquakes it is assumed that sufficient data will be collected to study validity of the low level excitation techniques for prediction of earthquake ground motions. It is assumed also that existing analytical methods will obtain experimental basis for their modification as well as development of an integral analytical method for prediction of local site effects during strong earthquake motions. Development of a new laboratory techniques for determination of dynamic soil properties in correlation with instrumental field evidence will be one of the important achievements of the research programme.

Soil-structure interaction problem in the past has been studied as an isolated problem of the integral part of local site effects and there is very little experimental evidence for this phenomena during strong ground motions. Particular instrumentation of structural systems is meant to study soil-structure interaction effects as a part of the entire dynamic response of the structural systems and soil media.

EXISTING METHODS AND TECHNIQUES FOR SEISMIC MICROZONING

Existing seismic microzoning methods are mainly based on the experience of earthquake damage studies in the past destructive earthquakes and on records of microtremors and small earthquakes. They are rather simple and with rapid procedure for estimating local seismicity. However, existing seismic microzoning methods have been developed from experience with low buildings and studies of the dynamic properties of the upper 10-20 m of soil layers (11, 13, 17). The value of microtremors as an aid in the development of microzoning seems to be questionable. Though some studies have shown that adequate analyses of microtremor recordings can be useful for better understanding of the site soil and geology, the very nature of their sources of energy that are located on the ground surface leads to the sampling of shallow site characteristics. Strong shaking, on the other hand, even when it results from shallow and surface earthquakes is caused by faulting which may extend

tens of kilometers into the earth's crust. As a result, the strong-motion waves also sample and depend on the characteristics of earth material at considerable depth. It seems then that microtremors that do not take into account the effects of variations in source mechanism may not even sample the complete geologic cross-section which influences the observed variations of surface shaking and damage (20).

Recently developed analytical methods for calculation of surface earthquake motions used to estimate earthquake design parameters for important facilities are requiring number of assumptions which are often uncertain and can involve large errors. Limited number of existing strong motion records in the epicentral areas (7) showed that actual behaviour of surface layers is inconsistent with the usual results of the calculation techniques. Present lack of sufficient observations of the bedrock, soil layers and surface motions, indicate that many available methods are over-simplified, and are not at this time capable of reliably predicting the surface motion in most practical cases.

Numerous analytical as well as numerical methods have proposed and used in the analysis of soil and geological calculus. Typically, a random function with broad band spectrum or recorded acceleration are being used as an input into such calculations whose output then reflects the influence of the site conditions. Several attempts for experimental verification of this approach or to provide an alternative for estimating the local site effects, with earthquake recording or microtremor studies were performed recently (13, 19, 21). While some of these studies have indicated that local soil and geologic site conditions can have a profound effect on the recorded motions, it has not been shown, so far, whether multiple recordings at the same station from different earthquakes lead to repeatable patterns of local site effects. This repeatable patterns are the most important requirements of the successful microzoning method leading to microzoning map which could predict relative effects repeatable from one earthquake to another. Existing experience is not qualitatively sufficient to understand the detailed nature of shaking and the resulting damage in relation to the soil and geological conditions. The fact that the consequences of an earthquake sometimes can be a simple site model does not in itself suggest that the same pattern of shaking may be repeated in the future (20). It appears therefore that until enough data is collected for shaking in the same area resulting from different small and strong earthquakes induced from different sources the current methods of microzoning for expected variations of strong motion amplitudes will rely more on judgement rather than on a proven observation fact.

THREE DIMENSIONAL STRONG MOTION ARRAY FOR STUDYING LOCAL SITE EFFECTS

To collect enough reliable data within a reasonable period of time as most efficient way at this time is to install three-dimensional instrument array in the carefully selected representative areas with specific soil conditions and significant frequency of earthquake occurrence. These three-dimensional arrays would be economically justified if there is an international cooperative effort and the installation is in countries with existing laboratory facilities and well trained staff for these specific studies.

Since 1976 the Institute of Earthquake Engineering and Engineering Seismology at the Skopje University has started with the research project of development of three-dimensional dense strong motion instrumentation array for studying local site effects on the modification of strong surface motions and dynamic response of structural systems and soil media. The project is

based on extensive monitoring of ground motion at low and high level of excitation.

The central concept of the project places the instrumentation as a nucleus of the system. A research cycle starts from the experiment design and progresses through instrumentation, definition of the immediate environment, data storing, handling and data interpretation back to possible adjustment of the experiment design. Each experiment is completed in one or more cycles. Studies of rare and random events (eg. earthquakes) involves one cycle at each event, whereas more persistent (planned) forced and ambient vibrations may be studied in more cycles.

The instrumentation program arranges ground motion measuring devices in three-dimensional satellite settings interconnected with time rewriter system of DCF-77 radio time code from radio broadcasting station in Frankfurt. Satellite instrumentation settings are design as very flexible consisting of three basic systems: instrumented buildings with down-hole instrumentation on the foundation level, along the height of a ground surface and down-hole consisting of total 10 three componental accelerometers; instrumented free field on a ground surface and down-hole up to the bed-rock, consisting of total 4 three componental accelerometers; and instrumented bed-rock with 1 three componental accelerometer. Each of the satellite settings has its own central reading system with digital cassette recorders. The integral instrumentation system at the first stage of development consists of instrumented two building sites, two free-field sites and one bed-rock site with total number of 87 channels. The block diagram showing distribution of the instruments in the three dimensional dense array at the first stage of development is presented in Figure 1 and the block diagram of the recording data processing and analysis system is shown in Figure 2.

Such a system can expand in space to encounter a variety of conditions. Each satellite setting may be arranged independently to fit best the local conditions under study. The recording system is very flexible and broad band response is achieved by force-balance accelerometers. The recording range of the system is continuously in the range of 5×10^{-4} g to 1 g with the option of manual adjustment into the 10^{-5} g to 2×10^{-2} g range.

Detailed studies of the seismicity and geology of the selected region for instrumentation have been already performed as well as geological and soil investigations of the selected sites.

The project is expected to be very heavy in data acquisition and a basic need will be for storing and handling this large volume of data. The data could be classified into two distinct categories: the data describing the immediate environment within which measurements are taken and the data acquired by the ground motion instruments. The second category of ground motion recording will be continuous monitoring of ground motion and will be regulated by setting a triggering level or by selective recording.

DATA INTERPRETATION

The preparation of this phase of the project is associated with the development of the necessary software. Modelling of realistic configurations of geometry and material properties is achieved by numerical analysis. In this analysis space and time are discretised into finite steps. Each step follows the equation of motion expressed in terms of realistic material behaviour.

The assembly of the steps satisfies the geometry and the appropriate boundary conditions. A finite step formulation cannot be applied to an open system without an appropriate boundary condition. In a case like this the following formulation seems promising: enclose the geometry irregularities and material non-linearities inside a regular boundary. Apply inside this boundary a finite step formulation and replace the medium outside the boundary by an appropriate boundary condition. If the boundary cuts through the infinite medium all the energy will be radiated to the surrounding space and the boundary will be a "transparent" one.

The finite step formulation can be done explicitly or implicitly. The two formulations are equivalent in the elastic domain whereas in the nonlinear case the implicit is more efficient than the explicit formulation. The formulation should allow for large deformations so that the software will be able to consider a broad strain range. General Codes are available; the main effort here will be to simplify the codes by adjusting them to the needs of the project as well as to transcribe them to the mini computer. Computer time will increase with increasing size of the model and increasing number of space dimensions.

ACKNOWLEDGEMENT

The author expresses his sincere thanks to Dr. D. Papastamatiou and Professors D. Petrovski, T. Paskalov, D. Jurukovski, V. Mihailov, M. Stojković and other collaborators from the Institute of Earthquake Engineering and Engineering Seismology, for their helpful suggestions and discussions during the development of the research project.

The work described in this paper is supported by the Self-Managed Community of Interest for Scientific Research of the S.R. of Macedonia in Skopje.

REFERENCES

1. Ambraseys, N.N., "Factors Controlling the Earthquake Response of Foundation Materials", Proc. 3rd ESEE, Vol.1, 1970, p.309, Sofia.
2. Ambraseys, N.N., "Dynamics and Response of Foundation Materials in Epicentral Region of Strong Earthquakes", Invited Paper, 5th WCEE, Rome, 1973.
3. Borchardt, R.D., "Effects of Local Geology on Ground Motion Near San Francisco Bay", Bulletin of the Seismological Society of America, Vol.60, No.1, February 1970.
4. Donovan, N.C. and Valera, J.E., "A Probabilistic Approach to Seismic Zoning of an Industrial Site", Proc. International Conference on Microzonation, Seattle, Vol.II, 1972, pp. 559-576.
5. Espinosa, A.F. and Algermissen, S.T., "A Study of Soil Amplification Factors in Earthquake Damage Areas, Caracas, Venezuela", NOAA - Environmental Research Laboratories, Earth Sciences Lab., Technical Report 280-ESL 31, Boulder, 1972.
6. Hudson, D.E., "Ground Motion Measurements", Earthquake Engineering, (Wiegel, R.L., ed.) Prentice-Hall Inc., Englewood Cliffs, New Jersey, 1970.

7. Hudson, D.E., "Local Distribution of Strong Earthquake Ground Motions", Bull. Seism. Soc. Am. 62, 1765-1786, 1972.
8. Kanai, K. and Tanaka, T., "On Microtremors, VIII", Bull. Earthquake Res. Institute, Vol. 39, 1961, pp. 97-114.
9. Kobayashi, H. and Kagami, H., "A Method for Local Seismic Intensity Zoning Maps on the Basis of Subsoil Conditions", Proc. of the International Conference on Microzonation, Seattle, Vol. II, 1972, pp. 513-528.
10. Medvedev, S.V., et al, "Recommendations for Seismic Microzoning", Stroyizdat, Moscow, 1971.
11. Ohsaki, Y., "Japanese Microzonation Methods", Proc. of the International Conference on Microzonation, Vol. I, 1972, pp. 161-182.
12. Penzien, J., "Predicting the Performance of Structures in Regions of High Seismicity", Invited Paper, Second Canadian Conf. in Earthquake Engineering, Hamilton, June, 1975.
13. Petrovski, J., "Seismic Microzoning and Related Problems", Invited Paper, UNESCO Intergovernmental Conference on the Assessment and Mitigation of Earthquake Risk, Paris, February 1976.
14. Seed, H.B. and Schnabel, P.B., "Soil and Geologic Effects on Site Response During Earthquakes", Proceedings of the International Conference on Microzoning, Seattle, Vol. I, 1972.
15. Seed, H.B., Lysmer, J. and Hwang, R., "Soil-Structure Interaction Analyses for Evaluating Seismic Response", Report No. EERC 74-6, University of California, Berkeley, 1974.
16. Seed, H.B., Ugas, C. and Lysmer, J., "Site Dependent Spectra for Earthquake Resistant Design", Report No. EERC 74-12, University of California, Berkeley, 1974.
17. Steinberg, V.V., "The Methods of Seismic Microzoning Developed in USSR", Report for UNDP/UNESCO Survey of the Seismicity of the Balkan Region, Skopje, 1973.
18. Trifunac, M.D., "A Note on Scattering of Plane SH Waves by a Semi-Cylindrical Canyon", Int. J. Earthquake Engr. Struct. Dynamics 1, 1973, p. 267-281.
19. Udwadia, F.E., "Investigation of Earthquake and Microtremor Ground Motions", Report EERL 72-02, Earthquake Engineering Research Laboratory, California Institute of Technology, 1972.
20. Udwadia, E.F. and Trifunac, M.D., "Problems in the Construction of Seismic Microzoning Maps", Preprints VI WCEE, New Delhi, January 1978, pp. 2-381-386.
21. Udwadia, F.E. and Trifunac, M.D., "Comparison of Earthquake and Microtremor Ground Motions in El Centro, California", Bull. Seism. Soc. Am. Vol. 63, 1973, pp. 1227-1253.

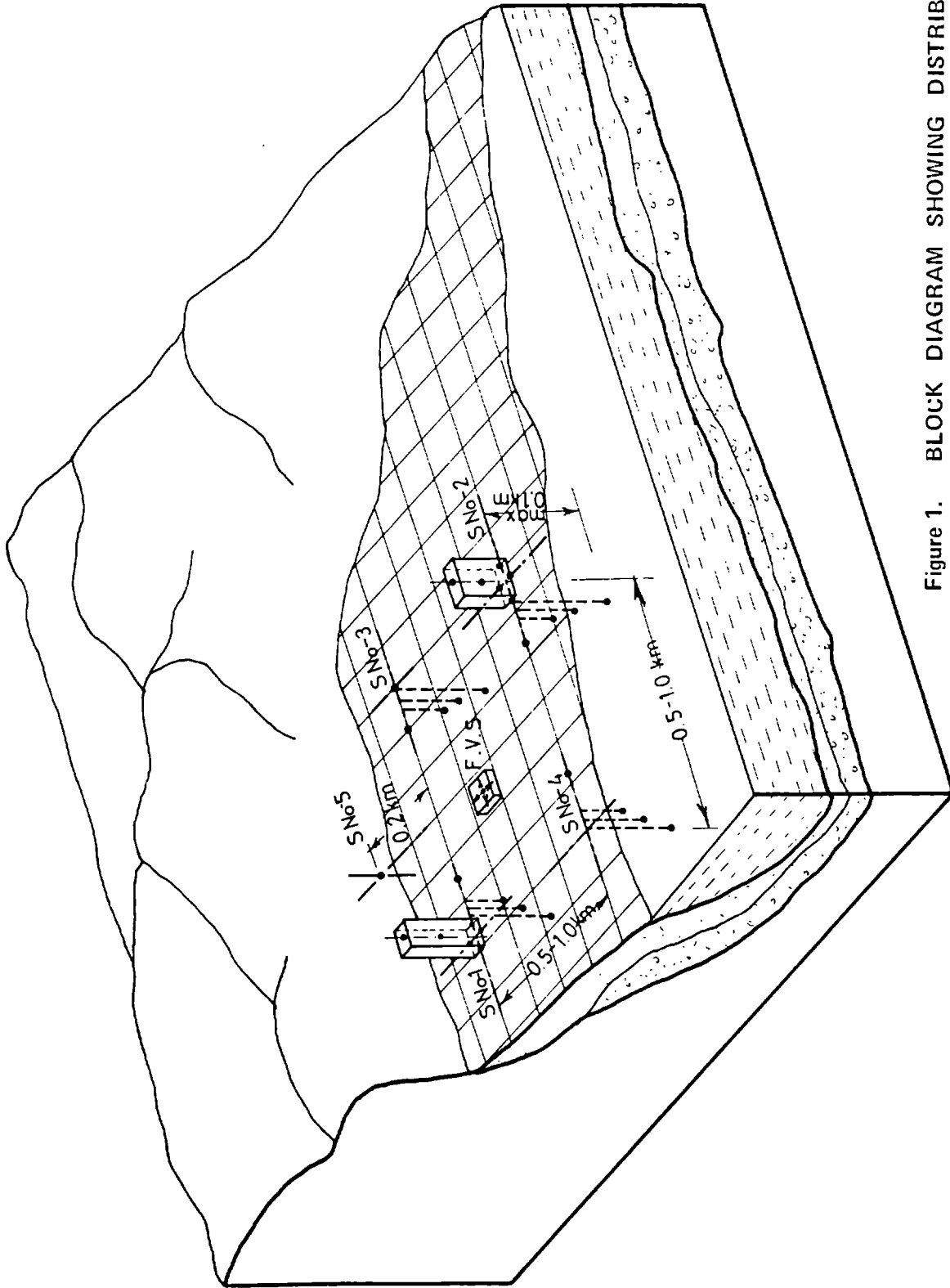


Figure 1.

BLOCK DIAGRAM SHOWING DISTRIBUTION OF THE INSTRUMENTS IN THE THREE DIMENSIONAL DENSE ARRAY

SNo - 1 & 2: Sites of Instrumented Buildings; SNo - 3 & 4: Sites of Instrumented Free Fields; SNo - 5: Site of Instrumented bedrock; FVS: Forced Vibration System

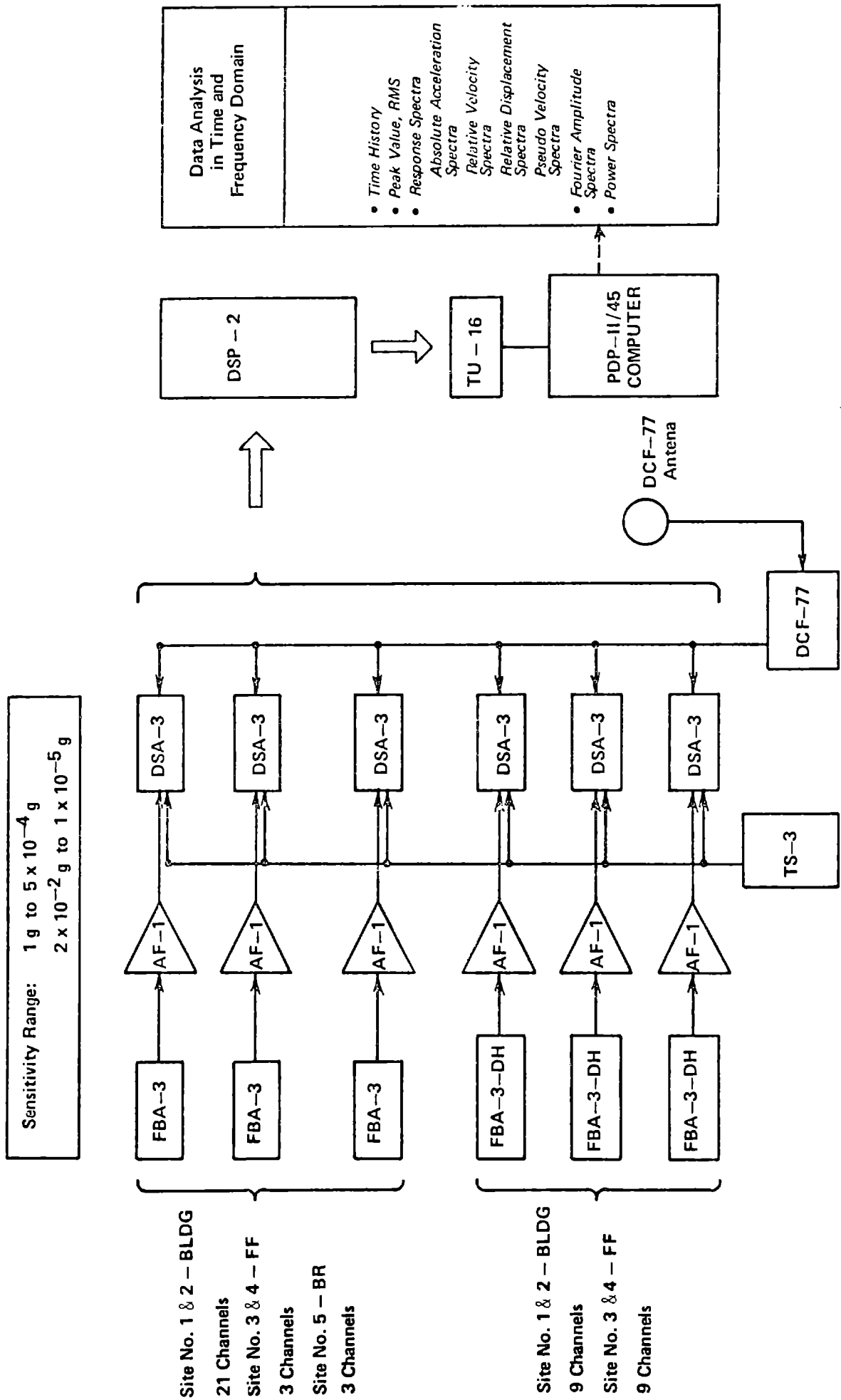


Figure 2 BLOCK DIAGRAM OF RECORDING, DATA PROCESSING AND ANALYSIS SYSTEM

A NEW PROPOSAL OF THE SEISMIC RISK MAP BASED ON THE MAXIMUM
EARTHQUAKE MOTIONS, THE GROUND CHARACTERISTICS AND
THE TEMPORAL VARIATIONS OF THE SEISMICITY

by

S. Hattori*

ABSTRACT

A new idea of the seismic risk map in the vicinity of Japan is proposed. It means combining (i) the expectations of the maximum earthquake motion at the base rock, (ii) the ground characteristics and (iii) the temporal variations of the seismicity. In order to get the expectations of the maximum earthquake motion for some return periods, (a) the earthquake data for the period 1885-1973, (b) Kanai's attenuation model and (c) Gumbel's asymptotic distribution are used. For the ground characteristics, use is made of seismic data obtained by strong motion seismographs of the Japan Meteorological Agency (JMA). The base rock is classified into the first one and the second one depending on the period range concerned. The temporal variations of the seismicity are estimated by the accumulative energy curves which are calculated by using the earthquakes that occurred in the region within a radius of 250 km centered the site concerned.

1. INTRODUCTION

It is not necessary to take the amount of the seismic risk newly into account, if (i) the earthquake prediction is made accurately and (ii) if the earthquake motions at any site due to earthquakes which occurred in a certain point are exactly estimated considering the characteristics of the ground. However, till the present, the problems of the above mentioned (i) and (ii) have not been clarified as to fully satisfy the demands of the earthquake engineering.

On the other hand, earthquake engineers, basing on the knowledge obtained up to now, have to design buildings and civil engineering structures which will remain for many decades and centuries. This is the reason why the amount of the seismic risk must be estimated by some methods.

The seismic risk $O(S)$ is related to (i) the spatial characteristics of the seismicity $S(S)$, (ii) the characteristics of the ground $M(S)$ and (iii) the temporal variations of the seismicity $S(T)$. The relation among them may be indicated in the following:

$$O(S) \sim S(S) \cdot M(S) \cdot S(T) \dots\dots\dots (1-1)$$

Many researches have been done on the seismic risk map up to the present (1, 2, 3, 4, 5). In these researches, however, many of the maps which are entitled to be the regional distributions of the seismic risk or the expectations of the maximum earthquake motions, only show the spatial characteristics of the seismicity, that is, $S(S)$ in eq.(1-1). Many of them keep from estimating $M(S)$, by indicating the values on the standard

* Head, Applied Seismology Division, International Institute of Seismology & Earthquake Engineering, Tokyo, Japan.

ground and those at the base which excludes the ground. None of them have much less dealt with S(T). This research was made to get S(S), M(S) and S(T), and to obtain a more reasonable seismic risk map in the vicinity of Japan.

2. EXPECTATIONS OF MAXIMUM EARTHQUAKE MOTION AT THE BASE ROCK (6)

2-1. Earthquake Data

The earthquake data which are considered to be available at present in Japan can be divided into five periods as follows.

(i) Data I; Period 416--1872.

Magnitudes M_k (Kawasumi's magnitude) and epicenters have been determined by Kawasumi using descriptions found in ancient documents. Errors are fairly large as for the magnitudes and even the relation between M_k and M (JMA's magnitude) is not clearly defined. No data except earthquakes with damages are included.

(ii) Data II; Period 1873--1884.

Both M_k and M have been shown in such a relation as $M_k = M + 0.5$. No data except earthquakes with damages are included.

(iii) Data III; Period 1885--1925.

Both M_k and M have been shown in the same relation as in the data II. In this period, however, also the data except earthquakes with damages have been included, and almost all the earthquakes with the magnitude $M \geq 5.5$ may be included.

(iv) Data IV; Period 1926--1960.

The results of the instrumental observations have been reported by JMA, and all the earthquakes with the magnitude $M \geq 5.0$ are considered to be included.

(v) Data V; Period in and after 1961.

The detection ability in this period being much advanced comparing with that in the period of the data IV, almost all the earthquakes with the magnitude $M \geq 4.0$ are considered to be included.

The data I-V can be classified into two parts of data A (data I + data II) and data B (data III + data IV + data V). The values of the mean annual energy (E /year) are $0.30 - 0.45 \cdot 10^{23}$ erg for the data A and $0.22 - 0.27 \cdot 10^{24}$ erg for the data B, respectively. The former is only about 10-20% of the latter. It means that there are remarkable differences between data A and B. Attentions must be paid to the facts that (i) the data A have been made according to the descriptions found in ancient documents and that (ii) the distribution of people in the age when the documents were made, must have been very uneven. It is easily inferred that the data A are not only (a) small in quantity and (b) low in accuracy but also (c) uneven regionally. Accordingly, it is not appropriate to treat the data A and the data B equally.

It is doubtful whether the period (89 years) of the data B is long enough for the seismic activity to be regarded as being constant. However, supposing that the deficiency of using only the data B is less than that of including the data A, only the data B are used in this research.

The data B are examined below. For high ranks of magnitude, the earthquake numbers for the period 1885--1925 are very large comparing with those of the period thereafter. The magnitudes for the period 1885--1925 have been determined on the strength of Kawasumi's magnitude, and those for the period thereafter have been determined on the instrumental observations. It is necessary, it seems, to modify the magnitudes for the period 1885-1925. Assuming that the gradient of the accumulative energy curve is nearly constant and that the gradient value for the period 1926--1973 is typical of the vicinity of Japan, the following modifications were made;

Modification; $M_m = M_o - 0.6$ for the period 1896--1915, and

$M_m = M_o - 0.5$ for the period 1885--1895 and 1916--1925;

where M_m and M_o are the modified and original magnitudes, respectively. The resultant accumulative energy curve makes almost a straight line. As the modification seems to be suitable from the above facts, the data with such a modification are used in this research. As solely for the Kanto earthquake, however, a re-determined magnitude 7.9 is used without such a modification.

2-2. Attenuation Model

It is necessary to calculate a maximum earthquake motion on the ground or at the base rock in arbitrary sites for each earthquake in the data. There are many attenuation models to calculate the maximum earthquake motion from the epicentral (focal) distance and the magnitude. In this research, the attenuation model by Kanai,

$\log v(\text{kine}) = 0.61M - (1.66 + 3.60/x)\log x - (0.631 + 1.83/x) \dots (2-1)$
is used because of the following reasons.

(i) It is more rational to indicate the values at the base rock than to indicate the values on the ground for such a kind of macrozoning as the seismic risk in the whole vicinity of Japan. The incident waves at a base rock are generally considered to be amplified by the ground on the base rock. As the amplification of the ground differs greatly from place to place, however, the regional distributions of the maximum earthquake motion on the ground are to become very complicated. Accordingly, it means that complicated regional characters of the ground are disregarded to obtain the regional distributions of the maximum earthquake motions on the ground from only one attenuation model and the seismicity. Therefore, the following way of expressing the seismic risk is more reasonable. That is, defining, as the base rock at a certain site, a certain underground surface at which the velocity contrast is large and the maximum earthquake motions depend on only the seismicity in the vicinity and, moreover, which is common in a fairly wide area, the regional distributions of the seismic risk ($O(S)$) are expressed by means of the maximum earthquake motions at the base rock and the maximum earthquake motions on the ground are calculated taking the ground characteristic ($M(S)$) in each site into consideration.

(ii) Kanai derived eq.(2-1) from Tsuboi's equation which had been made to determine the magnitude in the vicinity of Japan. The magnitudes used in this report, that is, the magnitudes by JMA, have been determined by the method based on Tsuboi's equation. Consequently in the case where eq.(2-1), that is, $A_K = f(M_J, r(\Delta))(M_J$; magnitude by JMA, $r(\Delta)$; focal (epicentral) distance, A_K ; maximum earthquake motion in Kanai's equation) is used, there is a certain continuity between A_K and M_J .

(iii) According to Kanai (2), the maximum velocity amplitude is nearly constant in the range of period between 0.05 sec and 5.0 sec. Consequently, if expressed by maximum velocity amplitudes, the seismic risk for a certain return period can be shown only in one map for the above range of period.

(iv) The maximum acceleration and displacement amplitude for some periods can also be derived from the value of the maximum velocity amplitude.

2-3. Estimation of Presumable Maximum Earthquake Motions

The maximum earthquake motions are estimated by the following method. Putting the probability that a certain variable x is equal to or larger than any of x_1, x_2, \dots, x_n ,

$$\Phi_n(x) = P(x_1 \leq x, x_2 \leq x, \dots, x_n \leq x) \dots\dots\dots(2-1)$$

the return period $T(x)$ and the reduced variable z are defined by the equations.

$$T(x) = 1/\{1 - \Phi_n(x)\} \dots\dots\dots(2-2)$$

$$z = - \ln \{ - \ln \Phi_n(x) \} \dots\dots\dots(2-3)$$

Gumbel's third asymptotic distribution is shown by the equation.

$$\Phi_n^{(3)}(x) = \exp \left\{ - \left(\frac{W-x}{W-V} \right)^K \right\} \dots\dots\dots(2-4)$$

The parameters W, K and V in eq.(2-4) are the upper limit of the maximum value, the shape parameter and the characteristic maximum value, and

$$\Phi_n^{(3)}(V) = 1/e \text{ and } \Phi_n^{(3)}(W) = 1.$$

We have the following equations.

$$\left. \begin{aligned} z_m &= - \ln \left(\frac{W-x_m}{W-V} \right)^K \\ \Phi_m &= \frac{m}{n+1} \\ y_m &= - \ln [- \ln(\Phi_m)] \\ \sigma &= \sum_{m=1}^n (z_m - y_m)^2 \end{aligned} \right\} \dots\dots\dots(2-5)$$

where x_m, n, y_m and z_m are the maximum value of the variable x in a unit-period m , the number of unit-period, the reduced variable corresponding to the observed data and the theoretical reduced variable of the third asymptotic distribution, respectively. The third asymptotic distribution most fit for n values of x_m can be gotten by determining the values of W, V and K so as to minimize σ .

The maximum velocity amplitudes v_m in every year for the period 1885-1973 are calculated by eq.(2-1), and the logarithms of these maximum values ($x_m = \log v_m$) are approximated by the Gumbel's third asymptotic distribution. The analytical results for Tokyo (Fig. 1) shows that the expected values for the return period 50, 75, 100 and 200 years are 8.3 kine, 10.4 kine, 12.2 kine and 17.5 kine, respectively.

Fig. 2 indicates the regional distribution of maximum velocity amplitudes (kine) at the base rock for the return period 100 years in the vicinity of Japan.

3. GROUND CHARACTERISTICS (7)

It is not easy to know the detailed underground structure throughout Japan. An alternative technique is proposed herein to know the ground characteristics without determining the underground structure.

In the Seismological Bulletin of Japan Meteorological Agency (SBJMA), the elements (magnitude, epicenter etc.) of each earthquake and the observed results (maximum amplitudes and their period) at each station have been reported. The magnitudes reported in SBJMA have been determined by Tsuboi's formula

$$M = (1/2)\log(A_{NS}^2 + A_{EW}^2) + 1.73\log\Delta - 0.38. \quad (3-1)$$

Since A_{NS} and A_{EW} for an earthquake are observed in many stations, the mean value of magnitudes determined at these stations has been reported in SBJMA as the magnitude of the earthquake.

Reversing the procedure, the following values are calculated at every station,

$$F(T) = \frac{1}{m} \sum_{i=1}^m \left[\frac{\sqrt{A_{NS}^2(T)_i + A_{EW}^2(T)_i}}{10^{M_i - 1.73\log\Delta_i + 0.38}} \right]. \quad (3-2)$$

Here A_{NS} , A_{EW} , T , M and Δ are the maximum amplitude (μ) in NS and EW components, their period (sec), the magnitude of the earthquake and the epicentral distance, respectively. And m denotes the total number of the data such as the periods of the phase giving maximum amplitudes are T . The discrepancy between the periods of A_{NS} and A_{EW} is reconciled by defining T as $T \pm (1/2)\Delta T$.

Eq.(3-1) is transformed to an equation of $\sqrt{A_{NS}^2 + A_{EW}^2} = 10^{M - 1.73\log\Delta + 0.38}$. As the magnitudes in SBJMA are the average of ones determined by eq.(3-1) at many stations, the value $10^{M - 1.73\log\Delta + 0.38}$ can be regarded as a standard value of maximum amplitudes. If it is assumed that this value can be always the standard value in the period range concerned ($T \leq 5.0$ sec), $F(T)$ means the average of "m" numbered ratios of the observed value $\sqrt{A_{NS}^2(T) + A_{EW}^2(T)}$ to the standard value. Consequently, we can say that $F(T)$ expresses the mean quakability in the period T at each site. Therefore, $F(T)$ in the period range less than 5.0 sec can be regarded as a kind of "spectrum" reflecting the ground characteristic.

To find the most proper period window ΔT from the viewpoint of the numbers of the data and resolving power, five cases of $\Delta T = 0.3, 0.5, 0.7, 0.9$ and 1.1 sec were examined. In the case of $\Delta T = 0.3$ sec, $F(T)$ curve shows remarkable changes with the variation of T owing to comparatively few available data. In the case of $\Delta T = 1.1$ sec, on the other hand, $F(T)$ curve changes too smoothly because of less resolving power. In Fig. 3, $F(T)$ curve ($\Delta T = 0.3, 0.5, 0.7$ sec) and the numbers of the data for $\Delta T = 0.9$ sec at Tokyo are shown. The numbers of the data are more than 50 at $T \leq 4.4$ sec, and $F(T)$ is a little larger than 1 at $T \leq 3.6$ sec and 2-9 at $T > 3.6$ sec. It is concluded that the quakability at Tokyo is a little more at $T \leq 3.6$ sec and fairly more at $T > 3.6$ sec comparing with the standard one.

$F(T)$ in short period range ($T \leq 1.0$ sec) corresponds to the ground characteristics just beneath the station. The total number of stations, which amounts to 110, is still too few to get the regional distribution of the short period ground characteristics throughout Japan. On the other hand, the long period $F(T)$ ($1.0 \text{ sec} < T$) corresponds to the ground

characteristics common to fairly large area including each station.

It seems to be most adequate to divide the whole region of Japan into five ranks of $F(T) \leq 1.0$, $1.0 < F(T) \leq 1.5$, $1.5 < F(T) \leq 2.0$, $2.0 < F(T) \leq 3.0$ and $3.0 < F(T)$. We can regard Fig. 4 as the regional distributions of the long period ground characteristic throughout Japan.

4. BASE ROCK (8)

Concerning influences of the ground on the seismic risk, the following points are generally agreed. (A) The seismic risk due to short period ground motions such as 1 sec or less shows frequent variations from place to place, that is, it varies with short wave-lengths two-dimensionally. This indicates "micro-zoning" is indispensable for the short period ground characteristics. (B) The seismic risk due to long period components (1-5 sec.), on the other hand, varies with long wave-lengths two-dimensionally. This necessitates "macro-zoning".

The relations between the above-mentioned points (A, B) and the underground structures are schematically shown in Fig. 5. The periods of ground motions are classified into the long period and the short period for simplicity's sake. Here "the short period" corresponds to the period range $T \leq 1.0$ sec. and "the long period" to the period range $1.0 \text{ sec} < T \leq 5.0 \text{ sec}$. The periods above than 5.0 sec are not taken into considerations, because the predominant periods of ordinary buildings may be less than 5.0 sec.

As shown in Fig. 5, it is assumed that a seismic input ① would be applied to a certain interface ② in the underground and the velocity spectrum of the input would be flat both in the short and long periods. These two assumptions are justified by the following observational and theoretical researches. (1) Kanai et al.(9) analysed seismic waves observed in the underground of Hitachi Mine, and found that the mean velocity spectra are flat in the period range between 0.1 sec and 1.6 sec. (2) Aki (10) studied the spectrum of seismic waves in farfield based on the dislocation theory and concluded that the velocity spectra of the earthquakes with magnitude $M \leq 6$ are flat in the frequency range higher than the corner frequency. For example, the corner frequency of the earthquake with magnitude $M = 6$ being about 0.1 cps, the velocity spectra are constant in the period less than 10 sec. (3) Shima et al.(11) made earthquake observations for the long period components in Inage and Kawasaki near Tokyo and obtained the results that while the velocity spectra for the earthquakes with magnitude $M < 5.5$ decrease with a fixed but fairly small gradient as the periods increase between 1.0 sec and 5.0 sec, the velocity spectra for the earthquakes with magnitude $M \geq 5.5$ are nearly constant.

The first base rock (interface ② in Fig. 5) is defined as follows: (1) The velocity contrast above and beneath it is fairly remarkable. (2) It exists in common over a fairly large area (for example, the whole Tokyo area). (3) The amplification characteristics both for the short and long period components depend on the ground condition above it. (4) Its depth ranges between a few hundred m and 1-2 km.

When the ground above the first base rock is uniform without layered structure, the ground and its predominant periods are represented by

$L_n (L_1, L_2, \dots, L_n \dots)$ as shown in Fig. 5, where n indicates the classification of the region. The spectra of the earthquake motion obtained on the ground surface, corresponding to the ground L_n , will have such predominant periods as shown by part ⑧ in Fig. 5.

However, it rarely occurs that the ground above the first base rock is uniform. In general, layered structures exist especially near the ground surface. The layered structure is considered to give a great influence upon the amplification in the short period range. Accordingly, introduction of additional base rock is needed. The second base rock ③ is thus defined as follows; (1) The velocity contrast above and below it is fairly remarkable. (2) It exists only in a limited area. (3) The amplification characteristics in the short period range are strongly influenced by the ground above it. (4) Its depth is less than 100 m.

When the seismic inputs ① at the first base rock are amplified in the ground L_n and S_n , the spectra of the earthquake motions on the ground surface will become such as shown by part ⑨ in Fig. 5. Here the ground above the second base rock and its predominant periods are represented by $S_n (S_1, S_2, \dots, S_n \dots)$. It is summarized as follows: (1) The seismic risk due to the short period ground motions depends on seismicity and also on the ground S_n above the second base rock. This corresponds to the above mentioned point A. (2) The seismic risk due to the long period ground motions depends on seismicity and also on the ground L_n above the first base rock. This corresponds to the point B.

By the above discussions, the notions of (i) the seismic risk of the short and long periods, (ii) macrozoning, (iii) microzoning, (iv) base rocks and (v) the ground could be related synthetically. Here the said macro- and micro- zoning have been interrelated only to the media, especially to the ground. Consequently, if the usual meaning of "-zoning" implies also that of seismicity, it differs distinctly from the meaning of "-zoning" used here.

5. TEMPORAL VARIATIONS OF SEISMICITY (12)

The temporal variations of the seismicity are presumed by using the accumulative energy curves. As mentioned before, high-quality earthquake data in the vicinity of Japan are those after 1885. The return periods of great earthquakes are said to be some decades at the short and some hundreds or thousands years at the long. The periods of the earthquake data stated above, therefore, are not long enough to cover the return periods of the great earthquakes. The attention should be paid to the fact that the following analyses and the results contain such a problem.

The accumulative energy curve (AE-curve) in an arbitrary point is calculated by using the earthquakes occurred within a radius of 250 km centered on the point. The AE-curves are obtained at every 0.5° in the latitude and the longitude in the whole of Japan. Suppose that a great earthquake occurs in a point just outside 250 km boundary of the point (i). This great earthquake does not produce any effect on the AE-curve of the point (i). However, the effects are seen on the AE-curve of the point (i+1) neighbouring it. Therefore, the AE-curves for two points, the distance between which is only 50 km, show remarkable discontinuity for this earthquake. This discontinuity is considered to be unnatural from the point of view that the temporal variations of the seismicity should not

show sudden changes regionally. To avoid this unnaturalness, the AE-curve is modified by the weight of two dimensions.

Taking the above-stated procedures the AE-curves in the whole vicinity of Japan were calculated. In Fig. 6, the results at every 1° in the latitude and the longitude, mainly those of the land part are shown. For example, the AE-curve at a point (①-a) offshore the east of Hokkaido is shown at "a" in diagram ① in Fig. 6. This figure can be said to be a four dimensional seismicity map in the vicinity of Japan in the period 1885-1975.

The values of $S(T)$ are estimated at every point according to the following respective cases: (i) Regular AE-curve, (ii) Semi-regular AE-curve, (iii) Irregular AE-curve. The $S(T)$ value implies that $S(T) \cdot T_r$ years have passed till the present from the previous great earthquake when the temporal variations of the seismicity are assumed to be repeated by the period T_r . The maximum earthquake motions ($S(S) \cdot M(S)$) are expected to occur after $(1-S(T)) T_r$ years. As stated above, T_r , not always being clarified in all the points, it may be one way to assume it, for example, as to be 100 years. Fig. 7 shows the regional distribution of $S(T)$ values in and around Japan.

6. DISCUSSIONS AND CONCLUSIONS

One of the most important problems in the earthquake engineering is to estimate when or how long and what kind of earthquake input work on buildings or civil engineering structures. For this purpose, the following many subjects have to be solved; (1) what is called earthquake prediction, that is, to forecast the magnitude, the hypocenter and the occurrence time of a great earthquake (ii) the seismic wave generations at the hypocenter and the propagations through such media as crust and ground.

If all of these problems are possible to be solved with such high accuracy as required by the earthquake engineering, there will be no need for further discussions. Though lots of views and knowledge on these subjects have been shown till now, the results are not always satisfactory from the viewpoint of the practical use of earthquake engineering.

Nevertheless, aseismatic designs for buildings or civil engineering structures which will remain for decades and centuries must be planned being based on the knowledge obtained up to the present.

The following procedures were proposed as a substitute for the perfect solution. (i) The seismic inputs at the base rock of arbitrary sites were estimated by the spacial characteristics of the seismicity in a certain period in the past ($S(S)$). (ii) The ground characteristics were presumed by seismic data by strong motion seismographs at each site ($M(S)$). (iii) The temporal variations of the seismicity were estimated by the accumulative energy curve at each point ($S(T)$). It was also proposed that a more reasonable seismic risk map $O(S)$ should be made by combining $S(S)$, $M(S)$ and $S(T)$ and Fig. 2, Fig. 4 and Fig. 7 were to be used as $S(S)$, $M(S)$ and $S(T)$.

REFERENCES

- (1) Kawasumi, H., Measures of Earthquake Danger and Expectancy of Maximum Intensity throughout Japan as inferred from the Seismic Activity in Historical Times, Bull. Earthq. Res. Inst., 21 (1951), 469-482.
- (2) Kanai, K. and T. Suzuki, Expectancy of the Maximum Velocity Amplitude of Earthq. Res. Inst., 46 (1968) 663-666.
- (3) Muramatu, I., Expectation of Maximum Velocity of Earthquake Motion within 50 years through Japan, Sci. Rep. Gifu. Univ., 3 (1966), 470-481.
- (4) Goto, H. and H. Kameda, A Statistical Study of the Maximum Ground Motion in Strong Earthquakes (in Japanese), Proceeding of the Japan Society of Civil Engineers, 159 (1968), 1-12.
- (5) Omote, S., H. Hanai and S. Nagamatsu, Occurrence Rate of Earthquake Motion in Japan, Bull. IISEE, 13 (1975), 101-118.
- (6) Hattori, S., Regional Distribution of Presumable Maximum Earthquake Motion at the Base Rock in the Whole Vicinity of Japan, Bull. IISEE, 14 (1976), 47-86.
- (7) Hattori, S., Regional Peculiarities on the Maximum Amplitudes of Earthquake Motion in Japan, Bull. IISEE, 15 (1977), 1-21.
- (8) Hattori, S., A Proposal of the Earthquake Danger Map Based on Seismicity and Ground Characteristics, Bull. IISEE, 15 (1977), 23-32.
- (9) Kanai, K., S. Yoshizawa, and T. Suzuki, An empirical formula for the spectrum of strong earthquake motions II, Bull. Earthq. Res. Inst., 41 (1963), 261-270.
- (10) Aki, K., Scaling law of earthquake source time function, Geophys. J. R. Astr. Soc., 31 (1972), 3-25.
- (11) Silva, B. and E. Shima, Spectra of Seismic waves in the period range from 1.0 to 10 seconds, Bull. IISEE, 13 (1975), 23-44
- (12) Hattori, S., Temporal variations of seismicity and seismic risk, Bull. IISEE, 16 (1978) (in press).

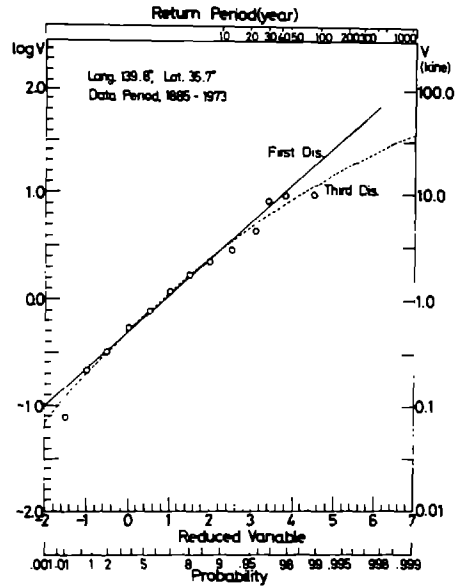


Fig. 1 Example of analytical result for Tokyo

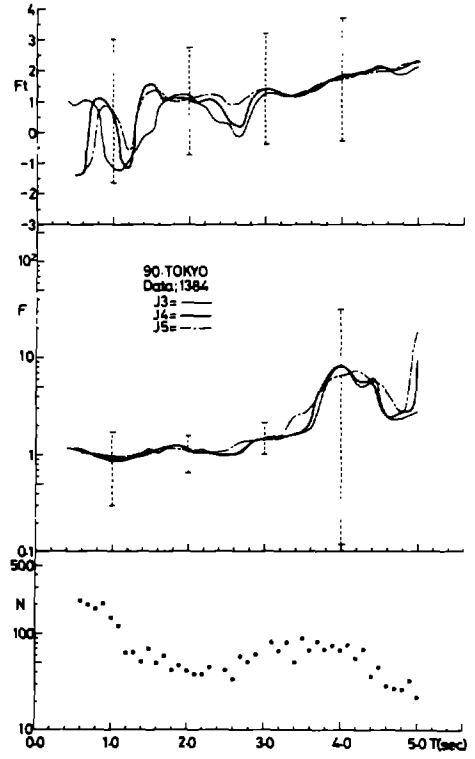


Fig. 3 F(T) curve and the number of data for the case $\Delta T = 0.9$ sec at Tokyo.



Fig. 2 An example of regional distribution of the maximum velocity amplitude (kine) expected at the base rock for return period 100 years.

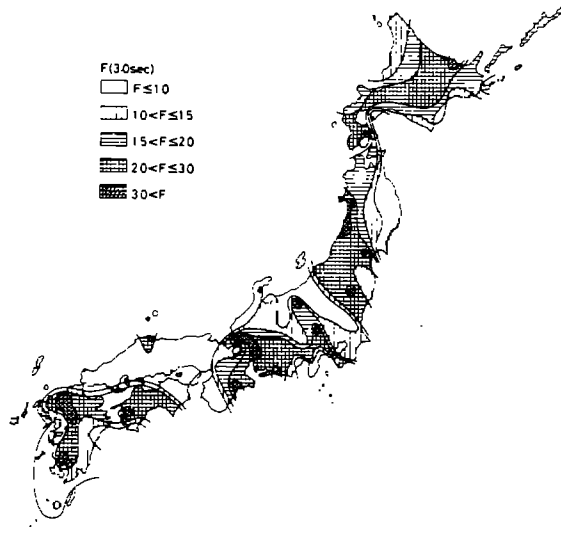


Fig. 4 An example of regional distribution of the ground characteristic above the first base rock (period $T = 3.0$ sec).

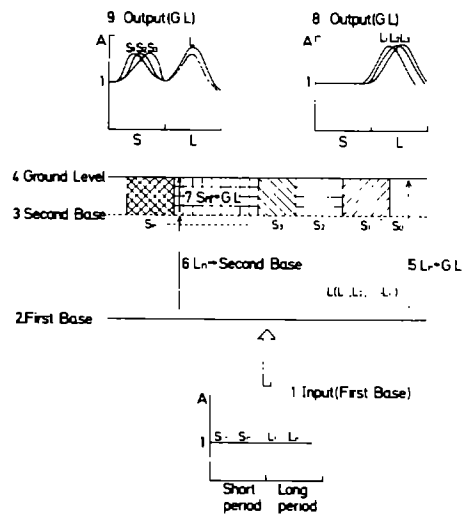


Fig. 5. A general idea of input, First base, Second base and Output.

SEISMIC MICROZONING MAP OF TOKYO

by

Etsuzo Shima^I

ABSTRACT

Geological sections published by the Tokyo Metropolitan Government were converted into the shear wave velocity sections using a large amount of shear wave velocity data. The amplification study employing the multiple reflection theory was then carried out at more than 800 points. Since we could not find the common base rock throughout the area, we assumed that the deepest formation at the site found in the geological section was the base rock. It was found that there is the linear relationship between the square roots of powers of responses and the ratios between the shear wave velocities of base rocks assigned at the sites and those of surface layers. The thickness of the subsoil had little effect in deriving the above results. Thus we could obtain approximately the relative magnitude of vibration at any site throughout the area without the information of the base rock.

INTRODUCTION

It has been well recognized that the shear wave velocity section at the site plays an important role in estimating the input seismic forces to the structures. This can be realized easily, since in general, the shear wave amplitudes in the near field are much larger than those of P waves or other types of waves such as surface waves. The shear wave velocity V_s in the elastic medium is given by the formula $V_s = \sqrt{G/\rho}$, where G and ρ are the rigidity and the density of the medium respectively. Since G is considered to be associated with the strength of material, and the increment of ρ with respect to the depth in the near surface is not so remarkable, we could say that the shear wave velocity itself is the measure of strength of the medium.

The shear wave velocity at the depth where the earthquake is generated is around 3-3.5 km/sec. On the other hand, it is as slow as 100-400 m/sec near the ground surface of the Tokyo Metropolis. Most of the big cities in Japan are situated on the Quaternary deposits, as Tokyo is. The shear wave velocities near the ground surface in such cities will be the same order which we found in case of Tokyo. And that is why structures in those cities are not strong enough to resist the forces due to the huge earthquakes.

Seismic waves generated at the origin change their waveforms gradually at the discontinuities which do exist on the way of propagation. Between the incident and refracted angles of the seismic waves at the boundary of two media, there is a law called Snell. That is: $\sin i/V_1 = \sin r/V_2$, where i and r are the incident and refracted angles, V_1 and V_2 are the wave velocities of two media respectively. In general, seismic wave velocity increases with depth, r becomes smaller and smaller when the seismic waves approach to the ground surface. According to this law, we can safely

^IProfessor, Earthquake Research Institute, The University of Tokyo.

assume that the seismic waves propagate normally upwards near the ground surface, since $r \neq 0$. When the seismic waves are incident from the hard medium (fast shear wave velocity) to the soft one (slow shear wave velocity), the refracted amplitudes becomes larger compared with the incident one. The softer the medium in which the seismic waves are refracted the bigger will be the amplification of refracted amplitudes. And due to the multiple reflections of seismic waves in the surface layers, the amplitude at certain frequency becomes very large and sometimes causes damage to the structures.

Let us assign the base rock in the depth which is common in the area we are interested in. Then the waveforms of incident waves to the base rock are assumed to be almost the same throughout the area provided that it is not so extensive compared with the epicentral distance. We often experience that the seismic intensities in the same area sometimes differ so much as to alter the degree of damage several times over. It was found through the comparative observations of earthquakes at such sites, the difference of seismograms was so remarkable that we could not believe us observing the same earthquake. As mentioned above, these events are due to the difference of the shear wave velocity sections at the sites. From the engineering point of view, we may assume that the velocity spectrum of seismic waves from the destructive earthquake incident to the base rock is white. Then we can easily synthesize the seismograms at any sites provided that we know the velocity sections above the base rock.

In the following, we will mention the effort of completing the seismic microzoning map of Tokyo employing the above-mentioned conception.

SHEAR WAVE VELOCITIES OF SOIL LAYERS IN 23 WARDS OF TOKYO

From the topographical point of view, the 23 Wards of Tokyo can be divided into two parts, the eastern and the western parts. Roughly speaking, the boundary of two parts is along the Keihin-Tohoku Line of Japanese National Railways which traverse the area almost NS direction passing through the Tokyo Station. The eastern part of Tokyo is called downtown or lowland, and the height at some parts of this area are as low as the mean sea level. The surface geology of this area is of the holocene deposits, mainly soft clays or sands of 10-50 m thickness. The western part (uptown or Yamate) is of mainly the terrace of pleistocene deposits, called Kanto loam. There are many small valleys due to the erosion of small rivers and their branches. Deposits at these sites are the peat or very soft clays of Holocene.

After the 1923 Great Kanto Earthquake, Tokyo Metropolitan Government has conducted the series of bore-hole survey mainly in the eastern part of Tokyo where the damage was remarkable. After the 2nd World War, a great deal of data associated with the subsoil layers were obtained through the investigations in relation to the constructions of the new subway systems and also of the express ways. Using these numerous soil data, Tokyo Metropolitan Government published the EW geological cross-sections of 23 Wards of Tokyo every 1 km interval from North to South (1).

To correlate these geological sections with the shear wave velocity sections, we have conducted energetically the shear wave velocity measurements in the typical formations which consist of the subsoils of Tokyo

(2). This project started in 1966 headed by late Professor H. Kawasumi who was the chairman of the Earthquake Prevention Committee of the Tokyo Metropolitan Government at that time. Although a convenient technique of shear wave generation was developed at that time in Japan already (3), the systematical survey of the shear wave velocities in various soils was the first one carried out in Japan as far as the author knows. In these measurements, we mainly adopted the down-hole method utilizing the bore-hole. It was proved to be quite apposite for our purpose compared with the conventional refraction survey inevitably requires wide open space which is hard to be found in the city area. In our method, only as much space where we could set the boring machine, say $5\text{m} \times 5\text{m}$ space, is needed. In addition to this advantage, we could detect the sandwiched low velocity layers at the depth, which can not be detected through the refraction survey (4). Above-mentioned geological structures are often found at the sites where the deep holocene deposits exist.

Figure 1 shows the example of pasted-up records obtained at Motokinishi, Adachi-ku. The end of the wooden plate placed firmly on the ground surface by means of the sufficient weight near the bore hole was hit horizontally by the hammer to produce the shear waves. The observations were made in the bore hole using the horizontally sensitive seismometer. One may easily notice that the shear wave arrivals are found as the first arrivals. Figure 2 shows the seismograms for P source at the same site. P waves were generated by the hammer blow of the ground surface very close to the bore hole and the observations were made by the vertically sensitive seismometer. The first arrivals in this pasted-up record are P waves. We notice the phases at the travel times of expected shear wave arrivals although the commencement is not so clear compared with Figure 1. Figures 3 and 4 are the travel time graphs for shear and P waves. Figure 5 shows the comparison of derived wave velocities and geological section. It is clear from the figure that the shear wave velocity section does reflect the geological section much better than the P wave velocity section does. This may be due to the fact that P wave velocities are very sensitive to the water content of the medium, but less sensitive in the cases of shear wave velocities.

Through the investigation, we found that, in general, the older the geological age the higher are the shear wave velocities. And if we compare the shear wave velocities of same age, the sand and gravel layers are the highest ones and then follow the sand layers. Clay layers show the slowest shear wave velocities among them. And if we exclude the sand and gravel layers, we could separate the shear wave velocities of holocene deposits from the pleistocene ones at 200 m/sec, and those of pleistocene ones from those of pliocene ones at 400 m/sec. However, we have to be careful when we talk about the weathered layers. For example, we found the shear wave velocity of mudstone (Pliocene) to be 300 m/sec in Tama District. This was found at the very top of the ground surface, where we may expect the strong effect of weathering. 600 m/sec was obtained just below this weathered layer as the shear wave velocity of fresh one. In the same way, the shear wave velocity of Kanto loam which is common in the uptown of Tokyo (Pleistocene) was found to be 150 m/sec. The weathering effect is also expected. So, we may conclude that, in the case of weathered layers, we can degrade the pliocene ones as pleistocene ones, and the pleistocene ones as holocene ones as far as the shear wave velocities in Tokyo are concerned.

As mentioned before, the shear wave velocities of holocene deposits are, generally, slower than 200 m/sec, we have subtracted the amount of times, depth (m)/ 200 (m/sec), from the travel times and constructed the so called reduced travel time graph of shear waves as shown in Figure 3. If the subsoils we are interested in are of the holocene deposits, then the right side of reduced travel time graphs for these media go up. This type of figure was extremely convenient in the case of subsoil research in Tokyo to discriminate the holocene deposits from the pleistocene ones by means of shear wave velocities.

In downtown Tokyo, the depth of the pliocene deposits (mainly mudstones) often exceeds 200 m (5). But in uptown Tokyo, we can find them in shallower depths. For example, in Yukigaya, Ota-ku, the depth of mudstones is around 5 m (1, 5). For convenience' sake, we have measured shear wave velocities of such deposits at such sites where we could find them in shallower depths in the early stage of our project. Recently, several shear wave velocity measurements down to deeper than 300 m depth were carried out (6). And the shear wave velocities of mudstones at the depths were proved to be the same with those we got before. More recently, a new project associated with the exploration of the deeper underground structure in Metropolitan area by means of the seismic refraction method down to the depth of 2-5 km has been started (Project of Yumenoshima Explosions). Through these experiments, the shear wave velocity of mudstone was reconfirmed to be around 600 m/sec (7).

Through these data, mean shear wave velocities in the typical soil layers in 23 Wards of Tokyo were determined and tabulated in Table 1.

VIBRATION CHARACTERISTICS OF THE TOKYO METROPOLIS

We are now ready to convert the geological sections into the shear wave velocity sections. Tokyo was divided into small lots (1 km \times 1 km) using the coordinates as shown in Figure 6. At 604 1 km-mesh points as well as at 212 supplementary points, in-between the mesh points, where the appreciable changes of the geological structures were found, the shear wave velocity sections were determined. The responses at these sites due to the multiple reflections of shear waves in the surface layers were then computed assuming that the spectra of incident seismic waves were white. The computations were made in the frequency range from 0 to 10 Hz at frequencies every 0.1 Hz interval. The loss of energy of seismic waves in the soil layers is also taken into consideration. Since we do not have much data associated with the attenuation of the seismic waves in the surface layers, we made the assumption that the Q-values of every surface layer were 20 consulting our data obtained during the shear wave velocity measurements (8). Our results are tabulated in Table 2. The assumption we made in the computations may result in the overestimation of the responses. We did so, from the view point of antiseismic designing, the overestimation of the input force would be safer than the underestimation. The results of computations were published in 1970 and 1975 respectively from the Tokyo Metropolitan Government (9).

Through the study, the vibration characteristics of the sites such as predominant frequencies and the amplification magnitudes were clarified to some extent. We may now compare the results within the area where we found the same geological formation as the base rock. But, we cannot extend this idea all through the 23 Wards. Since, we could not find the

TABLE 1

SHEAR WAVE VELOCITIES USED IN THE COMPUTATION

Notation	Density (gr/cm ³)	Velocity (m/sec)	Note
AL	1.4	80	Peat
ALO	1.5	100	Clay, N < 5
ALP	1.5	90	Humus Soil
* BL	1.4	150	Buried Loam
* ED	2.0	400	Gravel, Sand and Gravel
* ED2	1.5	200	Clay, Silt, Clayey Soil
* ED6	1.8	250	Sand, Sandy Soil, 10 < N < 30
* HO	2.0	400	Gravel, Sand and Gravel
* HO5	1.8	250	Sand, Sandy Soil, 10 < N < 30
* HO6	1.8	250	Sand, Sandy Soil, 30 < N
** KA3	1.9	400	Clay, Clayey Soil, 30 < N
** KA6	2.0	600	Sand, Sandy Soil, 30 < N
* LC	1.5	200	Loamy Clay
* MG	2.0	300	Gravel, Sand and Gravel
NA1	1.5	150	Alternation of Loose Clay and Sand, 5 < N < 10
NA2	1.5	170	Clay, Silt, Clayey Silt, 10 < N < 30
NA5	1.8	250	Sand, Sandy Soil, 10 < N < 30
NA6	1.8	250	Sand, Sandy Soil, 30 < N
* TG	2.0	300	Gravel, Sand and Gravel
* TG1	2.0	300	Gravel, Sand and Gravel
* TG2	2.0	300	Gravel, Sand and Gravel
* TML	1.4	150	Kanto Loam
* TO	2.0	400	Alternation of Fine Sand and Hard Clay
* TO1	1.5	150	5 < N < 10
* TO6	1.9	300	Sand, Sand with Gravel, 30 < N
* TOG	2.0	400	Gravel, Sand and Gravel
TS	1.5	100	Top Soil
YLO	1.5	100	N < 5
YU4	1.8	170	N < 10

N: Number of blows, Standard Penetration Test.

* Pleistocene, ** Pliocene, otherwise Holocene.

ED: Edogawa Formation, HO: Hongo Formation, KA: Miura Group, NA: Nanago Formation, TO: Tokyo Formation, YL, YU: Yurakucho Formation.

TABLE 2
Q-VALUES OF SOILS

No.	Location	S-wave Velocity	Q	Geology
1	Adachi	260 m/sec	8	Pleistocene Sand
2	Sunamachi	102	20	Holocene Silt
3	Yukigaya	420	6.5	Pliocene Mudstone
4	Yayoi	150	5	Kanto Loam

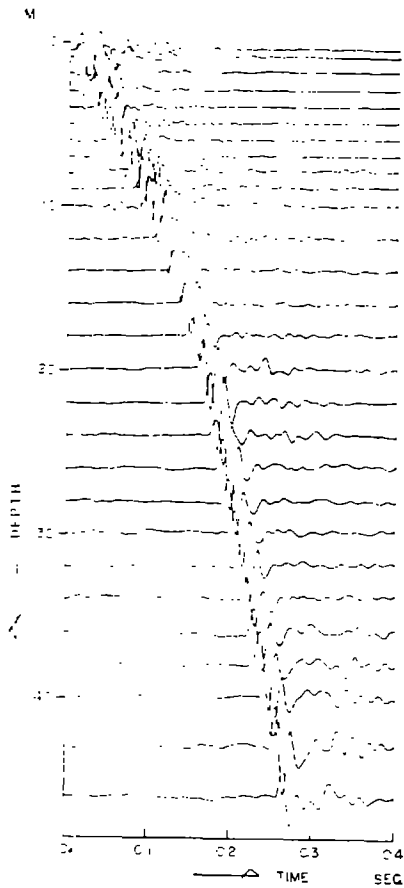


Figure 1. Pasted-up seismograms of shear arrivals.

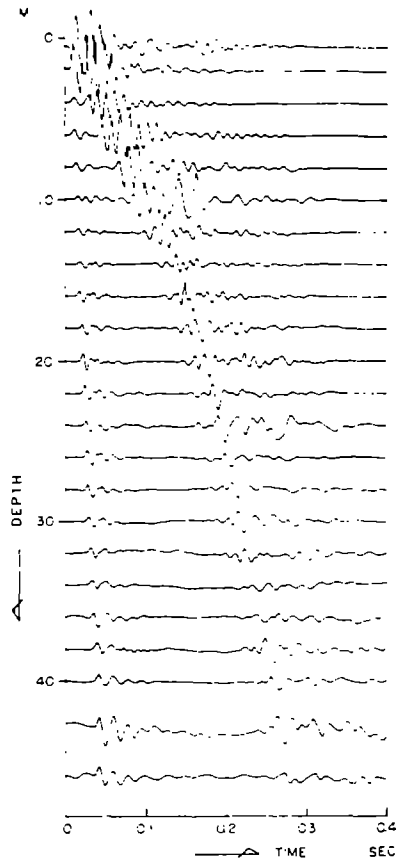


Figure 2. Pasted-up seismograms of P arrivals.

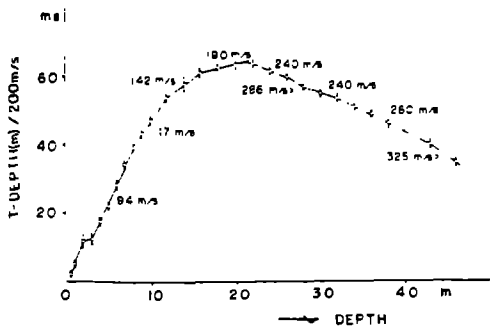


Figure 3. Reduced travel time graph of shear waves. Bars show 95 % confidence interval.

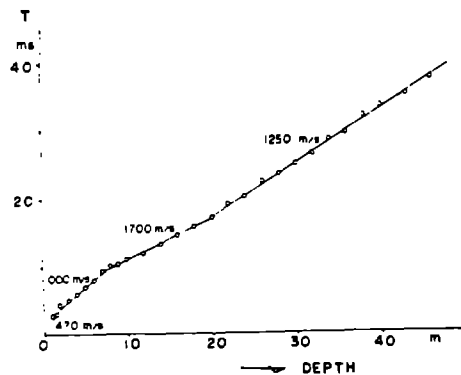


Figure 4. Travel time graph of P waves.

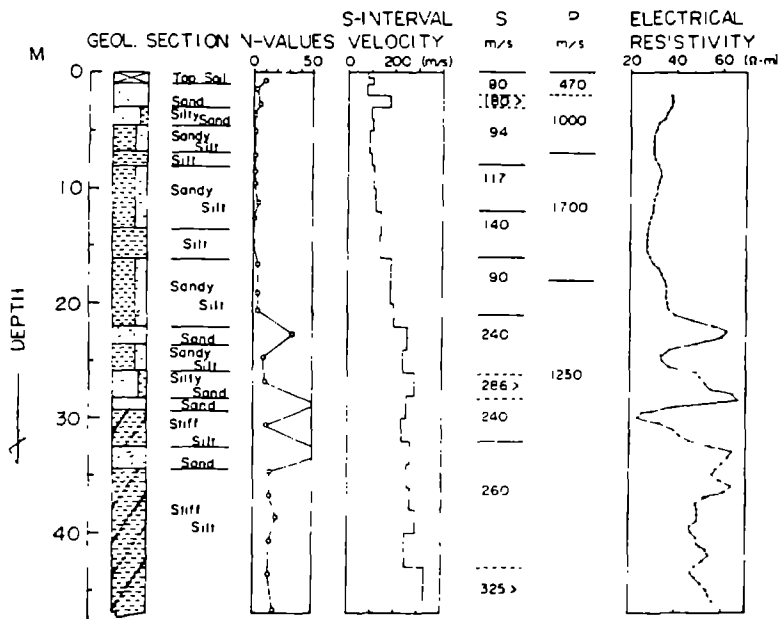


Figure 5. Comparison of derived wave velocities and geological section.

common base rock from the geological sections all through the area. This is inconvenient from the political point of view, since we have to consider the counterplan for the future earthquake damage expected in Tokyo as a whole. And it will take a lot of time until we get the sufficient information down to the pliocene mudstone formation all through the area.

The following attempt was made to get rid of the above-mentioned difficulty. Figure 7 shows the relation between the shear wave velocity ratios of surface and the basement formations and the amplification magnitudes taken from the data of former computations. "o" and "x" in the figure show the magnitudes of longest period predominant responses and those of largest predominant responses respectively. Although plots were made all for 816 points, the mean values of amplification magnitudes for each velocity ratio are shown in Figure 7 for simplicity. There is a fairly good linear relation between two variables. It is interesting to note that, in deriving the above-mentioned relation, we did not care anything about the thickness or number of layers which consist of the velocity section at the site. Thus, we may estimate the relative magnitudes of peak spectral densities approximately by comparing the surface shear wave velocities at the sites even if we do not know the shear wave velocity of the base rock, since it is common. The predominant frequency at the site is an important information in estimating the input force to the structure due to the earthquake. However, in the relation above, the information related to the predominant frequency is lost completely. So, to take care of this information, we computed the square roots of the powers of responses to estimate the relative magnitudes of vibrations at the sites. Then we compared them with the velocity ratios as we did before. The relation is shown in Figure 8. Consulting the figure, the seismic micro-zoning map of 23 Wards of Tokyo shown in Figure 9 was proposed for the counterplan of future earthquake hazard. To get the relative magnitudes of the vibrations, we selected the site of Kanto loam as the standard site.

To prove the validity of this map, we have correlated this with the damage distribution map of 1923 Kanto Earthquake (10). A good correlation was found between them.

CONCLUDING REMARKS

It is reasonable to consider that the relative vibration magnitudes are associated with the ground velocity, since the incident wave spectrum is assumed to be white with respect to the ground velocity from the view point of engineering seismology. It follows from Figure 9 that the site of peat will receive about 4 times more seismic energy compared with the site of sand. The risk of damage due to the earthquake is thus much higher at the peat site than at the sand site. According to Imamura (11), the maximum amplitude of 1923 Kanto Earthquake observed at Hongo, University of Tokyo campus (surface geology is Kanto loam), was 4.45 cm with 1.35 sec period. He also stated that the amplitude of 0.3 sec wave was about 5.3 mm. From these data, we could obtain the maximum velocity values as 20 kine (= cm/sec) and 11 kine respectively. May be 15 kine, taking the mean value of above derivings, would be the realistic value of maximum velocity in Hongo at that time. If we use this value, we may estimate the maximum velocity at the other site consulting the map. Associated with the displacement amplitudes, we may expect larger one in downtown Tokyo compared with that of uptown, since the predominant period in downtown is much longer than that of uptown. On the other hand, we may

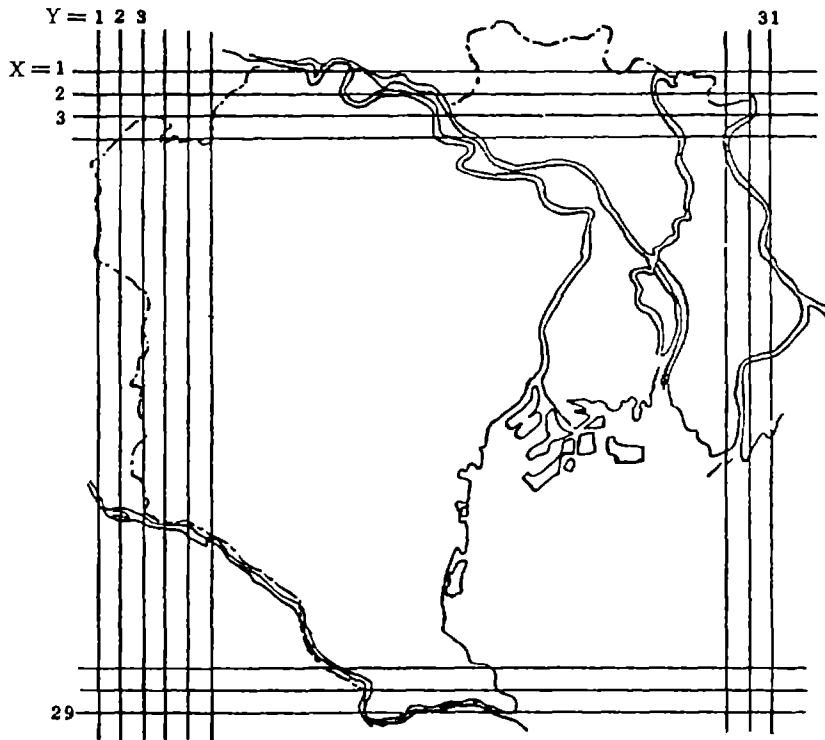


Figure 6. Coordinate.

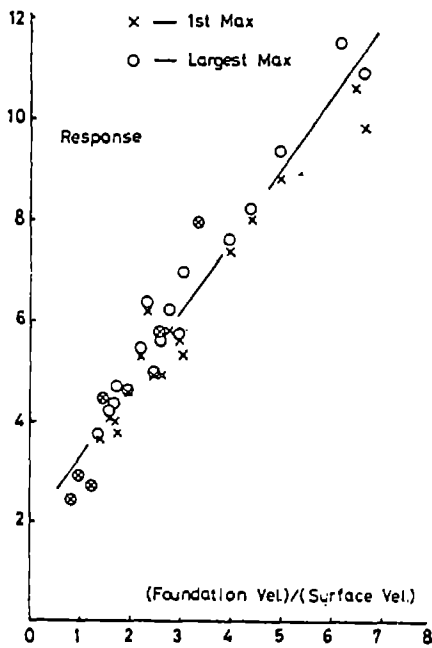


Figure 7. Relation between the shear wave velocity ratios of surface and the basement formations and the amplification magnitudes.

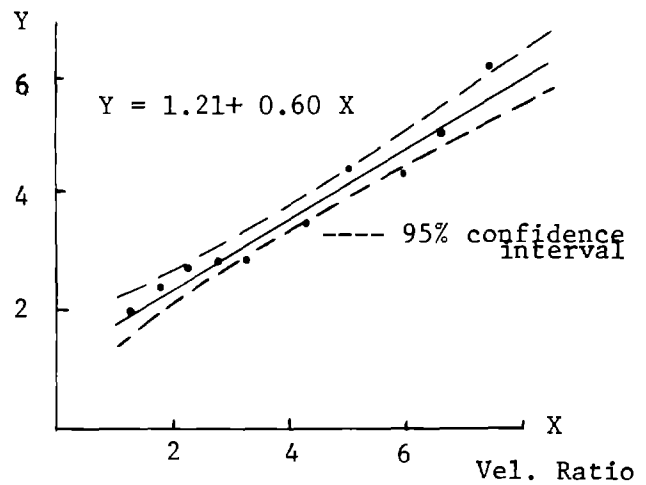


Figure 8. Relation between the shear wave velocity ratios of surface and the basement formations and the square roots of powers of responses.

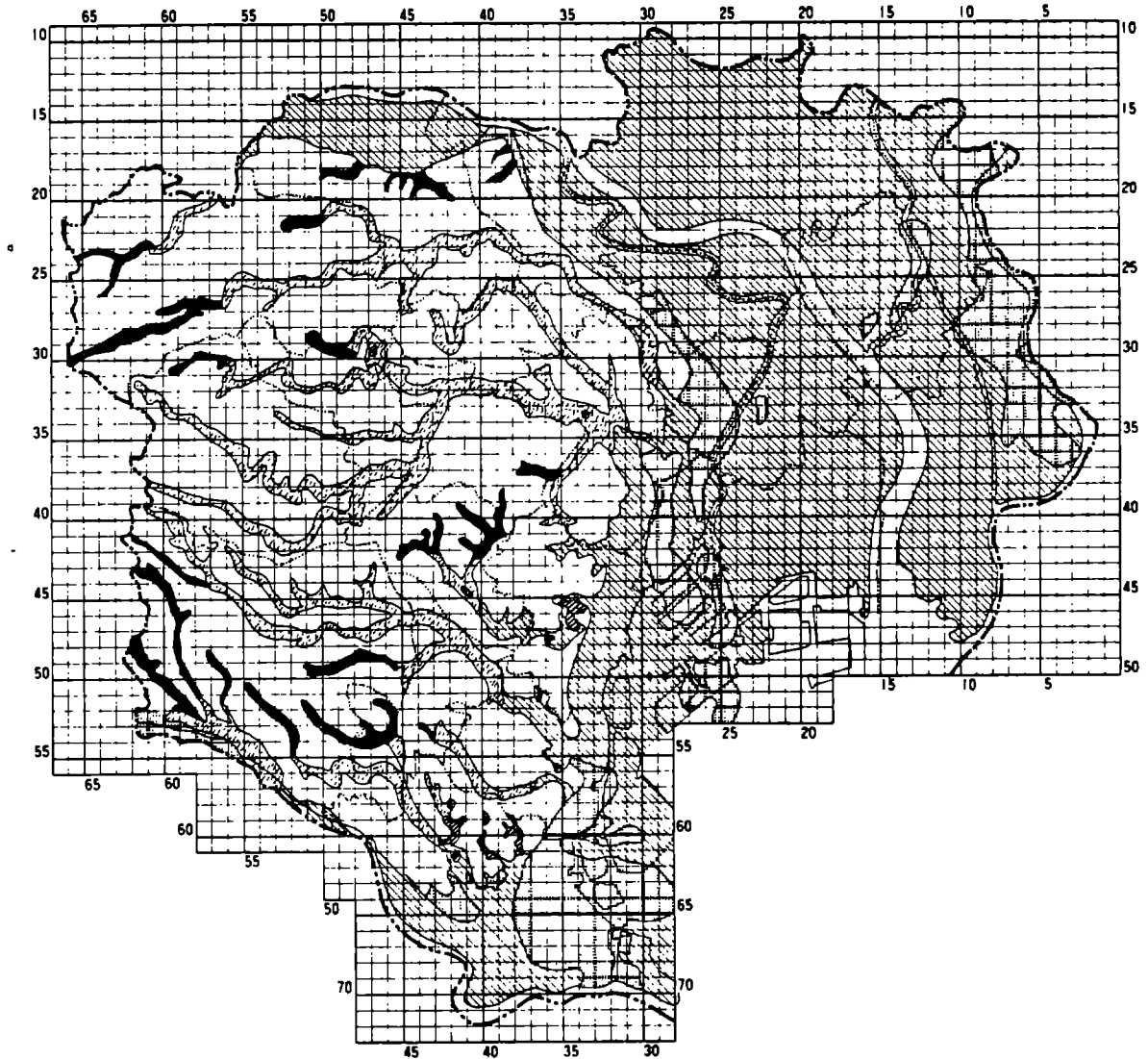

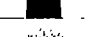
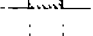




Figure 9. Seismic microzoning map
of 23 Wards of Tokyo.

Geology	Indication	S-Velocity m/sec	Relative Ampl.
Peat		80	1.6
Humus Soil		90	1.4
Clay A, B		100	1.3
Kanto Loam		150	1.0
Sand		170	0.9

expect larger acceleration in uptown because of the shorter natural period than that of downtown.

It should be noted that the longest predominant period expected in Tokyo due to the multiple reflections of shear waves in the soil layers above the pliocene mudstone assigned as the base rock in this study is around 2 sec. The seismic microzoning map proposed in this study is thus applicable to estimate the damage of structures having the natural periods shorter than 2 sec.

Recently, we are having more and more structures of longer natural periods. If we are interested in the damage estimation of such structures, we have to assign the base rock in the depth deeper than the mudstone formation. The information associated with the shear wave velocities in the depths is thus inevitable. For this purpose, the Project of Yumenoshima Explosions is now in progress to explore deep underground structure down to 2-5 km depth in Tokyo Metropolitan area.

REFERENCES

- 1) Institute of Civil Engineering, Tokyo Metropolitan Government, Geology of Tokyo Metropolitan, No. 2 (1969).
- 2) H. Kawasumi et al., S Wave Velocities of Subsoil Layers in Tokyo, Bull. Earthq. Res. Inst., 44 (1966), 731-747.
E. Shima et al., S Wave Velocities of Subsoil Layers in Tokyo, Bull. Earthq. Res. Inst., 46 (1968), 759-772; 46 (1968), 1301-1312; 47 (1969), 819-829.
- 3) N. Kobayashi, A Method of Determining of the Underground Structure by Means of SH Waves, Zisin, ii, 12 (1959), 19-24.
E. Shima and Y. Ohta, Experimental Study on Generation and Propagation of S Waves I, Bull. Earthq. Res. Inst., 45 (1967), 19-31.
- 4) E. Shima et al., Experimental Study on Generation and Propagation of S Waves IV, Bull. Earthq. Res. Inst., 46 (1968), 517-528.
- 5) Institute of Civil Engineering, Tokyo Metropolitan Government, Geology of Tokyo Metropolitan, No. 1 (1963).
- 6) Investigation Committee of Geology and Subsoils in Koto District, Geology and Subsoils in Koto District, (1977).
- 7) E. Shima et al., On the Base Rock of Tokyo, Bull. Earthq. Res. Inst., 51 (1976), 1-11; 51 (1976), 45-61; 53 (1978), 305-318.
- 8) K. Kudo and E. Shima, Attenuation of Shear Waves in Soil, Bull. Earthq. Res. Inst., 48 (1970), 145-158.
- 9) H. Kawasumi et al., Vibration Characteristics of 23 Wards of Tokyo (Tokyo-to 23-ku no Ziban no Response oyobi Shindo-Bunpu ni kansuru Chosa Kenkyu), Earthquake Prevention Committee of Tokyo Metropolitan Government.
- 10) H. Kawasumi, Relation between the Damage Distribution and the Nature of Subsoils in Tokyo and Osaka (Tokyo, Osaka Ryo-toshi no Shingai-Bunpu to Ziban), Shigen Data Book, No. 6 (1952), 18-25, Shigen-Chosa Kai.
- 11) A. Imamura, Reports of the Imperial Earthquake Investigation Committee, No. 100 A (1925), Iwanami Shoten.

444

INTENTIONALLY BLANK

MICROZONING OF OSAKA REGION

by

S.Yoshikawa^I, Y.T.Iwasaki^{II} and M.Tai^{III}

ABSTRACT

Microzoning of Osaka region has been studied in several respects from geological ground condition to social effects due to earthquake disaster. In this paper, the results of the following research works are summarized.

1. Tectonic conditions and active fault system
2. Design earthquakes
3. Dynamic characteristics of local soils
4. Earthquake response of Osaka ground
5. Vulnerability against earthquake disaster

INTRODUCTION

Damages of earthquake has been realized and stressed to depend upon various local factors of ground conditions as well as social environments. In Osaka, microzonation technique has been used to give basic data to clarify the nature of the hazards and the problem concentrated zones. The results are to be used to establish methodology of the short and long term planning to prevent earthquake disaster and to make aseismic urban structure.

On microzonig of Osaka, the authors have reported the basic characteristics of the area and a method to assess the building vulnerability based upon response spectral technique applied for elasto-plastic soil-structure system(1). In this report, seismic activity, geological and soil conditions of Osaka region is reviewed based on recent results of the research works and the some applications on vulnerability of the region is discussed.

TECTONIC AND ACTIVE FAULT SYSTEM

South-west of Japan, where Osaka is located, is considered in a stress state caused by the surrounding tectonic plates of Pacific Ocean and Philippine Sea plates. The distribution of the historical damage earthquakes near Osaka is shown in Fig.1 as well as the active fault system in the area. The epicenters of the earthquakes are found to have good coincidence to the present active fault sytem in south-west Japan. The fault system causing the great damage earthquakes in the region are considered to be divided into two major groups; one is related with the direct geotectonic movement of plate subduction at the Pacific Ocean side of Japan island and the other is related with the fault block movement in the island induced by the tectonic stress due to the plate subduction.

The axis of principal compression stress, which have been obtained by the analysis of the earthquake mechanism based upon the initial motion of the seismic P-wave from the earthquakes occurred in the area, is east-west direction for the shallow earthquakes within the depth of 30 km and north-south direction for the deep earthquakes deeper than 30 km. The each different direction of the compression stress is considered due to Pacific Ocean and Philippine Sea plate respectively as shown in Fig.2(2).

East part of the south-west of Japan is particularly characterized by triangular shape of the geological formation of the Kinki Triangle

I Prof. Disaster Prevention Research Inst., Kyoto Univ.

II Act. Director, Osaka Soil Test., Geo-Research Inst., Osaka

III Research St., Osaka Soil Test., Geo-Research Inst., Osaka

Structure". The geological formation of the inside and outside of the structure is different each other. The inside of the structure is composed of granitic rock which is much softer and more plastic than the outside zone of paleozoic rock formation. The difference of the mechanical characteristics have resulted in special feature of the tectonic structure in the area as shown in Fig.3. In the surrounding part of the outside of the Kinki Triangle Structure, the present active fault system is two sets of strike slip faults shown in Fig.4. One is left lateral strike slip with NW-SE direction and the other is right lateral with SW-NE direction as the conjugate system to the former one. The boundary of the triangular structure is complicated with strike slip as well as dip slip of reverse type faults. Those faults system shown in Fig.4 are well correspondent to the general pattern caused by westwards tectonic stress field by two plates.

The magnitude of the earthquakes by direct subduction of the plates have ranged over $M = 8$, while that of the earthquakes occurred in the island of south-west Japan by block movements have resulted $M=7.5$ as the maximum magnitude in the history of the damage earthquakes since 416A.D..

The seismicity associated with the above two types of tectonic structures are considered to be major damage potential earthquakes to Osaka region.

DESIGN EARTHQUAKES

A probabilistic approach was made to estimate design earthquakes to Osaka site in terms of magnitude, epicentral distance and return period. In the analysis, Gumbel's model is introduced to simulate the occurrence of the maximum magnitude earthquake in a given time and in a given epicentral distant zone (3). Data used for the analysis are from two sources, one is historically documented damage earthquakes from 599 A.D. to 1773(4) and the other is instrumentally observed earthquake data reported by Japan Meteorological Agency from 1925 to 1970. The historical earthquakes consist of magnitude 5 to 8.5, while the observed earthquakes consist of mainly much smaller scaled magnitude of 4 to 6.

The earthquakes to be analysed are grouped into two types according to the above mentioned different geotectonic zones of inside of the island and the plate subduction at marginal side of the Pacific Ocean.

Some of the results are shown in Fig.5, where the equireturn period lines of earthquake with a magnitude and at an epicentral distance are estimated for each zone. In each geotectonic zone analysed, earthquake occurrence are realized to have the higher possibility at a specified epicentral distance. The earthquake of block movements type are found to have higher possibility (or shorter return period for a given magnitude) at epicentral distance of about 40, 80, 130 and 170 km. Based on the above results, two types of the most likely possible damage earthquakes for the Osaka region are selected. One is inside of the island type with epicentral distance of about 30 - 50 km. The other is plate subduction type earthquake with epicentral distance of about 130 km. The magnitude of the above earthquakes may be determined according to the design return period. The estimated magnitude based on the return period $T_r=1,000$ years is Mag.7 -7.3 for the block movements type and Mag.8.3 for the subduction type.

The characteristics of the bed rock motions for the above two design earthquakes are estimated based on several proposals(5,6,7) of the relationship among the magnitude, epicentral distance and the ground motion characteristics of maximum acceleration, velocity, predominant period of the motion and the duration time of the motion. The shape of the response spectra as well as the shape of the envelope of the acceleration time history (8) is introduced to obtain artificially composed time history of the acceleration wave.

DYNAMIC CHARACTERISTICS OF SOILS IN OSAKA

Osaka ground is principally delta plane open to Osaka Bay with soft alluvial formation of thickness about 10 - 20 m and less than 35 m. The depth of granitic base rock varies in the area from 600 to 1,500 m. Above the base rock, sedimentary formations of tertiary and quarternary cover the most part of the Osaka basin as shown in geological map of Fig.6.

In the central part of the Osaka basin, anticline structure with axis of north-south direction divides the delta plane into two part of east and west sides of Osaka basin. The top subsurface of alluvial layer consists from loose sand(S.P.T. value $N=5-10$) and soft clay(L.L.=60-120, P.L.=20-40 $w=40-100$, $q_u=0.4-1.0\text{kg/cm}^2$) . Diluvial layers consists of very dense sand and gravel(N more than 50) and very stiff clay($q_u= 2-10 \text{ kg/cm}^2$).

The in-situ shear velocity measurement for various geological formations have been carried out in the Osaka area. The most conventional method have been the down hole measurement with surface source and borehole geophone fixed to the wall of the borehole.(9) Recent developement of the shear wave velocity determination by downhole method does not require the geophone to be fixed to the borehole wall. This method is based upon to measure the horizontal water movement in the borehole which is the same as that of the surrounding media, provided that the shear wave travels vertically upward or downward and the wave length of the shear wave is much longer than the diameter of the borehole, which are satisfied in most cases of in-situ conditions (10).

These measured S-wave velocities for various geological formations are shown in Tab.1. The measured velocity ranges from 90-150m/sec of recently reclaimed filled layer, 200-400m/sec. of diluvial clay, 300-600m/sec. of diluvial sand and gravel to 500-1,000m/sec. of tertiary formation.

Osaka alluvial clays are found to have the ratio of initial rigidity at small strain to the shear strength in rather wide range of 500 to 1,500 (11).

The strain effects on the rigidity for Osaka soils have been studied through laboratory tests. It is shown that the elastic limit strain level at which the strain softening starts depends upon physico-chemical micro structural characteristics of the soil (12). The elastic limit shear strain levels are found from 10^{-5} for sand to 10^{-3} for highly plastic clay as shown in Fig.7 (13). Damping characteristics of soils is found to increase with decrease of rigidity due to softening (13). The following expression of Hardin-Drnevich model(14) is assumed for soils in Osaka.

$$D = D_f(1 - G/G_0)$$

where D_f : damping ratio at failure
 G_0 : initial rigidity at small strain level

EARTHQUAKE RESPONSE OF OSAKA GROUND

Response of the Osaka ground due to two types of the design earthquakes were obtained through computer simulation technique.

For the first approximation, one dimensional upwards wave propagation is considered. The direction of the wave propagation in the Osaka ground assuming horizontally incoming body wave through base rock is shown in Fig.8. Fig.8 shows the clear tendency that the horizontally incoming body wave is to become almost vertically upwards direction. However, incoming surface wave and induced surface waves in the Osaka basin are considered to have different features of its characteristics and is to be discussed in the future. For the present study, one dimensional upwards wave propagation is studied to clarify the characteristics of earthquake response due to horizontally incoming body waves.

Osaka ground has two major different formations based on the comparison

of the wave impedance ratio as well as soil mechanical characteristics. One is shallow surface structure of the soft alluvial layers and the other is deeper structures of diluvial and tertiary formation down to the base rock. 8 models of the alluvial structures to present for various thickness and its components are considered. 5 models are also considered to simplify various conditions of the deeper structure of the diluvial and tertiary formation. Thus Osaka grounds are expressed as the combination of the above shallow and deep structural models.

Computer simulation for earthquake ground motion is based upon wave equation using strain dependent rigidity and damping factor. The maximum ground motions and the predominant period of the surface motions as well as the maximum shear strains induced in the alluvial layer.

The results of the computation of the maximum acceleration and velocity is plotted against the thickness of the shallow structure of alluvial layer and shown in Fig.9. The maximum acceleration at the surface increases with the thickness of the alluvial layer upto 5 - 10m then decreases with the increase of the thickness of the layer. The maximum velocity at the surface increases with the thickness of the alluvial layer upto 10 m and keeps rather constant for the thicker layer. The response spectra of the top surface motions are found to have much effects of the deeper structures as well as shallow structures than the maximum values of the surface motion of acceleration and velocity.

Osaka ground has some experiences of sand liquefaction (Ansei earthquake Dec.23 and 24,1854, M=8.4, epicentral distance=160km, Tango earthquake March 7,1927, M=7.5, epicentral distance=110km, Kawachi earthquake Feb.20,1936, M=6.7, epicentral distance=10 - 30km). Eventhough the liquefaction have been reported without severe damages in the case of the above historical earthquakes, the present enlarged urbanized area onto the softer and thicker alluvial plane and therefore the ground failure due to liquefaction may cause structural damages in the area. The liquefaction potential in Osaka area is estimated through a modified method based on a simplified procedure (15).

The relation between the cyclic number n_L and stress ratio τ_L/σ_V is given by the following equation (16).

$$n_L = \left(\frac{3}{4} - f\left(\frac{\tau_L}{\sigma_V}\right) \operatorname{cosec} \psi_L^* \right) / a \left(f\left(\frac{\tau_L}{\sigma_V}\right) - \frac{1}{4} \right)^2$$

$$f\left(\frac{\tau_L}{\sigma_V}\right) = \left(\left(\frac{\tau_L}{\sigma_V}\right)^2 + \frac{1}{16} \right)^{1/2}$$

where

ψ_L^* = internal friction angle for liquefaction

The area is divided into meshes of 1,000x1,000 or 500x500m and the liquefaction potential for each mesh was estimated based on the design earthquakes. The results are shown in Fig.10 as the degree of the liquefaction potential. (see Fig.6 for meshed zone)

VULNERABILITY AGAINST EARTHQUAKE DISASTER

There are many factors to be considered related with earthquake disaster in Osaka region. The earthquake damage may consist of two steps of primary and secondary phases. Damages of the primary phase is the direct hazards from earthquake ground motions for buildings, structures, life line systems and etc. The secondary phase consists of fire, panic and econo-social hazards as a later phase effects due to primary damages.

In Osaka area, among the many uncertain factors to widen the secondary phase damages, the failure of the wooden residential houses is considered as the most important damage in the primary phase to increase loss of life

as well as the number of burnt houses.

The long term disaster prevention plan aiming at making earthquake resistive urban structure should be based on the present failure possibility of the wooden houses. The short term disaster prevention plan, on the other hand, which is rather refuge planning, needs to assess the problem concentrated area in the region based upon the failure of the wooden house as primary phase.

The failure of the wooden houses are considered due to two main factors; one is structural failure due to vibration of the superstructure and the other is foundation failure due to failure of ground.

The superstructural damage of the houses are estimated based on the response spectral value and the damage criteria. The experimental results of wooden house failure due to cyclic loading are summarized as follows; the relative displacement exceeding 7 - 10 cm begins to fail and reaching 15-20 cm make the wooden houses in complete failure state. The estimated number of the failed houses in meshes of 500x500m are shown in Fig.11 as the failure density in a mesh.

The degree of the foundation failure may increase with the increase of the shear strain induced in subsurface alluvial layer and the liquefaction susceptibility. In the area, the shear strain level of 1 % is considered as large enough to cause the foundation failure and the estimated results are shown in Fig.12. The total failure estimated for superstructure and foundation are shown in Fig.13 as total failure intensity. The results clearly indicate the existence of some zones with concentration of anticipated failure.

Osaka region as developed as time and becoming big-urbanized has not enough space available for shelter in case of the earthquake emergency. The refuge allocation planning from hazardous residential areas to several selected and arranged shelter zones have been studied with respect to acceptable number of the refuge of each shelter zone and time necessary for citizen in some area to reach the shelter zone. Some zones are pointed out too far to walk or too crowded by narrow street on the way. Emergent refuge planning to prepare enough shelter spaces and safety route to the zone is to be carried out based on the above assessment of the primary hazards.

Longterm base project of disaster prevention planning is being proposed to connect the results of microzonation with redevelopment plans for the urbanized area in Osaka.

CONCLUSIONS

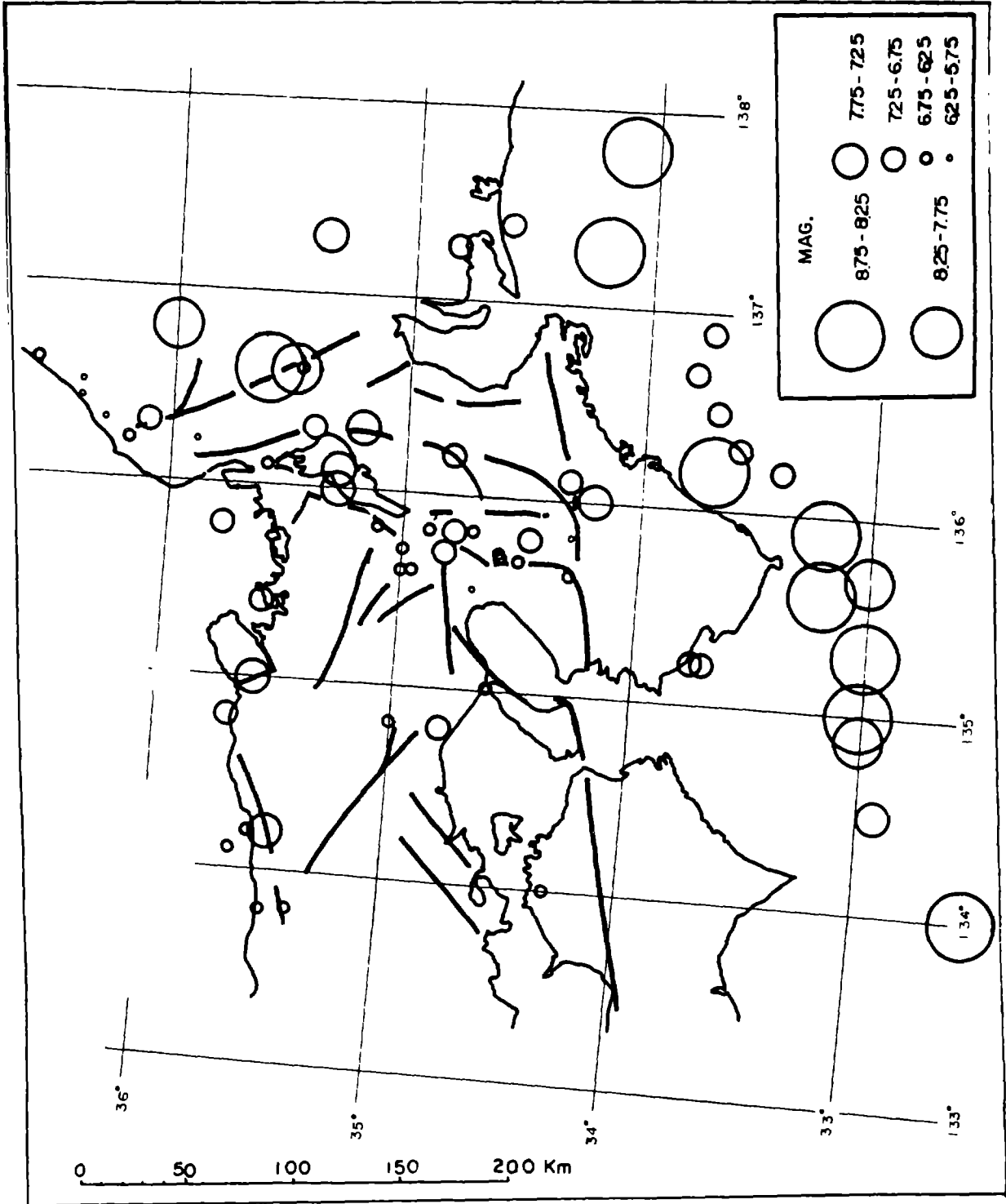
Some results of the present microzonation studies for Osaka region are presented. The conclusions obtained are as follows;

1. Based on the geotectonic activity near Osaka, two types of the design earthquakes are considered.
2. Sedimentary formation of about 1,500 - 600 m in thickness on the granitic base rock is considered as subsurface structure in the region.
3. Earthquake response of the ground is calculated assuming non-linear characteristics based on the shear wave velocity and laboratory test results.
4. Liquefaction potential in the region is estimated and some places are found to be likely to liquefy.
5. The failure of wooden houses is considered as one of the major primary hazards to be considered resulting in severe secondary phase damages.
6. The main factors to cause failure of the wooden houses are that of superstructure due to vibration and that of foundation due to ground failure.
7. Zoning map for estimation of damages of wooden houses is presented and problem concentrated zones are clarified.
8. The emergency refuge plan is briefly discussed based upon the results of the zoning map above described.

BIBLIOGRAPHY

1. Kobori, T., Yoshikawa, S., Minai, R., Suzuki, T. and Iwasaki, Y.T. (1972) "Effects of Soil and Geological Conditions on Structural Responses in the Osaka Area", Proc. of Inter. Conf. on Microzonation, Seattle, Nov., 1972
2. Huzita, K., Kishimoto, Y. and Shiono, K. (1973) "Neotectonics and Seismicity in the Kinki Area, Southwest Japan", Jour. of Geoscience, Osaka City Univ. Vol. 16, Art. 6 pp. 93-125
3. Yoshikawa, S., Iwasaki, Y.T. and Ishii, E. (1977) "A Probabilistic Approach to estimate Design Earthquake For a Site in Terms of Magnitude, Epicentral Distance and Return Period", Preprint, Proc. of Sixth World Conference on Earthquake Eng., Vol. 2, pp. 2-337 - 2-242, New Delhi, Jan., 1977
4. Usami, T. (1975) "Japanese Damage Earthquake Manual", Univ. of Tokyo Press.
5. Kanai, K. (1957) "Semi-Empirical Formula for the Seismic Characteristics of the Ground." Bull. of E.R.I., Univ. of Tokyo, 35(2), pp. 309-325
6. Kanai, K. (1961) "An Empirical Formula for the Spectrum of Strong Earthquake Motions", Bull. of E.R.I., Univ. of Tokyo, 39(1) pp. 85-96
7. Schnabel, P.B. and Seed, H.B. (1972) "Acceleration in Rock for Earthquakes in the Western United States", EERC 72-2, University of Calif., Berkeley
8. Jennings, R.C., Housner, G.W. and Tsai, N.C. (1969) "Simulated Earthquake Motions for Design Purpose", Proc. of 4th World Conf., Earthquake Engineering, Santiago, Chile, 1, A-1, pp. 145-160
9. Kitsunezaki, C. (1966) "Observation of S-wave by the Special Borehole Geophone", Geophysical Exploration, VOL. XX, No. 1, The Soc. of Exploration Geophysicists of Japan
10. Kitsunezaki, C. (1975) "Shear Wave Logging by Suspension-type Geophone", Geophysical Exploration, Vol. XXVIII, No. 1, pp. 13-21
11. Shibata, T. and Iwasaki, Y.T. (1977) "Seismic Problems of Soft Clay Deposits" Preprint of State of the Art Report, Int. Symp. on Soft Clay, Bangkok, 1977
12. Nakagawa, K., Iwasaki, Y.T., Okuda, T. and Tsurumaki, M. (1977) "Elastic Moduli of Undrained Clayey Soils based on Clay-Water-Electrolyte System", Proc. of Specialty Session No. 9, 9th ICSMFE, Tokyo
13. Nakagawa, K. (1975) "Measurement of Shear Wave Velocity in Soils", Jour. of Geoscience, Osaka City Univ., Vol. 19, Art. 7
14. Hardin, B.O. and Drnevich, L.P. (1970) "Shear Modulus and Damping in Soils; Design Equations and Curves, Techn. Rep., UKY27-30-CE3, Univ. of Kentucky
15. Seed, H.B. and Idriss, I.M. (1970) "A Simplified Procedure for Evaluating Soil Liquefaction Potential", EERC 70-9, Univ. of Calif., Berkeley
16. Shibata, T. and Yukiwaka, H. (1970) "Liquefaction of Saturated Sands During Cyclic Loading", Proc. of Japanese Soc. of Civil Eng., Vol. No. 180, Aug., 1970

Fig.1
 Distribution of
 Historical
 Damage Earthquakes
 near Osaka Region
 and Active Fault
 System



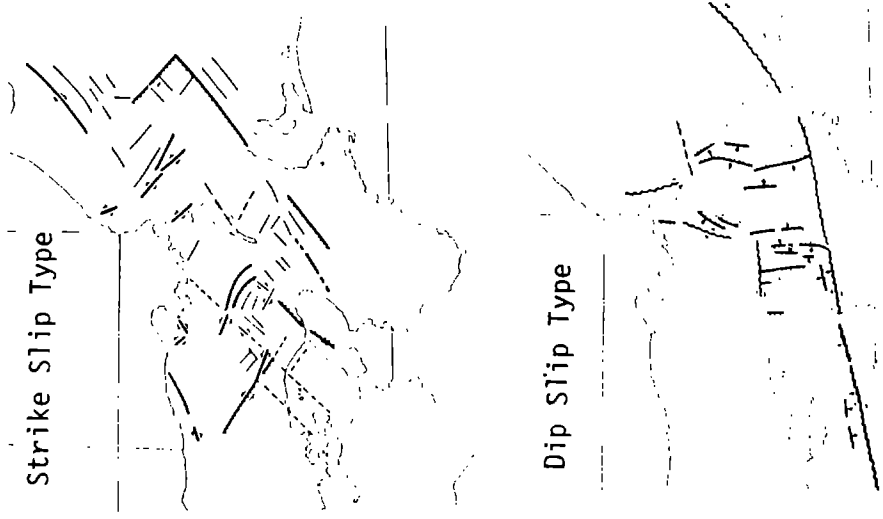


Fig.4 Fault System around Kinki Triagle Structure (after Huzita(1973))

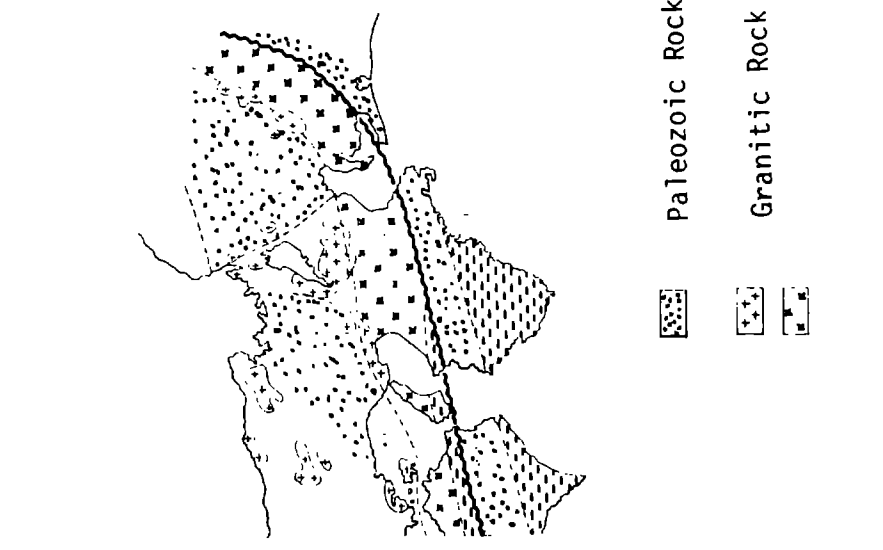


Fig.3 Kinki Triangle Geological Structure (after Huzita(1973))

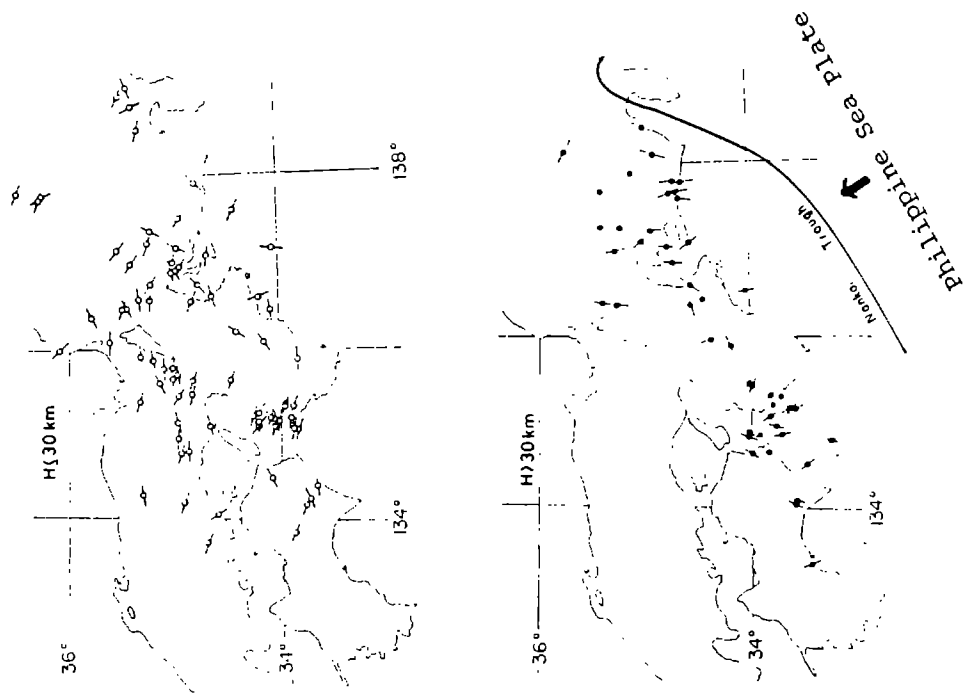


Fig.2 Distribution of the Directions of Axis of Compressional Principal Stress Analysed by Earthquake Source Mechanics(after Shiono(1973))

Fig.5 Equi-Return Period Lines of Earthquakes near Osaka

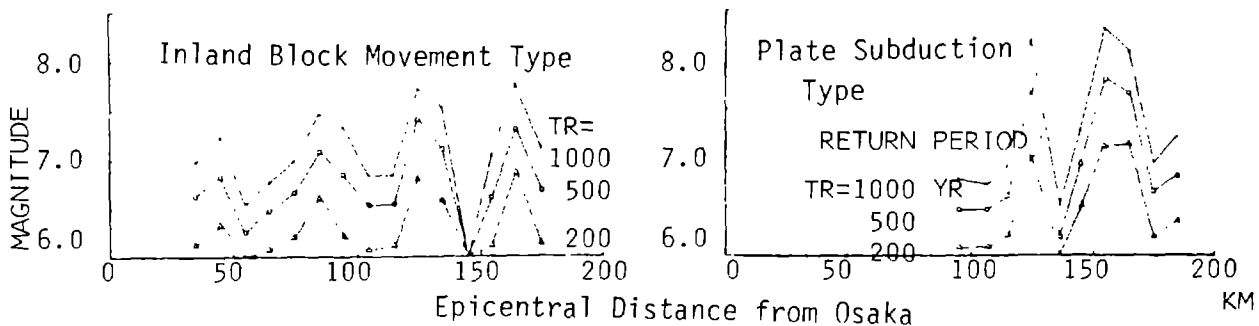


Fig.6 Geological Map of Osaka Area

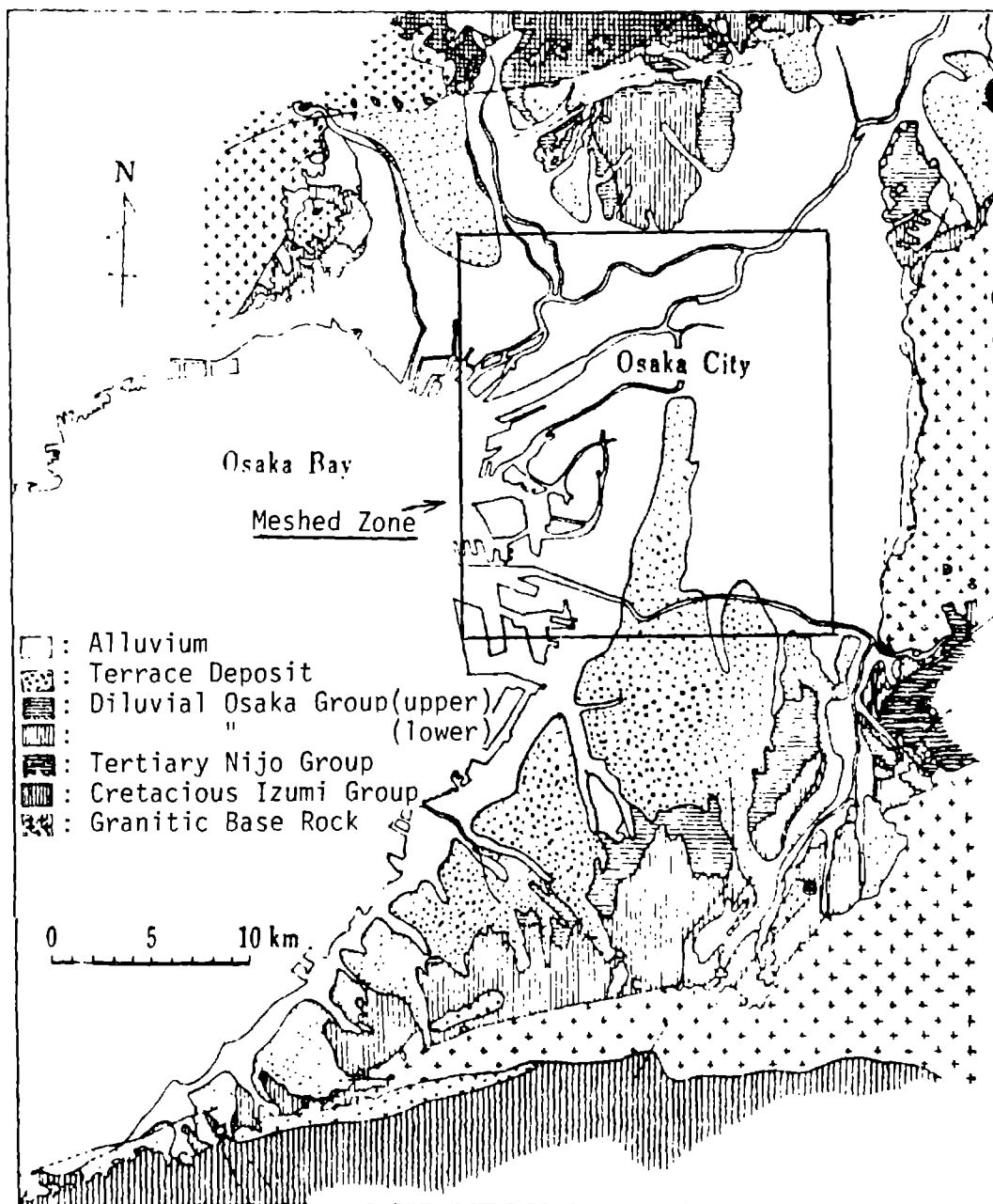


Table-1 Shear Wave Velocity of Geological Formation in Osaka Area

formation	V_s m/sec	unit weight
reclaimed clay	90-110	1.4-1.5
reclaimed sand	110-150	1.6-1.7
alluvial clay	90-190	1.5-1.6
alluvial sand	110-200	1.7-1.8
diluvial clay	200-400	1.6-1.7
diluvial sand	300-600	1.8-1.9
tertiary	500-1,000	1.9-2.1
granite	2,700-3,000	2.7

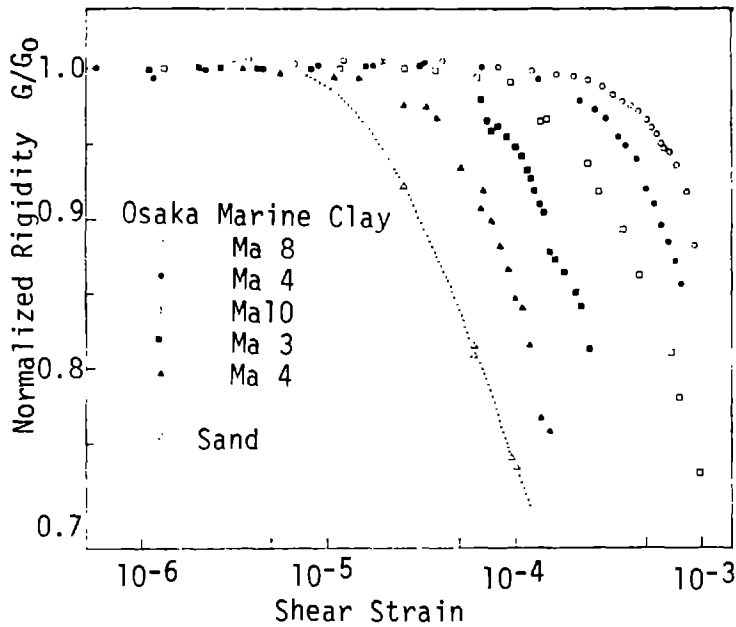


Fig.7 Normalized Rigidity vs Shear Strain Obtained by Resonant Colum Method (after Nakagawa (1975))

Fig.8 Computed Max. Acceleration at Ground Surface

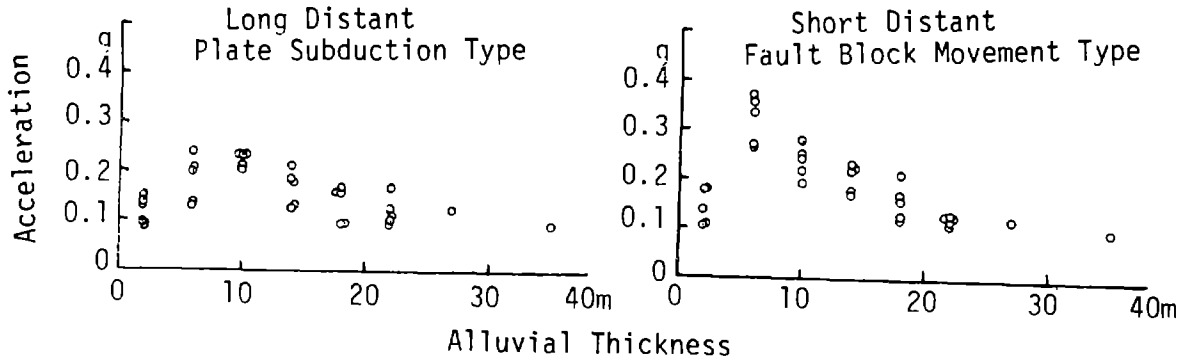


Fig.9 Earthquake Wave Path into Osaka Ground

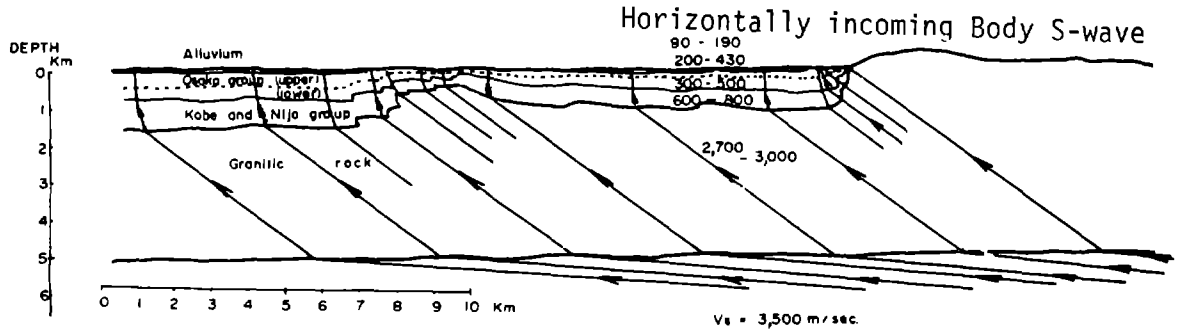


Fig.11 Degree of Failure of Superstructure of Wooden Houses

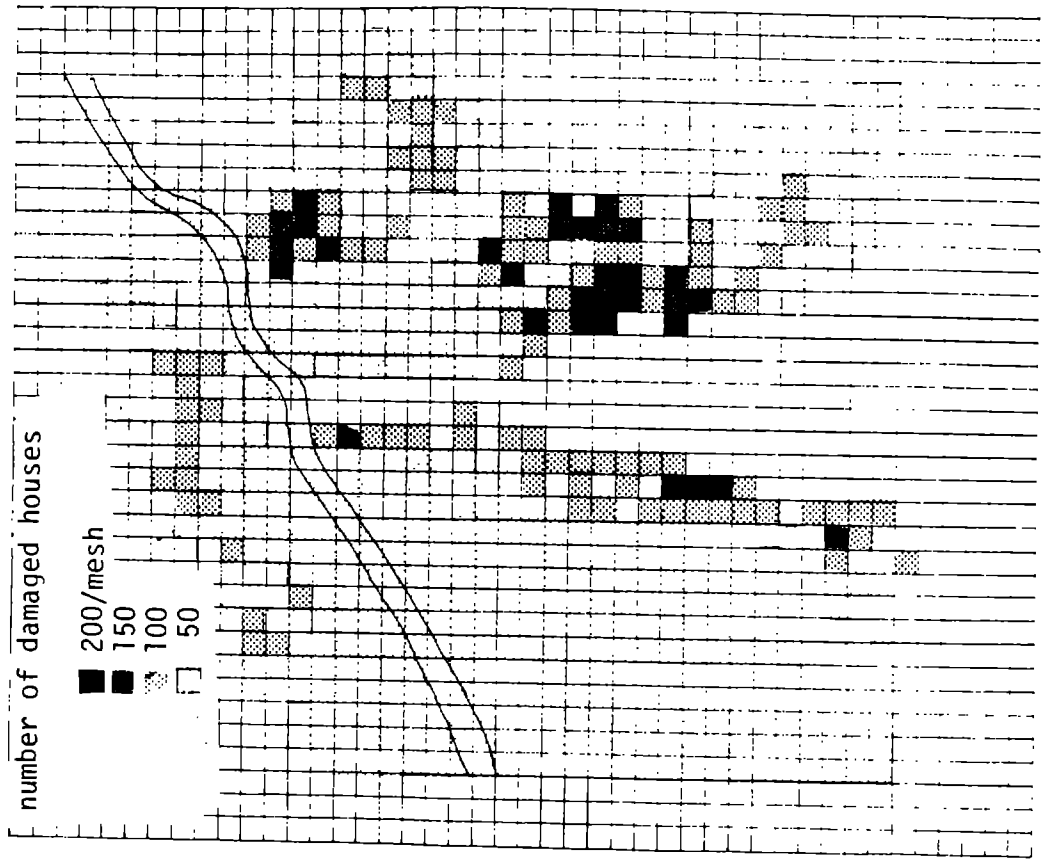


Fig.10 Degree of Susceptibility for Liquefaction

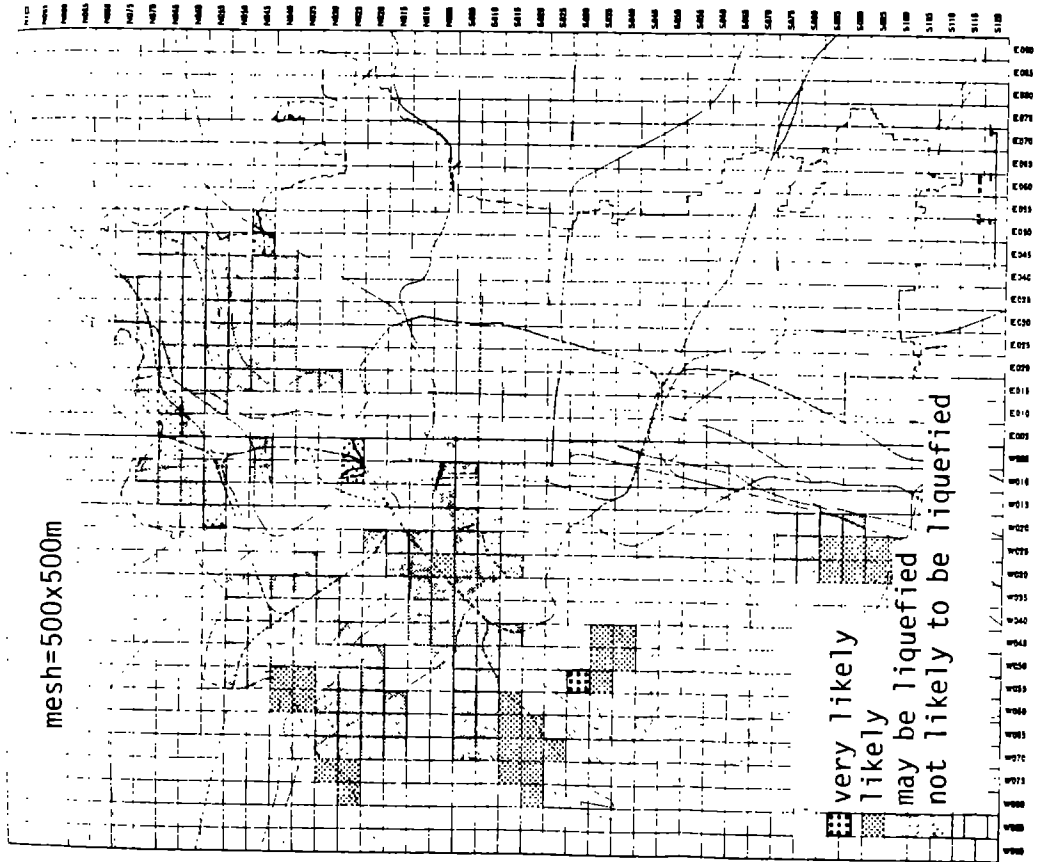


Fig.12 Degree of Failure of Foundation of Wooden Houses

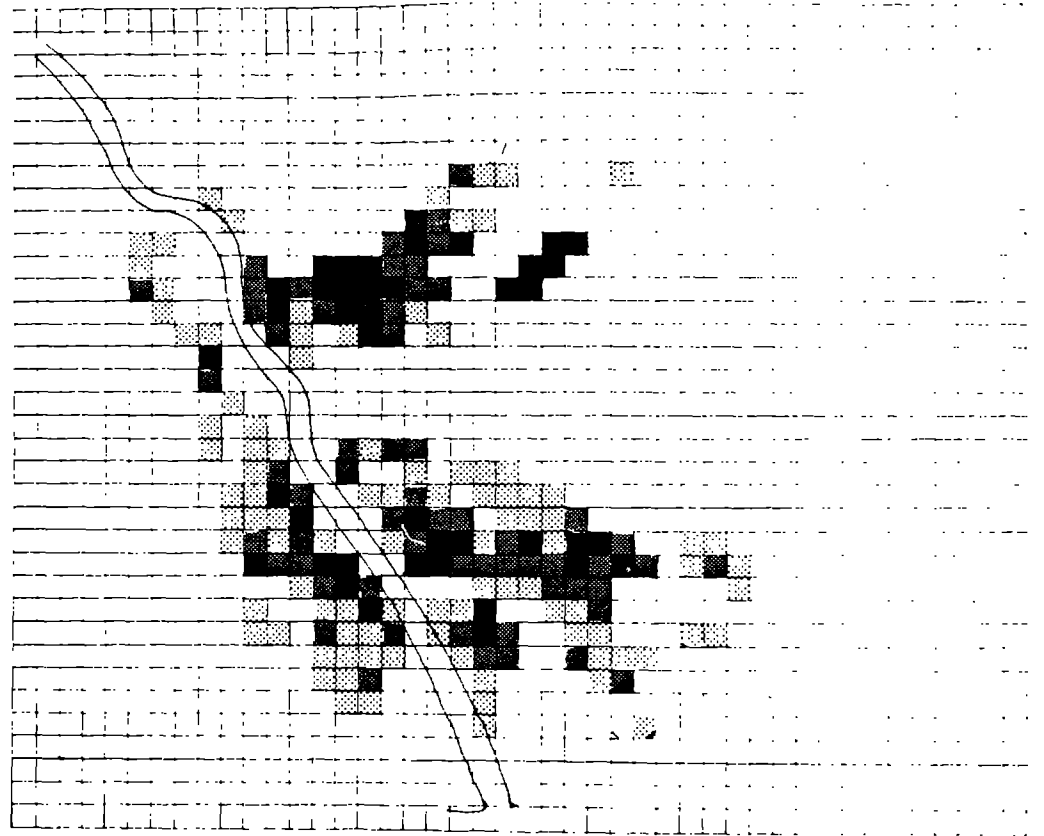
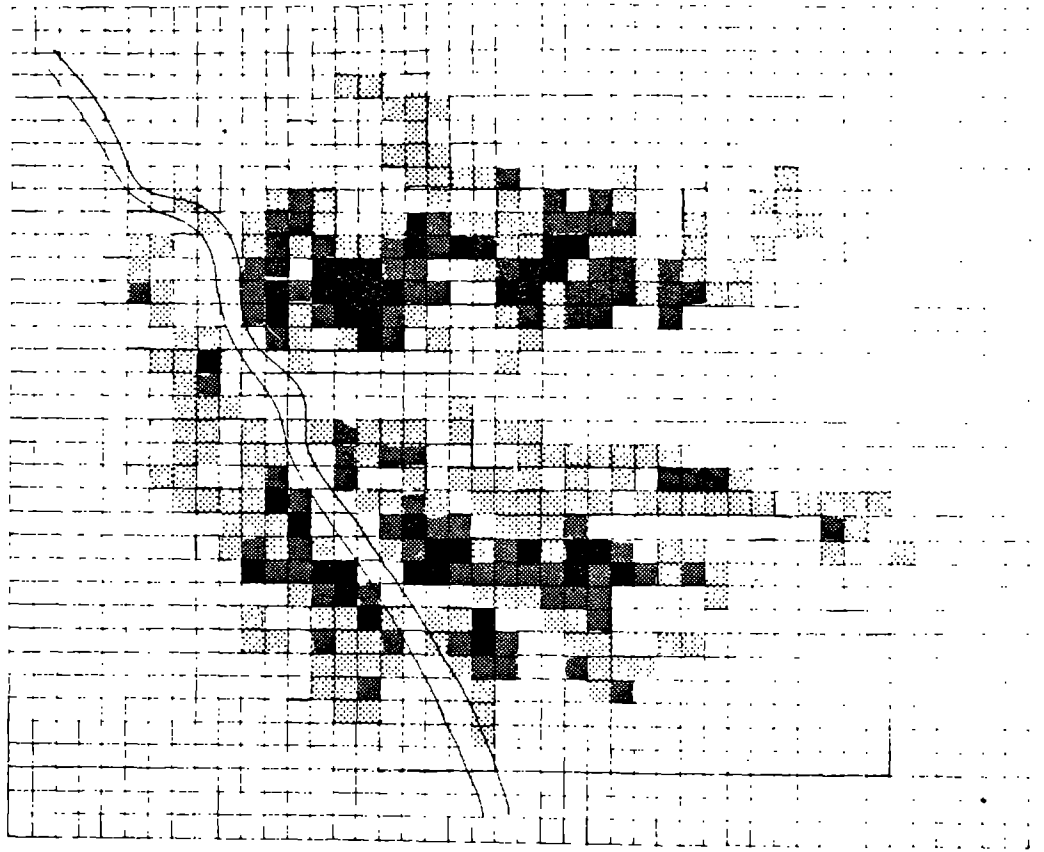


Fig.13 Degree of Failure of Wooden Houses in Total



AUBURN DAM - A CASE HISTORY OF EARTHQUAKE
EVALUATION FOR A CRITICAL FACILITY

By

D. R. Packer^I; L. S. Cluff^{II}; D. P. Schwartz^{III};
F. H. Swan, III^{III}; and I. M. Idriss^{IV}

ABSTRACT

The proposed Auburn Dam is to be located on the north fork of the American River near Auburn, California on the western margin of the Sierran foothills, an area of few damaging earthquakes during historical time. On August 1, 1975, a magnitude 5.7 earthquake and associated surface faulting occurred in the Sierran foothills near Oroville, 70 km northwest of Auburn Dam. Subsequent investigations revealed evidence of previous Quaternary displacements along this fault.

Because of the possibility of surface faulting and earthquakes along other faults in the western Sierran foothills, the U.S. Bureau of Reclamation chose to have an independent and objective reexamination of fault activity in the region to evaluate a) maximum credible earthquakes of significance to Auburn Dam, b) earthquake ground motions to which the proposed Auburn Dam may be subjected, c) the potential for reservoir induced seismicity resulting from impoundment of the proposed reservoir, and d) the potential for surface faulting in the foundation of the proposed Auburn Dam.

As a result of these studies, significant contributions have been made to several aspects of earthquake evaluation studies, including a) detection and evaluation of low-level fault activity along zones of older faulting, b) evaluation of the potential for reservoir induced seismicity, c) use of multiple parameters in evaluating maximum credible earthquakes, d) use of probabilities and probabilistic evaluations in hazard assessments. In addition, the results indicate the need to consider degree of fault activity in evaluating earthquake hazards to allow judgments to be made regarding acceptable risk.

INTRODUCTION

The proposed Auburn Dam is to be located along the western margin of the Sierran foothills on the North Fork of the American River immediately southeast of Auburn, California (Figure 1). On August 1, 1975, a magnitude 5.7 earthquake occurred in the foothills near Oroville, 70 km northwest of Auburn Dam. The earthquake caused moderate damage to Oroville and nearby communities (1).

Prior to the 1975 Oroville earthquake, geologic studies of the western Sierran foothills generally were not concerned with the

-
- I Associate, Woodward-Clyde Consultants, San Francisco, CA
 II Chief Geologist, Woodward-Clyde Consultants, San Francisco, CA
 III Project Geologist, Woodward-Clyde Consultants, San Francisco, CA
 IV Chief Earthquake Engineer, Woodward-Clyde Consultants,
 San Francisco, CA

evaluation of fault activity and earthquake hazards. The earthquake history of the foothills region indicates there were few damaging earthquakes in the region during historical time prior to the 1975 Oroville earthquake. The earthquake activity of the Sierran foothills, compared with other, more historically active regions, appears to be almost aseismic (2). The virtual absence of significant historical seismicity and the lack of known active faulting within the Sierran foothills led to the general conclusion that there were no active faults in the western Sierran foothills.

The fault that generated the August 1, 1975 Oroville earthquake is part of the complex system of faults that extends from Chico on the north to Mariposa on the south (Figure 1). The relatively moderate earthquake at Oroville was caused by slip along a fault that had not been previously recognized as active (3). Detailed studies along the fault, now named the Cleveland Hill fault, revealed ground cracks near Cleveland Hill that were the result of surface faulting, and evidence that previous Quaternary displacements had occurred along this fault (4, 5, 6). The Oroville earthquake and related surface faulting implied that other active faults may be present in the western Sierran foothills. In addition, because of the proximity of Lake Oroville and the 1975 Oroville earthquake, the question of reservoir induced seismicity in the Sierran foothills was introduced.

Because the Oroville earthquake and related surface faulting implied that other faults in the western Sierran foothills may be active, earthquake evaluation studies for the proposed Auburn Dam were undertaken by Woodward-Clyde Consultants for the U.S. Bureau of Reclamation to provide an independent, objective reexamination of fault activity in the Sierran foothills. The primary objectives of these studies were:

- 1) To evaluate the maximum credible earthquakes of significance to the dam site.
- 2) To characterize earthquake ground motions to which the proposed Auburn Dam site may be subjected and the probability of exceedance of response spectra developed for the site.
- 3) To evaluate the potential for reservoir induced seismicity as a result of impoundment of the proposed Auburn Reservoir.
- 4) To evaluate the potential for surface faulting in the foundation of the proposed dam.

The results of the earthquake evaluation studies are discussed in the following sections. An evaluation of the implications of the estimated ground motions, the potential for reservoir induced earthquakes, and possible surface fault displacement in the foundation of the proposed dam was not part of this study. It was also not an objective of this study to make judgments regarding the overall safety of the proposed Auburn Dam, or the level of risk that may be acceptable. The implications of these geologic considerations and the safety of the dam are being assessed by the U. S. Bureau of Reclamation and by state and federal review agencies.

METHOD OF STUDY

The surface faulting and earthquake potential at the Auburn Dam site was evaluated by applying the active fault concept, using the U.S. Bureau of Reclamation Proposed Fault Classification and Investigation Criteria (6). According to these criteria, faults that have experienced displacement within the past 100,000 years are classified as active. Where definitive evidence has not been found concerning the activity of a fault during the past 100,000 years, the fault may be classified as either indeterminate, indeterminate (active), or indeterminate (inactive), based on a judgmental evaluation of the data.

Typically, fault activity is assessed by evaluating the age of the youngest deposits that are displaced by a fault and/or by evaluating the age of the oldest deposits that overlie the fault and are not displaced. However, in the Auburn Dam site vicinity, there is an absence of geologic evidence for conclusively assessing the activity of faults. This lack of sufficient evidence at the site required that the assessment of fault activity be based on an understanding of the tectonic environment and the behavior and characteristics of late Cenozoic and active faults in the western Sierran foothills. Late Cenozoic faults were defined as faults that had experienced displacement during the present tectonic stress regime. Investigations were conducted of the zone of surface fault rupture produced by the August 1, 1975 Oroville earthquake to develop an understanding of the physical characteristics (bedrock characteristics and soil features) associated with this active fault that could be used to assess fault activity and the potential for surface faulting elsewhere in the foothills (3, 4, 5, 6, 7).

To identify the most probable locations of active faults for detailed investigations, an analysis of lineaments was made using various types of imagery of an area from Oroville southeastward to Table Mountain near Sonora. Geologic mapping was done and, at some places, geophysical surveys were made and test pits were excavated to locate areas along selected lineaments most likely to contain Quaternary deposits and soils of suitable thickness and age that could be used to assess fault activity. The assessments of fault activity made at selected exploration localities were based primarily on observations made in exploration locality trenches compared with observations of features along the Cleveland Hill fault.

SUMMARY OF EARTHQUAKE STUDIES

Investigation of Active Faults

The regional geologic studies and detailed investigations of 22 exploration localities indicate that late Cenozoic and active faulting has occurred throughout the Sierran foothills (Figure 1) (6, 8). At least six faults classified as active and indeterminate (active) (USBR criteria) occur within 32 km of the Auburn Dam site; the closest of these, the Maidu East fault zone, is within 0.8 km of the site. The displacements have occurred along segments of some preexisting planes of weakness associated with the Mesozoic Foothills fault system (9, 10). Most of the late Cenozoic and active faults are high-angle normal faults that are a result of an east-west extensional stress environment. Late Cenozoic and active faults having reverse and oblique slip were observed

locally. The pattern of surface fault rupture associated with extensional faulting typically consists of discontinuous, en echelon and locally branching fault traces that comprise fault zones hundreds to thousands of feet wide. Because of the limited extent of late Cenozoic deposits in the Sierran foothills, the lengths of the fault segments that have experienced late Cenozoic and active faulting can only be estimated. The geologic evidence and the data from the 1971 Oroville earthquake suggest individual fault lengths are several thousands of feet. The geologic evidence from areas where there are late Cenozoic deposits indicate the rate of displacement has been gradual throughout late Cenozoic time and that episodic slips have occurred along active faults during the past 100,000 years.

The maximum observed cumulative net displacement of a buried paleosol that is at least 100,000 years old (11, 12, 13) is 0.7 m. On the basis of cumulative displacements of dated geologic units and estimated recurrence intervals, the maximum net slip per event is judged to be 0.24 m. The maximum length of segments of active faults in the Sierran foothills that have the potential for slip during a single earthquake is judged to be approximately 16 km.

Maximum Credible Earthquakes

Estimates of the maximum credible earthquakes that may occur along active (USBR criteria) faults significant to the Auburn Dam site were based on evaluations of the following: a) the regional geologic and tectonic framework; b) the historical seismic activity along the faults and in the surrounding region; c) the geologic history of displacement along the faults; d) the relationship between earthquake magnitude and fault rupture length; and e) the relationship between earthquake magnitude and amount of fault displacement (14, 15).

Estimated magnitudes of maximum credible earthquakes on distant faults include: a magnitude 8 1/2 earthquake at a distance of 185 km on the San Andreas fault; a magnitude 7 1/2 earthquake at 80 km on the northern portion of the Sierra Nevada frontal fault system; and a magnitude 7 earthquake at 80 km on the Little Grass Valley fault in the northeastern Sierran block.

The nearby maximum credible earthquake is based on an evaluation of the maximum displacement (0.24 m) and length (10 km) compared to geologic parameters (16), seismologic parameters (17), and to similar types of active faults (16). The nearby maximum credible earthquake, based on this evidence, is estimated to be a magnitude 6 to 6 1/2 earthquake at a focal depth of approximately 10 km. At least six faults judged active and indeterminate (active) (USBR criteria) occur within 32 km of the Auburn Dam site; the closest of these is within 0.8 km of the site.

Earthquake Ground Motions

The method of characterizing earthquake ground motions that may occur at the Auburn Dam site consisted of developing smooth response spectra for the nearby and distant maximum credible earthquakes, assessing the probability of exceedance of the smooth response spectra developed for the nearby maximum credible earthquake, and identifying appropriate natural acceleration time histories that could be used in dynamic time-history analyses of the dam (18).

For this study, ground motions associated with the nearby maximum credible earthquake (magnitude 6 1/2) were characterized on the basis of analyses of strong-motion data recorded during selected historical earthquakes at Oroville, San Fernando, and Parkfield, California; Koyna, India; and Helena, Montana. The data used were selected to correspond as closely as possible to the conditions of the estimated maximum credible earthquakes for the Auburn Dam site in terms of magnitude, distance from earthquake source, and geologic conditions at the site. The statistical analyses resulted in a mean (average) and an 84th-percentile response spectrum.

Eighty-fourth-percentile smooth response spectra were also developed for the distant maximum credible earthquakes (magnitude 7 1/2 at 80 km, and magnitude 8 1/2 at 185 km). It was found that the smooth response spectrum for the nearby event greatly exceeds the spectra developed for the two distant events (14, 19).

The statistical analyses and probability studies used to evaluate the probabilities of exceeding the smooth response spectra developed for the nearby maximum credible earthquake take into account both the variability of ground motions and the uncertainties involved in their prediction. In addition, the following factors were considered: recurrence of naturally occurring earthquakes along faults in the Sierran foothills; potential for an earthquake associated with impoundment of the reservoir (reservoir induced seismicity); distances from the site at which earthquakes might occur; and peak ground accelerations and spectral accelerations at the site resulting from the earthquakes. The probability of exceeding the mean response spectrum in the period range 0.5 to 2 seconds within the next 100 years varies from approximately 0.04 to 0.07 (that is, 4 to 7 percent chance of exceedance); the probability of exceeding the 84th-percentile response spectrum in the same period range within the next 100 years varies from approximately 0.02 to 0.03 (that is, 2 to 3 percent chance of exceedance). The structural period range of 0.5 to 2 seconds is understood to be the range of greatest significance to the proposed dam. A major portion of the probability of exceedance was found to be attributable to reservoir induced earthquakes. For example, at a period of 1 second, approximately 90 percent of the probability of exceeding the 84th-percentile response spectrum is due to reservoir induced earthquakes.

Acceleration time histories (accelerograms) of recorded motions were identified for possible use in dynamic analyses of the dam for the nearby maximum credible earthquake. These accelerograms were scaled to provide response spectral values that, taken together, would approximately envelope the smooth 84th-percentile response spectrum. Possible time histories to represent distant maximum credible earthquakes were also identified.

Reservoir Induced Seismicity

The method of evaluating the potential for reservoir induced earthquakes at the Auburn Dam site was to review the available literature regarding reported cases of reservoir induced seismicity throughout the world (20). The reported cases were classified as acceptable cases, questionable cases, or cases that were not reservoir induced. The theoretical mechanisms of triggering a reservoir induced seismic event

and the parameters involved were considered. The geology and seismicity at the dam sites associated with the acceptable and questionable cases of reservoir induced seismicity were reviewed. The study was approached from the standpoints of worldwide cases of reservoir induced seismicity, deep reservoirs, and reservoirs in the Sierran foothills. Selected parameters associated with reported cases of reservoir induced seismicity were compiled and then systematically analyzed to assess the significance of these parameters to the occurrence of reservoir induced seismicity. The parameters included water depth, reservoir volume, geologic setting, faulting, regional tectonic stress regime, rate of change in water level, and duration of maximum loading. Comparison of these parameters was also made between the Auburn Dam site and Sierran foothills reservoirs selected because they are large and in the same tectonic environment.

Evaluation of the available data regarding the world's reservoirs indicates there have been 55 reported cases of reservoir induced seismicity. During this study, 16 of these have been classified as accepted cases of reservoir induced seismicity, 35 as questionable cases, and four as not being reservoir related (14).

Evaluation of the data for accepted and questionable cases of reservoir induced seismicity indicates that as water depth and reservoir volume increase, there is an increase in the occurrence of reservoir induced seismicity. There is also an increase in the occurrence of reservoir induced seismicity among reservoirs impounded in an extensional regional tectonic stress regime, where active faults are present, and where sedimentary strata predominate.

Geologic and seismologic data for 16 selected dams and reservoirs in the Sierran foothills show no definitive spatial or temporal relationship between seismicity and reservoir impoundment. Of these 16, there are six reservoirs that are deep to very deep or large to very large and are impounded in a geologic and structural setting similar to that of the proposed Auburn Dam and reservoir. Among these six dams and reservoirs, one, Oroville, has experienced seismicity that has been classified as a questionable case of reservoir induced seismicity (1975 Oroville earthquake).

The reservoir to be impounded by Auburn Dam is to be very deep, large in volume, located in an extensional stress environment, near active faults (USBR criteria), and in an area of dominantly metamorphic geology. The estimation of the likelihood of reservoir induced seismicity at the proposed Auburn Dam was based on the present understanding of faulting and fault activity in the Sierran foothills and on the judgment there are active faults in the hydrologic regime of the proposed Auburn Reservoir.

The seismic activity near the Oroville Reservoir in 1975 is also important to an evaluation of the likelihood of a reservoir induced earthquake occurring near Auburn Dam because the geologic and tectonic settings of the two areas are similar and the reservoir at Oroville is large and very deep. The present data regarding the relationship of the 1975 Oroville earthquake to Lake Oroville is inconclusive; therefore, the evaluation of the likelihood of reservoir induced seismicity at the proposed Auburn Reservoir was made first by assuming that the Oroville earthquake was not a reservoir induced seismic event, and then by assuming that it was a reservoir induced seismic event.

If the 1975 Oroville earthquake is assumed not to be reservoir induced, the likelihood of a reservoir induced earthquake greater than magnitude 3.0 occurring near Auburn Dam during the design life of the dam is 20 percent to 30 percent; the likelihood of a reservoir induced earthquake of the magnitude of the Oroville earthquake (5.7) or larger is 2 percent to 5 percent.

If the 1975 Oroville earthquake is assumed to be reservoir induced, the likelihood of a reservoir induced earthquake greater than magnitude 3.0 occurring near Auburn Dam during the design life of the dam is 50 to 80 percent; the likelihood of a reservoir induced earthquake of the magnitude of the Oroville earthquake (5.7) or larger is 30 percent.

Assessment of Fault Activity in the Dam Foundation and the Potential for Surface Fault Rupture

At six localities within 32 km of the Auburn Dam site, active or indeterminate (active) (USBR criteria) faults were located along preexisting faults in the Sierran foothills. One of these faults, the Maidu East fault zone, is located within 0.8 km of the excavation for the foundation (Figure 2).

The Maidu East fault zone displaces the Mehrten Formation (Miocene-Pliocene) at the Auburn Dam site and trends toward the foundation excavation for the right abutment. Approximately 800 m south of the dam foundation, the fault zone has approximately 5.5 m of late Cenozoic (post-Mehrten Formation) vertical displacement across a zone approximately 2.3 m wide. The faults are predominantly high-angle faults having down-to-the-east displacement. The vertical displacement apparently dies out 150 m southwest of the foundation excavation for the right abutment. The late Cenozoic faulting is coincident with a Mesozoic bedrock structure that trends northwestward and is approximately 68 m west of the right abutment foundation excavation at its closest point (T-26 on Figure 2). An indeterminate (active) (USBR criteria) classification was made at one point along a trace of the Maidu East fault zone, approximately 275 m south of the right abutment. Approximately 136 m north of this location, the Quaternary displacements along this trace have either died out or they are too small to be detected in the buried paleosol that overlies the fault.

The pattern of surface fault rupture associated with extensional faulting (normal faulting) typically consists of discontinuous, en echelon and locally branching fault traces that together comprise fault zones hundreds to thousands of feet wide. Such a pattern of surface fault rupture may be associated with the Maidu East fault zone at the Auburn Dam site and indicates displacements could occur along limited lengths of the preexisting Mesozoic bedrock structures (T-zones and F-zones in Figure 2).

T-zones and F-zones are the dominant bedrock structures in the Auburn Dam foundation. T-zones are generally north-northwest-striking, steeply dipping zones that characteristically contain talc and chlorite schist. Locally, these zones are crenulated and sheared. F-zones are generally northwest-striking, southwest-dipping fault zones that systematically cut across and displace the apparently older T-zones. Locally, F-zones refract along T-zones and may be coincident with them, and then resume

cross-cutting relationships with the T-zones. Where relative displacements along the F-zones were identified, the displacements show reverse faulting with the southwest block faulted up relative to the northeast block.

Segments of some T-zones and F-zones exposed in the foundation excavation (Figure 2) have bedrock characteristics similar to those of late Cenozoic and active (USBR criteria) faults in the western Sierran foothills, including the faults associated with the 1975 Oroville earthquake, and the faults in the Auburn Dam site vicinity that have been classified as active and indeterminate (active) (USBR criteria). The bedrock characteristics include well defined zones of multiply deformed rock having two and sometimes three foliation directions that are cross-cut and disrupted by narrow planes containing clay gouge. In many places, these zones are associated with brecciated quartz veins. The late Cenozoic and active displacements occur along the narrow, cross-cutting planes.

At the Auburn Dam site, there is an absence of Quaternary deposits, soils, or other geologic materials that can be used to conclusively assess the activity or inactivity (USBR criteria) of the faults in the foundation excavation of the proposed Auburn Dam. Therefore, assessment of the activity along these faults is based on an understanding of the behavior and characteristics of active and late Cenozoic faults in the western Sierran foothills. The following factors: the regional geologic setting; the seismicity of the Auburn area; the similarity between the bedrock characteristics of faults in the dam foundation and the bedrock characteristics of late Cenozoic and active faults in the foothills; the bedrock structural relationships at the dam site; the close proximity of the indeterminate (active) (USBR criteria) Maidu East fault zone to the dam foundation; and the pattern of late Cenozoic and active faulting in the foothills suggest there could be active faults (USBR criteria) in the dam foundation excavation.

Figure 3 summarizes the major factors affecting the assessment of the probability that faults in the Auburn Dam foundation have had displacement during the past 100,000 years. The impact of each factor on the overall activity assessment is indicated by a range of probabilities shown by the dark bars. The overall assessment is expressed as a probability because the lack of conclusive evidence at the dam foundation for either activity or inactivity makes a deterministic expression of fault activity insufficient. Most of the factors that affect the overall activity assessment of faults in the dam foundation are interdependent, or, in probabilistic terms, they are probabilistically dependent. Since the interrelationships are not known well enough to be accurately modeled, the overall assessment of the probability of active faults (USBR criteria) in the dam foundation cannot be derived mathematically from the probabilities suggested by the individual factors shown on Figure 3. The overall assessment of fault activity based on the available data is that there is a very low to low probability that faults in the Auburn Dam foundation have had displacement in the past 100,000 years. For the purpose of this study, very low to low probability is 1 in 100 to 1 in 10.

The most likely locations of future surface fault rupture in the foundation excavation are along segments of F-zones and T-zones that have

bedrock characteristics similar to those of late Cenozoic and active faults in the western Sierran foothills (Figure 2). The most likely type of future displacement along faults in the dam foundation excavation is predominantly dip slip. The maximum net slip along faults in the dam foundation excavation during a single event is estimated to be 0.24 m.

DISCUSSION

Significant contributions to the state of the art of evaluating earthquake hazards that have resulted from these studies include: a) the detection of low-level fault activity along zones of older faulting; b) evaluation of the potential for reservoir induced seismicity; c) use of multiple parameters in evaluating maximum credible earthquakes; and d) the use of probabilistic evaluations in hazard assessments. In addition, the results indicate the need to consider degree of fault activity in evaluating the potential for earthquake hazards.

The results of this study indicate that low levels of fault activity can be detected. Regional geologic studies made in conjunction with detailed site investigations, including trenching, geomorphic analysis, and soil stratigraphic studies are necessary to identify potential locations of late Cenozoic faulting and to assess the activity of these faults. Comprehensive regional studies in support of detailed site investigations are particularly important in areas such as the western Sierran foothills, where there is a paucity of late Cenozoic strata that can be used to evaluate recent fault activity. Similar situations occur in the eastern U. S.; for example, the Appalachian Piedmont, where there are extensive areas of bedrock that are overlain only by colluvium and residual soils.

Induced seismicity has the potential to influence in a significant way the probability of a seismic event in a particular area. The state of knowledge about the influence of a reservoir on faulting and earthquakes is poor. This study is the first detailed compilation of data on reservoir induced seismicity that systematically compares selected factors among the world's deepest reservoirs. The results of this study confirm that the potential for reservoir induced seismic events should be considered in the earthquake evaluation of reservoirs, particularly those reservoirs that are deep and located in certain tectonic environments.

Multiple parameters should be used to evaluate the maximum credible earthquake that can occur along a given fault. Estimates based on only one parameter can result in unrealistic faults being hypothesized. For example, using only the relationship between fault length and earthquake magnitude in the foothills can lead to unrealistically high values because only short segments of the preexisting Paleozoic and Mesozoic faults have been reactivated under the late Cenozoic stress regime. In addition to fault length, the following factors should be considered: the regional tectonic framework, the historical seismicity, the geologic history of slip along the fault, and the amount of slip that can occur during a single event.

Judgments and subjective evaluations are made in reaching any conclusions. In this study, these judgments and subjective evaluations are expressed in terms of subjective probabilities and likelihoods to

promote more complete communication. The use of subjective probabilities provides an opportunity to express the degree of certainty or uncertainty in a conclusion. Use of probability more accurately expresses the degree of confidence in the data supporting a conclusion.

Although it was not within the scope of the earthquake evaluation studies for Auburn Dam to evaluate the level of risk that might be acceptable, the results of the study suggest that deterministic assessments of fault activity using the "active fault concept" are not completely satisfactory for assessing the potential earthquake hazards. The existing criteria for defining fault activity do not consider the degree of fault activity. This results in all active faults being regarded as equal even though there may be significant differences in the potential for slip. Comparing the relative activity of faults is a means for more realistically assessing the relative hazard. The degree of activity of faults may be expressed in terms of slip rate (centimeters per year), cumulative slip during a given interval, the amount of slip during one slip event, and the recurrence interval between slip events. Comparing the activity of faults in the western Sierran foothills with the activity of other active faults results in a spread of four orders of magnitude in degree of activity, as expressed by the slip rate (Table 1). High and low rates of activity emphasize differences in tectonic environments (21) (see paper by Cluff, this volume).

Table 1
DEGREE OF FAULT ACTIVITY

FAULT	SLIP RATE (CM/YEAR)	ESTIMATED MAX SLIP /EVENT (METERS)	CALCULATED RECURRENCE INTERVAL (YRS.) ASSUMING MAX. SLIP/EVENTS
FAIRWEATHER, AK.	5.8	10	170
SAN ANDREAS, CA.	3.7	10	270
HAYWARD, CA.	.6	2	300
COYOTE CREEK, CA.	.3	1.5	500
LOWER RHINE GRABEN, GER.	.023	.5	2000
UPPER RHINE GRABEN, GER.	.005	.3	6000
CLEVELAND HILL, CA.	.0006	.24	30000

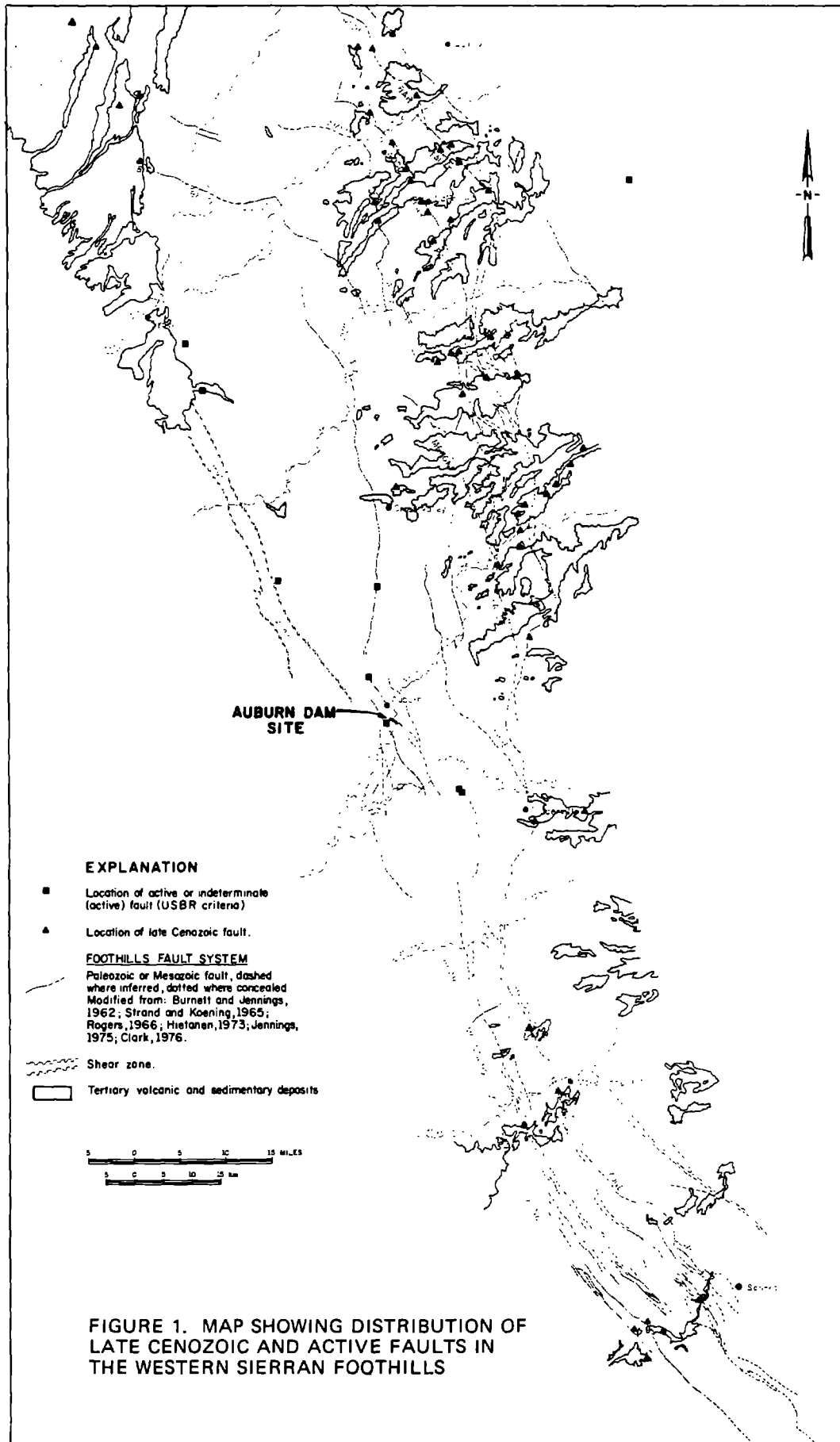
REFERENCES

1. Sherburne, R. W., and Hauge, C. J., (eds.), 1975, Oroville, California, Earthquake, 1 August, 1975; California Division of Mines and Geology, Special Report 124, 151 p.
2. McNalley, K. C., and Savage, W. U., 1978, Seismological characteristics of the Sierran block, California (abs.): Seismological Society of America, 73rd Annual Meeting, Earthquake Notes, Eastern Section, v. 49, no. 1, p. 83.
3. Hart, E. W., and Rapp, J. S., 1975, Ground rupture along the Cleveland Hill fault, in Sherburne, R. S., and Hauge, C. J. (eds.), Oroville, California, Earthquake, 1 August 1975: California Division of Mines and Geology, Special Report 124, p. 61-72.

4. Woodward-Clyde Consultants, 1976, Evaluation for potential for earthquakes and surface faulting, Parks Bar Afterbay Dam: unpublished report prepared for U. S. Army Corps of Engineers, Sacramento District, California, by Woodward-Clyde Consultants, San Francisco, Calif., 45 p.
5. Harpster, R. E., Biggar, N. E., and Taylor, C. L., 1978, Identification of distinguishing characteristics of late Quaternary faults in the western Sierran foothills, California (abs.): Seismological Society of America, 73rd Annual Meeting, Earthquake Notes, Eastern Section, v. 49, no. 1, p. 88.
6. Schwartz, D. P., Swan, F. H., III, Harpster, R. E., Rogers, T. H., and Hitchcock, D. E., 1977, Surface Faulting Potential, Earthquake Evaluation Studies of the Auburn Dam Area: Report prepared for the U. S. Bureau of Reclamation, Denver, Colo., by Woodward-Clyde Consultants, San Francisco, Calif., v. 2, 405 p.
7. Hart, E. W., and Harpster, R. E., 1978, Surface faulting associated with the Oroville, California, earthquake of August 1975 (abs.): Seismological Society of America, 73rd Annual Meeting, Earthquake Notes, Eastern Section, v. 49, no. 1, p. 87.
8. Swan, F. H., III, Hitchcock, D. M., and Rogers, T. H., 1978, Late Cenozoic faulting from Oroville to Placerville, California (abs.): Seismological Society of America, 73rd Annual Meeting, Earthquake Notes, Eastern Section, v. 49, no. 1, p. 91.
9. Schwartz, D. P., Alt, J. N., and Packer, D. R., 1977, Relationship of Paleozoic and Mesozoic structures to late Cenozoic faulting in the northern and western Sierra Nevada, California (abs.): The Geological Society of America, Abstracts with Programs, v. 9, no. 7, p. 1165.
10. Schwartz, D. P., Hitchcock, D. M., and Perkins, M. E., 1978, Basement control of late Cenozoic extensional faulting in the Sierran foothills, California (abs.): Seismological Society of America, 73rd Annual Meeting, Earthquake Notes, Eastern Section, v. 49, no. 1, p. 89.
11. Swan, F. H., III, and Hanson, K., 1977, Quaternary Geology and Age Dating, Earthquake Evaluation Studies of the Auburn Dam Area: Report prepared for the U. S. Bureau of Reclamation, Denver, Colo., by Woodward-Clyde Consultants, San Francisco, Calif., v. 4, 251 p.
12. Swan, F. H., III, and Hanson, K. L., 1978, Origin and ages of late Quaternary deposits and buried paleosols in the western Sierra Nevada foothills, California (abs.): Abstracts with Programs (Cordilleran Section), v. 10, no. 3, p. 149.
13. Swan, F. H., III, Hanson, K. L., and Page, W. D., 1977, Landscape evolution and soil development in the western Sierra Nevada foothills, California, in Singer, M. J., (ed.), Soil

Development, Geomorphology, and Cenozoic History of the Northwestern San Joaquin Valley and Adjacent Areas, California: A guidebook for the joint field session of the American Association of Agronomy, Soil Science Society of America and the Geological Society of America, p. 300-312.

14. Packer, D. R., Alt, J. N., and Patwardhan, A., 1977, Maximum Credible Earthquakes, Earthquake Evaluation Studies of the Auburn Dam Area: Report prepared for the U. S. Bureau of Reclamation, Denver, Colo., by Woodward-Clyde Consultants, San Francisco, Calif., v. 7, 49 p.
15. Anttonen, G. J., and Packer, D. R., 1978, Estimating magnitudes of future earthquakes along the western Sierran foothills, California: a geologic evaluation (abs.): Seismological Society of America, 73rd Annual Meeting, Earthquake Notes, Eastern Section, v. 49, no. 1, p. 92.
16. Slemmons, D. B., 1977, State-of-the-art for assessing earthquake hazards in the United States; Part 6: faults and earthquake magnitude, with an appendix on geomorphic features of active fault zones: U. S. Army Engineer Waterways Experiment Station, Vicksburg, Contract No. DACW 39-76-C-0009, 129 p., plus 37 p. Appendix.
17. Tocher, D., and Sommerville, P., 1978, Constraints from theoretical seismology on maximum earthquake magnitude and ground motions in the western Sierran foothills, California (abs.): Seismological Society of America, 73rd Annual Meeting, Earthquake Notes, Eastern Section, v. 49, no. 1, p. 93.
18. Idriss, I. M., Sadigh, K., and Power, M. S., 1978, Characteristics of ground motions near sources in the western Sierran foothills (abs.): Seismological Society of America, 73rd Annual Meeting, Earthquake Notes, Eastern Section, v. 49, no. 1, p. 93.
19. Idriss, I. M., Power, M. S., Sadigh, K., and Kulkarni, R., 1977, Earthquake Ground Motions, Earthquake Evaluation Studies of the Auburn Dam Area: Report prepared for the U. S. Bureau of Reclamation, Denver, Colo., by Woodward-Clyde Consultants, San Francisco, Calif., v. 8, 118 p.
20. Packer, D. R., Lovegreen, J. R., and Born, J. L., 1977, Reservoir Induced Seismicity, Earthquake Evaluation Studies of the Auburn Dam Area: Report prepared for the U. S. Bureau of Reclamation, Denver, Colo., by Woodward-Clyde Consultants, San Francisco, Calif., v. 6, 345 p.
21. Packer, D. R., and Cluff, L. S., 1978, Comparison of activity of late Cenozoic faults in the western Sierran foothills, California with other active faults (abs.): Seismological Society of America, 73rd Annual Meeting, Earthquake Notes, Eastern Section, v. 49, no. 1, p. 89.



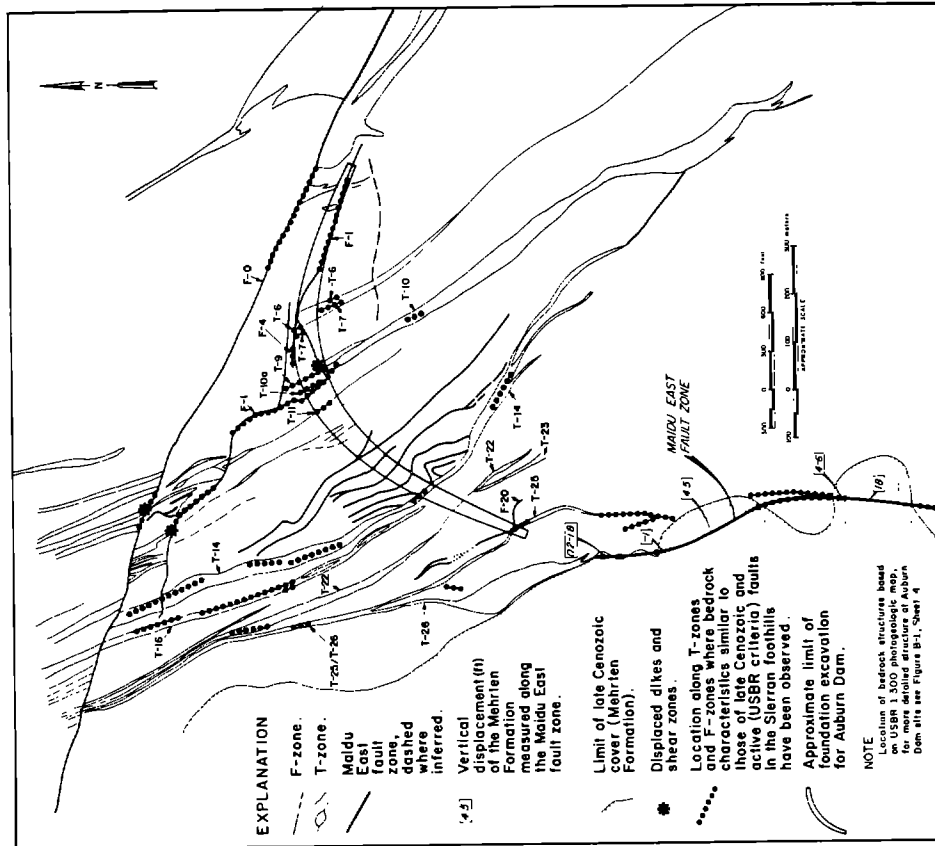


FIGURE 2. MAP OF AUBURN DAM SITE SHOWING LOCATIONS WHERE FAULTS HAVING BEDROCK CHARACTERISTICS SIMILAR TO THOSE OF LATE CENOZOIC FAULTS IN THE SIERRAN FOOTHILLS HAVE BEEN OBSERVED

MAJOR FACTORS THAT AFFECT THE ACTIVITY ASSESSMENT OF FAULTS IN THE DAM FOUNDATION	PROBABILITY THAT FAULTS IN THE DAM FOUNDATION HAVE HAD DISPLACEMENT IN THE PAST 100,000 YEARS						
	Zero	Extremely low ≤.001	Very low .01	Low .1	Moderate .5	High .8	Absolute 1
REGIONAL GEOLOGIC SETTING			█	█			
SEISMICITY OF AUBURN AREA		█					
BEDROCK CHARACTERISTICS OF FAULTS IN DAM FOUNDATION COMPARED WITH THOSE OF LATE CENOZOIC AND ACTIVE FAULTS IN THE SIERRAN FOOTHILLS			█	█			
FAULTING AND STRUCTURAL RELATIONSHIPS AT DAM SITE			█	█			
<ul style="list-style-type: none"> • Fault zone F-1 • T-zones • Structural relationships between F-1 and T-zones at the dam site • Maidu East fault zone 			█	█			
PATTERN OF LATE CENOZOIC FAULTING IN THE WESTERN SIERRAN FOOTHILLS			█	█			
OVERALL ASSESSMENT			█	█			

FIGURE 3. ASSESSMENT OF THE PROBABILITY THAT FAULTS IN THE DAM FOUNDATION HAVE HAD DISPLACEMENT IN THE PAST 100,000 YEARS

COMPUTER-SIMULATED COMPOSITE EARTHQUAKE HAZARD MODEL FOR RENO, NEVADA

Bell, E. J.¹, Trexler, D. T.², and Bell, J. W.²

ABSTRACT

A computer-simulated earthquake hazard model was developed for the Reno 7½-minute quadrangle in western Nevada. Relevant geologic, geophysical and engineering data for the Reno quadrangle were compiled to develop specific knowledge of the physical environment of seismic loading, including depth to the water table, distribution of potentially unstable slopes (defined by topography, microclimate, and bedrock and soil characteristics), and the space-time characteristics of faults. Probable range and finite limits for geologic processes as sources of earthquake-related hazard parameters were determined. Seismic response of the geologic units was estimated by the rigidity product, (i.e., the product of the shear wave velocity and density) with three alluvial unit groups (I, II, III) and one bedrock group (IV) defined by similar rigidity product values. Alluvial units II and III were modified to indicate areas with less than 200 ft depth to bedrock. Faults ranked on the basis of age of last movement, slopes of 25% or greater, and areas of depth to ground water less than 60 ft (18 m) were combined with the seismic response to produce three individual hazard elements. The potential for slope instability, the potential for liquefaction and differential compaction and the potential for surface faulting maps are the specific seismically-induced hazard elements considered for the Reno area. The composite earthquake hazard map depicts the best estimate of the total potential seismic hazard for a particular area within the Reno 7½-minute quadrangle by summing the individual hazard elements.

The model can be adapted to other regions for use at detailed scales of 1:24,000 or larger. The dynamic nature of the model allows the seismic zonation to be updated as new data become available. The sequential structural format can expand to incorporate all locally significant site parameters without minimizing the dynamic range of parameter values or the scaling factors for each hazard element in the composite earthquake hazard analysis.

INTRODUCTION

Most previous seismic risk maps are regional in scale and are based on historic seismicity patterns, on probabilistic prediction of future events (1, 10), or interpretation of regional tectonic regimes (11). Other risk mapping approaches incorporate site conditions as factors of risk (13, 24). Slemmons (22) proposes microzonation methods for active faults. Borchardt (6) presents a series of studies evaluating individual seismic hazards. While acknowledging the importance of specific site characteristics, these studies do not provide a systematic and dynamic technique for appraisal of individual seismic hazards at detailed scales and, more importantly, for developing an integrated or "composite" assessment of the seismic hazards significant to a given area.

The computer program described in this report evaluates earthquake hazard and assesses seismic risk for large-scale areas of investigation. It is based on phenomenologic and probabilistic data incorporating the best available geophysical, geologic and engineering information. The program addresses such significant factors as: physical properties of geologic units; depth to bedrock; slope of the terrain; depth to ground water; and proximity to fault traces of known length, displacement, and movement history. This technique is applied to the Reno 7½-minute quadrangle.

The program addresses major factors which influence seismically-induced hazards and can be readily modified to add, or delete, a particular hazard element which may, or may not, be pertinent to the specific area. For example, inland areas are less subject to flooding; however, for coastal areas, the assessment of flooding (tsunamis) potential may be critical. Each hazard element can be ranked individually, relative to its contributing effect on the total seismic hazard. This method of construction allows for the maximum degree of freedom in assessing and delineating each specific hazard or combination of seismically induced hazards that will affect a given area. All locally significant parameters can be incorporated without minimizing the dynamic range of individual hazard elements.

The program is designed to generate three specific hazard element maps for the Reno area: 1) potential for slope instability; 2) potential for liquefaction and differential compaction, and 3) potential for surface faulting. The final product, a combination of these individual hazard elements, is a composite earthquake hazards map of the Reno 7½-minute quadrangle.

¹ Mackay School of Mines, University of Nevada, Reno, Nevada 89557

² Nevada Bureau of Mines and Geology, University of Nevada, Reno, Nevada 89557

THE PROGRAM

A Fortran IV computer program was prepared in sequential structural format and is available upon request to provide potential users with a direct approach to the production of seismic zonation maps based on multiple factors. Parameters that are significant in evaluating seismic hazards include physical properties of units, slope, depths to ground water and bedrock, and the activity and capability of faults. Data defining these parameters are digitized to form basic data files; the files listed in Table 1 are available in the program.

TABLE 1. Basic data files

- 1) Seismic response classification
- 2) Slope of the terrain
- 3) Depth to ground water
- 4) Faults

Seismic response should, ideally, be based on strong-motion instrumental monitoring of high-strain events, namely large-magnitude earthquakes. The empirical measurements of shaking intensities reflect both the physical properties of the underlying deposits and the characteristics of the input seismic motion. Each unit is assigned an integer value representing its seismic response relative to the response of the other units within the given study area. In areas where empirical measurements based on monitoring of local, large-magnitude earthquakes are lacking, units may be grouped into broad relative response categories based on their physical properties (14, 15). In all cases the seismic response classification should be based on empirical data rather than intuitive judgement.

Slope can be evaluated in percent or gradient. Integer values are assigned to represent each of the slope intervals (i.e., ranges in percent or gradient).

This data file is used in conjunction with Medvedev's (15) equation that relates liquefaction potential to depth to ground water in meters. The increase in seismic intensity (n) is calculated from the equation $n = e^{-.04h^2}$, where h is the depth to ground water in meters (15). The depth to ground water in meters is determined for the center of each cell and is digitized.

The length of the fault trace and age of last movement on the fault should be considered simultaneously. Data related to the recurrence interval for large earthquakes of sufficient magnitude to cause surface disruption should also be considered. Fault data are digitized in integer format representing the trace length and the best estimate of the age of last movement and capability. In addition, geodetic deformation and ground acceleration, both of which attenuate with distance from the fault, should be evaluated and, where necessary, be represented by digitized integers of decreasing value with distance from the fault. Geodetic deformation should be evaluated with respect to the style of faulting, i.e., strike-slip, normal or reverse (12, 17, 18, 19).

Additional basic data files could be developed to indicate areas of low elevation along coastal margins that may be susceptible to flooding due to tsunamis. For urban areas that have upstream water storage reservoirs, slope failure into reservoirs initiating dam failure and subsequent flooding could also be incorporated into a basic data file. The development of these or other files would adapt the program to other geographic regions.

The parameters are evaluated for a geographic area based on a matrix with a cell as the fundamental unit of evaluation and digitization. The minimum cell size, or number of cells in the matrix, should be consistent with the detail of the individual basic data sets. The digitized basic data represent the areally predominant condition in any particular cell. The parameters are assigned integer values representing the areally predominant condition within a cell, and these values are digitized for the matrix. The files are in I2 format and can accommodate integer values ranging from 0 to 99.

Individual hazard elements are produced by algebraic summation of the digitized values in the seismic response classification with each of the other basic data files (fig. 1). The program is designed to produce the following hazard elements: 1) potential for slope instability, 2) potential for liquefaction and differential compaction, and 3) potential for surface faulting.

The program allows the operator to vary the dynamic range of values internally to produce potential values for each hazard element. A scaling factor is available and can be varied, depending on the particular parameters encountered, to reflect the actual (if known) or suspected degree of hazard each element should have in a composite earthquake hazard assessment. For example, the potential for liquefaction and differential compaction, in the worst case, was considered to have a greater effect than indicated by the maximum hazard element potential of 7 when compared to other hazard elements which had maximum values as high as 14. Therefore, a scaling factor of 10 was included in calculating the potential for liquefaction and differential compaction for the Reno 7½-minute quadrangle.

Each individual hazard element is produced in digital format so that the interpreter can verify the completeness of the summing operations. For example, Figure 2A depicts an area at the southern margin of the Reno 7½-minute quadrangle where post-Illinoian age faults offset Donner Lake and Tahoe Outwash as well as

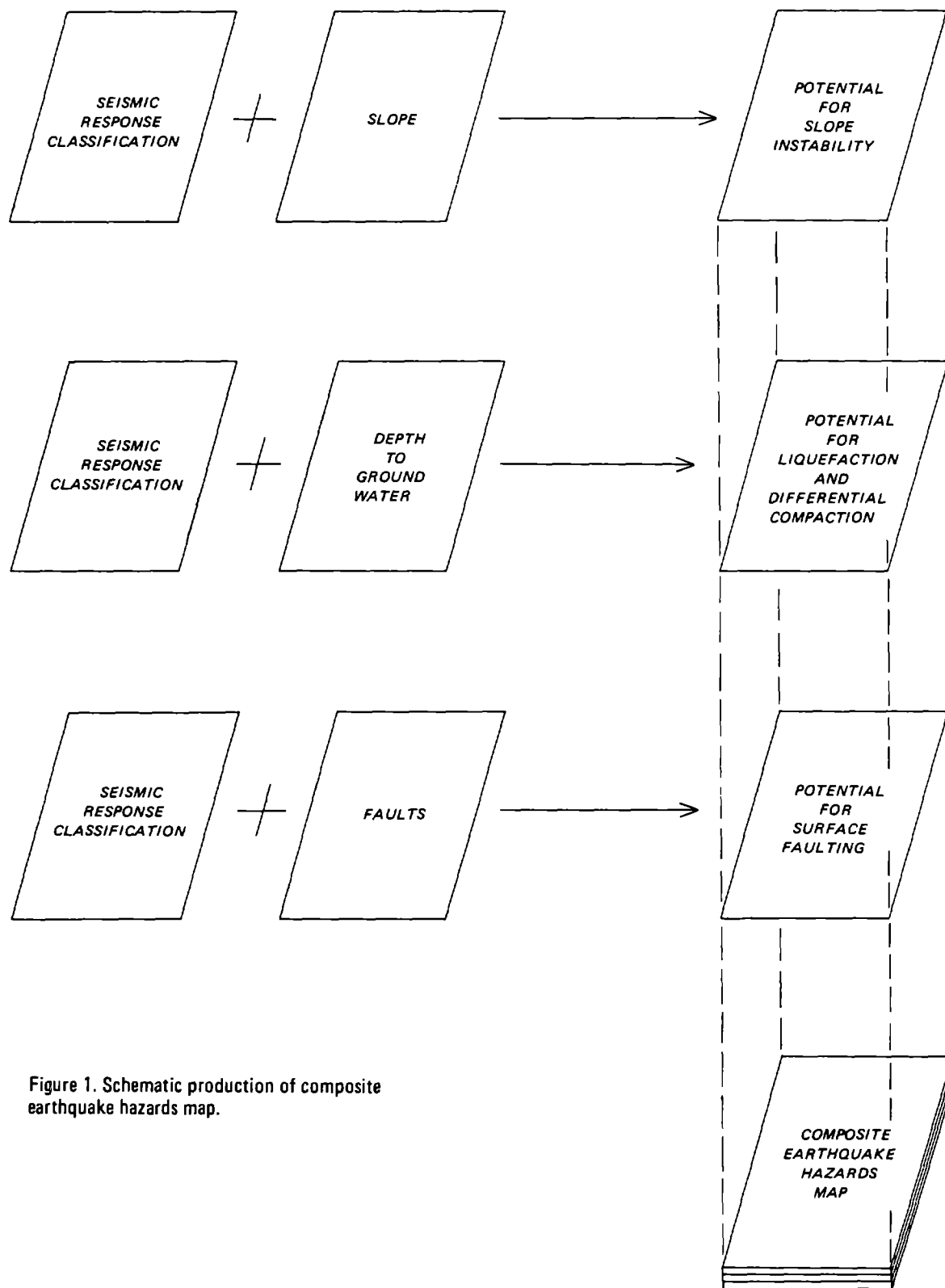


Figure 1. Schematic production of composite earthquake hazards map.

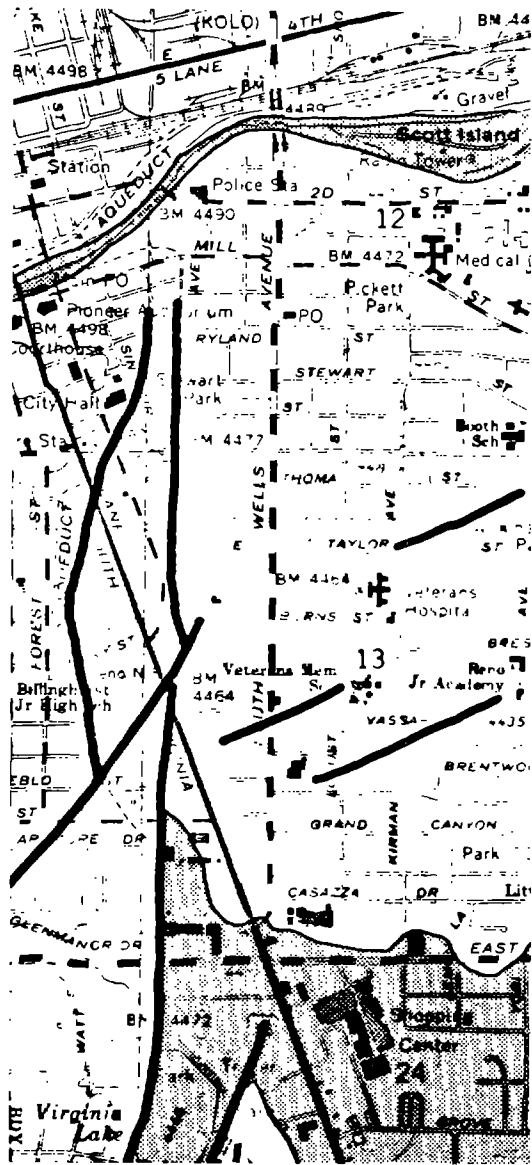


Figure 2A. A portion of the seismic hazard map prepared from seismic response values and faults.

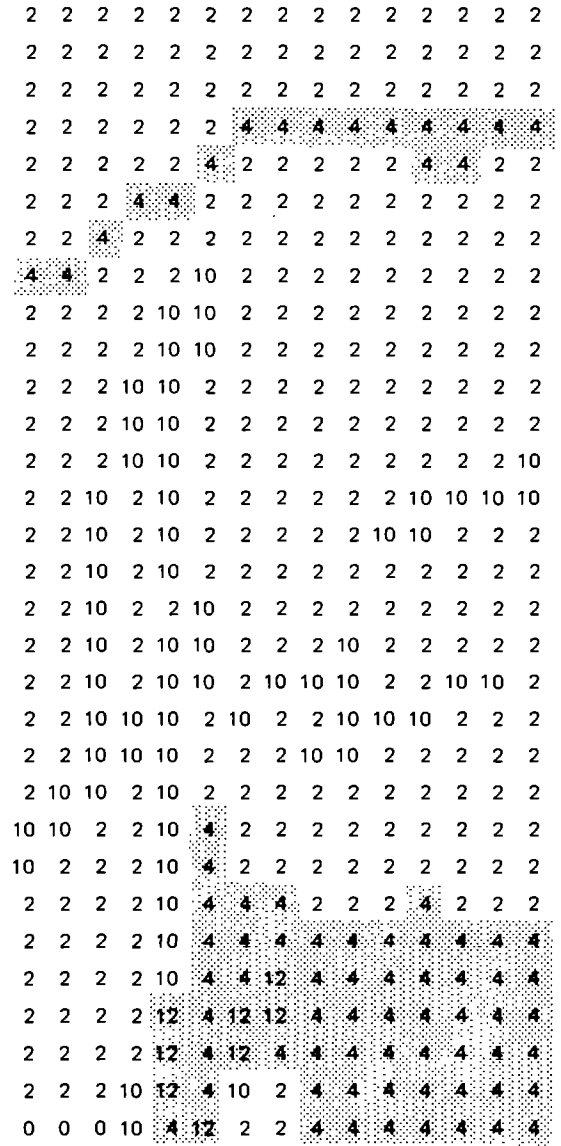


Figure 2B. A portion of the digital seismic hazard map produced from seismic hazard file and fault file.

Mainstream Gravel and Alluvium (shaded area). Figure 2B is the digitized portion of the same area produced by the combination of the seismic response classification and fault basic data files.

The digitized hazard elements are algebraically summed to produce the composite earthquake hazard potential. The composite earthquake hazards map may be produced in digital format or plotted as hazard domains. Density contouring was found to be more suitable than conventional line contours for visual representation of the map. Software packages for plotting routines are available in NCAR (National Center for Atmospheric Research) and GDS (Graphic Display System, U. C. Berkeley). Conventional line contour routines are not recommended since the map contains areas or domains representing degrees of potential hazard. The magnitude of the degree of hazard can vary greatly between adjoining cells, and in many cases, the domains represent isolated hazards. Density contouring is superior to line contouring since it graphically represents the value of individual cells within the range of the contour interval selected. Figures 3 through 6 are small-scale representations of the individual hazard element maps and the composite earthquake hazards map of the Reno 7½-minute quadrangle and show the use of density contouring as a means of graphic representation.

EARTHQUAKE HAZARD MODEL FOR RENO, NEVADA

The computer-simulated hazards mapping technique was applied to the Reno 7½-minute quadrangle. Development of the four basic data files, the three individual hazard elements, and the composite earthquake hazard model is discussed in the following sections.

A matrix of 10,602 cells, with each cell representing a 160,000 square foot area on the ground surface (400 x 400 ft), served as the digitization base for the Reno area. On the Reno 7½-minute quadrangle map each cell is 0.4 inches square and is considered small enough to provide a realistic representation of the hazard components at a scale of 1:24,000.

The basic data files were prepared by Comarc Design Systems by digitizing the geologic, hydrologic and slope maps of the Reno 7½-minute quadrangle. Digitizing was performed manually using a CALMA Graphic III System in conjunction with a Data General NOVA 1200 mini-computer. Digital data were encoded on cards and read into files on the University of Nevada, Reno, Control Data Corporation 6400 computer for manipulation and file integration.

BASIC DATA FILES: RENO QUADRANGLE

File 1: Seismic Response of Units

During large magnitude earthquakes, significant differences in shaking intensities can occur at sites with differing soil or material characteristics. Detailed modeling or calculation of soil (geologic unit) amplification values is difficult, and may not be valid, in areas lacking observational or instrumental data bases. Soil column response is dependent on numerous variables, including: thickness, density, degree of saturation, elastic modulus, fundamental period, lithologic discontinuities, and the characteristics of the input seismic motion. Seed and Schnabel (21) present a concise summary of the problems inherent in accurately modeling soil responses.

Past observations have shown, however, that geologic or soil units may be grouped into broad relative response categories based on specific physical characteristics (14, 15). Assuming that severe surficial shaking is due primarily to earthquake induced shear wave propagation (5, 8, 16, 21), the physical properties of interest are the rigidity or shear modulus (μ) and the density (ρ). Units with significantly contrasting rigidity and density characteristics should exhibit different relative degrees of shear wave amplification and different levels of shaking intensity. Medvedev (15) demonstrated this relationship based on empirical observation of large magnitude earthquakes in the Soviet Union. Units were grouped into preliminary shaking intensity categories based on the seismic rigidity, defined as the product of the rate of propagation of longitudinal (P) seismic waves and the density of the unit (15). Borchardt and others (7) substantiated similar interpretations to Lajoie and Helley (14) by strong motion instrumental monitoring of low-strain (nuclear blasts) and high strain (earthquakes) events in the San Francisco Bay area. Spectral amplifications were found by Borchardt and others (7) to be greatest between deposits having the greatest seismic impedance value contrasts (i.e., the product of S-wave velocity and relative bulk density).

The lack of both instrumental and empirical observation data for large-magnitude earthquakes in the Reno area necessitated the development of semiquantitative relations based on empirical data from geophysical and geotechnical studies. Using the methods of Lajoie and Helley (14), as modified after Medvedev (15), the expected seismic response or "rigidity" of the units to seismic shaking was calculated from seismic shear wave velocities and bulk density data. The rigidity products derived for each geologic unit allow categorization of units into rigidity groups (Table 2).

Longitudinal and transverse seismic wave velocity data were derived from near-surface seismic studies conducted by the Nevada Bureau of Mines and Geology. Density data were obtained from unpublished consultant's reports on file at the Nevada Bureau of Mines and Geology. These data are listed in Table 2 with ranges

TABLE 2. Seismic and Density Data
Upper 30 Ft (10 m) of Deposit

Geologic Unit (4)	Seismic Velocities		Density (ρ)		Rigidity Product (V_{sp})*	Rigidity Group
	Longitudinal Wave (Vp) Range (ft/sec)	Transverse Wave (Vs) Range (ft/sec)	Range (gm/cc)	Mean (gm/cc)		
Q1l	850-1100	250-600	1.4-1.8	1.6	650	I
Qs Qp, Qps Qa Qg Th Thd	1000-2800	1000-1600	0.8-2.0	1.6	1400-1800	II
Qpf Qgr, Qgrs Qdo, Qto Ta(w) Tg(w)	1100-7100	80-1800	1.3-2.1	1.8	2250-2700	III
Tir Mzgd(w) Mzgm(w) Mzv(w) Mzgd Tg Ta Mzv Thh	2000-8000	1200-2700	-	2.5	5410	IV

Note: (w) = weathered

$$\rho = \frac{\text{dry unit weight (}\gamma_d\text{) in pcf}}{62.4}$$

* represents ranges of values calculated for individual units

Decreasing Rigidity

and average mean values given for each group of geologic units.

Four rigidity groups were defined for the Reno area:

Group I	Poorly consolidated, young (Holocene) flood-plain alluvium
Group II	Poorly consolidated late Pleistocene alluvium and low density Tertiary sediments
Group III	Moderately consolidated older Pleistocene alluvium and weathered bedrock
Group IV	Bedrock and weathered bedrock

A SHAKE III computer program (20) for evaluating the earthquake response of soil materials by equivalent linear analysis was used to evaluate this rigidity group classification. Soil period, maximum amplification factor, and maximum surface acceleration were computed for standard logs consisting of a 200-foot column of material with mean density and shear wave velocity representative of each rigidity group. In general the results of the SHAKE program analysis verified the rigidity group sequence.

A map defining four domains based on groups of geologic units with similar rigidity values was prepared from the geologic map of the Reno 7½-minute quadrangle (4). The possible amplification of seismic energy in areas where the geologic units in Groups II and III overlie shallow bedrock was considered significant; thus, two additional domains are defined by the presence of Groups II and III in areas where the depth to bedrock is less than 200 feet (i.e., Group IIa and Group IIIa). Integer values were assigned each of the six domains: Group I – 6; Group IIa – 5; Group II – 4; Group IIIa – 3; Group III – 2; and Group IV – 1. These six domains were digitized as the seismic response classifications.

File 2: Slope of the Terrain

For the Reno area, the 7½-minute quadrangle slope map (23) was digitized based on the slope values listed in Table 3. In general, areas within the Reno quadrangle with slopes of 25 percent or greater have limited geographic extent; they do not constitute the areally predominant condition within a matrix cell, and therefore were not reflected in the digitized data file. However, since these slopes are potentially hazardous, the basic data file was modified by hand to reflect the existence of slopes of 25 percent or greater.

TABLE 3. Slope values.

<u>Percent Slope</u>	<u>Slope Angle</u>	<u>Slope Value</u>
>50	> 26.5°	7
30-50	16.5°-26.5°	6
20-30	11.3°-16.5°	5

File 3: Depth to Ground Water

For the Reno area, depth to ground water was obtained from the 7½-minute quadrangle hydrologic map (9). Depth to ground water was converted to meters and digitized for each cell. Only areas with depths to ground water of less than 18 m (60 ft) were included; this value was considered conservative since Medvedev (15) assumes negligible increase in seismic intensity for depths to ground water greater than 10 m.

File 4: Faults

Faults in the Reno quadrangle less than 600,000 years in age were considered active and were digitized into a file indicating length of the fault trace with numerical values representing the age of last movement. Four categories for the ages of faults used by Bingler (2, 3) were adopted in this analysis; these include: 1) Holocene, 2) post-Wisconsinan, 3) post-Illinoian, and 4) early to middle Quaternary. Numerical values were assigned each category with the youngest faults given the highest value (10) and with decreasing values given to the older faults.

Post-Tertiary faults lacking morphologies suggestive of recent activity were not digitized. Geodetic deformation and ground acceleration that could be generated by movement along the faults are considered to be only locally significant, and therefore are not represented by digitized values beyond the respective cells transected by the faults.

HAZARD ELEMENTS

The basic data files are combined to produce individual hazard elements. The seismic response classification of the geologic units is combined with the slope of the terrain, the depth to ground water, and the fault files, respectively, to produce the following hazard elements: 1) potential for slope instability, 2) potential for liquefaction and differential compaction, and 3) potential for surface faulting. The digitized data are algebraically summed for each cell in the matrix to produce the relative hazard element potential.

1) Potential for Slope Instability

The slope instability map (fig. 3) depicts areas which are susceptible to slope failure during seismic load-

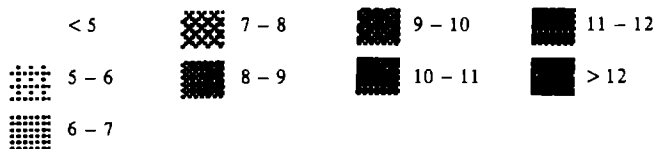
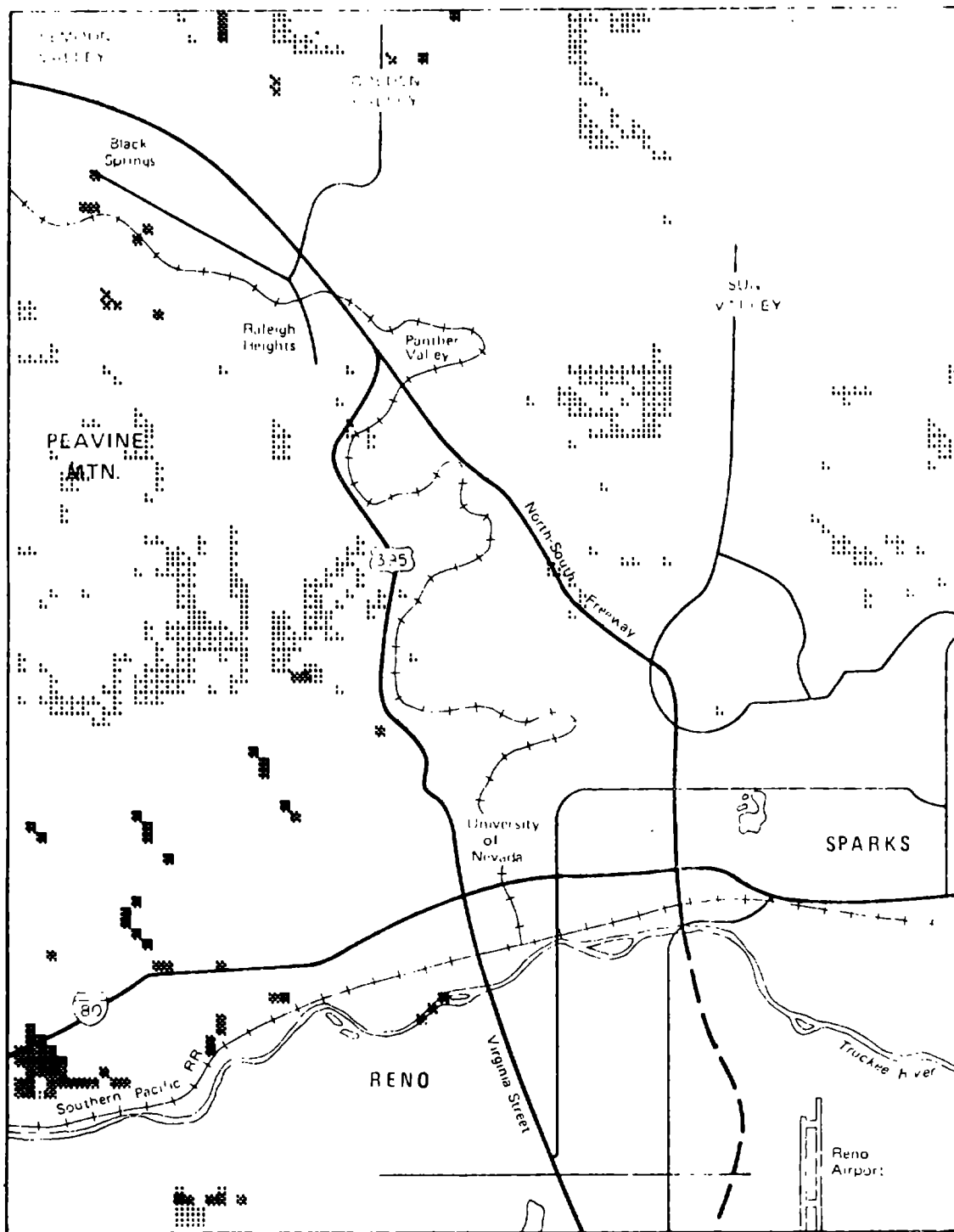


Figure 3. Potential for slope instability hazard element.

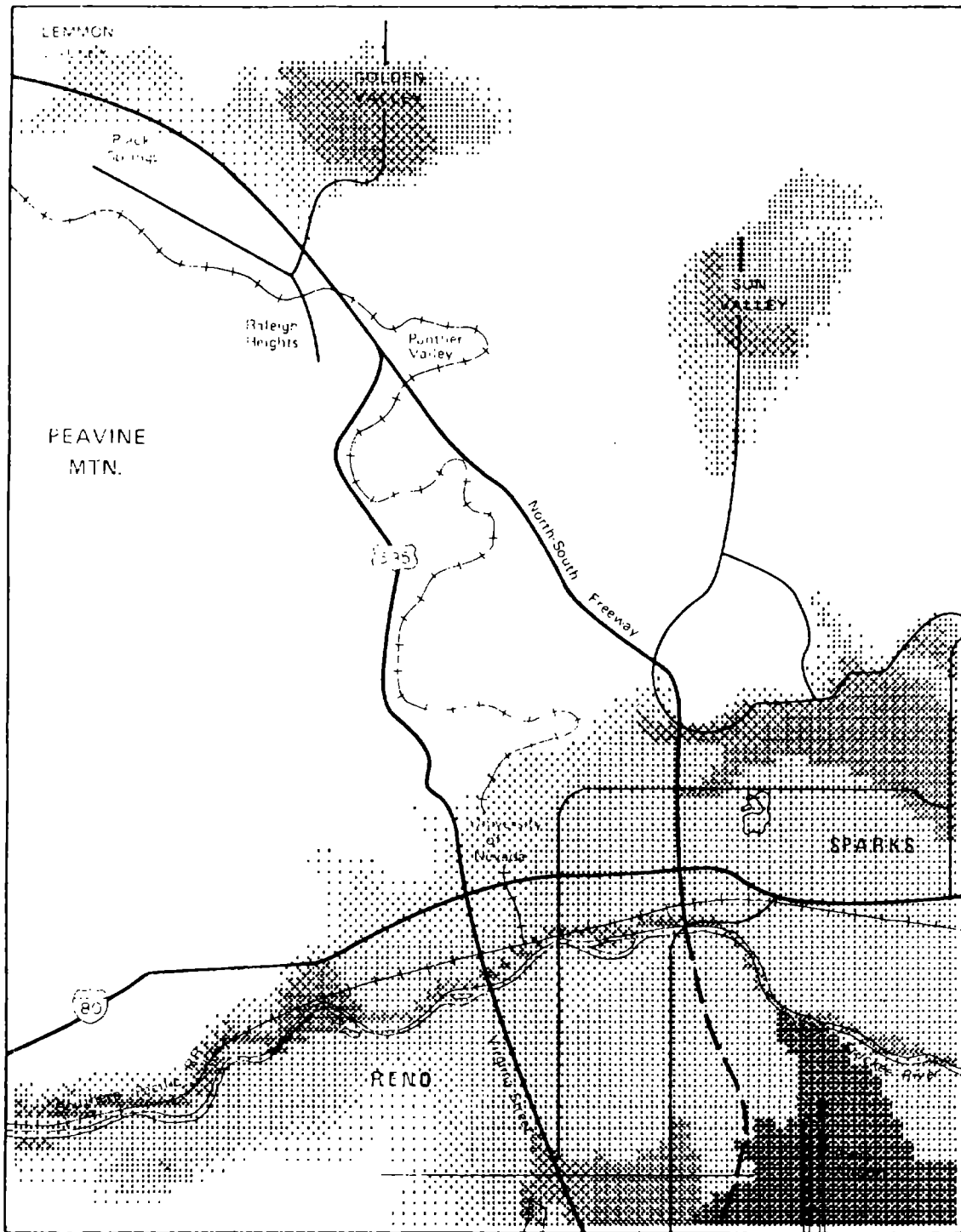


Figure 4. Potential for liquefaction hazard element.

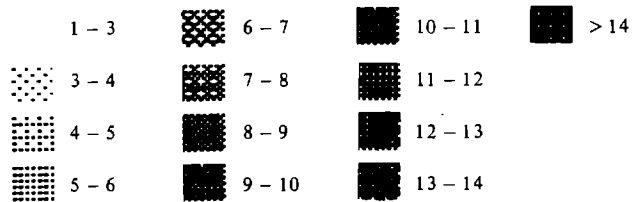
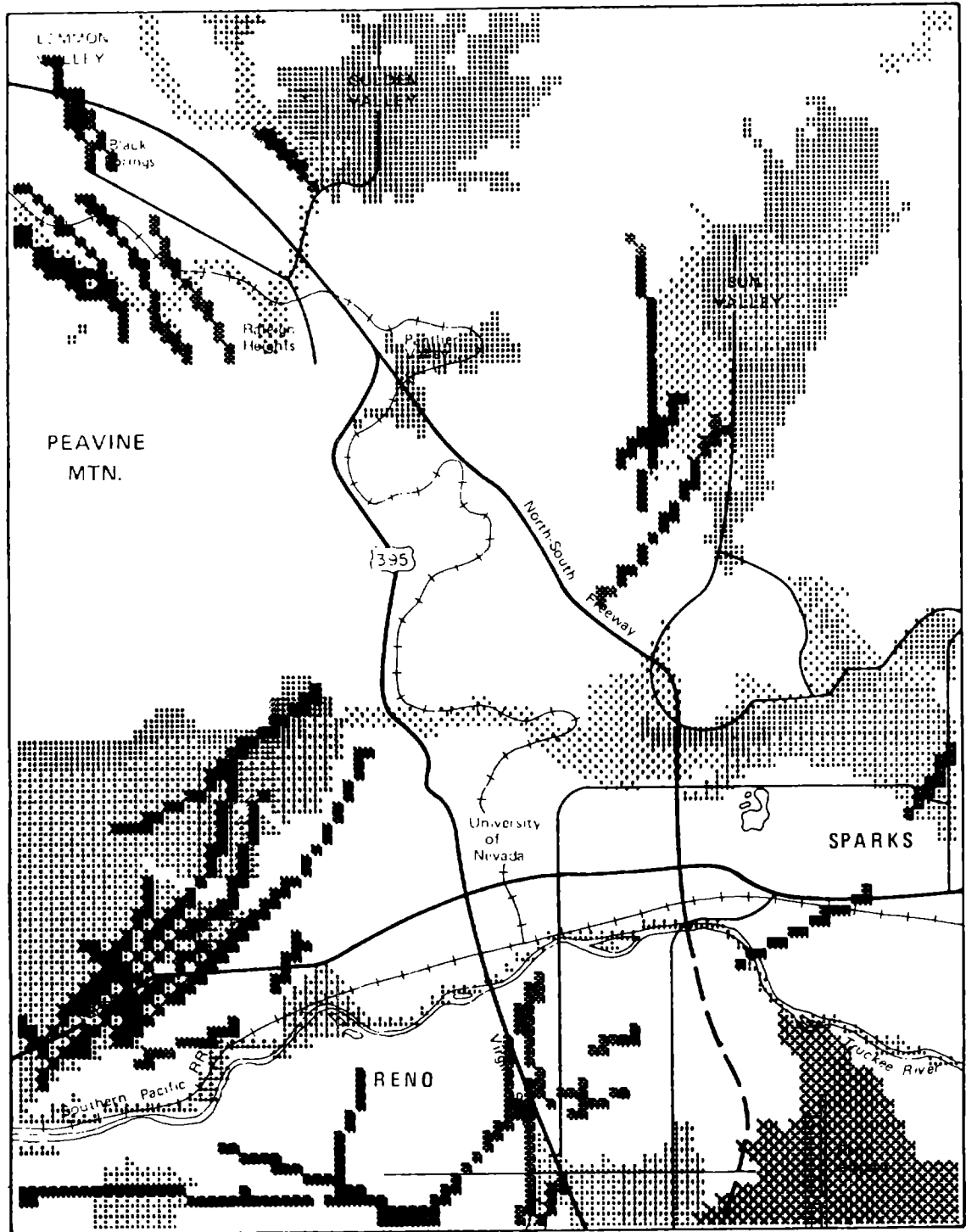


Figure 5. Potential for surface faulting.

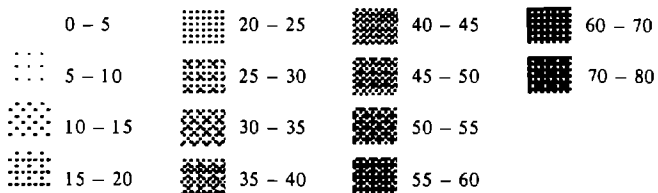
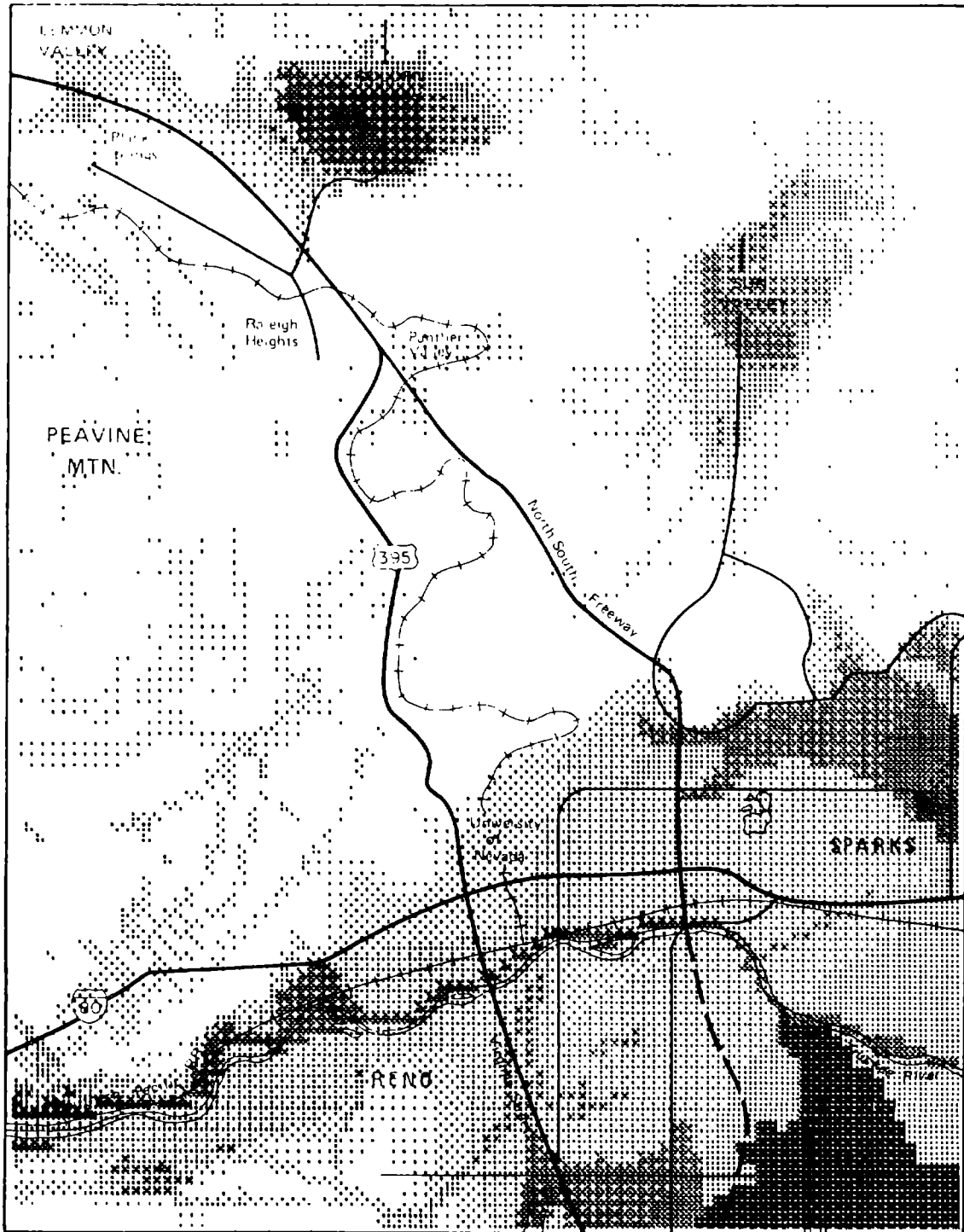


Figure 6. Composite earthquake hazard map.

ing. Slope instability values for the Reno quadrangle range from a low of 6 for areas of bedrock (hazard element potential = 1) with 20 to 30 percent slope (hazard element potential = 5) to maximum values of 11 representing several combinations of slope values and seismic response classifications.

2) Potential for Liquefaction and Differential Compaction

The potential for liquefaction map (fig. 4) represents the probable response of the various seismic response classifications as a function of depth to ground water in meters (h). Seismic intensity (n), calculated from the equation $n = e^{-0.4h}$, is algebraically summed with the seismic response classification value and is then scaled by a factor of 10. The resulting value represents the hazard element potential for liquefaction and differential compaction. For the Reno area, these values range from 69 for flood-plain and lake deposits located in areas of ground water discharge to 2 for more competent material with depths to ground water greater than 18 m. Unconsolidated outwash deposits are less likely to liquefy, but water-saturated lenses of clean, fine sand within these deposits may compact differentially and cause local surface disruption.

3) Potential for Surface Faulting

The potential for surface faulting presented in figure 5 is based on the length and relative ages of the faults in combination with the seismic response classifications. Values for the potential for surface faulting in the Reno area range from 8 where early to middle Quaternary age faults (hazard element potential = 7) transect units in seismic response classification IV (hazard element potential = 1) to 14 where Holocene age faults (hazard element potential = 10) transect units in seismic response classification II (hazard element potential = 4).

COMPOSITE EARTHQUAKE HAZARDS MAP

The composite earthquake hazards map of the Reno 7½-minute quadrangle is shown in figure 6 and represents the summation of the three hazard elements presented above. This map was produced using the best available data on the physical properties of the geologic units, the slope of the terrain, the depth to ground water, the depth to bedrock, and the known length, displacement, and movement history of faults. The lack of deep subsurface seismic velocity data and empirical post-earthquake strong motion data severely limits the evaluation of the potential seismic response of thick sequences of unconsolidated materials common in the southern portion of the quadrangle.

The map represents the best estimate of potential seismic hazards in the Reno 7½-minute quadrangle. The hazard element maps can be used in conjunction with the composite hazards map to evaluate the relative significance of each hazard element for a particular area. The map is intended to be a dynamic seismic zonation of the Reno quadrangle—it can be updated when new data become available, and it can be tested and modified after a large magnitude earthquake occurs in the Reno area.

ACKNOWLEDGMENTS

The authors thank Dennis P. Bryan and David B. Slemmons for their review of the manuscript and their valuable comments. The research was supported by U. S. Geological Survey Earthquake Hazards Reduction Program Grant 14-08-0001-G-358.

REFERENCES

- (1) Algermissen, S. T. (1975) Hazard maps, risk maps, and zoning maps for use by seismologists, engineers, and public agencies: *Geol. Soc. America Abstracts with Programs*, v. 7, no. 3, p. 393.
- (2) Bingler, E. C. (1974) Earthquake hazards map, Reno folio: Nevada Bur. of Mines and Geology Environmental Map 4A i.
- (3) _____ (1976) Earthquake hazards map, *in* Environmental Folio Series, Reno quadrangle: Nevada Bur. Mines and Geology Pub., p. 42–48.
- (4) Bonham, H. F., Jr., and Bingler, E. C. (1973) Geologic map of the Reno quadrangle, Reno folio: Nevada Bur. Mines and Geology Environmental Map 4Ag.
- (5) Bolt, B. A. (1972) Seismicity: *Proc. Internat. Conf. on Microzonation*, Seattle, Washington, p. 13–23.
- (6) Borchardt, R. D., ed., (1975) Studies for seismic zonation of the San Francisco Bay region: U. S. Geol. Survey Prof. Paper 941–A, 102 p.
- (7) Borchardt, R. D., Joyner, W. B., Warrick, R. E., and Gibbs, J. F. (1975) Response of local geologic units to ground shaking, *in* Borchardt, R. D., ed., Studies for seismic zonation of the San Francisco Bay region: U. S. Geol. Survey Prof. Paper 941–A, p. A52–A67.
- (8) Bullen, K. E. (1963) An introduction to the theory of seismology: London, Cambridge Univ. Press, 381 p.
- (9) Cooley, R. L., Spane, F. A., Jr., and Scheibach, R. B. (1974) Hydrologic map, Reno folio: Nevada Bur. Mines and Geology Environmental Map 4Af.
- (10) Dewey, J. W., Dillinger, W. H., Taggart, James, and Algermissen, S. T. (1972) A technique for seismic zoning: analysis of earthquake locations and mechanism in northern Utah, Wyoming, Idaho and

- Montana: Proc. Internat. Conf. on Microzonation, Seattle, Washington, p. 879–895.
- (11) Greensfelder, R. W. (1976) Maximum probable earthquake acceleration in bedrock in the state of Idaho: Idaho Dept. Transportation—Division of Highways, Boise, Research Project No. 79, 69 p.
 - (12) Hastie, L. M., and Savage, J. C. (1970) A dislocation model for the 1964 Alaska earthquake: *Bull. Seis. Soc. America*, v. 60, no. 4, p. 1389–1392.
 - (13) Howell, B. F., Jr. (1974) Average regional seismic hazard index in the United States: *Geol. Soc. America Abstracts with Programs*, v. 6, no. 3, p. 296.
 - (14) Lajoie, K. R., and Helley, E. J. (1975) Differentiation of sedimentary deposits for purposes of seismic zonation, *in* Borcherdt, R. D., ed., *Studies for Seismic Zonation of the San Francisco Bay Region*: U. S. Geol. Survey Prof. Paper 941–A, p. A39–A51.
 - (15) Medvedev, S. V. (1965) Engineering seismology: National Tech. Inf. Serv., NTIS No. TT65-50011, 260 p.
 - (16) Power, J. H., and Real, C. R. (1975) Shear wave velocity—propagation and measurement: *California Geol.*, v. 29, no. 2, p. 27–29.
 - (17) Savage, J. C., and Hastie, L. M. (1966) Surface deformation associated with dip-slip faulting: *Jour. Geophys. Res.*, v. 71, p. 4896–4904.
 - (18) _____ (1969) A dislocation model for the Fairview Peak, Nevada, earthquake: *Bull. Seis. Soc. America*, v. 59, no. 5, p. 1937–1948.
 - (19) Savage, J. C., Church, J. P., and Prescott, W. H. (1975) Geodetic measurement of deformation in Owens Valley, California: *Bull. Seis. Soc. America*, v. 65, no. 4, p. 865–874.
 - (20) Schnabel, P. B., Lysmer, J., and Seed, H. B. (1972) SHAKE—a computer program for earthquake response analysis of horizontally layered sites: EERC Rept. No. 72–12, Univ. California, Berkeley. Modified by California State Highway Department (1976): SHAKE III.
 - (21) Seed, H. B., and Schnabel, P. B. (1972) Soil and geologic effects on site response during earthquakes: Proc. Internat. Conf. on Microzonation, Seattle, Washington, p. 61–85.
 - (22) Slemmons, D. B. (1972) Microzonation for surface faulting: Proc. Internat. Conf. on Microzonation, Seattle, Washington, p. 347–361.
 - (23) U. S. Geological Survey (1973) Slope map, Reno Folio: Nevada Bur. of Mines and Geology Environmental Map 4Ab.
 - (24) Whitham, K., Milne, W. G., and Smith, W. E. T. (1970) The new seismic zoning map for Canada—1970 edition: The Canadian Underwriter, June, 1970.

484

INTENTIONALLY BLANK

ZONATION FOR CRITICAL FACILITIES BASED ON TWO-LEVEL EARTHQUAKES

By

Ashok S. Patwardhan^I, David D. Tillson^{II}, and Robert L. Nowack^{III}

ABSTRACT

The seismic design of critical facilities is based on two levels of earthquakes. Seismic zonation can be used in the siting of such facilities to identify areas that have a higher potential for containing suitable sites than those outside. The criterion for exclusion is a ground motion value beyond which the cost of construction of a safe facility increases substantially. Areas within which this ground motion may be experienced are established by a deterministic procedure. If a probabilistic analysis is used to identify suitable areas, different boundaries are obtained. If a probabilistic approach is to be utilized as one of the bases for assessing ground motion parameters for the two earthquakes, those for the higher level earthquake may be based on a reasonably long return period (in the order of 10,000 years) and those for the lower level earthquake based on 100- to 500-year return periods. However, we recommend that a firm ratio between the two values should not be utilized. An example area consisting of a portion of eastern Washington and Oregon is utilized to examine the relationship between ground motion values for different return periods.

INTRODUCTION

The seismic design of critical facilities such as nuclear and fossil power plants, LNG terminals, and offshore platforms is rarely based on zonation. Detailed site-specific studies are required for the selection of the seismic design bases and, in some cases, even the procedures for establishing the design bases is specified by regulations; e.g., see 10 CFR 100 App A and USNRC Regulatory Guide 1.60 for nuclear power plants (1, 2).

In practically all cases, the seismic design of such facilities is based on two earthquakes:

(a) A higher level earthquake defined as the maximum earthquake on a source assumed to occur at a point closest to the site. Estimated ground motions due to this earthquake are used for inelastic design to preclude failure of critical elements. The probability of occurrence of the motions is generally not calculated or taken into account.

-
- I Associate, Woodward-Clyde Consultants, San Francisco, California
II Principal Geologist, Washington Public Power Supply System,
Richland, Washington
III Formerly Staff Seismologist, Woodward-Clyde Consultants,
San Francisco, California

(b) A lower level earthquake defined as the earthquake that can reasonably be expected to occur within the lifetime of the facility. Estimated ground motions due to this earthquake are used in the elastic design of the facility. The probability of exceeding the motions within the useful lifetime of the facility is computed either formally or is estimated by simplified procedures.

In the case of nuclear plants, the U.S. regulations specify a definite relationship between the higher level (safe shutdown earthquake, SSE) and the lower level (operating basis earthquake, OBE) earthquakes; i.e., the peak acceleration $a_{OBE} \geq 0.5 a_{SSE}$.

Although the seismic design is site specific in nature, the selection of sites for the facilities themselves is often based on a zonation approach. Most siting studies utilize a screening process in which suitable criteria are applied to a large area to focus attention on progressively smaller areas which have a higher probability of containing suitable sites. In case of seismicity, the screening criteria can be readily based on current technological limitations (difficulty in designing for surface fault displacement) and on economic considerations (cost of constructing a facility to withstand the design ground motions).

ZONATION CRITERIA

Zonation to meet the first criterion is accomplished by excluding areas close to active (capable) faults (usually within approximately 5 miles). Such an approach does not consider the probability of experiencing a surface rupture at the site based on the degree of activity of faults. However, the area excluded is not large, is generally included within areas excluded for other reasons discussed below, and a more refined analysis does not provide any additional benefit.

Zonation criteria for seismic ground motions can also be based on the cost of designing the facility to withstand the design motions. In case of 1100-MW nuclear plants, a recent study (3) suggests a relationship between a_{SSE} and cost as shown in Fig. 1 for meeting seismic design requirements. A representative cost versus a_{SSE} curve is not continuous and shows two steps at approximately $a_{SSE} \approx 0.25$ g and 0.40 to 0.50 g. The first step is the approximate upper limit of standard design of major reactor components and equipment, while the second step at approximately 0.40 to 0.50 g represents a change in the design strategy and/or the cost of additional foundation treatment and the cost of providing additional structural supports for critical equipment.

The issue to be resolved is: "how does one select zonation criteria when the facility design will be based on two different earthquake levels?" Based on stepwise jumps in construction cost shown in Fig. 1, an appropriate zonation criterion appears to be $a_{SSE} = 0.40$ g. If in addition the relationship between a_{SSE} and a_{OBE} required by NRC is to be maintained, the same criterion may be stated as $(a_{OBE})_{min} = 0.20$ g. Therefore, other factors being equal, areas with peak SSE accelerations greater than 0.40 g may be excluded from further consideration. The criterion is applied by utilizing an attenuation which is stated either as a magnitude-acceleration-distance or intensity-acceleration-distance

relationship. During screening, the ground motion criterion is applied to large areas and for the selection of candidate areas is generally not reapplied in the progressive exclusion of areas until a number of candidate sites are selected. At this stage, site-specific estimates of peak SSE accelerations are made using, if appropriate, additional information on smaller capable faults that were not included in the earlier regional evaluation. Mean attenuation relationships are used to estimate the accelerations, and the uncertainty associated with the relationship may not be included in the estimate.

Analyses from a number of nuclear plants have indicated that the OBE ground motions rather than the SSE may govern the plant design above $a_{SSE} \approx 0.20$ g. The specified criteria for OBE selection given by 10 CFR 100 App A (1) imply that the OBE is an earthquake (and associated motions) that may be expected in a useful plant life of 30 to 40 years. Generally, motions with a 100- to 150-year return period at the site are considered reasonable. An OBE design acceleration with a 100-year return period may be the combined effect of different magnitude earthquakes from a number of sources. No similar probability evaluation is made for the SSE design acceleration on the basis of the occurrence of the "maximum credible" earthquake. The SSE is usually associated with the closest earthquake source, which may suggest a considerably longer return period in the range of 10^4 years or so. If the SSE peak acceleration is evaluated probabilistically, it may be anticipated that an acceleration corresponding to twice the OBE peak acceleration may have a return period smaller than the 10^4 years. Conversely, the return period of an acceleration corresponding to a value one half of the SSE with a return period 10^4 years may be considerably higher than the value corresponding to a 100-year return period. Also, when design values are chosen, the recurrence of those values can often be different from the return periods noted above.

Clearly, several alternatives exist for the selection of seismic zonation criteria which can lead to different results. The effects of using the different criteria are examined in the following paragraphs with the aid of an example.

ZONATION OF EXAMPLE AREA

The model utilized in the seismic exposure evaluation is shown in Fig. 2. Inputs to the model include source seismicity characterization, attenuation characteristics, and criteria for the evaluation of seismic exposure. Source characterization includes location and geometry of the earthquake sources and establishment of the recurrence relationship for each source.

The example area is a portion of eastern Washington and Oregon (see Fig. 3) and is characterized by low to moderate seismicity with areas of higher seismicity along the western boundary. Twenty source areas based on the USNRC criteria for capable structures (1) were identified from the geology and seismicity in the region (4). Names of these sources and the applicable source depths are given in Table 1, and their location is shown in Fig. 3. Since the boundaries of some sources are not well defined, envelopes were drawn around them to enclose the probable source locations.

To recognize the possibility of occurrence of sources of unknown location, random sources were included (see Table 1) at relatively shallow depths. The recurrence relationships and maximum earthquakes on sources were established in a conservative manner. The sources were modelled as horizontal or dipping planes. Individual earthquake events were modelled as rectangular areas of sizes dependent upon the magnitude of the postulated event.

For calculation of seismic exposure, both the earthquake source surface and the study region were discretized into grid cells. Each grid cell corner on the study region was considered as a "site". An earthquake event was postulated to occur on a hypocentral on the source. Vibratory ground motion was assumed to be generated along the rupture surface and propagate towards the site. Mean peak accelerations at the site were calculated by using an attenuation relationship proposed by McGuire (5).

$$a = 472.3(10)^{0.278M} (R + 25)^{-1.301} ; \sigma_{\log a} = 0.22 \quad (1)$$

Utilizing the attenuation relationship, the expected peak acceleration due to a given magnitude earthquake at each "site" was estimated. Utilizing the recurrence relationship defined for the source (such as in Fig. 4), expected ground motions for all earthquakes and all locations on the source were calculated. The process was continued until all sources were covered. The combined result was a relationship showing the probability of exceeding a given acceleration at the site due to all sources and magnitudes.

$$P(a \geq a_i) = 1 - \prod_{\text{all sources}} [1 - P[a \geq a_i]_{\text{one source}}] \quad (2)$$

The results were plotted as a cumulative distribution function (see Fig. 8) for a given site. The process was repeated for all "sites" in the study region.

To study trends of expected peak acceleration values over the study region, contours were plotted for selected probabilities of exceedance. Considering a 40-year economic life, the accelerations corresponding to selected probabilities of nonexceedance during a given year were calculated using Bernoulli's binominal probability law,

$$P_R(r/n) = C_R^n p^r (1 - p)^{n-r} \quad (3)$$

where n is total number of trials (40 years, period of interest), r is number of successes (0 in this case), and p is probability of success in any trial (one year).

Three probabilities of exceedance ($1 - P_R$) were selected for analysis (i.e., 0.003, 0.033, and 0.33) corresponding to return periods of approximately 13,100; 1,200; and 100 years, respectively.

Contour maps shown in Figs. 5, 6, and 7 were plotted to depict the variation of peak accelerations corresponding to the three probabilities of exceedance in the study area. The contours show similar trends. A closer spacing of contours is seen in the western portion of the region,

which reflects the larger maximum magnitudes, proximity, and higher earthquake recurrence from earthquake sources in that portion of the study area. As discussed in the section on sensitivity below, the values shown in the map are influenced by the input parameters and by themselves are relatively less significant; the chief value of the maps is in their use for comparative purposes.

The maps can be used for zonation by selecting a peak acceleration value for a given return period as a criterion. If, as discussed above, the zonation criterion chosen is that the peak SSE acceleration should have a long return period ($\approx 10^4$ years), the boundary of a zone within which a site may be located is identified by the 0.40 g contour in Fig. 5. In conjunction, if the zonation criterion is selected as an OBE acceleration of 0.20 g with a 100-year return period, the boundaries of the zone within which sites may be selected is defined by the 0.20 g contour in Fig. 7. If a different return period is selected for the OBE (e.g., $\approx 1,000$ years), the zone suitable for siting is shown by the 0.20 g contour in Fig. 6. In addition, if a deterministic procedure is used, the distance at which 0.40 g peak acceleration can be expected from the maximum earthquake on each source can be calculated from equation 1. Using this distance, an envelope can be drawn around each source to define areas which can be excluded from further consideration. These envelopes are shown by dashed lines around each source in Fig. 3.

A comparison can be made between Figs. 3, 5, 6, and 7. The figures identify areas that may be excluded from further consideration based on three different criteria. The areas to be excluded differ in size and location in each case. The zonation based on the deterministic procedure may exclude areas that may contain some suitable sites. However, if the remaining areas still contain an adequate number of sites, this exclusion may not be significant. The peak SSE acceleration in the remaining areas in Fig. 3 will be less than 0.40 g when established by a deterministic procedure. If the earthquake location, recurrence, and attenuation of ground motions are included to evaluate the combined effect of various sources on a given site, the peak acceleration corresponding to a 10^4 -year return period may exceed the value calculated by a mean deterministic relationship.

ACCELERATION VALUES AT SPECIFIC SITES

Acceleration values for various return periods were calculated for three sites, A, B, and C (see Fig. 2), in the area outside the exclusion boundaries shown in Fig. 3. The locations of the sites are shown in Fig. 3. Figure 8 shows the cumulative distribution function for maximum accelerations at sites A and B. Values of peak acceleration corresponding to selected return periods for a 40-year period of interest are summarized in the table below:

return period (yrs)	peak acceleration values at sites (cm/sec ²)		
	A	B	C
100	170	110	90
500	250	170	130
10,000	470	320	250
mean acceleration due to largest earthquake on closest source at closest point	290	150	111

The values tabulated above are instructive in showing the relationship between values for different return periods. The ratio between the 10,000-year and 100-year return period values lies between 2.75 and 2.91 (i.e., greater than 2). If the 10,000-year return period value is used as a basis for selecting the SSE acceleration, the corresponding OBE acceleration at one half of the SSE acceleration will be higher than the value calculated for a 100-year return period. This is to be anticipated from the shape of the cumulative distribution function and the fact that a significant contribution to the acceleration values at longer return periods is due to the larger earthquakes on each source, while the shorter return period acceleration values are influenced by smaller magnitude earthquakes. A ratio of approximately two can be obtained between the accelerations for the higher and lower level earthquakes by choosing values with return periods of approximately 500 and 10,000 years. If the acceleration level corresponding to the higher level earthquake is chosen by calculating the mean acceleration due to the largest earthquake on a source assumed to occur at a point closest to the site, the values so obtained are lower than the accelerations for a longer return period (such as 10,000 years). This is the case of all three sites in the above table. The difference is attributable to the fact that the calculated mean value is the estimated effect of one earthquake from one source without taking into account the uncertainty in the attenuation relationship while the 10,000-year value is the combined effect of earthquakes of all magnitudes that may be expected to occur within the period of interest from all sources including the effect of variation in the attenuation relationships.

SENSITIVITY

The calculated seismic exposure values are significantly influenced by three input parameters (i.e., earthquake recurrence, attenuation relationships, and the exposure evaluation model). Sensitivity analyses suggest that an increase in the overall seismicity by a factor of two increases the calculated values by 15 to 25 percent. A comparison of exposure evaluation models indicates that, for low seismicity areas such as the one discussed here, models that associate a rupture surface with an earthquake event give approximately 10 percent higher acceleration values as compared to the models that do not associate a rupture surface with an earthquake but consider all earthquakes to originate at a point (6; see Fig. 9). The largest variation in calculated values is obtained by the choice of the attenuation relationship and the dispersion associated with the mean relationship. Recent studies have shown that the calculated values can vary by a factor 1 to 2.5 depending upon the relationship used and the magnitude and distance of the site from the source (7).

SUMMARY

Seismic zonation can be used in the siting of critical facilities to identify areas that have a higher potential for containing suitable sites than those outside. The criterion for exclusion is a ground motion value beyond which the cost of construction of a safe facility increases substantially. Areas within which this ground motion may be experienced

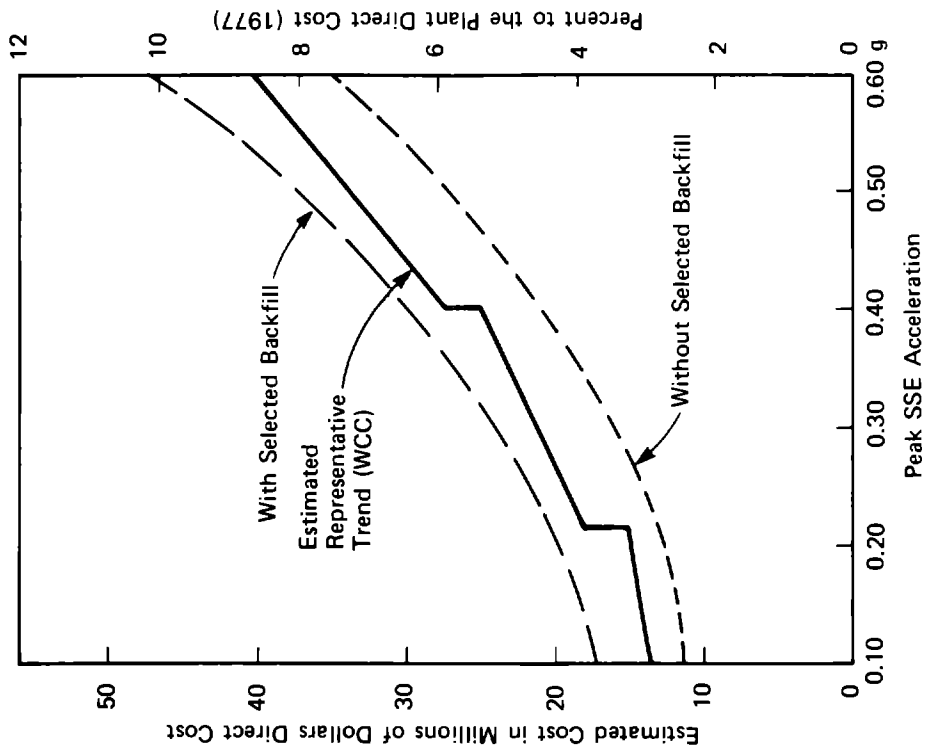
are established by a deterministic procedure. If a probabilistic analysis is used to identify suitable areas, different boundaries are obtained. If a probabilistic approach is to be utilized as one of the bases for the selection of design values, ground motions for the higher level earthquake may be based on a reasonably long return period (in the order of 10,000 years), and the ground motions for the lower level earthquakes based on 100- to 500-year return periods. However, we recommend that a firm ratio between the two values should not be utilized.

ACKNOWLEDGEMENTS

A portion of the work reported here was conducted by Woodward-Clyde Consultants for United Engineers & Constructors (UE&C) in connection with the earthquake studies for the Washington Public Power Supply System Nuclear Project Nos. 1 and 4. The support from WPPSS and UE&C is acknowledged. The authors wish to thank Dr. Don Tocher, Dr. Thomas Turcotte, and Mr. John Hobgood of Woodward-Clyde Consultants, who participated in the characterization of earthquake sources, and Dr. Christian P. Mortgat of Stanford University, who assisted in computer analyses.

BIBLIOGRAPHY

1. U. S. Code of Federal Regulations, Title 10, Chapter 1, Part 100-- Reactor Site Criteria, Appendix A--Seismic and Geologic Siting Criteria for Nuclear Power Plants.
2. U. S. Nuclear Regulatory Commission, 1973, Regulatory Guide 1.60, "Design Response Spectra for Seismic Design of Nuclear Power Plants", Revision 1, December.
3. Stevenson, John D., 1978, Selection of seismic input level and its impact on costs of nuclear power plants: Nuclear Engineering and Design, North Holland Publishing Co., v. 48, no. 1, June.
4. Washington Public Power Supply System, 1977, WPPSS Nuclear Project Nos. 1 and 4 PSAR, Docket Nos. 50-460 and 50-513.
5. McGuire, Robin K., 1974, Seismic structural response risk analysis, incorporating peak response regressions on earthquake magnitude and distance: Massachusetts Institute of Technology, Dept. of Civil Engineering, Research Report R74-51.
6. Mortgat, Christian P., Patwardhan, Ashok S., and Idriss, I. M., 1978, Influence of seismicity modeling on seismic exposure evaluation: Seismological Society of America, Earthquake Notes, v. 49, no. 1, p. 51.
7. Alaska Subarctic Offshore Committee, 1978, Offshore Alaska Seismic Exposure Study, Vols. I through V: prepared by Woodward-Clyde Consultants, San Francisco, California.



Based on Stevenson 1978.

Fig. 1. Relationship Between Peak SSE Acceleration and Cost for Nuclear Plant

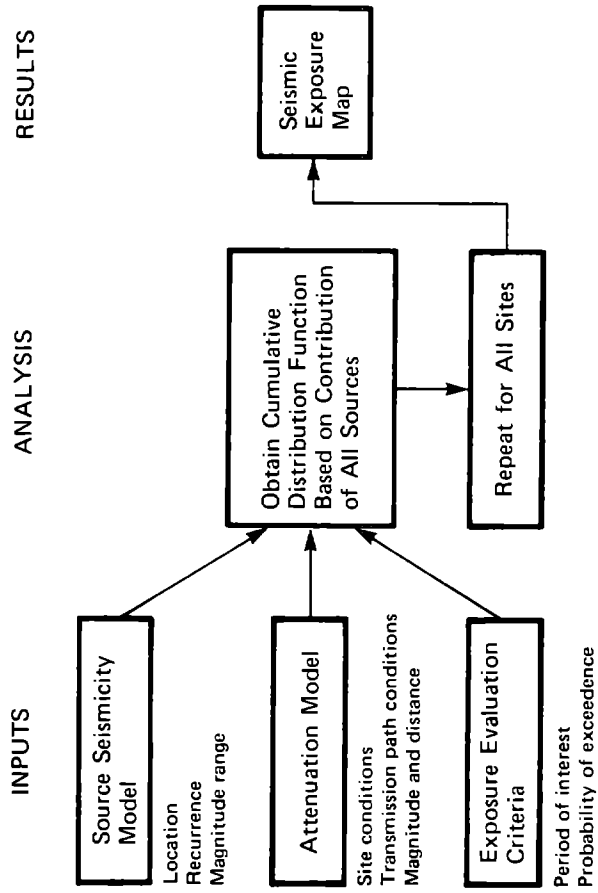


Fig. 2. Seismic Exposure Evaluation Model Used in Analysis

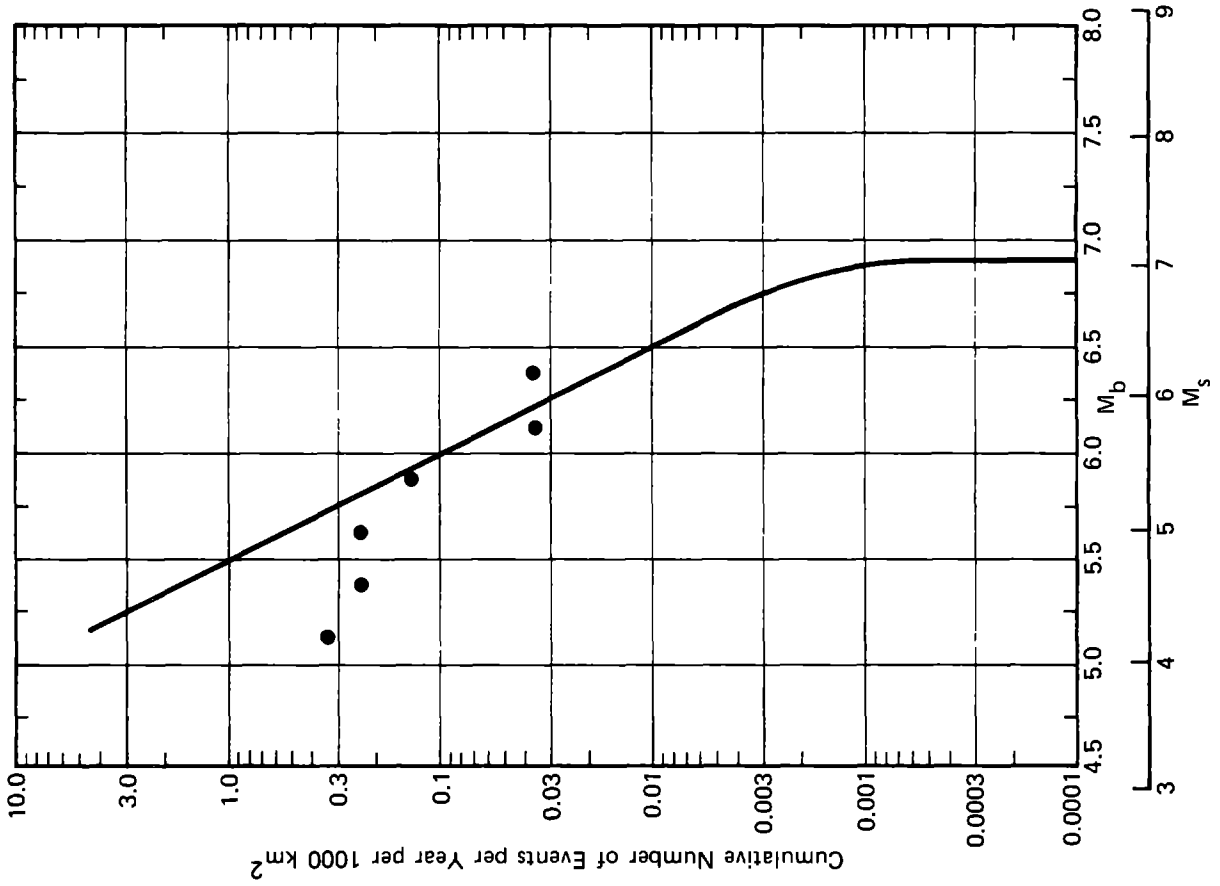


Fig. 4. Typical Earthquake Recurrence Relationship Used in Analysis

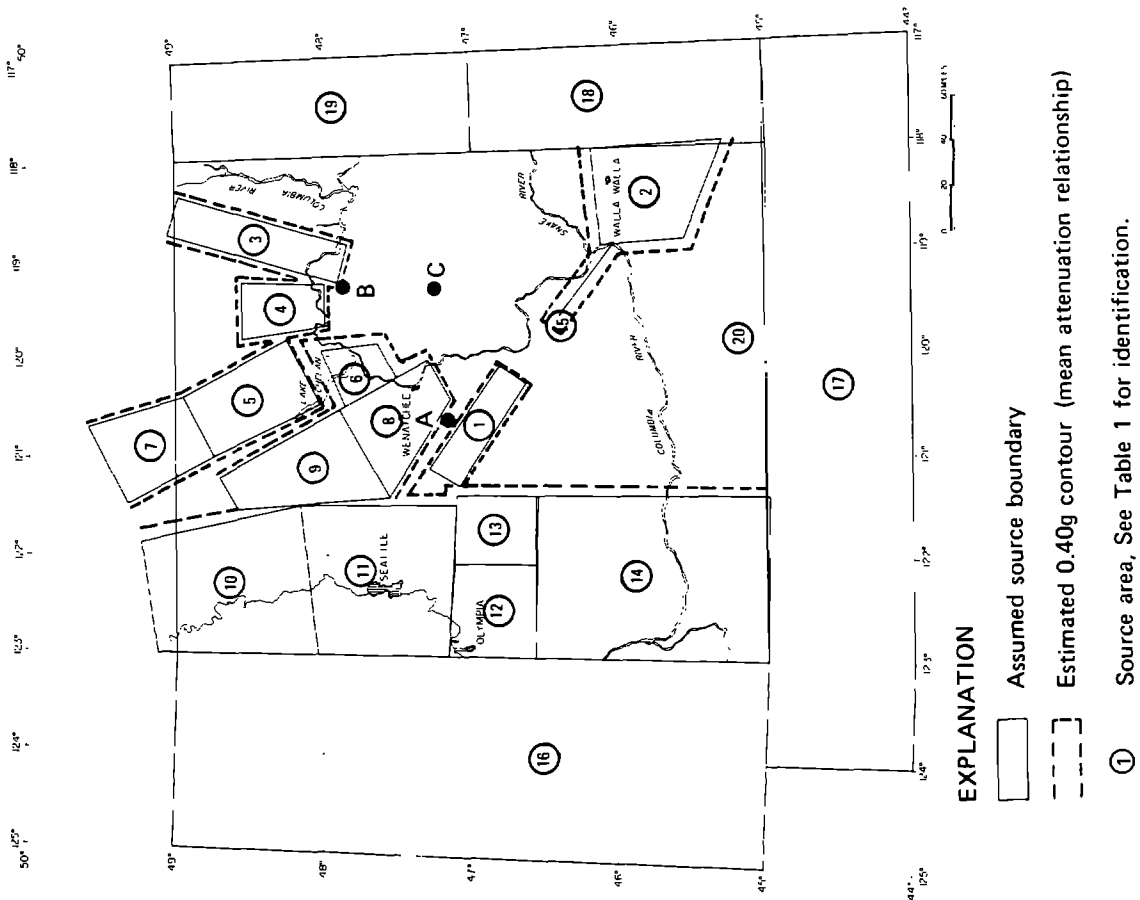
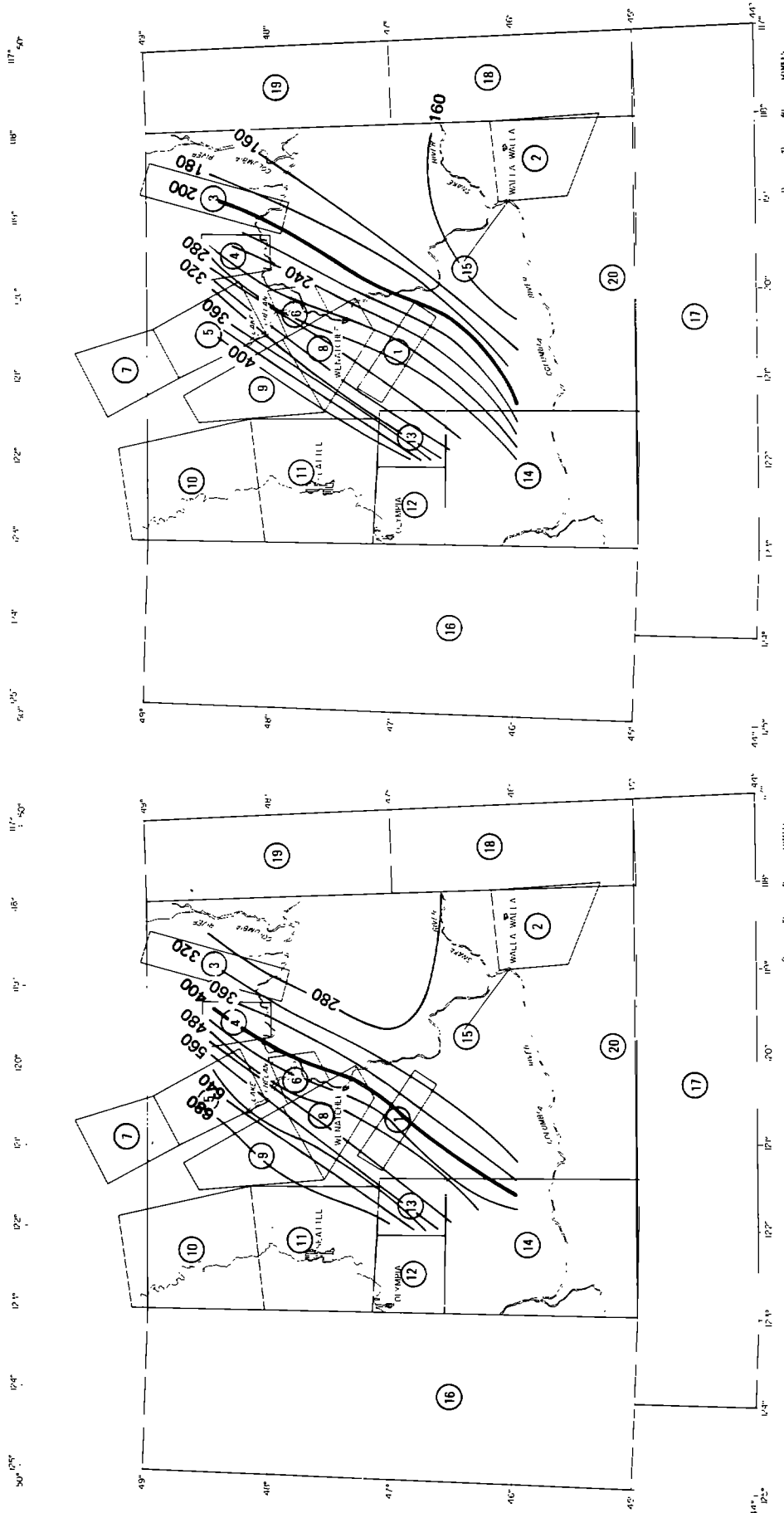


Fig. 3. Example Area Earthquake Sources and Exclusion Area Boundaries Based on Mean Attenuation Values; $a_{max} < 0.40g$



EXPLANATION

—680 — Contours of peak acceleration, cm/sec²

⑩ Source area, See Table 1 for identification

Note:

Acceleration values in maps are based on input relationships for source seismicity and attenuation.

Fig. 5. Contours of Peak Acceleration for Return Period of 13,100 Years

Fig. 6. Contours of Peak Acceleration for Return Period of 1200 Years

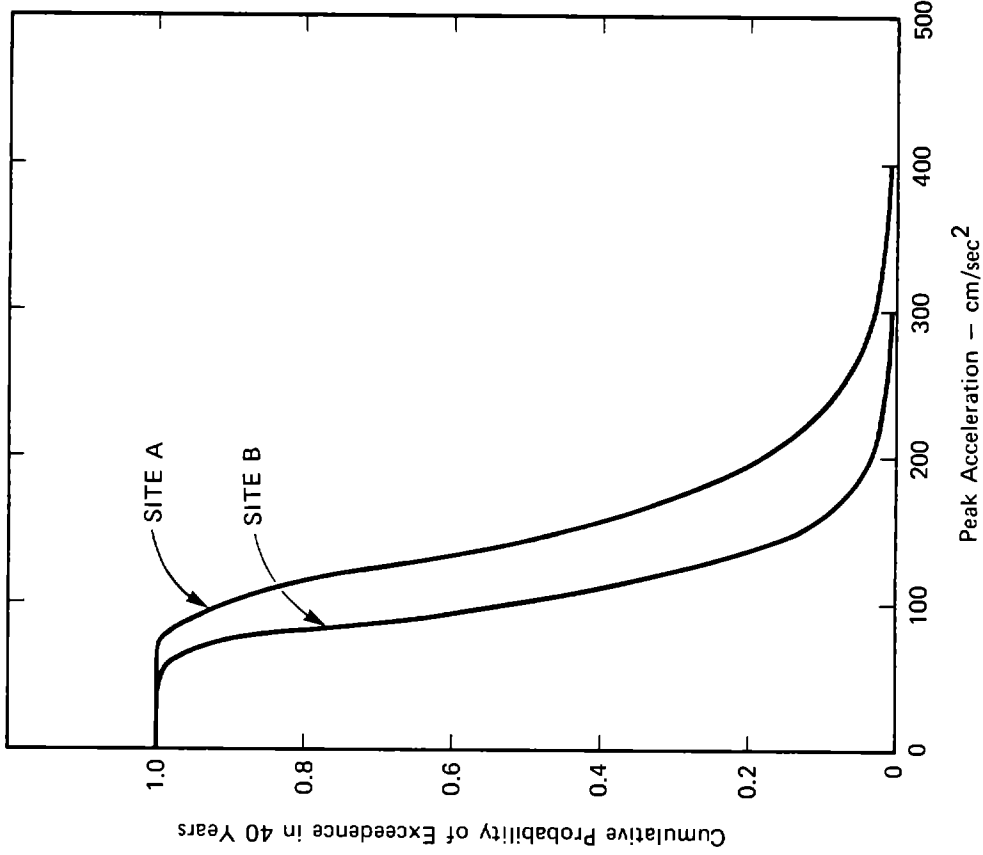
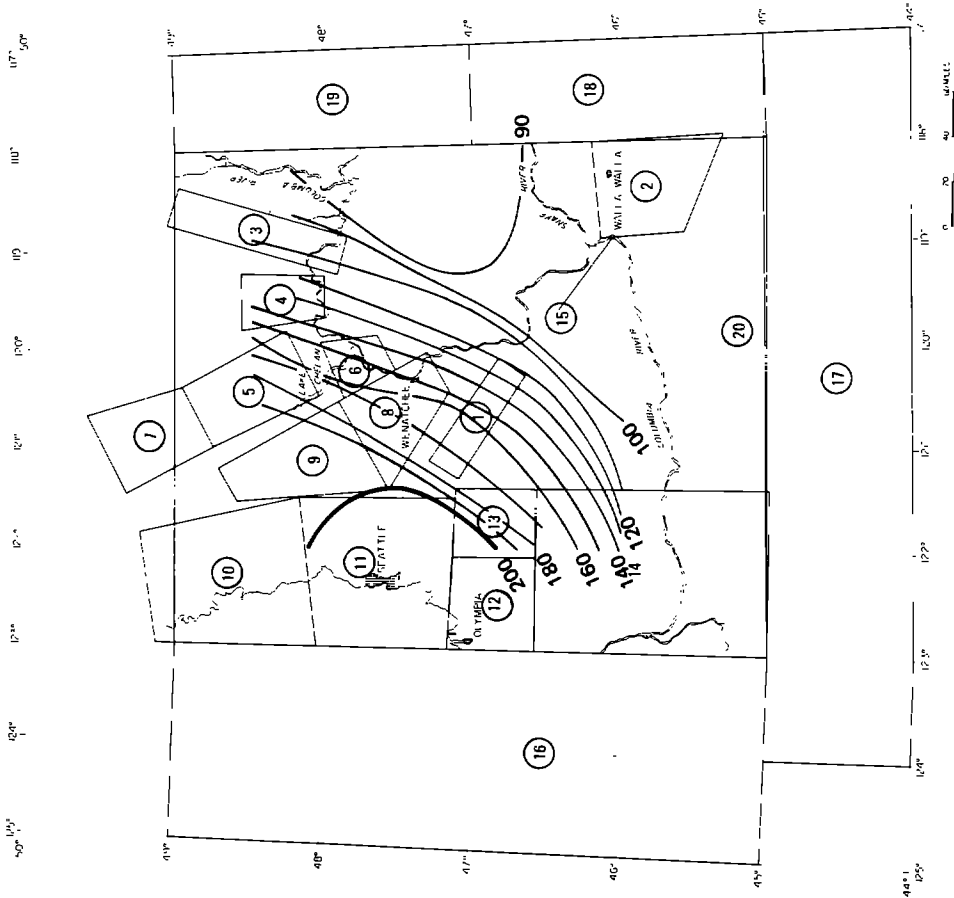


Fig. 8. Cumulative Distribution Function for Sites A and B



EXPLANATION

—100— Contours of peak acceleration, cm/sec²

⊙ Source area, See Table 1 for identification

See Note in Fig. 5 and 6

Fig. 7. Contours of Peak Acceleration for Return Period of 100 Years

Table 1 – Earthquake Source Identification

Source	Name	Maximum Magnitude (M_s)	Source Depth – km
1	Ellensburg Area	5.75	10
2	Walla Walla Area	6.75	10
3	Republic Graben	5.75	10
4	Okanogan Area	6	10
5	Lower Chewack Area	6	15
6	Chelan Area	6–7.5	10
7	Upper Chewack Area	5.5–7.5	15
8	Leavenworth Fault Area	6.75	10
9	Straight Creek Area	6.75	10
10	Bellingham Area	7.25	25
11	Seattle Area	7.25	25
12	Olympia Area	6.75	25
13	Mt. Rainier Area	6.75	15
14	Portland Area	7.25	25
15	Rattlesnake Structure	6.75	10
16	Random West	7.5	25
17	Random South	5.75	15
18	Random East 1	5.75	15
19	Random East 2	5.25	15
20	Random Central	6.00	10

(See Fig. 3 for location)

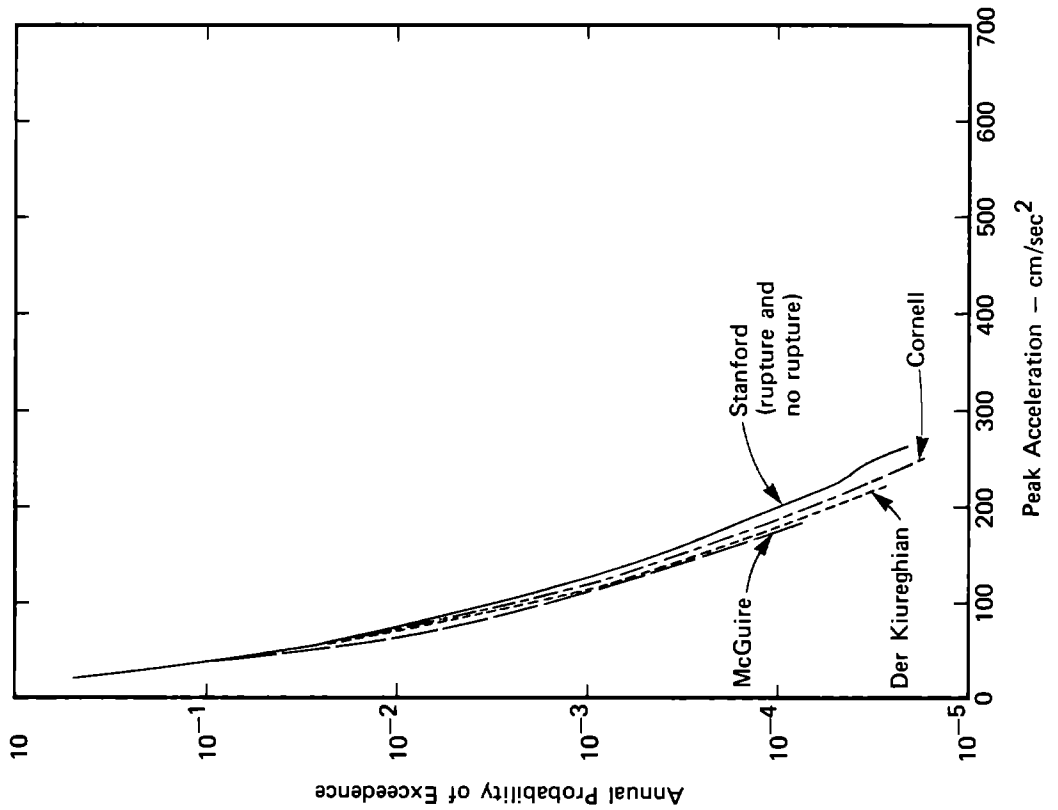


Fig. 9. Sensitivity of Seismic Exposure to Evaluation Model

PRELIMINARY GROUND RESPONSE MAPS FOR THE SALT LAKE CITY, UTAH, AREA

by

W. W. Hays^I, S. T. Algermissen^I, R. D. Miller^{II}, and K. W. King^{III}

ABSTRACT

Preliminary maps of relative ground response were constructed for the Salt Lake City area using nuclear-explosion ground motion data recorded at 27 sites. These maps demonstrate that large differences in ground response relative to rock occur throughout the area at sites underlain by unconsolidated water-saturated materials. These maps provide a basis for evaluating the risk from ground shaking in the Salt Lake City area.

INTRODUCTION

This paper describes a procedure used to construct preliminary ground response maps for the Salt Lake City, Utah, area. Salt Lake City, which has a population of about 170,000, is the major urban center of Utah. This procedure utilized nuclear explosion ground-motion data recorded simultaneously on an array of broad-band seismographs. Each seismic station was located at a site where the surficial geology was well defined, permitting the relative ground response to be correlated with the geology.

These maps are intended to provide preliminary guidance for evaluating the ground shaking hazard in the Salt Lake City area. They can be incorporated with other earthquake hazard maps (e.g., surface fault rupture, liquefaction potential, and landslide susceptibility), to evaluate the seismic risk.

PROBLEMS IN CONSTRUCTING EARTHQUAKE GROUND RESPONSE MAPS

Evaluation of the ground shaking hazard in any area is a complex research problem. The variety of information needed to develop meaningful earthquake ground response maps includes: regional and local geology, seismicity, the spatial distribution and physical properties of soils and rock in the area, and empirical ground response data.

The most important requirement for a ground response map is that it be useful for making engineering, social, or political decisions. From a scientific viewpoint, the map must correspond to a small enough area that source and path effects are negligible and the relative site responses are essentially repeatable from earthquake to earthquake. At the present time, the repeatability of relative ground response has been demonstrated for only a few places in the United States. It is prudent, therefore, to classify a ground response map as "preliminary" until adequate ground motion data have been recorded in the area.

I Geophysicists, U.S. Geological Survey, Denver, Colorado
II Geologist, U.S. Geological Survey, Denver, Colorado
III Geophysicist, U.S. Geological Survey, Las Vegas, Nevada

SUMMARY OF THE ELEMENTS USED IN CONSTRUCTING GROUND RESPONSE MAPS FOR THE SALT LAKE CITY AREA

GEOLOGIC SETTING - Salt Lake City is located at the eastern margin of the Basin and Range province and adjacent to the Rocky Mountains. The city is situated near the southern end of the Intermountain Seismic Belt, a north-south trending zone of seismicity that extends from the Montana-Canada border to Arizona (1).

The Wasatch fault zone, a north-south trending zone of young, active, normal faulting that can be traced for about 370 km, is the most striking tectonic feature of the area. Vertical displacement of more than 30 m in the late Pleistocene and Holocene material has occurred within the fault zone (2). Although large earthquakes have not occurred in historic time, the geologic record contains clear evidence that the Wasatch fault zone has apparently been active for millions of years and that the faults within this extensive zone have the potential for generating a large earthquake (3).

The Wasatch fault system is visible along the escarpment of the Wasatch Range in the Salt Lake City area. Three segments are shown in Figure 1; the Wasatch Fault south of Salt Lake City, the East Bench Fault group in Salt Lake City, and the Warm Springs Fault in the northern part of Salt Lake City. These faults are marked by prominent surface scarps that cut the surficial deposits and dislocate some surfaces upward or downward. At present, the history of fault movement is uncertain, and studies are underway to develop additional data regarding ages of and recurrence intervals between movements.

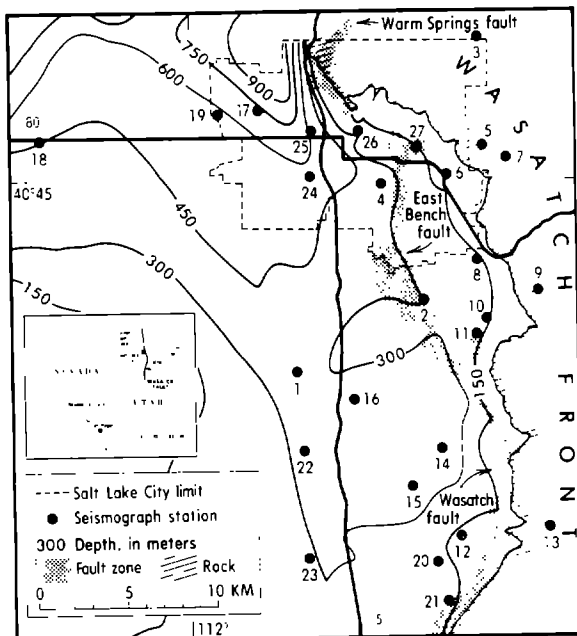


Figure 1. Map showing location of seismograph stations, thickness of unconsolidated materials and Wasatch Fault zone (4,5).

The urbanized portion of the Salt Lake City area lies within the Jordan Valley, a north-south graben about 40 km long and 28 km wide. The east side of the Jordan Valley is almost completely urbanized, utilizing the unconsolidated sediments as foundation materials. The valley is bounded on the east by faults within the Wasatch fault system (see Figure 1) and on the west by the Oquirrh Mountains. The Oquirrh Mountains (not shown) are the northern portion of the Basin and Range eastward-tilted Oquirrh-Boulter-Tintic fault block.

The rocks to the east and west of the graben are lithified sedimentary and crystalline rocks of Tertiary and older ages. The graben is filled with unconsolidated sediments up to about 760 m thick resting on sedimentary limestone, shale, conglomerate, quartzite, and volcanic tuff and andesite of Tertiary and Paleozoic ages (4, 5).

The materials of interest for this paper are the unconsolidated sediments in the Jordan Valley graben. The graben was inundated by several lakes that filled the Great Salt Lake Basin during the Pleistocene epoch, the

last being Lake Bonneville. It fluctuated in size and level during its existence, and perhaps was nearly dry before the basin filled again to within 100 m of the highest previous level (6), a fluctuation of almost 300 m. The deposits exposed at the surface in the Salt Lake City area accumulated during those fluctuations and represent offshore, nearshore, and onshore depositional environments (Table 1).

Table 1. Description of site geology (see Figure 1)

STATION	LOCATION	DEPOSITIONAL ENVIRONMENT	SITE DESCRIPTION
1	West bank of Jordan River	Onshore	Sand/silt, clay/alternating gravel and clay
2	Near East Bench fault	Offshore	Clay/alternating clay and gravel
3	Rotary Park in City Creek	Rock	Fitchville limestone
4	Liberty Park	Nearshore	Clay alternating with sand
5	Georges Hollow, Fort Douglas	Rock	Nugget sandstone
6	Utah Geological and Mineralogical Survey Bldg.	Offshore	Silt and clay/gravel/sandy silt
7	Emigration Canyon	Rock	Twin Creek limestone
8	South side of Parleys Creek	Onshore	Gravel/alternating silt and clay
9	Mill Creek Canyon	Rock	Weber quartzite
10	4500 South street near Wasatch Blvd.	Nearshore	Sand
11	Castro Springs	Offshore	Silt and clay
12	North bank of Dry Creek	Onshore	Windblown sand/gravel/sand and silt
13	Little Cottonwood Canyon (Terra Tech. Annex)	Rock	Quartz monzonite
14	1932 Parkridge	Onshore	Windblown sand/sand and gravel
15	Sandy City fire station (9400 South street)	Nearshore	Sand and gravel
16	Murray City	Nearshore	Sand and gravel
17	Salt Lake City International Airport (Air National Guard hanger)	Nearshore	Silty clay/alternating clay, silt and sand
18	Morton Salt Plant, Saltair	Nearshore	Silty clay/alternating clay, silt and sand
19	Salt Lake City International Airport (fire station)	Nearshore	Silty clay/alternating clay, silt and sand
20	South bank of Dry Creek (Memorial Gardens)	Nearshore	Sand/sand and gravel
21	Draper, Hidden Valley Country Club	Nearshore	Sand/sand and gravel/gravel
22	West side of Jordan River, Midvale	Offshore	Sandy silt/clayey silt/gravel and clay
23	South Jordan Cemetary	Offshore	Silty sand/silt
24	North of Jordan Park, east bank of Jordan River	Nearshore	Silt/sand/silt
25	Northeast corner, state fairgrounds	Onshore	Silt/sand
26	South of state capitol	Onshore	Gravel, sand
27	University of Utah campus	Nearshore	Gravel, sand

Offshore deposits are lacustrine in origin, and consist of very fine to fine sand, silt, and clay. For the most part, these fine-grained sediments accumulated in quiet, relatively deep water. The sand, silt, and clays probably represent the finer portion of debris being carried into the lake from the mountains. Natural exposures and cores from drill holes reveal that in many places the finer-grained deposits alternate as thin (1 mm) laminae or layers (5-20 cm) that are periodically separated by about 0.5-2 m of fine sand. In some places the deposits are more massive, and consist of sandy-silt and silt beds with a combined thickness of 3-5 m.

Nearshore deposits occur as beaches, long-shore spits and bars, deltas, and marsh deposits that accumulated in shallow water along the lakeshore, near what is now the Jordan River. The deposits include sediments of the earliest and the latest stages of Lake Bonneville. Except for the humic silt and very fine sand in the marsh sediments, the older near-shore materials are generally medium- to coarse-grained sediments that consist of sand and pebble and cobble gravels. The deltaic sediments are the largest and most widespread of the nearshore deposits. The thickest deltaic accumulations lie close to the mountain escarpment where streams exit into the Jordan Valley. Salt Lake City

is founded on several different nearshore deposits. The city covers most of a large delta, but also extends onto beach deposits, on shores that form benches along the mountain front, and a marsh deposit near the Jordan River.

Although most of the nearshore deposits are part of the earlier lake cycles, a portion of the sediments accumulated during the later part of the Lake Bonneville cycle. These are the sediments that underlie the broad flat surface west of Salt Lake City and constitute the materials in the upper part of the Jordan River delta. Cores from holes in that area indicate that fine-grained sands, silt, and clay comprise the lakeward delta to considerable depth. One core (7) showed fine-grained sediments the entire depth of almost 200 m. The natural moisture content by weight ranged from 24 to 52-percent and averaged 43-percent in a USGS hole drilled near site 18 (Figure 1). This range is believed to be typical of the nearshore deposits in the area.

Onshore deposits are mostly fluvial in origin. Alluvium is the dominant material, and extends under modern flood plains, fans, and terraces bounding the streams flowing from the mountains and along the Jordan River. The terraces are graded sequentially to lake levels marked by shorelines and beaches and lie within channels cut into older deposits. In all cases the sediments coarsen toward their sources. Small local deposits of windblown sand are scattered throughout the area. These deposits are derived from nearby sources and lie along banks or streams, or on broad plains underlain by silty sand or sand.

Representative values for shear-wave velocities in unconsolidated materials are generally less than 500 m/s. According to C. H. Miller*, shear-wave velocities measured in a USGS borehole near station 18 average about 200 m/s. These velocities are intermediate compared to the full-range of velocities (55-310 m/s) for soils reported by Gibbs and others (8) for the San Francisco Bay region. This suggests that the shear strength (at failure) of the soil in this borehole is comparable with that of similar materials in the Bay region.

SEISMICITY - Historical seismicity of Utah, documented since 1850, indicates sporadic activity concentrated on the southern and northern segments of the Wasatch Front. Six damaging earthquakes have occurred with Modified Mercalli intensity ranging from VII to IX. The only historical earthquake in Utah that produced ground displacement was the magnitude 6.6, 1934, Hansel Valley earthquake with an epicenter at the northern end of the Great Salt Lake.

Algermissen and Perkins (9) defined seismic source zones in terms of the historical seismicity and the patterns and orientations of fault systems known to have had Holocene faulting. The area parallel to and along the extent of the Wasatch Fault zone contains about 90 percent of Utah's seismicity.

GROUND RESPONSE DATA - For this study, ground motion measurements were obtained at 27 locations (Table 1) from three Nevada Test Site explosions (Bulkhead, Bañon, and Scantling), having magnitudes (M_L) in the 5.2-5.6 range. Five of the seismograph stations were located on rock (limestone, sandstone, quartz monzonite) to establish a reference site for comparing ground response. The peak horizontal ground motion levels recorded in Salt Lake City from the

*Geophysicist, U.S. Geological Survey, Denver, Colorado

nuclear explosions were: acceleration-0.001 g; velocity-0.26 cm/s; and displacement-0.06 cm. The strain levels of the ground motions were about 10^{-5} .

The range of relative ground response for the sites underlain by unconsolidated materials is shown in Figure 2. The ground response, shown in terms of the ratio of velocity response spectra, an approximate site transfer function, tends to be high (factor of 3-10) for sites underlain by thick lake and deltaic deposits. The ratios vary considerably over the period range 0.6-6.0 seconds with the largest variation occurring at the short periods where the signal/noise ratio is also smallest. Ground response at sites underlain by thinner surficial materials is smaller than the response for sites underlain by thicker deposits. The largest values of ground response tend to correlate with thick, saturated-to-semisaturated clay-rich (lacustrine and deltaic) deposits, and the lowest values of ground response tend to correlate with thin, semi-saturated, gravel and clay or beach-sand deposits. The response of the rock sites is roughly unity across the entire period band.

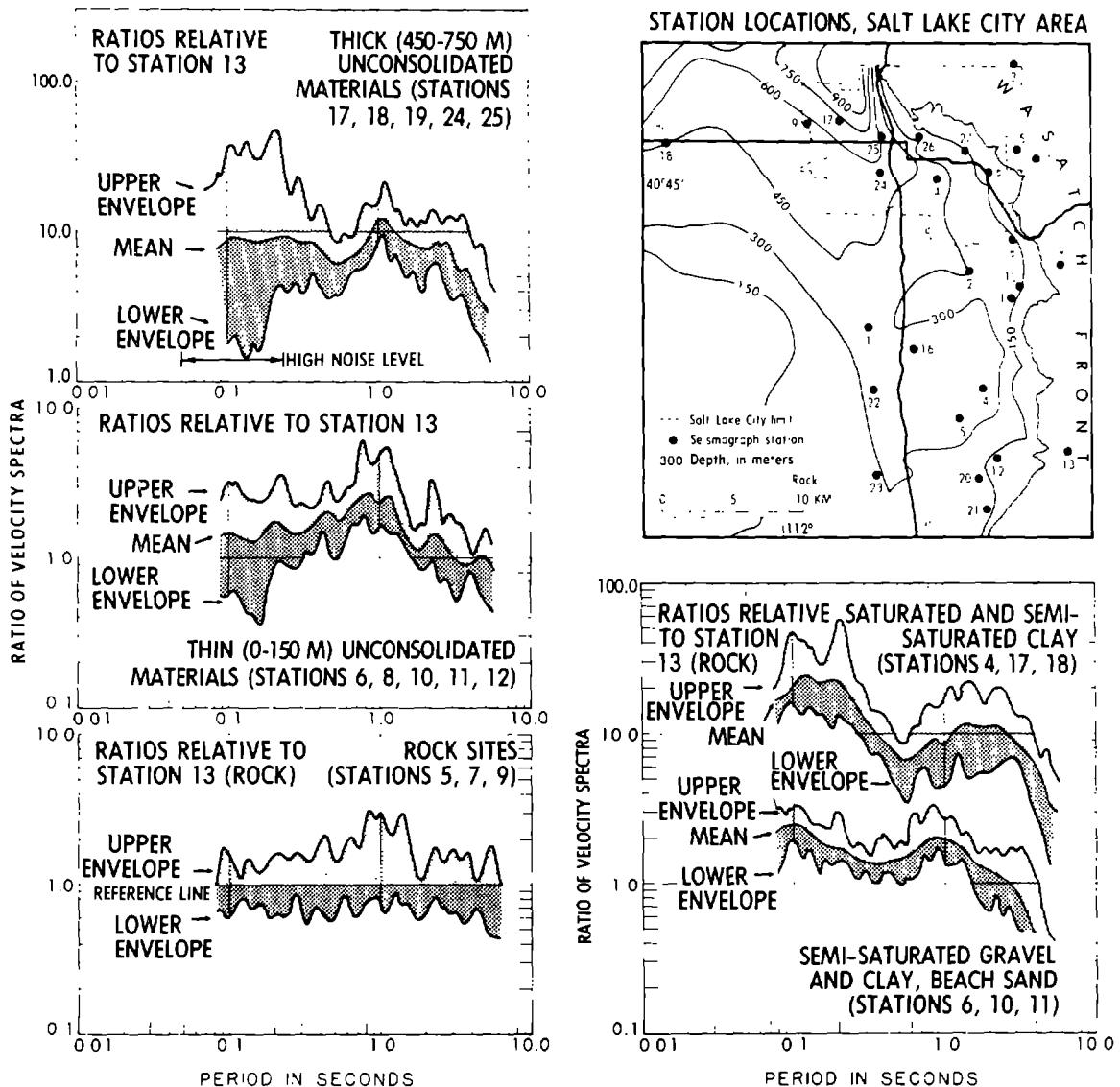


Figure 2. Graphs showing range of relative ground response in terms of thickness and relative water content of the unconsolidated materials.

The reproducibility of the site transfer function (10) for stations 1 and 7, is shown in Figure 3 for events Bañon and Bulkhead. The degree of reproducibility shown is representative of that determined for other stations.

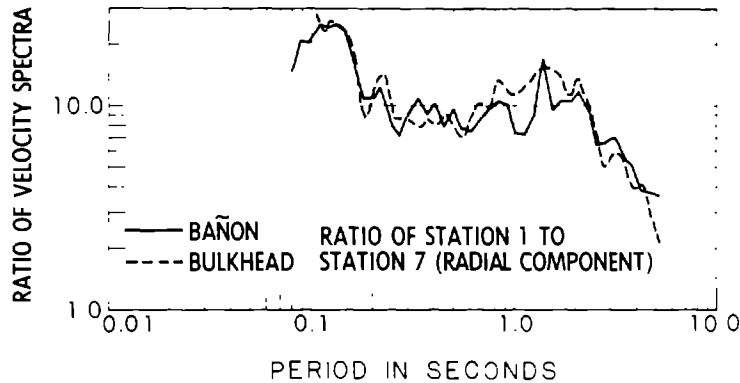


Figure 3. Reproducibility of site transfer function

PRELIMINARY GROUND RESPONSE MAPS

For earthquake hazard evaluation, it is reasonable to ignore the fine details of the ground response depicted by the spectral ratios and to characterize only the dominant trends. Figures 4 and 5 show preliminary maps of ground response for two period bands: (1) 0.1-0.2 second - the upper end of the range of the natural period of the fundamental mode of response for 1-2 story structures and (2) 0.2-0.7 second - the natural period range for 3-7 story structures. These contour maps show ground response values relative to rock (station 7) and are based on the site transfer functions. These maps do not show the effects of surface faulting, the seismic radiation pattern, and high-strain ground motion (11) that might occur in Salt Lake City during some earthquakes. However, one can reasonably expect that many of the potential earthquakes originating in the area encompassing the Wasatch Fault zone would produce low-strain ground motions in the Salt Lake City area and generate ground response patterns similar to those shown in Figures 4-5. One can use the mean curve proposed by Seed and others (12) for the attenuation of peak particle velocity and a value of 200 m/s for the approximate shear wave velocity of the unconsolidated deposits to calculate a distance of about 5 km as the radius to the 1×10^{-5} strain level. For distances from the energy center greater than about 5 km, the ground response would be essentially linear.

ESTIMATED EARTHQUAKE SHAKING IN SALT LAKE CITY

Algermissen and Perkins (9) and Whitman and others (13) developed, respectively, a ground shaking hazard map and a seismic design regionalization map for the United States. Both maps provide an estimate of about 0.20 g for the 90 percent probable, peak horizontal acceleration that would be expected at rock sites in Salt Lake City within a 50-year period of time. The corresponding value of Modified Mercalli intensity is VII. These values correspond to a return period of 475 years (figure 6).

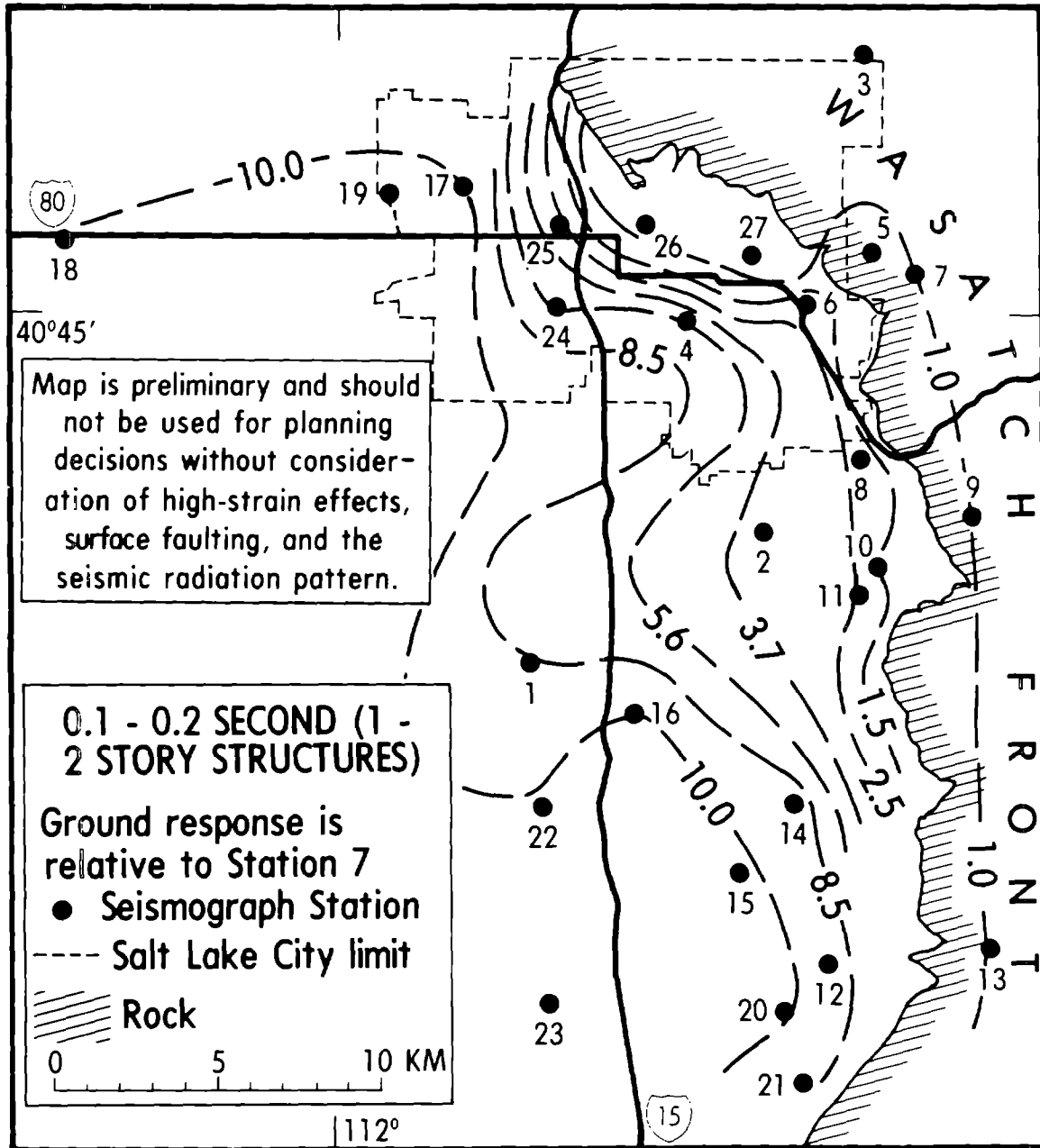


Figure 4. Preliminary map of ground response (0.1-0.2 second)

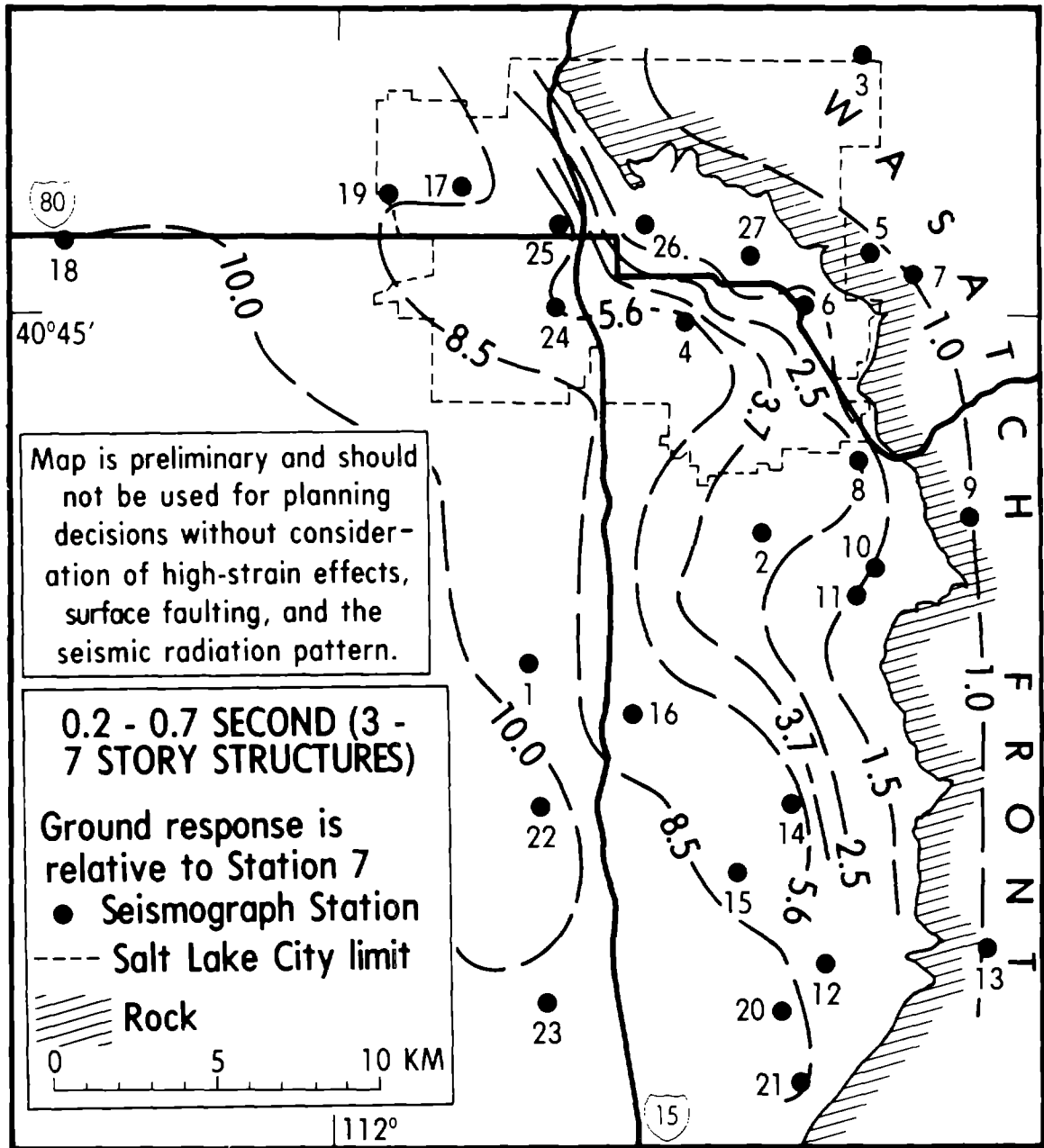


Figure 5. Preliminary map of ground response (0.2-0.7 second)

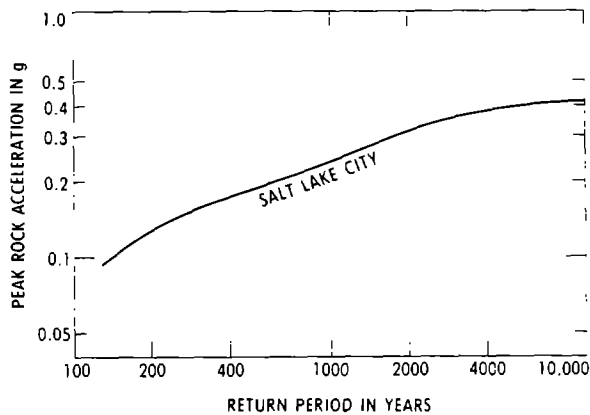


Figure 6. Variation of peak rock acceleration with return period. There is a 90 percent probability that 0.20 g will be observed in Salt Lake City in a 50-year period of time. The values shown can also be stated in terms of probability levels and exposure times (see reference 9).

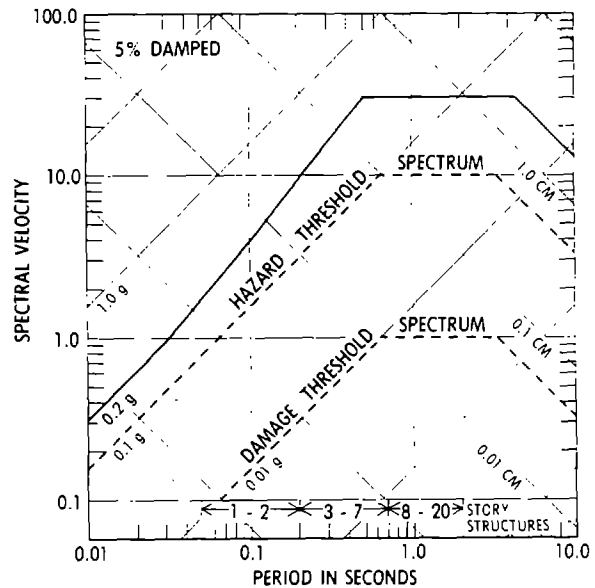


Figure 7. Estimated spectrum for rock sites produced by an earthquake causing 0.20 g peak acceleration.

The value of 0.20 g can be used to define the high-frequency asymptote of a design response spectrum for rock sites in Salt Lake City. The spectrum shape can be established on the basis of Nuclear Regulatory Commission Reg. Guide 1.60 (14) and the level from actual response spectra for rock sites from the 1971, San Fernando earthquake. The smooth spectrum shown in Figure 7 is a reasonable estimate of the earthquake ground shaking expected at a rock site such as station 7. Superposed on Figure 7 for comparison are the damage and hazard threshold spectra (15). The boundary of the hazard spectrum represents a postulated level of motion below which serious injury or death due to structural damage is considered unlikely.

To evaluate the ground shaking hazard from an earthquake that produces an acceleration of 0.20 g at rock sites in Salt Lake City, the preliminary ground response maps (Figs. 4-5) must be adjusted to account for high-strain (i.e., 10^{-2} to 10^{-3}) effects on the unconsolidated materials (soil) in the area. On the basis of laboratory analysis and ground motion data obtained from past earthquakes, Seed (11) and others have suggested that, on the average:

- (1) the maximum acceleration developed at the ground surface will vary from soil deposit to another because there is a physical limit to the peak acceleration that each type of soil deposit can transmit (Fig. 8),
- (2) for peak rock accelerations equal to or exceeding 0.20 g, soft soil deposits tend to attenuate rock accelerations (Fig. 8),
- (3) for peak rock accelerations less than 0.1 g, almost all soil deposits amplify the rock accelerations, especially for periods larger than 0.5 second (Fig. 8).

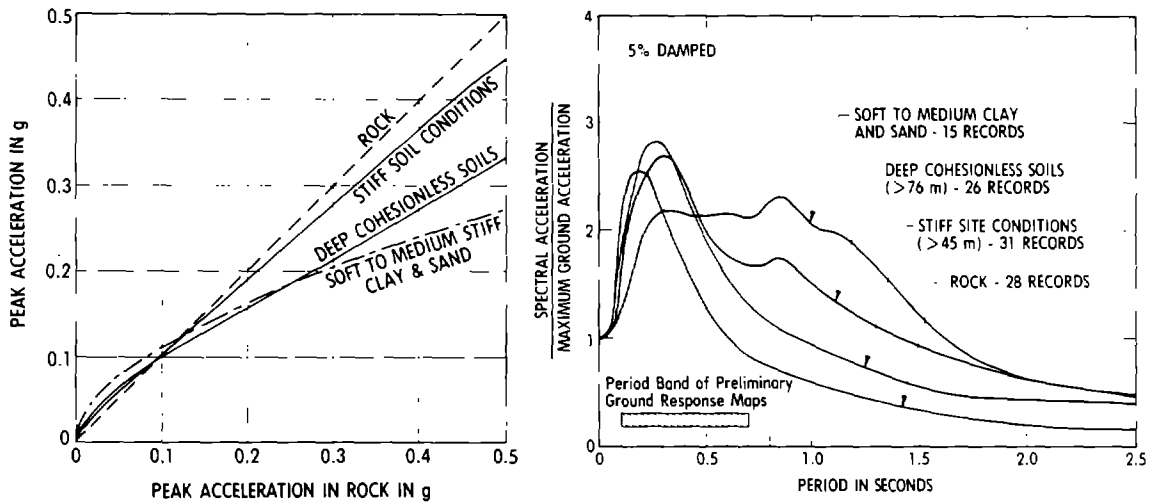


Figure 8. Average effect of peak rock acceleration level on the peak ground acceleration and spectra for four site classifications (11).

The values shown on the preliminary maps of ground response were adjusted by using the empirical factors shown in Figure 8. Multiplication of the smooth spectrum for a rock site and the adjusted ground response values gives the estimated ground response under high-strain conditions for sites underlain by unconsolidated materials. The range of spectral velocity values is shown in Figure 9.

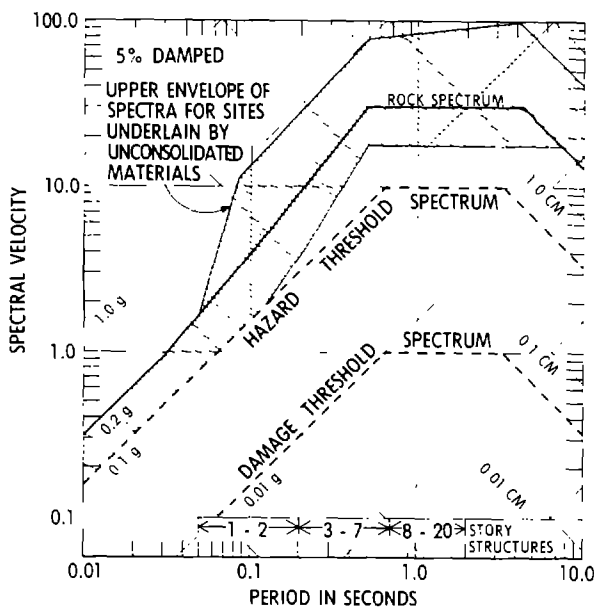


Figure 9. Range of spectral velocity values for sites on rocks and unconsolidated materials.

The considerations for lower levels of rock acceleration (e.g., 0.05 g, or 0.10 g) will not be developed in this paper.

POTENTIAL RISK TO SINGLE FAMILY DWELLINGS FROM GROUND SHAKING

An earthquake producing a peak rock acceleration of 0.20 g in Salt Lake City would have a significant impact on all types of structures. A detailed evaluation of loss from ground shaking is beyond the scope of this paper. However, a general idea of the types of losses that might occur in the Salt Lake City area can be obtained from the study by Rogers and others (16).

CONCLUSIONS

The preliminary maps of ground response for the Salt Lake City area

show that large differences in ground response (relative to rock) occur at sites underlain by unconsolidated materials. These differences appear to be caused primarily by lateral changes in lithology, grain size, thickness, geometry, and water content. The controlling physical parameters at each site are not known at this time; however, it appears that water content is one of the most important parameters.

REFERENCES

1. Smith, R. B., and Sbar, M. L., 1974, Contemporary tectonics and seismicity of the western United States with emphasis on the intermountain seismic belt: *Geol. Soc. America Bull.*, v. 85, p. 1205-1218.
2. Cluff, L. S., Hintz, L. F., Brogan, G. E., and Glass, C. E., 1975, Recent activity of the Wasatch Fault, northeastern Utah, USA: *Tectonophysics*, v. 29, p. 161-168.
3. Hamblin, W. K., 1976, Patterns of displacement along the Wasatch fault: *Geology*, v. 4, p. 619-622.
4. Van Horn, Richard, 1975, Unevaluated reconnaissance geologic maps of Salt Lake and Davis counties west of the Wasatch Front, Utah: U.S. Geological Survey Open-File report 75-616, 23 maps.
5. Arnow, Ted, Van Horn, Richard, and LaPray, R., 1970, The pre-Quaternary surface in the Jordan Valley, Utah: in *Geological Survey Research, 1970*, Prof. Paper 700-D, p. D257-D261.
6. Morrison, Roger B., 1965, Lake Bonneville: Quaternary stratigraphy of eastern Jordan Valley, south of Salt Lake City, Utah: U.S. Geological Survey Prof. Paper 477, 80 p.
7. Eardley, S. S. and Gvosdetsky, Vasyi, 1960, Analysis of Pleistocene core from Great Salt Lake, Utah, *Geol. Soc. America Bull.*, v. 71, p. 1323-1344.
8. Gibbs, J. F., Fumal, T. E., and Borchardt, R. E., 1976, In-situ measurements of seismic velocities in the San Francisco Bay Region, Part III, U.S. Geological Survey Open-File Report 76-731, 145 p.
9. Algermissen, S. T., and Perkins, D. M., 1976, A probabilistic estimate of maximum acceleration in rock in the contiguous United States: U.S. Geological Survey Open-File Report 76-416, 45 p.
10. Rogers, A. M., and Hays, W. W., 1978, Preliminary evaluation of site transfer functions developed from nuclear explosions and earthquakes: 2nd Intl. Conf. on Microzonation, San Francisco, Calif., Proc. (in press).
11. Seed, H. B., 1975, Design provisions for assessing the effects of local geology and soil conditions on ground and building response during earthquakes: Seminar, Structural Engineers Assoc. Northern Calif., Proc., 26 p.
12. Seed, H. B., Murarka, R., Lysmer, J., and Idriss, I. M., 1976, Relationships of maximum acceleration, maximum velocity, distance from source, and local site conditions for moderately strong earthquakes: *Seismol. Soc. America Bull.*, v. 66, p. 1323-1342.
13. Whitman, R. V., Donovan, N. C., Bolt, B., Algermissen, S. T., and Sharpe, R. L., 1977, Seismic design regionalization maps for the United States: World Conf. on Earthquake Engineering, 6th New Delhi, India, Proc., v. 2, p. 387-392.

14. U.S. Atomic Energy Commission, 1973, Design response spectra for seismic design of nuclear power plants: Directorate of Regulatory Standards, Regulatory Guide 1.60, Rev. 1, 6 p.
15. Blume, J. A., and Skjei, R. E., 1970, Seismic motion thresholds for damage to structures [abs.]: 65th Ann. Mtg. of the Seismol. Soc. America, Riverside, Calif.
16. Rogers, A. M., Algermissen, S. T., Hays, W. W., Perkins, D., (geologic and seismological portion), Van Strien, D. O., Hughes, H. C., Hughes, R. C., Lagorio, H. J., and Steinbrugge, K. V., (engineering analysis portion), 1976, A study of earthquake losses in the Salt Lake City, Utah, area: U.S. Geol. Survey Open-file Rept. 76-89, 357 p.

APPLICATION OF REGIONALIZED VARIABLES TO MICROZONATION

by

Charles E. Glass^I

ABSTRACT

Historical sampling of earthquake ground motions has been spatially irregular and displays two contradictory aspects; (1) a random aspect characterized by unpredictable variations from point to point, and (2) a structured aspect characterized by a degree of spatial correlation. Because of these difficulties actual ground motion records are seldom quantitatively used in microzonation.

The theory of regionalized variables provides a method by which earthquake ground motion measurements may be used as a tool in microzonation. Using this theory the spatial correlation of ground motion parameters is captured in a function called a variogram which displays the degree of similarity between two samples separated by some distance. Given the variogram function, the ground motion at other points may be estimated through a process called kriging. Kriging calculates a set of weights that minimizes the estimation variance at all points according to the geometry of the problem and characteristics of the ground motion. The technique is demonstrated using intensity data from the 1872 Pacific Northwest earthquake.

Once the spatial distribution of surface motions is estimated for each event affecting the site, conventional techniques must be applied in the time domain to calculate the earthquake hazard.

INTRODUCTION

Microzonation involves a stochastic process in that there is error and uncertainty both in the temporal domain (probability that earthquake ground motion at a site will exceed a given level in a specified period of years) and in the spatial domain (probability that the ground motion will be the same at two sites separated by some distance h). Heretofore, microzonation studies have ignored the uncertainty in the local spatial distribution of earthquake ground motion by approximating local bedrock accelerations using a catalog of nearby historical earthquake magnitudes and a combination of geometric and anelastic attenuation relationships (18, 3, 12, 7, 5 and others). The resulting catalog of ground motions is then incorporated into a probabilistic analysis using various statistical techniques in the temporal domain such as expected value techniques (1, 3, 13), Bayesian techniques (15) or extreme value techniques (9). In effect, the use of the attenuation relationships considers the local ground motion to be absolutely determined; thus, a stochastic variable only in time. Donovan (6) has pointed out the importance of considering the uncertainty in the attenuation relationships when assessing earthquake hazard. However, this still does not fully account for the uncertainty in local ground motion which is due not only to the

^IAssistant Professor of Geological Engineering, University of Arizona, Tucson, Arizona, 85721.

character of the earthquake source and transmission path but also to local site conditions. An ideal microzonation approach would be one which involves calculating earthquake hazard based on a history of ground motions measured at each point in a grid. Unfortunately, such a complete history does not exist and the ground motion parameters that have been recorded exhibit a very irregular spatial sampling. In addition, measured ground motion variables (e.g., acceleration) display two contradictory aspects; (1) a random aspect characterized by irregular and unpredictable variations from point to point, and (2) a structured aspect characterized by a degree of spatial correlation. Because of these difficulties actual records of historical earthquake ground motions or intensities are seldom quantitatively used in microzonation studies. The purpose of this paper is to suggest a technique by which ground motion measurements may be used as a tool for microzonation.

THEORY OF REGIONALIZED VARIABLES

The theoretical basis of regionalized variables was developed by Georges Matheron (10) in the late 1950's and early 1960's in an effort to improve ore reserve estimations given assay data from drill holes. Within the framework of Matheron's theory regionalized variables are variables which display a degree of spatial correlation. Examples include ore grade, elevation of the earth's surface, earthquake accelerations, intensities, etc. Matheron noted the inability of classical statistical techniques to account for the spatial correlation of these variables, which in microzonation is a very important feature. Matheron's theory of regionalized variables has two basic purposes (11); (1) to express the structural properties of the regionalized variable in some form, and (2) to estimate the spatial distribution of regionalized variables from fragmentary sample data. Expression of the structural (spatial) properties of the regionalized variable is made possible through the use of the "variogram" function.

The Variogram

The variogram is a curve which represents the degree of continuity of ground acceleration (or any other regionalized variable) separated by some distance h . Specifically, the squared difference between the accelerations is calculated. The calculation is repeated for all samples separated by distance h , and the average squared difference is calculated. The distances (h) are plotted along the abscissa and the mean squared differences $\gamma(h)$ for different values of (h) are plotted along the ordinate. Thus, for each (h), the function

$$\gamma(h) = \frac{1}{2\ell} \int_{\ell} [f(x+h) - f(x)]^2 dx \quad (1)$$

is plotted (Figure 1), where

- ℓ = length of the traverse; if an area is evaluated, the area $\frac{1}{A}$ and surface integral are used; for a volume as in ore deposits, a volume integral is used,
- $\gamma(h)$ = value of the variogram for distance h ,
- $f(x)$ = acceleration at point x ,
- $f(x+h)$ = acceleration at point $x+h$.

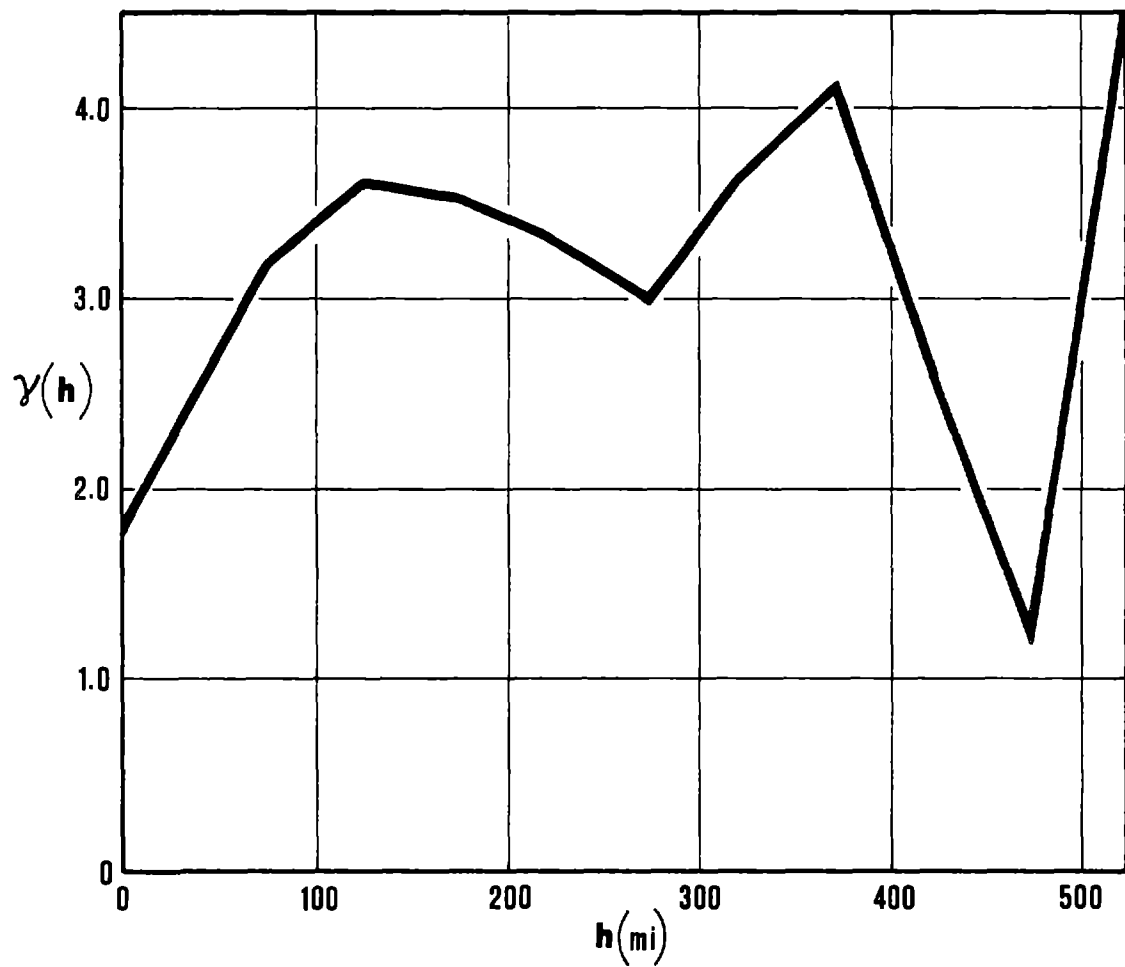


Figure 1. Variogram calculated using earthquake intensity values from the 1872 Pacific Northwest earthquake. The squared difference in intensity values $\gamma(h)$ for samples separated by class size $h = (50)(N)$ mi. where $N = 1, 2, \dots, 10$, is plotted against the separation distance h . The variogram shows that samples within 145 miles (230 km) are correlated to some degree.

Matheron noted four basic shapes for the variogram function (Figure 2). The first type exhibits a parabolic trend at the origin and represents a regionalized variable having a high degree of continuity. The second type is characterized by an oblique tangent at the origin and represents a variable having an "in average" (10) continuity. The third type has a discontinuity at the origin indicating less than "in average" continuity and corresponds to the type of variogram calculated using the 1872 Pacific Northwest earthquake intensity values (2) shown on Figure 1. The fourth type is a limiting case corresponding to the classical notion of a random variable. From Figure 1 it is seen that $\gamma(h)$ (mean difference in intensity squared at points h apart) increases with increasing separation until it becomes level, indicating that neighboring intensity values are similar while samples some distance away are quite different. The variogram thus numerically describes the continuity of intensities. The distance at which the variogram becomes level is termed the range; beyond the range samples are no longer correlated. The value of the variogram at the range is termed the sill which corresponds to the variance of all samples used in the variogram development. Just as the variance of an estimate in classical statistics is often considered to represent the uncertainty associated with the estimate, the variogram may be viewed as a measurement of the uncertainty that exists when a sample acceleration has been extended some distance. The value of the variogram at $h=0$ is termed the nugget value. Ideally the nugget value should be zero since two accelerations measured at the same point should be equal. However, in actual calculations errors in sampling, instrument characteristics, etc. result in non-zero nugget values.

In addition to expressing the continuity of the regionalized variable, the variogram also expresses the zone of influence of the variable through the range, and anisotropy of the variable by exhibiting varying shapes when computed in different directions.

One of the more important uses of the variogram is the calculation of the estimation variance of ground motion estimates. While the central limit theorem is not useful for samples which are dependent, the estimation variance can be calculated for dependent variables using the variogram through equation (2) (8)

$$\sigma_E^2 = \frac{2}{\ell N} \sum_{i=1}^N \int_{\ell} \gamma(x_i - p) dx - \frac{1}{\ell^2} \int_{\ell} dx \int_{\ell} \gamma(h) dy - \frac{1}{N^2} \sum_{i=1}^N \sum_{j=1}^N \gamma(x_i - x_j) \quad (2)$$

where σ_E^2 = the estimation variance,
 $\gamma(x_i - p)$ = the variogram using distances between each sample x_i and the point to be estimated (p),
 N = total number of samples used for the estimate.

This feature of the variogram (calculation of the probable error of an estimate) enables one to accomplish the second basic purpose of regionalized variables, i.e., to estimate the spatial distribution of the variable from fragmentary sampling data. This estimate should be unbiased and have a minimum estimation variance. Kriging is a technique by which such an estimate can be made.

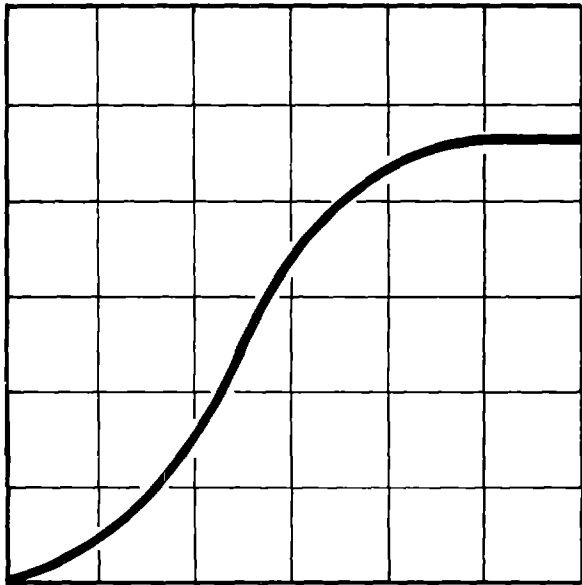
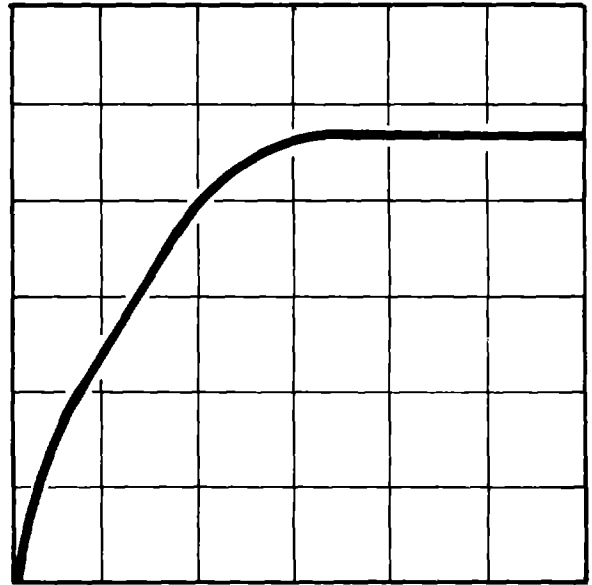
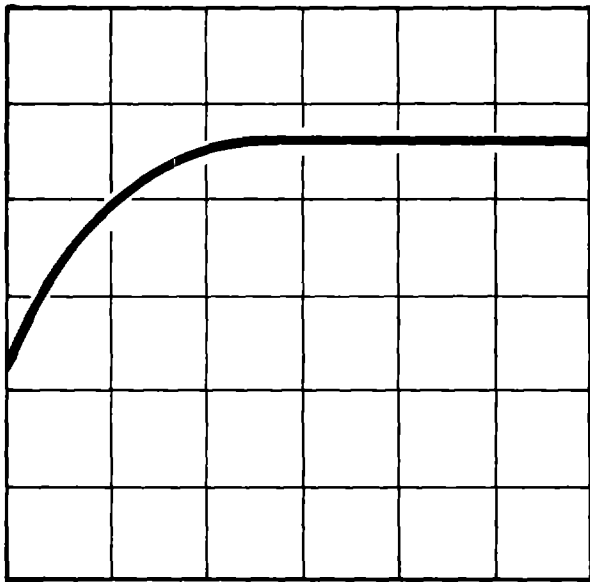
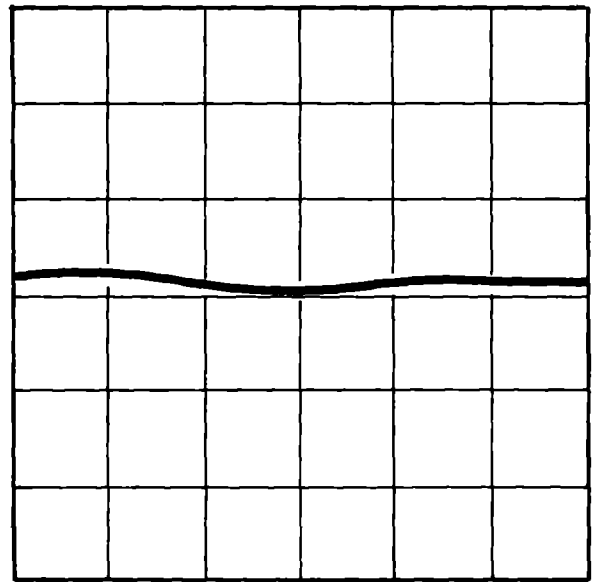
**2a****2b****2c****2d**

Figure 2. Typical variograms. 2a corresponds to a regionalized variable having a high degree of correlation; 2b corresponds to a variable having "in average" continuity; 2c corresponds to a variable having less than "in average" correlation similar to Figure 1; and 2d corresponds to a random, uncorrelated variable.

Kriging

Kriging is a tool for estimating the acceleration at a point as a linear combination of the available samples near the point such that the estimate is unbiased and has minimum variance. To accomplish this kriging finds a set of weights that minimizes the estimation variance according to the geometry of the problem and the character of the ground motion. In terms of the kriging weights, the estimation variance is given by equation (3) (8)

$$\sigma_E^2 = \sigma_a^2 - 2 \sum_{i=1}^N \lambda_i \sigma_{px_i} + \sum_{i=1}^N \sum_{j=1}^N \lambda_i \lambda_j \sigma_{x_i x_j} \quad (3)$$

where σ_a^2 = variance of all of the acceleration recordings,

N = number of data points used in kriging,

λ_i 's = kriging weights,

σ_{px_i} = covariance between point of interest (p) and the i^{th} data point,

$\sigma_{x_i x_j}$ = covariance between i^{th} and j^{th} data points.

In minimizing the estimation error of equation (3) the weights λ_i are constrained so that the sum of the weights is equal to 1

$$\sum_{i=1}^N \lambda_i = 1. \quad (4)$$

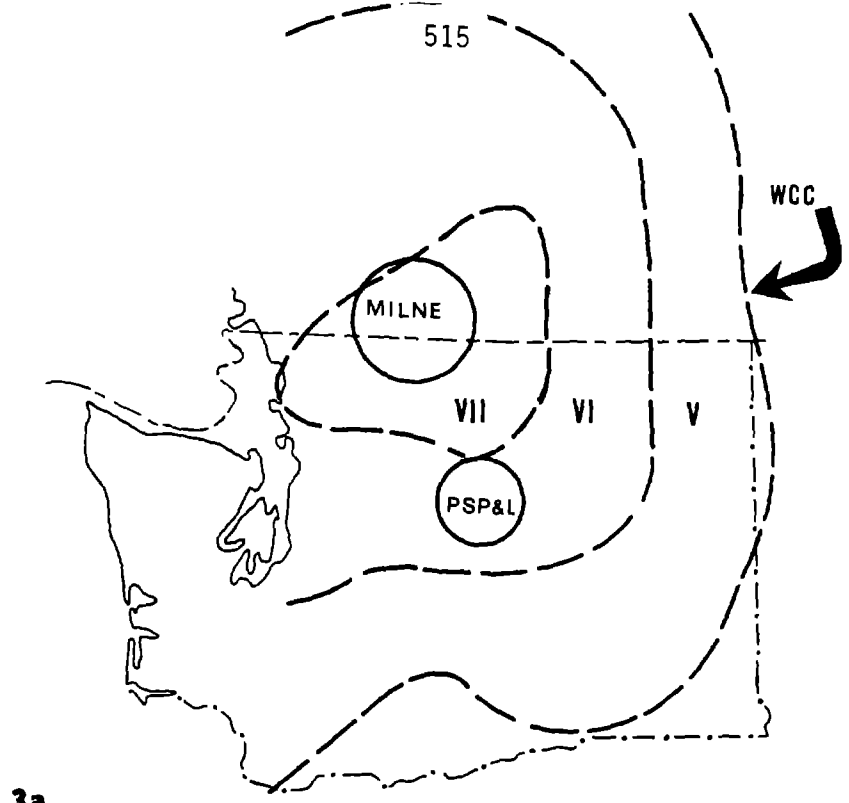
The kriging problem is thus a constrained optimization problem having N variables. The optimization process assigns lower weights to distant samples and higher weights to nearby samples and considers the relative position of the samples to the point being kriged and to each other. Since kriging calculates the estimation variance of each point kriged, confidence limits for these points may be determined, as well as the improvement that additional measurements would make in the estimation variance. Since kriging is an interpolation algorithm, the distribution of local ground motion is smoothed and appears less variable than the true distribution. David (4) has shown that the variance of the ground motion parameters σ_p^2 is approximately related to the variance of estimated values σ_{*p}^2 and the kriging variance by the following relationship

$$\sigma_p^2 = \sigma_{*p}^2 + \sigma_k^2 - \sigma_m^2, \quad (5)$$

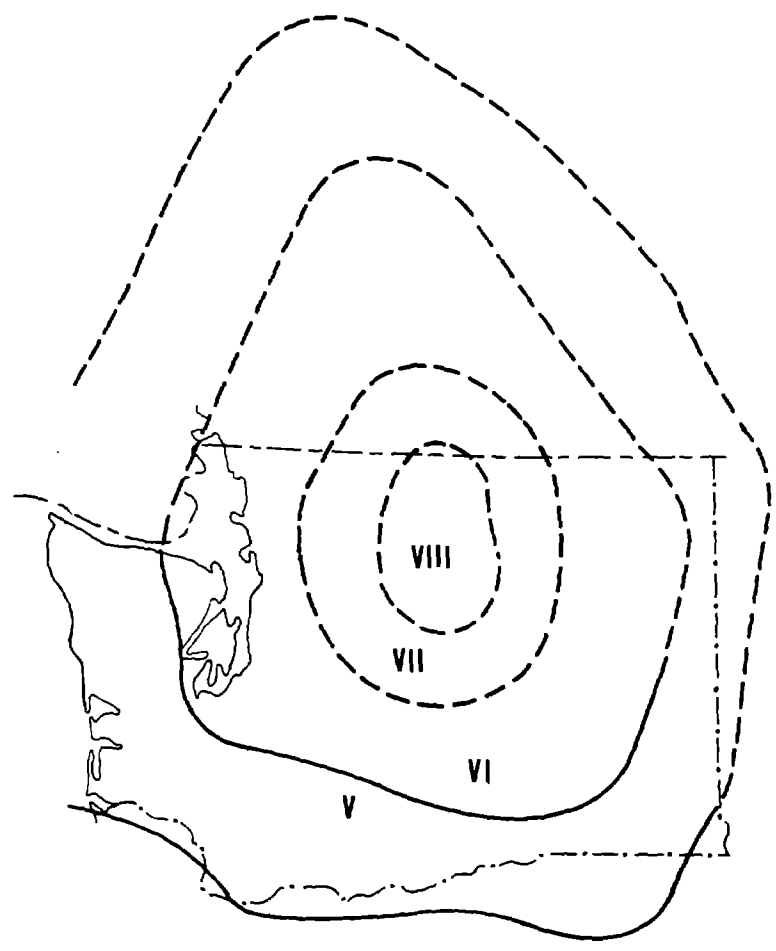
where σ_m^2 is the estimation variance of the average of the entire felt area which is generally very small.

APPLICATION TO 1872 PACIFIC NORTHWEST EARTHQUAKE

Numerous attempts have been made to construct isoseismal maps to represent the spatial distribution of strong ground motion accompanying the 1872 Pacific Northwest earthquake (Figure 3). All have relied upon qualitative



3a



3b

Figure 3. Isoseismal maps for the 1872 Pacific Northwest earthquake. Figure 3a shows interpretations by Milne (14), Puget Sound Power & Light (16) and Woodward-Clyde Consultants (19). Figure 3b is from Coombs (2).

contouring of the intensity values. The catalog of intensities utilized for this example is from Coombs et al (2) which represents an exhaustive search of published and unpublished eyewitness accounts of the earthquake. Variograms were computed for the intensity distribution using several class sizes (h) and directions. The variograms displaying the best spatial correlation correspond to a class size of 80 km (Figure 4). The north direction was chosen for kriging and a curve fitted to the variogram (Figure 1), though the variogram of Figure 4d could have also been used. From Figure 1, the range is found to be 230 km indicating that within 230 km the intensities are correlated to some degree; the sill value is 1.77. The isoseismal map shown on Figure 5 was contoured using the kriged data on a grid spacing of 36 km. Comparison of Figure 5 with Figure 3b indicates the following:

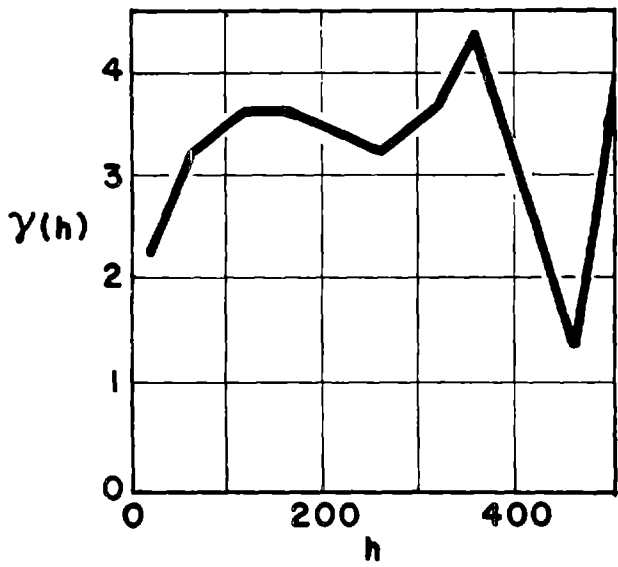
- (1) The areas enclosed by the Intensity VIII and VII isoseismals are much smaller on Figure 5. The only Intensity VIII listed by Coombs et al occurred at Lake Chelan and Entiat, Washington. The kriging procedure, which considered intensities within 200 km of each grid point, did not assign high weights to these two intensities when considering grid points some distance away.
- (2) The area enclosed by the Intensity VI isoseismal is stretched to the north on Figure 5 which may be due to the influence of the crystalline rocks of the northern Cascades, though, as Figure 6 indicates, the estimation variance increases rapidly to the north decreasing confidence in those values.

APPLICATION TO GENERAL MICROZONATION AND EARTHQUAKE ENGINEERING

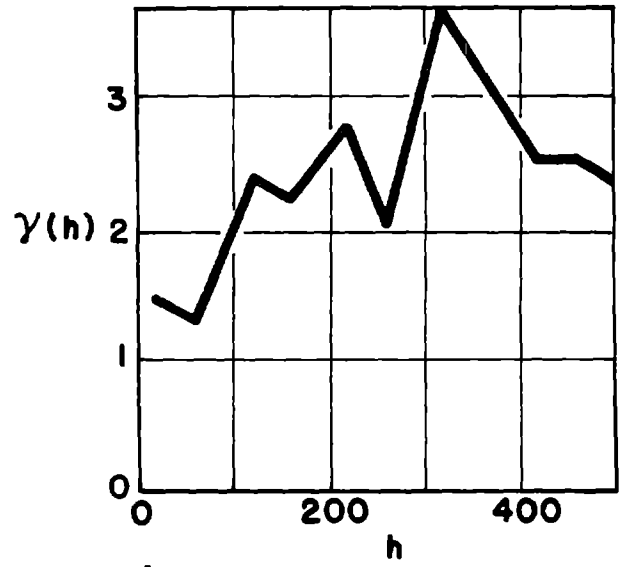
In a microzonation application the regionalized variable technique would be applied to all earthquakes causing ground motion in the area to be zoned, in a similar way as in the example above, constructing a catalog of ground motions at each grid point. Initially, intensity values would have to be utilized through some empirical relationship to acceleration (or velocity, etc.), however, as the data improves, actual acceleration values could be included. Actual earthquake records provide the best data; however, ground motion parameters developed during specific site studies using site response programs (17) could also be used. Since the regionalized variable technique is applied only to the spatial domain, a statistical technique suitable to the temporal domain (such as one of those mentioned earlier) must be applied to calculate the earthquake hazard at each point within the microzonation network.

The regionalized variable technique is valid for any variable which exhibits spatial correlation. Thus, the thickness and density of sand units from exploratory borings could be used in the technique to assess liquefaction hazard. In a case such as this, the calculation of the estimation variance is especially useful since it can be used to determine locations for additional borings so that maximum improvement in the estimation error may be realized.

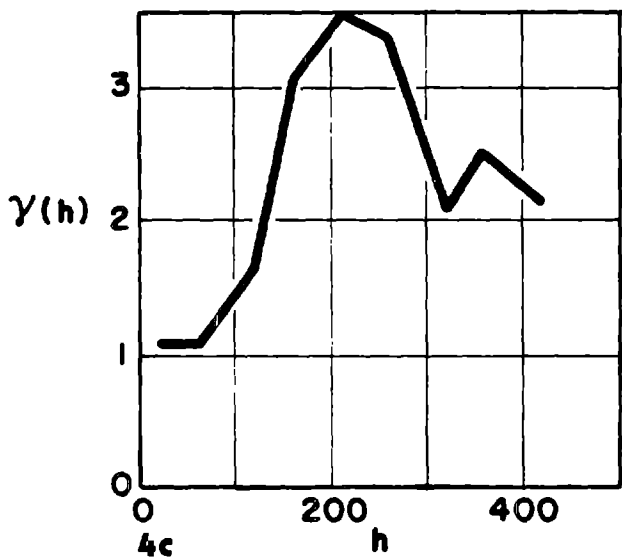
The technique has very limited value for handling earthquake epicenter data since these are rigidly confined to tectonic structures. However, it could be used in assessing earthquake hazard for projects in the central and eastern United States. In this area the seismicity is dominated by three



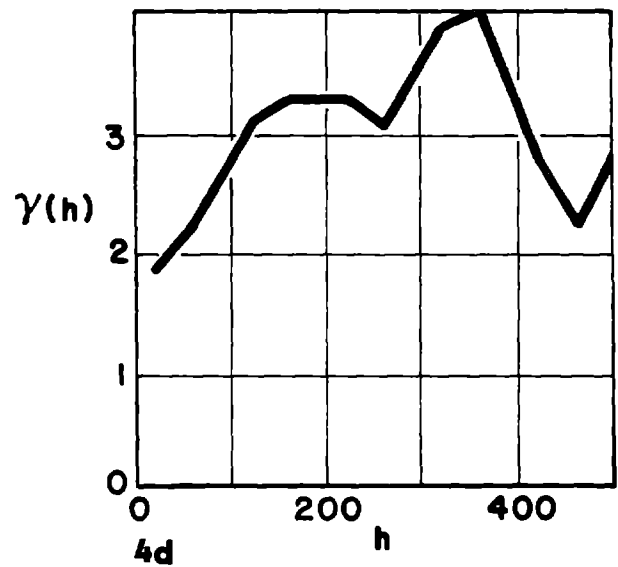
4a



4b



4c



4d

Figure 4. Variograms showing best spatial correlation for 1872 Pacific Northwest earthquake; the class size is 50 miles (80 km). Figure 4a was calculated in the north-south direction, 4b in the east-west direction, 4c in the northeast-southwest direction, and 4d using all samples (all directions).

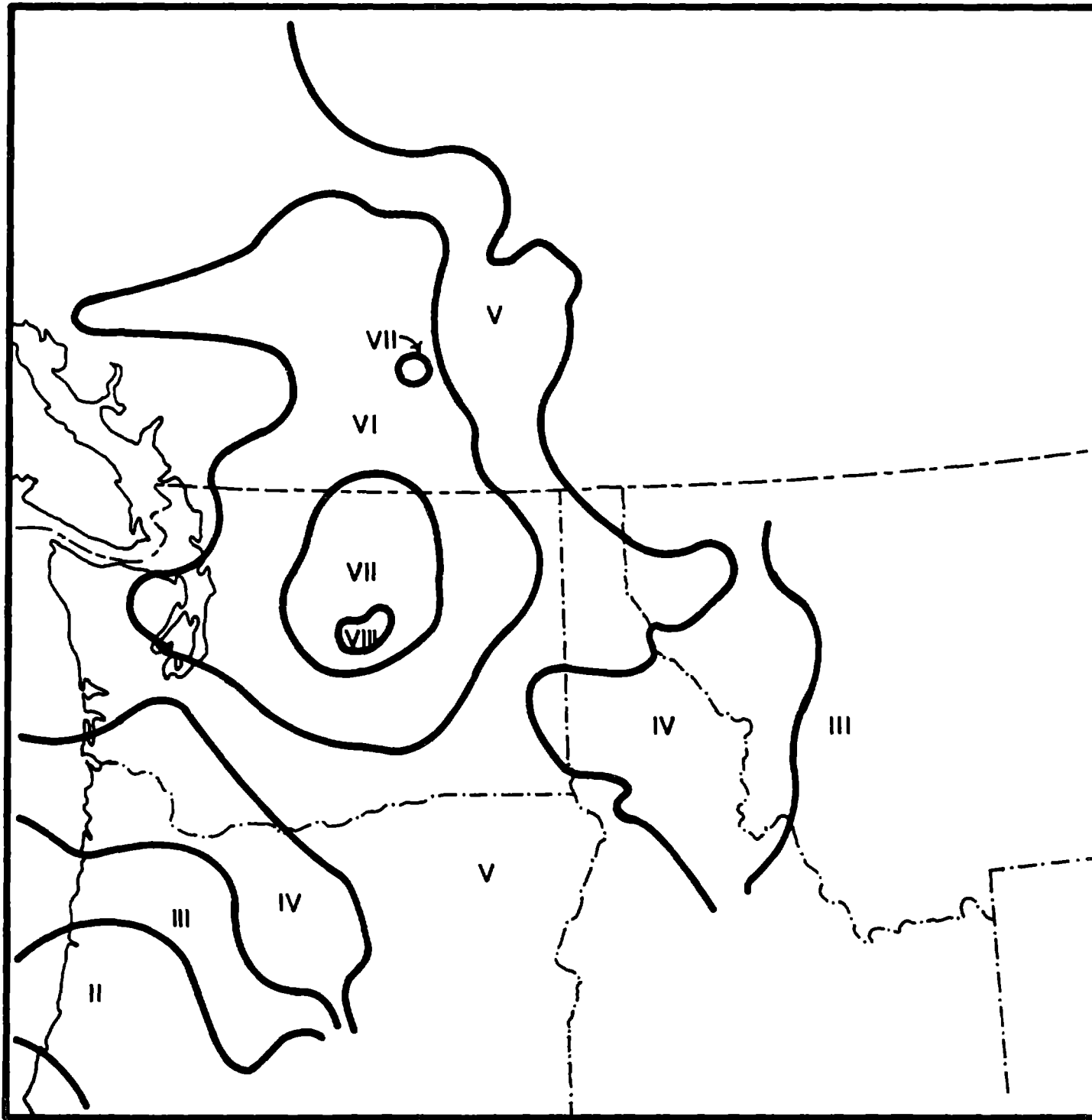


Figure 5. Isoseismal map calculated using the variogram of Figure 1 (Fig. 4a) and kriging to a grid with a spacing of 36 km. Compare with Figure 3b.

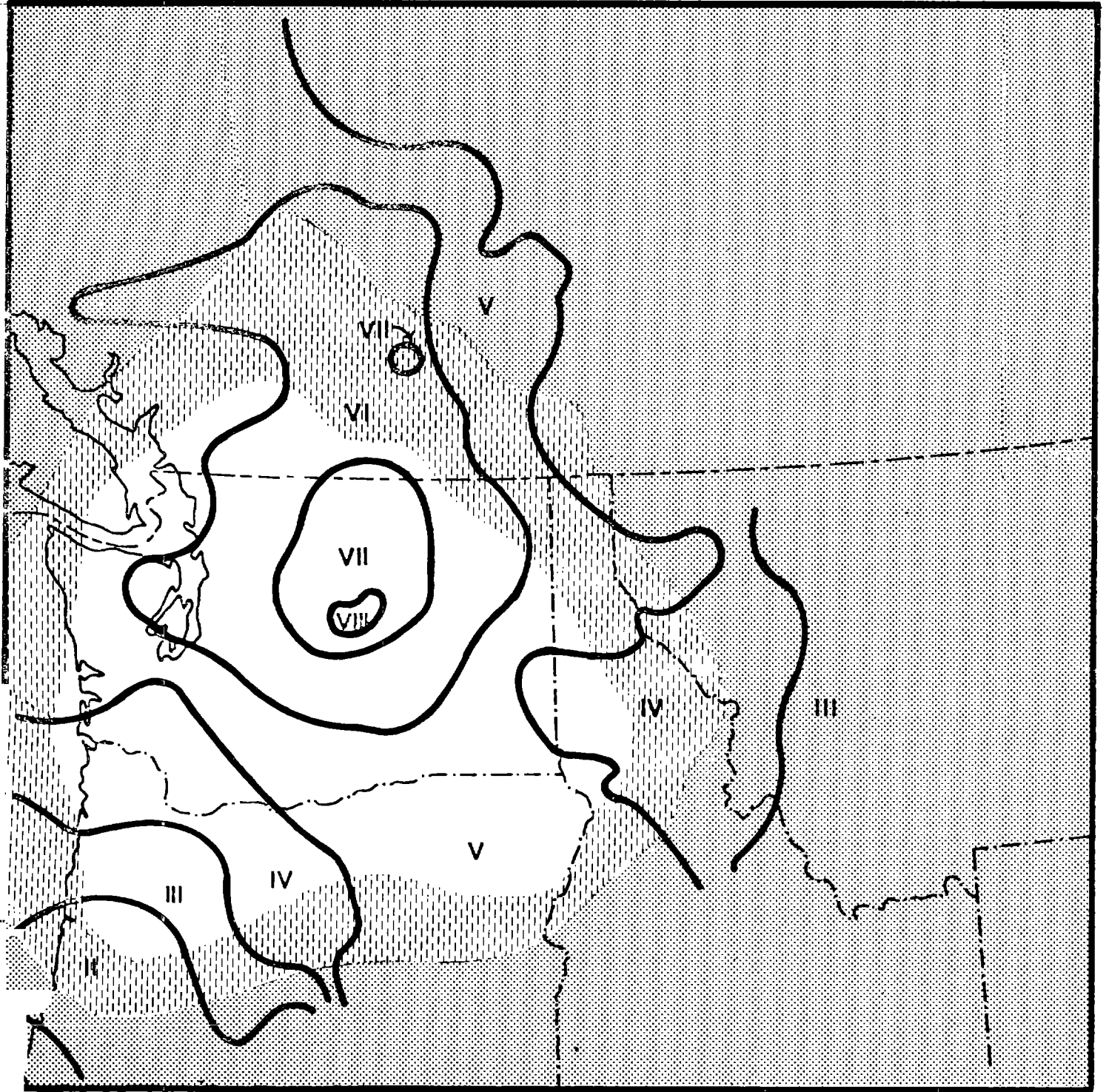


Figure 6. Isoseismal map of Figure 5, depicting confidence in intensity assignments. The clear area is characterized by a confidence of 95% that the intensities are within one intensity value of the value assigned. The confidence decreases to ± 2 intensity values for the dashed area, and to ± 3 or more for the other isoseismal lines.

major seismic zones; the New Madrid zone, the Charleston, S. C. zone, and the St. Lawrence zone. Seismic design for areas located great distances from these centers usually must contend with lower magnitude "floating earthquakes" which could conceivably occur under the site. Still, it seems reasonable to expect that the probability of experiencing one of these lower magnitude events would be higher in areas which have experienced them previously. Thus, while the historical epicenters themselves do not constitute a regionalized variable, the probability of occurrence of these earthquakes within a given design period does (being higher in areas having higher historical seismicity and lower in other areas). By treating the probability of occurrence within a given design period (earthquake hazard) of a "floating earthquake" as a regionalized variable, the earthquake hazard at sites characterized by low historical seismicity and lack of surface geologic structure may be approached.

SUMMARY

In summary, the theory of regionalized variables provides a way in which variables exhibiting spatial correlation may be evaluated statistically. Since many of the variables associated with earthquake engineering possess such a spatial correlation, the theory should prove to be a useful tool for microzonation and other earthquake engineering studies especially when used in conjunction with other conventional statistical, mathematical, and field techniques.

ACKNOWLEDGEMENTS

I am grateful to H. Peter Knudsen of the Department of Mining and Geological Engineering, University of Arizona, for his review of this paper. His comments and suggestions were extremely useful.

REFERENCES

1. Algermissen, S. T., and Perkins, D. M., (1972) "A technique for seismic zoning: general consideration and parameters," Proc. of the International Conference on Microzonation for Safer Construction Research and Application, Seattle, 1972.
2. Coombs, H. A., Milne, W. G., Nuttli, O. W., and Slemmons, D. B., (1976) "Report of the review panel on the December 14, 1872 earthquake," Preliminary Safety Analysis Report, Amendment 23, Washington Public Power Supply System, Subappendix 2RA.
3. Cornell, C. A., (1968) "Engineering seismic risk analysis," Seismological Society of America Bull., v. 58, no. 5, pp. 1503-1606.
4. David, M., (1977) Geostatistical Ore Reserve Estimation, Elsevier Scientific Publishing Co., Amsterdam, The Netherlands.
5. Donovan, N. C., (1974) "A statistical evaluation of strong motion data including the February 9, 1971, San Fernando earthquake," World Conference on Earthquake Engineering, 5th, Rome 1973, Proc. v. 1, pp. 1252-1261.
6. Donovan, N. C., and Bornstein, A. E., (1977) "The problems of uncertainties in the use of seismic risk procedures," Dames and Moore Technical Report EE77-4.
7. Esteva, L., and Villaverde, R., (1974) "Seismic risk, design spectra, and structural reliability," World Conference on Earthquake Engineering, 5th, Rome 1973, Proc., v. 2, pp. 2586-2596.

8. Knudsen, H. P., and Kim, Y. C., (1977) "A short course on geostatistical ore reserve estimation," Dept. of Mining and Geological Engineering, University of Arizona, Tucson, Arizona.
9. Lomnitz, C., (1974) "Global tectonics and earthquake risk," In Developments in Geotectonics 5, Elsevier Publishing Co., New York.
10. Matheron, G., (1963) "Principles of geostatistics," *Economic Geology*, v. 58, pp. 1246-1266.
11. Matheron, G., (1971) "The theory of regionalized variables and its applications," *Les Cahiers du Centre de Morphologie Mathematique*, Fontainebleau, no. 5.
12. McGuire, R. K., (1974) "Seismic structural response risk analysis, incorporating peak response regressions on earthquake magnitude and distance," Massachusetts Institute of Technology Research Report R74-51, 371 pp.
13. McGuire, R. K., (1976) "Fortran computer program for seismic risk analysis," U. S. Geological Survey Open File Report 76-67.
14. Milne, W. G., (1956) "Seismic activity in Canada west of the 113th meridian 1841-1951," *The Dominion Observatory Publications*, Ottawa, Canada, v. 18, no. 7, pp. 126-127.
15. Mortgat, C. P., (1976) "A Bayesian approach to seismic risk, development of stable response parameters," Ph. D. Dissertation, Department of Civil Engineering, Stanford University, Stanford, Calif.
16. Puget Sound Power and Light (1977) "Skagit Nuclear Project Preliminary Safety Report," Submitted to Nuclear Regulatory Commission, Amendment No. 15.
17. Schnabel, P. B., Lysmer, J., and Seed, H. B., (1972) "SHAKE a computer program for earthquake response analysis of horizontally layered sites," Report No. EERC72-12, University of California, Berkeley.
18. Seed, H. B., Idriss, I. M., and Kiefer, F. W., (1968) "Characteristics of rock motions during earthquakes," EERC68-5, University of California, Berkeley.
19. Woodward-Clyde Consultants (1977) "Review of the North Cascade earthquake of 14 December 1872," Preliminary Safety Analysis Report, Amendment 23, Washington Public Power Supply System, Subappendix 2RA.

522

INTENTIONALLY BLANK

A NEW MICROZONATION TECHNIQUE FOR DESIGN PURPOSES

by

JOSE LUIS ALONSO* and LUIS URBINA**

ABSTRACT

Spectral shapes from recorded motions change in a consistent fashion pattern depending on local soil conditions, characteristics of earthquake motions - and distances from zones of energy release. It has also been long recongnized the influence of geologic and soil conditions on the associated damage to buildings. Since within the area of a city or so, there may be no significant differences in seismicity, one of the most important aspects in urban planning and earthquake design, is to establish for different earthquakes the variation of the acceleration spectral shapes with local site conditions.

It is the purpose of this investigation to suggest a simple technique for the evaluation of both, normalized acceleration spectrum curves, and the fundamental period of soil deposits at the recording station directly from the recorded spectral shapes. This technique has been already applied to the seismic microzonation of cities of Mérida and Caracas in Venezuela.

PREVIOUS STUDIES

For structural design purposes, several attempts have been made to establish the relationship between the general characteristics of recorded spectral shapes and the local soil conditions at the recording stations, showing that in spite of the differences in records used, the spectral shapes are in fact site-dependent.

By multiplying the ordinates of certain normalized acceleration spectral shapes either by factors representative of the spectrum intensities, or by the expected maximum peak ground accelerations, representative response spectra for different site conditions and for different earthquakes could readily be obtained. For example, Figs 1A, 1B and 1C show a comparison between the recorded normalized acceleration spectra at different sites and their corresponding anticipated spectral shapes obtained by using the mean spectral curves proposed by Seed, Ugas and Lysmer (1) for soft to medium clay with sand, deep cohesionless and rock sites.

A NEW APROACH

From the observed differences in spectral shapes (mean-VS-recorded) shown in Figs. 1A,1B, it should be recongnized that spectral shapes can not be always

* Professor of Civil Engineering at Simon Bolivar and Central Universities; Consulting Engineer at FUNVISIS and GRID-APM, Caracas, Venezuela.

** Chairman of the Venezuelan Foundation for Seismic Research, FUNVISIS, Caracas, Venezuela.

properly reproduced (see Fig 1C) by simply scaling a set of statistical normalized acceleration spectral curves representative of different site conditions. Spectral shapes are in fact quite complicated to anticipate since - they vary, not only as a function of the local type of soil, but also as a function of other important parameters, such as: distance from zone of energy release, stiffness of soil deposit at the recording station, source mechanism, etc.

Based on the observed behavior of the spectral shapes of 104 records used by Seed, Ugas and Lysmer, and also, on analytical soil-response studies performed at different sites in Venezuela (2,3,4,5), it was decided in this paper to classify soils by their spectral shapes into two major groups:

Group A: Soft to medium clay and sand soils, and

Group B: Everything else, (rock, stiff, deep cohesionless, etc.)

It has been found that spectral shapes of soils in groups A and B depend primarily on the fundamental period of the soil deposit, T_s , at the recording station, and also, on the distance, D , from the zone of energy release. It was also found, that the range of periods at which maximum spectral accelerations take place, (so-called predominant period range, T_p), varies as a function of T_s , and D , in soils of group B, whereas for soils of group A, T_p range varies only as function of distance D .

In this paper, a simple graphical method is proposed to serve as a tool for:

- a) Anticipating normalized acceleration spectra (only for $\lambda=5\%$) for the two groups of soils herein considered, when T_s and D are known parameters, and
- b) Evaluating directly from any given recorded spectral shape, the fundamental period of the deposit at the recording station, when the type of soil and the distance D , are known.

Graphs 2A, 2B, 3A and 3B, in figures 2 and 3, provide the basic tools for - such evaluations. The relative position of the so-called predominant period range T_p , is governed by the "shift factor F_t ". This factor, whose units are given in seconds, depends on:

- a) The distance D , from the source of energy release, for soils of group A, (see graph 2B), and
- b) The fundamental period of soil deposit at the recording station T_s , and the distance D , for soils of group B, (see graph 3B).

For soils of group B, the values of factor F_t associated to a given distance D and to a known soil period T_s , can be obtained directly from curves shown in graph 3B, or more accurately from the following relationships:

$$F_t = \beta \cdot F_t \text{ base} \quad (1)$$

$$\text{and} \quad \beta = 1.5 - 0.0791 \sqrt{D - 10} \quad (2)$$

where β is an empirical equation and F_t base represents the base curve of reference, (see table I for $D = 50$ km).

However, for soils of group A, factor F_t is obtained from graph 2B only as a function of the distance D from the zone of energy release.

TABLE I

T_s	0.00	0.55	0.8	0.95	1.20	1.40	1.70	2.00	2.40	3.00
F_t base	0.35	0.35	0.8	1.00	1.26	1.38	1.48	1.53	1.55	1.56

The abscise \bar{T} in graphs 2A and 3A of Figs 2 and 3 will be identified in this paper as the "Equivalent Period" which is related to the fundamental periods of structures by means of the following equation:

$$\bar{T} = (F_t / T_s) \cdot T \quad (3)$$

Since for a particular earthquake at a given site, the factor F_t and the soil period T_s are constants, then, the equivalent period \bar{T} becomes proportional - to T . Therefore, with the aid of equation 3, it is a simple matter to evaluate for a given structure with a known fundamental period T , the corresponding normalized spectral acceleration, S_a^n , directly from graphs 2A and/ or - 3A depending of the soil group. Clearly, similar computations can be made - for structures with other fundamental periods. The acceleration spectrum is then obtained multiplying the normalized S_a^n values by the expected maximum - peak ground acceleration \ddot{U}_{gmax} . By virtue of the existent analogy among graphs 2A and 3A and a normalized acceleration spectrum, it has been decided in this paper to identify such graphs as the "Equivalent Normalized Acceleration Spectrum".

In the construction process of a desired normalized acceleration spectrum - from equation 3 and graphs 2A / or 3A, it becomes necessary to evaluate the structural periods associated to certain equivalent periods at some points of interest, such as points A,B,C, and D. Solving for T in equation 3, for any i value of \bar{T} , it can be written that:

$$T_i = \bar{T}_i (T_s / F_t) \quad (4)$$

Therefore, T_A , T_B , T_C and T_D are computed from equation 4 by simply substituting \bar{T}_i by the known values of \bar{T}_A , \bar{T}_B , \bar{T}_C and \bar{T}_D , which are tabulated in - graphs 2A and 3A.

Similarly, the "Equivalent Predominant Period", \bar{T}_p , will be defined as the - equivalent period (s) associated to the maximum normalized spectral acceleration (s) of the equivalent normalized acceleration spectrum. By substituting \bar{T} by \bar{T}_p , and T by T_p in equation 3, it can be now written that:

$$\bar{T}_p = (F_t / T_s) \cdot T_p \quad (5)$$

where T_p is the predominant period of the acceleration spectrum.

Note that values of the abscises \bar{T}_A and \bar{T}_B in graphs 2A and 2B define the range of variation of the equivalent predominant period \bar{T}_p , and they are fixed values, (see tables in Figs 2A and 3A). For practical purposes, however, \bar{T}_p can be directly obtained from the equation:

$$\bar{T}_p = (\bar{T}_A + \bar{T}_B) / 2 \quad (6)$$

By substituting the values of \bar{T}_A and \bar{T}_B into equation 6, \bar{T}_p becomes equal to 0.50 for soils of group A, and equal to 0.475 for soils of group B, and therefore, equation 5 can be then written as follows:

$$T_p = 0.5 (T_s / F_t) \quad (7) \quad T_p = 0.475 (T_s / F_t) \quad (8)$$

Equation 7 is valid only for soils of group A, whereas, eq. 8, is valid for soils of group B. These equations will be used for the evaluation of the fundamental period of soil deposit at the recording station (see next section, problem B).

Finally, in this paper, the spectral amplification factor, A, has been set equal to 3.55 (see graphs 2A and 3A), although it can be set to any desired value.

POTENTIAL USES OF PROPOSED METHOD

The information presented in Figs. 2 and 3 can be readily incorporated to the process of seismic microzonation of a city. In effect, with the aid of such graphs, the following earthquake problems can be solved:

- a) Anticipation of acceleration spectrum curves for the two groups of soils A and B herein considered ($\lambda = 5\%$ only), when the fundamental period of the soil deposit and the distance from the zone of energy release, are known parameters, and
- b) Estimation of the fundamental period of soil deposit at the recording station directly from the shape of the recorded normalized acceleration spectrum.

PROBLEM A: Figures 4 and 5 for example show a comparison of recorded-VS-anticipated normalized acceleration spectral shapes obtained using different techniques, at sites where the fundamental period of soil deposit had been previously evaluated by soil-response analyses (1,6). Notice the good agreement obtained with the aid of graphs 2A, 2B and 3B herein proposed.

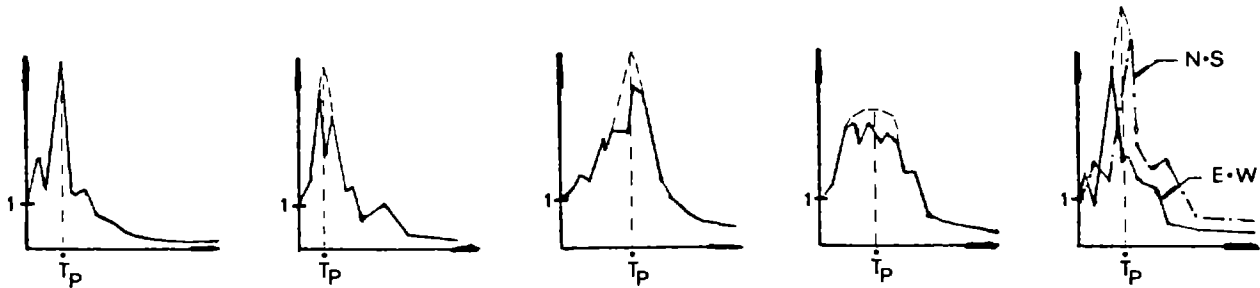
Figures 6-A through 6-H, show two cases in which this new technique have been applied to the seismic microzonation of the cities of Mérida and Caracas in-Venezuela (4,6). Figure 6-H, for instance shows a family of acceleration spectra at the surface of deposits of variable depth in the Caracas Valley, anticipated for a 7.2 magnitude earthquake at a distance of 80 km. This was obtained with the aid of graphs 3A and 3B, and with the information contained in figures 6-E and 6-F. It should be noted that neither the urban planner nor the designer engineer need to be experts in earthquake engineering in order to anticipate spectral shapes at any desired site of the city for a given earthquake. All it is needed is a very simple information, such as the one provided in Figs. 6-E, 6-F and 6-G, which had been previously evaluated, anyway, from sophisticated soil-response analyses, by experts.

PROBLEM B: The only information needed to evaluate the fundamental period of the soil deposit at the recording station directly from the recorded acceleration spectral shape are: The distance D from the zone of energy release and the type of soil, (A or B in our discussion). We shall distinguish two cases:

a) For soils of group A, T_s can be obtained from eq. 7 as follows:

$$T_s = (F_t/0.5) \cdot T_p \quad (9)$$

where T_p is the predominant period of the recorded acceleration spectrum, and F_t is obtained from graph 2-B in Fig. 2 for a given distance D . Note that - for distances greater than 125 km. T_s is virtually equal to the predominant period, i.e., $T_s \approx T_p$. In selecting the value of T_p from the recorded spectrum, the next suggestions should be taken into account:



The accuracy of equation 9, is then checked, evaluating, with the aids of - graphs 2A and 2B, the resulting spectral shape, and comparing it to the recorded one. If they look reasonably similar, then T_s is the right value. Otherwise, a new value of T_p should be selected, and the whole process repeated. Normally only a couple of trials are needed. For example, graphs A, B and C in Fig. 7-I, show the excellent accuracy obtained when the so - computed T_s values are compared to the "exact ones" obtained from expensive field surveys and soil-response analyses (1).

b) For soils of group B, however, a trial and error procedure must be performed by assuming different values of T_s and their corresponding F_t values (from graph 3B), until the value of T_p (associated to - the assumed T_s value) in equation 8 comes as close as possible to the value of T_p selected directly from the recorded acceleration spectrum. From then on, the checking process is the same as for group A soils. Graphs A, B and C of Fig. 7-II, show results obtained for group B soils. Table II contains the mathematical computations required to evaluate the fundamental period of the soil deposit at the recording station (INCERC) of the 1977 Bucarest earthquake, in Rumania. (NS-Component).

In the preliminar stages of the microzoning process, the evaluation of the - fundamental period of a soil deposit by means of this technique, would be - particularly useful in the event that a city, on which a net of strong motion accelerographs are already installed, were hit by an earthquake. In this - case, it would be possible, directly from the recorded ground motion, to detect within the city, soil deposits of different depths and/ or stiffnesses, simply by comparing the so-evaluated periods at the recording stations.

A table containing the fundamental period of soil deposits at the recording stations of the most important events used by Seed, Ugas and Lysmer, will be published quite soon (see ref. 6).

TABLE II

($\beta = 0.515$ for $D = 165$ km.; $T_p = 1.35$ -sec-)

	j	T_s	F_t	T_p^j	$T_p^j - T_p$	% Error

	8	2.35	0.850	1.313	-0.037	-2.726
best value	9	2.40	0.855	1.333	-0.017	-1.237
→	10	2.45	0.857	1.358	0.008	0.585
	11	2.50	0.858	1.384	0.034	2.519
	12	2.55	0.859	1.410	0.060	4.452
	:	:	:	:	:	:

CONCLUSION

The seismic microzonation of a city deals with a great volume of information concerning with the evaluation of seismic risk, geological hazards, classification and characterization of local soils, soil-response analyses, soil - structure interaction effects, code provisions, urban planning, earthquake insurance and government responsibility, among others. When this information is combined with good engineering judgment based on observed building performance during earthquakes, then it becomes possible to reduce the potential - seismic hazards of an urban area. It is hoped that the information presented in graphs 2A, 3A and 3B of Figs. 2 and 3 will prove to be a useful tool for the urban planner and the designer to accomplish above objectives.

ACKNOWLEDGEMENT

This investigation was supported in part by the Venezuelan Foundation for - Seismic Research "FUNVISIS", and by the Civil Engineering Department of the Universidad Central of Venezuela. The computer time and facilities were - provided by the Computer Center of GRID-APM. The authors wish to thank Miss Gloria Inés Quintero for typing and Miss Inés López for reviewing the manuscript, and also Mr. C. Ugas, who provided us with the recorded data.

REFERENCES

- 1.- Seed H.B., Ugas C. and Lysmer J., "Site-Dependent Spectra for Earth - quake Resistant Design"., Report N° EERC-74-12, University of California, Berkeley, 1974.
- 2.- Seed H.B., Idriss I.M., and Dezfulian H. "Relationships Between Soil- Conditions and Building Damage in the Caracas EQ. of 1967", Report N° EERC-70-2- Berkeley, 1970.

- 3.- Alonso J.L., and Larotta J., "Seismic Risk and Seismic Zoning of the Caracas Valley", VI World Congress on Earthquake Engineering, New - Delhi, India, January 1977, (1977-I).
- 4.- Alonso J.L., "Microzonificación Sísmica de Mérida, Recomendaciones Finales", Tomo III, Ministerio de Desarrollo Urbano, Caracas, Sept. 1977, (1977-II).
- 5.- Alonso J.L., "Estudio Sísmico de las Unidades 3 y 4 de Planta Centro, Morón", CADAPE, Caracas, Nov. 1977, (1977-III).
- 6.- Alonso J.L., "Generación de Espectros de Aceleración y Evaluación del Período Fundamental de Depósitos a partir de Registros Reales", Trabajo en preparación.

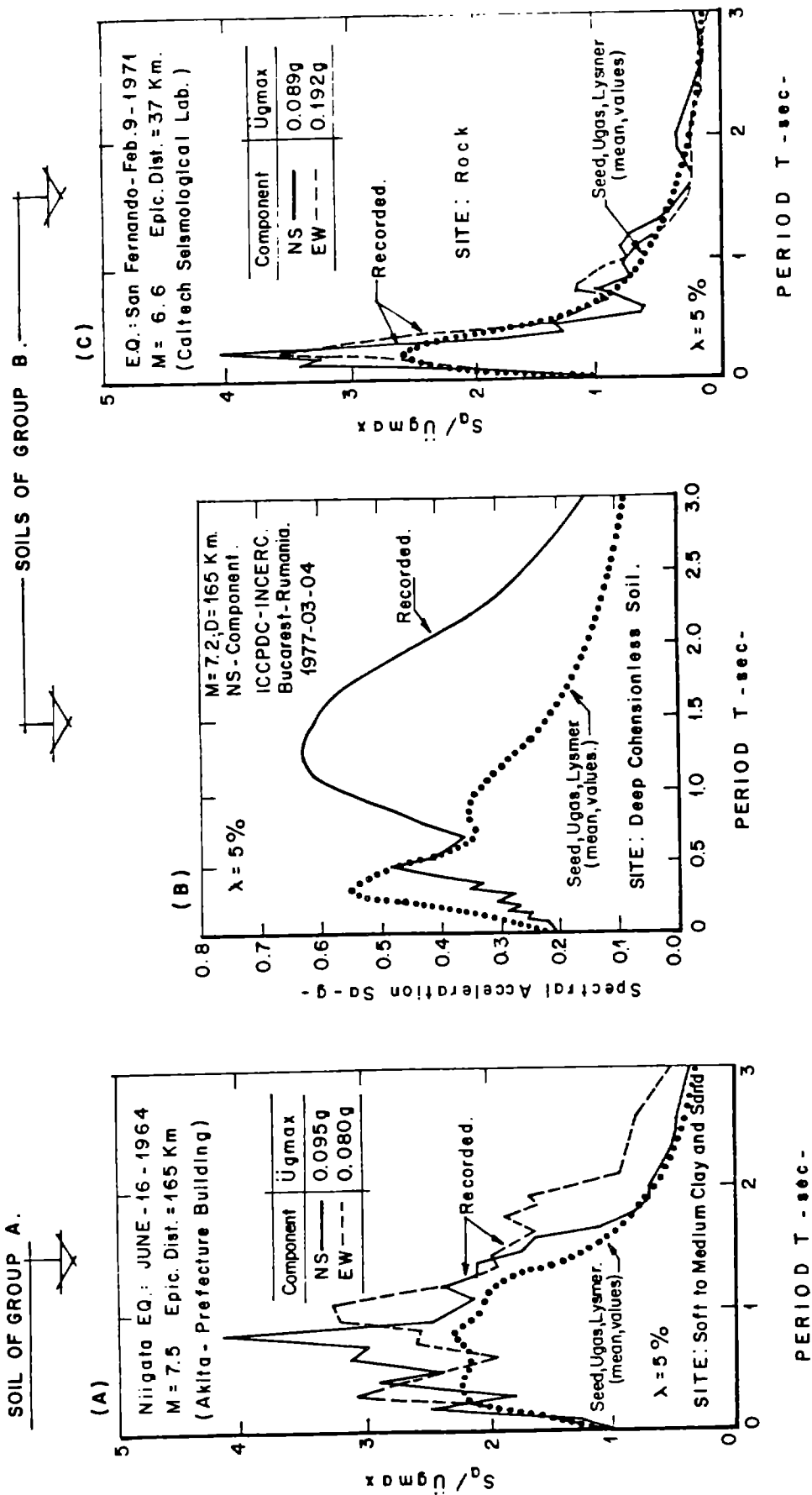
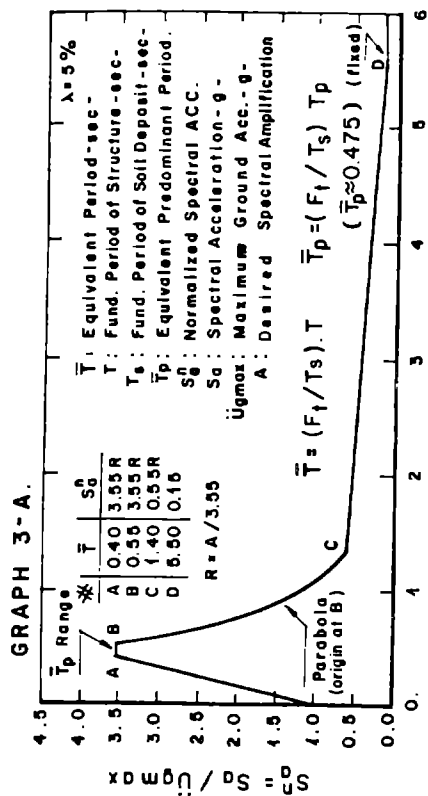


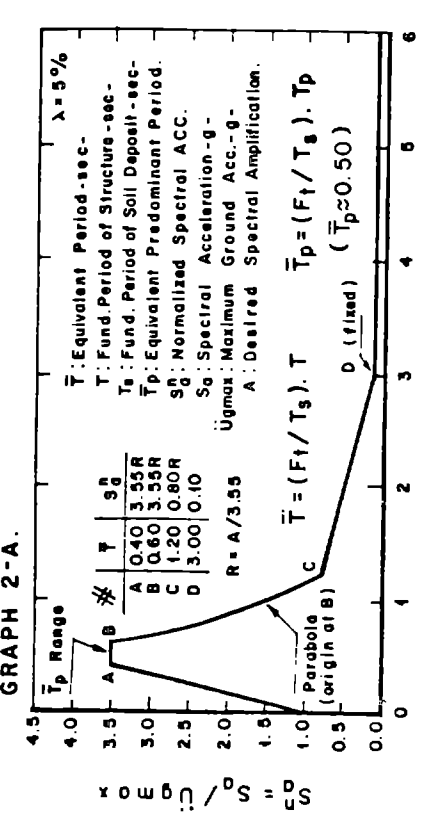
FIG. 1 ANTICIPATED MEAN SPECTRA AT DIFFERENT SITES (Seed, Ugas, Lysmer) -VS- SPECTRAL SHAPES AT THE RECORDING STATIONS.

SOILS OF GROUP B.
(Everything Else: rock, stiff, deep cohesionless, etc.)



EQUIVALENT PERIOD \bar{T} - sec -

SOILS OF GROUP A.
(Soft to Medium Clay and Sand)



EQUIVALENT PERIOD \bar{T} - sec -

FIG. 2 PROPOSED METHOD FOR THE EVALUATION OF NORMALIZED SPECTRAL ACCELERATION SHAPES FOR SOILS OF GROUP A.
(After Alonso J.L., 1977-III)

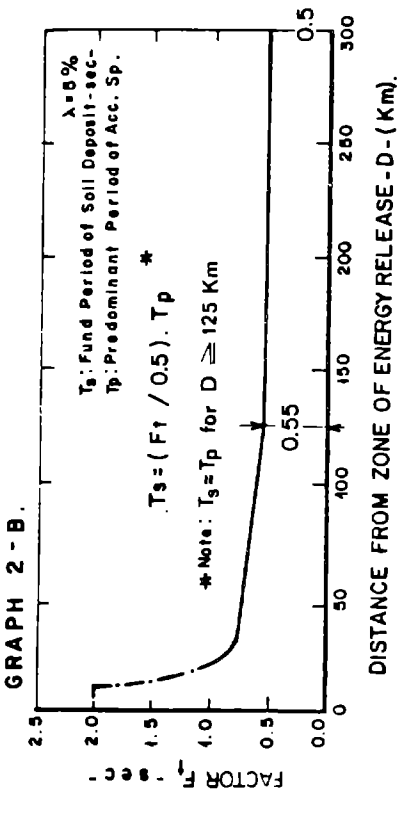
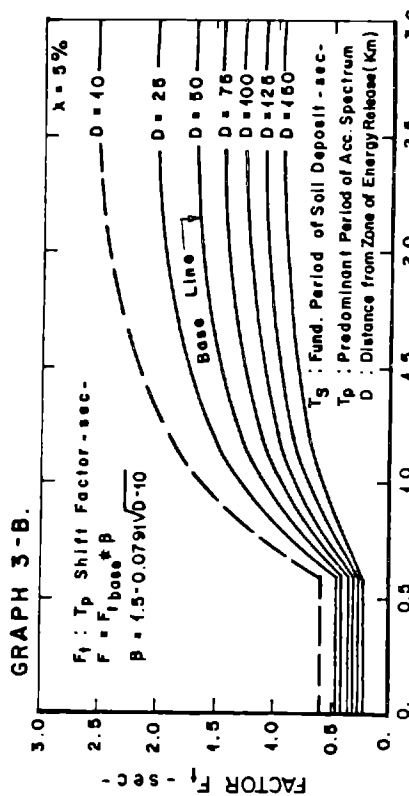


FIG. 3 PROPOSED METHOD FOR THE EVALUATION OF NORMALIZED SPECTRAL ACCELERATION SHAPES FOR SOILS OF GROUP B.
(After Alonso J.L., 1977-II)



FUND PERIOD OF SOIL DEPOSIT T_s - (sec) .

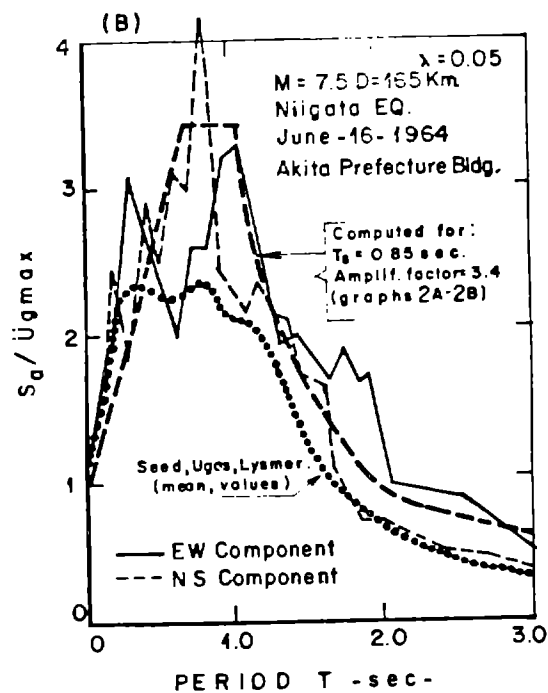
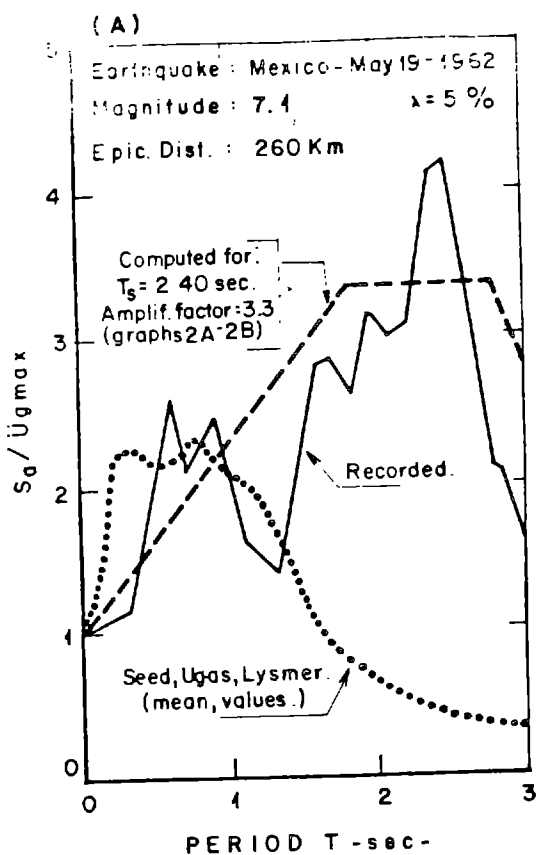


FIG. 4 COMPARISON OF NORMALIZED RESPONSE SPECTRA USING DIFFERENT TECHNIQUES. SOILS OF GROUP A (Soft to medium clay and sands).

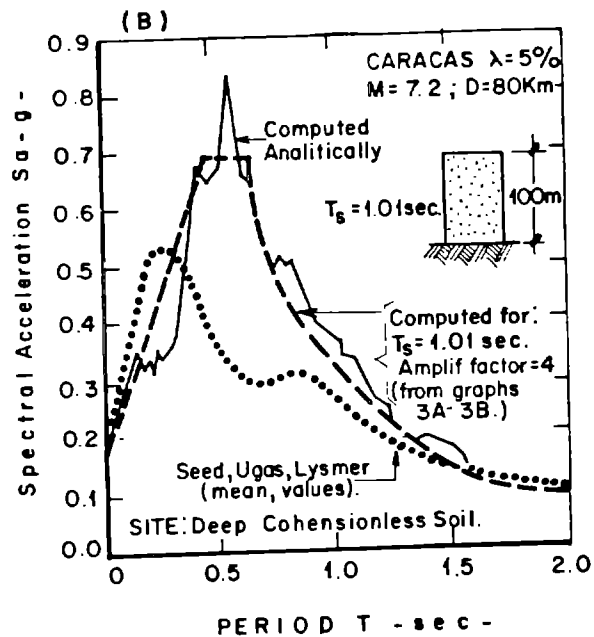
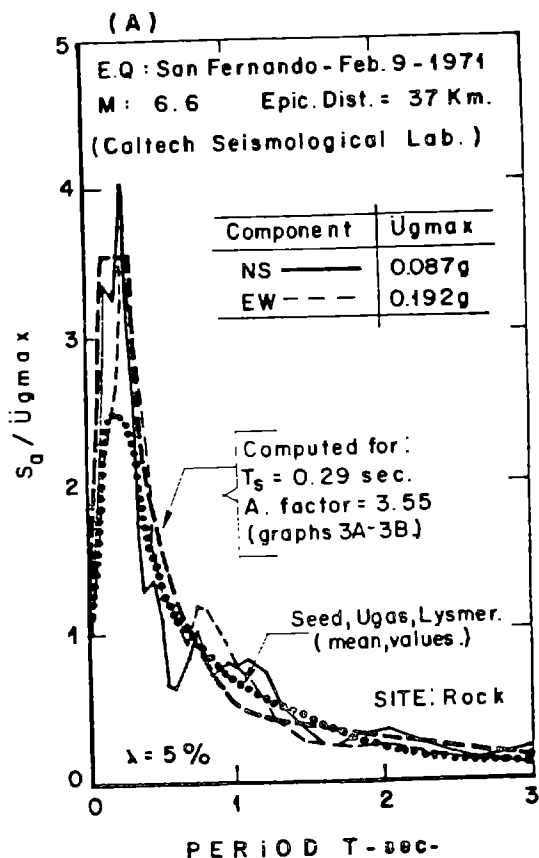


FIG. 5 COMPARISON OF ACCELERATION RESPONSE SPECTRA USING DIFFERENT TECHNIQUES. SOILS OF GROUP B. (Rock, stiff, deep cohesionless, etc.)

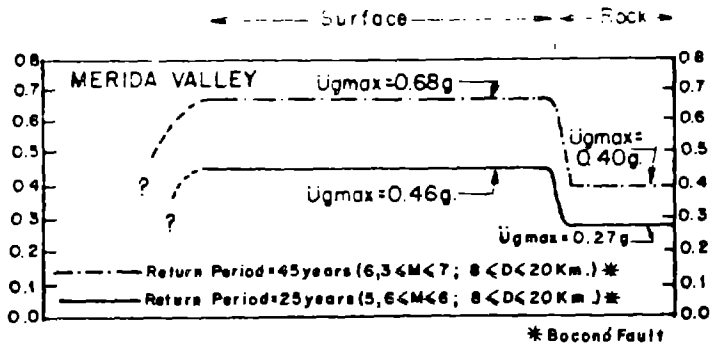


FIG. 6-A COMPUTED MAX. GROUND ACCELERATION FOR THE CITY OF MERIDA.

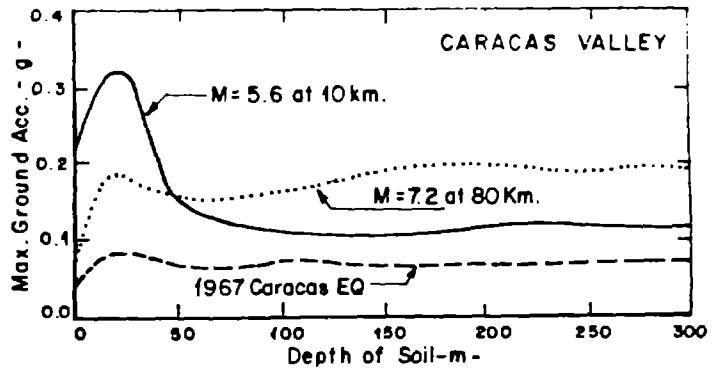


FIG. 6-E. COMPUTED MAX. GROUND ACCELERATION

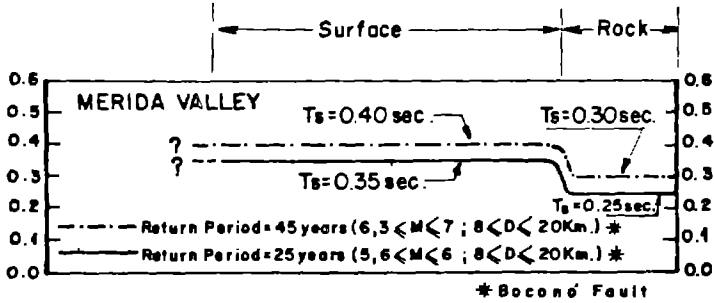


FIG. 6-B: COMPUTED VARIATION OF FUNDAMENTAL PERIOD OF DEPOSITS FOR CITY OF MERIDA.

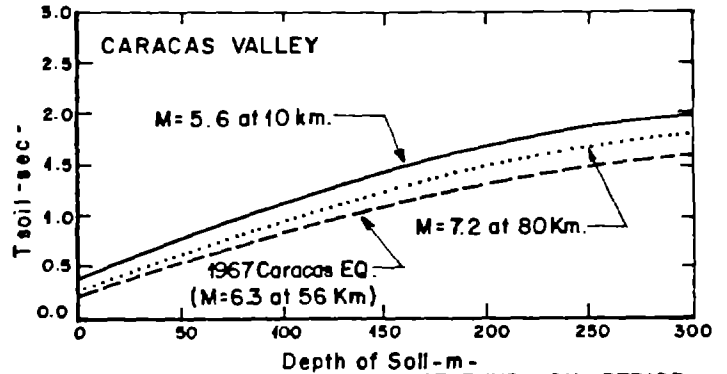


FIG. 6-F. COMPUTED VARIATION OF FUND. SOIL PERIOD

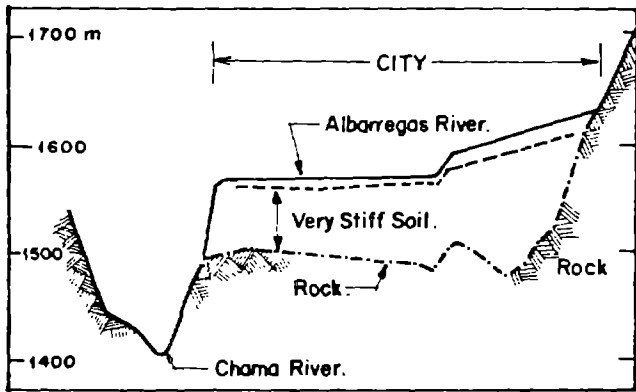


FIG. 6-C. TYPICAL CROSS SECTION OF THE MERIDA VALLEY.

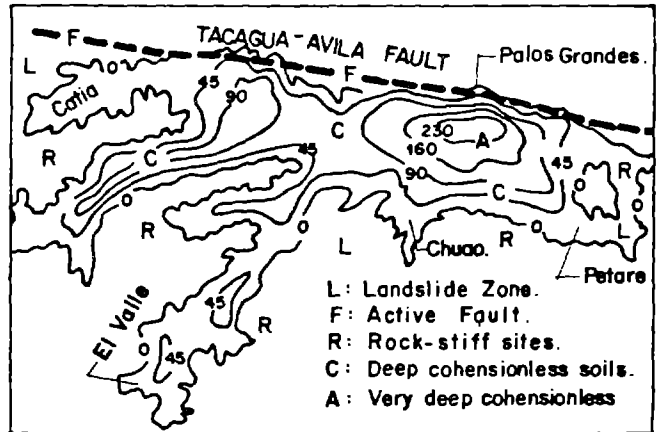


FIG. 6-G. MAP SHOWING DEPTH IN METERS OF SOIL DEPOSITS AND HAZARD ZONES-CARACAS VALLEY.

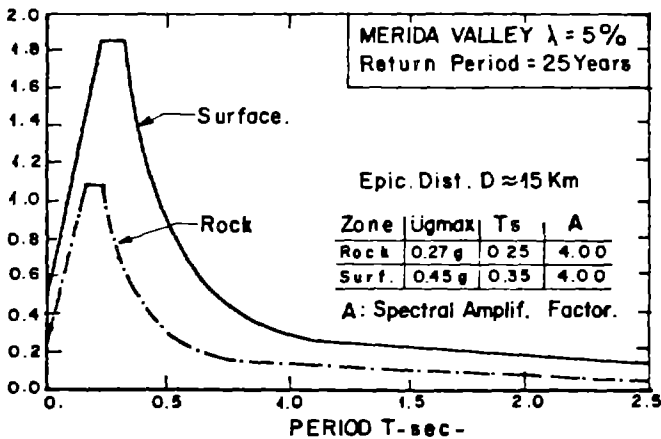


FIG. 6-D. ANTICIPATED ACCELERATION SPECTRA FOR A RETURN PERIOD OF 25 YEARS. (from graphs 3A and 3B)

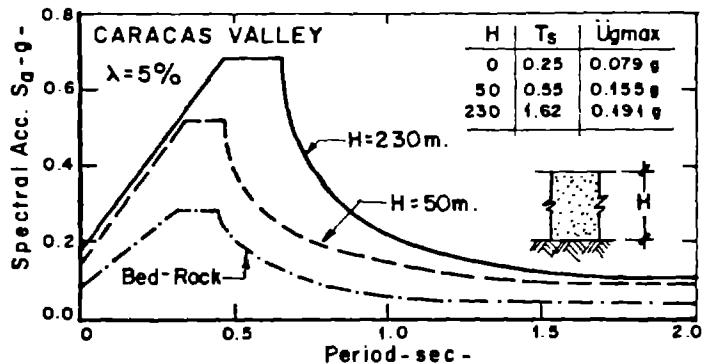


FIG. 6-H. ANTICIPATED ACCELERATION SPECTRA FOR A MAGNITUDE 7.2 EQ. AT 80 KM. (from graphs 3A and 3B)

FIG. 6 EXAMPLES OF THE POTENTIAL USES OF PROPOSED METHOD IN THE SEISMIC MICROZONATION OF THE CITIES OF MERIDA AND CARACAS.

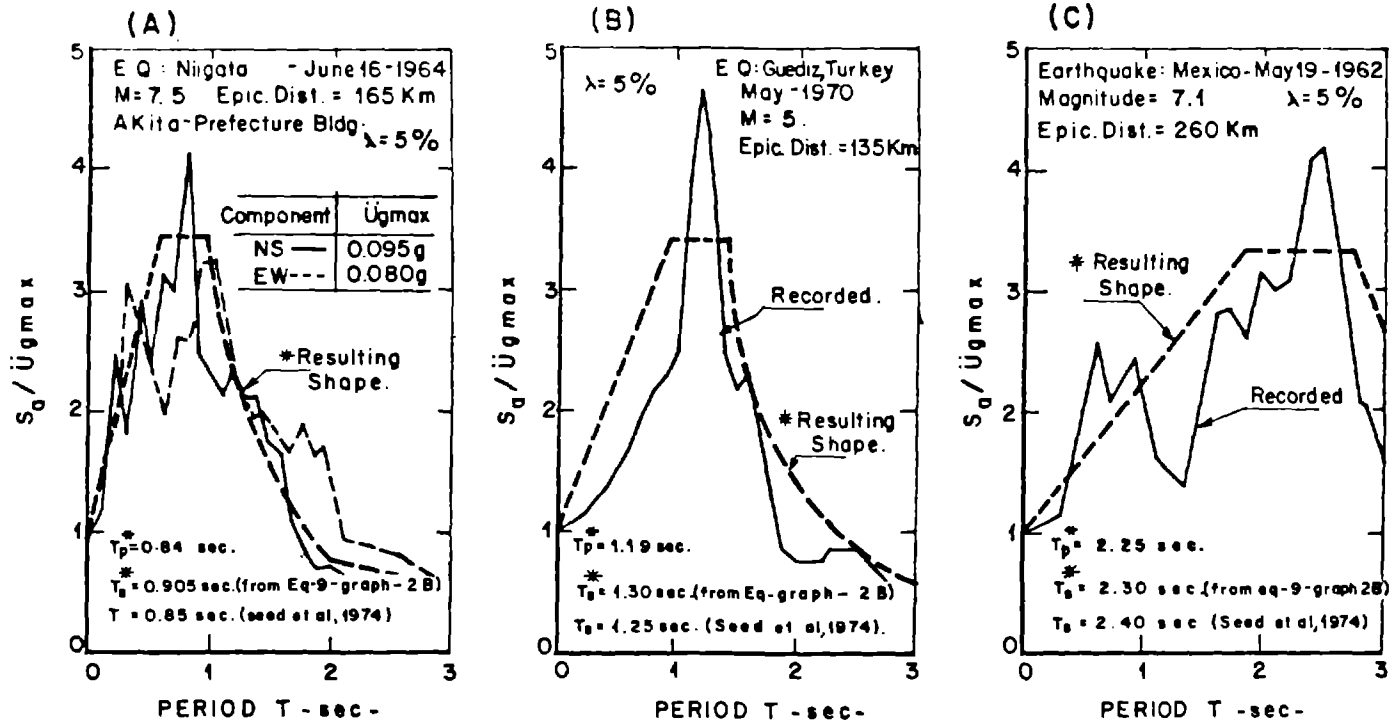


FIG. 7-I APPLICABILITY OF PROPOSED METHOD TO SOILS OF GROUP A.

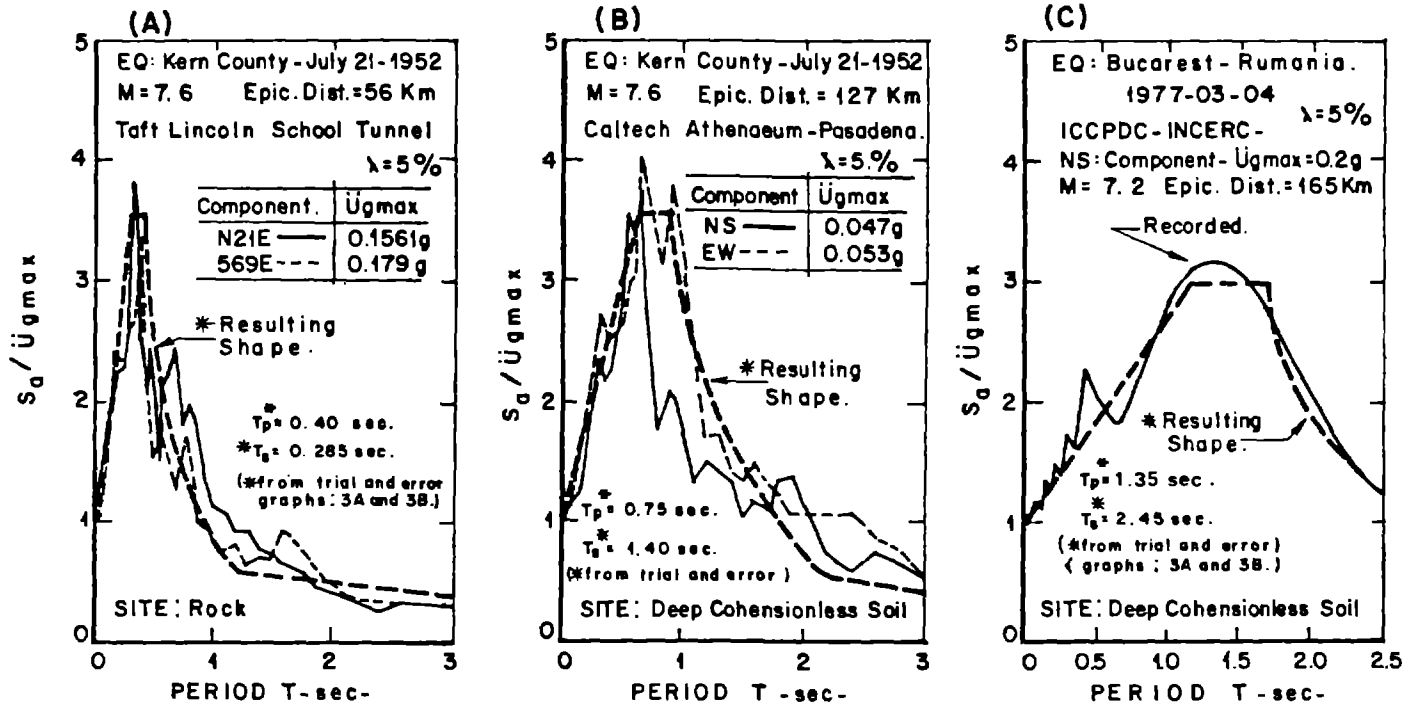


FIG. 7 - II APPLICABILITY OF PROPOSED METHOD TO SOILS OF GROUP B.

FIG.7 EVALUATION OF FUNDAMENTAL PERIOD OF SOILS DEPOSIT AT THE RECORDING STATION DIRECTLY FROM THE ACC.SPECTRAL SHAPES BY USING THE GRAPHS 2A,2B, 3A, and 3B HEREIN PROPOSED. CHECK OF ACCURACY

THE CONCEPT OF RESIDUAL RISK IN EARTHQUAKE RISK ASSESSMENTS

By

Ashok S. Patwardhan^I and Lloyd S. Cluff^{II}

ABSTRACT

The concept of residual risk has application in earthquake risk assessment. Residual risk is a quantitative portion of the calculated risk for a given probability that needs to be managed. It is time dependent, and all risk estimates must be updated periodically. Besides time dependence, earthquake risk estimates are sensitive to degree of fault activity, site conditions, and relationships between ground motions and expected losses. Earthquake risk assessments can provide the basis for establishing the level of earthquake hazard mitigation, insurance coverage, and contingency planning for single and multiple events. Current earthquake microzonation procedures may be enhanced by expanding to include risk-based assessments.

INTRODUCTION

The objective of the recently enacted Earthquake Hazards Reduction Act of 1977 (Public Law 95-124) (1) is "... to reduce the risks of life and property from future earthquakes in the United States through the establishment and maintenance of an effective earthquake hazards reduction program." The act "recommends appropriate roles for state and local units of government, individuals and private organizations in carrying out the plan." One of the objectives of earthquake microzonation is to provide a basis for earthquake hazard reduction and earthquake risk management. The management of earthquake risk is a complex issue that involves many disciplines and value judgments from different individuals. A program of earthquake hazard reduction necessarily has to be spread over a period of years.

A recent report by the Working Group on Earthquake Hazards Reduction (1) states that (a) the role of and the effect of earthquake hazards reduction on private institutions has not been explored or understood; (b) issues related to public and private financial institutions require much more study before definite policies can be recommended; and (c) a systematic risk-based procedure for planning earthquake hazards reduction programs is highly recommended but is not available at present. The public and private groups referred to may include individual owners, insurance companies, financial institutions, and local/state governments.

Figure 1 illustrates the steps in a risk-based assessment of earthquake effects; the steps are:

I Associate, Woodward-Clyde Consultants, San Francisco, California

II Chief Engineering Geologist, Woodward-Clyde Consultants,
San Francisco, California

- (a) evaluation of seismic exposure;
- (b) risk evaluation consisting of probabilities of various amounts of losses from all earthquake effects;
- (c) selection of microzonation criteria and identification of microzones;
- (d) evaluation of alternate strategies for risk management and hazard reduction.

Several workers have partially addressed some of the above steps. To name a few examples: step (a), the seismic exposure map of United States prepared by Algermissen and Perkins (2); step (b), the approach and application of methods for evaluation of seismically induced losses proposed by Whitman (3), and NOAA (4). Published literature for steps (c) and (d) has generally utilized a qualitative evaluation (5, 6) of earthquake risk. We examine in this paper some aspects that could contribute to a quantitative evaluation.

DEFINITION OF EARTHQUAKE RISK

In this paper, earthquake risk is defined as the probability of experiencing a certain amount of loss due to the effects of an earthquake. The definition of loss may vary from one group to another and from structure to structure. The loss may be either a physical loss (for example, damage to a building) or a consequential loss (for example, loss of business). It may be expressed either in quantifiable terms, such as dollars or number of lives lost, or in qualitative terms, as change in quality of life.

In the case of quantifiable risks, three different types may be defined. The calculated risk (R_c) is the expected loss for a given probability of occurrence. The acceptable risk (R_a) is often based on a value judgment and may be defined as the probable loss(es) that can be tolerated without adverse consequences. The residual risk (R_r) is the difference between the calculated and acceptable risk and is the risk that needs to be managed. The relationship between the three risks may be expressed as:

$$R_r = R_c - R_a \quad (1)$$

Other workers have described residual risk somewhat differently. It may be identified as the difference between calculated risk and the risk mitigated either by insurance or through hazard reduction. According to this definition, residual risk is synonymous with acceptable risk. In a given area, factors contributing to the calculated risk (R_c) are the size, location, and frequency of earthquakes; expected ground motions; site response; structural response; the potential for fault displacement through a structure; and the expected loss from all effects (Fig. 2). Calculated risks are high (a) if the site response is such that it will lead to ground failure such as liquefaction or landslides, (b) if the structures are not strong enough to withstand the expected ground motions, or (c) if the structure is located across an active fault and has not been

designed to accommodate the expected slip on the fault. Other factors being equal, the calculated risks may be lower for structures designed to modern codes, although the risks may not be eliminated entirely because the primary intent of codes is to minimize danger to life and property and not minimize damage, and the codes pertain to the shaking exposure only.

Factors comprising the acceptable risk (R_a) are the amounts of loss that may be accepted through self-insurance, contingency planning, and other financial arrangements (R_{si}). The acceptable risk may be supplemented by external insurance coverage (R_k),

$$R_a = R_{si} + R_k \quad (2)$$

The assessment of acceptable risk depends on value judgments, and the risk that is acceptable may vary within wide limits depending upon the risk-taking posture of the owner-individual or organization. The acceptable risk may be very small if there is no self insurance and no external coverage. On the other hand, it may equal or exceed the calculated risk if the combined coverage is high. In case of certain important structures such as dams and nuclear power plants, acceptable risks may be influenced significantly by regulatory actions. Acceptable risks may be constant (that is, independent of probability), or they may vary depending upon the probability of occurrence of the calculated risk (see Fig. 3).

The residual risk (R_r) may vary widely depending upon the difference between the calculated and acceptable risks. It is low if the calculated risks are low and the acceptable risks are high. It may even be negative if the acceptable risks exceed the calculated risks, as in the case of very conservatively designed structures; this may be the case for some nuclear reactors. Conversely, the residual risks may be very high if the calculated risks are high and the acceptable risks are small. An example is the case of certain older high-density urban areas in California where the calculated risks are high, the losses covered by self insurance are low, and the number of owners who have supplemented their coverage by external earthquake insurance is small (typically less than 10 percent). In such cases, the residual risk may be very nearly equal to the calculated risk.

It should be noted that different groups may evaluate residual risks differently. To an individual, residual risk may have the meaning given in equation (2). To an insurer, the residual risk may signify the difference between the premiums and amounts paid. A regulator may view residual risk as the risk that needs to be managed both individually and collectively. Similarly, different meanings may be attributed to the term "loss" such as cost of replacements, depreciation costs, and cost of replacement in conformance with current codes.

Figure 3 shows a typical distribution of risk at a given location. If the acceptable risk having a 10 percent probability is \$10,000 and the calculated risk for the same probability is \$50,000, the residual risk will be \$40,000. If supplemental coverage is acquired in the amount of \$20,000, the net residual risk is \$20,000. Similar calculations can be made for other probabilities of occurrence to obtain the risk versus loss relationship illustrated in Fig. 3.

The objective of an earthquake hazard reduction program is to reduce the residual risk (R_r) to a specific group or to society. This can be accomplished by reducing the calculated risk (via engineering, land-use planning) or by supplementing the acceptable risk with additional risk coverage (via insurance, contingency planning). The objective of earthquake risk management is to manage the residual, acceptable, and calculated risks.

TIME DEPENDENCE OF RISK

The relationship shown in Fig. 3 describes the risk picture at any point in time if the contributory factors do not change. However, earthquake risks are particularly time dependent (see Fig. 4).

The calculated risk (R_c) depends upon seismic exposure, site response, structural response, and the states of damage associated with a given state of response. One reason for change in the calculated risk is the identification of new earthquake sources or additional geologic information. Another reason for change in the risk may be a change in the level of seismic exposure due to a change in the expected number of earthquakes of different magnitudes. The effect may be significant if a significant component of the calculated risk at the given location is due to large magnitude earthquakes (magnitude $M_s \geq 7.5$). In many seismic areas, the occurrence of large earthquakes is not a random process but follows a law wherein the size and holding time to the next large earthquake are influenced by the size of and the time elapsed since the previous large earthquake. Figure 5 shows an example (7) of a case in which the probability of a given large magnitude earthquake increases above the level indicated by a random (Poissonian) process if the time elapsed since the last large earthquake increases and decreases during the period immediately following it.

Other reasons for change in the calculated risk may include the change in damage probability due to a change in strength (such as with age), change in the number of people at risk (such as population downstream from a dam), and change in the cost of repair.

The calculated risk may increase sharply in the case of a predicted earthquake, depending upon the magnitude of the predicted earthquake, its probability of occurrence, and the time window (see Fig. 6). On the other hand, it may decrease sharply just after the occurrence of an earthquake if effective earthquake hazard reduction measures are implemented.

Acceptable risks may or may not vary depending upon the choice of the owner and the underwriter. The risks may be increased by providing a combination of self insurance and external insurance coverage or they may be decreased to adjust to changed circumstances (for example, decrease in the functional utility of the structure). Consequently, the residual risk may increase or decrease depending upon whether the rate of change of calculated risks is higher or lower than the rate of change of acceptable and covered risks. Figure 4 shows a diagrammatic representation of time dependence for an individual structure.

Similar considerations may be applied to a group of structures, as in a portion of a city. Each structure may have a different level of risk. The combined risk may be evaluated by convolving the respective risks. The combined calculated risk in the area may show similar trends for time dependence, as in Fig. 4. In addition to the contributory factors noted above, an additional reason for the increase in the combined risk may be the increase in the number of structures and the number of people at risk in the area.

RISK EVALUATION

The calculated and residual risks defined above provide a useful basis for assessing earthquake effects. Usually, risk assessments are desired for a single earthquake or for the combined effects of a number of events expected during a certain period of time. The following table shows the utilization of risk assessment for single and multiple events.

<u>single event:</u>	(a) probability of different amounts of loss
	(b) probability of maximum loss on one structure
	(c) probability of different amounts of losses in a given area
<u>multiple events:</u>	(a) risk exposure for an individual structure for a given time period
	(b) combined risk exposure for an area

Risk evaluations for single events can be utilized for contingency planning, for assessing insurance coverages required, and assessing the total risk in an area. Risk evaluations for the combined effect of multiple events can be utilized for earthquake hazard reduction planning, for assessing frequency of insurance payments, and for contingency planning.

Within certain limits, the general relationship between ground motion and loss may be defined by an expression of the type:

$$L = A(1 - e^{-\beta a}) \quad (3)$$

where L is the loss, a is the ground motion at the site associated with the event, and A and β are coefficients dependent upon the site conditions and structure type (see Fig. 2). Based on this relationship and the associated uncertainty, the probability that a loss, L_i , may be incurred during the event is given by:

$$P(L = L_i) = \sum_{L_j > L_i} \sum_k \sum_l P(L_i | a_k) \cdot P(a_k | M_l) \cdot P(M_l | E) \cdot P(E) \quad (4)$$

where $P(L_i | a_k)$, $P(a_k | M_l)$, and $P(M_l | E)$ are the conditional probabilities of the occurrence of the ground motion (a_k), the magnitude (M_l), and the event (E), respectively.

Using equation (4), the probability distribution function shown in Fig. 3 for calculated risk and for residual risk for an individual structure can be constructed.

By setting $L_i = L_{\max}$, the probability of incurring the maximum loss (referred to as the probable maximum loss, PML) on a given structure can be ascertained.

In the case of a group of n similar structures subjected to similar ground motions, the probability that m structures will experience a loss L_i can be calculated by establishing correlative relationships (see equation 3) and estimating the dispersion associated with it.

If the acceptable risk for each structure is R_a , the residual risk for one structure for the probability p from equation (4) associated with the loss L_i is:

$$R_r = L_i - R_a \quad (5)$$

For a group of structures, the combined residual risk associated with the probability from equation (5) is:

$$R_{rc} = m(L_i - R_a) \quad (6)$$

Similarly, the residual risk for other probabilities and losses can be calculated.

Typically, an area will have a finite geographic extent and experience a range of ground motions resulting in different site responses. The types of structures also differ. The combined effect will be one of a range of structural responses and different loss versus ground motion relationships of the type shown in Fig. 2. The probabilities of different losses for both individual structures and groups of structures can be calculated in the same manner as above by discretizing the range of ground motions and creating subgroups of loss types based on structures and site conditions and defining a separate loss versus ground motion relationship for each subgroup. The probability of having a given residual risk R_r in an area can be determined by calculating the probability distributions separately and convolving them to obtain the combined probabilities and risk.

Similar calculations can be made for multiple events for a period of time, say 5 to 10 years, to obtain the probability distribution of risks over the area.

The probability distributions for individual and combined risks can be utilized for a number of purposes. To an individual owner, the distribution provides a basis for the various options including insurance coverage that must supplement the acceptable risk to reduce the residual risk to a minimum or eliminate it.

To an insurance carrier, it provides an estimate of probability that the loss (or amount payable) during a single event will exceed a given amount per structure or will attain a given total limit for the event. The probability distribution for the multiple event case provides an estimate of expected losses over a period of time. A calculation of the expected losses in different areas can be useful in making a comparison of the expected premiums and losses and in establishing the optimum number

and distribution of structures that an individual carrier may provide coverage for.

In the case of a financial institution, the acceptable risk on an individual structure is the ability of the borrower to repay the mortgage either through self insurance and/or through external insurance. The residual risk to the institution is the difference between the amount in calculated risk and the amount recoverable from the owner. The range of residual risks and associated probabilities may provide a basis for establishing limits on the size of individual loans and the total amount invested in a given area either during a single event or multiple events.

In the case of a local or state governmental organization, the distribution of residual risks during a single event is a good basis for contingency planning. The distribution of risks for multiple events is a good basis for comparison between different areas for earthquake hazard mitigation. For example, if the residual risks can be separated between those due to larger but rarer events ($M_s > 7.5$) and those due to smaller but more frequent events, a decision could be made regarding the scope of a contingency plan.

SEISMIC ZONATION

A risk-based zonation procedure is the last step of a zonation process shown in Fig. 1. Risk-based zonation utilizes the information developed in earlier steps and can be based either on the calculated risks or the residual risks within an area.

Information required for risk-based zonation includes the following:

(a) Evaluation of Seismic Exposure - The evaluation is based on an assessment of seismicity in the area including location, geometry, and degree of activity of earthquake sources and attenuation characteristics in the region. Results may be a seismic exposure map showing the variation of a ground motion parameter, such as peak acceleration.

(b) Evaluation of the Potential for Surface Fault Displacement - This evaluation consists of a probabilistic evaluation of the potential for and extent of surface fault rupture.

(c) Evaluation of Potential for Ground Failure - This evaluation consists of a probabilistic evaluation of the potential for and extent of liquefaction, landsliding, and other seismically induced hazards. The evaluation is based on an assessment of the properties of subsurface materials and their response to earthquake ground motions.

(d) Evaluation of Damage Potential - The probability of various amounts of damage due to shaking as well as fault displacement and ground failure is assessed. For this purpose the area is divided into a number of small cells and a damage probability relationship is established for each cell based on the seismic exposure, subsurface conditions, type of seismic hazard, and structural characteristics. The combined calculated risk for each cell is calculated based on the number of structures of different types at risk. If the acceptable and covered risks are known,

the combined probability of residual risks within each cell can also be calculated.

In the calculation of risks, a distinction should be made between risks for existing structures and risks for future structures in presently undeveloped areas. Before damage estimates could be made, assumptions will be required regarding the nature and density of construction. Risk assessments can be made for different alternatives.

The result of this step is a distribution function for the probability of various amounts of losses for each cell. Utilizing these relationships, a zonation map may be prepared to show the distribution of residual risk in the area for a selected probability of occurrence.

As discussed above, the residual risks are time dependent. Therefore, maps prepared in this step will be applicable for a specific time period, after which they should be revised. They should also be revised if the calculated risks change--either a decrease due to an earthquake hazards reduction program, or increase due to a predicted earthquake or increase in the size of investment or population at risk.

Utilization: A risk-based zonation map provides a reasonable quantitative basis for both earthquake hazard reduction and earthquake risk management.

The probability distribution functions for residual risk for different areas can be used to establish priorities for earthquake hazard reduction and to make quantitative benefit-cost evaluations for various options; for example, strengthening structures, engineering solutions to improvement of landslide susceptibility, and improving slope stability. Obviously, the available options are generally greater for future structures than for existing structures. In the case of future construction in undeveloped areas, the residual risk can be reduced by controlling the calculated risk through land use planning and requiring the use of appropriately conservative design practices.

Earthquake risk management will be required as long as residual risks exist. Even when an earthquake hazard reduction program is in progress, the implementation of the program will require a certain period of time and residual risks will exist, albeit on a diminishing scale. The cumulative distribution function for residual risk can be utilized for evaluating the size and nature of risk coverage on an individual structure and for a group of structures.

Earthquake risk management can be based on self insurance, external insurance or contingency planning. If a combination is used, the appropriate balance between the different means has to be established for analyzing benefits and costs. The information most often required for both contingency planning and external insurance coverage is the residual risk due to a single earthquake. This is so because if the loss due to that earthquake is significant, the basis for obtaining insurance coverage and the normal mode of operation may undergo substantial changes, which will result in a change in the residual risk probability for future earthquakes.

SENSITIVITY

All risk evaluations are sensitive to the parameters and the assumptions used in the model. Parameters that influence risk assessments are the degree of fault activity, the attenuation relationships, and the relationship between ground motion levels and losses. Sufficient data are not available at present for defining the mean relationship and dispersion about the mean for the ground motion versus loss relationship.

ACKNOWLEDGEMENTS

The authors acknowledge the useful discussions with Karl V. Steinbrugge of Insurance Services Office, Edward B. Howell of Risk Analysis and Research Corporation, and Ram B. Kulkarni and Thomas H. Rogers of Woodward-Clyde Consultants on different aspects of earthquake hazard evaluation and risk.

BIBLIOGRAPHY

1. Working Group on Earthquake Hazards Reduction, 1978, Earthquake hazards reduction: issues for an implementation plan: Office of Science and Technology Policy, Executive Office of the President, Karl V. Steinbrugge, chairman.
2. Algermissen, S. T., and Perkins, D. M., 1976, A probabilistic estimate of maximum acceleration in rock in the contiguous United States: U. S. Geological Survey Open-File Report 76-416, 45 p.
3. Schumacker, B., and Whitman, R. V., 1977, Models of threshold exceedance and loss computations of non-homogeneous, spatially distributed facilities: Department of Civil Engineering, Massachusetts Institute of Technology, Seismic Design Decision Analysis Report No. 30, R77-9, Order No. 567, March.
4. National Oceanic & Atmospheric Administration, 1972, A study of earthquake losses in the San Francisco Bay Area; data and analysis: prepared for The Office of Emergency Preparedness.
5. Borchardt, R. D., ed., 1975, Studies for seismic zonation of the San Francisco Bay region: U. S. Geological Survey Professional Paper 941-A.
6. Rogers, T. H., and Williams, J. W., 1974, Potential seismic hazards in Santa Clara County, California: California Division of Mines and Geology, Special Report 107.
7. Patwardhan, A. S., Kulkarni, R. B., and Tocher, D., 1978, A semi-Markov model for characterizing recurrence of great earthquakes: paper presented at EHRP Conference on Methodology for Defining Seismic Gaps and Soon-to-Break Gaps, sponsored by U. S. Geological Survey, Menlo Park, California.

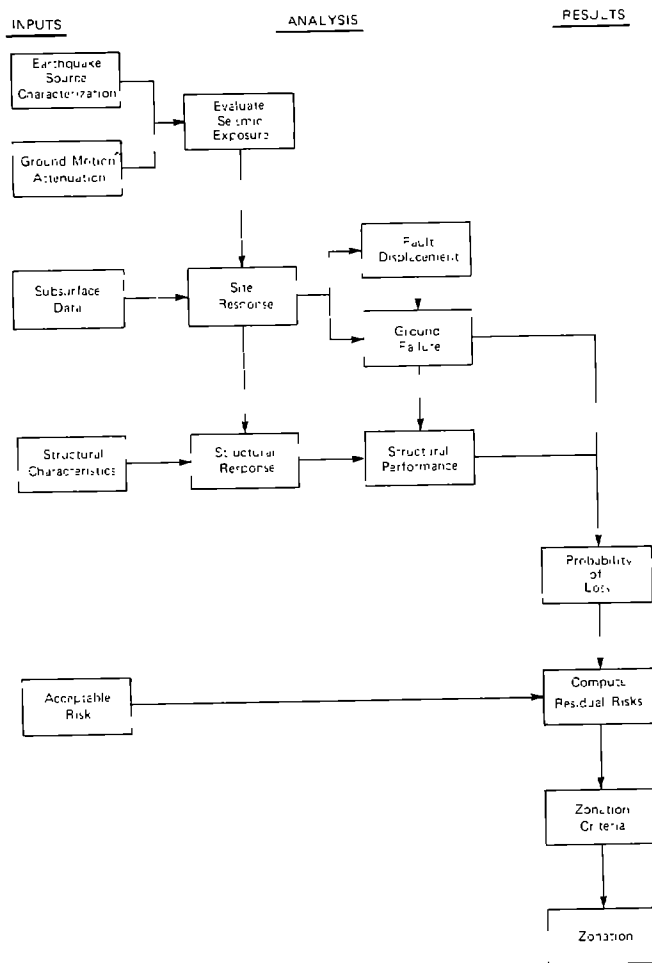


Fig. 1. Flow Diagram - Risk-based Zonation Process

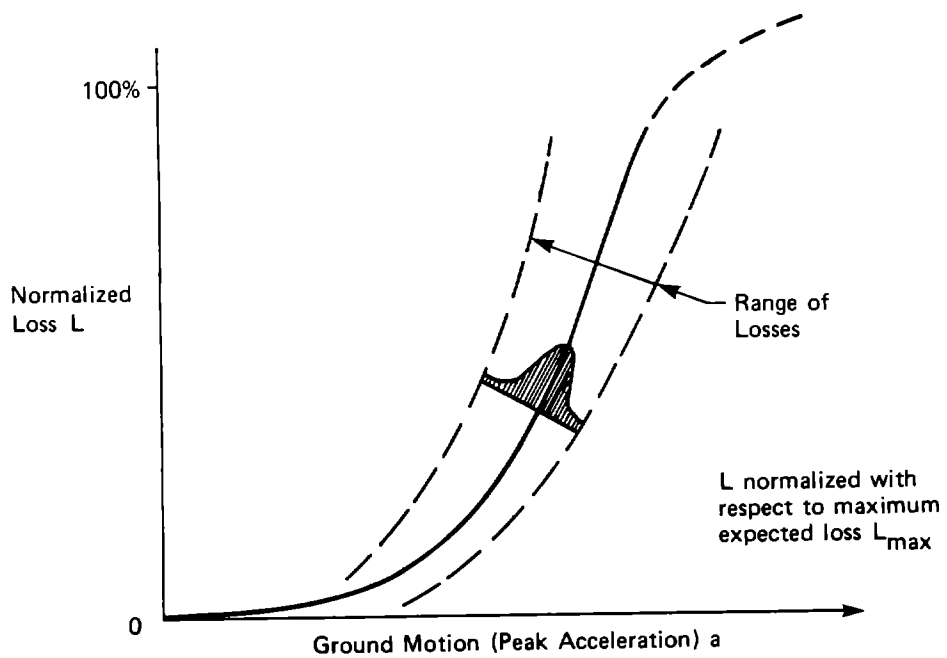


Fig. 2. Relationship Between Loss and Ground Motion

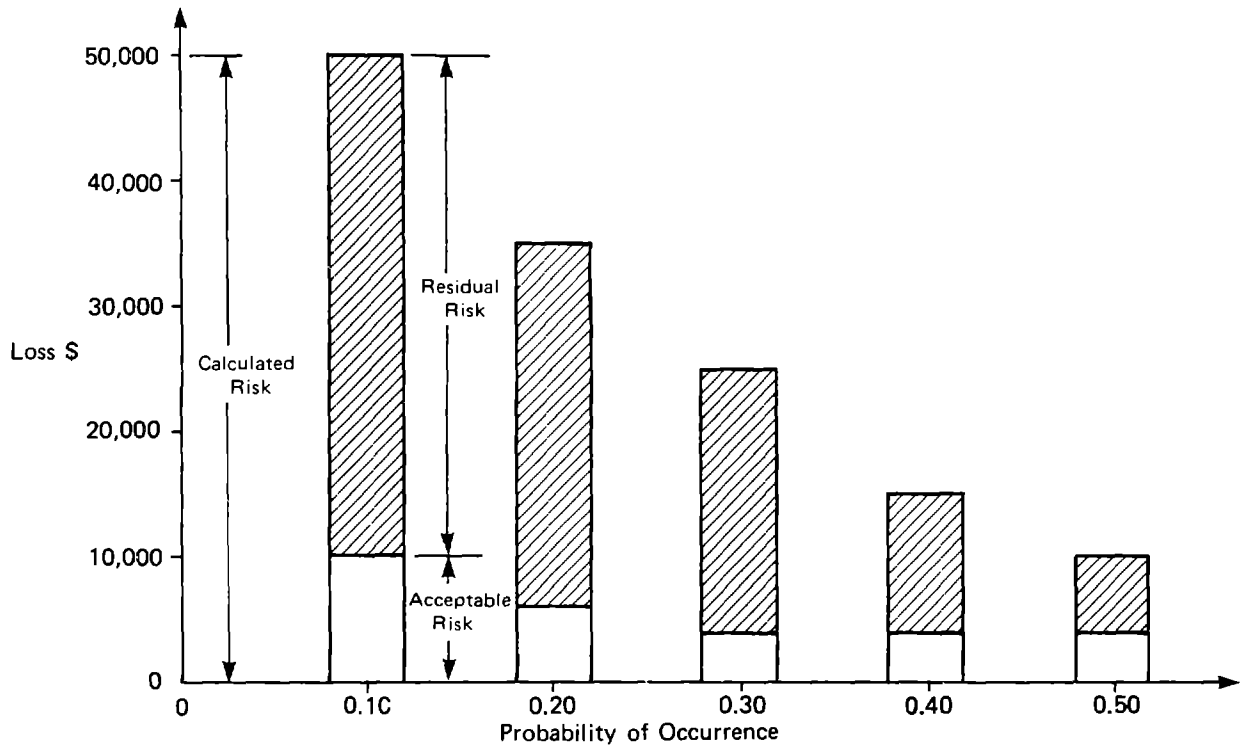


Fig. 3. Probability Distribution of Risks

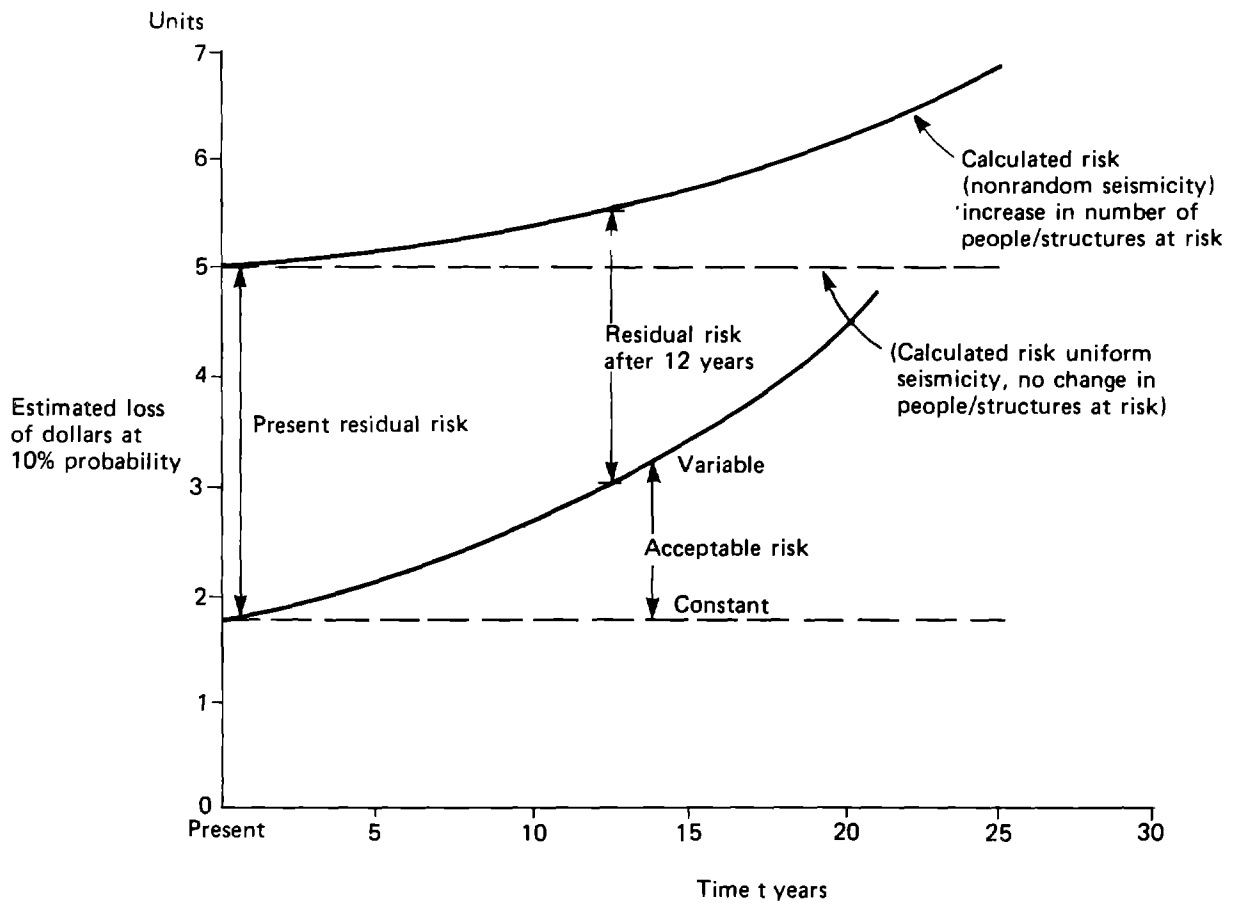


Fig. 4. Variation of Residual Risk with Time

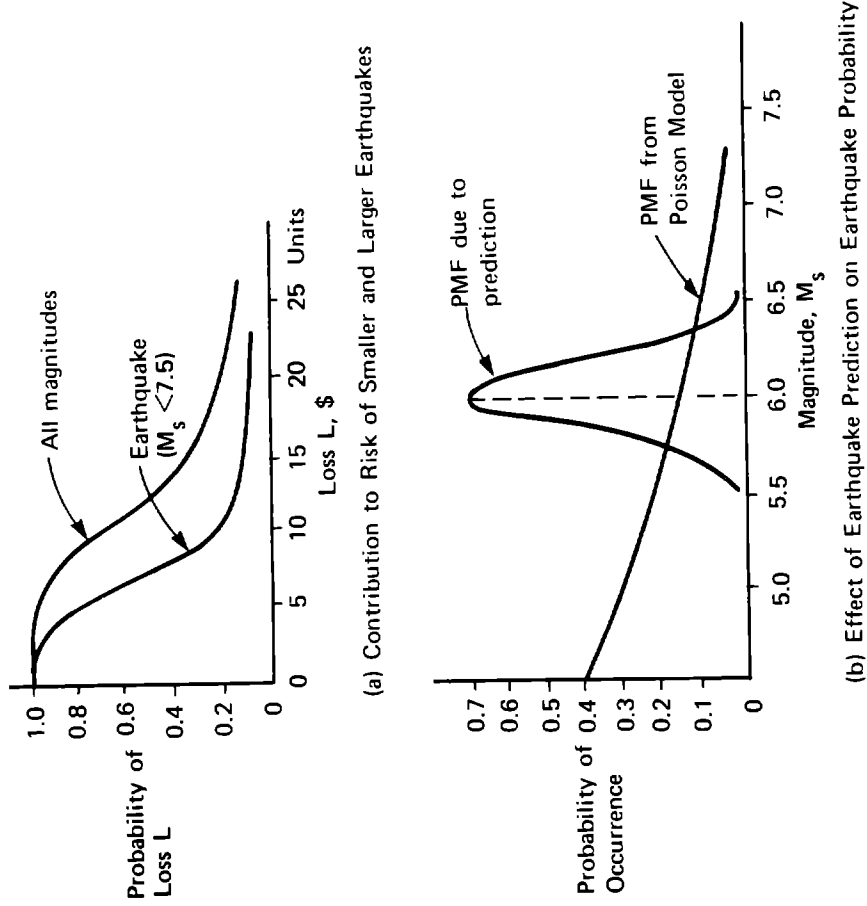


Fig. 6. Components of Risk and Effect of Earthquake Prediction on Magnitude Distribution

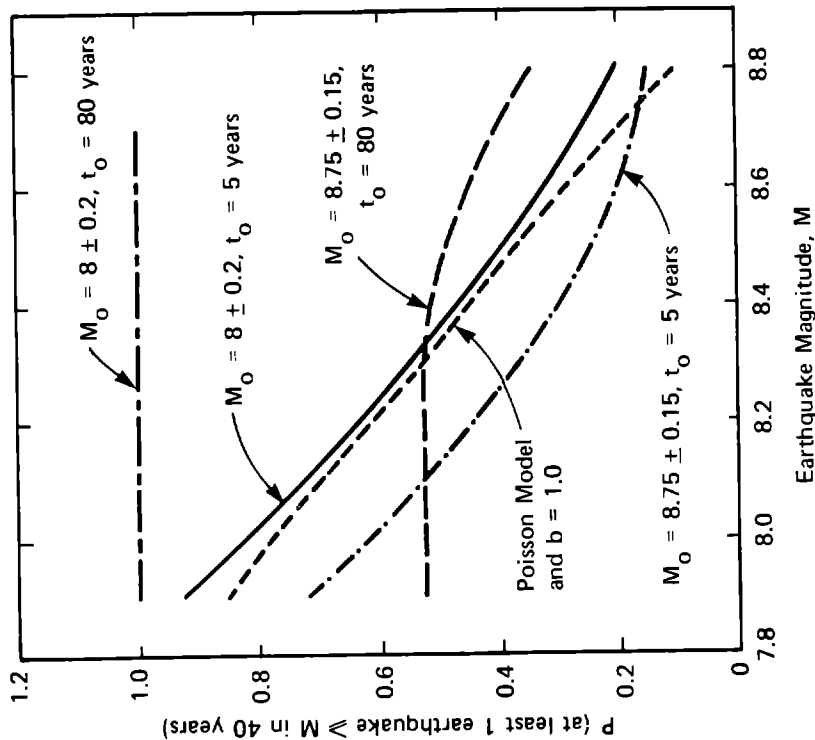


Fig. 5. Example of Variation in Earthquake Probability with Elapsed Time Since the Last Great Earthquake

LAND USE TECHNIQUE FOR MICROZONATION

by

S. Murakami^I and K. Midorikawa^{II}

ABSTRACT

Japanese cities have special character that is the high closely built-up area constructed by wooden houses. Its character has brought us many serious disasters in which many people has been killed by simultaneous fires to lose their escape ways. The collapse rate of wooden houses is related to the rate of fire occurrence, so construction of city to profit the ground condition is most important.

In this paper we will report the symple techniques of Microzonation which is usable by administration, and the land use techniques by which we controll the land use factors, ex. density of population, utility of buildings, and disposition of the urban facilities, etc. Its purposes are three, that are to develop the techniques to research soil conditions, to analyze the seismic intensity of the ground, and to make the land use planning.

INTRODUCTION

Many cities in Japan have suffered from earthquakes. In recent years RC-buildings, collapsed in Niigata (1964) and Tokachi (1968). But, Japanese cities consist of almost wooden houses and most terrible disaster is the fires which occurred in many places at the same time. We experienced such fires at Nobi (1891), Kwanto (1923), Fukui (1948), but in recent years we have no experience because we have not great earthquake by which many wooden houses will collapse. When we have such many collapse of wooden houses, there must be many fires to occur. Because the rate of fire occurrence grows accompanied with the collapse rate of wooden houses. Therefore we must controll the land use on which many buildings are expected to collapse, in the aspect of Microzonation.

For it, we have prepared the committee^{III}, which have been held in The Architectural Institute of Japan, constituted of the specialists of seismology, soil-engineering, geology, architecture and urban planning. One of the purposes of this committee is to develop the symple techniques to apply Microzonation to urban planning. Authors have participated this committee, and take a share in the subject of urban planning. So we introduce the consequence of its committee, and the land use techniques which in Japan are characterized by the fires in the earthquake.

-
- I. Director of Laboratory of Urban Safety Planning
 - II. Planner of Laboratory of Urban Safety Planning
 - III. Members of the committee are; Kiyoshi Kanai (Chairman), Eika Takayama (Adviser), Sachio Otani, Sohei Kaizuka, Shunji Kawana, Hiroyoshi Kobayashi, Etsuzo Shima, Kande Sugiyama, Masayoshi Takasaki, Kohei Doi, Suminao Murakami, Yoshiaki Yoshimi.

PURPUSES

Our purposes are that —

1. To develop techniques to research soil condition

To apply the Microzonation to urban planning, there must be the informations about comparatively wide area which is enough to cover the land intended to use. But it is difficult to gain the information around the whole area, because boring data, which are only means to know the soil conditions of profound stratifications, are not enough obtained when the land have not been used yet.

2. To develop techniques to analyze seismic intensity of the ground intended to use.

Several techniques of seismic intensity have been developed in recent years. But even if each techniques, which is intended to construct buildings safety to expected seismic intensity, will be high developed, when seismic intensity will be over the expected standard, the buildings would collapse. Those techniques are so complex and expensive to apply that many buildings which are out of those techniques will remain dangerous. So, we must control the buildings to fit the ground to use the land reasonably.

3. To develop techniques of urban planning to make the land use planning

Microzonation have no place in regal system of land use planning of Japan. And, when ideal of Microzonation will be promoted to influence urban planning, all land use system, ex. "Built-up promotion area" which is authorized by City Planning Act (1965) or land use zoning, or Road-planning, or other action planning, will have to be changed. To exercise the Microzonation to fit current regal system is defficult, but students who study the structure of buildings, though only study to build safe to any ground condition, should insist the danger of the buildings and promote the Microzonation.

AREA OF CASE STUDY

In that purposes, we chose the area as case study. This area, which center is Koshigaya-City, is in 20~30 Km from Tokyo, and had not growed yet to built-up area than other simulous areas. But, it became easy to reach to Tokyo in short time by railway, and cheaper land prices induced the intensive growness of population. Only this area in metropolitan region have held the 40% rate of population growness in 5 years from 1970 to 1975. Industries have been increasing on this area, as near to Koto District which is the great assembled industry area of Tokyo. This area has been constructed as the closely mixed land use with the ready-built houses on the reclaimed land from the paddy fields.

This area was in past the streams of Tonegawa Riv. and Arakawa Riv., therefore there were many swamps in the beginning of Tokugawa period. The swamps have been reclamated gradually to be called "Shinden" which meaning is "new paddy field." And geologically, soft ground as peat soil were formed, which lack safety by nature, i.e. unequally settling of foundation, futhermore, weak to flood.

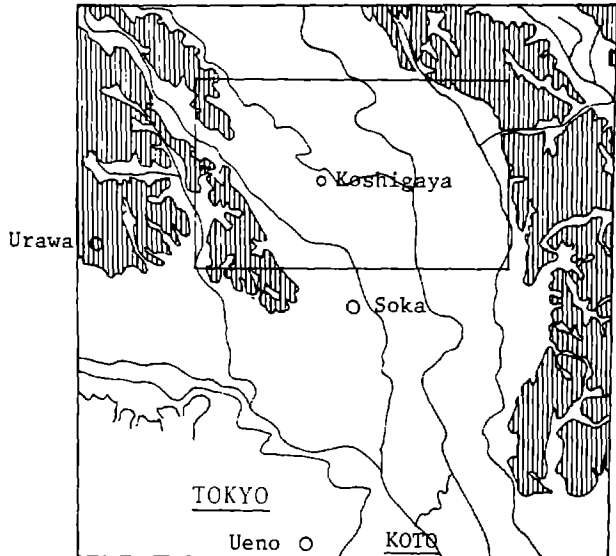


Fig. 1. Information Map of the area Fig. 2. Disposition of the swamps in Past

METHOD OF SOIL CONDITION RESEARCH

About reserching soil condition, we obtain the next conclusion.

1. By existing data, suppose the soil structure of chosed points, which distance of each other is 1 Km or 500 m.

Though there are dispersion of soil structure, the distance seems to be enough to use it for urban planning. In the case of complex configuration of ground, it is necessary to do in 500 m and to be amended by geological informations.

2. Suppose the soil dynamic factors (Velocity of P and S wave and density) of each layer.

In recent years we obtain several informations from measurement of S-wave, and other factors. This value are thought as similar at the near area, so we select same points to measure the soil dynamic factors of each layer, which we assume the representation of the layer of the near point.

3. Amend the supposed soil structure by observation of the Microtremors at each point.

The consequence which are obtained from upper method are supported by

the near boring data, therefore the points do not necessarily represent that one. However, it is difficult to obtain the boring data, from this point of view microtremors is easy because it is able to get from ground surface. But amplification of microtremor is not dependable, so we amend with its period which concerns the velocity and thickness of layers.

METHOD OF SEISMIC INTENSITY ANALYSIS

1. Obtain the expectation of bed-rock velocity spectrum from past earthquake records.

Expectation of bed-rock velocity spectrum in Japan was obtained by K. Kanai (1).

2. Obtain acceleration-frequency curve from Response Spectrum gained from soil structure.

We have the theory by which we gained the Response Spectrum curve from repetitional reflection theory.

3. By the distribution of natural period and strength of wooden houses and reinforced concrete building, at each story and structure, decide the seismic intensity of the ground.

The distribution of natural period of wooden houses are gained by K. Kanai. But the strength of existing houses have not been gained yet. So we try to gain statistically the ultimate strength by reserching the rate of collapse wooden houses at Kwanto earthquake. The strength which is seeked by this method is the one of existing in that time. So, we change the value relating to the period subduplicated. By the strength and natural period, we obtain the collapse rate of houses which are over the strength, and this rate is regarded as seismic intensity. (Fig. 3)

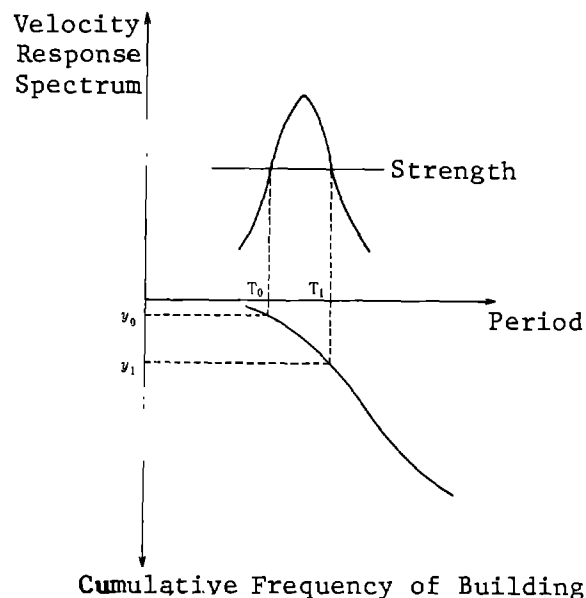


Fig. 3 Method of seismic intensity analysis

METHOD OF URBAN PIANNING

1. Regard the ground condition when to authorize "Built-up promotion area", in which development should be promoted. In City Planning Act, two areas are provided, that are "Built-up promotion area" and "Built-up controll area". The former is the area which should be promoted to built up from the point of view of investment of governmental facilities, road, water supply, etc., the later is not so. When designating this area, in existing legal system, ground condition is not considered. We have maintained that soil condition research should be obligated in "City Planning Research" and ground condition also should be considered in delineation of these area.

2. Regard the ground condition when to authorize "zoning"

The basic zoning in Janenese city planning regal system include that; Residential Area (Low-density Exclusive Residential, Exclusive Residential, and Mixed Residential), Commercial Area (Neiborhood Commercial and Commercial), Industrial Area (Light Industry, Industry, and Exclusive Industry). These zoning should be of course, applied to adequate ground condition. For example in Commercial Area, relationaly high and large buildings are relatively apt to be constructed and therefore if ground condition are not adequate to high building, its area should not be applied. But, other special zoning areas are more important for Microzonation, ex. Fire Area, Hight Area, High Utilization Area, and Green Conservation Area. In Fire Area, it is obligated to construct the fire resistive buildings, ex, RC buildings. So, if the ground condition is not profit to the wooden houses, we apply this zoning area to construct the non-wooden houses. In Hight Area, building height is limited at the lower lebel and/ or the upper lebel, by which we can the building hight at adquate lebel to the ground condition, although the purpose of this zoning area is to maintain the environment profitable. At more limited sense, in High Utilization Area, which purpose is to promote re-development with proper scale buildings, the minimum of the several factors of buildings can be limited. This Area is efficient to renew built-up area which are not adequate to ground condition.

3. In built-up area, positive investment should be taken to the area on the ground in which the second disasters will be expected.

The consequence of the research of Microzonation is immediately the control of the building characters, building structure, height or stores, or strength. But, it is special character of Japanese cities that almost buildings are the wooden houses, moreover which form the high closely built-up area. So, it is the most terrible disaster that many fires occur at same time and many people lost their way to escape in the great city where such flammable materials are spread over the 20 ~ 30 Km at radius. So the many people would be expected to be killed in the next great earthquake which is prospected to attack in recent years. We must make it the most important policy to make the cities safety to the lebel of 0.1% rate of the dead. For that purpose, we controll the utility factors in relation to the ground condition, ex. population rate, building coverage rate, land use, and the disposition of urban safety facilities such as the place to refuge, escape route, and the line of fire resistive buildings, open space and others, which should be promoted by positive investment. We try

to make method to controll these urban factors in the next paragraph.

LAND USE TECHNIQUES TO PROTECT THE SECOND DISASTER

In this paragraph, we try to seek the death rate in function of the ground condition in the parameters of urban factors.

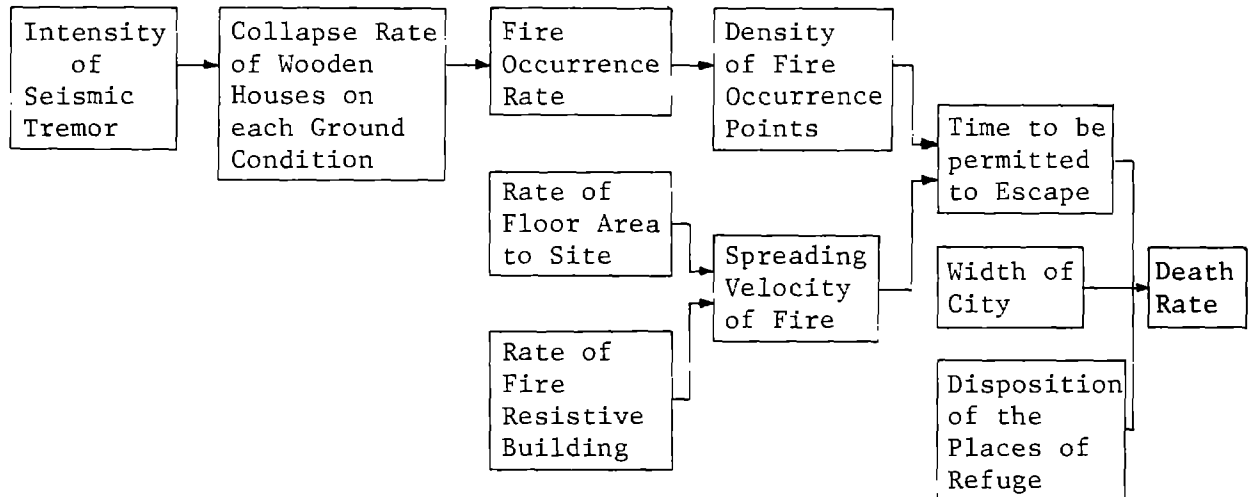


Fig. 4 Flow Chart of Procedures

This procedures are consist of 9 steps.

1. Intensity of seismic tremor is given by statistic data at the objective city.
2. From the given intensity is gained the collapse rate of wooden houses on each ground condition, by the former written method.
3. From the collapse rate and the seismic intensity, is gained the occurrence rate, in deferentiation of the fires from collapse houses and the other.
4. Density of fire occurrence points are obtained by the density of population.
5. The spreading velocity of fire is given by statistic data in relation to the rate of floor area to site in gross.
6. The decrease rate of the former velocity which come from the rate of the fire resistive buildings are obtained by the simulation model.
7. The average time to be permitted to escape to the safe area, such as the place of refuge or the suburbs, are obtained at parameter from the density of fire occurrence points and the spreading velocity of fire.
8. By adequate assumption about the behavior of escaper, death rate of a given area is obtained at parameter of the time to escape, the greatness

of city width and the disposition of the place of refuge.

9. By seeking the factors which mainly contribute the death rate, we efficiently choose the policy to make the city secure to earthquake, especially we can have techniques to use the land to profit the ground condition.

Now, we will describe the upper mentioned methods.

1. From the literature (1), is given the objective city's seismic intensity.
2. By Fig. 5 the collapse rate of wooden houses is given at the depth of each layer.

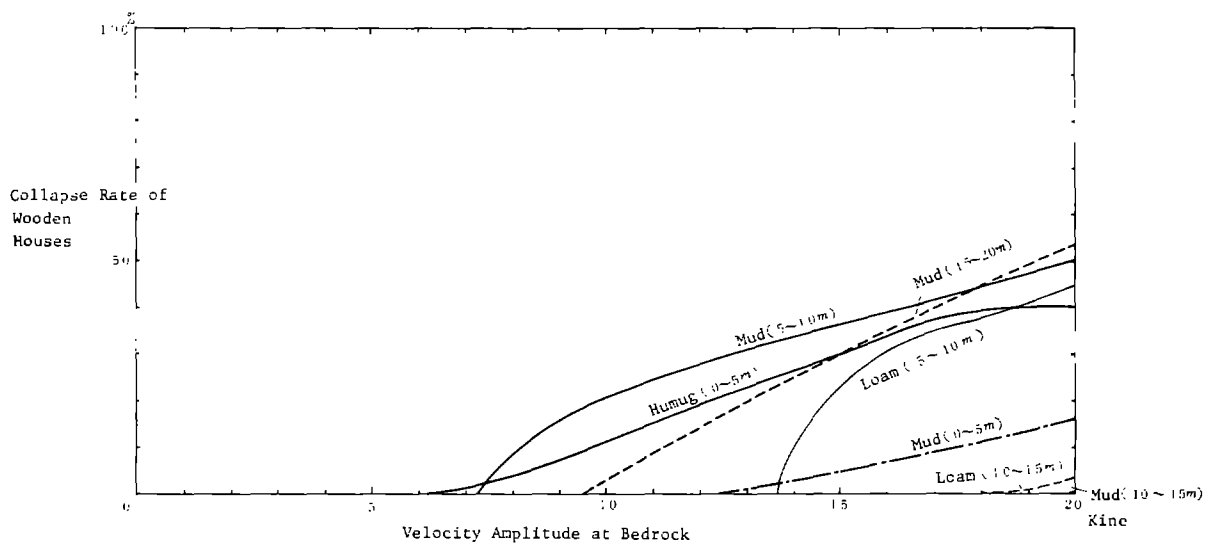


Fig. 5 Average Rate of Collapse Wooden Houses

3. From Fig. 6, the rate of fire occurrence is given in relation of the collapse rate of wooden houses.^I

I Step of 3, 5, 6 are the results of study by Akihiko Tsuji, a student of Laboratory of Urban Safety Planning.

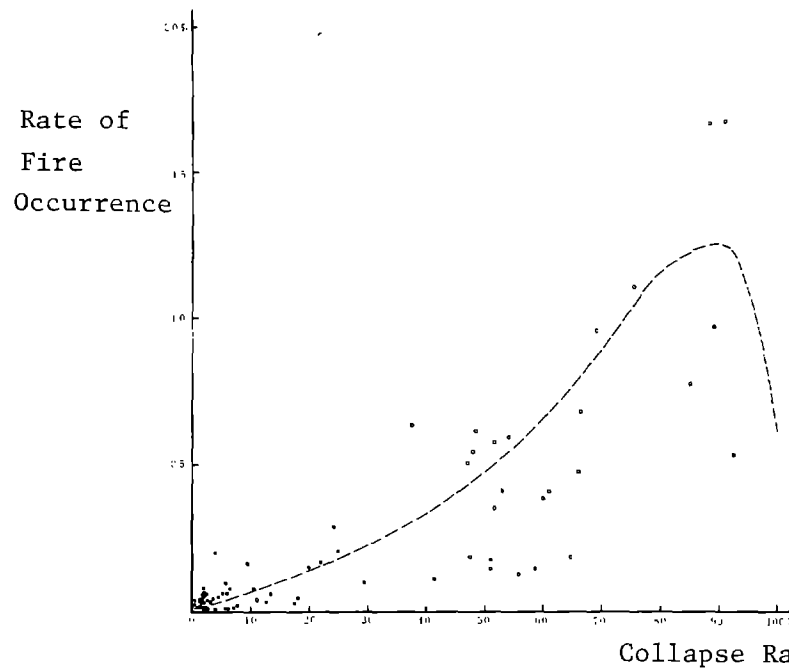


Fig. 6 Rate of Fire Occurrence

This rate is described as the following.

$$\gamma = \alpha x + \beta (1-x)$$

- x ; the rate of collapse wooden houses
- α ; the rate of fire occurrence from collapse houses
- β ; the rate of fire occurrence from non collapse houses
- γ ; the rate of fire occurrence (number/household)

α is expected constant for the seismic intensity, but β is the variable to it. So, we have gained the most adequate formula, as that —.

$$\gamma = 6.05 \times 10^{-5x} + 8.31 \times 10^{-7} e^{75x} (1-x)$$

4. The density of fire occurrence is given as that —

$$\rho = \gamma \times p/n$$

- ρ ; the density of fire occurrence
- p ; the density of population
- n ; average number of men in one household.

5. From Fig. 7, the spreading velocity of fire is gained in the relation of the rate of floor area to site.

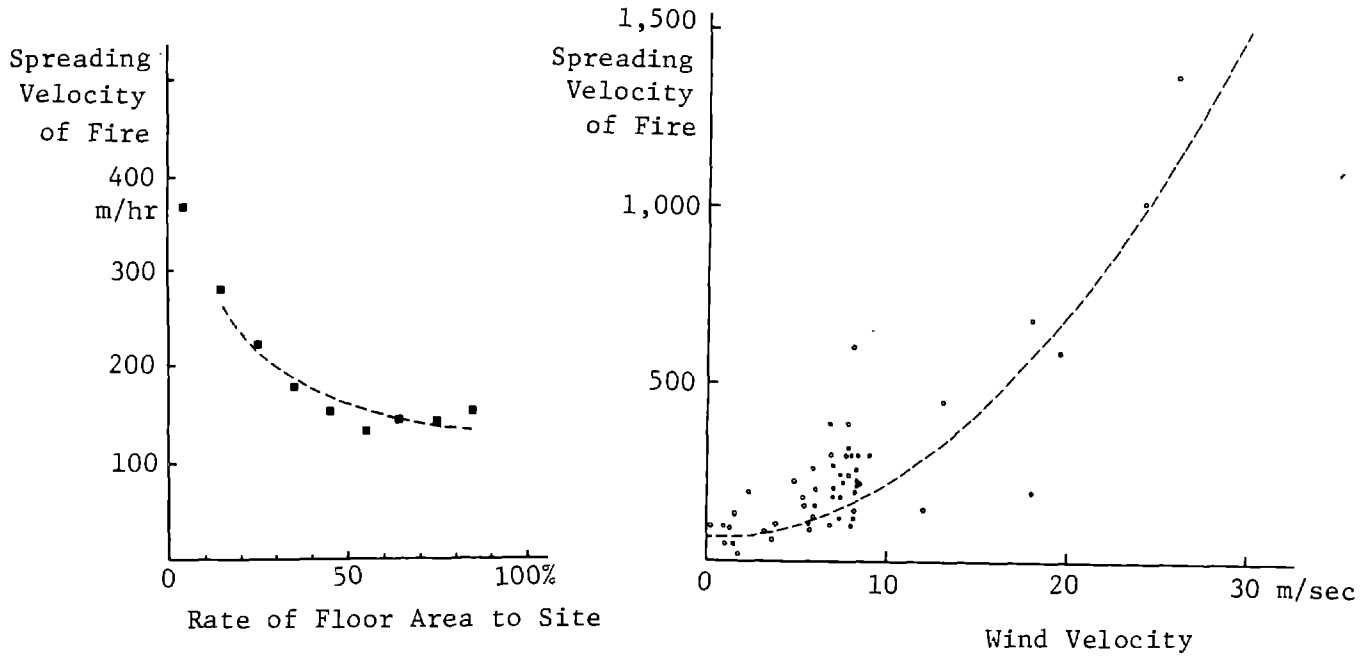


Fig. 7 Spreading Velocity of Fire

This formula, obtained statistically, is that

$$V = \frac{4.55\delta + 4.50v^2}{228\delta + 23.7(100-\delta) + 4.50v}$$

V ; Spreading Velocity of Fire (m/sec.)

δ ; Rate of Floor Area to Site (%)

v ; Wind Velocity (m/sec.)

6. The decrease rate of the spreading velocity of fire by mixing with fire registive buildings is given in Fig. 8.

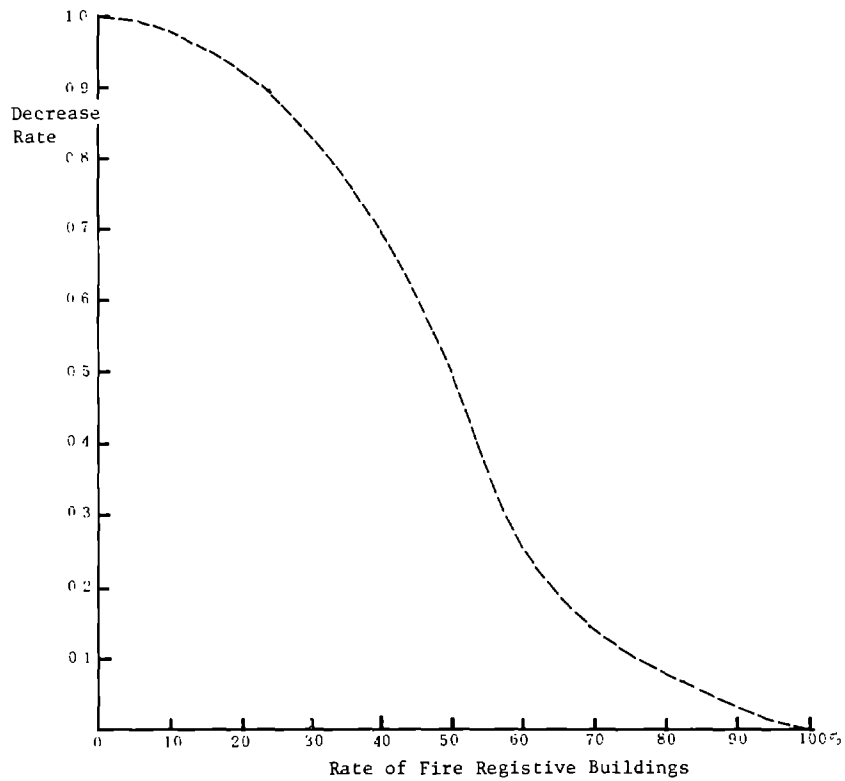


Fig. 8 Decrease Rate of Spreading Velocity of Fire

This curve is obtained by simulation analysis in random delivration of unfireable units.

7. The average time to be permitted to escape to the secure area is given in that formula.

$$t = \frac{1}{\sqrt{\rho} V}$$

t ; Time to be Permitted to Escape (hr.)
 ρ ; Density of Fire Occurrence Points (number/km²)
 V ; Spreading Velocity of Fire (km/hr.)

7. The death rate of the city is given in Fig. 9.

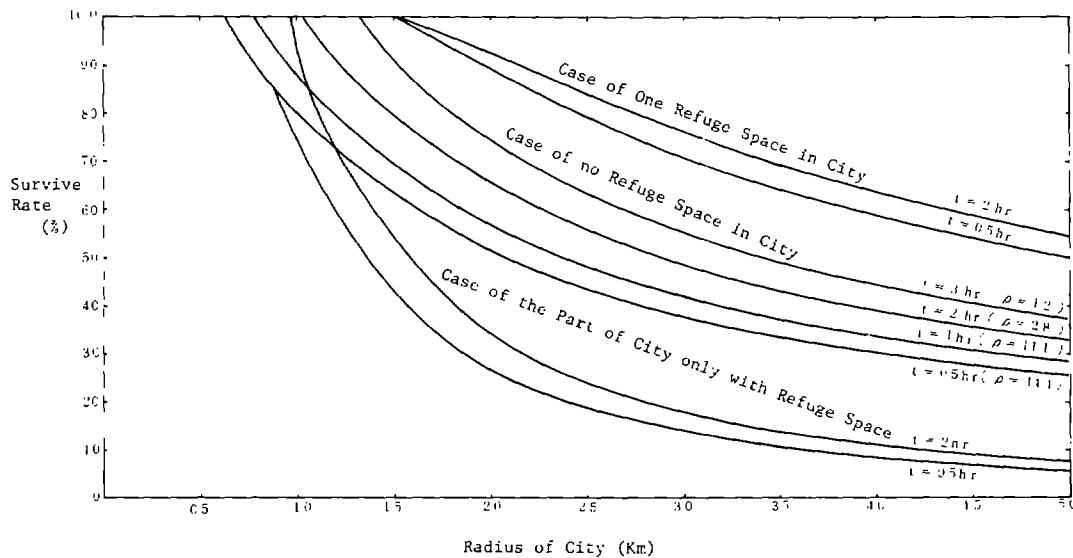

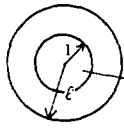
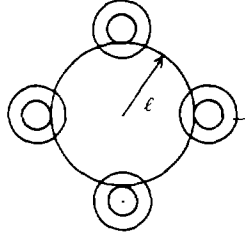


Fig. 9 Death Rate (Survive Rate) of City

Element Fomula : $\phi_L = 1 - (1 - \frac{0.5}{\ell})^2 \left(1 - \frac{1}{100} \left(\frac{0.114}{\sqrt{\rho}} + 0.576 \right) e^{4.53 \left\{ (\ell - 0.5) \sqrt{\rho} \right\}^{-0.222}} \right)$ 

$\phi_L^1 = 1 - \left(1 - \frac{1}{\pi} \sin^{-1} \frac{2}{\ell - 0.5} \right) \left(\frac{(\ell - 0.5)^2 - 1}{\ell^2} \right) (1 - \phi_L)$ 

$\phi_L^0 = \frac{4 \phi_L}{\pi} \sin^{-1} \frac{1}{\ell + 0.5}$ 

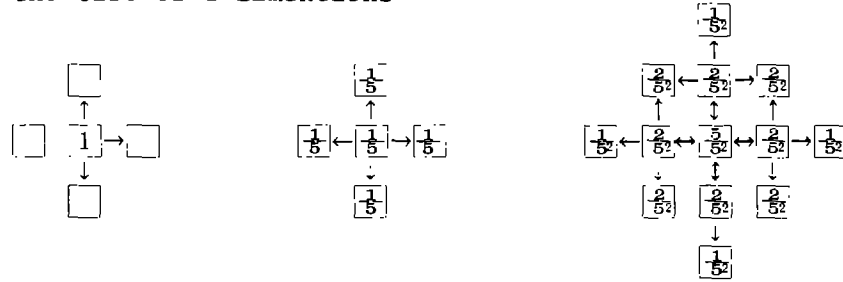
Area of Safety Around the Space of Refuge

Area of Safety around the Space of Refuge

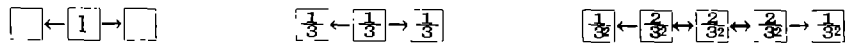
This figure is obtained by the assumption, that is —

- (1) The escaper may move to the direction which he may think the distance of each fire point as the nearest from his view point. Therefore, if the fire points are deposited at random, the escape direction is also at random.
- (2) The fire points scattered equally. Here, they have places on the grid point.
- (3) The behavior of escaper is assumed to next figure.

the Case of 2 dimentions



the Case of 1 dimation



(4) The unit of moving is the distance of the fire point.

(5) In the time to be permitted to escape, people who have not reached the safety area yet are assumed to be dead.

CONCLUSION

From upper method, we try to develop the controll techniques to use the land to profit the ground condition. We can controll the urban factors, density, land use and deposition, etc. in relation to ground condition.

In this method the non-wooden houses are not considered. This problem, ex. that RC building will be collapse easily, is important, for we have just experienced the earthquake, Miyagioki (1979.6), there occurred that many city functions, electricity, gass, water-supply, were paralysed and yet, gass has now been so. It is proved that even if the structure of building do not collapse, there must be sereous effects. And in this earthquake the collapse of RC buildings seem to be related to ground condition, especially to the depth of the layer, although detailed research has not done yet. From this point of view, such researches is hoped to do.

(1) Kanai, Kiyoshi, Engineering Seismology, 1969, Tokyo, p42.

APPLICATION OF SEISMIC RISK PROCEDURES TO
PROBLEMS IN MICROZONATION

by

J.G. Anderson* and M.D. Trifunac*

ABSTRACT

This study considers the seismic risk for the Los Angeles, California, metropolitan region. For sites there, the spectral amplitudes of shaking with a selected probability of exceedance are a function of location and geologic site conditions (but not including soil types or water table elevations, for example). However, the maximum difference, for the sites selected, among these amplitudes is smaller than the uncertainty involved in the estimate of shaking for a single site. It is difficult to justify contouring the expected amplitudes of ground motion with a contour interval which is significantly smaller than the uncertainty in ground motion for a single site. Thus, at most, only a small number of risk zones (e.g., 2 or 3) may be justified for the Los Angeles metropolitan area.

These results suggest that for metropolitan regions in similar locations it may be better to adopt a uniform level for estimated future amplitude of strong motion for the entire area or for large sub-areas. When and if methods for reducing the uncertainty in estimates of future amplitudes of strong shaking become available, the associated smaller uncertainties in the final result may allow a more detailed zoning of the Los Angeles region.

INTRODUCTION

This paper discusses how accurately seismic risk analysis can estimate probable amplitudes of future ground motion. The result is relevant to all aspects of seismic risk analysis, including microzonation.

The problem is studied by evaluating the accuracy for calculations which are based on one particular set of correlation functions, and in one particular region. One might expect that the results also apply to some other cases as well.

METHOD AND PRELIMINARY RESULTS

The study is for a portion of southern California. Figure 1 shows the major faults in southern California, after Jennings (1975), and a grid of points in the vicinity of Los Angeles. The seismic risk was found at each of the 210 points in this grid using the procedure described by Anderson and Trifunac (1977, 1978a). Their procedure is similar to that of Cornell (1968) to find the risk at each site. It is re-applied at several frequencies for each site as also suggested by McGuire (1974), but for brevity, the results here are discussed at only two frequency bands.

* Department of Civil Engineering, University of Southern California, Los Angeles, CA 90007

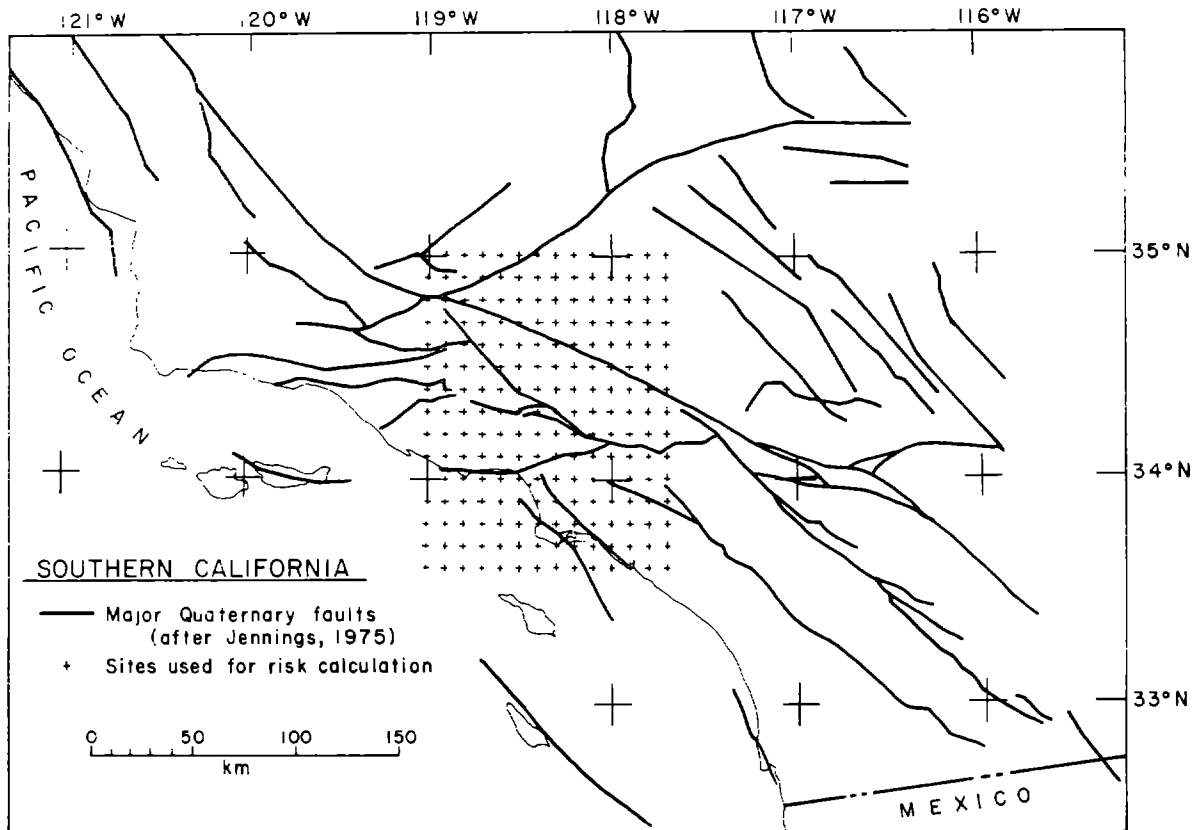


Figure 1

Let us regard the seismic risk analysis as a black box computer program. There are two sets of inputs for this program. The output is the risk at a site.

The first set of inputs is a description of the seismicity in the region. For that input the model of Anderson (1978) was used. His model finds a slip rate for most of the faults in Figure 1 which is consistent with the geology in the region, and then finds a rate of occurrence of earthquakes for these faults which is consistent with the slip rate at each fault. The resulting earthquake occurrence rates are consistent with historical seismicity.

The second input is a description of the attenuation of seismic waves as a function of distance from the seismic source. We use either the model by Trifunac and Anderson (1978) or by Trifunac and Lee (1979) for the attenuation of the amplitude of the pseudo-relative velocity spectrum (PSV) at period T . The first (Trifunac and Anderson, 1978) is:

$$\log_{10} \text{PSV}(T) \Big|_{P_{\ell}} = \begin{cases} M + \log_{10} A_o(R) - a(T)p_{\ell} - b(T)M_{\min} - c(T) - d(T)s \\ - e(T)v - f(T)M_{\min}^2 - g(T)R & M \leq M_{\min} \\ M + \log_{10} A_o(R) - a(T)p_{\ell} - b(T)M - c(T) - d(T)s - e(T)v \\ - f(T)M^2 - g(T)R & M_{\min} < M \leq M_{\max} \end{cases}$$

$$\log_{10} \text{PSV}(T) \Big|_{p_\lambda} = \begin{cases} M_{\max} + \log_{10} A_o(R) - a(T)p_\lambda - b(T)M_{\max} - c(T) - d(T)s \\ - e(T)v - f(T)M_{\max}^2 - g(T)R \end{cases} \quad M_{\max} \leq M \quad (1)$$

In equation (1), M is the local magnitude of the earthquake, $\log_{10} A_o(R)$ is a description of the attenuation with distance (R) used by Richter (1958) to define the local magnitude, and v is a site condition variable set to 0 for horizontal motion and 1 for vertical motion. The other site condition variable s is set to zero for alluvial sites, 2 for sites on hard igneous rocks, and 1 for sites which are on consolidated sediments or are uncertain because of confusing geologic relationships. The values of M_{\max} and M_{\min} are $1-b(T)/2f(T)$ and $-b(T)/2f(T)$, respectively; these cause the spectral amplitudes to grow less rapidly as magnitude increases, and to stop increasing for $M > M_{\max}$. The terms $a(T)$, $b(T)$, ..., $g(T)$ are empirical constants found in the regression analysis. Finally, p_λ is a linear approximation, for $0.1 < p_\lambda < 0.9$, to the probability (p_a , say) that the spectral amplitude $\text{PSV}(T) \Big|_{p_\lambda}$ will not be exceeded. Trifunac and Anderson (1978) have suggested a way to recover p_a from p_λ .

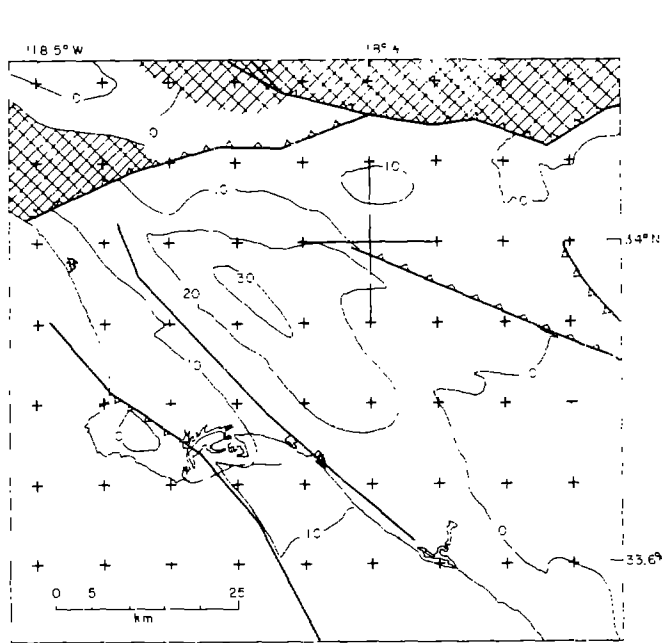
Trifunac and Lee (1979) have developed a more refined correlation function, which for $M_{\min} < M < M_{\max}$ becomes

$$\log_{10} \text{PSV}(T) = M + \log_{10} A_o(R) - b(T)M - c(T) - d(T)h - e(T)v - f(T)M^2 - g(T)R \quad (2)$$

The term $a(T)p_\lambda$ is dropped from this correlation, and the result is the mean value of $\text{PSV}(T)$. Trifunac and Lee found coefficients which allow a direct determination of p_a . Also, the term s in equation (1) has been replaced by h in equation (2), where h is the depth to the geological basement rock. For $M < M_{\min}$ and $M > M_{\max}$, Trifunac and Lee (1979) recommend equations analogous to equation (1). This study uses the coefficients $a(T)$, ..., $g(T)$ appropriate for PSV spectra with damping at 5% critical.

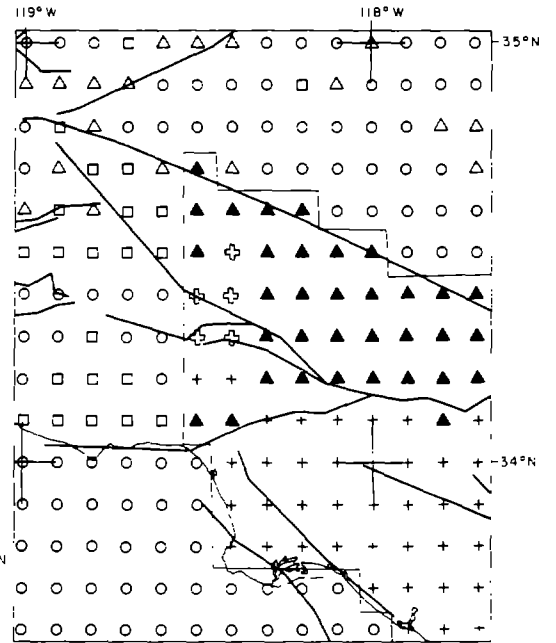
Equations (1) and (2) have complementary uses, since in some cases, h can be determined, while in others, only the surficial geology, s , is known. Figures 2 and 3 show where, for the sites on Figure 1, the depth to basement h could be found, and where s had to be used. In the south-east corner of the study region (Figure 2), the depth to basement is known from results of Yerkes, et. al. (1965), and therefore, h can be assigned in this region. (The contour interval in Figure 2 is 10,000 feet, but the original figure in Yerkes, et. al. has a 1000 ft contour interval.) Outside of this region, s was picked using the 1:250,000 scale geologic map of California sheets (Rogers, 1967; Jennings and Strand, 1969). A site condition of $s=2$ is equivalent to $h=0$. Thus, for the region north of Figure 2, but south of the San Andreas fault, the correlation (2) could still be applied. Figure 3 shows a summary of all the site conditions used in the risk analysis.

Figures 4 and 5 are risk maps based on the above correlations and seismicity model. They represent one approximation to the actual risk, and should not be accepted uncritically. Figure 4 shows contours of equal value of $SA(T) \approx 2\pi/T \text{PSV}(T)$ (Anderson and Trifunac, 1978b) in units



- Major Quaternary fault (Jenning's, 1975)
- ▲▲▲▲▲ Reverse fault teeth on up thrown side
- Structure contour-basement (Yerkes et al., 1965)
- + Sites used in risk calculations
- XXXXXX Basement

Figure 2



Site Classification

- | | | | |
|---|-------|---|------------------------------------|
| ○ | S = 0 | ▲ | h = 0 (geology) |
| □ | S = 1 | + | h > 0 (from Yerkes et al, 1965) |
| △ | S = 2 | ⊕ | used h = 0 site on secondary rocks |

Figure 3

of fraction of the acceleration of gravity at a period $T = 0.04$ sec. At this high frequency, it approximates peak acceleration. The contoured

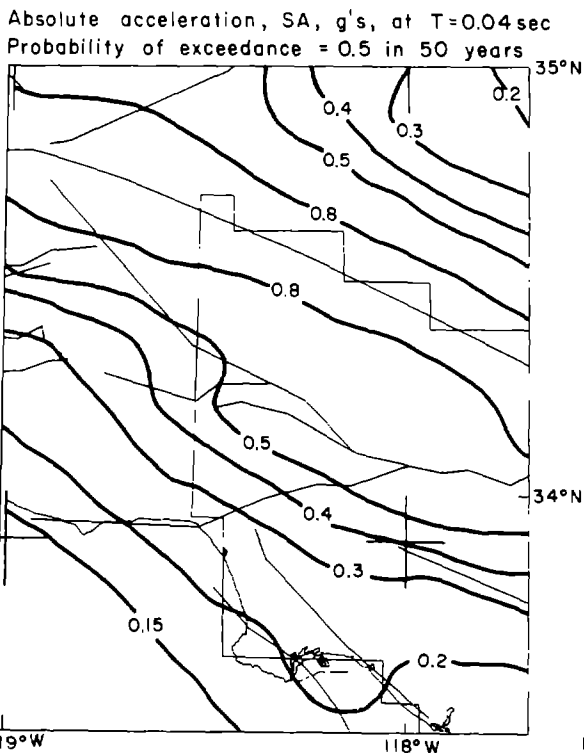


Figure 4

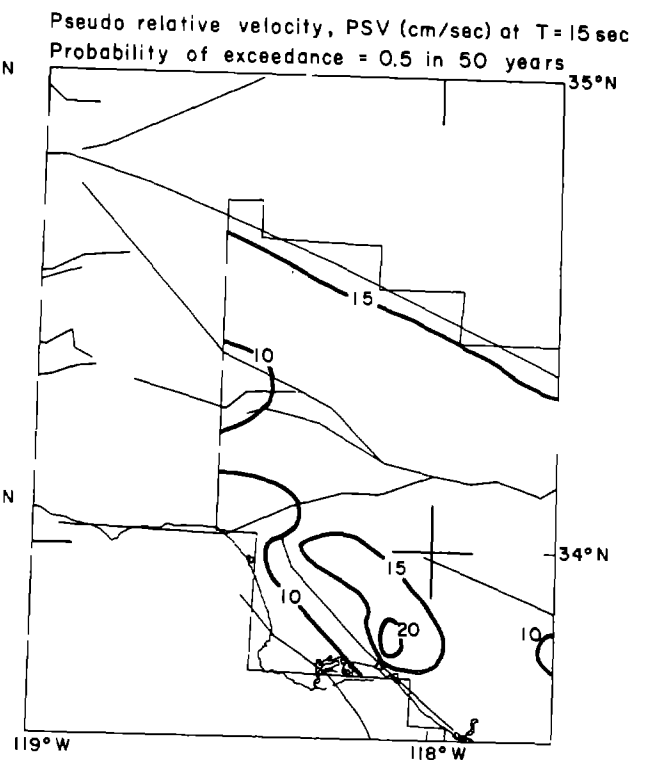


Figure 5

values have a probability of 0.5 of being exceeded once in a time interval of 50 years. There is no apparent discontinuity between the regions where equations (1) or (2) are used for scaling. Extreme values of SA (0.04 sec) range from about 1.2g for sites near the junction of the Garlock and the San Andreas faults, to about 0.1g in the extreme southwest corner of the map.

Figure 5 shows contours of $PSV(T)$ at $T = 15$ sec. These were only found for sites which used correlation (2). The contoured values have probability $p = 0.5$ of being exceeded once in 50 years. While Figure 4 suggests that at high frequencies the predominant influence to the risk is nearness to the highly active faults, in Figure 5 the depth to geologic basement is a more important factor. This could have been predicted directly from the correlations, as the quantity $d(T)$ in equation (2) does not differ significantly from zero at high frequencies, but it does at long periods.

SIGNIFICANCE OF THE RESULTS

The locations of contours shown in Figures 4 and 5 are determined to within about 2 to 3 kilometers. With a smaller grid spacing, one could draw more contours with more precisely determined locations. But such numerical precision would overlook significant uncertainties which are involved in the input to the computer program. This portion of the paper addresses these uncertainties, and examines how they may affect the results.

For each site the seismic risk can be described by a probability distribution function or its derivative density function of a desired strong motion functional. Examples of these density functions are shown in Figures 6 and 7. Figures 6 and 7 give the results for the probability density of the largest value of $\log_{10}(PSV)$ observed in one year at three sites. Figure 6 is for an oscillator with $T = 0.04$ sec, Figure 7 is for an oscillator with $T = 15$ sec.

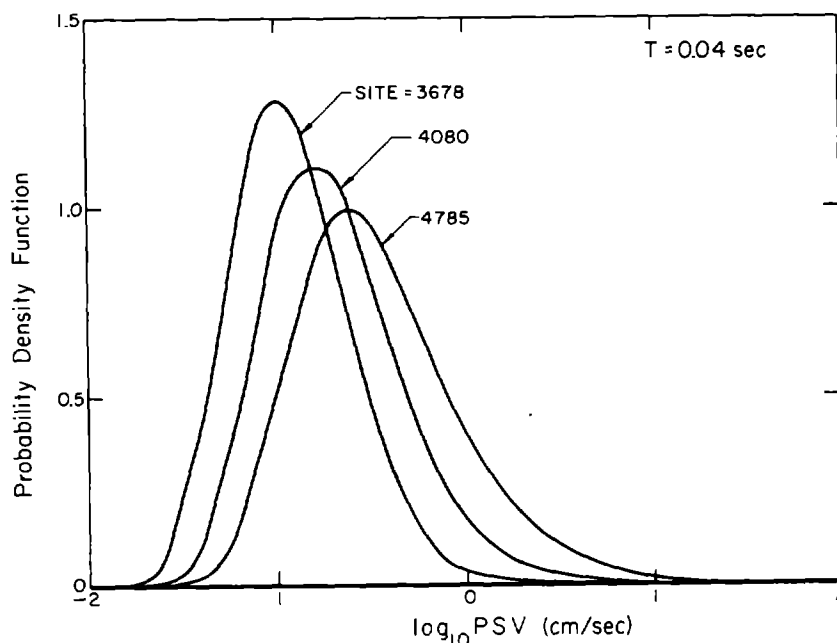


Figure 6

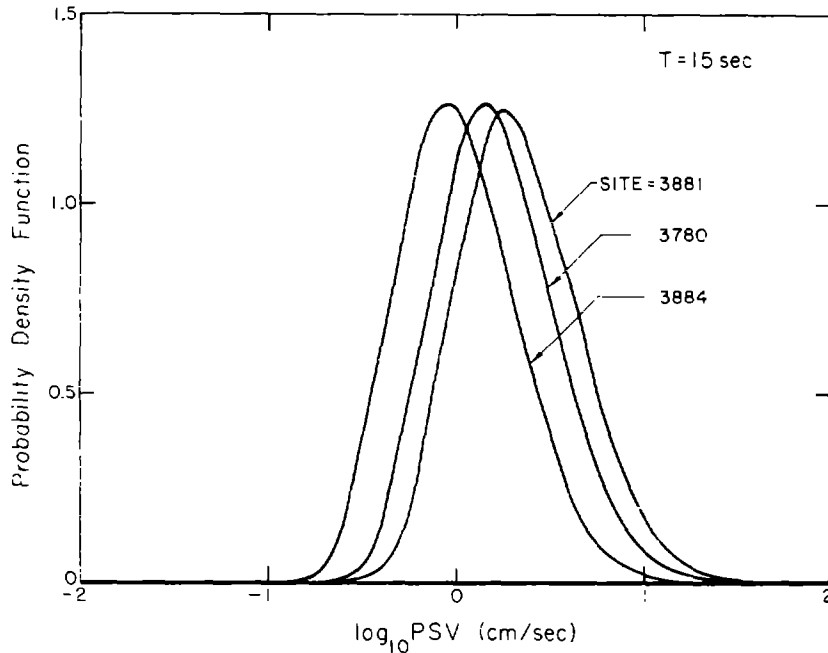


Figure 7

The distributions in Figure 6 are for three sites for which equation (2) was used in the risk calculations (Site 3678 is at latitude 33.6°N , and longitude 117.8°W). Site 3678 has the smallest spectral amplitude, Site 4785 the largest, and Site 4080 is about half-way between. The three sites in Figure 7 were chosen in the same way, again among those where the site condition was given by depth to basement h .

The inputs can affect these density functions in one of two ways: There can be systematic errors in the attenuation functions which may affect the absolute level of these distributions (i.e., the location on the longitudinal axis) or the shapes of the distributions. These would not necessarily affect the relative risk at two sites. There can also be errors in the model for the seismicity which affect the relative risks of sites. We therefore would like to know first what the absolute errors for the risk may be, and second, under what circumstances can we say with confidence that one site has significantly higher risk than another site.

There is the possibility that systematic errors coming from the attenuation functions will be large. At $T = 0.04$ sec, for example, Trifunac and Lee (1979) find that the one standard deviation bound for $c(T)$ is $\sigma_c = 0.7$. At $T = 15$ sec, $\sigma_c = 1.7$. Since $c(T)$ is an additive constant in equation (2), uncertainties in $c(T)$ could apply directly to the uncertainty in $\log \text{PSV}(T)$. If the uncertainty in $\log \text{PSV}(0.04 \text{ sec})$ were as large as 0.7, this would correspond to a multiplicative factor of 5, and this would imply that the uncertainty could be greater than the differences between the density functions for the extreme sites in Figure 6. Similarly, the uncertainties implied from the equation (2) are greater than the differences between the extreme sites in Figure 7. At 25Hz, if we cannot rule out the possibility that there is a multiplicative factor of 5 uncertainty in the amplitudes of PSV, then the usefulness of Figure 4 is open to question when applied to the design of structures.

When the attenuation functions (2) were found, the distribution of spectral amplitudes about the mean values were found. These distributions would supposedly be different if the best estimate of $c(T)$, for example, had been different. Therefore, the risk at the site may be uncertain by less than what the uncertainty of $c(T)$ implies. But even if the attenuation function is assumed to be known exactly, significant uncertainties remain.

Suppose we ask how many observations (N , say) would be needed to prove statistically that the hypothetical distributions at two sites differed significantly. To determine N , one can use the non-parametric Kolmogorov-Smirnov test (Hoel, 1971). To apply this, one finds the maximum difference between the two distribution functions from which the density functions in Figure 6 or 7 were derived. This difference can, for a selected confidence level, be associated with N by referring to a table of the numerical values of the Kolmogorov-Smirnov Distribution (e.g., in Hoel).

Figure 8 shows an example for sites 3678 and 4785. The maximum difference between these probability functions is 0.45; the corresponding value of N is 9. By this test, we have derived N for each pair of sites represented by density functions on Figures 6 and 7; the results are compiled in Table I. These distributions are derived from input data, however, and so it is appropriate to ask if there is some number N which characterizes this input. If so, this would be a measure of the intrinsic reliability of the distributions.

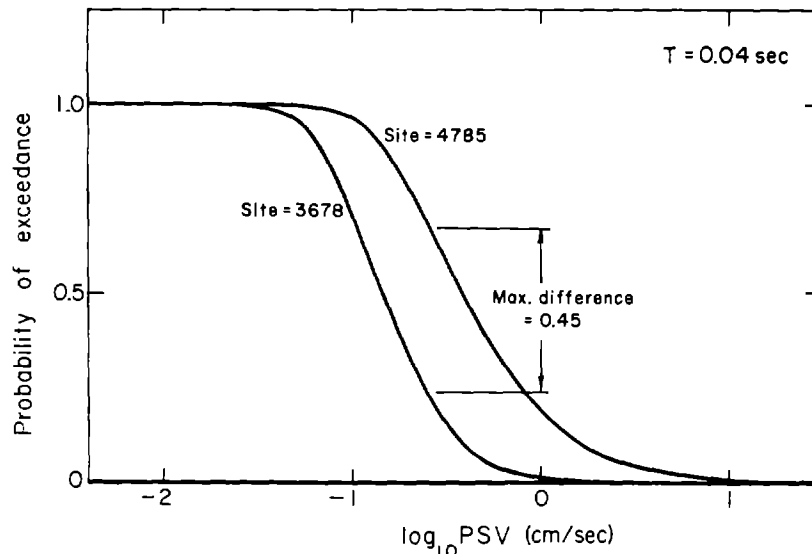


Figure 8

We can propose one method of finding a minimum value for N appropriate to these distributions. It is straight forward (but tedious) to eliminate from the seismicity model all the events which do not contribute significantly to the distribution of 1 year extreme amplitudes (such as Figures 6 and 7). When that is done for the model used here for a site near central Los Angeles (3881) about 15 events remain. Since at least 15 events are needed to compute these distributions, we suggest that at least 15 events have to be recorded so that these distributions would represent in some way all of the data, and therefore N is at least 15.

TABLE I

Site	T = 0.04 sec			Site	T = 15 sec		
	3678	4080	4785		3884	3881	3780
3678	-	30	9	3884	-	11	26
4080	-	-	35	3881	-	-	87
4785	-	-	-	3780	-	-	-

Assuming $N=15$, then the extreme density functions in both Figures 6 and 7 are significantly different, but the intermediate functions do not differ significantly from either extreme. Thus, by this test, we could support the division of the map into two zones: one with high risk and the other with low risk.

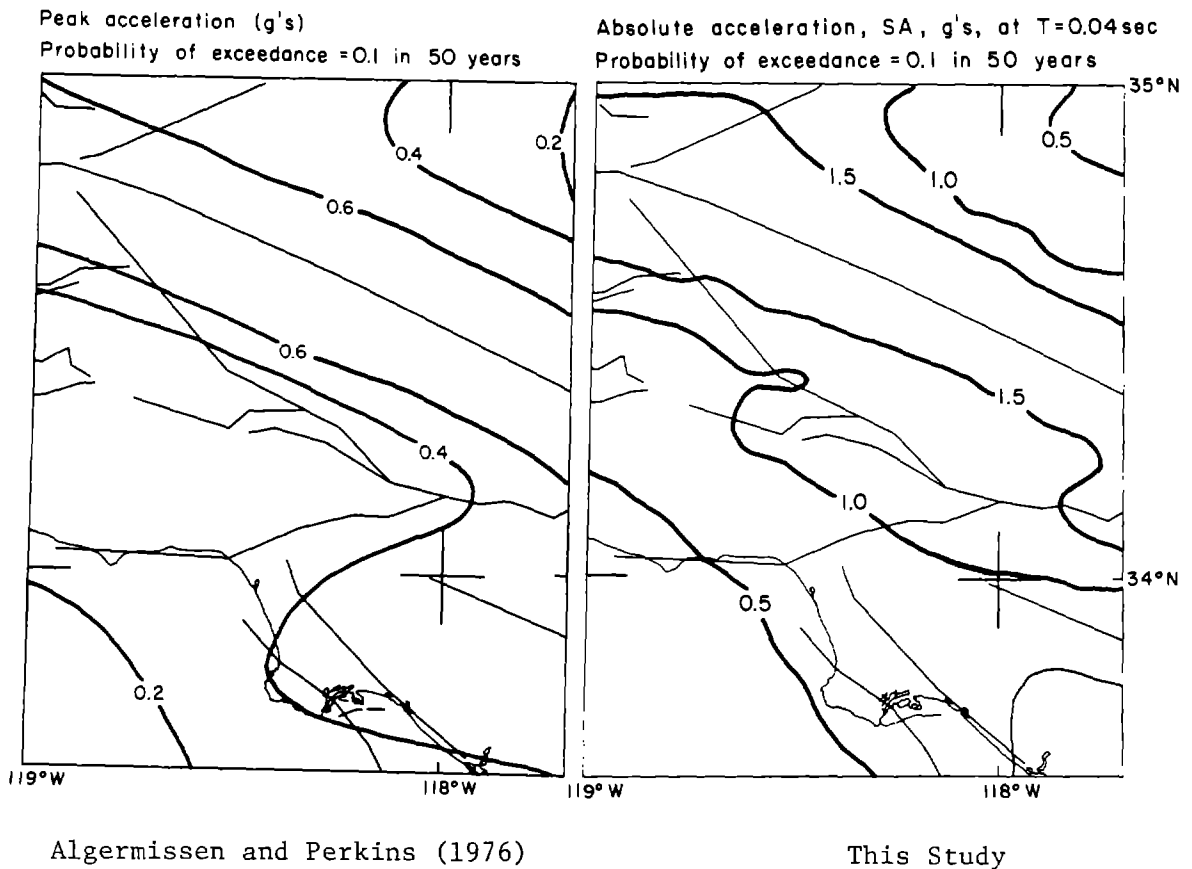


Figure 9

To carry these ideas one step further, we compare these results with results of the risk analysis by Algermissen and Perkins (1976). Figure 9 shows the maps derived by Algermissen and Perkins and by this study for the peak acceleration which has probability of 0.1 of being exceeded once in 50 years. It is assumed that the spectral response at 25 Hz is nearly the same as peak acceleration. The absolute levels of the amplitudes differ by about a factor of two; this is somewhat less than the factor of 5 discussed earlier as a possible limit to the systematic error at this frequency. In the northern section of the map, the contours generally have

similar shapes, so that the relative risks are similar. In the southern section, the contours have significantly different shapes.

We examined sites near Algermissen and Perkins' contour for a peak acceleration of 0.4g. Among these, sites 4279 and sites 3874 represented approximately the extremes in our model of highest and lowest risk. The ratio of the peak accelerations at the two sites by our model is about 2.5. The density functions for these two sites are plotted in Figure 10; one would predict that $N=8$ data points would be sufficient to determine whether the two sites differ significantly.

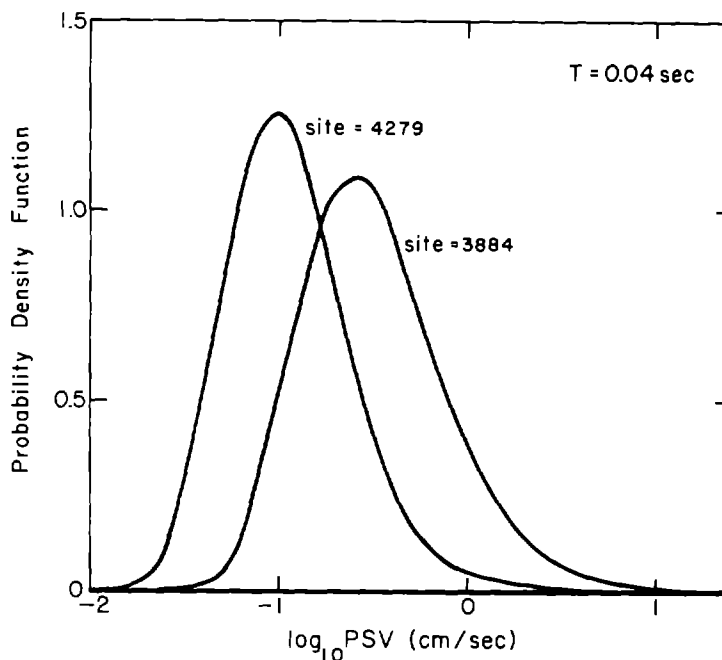


Figure 10

These density functions thus differ by more than sites 3678 and 4785 (Figure 6) at large probabilities, although their small probability tails differ by less. This result suggests that in the test suggested above, N may be smaller than the estimate of 15 which we found. The Kolmogorov-Smirnov test assumed that the seismicity model was known exactly; this result illustrates the important effect of judgement in defining the seismicity model.

Some seismic zonation studies (e.g., Fischer and McWhorter, 1972) have defined zones which correspond to units on Modified Mercalli, or an equivalent, intensity scales. An increase in one unit on the MMI scale corresponds to about a doubling of amplitudes (e.g., Trifunac and Brady, 1975). It seems from our results that the uncertainties of risk in the Los Angeles area may exceed a factor of 2. However, it is interesting to note that if a factor of 2 difference is assumed to be significant, then the smallest zone within the region would have a dimension of 10-20 km (10 km for the $T=15$ sec data, 20 km for the $T=0.04$ sec data).

CONCLUSIONS

This paper has addressed the question of how many zones of differing seismic risk could be justified within a selected region of southern

California. In general, it seems hard to justify more than two or three large zones. Uncertainties in the attenuation relationship for strong ground motion seem to be comparable to, or greater than, the extreme range of spectral amplitudes which are found with any selected probability of exceedance. If it is assumed that the attenuation model is known exactly, one can again look for relative differences in risk. Then the amount of information contained in the seismicity model seems to allow at least 2 zones, but differing interpretations of the tectonic relationships and historical seismicity of the region can lead to different patterns of relative risk throughout the study region. If it is assumed that the results from the model can be taken literally, and that a multiplicative factor of two difference is significant, then it is possible to define three zones within the study region; the minimum dimension of a zone is about 10 km.

These results depend on the model for the attenuation of strong motion. Our model does not consider details of the soil conditions or water table, for example, and thus does not consider all the factors that may be involved in a microzonation study. However, it suggests that the uncertainties involved in risk models can be larger than a factor of 2. This possibility should be considered in any microzonation analysis.

REFERENCES

- Algermissen, S.T., and D.M. Perkins (1976). A probabilistic estimate of maximum acceleration in rock in the contiguous United States, U.S. Geological Survey, Open file report 76-416.
- Anderson, J.G. (1978). Estimating the seismicity from geological structure for seismic risk studies, submitted to Bull. Seism. Soc. Am.
- Anderson, J.G., and M.D. Trifunac (1977). On uniform risk functionals which describe strong ground motion: definition, numerical estimation, and application to the Fourier amplitude spectrum of acceleration, Report No. CE 77-02, Department of Civil Engineering, University of Southern California, Los Angeles, California.
- Anderson, J.G., and M.D. Trifunac (1978a). Uniform risk functionals for characterization of strong earthquake ground motion, Bull. Seism. Soc. Am., 68, 205-218.
- Anderson, J.G., and M.D. Trifunac (1978b). A note on probabilistic computation of earthquake response spectrum amplitudes, Nuclear Engineering and Design, in press.
- Cornell, C.A. (1968). Engineering seismic risk analysis, Bull. Seism. Soc. Am., 58, 1583-1606.
- Fischer, J.A., and J.G. McWhorter (1972). The microzonation of New York State, Proc. of the International Conference on Microzonation for Safer Construction Research and Application, Seattle, 283-298.
- Hoel, P.G. (1971). Introduction to mathematical statistics, fourth edition, John Wiley and Sons, New York, 409p.

- Jennings, C.W. (1975). Fault map of California, California Division of Mines and Geology, Sacramento, California.
- Jennings, C.W., and R.G. Strand (1969). Geologic map of California, Los Angeles Sheet, 1:250,000, Division of Mines and Geology, Sacramento, California.
- McGuire, R.K. (1974). Seismic structural response risk analysis, incorporating peak response regressions on earthquake magnitude and distance, Research Report R74-51, Department of Civil Engineering, Mass. Inst. of Technology, Cambridge.
- Richter, C.F. (1958). Elementary Seismology, W.H. Freeman and Co., San Francisco.
- Rogers, T.H. (1967). Geologic map of California, San Bernardino Sheet, 1:250,000, Division of Mines and Geology, Sacramento, California.
- Trifunac, M.D., and J.G. Anderson (1978). Preliminary empirical models for scaling pseudo relative velocity spectra, Report No. CE78-04, Dept. of Civil Engineering, Univ. of Southern California, Los Angeles, Calif.
- Trifunac, M.D., and A.G. Brady (1975). On the correlation of seismic intensity scales with the peaks of recorded strong ground motion, Bull. Seism. Soc. Am., 65, 139-162.
- Trifunac, M.D., and V.W. Lee (1979). Dependence of the pseudo relative velocity spectra of strong motion acceleration on depth of sedimentary deposits, Dept. of Civil Eng., Report No. 79-02, Univ. of Southern California, Los Angeles (in preparation).
- Yerkes, R.F., T.H. McCulloh, J.E. Schoellhamer and J.G. Vedder (1965). Geology of the Los Angeles Basin, California -- an introduction, U.S. Geological Survey Professional Paper 420-A.

INTENTIONALLY BLANK



SEISMOTECTONIC MICROZONING FOR EARTHQUAKE RISK REDUCTION

by

Bruce A. Schell^I

ABSTRACT

Seismic-risk evaluations for proposed critical facilities have shown that existing seismic-risk maps are generally inadequate because they are based on a record of seismicity that is too short to assess the potential for future earthquakes. This has led to the development of seismotectonic zonations and microzonations of the type discussed in this paper which are based on a broader data base comprised of both seismologic and geologic parameters. Investigations conducted in the Middle East and western United States are outlined to illustrate the differences in the two types of seismic-risk maps.

INTRODUCTION

Seismic risk evaluations for proposed critical facilities such as nuclear power, rad-waste disposal, liquefied natural gas, offshore oil platforms, and dam sites have shown that many existing seismic-risk maps are largely inadequate for realistic earthquake-resistant design. Most seismic-risk zonation methods are based on too short an earthquake record and cannot adequately assess the potential for future earthquakes, especially in areas that have not shown much seismic activity in the last several hundred years. Geologic investigations conducted after the occurrence of large earthquakes, even in areas with relatively low levels of previous seismicity, commonly find that the earthquakes are associated with faults that had evidence of previous activity in Quaternary time.

The recognition of this fact has led to the development of seismotectonic zonations which subdivide regions into zones and/or provinces on the basis of their geologic characteristics as well as their seismicity. This paper will discuss seismic-risk zoning or microzoning techniques and compare the relative merits of zonations derived from the approach utilizing both geologic and seismologic criteria to those based mostly on seismicity.

Earthquakes are a result of present-day tectonic stresses (neotectonic) and the purpose of seismotectonic maps is to characterize this neotectonic activity. Meaningful seismic-risk zonations, therefore, must be based on data that actually characterizes the present and near-future potential for earthquakes and surface faulting. Seismotectonic zones resulting from detailed geologic investigations commonly differ from existing zones of studies which often cite their use of geology but which really are based primarily on seismicity and inactive tectonic features. The major shortcoming of the zonations based only on seismicity is that they statistically manipulate an incomplete data set which all too often is biased by recent earthquakes. The result is that they falsely assume that future earthquakes

I Fugro, Inc., Long Beach, California

will occur exactly where they have in the past couple hundred years. The strength of seismotectonic zonations is that they utilize a broader data base covering thousands and even millions of years and this represents a truer picture of the earthquake potential.

A well constructed seismotectonic map best serves as a guide to basic planning for critical facilities which will eventually require site-specific risk analysis. With the increased detail required for the site specific investigation, they can be further subdivided into smaller zones or microzones. Such seismotectonic microzonations from the Middle East, and the western United States will be compared to existing seismic-risk maps, hopefully, to increase the awareness of the shortcomings of existing seismic-risk maps and provide insight into the necessity for considering geologic data.

PARAMETERS USED TO ESTABLISH SEISMOTECTONIC MICROZONES

A seismotectonic zone map is a seismic-risk map which bases subdivisions on similarity of both seismicity and tectonic conditions. The term tectonic refers to geologic deformations, such as folds and faults, of regional dimensions. Features such as minor localized faults, landslides, and small-scale subsidence features usually are not tectonic features. The term microzone is a relative term which to the plate tectonist, would probably mean subdividing a lithospheric plate of continental proportions, but to a county agency it might mean subdivision of the county.

Seismotectonic-map subdivisions fall into two basic categories:

1) seismotectonic zones which are linear features with a relatively clear-cut correspondence between seismicity and geologic faults, and 2) seismotectonic zones with poorly defined or obscure relationships between seismicity and geology.

The essential aspects or parameters considered in the construction of a seismotectonic map are:

1. distribution of earthquake hypocenters,
2. distribution of historical seismicity,
3. magnitude or intensity of past earthquakes,
4. distribution and style of neotectonic faults and folds,
5. amount and characteristics of fault displacements, and
6. characteristics of stress release associated with earthquakes (focal mechanism solutions).

Factors such as the characteristics of the travel path of seismic waves and the soil conditions at the site are not taken into consideration because they are too widely variable and apply only to a specific site. Those factors are considered by the earthquake engineer when he applies the seismotectonic map in the final design. Other important parameters that may be taken into consideration, depending upon the area under study, are the distribution and history of volcanic activity and the distribution and type of younger rocks.

Seismologic Parameters

Seismicity data generally exist in several forms (instrumental, historical, microseismicity), each of which has inherent problems with respect to

its application to seismic-risk analysis. The best data generally are instrumental data recorded within the last 15 to 20 years because they are the most accurately located. The major problem with these instrumental records is that they represent a time period which is too short to adequately represent geologic phenomena which is measured in thousands or even millions of years. To compensate for this shortcoming, most investigators use the older instrumental data and the historical data. It would seem that the use of this longer record would add to the credibility of their studies, but many times it is preferable not to use the older data because it has a tendency to be poorly located and unrepresentative of present seismicity characteristics. Earthquake relocation techniques (14) can enhance the location accuracy of the older data and sometimes allow an increased measure of confidence in its use.

The hypocenter distribution of earthquakes are as important a factor as as epicentral distribution because seismotectonic zones are three-dimensional features. Commonly the depth range of earthquakes is small enough that it is not a factor, but in some areas such as at major lithospheric plate boundaries one may be required to differentiate deep zones of earthquakes from the surficial zones.

Microseismicity studies can be useful because they can provide a lot of data in a very short time and can indicate areas with an unrecognized seismic hazard. Care must be used in the application of microseismicity, however, because it is not clear how it related to macroseismicity.

Pre-instrumental earthquakes, commonly referred to as "historical earthquakes", are those documented prior to the establishment of seismograph networks. The lengths of these records and their completeness varies widely from region to region. Middle Eastern and far eastern countries have records of earthquakes that extend a few thousand years back in time, whereas in the western United States the record is only a couple hundred years long. An interesting aspect of historical earthquakes is that they are fewer in number but larger in magnitude backwards in time. This commonly has no real significance with respect to tectonic processes but is a result of a low population density, poor recording practices, and a lack of understanding of the mechanism causing the destruction. The quality of historical records is highly dependent on local culture and population density because earthquakes were usually recorded only at educational or religious institutions. This results in a distribution of historical earthquakes that is heavily biased towards major cities and towns. Estimates of the intensity or magnitude of historical earthquakes are usually based on reports of destruction and loss of life, thus local building practices probably play a more important role in the magnitude assigned than the actual size of the earthquake. Investigators commonly try to take construction practices into account when assigning Modified Mercalli (MM) intensities to earthquakes, but there is little consistency from person to person and this may lead to additional uncertainties if the criteria used are not documented. The conclusion is that historical records serve as useful indicators of past seismicity trends, but alone are not reliable indicators of present or near-future seismic activity.

Geologic Parameters

Most of the destruction caused by earthquakes is due to ground shaking, but considerable damage may also be caused by the actual fault displacement

of the ground surface. Therefore a most important parameter for earthquake-hazard evaluation is the location of active faults. Investigations in areas that have recently sustained large earthquakes but which previously were seismically quiescent have shown geologic evidence that could have alerted geologists to the potential for those earthquakes if the proper studies had been conducted. The North Anatolian fault area in northern Turkey and the Buyin-Zahra and Dash-e Bayaz areas of Iran provide good examples of the need for geologic fault studies. These earthquakes occurred in areas which previously had been relatively quiet seismically, but geologic studies of the damaged areas after the earthquakes revealed that the earthquakes, indeed, had occurred along large pre-existing faults (2, 6, 8, 40).

Assignment of Maximum Earthquakes

The ideal map for seismic-risk reduction would be one with a maximum earthquake and recurrence data for every active or Quaternary fault. Considering the present state of knowledge this is not possible. However, an experienced geologist can generally recognize the potentially troublesome faults and can establish seismotectonic zones and assign maximum credible earthquakes that indicate the potential for damaging earthquakes. The maximum credible event, which is defined as the largest earthquake to be expected, is based on the largest previous earthquake unless there is evidence to suggest that a larger event should be expected.

Where major Quaternary faults are present, but which have not moved during recorded history, application of the relationships of fault length and displacement to earthquake magnitude (1, 10, 21, 41) can be used to estimate the maximum credible magnitude. The data upon which these relationships are based sometimes have considerable uncertainty thus the magnitudes derived from them usually are not directly incorporated into the seismotectonic model. They must undergo close scrutiny and analysis regarding all of the existing geologic and seismic data. In these analyses, the investigator must determine all of the unknowns and variables that may have an effect on the calculations. For example, how well known is the fault length? Very seldom can the exact length of a fault be determined; they usually splay and merge with other faults. Is the length as shown on existing maps a representation of a single fracture or of a series of smaller fractures? If a field investigation is not conducted, the investigator must use his judgment to arrive at fault lengths that will be characteristic and realistic, but still conservative. When dealing with critical facilities conservatism is usually applied at several stages and assures that the magnitudes assigned are indeed the largest to be expected. For example, the fault length used is the maximum possible length. This length is then applied to fault length/displacement/magnitude graphs or formulae to determine the appropriate earthquake magnitude. After a reasonable and conservative earthquake magnitude has been determined, a somewhat arbitrary increase in magnitude may be tacked on as a final effort towards conservatism. The amount of this final increase should range from one-tenth magnitude to one-quarter magnitude, depending on the reliability of the data.

Other fault-magnitude data such as scarp height has been used but caution must be exercised because of the difficulty in judging whether the observed displacement occurred during only one earthquake or several. Such relationships, however, can be useful measures of the credibility or conservatism of the conclusions drawn from other data.

EXAMPLES OF SEISMOTECTONIC MICROZONING

In order to illustrate the application of the above principles two examples will be discussed. It must be borne in mind that further subdivision of some of the zones may be possible when more detailed data become available. The main purpose in presenting the seismotectonic maps is to illustrate how the data discussed above has been applied to siting of critical facilities and the differences that result from using both geologic and seismologic data rather than seismologic data alone.

Middle East

The long-term civilizations in the Middle Eastern countries have left a record of earthquakes spanning nearly 3,000 years. In spite of this long record, the major difficulty in seismotectonic zoning of most Middle Eastern countries is a paucity of data. Geologic investigations have been primarily for oil and mineral exploration and up until recently not much attention has been directed to the reduction of earthquake risks. Modern seismograph stations are widely spaced and most of them have been in operation only a short time. Prior to establishment of the Worldwide Standardized Seismograph Network in the early 1960's, epicenter location errors in this region were often as much as 1 degree (110 km) (29) and hypocenter locations were no better than 50 km (24). The data being recorded now seem to be more accurate but small earthquakes ($M < 5$) probably are not recorded unless they occur near a seismograph station.

The majority of earthquakes in the Middle East are associated with a broad zone of collision between the Afro-Arabian and Eurasian lithospheric plates. Figure 1 is a microzone map of a portion of this collision zone between the Caspian Sea and the Persian Gulf. The parallelism of the seismotectonic zones is a result of northeast-southwest convergence between the two plates. The greatest number and most destructive earthquakes occur in the Alborz, Tabriz-Nain, and Zagros seismotectonic zones. In spite of their abundant seismicity, the Zagros and Alborz belts have few faults with documented Quaternary movement or historic surface ruptures. This is believed to be partly due to the difficulty in recognizing such features in so rugged a terrain. Reconnaissance field studies in the Zagros Mountains, by the author, revealed the presence of numerous, young-looking faults but poor accessibility, lack of cross-cutting relationships, and a poorly known Quaternary stratigraphy did not allow determination, with certainty, that the faults are indeed Quaternary in age.

The largest historical earthquake associated with the Zagros appears to be the 1909 Silakhor event ($M=7.4$) which occurred along the northeastern margin of the range on the Main Recent fault (7, 18, 39). This fault is the most dominant fault in the Zagros region and appears to have a slightly higher rate of activity than the mountains to the west, thus it is set out as a separate seismotectonic zone. The Main Recent fault is a 1,700-km-long linear zone of near-vertical faults, which individually are no greater than about 100 km in length. Because the smaller faults are discrete features of relatively short length, a maximum credible earthquake of about 7.5 is believed to be conservative and reasonable for this seismotectonic zone. The maximum historical event in the Zagros seismotectonic province then becomes the 1977 Bandar Abbas earthquake ($M=7.0$). Based on the lack of significant Quaternary faults it is difficult to justify a maximum credible event much larger than $M=7.25$ but the high recurrence interval of moderate to large

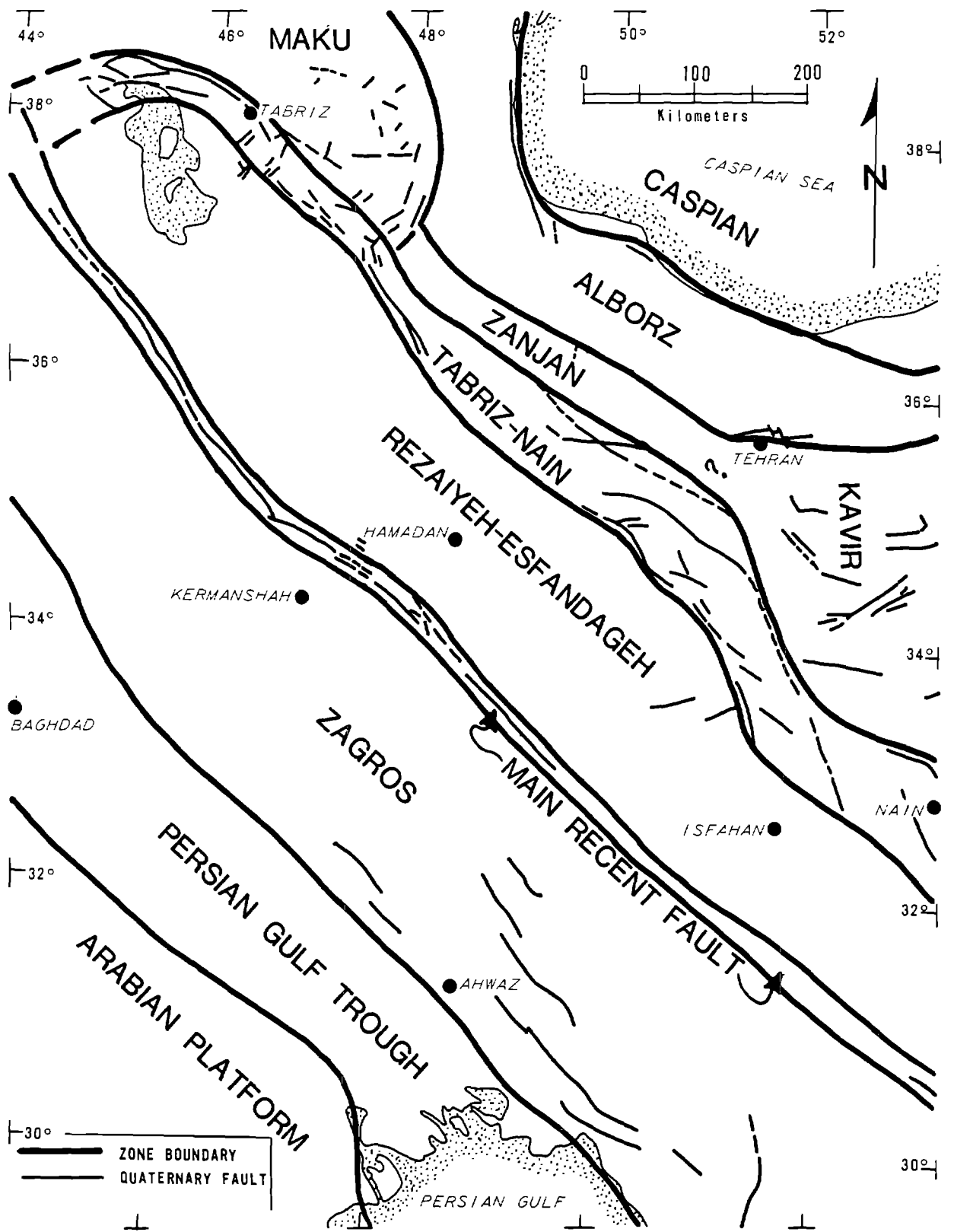


Figure 1. Seismotectonic zones in the Persian Gulf-Caspian Sea region.

earthquakes in this area indicates that the probability of the occurrence of such an event is quite high. If the present higher rate of seismicity in the southern Zagros truly represents greater tectonic activity than the northern Zagros, then the Zagros should be subdivided into smaller seismotectonic zones (9, 31).

The Alborz seismotectonic province is similar to the Zagros in that it has abundant seismicity but few documented Quaternary faults except at its margins. The maximum historical event is the Mazandaran event ($M=7.38$) of 1957. Surface rupture was reported with this event (5, 33) but based on subsequent field investigations (9) they were attributed to landsliding. Based on this province's history of large, destructive events and on the premise that the region is so rugged that Quaternary faults could not be easily recognized if they exist, a maximum credible event of magnitude 7.5 is believed to be reasonable and conservative.

The other major seismogenic zone shown on Figure 1 is the Tabriz-Nain seismotectonic zone. This zone is a linear zone of Quaternary faults that extends southeasterly from the Tabriz area in northwestern Iran to the Nain area. This system of faults separates the Rezaiyeh-Esfandagheh belt from the Quaternary depressions of central Iran and lies almost entirely within a Tertiary volcanic belt. This zone provides a good example of high-risk area that probably would not be delineated on the basis of seismicity alone. However, two large earthquakes ($M=7.2$ at Salmas in 1930 and $M=7.25$ at Buyin-Zahra in 1962) have demonstrated the high seismic potential of this zone. Fault-length/magnitude relationships suggest that a $M=7.4$ may be more appropriate but the recurrence interval of such an event would be longer than in the Zagros or Alborz zones.

The remaining seismotectonic zones have much lower levels of seismicity than the provinces discussed above. Their maximum earthquakes and tectonic character are summarized on Table 1.

The seismicity and seismic risk studies of portions of the area shown on Figure 1 (22, 27-31, 38) provide valuable information regarding the characteristics of the seismicity but, with the possible exception of Nowroozi's (31), cannot be used directly for seismotectonic zoning for critical facilities. Comparison of Figure 1 with the previous seismicity studies represented on Figure 2 shows some general similarities but also some differences which could be important to the siting of critical facilities. The differences are due to the previous studies not taking advantage of the information that the neotectonic features offer. The contour lines drawn on Figure 2 suggest a connection between the Zagros and the Alborz Mountain chains through the Kermanshah-Hamadan-Tehran region. The delineation of this zone is strongly influenced by the 1962 Buyin-Zahra earthquake in the Tabriz-Nain zone and the 1957 Farsinaj earthquake which was felt in Hamadan but which occurred along the eastern margin of the Zagros Mountains most probably on the Main Recent fault. The correlation of these earthquakes to their respective seismotectonic zones is very important to an accurate assessment of the seismic risk. Seismic design in regions near the borders of the Reziyeh-Esfandagheh zone would probably be controlled by earthquakes in the bordering seismotectonic zones, whereas design in the central area of the Rezaiyeh-Esfandagheh zone would be controlled by the low-magnitude random earthquake occurring within the zone.

TABLE 1

SEISMOTECTONIC ZONE	MAXIMUM PREVIOUS EARTHQUAKE	MAXIMUM CREDIBLE EARTHQUAKE	TECTONIC CHARACTER AND SEISMICITY (1)
MAKU	6.5	6.75	Numerous minor Quaternary faults. Seismicity common.
KAVIR	6.5	6.75	Numerous Quaternary faults; bounded by major active faults. Seismicity low to moderate.
PERSIAN GULF TROUGH	5.6-5.9	6.0	Gentle downwarp near edge of Arabian plate. Seismicity low; several destructive historical events near Baghdad.
ZANJAN	5.7	6.0	Neogene downwarp; may be salient of Kavir zone. No major Quaternary faults. Low seismicity.
CASPIAN	5.5	6.0	Oceanic crust surrounded by folds concordant with Alborz trends. Seismicity rare in center; common near coast.
REZAIYEH-ESFANDAGHEH	<5.0 magnitudes not reported	5.0	Stable plateau. No major Quaternary faults. Seismicity rare.
ARABIAN PLATFORM	None Recorded	?	Stable platform. Rare seismic activity restricted to boundaries.

(1) Seismicity terms indicate relative number of earthquakes from most to fewest; abundant, common, moderate, low, rare. Abundant seismicity occurs in Zagros and Alborz zones.

Western United States

Less is known, perhaps, about the earthquake history of the western United States than any other part of the U.S. Because the region was largely unsettled before the mid 1800's, the earthquake record is only a couple hundred years long, a very short time compared to other regions of the world. The potential for destructive earthquakes has been dramatically demonstrated by events such as the 1906 San Francisco (M=8.3), the 1969 Hebgen Lake (M=7.1), and the 1971 San Fernando (M=6.4) earthquakes. The California area has the largest and most abundant earthquakes and much is known about its Quaternary fault and seismicity characteristics. Other areas such as the Basin and Range area are less understood and require much more detailed work before final seismotectonic zones can be established. The seismotectonic zones shown on Figure 3 are generalized from regional data (for example, 20, 36, 37) and undoubtedly will change as more detailed information becomes available. Comprehensive attempts to determine the seismic risk of this vast area (3, 4, 32, 42) are based primarily on present-day seismicity trends. Analysis of Quaternary fault trends indicate that these seismic risk maps may not be adequate for siting critical facilities. The areas of highest seismicity (zone 3 on Fig. 4) are certainly areas which require the utmost care when constructing critical facilities, but the risk in Nevada is probably not as great as in California. What about the seismic

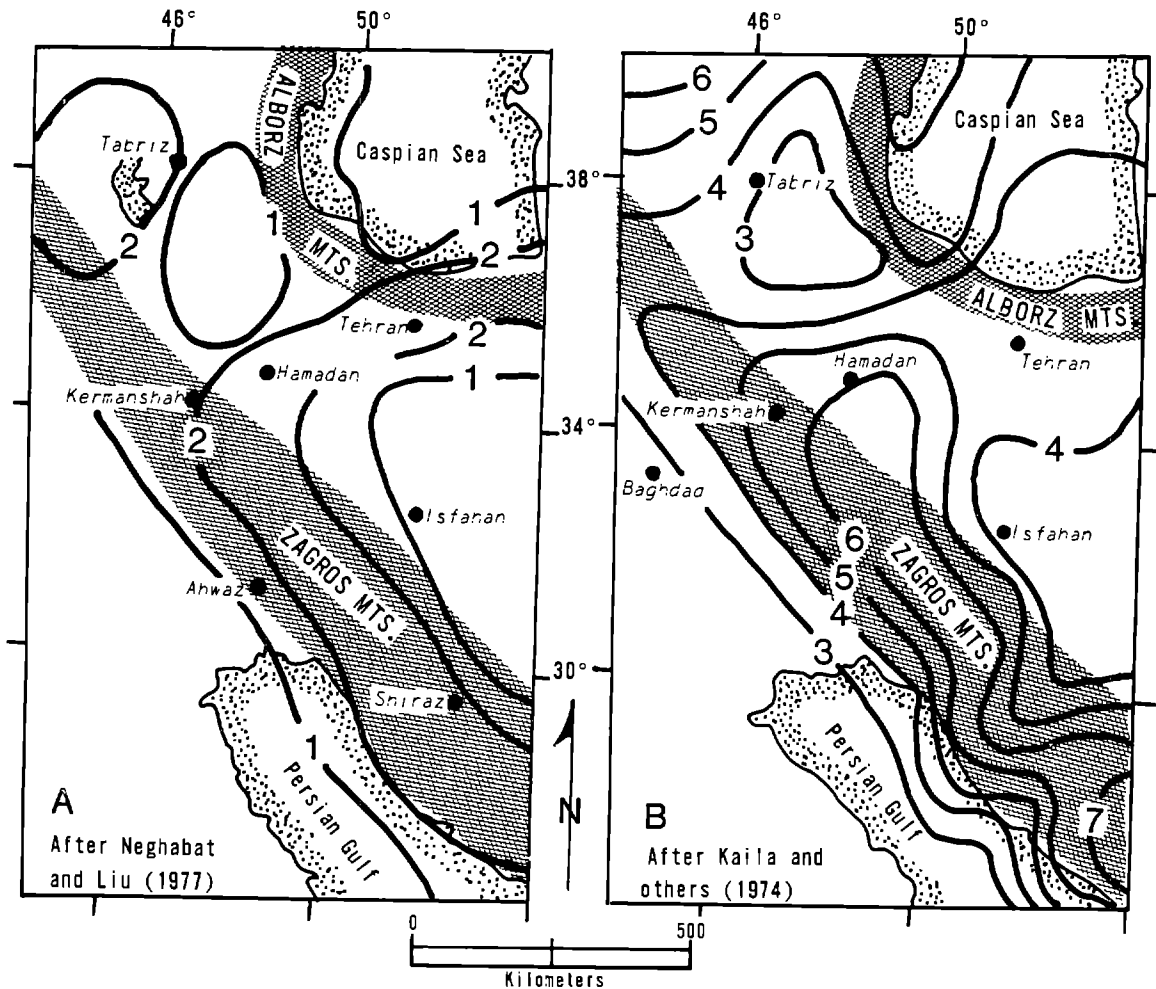


Figure 2. Maps of Persian Gulf-Caspian Sea region based on seismological data. A shows earthquake intensity contours; considering a return period of 100 years, 1 represents MM intensity VII, 2=MM VIII, and 3=MM IX. B is a quantitative seismicity map of A values based on a 14-year observation period.

risk in areas such as eastern Nevada, western Utah, and southeastern Arizona? In the recent past (the last 100 years or so) the general frequency and size of earthquakes in these areas has been less than in the areas designated as zone 3. Does this infrequent seismicity indicate a lack of earthquake danger or does it merely indicate that the area is in a temporary, inactive cycle? Significant earthquakes (for example, the 1887 Sonora Mexico earthquake with a magnitude estimated to be in the neighborhood of 7.5 to 8.0) have occurred outside of zone 3. A detailed analysis of the geology with emphasis on Quaternary faults and earthquakes allows some preliminary seismotectonic zones and microzones to be established (Fig. 3). Some of these zones can probably be subdivided, but as presently shown they do illustrate some general and important trends. Table 2 lists the maximum previous earthquake in each zone. These are the earthquakes upon which the maximum credible event will be based. Some of them can be associated with specific geologic structures but others will be random events.

One of the most prominent seismicity trends is a band of earthquakes that stretches from the city of Ventura in southern California to the

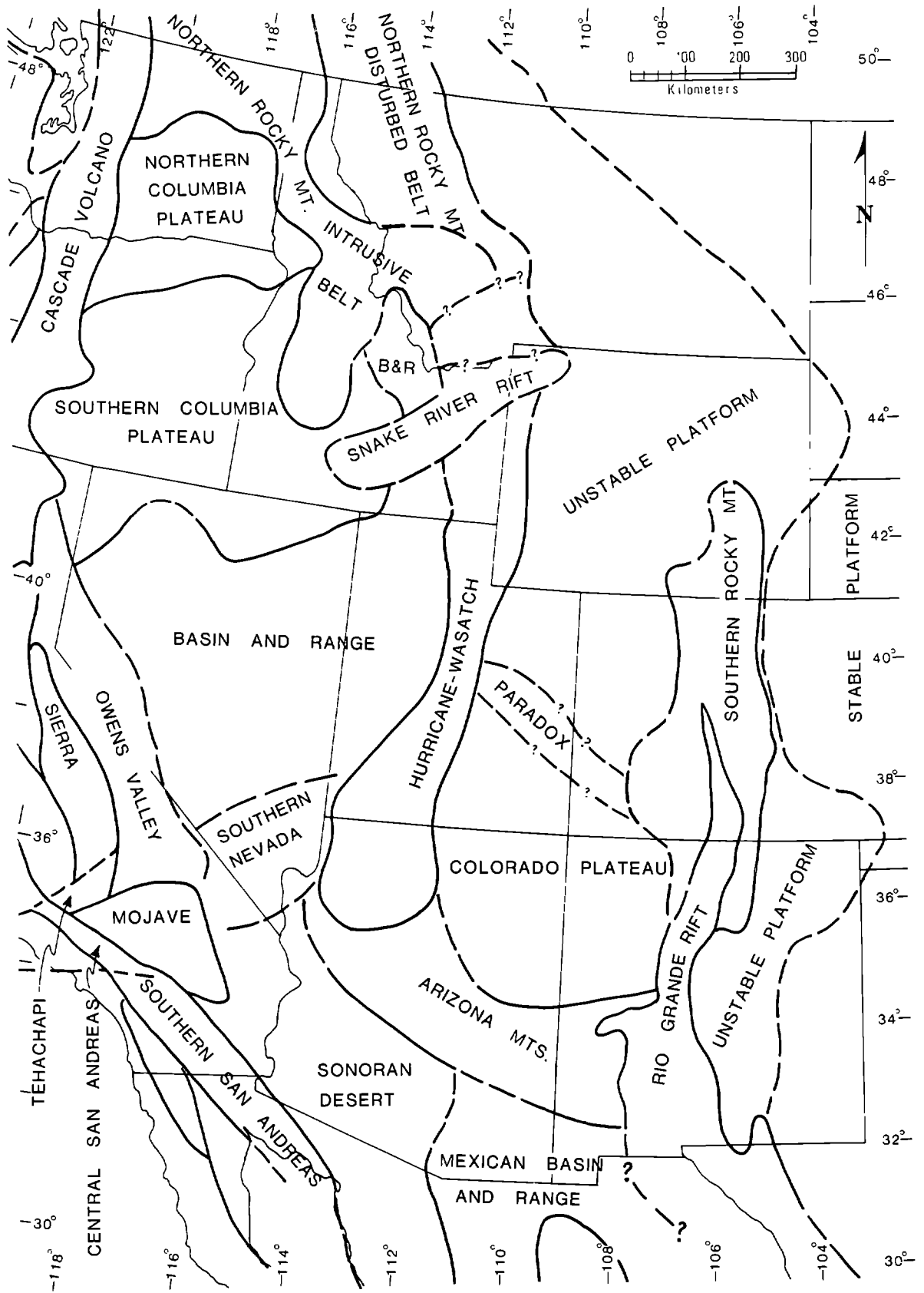


Figure 3. Preliminary seismotectonic zones of the western United States.

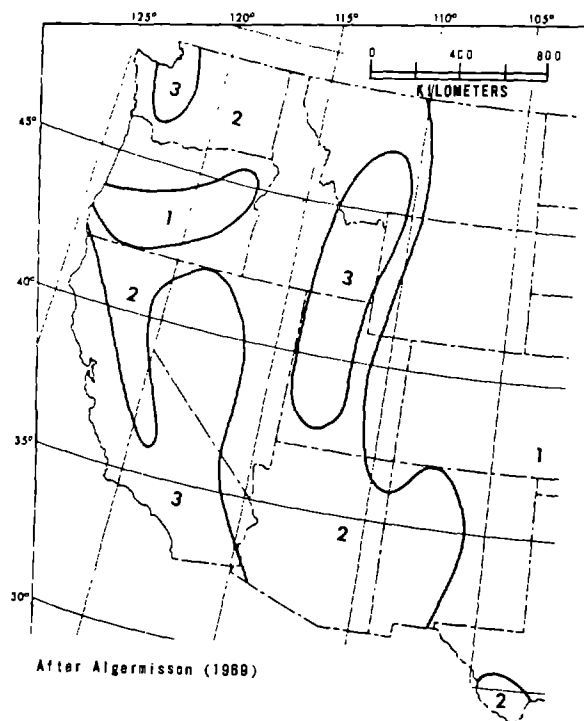


Figure 4. Seismic-risk map of the western United States.

Zone 1 - Minor damage; corresponds to intensities V and VII of the Modified Mercalli scale (MM).

Zone 2 - Moderate damage; MM intensity VII.

Zone 3 - Major damage; MM intensity VIII and higher.

TABLE 2

SEISMOTECTONIC ZONE	MAXIMUM PREVIOUS EARTHQUAKE
ARIZONA MOUNTAIN	5.5
BASIN AND RANGE	7.75
CASCADE VOLCANO	5.5
CENTRAL SAN ANDREAS	8.0*
COLORADO PLATEAU	5.1
HURRICANE-WASATCH	6.7*
MEXICAN BASIN AND RANGE	8.0*
MOJAVE	6.4
NORTHERN COLUMBIA PLATEAU	5.75
NORTHERN ROCKY MOUNTAIN DISTURBED BELT	6.7
NORTHERN ROCKY MOUNTAIN INTRUSIVE BELT	6.1
OWENS VALLEY	8.3*
PARADOX	4.6
RIO GRANDE RIFT	6.4
SIERRA	< 5.0
SNAKE RIVER RIFT	6.5-7.1
SONORAN DESERT	5.0
SOUTHERN COLUMBIA PLATEAU	5.25
SOUTHERN NEVADA	6.1
SOUTHERN ROCKY MOUNTAIN	5.5
SOUTHERN SAN ANDREAS	7.1
TEHACHAPI	7.7
UNSTABLE PLATFORM	5.5

* Estimates of earthquake magnitude based on felt reports. These events are cited because the maximum instrumental magnitude is much less than geologic data indicates is possible.

Nevada-Oregon border. Geologic analysis indicates that this alignment is largely coincidental and really represents several different tectonic regimes. The southern earthquakes are related to the compressional and left-lateral tectonics of the Transverse Ranges and Tehachapi Mountains and the northern earthquakes are associated with Basin and Range tensional tectonics. Even the Basin and Range area has important internal differences and has three or four major zones of earthquake activity. Two of these are linear trends along the eastern and western margins. The third and fourth are in west-central and southern areas. The eastern and western bounding zones have abundant geologic evidence to explain their existence. Very little geologic or geophysical support for separate and discrete west-central and southern zones can be found. Analysis of faults in eastern Nevada and western Utah reveals numerous Quaternary fault zones, some in the 50- to 100 km-length range. According to relationships between fault length and earthquake magnitude (10, 11, 19, 41) faults of these dimensions could generate earthquakes in the $M=6\text{-}3/4$ to $7\text{-}1/2$ range. There is no strong geologic evidence to suggest different seismotectonic regimes between the west-central Basin and Range area and the eastern area, therefore earthquakes such as the Fairview Peak ($M=7.1$) or Pleasant Valley ($M=7.6$) events should be considered in the seismic risk analysis of the eastern Basin and Range area. A Southern Nevada zone is delineated (Fig. 3) because there are Quaternary fault trends transverse to normal Basin and Range trends in the area. However, earthquakes in both the west-central and southern seismic zones may represent typical Basin and Range activity which at the present is more active in these areas than others. Ryall (34) has suggested that earthquakes in the Basin and Range area occur in cycles of about 1,000 years, therefore, the west-central and southern Basin and Range may be experiencing a temporary localized increase in activity.

The Hurricane-Wasatch zone (Fig. 3) has abundant seismicity and semi-parallel Quaternary faults and forms the transition from highly active Basin and Range tectonics to the less active areas of the east. This seismotectonic zone is part of the Intermountain Seismic belt (ISB) (36). Tectonic features, seismicity, and focal mechanisms suggest that the ISB is comprised of several seismotectonic zones or microzones. The microzone boundaries are difficult to determine with precision but a major discontinuity appears to lie near the zone of high seismicity at the intersection of this zone with the Snake River Rift zone. Focal mechanism solutions south of the Snake River Rift zone have tensional axes oriented in a general east-west direction; tensional axes in the Snake River Rift area trend north-south, and those in the Northern Rockies trend northeast-southwest or east-west (15, 16, 36). The maximum previous earthquake in the ISB is the $M=7.1$ Hebgen Lake earthquake. Based on present knowledge, it is difficult to confidently associate the Hebgen Lake earthquake with a specific seismotectonic zone (see 15, 16, 26) but it does not appear to be related to the same tectonic regime that causes earthquakes in the Hurricane-Wasatch zone thus it is restricted to the Snake River-Yellowstone area. The maximum previous earthquake in the Hurricane-Wasatch zone is estimated to be $M=6.7$ (13) but judging from the length and displacement of Quaternary faults, earthquakes as large as 7.1 to 7.2 can be expected (12).

The vast area east of the ISB (Fig. 3) has a wide variety of structural provinces of different characteristics (for example, the Wind River Uplift, Bighorn Basin, Uinta Uplift, Wyoming Basin, and the Colorado Plateau). Due to the present uniform low level of seismicity and scarcity of Quaternary fault trends, the basins and uplifts of this region are classified as one

zone, the Unstable Platform zone. The Colorado Plateau is separated from this zone by a zone of northwest-southeast trending faults in the Paradox zone.

The Rio Grande Rift appears to be a major neotectonic feature but its relatively abundant seismicity is characteristically of low magnitude (generally less than 5.0). The maximum historical earthquake is the 1964 Valentine, Texas event of $M=6.4$. Fault lengths and displacements, however, suggest that earthquakes in the 7 to 8 magnitude range are possible (38). The occurrence of the 1887 Sonoran earthquake also may bear on the maximum credible event for the Rift. South of the U.S.-Mexico border, there is no strong geologic evidence to distinguish the Mexican Basin and Range zone from the Rio Grande Rift zone. If no such evidence can be found, they may have to be considered one zone and then the maximum historical event and the length/magnitude relationships would be mutually supportive and a great earthquake ($M=8$) would have to be considered credible for the rift zone in New Mexico.

The above discussion just touches upon a few of the important aspects of the earthquakes and tectonic characteristics of the western U.S. to illustrate the great complexity of the area and the need for exhaustive geologic studies before sites for critical facilities can be picked.

BIBLIOGRAPHY

- 1) Albee, A. L., and Smith, J. L., 1966, Earthquake characteristics and fault activity in southern California: Spec. Pub. of the Los Angeles Section of the Assoc. of Engr. Geologists, 9-13.
- 2) Allen, C. R., 1975, Geological criteria for evaluating seismicity: Geol. Soc. Am. Bull., 86, 1041-1057.
- 3) Algermissen, S. T., 1969, Seismic risk studies in the United States: Proc. Fourth World Conf. on Earthquake Engineering, I, Santiago, Chile.
- 4) Algermissen, S. T., and Perkins, D. M., 1976, A probabilistic estimate of maximum acceleration in rock in the contiguous United States: U.S. Geol. Survey Open File Rept. 76-416.
- 5) Ambraseys, N. N., 1975, Studies in historical seismicity and tectonics: Geodynamics Today, ch. 2, Roy. Soc. London, 7-16.
- 6) Ambraseys, N. W., Anderson G., Bubnow, S., Crampin, S., Shahidi, M., Tassios, T. P., and Tchalenko, J. S., 1969, Dasht-e Bayaz earthquake of 31 August 1968: UNESCO Publ. 1214/BMS, RD/SCE.
- 7) Ambraseys, W. N., and Moinfar, A., 1973, The seismicity of Iran: the Silakhor, Lurestan earthquake of 23 January 1909: Annali di Geofisica, 26, 4.
- 8) Berberian, M., 1971, Preliminary report on structural analysis of Ipak active fault: Geol. Survey Iran, Internal Rept.
- 9) _____, 1976, Seismotectonic map of Iran: Geol. Surv. Iran.
- 10) Bonilla, M. G., 1970, Surface faulting and related effects, in Weigel, R. L., ed., Earthquake engineering: New Jersey, Prentice-Hall, Inc., 47-74.
- 11) Bonilla, M. G., and Buchanan, J. M., 1970, Interim report on worldwide historic surface faulting: U.S. Geol. Surv. Open-File Rept.
- 12) Cook, K. L., 1971, Earthquakes along the Wasatch Front, Utah - the record and the outlook: Utah Geol. Assoc. Publ. 1-H.
- 13) Cook, K. L., and Smith, R. B., 1967, Seismicity in Utah, 1850 through 1965: Seismol. Soc. Am. Bull., 57, 689-718.

- 14) Dewey, J. W., 1971, Seismicity studies with the method of joint hypocenter determination [Ph.D. thesis]: Berkeley, Univ. Calif.
- 15) Dewey, J. W., Dillinger, W. H., Taggart, J., and Algermissen, S. T., 1972, A technique for seismic zoning: analysis of earthquake locations and mechanisms in northern Utah, Wyoming, Idaho, and Montana: First Int. Conf. on Microzonation, Seattle, Washington.
- 16) Frazer, G. D., Witkind, I. J., and Nelson, W. H., 1964, A geological interpretation of the epicentral area - the dual basin concept: U.S. Geol. Surv. Prof. Paper 435-J.
- 17) Friedline, R. A., Smith, R. B., and Blackwell, D. D., 1976, Seismicity and contemporary tectonics of Helena, Montana area: Seismol. Soc. Am. Bull., 66, 81-95.
- 18) Golitsin, B. B., 1909, Kratkoe soobshenie o zemletriasenii 10/23 vo iranaria 1909 goda: Izv. Imp. Akad. Navk., 3, 159-160.
- 19) Housner, G. W., 1970, Strong ground motion, *in* Wiegel, R. L., ed., Earthquake engineering: New Jersey, Prentice-Hall, Inc., 75-91.
- 20) Howard, K. A., Aaron, J. M., and others, 1978, Preliminary map of young faults in the United States as a guide to possible fault activity: U.S. Geol. Surv. Misc. Field Studies Map MF-916.
- 21) Iida, K., 1965, Earthquake magnitude, earthquake fault, and source dimensions: Nagoya Univ., Jour. Earth Sci., 13, 115-132.
- 22) Kaila, K. L., Madhava, R. N., and Narain, H., 1974, Seismotectonic maps of southwest Asia region comprising eastern Turkey, Caucasus, Persian plateau, Afghanistan, and Hindukush: Seismol. Soc. Am. Bull., 64, 657-669.
- 23) Mark, R. K., and Bonilla, M. G., 1977, Regression analysis of earthquake magnitude and surface fault length using the 1970 data of Bonilla and Buchanan: U.S. Geol. Surv. Open File Rept. 77-614.
- 24) McKenzie, D. P., 1972, Active tectonics of the Mediterranean region: Royal Astron. Soc. Geophys. J., 30, 109-185.
- 25) Molnar, P., and Sykes, L. R., 1969, Tectonics of the Caribbean and middle America regions from focal mechanisms and seismicity: Geol. Soc. Am. Bull., 80, 1639-1684.
- 26) Myers, W. B., and Hamilton, W., 1964, Deformation accompanying the Hebgen Lake earthquake of August 17, 1959: U.S. Geol. Surv. Prof. Paper 435-I.
- 27) Neghabat, F., and Liu, S. C., 1977, Earthquake regionalization of Iran: New Delhi, Sixth World Conf. on Earthquake Engineering, 2-531 to 2-536.
- 28) Niazi, M., and Basford, J. R., 1968, Seismicity of Iranian plateau and Hindlu Kush region: Seismol. Soc. Am. Bull., 58, 417-426.
- 29) Nowroozi, A. A., 1971, Seismotectonics of the Persian plateau, eastern Turkey, Caucasus, and Hindu-Kush regions: Seismol. Soc. Am. Bull., 61, 317-341.
- 30) _____, 1972, Focal mechanism of earthquakes in Persia, Turkey, west Pakistan, and Afghanistan and plate tectonics of the Middle East: Seismol. Soc. Am. Bull., 62, 823-850.
- 31) _____, 1976, Seismotectonic provinces of Iran: Seismol. Soc. Am. Bull., 66, 1249-1276.
- 32) Richter, C. F., 1959, Seismic regionalization: Seismol. Soc. Am. Bull., 49, 123-162.
- 33) Rothe, J. P., 1969, The seismicity of the earth, 1953-1965: Paris, UNESCO, SC.68/D, 67/4F.
- 34) Ryall, A., 1977, Earthquake hazard in the Nevada region: Seismol. Soc. Am. Bull., 67, 517-532.

- 35) Sanford, A. R., Budding, A. J., Hoffman, J. P., Alptekin, U. S., Rush, C. A., and Topozada, T. R., 1972, Seismicity of the Rio Grande rift in New Mexico: New Mexico Bur. Mines and Min. Res. Circ. 120.
- 36) Smith, R. B., and Sbar, M. L., 1974, Contemporary tectonics and seismicity of the western United States with emphasis on the intermountain seismic belt: Geol. Soc. Am. Bull., 85, 1205-1218.
- 37) Stover, C. W., 1977, Seismicity map of the conterminous United States and adjacent areas, 1965-1974: U.S. Geol. Surv. Misc. Field Studies Map MF-812.
- 38) Tchalenko, J., 1974, Outline of seismotectonic provinces of North-Central Iran: Geol. Survey of Iran Rept. 29, 117-126.
- 39) Tchalenko, J. S., and Braud, J., 1974, Seismicity and structure of the Zagros (Iran) - the main recent fault between 33° and 35°N: Phil. Trans. Roy. Soc. London, 277, 1-25.
- 40) Tchalenko, J. S., and Berberian, M., 1975, Dasht-e Bayaz fault, Iran: earthquake and earlier related structures in bedrock: Geol. Soc. Am. Bull., 86, 703-709.
- 41) Tocher, D., 1958, Earthquake energy and ground breakage: Seismol. Soc. Am. Bull., 48, 147-153.
- 42) Ulrich, F. P., 1948, Zones of earthquake probability in the United States: Building Standards Monthly, 17, 11-12.

INTENTIONALLY BLANK



A REPORT ON THE MIYAGIKEN-OKI, JAPAN, EARTHQUAKE OF JUNE 12, 1978

by

H.Kobayashi, K.Seo, S.Midorikawa, Y.Yoshimi, I.Tohno,
K.Tokimatsu, T.Katayama and H.Shibata

ABSTRACT

On June 12, 1978, a severe earthquake broke out in the north-eastern part of Japan. Heavy damages was caused by this earthquake, 27 persons were killed and more than 110,000 houses suffered damage by the earthquake.

Part I: Seismicity of this source area were discussed, Isoseismal map and peak acceleration recorded by SMAC were discussed by an attenuation law and amplification of seismic waves in the layered soil structure. Geological maps and measurements of microtremor were refered for these discussions.

Part II: Sand deposits were liquefied at a number of places causing ground subsidence, settlement of buildings, and displacement of earth-retaining structures. There were some slope failures as well as numerous failures of embankments. The liquefaction potential and settlement of level sand evaluated by previously published methods were in good agreement with the field behavior.

Part III: The damage to lifeline utility systems were described. Extent of damage and process of restoration were summarized for electric power, water supply, city gas and sewerage systems for mostly in the city of Sendai. The distributions of utility damages plotted on maps were qualitatively related to the subsurface site conditions of respective area in Sendai.

Part IV: Detailed damages of lifeline systems, which are telephone communication system, electric power network, and oil storage tanks, were reported.

GENERAL ASPECTS

On June 12, 1978, at 17h 14m of the Japanese Standard Time, Tohhoku Districts, Japan were heavily shaken by a strong earthquake motion. Determination of hypocenter and magnitude of this earthquake were performed by the Japan Meteorological Agency (JMA) and Observation Center for Earthquake Prediction, Faculty of Science, Tohhoku University as follows;

	J.M.A.	Tohhoku Univ.
Longitude	142°13'E	142°.23 E
Latitude	38°09'N	38°.17 N
Depth of focus	40 km	25 km
Magnitude	7.4	-

This earthquake was named as the Miyagiken-Okai Earthquake of 1978 by JMA. The length and width of fault plane were estimated by Seno(1) as 30 km and 80 km, respectively. The source area, isoseismal map by JMA and peak acceleration values of individual site were shown in Fig.1.1.

The damage to persons and houses reported by Miyagi Prefectural Government was as follows;

Sendai City	13 killed	59,912 houses damaged
Miyagi Pref.(except Sendai City)	14	51,080

PART I. STRONG GROUND MOTIONS AND SEISMIC MICROZONING

by
 Hiroyoshi Kobayashi^I, Kazuoh Seo^{II} and Sabroh Midorikawa^{III}

1. SEISMICITY OF THE SOURCE AREA

The seismicity of the source area, off Miyagi prefecture, is high and many large earthquakes have occurred in the past. Two earthquakes of magnitude 7 or more occurred in 1897 and in 1936 to 1937 respectively. And in advance to the earthquake of June 12, 1978, an earthquake of magnitude 6.8 occurred on Feb. 20, 1978. (see Fig.1.2) Therefore, it would be considered that the earthquake of magnitude 7 or more in this area occurs with about 36 years period.

To determine the dimensions of the seismic source zone in this area, authors made a calculation as following. Changing the length of the major and minor axis of the ellipse, whose center is $141^{\circ}.9E$, $38^{\circ}.2N$ and direction of the major axis is $N30^{\circ}E$, they calculated the total accumulated energy of the earthquakes, whose epicenters are located in the ellipse. The left part of Fig.1.3 shows the relation between the length of the major axis of the ellipse and the total accumulated energy of earthquakes. The total energy increase with length of the major axis moderately in the length of 100 to 130 km and gradually in 130 to 160 km and suddenly in over 160 km. It means that the ellipse has entered into another seismic source zone in the length of over 160 km. Consequently the major axis of this seismic source zone should be about 160 km long. The right part of Fig.1.3 shows the relation between the length of the minor axis and the total accumulated energy in case of that the major axis is 160 km. In the same way, the minor axis should be 100 km long. Therefore the size of this seismic source zone is $13,000 \text{ km}^2$ and corresponds to the aftershock area for the main shock of magnitude 8.1 according to the Utsu's formula (2).

The broken line and the circle in Fig.1.2 indicate the seismic source zone and the epicenter in this area respectively. The area of the circle corresponds to the aftershock area obtained from the Utsu's formula. The epicenters of the earthquakes of magnitude 7 or more are located not so far from the fault plane of the earthquake of June 12, 1978. Figs.1.4 and 1.5 show the accumulated frequency curve and the accumulated energy curve of this seismic source zone respectively. Judging from these curves and the size of this seismic source zone, a probable maximum earthquake magnitude in this zone can be regarded as 7.8 approximately.

2. FOCAL MECHANISM, ISOSEISMAL MAP AND GEOLOGICAL CONDITIONS

The Miyagiken-Oki Earthquake of 1978 can be comprehended as the inter-plate earthquake occurred along the Japan Trench. The fault model of this earthquake was proposed by Seno(1) as follows, fault length (L) is 30 km, fault width (W) is 80 km, dip angle is 20° , and dip direction is $W10^{\circ}N$. (see Fig.1.1) The rupture is considered to start at the eastern end and propagate unilaterally. Using this model, the peak accelerations of the incident waves from the seismic bedrock of individual site were calculated

^I Professor of Earthquake Engineering, Dr. of Engineering

^{II} Assistant, ^{III} Graduate student

Graduate School of Engineering and Science, Tokyo Institute of Technology

by using the shear wave velocity of 4.5km/sec.(3) The broken lines in Fig.1.1 indicate the contours of these values and can be regarded as the concentric circles centering around the specified point that is located 0.1W inside from the rupture terminus. The broken line which indicates 30 gals should be compared with the upper boundary of JMA intensity IV. The peak accelerations recorded by strong motion accelerographs, which were indicated by arabic numbers in Fig.1.1, do not always attenuate with distance from the source area and seem to be affected by the subsoil conditions.

Fig.1.6 shows the attenuation of peak accelerations against the distance from the specified point mentioned above. The marks of circle, square and triangle in the figure indicate the estimated value from overturning of the simple bodies, the recorded value of strong motion accelerographs and the calculated value by Midorikawa and Kobayashi's method (3), respectively. The subsoil structure models used in this calculation were shown in Fig.1.7. The calculated peak accelerations of the incident waves attenuate with distance from the source and the estimated and recorded accelerations on the ground surface, on the contrary, do not attenuate in proportion to distance. The calculated values show good agreements with the estimated or recorded values and this result shows that the ratio of amplification of the ground in the eastern part of Sendai City is very large.

Figs. 1.8.a and 1.8.b show the geological map of Ishinomaki and Sendai area respectively. The mark of circle, square and triangle in these figures correspond to those in Fig.1.6 respectively. In the Oshika peninsula that is located on the pre-Neogene formation, the peak acceleration is estimated to be less than 300 gals and the damage of the structures is very little in spite of little distance from the source. In the central part of Sendai City on the diluvium and the eastern part of Sendai City on the alluvium, the peak accelerations are considered to be 350 to 400 gals and over 400 gals respectively. From these results, it was confirmed that the peak accelerations were influenced by the subsoil condition strongly in this earthquake and the importance of the seismic microzoning was reconfirmed.

3. SEISMIC MICROZONING

In Sendai and Ishinomaki districts where damages by this earthquake were the most tremendous, measurements of microtremors were carried out to compare these results with geological conditions and with extents of real damages to buildings and houses. Kind of ground in those area was investigated by Kanai (4) and the authors using the Kanai's method (5) as shown in Figs.1.9.a and 1.9.b. In these figures, geological conditions (6) and locations of severe damaged buildings (instructed by Profs. Izumi and Shibata, Tohhoku University) were indicated together. Existence of poor-ground consisted of Peat was stressed by Okutsu (7), and which was shown in Fig.1.9.a.

The area where the measurements of microtremors were performed can be divided into four types of geological conditions, these are outcrop of Neogene, diluvium, alluvial fan and alluvium. In all measuring points of microtremor, only three points, that is Nos. 16,18 and 22 in Fig.1.9, were regarded as kind of ground I. These points situated on the Neogene formation. The majority of points on the diluvium, Nos. 1, 2 and 4, or alluvial fan, Nos.6 and 7, were decided as ground kind-II. On the other hand, points on the alluvium were seemed to belong to any one of kind-II, III or IV. Then, both area where Peat exists and where kind of ground is IV is not always

coincident. Fig.1.10 shows typical results of microtremor measurement. The upper part of the figure shows Fourier spectrum and the lower part shows period distribution curve by Kanai's method.

4. EXTENTS OF DAMAGES TO BUILDINGS

Damages to reinforced concrete structures were mainly seen on diluvium and alluvial fan in the city of Sendai. In Oroshi-choh, Point O in Fig.1.8.b and No.7 in Fig.1.9.a, three-storied buildings were exhaustively damaged by shear failure of the first story columns as shown in Photos.1.1, 1.2 and 1.3. Photo.1.4. shows a typical example of shear failure with X-shaped cracks. In Nigatake, Point N in Fig.1.8.b and No.6 in Fig.1.9.a, also, three-storied buildings collapsed entirely as shown in Photo.1.5. Photo.1.6 shows a damaged column of a school building in Izumi City.

Damages to steel structures were seen almost in the similar sites mentioned above. Almost all of damages to steel structures brought about buckling and breaking of bracings and failure of anchorings. Photo.1.7 shows an example of broken bracing in Izumi City.

Damage to wooden houses can be divided into two types. Damages due to ground motions were seen distinctly in Rokugo of Sendai districts (Photo.1.8) and in Yamoto of Ishinomaki districts. Damaged area of this type situated on the alluvium. On the other hand, damages due to slope failure of embankment were seen on the terrace, such as Midorigaoka, which is shown in Photo.1.9 and Point M in Fig.1.8.b, for example.

As for damages to special structures, gas storage tank in Haramachi, Photo.1.10, Point H in Fig.1.8.b, blasted and was destroyed by fire, and heavy oil storage tanks in Shichigahama, Photo.1.11, Point S in Fig.1.8.b, were broken out. These facts should be given much attention in all disasters by this earthquake for the reason of immense influence to circumstances.

In Kinka-zan and Oshika-peninsula, in spite of the most adjacent parts to the source area, buildings were not so damaged as Sendai. It was considered as the reason, that those area situated on the firm rock of pre-Neogene and ground motions during main shock seemed to be extremely short-period, notwithstanding large amplitude of acceleration. Difference of damages to simple bodies between in Kinka-zan, Photo.1.12, Point K in Fig. 1.8.a, and in Sendai, Photo.1.13, Point C in Fig.1.8.b, was suggested this fact well.

REFERENCES

- (1) Seno, T. et al; "Focal Mechanism of the Miyagi-ken-oki Earthquake of 1978", Proc. of Seism. Soc. Japan, Oct. 1978 (in Japanese)
- (2) Utsu, T. and A.Seki;"A Relation between the Area of after-shock Region and the Energy of Main-shock", Zisin, Vol.7, 1955 (in Japanese)
- (3) Midorikawa, S. and H.Kobayashi;"On Estimation of Strong Earthquake Motions with Regard to Fault Rupture", Proc. of 2nd Int. Conf. Microzonation, 1978
- (4) Minst. of Construction,"Ground in the Coastal Region of the Bay of Sendai", Oct. 1965 (in Japanese)
- (5) Kanai, K. et al,"On Microtremors VIII", Bull. Earthq. Res. Inst.,Vol.39
- (6) "Hydrogeological Map of the Coastal Region of Bay of Sendai", Hydrogeological Maps of Japan Vol.16, 1968
- (7) Okutsu, H.,"Ground and Groundwater of Great Sendai Sphere",Hobun-do, 1977

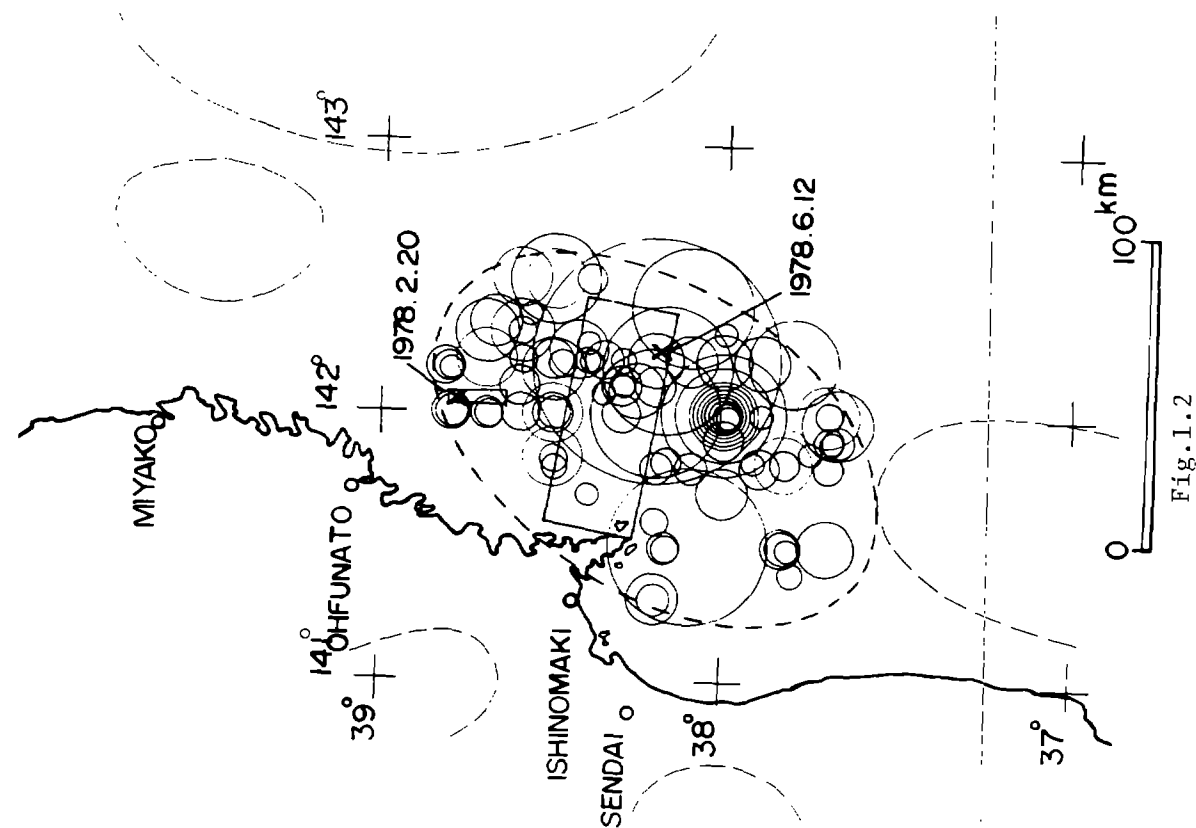


Fig.1.1.2

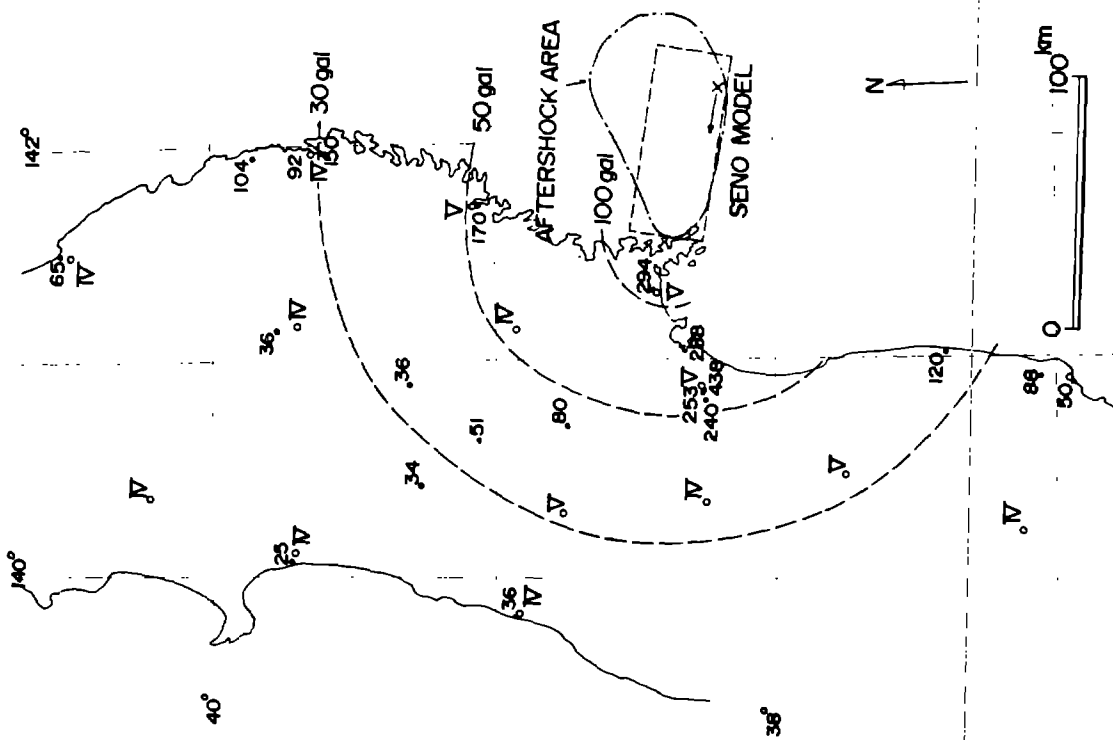


Fig.1.1

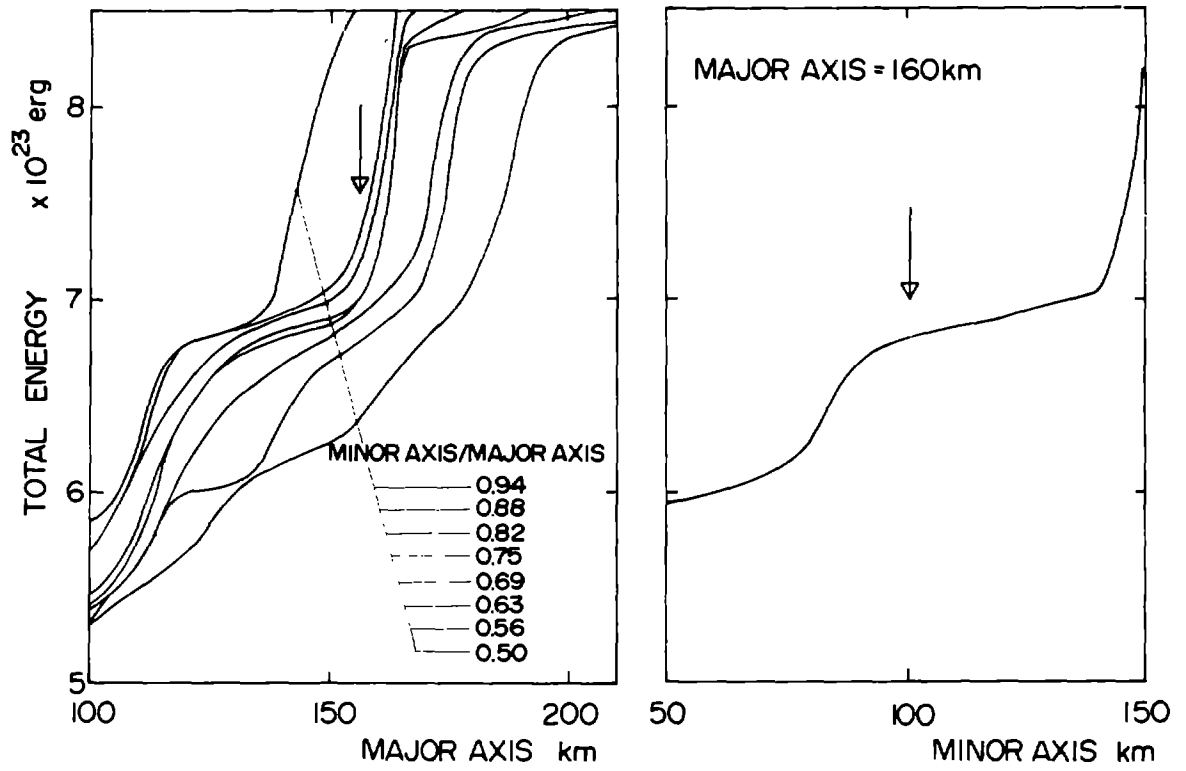


Fig.1.3

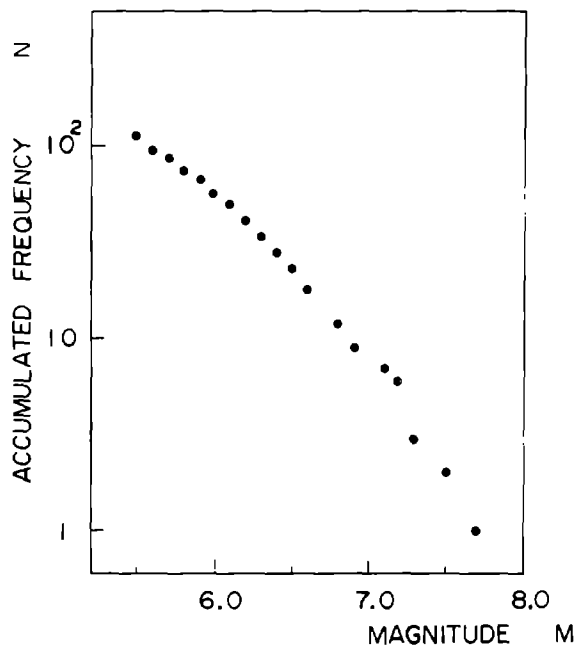


Fig.1.4

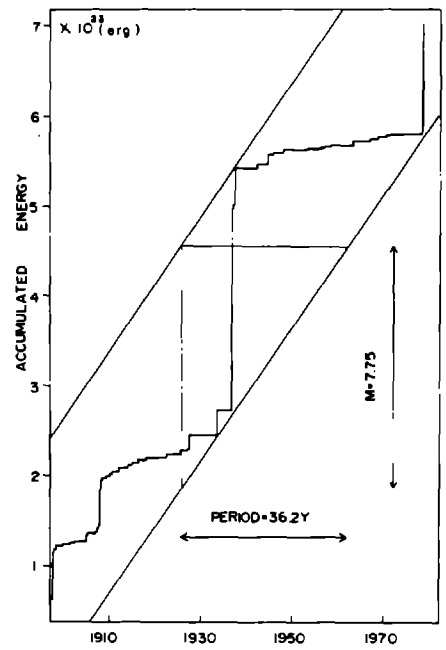
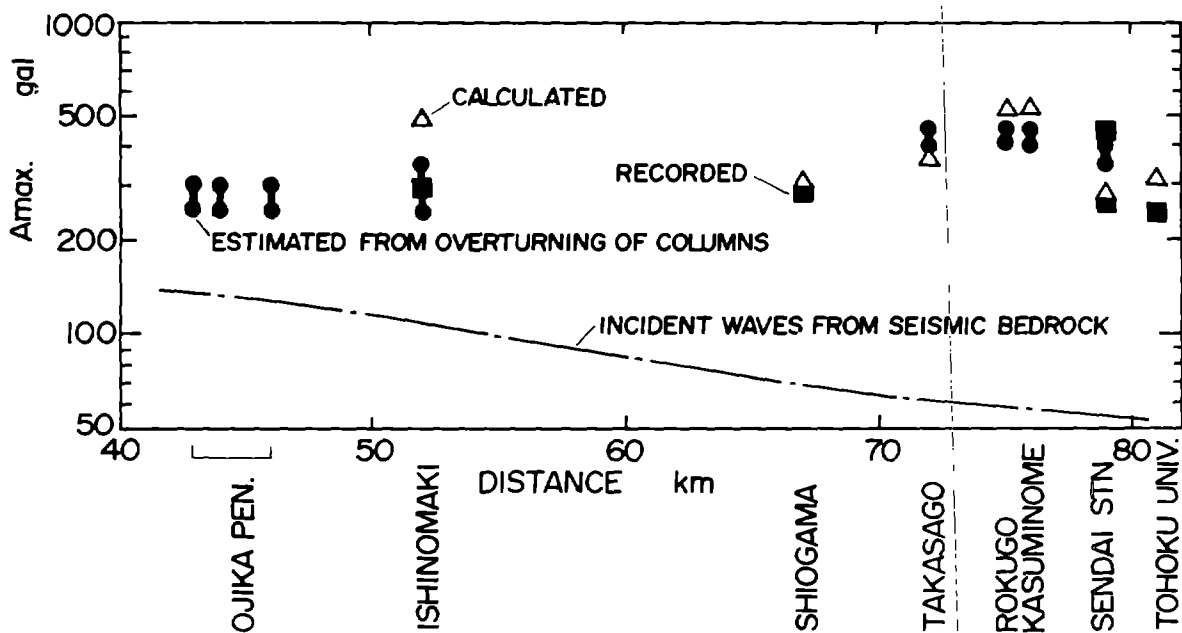


Fig.1.5



ATTENUATION OF PEAK ACCELERATIONS

Fig.1.6

ISHINOMAKI				SHIOGAMA				TAKASAGO			
P	Vs	H	Q	P	Vs	H	Q	P	Vs	H	Q
t/m ³	km/s	m		t/m ³	km/s	m		t/m ³	km/s	m	
1.9	0.40	25	10	1.6	0.08	24	8	1.7	0.16	23	10
				1.8	0.30	3	10	1.8	0.40	29	20
2.0	0.80	200	30	2.0	0.70	93	30	2.0	0.70	28	50
				2.3	1.50	80	100	2.3	1.50	920	100
2.5	3.00	-	200	2.5	3.00	-	200	2.5	3.00	-	200

ROKUGO				KASUMINOME				SENDAI STN.				TOHOKU UNIV.			
P	Vs	H	Q	P	Vs	H	Q	P	Vs	H	Q	P	Vs	H	Q
t/m	km/s	m		t/m	km/s	m		t/m	km/s	m		t/m	km/s	m	
1.6	0.10	7	10	1.6	0.10	6	10	1.8	0.25	8	20	1.9	0.30	23	20
1.7	0.23	11	10	1.7	0.23	11	10								
1.8	0.40	17	20	1.8	0.40	19	20	2.0	0.70	132	50	2.0	0.70	157	50
2.0	0.70	65	50	2.0	0.70	64	50								
2.3	1.50	900	100	2.3	1.50	900	100	2.3	1.50	860	100	2.3	1.50	820	100
2.5	3.00	-	200	2.5	3.00	-	200	2.5	3.00	-	200	2.5	3.00	-	200

PROFILE OF UNDERGROUND STRUCTURES

Fig.1.7

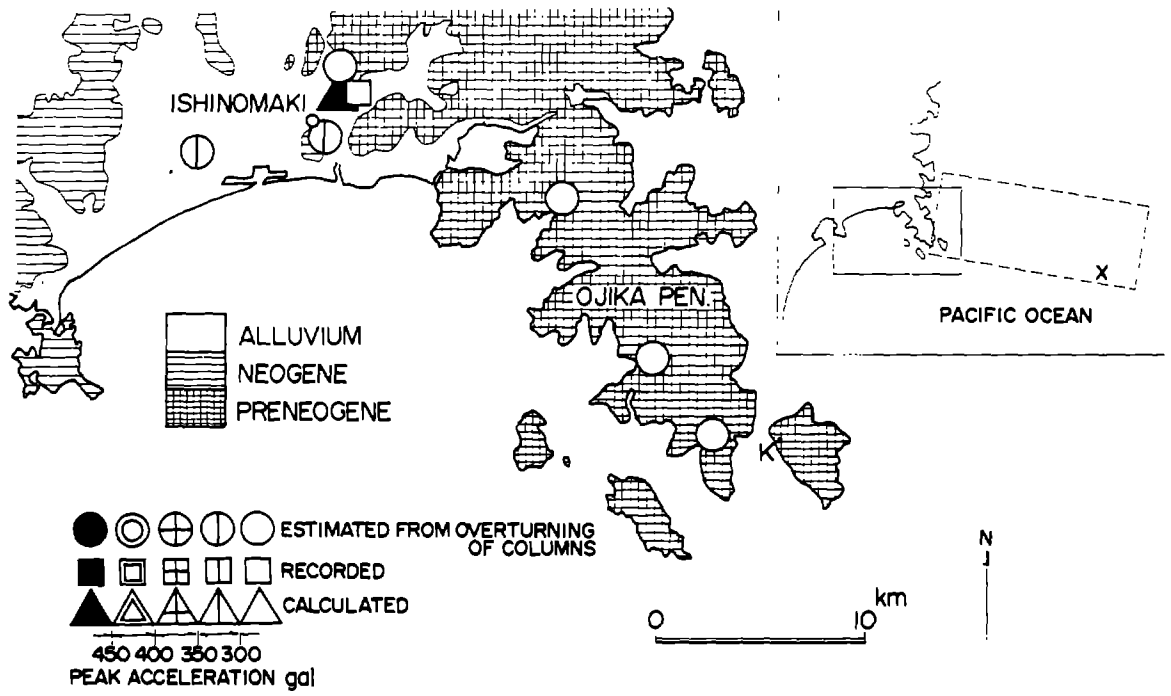


Fig.1.8.a

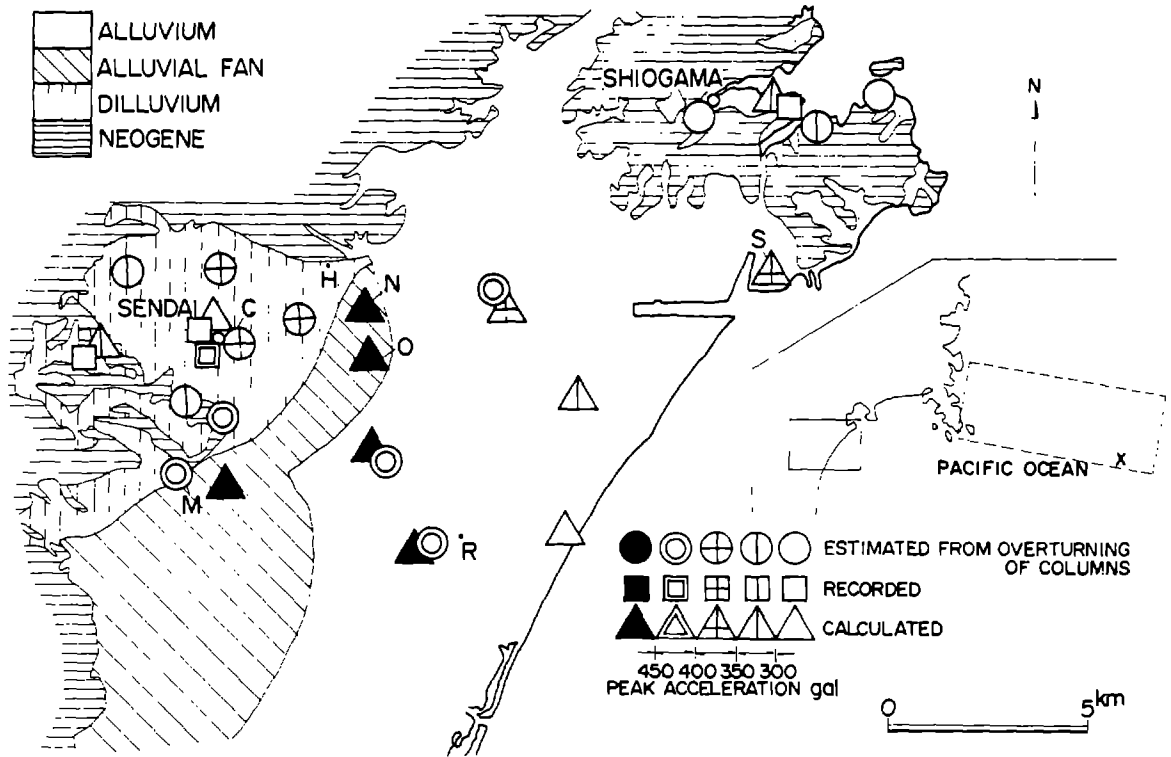


Fig.1.8.b

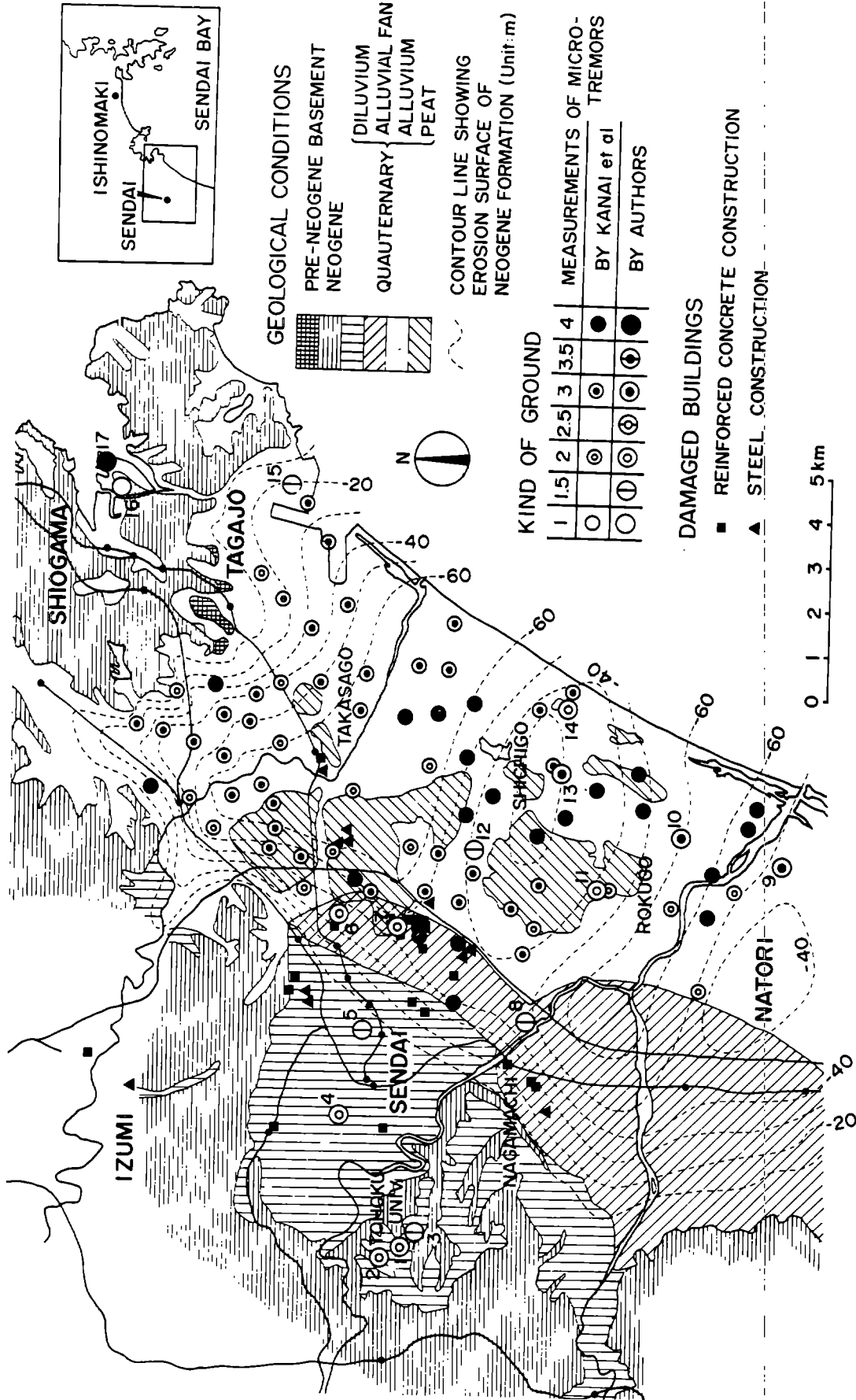
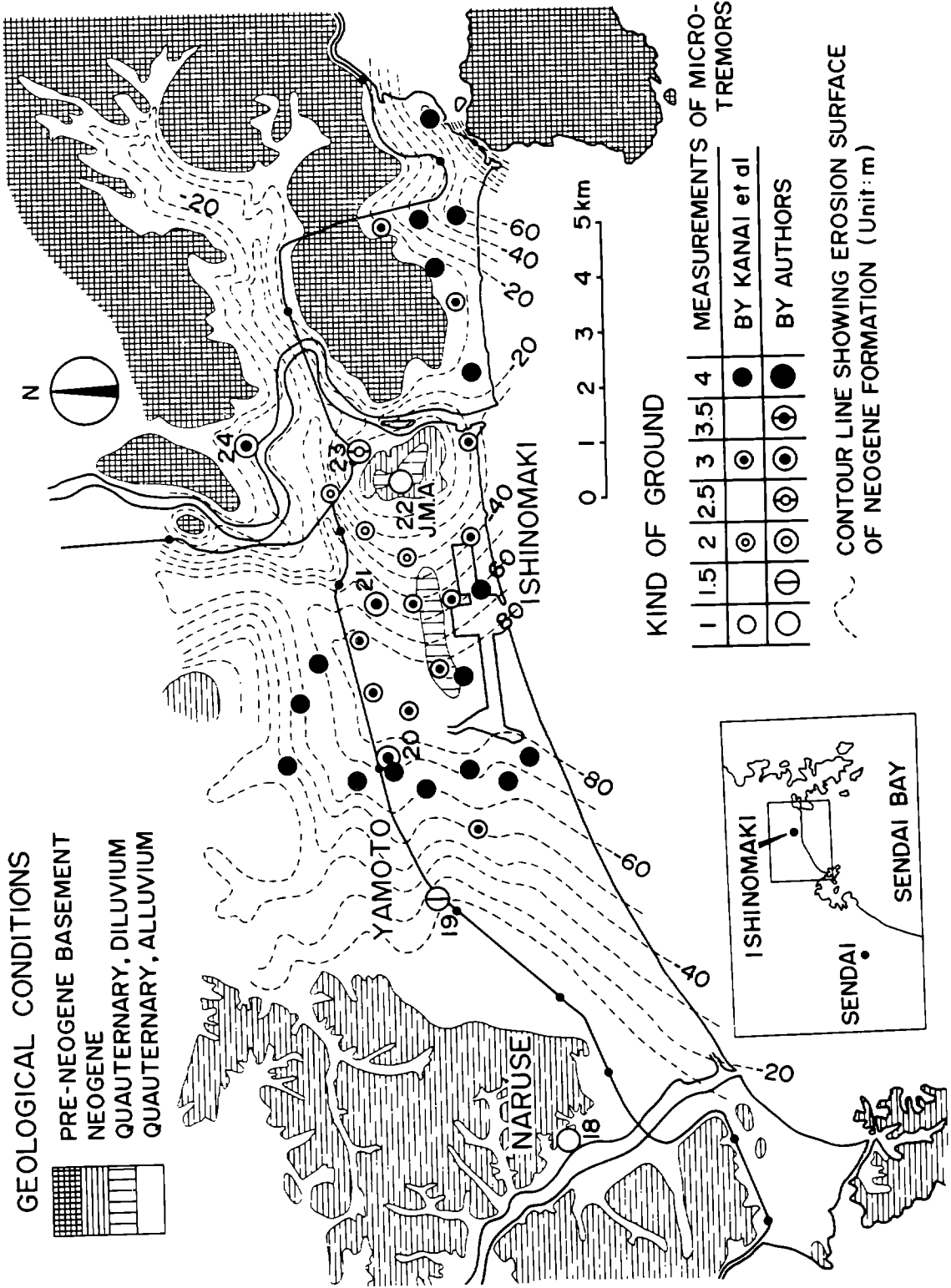
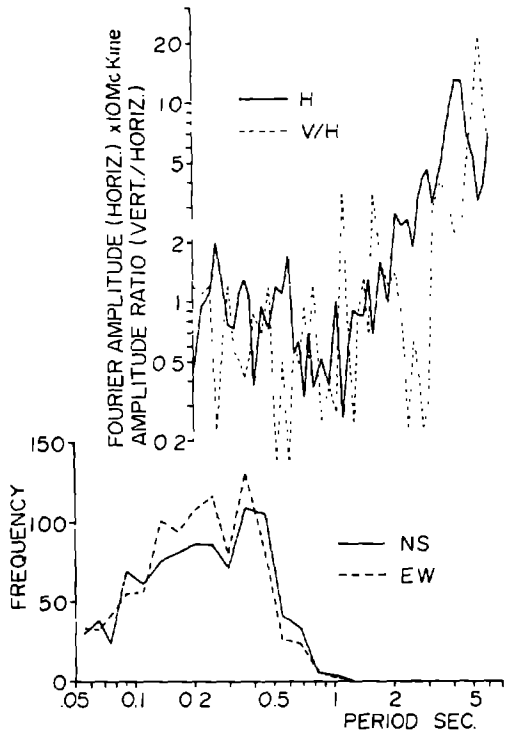


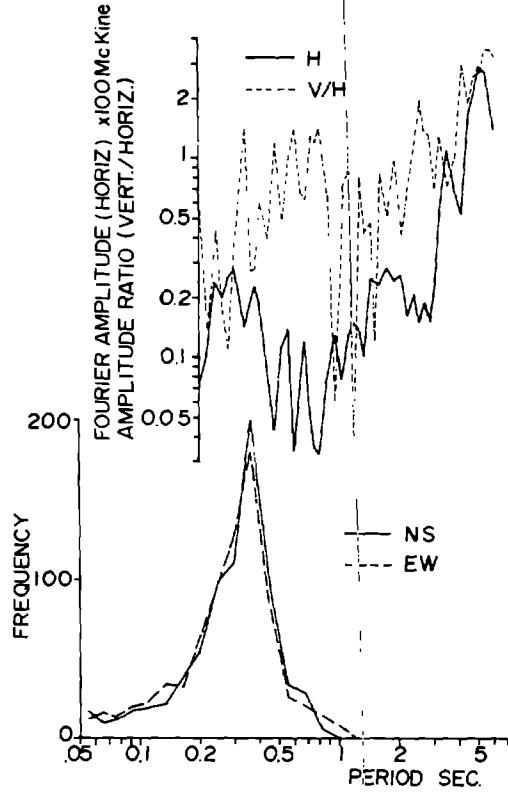
Fig.1.9.a





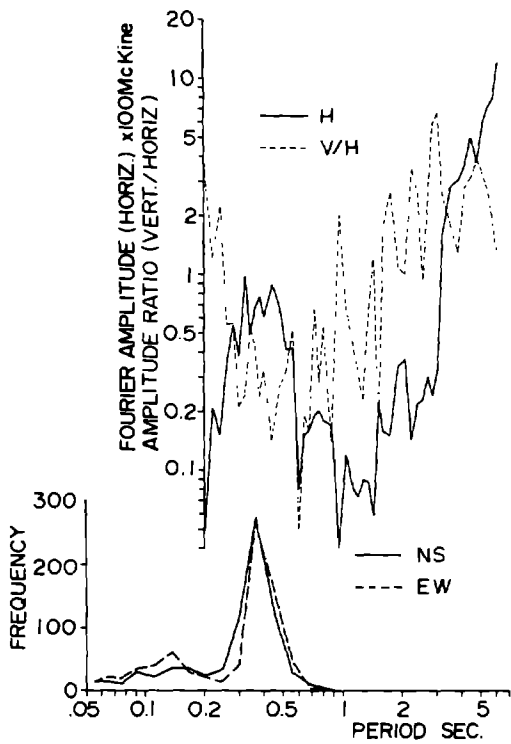
I TOHOKU UNIV. ARCH GL

Fig.1.10.a



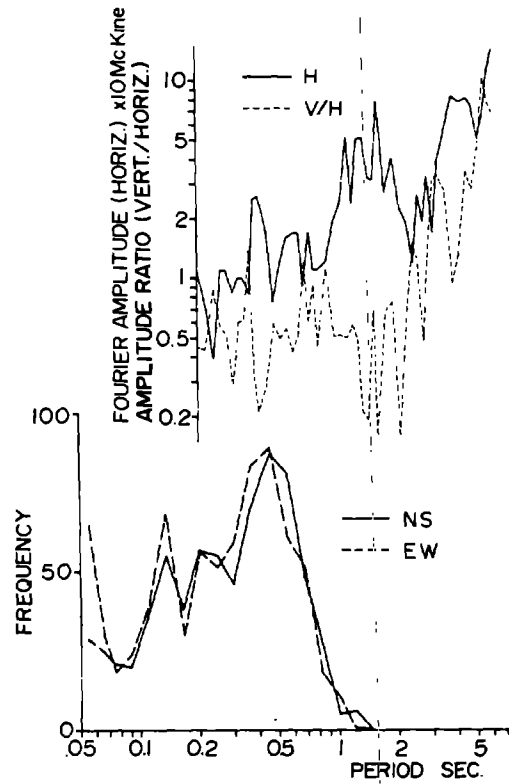
6 NIGATAKE TAIYO-GYOGYOH

Fig.1.10.b



II ROKUGO PRIMARY SCHOOL

Fig.1.10.c



10 HIGASHI-ROKUGO PRIMARY SCHOOL

Fig.1.10.d

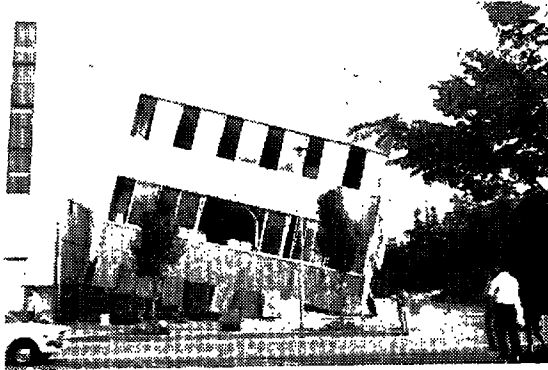


Photo.1.1



Photo.1.2 *

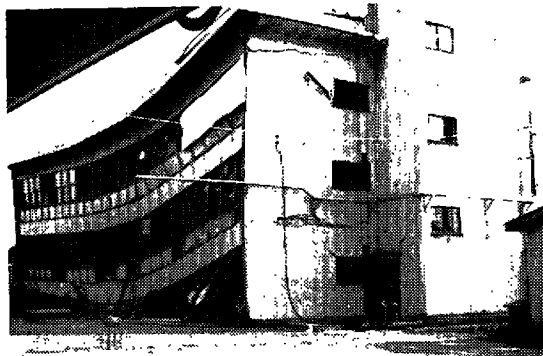


Photo.1.5



Photo.1.3



Photo.1.4 *



Photo.1.6 *

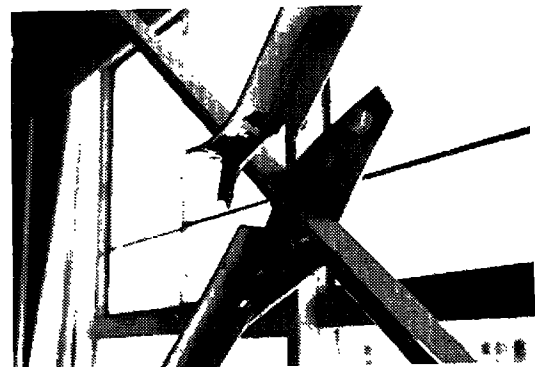


Photo.1.7 *

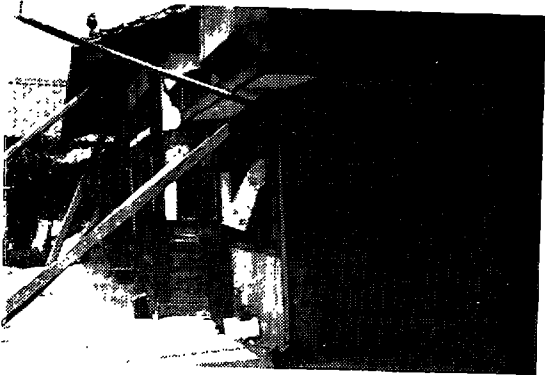


Photo.1.8



Photo.1.9

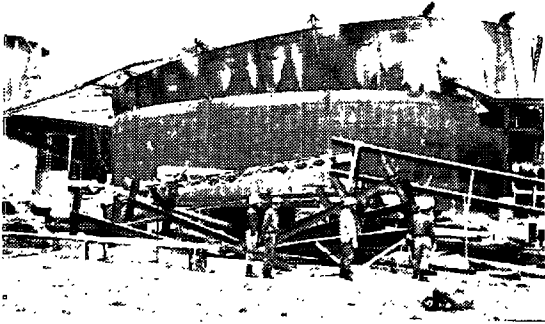


Photo.1.10 *

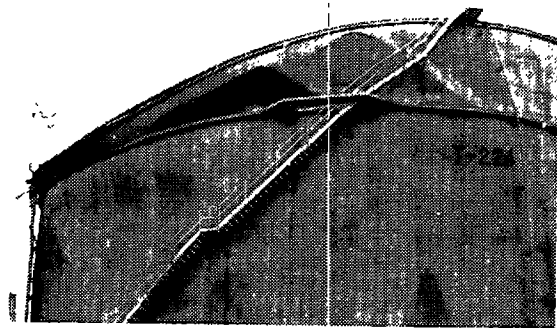


Photo.1.11 *



Photo.1.12



Photo.1.13

* after Prof.M.Fujimoto,
Tokyo Institute of Technology

PART II Geotechnical Aspects of Damage

by

Yoshiaki Yoshimi^I, Ikuo Tohno^{II} and Kohji Tokimatsu^{III}

SAND LIQUEFACTION AND RELATED DAMAGE

The encircled letters from a to r in Fig. 2.1 show the locations where signs of sand liquefaction such as sand blows or flotation of buried sewage treatment tanks were observed. The geological conditions at these sites may be classified as follows: Recent fill: a, e, g, j, q; old riverbed or floodplain: h, n, o; riverbank or sandbar: b, c, d, i, l, m, n, r; lagoon: g. The damage at these locations are shown in Photos 2.1 and 2.2, and summarized in Table 2.1. Concerning Photo 2.2, the ground around a building on piles settled about 40 cm, whereas the ground away from the building settled about 20 cm.

The dashed arc in Fig. 2.1 shows the maximum epicentral distance of liquefied sites, $R=125$ km, which is computed from the following empirical relationship proposed by Kuribayashi and Tatsuoka (1):

$$\log_{10} R = 0.77 M - 3.6 \quad (2.1)$$

in which M is the earthquake magnitude assigned by the Japanese Meteorological Agency. The distance, R , shown in Fig. 2.1 is based on the epicenter announced by the JMA rather than the fault plane location as discussed in Part I of this report because R in Eq. (2.1) is measured from the JMA epicenters. It can be seen in the figure that all the liquefied sites fall within this boundary.

The numbers in solid boxes are the maximum horizontal acceleration observed on the ground surface or in building basement, and the numbers in dotted boxes are approximate values of horizontal acceleration estimated using the method proposed by Midorikawa and Kobayashi (3). The results of the standard penetration tests and the sieve analyses are shown in Figs. 2.2 and 2.3, respectively.

The estimated acceleration and the soil data were used to evaluate the liquefaction potential of level sandy ground at three sites (a, e and c) using the methods proposed by Seed (4) and Tatsuoka et al (5). The results are summarized in Table 2.2, in which the thickness of soil that the methods would predict to liquefy is shown in the second and third lines from bottom. Both methods would have predicted the field behavior correctly, although the method by Tatsuoka et al was better able to differentiate the comparative field behavior.

The settlement of the level ground at Site a was about 20 cm. If this settlement is attributed to consolidation of the sand following liquefaction, the vertical strain is the settlement divided by the thickness of the liquefied sand, i.e., $20 \text{ cm} \div (5 \text{ to } 9 \text{ m}) = 2.2 \text{ to } 4$ percent, which is compatible with the values estimated previously (2, 6).

I Professor, Tokyo Institute of Technology, Tokyo, Japan.

II Assistant, Tokyo Institute of Technology, Tokyo, Japan.

III Graduate Student, Tokyo Institute of Technology, Tokyo, Japan.

SLOPE FAILURES

A number of slope failures occurred as a result of the earthquake. Photo 2.3 shows a typical example of numerous road fill failures. Photo 2.4 shows an extensive failure of stepped subdivisions at Site A (Shiroishi-shi) which is located within the Green Tuff region. The site was developed in 1976 from a natural slope of about 16 degrees. The slide involved an area of 25,000 m² and a volume of 100,000 m³, and the soil near the sliding surface is primarily sand as shown in Fig. 2.3. Considering the gentle slope and the considerable distance from the hypocentral region, it is conceivable that the slide might be attributed to development of pore water pressures in the granular soil, although no direct evidence has been reported yet.

CONCLUSIONS

Sand deposits in recent fills, in old riverbeds, and along riverbanks were liquefied at a number of locations within a radius of about 125 km from the JMA epicenter. The liquefaction caused ground subsidence, settlement of buildings, and displacement of earth-retaining structures. There were some slope failures as well as numerous embankment failures. The above soil behavior was similar to that observed during the Niigata earthquake of 1964 and the Tokachioki earthquake of 1968. The liquefaction potential and settlement of level sand deposits evaluated by previously published methods were in good agreement with the actual field behavior.

REFERENCES

1. Kuribayashi, E. and Tatsuoka, F. (1975), "Brief Review of Liquefaction During Earthquakes in Japan," *Soils and Foundations*, Vol. 15, No. 4, pp. 81 - 92.
2. Lee, K. L. and Albaisa, A. (1974), "Earthquake Induced Settlements in Saturated Sands," *Journal of the Geotechnical Engineering Division, ASCE*, Vol. 100, No. GT4, pp. 387 - 406.
3. Midorikawa, S. and Kobayashi, H. (1978), "On Estimation of Strong Earthquake Motions with Regard to Fault Rupture," *Proc. 2nd International Conf. on Microzonation, San Francisco*.
4. Seed, H. B. (1976), "Evaluation of Soil Liquefaction Effects on Level Ground During Earthquakes," *Proceedings of Geotechnical Engineering Division Specialty Session on Liquefaction Problems in Geotechnical Engineering, ASCE*, pp. 1 - 104.
5. Tatsuoka, F. et al (1978), "A Method for Estimating Undrained Cyclic Strength of Sandy Soils Using Standard Penetration Resistances," *Soils and Foundations*, Vol. 18, No. 3, pp. 43 - 58.
6. Yoshimi, Y., Kuwabara, F., and Tokimatsu, K. (1975), "One-Dimensional Volume Change Characteristics of Sands under Very Low Confining Stresses," *Soils and Foundations*, Vol. 15, No. 3, pp. 51 - 60.

Table 2.1 Geotechnical Damage

	Damage	Location
Liquefaction of sand deposits	Ground subsidence	a, e, f, g, q
	Flotation of sewage treatment tanks	a, e, j
	Settlement/tilting of wooden buildings	a, j
	Cracking/slumping of embankments	a, b, f, g, h, l, m, n, o, r
	Failure of retaining walls	a
	Displacement of revetments	a, b, c
Others	Slope failures	A, B, C
	Mud blows	D, E

a and p: Watari-cho, b: Iwanuma-shi, c and d: Natori-shi, e: Matsushima-cho, f: Naruse-cho, g: Yamoto-cho, h, i and r: Kahoku-cho, j and q: Ishinomaki-shi, k: Miyagi-gun, l: Ohsato-cho, m and n: Kanan-cho, o: Sendai-shi, A: Shiroishi-shi, B: Sendai-shi, C: Izumi-shi, D: Hazama-cho, E: Wakayanagi-cho

Table 2.2 Evaluation of Liquefaction Potential

Site	a Arahama	e Matsushima	c Yuriage		
Estimated acceleration (gal)	240	290	290	290	
Soil type	coarse sand	fine sand	coarse sand	coarse sand	
Mean grain size, D_{50} (mm)	1.0	0.2	0.6	0.6	
Avg N-value	10	4	11	18	
Ground water table (m)	2	0.4	2	2	
Thickness of liquefiable soil (m)	Seed (1976)	6~9	4	12	0
	Tatsuoka et al (1978)	5~9	4	2	0
Field behavior	Liquefaction	Liquefaction (moderate)	Liquefaction (slight)	No liquefaction	

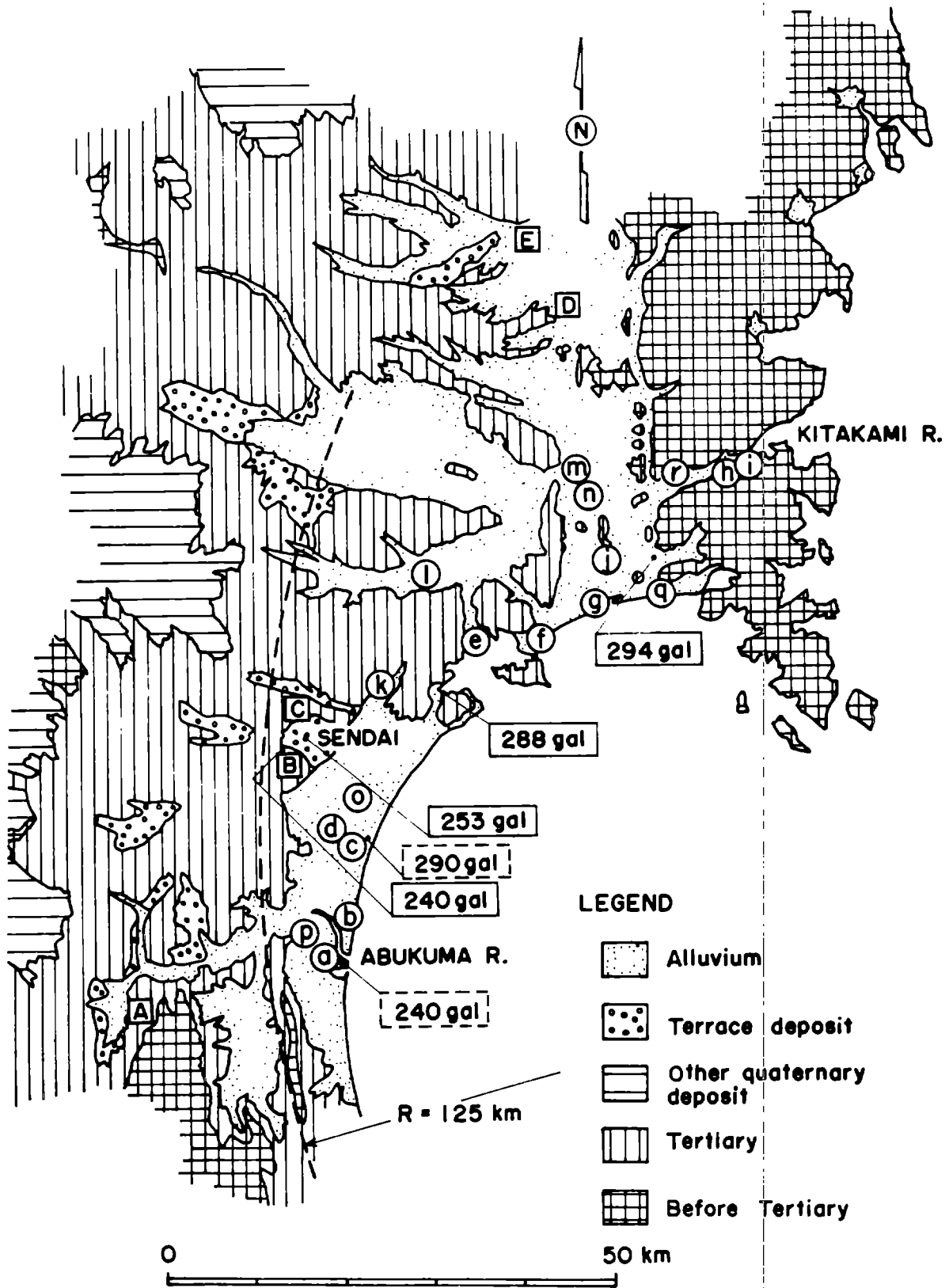


Fig. 2.1 Distribution of damage

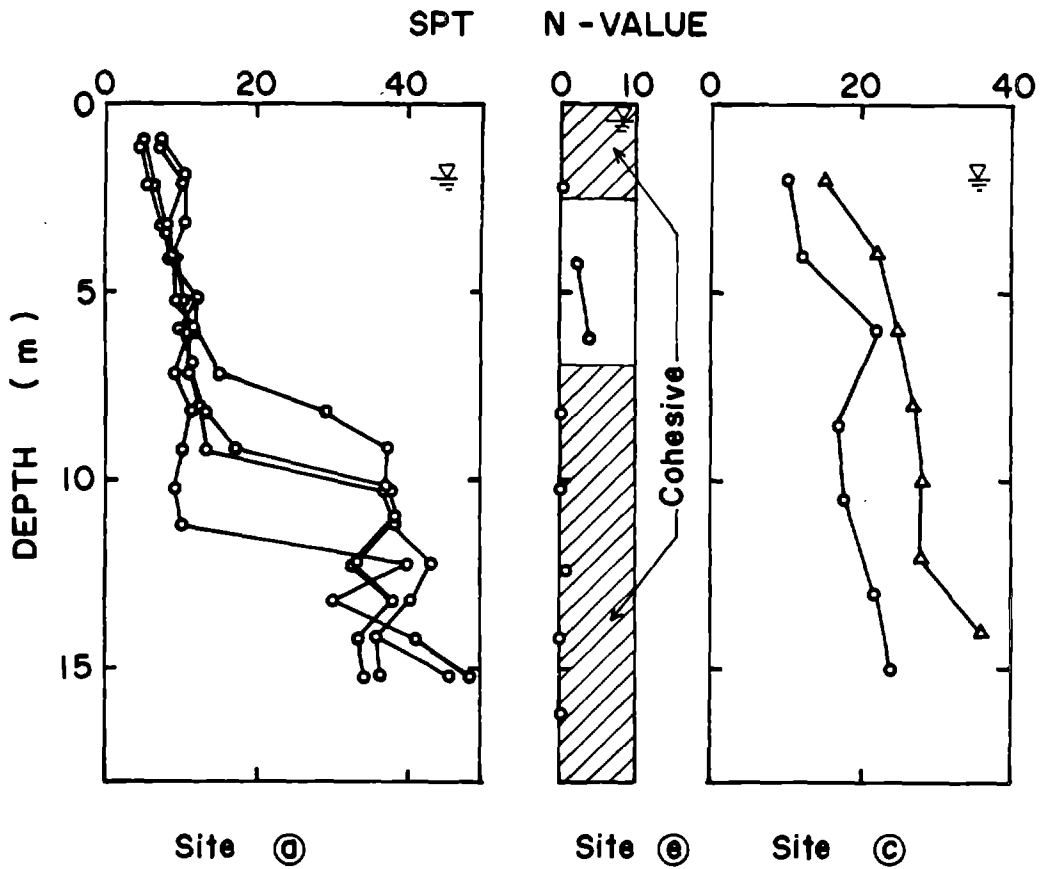


Fig. 2.2 Standard penetration test data obtained before the earthquake

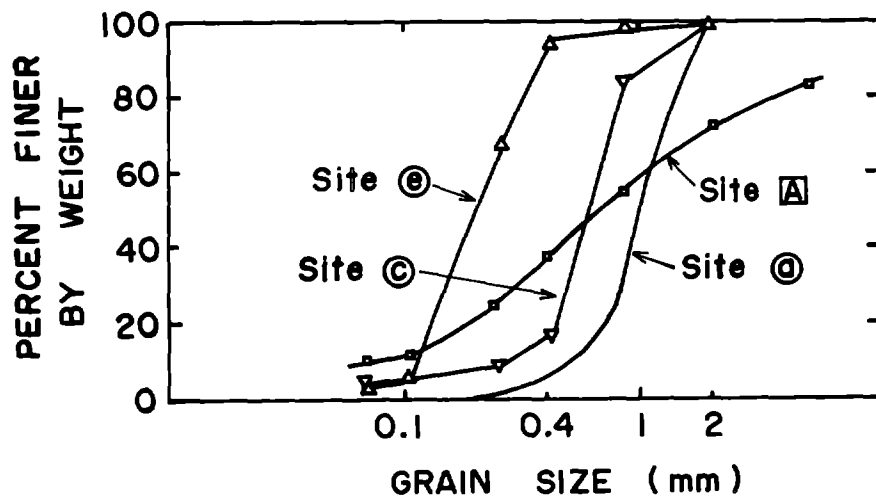


Fig. 2.3 Grain size distribution curves

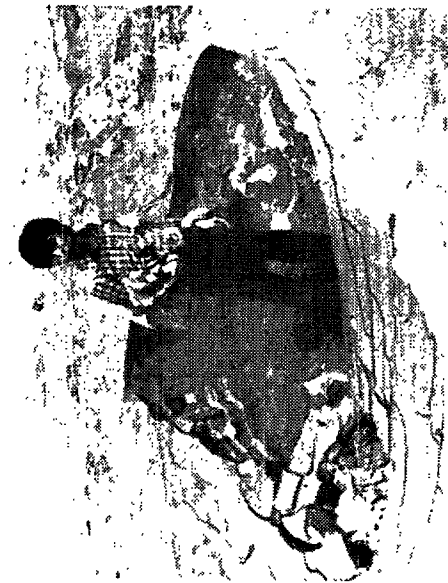


Photo 2.1 Sandblow at Site a

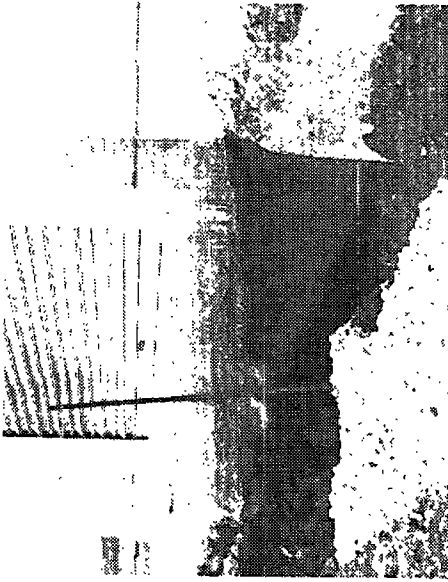


Photo 2.2 Ground subsidence at Site a



Photo 2.3 Typical failure of roadside fill



Photo 2.4 Large slide at Site A

PART III. DAMAGE TO LIFELINE UTILITY SYSTEMS (A)

by
Tsuneo Katayama^I

INTRODUCTION

The 1978 Miyagiken-Oki earthquake of June 12 caused damage to a variety of utility systems in the city of Sendai and several surrounding smaller cities. Degrees of damage generally varied from moderate to severe according to different utilities but it was never catastrophic as experienced in the city of Niigata at the time of the 1964 Niigata earthquake. Although damage was sustained by almost all the lifeline systems such as water, power, transportation and communications systems, this report only describes the damages to electric power, water supply, sewerage and city gas systems. Description is also limited to the city of Sendai, the 14th largest city in Japan with a population of 617,000 on 237 km².

1. EXTENT OF DAMAGE AND ITS RESTORATION

Immediately following the main shock at 5:14 p.m. power service was disrupted and an estimated 680,000 customers were affected in the service area of the Tohoku Electric Power Company. Service was restored to 90 percent of the customer within the same day but blackout to about 80,000 customers remained on the following morning, approximately 15 hours after the occurrence of the earthquake, mostly in the city of Sendai and several surrounding cities. Emergency restoration is reported to have been completed about 38 hours after the earthquake occurrence.

Main causes for the extensive power outages may be summarized as follows:

(1) Electrical equipment was severely damaged at two of the key bulk power substations disrupting a 275-kv trunk line. Most of the equipment damage at these substations was associated with failures of porcelain components and damage caused by inadequate anchorage was minimal. Relays were reported to have normally operated and protected the equipment from electrical faults in the system before equipment was structurally damaged.

(2) Two steam powerplants serving most of the customer load in the Sendai area sustained equipment damage. Five generating units with a total of 1,475,000-kw suffered damage from intense shaking at these plants. Principal damage was sustained by piping systems in a boiler, various supporting structures and a valve within an emergency cooling water pipe.

Early restoration by 275-kv lines was judged impossible because of the damages mentioned above and emergency service was recovered by connecting intact lower voltage (154 and 66-kv) lines. A 250,000-kvA transformer was restored by June 14 and two more (250,000 and 100,000-kvA) were back in service by June 15, all at the most heavily damaged Sendai Susstation. With respect to generating facilities, a 175,000-kw and a 350,000-kw unit were paced in service by June 16 and 18, respectively, at each of the damaged steamplants. Curtailment of customer load become minimal within less than a week.

^I Associate Professor. Institute of Industrial Science, University of Tokyo, Tokyo, Japan

The Sendai City Bureau of Water Supply provides potable water to some 200,000 customers with a total population of 620,000 from its three treatment facilities having a maximum daily capacity of 320,000 m³. Damage was restricted to minor distribution, and pipings and facilities for collection, storage, transmission and treatment works came through the earthquake without any substantial damage. Since the Sendai water supply network uses gravity flow for most of its service area, pumping facilities were minimal and they were not damaged. Power required at treatment facilities was obtained from emergency power units and the power outages did not affect service to customers.

A total of 130 failures are reported to have occurred in the water distribution mains, of which 111 failures were for smaller diameter pipes with 50-100 mm. The emergency operations were primarily concentrated on stopping any uncontrolled flows of water from these broken mains. Consequently, approximately 7,000 services were without water on the morning following the earthquake. The restoration of water service in Sendai was generally fast and the number of customers without water decreased to 5,800 by June 14 and to 800 by June 15, during which normal service was restored in the city of Sendai except for several newly developed residential districts where the stability of fills and slopes came into grave question. Over 4,000 damages to service connections, meters and domestic pipings were reported to the Bureau during June.

The city of Sendai and parts of several surrounding cities are supplied with city gas by the Sendai City Bureau of Gas. City gas is served to approximately 136,000 customers from the Bureau's two factories, one of which produces more than 90 percent of the total supply. Generally speaking, damage to production facilities was light although an old water-sealed gas holder suffered structural damage and was destroyed by the ensuing fire at the smaller factory. All of the three production units at the larger factory stopped due to power outages but equipment damage was slight. Service to customers was maintained for nearly an hour after the earthquake by using the reserved gas in holders. During this period, however, over 200 calls from customers were received informing gas leakage and supply was eventually closed down at 6:15 to all the 136,000 customers.

Approximately 200 km transmission lines, mostly of arc-welded steel pipes, were found intact except for several loosened joints. Repair of these joints was completed by June 15. Four days beginning on June 15 were used to turn off the customers' meters. Leakage surveys and repairs started on a full scale from June 16 for some 1,200 km distribution lines. The service area was broken down into 8 sections by cutting off mains to isolate each section. The 8 isolation areas varied in number of customers from 9,000 to 27,000. The first 350 customers had their services restored by June 16, the fourth day after the earthquake. As surveys and repairs progressed, however, damage in several newly developed residential districts was found much heavier than earlier expected and several sections had to be further divided into smaller subisolation areas. Accumulated percentages restored were 30 percent by June 22, 50 percent by June 24, 70 percent by June 26, and 90 percent by June 28. It was about four weeks after the earthquake that all restorable meters were returned to service. A total of 533 breaks and leaks were found including 212 for mains, 143 for services, and 178 for domestic buried pipes from street boundary to customer's meter.

The sewer system of Sendai serves to approximately 60 percent of the

city's total population. The length of sewers amounts to about 700 km. Sewage is boosted at 11 main pumping stations to a single treatment plant where a daily amount of 260,000 m³ is treated before discharged to shore. Two stations continued pumping after the earthquake by using emergency power units, but at the rest of the stations sewage had to be temporarily discharged to rivers or other water courses because of several causes which were often combined. Power outage was one of the primary causes. Emergency power unit was not installed at one station, and power units did not work properly at six stations mainly because supply of cooling water stopped. At one of the pumping stations where equipment damage was most severe, discharge to river continued for eleven days. The total amount of sewage discharged from the nine pumping stations was some 473,000 m³. Damage to manholes and sewers was numerous. For the trunk sewers alone with a total length of about 50 km, 119 manholes and 454 joints are reported to have suffered damage and a total of approximately 200 m sections had to be replaced.

2. DAMAGE AND SUBSOIL CONDITIONS

The general geologic setting of the Sendai area is shown in Fig.3.1*. The district NE-SW line passing near the center of the map is called the Rifu-Nagamachi tectonic line. The Sendai Plain develops to the east of this line and is bounded by the Pacific Ocean. The alluvial plain is mostly of sand, silt and gravels. Its depth of the Tertiary basement rocks varies abruptly near the tectonic line but is generally between 30 and 60 m. There are several areas in this plain which are covered by 2-5 m thick, very soft peat or mud. The general topography of the area to the west of the tectonic line is characterized by hilly terrain and several levels of terraces. The central part of Sendai including office and business quarters and older residential districts is located on the terrace structure on the north of the Hirose River. The surface deposit of this terrace is loam with its thickness rarely exceeding 2 m. This surface deposit is underlain by gravels and gravels & sand with the standard penetration *N*-value varying from 20 to 60. The tertiary basement rocks, mostly of tuff, is usually found at the depth of 5 to 7 m. The hills are either of very hard andesite or agglomerate, or of workable tuff, shale, mudstone or sandstone. At several places, the tops of hills are covered with loam deposits. A number of residential districts have been developed in the last 30 years on the slopes of the hills with softer workable rocks.

Figures 3.2 to 3.4 are presented to discuss the effect of subsurface site conditions on seismic damage to some utility systems. Note that the lines bounding different site conditions in Fig.3.1 are retained in Figs.3.2 to 3.4 so that easier reference can be made. Figures 3.2 and 3.3 show the distributions of damages to buried gas pipes and water pipes, respectively. Figure 3.4 shows the distribution of damage to electric poles, overhead distribution transformers and overhead wires.

The discussions in the following paragraphs are mostly qualitative and macroscopic in nature, because quantitative analysis should incorporate various factors such as the difference in the densities of facilities in respective areas according to the difference in land use.

* This map was taken with minor modifications from "Subsoil Conditions and Groundwater of the Greater Sendai Area (in Japanese)" by H.Okutsu, Hohbundo Publishing Co., 1975.

It is seen from Figs.3.2 and 3.3 that the distributions of damages to gas and water pipes are similar. The damages is generally very slight in the central part of the city located on geologically stable terrace. Pipe failures concentrated to the newly developed residential districts, where large-scaled cut and fill have extensively altered the original ground profile in order to create shapes and physical condition desired for this particular purpose. Widespread damage was noted for natural and artificial slopes and retaining walls in these cut-and-fill districts, and consequently a number of residential houses were severely damaged. Although houses were also severely damaged on the alluvial plain, the extent of damage to buried pipes was relatively low in this area except for the area in the vicinity of the Japanese National Railways' Nagamachi Station. This area is characterized by an alluvial fan with alteration of silt and gravels. Figure 3.2 shows a concentration of gas pipes damage in this area but the reason for this heavy damage is not clear at present.

According to Fig.3.4 damage to electric distribution facilities is found both in some cut-and-fill areas and on the alluvial plain. Unlike the damage to buried pipes, the damage to poles and pole-mounted transformers is more pronounced on the alluvial plain, where, as mentioned previously, residential houses also sustained heavy damage. Since aboveground structures such as houses and poles are more liable to be influenced by inertia effect caused by seismic ground acceleration, the widespread damage to these structures on the alluvial plain may be accounted for by the amplification effect of thick alluvium.

CONCLUDING REMARKS

Although one could obtain, by examining in depth the extent of damage to utilities and its restoration process, numerous lessons which are extremely important for the mitigation of earthquake-induced disaster in urban areas, only those explicitly related to subsurface site conditions are summarized here.

(1) As exemplified by the distribution of damage to electric power distribution facilities as well as to residential houses, the subsoil amplification effect seems to have major influence on the seismic damage to aboveground structures. Their damage was definitely heavier on the alluvial plain where the depth to the basement rocks is greater than in the terrace area where the soft topsoil is thin and the basement rocks are found at a shallow depth.

(2) Damage to buried pipes concentrated to newly developed residential districts where large-scaled earthwork was recently made. In these areas, because of inherent instability of artificial slopes, insufficient desiccation of fills, and abrupt change in subsoil properties at the boundary between cut and fill, strong seismic shaking easily produces fissures, local settlement, slippage, and relative displacement over short horizontal distances. These were the main causes of buried pipes failures, and the soil amplification effect seems to have played only a minor role.

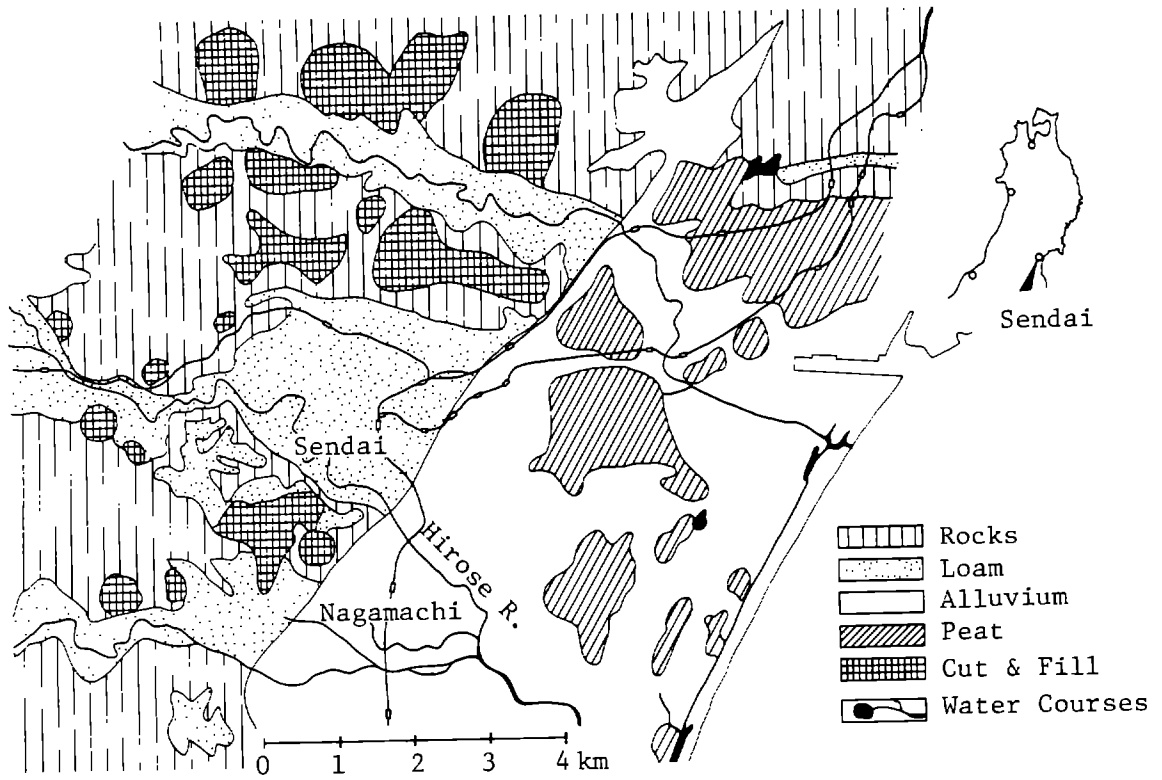


Fig.3.1. General Geologic Setting of the Sendai Area.

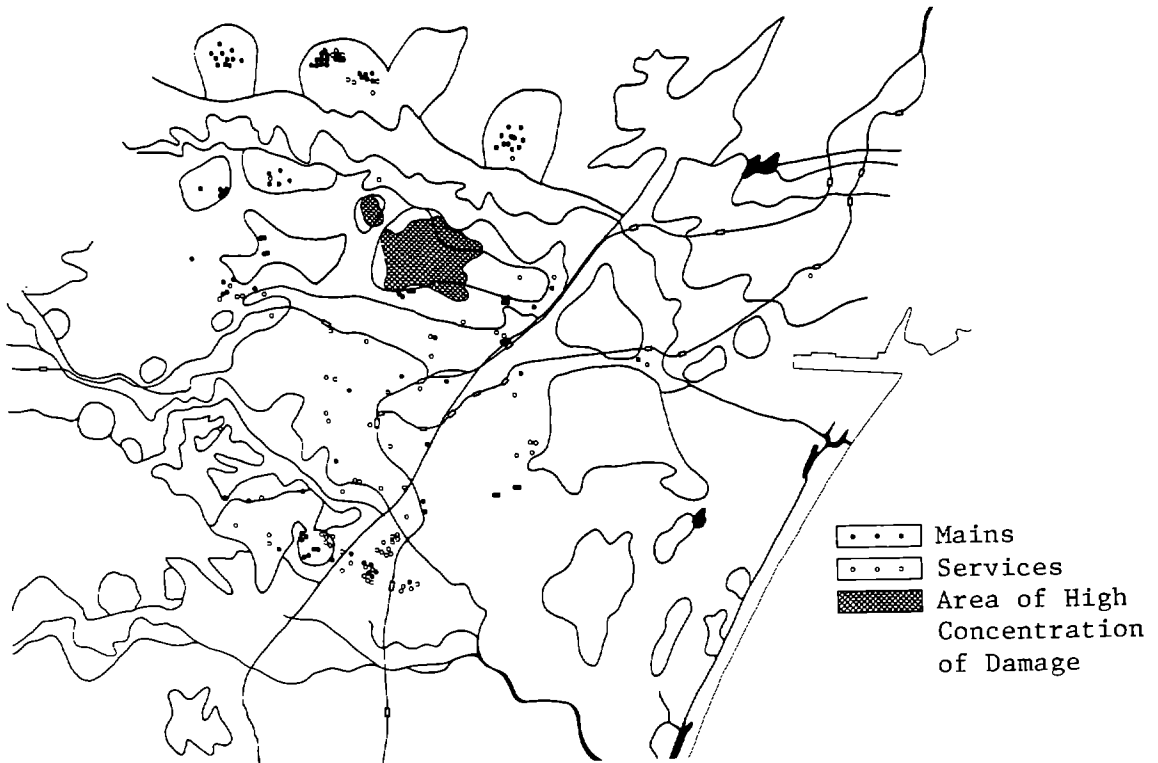


Fig.3.2. Location of Breaks and Leaks of Gas Distribution System.



Fig.3.3. Location of Ruptures in Water Distribution Mains.



Fig.3.4. Location of Areas with Heavy Damage to Power Distribution Facilities.

PART IV. DAMAGE TO LIFELINE UTILITY SYSTEMS (B)

by
Heki Shibata^I

INTRODUCTION

Lifeline systems were typically damaged in this earthquake. Here, the lifeline systems cover water supply, city gas supply, electric power supply, telephone communication and other facilities like oil refineries and storages, a sewer treating factory and so on. The damages of these facilities were mainly observed in a circumbelt from north to south via east of Sendai City. It is quite similar to the distribution of damages of ordinary buildings. Installations and equipment of lifeline system have variety of their failure modes, and some of them are very sensitive to local soil conditions and others are not.

Porcelain insulation is very sensitive to the vibration characteristics of ground motions in a high frequency range. On the other hand, sloshing phenomenon is depending on long period ground motions which are induced in the stratum on the very deep, complete base such in a sense of vibration transmission. The damages of water tanks made by plastics, which were installed on roof of reinforced concrete buildings are worth while to note in the contract of those on the ground.

1. TELEPHONE COMMUNICATION SYSTEM

Author was a member of a technical committee to improve earthquake resistant capacity of the telephone communication system immediately after the Tokachi-oki Earthquake of 1968. The committee described the following criteria in their report,

- i) important line should be double under the consideration of the areal effect of the potential earthquakes,
- ii) building should be designed stronger than ordinary buildings,
- iii) all racks of exchangers should be supported by steel lattice at their top,
- iv) electric power supply to exchangers should be designed stronger than ordinary equipment, especially emergency diesel-generator units and batteries,
- v) towers for the micro-wave communication system on the top of building should be designed with more care on the high acceleration of floor response of the supporting building.

The criterion(iii) brought us unexpected damage of supporting structures. In general, building structures for the equipment were damaged more severely than other ordinary buildings. The author estimated the reasons as follow, that is the weight of equipment on each floor is heavier than the load of ordinary buildings and the layout of windows is different from ordinary buildings and it is easy to have shear type failure on their walls. Therefore, the stiffness of the building was lowered. On the other hand, the stiffness of supporting lattice and rack system is relatively high to that of building. Then they are barging each other, and then anchor points, cable rack along the structure and other supporting devices were damaged. This result was a quite unexpected matter.

^I Professor, Institute of Industrial Science, University of Tokyo, Tokyo, Japan

Other damages of some important parts of systems were coming from somehow care-less designs, that is, the wave guide tube at the foot of a tower, the supporting points of a parabolic antenna, the elbow of cooling water piping of an emergency diesel-generator unit and so on. These damages mainly came from insufficient estimation of mode of failure of each component.

In conclusion, the distribution of damages was wider than that of ordinary buildings, even though there was no critical result.

2. ELECTRIC POWER NETWORK

Electric power network system can be divided into three portions, one is a power generating station, the second is a switching station including transformer, and the third is transmission network. The north switching station, Nanakita, is on a hill of northern part of Sendai City, and it was severely damaged. This station is connecting point of 270 KV line, 150 KV line and 60 KV line. All bushings of two huge transformers of 270 KV line were failed at their roots, and many switch gears, that is, air circuit breakers (ABB), current transformers (CT), lightning arrestors (AR) and capacitor banks were failed. Most of failures showed typical common mode failure.

The manufacturer of the transformer tried the vibration test on a set of a bushing and a part of housing of the 270 KV transformer. According to the specification, they vibrated it by three 0.5g sinusoidal waves at the natural frequency of the bushing system at first. Then, they made continuous resonance test more than 0.5g horizontal input with some vertical ground motions. However, it has never failed.

Most of failures of ABB, CT and AR were at porcelain parts, however, also cast iron parts and aluminium bronze parts. Although both materials are brittle, their strengths are better known than that of porcelain. We made ordinary dynamic design analysis and also vibration tests imposed three resonate waves of level 0.5g on all these items. Nevertheless, they failed under the condition where the estimated maximum acceleration of ground surface was less than 400 gals. Author has a doubt on a shock effect, that is, the maximum ground velocity might exceed some certain value, maybe 100 kine(cm/sec). He has planning to build a high velocity shaking table, whose maximum velocity will be 250 to 300 kine at 1 Hz. Through such testing, the mechanism of failures of brittle materials using in electrical equipment will be clarified.

Such types of damages were also observed at another switching station, Sendai Controlling Station, which is located in the southern part of the city, and a switching yard of Sendai Power Station, in the south-western part. The later one is situated on a hill again, however the former one is situated in rather soft soil area. At Sendai Controlling Station, bushings of the main transformers of 150 KV were partly broken and damages of ABB, CT and AR were observed. Most of them were failed in NS plane. The main transformers moved to northward by the failure of anchor parts, and their bushings which were failed are those of the third bank, that is, the smallest ones of this transformer's bushings. The damages in this station seemed to be induced relatively high acceleration ground motions.

Most of transformers for high tension voltage networks provide rupture

discs for unexpected electric arcs in their oil. It was reported that the mechanism of such rupture discs was very often activated and brought the unnecessary rupturing of the disc. Author is not sure which this was coming from the sloshing phenomenon of insulation oil or from the shock effect of its mechanism.

Sendai Steam Power Plant(175 MW x3 units) and Shin-Sendai Steam Power Plant(350 MW + 600 MW) were subjected to some failures, for examples, rupture of boiler tubers, failures of piping supports and so. These were brought by high acceleration and lower design levels.

3. CYLINDRICAL TANKS

The modes of failure of cylindrical tanks can be classified in three types. Ordinary sloshing phenomena, acceleration response and higher mode coupled vibration between shell and liquid. Sloshing phenomena were observed on tanks of the diameter from 10 to 12 m mainly, that means their natural periods are less than 4 seconds. Some are on fill ground, however, one of them has a very hard foundation soil. It is quite clear that the sloshing phenomenon has no relation to surface soil condition as the author has been pointing out.

On the other hand, we observed higher mode response of oil and shell of a 100,000 kl floating roof tank. The trace of splashed oil on inside of tank wall clearly showed this fact. Three tanks of Tohhoku Oil Refinery were failed at the corner welding lines between side wall and bottom annular plate. Their capacities were 30,000 kl and 20,000 kl. And their natural periods are longer than those of the tanks on which we observed the sloshing phenomenon. The mechanism of failure has not been explained completely, however, it might be that rocking motion of tanks caused local subsidence of their foundation and finally broke it along the welding line of unsupported part of annular (bottom) plate.

Box-shaped water tanks, made by plastics, on roof floor of R.C.buildings were mainly damaged by the acceleration effects. However, some of them were settled on ground foundation, and they seemed to be damaged by sloshing effect.

INDEX OF AUTHORS

- Abdel-Ghaffar, A.M.II-1037
 Abolafia, M.III-1489
 Acharya, H.K.I-379
 Alarcón, E.II-921
 Aki, K.II-1051
 Akky, M.R.III-1307
 Algermissen, S.T.I-291, 497
 Alonso, J.L.I-523
 Alt, J.N.II-669
 Anderson, J.G.I-559
 Apsel, R.II-693
 Arango, I.II-983
 Archuleta, R.J.I-255
 Arya, A.S.II-865

 Ballard, R.F. Jr.II-1013
 Bazán, E.II-657
 Bea, R.G.III-1307
 Bell, E.J.I-471
 Bell, J.W.I-471
 Benjamin, J.R.III-1369
 Bertero, V.V.III-1145
 Bhatia, S.K.II-839
 Bolt, B.A.II-617
 Boore, D.M.I-255; III-1447
 Borchardt, R.D.I-229, 241
 Botsai, E.E.I-193
 Brabb, E.E.I-229, 303
 Brune, J.II-1051
 Byrd, R.C.III-1409

 Campbell, K.W.II-1063
 Chandrasekaran, A.R.III-1157
 Chen, J.H.III-1169
 Chen, P.C.III-1169
 Clayton, D.N.II-983
 Cluff, L.S.I-135, 457, 535;
 II-669; III-1281
 Cochrane, H.C.III-1511
 Cooper, S.S.II-1013
 Crouse, C.B.II-1117

 Delfosse, G.C.III-1223
 Deza, E.I-341
 Dezfalian, H.II-873
 Dobry, R.II-945
 Dominguez, J.II-921
 Donovan, N.C.I-55
 Doyle, E.H.III-1433
 Duke, C.M.II-1025

 Eguchi, R.T.III-1341
 England, R.II-813
 Eskijian, M.L.III-1257
 Esteva, L.II-657

 Finn, W.D.L.II-839
 Fischer, J.A.I-329; III-1329
 Frazier, G.A.II-693
 Fumal, T.E.I-241
 Furuya, T.II-1001

 Gardner, W.S.II-945
 Gibbs, J.F.I-241
 Glass, C.E.I-509
 Goto, N.II-793
 Grant, W.P.II-983

 Hadjian, A.H.III-1199
 Hall, W.J.III-1235
 Harp, E.L.I-279, 353
 Hart, E.W.II-635
 Hart, G.C.III-1135
 Hasselman, T.K.III-1341
 Hattori, S.I-421
 Hayes, R.A.III-1383
 Hays, W.W.I-497; II-753
 Helmberger, D.V.I-27
 Herd, D.G.I-231
 Herrera, I.II-813
 Hisada, T.III-1187
 Hutton, J.R.I-179

 Idriss, I.M.I-457; III-1281
 Isenberg, J.II-911
 Ishibashi, I.I-81
 Ishihara, K.II-897
 Iwasaki, T.II-705, 885; III-1211
 Iwasaki, Y.T.I-445

 Jaén, H.I-341
 Jennings, P.C.I-27
 Joyner, W.B.I-255

 Kafka, A.L.III-1489
 Kagami, H.II-793
 Kallaby, J.III-1459
 Kao, C.S.I-367
 Kappler, H.III-1399
 Katayama, T.I-606; II-705
 Kawashima, K.II-705; III-1211
 Keefer, D.K.I-279, 353
 King, E.J.I-267
 King, J.II-1051
 King, K.W.I-497
 Kircher, C.III-1369
 Kisslinger, C.I-3
 Kobayashi, H.I-588; II-825
 Kockelman, W.J.I-303
 Kogan, J.I-341
 Kudo, K.II-765

- Kuribayashi, E.III-1499
 Kuroiwa, J.I-341

 Lagorio, H.J.I-193
 Lam, I.II-1089
 Liang, G.C.II-1025

 Mahin, S.A.III-1145
 Mândrescu, N.I-399
 Marcuson, W.F. IIIII-1013
 Mardiross, E.II-739
 Martín, A.II-921
 Martin, G.R.II-1089
 Matthews, R.A.III-1531
 Mau, S.T.I-367
 McWhorter, J.G.I-329
 Midorikawa, K.I-547
 Midorikawa, S.I-588; II-825
 Mileti, D.S.I-179
 Miller, R.D.I-497
 Milne, W.G.I-323
 Miranda, J.C.III-1223
 Mitchell, W.W.III-1459
 Moazami-Goudarzi, K.I-391
 Mohraz, B.III-1257
 Morgan, J.R.III-1235
 Moriwaki, Y.III-1433
 Mukerjee, S.II-865
 Murakami, S.I-547
 Murphy, V.J.I-153

 Nair, D.III-1383
 Nandakumaran, P.II-865
 Negmatullaev, S.Kh.II-681
 Nemat-Nasser, S.II-957
 Nersesov, I.II-1051
 Newmark, N.M.III-1235
 Nichols, D.R.III-1531
 Nishi, M.II-971
 Noda, T.II-971
 Nowack, R.L.I-485

 Ogawa, K.II-897
 Ohsaki, Y.III-1187
 Ohta, T.III-1187
 Ohta, Y.II-793
 Okahara, M.II-1001
 Olson, R.A.III-1475
 Oweis, I.S.II-777

 Packer, D.R.I-457
 Page, W.D.II-669
 Parhikhteh, H.I-391
 Paris, F.II-921
 Patwardhan, A.S.I-485, 535;
 III-1281, 1291
 Paul, D.K.III-1157

 Perkins, D.M.I-267
 Perkins, J.B.I-315
 Petrovski, J.I-413; III-1269
 Ploessel, M.R.II-647
 Power, M.S.II-801
 Prager, S.R.II-873
 Preston, R.F.I-267
 Prothero, W.II-1051
 Puri, V.K.II-865

 Remmer, N.S.I-215
 Rogers, A.M.II-753
 Rojahn, C.II-681; III-1135
 Roth, W.H.II-1105

 Sabina, F.A.II-813
 Sadigh, K.II-801
 Saeki, M.II-705
 Sánchez-Sesma, F.J.II-729
 Savage, W.U.II-669
 Schell, B.A.I-571
 Schuëller, G.I.III-1399
 Schwartz, D.P.I-457
 Scott, R.F.II-1037
 Seleznyov, G.S.II-681
 Self, G.II-1051
 Selzer, L.A.III-1341
 Seo, K.I-588
 Shakal, A.F.II-717
 Sherif, M.A.I-81
 Shibata, H.I-612
 Shima, E.I-433
 Shioi, Y.II-1001
 Shokooh, A.II-957
 Shpilker, G.II-1051
 Simpson, D.W.II-681
 Singh, R.D.II-945
 Spiker, C.T.III-1329
 Steinbrugge, K.V.I-203, 291
 Sugimura, Y.II-933
 Swan, F.H. IIII-457
 Swanger, H.J.III-1447
 Sweet, J.II-693

 Tai, M.I-445
 Tanimoto, K.II-971
 Tatsuoka, F.II-885
 Tazaki, T.III-1499
 Themptander, R.III-1525
 Tillson, D.D.I-485
 Tinsley, J.C.I-267
 Tocher, D.II-669
 Tohno, I.I-600
 Tokida, K.II-885
 Tokimatsu, K.I-600; II-853
 Toksöz, M.N.II-717
 Traubenik, M.L.II-1105

Trexler, D.T.	I-471
Trifunac, M.D.	I-559
Tsai, C.F.	II-1089
Ts'ao, H.S.	II-1077
Tucker, B.	II-1051
Tuel, D.G.	I-279
Turner, B.E.	II-1117
Urbina, L.	I-523
Vaid, Y.P.	II-839
Valera, J.E.	II-1105
Vaughan, D.K.	II-911
Veletsos, A.S.	I-111
Watabe, M.	III-1187
Watt, B.J.	III-1409
Webster, F.A.	III-1369
Weichert, D.H.	I-323
Weidler, J.B.	III-1383
Werner, S.D.	II-1077
Whitman, R.V.	III-1247
Wieczorek, G.F.	I-279, 353
Wiggins, R.A.	II-693
Wilson, R.C.	I-353
Wu, F.T.	II-701
Yasuda, S.	II-885
Yoshikawa, S.	I-445
Yoshimi, Y.	I-600; II-853
Youd, T.L.	I-267
Youngs, R.R.	II-801

REPORT DOCUMENTATION PAGE	1. REPORT NO. NSF/RA-780617	2.	3. Recipient's Accession No. PB300308
4. Title and Subtitle Microzonation for Safer Construction, Research and Application, Proceedings of the Second International Conference, Volume I, San Francisco, November 26 - December 1, 1978		5. Report Date December 1978	
7. Author(s)		8. Performing Organization Rept. No.	
9. Performing Organization Name and Address University of Washington at Seattle Seattle, Washington 98105		10. Project/Task/Work Unit No.	
12. Sponsoring Organization Name and Address Engineering and Applied Science (EAS) National Science Foundation 1800 G Street, N.W. Washington, D.C. 20550		11. Contract(C) or Grant(G) No. (C) (G) PFR7723228	
15. Supplementary Notes		13. Type of Report & Period Covered Conference proceedings	
16. Abstract (Limit: 200 words) This first of three volumes of technical papers presented at the Second International Conference summarizes the state of knowledge in the zoning areas for earthquake effects and identifies future research needs in seismic microzonation. Although the titles of papers contained in all three volumes are listed and represent diverse fields of interest such as geology, seismology, engineering, sociology, economics, and architecture, this volume contains only those papers on the state-of-the-art and microzonation which make up the first two sessions of the conference. The first session consists of eleven papers in areas such as global tectonics, strong motion seismology, soil dynamics, social aspects of earthquakes, urban design, earthquake insurance and government responsibility in microzonation. Included in the second session are a total of thirty-six papers, nine of which concentrate on progress on seismic zonation in the San Francisco Bay region. Other areas reported in relation to microzonation are British Columbia, Peru, Guatemala, Taiwan, the Phillipines, Iran, Vrancea, Japan, Nevada, and Utah. This volume also contains a four-paper report on the Miyagiken-oki, Japan Earthquake of June 12, 1978. An index of authors is included.		14.	
17. Document Analysis a. Descriptors Earthquakes Earthquake resistant construction Utah Seismology Soil dynamics Technical reports Meetings Nevada Geologic processes California b. Identifiers/Open-Ended Terms c. COSATI Field/Group			
18. Availability Statement NTIS		19. Security Class (This Report) 21. No. of Pages 613	
		20. Security Class (This Page) 22. Price PCA99/105	

